

Enantioselective Radical Strategy
for the Stereoselective Synthesis of
Three-Membered Heterocycles via
Co(II)-Based Metalloradical Catalysis

Xavier Riart-Ferrer

A dissertation for PhD
submitted to the Faculty of
the department of Chemistry
in partial fulfillment
of the requirements for the degree of
Doctor of Philosophy

Boston College
Morrissey College of Arts and Sciences
Graduate School

April 2021

Enantioselective Radical Strategy for the Stereoselective Synthesis of Three-Membered Heterocycles via Co(II)-Based Metalloradical Catalysis

Xavier Riart-Ferrer

Advisor: Professor X. Peter Zhang, PhD

Highly strained three membered heterocycles are a common motif in many biologically relevant molecules and represent a versatile building block for organic synthesis. Of special interest for asymmetric synthesis is the construction of enantioenriched aziridines and epoxides, which are often used as chiral synthons to introduce heteroatoms in a stereoselective fashion. Among different elegant strategies, the direct aziridination and epoxidation of the ubiquitous alkene functionality represents one of the most powerful methods to access these motifs. Given the synthetic importance of the enantioenriched smallest aza- and oxaheterocycles, the focus of this dissertation is centered on the design and use of chiral cobalt porphyrins as catalysts to develop new methodologies for the asymmetric radical aziridination and epoxidation of alkenes.

In the first part of this dissertation, we focused on using carbonyl azides as nitrogen source for the enantioselective radical aziridination of alkenes. Despite its high functionality and versatility for further derivatization, carbonyl azides have never been reported as nitrogen source for intermolecular asymmetric alkene aziridination. In the second part of this dissertation, we focused on opening up a new area of research, which involves the generation and characterization of the unprecedented cobalt porphyrin-supported oxygen-centered radical species. Finally, we demonstrated the synthetic utility of these new radical species by developing a new system for the asymmetric epoxidation of alkenes through the design and development of a novel family of catalyst named “JesuPhyrin”.

TABLE OF CONTENTS

Table of Contents.....	i
List of Schemes.....	vi
List of Tables.....	ix
List of Figures.....	x
Table of Abbreviations.....	xii
Acknowledgements.....	xv
Preface.....	1

Chapter 1: Review on Catalytic Systems for Enantioselective Radical Aziridination of Alkenes

1.1 Introduction.....	4
1.2 Phosphoryl Azides as Nitrogen Source for the [Co(Por)] Catalyzed Enantioselective Aziridination of Alkenes	6
1.3 Sulfonyl Azides as Nitrogen Source for the [Co(Por)] Catalyzed Enantioselective Aziridination of Alkenes.....	8
1.4 Fluoroaryl Azides as Nitrogen Source for the [Co(Por)] Catalyzed Enantioselective Aziridination of Alkenes	10
1.5 Allyl Azidoformates as Nitrogen Source for the [Co(Por)] Catalyzed Asymmetric Intramolecular Aziridination.....	13
1.6 Summary and Outlook.....	16

Chapter 2: Enantioselective Radical Aziridination of Alkenes with Carbonyl Azides

2.1	Introduction	18
2.2	Results and Discussion.....	22
2.2.1	Reaction Optimization	22
2.2.2	Substrate Scope.....	25
2.2.3	Mechanistic Studies	28
2.2.4	Synthetic Applications	39
2.3	Conclusions.....	43
2.4	Experimental Section	45
2.4.1	General Considerations.....	45
2.4.2	TrocN ₃ Synthesis	46
2.4.3	General Procedure for Enantioselective Aziridination of Styrenes	47
2.4.4	Characterization of <i>N</i> -Troc Aziridine Products	47
2.4.5	General Procedure for the Deprotection of <i>N</i> -Troc Aziridines.....	60
2.4.6	Characterization Data of <i>N</i> -H aziridines.....	60
2.4.7	General Procedure for the Ring-opening Reactions of <i>N</i> -Troc Aziridines with Different Nucleophiles.....	61
2.4.8	Characterization Data of Ring-Opening Products	62
2.4.9	General Procedure and Characterization Data for the Reaction of <i>N</i> -Troc Aziridines with Primary Amines	65
2.4.10	Mechanistic Study of the Proposed Stepwise Radical Mechanism	67
2.4.11	X-ray Crystallographic Information	72
2.4.12	DFT Calculations	76

Chapter 3: Generation and Characterization of Unprecedented α -Co(III)-Oxyl Radicals by Metalloradical Activation of Oxygen Radical Precursors

3.1	Introduction	113
3.2	Results and Discussion.....	116
3.2.1	Initial Investigation	116
3.2.2	Characterization Studies of α -Co(III)-Oxyl Radicals with NaOCl.....	119
3.2.2.1	UV-Vis Spectroscopy.....	119
3.2.2.2	Electron Paramagnetic Resonance (EPR)	120
3.2.2.3	High Resolution Mass Spectrometry.....	121
3.2.2.4	Reactivity Towards Epoxidation.....	123
3.2.2.5	Isotope Labeling studies.....	124
3.2.2.6	Computational Studies	127
3.3	Conclusions	132
3.4	Experimental Section	133
3.4.1	General Considerations.....	133
3.4.2	Characterization of α -Co(III)-Oxyl Radicals by UV-Vis Using Different Oxygen Radical Precursors.....	134
3.4.3	Characterization of α -Co(III)-Oxyl Radicals by UV-Vis Using NaOCl ..	134
3.4.4	Characterization of α -Co(III)-Oxyl Radicals by EPR Using Different Oxygen Radical Precursors.....	136
3.4.5	Characterization of α -Co(III)-Oxyl Radicals by EPR using NaOCl	137
3.4.6	Characterization of α -Co(III)-Oxyl Radicals by HRMS	143

3.4.7	General Procedure for Enantioselective Epoxidation of Styrene	147
3.4.8	DFT Calculations	148

**Chapter 4: New Catalytic System for Enantioselective Radical Epoxidation
of Alkenes: Catalyst Development, Substrate Scope, and Reaction
Mechanism**

4.1	Introduction	157
4.2	Results and Discussion.....	160
4.2.1	Ligand Screening	160
4.2.2	Design of New Ligands	163
4.2.3	New Catalyst Synthesis.....	165
4.2.4	Reaction Optimization	167
4.2.5	Substrate Scope.....	168
4.2.6	Mechanistic Studies	171
4.3	Conclusions	174
4.4	Experimental Section	175
4.4.1	General Considerations.....	175
4.4.2	Catalysts Synthesis.....	176
4.4.3	General Procedure for Enantioselective Epoxidation of Styrenes	207
4.4.4	Characterization of Styrene Oxide Products.....	208
4.4.5	X-ray Crystallographic Information	218
5.	References	217
6.	Spectral Data.....	240
6.1	Spectral Data for Chapter 2.....	S1

6.2	Spectral Data for Chapter 3.....	S178
6.3	Spectral Data for Chapter 4.....	S188

LIST OF SCHEMES

Scheme 1.1 Co(II)-MRC Activation of Diazo and Azide Compounds	2
Scheme 1.2 General Proposed Catalytic Cycle for the [Co(Por)] Catalyzed Aziridination of Alkenes with Organic Azides as Nitrogen Source via MRC.....	6
Scheme 1.3 Phosphoryl Azides as Nitrogen Source for the [Co(Por)] Catalyzed Enantioselective Aziridination of Alkenes	7
Scheme 1.4 Tces-Azide as Nitrogen Source for the [Co(Por)] Catalyzed Enantioselective Aziridination of Alkenes.....	9
Scheme 1.5 Fluoroaryl Azides as Nitrogen Source for the [Co(Por)] Catalyzed Enantioselective Aziridination of Alkenes	12
Scheme 1.6 Mechanistic Proposal for the Enantioselective Radical Bicyclic Aziridination via Co(II)-MRC	14
Scheme 1.7 Scope and <i>in-situ</i> Nucleophilic Ring-Opening of Optically Active [3.1.0]-Bicyclic Aziridines.....	15
Scheme 1.8 Diastereoconvergent Bicyclization to Probe Radical Mechanism of the Intramolecular Bicyclization.....	16
Scheme 2.1 Proposed Mechanism for the Radical Aziridination of Alkenes with Carbonyl Azide TrocN ₃ via Co(II)-MRC	19
Scheme 2.2 Precedents for the Synthesis of <i>N</i> -Carbonyl Aziridines.....	21
Scheme 2.3 DFT Study on the Catalytic Pathway for Aziridination of Styrene with TrocN ₃ by [Co(P5)]	30

Scheme 2.4 Aziridination of (<i>E</i>)- or (<i>Z</i>)- β -Deuterostyrenes to Probe Radical Mechanism	35
Scheme 2.5 Upfield ^2H NMR and ^1H NMR for Aziridine Isomers 3_{aD} from [Co(P6)]- Catalyzed Aziridination	37
Scheme 2.6 Upfield ^2H NMR and ^1H NMR for Aziridine Isomers 3_{aD} from [Co(P1)]- Catalyzed Aziridination	38
Scheme 2.7 Upfield ^2H NMR and ^1H NMR for Aziridine Isomers 3_{aD} from [Co(P5)]- Catalyzed Aziridination	39
Scheme 2.8 Troc-Deprotection and Nucleophilic Ring Opening of the Resulting Enantioenriched <i>N</i> -Carbonyl Aziridines.....	41
Scheme 2.9 Synthesis of Aziridine-Based Chiral Ureas.....	42
Scheme 2.10 Troc-Deprotection and Nucleophilic Ring Opening of the Resulting Enantioenriched <i>N</i> -Carbonyl Aziridines with Different Substrate	43
Scheme 2.11 Calculated Energy Diagram for [Co(P5)] Radical Aziridination of Styrene with Troc Azide	77
Scheme 3.1 Generation of Cobalt-Bound Organic Radicals and Catalytic Applications for Selective Radical Reactions.....	114
Scheme 3.2 Characterization of α -Co(III)-Oxyl Radicals by Mass Spectrometry	122
Scheme 3.3 Relevance of the New α -Co(III)-Oxyl Radicals to Catalytic Radical Epoxidation.....	124
Scheme 3.4 Epoxidation of (<i>E</i>)- or (<i>Z</i>)- β -Deuterostyrenes to Probe Radical Mechanism	125

Scheme 3.5 Upfield ^2H NMR and ^1H NMR for Epoxide Isomers 13_{D} from [Co(P1)]-Catalyzed Epoxidation	126
Scheme 3.6 Oxygen Isotope Labeling Epoxidation: Characterization by HRMS	127
Scheme 3.7 Calculated Energy Diagram of the [Co(Por)] Activation of NaOCl	128
Scheme 3.8 Computational Study on the Generation of α -Co(III)-Oxyl Radicals through [Co(Por)] Activation of NaOCl	131
Scheme 4.1 Working Proposal for Catalytic Radical Epoxidation Involving α -Co(III)-Oxyl Radicals via Co(II)-MRC.....	159
Scheme 4.2 General Synthesis of the New Family of Bridged Amidoporphyrins JesuPhyrin.....	166
Scheme 4.3 Epoxidation of β -Deuterostyrenes with New Catalyst to Probe Radical Mechanism.....	172
Scheme 4.4 Upfield ^2H NMR and ^1H NMR for Epoxide Isomers 13_{D} from [Co(P16)]-Catalyzed Epoxidation	173

LIST OF TABLES

Table 2.1 Enantioselective Aziridination Reaction of Styrene with Carbonyl Azide TrocN ₃ by [Co(Por)]	24
Table 2.2 Co(II)-Catalyzed Enantioselective Aziridination of Styrene Derivatives with Carbonyl Azide TrocN ₃	26
Table 2.3 Crystal Data and Structure Refinement for 3p.....	73
Table 2.4 Crystal Data and Structure Refinement for 3w	74
Table 2.5 Crystal Data and Structure Refinement for 6p.....	75
Table 4.1 Ligand Effect on the Co(II)-Catalyzed Enantioselective Epoxidation of Styrene with NaOCl	162
Table 4.2 Effect of the New Ligands on the Co(II)-Catalyzed Enantioselective Epoxidation of Styrene with NaOCl.....	164
Table 4.3 Optimization of the [Co(P16)] Catalyzed Epoxidation of Styrene Reaction.	167
Table 4.4 [Co(P16)]-Catalyzed Enantioselective Radical Epoxidation of Different Alkenes with NaOCl	170
Table 4.5 Crystal Data and Structure Refinement for P16.....	216

LIST OF FIGURES

Figure 2.1 Select Examples of Biologically Important Molecules Containing <i>N</i> -Carbonyl and <i>N</i> -H Aziridines.....	20
Figure 2.2 X-ray Structures of Compounds 3p and 3w	27
Figure 2.3 Optimized Geometries for Intermediates and Transition States.....	31
Figure 2.4 Spin Density Distribution for Optimized Geometries	32
Figure 2.5 Generation and Detection of α -Co(III)-Aminyl Radical Intermediate by EPR and HRMS	34
Figure 2.6 High Resolution Mass Spectroscopy (HRMS) Spectrum for Co(III)-Supported Aminyl Radical Intermediate I.....	71
Figure 3.1 UV-vis Spectrum of [Co(P1)] only and [Co(P1)] Exposed to Different Oxygen Radical Precursors	117
Figure 3.2 EPR Spectrum of [Co(TPP)] only and [Co(TPP)] Exposed to Different Oxygen Radical Precursors	118
Figure 3.3 UV-Vis Studies on Activation of NaOCl by [Co(Por)].....	119
Figure 3.4 EPR Studies on Activation of NaOCl by Co(II)-Metalloradicals [Co(Por)]	121
Figure 3.5 Optimized Geometries for Intermediates and Transition States.....	129
Figure 3.6 UV-Vis Spectrum for Co(III)-Supported Oxyl Radical Intermediate	135
Figure 3.7 High Resolution Mass Spectroscopy (HRMS) Spectrum for α -Co(III)-oxyl radical I _[Co(TPP)]	143
Figure 3.8 High Resolution Mass Spectroscopy (HRMS) Spectrum for Isotopically Labeled α -Co(III)-oxyl radical I _[Co(TPP)]	144

Figure 3.9 High Resolution Mass Spectroscopy (HRMS) Spectrum for α -Co(III)-oxyl radical I _[Co(P1)]	145
Figure 3.10 High Resolution Mass Spectroscopy (HRMS) Spectrum for Isotopically labeled α -Co(III)-oxyl radical I _[Co(P1)]	146

TABLE OF ABBREVIATIONS

Por: porphyrin	Hex: hexane
TrocN ₃ : 2,2,2-trichloroethoxycarbonyl azide	EtOH: ethanol
DDQ: 2,3-dichloro-5,6-dicyano-1,4-benzo quinone	SiO ₂ : silica gel
Xanthphos: 4,5-Bis(diphenylphosphino)-9,9-dimethylxanthene	TBME: tert-butyl methyl ether
THF: tetrahydrofuran	DME: Dimethoxyethane
DMAP: 4-dimethylaminopyridine	TCE: 1,1,2,2-tetrachloroethane
DMF: dimethyl formamide	TFA: trifluoroacetic acid
MeO: methoxy	TS: transition state
Me: methyl	Å: angstrom
^t Bu: tert-butyl	MRC: metalloradical catalysis
Et: ethyl	es: estereospecificity
Ar: aryl	ee: enantiomeric excess
Ph: phenyl	de: diastereomeric excess
TPP: tetraphenyl porphyrin	dr: diastereomeric ratio
TEMPO: 2,2,6,6-Tetramethyl-1-piperidinyloxy	equiv.: equivalent(s)
PhMe: toluene	eq: equation
PhCF ₃ : trifluorotoluene	rt: room temperature
EtOAc: ethyl acetate	HPLC: high performance liquid chromatography
PhH: benzene	HRMS: high resolution mass spectrometry
PhCl: chlorobenzene	y: yield
DCM: dichloromethane	IR: infrared spectroscopy
MeOH: methanol	TOF: time of flight
MeCN: acetonitrile	ESI: electrospray ionization
	EPR: electron paramagnetic resonance
	M: molar or mass

NMR: nuclear magnetic resonance

DART: direct analysis in real time

HAA: hydrogen atom abstraction

MHz: megahertz

M.S.: molecular sieves

$\text{BF}_3 \cdot \text{OEt}_2$: boron trifluoride diethyl
etherate

Al foil; aluminum foil

CAM: ceriumammonium-molybdate

TLC: thin layer chromatography

[O]: oxygen radical precursor

G: gauss

UV-Vis: ultraviolet visible

B: magnetic field

DMPO: 5,5-dimethyl-1-pyrroline N-
oxide

DFT: density-functional theory

Rad: radical species

Nu^- : nucleophile

nm: nanometers

DEDICATED TO:

I would like to dedicate this dissertation to my mother, Neus, and my recently deceased father, Jesus (*in caelis est*), after whom a new catalyst reported in this dissertation has been named. Their unconditional love and support have made me who I am and have been a continuous source of confidence and inspiration to stay strong, stubborn, and achieve my goals throughout my life. I feel extremely fortunate to have been raised by them.

I would also like to dedicate this dissertation to my beloved wife Loraine, who with her patience, continuous support, and unconditional love has made this long PhD journey possible, pleasant, and enjoyable.

Lastly, I would like to also dedicate this dissertation to my siblings Judit, Jordi, and Nuria for being great role models growing up together.

ACKNOWLEDGEMENTS

First, I would like to express my most sincere gratitude to my advisor, Professor X. Peter Zhang, for his continued support, guidance, and encouragement throughout the PhD journey. Thank you for challenging me to be a better scientist and helping me achieve my potential as researcher. I really appreciate all the time and effort you have put on helping me throughout my PhD degree; in the laboratory, in manuscript writing (specially the revision process), and in achieving the next step of my career as medicinal chemist.

Next, I would also like to give a special thanks to my PhD committee, Professor Jeff Byers and Professor James Morken. Thank you for serving as my PhD committee and for reading my dissertation. Thank you, Professor Byers, for serving as the chair in my second year PhD candidacy exams and for providing constructive feedback. I would also like to thank Professor James Morken, Professor Amir Hoveyda, and Professor Marc Snapper for supporting my job applications with valuable recommendation letters.

I would like to thank all my lab mates in the Zhang Group and colleagues with whom I have had the pleasure to work with and from whom I learned a lot, especially Dr. Yong Wang, Dr. Arghya Deb, Dr. Pan Xu, and Dr. Xin Wen. Special thanks to my wife for carefully proofreading this dissertation and to Hao Xu for his contribution to my research from a computational point of view.

Lastly, I am very grateful for the amazing friendships I have been able to establish at BC during this journey, so a big thanks to Lucas, Juan, Yong, Xin, Katie, Filipino, Michael, Paulo, Stella, Cris, Elsie, Katie, Adam, Xiaoxu, Pan, Arghya, and Hao for making the PhD more enjoyable.

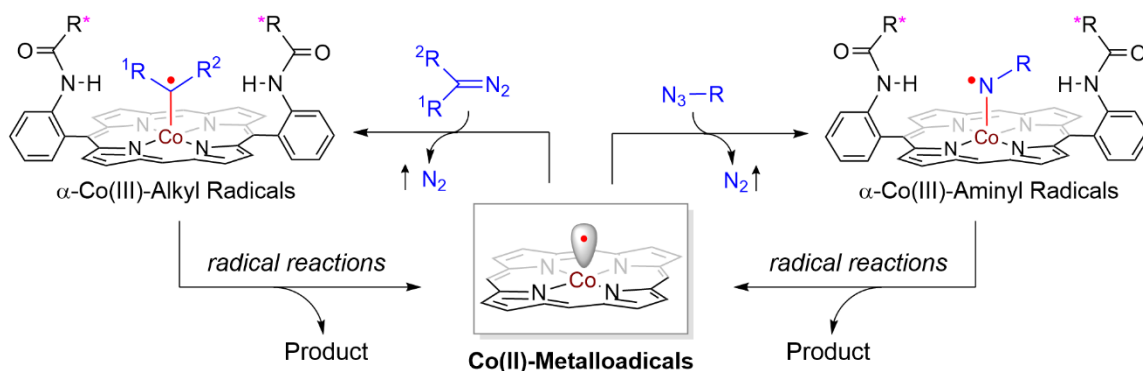
PREFACE

The chemistry of free radical species has been a latent field of study for the last century. Usually regarded as fleeting and highly reactive intermediates, species including carbon-, nitrogen-, and oxygen-centered radicals have been found to initiate and/or participate in a myriad of chemical reactions such as radical addition, atom abstraction, radical substitution, and fragmentation.¹ Given the inherent synthetic advantages associated with radical chemistry (typically rapid reaction rates, mild reaction conditions in a broad range of solvents), growing research interest has been attracted to the development of radical reactions for applications in organic synthesis.¹⁻² Despite significant recent advancements, the control of reactivity and selectivity in radical reactions still poses significant challenges, especially in the context of enantioselectivity.³ This is in part due to the highly reactive nature of the short-lived “free” radical intermediates.

Metalloradical Catalysis (MRC), which aims at the development of metalloradical-based systems for both catalytic initiation and selective control of radical processes, represents a new approach to address long-standing challenges associated with radical chemistry.^{2b,4,5,6} As stable 15e-metalloradicals, cobalt(II) complexes of porphyrins [Co(Por)] have been shown with particular capability to homolytically activate diazo compounds and organic azides for the formation of fundamentally new α -Co(III)-alkyl radicals⁷ and α -Co(III)-aminyl radicals,⁸ respectively. (Scheme 1.1) Upon activation, which results in the evolution of nitrogen gas as the only byproduct and serves as

thermodynamic driving force, these new organic radical species remain complexed with the [Co(Por)] and can undergo archetypal radical reactions such as addition to alkenes or hydrogen atom abstraction. With the employment of D_2 -symmetric chiral amidoporphyrin ligands, these well-defined cobalt-supported carbon- and nitrogen-centered radicals have been used as key intermediates in a number of new catalytic asymmetric radical processes, including olefin cyclopropanation,⁹ C–H alkylation,¹⁰ olefin aziridination,¹¹ and C–H amination.^{8c,12}

Scheme 1.1| Co(II)-MRC Activation of Diazo and Azide Compounds



Highly strained three-membered heterocycles are a common motif in biologically relevant molecules and represent a versatile building block for organic synthesis. Furthermore, its enantioenriched versions serve as common chiral synthons to introduce ubiquitous heteroatoms in a stereoselective fashion. Given the synthetic importance of aziridines and epoxides, the focus of my PhD research has been centered on the design and use of chiral cobalt porphyrins as metalloradical catalysts to develop new methodologies for asymmetric radical aziridination and epoxidation of alkenes. The first part of this dissertation is focused on using carbonyl azides for the radical aziridination of alkenes (Chapter 2). Despite its potential functionality and versatility for further derivatization,

carbonyl azides have never been reported as nitrogen sources for intermolecular asymmetric alkene aziridination. To put some context on the use of organic azides as nitrogen source for the [Co(Por)] catalyzed enantioselective radical aziridination of alkenes, the first chapter of this dissertation attempts to review these types of methodologies reported so far (Chapter 1).

The second part of this dissertation is focused on opening a new area of research, which involves the generation and characterization of the unprecedented cobalt-supported oxygen-centered radical species (Chapter 3) and its use in the asymmetric epoxidation of alkenes through the design and development of a novel family of catalysts (Chapter 4).

1. CHAPTER 1: REVIEW ON CATALYTIC SYSTEMS FOR ENANTIOSELECTIVE RADICAL AZIRIDINATION OF ALKENES

As the smallest saturated azaheterocycles, aziridines have been the subject of study by several chemists given their vast potential in synthetic organic and medicinal chemistry.¹³ In view of the recent advancements in enantioselective synthesis, several methodologies have been developed that allow for the highly enantio- and diastereoselective synthesis of aziridines. In this context, excellent reviews on the topic have been reported, from methodologies for their synthesis, to applications in construction of complex molecules.¹⁴

The recent renaissance in developing diversified means for effective and selective radical reactions has attracted increasing attention amongst the academic community and pharmaceutical industry.^{1-2,2i,2j} In view of the interest in the use of radical chemistry for catalytic and enantioselective organic synthesis, this first chapter will serve as a review to cover the recent development of methodologies for the catalytic and enantioselective aziridination of alkenes through a well-defined stepwise radical mechanism. More specifically, it will cover recent reports on cobalt(II) porphyrin catalyzed enantioselective radical aziridination of alkenes using organic azides as nitrogen source.

1.1 INTRODUCTION

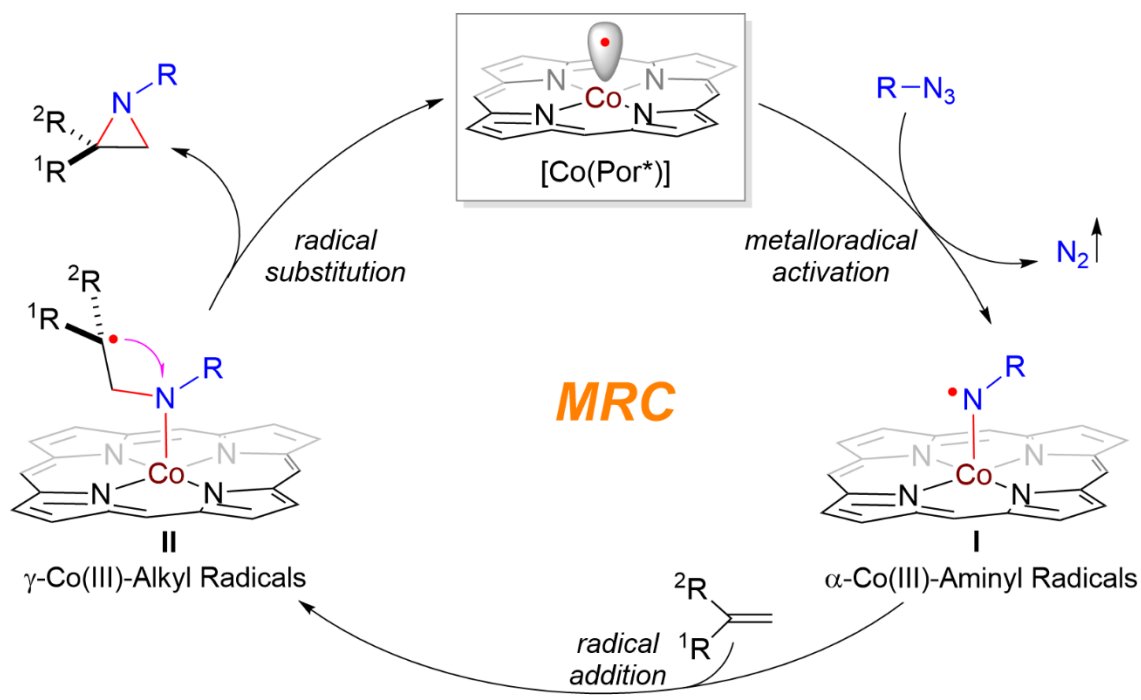
Transition metal catalyzed aziridination of alkenes with nitrene sources through a “C2+N1” paradigm represents a general approach for the direct synthesis of the smallest

three membered azaheterocycles.¹⁵ Over the years, several types of nitrogen-containing reagents have been explored as potential nitrene sources for this paradigm. One of the most widely utilized nitrene sources are hypervalent iodine nitrenes (PhINTs) and related iminoiodane derivatives,¹⁶ including its *in situ* generated variants. However, their instability and generation of iodobenzene as a byproduct represent a major drawback and hamper their broad applicability. While significant efforts have been made to overcome and mitigate the several limitations associated with the use of these hypervalent iodine reagents, on a different avenue, growing efforts have also been devoted to developing alternative nitrene sources such as chloramine- and bromamine-T,¹⁷ and tosyloxycarbamates.¹⁸ These nitrene precursors have been used successfully in different types of nitrene transfer reactions, albeit the drawbacks associated with their use (instability, oxidative or basic conditions) still make it challenging to develop broad methodologies, especially given the limited access to their derivatives. Among recent developments aspiring to move away from hypervalent iodine reagents, organic azides have been increasingly employed as nitrogen sources for catalytic nitrene insertion reactions due to their attractive attributes such as ease of preparation and derivatization, and generation of benign N₂ as the only byproduct.^{17c,19}

As stable metalloradicals, cobalt(II) complexes of *D*₂-symmetric chiral amidoporphyrins [Co(*D*₂-Por*)] have emerged as a family of open-shell transition metal catalysts for enantioselective radical transformations through catalytic generation of metal-supported organic radical intermediates via metalloradical catalysis (MRC).^{2b,4} Specifically, metalloradical catalysts [Co(*D*₂-Por*)] have shown to be particularly effective in activating organic azides for the catalytic radical aziridination of alkenes,^{11,20} producing

the smallest three-membered N-heterocycles with effective control of reactivity and enantioselectivity through a postulated stepwise radical mechanism (Scheme 1.2).

Scheme 1.2| General Proposed Catalytic Cycle for the [Co(Por)] Catalyzed Aziridination of Alkenes with Organic Azides as Nitrogen Source via MRC

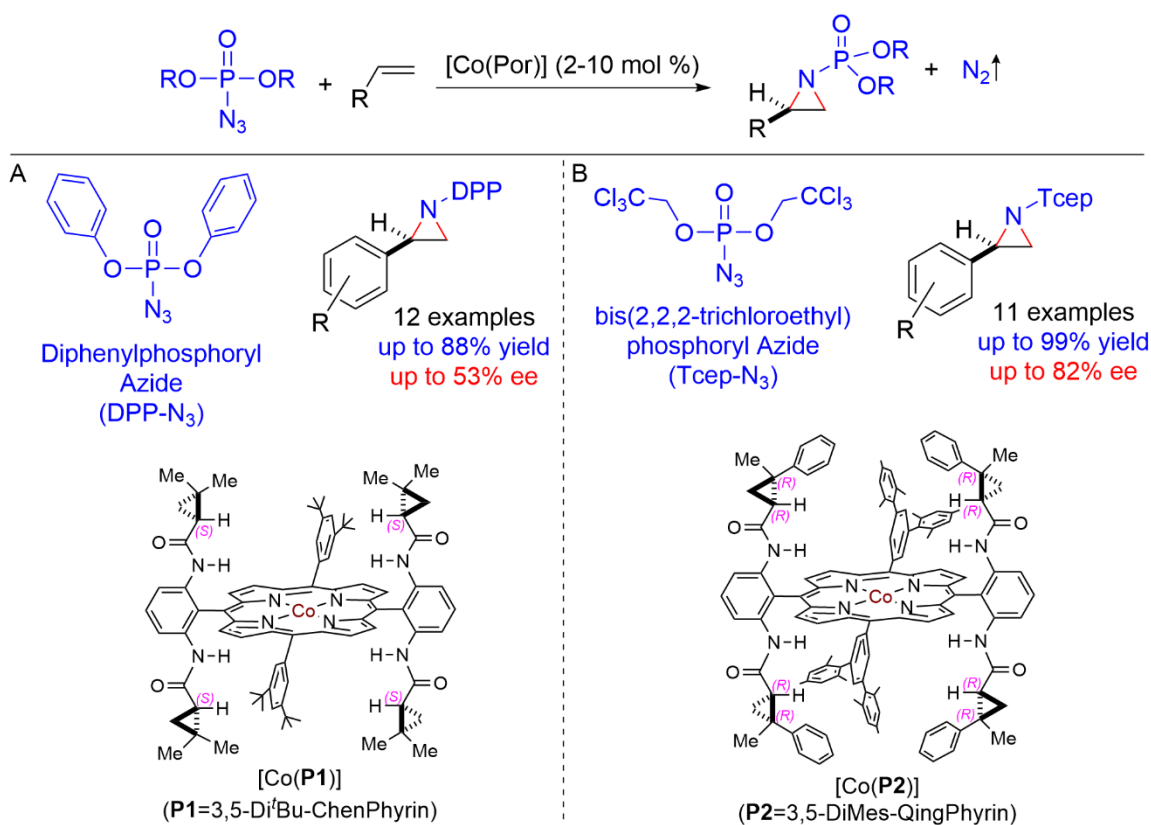


1.2 PHOSPHORYL AZIDES AS NITROGEN SOURCE FOR THE [Co(POR)] CATALYZED ENANTIOSELECTIVE AZIRIDINATION OF ALKENES

In 2008, the Zhang group demonstrated the catalytic activation of phosphoryl azides by cobalt porphyrins for the asymmetric aziridination of a broad array of styrene and styrene derivatives (Scheme 1.3A).^{11b} Compared with the more typical *N*-sulfonyl aziridines, *N*-phosphorylated and the related *N*-phosphinylated aziridines are more

advantageous synthetic building blocks due to the easier deprotection of the *N*-phosphoryl and *N*-phosphinyl groups.²¹

Scheme 1.3| Phosphoryl Azides as Nitrogen Source for the [Co(Por)] Catalyzed Enantioselective Aziridination of Alkenes



Upon evaluation of different catalysts, the cobalt(II) complex of 3,5-Di^tBu-ChenPhyrin^{9b} [Co(P1)] proved to be an effective catalyst for the aziridination of a range of aromatic olefins with diphenylphosphoryl azide (DPPA) under mild conditions, affording the synthetically valuable *N*-phosphorylated aziridines in moderate to good yields with an acceptable degree of asymmetric induction (Scheme 1.3A). It represented the first Co-catalyzed asymmetric olefin aziridination system that could employ the commercially available DPPA as a convenient nitrogen source for enantioselective aziridination. The

scope included styrene derivatives with both electron donating and withdrawing in different positions. Despite its practicality, the catalytic system was limited to terminal aromatic alkenes, as it proved to be ineffective for internal aromatic olefins and any kind of aliphatic alkenes.

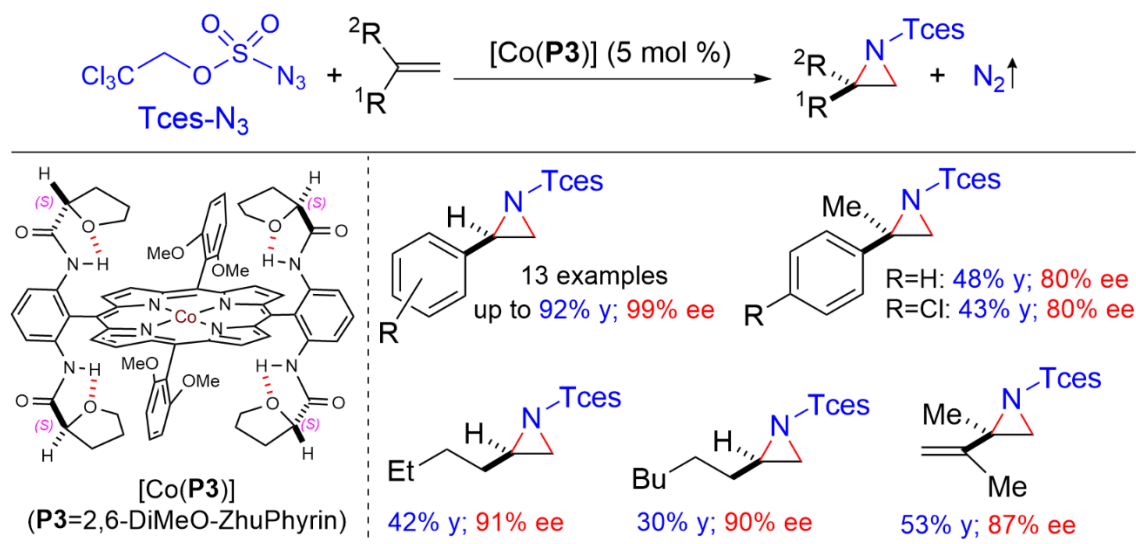
While this [Co(**P1**)]/DPPA catalytic system represented the first asymmetric version of olefin aziridination with phosphoryl azides, both the yields and enantioselectivities were moderate even using 10 mol % catalyst loading. To improve the reactivity and selectivity, the Zhang group later developed a new system involving a Co(II) complex of the new *D*₂-symmetric chiral porphyrin 3,5-DiMes-QingPhyrin, [Co(**P2**)] as an effective metalloradical catalyst for asymmetric olefin aziridination employing bis(2,2,2-trichloroethyl)phosphoryl azide (TcepN₃) as a new nitrogen source (Scheme 1.3B).^{20b} The overall yields and enantioselectivities were significantly improved, even using only 2 mol % of catalyst loading. Although TcepN₃ is not commercially available, it can be easily synthesized in multigram scale from readily available starting materials.^{12e} Despite the notable improvement, the scope of this new catalytic system is still limited to mono-substituted styrene derivatives with varied electronic and steric patterns.

1.3 SULFONYL AZIDES AS NITROGEN SOURCE FOR THE [Co(POR)] CATALYZED ENANTIOSELECTIVE AZIRIDINATION OF ALKENES

A year later, in 2009, the Zhang group demonstrated the ability of Co(II) complexes of chiral porphyrins to catalytically activate trichloroethoxysulfonyl azide (TcesN₃) as a new nitrogen source for a highly asymmetric aziridination system of a broad range of alkenes

(Scheme 1.4).^{11d} Using the D_2 symmetric chiral amidoporphyrin **P3** (**P3** = 2,6-DiMeO-ZhuPhyrin)^{9f} as supporting ligand, the [Co(Por)]-TcesN₃-based system proved to be operationally simple and suitable for the aziridination of both aromatic and aliphatic olefins under mild conditions, forming the corresponding *N*-Tces-aziridines in high yields and excellent enantioselectivities.

Scheme 1.4| Tces-Azide as Nitrogen Source for the [Co(Por)] Catalyzed Enantioselective Aziridination of Alkenes



It is worth noting that in this system, the catalyst was recycled and reused multiple times without significant loss of reactivity and selectivity. In addition, a noteworthy additive effect of palladium(II) acetate, Pd(OAc)₂, on the yield of the Co-catalyzed aziridination was described, presumably due to the activation of the alkenes by the p-electrophilic Lewis acid, Pd(OAc)₂.²² This represented the first highly effective and enantioselective catalytic system for the asymmetric aziridination of a broad range of simple olefins beyond mono-substituted styrenes, including 1,1-disubstituted styrenes and aliphatic alkenes without the

need of additional functional and/or directing groups in the substrates for secondary binding interactions.

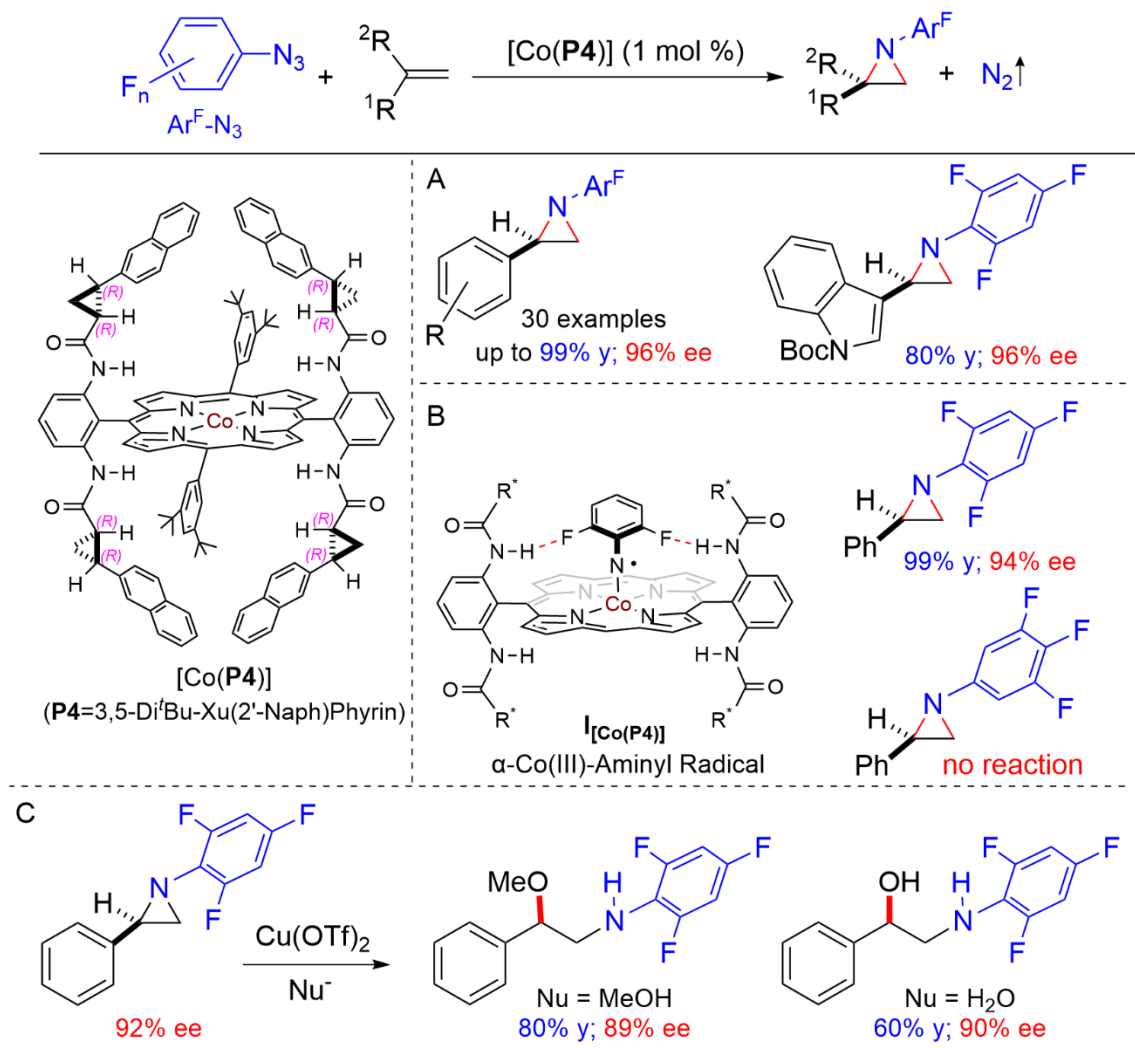
1.4 FLUOROARYL AZIDES AS NITROGEN SOURCE FOR THE [Co(POR)] CATALYZED ENANTIOSELECTIVE AZIRIDINATION OF ALKENES

A different class of organic azides that had not been previously employed as nitrene source for asymmetric aziridination are fluoroaryl azides. These organic azides can be easily prepared from a myriad of commercially available fluoroanilines and are particularly attractive since the resulting enantioenriched *N*-fluoroaryl aziridines could serve as effective chiral synthons for ring-opening and ring-expansion methodologies for the preparation of chiral fluoroarylamine-containing compounds, which can find many applications in the pharmaceutical and related industries.²³

In 2013, the Zhang group reported a highly asymmetric aziridination of alkenes using fluoroaryl azides as nitrogen source.^{11e} Using **P4** (**P4**= 3,5-Di^tBu-Xu(2'-Naph)Phyrin) as the chiral amidoporphyrin ligand, the [Co(**P4**)]-catalyzed asymmetric aziridination was successfully applied to a wide range of aromatic olefins with varied steric and electronic properties (Scheme 1.5). Notably, heteroaromatic alkenes such as Boc-protected 3-vinylindole could also be aziridinated to generate the desired aziridinylindole in high yield and excellent enantioselectivity (Scheme 1.5A). Besides the synthetic interest for potential further applications, fluorine-containing aryl azides proved to be key for the effectiveness and enantioselectivity of this new aziridination reaction, as significant variations in the results were observed when changing the position of the fluorine atom substituent around

the phenyl ring. To study the effects of the fluorination patterns in the aryl azide, several fluoroaryl azides were tested. Presumably as a result of additional NH \cdots F hydrogen-bonding interactions in the postulated α -Co(III)-aminyl radical intermediate **I**_[Co(P4)] (Scheme 1.5B), di-*ortho*-fluoro-substituted aryl azides were found to be more selective and effective aziridinating agents than mono-*ortho*-fluoro-substituted aryl azides. To test this hypothesis, 3,4,5-trifluorophenyl azide, which contains three F atoms but none of them in *ortho* position, was used as nitrogen source and yielded no reaction under the same conditions (Scheme 1.5B). This observation suggests the important role the NH \cdots F hydrogen bond plays in this Co(II)-based metalloradical aziridination process, representing the first catalytic system for asymmetric olefin aziridination using aryl azides as the nitrogen source. Among other attributes, this methodology could be performed at room temperature using olefin as the limiting reagent without the need of any additives, resulting in the generation of nitrogen gas as the only by-product. Furthermore, the practicality of the methodology was showcased by the synthesis of highly enantiomerically enriched *N*-fluoroaryl-containing compounds through stereoselective nucleophilic ring opening under Lewis acid catalysis (Scheme 1.5C). The major shortcoming of this new methodology is that the scope is limited to terminal monosubstituted aromatic alkenes, and that the deprotection of the fluoroaryl group has not been demonstrated or reported.

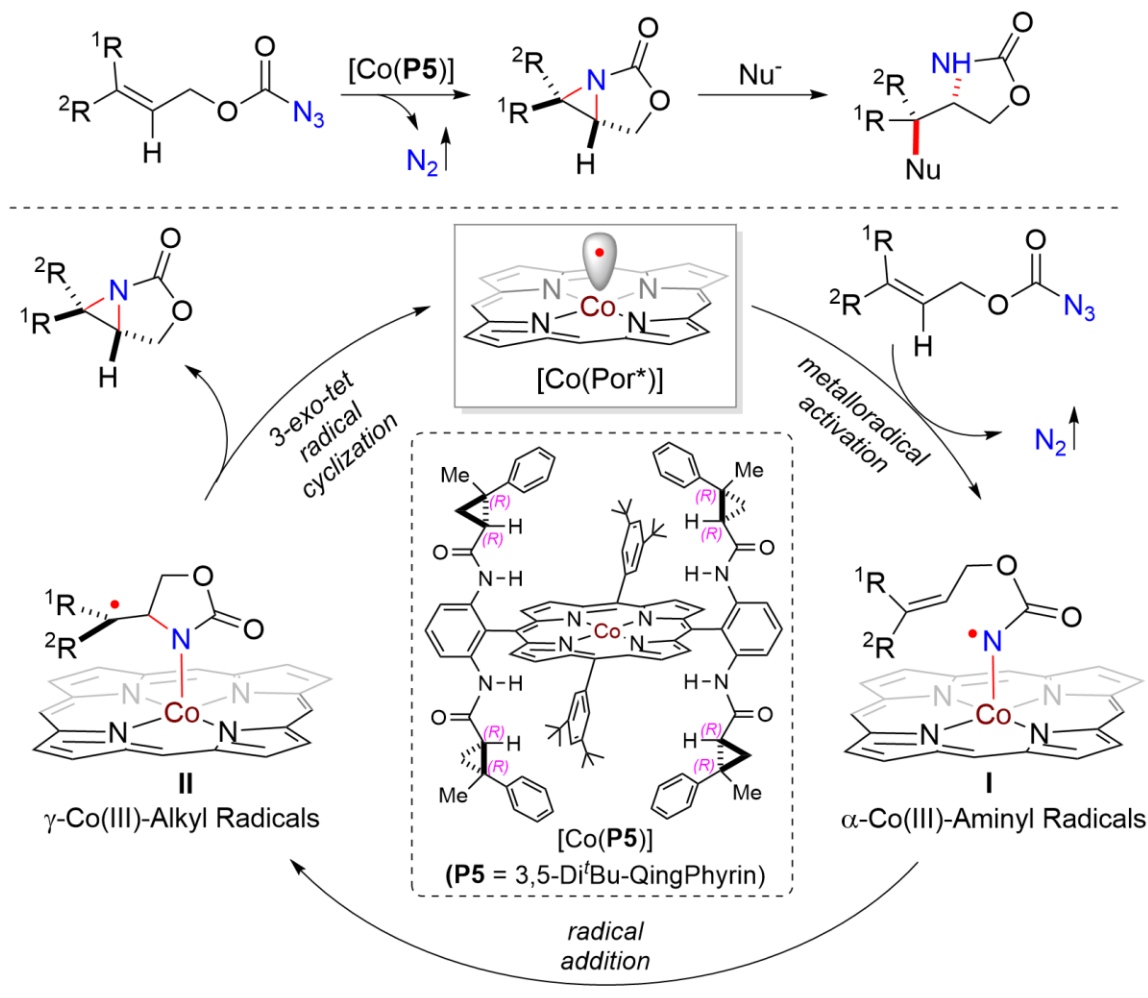
Scheme 1.5| Fluoroaryl Azides as Nitrogen Source for the [Co(Por)] Catalyzed Enantioselective Aziridination of Alkenes



1.5 ALLYL AZIDOFORMATES AS NITROGEN SOURCE FOR THE [Co(POR)] CATALYZED ASYMMETRIC INTRAMOLECULAR AZIRIDINATION

Catalytic intramolecular olefin aziridination represents one of the most attractive approaches for the construction of fused bicyclic aziridines.^{14c-e} These highly strained motifs represent a synthetically useful family of compounds, given that the resulting chiral [3.1.0]-bicyclic aziridines are versatile intermediates for the synthesis of chiral oxazolidinone and vicinal amino alcohol derivatives, which are ubiquitous motifs in many biologically relevant and complex molecules.^{11h} To that end, the Zhang group employed allyl azidoformates as nitrogen source for the [Co(Por)] catalyzed asymmetric construction of a broad range of fused bicyclic aziridines via a postulated step-wise radical mechanism (Scheme 1.6).^{11h} Ligand optimization revealed that the cobalt(II) complex of *D*₂-symmetric chiral amidoporphyrin 3,5-Di^tBu-QingPhyrin⁹ⁱ (**P5**) proved to be an efficient catalyst that could activate allyl azidoformates for the construction of fused bicyclic aziridines in high yields with excellent stereoselectivities (Scheme 1.7A).

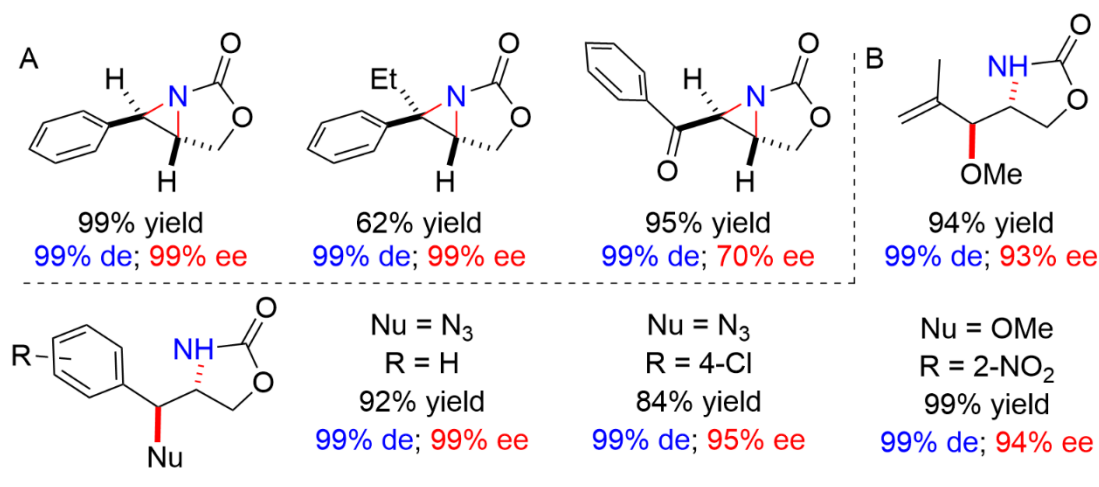
Scheme 1.6| Mechanistic Proposal for the Enantioselective Radical Bicyclic Aziridination via Co(II)-MRC



Due to the high reactivity associated with the strain of 3-oxa-1-azabicyclo[3.1.0]hexan-2-one structures, some of the resulting bicyclic aziridines were difficult to isolate in high yields, as certain product decomposition was observed after common chromatographic purification. Taking advantage of this reactivity, the resulting aziridines could be directly transformed to the corresponding 2-oxazolidinones via *in situ* ring-opening reactions by a myriad of nucleophiles of different nature (Scheme 1.7B), showcasing the versatility of the

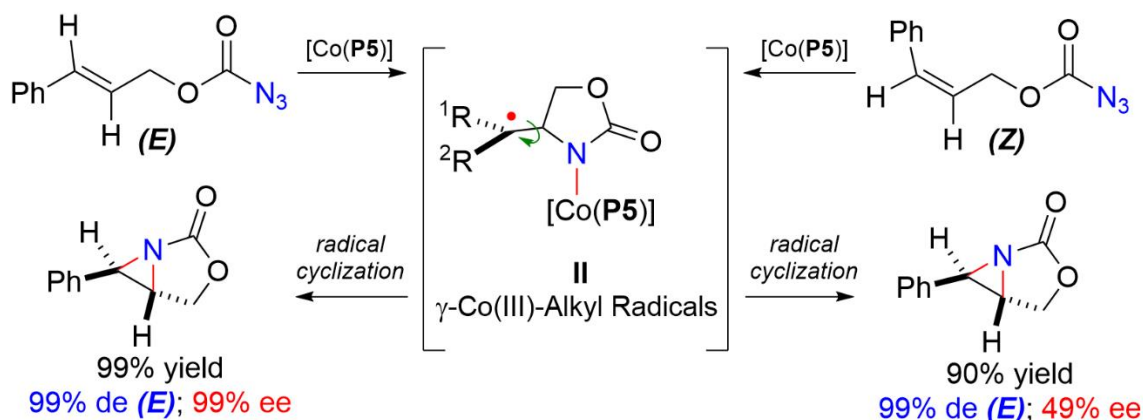
resulting optically active [3.1.0]-bicyclic aziridines as chiral building blocks for stereoselective organic synthesis.

Scheme 1.7| Scope and *in-situ* Nucleophilic Ring-Opening of Optically Active [3.1.0]-Bicyclic Aziridines



To probe the proposed stepwise radical mechanism, two pairs of (*E*)- and (*Z*)-allyl azidoformates were employed as the substrates for the aziridination reaction (Scheme 1.8). Under standard conditions, both reactions of the disubstituted allyl azidoformates (*E*) and (*Z*) produced the same (*E*)-aziridine as a single diastereomer in similar yields but with different enantioselectivities. The observed diastereoconvergence is attributed to the facile interconversion between the corresponding intermediates **II** generated from (*E*) and (*Z*) allyl azidoformate, respectively, due to the low-barrier rotation of the α -C–C bond of the C-centered radical (Scheme 1.8), leading to the formation of the more stable (*E*)-aziridine after the second radical cyclization.

Scheme 1.8| Diastereoconvergent Bicyclization to Probe Radical Mechanism of the Intramolecular Bicyclization



1.6 SUMMARY AND OUTLOOK

In summary, this review shows the potential of cobalt porphyrins as metalloradical catalysts to activate organic azides for the enantioselective aziridination of alkenes. The combination of [Co(D_2 -Por*)] with phosphoryl, sulfonyl, and fluoroaryl azides is a powerful tool for the highly effective and enantioselective intermolecular aziridination of terminal alkenes. These methodologies represent the first examples of asymmetric aziridination with the respective azides and they have salient attributes including low catalyst loading, catalyst recycling, and mild conditions; however, there remain significant unsolved problems. In general, the scope is limited to aromatic monosubstituted-terminal alkenes. Furthermore, the azides that have been reported so far do not offer a handle for further transformation or easy deprotection, hindering the synthesis of the highly desired *N*-H aziridines. It remains to be seen whether more functional organic azides can be utilized as nitrogen source for new [Co(D_2 -Por*)] catalyzed aziridination reactions. We envision

that designing judicious catalyst and reaction conditions as well as finding the right organic azide can provide potential solutions to address the aforementioned unsolved issues in the enantioselective radical aziridination of alkenes.

2. CHAPTER 2: ENANTIOSELECTIVE RADICAL AZIRIDINATION OF ALKENES WITH CARBONYL AZIDES

2.1 INTRODUCTION

As shown in Chapter 1 (*vide supra*), metalloradical catalysts [Co(*D*₂-Por*)] have shown to be particularly effective in activating organic azides to generate the corresponding α -Co(III)-aminyl radicals as key intermediates for catalytic radical aziridination of alkenes, producing the smallest three-membered *N*-heterocycles with effective control of reactivity and enantioselectivity. While previous reports involved the use of phosphoryl, sulfonyl and aryl azides, we were attracted to the possibility of using carbonyl azides such as 2,2,2-trichloroethoxycarbonyl azide (TrocN₃) for radical olefin aziridination via Co(II)-MRC, especially its asymmetric variant by [Co(*D*₂-Por*)] (Scheme 2.1). Although [Co(TPP)] (TPP = 5,10,15,20-tetraphenylporphyrin) was previously shown to activate TrocN₃, it required elevated temperature and elongated reaction time as well as the use of high catalyst loading.²⁴ We reasoned that the metalloradical activation of TrocN₃ to generate α -2,2,2-trichloroethoxycarbonyl- α -Co(III)-aminyl radical intermediate **I** could be facilitated by [Co(*D*₂-Por*)] as a result of the putative H-bonding interaction between the carbonyl moiety in the azide and the amide unit of the catalyst (Scheme 2.1).^{11c,11e} In view of the spin delocalization in the α -carbonylaminy radical intermediate **I**, however, it was unclear whether it could function as effective nitrogen-centered radical to proceed to radical addition to olefins for the generation of γ -Co(III)-alkyl radical intermediate **II** (Scheme 2.1). Moreover, in order to form the expected aziridines, the resulting carbon-centered

radical in intermediate **II** must undergo competitive *3-exo-tet* radical cyclization over *5-endo-trig* radical cyclization,²⁵ which would produce oxazolines after subsequent β -scission. More importantly, could the desired *3-exo-tet* radical cyclization proceed in an enantioselective fashion? We envisioned to address these and related issues of reactivity and selectivity through the judicious choice of metalloradical catalysts [Co(*D*₂-Por*)]. If successful, it would offer a new radical protocol for the stereoselective synthesis of chiral *N*-carbonyl aziridines (Scheme 2.1), which have found many synthetic and biologic applications^{13d,14d,14e,26} (see Figure 2.1).

Scheme 2.1| Proposed Mechanism for the Radical Aziridination of Alkenes with Carbonyl Azide TrocN₃ via Co(II)-MRC

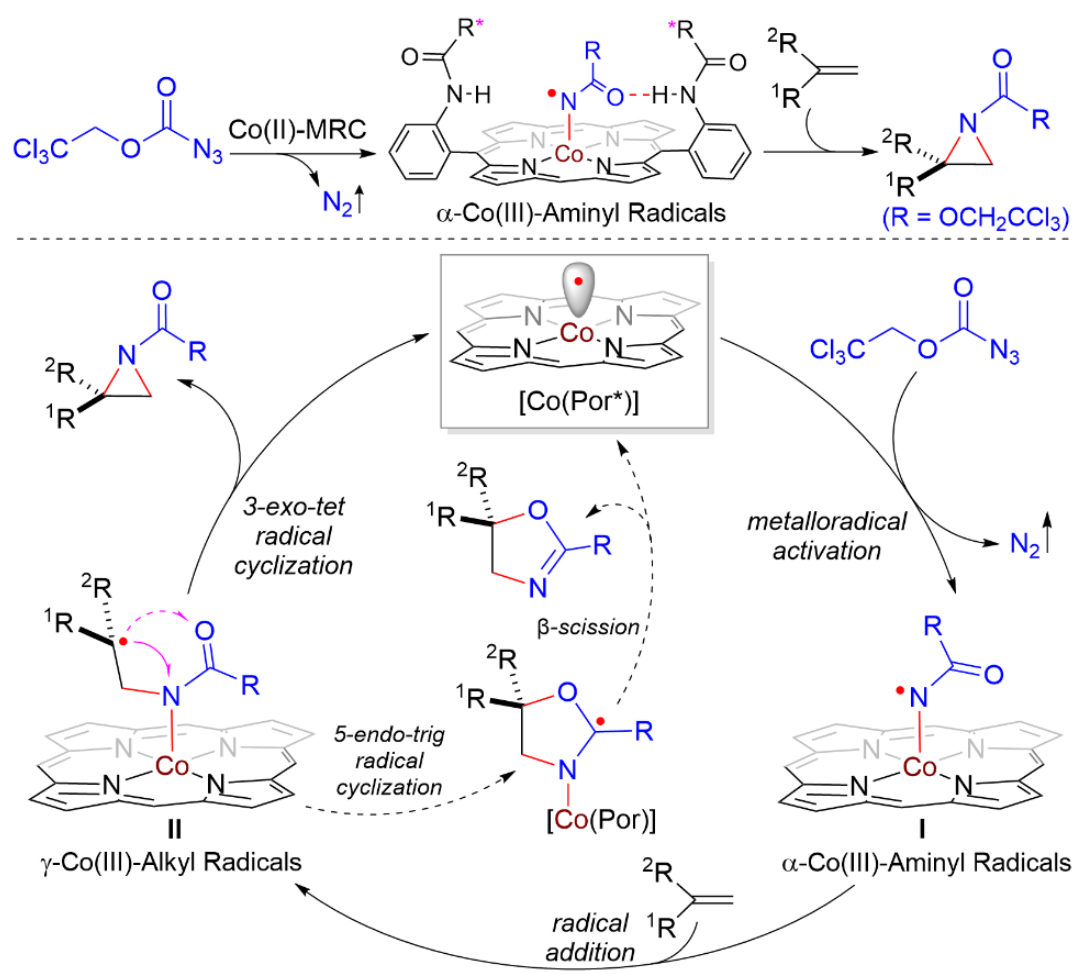
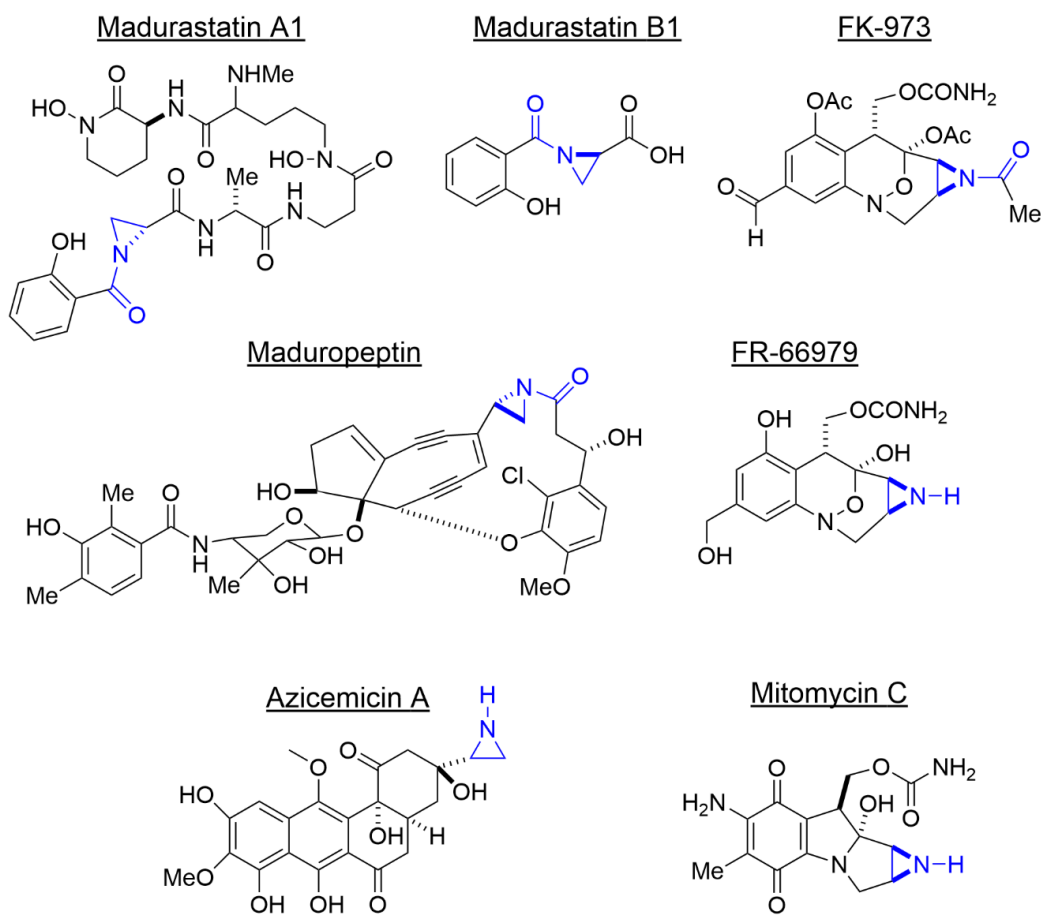


Figure 2.1| Select Examples of Biologically Important Molecules Containing *N*-Carbonyl and *N*-H Aziridines

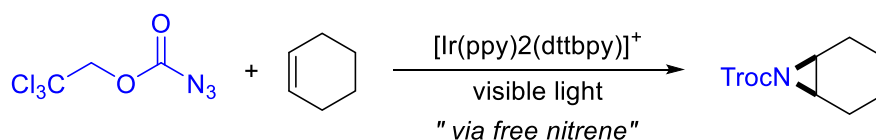


Organic azides have been increasingly employed as nitrogen sources for catalytic aziridination of alkenes due to their attractive attributes, such as ease of preparation and generation of benign N_2 as the only byproduct.^{17c,19} Among common organic azides, carbonyl azides have not been previously demonstrated as effective nitrogen sources for intermolecular olefin aziridination,^{11h,27} despite the potential formation of useful aziridines bearing the versatile *N*-carbonyl functionality, which can also be easily deprotected to yield *N*-H aziridines (Figure 2.1).^{26a} This underdevelopment is mainly attributed to the well-known challenges associated with the high lability of carbonyl azides toward thermal and photolytic rearrangements.²⁸ Yoon and coworkers recently reported the use of Ir-based

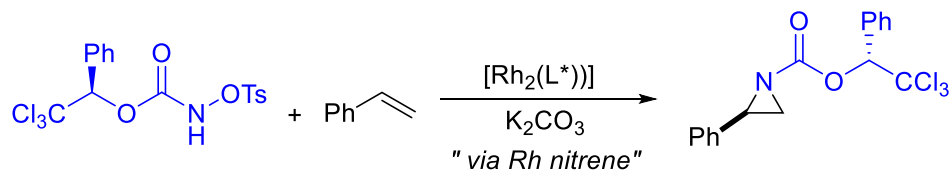
catalysts as photosensitizers for activation of TrocN₃ with visible light to generate triplet free nitrenes that can be selectively trapped by various alkenes for aziridination that proceeds without asymmetric induction (Scheme 2.2 A).²⁹ As a novel alternative to carbonyl azides, Lebel and coworkers successfully employed chiral *N*-tosyloxycarbamates as nitrogen sources for the Rh₂-catalyzed diastereoselective aziridination of alkenes (Scheme 2.2B).^{18b,18c}

Scheme 2.2| Precedents for the Synthesis of *N*-Carbonyl Aziridines

A. Yoon and coworkers



B. Lebel and coworkers



To the best of our knowledge, there has been no previous report on an asymmetric catalytic system for olefin aziridination using TrocN₃ as nitrogen source. In comparison to other nitrene precursors, Troc-N₃ offers several advantages: (i) straightforward synthesis from the commercially available 2,2,2-trichloroethoxy chloroformate in near quantitative yield; (ii) generation of environmentally benign dinitrogen as the only byproduct; and (iii) ease of deprotection from the resulting aziridine products to afford *N*-H aziridines. As a new application of Co(II)-MRC, we herein report the development of the first asymmetric catalytic system that can effectively employ TrocN₃ for the highly asymmetric aziridination of alkenes. Supported by *D*₂-symmetric chiral amidoporphyrin ligands, the Co(II)-based catalytic process allows for efficient synthesis of chiral *N*-Troc-aziridines with a high degree of enantiocontrol. In addition to the convenient access to chiral *N*-H-aziridines

through mild deprotection, the utility of the resulting chiral *N*-Troc-aziridines is further showcased by the synthesis of chiral amines through stereospecific ring-opening with nucleophiles of different nature without erosion of the original enantiopurity. We also describe our mechanistic studies on the proposed stepwise radical mechanism of the Co(II)-catalyzed aziridination.

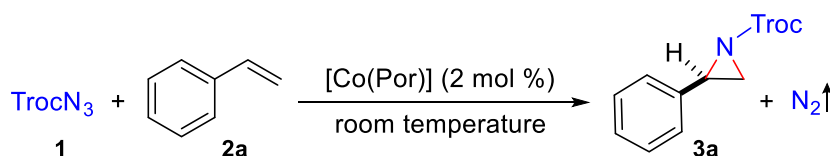
2.2 RESULTS AND DISCUSSION

2.2.1 Reaction Optimization

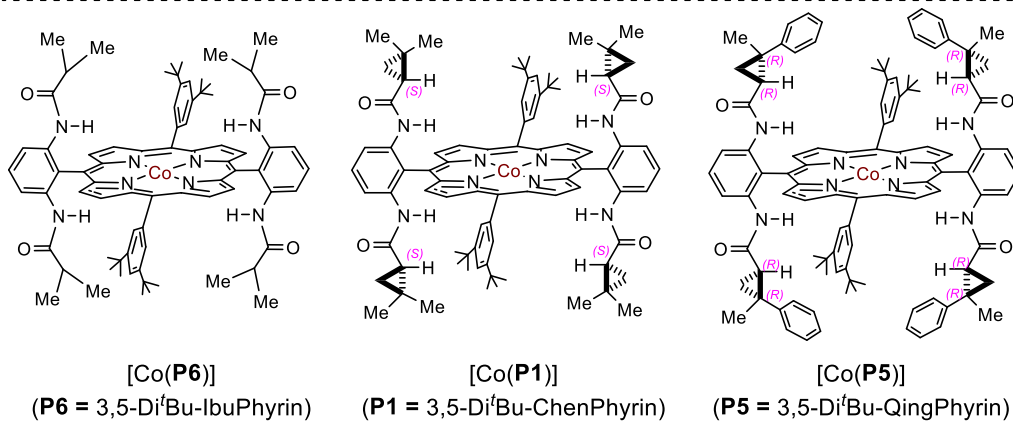
Our efforts started with the use of styrene (**2a**) as the model substrate for asymmetric aziridination with TrocN₃ (**1**) by metalloradical catalysts [Co(Por)] (Table 2.1). While [Co(TPP)] was ineffective (Table 2.1; entry 1), the Co(II) complex of *D*_{2h}-symmetric achiral amidoporphyrin [Co(**P6**)] (**P6** = 3,5-Di^tBu-IbuPhyrin)^{11c} could catalyze the reaction even at room temperature to form the desired *N*-Troc-aziridine **3a** in a low but significant yield (Table 2.1; entry 2), indicating ligand-accelerated catalysis as a result of the putative H-bonding interaction between the carbonyl moiety in the azide and the amide unit of the catalyst. The first-generation chiral metalloradical catalyst [Co(**P1**)] (**P1** = 3,5-Di^tBu-ChenPhyrin)^{9b} could give rise to significant asymmetric induction for the formation of chiral aziridine **3a** while slightly improving the yield (Table 2.1; entry 3). Taking advantage of the modularity and tunability of the *D*₂-symmetric chiral amidoporphyrin ligand platform, we synthesized the second-generation metalloradical catalyst [Co(**P5**)] (**P5** = 3,5-Di^tBu-QingPhyrin) by replacing one of the methyl groups on the chiral amide units of

[Co(**P1**)] with a phenyl group, resulting in a [Co(*D*₂-Por*)] complex bearing chiral amides with two contiguous stereogenic centers.⁹ⁱ Gratifyingly, [Co(**P5**)] could further enhance both reactivity and enantioselectivity of the catalytic aziridination reaction, affording **3a** in 50% yield with 94% ee (Table 2.1; entry 4). Since all the azide was consumed in the reaction, the remaining mass balance was attributed to the formation of oxazoline and other side products detected in the crude HNMR analysis. On the assumption that the presence of adventitious water might negatively affect the yield of the aziridine product, molecular sieves were employed as additives in the catalytic system and the yield of aziridine **3a** was improved to 81% with preservation of the 94% ee (Table 2.1; entry 5). It was further found that addition of anhydrous K₂CO₃ could lead to quantitative formation of the desired aziridine **3a** with the same excellent enantioselectivity (Table 2.1; entry 6). While its exact role was difficult to ascertain, we speculate that anhydrous K₂CO₃ might, in addition to the removal of adventitious water like molecular sieves, prevent Co(III)-intermediates from functioning as potential Lewis acids to promote aziridine isomerization.³⁰ In a similar trend, the use of comparable additives such as Cs₂CO₃, NaI, or KF afforded aziridine **3a** with the same excellent yields and enantioselectivity (Table 2.1, entries 12–14). Switching the ratio of **2a**:**1** from 3:1 to 1:1.2 resulted in decrease in the yield of **3a** without affecting the enantioselectivity (Table 2.1; entry 7). Among different solvents tested, chlorobenzene proved to be the choice of reaction medium, affording aziridine **3a** in high yield with excellent enantioselectivity at room temperature (Table 2.1; entries 6–10). As expected, no reaction was observed in the absence of a catalyst (Table 2.1; entry 11).

Table 2.1| Enantioselective Aziridination Reaction of Styrene with Carbonyl Azide TrocN₃ by [Co(Por)]^a



entry	[Co(Por)]	solvent	additive	yield (%) ^b	ee (%) ^c
1	[Co(PPP)]	chlorobenzene	--	trace	0
2	[Co(P6)]	chlorobenzene	--	15	0
3	[Co(P1)]	chlorobenzene	--	22	76
4	[Co(P5)]	chlorobenzene	--	50	94
5	[Co(P5)]	chlorobenzene	M.S. ^d	81	94
6	[Co(P5)]	chlorobenzene	K₂CO₃^e	99	94
7 ^f	[Co(P5)]	chlorobenzene	K ₂ CO ₃ ^e	43	94
8	[Co(P5)]	trifluorotoluene	K ₂ CO ₃ ^e	84	94
9	[Co(P5)]	hexanes	K ₂ CO ₃ ^e	79	94
10	[Co(P5)]	dichloromethane	K ₂ CO ₃ ^e	trace	nd ^g
11	--	chlorobenzene	K ₂ CO ₃ ^e	--	--
12	[Co(P5)]	chlorobenzene	Cs ₂ CO ₃ ^h	99	94
13	[Co(P5)]	chlorobenzene	NaI ^h	99	94
14	[Co(P5)]	chlorobenzene	KF ^h	99	94

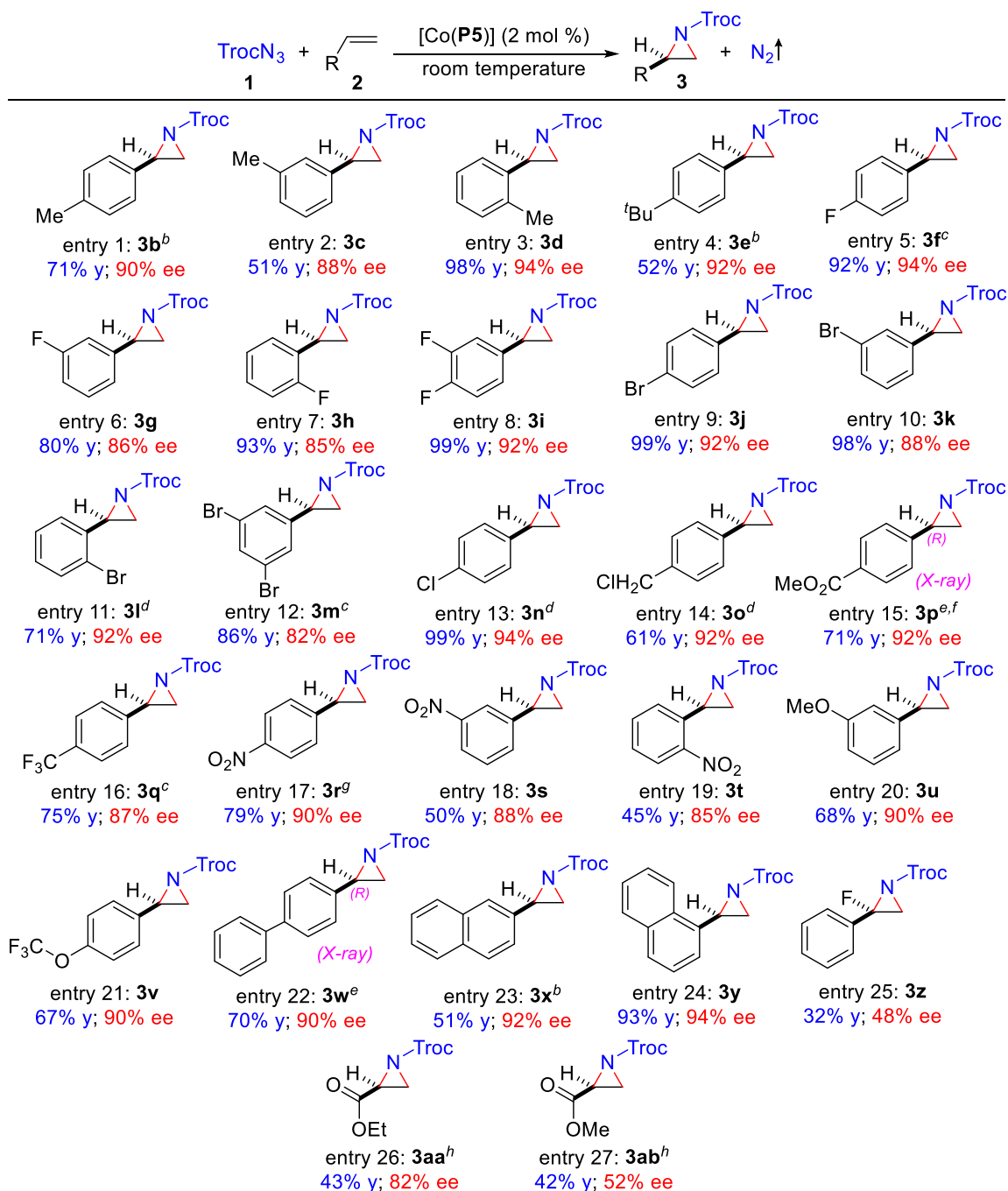


^a Carried out at room temperature for 24 h with TrocN₃ (0.1 mmol) and styrene (0.3 mmol); [TrocN₃] = 0.10 M. ^b Isolated yields. ^c Enantiomeric excess determined by chiral HPLC. ^d With 50 mg of 4 Å molecular sieves. ^e With 0.5 mmol of anhydrous K₂CO₃. ^f TrocN₃ (0.12 mmol) and styrene (0.1 mmol) were used. ^g Not determined. ^h 0.5 mmol of additive.

2.2.2 Substrate Scope

Under the optimized reaction conditions, the [Co(**P5**)]/TrocN₃-based system was found to be effective for the enantioselective aziridination of various styrene derivatives (Table 2.2). Like styrene, the Co(II)-catalyzed aziridination was suitable for styrene derivatives bearing alkyl substituents at the *para*-, *meta*-, and *ortho* positions, affording the desired aziridines **3b–3e** in moderate to high yields with excellent enantioselectivities (Table 2.2; entries 1–4). Similarly, fluorinated styrenes having different substitution patterns could be employed as effective substrates, providing the corresponding fluorinated aziridines **3f–3i** in high yields with excellent enantioselectivities (Table 2.2; entries 5–8). Other halogenated aromatic olefins such as brominated and chlorinated styrenes could also be effectively aziridinated with TrocN₃, affording the halogenated aziridines **3j–3n** in high yields with excellent enantioselectivities (Table 2.2; entries 9–13), which may be potentially transformed to other aziridine derivatives by cross-coupling and related reactions. Furthermore, the Co(II)-based system could tolerate functional groups as exemplified by productive formation of the desired aziridine **3o** and **3p** with high enantioselectivities (Table 2.2; entries 14 and 15). To demonstrate the synthetic practicality, a gram-scale synthesis of aziridine **3p** was performed using 1 mol % of [Co(**P5**)] under otherwise the same conditions, affording the desired product with the same high enantioselectivity (92% ee) but in a relatively lower yield (from 71% to 51%), likely due to the reduction of the catalyst loading. Additionally, styrene derivatives containing electron-withdrawing substituents such as –CF₃ and –NO₂ groups at different positions could serve as suitable substrates, affording the corresponding three-membered *N*-heterocycles **3q–3t** in enantioenriched forms although in relatively lower yields (Table 2.2; entries 16–19).

Table 2.2| Co(II)-Catalyzed Enantioselective Aziridination of Styrene Derivatives with Carbonyl Azide TrocN₃^a

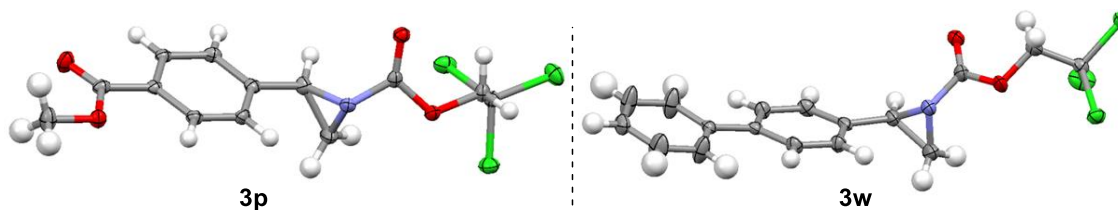


^a Carried out with **1** (0.1 mmol), **2** (0.3 mmol), and K₂CO₃ (0.5 mmol) by [Co(**P5**)] (2 mol %) in chlorobenzene at room temperature for 24 h; [TrocN₃] = 0.10 M; Isolated yields; Enantiomeric excess determined by chiral HPLC. ^b Used [Co(**P5**)] (5 mol %), **2** (0.5 mmol), and Cs₂CO₃ (0.5 mmol). ^c At 0 °C for 24 h. ^d At 40 °C for 24 h. ^e Absolute configuration determined by anomalous

dispersion effects in X-ray diffraction measurements on the crystal. ^f 51% Yield (815 mg); 92% ee when carried out on a gram scale with **1** (4.6 mmol), **2** (13.7 mmol), and K₂CO₃ (22.9 mmol) with [Co(**P5**)] (1 mol %). ^g At -20 °C for 48 h. ^h Used [Co(**P5**)] (5 mol %) with addition of Pd(OAc)₂ (10 mol %) in the presence of 4Å molecular sieves (50 mg) instead of K₂CO₃ at 40 °C for 48 h.

The Co(II)-catalyzed aziridination could also be applied for styrene derivatives bearing electron-donating groups as demonstrated by the highly asymmetric formation of **3u** and **3v** albeit in lower yields (Table 2.2; entries 20 and 21). In addition, the aziridination system catalyzed by [Co(**P5**)] could be applied to extended aromatic olefins as shown by the construction of aziridines **3w–3y** in moderate to high yields with excellent enantioselectivities (Table 2.2; entries 22–24). The absolute configurations of the newly-generated stereogenic centers in both **3p** and **3w** were established as (*R*) by X-ray crystallography (Figure 2.2).

Figure 2.2 | X-ray Structures of Compounds **3p** and **3w**



Besides mono-substituted styrene derivatives, the catalytic system could be applicable to 1,1-disubstituted styrenes as exemplified by the productive formation of aziridine **3z** bearing a tertiary fluoride stereocenter from the reaction of α -fluorostyrene although in lower yield and enantioselectivity (Table 2.2; entry 25). Assisted by a catalytic amount of Pd(OAc)₂ that presumably acts as p-electrophilic Lewis acid to activate the alkene,²² we found that the Co(II)-based metalloradical system could also aziridinate electron-deficient alkenes as shown for the successful reactions of ethyl and methyl acrylates to form the

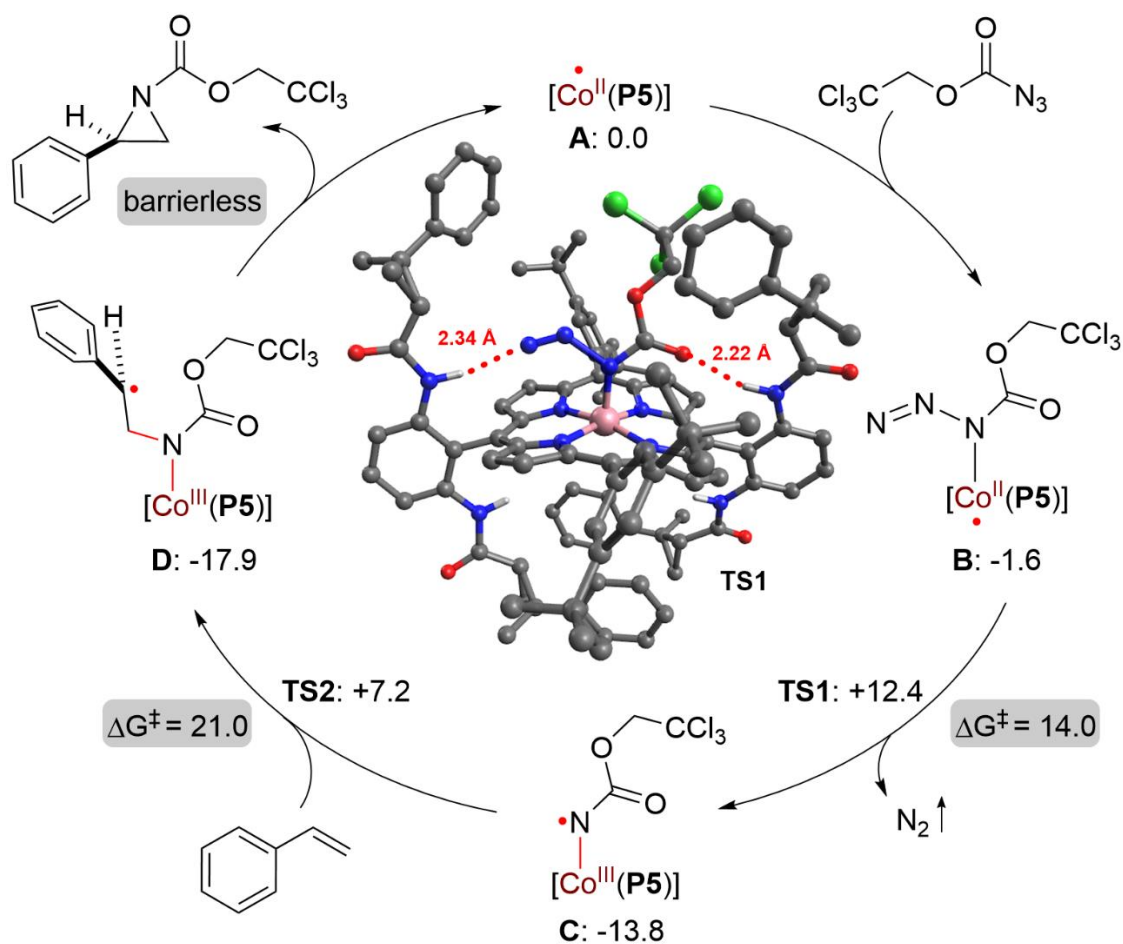
corresponding aziridines **3aa** and **3ab**, respectively, in moderate yields but with significant levels of enantiocontrol (Table 2.2; entries 26–27). It is worth mentioning that electron-deficient alkenes are known to be challenging substrates for aziridination by existing catalytic systems involving electrophilic metallonitrenes as the key intermediate. When heteroaromatic olefins were used, however, it generated an unidentified mixture of products in low yields without observation of the corresponding aziridines. Catalyst [Co(**P5**)] was found to be ineffective for aziridination reactions of aliphatic and internal olefins with TrocN₃ as well as dienes. We hope to address these shortcomings in the future by developing a new catalytic system involving a more effective catalyst for the asymmetric aziridination of a broader scope of alkenes.

2.2.3 Mechanistic Studies

Combined computational and experimental studies were performed for the proposed stepwise radical mechanism of the Co(II)-catalyzed aziridination (Scheme 2.1). First, with the help of my colleague Hao Xu as computational chemist, DFT calculations were carried out to study the catalytic pathway for the aziridination reaction of styrene with TrocN₃ with the use of the actual catalyst [Co(**P5**)] (Scheme 2.2).³¹ The computational study indicates the existence of intermediate **B**, which is formed upon coordination of the internal nitrogen atom in TrocN₃ to the cobalt center of the catalyst. The formation of intermediate **B** is slightly exergonic by –1.6 kcal/mol due to additional H-bonding stabilization (see Figures 2.3 and 2.4). Upon further activation, the coordinated azide undergoes dinitrogen elimination to generate α -Co(III)-aminyl radical **C**. The metalloradical activation step, which is exergonic by –12.2 kcal/mol, has a relative low activation energy (**TS1**: $\Delta G^\ddagger =$

14.0 kcal/mol). As shown in the middle of the catalytic cycle (see also Figures 2.3 and 2.4), the optimized **TS1** structure reveals strong double H-bonding interactions (N–H---N: 2.34 Å; N–H---O: 2.22 Å) between [Co(**P5**)] and TrocN₃ as well as the strengthening of Co–N bonding interaction (as indicated by the decrease of bond distance from 2.10 Å to 1.90 Å). According to the DFT calculations, the subsequent radical addition of radical intermediate **C** to styrene is associated with a relatively high but accessible activation barrier (**TS2**: $\Delta G^\ddagger = 21.0$ kcal/mol), leading to the formation of γ -Co(III)-alkyl radical intermediate **D** as the rate determining step (Scheme 2.2). The final step of *3-exo-tet* cyclization via radical substitution, which is highly exergonic by -27.2 kcal/mol, is found to be almost barrierless, resulting in the formation of the three-membered aziridine **3a** and the regeneration of catalyst [Co(**P5**)]. See Figures 2.3 and 2.4 for details on optimized geometries and spin density plots for intermediates and transition states.

Scheme 2.3| DFT Study on the Catalytic Pathway for Aziridination of Styrene with TrocN₃ by [Co(P5)]^a



^aCalculations performed with the Gaussian 09 at the unrestricted BP86 /lanl2dz level of theory. See Experimental Section for further details. All relative Gibbs free energies (ΔG°) for intermediates and transition states as well as activation energies (ΔG‡) are reported in kcal/mol.

Figure 2.3| Optimized Geometries for Intermediates and Transition States

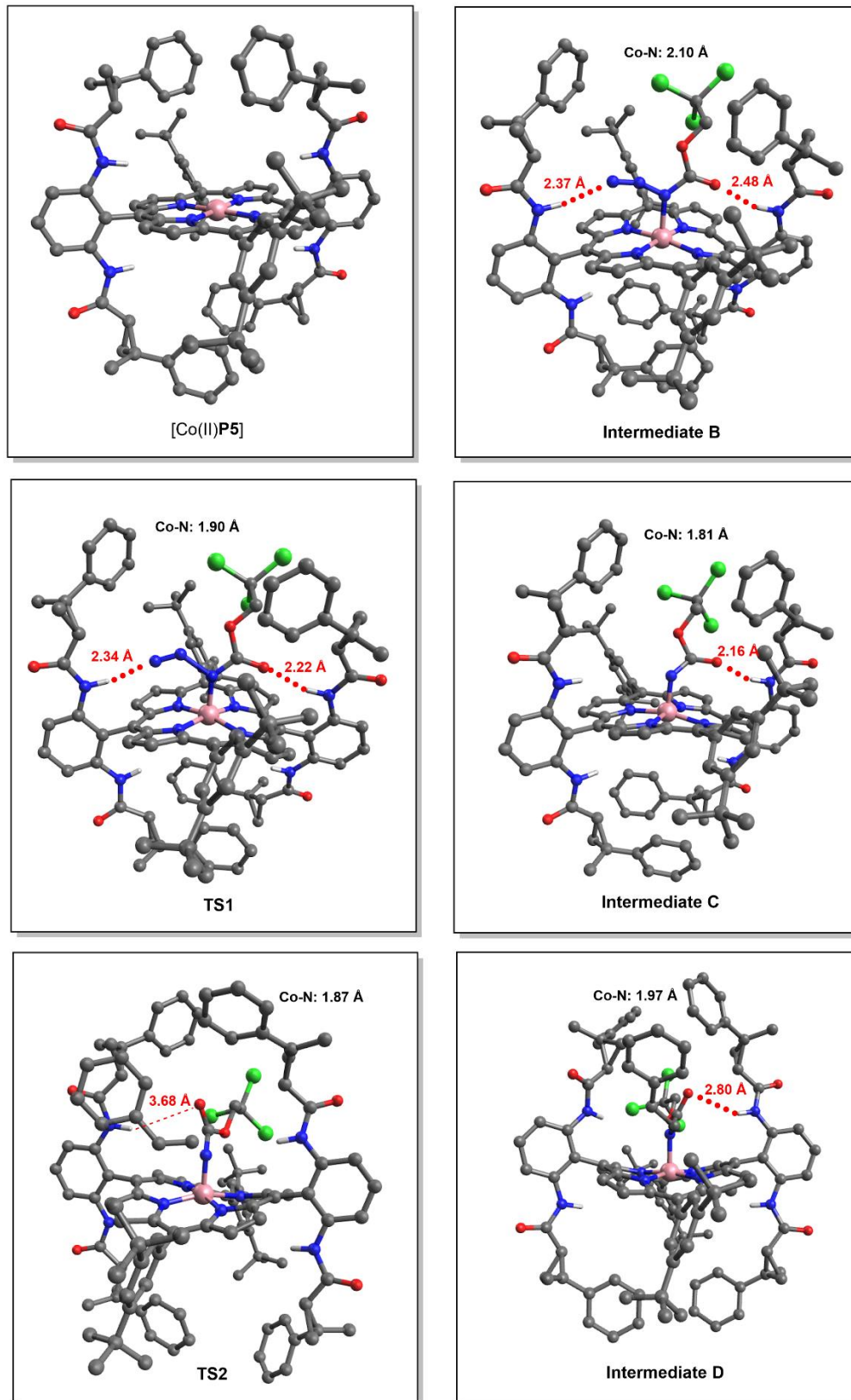
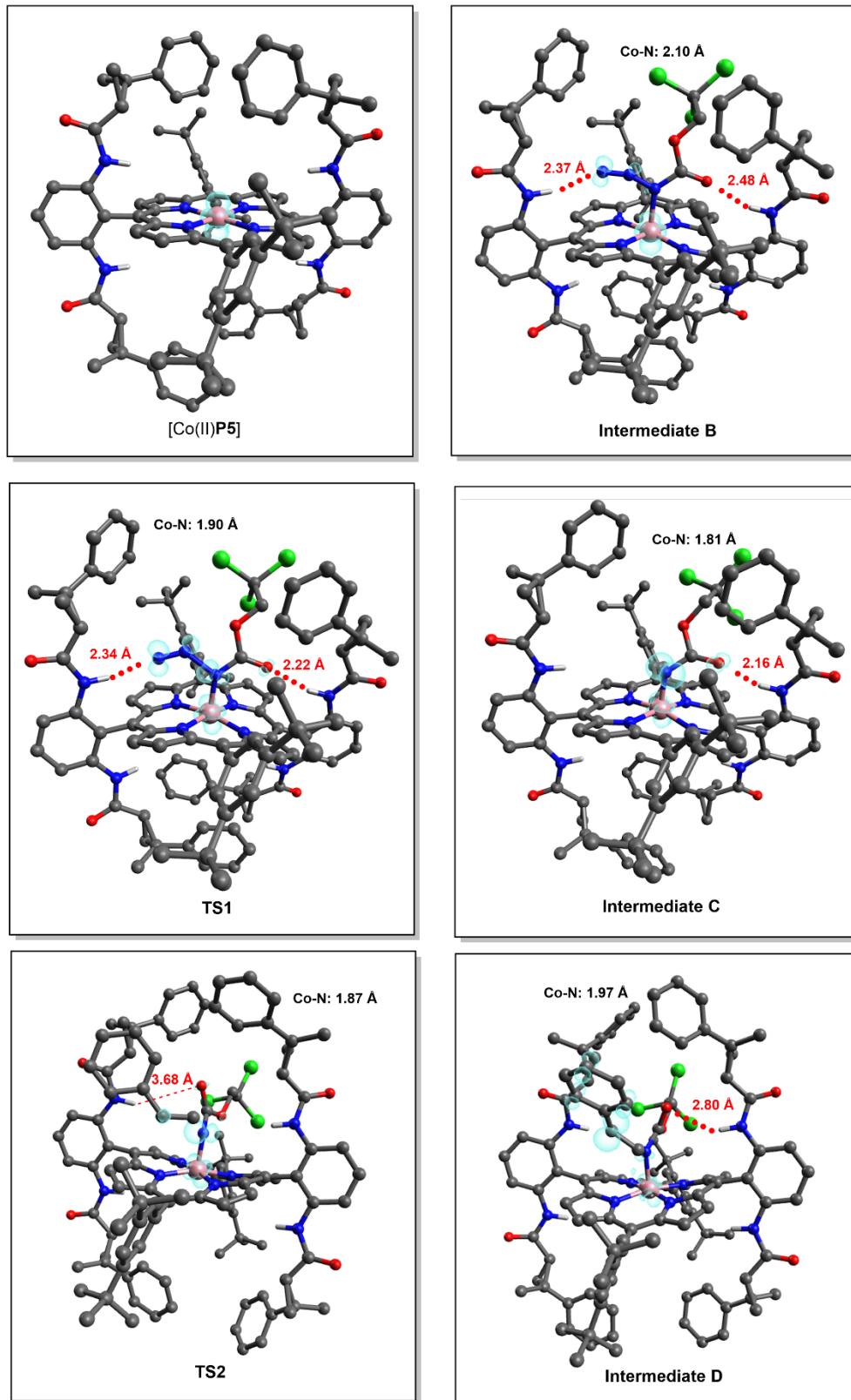


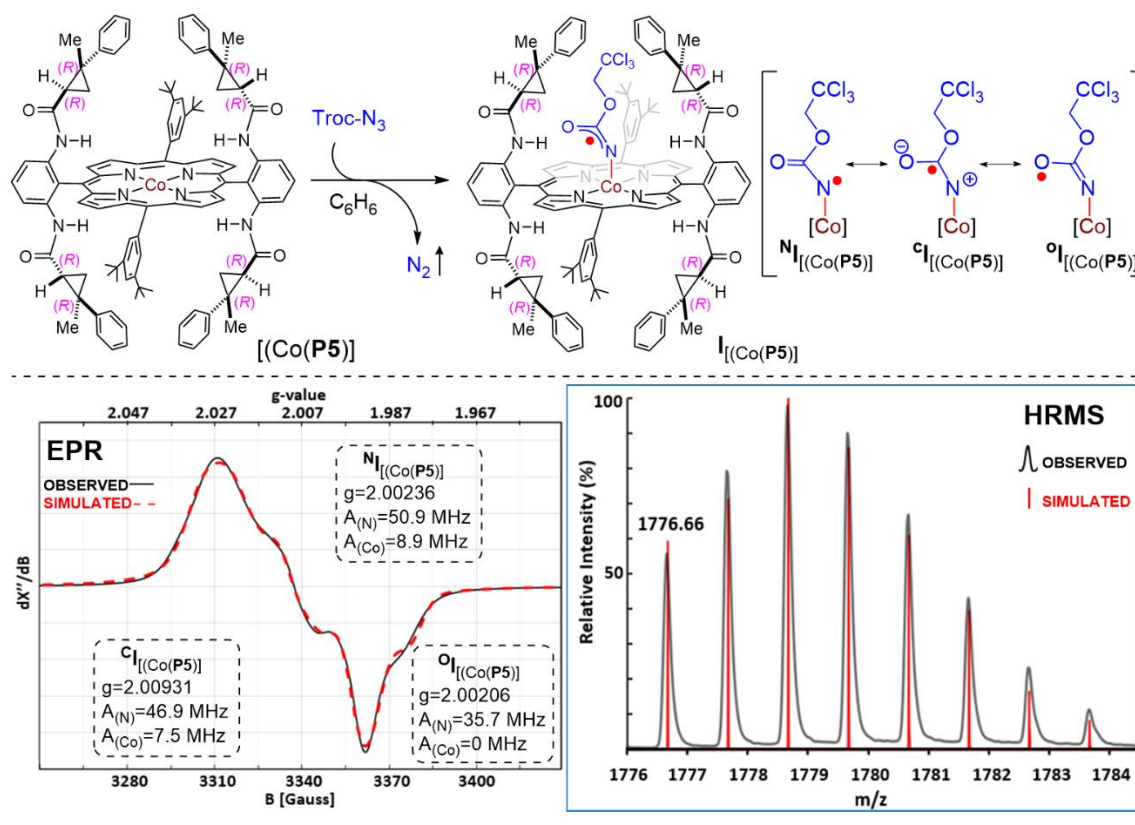
Figure 2.4| Spin Density Distribution for Optimized Geometries



Second, in an effort to detect the α -Co(III)-aminyl radical intermediate **I** experimentally, the isotropic X-band EPR (Electron Paramagnetic Resonance) spectrum was recorded at room temperature for the reaction mixture of [Co(**P5**)] with TrocN₃ (**1**) in benzene without alkene substrate (Figure 2.5). The spectrum displays salient signals akin to those characteristics of α -Co(III)-aminyl radicals (Figure 2.5).⁸ The observed isotropic g value of 2.00 is consistent with the formation of organic radical **I**_[Co(**P5**)] upon spin translocation from the Co(II) to the N-atom during metalloradical activation of the azide. Consistent with the spin delocalization in the α -carbonylaminy radical intermediate **I**_[Co(**P5**)], the observed broad signals could be simulated by invoking its three resonance forms on the basis of hyperfine coupling by both ¹⁴N (I = 1) and ⁵⁹Co (I = 7/2): 17% of N-centered radical ^N**I**_[Co(**P5**)] (g: 2.00236; A_(Co): 8.9 MHz; A_(N): 50.9 MHz), 78% of C-centered radical ^C**I**_[Co(**P5**)] (g: 2.00931; A_(Co): 7.5 MHz; A_(N): 46.9 MHz), and 5% of O-centered radical ^O**I**_[Co(**P5**)] (g: 2.00206; A_(Co): 0 MHz; A_(N): 35.7 MHz) (see Experimental Section for details and for the individual spectrum of each species without the other resonance structures). Furthermore, the α -Co(III)-aminyl radical **I**_[Co(**P5**)] from the reaction mixture of [Co(**P5**)] with azide **1** could be detected by high-resolution mass spectrometry (HRMS) with electrospray ionization (ESI) (see Experimental Section for details). The obtained spectrum (Figure 2.5) exhibited a signal corresponding to [**I**_[Co(**P5**)]]⁺ (m/z = 1776.6666), which resulted from the neutral α -Co(III)-aminyl radical **I**_[Co(**P5**)] by the loss of one electron. Both the exact mass and the isotope distribution pattern measured experimentally matched well with those calculated from the formula of [(**P5**)Co(NCO₂CH₂CCl₃)]⁺. The successful detection of α -Co(III)-aminyl radical intermediate **I**_[Co(**P5**)] by EPR and HRMS provided

experimental evidence to support the first step of metalloradical activation in the proposed mechanism of radical aziridination (Scheme 2.1).

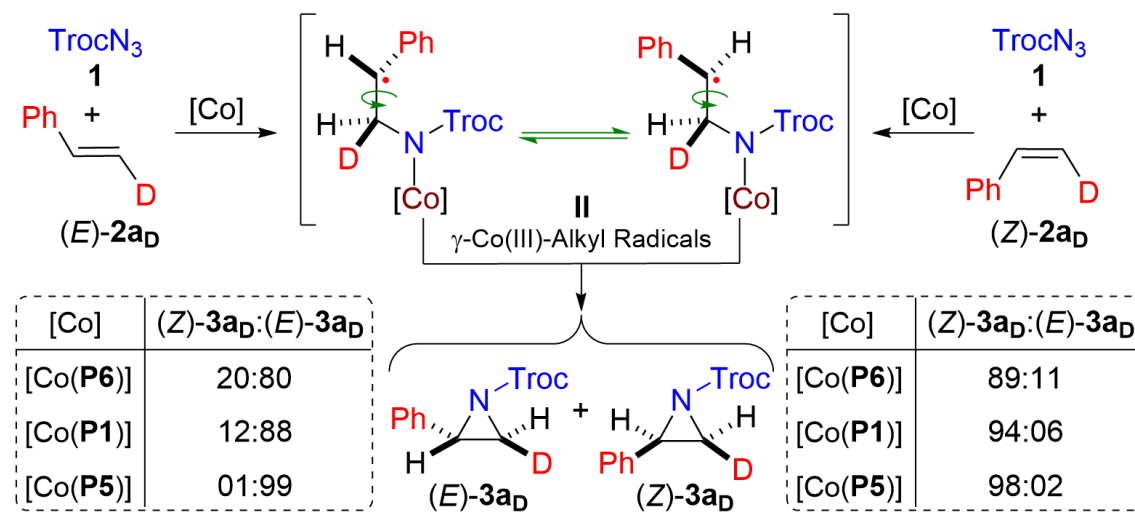
Figure 2.5| Generation and Detection of α -Co(III)-Aminyl Radical Intermediate by EPR and HRMS



Finally, to probe the subsequent steps of radical addition and radical cyclization in the proposed mechanism (Scheme 2.1), both isotopomers of β -deuterostyrene (*E*)-**2a_D** and (*Z*)-**2a_D** were applied as substrates for Co(II)-catalyzed aziridination with TrocN₃ (**1**) (Scheme 2.4). While a concerted mechanism associated with metallonitrene intermediates is usually stereospecific, a stepwise mechanism involving α -Co(III)-aminyl radical intermediates may lead to the formation of aziridines as a mixture of both diastereoisomers (*E*)-**3a_D** and

(*Z*)-**3a_D** from either (*E*)-**2a_D** or (*Z*)-**2a_D** as a result of the β-C–C bond rotation in the resulting γ-Co(III)-alkyl radical intermediate **II** before cyclization (Scheme 2.4). The aziridination of (*E*)-**2a_D** with azide **1** by the achiral catalyst [Co(**P6**)] produced an isotopomeric mixture of (*Z*)-**3a_D** and (*E*)-**3a_D** in a ratio of 20:80. Under the identical conditions, aziridination of (*Z*)-**2a_D** yielded the isotopomeric mixture in a ratio of 89:11. (Scheme 2.5) The formation of an isotopomeric mixture of aziridine **3a_D** from isomerically pure **2a_D** is attributed to the rotation around the β-C–C bond in the γ-Co(III)-alkyl radical intermediate **II**.

Scheme 2.4| Aziridination of (*E*)- or (*Z*)-β-Deuterostyrenes to Probe Radical Mechanism^a

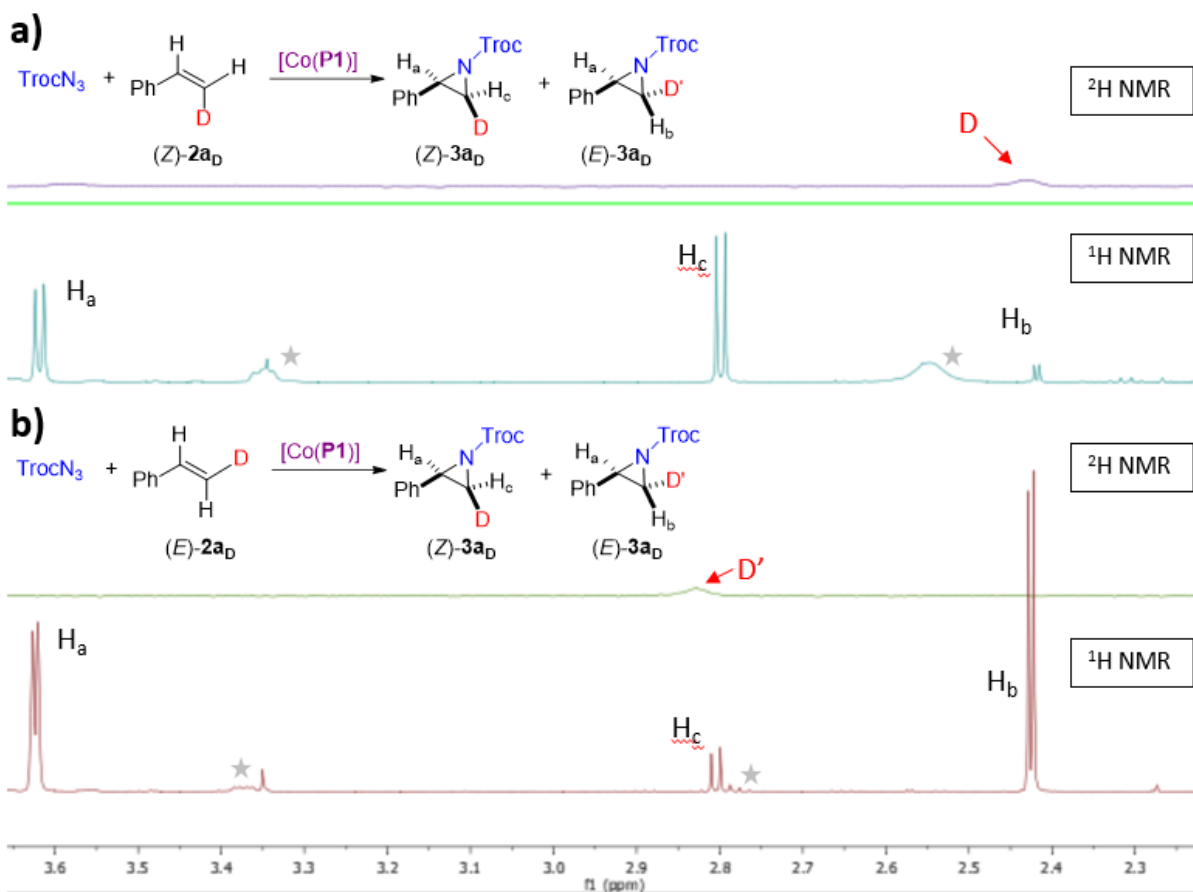


^aCarried out with **1** (0.1 mmol), **2a_D** (0.3 mmol), and K₂CO₃ (0.5 mmol) by [Co(Por)] (2 mol %) in chlorobenzene at 40 °C for 24 h; [TrocN₃] = 0.10 M; (*Z*)-**3a_D**:(*E*)-**3a_D** ratio determined by ¹H-NMR and ²H-NMR analysis of crude reaction mixture; see Schemes 2.5, 2.6, and 2.7.

It was found that the degree of the bond rotation could be influenced by the environment of the supporting ligand. For example, when the two reactions were carried out under the

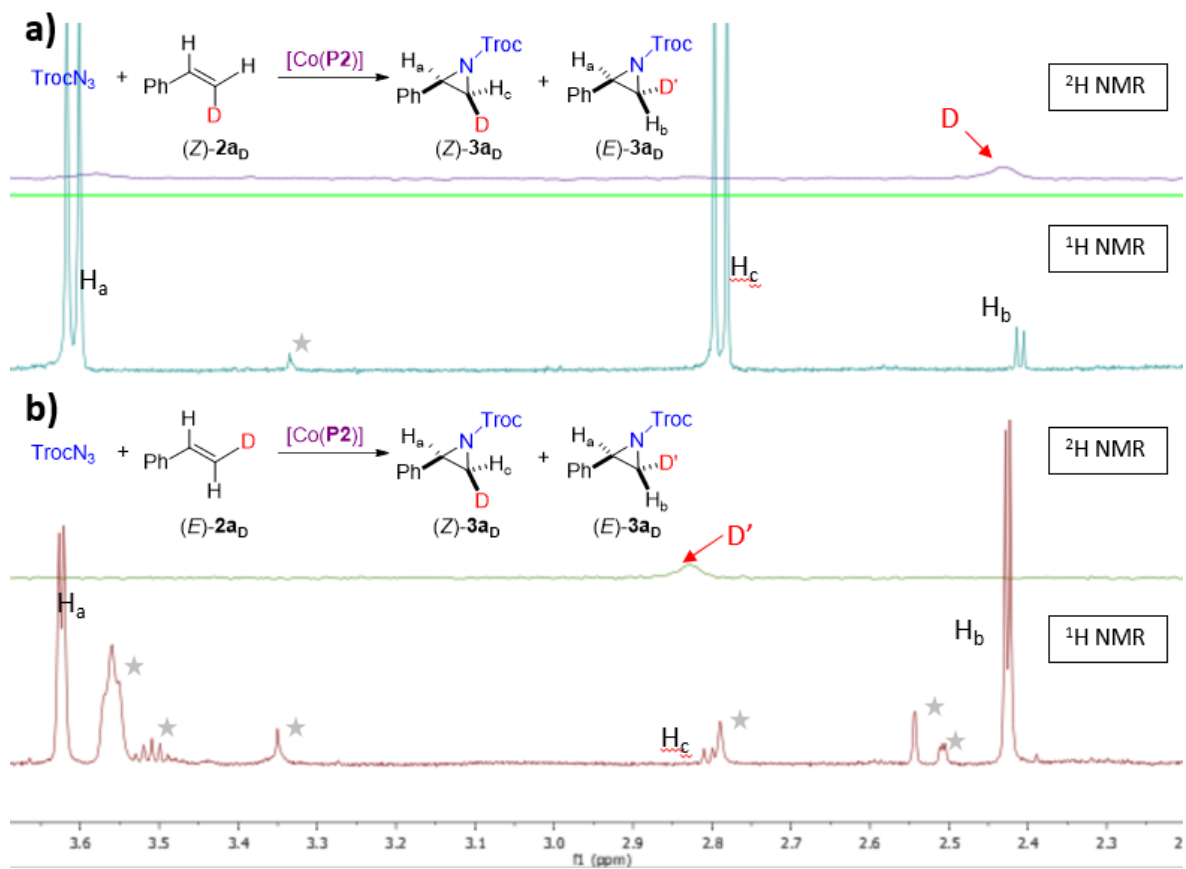
same condition but using the chiral catalyst [Co(**P1**)] (Scheme 2.6), the isotopomeric ratio of (*Z*)-**3aD** and (*E*)-**3aD** changed from 20:80 to 12:88 for the reaction of (*E*)-**2aD** and from 89:11 to 94:06 for the reaction of (*Z*)-**2aD**, indicating a lower degree of rotation in a more hindered ligand environment (Scheme 2.4). In a similar trend, when the optimized catalyst [Co(**P5**)], which has an even more confined ligand environment, was employed for the aziridination reactions of (*E*)-**2aD** and (*Z*)-**2aD**, minimal isotopomeric distributions were observed (Scheme 2.7), as a result of a faster radical cyclization than the β -C–C bond rotation, leading to a stereospecific process (Scheme 2.4). This high stereospecificity for β -deuterostyrenes, together with the high enantioselectivity observed for styrene (Table 2.1, entry 6), suggests that the [Co(**P5**)]-catalyzed olefin aziridination with TrocN₃ involves radical addition as the enantiodetermining step, followed by a stereoretentive radical cyclization. It is worth mentioning that no erosion of the original isomeric purity was observed in the recovered starting materials (*E*)-**2D** and (*Z*)-**2D** after the reaction. As anticipated for a radical process, it was found that the catalytic aziridination process could be significantly inhibited when a large excess of TEMPO (2,2,6,6-Tetramethylpiperidine 1-oxyl) was added. Together with the detection of the α -Co(III)-aminyl radical intermediate **I** by EPR and HRMS, these results are in good agreement with the proposed stepwise radical mechanism for the Co(II)-based metalloradical aziridination (Scheme 2.1).

Scheme 2.5| Upfield ^2H NMR and ^1H NMR for Aziridine Isomers $3a_D$ from $[\text{Co}(\text{P}6)]$ -Catalyzed Aziridination between: a) Troc- N_3 (1) and (*Z*)- β -Deuterostyrene ((*Z*)- $2a_D$); b) Troc- N_3 (1) and (*E*)- β -Deuterostyrene ((*E*)- $2a_D$)



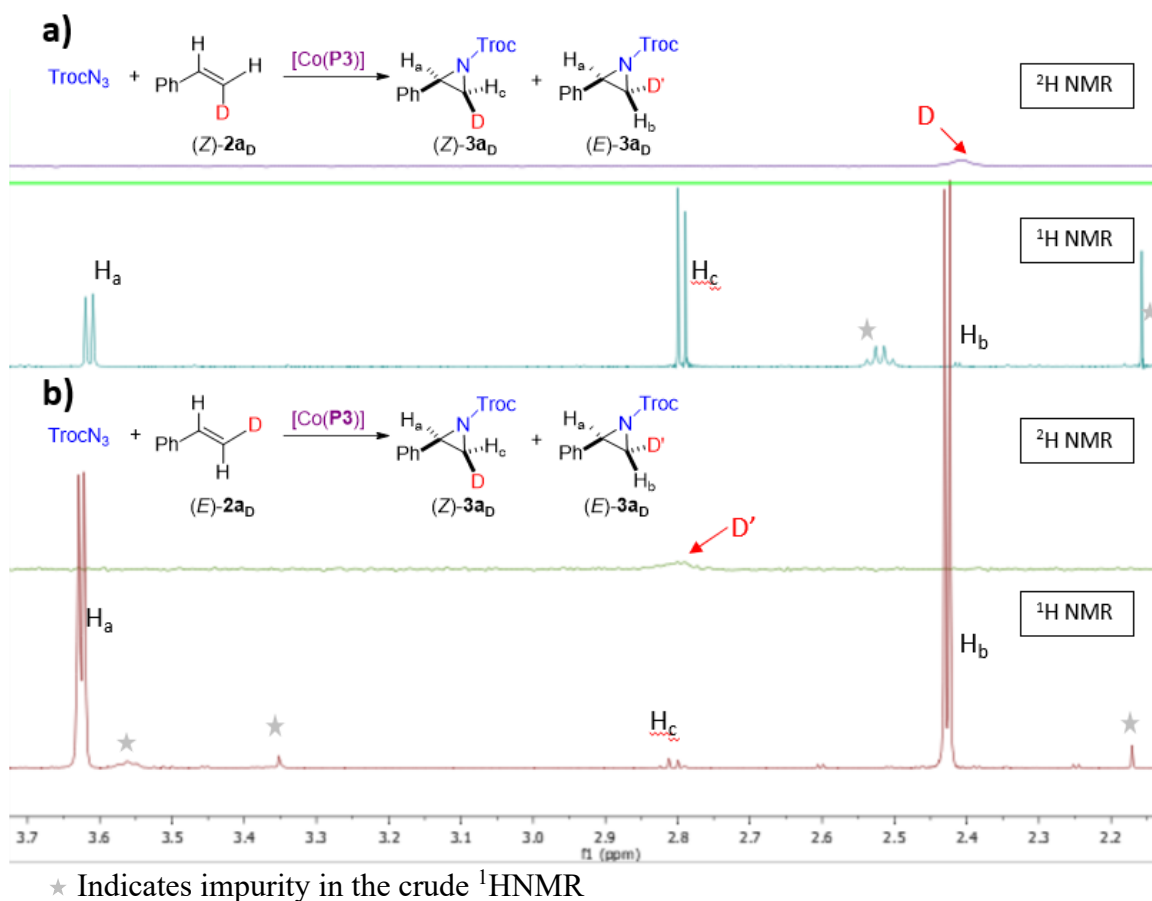
★ Indicates impurity in the crude ^1H NMR

Scheme 2.6| Upfield ^2H NMR and ^1H NMR for Aziridine Isomers 3_{aD} from $[\text{Co}(\text{P}1)]$ -Catalyzed Aziridination between: a) TrocN $_3$ (1) and (*Z*)- β -Deuterostyrene ((*Z*)- 2_{aD}); b) Troc-N $_3$ (1) and (*E*)- β -Deuterostyrene ((*E*)- 2_{aD})



★ Indicates impurity in the crude ^1H NMR

Scheme 2.7| Upfield ^2H NMR and ^1H NMR for Aziridine Isomers $3a_D$ from $[\text{Co}(\text{P}5)]$ -Catalyzed Aziridination between: a) TrocN₃ (1) and (*Z*)- β -Deuterostyrene ((*Z*)- $2a_D$); b) Troc-N₃ (1) and (*E*)- β -Deuterostyrene ((*E*)- $2a_D$)

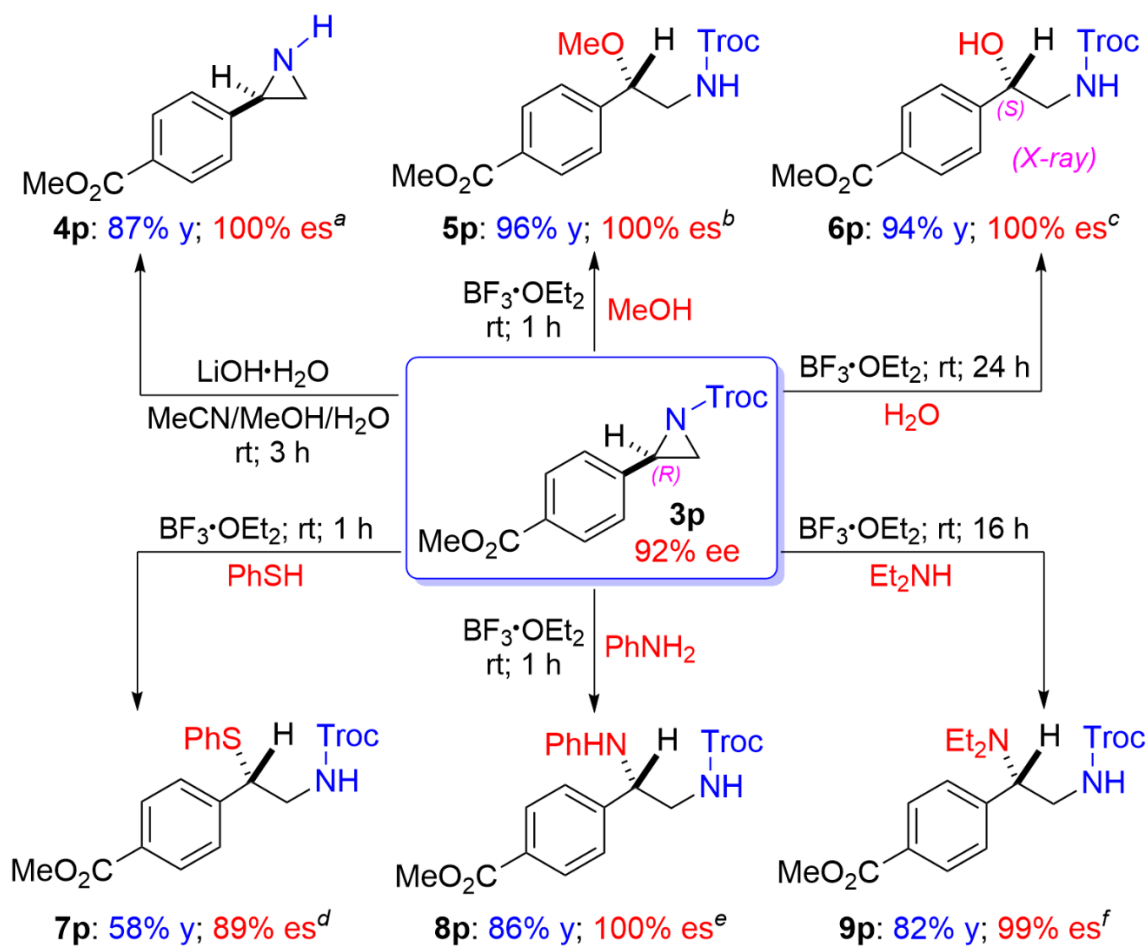


2.2.4 Synthetic Applications

To access aziridine derivatives with various *N*-substituents for different applications, it would be desirable that the aziridine products from a catalytic aziridination process could be effectively converted to the corresponding *N*-H aziridines through simple deprotection without opening the three-membered ring structures.^{13c,26a,32} In contrast to aziridines with

N-protecting groups that require harsh conditions for deprotection,^{21,33} *N*-carboalkoxy aziridines have been known to undergo facile *N*-deprotection under mild conditions.³⁴ To showcase the synthetic utility of the resulting chiral *N*-Troc-aziridines from the Co(II)-catalyzed process, it was demonstrated that enantioenriched *N*-Troc-aziridine (*R*)-**3p** could be readily converted to the corresponding *N*-H aziridine **4p** in 87% yield without erosion of its optical purity when treated with lithium hydroxide at room temperature (Scheme 2.8). In addition to *N*-deprotection, chiral *N*-Troc-aziridines were shown to undergo facile ring-opening reactions at room temperature by a wide range of nucleophiles in the presence of Lewis acids with preservation of the high enantiomeric purity (Scheme 2.8). For instance, methanol could effectively open the three-membered ring in (*R*)-**3p** in the presence of boron trifluoride diethyl etherate, generating chiral β -amino ether **5p** in 96% yield without any racemization. Notably, even water could function as an effective nucleophile for ring-opening of (*R*)-**3p** under similar conditions, resulting in the highly stereospecific formation of chiral β -amino alcohol **6p** in 94% yield. The absolute configuration of **6p** was established by X-ray crystallography as (*S*), indicating an S_N2-type mechanism of the ring-opening reaction. Sulfur-based nucleophiles could also be applied for the ring-opening process as exemplified by the reaction of (*R*)-**3p** with thiophenol, affording the chiral β -amino thioether **7p** in 58% yield with some loss of the original enantiopurity. Similarly, the three-membered ring in chiral *N*-Troc-aziridines could be readily opened by nitrogen-based nucleophiles, including both aromatic and aliphatic amines at room temperature to provide valuable vicinal diamines.³⁵ For example, both aniline and diethylamine could effectively react with (*R*)-**3p** to afford chiral vicinal diamines **8p** and **9p**, respectively, in high yields with no erosion of the original enantiopurity.

Scheme 2.8| Troc-Deprotection and Nucleophilic Ring Opening of the Resulting Enantioenriched *N*-Carbonyl Aziridines

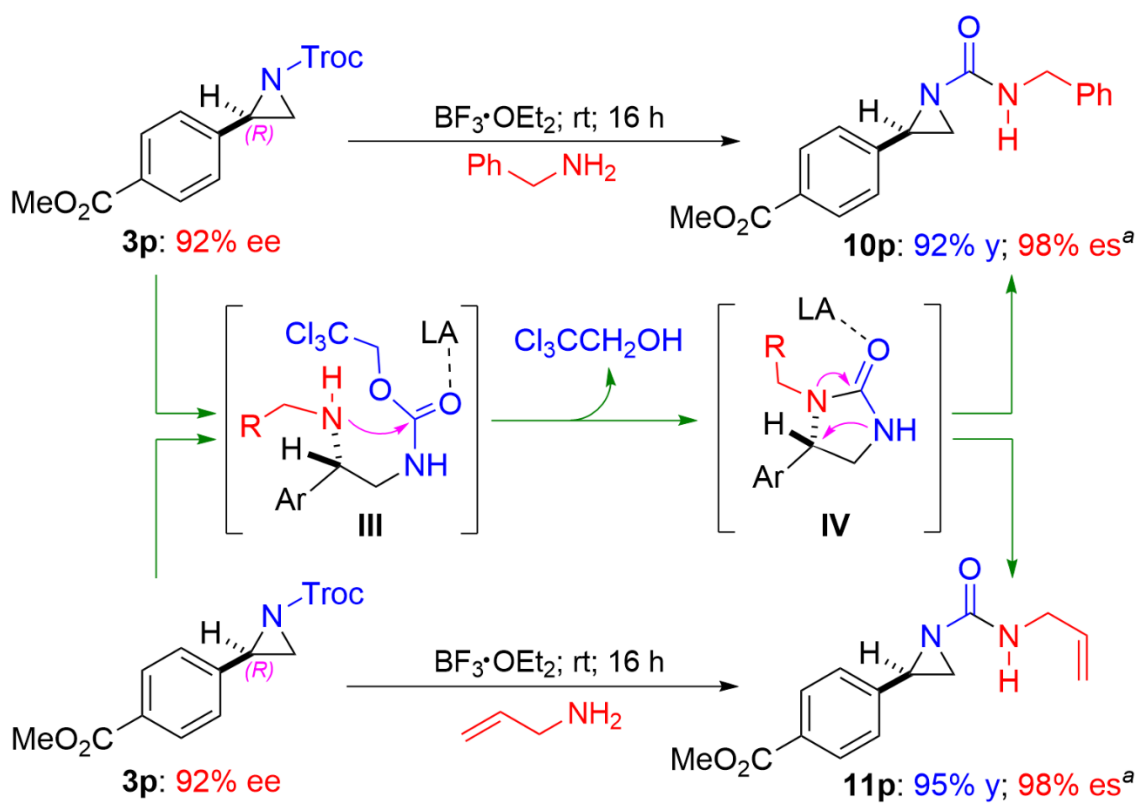


^a Conditions as reported in the literature.³⁴ ^b MeOH (0.10 M), BF₃·OEt₂ (10 mol %). ^c H₂O (0.10 M), BF₃·OEt₂ (10 mol %). ^d PhSH (0.10 M), BF₃·OEt₂ (10 mol %). ^e PhNH₂ (0.10 M), BF₃·OEt₂ (10 mol %). ^f CH₂Cl₂ (0.10 M), BF₃·OEt₂ (20 mol %), amine (20 equiv).

Interestingly, when primary aliphatic amines were employed as the nucleophiles, the reactions of *N*-Troc-aziridines were found to proceed further to generate aziridine-based chiral ureas, a formal process that transforms carbamates to ureas via amide bond formation (Scheme 2.9).³⁶ As two examples, benzylamine and allylamine reacted readily with (*R*)-**3p** under the similar conditions to form aziridine-based chiral ureas **10p** and **11p**, respectively,

in excellent yields without apparent racemization. Presumably due to the combined high nucleophilicity of the resulting secondary amines and good leaving ability of the trichloroethyl group, the initial ring-opening products **III** of (*R*)-**3p** by the primary amines proceeded further intramolecular amide bond formation in the presence of Lewis acid to generate imidazolidinones **IV**, which then underwent ring-contraction under Lewis acid catalysis³⁷ to yield the final products **10p** and **11p**.

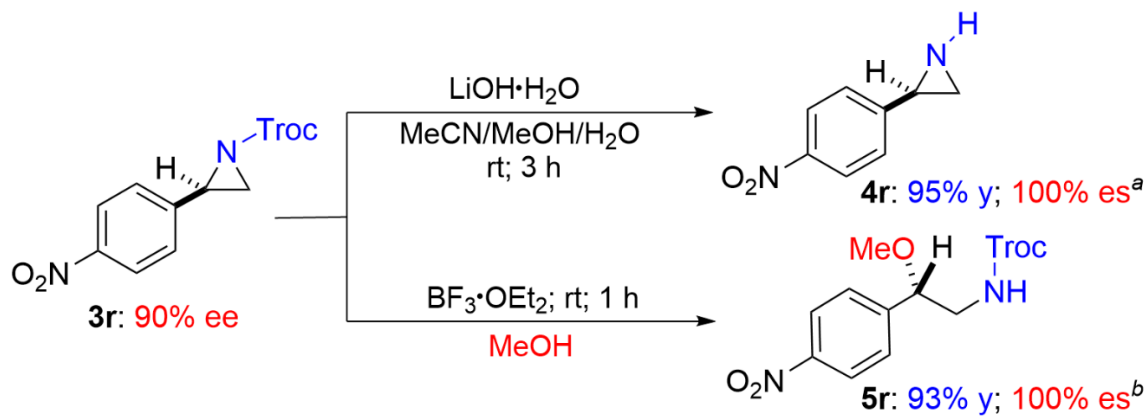
Scheme 2.9| Synthesis of Aziridine-Based Chiral Ureas



^a CH₂Cl₂ (0.10 M), BF₃·OEt₂ (20 mol %), amines (20 equiv).

The *N*-deprotection and ring-opening reactions could proceed equally well with other chiral *N*-Troc-aziridines as exemplified by the stereospecific formations of *N*-H aziridine **4r** and β-amino ether **5r** from enantioenriched aziridine **3r** (Scheme 2.10).

Scheme 2.10| Troc-Deprotection and Nucleophilic Ring Opening of the Resulting Enantioenriched *N*-Carbonyl Aziridines with Different Substrate



^a Conditions as reported in the literature.³⁴ ^b MeOH (0.10 M), BF₃·OEt₂ (10 mol %).

2.3 CONCLUSIONS

In summary, we have developed the first catalytic system that can employ the carbonyl azide TrocN₃ as the nitrogen source for the asymmetric aziridination of alkenes via Co(II)-based metalloradical catalysis. With the support of 3,5-Di^tBu-QingPhyrin as the chiral ligand, the Co(II)-based aziridination system with TrocN₃, which proceeds with the underlying stepwise radical mechanism as evidenced by the combined computational and experimental studies, provides a new methodology for the stereoselective synthesis of chiral *N*-Troc-aziridines from styrene derivatives with varied steric and electronic properties in high yields with high enantioselectivities. Assisted by a catalytic amount of Pd(OAc)₂, this new [Co(3,5-Di^tBu-QingPhyrin)]/TrocN₃-based system can further catalyze the asymmetric aziridination of electron-deficient alkenes such as methyl and ethyl acrylates, which are challenging substrates for catalytic systems involving

electrophilic metallonitrene intermediates. Among several salient features, the Co(II)-catalyzed radical aziridination can operate efficiently at room temperature and has good functional group tolerance. The resulting enantioenriched *N*-Troc-aziridines have been showcased as valuable chiral synthons for the stereoselective synthesis of other chiral aziridines and various chiral amine derivatives. Through fine-tuning the environments of *D*₂-symmetric chiral amidoporphyrins as the supporting ligand, we hope to develop a more general Co(II)-based catalytic system for enantioselective radical aziridination of different alkenes with TrocN₃.

2.4 EXPERIMENTAL SECTION

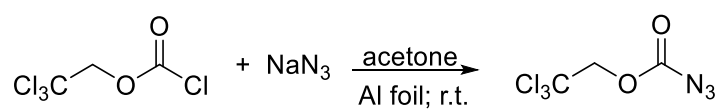
2.4.1 General Considerations

Unless otherwise stated, all reactions were carried out under a nitrogen atmosphere in oven-dried glassware following standard Schlenk techniques. Gas tight syringes were used to transfer liquid reagents and solvents in catalytic reactions. 4Å MS, potassium carbonate, potassium fluoride and sodium iodide were dried in a vacuum oven prior to use. Solvent was freshly distilled/degassed prior to use unless otherwise noted. Thin layer chromatography was performed on Merck TLC plates (silica gel 60 F254), visualizing with UV-light 254 nm or ceriumammonium-molybdate (CAM) stain (ammonium pentamolybdate, cerium(IV) sulfate, sulfuric acid aqueous solution). Flash column chromatography was performed with ICN silica gel (60 Å, 230-400 mesh, 32-63 µm). ¹H and ²HNMR, and ¹³C NMR were recorded on a Varian600 (600 MHz), Varian500 (500 MHz), Varian Inova400 (400 MHz) instrument with chemical shifts reported relative to residual solvent. ¹⁹F spectra were recorded on a Bruker 400 spectrometer (376 MHz), using CFC_l₃ (δ=0) as internal standard. Infrared spectra were measured with a Nicolet Avatar 320 spectrometer with a Smart Miracle accessory. HPLC measurements were carried out on a Shimadzu HPLC system with Chiralcel OD-H, OJ-H, AD-H, IC, ID, and Whelk columns. Optical rotations were measured on a Rudolph Research Analytical AUTOPOL[®] IV digital polarimeter. High resolution mass spectra were obtained on an Agilent 6220 using electrospray ionization time-of-flight (ESI-TOF). The X-ray diffraction data were collected using Bruker-AXSSMART-APEXII CCD diffractometer (CuKα, λ = 1.54178 Å). Co(3,5-

Di^tBu-IbuPhyrin), Co(3,5-Di^tBu-ChenPhyrin) and Co(3,5-Di^tBu-QingPhyrin) were synthesized following literature reported procedures.^{9b,9i}

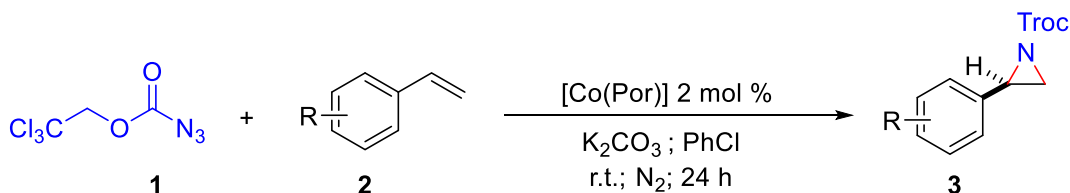
Note: TrocN₃ could be explosive and should be handled carefully. Store in freezer and avoid temperatures above 40 °C during solvent evaporation under reduced pressure.

2.4.2 TrocN₃ Synthesis^{12d}:



To a well-stirred suspension of sodium azide (1.95 g, 30 mmol) in acetone (40 mL) was added 2,2,2-Trichloroethyl chloroformate (4.237 g, 20 mmol) at room temperature. The flask was protected from light by using aluminum foil. TLC analysis after a total of 3 h indicated the reaction was complete. The reaction mixture was then poured into a flash chromatography column filled with Celite (dry) and was washed with dichloromethane until all the product was washed out. The filtrate was collected and concentrated *in vacuo* at room temperature to give the product, which was further purified by flash chromatography column on silica gel using hexanes/EtOAc (10:1) as eluent to provide TrocN₃ as a colorless oil (4.33 g, 99%). *R_f* = 0.5 (Eluent: hexanes/ethyl acetate 10:1); ¹H NMR (500 MHz, CDCl₃) δ: 4.82 (s, 2 H). ¹³C NMR (125 MHz, CDCl₃) δ: 156.7, 93.9, 76.7. IR (neat, cm⁻¹): 2177, 2141, 1732, 1222, 712.

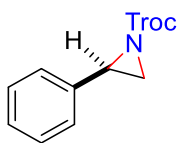
2.4.3 General Procedure for Enantioselective Aziridination of Styrenes



To an oven-dried Schlenk tube, [Co(Por)] (2 mol %) and K₂CO₃ (0.5 mmol) were added. The Schlenk tube was then evacuated and backfilled with nitrogen 3 times. The Teflon screw cap was replaced with a rubber septum and TrocN₃ (0.1 mmol), styrene (0.3 mmol) and PhCl (1 mL) were added. The Schlenk tube was then purged with nitrogen for 2 minutes and the rubber septum was replaced with a Teflon screw cap. The mixture was then stirred at room temperature for 24 h. After the reaction finished, the resulting mixture was concentrated *in vacuo* and the residue was purified by flash silica gel chromatography to afford the desired products. The silica gel was pre-treated with 1% Et₃N/hexanes. In most cases, the product was visualized on TLC using UV lamp and/or the cerium ammonium molybdate (CAM) stain.

2.4.4 Characterization of *N*-Troc Aziridine Products

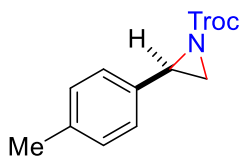
2,2,2-Trichloroethyl 2-phenylaziridine-1-carboxylate (3a), known compound.³⁴



Colorless solid. $R_f = 0.5$ (Eluent: hexanes/ethyl acetate 5:1). $[\alpha]_D^{20} = -82.590$ ($c = 1$, CHCl₃). ¹H NMR (400 MHz, CDCl₃): δ 7.30–7.38 (m, 5H), 4.82, 4.75 (AB q, $J = 12.00$ Hz, 2H), 3.63 (dd, $J = 6.40, 3.60$ Hz, 1H), 2.82 (d, $J = 6.40$ Hz, 1H), 2.44 (d, $J = 3.60$ Hz, 1H). ¹³C NMR (100 MHz, CDCl₃): δ 161.4, 136.2, 128.6,

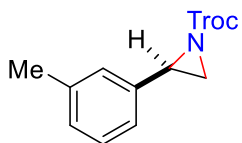
128.1, 126.3, 94.9, 75.4, 39.8, 35.2. HPLC analysis: $ee = 94\%$. IC (98% hexanes: 2% isopropanol, 1.0 ml/min) $t_{major} = 11.30$ min, $t_{minor} = 9.57$ min.

2,2,2-Trichloroethyl 2-p-tolylaziridine-1-carboxylate (3b), known compound.³⁴



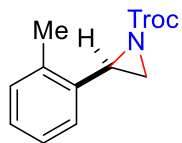
Colorless oil. $R_f = 0.3$ (Eluent: hexanes/ethyl acetate 10:1); $[\alpha]_D^{20} = -70.331$ ($c = 1$, CHCl_3). $^1\text{H NMR}$ (400 MHz, C_6D_6): δ 7.06 (d, $J = 8.00$ Hz, 2H), 6.91 (d, $J = 7.60$ Hz, 2H), 4.51, 4.43 (AB q, $J = 12.00$ Hz, 2H), 3.27 (dd, $J = 6.40, 3.60$ Hz, 1H), 2.32 (d, $J = 6.00$ Hz, 1H), 2.06 (s, 3H), 1.95 (d, $J = 3.60$ Hz, 1H). $^{13}\text{C NMR}$ (100 MHz, C_6D_6): δ 161.4, 137.8, 133.9, 129.5, 126.6, 95.7, 75.4, 39.9, 35.1, 21.1. HRMS (ESI) ($[\text{M}+\text{H}]^+$) Calcd. for $\text{C}_{12}\text{H}_{13}\text{Cl}_3\text{NO}_2^+$: 308.0004, found: 308.0006. HPLC analysis: $ee = 90\%$. IC (98% hexanes: 2% isopropanol, 1.0 ml/min) $t_{major} = 35.80$ min, $t_{minor} = 30.99$ min.

2,2,2-Trichloroethyl 2-m-tolylaziridine-1-carboxylate (3c). Colorless oil. $R_f = 0.4$



(Eluent: hexanes/ethyl acetate 10:1). $[\alpha]_D^{20} = -96.454$ ($c = 1$, CHCl_3). $^1\text{H NMR}$ (600 MHz, C_6D_6): δ 6.99 – 7.05 (m, 3H), 6.88 (d, $J = 8.00$ Hz, 1H), 4.52, 4.44 (AB q, $J = 12.00$ Hz, 2H), 3.28 (dd, $J = 6.40, 3.60$ Hz, 1H), 2.34 (d, $J = 6.80$ Hz, 1H), 2.06 (s, 3H), 1.94 (d, $J = 4.00$ Hz, 1H). $^{13}\text{C NMR}$ (100 MHz, C_6D_6): δ 161.4, 138.3, 136.8, 129.0, 128.7, 127.3, 123.8, 95.7, 75.3, 40.0, 35.3, 21.3. IR (neat, cm^{-1}): 2955.09, 1732.99, 1275.97, 1187.09, 827.27, 715.76, 698.65, 564.45. HRMS (ESI) ($[\text{M}+\text{H}]^+$) Calcd. for $\text{C}_{12}\text{H}_{13}\text{Cl}_3\text{NO}_2^+$: 308.0004, found: 308.0006. HPLC analysis: $ee = 88\%$. IC (98% hexanes: 2% isopropanol, 1.0 ml/min) $t_{major} = 10.72$ min, $t_{minor} = 9.48$ min.

2,2,2-Trichloroethyl 2-o-tolylaziridine-1-carboxylate (3d). Colorless oil. $R_f = 0.4$



(Eluent: hexanes/ethyl acetate 10:1). $[\alpha]_D^{20} = -180.371$ ($c = 1$, CHCl_3). ^1H

NMR (500 MHz, CDCl_3) δ 7.32 – 7.27 (m, 1H), 7.25 – 7.15 (m, 3H), 4.81,

4.79 (AB q, $J = 11.9$ Hz, 2H), 3.71 (dd, $J = 6.3, 3.9$ Hz, 1H), 2.84 (d, $J = 6.4$ Hz, 1H), 2.46

(s, 3H), 2.40 (d, $J = 3.8$ Hz, 1H). ^{13}C NMR (150 MHz, CDCl_3): δ 161.9, 136.9, 134.5, 130.0,

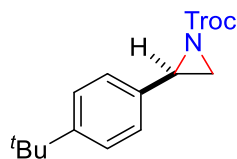
128.1, 126.3, 126.0, 95.1, 75.7, 38.6, 34.3, 19.2. IR (neat, cm^{-1}): 2956.09, 1735.17,

1264.97, 1173.9, 895.63, 714.54, 704.02, 571.33. HRMS (ESI) ($[\text{M}+\text{H}]^+$) Calcd. for

$\text{C}_{12}\text{H}_{13}\text{Cl}_3\text{NO}_2^+$: 308.0004, found: 308.0006. HPLC analysis: $ee = 94\%$. IC (98% hexanes:

2% isopropanol, 1.0 ml/min) $t_{\text{major}} = 9.40$ min, $t_{\text{minor}} = 10.74$ min.

2,2,2-Trichloroethyl 2-(4-tert-butylphenyl)aziridine-1-carboxylate (3e). Colorless



solid. $R_f = 0.5$ (Eluent: hexanes/ethyl acetate 10:1). $[\alpha]_D^{20} = -79.775$

($c = 1$, CHCl_3). ^1H NMR (400 MHz, C_6D_6): δ 7.19 – 7.22 (m, 2H), 7.14

– 7.16 (m, 2H), 4.51, 4.46 (AB q, $J = 12.00$ Hz, 2H), 3.30 (dd, $J = 6.40, 3.60$ Hz, 1H), 2.35

(d, $J = 6.40$ Hz, 1H), 2.00 (d, $J = 3.60$ Hz, 1H), 1.18 (s, 9H). ^{13}C NMR (100 MHz, C_6D_6):

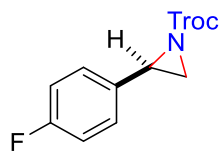
δ 161.5, 151.1, 133.9, 126.4, 125.8, 95.7, 75.4, 39.9, 35.1, 34.5, 31.4. IR (neat, cm^{-1}):

2964.34, 1732.40, 1281.04, 1164.23, 818.51, 710.00, 565.75. HRMS (ESI) ($[\text{M}]^+$) Calcd.

for $\text{C}_{15}\text{H}_{18}\text{Cl}_3\text{NO}_2^+$: 349.0403, found: 349.0401. HPLC analysis: $ee = 92\%$. ADH (99%

hexanes: 1% isopropanol, 1.0 ml/min) $t_{\text{major}} = 11.10$ min, $t_{\text{minor}} = 9.18$ min.

2,2,2-Trichloroethyl 2-(4-fluorophenyl)aziridine-1-carboxylate (3f), known



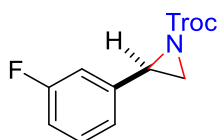
compound.³⁴ Yellow oil. $R_f = 0.4$ (Eluent: hexanes/ethyl acetate 10:1).

$[\alpha]_D^{20} = -81.182$ ($c = 1$, CHCl_3). ^1H NMR (400 MHz, CDCl_3): δ 7.30

(dd, $J = 8.0, 4.0$ Hz, 2H), 7.04 (t, $J = 8.0$ Hz, 2H), 4.81, 4.76 (AB q, $J = 12.0$ Hz, 2H), 3.61

(dd, $J = 6.4, 3.6$ Hz, 1H), 2.81 (d, $J = 6.4$ Hz, 1H), 2.39 (d, $J = 3.6$ Hz, 1H). ^{13}C NMR (100 MHz, CDCl_3): δ 162.6 (d, $J_{\text{CF}} = 246.0$ Hz), 161.3, 132.1 (d, $J_{\text{CF}} = 3.0$ Hz), 128.0, 127.9, 115.7, 115.4, 94.9, 75.4, 39.2, 35.2. ^{19}F NMR (376 MHz, CFCl_3 , CDCl_3): -114.4 (m). HRMS (ESI) ($[\text{M}+\text{H}]^+$) Calcd. for $\text{C}_{11}\text{H}_{10}\text{Cl}_3\text{FNO}_2^+$: 311.9756, found: 311.9741. HPLC analysis: ee = 94%. ODH (98% hexanes: 2% isopropanol, 1.0 ml/min) : $t_{\text{major}} = 33.19$ min, $t_{\text{minor}} = 23.61$ min.

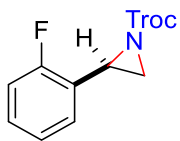
2,2,2-Trichloroethyl 2-(3-fluorophenyl)aziridine-1-carboxylate (3g). Yellow oil. $R_f =$



0.4 (Eluent: hexanes/ethyl acetate 10:1). $[\alpha]_D^{20} = -18.935$ ($c = 0.5$, CHCl_3).

^1H NMR (500 MHz, CDCl_3) δ 7.32 (m, 1H), 7.13 (d, $J = 7.6$ Hz, 1H), 7.06 – 6.97 (m, 2H), 4.82, 4.76 (AB q, $J = 12$ Hz, 2H), 3.61 (dd, $J = 6.1, 3.7$ Hz, 1H), 2.83 (d, $J = 6.3$ Hz, 1H), 2.40 (d, $J = 3.6$ Hz, 1H). ^{13}C NMR (125 MHz, CDCl_3): δ 163.2 (d, $J_{\text{CF}} = 246.4$ Hz), 161.4 (s), 139.1 (d, $J = 7.7$ Hz), 130.4 (d, $J = 8.3$ Hz), 122.2 (d, $J = 2.9$ Hz), 115.3 (d, $J_{\text{CF}} = 21.2$ Hz), 113.3 (d, $J_{\text{CF}} = 22.6$ Hz), 95.0, 75.6, 39.3, 35.6. ^{19}F NMR (470 MHz, CFCl_3 , CDCl_3): -112.7 (m). IR (neat, cm^{-1}): 2959.09, 1735.34, 1264.12, 895.64, 721.16, 704.18. HRMS (ESI) ($[\text{M}+\text{H}]^+$) Calcd. for $\text{C}_{11}\text{H}_{10}\text{Cl}_3\text{FNO}_2^+$: 311.9756, found: 311.9740. HPLC analysis: ee = 88%. Whelk (99% hexanes: 1% isopropanol, 0.8.0 ml/min) : $t_{\text{major}} = 14.21$ min, $t_{\text{minor}} = 22.88$ min.

2,2,2-Trichloroethyl 2-(2-fluorophenyl)aziridine-1-carboxylate (3h). Yellow oil. $R_f =$

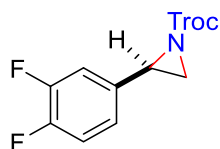


0.4 (Eluent: hexanes/ethyl acetate 10:1). $[\alpha]_D^{20} = -85.180$ ($c = 1$, CHCl_3).

^1H NMR (500 MHz, CDCl_3) δ 7.25 – 7.31 (m, 2H), 7.15 – 7.06 (m, 2H), 4.81, 4.78 (AB q, $J = 11.9$ Hz, 2H), 3.85 (dd, $J = 6.2, 3.7$ Hz, 1H), 2.86 (d, $J = 6.4$ Hz, 1H), 2.42 (d, $J = 3.6$ Hz, 1H). ^{13}C NMR (125 MHz, CDCl_3): δ 161.7 (d, $J_{\text{CF}} = 247.4$ Hz), 161.6, 129.8 (d, $J_{\text{CF}} = 8.1$ Hz), 127.4 (d, $J_{\text{CF}} = 3.5$ Hz), 124.6 (d, $J_{\text{CF}} = 3.5$ Hz), 123.9 (d, $J_{\text{CF}} =$

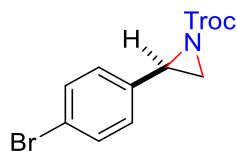
13.3 Hz), 115.5 (d, $J_{CF} = 20.8$ Hz), 95.0, 75.7, 34.8, 34.6 (d, $J_{CF} = 5.5$ Hz). ^{19}F NMR (470 MHz, CFCl_3 , CDCl_3): -120.1 (m). IR (neat, cm^{-1}): 2958.19, 1738.42, 1264.29, 1174.37, 895.74, 720.76, 703.74, 565.52. HRMS (ESI) ($[\text{M}+\text{H}]^+$) Calcd. for $\text{C}_{11}\text{H}_{10}\text{Cl}_3\text{FNO}_2^+$: 311.9756, found: 311.9748. HPLC analysis: $ee = 85\%$. ODH (98% hexanes: 2% isopropanol, 1.0 ml/min) : $t_{\text{major}} = 10.27$ min, $t_{\text{minor}} = 16.25$ min.

2,2,2-Trichloroethyl 2-(3,4-difluorophenyl)aziridine-1-carboxylate (3i). Colorless oil.



$R_f = 0.3$ (Eluent: hexanes/ethyl acetate 10:1). $[\alpha]_D^{20} = -95.549$ ($c = 1$, CHCl_3). ^1H NMR (400 MHz, CDCl_3): δ 7.06 – 7.18 (m, 3H), 4.84, 4.77 (AB q, $J = 11.60$, 2H), 3.58 (dd, $J = 6.40$, 3.60 Hz, 1H), 2.82 (d, $J = 6.40$ Hz, 1H), 2.35 (d, $J = 3.60$ Hz, 1H). ^{13}C NMR (100 MHz, CDCl_3): δ 161.1, 151.6 (dd, $J_{CF} = 30.8$, 12.7 Hz), 149.1 (dd, $J_{CF} = 30.7$, 12.8 Hz), 133.4, 122.4 (dd, $J_{CF} = 5.9$, 3.5 Hz), 117.5 (d, $J_{CF} = 17.5$ Hz), 115.2 (d, $J_{CF} = 18.2$ Hz), 94.8, 75.4, 38.6, 35.4. ^{19}F NMR (376 MHz, CFCl_3 , CDCl_3): -137.5 (m, 1F), -138.87 (m, 1F). IR (neat, cm^{-1}): 2957.74, 1737.04, 1520.65, 1278.36, 1184.05, 772.19, 715.22, 569.45. HRMS (ESI) ($[\text{M}]^+$) Calcd. for $\text{C}_{11}\text{H}_8\text{Cl}_3\text{F}_2\text{NO}_2^+$: 328.9589, found: 328.9573. HPLC analysis: $ee = 92\%$. Whelk (99% hexanes: 1% isopropanol, 1.0 ml/min) $t_{\text{major}} = 12.21$ min, $t_{\text{minor}} = 9.38$ min.

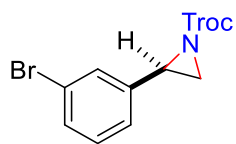
2,2,2-Trichloroethyl 2-(4-bromophenyl)aziridine-1-carboxylate (3j). known



compound.³⁴ Colorless oil. $R_f = 0.3$ (Eluent: hexanes/ethyl acetate 10:1). $[\alpha]_D^{20} = -102.48$ ($c = 1$, CHCl_3). ^1H NMR (400 MHz, CDCl_3): δ 7.47 – 7.49 (m, 2H), 7.20 – 7.22 (m, 2H), 4.81, 4.73 (AB q, $J = 11.60$ Hz, 2H), 3.57 (dd, $J = 6.40$, 3.60 Hz, 1H), 2.81 (d, $J = 6.40$ Hz, 1H), 2.37 (d, $J = 3.60$ Hz, 1H). ^{13}C NMR (100 MHz, CDCl_3): δ 161.2, 135.4, 131.7, 127.9, 122.1, 94.7, 75.4, 39.2, 35.3. HRMS (ESI) ($[\text{M}]^+$) Calcd. for $\text{C}_{11}\text{H}_9\text{BrCl}_3\text{NO}_2^+$: 370.8882, found: 370.8875. HPLC analysis: ee

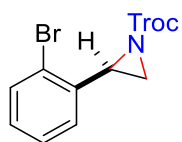
= 92%. Whelk (99% hexanes: 1% isopropanol, 1.0 ml/min) $t_{major} = 17.31$ min, $t_{minor} = 11.95$ min.

2,2,2-Trichloroethyl 2-(3-bromophenyl)aziridine-1-carboxylate (3k). Colorless oil. R_f



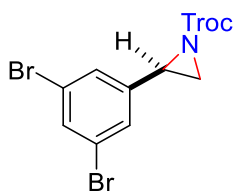
$R_f = 0.6$ (Eluent: hexanes/ethyl acetate 5:1). $[\alpha]_D^{20} = -88.617$ ($c = 1$, CHCl_3). $^1\text{H NMR}$ (400 MHz, CDCl_3): δ 7.41 – 7.47 (m, 2H), 7.19 – 7.27 (m, 2H), 4.81, 4.75 (AB q, $J = 12.00$ Hz, 2H), 3.58 (dd, $J = 6.40, 3.60$ Hz, 1H), 2.81 (d, $J = 6.40$ Hz, 1H), 2.38 (d, $J = 3.60$ Hz, 1H). $^{13}\text{C NMR}$ (100 MHz, CDCl_3): δ 161.1, 138.7, 131.2, 130.1, 129.3, 125.0, 122.7, 94.8, 75.5, 39.0, 35.4. IR (neat, cm^{-1}): 2958.31, 1732.88, 1288.50, 1172.44, 1163.23, 812.47, 782.26, 692.99, 572.12. HRMS (ESI) ($[\text{M}]^+$) Calcd. for $\text{C}_{11}\text{H}_9\text{BrCl}_3\text{NO}_2^+$: 370.8882, found: 370.8872. HPLC analysis: $ee = 88\%$. OJH (98% hexanes: 2% isopropanol, 1.0 ml/min) $t_{major} = 28.06$ min, $t_{minor} = 25.09$ min.

2,2,2-Trichloroethyl 2-(2-bromophenyl)aziridine-1-carboxylate (3l). Colorless oil. $R_f =$



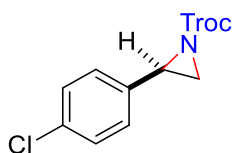
$R_f = 0.5$ (Eluent: hexanes/ethyl acetate 5:1). $[\alpha]_D^{20} = -131.172$ ($c = 1$, CHCl_3). $^1\text{H NMR}$ (400 MHz, CDCl_3): δ 7.55 (dd, $J = 8.0, 1.2$ Hz, 1H), 7.40 (dd, $J = 7.7, 1.7$ Hz, 1H), 7.32 (td, $J = 7.6, 1.2$ Hz, 1H), 7.18 (td, $J = 7.7, 1.8$ Hz, 1H), 4.81 (s, 2H), 3.86 (dd, $J = 6.5, 3.7$ Hz, 1H), 2.89 (d, $J = 6.5$ Hz, 1H), 2.29 (d, $J = 3.7$ Hz, 1H). $^{13}\text{C NMR}$ (100 MHz, CDCl_3): δ 161.4, 135.9, 132.3, 129.4, 127.7, 127.6, 122.7, 94.8, 75.5, 39.8, 34.9. IR (neat, cm^{-1}): 2969.19, 1746.07, 1466.08, 1377.95, 1300.71, 1160.19, 1127.77, 895.63, 816.04, 721.15. HRMS (ESI) ($[\text{M}+\text{H}]^+$) Calcd. for $\text{C}_{11}\text{H}_{10}\text{BrCl}_3\text{NO}_2^+$: 371.8955, found: 371.8962. HPLC analysis: $ee = 92\%$. IC (98% hexanes: 2% isopropanol, 1.0 ml/min) $t_{major} = 7.98$ min, $t_{minor} = 8.66$ min.

2,2,2-Trichloroethyl 2-(3,5-dibromophenyl)aziridine-1-carboxylate (3m). Yellow oil.



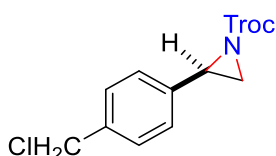
$R_f = 0.3$ (Eluent: hexanes/ethyl acetate 10:1). $[\alpha]_D^{20} = -76.961$ ($c = 1$, CHCl_3). $^1\text{H NMR}$ (400 MHz, CDCl_3): δ 7.60 – 7.61 (m, 1H), 7.41–7.42 (m, 2H), 4.85, 4.81 (AB q, $J = 12.00$, 2H), 3.55 (dd, $J = 6.40$, 3.60 Hz, 1H), 2.81 (d, $J = 6.00$ Hz, 1H), 2.35 (d, $J = 3.20$ Hz, 1H). $^{13}\text{C NMR}$ (100 MHz, CDCl_3): δ 161.1, 140.5, 133.9, 128.3, 123.3, 94.8, 75.7, 38.4, 35.7. IR (neat, cm^{-1}): 2955.10, 1736.30, 1165.48, 743.18, 716.03, 565.29. HRMS (ESI) ($[\text{M}]^+$) Calcd. for $\text{C}_{11}\text{H}_8\text{Br}_2\text{Cl}_3\text{NO}_2^+$: 448.7987, found: 448.7967. HPLC analysis: $ee = 82\%$. Whelk (99% hexanes: 1% isopropanol, 1.0 ml/min) $t_{\text{major}} = 18.42$ min, $t_{\text{minor}} = 10.32$ min.

2,2,2-Trichloroethyl 2-(4-chlorophenyl)aziridine-1-carboxylate (3n), known



compound.³⁴ Colorless oil. $R_f = 0.3$ (Eluent: hexanes/ethyl acetate 10:1). $[\alpha]_D^{20} = -65.609$ ($c = 1$, CHCl_3). $^1\text{H NMR}$ (400 MHz, CDCl_3): δ 7.30 – 7.33 (m, 2H), 7.24 – 7.26 (m, 2H), 4.80, 4.75 (AB q, $J = 12.00$ Hz, 2H), 3.58 (dd, $J = 6.40$, 3.60 Hz, 1H), 2.81 (d, $J = 6.40$ Hz, 1H), 2.37 (d, $J = 3.60$ Hz, 1H). $^{13}\text{C NMR}$ (100 MHz, CDCl_3): δ 161.2, 134.8, 134.0, 128.8, 127.6, 94.8, 75.4, 39.1, 35.3. HPLC analysis: $ee = 94\%$. Whelk (99% hexanes: 1% isopropanol, 1.0 ml/min) $t_{\text{major}} = 16.52$ min, $t_{\text{minor}} = 11.34$ min.

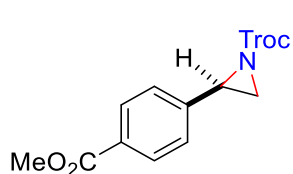
2,2,2-Trichloroethyl 2-(4-(chloromethyl)phenyl)aziridine-1-carboxylate (3o).



Colorless oil. $R_f = 0.4$ (Eluent: hexanes/ethyl acetate 10:1). $[\alpha]_D^{20} = -98.161$ ($c = 1$, CHCl_3). $^1\text{H NMR}$ (600 MHz, CDCl_3) δ 7.38 (d, $J = 7.9$ Hz, 2H), 7.33 (d, $J = 8.0$ Hz, 2H), 4.81, 4.79 (AB q, $J = 12.00$ Hz, 2H), 4.58 (s, 2H), 3.63 (dd, $J = 5.8$, 3.8 Hz, 1H), 2.82 (d, $J = 6.3$ Hz, 1H), 2.41 (d, $J = 3.5$ Hz, 1H). $^{13}\text{C NMR}$

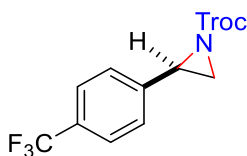
(100 MHz, CDCl₃) δ 161.4, 137.6, 136.8, 129.0, 126.8, 95.0, 75.6, 45.9, 39.6, 35.5. IR (neat, cm⁻¹): 2955.70, 2102.57, 1732.14, 1281.20, 1164.24, 799.31, 712.09, 566.32. HRMS (ESI) ([M]⁺) Calcd. for C₁₂H₁₁Cl₄NO₂⁺: 340.9544, found: 340.9539. HPLC analysis: *ee* = 90%. IA (99% hexanes: 1% isopropanol, 1.0 ml/min) *t*_{major} = 35.51 min, *t*_{minor} = 38.43 min.

2,2,2-Trichloroethyl 2-(4-(methoxycarbonyl)phenyl)aziridine-1-carboxylate (3p).



Colorless solid. *R*_f = 0.3 (Eluent: hexanes/ethyl acetate 5:1). $[\alpha]_D^{20}$ = -125.49 (*c* = 1, CHCl₃). ¹H NMR (400 MHz, CDCl₃): δ 8.03 (d, *J* = 8.3 Hz, 2H), 7.40 (d, *J* = 8.3 Hz, 2H), 4.77, 4.82 (AB q, *J* = 11.96 Hz, 2H), 3.92 (s, 3H), 3.66 (dd, *J* = 6.40, 3.60 Hz, 1H), 2.86 (d, *J* = 6.40 Hz, 1H), 2.42 (d, *J* = 3.60 Hz, 1H). ¹³C NMR (100 MHz, CDCl₃): δ 166.8, 161.3, 141.6, 130.1, 126.6, 126.1, 94.9, 75.6, 52.4, 39.6, 35.7. IR (neat, cm⁻¹): 2954.65, 1732.48, 1713.53, 1271.82, 1101.31, 715.11, 585.31, 559.91. HRMS (ESI) ([M]⁺) Calcd. for C₁₃H₁₂Cl₃NO₄⁺: 350.9832, found: 350.9822. HPLC analysis: *ee* = 92%. IC (98% hexanes: 2% isopropanol, 1.0 ml/min) *t*_{major} = 60.83 min, *t*_{minor} = 47.06 min.

2,2,2-Trichloroethyl 2-(4-(trifluoromethyl)phenyl)aziridine-1-carboxylate (3q),



known compound.²⁹ Colorless solid. *R*_f = 0.3 (Eluent: hexanes/ethyl acetate 10:1). $[\alpha]_D^{20}$ = -70.532 (*c* = 1, CHCl₃). ¹H NMR (400 MHz, CDCl₃): δ 7.61 (d, *J* = 8.00, 2H), 7.45 (d, *J* = 8.00, 2H), 4.78, 4.75 (AB q, *J* = 12.00 Hz, 2H), 3.66 (dd, *J* = 6.40, 3.60 Hz, 1H), 2.86 (d, *J* = 6.40 Hz, 1H), 2.41 (d, *J* = 3.60 Hz, 1H). ¹³C NMR (100 MHz, CDCl₃): δ 161.1, 140.4, 136.5 (q, *J*_{CF} = 32.4 Hz), 126.6, 125.6 (q, *J*_{CF} = 3.4 Hz), 123.9 (q, *J*_{CF} = 270.6 Hz), 94.8, 75.5, 39.1, 35.6. ¹⁹F NMR (376 MHz, CFCl₃, CDCl₃): -63.15 (s). IR (neat, cm⁻¹): 2922.00, 1738.38, 1323.70, 1123.12, 1111.82, 829.47, 738.45, 717.17, 562.70. HRMS (ESI) ([M]⁺)

Calcd. for $C_{12}H_9Cl_3F_3NO_2^+$: 360.9651, found: 360.9646. HPLC analysis: $ee = 86\%$. Whelk (99% hexanes: 1% isopropanol, 1.0 ml/min) $t_{major} = 11.61$ min, $t_{minor} = 8.81$ min.

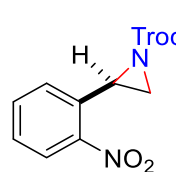
2,2,2-Trichloroethyl 2-(4-nitrophenyl)aziridine-1-carboxylate (3r), known

compound.³⁴ Yellow oil. $R_f = 0.4$ (Eluent: hexanes/ethyl acetate 5:1). $[\alpha]_D^{20} = -135.54$ ($c = 1$, $CHCl_3$). 1H NMR (400 MHz, $CDCl_3$): δ 8.20 – 8.24 (m, 2H), 7.49 – 7.52 (m, 2H), 4.82, 4.79 (AB q, $J = 12.00$ Hz, 2H), 3.71 (dd, $J = 6.40, 3.60$ Hz, 1H), 2.91 (d, $J = 6.40$ Hz, 1H), 2.41 (d, $J = 3.60$ Hz, 1H). ^{13}C NMR (100 MHz, $CDCl_3$): δ 160.9, 147.8, 143.7, 127.1, 123.9, 94.7, 75.5, 38.7, 35.9. HRMS (ESI) ($[M+H]^+$) Calcd. for $C_{11}H_{10}Cl_3N_2O_4^+$: 338.9701, found: 338.9708. HPLC analysis: $ee = 90\%$. Whelk (99% hexanes: 1% isopropanol, 1.0 ml/min) $t_{major} = 34.79$, $t_{minor} = 27.94$ min.

2,2,2-Trichloroethyl 2-(3-nitrophenyl)aziridine-1-carboxylate (3s). Yellow oil. $R_f = 0.4$

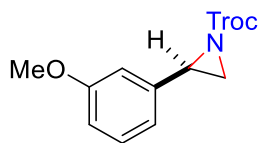
(Eluent: hexanes/ethyl acetate 5:1). $[\alpha]_D^{20} = -67.785$ ($c = 1$, $CHCl_3$). 1H NMR (500 MHz, $CDCl_3$) δ 8.21 – 8.17 (m, 2H), 7.68 (d, $J = 7.7$ Hz, 1H), 7.55 (t, $J = 7.9$ Hz, 1H), 4.83, 4.79 (AB q, $J = 11.9$ Hz, 2H), 3.72 (dd, $J = 6.3, 3.6$ Hz, 1H), 2.91 (d, $J = 6.4$ Hz, 1H), 2.44 (d, $J = 3.6$ Hz, 1H). ^{13}C NMR (150 MHz, $CDCl_3$): δ 161.1, 148.7, 138.9, 132.5, 129.8, 123.3, 121.6, 94.9, 75.7, 38.8, 35.8. IR (neat, cm^{-1}): 2967.09, 1728.92, 1456.39, 1264.19, 1070.12, 895.85, 725.22. HRMS (ESI) ($[M+H]^+$) Calcd. for $C_{11}H_{10}Cl_3N_2O_4^+$: 338.9701, found: 338.9709. HPLC analysis: $ee = 88\%$. IC (98% hexanes: 2% isopropanol, 1.0 ml/min) $t_{major} = 58.18$, $t_{minor} = 60.82$ min.

2,2,2-Trichloroethyl 2-(2-nitrophenyl)aziridine-1-carboxylate (3t). Yellow oil. $R_f = 0.5$

(Eluent: hexanes/ethyl acetate 5:1). $[\alpha]_D^{20} = -160.135$ ($c = 1$, $CHCl_3$). 

^1H NMR (500 MHz, CDCl_3) δ 8.15 (d, $J = 8.2$ Hz, 1H), 7.78 (d, $J = 7.7$ Hz, 1H), 7.68 (t, $J = 7.5$ Hz, 1H), 7.51 (m, 1H), 4.86, 4.82 (AB q, $J = 11.9$ Hz, 2H), 4.23 (dd, $J = 6.6, 3.7$ Hz, 1H), 3.00 (d, $J = 6.7$ Hz, 1H), 2.30 (d, $J = 3.6$ Hz, 1H). ^{13}C NMR (150 MHz, CDCl_3): δ 161.4, 148.3, 134.4, 132.9, 129.4, 129.1, 124.9, 94.9, 75.7, 38.7, 35.3. IR (neat, cm^{-1}): 2965.09, 1722.94, 1466.39, 1378.93, 1161.82, 1130.19, 954.26. HRMS (ESI) ($[\text{M}+\text{H}]^+$) Calcd. for $\text{C}_{11}\text{H}_{10}\text{Cl}_3\text{N}_2\text{O}_4^+$: 338.9701, found: 338.9696. HPLC analysis: $ee = 85\%$. IC (98% hexanes: 2% isopropanol, 1.0 ml/min) $t_{\text{major}} = 17.86$ min, $t_{\text{minor}} = 41.99$ min.

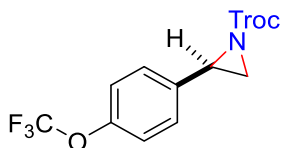
2,2,2-Trichloroethyl 2-(3-methoxyphenyl)aziridine-1-carboxylate (3u), known



compound.³⁴ Colorless oil. $R_f = 0.3$ (Eluent: hexanes/ethyl acetate 10:1). $[\alpha]_D^{20} = -88.818$ ($c = 1$, CHCl_3). ^1H NMR (400 MHz, C_6D_6):

δ 7.03 (t, $J = 8.00$ Hz, 1H), 6.85 – 6.86 (m, 1H), 6.79 – 6.81 (m, 1H), 6.66 – 6.71 (m, 1H), 4.44, 4.41 (AB q, $J = 12.00$ Hz, 2H), 3.27 (s, 3H), 3.25-3.27 (m, 1H), 2.30 (d, $J = 6.40$, 1H), 1.92 (d, $J = 3.60$ Hz, 1H). ^{13}C NMR (100 MHz, C_6D_6): δ 161.4, 160.5, 138.5, 129.8, 118.9, 114.1, 111.9, 95.7, 75.4, 54.8, 39.9, 35.3. HPLC analysis: $ee = 90\%$. Whelk (99% hexanes: 1% isopropanol, 1.0 ml/min) $t_{\text{major}} = 35.51$ min, $t_{\text{minor}} = 18.02$ min.

2,2,2-Trichloroethyl 2-(4-trifluoromethoxyphenyl)aziridine-1-carboxylate (3v).



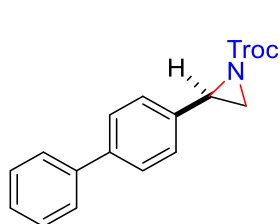
Colorless oil. $R_f = 0.4$ (Eluent: Hexane: Ethyl acetate = 15:1).

$[\alpha]_D^{20} = -111.570$ ($c = 0.5$, CHCl_3). ^1H NMR (500 MHz, CDCl_3):

δ 7.36 (d, $J = 7.8$ Hz, 2H), 7.21 (d, $J = 8.1$ Hz, 2H), 4.82, 4.76 (AB q, $J = 11.9$ Hz, 2H), 3.62 (d, $J = 3.9$ Hz, 1H), 2.83 (d, $J = 6.1$ Hz, 1H), 2.40 (d, $J = 2.6$ Hz, 1H). ^{13}C NMR (100 MHz, CDCl_3): δ 161.4, 149.2, 135.2, 127.9, 121.3, 120.6 (q, $J = 257.4$ Hz), 94.9, 75.6, 39.2, 35.5. ^{19}F NMR (376 MHz, CFCl_3 , CDCl_3): -57.9 (s). IR (neat, cm^{-1}): 2952.45, 1739.87, 1264.09, 895.96, 748.63, 703.18. HRMS (ESI) ($[\text{M}+\text{H}]^+$) Calcd. for

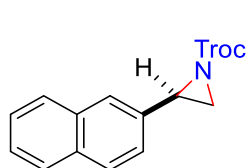
$C_{18}H_{10}Cl_3F_3NO_3^+$: 377.9673, found: 377.9679. HPLC analysis: $ee = 90\%$. ADH (99% hexanes: 1% isopropanol, 1.0 ml/min) $t_{major} = 21.34$ min, $t_{minor} = 23.97$ min.

2,2,2-Trichloroethyl 2-(4-phenyl)aziridine-1-carboxylate (3w). Colorless oil. $R_f = 0.5$



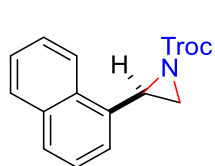
(Eluent: Hexane: Ethyl acetate = 10:1). $[\alpha]_D^{20} = -25.965$ ($c = 1$, $CHCl_3$). 1H NMR (500 MHz, $CDCl_3$) δ 7.59 – 7.57 (m, 4H), 7.45 – 7.35 (m, 5H), 4.83, 4.76 (AB q, $J = 11.9$ Hz, 2H), 3.67 (dd, $J = 6.3, 3.7$ Hz, 1H), 2.85 (d, $J = 6.3$ Hz, 1H), 2.48 (d, $J = 3.7$ Hz, 1H). ^{13}C NMR (125 MHz, $CDCl_3$): δ 161.6, 141.4, 140.8, 135.4, 128.9, 127.6, 127.5, 127.2, 126.9, 95.1, 75.6, 39.9, 35.4. IR (neat, cm^{-1}): 2921.42, 1742.69, 1391.09, 1295.22, 1167.48, 828.15, 717.28, 697.54. HRMS (ESI) ($[M+H]^+$) Calcd. for $C_{17}H_{15}Cl_3NO_2^+$: 370.0163, found: 370.0155. HPLC analysis: $ee = 90\%$. IC (98% hexanes: 2% isopropanol, 0.8 ml/min) $t_{major} = 16.39$ min, $t_{minor} = 13.52$ min.

2,2,2-Trichloroethyl 2-(naphthalen-2-yl)aziridine-1-carboxylate (3x). Colorless solid.



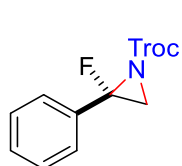
$R_f = 0.4$ (Eluent: Hexane: Ethyl acetate = 10:1). $[\alpha]_D^{20} = -84.096$ ($c = 1$, $CHCl_3$). 1H NMR (400 MHz, C_6D_6): δ 7.47 – 7.56 (m, 4H), 7.13 – 7.20 (m, 3H), 4.50, 4.42 (AB q, $J = 12.00$ Hz, 2H), 3.36 (dd, $J = 6.40, 3.60$ Hz, 1H), 2.34 (d, $J = 6.40$ Hz, 1H), 1.94 (d, $J = 3.60$ Hz, 1H). ^{13}C NMR (100 MHz, C_6D_6): δ 161.4, 134.3, 133.7, 133.6, 128.7, 126.6, 126.3, 126.2, 123.8, 95.7, 75.4, 40.2, 35.3. IR (neat, cm^{-1}): 2954.45, 2102.65, 1732.69, 1285.93, 1188.86, 815.69, 746.60, 715.34, 564.23, 475.61. HRMS (ESI) ($[M]^+$) Calcd. for $C_{15}H_{12}Cl_3NO_2^+$: 342.9934, found: 342.9921. HPLC analysis: $ee = 92\%$. ODH (99% hexanes: 1% isopropanol, 1.0 ml/min) $t_{major} = 29.98$ min, $t_{minor} = 36.05$ min.

2,2,2-Trichloroethyl 2-(naphthalen-1-yl)aziridine-1-carboxylate (3y). Yellow solid. R_f



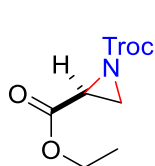
$R_f = 0.4$ (Eluent: Hexane: Ethyl acetate = 10:1). $[\alpha]_D^{20} = -13.598$ ($c = 0.5$, CHCl_3). $^1\text{H NMR}$ (500 MHz, CDCl_3) δ 8.34 (d, $J = 8.3$ Hz, 1H), 7.90 (d, $J = 8.0$ Hz, 1H), 7.84 (d, $J = 8.1$ Hz, 1H), 7.62 – 7.53 (m, 3H), 7.47 (t, $J = 7.6$ Hz, 1H), 4.87 (s, 2H), 4.21 – 4.19 (m, 1H), 3.01 (d, $J = 6.2$ Hz, 1H), 2.57 (d, $J = 3.5$ Hz, 1H). $^{13}\text{C NMR}$ (125 MHz, CDCl_3): δ 162.1, 133.5, 132.3, 131.9, 128.8, 128.8, 126.7, 126.2, 125.6, 124.6, 123.4, 95.1, 75.8, 38.8, 34.1. IR (neat, cm^{-1}): 2951.25, 2363.88, 1746.26, 1377.27, 1188.32, 575.49. HRMS (ESI) ($[\text{M}+\text{H}]^+$) Calcd. for $\text{C}_{15}\text{H}_{13}\text{Cl}_3\text{NO}_2^+$: 344.0006, found: 344.0017. HPLC analysis: $ee = 94\%$. IC (98% hexanes: 2% isopropanol, 0.8 ml/min) $t_{\text{major}} = 11.69$ min, $t_{\text{minor}} = 14.87$ min.

2,2,2-trichloroethyl 2-fluoro-2-phenylaziridine-1-carboxylate (3z). Colorless oil. $R_f =$



$R_f = 0.5$ (Eluent: Hexane: Ethyl acetate = 5:1). $[\alpha]_D^{20} = -7.742$ ($c = 0.5$, CHCl_3). $^1\text{H NMR}$ (600 MHz, CDCl_3) δ 7.49 – 7.39 (m, 5H), 4.68, 4.50 (AB q, $J = 11.88$ Hz, 2H), 3.06 (dd, $J = 3.3, 1.3$ Hz, 1H), 3.05 (dd, $J = 2.7, 1.3$ Hz, 1H). $^{13}\text{C NMR}$ (125 MHz, CDCl_3): δ 156.96 (d, $J_{\text{CF}} = 3.9$ Hz), 131.32 (d, $J_{\text{CF}} = 27.0$ Hz), 130.24 (d, $J_{\text{CF}} = 0.9$ Hz), 128.96 (s), 126.08 (d, $J_{\text{CF}} = 5.9$ Hz), 94.24 (s), 84.48 (d, $J_{\text{CF}} = 251.4$ Hz), 76.03 (s), 36.34 (d, $J_{\text{CF}} = 16.6$ Hz). $^{19}\text{F NMR}$ (376 MHz, CFCl_3 , CDCl_3): -145.1 (s). IR (neat, cm^{-1}): 2924.86, 1969.66, 1741.56, 1512.08, 1219.61, 576.16. HRMS (ESI) ($[\text{M}+\text{H}]^+$) Calcd. for $\text{C}_{11}\text{H}_{10}\text{Cl}_3\text{FNO}_2^+$: 311.9756, found: 311.9765. HPLC analysis: $ee = 48\%$. IA (99.5% hexanes: 0.5% isopropanol, 0.8 ml/min) $t_{\text{major}} = 29.30$ min, $t_{\text{minor}} = 26.69$ min.

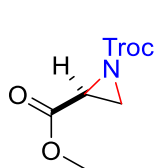
2-ethyl-1-(2,2,2-trichloroethyl) aziridine-1,2-dicarboxylate (3aa). Yellow oil. $R_f = 0.5$



(Eluent: Hexane: Ethyl acetate = 10:1). $[\alpha]_D^{20} = -12.781$ ($c = 0.5$, CHCl_3).

$^1\text{H NMR}$ (500 MHz, CDCl_3) δ 4.80, 4.68 (AB q, $J = 12.00$ Hz, 2H), 4.30 – 4.20 (m, 2H), 3.20 (dd, $J = 5.3, 3.2$ Hz, 1H), 2.68 (dd, $J = 3.2, 1.2$ Hz, 1H), 2.56 (dd, $J = 5.3, 1.2$ Hz, 1H), 1.31 (t, $J = 7.2$ Hz, 3H). $^{13}\text{C NMR}$ (150 MHz, CDCl_3): δ 168.0, 159.3, 94.6, 75.9, 62.3, 35.4, 31.7, 14.3. IR (neat, cm^{-1}): 2169.37, 2040.58, 1749.50, 1376.68, 1323.43, 1219.42, 1179.49. HRMS (ESI) ($[\text{M}+\text{H}]^+$) Calcd. for $\text{C}_8\text{H}_{11}\text{Cl}_3\text{NO}_4^+$: 288.9675, found: 289.9757. HPLC analysis: $ee = 82\%$. IA (98% hexanes: 2% isopropanol, 0.8 ml/min) $t_{\text{major}} = 17.75$ min, $t_{\text{minor}} = 14.63$ min.

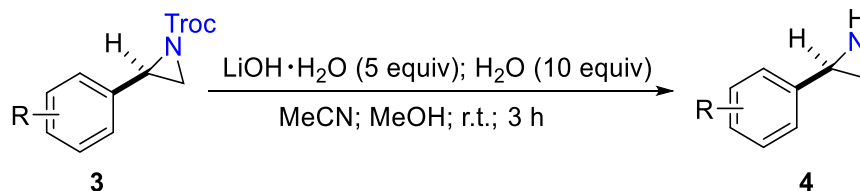
2-methyl-1-(2,2,2-trichloroethyl) aziridine-1,2-dicarboxylate (3ab). Yellow oil. $R_f =$



0.5 (Eluent: Hexane: Ethyl acetate = 10:1). $[\alpha]_D^{20} = -20.597$ ($c = 0.5$, CHCl_3).

$^1\text{H NMR}$ (500 MHz, CDCl_3) δ 4.80, 4.68 (AB q, $J = 12.00$ Hz, 2H), 3.80 (s, 3H), 3.22 (dd, $J = 5.3, 3.2$ Hz, 1H), 2.68 (dd, $J = 3.2, 1.2$ Hz, 1H), 2.58 (dd, $J = 5.3, 1.2$ Hz, 1H). $^{13}\text{C NMR}$ (150 MHz, CDCl_3): δ 168.4, 159.3, 94.6, 76.0, 53.1, 35.2, 31.7. IR (neat, cm^{-1}): 2159.61, 1748.55, 1395.97, 1325.30, 1224.67, 1173.87. HRMS (ESI) ($[\text{M}+\text{H}]^+$) Calcd. for $\text{C}_7\text{H}_9\text{Cl}_3\text{NO}_4^+$: 275.9592, found: 275.9597. HPLC analysis: $ee = 52\%$. IA (98.5% hexanes: 1.5% isopropanol, 0.8 ml/min) $t_{\text{major}} = 47.59$ min, $t_{\text{minor}} = 42.09$ min.

2.4.5 General Procedure for the Deprotection of *N*-Troc Aziridines



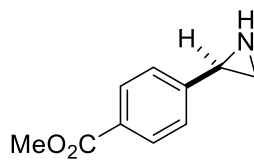
To a solution of *N*-Troc Aziridine **3** (0.250 mmol) in MeCN (2.5 mL) and MeOH (1.0 mL) was added LiOH·H₂O (53 mg, 1.3 mmol) and H₂O (45 μL, 2.5 mmol). After 3 hours of stirring at room temperature, H₂O (3 mL) and EtOAc (10 mL) were added. The two layers were separated and the aqueous layer was extracted with EtOAc (3×10 mL). The combined organic layers were washed with brine (10 mL), dried over anhydrous Na₂SO₄ and concentrated. The residue was purified by column chromatography on pretreated (5% Et₃N/hexanes) silica gel using ethyl acetate / hexanes as eluent to afford the desired products **4**.

2.4.6 Characterization Data of *N*-H aziridines

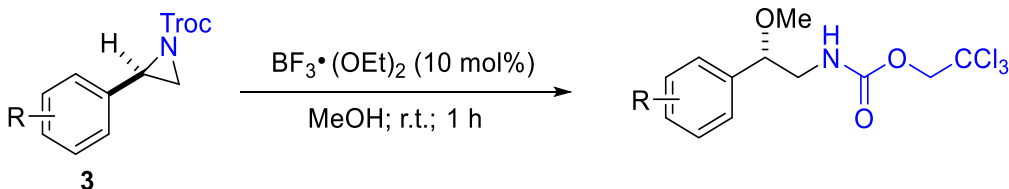
2-(4-Nitrophenyl)aziridine (4r), known compound.³⁴ Yellow solid. *R*_f = 0.3 (Eluent: Ethyl

acetate). $[\alpha]_D^{20} = -50.939$ (*c* = 1, CHCl₃). ¹H NMR (400 MHz, CDCl₃): δ 8.14 (d, *J* = 8.70 Hz, 2H), 7.39 (d, *J* = 8.70 Hz, 2H), 3.13 (br, 1H), 2.35 (d, *J* = 5.52 Hz, 1H), 1.71 (br 1H), 1.24 (s, 1H). ¹³C NMR (125 MHz, CDCl₃): δ 148.6, 147.2, 126.6, 123.8, 31.2, 30.7. HPLC analysis: *ee* = 90%. ODH (98% hexanes: 2% isopropanol, 1.0 ml/min) *t*_{major} = 58.63 min, *t*_{minor} = 52.33 min.

Methyl 4-(aziridin-2-yl)benzoate (4p). Yellow oil. $R_f = 0.5$ (Eluent: Ethyl acetate). $[\alpha]_D^{20}$

 $= -59.781$ ($c = 1$, CHCl_3). $^1\text{H NMR}$ (400 MHz, CDCl_3): δ 7.95 (d, $J = 8.20$ Hz, 2H), 7.26 (d, $J = 8.08$ Hz, 2H), 3.87 (s, 3H), 3.04 (br, 1H), 2.26 (d, $J = 5.52$ Hz, 1H), 1.74 (br, 1H), 1.22 (br, 1H). $^{13}\text{C NMR}$ (125 MHz, CDCl_3): δ 167.1, 146.2, 129.9, 129.0, 125.8, 52.2, 30.2, 29.8. IR (neat, cm^{-1}): 3305.18, 2996.07, 1738.63, 1264.64, 731.93, 561.14. HRMS (ESI) ($[\text{M}]^+$) Calcd. for $\text{C}_{10}\text{H}_{11}\text{NO}_2^+$: 177.0790, found: 177.1136. HPLC analysis: $ee = 92\%$. ODH (93% hexanes: 7% isopropanol, 1.0 ml/min) $t_{\text{major}} = 35.72$ min, $t_{\text{minor}} = 32.37$ min.

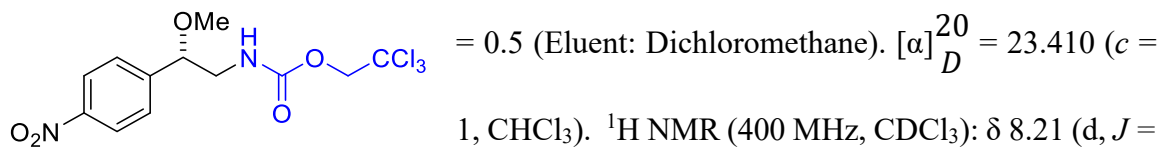
2.4.7 General Procedure for the Ring-opening Reactions of N-Troc Aziridines with Different Nucleophiles



To a solution of N-Troc Aziridines **3** in MeOH (2 mL, 0.1 M) was added $\text{BF}_3 \cdot (\text{OEt})_2$ (10 mol %) and the mixture was stirred at room temperature for 1 h. After the reaction finished, the solvent was removed in vacuo to provide a crude product, which was purified by column chromatography on silica gel to afford pure products.

2.4.8 Characterization Data of Ring-Opening Products

2,2,2-Trichloroethyl 2-methoxy-2-(4-nitrophenyl)ethylcarbamate (5r). Colorless oil. R_f



8.40 Hz, 2H), 7.50 (d, $J = 8.40$ Hz, 2H), 5.50 (br, 1H), 4.71 (s, 2H), 4.42 (dd, $J = 8.00$,

3.60 Hz, 1H), 3.53 – 3.59 (m, 1H), 3.31 (s, 3H), 3.24-3.30 (m, 1H). $^{13}\text{C NMR}$ (100 MHz,

CDCl_3): δ 154.6, 147.9, 146.3, 127.5, 123.9, 95.5, 81.6, 74.5, 57.4, 47.1. IR (neat, cm^{-1}):

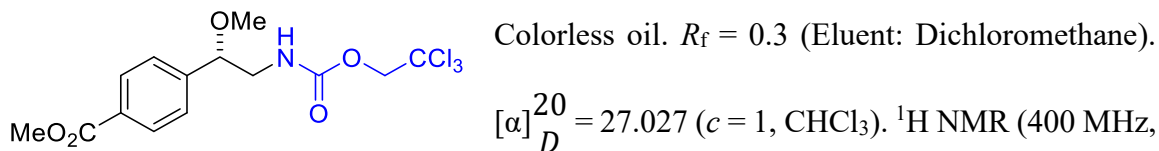
3341.08, 2939.09, 1723.63, 1520.37, 1344.61, 1109.09, 853.85, 752.49, 700.37, 560.35.

HRMS (ESI) ($[\text{M}]^+$) Calcd. for $\text{C}_{12}\text{H}_{13}\text{Cl}_3\text{N}_2\text{O}_5^+$: 369.9890, found: 369.9881. HPLC

analysis: $ee = 90\%$. ADH (93% hexanes: 7% isopropanol, 1.0 ml/min) $t_{\text{major}} = 20.01$ min,

$t_{\text{minor}} = 15.52$ min.

Methyl 4-(1-methoxy-2-((2,2,2-trichloroethoxy)carbonylamino)ethyl)benzoate (5p)



CDCl_3): δ 8.02 (d, $J = 8.00$ Hz, 2H), 7.38 (d, $J = 8.40$ Hz, 2H), 5.50 (br, 1H), 4.72 (s, 2H),

4.35 (dd, $J = 8.00, 3.60$ Hz, 2H), 3.90 (s, 3H), 3.52-3.58 (m, 1H), 3.27 (s, 4H). $^{13}\text{C NMR}$

(100 MHz, CDCl_3): δ 166.7, 154.5, 143.9, 130.1, 129.9, 126.6, 95.5, 82.0, 74.5, 57.1, 52.1,

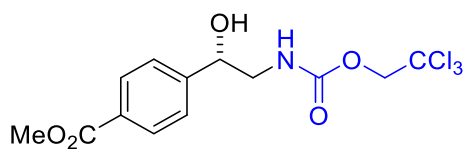
47.2. IR (neat, cm^{-1}): 3347.19, 2952.27, 1720.56, 1276.06, 1103.93, 766.29, 707.69,

564.39. HRMS (ESI) ($[\text{M}]^+$) Calcd. for $\text{C}_{14}\text{H}_{16}\text{Cl}_3\text{NO}_5^+$: 383.0094, found: 383.0077. HPLC

analysis: $ee = 92\%$. ADH (93% hexanes: 7% isopropanol, 1.0 ml/min) $t_{\text{major}} = 15.88$ min,

$t_{\text{minor}} = 13.43$ min.

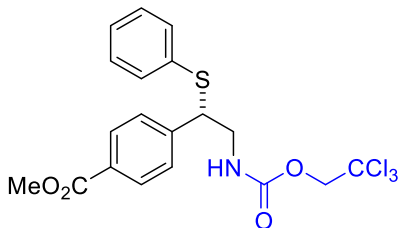
Methyl 4-(1-hydroxy-2-((2,2,2-trichloroethoxy)carbonylamino)ethyl)benzoate (6p)



Modification from general procedure: stirred for 24 hours. Colorless solid. $R_f = 0.6$ (Eluent: Ethyl

acetate: Hexane = 2:1). $[\alpha]_D^{20} = 15.573$ ($c = 1$, CHCl_3). $^1\text{H NMR}$ (400 MHz, CDCl_3): δ 7.95 (d, $J = 8.00$ Hz, 2H), 7.40 (d, $J = 8.40$ Hz, 2H), 5.65 (br, 1H), 4.90 (dd, $J = 7.20, 2.80$ Hz, 1H), 4.69 (s, 2H), 3.88 (s, 3H), 3.55-3.61 (m, 1H), 3.29-3.36 (m, 2H). $^{13}\text{C NMR}$ (100 MHz, CDCl_3): δ 166.9, 155.2, 146.3, 129.8, 129.7, 125.8, 95.4, 74.6, 72.9, 52.2, 48.3. IR (neat, cm^{-1}): 3444.78, 3362.25, 2948.53, 1699.91, 1257.18, 1110.58, 815.94, 707.18, 558.74. HRMS (ESI) ($[\text{M}]^+$) Calcd. for $\text{C}_{13}\text{H}_{14}\text{Cl}_3\text{NO}_5^+$: 368.9938, found: 368.9955. HPLC analysis: $ee = 92\%$. ODH (93% hexanes: 7% isopropanol, 1.0 ml/min) $t_{\text{major}} = 28.34$ min, $t_{\text{minor}} = 23.86$ min.

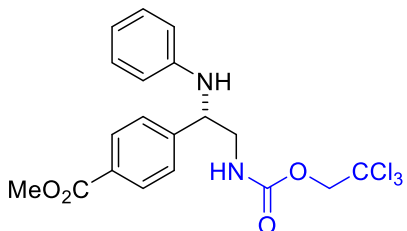
Methyl 4-(1-(phenylthio)-2-((2,2,2-trichloroethoxy)carbonylamino)ethyl) benzoate (7p)



(7p). Colorless oil; $R_f = 0.3$ (Eluent: Hexanes: Ethyl

acetate = 5:1); $[\alpha]_D^{20} = 60.183$ ($c = 1$, CHCl_3). $^1\text{H NMR}$ (400 MHz, CDCl_3): δ 7.95 (d, $J = 8.40$ Hz, 2H), 7.27 – 7.32 (m, 4H), 7.21 – 7.23 (m, 3H), 5.26 (t, $J = 5.20$ Hz, 1H), 4.68 (s, 2H), 4.38 (t, $J = 7.60$ Hz, 1H), 3.89 (s, 3H), 3.61-3.75 (m, 2H). $^{13}\text{C NMR}$ (100 MHz, CDCl_3): δ 166.6, 154.4, 144.2, 133.13, 132.8, 130.0, 129.6, 129.1, 128.0, 95.4, 74.5, 52.7, 52.2, 45.5. IR (neat, cm^{-1}): 3343.84, 2951.67, 1716.93, 1277.02, 1110.83, 750.13, 563.56. HRMS (ESI) ($[\text{M}]^+$) Calcd. for $\text{C}_{19}\text{H}_{18}\text{Cl}_3\text{NO}_4\text{S}^+$: 461.0022, found: 461.0033. HPLC analysis: $ee = 82\%$. Whelk (93% hexanes: 7% isopropanol, 1.0 ml/min) $t_{\text{major}} = 25.56$ min, $t_{\text{minor}} = 22.29$ min.

Methyl 4-(1-(phenylamino)-2-((2,2,2-trichloroethoxy)carbonylamino)ethyl) benzoate



(8p). Yellow oil. $R_f = 0.2$ (Eluent: Hexanes: Ethyl acetate

= 5:1). $[\alpha]_D^{20} = 21.099$ ($c = 1$, CHCl_3). $^1\text{H NMR}$ (500

MHz, CDCl_3): δ 8.02 (d, $J = 8.40$ Hz, 2H), 7.46 (d, $J =$

8.20 Hz, 2H), 7.08 (t, $J = 7.90$ Hz, 2H), 6.68 (t, $J = 7.30$ Hz, 1H), 6.48 (d, $J = 7.80$ Hz,

2H), 5.34 (t, $J = 6.20$ Hz, 1H), 4.77 (AB q, $J = 12.00$ Hz, 2H), 4.58 (dd, $J = 7.70, 4.40$ Hz,

1H), 3.90 (s, 3H), 3.53-3.66 (m, 2H). $^{13}\text{C NMR}$ (100 MHz, CDCl_3): δ 166.7, 155.7, 146.6,

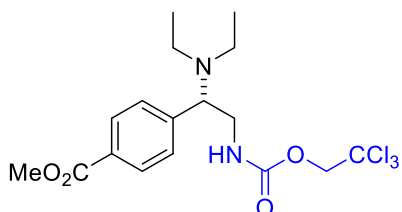
145.9, 130.2, 129.7, 129.2, 126.6, 118.0, 113.3, 95.3, 74.7, 59.2, 52.1, 47.4. IR (neat, cm^{-1})

1): 3383.55, 2951.38, 1705.56, 1277.16, 748.93, 565.25. HRMS (ESI) ($[\text{M}]^+$) Calcd. for

$\text{C}_{19}\text{H}_{19}\text{Cl}_3\text{N}_2\text{O}_4^+$: 444.0410, found: 444.0420. HPLC analysis: $ee = 92\%$. Whelk (93%

hexanes: 7% isopropanol, 1.0 ml/min) $t_{\text{major}} = 33.00$ min, $t_{\text{minor}} = 27.79$ min.

Methyl 4-(1-(N,N-diethylamino)-2-((2,2,2-trichloroethoxy)carbonylamino)ethyl) benzoate (9p)



benzoate (9p). Modification from general procedure:

Methylene Chloride was used as solvent (0.1 M),

diethylamine (20 equiv), 16 hours. Colorless oil; $R_f = 0.3$

(Eluent: Hexanes: Ethyl acetate = 5:1); $[\alpha]_D^{20} = -7.199$ ($c = 1$, CHCl_3). $^1\text{H NMR}$ (500 MHz,

CDCl_3): δ 8.01 (d, $J = 8.2$ Hz, 2H), 7.33 (d, $J = 7.8$ Hz, 2H), 5.40 (s, 1H), 4.73 (s, 2H),

3.92 (s, 4H), 3.69 (s, br, 1H), 3.58 – 3.47 (m, 1H), 2.67 (dd, $J = 13.1, 6.8$ Hz, 2H), 2.35 (d,

$J = 5.0$ Hz, 2H), 1.05 (t, $J = 7.0$ Hz, 6H). $^{13}\text{C NMR}$ (125 MHz, CDCl_3): δ 166.9, 154.7,

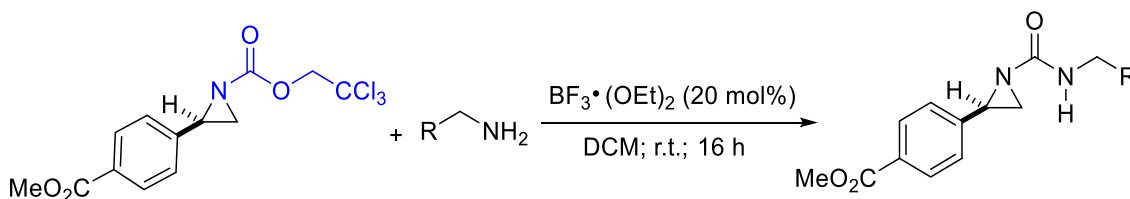
129.8, 128.6, 95.8, 74.6, 62.9, 52.3, 43.3, 42.5, 29.9, 25.5, 12.9. IR (neat, cm^{-1}): 3354.14,

2969.09, 1721.14, 1527.20, 1280.27, 1111.03, 818.02. HRMS (ESI) ($[\text{M}-\text{H}]^+$) Calcd. for

$\text{C}_{17}\text{H}_{24}\text{Cl}_3\text{N}_2\text{O}_4^+$: 425.07962, found: 425.08014. HPLC analysis: $ee = 91\%$. IA (95%

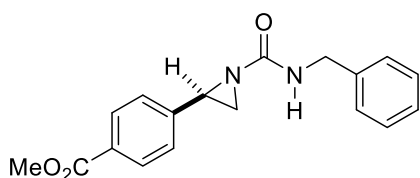
hexanes: 5% isopropanol, 1.0 ml/min) $t_{\text{major}} = 18.77$ min, $t_{\text{minor}} = 16.81$ min.

2.4.9 General Procedure and Characterization Data for the Reaction of N-Troc Aziridines with Primary Amines



N-Troc Aziridine (0.200 mmol) was dissolved in methylene chloride (0.1 M) and the primary amine (20 equiv) was added. Upon stirring, BF₃·(OEt)₂ (20 mol %) was added and the mixture was stirred at room temperature for 16 h. After the reaction finished, the solvent was removed *in vacuo* to provide a crude product, which was purified by column chromatography on pretreated (1% Et₃N/hexanes) silica gel using ethyl acetate/hexanes as eluent to afford the desired products.

Methyl 4-(1-(benzylcarbamoyl)aziridin-2-yl)benzoate (10p). White solid; $R_f = 0.2$



(Eluent: Hexanes: Ethyl acetate = 4:1); $[\alpha]_D^{20} = -129.77$

($c = 0.5$, CHCl₃). ¹H NMR (500 MHz, CDCl₃): δ 7.98

(d, $J = 8.3$ Hz, 2H), 7.35 – 7.30 (m, 4H), 7.30 – 7.24 (m,

4H), 5.78 (s, 1H), 4.41 (dd, $J = 14.2, 5.9$ Hz, 2H), 3.90 (s, 3H), 3.43 (dd, $J = 6.7, 3.8$ Hz,

1H), 2.82 (d, $J = 6.7$ Hz, 1H), 2.15 (d, $J = 3.7$ Hz, 1H). ¹³C NMR (125 MHz, CDCl₃): δ

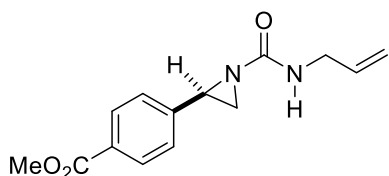
166.9, 164.4, 143.2, 138.2, 129.9, 129.7, 128.9, 127.8, 127.7, 126.3, 52.2, 45.1, 39.8, 35.8.

IR (neat, cm⁻¹): 3309.30, 2950.63, 1717.26, 1666.91, 1526.89, 1270.02, 1109.15, 701.06.

HRMS (ESI) ([M-H]⁺) Calcd. for C₁₈H₁₉N₂O₃⁺: 311.13902, found: 311.13868. HPLC

analysis: $ee = 90\%$. IC (80% hexanes: 20% isopropanol, 0.8 ml/min) $t_{\text{major}} = 41.09$ min ,
 $t_{\text{minor}} = 38.64$ min.

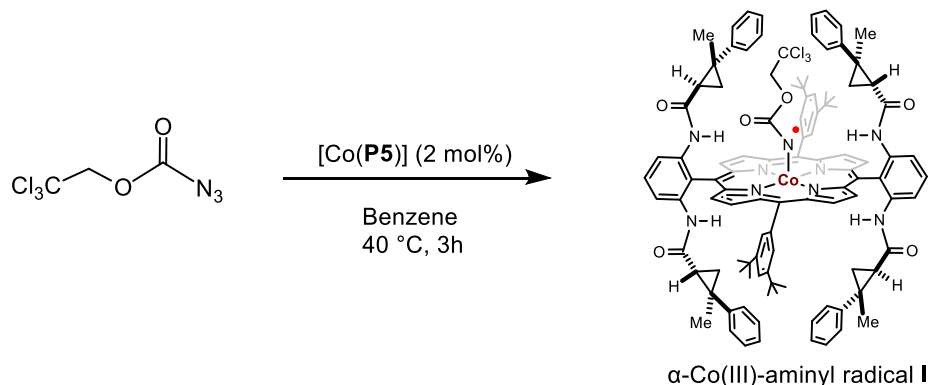
Methyl 4-(1-(allylcarbamoyl)aziridin-2-yl)benzoate (11p). White solid; $R_f = 0.2$ (Eluent:



Hexanes: Ethyl acetate = 3:1); $[\alpha]_D^{20} = -57.783$ ($c = 0.5$,
 CHCl_3). $^1\text{H NMR}$ (500 MHz, CDCl_3): δ 7.99 (d, $J = 8.2$
Hz, 2H), 7.34 (d, $J = 8.2$ Hz, 2H), 5.83 (ddd, $J = 22.6, 10.7,$
5.6 Hz, 1H), 5.53 (s, 1H), 5.19 (dd, $J = 17.1, 0.9$ Hz, 1H), 5.13 (d, $J = 10.2$ Hz, 1H) 3.91
(s, 3H), 3.85 (dd, $J = 10.9, 5.6$ Hz, 2H), 3.41 (dd, $J = 6.7, 3.8$ Hz, 1H), 2.80 (d, $J = 6.8$ Hz,
1H), 2.14 (d, $J = 3.7$ Hz, 1H). $^{13}\text{C NMR}$ (125 MHz, CDCl_3): δ 166.9, 164.3, 143.3, 134.2,
129.9, 129.7, 126.3, 116.7, 52.3, 43.4, 39.8, 35.8. IR (neat, cm^{-1}): 3308.66, 2951.89,
1717.12, 1665.69, 1528.63, 1435.11, 1271.01, 1108.05, 769.83, 704.99. HRMS (ESI) ($[\text{M}-$
 $\text{H}]^+$) Calcd. for $\text{C}_{14}\text{H}_{17}\text{N}_2\text{O}_3^+$: 261.12337, found: 261.12291. HPLC analysis: $ee = 90\%$. IC
(80% hexanes: 20% isopropanol, 0.8 ml/min) $t_{\text{major}} = 35.75$ min, $t_{\text{minor}} = 32.55$ min.

2.4.10 Mechanistic Study of the Proposed Stepwise Radical Mechanism

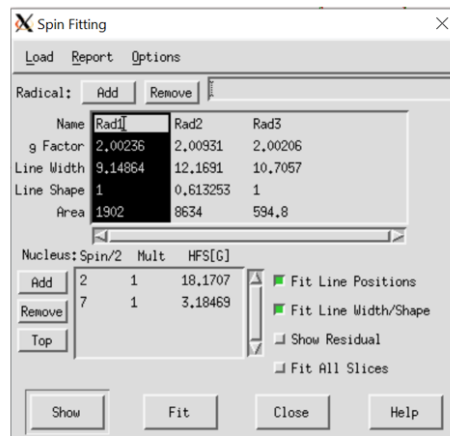
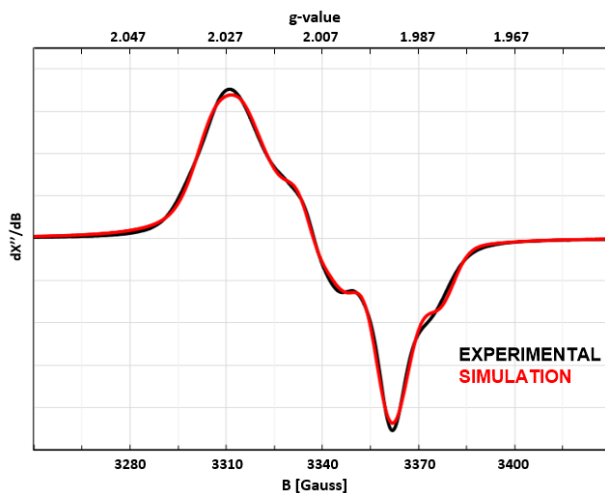
Characterization of α -Co(III)-Aminyl Radical I by EPR



Procedure for EPR Experiment: To an over-dried Schlenk tube, $[\text{Co}(\mathbf{P5})]$ (2 mol %) was added. The Schlenk tube was then evacuated and backfilled with nitrogen for 3 times. The Teflon screw cap was replaced with a rubber septum, and TroCN_3 (0.1 mmol) and Benzene (0.5 mL) were added via a gas-tight syringe. The mixture was then stirred at $40\text{ }^\circ\text{C}$ for 3h and transferred into a degassed EPR tube (filled with argon) through a gas tight syringe. The sample was then carried out for EPR experiment at room temperature (EPR settings: $T = 298\text{ K}$; microwave frequency: 9.37762 GHz ; power: 20 mW ; modulation amplitude: 1.0 G).

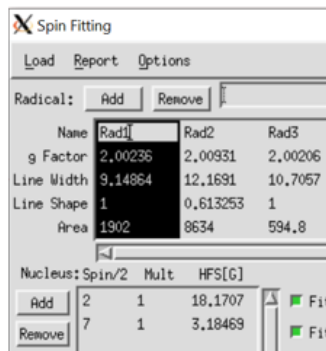
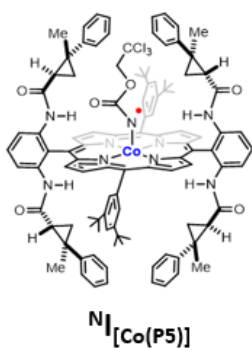
X-band EPR spectra were recorded on a Bruker EMX-Plus spectrometer (Bruker BioSpin). Simulations of the EPR spectra were performed by iteration of the isotropic g -values and line widths using the EPR simulation program SpinFit in Xenon.

EPR simulation details:



Species simulated:

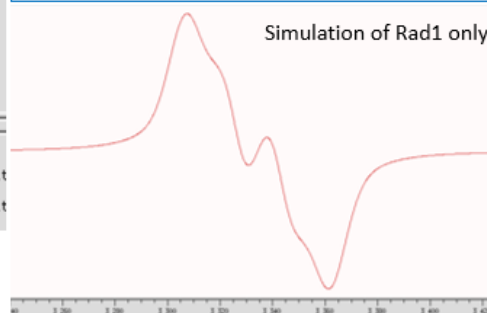
Rad1: $(1902 / (1902 + 8634 + 594.8)) \times 100 = 17\%$



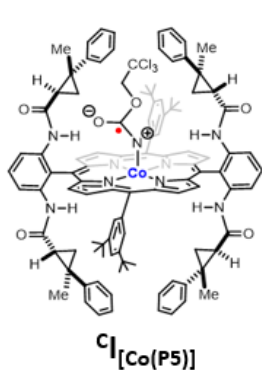
$$g_{\text{iso}} = 2.00236$$

$$A_{\text{iso}}(\text{N}) = 18.1707 \times 2.00236 \times 1.399611451 = 50.92 \text{ MHz}$$

$$A_{\text{iso}}(\text{Co}) = 3.1847 \times 2.00236 \times 1.399611451 = 8.92 \text{ MHz}$$



Rad2: $(8634 / (1902 + 8634 + 594.8)) \times 100 = 78\%$



Spin Fitting

Load Report Options

Radical: Add Remove

Name	Rad1	Rad2	Rad3
g Factor	2.00236	2.00931	2.00206
Line Width	9.14864	12.1691	10.7057
Line Shape	1	0.613253	1
Area	1902	8634	594.8

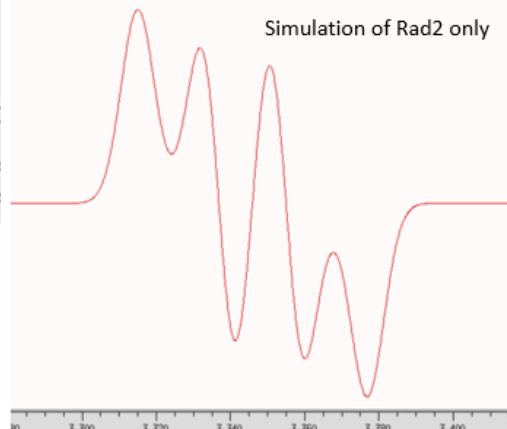
Nucleus: Spin/2 Mult HFS[G]

Add	2	1	16.6708	<input checked="" type="checkbox"/> Fit
Remove	7	1	2.67594	<input checked="" type="checkbox"/> Fit

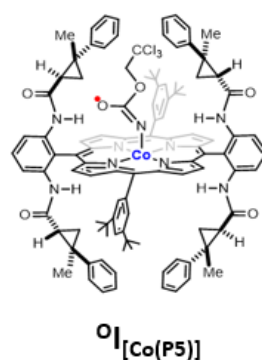
$$g_{\text{iso}} = 2.00931$$

$$A_{\text{iso}}(\text{N}) = 16.6708 \times 2.00931 \times 1.399611451 = 46.88 \text{ MHz}$$

$$A_{\text{iso}}(\text{Co}) = 2.67594 \times 2.00931 \times 1.399611451 = 7.52 \text{ MHz}$$



Rad3: $(594.8 / (1902 + 8634 + 594.8)) \times 100 = 5\%$



Spin Fitting

Load Report Options

Radical: Add Remove

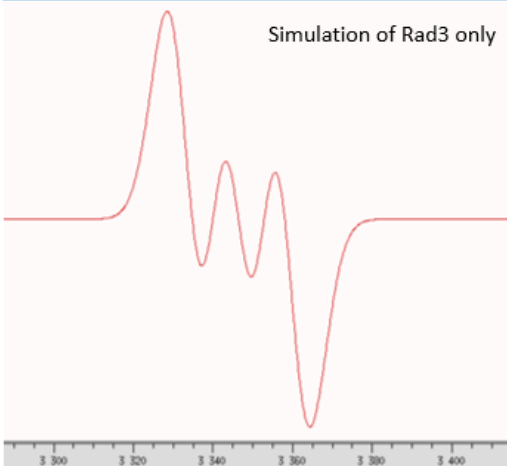
Name	Rad1	Rad2	Rad3
g Factor	2.00236	2.00931	2.00206
Line Width	9.14864	12.1691	10.7057
Line Shape	1	0.613253	1
Area	1902	8634	594.8

Nucleus: Spin/2 Mult HFS[G]

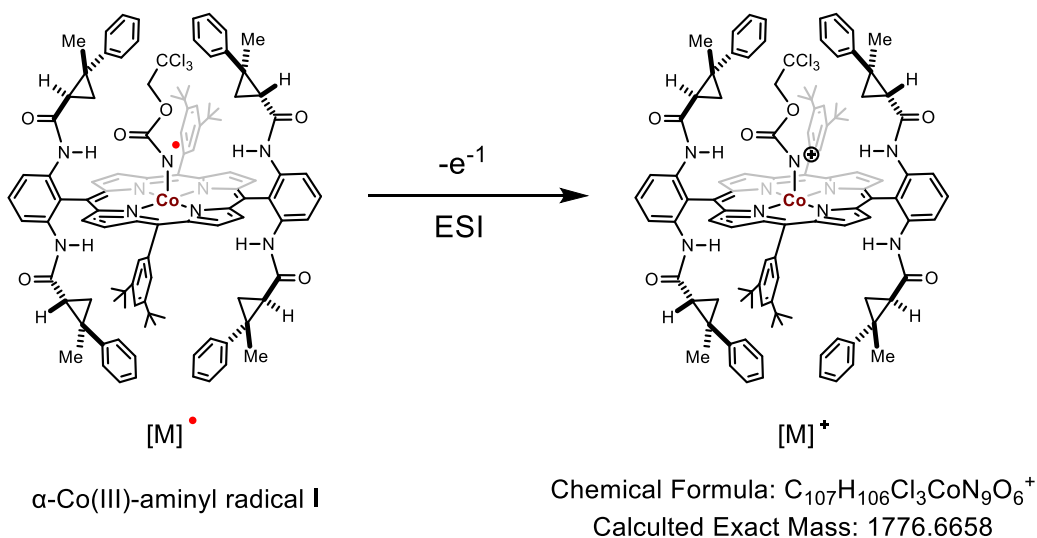
Add	2	1	12.7436	<input checked="" type="checkbox"/> Fit
Remove				<input checked="" type="checkbox"/> Fit

$$g_{\text{iso}} = 2.00206$$

$$A_{\text{iso}}(\text{N}) = 12.7436 \times 2.00206 \times 1.399611451 = 35.71 \text{ MHz}$$



Characterization of α -Co(III)-Aminyl Radical I by HRMS



Procedure for HRMS Experiment: To an over-dried Schlenk tube, [Co(P5)] (2 mol %) was added. The Schlenk tube was then evacuated and backfilled with nitrogen for 3 times. The Teflon screw cap was replaced with a rubber septum, and TrocN₃ (0.1mmol) and CH₃CN (0.5 mL) were added via a gas-tight syringe. The mixture was then stirred at room temperature for 30 min. The resulting solution was collected in a HPLC vial (degassed and backfilled with argon). The sample was further diluted with CH₃CN and immediately injected into HRMS instrument. The HRMS experiment was carried out in the absence of any additives such as formic acid, commonly act as electron carriers for ionization, allowing the detection of the molecular ion signals corresponding to Co(III)-aminyl radical ($C_{107}H_{106}Cl_3CoN_9O_6^+$) ($[M]^+$ $m/z = 1776.6666$ (observed)) by the loss of one electron, Figure 2.2.

Figure 2.6| High Resolution Mass Spectroscopy (HRMS) Spectrum for Co(III)-Supported Aminyl Radical Intermediate I

sCLIPS Report - F:\Agilent6220_0752.d\AcqData\MSProfile.bin

Self-Calibration Mass Range (Da)
 Start: -0.50
 End: 0.50

RT Windows

Average of Scans 22 thru 43 (0.3600 to 0.7080)

sCLIPS Parameters

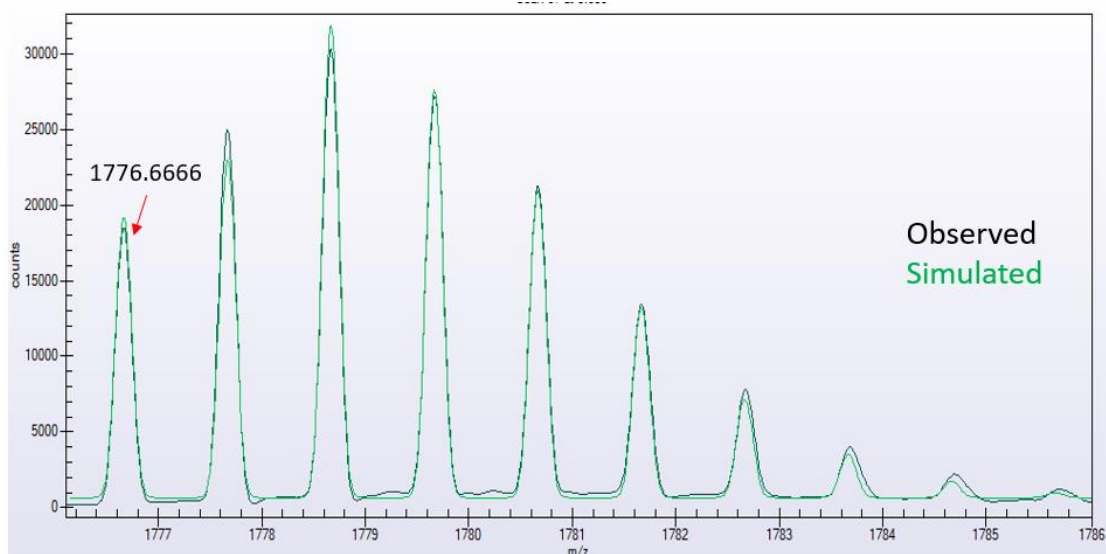
Accurate Mass: 1776.6666
 Charge: 1
 Mass Tolerance (PPM): 300.00
 Electron State: Both
 Double Bond Equivalent Range
 Minimum: -30.00
 Maximum: 300.00
 Profile Mass Range (Da)
 Start: -2.00
 End: 10.00
 Empirical Rules: Enabled
 Empirical Elemental Limits: DNP
 H/C Ratio: Common
 Heteroatom Ratios: Common

Chemical Formula: $C_{107}H_{106}Cl_3CoN_9O_6+$
 Calculated Mass: 1776.6658
 Found Mass: 1776.6666

Element	Minimum	Maximum
C	100	110
H	100	110
N	5	9
O	4	6
Co	1	1
Cl	1	3

sCLIPS Search Results

	Formula	Mono Isotope	Mass Error (mDa)	Mass Error (PPM)	Spectral Accuracy	RMSE	DBE
1	C110H102N9O4CoCl3	1,776.6447	21.9124	12.3335	90.4347	1,074	63.0
2	C110H100N8O5CoCl3	1,776.6209	45.7219	25.7346	90.4030	1,078	63.5
3	C109H110N7O6CoCl3	1,776.6910	-24.3691	-13.7162	90.2314	1,097	67.0
4	C108H110N9O5CoCl3	1,776.7022	-35.6024	-20.0389	90.1470	1,106	67.0
5	C108H108N8O6CoCl3	1,776.6784	-11.7930	-6.6377	90.1120	1,110	67.5
6	C107H108N9O6CoCl3	1,776.6659	0.7981	0.4496	89.9863	1,125	67.0
7	C107H106N9O6CoCl3	1,776.6661	-0.6302	-0.3547	79.9861	9,326	67.0



2.4.11 X-ray Crystallographic Information

The X-ray diffraction data for **3p**, **3w**, and **6p** were measured on a Bruker D8 Venture PHOTON 100 CMOS system equipped with a Cu K α INCOATEC Imus micro-focus source ($\lambda = 1.54178 \text{ \AA}$). Indexing was performed using *APEX2*³⁸ (Difference Vectors method). Data integration and reduction were performed using SaintPlus 6.01³⁹. Absorption correction was performed by multi-scan method implemented in SADABS⁴⁰. Space groups were determined using XPREP implemented in APEX2³⁸. The structure was solved using SHELXS-97 (direct methods) and refined using SHELXL-2013³⁸ (full-matrix least-squares on F^2) contained in APEX2^{38,41} WinGX v1.70.01⁴¹⁻⁴² and OLEX2.⁴³ All non-hydrogen atoms were refined anisotropically. Hydrogen atoms of -CH, -CH₂ and -CH₃ groups were placed in geometrically calculated positions and included in the refinement process using riding model with isotropic thermal parameters: $U_{iso}(H) = 1.2(1.5)U_{eq}(-CH, -CH_2(-CH_3))$ There are two molecules in the asymmetric unit of structure **3p**. Crystal data and refinement conditions are shown in Tables 2.4-2.6.

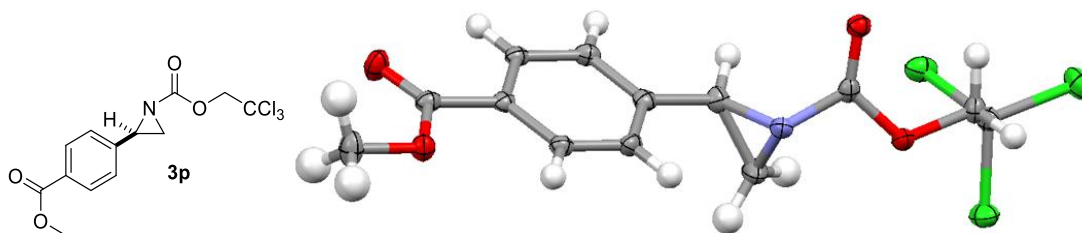


Table 2.3| Crystal Data and Structure Refinement for 3p

Identification code	3p
Empirical formula	C ₁₃ H ₁₂ Cl ₃ NO ₄
Formula weight	352.59
Temperature/K	100.01
Crystal system	orthorhombic
Space group	P2 ₁ 2 ₁ 2 ₁
a/Å	6.8851(1)
b/Å	13.3886(3)
c/Å	32.1552(7)
α/°	90
β/°	90
γ/°	90
Volume/Å ³	2964.13(10)
Z	8
ρ _{calc} /g/cm ³	1.580
μ/mm ⁻¹	5.745
F(000)	1440.0
Crystal size/mm ³	0.05 × 0.02 × 0.01
Radiation	CuKα (λ = 1.54178)
2θ range for data collection/°	7.152 to 138.636
Index ranges	-8 ≤ h ≤ 8, -16 ≤ k ≤ 15, -39 ≤ l ≤ 37
Reflections collected	26929
Independent reflections	5506 [R _{int} = 0.0510, R _{sigma} = 0.0386]
Data/restraints/parameters	5506/0/381
Goodness-of-fit on F ²	1.013
Final R indexes [I ≥ 2σ (I)]	R ₁ = 0.0270, wR ₂ = 0.0577
Final R indexes [all data]	R ₁ = 0.0324, wR ₂ = 0.0594
Largest diff. peak/hole / e Å ⁻³	0.22/-0.21
Flack parameter	0.024(7)

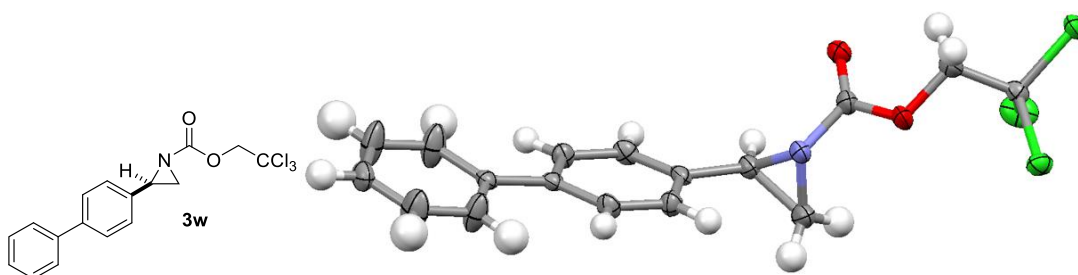


Table 2.4| Crystal Data and Structure Refinement for 3w

Identification code	3w
Empirical formula	C ₁₇ H ₁₄ Cl ₃ NO ₂
Moiety Formula	C ₁₇ H ₁₄ Cl ₃ NO ₂
Formula weight	370.6540
Temperature/K	123
Crystal system	Monoclinic
Space group	P2 ₁
a/Å	10.4899(3)
b/Å	5.60680(10)
c/Å	14.1047(3)
α/°	90
β/°	92.116
γ/°	90
Volume/Å ³	829.00(3)
Z	2
ρ _{calc} Mg/cm ³	1.485
μ/mm ⁻¹	5.076
F(000)	380.0
Crystal size/mm ³	0.320 × 0.080 × 0.050
Radiation	CuKα (λ = 1.54178)
2θ range for data collection/°	3.135 to 66.674
Index ranges	-12 ≤ h ≤ 12, -6 ≤ k ≤ 6, -16 ≤ l ≤ 16
Reflections collected	8557
Independent reflections	2910 [R _{int} = 0.0283]
Data/restraints/parameters	2910 / 1 / 208
Goodness-of-fit on F ²	1.069
Final R indexes [I ≥ 2σ (I)]	R ₁ = 0.0361, wR ₂ = 0.0956
Final R indexes [all data]	R ₁ = 0.0375, wR ₂ = 0.0968
Largest diff. peak/hole / e Å ⁻³	0.625/-0.265
Flack parameter	0.001(10)

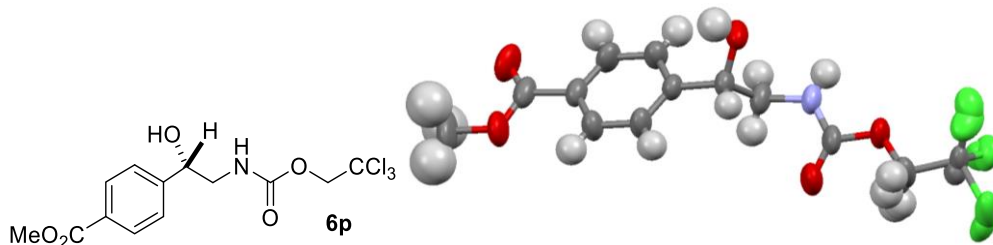


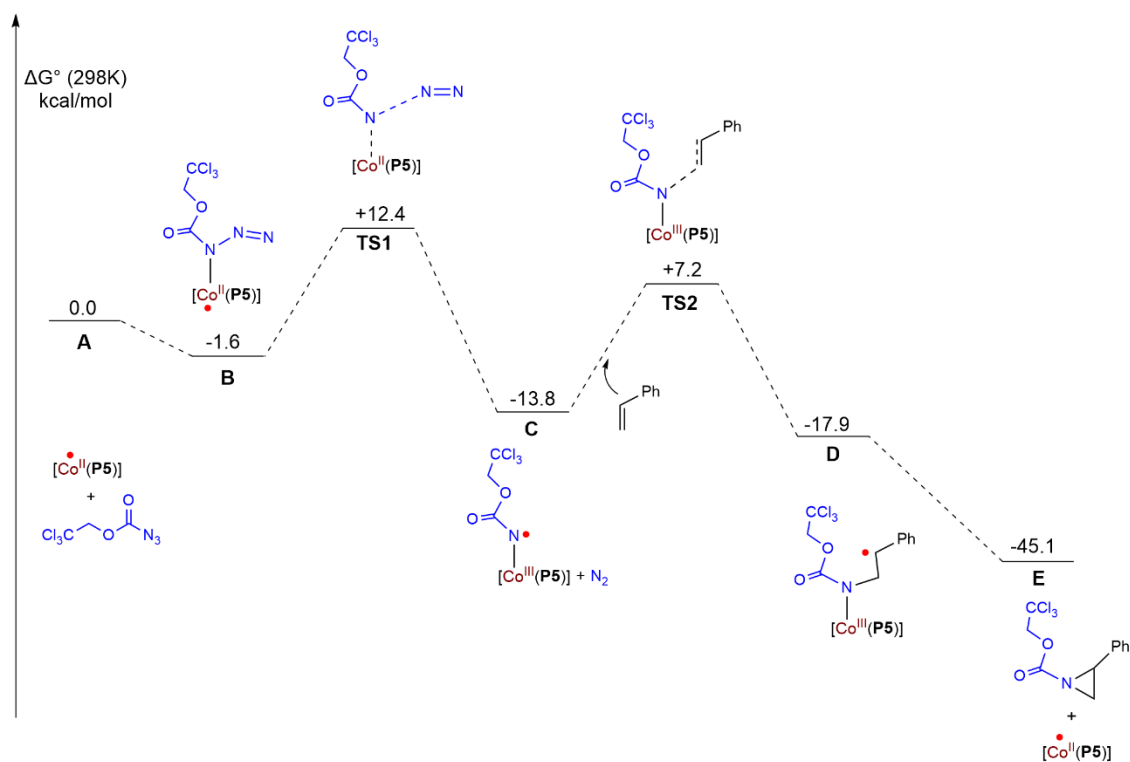
Table 2.5| Crystal Data and Structure Refinement for 6p

Identification code	6p_disorder
Empirical formula	C ₁₃ H ₁₄ Cl ₃ NO ₅
Formula weight	370.60
Temperature/K	296.15
Crystal system	orthorhombic
Space group	P2 ₁ 2 ₁ 2 ₁
a/Å	9.2565(2)
b/Å	9.7710(2)
c/Å	18.3117(4)
α/°	90
β/°	90
γ/°	90
Volume/Å ³	1656.21(6)
Z	4
ρ _{calc} /cm ³	1.486
μ/mm ⁻¹	5.215
F(000)	760.0
Crystal size/mm ³	0.27 × 0.05 × 0.03
Radiation	CuKα (λ = 1.54178)
2θ range for data collection/°	9.66 to 142.508
Index ranges	-11 ≤ h ≤ 11, -11 ≤ k ≤ 11, -21 ≤ l ≤ 22
Reflections collected	19787
Independent reflections	3119 [R _{int} = 0.0513, R _{sigma} = 0.0324]
Data/restraints/parameters	3119/72/254
Goodness-of-fit on F ²	1.062
Final R indexes [I >= 2σ (I)]	R ₁ = 0.0310, wR ₂ = 0.0833
Final R indexes [all data]	R ₁ = 0.0339, wR ₂ = 0.0854
Largest diff. peak/hole / e Å ⁻³	0.18/-0.18
Flack parameter	0.019(7)

2.4.12 DFT Calculations

Considering the cost of time and computing resources for the large system with [Co(II)P5], the geometry optimizations were performed with the Gaussian 09⁴⁴ at the unrestricted BP86^{31a,45} /lanl2dz^{121,46} level of theory in the gas phase at room temperature. Gas-phase Hessian matrix calculations were applied to the characterization of all minima (without imaginary frequency) and transition states (with only one imaginary frequency). Thermochemical parameters such as internal energy, enthalpy, entropy, Gibbs free energy and thermal corrections (entropy and enthalpy, 298.15 K, 1 Atm) were obtained from these calculations. To further improve the accuracy of energies, single point energies were carried out at the B3LYP⁴⁷/def2-tzvp^{121,46} level of theory along with Grimme's dispersion correction⁴⁸ (D3BJ) and SMD⁴⁹ solvation model (in PhCl).

Scheme 2.11| Calculated Energy Diagram for [Co(P5)] Radical Aziridination of Styrene with Troc Azide. [Co^{II}(P5)]= [Co(P5)] = [Co(3,5-Di^tBu-QingPhyrin)]



Intermediate A

A_[Co(II)P5]:

Temperature: 298.15 Kelvin

G_{corr}: 1.631957 Hartree

H_{corr}: 1.911187 Hartree

S: 587.689 Cal/Mol-Kelvin

SCF: -6149.929174 Hartree

H: -6148.017987 Hartree

G: -6148.297217 Hartree

Cartesian Coordinates:

Co	-0.00000300	-0.00004200	0.00007100
O	0.64213800	-4.05086500	6.61130500
O	-0.64494700	4.05112100	6.61146200
N	-1.41132400	-0.02603300	1.39939400
N	-1.41054900	0.02865600	-1.39998100
N	0.31991200	-2.41140000	4.94877500
H	0.28223300	-2.27438900	3.93342500
N	-0.32217600	2.41177400	4.94891500
H	-0.28405100	2.27487500	3.93356600
C	-0.00088400	0.00025900	3.48252100
C	-1.23009100	-0.08063600	2.79975700
C	-2.50942200	-0.19759000	3.48402500
H	-2.62333100	-0.27158500	4.56463000
C	-3.48642900	-0.19654200	2.51161700
H	-4.56470800	-0.27685700	2.63585700
C	-2.81426400	-0.07218400	1.22503900
C	-3.50185100	0.00439700	-0.00082100
C	-2.81345300	0.07875700	-1.22635300
C	-3.48464000	0.20406000	-2.51335700
H	-4.56262700	0.28728100	-2.63822300
C	-2.50715000	0.20153800	-3.48527900
H	-2.62030200	0.27498600	-4.56599900
C	-1.22848300	0.08169500	-2.80028200
C	-0.00125000	0.00017700	4.99220800
C	0.16555200	-1.22171600	5.71627200
C	0.16767300	-1.22314500	7.13775000
H	0.30049100	-2.16754400	7.66799600
C	-0.00188700	0.00000000	7.82056400
H	-0.00213100	-0.00006000	8.91675800
C	-0.17110200	1.22323500	7.13782300
H	-0.30410900	2.16756700	7.66813900
C	-0.16833000	1.22198500	5.71634600
C	0.54040900	-3.72409500	5.38524400
C	0.65854500	-4.71505000	4.26032000
H	0.24473800	-4.39421000	3.29562000

C	0.53226900	-6.21915500	4.58506900
H	-0.04648900	-6.83078300	3.88530700
H	0.39958900	-6.45306700	5.64677300
C	1.89671300	-5.68078900	4.15485600
C	2.38267800	-5.98977400	2.74971500
C	2.50345200	-7.33695100	2.31670000
H	2.19322800	-8.14566100	2.99048000
C	3.00875500	-7.64092700	1.03070700
H	3.09242100	-8.68605500	0.70932300
C	3.40127600	-6.59843900	0.15640600
H	3.78681300	-6.83169300	-0.84311700
C	3.28658100	-5.25164300	0.57913000
H	3.57783600	-4.43906900	-0.09770600
C	2.78573700	-4.95210900	1.86796800
H	2.69709100	-3.90675100	2.19097300
C	3.01830800	-5.58610700	5.19918000
H	3.54873800	-6.55479000	5.26573600
H	2.61307300	-5.33444800	6.19387900
H	3.75825400	-4.81495300	4.91332100
C	-0.54264300	3.72446300	5.38541900
C	-0.65991100	4.71558400	4.26055100
H	-0.24582500	4.39469100	3.29598800
C	-0.53303500	6.21960100	4.58553500
H	-0.40071400	6.45330200	5.64732900
H	0.04632900	6.83102900	3.88610200
C	-1.89754900	5.68192800	4.15465300
C	-2.38271800	5.99134600	2.74933100
C	-2.78527000	4.95399600	1.86699000
H	-2.69681400	3.90852400	2.18967900
C	-3.28540200	5.25399000	0.57798000
H	-3.57626400	4.44165400	-0.09931100
C	-3.39987700	6.60093300	0.15567400
H	-3.78485000	6.83454000	-0.84398300
C	-3.00784400	7.64311300	1.03056400
H	-3.09132200	8.68835400	0.70949700
C	-2.50326200	7.33868300	2.31672900
H	-2.19341900	8.14715800	2.99096800
C	-3.01963300	5.58770300	5.19849500
H	-3.54958000	6.55665500	5.26497200
H	-2.61492200	5.33569500	6.19331900
H	-3.75986700	4.81697400	4.91223700
C	-5.00671700	0.00646200	-0.00116900
C	-5.72222600	1.10743400	0.53430800
C	-7.14197300	1.13097100	0.53896100
C	-7.82652200	0.01023700	-0.00166200
H	-8.91883400	0.01167700	-0.00182800

C	-7.14478000	-1.11231300	-0.54205700
C	-5.72498300	-1.09258200	-0.53690700
O	-0.65084400	-4.05440400	-6.60828100
O	0.65361600	4.04492800	-6.61407500
N	1.41126300	-0.02979800	-1.39923100
N	1.41059700	0.02704800	1.40011600
N	-0.32516000	-2.41442400	-4.94690900
H	-0.28733500	-2.27676600	-3.93165200
N	0.32750400	2.40730200	-4.95046000
H	0.28933700	2.27112900	-3.93501400
C	0.00088500	-0.00238800	-3.48237000
C	1.22994000	-0.08508000	-2.79955100
C	2.50905500	-0.20494800	-3.48372700
H	2.62282900	-0.27990900	-4.56427800
C	3.48605800	-0.20504900	-2.51131400
H	4.56419200	-0.28742500	-2.63548500
C	2.81410900	-0.07853200	-1.22482900
C	3.50182900	-0.00244100	0.00097300
C	2.81359300	0.07417200	1.22644900
C	3.48504400	0.19902100	2.51335400
H	4.56320800	0.28008300	2.63811400
C	2.50756800	0.19921600	3.48529100
H	2.62088900	0.27321300	4.56595600
C	1.22864600	0.08148500	2.80038400
C	0.00122800	-0.00358200	-4.99205400
C	-0.16825000	-1.22561100	-5.71524800
C	-0.17036300	-1.22804100	-7.13672600
H	-0.30519500	-2.17253300	-7.66629500
C	0.00181800	-0.00575200	-7.82042000
H	0.00204800	-0.00660600	-8.91661400
C	0.17370300	1.21759800	-7.13855100
H	0.30870100	2.16129100	-7.66950300
C	0.17098500	1.21734500	-5.71707400
C	-0.54873300	-3.72691600	-5.38244500
C	-0.66971400	-4.71668000	-4.25678700
H	-0.25565800	-4.39600100	-3.29213500
C	-0.54685000	-6.22135900	-4.58022500
H	0.03002300	-6.83379400	-3.87961700
H	-0.41415600	-6.45644400	-5.64166600
C	-1.91022000	-5.67937600	-4.15119500
C	-2.39767300	-5.98611800	-2.74607400
C	-2.52145700	-7.33267800	-2.31199200
H	-2.21254900	-8.14257900	-2.98494700
C	-3.02803900	-7.63451700	-1.02600400
H	-3.11400900	-8.67919100	-0.70375500
C	-3.41884100	-6.59047500	-0.15278100

H	-3.80534600	-6.82210000	0.84674700
C	-3.30115500	-5.24427800	-0.57658200
H	-3.59100500	-4.43052500	0.09944500
C	-2.79903800	-4.94687200	-1.86542200
H	-2.70805300	-3.90198300	-2.18929300
C	-3.03107500	-5.58284100	-5.19617400
H	-3.56398200	-6.55021600	-5.26198200
H	-2.62473900	-5.33321500	-6.19093500
H	-3.76913600	-4.80948200	-4.91141600
C	0.55094900	3.71921100	-5.38781800
C	0.67107600	4.71062200	-4.26353200
H	0.25661000	4.39120600	-3.29863600
C	0.54791400	6.21480700	-4.58914300
H	0.41569400	6.44837800	-5.65097700
H	-0.02954300	6.82804600	-3.88971900
C	1.91121300	5.67384200	-4.15861100
C	2.39773900	5.98261800	-2.75361100
C	2.79896100	4.94460100	-1.87143500
H	2.70849300	3.89928000	-2.19405400
C	3.30025400	5.24378200	-0.58269300
H	3.58995900	4.43097700	0.09453800
C	3.41728000	6.59055000	-0.16051600
H	3.80315600	6.82354800	0.83893600
C	3.02660700	7.63336600	-1.03525200
H	3.11204700	8.67847000	-0.71426000
C	2.52082900	7.32975400	-2.32114400
H	2.21202600	8.13871800	-2.99527300
C	3.03268400	5.57618700	-5.20281200
H	3.56536600	6.54361100	-5.26967700
H	2.62696400	5.32506100	-6.19745000
H	3.77080500	4.80342200	-4.91658400
C	5.00670700	-0.00337400	0.00132100
C	5.72442200	1.09597400	-0.53450200
C	7.14421800	1.11667100	-0.53908800
C	7.82650000	-0.00524700	0.00194100
H	8.91881400	-0.00596300	0.00219700
C	7.14249800	-1.12626800	0.54266000
C	5.72273900	-1.10369500	0.53743100
C	7.89101800	2.34823100	-1.11803400
C	7.88741100	-2.35885100	1.12184200
C	9.43563300	2.18897300	-1.06226100
H	9.78111400	1.31806700	-1.65115500
H	9.91438000	3.09096000	-1.48732000
H	9.80055800	2.07589700	-0.02372600
C	7.47662800	2.55444300	-2.61016700
H	7.75506100	1.67596800	-3.22247600

H	6.38774000	2.71213800	-2.71544000
H	7.98736500	3.44338900	-3.02734900
C	7.50139300	3.61872700	-0.29584800
H	6.41426500	3.81381400	-0.33481800
H	7.79087700	3.50441000	0.76586600
H	8.01756900	4.50926900	-0.70292500
C	9.43226100	-2.20161300	1.06680800
H	9.90963400	-3.10424000	1.49204800
H	9.79782300	-2.08895300	0.02845300
H	9.77860000	-1.33118900	1.65591400
C	7.49648700	-3.62874200	0.29932000
H	6.40909100	-3.82243300	0.33783600
H	7.78652100	-3.51466100	-0.76226700
H	8.01137700	-4.51999500	0.70647600
C	7.47206700	-2.56470200	2.61375600
H	7.75141800	-1.68669000	3.22631200
H	6.38292100	-2.72094100	2.71855300
H	7.98142000	-3.45439000	3.03105300
C	-7.88630100	2.36424200	1.11743700
C	-7.49423200	3.63360800	0.29465500
H	-6.40671600	3.82655600	0.33342400
H	-7.78405400	3.51940800	-0.76697800
H	-8.00861500	4.52534200	0.70140000
C	-7.47141100	2.57030200	2.60945100
H	-7.75145700	1.69261100	3.22215300
H	-6.38222400	2.72600300	2.71460900
H	-7.98045600	3.46037300	3.02630400
C	-9.43123000	2.20801200	1.06181800
H	-9.77839900	1.33804100	1.65110400
H	-9.90817700	3.11111700	1.48652400
H	-9.79642500	2.09522500	0.02334800
C	-7.89216500	-2.34350300	-1.12104200
C	-7.50335800	-3.61421800	-0.29881400
H	-6.41634600	-3.80997100	-0.33765700
H	-7.79288300	-3.49973800	0.76287100
H	-8.02001500	-4.50445600	-0.70594200
C	-9.43670300	-2.18341300	-1.06549300
H	-9.78165800	-1.31241800	-1.65456500
H	-9.91587600	-3.08520600	-1.49048100
H	-9.80169700	-2.06997600	-0.02702100
C	-7.47764500	-2.54990500	-2.61311500
H	-7.75562600	-1.67132100	-3.22547500
H	-6.38879600	-2.70801100	-2.71820600
H	-7.98867400	-3.43864600	-3.03037600
H	-5.15508700	1.95495600	0.93782900
H	-5.15997900	-1.94165900	-0.94016700

H	5.15899400	1.94449900	-0.93832800
H	5.15601600	-1.95147300	0.94100100

A_{Troc Azide}:

Temperature: 298.15 Kelvin

G_{corr}: 0.020608 Hartree

H_{corr}: 0.073989 Hartree

S: 112.35 Cal/Mol-Kelvin

SCF: -1811.021952 Hartree

H: -1810.947963 Hartree

G: -1811.001344 Hartree

Cartesian Coordinates:

N	3.16445000	0.54883300	-0.08724600
N	3.32923000	-0.72188800	-0.04052200
N	3.69561900	-1.84033200	-0.07073000
O	1.66115400	2.32521700	0.23326800
O	1.00111000	0.09444200	0.68613700
C	-0.36426100	0.53664800	1.02102700
H	-0.58125600	0.17458700	2.03934900
H	-0.42694500	1.63889700	0.97176000
C	-1.37607900	-0.08562600	0.04330700
Cl	-3.07141500	0.50445200	0.57907500
Cl	-1.04591300	0.47077700	-1.69909200
Cl	-1.32967600	-1.94253200	0.12144800
C	1.90435000	1.11016300	0.26879800

Intermediate B

Temperature: 298.15 Kelvin

G_{corr}: 1.681291 Hartree

H_{corr}: 1.986349 Hartree

S: 642.048 Cal/Mol-Kelvin

SCF: -7960.982339 Hartree

H: -7958.995990 Hartree

G: -7959.301048 Hartree

Cartesian Coordinates:

Co	0.36242600	-0.30840700	0.08977600
O	-2.54138300	0.83503600	7.55496000
O	2.60694200	-5.07802300	5.34445700
N	1.23920400	0.18346500	1.80543900
N	1.89561400	0.45719400	-0.88775100
N	-1.72714000	0.10266100	5.46765900
H	-1.69766800	0.33977000	4.46921200
N	1.35340500	-3.45683500	4.17587800

H	1.22205900	-3.04988300	3.24442200
C	-0.10551700	-1.18166500	3.43560400
C	0.89462200	-0.24145400	3.10777100
C	1.70044000	0.45125900	4.10128600
H	1.61334500	0.30091200	5.17649000
C	2.52956900	1.31727000	3.41708600
H	3.25670600	2.01651400	3.82523200
C	2.28517700	1.11518000	1.99443100
C	3.08885400	1.66292900	0.97227900
C	2.92864700	1.26922500	-0.37354300
C	3.89966800	1.57167400	-1.41899900
H	4.80304900	2.15971300	-1.26701800
C	3.47151100	0.94099900	-2.56918000
H	3.94155600	0.92576600	-3.55162900
C	2.21333700	0.28047000	-2.24938500
C	-0.18346900	-1.69283700	4.85285000
C	-0.97170400	-1.04476400	5.85448900
C	-0.98254500	-1.54422500	7.18728200
H	-1.57951000	-1.02958700	7.94093700
C	-0.20588700	-2.67784800	7.50501600
H	-0.21494200	-3.05450400	8.53444500
C	0.58232600	-3.33961100	6.54092400
H	1.19271500	-4.20979400	6.78807700
C	0.58992900	-2.84501200	5.20966300
C	-2.45324500	0.97682300	6.29184600
C	-3.11103900	2.11074100	5.55998900
H	-2.82547500	2.23609600	4.51003000
C	-3.39253700	3.41405400	6.34857500
H	-3.17572900	4.35744500	5.83637800
H	-3.12872900	3.37814600	7.41077700
C	-4.58018600	2.56910200	5.90045400
C	-5.41514600	3.05778800	4.73031700
C	-5.89916200	4.39219400	4.69456300
H	-5.61159600	5.08790300	5.49277900
C	-6.74752000	4.82651600	3.64838600
H	-7.11403200	5.86009100	3.63513700
C	-7.12772800	3.92828000	2.62198100
H	-7.78925900	4.26135400	1.81349200
C	-6.64987900	2.59444600	2.64883200
H	-6.93831600	1.89417800	1.85609900
C	-5.80237400	2.16480000	3.69575100
H	-5.43357600	1.13116300	3.71417000
C	-5.39740300	1.80911800	6.95598200
H	-6.16163100	2.48373400	7.38649900
H	-4.74962200	1.43493200	7.76586100
H	-5.92528800	0.95000400	6.50069000

C	2.29249000	-4.49415400	4.25842200
C	2.90715100	-4.83126800	2.92881400
H	2.31195300	-4.55506500	2.04921600
C	3.74734300	-6.11486300	2.78840500
H	3.87114200	-6.69465200	3.70948700
H	3.60146700	-6.69756600	1.87320300
C	4.46402100	-4.76527900	2.71670100
C	4.93293800	-4.25161400	1.36784900
C	4.55867600	-2.96004800	0.90959900
H	3.87639200	-2.34957800	1.51544500
C	5.04998800	-2.45554300	-0.31779500
H	4.75281900	-1.45565400	-0.65692500
C	5.93081600	-3.23801300	-1.10453400
H	6.31050500	-2.85116400	-2.05734100
C	6.31328900	-4.52558800	-0.65530100
H	6.99373400	-5.13582800	-1.26126800
C	5.81825600	-5.02634700	0.57223800
H	6.11378800	-6.02462700	0.91926000
C	5.36602500	-4.35115000	3.88891200
H	6.38035100	-4.76904500	3.74482800
H	4.96502600	-4.71937500	4.84883700
H	5.45978900	-3.25009600	3.94484800
C	4.23859300	2.56523400	1.32956400
C	5.32338600	2.06599200	2.09565100
C	6.43430500	2.88556900	2.42416300
C	6.42840900	4.22839500	1.96255900
H	7.27641200	4.87180700	2.20730200
C	5.36308800	4.76422500	1.19138200
C	4.27185100	3.90966900	0.87983600
O	1.48154000	3.31242400	-6.85373000
O	3.32283800	-4.54024000	-5.49158400
N	-0.41484500	-0.97789300	-1.60201600
N	-1.01523100	-1.32895600	1.09664200
N	1.12895500	1.81730600	-5.05977100
H	0.70873300	1.74815300	-4.12341200
N	2.61237900	-2.73698800	-4.14847100
H	2.32068000	-2.50044100	-3.19459200
C	1.40790900	-0.35957100	-3.21233400
C	0.13400600	-0.87272600	-2.89374700
C	-0.82244400	-1.32462000	-3.89424800
H	-0.63137900	-1.33397800	-4.96658100
C	-1.97263000	-1.68237000	-3.22104300
H	-2.91188800	-2.04373300	-3.63528700
C	-1.70889400	-1.51136900	-1.79680900
C	-2.58217600	-1.93895900	-0.77594100
C	-2.18541900	-1.92358400	0.58009100

C	-2.89663800	-2.63831300	1.63254100
H	-3.82082900	-3.19342000	1.48082300
C	-2.15878500	-2.50127100	2.79217700
H	-2.36503200	-2.90635600	3.78226100
C	-1.01397700	-1.66261400	2.47059600
C	1.90266900	-0.45836900	-4.63312100
C	1.78191800	0.64306100	-5.53694000
C	2.27419900	0.53433600	-6.86718000
H	2.18935500	1.39136100	-7.53664100
C	2.85828400	-0.67964200	-7.28590200
H	3.22961200	-0.76235600	-8.31400200
C	2.97684200	-1.79043400	-6.42451700
H	3.41704700	-2.73317100	-6.75355200
C	2.50259700	-1.67507100	-5.09030700
C	0.98058900	3.04715300	-5.71282700
C	0.15426200	4.03727500	-4.94167400
H	-0.42550300	3.60678400	-4.11881500
C	-0.48203900	5.21977800	-5.70482000
H	-1.51781400	5.47678100	-5.45855800
H	-0.22038700	5.27570000	-6.76667900
C	0.63219800	5.51572800	-4.70229000
C	0.25018000	6.11011100	-3.35857900
C	-0.59475700	7.24877200	-3.27839200
H	-1.00235600	7.67948200	-4.20116100
C	-0.91271100	7.82951300	-2.02634900
H	-1.56474900	8.70989500	-1.98263400
C	-0.38739800	7.27777000	-0.83213600
H	-0.63007500	7.72703000	0.13787600
C	0.45866900	6.14220600	-0.90153400
H	0.86430200	5.70746000	0.02014200
C	0.77600300	5.56696800	-2.15418400
H	1.42598500	4.68440700	-2.20493500
C	2.00355000	5.96640500	-5.22422900
H	2.00168600	7.06059800	-5.38865700
H	2.24448200	5.46263200	-6.17560200
H	2.80070500	5.73508100	-4.49267000
C	2.98763100	-4.07119700	-4.35719200
C	2.92624200	-4.90022000	-3.10460800
H	3.02876700	-4.34483300	-2.16383600
C	3.52195600	-6.32018700	-3.11161600
H	3.93598400	-6.64856500	-4.07106000
H	4.08346000	-6.62021900	-2.22121100
C	2.00200600	-6.17099200	-3.02615500
C	1.31303300	-6.41260300	-1.69577100
C	0.41658200	-5.45110100	-1.15666500
H	0.26721700	-4.49939900	-1.68334100

C	-0.27414500	-5.70138300	0.05264000
H	-0.95904600	-4.94672200	0.45845300
C	-0.08062600	-6.92509400	0.73974800
H	-0.61065500	-7.11974200	1.67938300
C	0.80805900	-7.89184400	0.20948300
H	0.96263900	-8.84030600	0.73791600
C	1.49765700	-7.63666700	-0.99996800
H	2.18651700	-8.38654100	-1.40917000
C	1.15670500	-6.56165100	-4.24742600
H	0.93588900	-7.64547800	-4.21773600
H	1.68777400	-6.33542100	-5.18800400
H	0.19141700	-6.02075300	-4.24897900
C	-3.91974900	-2.52884900	-1.12546500
C	-4.01287800	-3.73562500	-1.86509500
C	-5.27223900	-4.31015300	-2.17983000
C	-6.44074400	-3.63635500	-1.73438900
H	-7.41706200	-4.06545800	-1.97142100
C	-6.38700000	-2.42931600	-0.98820500
C	-5.10804900	-1.89083600	-0.68791200
N	-0.80594100	1.43107600	0.05915300
N	-1.43817000	1.70823200	1.17366600
N	-1.76220400	1.56804200	2.30184200
O	-0.54661900	2.18101400	-2.16434000
O	-2.04293200	3.25157500	-0.68532800
C	-2.51204800	4.18270100	-1.72793700
H	-2.33161500	5.20422400	-1.35417800
H	-1.95891400	4.01626100	-2.66735100
C	-4.01514500	3.96997100	-1.96530700
Cl	-4.54993800	5.22883200	-3.24556200
Cl	-4.33966600	2.25429100	-2.61942000
Cl	-4.99125300	4.23058300	-0.40788300
C	-1.08702400	2.28244100	-1.05036700
H	3.42801400	4.28566800	0.28839600
H	5.29866100	1.01799500	2.41727000
H	-5.01933100	-0.95898800	-0.11648000
H	-3.08643600	-4.23493900	-2.17253400
C	-7.66141300	-1.69604900	-0.49078200
C	-5.32830800	-5.64073000	-2.97693200
C	5.35510300	6.23460000	0.69302100
C	7.60067500	2.29224700	3.25878400
C	6.64027800	7.00909100	1.09785800
H	7.55090100	6.54686400	0.67182200
H	6.58063400	8.04485800	0.71431900
H	6.75825100	7.06672400	2.19657600
C	4.12616000	6.97860800	1.30696200
H	3.17407300	6.49834300	1.01619300

H	4.18157600	6.98636700	2.41177700
H	4.09790700	8.02663200	0.95167300
C	5.24498500	6.25794400	-0.86516100
H	6.10963600	5.74704800	-1.32911500
H	4.32365300	5.76032000	-1.21907600
H	5.22321400	7.30298100	-1.22919200
C	8.72629800	3.32823700	3.52967900
H	9.18633900	3.69067400	2.59074800
H	8.35320100	4.20198900	4.09695000
H	9.52506600	2.85600100	4.13169900
C	8.22394500	1.08284300	2.49020700
H	7.48029500	0.28700200	2.30290600
H	8.63013400	1.40381200	1.51257000
H	9.04977600	0.64193100	3.08085600
C	7.05050100	1.79911500	4.63553400
H	6.62376900	2.64015700	5.21424100
H	6.26072500	1.03547000	4.51200000
H	7.86608700	1.34758800	5.23235800
C	-8.97055000	-2.41537700	-0.91811300
H	-9.03264300	-3.43973200	-0.50418900
H	-9.84195800	-1.84922200	-0.53901600
H	-9.06532900	-2.47672400	-2.01881300
C	-7.68907400	-0.24794100	-1.07588100
H	-6.79333700	0.33051100	-0.78578900
H	-7.73149600	-0.27078800	-2.18089600
H	-8.58070000	0.29492700	-0.70675700
C	-6.78382300	-6.11297000	-3.24676600
H	-7.33680200	-6.29992300	-2.30659300
H	-7.35200900	-5.37686100	-3.84677900
H	-6.76361800	-7.06209000	-3.81445300
C	-4.59554200	-6.75784200	-2.16621500
H	-3.53826700	-6.50044400	-1.97338400
H	-5.08867500	-6.92317300	-1.18975900
H	-4.61418600	-7.71080600	-2.72930000
C	-4.61493200	-5.45114400	-4.35384400
H	-5.12253000	-4.67522500	-4.95764800
H	-3.55830300	-5.15062700	-4.23019500
H	-4.63068400	-6.39902900	-4.92503700
C	-7.63348800	-1.62126600	1.06963800
H	-7.63407700	-2.63470700	1.51339900
H	-6.73456500	-1.09177700	1.43618000
H	-8.52397200	-1.07974100	1.44290800

Transition State TS1

Temperature: 298.15 Kelvin

Imaginary Frequency: -390.3109 cm⁻¹

G_corr: 1.671489 Hartree

H_corr: 1.983073 Hartree

S: 655.784 Cal/Mol-Kelvin

SCF: -7960.953973 Hartree

H: -7958.97090 Hartree

G: -7959.282484 Hartree

Cartesian Coordinates:

Co	-0.26017900	0.31184600	0.10900300
O	2.30536800	-1.34088900	7.54348200
O	-1.28076700	5.61689100	5.34236900
N	-1.20669300	0.07258000	1.84092100
N	-1.95837700	0.00088700	-0.80962600
N	1.69945200	-0.44666200	5.44687000
H	1.61515900	-0.68195200	4.44985800
N	-0.47884500	3.73593600	4.16691300
H	-0.46777500	3.30560100	3.23696200
C	0.39641700	1.17290600	3.42964700
C	-0.77091200	0.44330300	3.13108900
C	-1.67575200	-0.07754900	4.14358900
H	-1.54846900	0.07118800	5.21486700
C	-2.65147800	-0.79679900	3.48287000
H	-3.48492800	-1.35133500	3.90930200
C	-2.39670600	-0.65550900	2.05518500
C	-3.31038400	-1.02904200	1.04831300
C	-3.11362800	-0.62073100	-0.28790500
C	-4.15451100	-0.67263700	-1.30413800
H	-5.15110500	-1.07847700	-1.13995800
C	-3.64563500	-0.08361300	-2.44460200
H	-4.13283500	0.06897200	-3.40649100
C	-2.26984800	0.28700500	-2.15621600
C	0.61148800	1.66228500	4.83855700
C	1.23791400	0.84687300	5.83336100
C	1.38275100	1.33693100	7.16222500
H	1.84863900	0.69790600	7.91296400
C	0.90164300	2.62359600	7.48081200
H	1.01359800	2.99128900	8.50740800
C	0.27959100	3.45009500	6.52232500
H	-0.10327300	4.44085700	6.77214200
C	0.13668600	2.96609900	5.19494500
C	2.19911300	-1.46293900	6.27967200
C	2.58674000	-2.71872000	5.55590500
H	2.30052500	-2.77216400	4.49976400
C	2.54396500	-4.05209100	6.34399900
H	2.12305400	-4.91832100	5.82281900

H	2.27672400	-3.95654600	7.40164500
C	3.90330300	-3.50707300	5.91994300
C	4.62169300	-4.17869500	4.76300900
C	4.77221000	-5.59009500	4.72777400
H	4.31011100	-6.19815600	5.51557400
C	5.51222500	-6.21353200	3.69506400
H	5.61936200	-7.30489900	3.68147700
C	6.11564300	-5.43097500	2.68146200
H	6.68904100	-5.91205700	1.88026100
C	5.97086800	-4.02199100	2.70752200
H	6.43159400	-3.41091400	1.92249000
C	5.23202100	-3.40286400	3.74174500
H	5.12046800	-2.31100300	3.75860800
C	4.85632700	-2.95686700	6.99162200
H	5.44354800	-3.78911100	7.42408100
H	4.29922700	-2.45137100	7.79744900
H	5.56986400	-2.23592200	6.54986400
C	-1.13964100	4.96943400	4.25634200
C	-1.68755900	5.43906800	2.93778500
H	-1.19893900	5.02662100	2.04583000
C	-2.20022500	6.88680700	2.81135000
H	-2.15620000	7.47789600	3.73243900
H	-1.94266200	7.41877800	1.89004500
C	-3.22113100	5.74965600	2.76483500
C	-3.83245200	5.36662900	1.42954800
C	-3.83705000	4.01452300	0.99331900
H	-3.34368100	3.24906700	1.60659500
C	-4.46413800	3.64614300	-0.22031400
H	-4.45925600	2.59791600	-0.54322400
C	-5.10371500	4.62903900	-1.01545000
H	-5.58839200	4.34727100	-1.95740400
C	-5.10865600	5.97907100	-0.58783200
H	-5.60249700	6.74376600	-1.19928400
C	-4.47813500	6.34321900	0.62577200
H	-4.48324100	7.38959200	0.95626200
C	-4.16584700	5.55879300	3.96055100
H	-5.05287500	6.20949500	3.84260200
H	-3.66351100	5.81473900	4.90910700
H	-4.52106400	4.51255800	4.02019000
C	-4.59456200	-1.71940100	1.41330400
C	-5.55040700	-1.05839500	2.22770500
C	-6.78393400	-1.67400000	2.56322500
C	-7.03231300	-2.97840600	2.06017700
H	-7.97657500	-3.46692400	2.31071100
C	-6.10237400	-3.67039400	1.23939100
C	-4.88165300	-3.01744000	0.91973800

O	-2.52208700	-2.78498400	-6.71807800
O	-2.22836800	5.26735600	-5.41808100
N	0.59336200	0.85615300	-1.57641800
N	1.29020000	1.06276500	1.08089500
N	-1.70881800	-1.44145700	-4.95410500
H	-1.24508500	-1.49172300	-4.03508000
N	-1.95124500	3.35437800	-4.06775900
H	-1.71786400	3.06107600	-3.11388700
C	-1.36827000	0.74692200	-3.13393100
C	0.00169000	0.91408100	-2.85094500
C	1.01583100	1.11202000	-3.87478300
H	0.80417900	1.18492900	-4.94063000
C	2.23819000	1.13734500	-3.23478500
H	3.22781200	1.23780400	-3.67571400
C	1.97840800	1.02622500	-1.80555300
C	2.94992500	1.21736100	-0.80387900
C	2.57131800	1.32867500	0.55338900
C	3.43812500	1.87360400	1.58684600
H	4.47088700	2.17683800	1.42440500
C	2.69025900	1.96065200	2.74633100
H	2.99222000	2.32936100	3.72585800
C	1.37689400	1.41706500	2.44738700
C	-1.85638400	0.96503200	-4.54126600
C	-2.04253200	-0.14027100	-5.43094400
C	-2.51715600	0.08650400	-6.75341400
H	-2.67307900	-0.76746000	-7.41365100
C	-2.77497600	1.40705800	-7.17628900
H	-3.13279300	1.57521000	-8.19872400
C	-2.58528500	2.51751000	-6.32734700
H	-2.77509400	3.53921400	-6.65982100
C	-2.13122500	2.29272200	-5.00043400
C	-1.92785000	-2.66891000	-5.59714100
C	-1.37374600	-3.84644800	-4.84851400
H	-0.69817600	-3.58729500	-4.02743300
C	-1.05312800	-5.12881800	-5.65077800
H	-0.11526000	-5.64492400	-5.42046300
H	-1.33058000	-5.09141900	-6.70964000
C	-2.19711000	-5.16405100	-4.63424900
C	-1.94580100	-5.89391800	-3.32560300
C	-1.75080700	-7.30204900	-3.33251600
H	-1.75212500	-7.83809000	-4.29005200
C	-1.53991100	-8.01137400	-2.12719400
H	-1.38515200	-9.09670200	-2.15154500
C	-1.51954600	-7.32103800	-0.88993500
H	-1.34778500	-7.86738600	0.04487400
C	-1.71663000	-5.91893400	-0.87102800

H	-1.68941900	-5.37550900	0.08136200
C	-1.93318400	-5.21300000	-2.07952500
H	-2.07808600	-4.12602100	-2.05956800
C	-3.64230000	-5.25597300	-5.14293500
H	-3.91111800	-6.31322100	-5.32867200
H	-3.76507300	-4.68741500	-6.08021500
H	-4.34851400	-4.85442100	-4.39171000
C	-2.00107800	4.73880200	-4.28317100
C	-1.73449100	5.53939700	-3.03916300
H	-1.93610800	5.02512700	-2.09101300
C	-2.01492800	7.05458500	-3.05204500
H	-2.36690500	7.45503800	-4.00888600
H	-2.48429800	7.47367500	-2.15642200
C	-0.56068100	6.58617100	-2.98874000
C	0.18456600	6.68842600	-1.67059100
C	0.85293500	5.56083700	-1.12295200
H	0.78146300	4.59213000	-1.63473000
C	1.59937100	5.67112000	0.07394800
H	2.10623100	4.79010800	0.48639400
C	1.69338600	6.91816500	0.73949700
H	2.26730400	7.00543600	1.66937000
C	1.03466500	8.04968400	0.19978800
H	1.10310000	9.01752300	0.71086800
C	0.28736000	7.93417600	-0.99657700
H	-0.22362200	8.81155200	-1.41293300
C	0.32874100	6.77954000	-4.22565500
H	0.77665000	7.79111400	-4.20916700
H	-0.25407800	6.66622500	-5.15579600
H	1.15589400	6.04462600	-4.23596400
C	4.38943400	1.43785900	-1.16890900
C	4.77973900	2.55935200	-1.94534200
C	6.14187800	2.78935500	-2.27101000
C	7.10500400	1.86015800	-1.79533000
H	8.15735800	2.02335500	-2.03868300
C	6.75249900	0.72942300	-1.01159400
C	5.38005300	0.53567900	-0.70384000
N	0.33850500	-1.48355700	0.01210600
N	1.29623300	-2.12898400	1.26856900
N	1.45754100	-1.72731700	2.35758900
O	-0.11854400	-2.09977800	-2.21653200
O	1.33998000	-3.40294100	-0.89922600
C	1.53883600	-4.30123000	-2.03779800
H	1.12573500	-5.28984400	-1.77290500
H	1.03557500	-3.90574700	-2.93732000
C	3.04170900	-4.44267900	-2.32174000
Cl	3.22105400	-5.65332600	-3.74728100

Cl	3.78354100	-2.80530400	-2.81815600
Cl	3.95829300	-5.11111100	-0.85087500
C	0.48631200	-2.27681300	-1.11639000
H	-4.13540200	-3.51767600	0.29080700
H	-5.32814100	-0.04362000	2.57851100
H	5.06134800	-0.33003200	-0.11134900
H	4.00860200	3.26708500	-2.27202300
C	7.80495900	-0.28197800	-0.48423200
C	6.52640500	4.03543100	-3.11287300
C	-6.37575100	-5.09896400	0.69792400
C	-7.80511100	-0.90798700	3.44621000
C	-7.77777800	-5.63228400	1.10430900
H	-8.59147900	-4.99096100	0.71529400
H	-7.92033400	-6.64504300	0.68326400
H	-7.88753700	-5.71022900	2.20271100
C	-5.29826400	-6.07680500	1.26718800
H	-4.27868100	-5.78021600	0.96205100
H	-5.33353000	-6.10224500	2.37275400
H	-5.47662300	-7.10156400	0.88878500
C	-6.29199700	-5.09160200	-0.86182700
H	-7.05055100	-4.41216800	-1.29464900
H	-5.29711800	-4.76892500	-1.21845600
H	-6.47332300	-6.10957900	-1.25621900
C	-9.08880800	-1.73688800	3.72812000
H	-9.62954400	-1.98835100	2.79604200
H	-8.86229000	-2.67703500	4.26609200
H	-9.77572800	-1.14628100	4.36270300
C	-8.22538300	0.41137000	2.72186900
H	-7.35729400	1.06666500	2.52527900
H	-8.71074000	0.19136700	1.75244200
H	-8.94190100	0.97764400	3.34735300
C	-7.14279400	-0.55525600	4.81662900
H	-6.84806900	-1.47269100	5.36030700
H	-6.24026700	0.07002000	4.68748900
H	-7.85456400	0.00807400	5.44997900
C	9.25332400	0.08845800	-0.90806400
H	9.55980000	1.07539100	-0.51211000
H	9.95722400	-0.66484800	-0.50745700
H	9.36947400	0.10084700	-2.00839900
C	7.48245800	-1.70459700	-1.04245000
H	6.47056000	-2.04209500	-0.75498000
H	7.53801600	-1.71652400	-2.14692500
H	8.21243800	-2.43992500	-0.65214100
C	8.05232100	4.11618100	-3.39495200
H	8.64017100	4.19641600	-2.46090900
H	8.41362900	3.23708100	-3.96173300

H	8.26669700	5.01591200	-4.00149300
C	6.10276000	5.32790600	-2.34345200
H	5.01585700	5.35083000	-2.14448600
H	6.62726300	5.39761600	-1.37188800
H	6.35643700	6.22589900	-2.93891400
C	5.78055300	3.98423600	-4.48476500
H	6.07188300	3.08465600	-5.05919800
H	4.68288400	3.96617900	-4.35453200
H	6.03265000	4.87682000	-5.08876700
C	7.74890200	-0.31368900	1.07692700
H	7.99096200	0.67915200	1.50103700
H	6.74726100	-0.60441900	1.44405800
H	8.48085200	-1.04482400	1.47050700

Intermediate C

C_[Co(II)P5]:

Temperature: 298.15 Kelvin

G_corr: 1.672229 Hartree

H_corr: 1.975012 Hartree

S: 637.262 Cal/Mol-Kelvin

SCF: -7851.418683 Hartree

H: -7849.443671 Hartree

G: -7849.746454 Hartree

Cartesian Coordinates:

Co	0.16803000	0.31095200	0.11401000
O	-1.35496100	-0.65406200	7.85701000
O	5.16500100	3.38000000	5.07301000
N	-0.36298200	1.60094700	1.54701000
N	-0.59798100	1.54194500	-1.20699000
N	-0.50996500	-0.22005400	5.70001000
H	-0.71696400	-0.33205600	4.70301000
N	3.33701100	2.29798200	4.04901000
H	2.91801300	2.09597800	3.13701000
C	1.02002600	0.78096100	3.47401000
C	0.03101800	1.60195100	2.90001000
C	-0.74999100	2.56494400	3.66201000
H	-0.62299300	2.75494500	4.72701000
C	-1.65199700	3.13393500	2.78701000
H	-2.41700400	3.87992800	2.99501000
C	-1.38399100	2.57093800	1.47101000
C	-1.96299600	3.04793200	0.28001000
C	-1.50999100	2.59493700	-0.97399000
C	-1.87199700	3.23393300	-2.22899000
H	-2.53100600	4.09592700	-2.30899000
C	-1.20499100	2.56794000	-3.23599000

H	-1.22099300	2.76193900	-4.30699000
C	-0.46098100	1.48794700	-2.61199000
C	1.44302300	1.01696500	4.90301000
C	0.68402800	0.49995700	6.00101000
C	1.12002600	0.71496100	7.33701000
H	0.52803000	0.30895600	8.15901000
C	2.29901900	1.45497300	7.56401000
H	2.63201800	1.61897600	8.59601000
C	3.06101400	1.99198000	6.50601000
H	3.96900900	2.57098800	6.68301000
C	2.63001600	1.77297600	5.17001000
C	-1.47596000	-0.71606300	6.59101000
C	-2.68295500	-1.30607400	5.92001000
H	-2.78595700	-1.10307500	4.84601000
C	-3.99895400	-1.34908700	6.73601000
H	-4.91895700	-1.07509600	6.20801000
H	-3.91295800	-0.98708600	7.76601000
C	-3.30994200	-2.66808000	6.39801000
C	-3.93093400	-3.53808600	5.32101000
C	-5.26592900	-4.00109900	5.47001000
H	-5.85393200	-3.66910400	6.33501000
C	-5.83792100	-4.87810400	4.51901000
H	-6.86991800	-5.22711400	4.64801000
C	-5.07891700	-5.30709700	3.40201000
H	-5.51891000	-5.98910100	2.66501000
C	-3.74892100	-4.84708400	3.24301000
H	-3.15591800	-5.17007900	2.37901000
C	-3.17992900	-3.97207900	4.19801000
H	-2.14993300	-3.61906900	4.06601000
C	-2.62893400	-3.46807400	7.51801000
H	-3.37392800	-4.11808100	8.01501000
H	-2.17994000	-2.79807000	8.27101000
H	-1.83492800	-4.11906600	7.10501000
C	4.52200400	3.04899400	4.02501000
C	4.95900100	3.43499800	2.64101000
H	4.49800600	2.87299300	1.81801000
C	6.42799700	3.86101200	2.42201000
H	7.03999600	3.88901700	3.33001000
H	6.92000000	3.47701600	1.52301000
C	5.33898700	4.92300100	2.28801000
C	4.95698200	5.39799800	0.89801000
C	3.59698200	5.44398500	0.49201000
H	2.81898500	5.07697800	1.17401000
C	3.23697700	5.95198100	-0.77799000
H	2.18397700	5.97597200	-1.08099000
C	4.23597200	6.43099100	-1.66099000

H	3.95996900	6.82398800	-2.64599000
C	5.59497300	6.39300400	-1.26399000
H	6.37396900	6.76601100	-1.93999000
C	5.95097800	5.88100700	0.00601000
H	7.00397800	5.85101700	0.31201000
C	5.22397600	6.00900000	3.36801000
H	5.91596900	6.84000700	3.13301000
H	5.47398000	5.60800300	4.36401000
H	4.19897200	6.42399100	3.40101000
C	-2.99600600	4.13892300	0.33101000
C	-2.65501800	5.42592600	0.82001000
C	-3.61102800	6.47391700	0.86101000
C	-4.92502500	6.19190400	0.40401000
H	-5.67303300	6.98789700	0.43301000
C	-5.30301300	4.91690100	-0.09499000
C	-4.31500400	3.89691000	-0.12999000
O	-3.58696200	-0.54008300	-6.72899000
O	4.11801300	2.08499000	-6.25299000
N	0.95804100	-0.79004000	-1.32299000
N	1.36203900	-0.62003600	1.40901000
N	-2.04696300	-0.36806800	-4.94599000
H	-1.95396200	-0.52306800	-3.92999000
N	2.47401900	1.47197400	-4.67799000
H	2.30802000	1.38197300	-3.66999000
C	0.19402900	0.48395300	-3.34499000
C	0.78603900	-0.62604200	-2.71199000
C	1.29605000	-1.78103700	-3.43199000
H	1.26905100	-1.88503700	-4.51499000
C	1.76205800	-2.67203200	-2.48799000
H	2.19006800	-3.66002800	-2.64499000
C	1.59205200	-2.04903400	-1.18399000
C	2.11105700	-2.57502900	0.01401000
C	2.04705000	-1.83703000	1.21501000
C	2.76705400	-2.21302300	2.42401000
H	3.39506200	-3.09601700	2.51501000
C	2.51304500	-1.24002500	3.36901000
H	2.87804400	-1.17302200	4.39301000
C	1.61303600	-0.27603400	2.75601000
C	0.21502800	0.57095300	-4.84699000
C	-0.91596900	0.16894200	-5.62699000
C	-0.87297000	0.29194300	-7.04499000
H	-1.74696700	-0.00106600	-7.62699000
C	0.29202600	0.79395400	-7.66199000
H	0.31602500	0.87995400	-8.75399000
C	1.42502200	1.18596400	-6.91999000
H	2.32601800	1.57297300	-7.39799000

C	1.38302300	1.07596400	-5.50499000
C	-3.28596000	-0.72508000	-5.50399000
C	-4.22995400	-1.36808900	-4.53099000
H	-3.76895100	-1.70608500	-3.59799000
C	-5.37394600	-2.23410000	-5.10799000
H	-5.58493700	-3.18210200	-4.60299000
H	-5.43494600	-2.24810000	-6.20099000
C	-5.72895800	-0.91910300	-4.40999000
C	-6.33895700	-1.00110900	-3.02099000
C	-7.62995200	-1.57312100	-2.85499000
H	-8.14694800	-1.98912600	-3.72899000
C	-8.24195200	-1.62312700	-1.58099000
H	-9.23694700	-2.07113600	-1.46899000
C	-7.57095700	-1.10012100	-0.44799000
H	-8.03995600	-1.14312500	0.54101000
C	-6.28396200	-0.52810800	-0.60299000
H	-5.75096600	-0.13410300	0.27101000
C	-5.67596200	-0.47510300	-1.88099000
H	-4.67496700	-0.04209300	-1.99499000
C	-6.24596900	0.25489200	-5.25299000
H	-7.33796800	0.15788200	-5.40399000
H	-5.75197000	0.27789700	-6.23899000
H	-6.05897800	1.21689400	-4.74099000
C	3.74501500	1.93398600	-5.04599000
C	4.63301200	2.22299500	-3.86799000
H	4.12101100	2.34899000	-2.90599000
C	5.89100400	3.09400700	-4.07599000
H	6.06900100	3.41400800	-5.10799000
H	6.10799700	3.83300900	-3.29899000
C	6.07601800	1.60800800	-3.76699000
C	6.53702200	1.20801300	-2.37599000
C	5.75903000	0.34000500	-1.56399000
H	4.78203300	-0.00300400	-1.92799000
C	6.22603400	-0.07599000	-0.29499000
H	5.60904000	-0.73799600	0.32501000
C	7.48603000	0.36402200	0.17801000
H	7.84903300	0.04402500	1.16201000
C	8.27202200	1.22502900	-0.62699000
H	9.25001800	1.56803800	-0.26699000
C	7.80001800	1.64202500	-1.89299000
H	8.40801100	2.31503000	-2.51299000
C	6.58502700	0.67801300	-4.87899000
H	7.69002600	0.70302400	-4.90999000
H	6.19502400	0.98800900	-5.86399000
H	6.27603700	-0.36699000	-4.68999000
C	2.83307000	-3.89202200	0.01501000

C	4.02907100	-4.06201100	-0.72899000
C	4.74108300	-5.29000400	-0.70599000
C	4.21809300	-6.34600900	0.08801000
H	4.75510200	-7.29700400	0.11901000
C	3.02609200	-6.21202100	0.84701000
C	2.34208000	-4.96802700	0.79801000
N	-1.31096000	-0.72206100	0.30101000
O	-2.28295700	-1.06207100	-1.86299000
O	-2.27794100	-2.73907100	-0.18799000
C	-3.38993500	-3.42508100	-0.85599000
H	-4.12193200	-3.68908800	-0.07299000
H	-3.85894100	-2.77008600	-1.61099000
C	-2.92792200	-4.72207700	-1.54199000
Cl	-4.46591500	-5.54409100	-2.24999000
Cl	-1.72392500	-4.39906500	-2.91599000
Cl	-2.14991100	-5.90306900	-0.32099000
C	-1.90995300	-1.44406700	-0.70499000
C	-6.74101000	4.61088700	-0.59199000
C	-3.19304100	7.87192100	1.39101000
C	-7.68002200	5.84587800	-0.49699000
H	-7.31703000	6.68888200	-1.11499000
H	-8.68502000	5.56986900	-0.86699000
H	-7.79302500	6.19787700	0.54601000
C	-4.36605100	8.89091000	1.37301000
H	-5.20804800	8.55990200	2.01001000
H	-4.01506000	9.86491300	1.76201000
H	-4.74905200	9.05990600	0.34801000
C	-2.68704000	7.73892600	2.86301000
H	-3.48803600	7.35491800	3.52301000
H	-1.82303400	7.05293400	2.94001000
H	-2.36704900	8.72592900	3.24701000
C	-2.04004700	8.43893200	0.50001000
H	-1.15504000	7.77794000	0.50701000
H	-2.37304800	8.55292900	-0.54899000
H	-1.72405600	9.43193500	0.87401000
C	-6.68700600	4.15488800	-2.08499000
H	-6.26601400	4.95189200	-2.72699000
H	-6.06699800	3.24889400	-2.21299000
H	-7.70500400	3.91787800	-2.44799000
C	-7.35300000	3.46488100	0.27501000
H	-6.75999100	2.53588700	0.19901000
H	-7.40000200	3.75888100	1.34001000
H	-8.37899700	3.23487200	-0.06899000
C	2.45410300	-7.36302600	1.71701000
C	6.05308400	-5.43199200	-1.52199000
C	1.03010600	-7.74103900	1.19901000

H	0.34209800	-6.87704600	1.22701000
H	1.07311000	-8.10203900	0.15401000
H	0.59711400	-8.54304300	1.82601000
C	3.34011500	-8.63901800	1.67701000
H	4.35911300	-8.44500800	2.06401000
H	2.88512200	-9.42102200	2.31301000
H	3.42611900	-9.05001700	0.65401000
C	2.35309800	-6.88802700	3.20201000
H	3.35109600	-6.62801700	3.60301000
H	1.70209000	-6.00103300	3.30501000
H	1.92710600	-7.69303100	3.83101000
C	6.68009800	-6.84898600	-1.40199000
H	7.60209800	-6.89497700	-2.00999000
H	6.95710000	-7.08898300	-0.35799000
H	5.99510500	-7.63399200	-1.77299000
C	5.75908200	-5.15699500	-3.03199000
H	5.03608900	-5.89200200	-3.43399000
H	5.34407200	-4.14599900	-3.19199000
H	6.69408300	-5.23498600	-3.61999000
C	7.09707500	-4.38998200	-1.00499000
H	6.73206500	-3.35198600	-1.10999000
H	7.32907600	-4.56298000	0.06401000
H	8.03907500	-4.47597300	-1.58099000
H	-4.56499400	2.89690800	-0.50399000
H	-1.62402000	5.60493600	1.15101000
H	1.41207900	-4.82603600	1.36001000
H	4.41306300	-3.21600700	-1.31199000

C_{P5-N2}:

Temperature: 298.15 Kelvin

G_{corr}: -0.013595 Hartree

H_{corr}: 0.008228 Hartree

S: 45.93 Cal/Mol-Kelvin

SCF: -109.560519 Hartree

H: -109.552291 Hartree

G: -109.574114 Hartree

Cartesian Coordinates:

N	0.00000000	0.00000000	0.57307500
N	0.00000000	0.00000000	-0.57307500

C_{P5-Styrene}:

Temperature: 298.15 Kelvin

G_{corr}: 0.099591 Hartree

H_{corr}: 0.138486 Hartree

S: 81.861 Cal/Mol-Kelvin

SCF: -309.798739 Hartree

H: -309.660253 Hartree

G: -309.699148 Hartree

Cartesian Coordinates:

H	-0.70823500	1.95657200	-0.00043400
C	-0.01429700	1.10760800	-0.00021100
C	1.80396400	-1.05993400	0.00020200
C	-0.52371800	-0.22493100	-0.00017400
C	1.37556300	1.34985700	-0.00008700
C	2.29346100	0.26811800	0.00011000
C	0.41132900	-1.30067800	0.00002000
H	1.74805200	2.38122000	-0.00016300
H	3.37271900	0.45998000	0.00018600
H	0.03719500	-2.33319800	0.00008500
H	2.50388400	-1.90378600	0.00037700
C	-1.97141600	-0.54000100	-0.00031800
H	-2.20874900	-1.61538600	-0.00101900
C	-3.01243600	0.33996100	0.00038500
H	-4.04936500	-0.01299200	0.00018100
H	-2.87021000	1.42759200	0.00122200

Transition State TS2

Temperature: 298.15 Kelvin

Imaginary Frequency: -164.7223 cm⁻¹

G_{corr}: 1.798031 Hartree

H_{corr}: 2.113972 Hartree

S: 664.953 Cal/Mol-Kelvin

SCF: -8161.210116 Hartree

H: -8159.096144 Hartree

G: -8159.412085 Hartree

Cartesian Coordinates:

Co	0.28773300	-0.12511800	0.02426900
O	-5.30730400	-2.81257800	-4.79961200
O	2.20767600	-1.05980800	-7.32606700
N	0.54560200	-1.67824000	-1.16413100
N	1.16106000	-1.13305700	1.48948800
N	-3.54171800	-1.62156300	-3.79719000
H	-3.24897800	-1.15951700	-2.92971600
N	1.02867600	-0.72255500	-5.30880200
H	1.14814700	-0.37748300	-4.35198400
C	-0.78176200	-0.90136100	-3.15173600
C	-0.07057100	-1.87778500	-2.41642000
C	0.26855800	-3.19148700	-2.94190100
H	-0.07956500	-3.57960800	-3.89797900

C	1.11931300	-3.78643900	-2.02970600
H	1.58521900	-4.76917200	-2.08086800
C	1.26245200	-2.86738600	-0.90824100
C	1.88775000	-3.21930400	0.30824500
C	1.75445500	-2.41139400	1.45702900
C	2.14247100	-2.81545900	2.80326200
H	2.65483800	-3.74434000	3.04607400
C	1.72692800	-1.81909900	3.66600100
H	1.83966900	-1.77035400	4.74834800
C	1.15902000	-0.75667600	2.84589600
C	-1.23305500	-1.25763800	-4.54984400
C	-2.56850700	-1.68019100	-4.83823900
C	-2.90892300	-2.11301900	-6.15245000
H	-3.92046500	-2.47078900	-6.34422800
C	-1.93164500	-2.09112700	-7.16639400
H	-2.20334300	-2.42950400	-8.17300900
C	-0.61857600	-1.63750400	-6.92631000
H	0.13855700	-1.61021400	-7.71154800
C	-0.27235200	-1.21460800	-5.61665300
C	-4.86091500	-2.10900500	-3.83544400
C	-5.71688800	-1.71934300	-2.66821000
H	-5.20346200	-1.30037500	-1.79340300
C	-6.96476000	-2.58561000	-2.38257500
H	-7.17469200	-2.80256700	-1.33135500
H	-7.12008500	-3.41529900	-3.08000400
C	-7.18683900	-1.17726200	-2.91434800
C	-7.69496000	-0.11325300	-1.95971500
C	-8.78315300	-0.38551400	-1.08941000
H	-9.20701700	-1.39717600	-1.06051400
C	-9.33164100	0.63304200	-0.27400600
H	-10.17162000	0.40595200	0.39346600
C	-8.79847300	1.94306000	-0.32101500
H	-9.22185000	2.73486500	0.30817200
C	-7.71206500	2.22506400	-1.18589100
H	-7.29131800	3.23579200	-1.22477000
C	-7.16600700	1.20424900	-1.99699200
H	-6.32373400	1.42827400	-2.66370000
C	-7.70720400	-0.98924000	-4.34774200
H	-8.81273400	-1.03954400	-4.34403100
H	-7.31462300	-1.76852700	-5.02083300
H	-7.41826900	0.00206900	-4.74506500
C	2.16450400	-0.64079900	-6.12517900
C	3.34242900	-0.01403300	-5.43228300
H	3.10506500	0.59968400	-4.55369800
C	4.54292600	0.45371100	-6.28112500
H	4.45853700	0.25127600	-7.35419400

H	4.99779300	1.41246900	-6.01173100
C	4.73097100	-0.75001000	-5.35757600
C	5.50658500	-0.55393600	-4.06752000
C	4.95675700	-0.95265100	-2.81979800
H	3.94231800	-1.37179000	-2.78731600
C	5.69255400	-0.79539900	-1.62168800
H	5.24598200	-1.08842500	-0.66365100
C	6.99689900	-0.24428500	-1.65464200
H	7.56230800	-0.10296300	-0.72651200
C	7.55827000	0.14326100	-2.89532700
H	8.56828200	0.56911100	-2.92826800
C	6.81842900	-0.01130100	-4.09157900
H	7.25257100	0.29792300	-5.05079400
C	4.88030700	-2.14463400	-5.98157300
H	5.93931800	-2.32331800	-6.24751400
H	4.26465600	-2.23854000	-6.89231800
H	4.57425900	-2.93118700	-5.26610600
C	2.60828300	-4.53541300	0.39904900
C	3.81677900	-4.73534100	-0.31446800
C	4.51253700	-5.97177000	-0.24934600
C	3.95294700	-7.00891900	0.54360700
H	4.47425100	-7.96711900	0.60088200
C	2.73799200	-6.84835400	1.26156300
C	2.07781600	-5.59458700	1.17845100
O	-3.00587800	1.88642700	6.27702500
O	5.00225100	0.96575000	6.39103000
N	0.57194600	1.51350100	1.03969600
N	-0.25021800	0.93949300	-1.52980100
N	-1.54828800	0.67348100	4.88980200
H	-1.48386600	0.15948400	4.00431900
N	3.34809100	0.91898400	4.71281600
H	3.20948500	0.81224100	3.70319600
C	0.85577900	0.53457400	3.33168600
C	0.68145700	1.61544100	2.44048100
C	0.77244300	3.01259200	2.83622500
H	0.84809200	3.35831500	3.86627000
C	0.77362100	3.76107400	1.67535800
H	0.83040700	4.84274100	1.56850900
C	0.60278600	2.83681200	0.56277800
C	0.35974300	3.24807700	-0.76544300
C	-0.15543600	2.33526700	-1.71045200
C	-0.66276000	2.70319100	-3.02605200
H	-0.66859700	3.71540300	-3.42399600
C	-1.11236300	1.54891000	-3.63301000
H	-1.54819800	1.42710800	-4.62389900
C	-0.79979400	0.44640400	-2.73218100

C	0.90235900	0.81778100	4.81139300
C	-0.31235000	0.93971600	5.55571800
C	-0.27705700	1.26525000	6.93922300
H	-1.21297500	1.38673600	7.48457000
C	0.96722500	1.44432600	7.57410400
H	0.99092300	1.68939000	8.64206700
C	2.18406400	1.31675300	6.87313900
H	3.14835400	1.44409800	7.36646700
C	2.15264600	1.01196400	5.48619500
C	-2.82562100	1.09199700	5.29831900
C	-3.96602800	0.52665600	4.49954800
H	-3.69858600	-0.01400100	3.58284800
C	-5.29926600	1.29473700	4.51293100
H	-5.87266200	1.36537600	3.58346500
H	-5.30626900	2.19202400	5.14094800
C	-5.25653900	-0.05243800	5.24602500
C	-5.94374600	-1.23137700	4.57846700
C	-6.54953500	-2.25216300	5.36482300
H	-6.48095600	-2.21426500	6.45629700
C	-7.25987000	-3.31822900	4.76506000
H	-7.71939200	-4.08650900	5.39867500
C	-7.38775200	-3.38944500	3.35901000
H	-7.95300600	-4.20615000	2.89438200
C	-6.77675500	-2.39095800	2.56243100
H	-6.86705600	-2.42117400	1.47033100
C	-6.05709100	-1.33360100	3.16116800
H	-5.58665800	-0.59442600	2.50172600
C	-5.28724000	-0.02424100	6.77556900
H	-6.33427600	0.00117000	7.13248100
H	-4.77011500	0.87071400	7.15478900
H	-4.79310400	-0.91351600	7.21079300
C	4.67682400	0.89405800	5.16190600
C	5.69223200	0.76395100	4.06263200
H	5.29859000	0.51184100	3.06960000
C	7.07224600	0.15824400	4.41915600
H	7.20935700	-0.08447100	5.47808000
H	7.49706300	-0.55790000	3.70802500
C	7.00474800	1.63631700	4.04805500
C	7.51224700	2.06191900	2.68214300
C	6.75018800	2.94145500	1.86767300
H	5.75547600	3.25940000	2.20597300
C	7.25882100	3.40694900	0.63335500
H	6.65684500	4.08059400	0.01242900
C	8.54445200	3.00383900	0.19664200
H	8.94044400	3.36688200	-0.75911600
C	9.31336300	2.12881700	1.00136100

H	10.31161300	1.81580300	0.67210600
C	8.79939400	1.66208400	2.23486000
H	9.39942200	0.98921900	2.86030700
C	7.23152000	2.69291800	5.13976000
H	8.31632700	2.87889400	5.25277900
H	6.82121200	2.35944700	6.10717200
H	6.75265900	3.65143300	4.86446000
C	0.65945200	4.66921400	-1.14771000
C	1.99798300	5.12091600	-1.03254200
C	2.36742700	6.44605500	-1.39177900
C	1.34756200	7.30858200	-1.85951500
H	1.60833600	8.33475100	-2.13699400
C	-0.01080500	6.89554300	-1.97902800
C	-0.33835400	5.56542600	-1.62154300
N	-1.41738300	-0.53422100	0.68052000
O	-3.76887200	-0.47519200	0.64995400
O	-2.56052400	1.55971700	0.61128800
C	-3.84179400	2.15774100	1.02785900
H	-4.68661700	1.57839000	0.61104700
H	-3.90833300	2.16311700	2.13247200
C	-3.93627400	3.60078700	0.54220000
Cl	-5.58006000	4.28944700	1.15602900
Cl	-2.58721200	4.67470400	1.23565200
Cl	-3.90850700	3.69227200	-1.32256000
C	-2.62329200	0.09750300	0.58866900
H	-4.50428200	-3.51291000	1.29939200
C	-4.36594500	-4.14975300	0.42012800
C	-4.03421500	-5.81951900	-1.85020400
C	-3.07857300	-4.24614100	-0.19686600
C	-5.45365500	-4.89147600	-0.07871600
C	-5.29758500	-5.72843000	-1.21408100
C	-2.93777900	-5.09536000	-1.34158100
H	-6.42705300	-4.83015000	0.42201500
H	-6.14962100	-6.30103900	-1.59846800
H	-1.95475000	-5.17667600	-1.82273000
H	-3.91045500	-6.45323700	-2.73547600
C	-1.88638000	-3.59285700	0.34022000
H	-0.94126300	-3.89326300	-0.13081600
C	-1.81998400	-2.68513000	1.39341100
H	-0.86352700	-2.48159900	1.87461400
H	-2.72264100	-2.37783800	1.93140500
H	1.13073300	-5.43436800	1.70730700
H	4.21564700	-3.90887900	-0.91499800
H	-1.37464100	5.22066300	-1.66728500
H	2.75746800	4.41482500	-0.67518100
C	-1.07218600	7.91105600	-2.48003000

C	3.84905300	6.88882400	-1.26220100
C	2.11300100	-7.98393000	2.11560000
C	5.84094900	-6.14255700	-1.03359300
C	-2.49371600	7.29163500	-2.56396500
H	-2.53061000	6.43789200	-3.26696600
H	-2.84996300	6.94241800	-1.57754100
H	-3.20753200	8.05428800	-2.92773000
C	-1.12725000	9.12533500	-1.49760700
H	-0.15131000	9.64024000	-1.42689500
H	-1.87531900	9.86304200	-1.84628400
H	-1.41310700	8.79676500	-0.48095900
C	4.06929600	8.36544100	-1.69274300
H	3.79615400	8.52929200	-2.75237800
H	3.48497100	9.06722300	-1.06783300
H	5.13794100	8.62782900	-1.57842600
C	4.30471500	6.74222600	0.22474200
H	3.70326000	7.39288400	0.88704600
H	4.19716300	5.70235100	0.58463000
H	5.36823000	7.03137300	0.32968400
C	4.73882100	5.97922400	-2.16887600
H	4.65100200	4.91245500	-1.89177600
H	4.44556800	6.07612900	-3.23104700
H	5.80277100	6.27138900	-2.07538300
C	-0.67664900	8.41823800	-3.90408700
H	0.31491500	8.90705100	-3.90845700
H	-0.64527300	7.58072800	-4.62632200
H	-1.41907200	9.15671400	-4.26294600
C	5.57943300	-5.90828000	-2.55590900
H	4.85990500	-6.64945400	-2.95228900
H	5.17480600	-4.89841200	-2.75116200
H	6.52504500	-6.00644100	-3.12274800
C	6.45763500	-7.55843100	-0.86117000
H	7.39378400	-7.62437200	-1.44646100
H	6.70846600	-7.77371400	0.19493800
H	5.77794800	-8.35091000	-1.22814700
C	2.96839700	-9.28096600	2.10313600
H	3.97916600	-9.11161500	2.52077600
H	2.47534700	-10.05198500	2.72425300
H	3.07607200	-9.69397300	1.08230800
C	0.69532200	-8.32909700	1.55587000
H	0.02196900	-7.45271100	1.57130300
H	0.76060600	-8.68799400	0.51145100
H	0.22785700	-9.12497900	2.16692700
C	6.87889100	-5.09149100	-0.52370900
H	6.52144000	-4.05669700	-0.67533600
H	7.08170900	-5.22985400	0.55509100

H	7.83292200	-5.20191900	-1.07414400
C	1.97809500	-7.50456100	3.59662600
H	2.96883700	-7.26162700	4.02499800
H	1.33956400	-6.60592300	3.68035900
H	1.52037600	-8.30092500	4.21434200

Intermediate D

Temperature: 298.15 Kelvin

G_corr: 1.800613 Hartree

H_corr: 2.116239 Hartree

S: 664.291 Cal/Mol-Kelvin

SCF: -8161.252813 Hartree

H: -8159.136574 Hartree

G: -8159.452200 Hartree

Cartesian Coordinates:

Co	-0.47124800	-0.00653000	-0.04213500
O	3.66755200	-3.72223200	4.13841900
O	-3.24842500	-1.32596200	7.32725700
N	-1.28640300	-1.38553200	1.08464700
N	-1.22376800	-0.87364300	-1.63937200
N	2.55239400	-1.67323100	3.88583100
H	2.49762100	-0.82677300	3.30984100
N	-2.00054900	-0.72838400	5.42001400
H	-2.06702300	-0.23922500	4.52170100
C	-0.13838700	-0.84043700	3.24015500
C	-0.90678400	-1.68596000	2.40736600
C	-1.56394000	-2.90744900	2.85295700
H	-1.42845000	-3.36097900	3.83374400
C	-2.38866700	-3.32287100	1.82403800
H	-3.04058100	-4.19430500	1.79184300
C	-2.18639400	-2.40522300	0.70918900
C	-2.67664700	-2.63583000	-0.59793500
C	-2.13875200	-1.94665500	-1.70898200
C	-2.33614600	-2.33820100	-3.09903500
H	-3.02520900	-3.11198900	-3.43171300
C	-1.48272700	-1.56917100	-3.86811000
H	-1.34666500	-1.58850300	-4.94865300
C	-0.82377300	-0.62932200	-2.96967700
C	0.22592200	-1.32556200	4.61943800
C	1.53047700	-1.84442400	4.87352900
C	1.82569900	-2.47456500	6.11091800
H	2.81621600	-2.90332000	6.27327900
C	0.82962900	-2.54747600	7.10489200
H	1.05696500	-3.03878300	8.05779400

C	-0.44782800	-1.97761400	6.91384100
H	-1.21470700	-2.01135800	7.68928300
C	-0.74670600	-1.35509200	5.67291000
C	3.62746200	-2.54707400	3.64382500
C	4.69176700	-1.98482100	2.75523200
H	4.48280400	-0.99317400	2.33589800
C	5.52120300	-2.93826300	1.86072600
H	5.70390900	-2.60848700	0.83355100
H	5.28981800	-4.00195200	1.97197100
C	6.23076600	-2.26369200	3.02358700
C	7.18532800	-1.11737100	2.74190000
C	8.07250400	-1.16050900	1.63434100
H	8.01648500	-1.99719000	0.92715100
C	9.03514400	-0.14066400	1.44020200
H	9.71385800	-0.19109200	0.58045700
C	9.12378100	0.93808000	2.35137600
H	9.86980500	1.72777600	2.20241500
C	8.23615000	0.99535600	3.45429500
H	8.29073500	1.83403700	4.15864000
C	7.27793000	-0.02493900	3.64695400
H	6.59408900	0.02461800	4.50413700
C	6.64988100	-3.11723700	4.23020100
H	7.63388800	-3.57888500	4.02269500
H	5.91143100	-3.90956800	4.43320000
H	6.75674200	-2.49536300	5.13874800
C	-3.15135400	-0.70690300	6.21961700
C	-4.26820600	0.11659500	5.64096200
H	-3.96916800	0.87513500	4.90643500
C	-5.45412100	0.48552000	6.55787500
H	-5.40072100	0.07044200	7.57007900
H	-5.84655700	1.50451600	6.47911800
C	-5.69691300	-0.49757900	5.41177700
C	-6.44813100	0.00040200	4.18975000
C	-5.86802600	-0.04389200	2.89451600
H	-4.83852500	-0.40612900	2.77610800
C	-6.59876500	0.38222500	1.76009600
H	-6.13222800	0.36429600	0.76790500
C	-7.92888800	0.84662800	1.90403600
H	-8.49190900	1.17729400	1.02365200
C	-8.51994800	0.88573000	3.19030600
H	-9.54920000	1.24498100	3.31002900
C	-7.78295100	0.46787300	4.32315900
H	-8.23817800	0.50916000	5.32092300
C	-5.94418200	-1.97633200	5.74167300
H	-7.01850000	-2.13850200	5.95040900
H	-5.36206700	-2.29021800	6.62489500

H	-5.66526100	-2.62056500	4.88650500
C	-3.67518200	-3.73958800	-0.80691500
C	-4.98779200	-3.61292300	-0.28560600
C	-5.95080100	-4.64222200	-0.46017000
C	-5.55510600	-5.81097600	-1.16369700
H	-6.28448500	-6.61216100	-1.30414000
C	-4.24524000	-5.97942800	-1.68607000
C	-3.31437800	-4.92516000	-1.49664500
O	4.33950200	0.85473000	-6.04282500
O	-3.56320000	1.94835500	-6.92644800
N	-0.05395400	1.55084100	-1.13329600
N	-0.05259400	1.01864100	1.56334800
N	2.56630800	0.15176800	-4.65996300
H	2.34868100	-0.23457500	-3.73421800
N	-2.20735100	1.29759900	-5.10692600
H	-2.24173800	1.09690300	-4.10339000
C	-0.07770100	0.49278200	-3.40771200
C	0.18999200	1.56233500	-2.52113700
C	0.55016800	2.90464900	-2.95668600
H	0.79629100	3.17546300	-3.98253800
C	0.46542300	3.72357300	-1.84828200
H	0.65619800	4.79334000	-1.78648900
C	0.12231600	2.88134300	-0.70790800
C	0.10352200	3.33630200	0.63136100
C	0.11816800	2.41039400	1.70012700
C	0.37967600	2.74059400	3.09598600
H	0.48946700	3.75020900	3.48495900
C	0.46242800	1.54980600	3.79309500
H	0.64501500	1.39893100	4.85709700
C	0.15022900	0.48503200	2.84822200
C	0.16360100	0.70192800	-4.88411100
C	1.46186900	0.55880000	-5.47352700
C	1.64115100	0.80135500	-6.86578400
H	2.63782700	0.70458400	-7.29459400
C	0.54434000	1.19503200	-7.65475500
H	0.69685300	1.38095100	-8.72408400
C	-0.74104500	1.36541700	-7.10379900
H	-1.59171500	1.68753500	-7.70608400
C	-0.93129200	1.11951400	-5.71920200
C	3.93493300	0.29408800	-4.97271200
C	4.88620200	-0.23617700	-3.93932100
H	4.44384600	-0.56111300	-2.99014200
C	6.28076900	0.44503100	-3.87748800
H	6.70006100	0.64331600	-2.88546800
H	6.45103300	1.21699500	-4.63592000
C	6.19302000	-1.00236500	-4.36390300

C	6.69894600	-2.08251500	-3.42002600
C	8.10493800	-2.25236900	-3.27781100
H	8.78340600	-1.57109500	-3.80756800
C	8.63558300	-3.27843900	-2.46402100
H	9.72224900	-3.39495200	-2.36955900
C	7.76412700	-4.15758400	-1.77322700
H	8.17092700	-4.95865600	-1.14427400
C	6.36480300	-3.99038200	-1.89881700
H	5.68085500	-4.66046200	-1.36504100
C	5.83655900	-2.96063500	-2.71581300
H	4.75140300	-2.83369000	-2.78971900
C	6.45852100	-1.31621300	-5.84392400
H	7.54514300	-1.43790200	-6.01351400
H	6.08453800	-0.50864400	-6.49389400
H	5.96558100	-2.26356700	-6.13332400
C	-3.42749000	1.65615600	-5.69449000
C	-4.58098500	1.66245300	-4.72843200
H	-4.42251100	1.11104700	-3.79278100
C	-6.01191500	1.61506900	-5.31126300
H	-6.06494800	1.62964000	-6.40514500
H	-6.73443300	0.96672000	-4.80496700
C	-5.54691600	2.89606700	-4.61759100
C	-6.09791700	3.19700900	-3.23490300
C	-5.24620900	3.32730100	-2.10684700
H	-4.16796600	3.15976100	-2.22448700
C	-5.77300700	3.66495800	-0.83751100
H	-5.10556900	3.74866300	0.02860400
C	-7.16234500	3.88843600	-0.68027800
H	-7.56928300	4.15103000	0.30314900
C	-8.02037900	3.76635100	-1.80079200
H	-9.09767900	3.93810200	-1.68756600
C	-7.49085600	3.42139800	-3.06611000
H	-8.15787400	3.31924000	-3.93158200
C	-5.27971300	4.14714200	-5.46713200
H	-6.22359900	4.70331700	-5.62164400
H	-4.86264400	3.87524100	-6.45144000
H	-4.56911200	4.82379000	-4.95611600
C	0.11570600	4.81352900	0.89752300
C	-0.93248400	5.61171200	0.37452500
C	-0.98184400	7.01488300	0.60168800
C	0.05854400	7.59558900	1.36616400
H	0.04047000	8.67447600	1.55060100
C	1.13494200	6.82991600	1.89974200
C	1.14660100	5.43650500	1.65597200
N	1.21191800	-1.01516100	-0.23567300
O	3.32265200	-1.15467300	-1.27725300

O	2.73194900	0.79793800	-0.12566000
C	4.13185800	1.15785300	-0.42666300
H	4.80832000	0.34201500	-0.11348600
H	4.27264400	1.33388800	-1.50854300
C	4.51960000	2.43217200	0.32115500
Cl	6.36057300	2.67942700	0.04854900
Cl	3.64200500	3.93248700	-0.33777400
Cl	4.20083900	2.28461400	2.15290800
C	2.43405700	-0.52443100	-0.59830600
H	2.19633200	-4.50630700	-2.12970400
C	2.56148100	-5.10139300	-1.28552800
C	3.54031800	-6.64921300	0.88564300
C	2.43620900	-4.58845200	0.05845300
C	3.15564000	-6.35237600	-1.52527300
C	3.64484100	-7.13812000	-0.44548400
C	2.95538900	-5.39725100	1.13939700
H	3.24732600	-6.72379300	-2.55255500
H	4.10325000	-8.11457500	-0.64009700
H	2.88193500	-5.02528300	2.16915700
H	3.91931700	-7.24951300	1.72062700
C	1.78630200	-3.35426900	0.36539300
H	1.73553700	-3.04492100	1.41909100
C	1.04921300	-2.47150800	-0.59898400
H	-0.02703600	-2.70137500	-0.53568200
H	1.36181100	-2.65068100	-1.64589500
H	-2.28645200	-5.02431300	-1.86487100
H	-5.25273700	-2.69311200	0.25015500
H	1.97781600	4.82333600	2.01233200
H	-1.72493200	5.12104200	-0.20343200
C	2.25218700	7.54259500	2.70742900
C	-2.15323500	7.84477200	0.01151800
C	-3.80022400	-7.26511200	-2.43376700
C	-7.38231300	-4.45702200	0.10971600
C	3.32780200	6.55340200	3.23480200
H	2.89222700	5.79336900	3.91128200
H	3.84439800	6.02829400	2.41040000
H	4.09185900	7.11144200	3.80759000
C	2.96149500	8.59035900	1.79018400
H	2.25150600	9.34578500	1.40589200
H	3.74960000	9.12272300	2.35690200
H	3.43447100	8.09555900	0.92143500
C	-2.04436200	9.35577600	0.35628400
H	-2.06843400	9.52986000	1.44882800
H	-1.11798500	9.80504500	-0.04945200
H	-2.90033600	9.89755500	-0.08774500
C	-2.15688400	7.69759100	-1.54395600

H	-1.21844500	8.08958500	-1.97958800
H	-2.26065300	6.64190500	-1.85494200
H	-3.00340200	8.26261000	-1.97914500
C	-3.50568300	7.31080400	0.58276100
H	-3.66533400	6.24723000	0.32810600
H	-3.53290200	7.40615500	1.68458000
H	-4.35174700	7.88715800	0.16186600
C	1.61952700	8.27589900	3.93350200
H	0.87302400	9.02963500	3.62233300
H	1.11492600	7.55700000	4.60628100
H	2.40582200	8.79788700	4.51191200
C	-7.30259500	-4.22742500	1.65274600
H	-6.84499600	-5.09869100	2.15854600
H	-6.70647500	-3.33124200	1.90369700
H	-8.31806400	-4.07958100	2.06742300
C	-8.29162300	-5.68979700	-0.15159900
H	-9.29222800	-5.50655900	0.28280500
H	-8.42740700	-5.87954100	-1.23342900
H	-7.88697000	-6.60721600	0.31659600
C	-4.95051100	-8.30036100	-2.57609000
H	-5.80406100	-7.89174500	-3.14963900
H	-4.57866700	-9.19009800	-3.11811300
H	-5.32143100	-8.64092400	-1.59087900
C	-2.63172900	-7.93956700	-1.64538400
H	-1.76555400	-7.26173600	-1.53739700
H	-2.95963600	-8.23400600	-0.63082400
H	-2.28851500	-8.84813000	-2.17653000
C	-8.04592200	-3.21138000	-0.56100900
H	-7.47087600	-2.28855200	-0.36405900
H	-8.11647900	-3.34453400	-1.65709400
H	-9.06752500	-3.06338400	-0.16130700
C	-3.30504900	-6.88880000	-3.86700300
H	-4.11670400	-6.41963000	-4.45457100
H	-2.45497900	-6.18272800	-3.83524100
H	-2.96959000	-7.79649000	-4.40453800

Intermediate E

$E_{[\text{Co}(\text{II})\text{P5}]} = A_{[\text{Co}(\text{II})\text{P5}]}$

$A_{\text{P5-Aziridine}}$:

Temperature: 298.15 Kelvin

G_{corr} : 0.139530 Hartree

H_{corr} : 0.205668 Hartree

S: 139.199 Cal/Mol-Kelvin

SCF: -2011.337842 Hartree

H: -2011.132174 Hartree

G: -2011.198312 Hartree

Cartesian Coordinates:

H	-5.19999100	-2.51519800	1.35076400
C	-4.78559500	-1.72341100	0.71595200
H	-6.29845500	-1.95207200	-0.84076100
C	-5.40374800	-1.40719700	-0.51789100
C	-3.62794200	-1.02378200	1.12860500
H	-3.14904700	-1.27676000	2.08353700
C	-4.85448900	-0.39098100	-1.33824500
H	-2.78301100	2.85777300	0.65128600
C	-3.08085200	0.00164500	0.31401600
H	-5.32263900	-0.15217700	-2.30038700
C	-1.88258700	2.30869200	0.94554400
C	-3.69892400	0.31024700	-0.92565700
H	-1.28683100	2.75732300	1.75028400
C	-1.87781600	0.75783200	0.79656800
H	-1.24736100	0.22499800	1.52166900
H	-3.25074600	1.07963200	-1.56534700
N	-1.15299100	1.64372400	-0.15421500
C	0.19398500	1.72884300	-0.45132000
O	0.89031600	2.76866200	-0.51306900
O	0.67502600	0.42219200	-0.78402900
C	2.09067700	0.34415200	-1.14821200
H	2.15563200	-0.17028900	-2.12188700
Cl	2.18860900	-2.21249700	0.02703200
H	2.52617000	1.35908700	-1.20817000
Cl	2.79947300	0.32766300	1.57296000
C	2.86374000	-0.48233000	-0.10474500
Cl	4.64637600	-0.57325300	-0.67954400

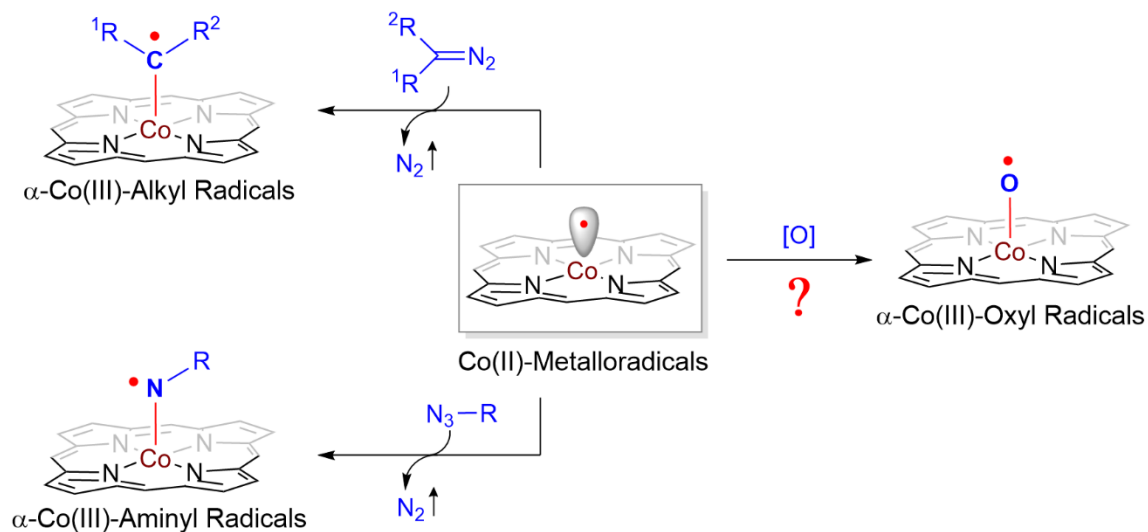
**3. CHAPTER 3: GENERATION AND CHARACTERIZATION OF
UNPRECEDENTED α -Co(III)-OXYL RADICALS BY METALLORADICAL
ACTIVATION OF OXYGEN RADICAL PRECURSORS**

3.1 INTRODUCTION

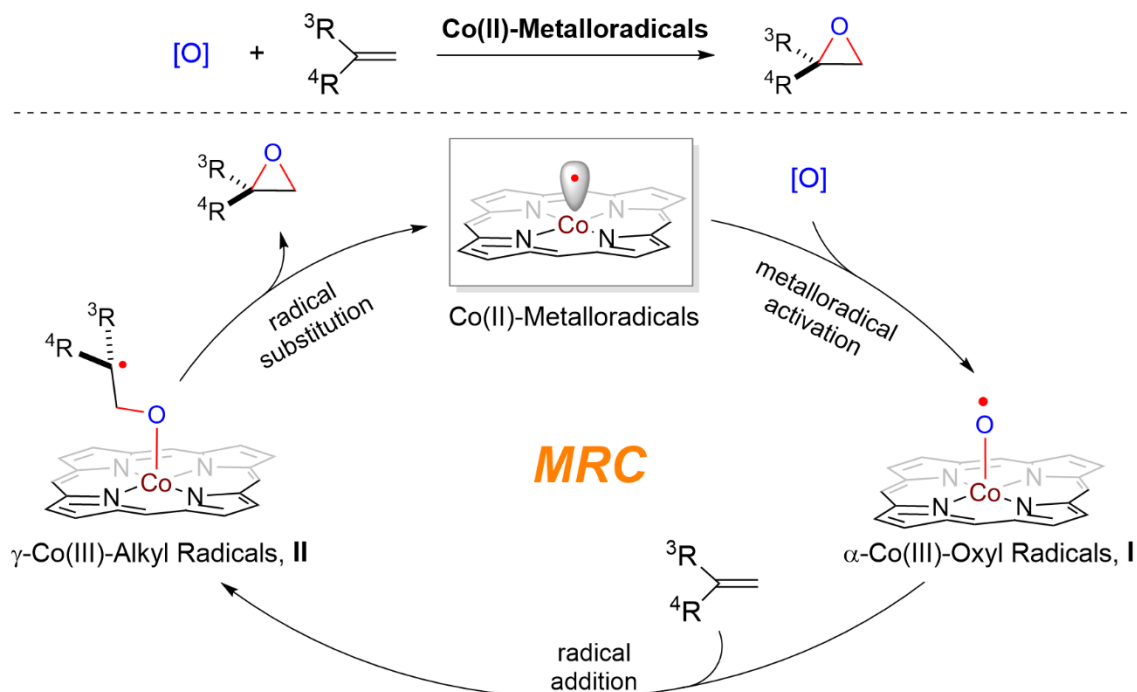
As mentioned in Chapters 1 and 2, cobalt(II) complexes of porphyrins [Co(Por)] have been shown to homolytically activate diazo compounds and organic azides for the formation of α -Co(III)-alkyl radicals and α -Co(III)-aminyl radicals, respectively (Scheme 3.1A). While these distinctive cobalt-bound organic radicals have been successfully utilized for stereoselective formation of C–C and C–N bonds, the generation of the analogous α -Co(III)-oxyl radicals **I** and related catalytic applications for C–O bond formation, such as olefin epoxidation (Scheme 3.1B), have remained to be realized. Relevant questions to address this unsolved problem include: i) what type of common oxygen-containing compounds could be homolytically activated by Co(II)-metalloradicals [Co(Por)] and might lead to generation of the largely unknown cobalt-bonded oxygen-centered radicals? ii) Would this class of unprecedented α -Co(III)-oxyl radicals be stable enough for detection and characterization? iii) Regarding the catalytic application, could the metal-stabilized oxygen-centered radicals act as competent intermediates to undergo radical reactions?

Scheme 3.1| Generation of Cobalt-Bound Organic Radicals and Catalytic Applications for Selective Radical Reactions

A. Generation of α -Metallorganic Radicals by Metalloradical Activation



B. Catalytic Radical Olefin Epoxidation Involving α -Co(III)-Oxyl Radicals



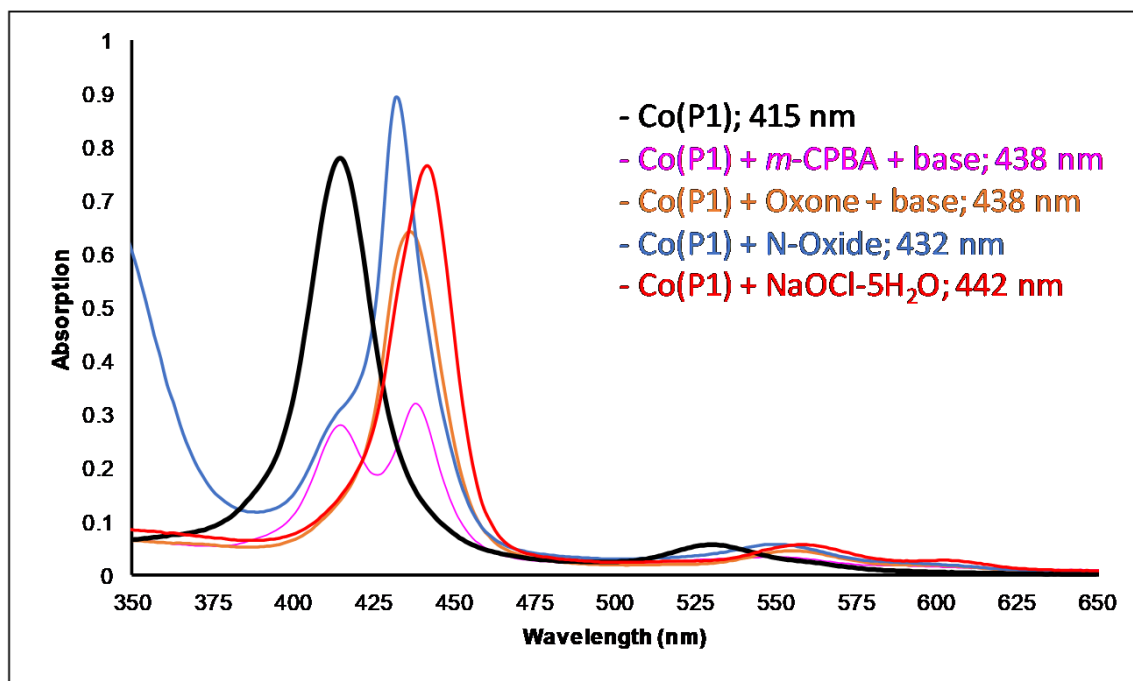
Oxidation reactions, such as olefin epoxidation and C–H hydroxylation, play crucial roles in many important biological processes⁵⁰ and represent cornerstones for chemical transformations in organic synthesis.⁵¹ Terminal oxo complexes ($M^{n+1}=O$) of transition metals have been widely demonstrated as key reactive intermediates in both biological and chemical oxidation processes.^{50d,52} Although they are often postulated as resonance structures of metal-oxo complexes, the electronically equivalent metal-oxyl radicals ($M^n-O\cdot$) have not been well established as genuine intermediates in catalytic oxidations, except in some cases with indirect evidence or on the basis of computational studies.⁵³ While the formation of the cobalt superoxo ($Co-O-O\cdot$) radicals has been well documented,^{52c,54} there are only few reports on cobalt catalysts in oxidation reactions that invoke the putative α -Co(III)-oxyl radical ($Co-O\cdot$) intermediate.⁵⁵ In those examples, where the radical species is proposed to explain side products or as potential active species based on calculations, however, no direct evidence was reported. Understanding the generation and characteristics of this ill-defined reactive intermediate is pivotal for the development of catalytic systems that are capable of unequivocally generating metal-supported oxyl radicals and potentially perform intrinsically difficult selective oxidations. To this end, we embarked on the investigation of potential oxygen radical precursors and analyzed its interplay with metalloradicals [Co(Por)] experimentally and computationally. Herein we report the results of this investigation, where three experimental parameters were chosen to study the interaction between [Co(Por)] and oxidants: i) UV-Vis spectroscopy, where changes in the absorption might be indicative of new species and/or oxidation state; ii) EPR, where new radical species can be detected; and iii) HRMS, where new species can be characterized based on mass.

3.2 RESULTS AND DISCUSSION

3.2.1 Initial Investigation

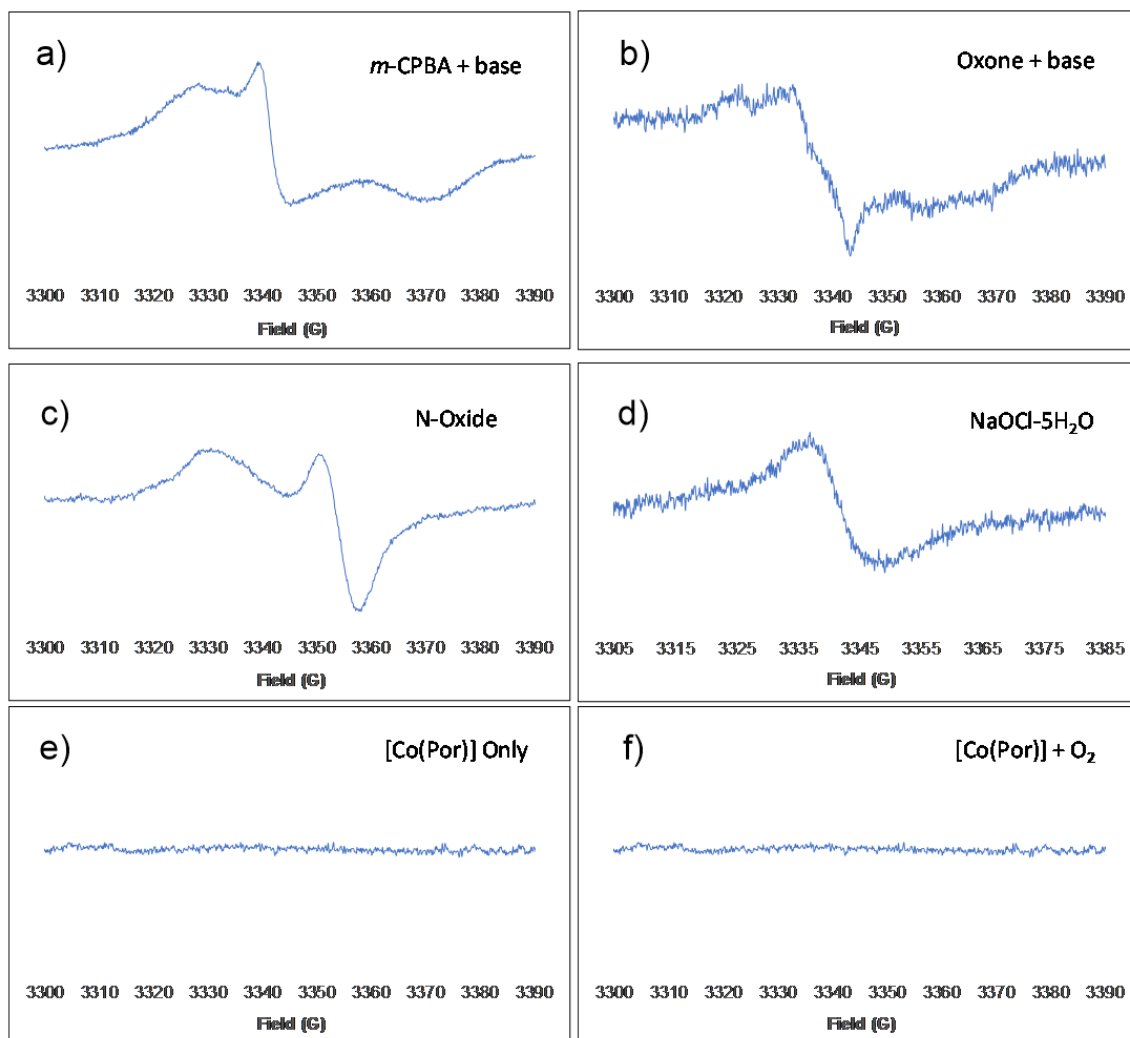
At the outset of our investigation, we focused our efforts on identifying suitable oxygen compounds as potential radical precursors that could be homolytically activated by Co(II)-metalloradicals [Co(Por)] for the generation of the desired α -Co(III)-oxyl radicals. Among common oxygen sources evaluated, changes in the UV-Vis (ultraviolet-visible spectroscopy) (Figure 3.1) and characteristic peaks in EPR (electron paramagnetic resonance spectroscopy) (Figure 3.2) studies indicated that *m*-CPBA (*meta*-chloroperoxybenzoic acid), Oxone (potassium peroxymonosulfate), PNO (pyridine-N-oxide) and NaOCl (sodium hypochlorite) could be activated by [Co(Por)] (See Experimental Section for details). Considering its commercial availability at low cost and the lack of organic components that could engage in further reactivity, sodium hypochlorite pentahydrate (NaOCl·5H₂O; hereafter abbreviated as NaOCl) was selected as the oxygen radical precursor of choice for subsequent detailed studies.

Figure 3.1| UV-vis Spectrum of [Co(P1)] only and [Co(P1)] Exposed to Different Oxygen Radical Precursors



Previous studies on the characterization of Co(II) porphyrins have established that the UV-vis spectra of these species consist of a Soret band ($\lambda \sim 400\text{nm}$) and a Q band ($\lambda \sim 500\text{nm}$).^{8b,56} One electron oxidation of the cobalt center from [Co(II)Por] to [Co(III)Por] is known to produce characteristic redshift of the Soret and Q bands.^{8b,56} Consistent with the aforementioned previous reports, the UV-vis spectrum (Figure 3.1) shows how the original Co(II) porphyrin undergoes a redshift of the Soret and Q bands upon mixing with different oxygen radical precursors. This change is indicative of potential interaction between the [Co(II)Por] and the oxidant, consistent with a one electron oxidation at the cobalt center. These experiments were carried out in an acetonitrile solution under nitrogen, using 1 equivalent of oxidant and 2 mol % of [Co(Por)]. See Experimental Section for details.

Figure 3.2| EPR Spectrum of [Co(TPP)] only and [Co(TPP)] Exposed to Different Oxygen Radical Precursors



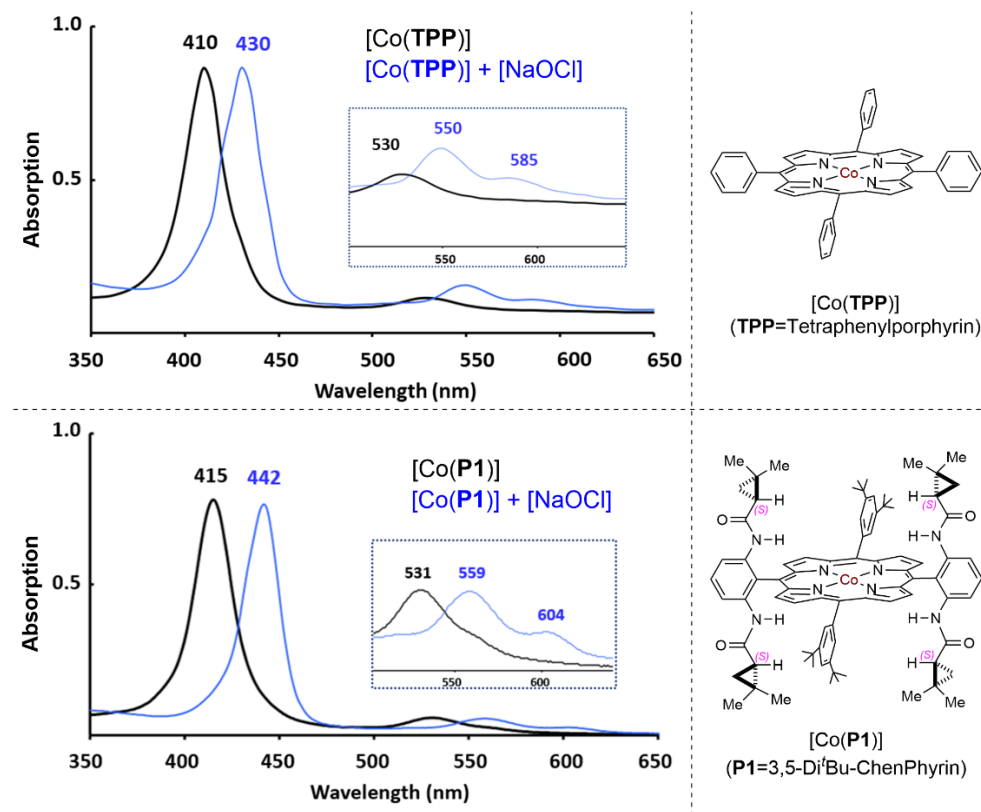
While it is known that Co(II) porphyrins are EPR silent at room temperature,⁷ EPR experiments shows how the originally EPR silent spectrum of Co(II) porphyrin (Figure 3.2 e) displays broad peaks upon mixing with different oxygen radical precursors, indicating the formation of a new radical species. Spectra were collected at room temperature with benzene as solvent, using 1 equivalent of oxidant and 2 mol % of [Co(Por)]. See Experimental Section for details.

3.2.2 Characterization Studies of α -Co(III)-Oxyl Radicals with NaOCl

3.2.2.1 UV-Vis Spectroscopy

When NaOCl was added into a solution of Co(II)-metalloporphyrin [Co(TPP)] in acetonitrile, significant bathochromic shifts of Soret (from 410 nm to 430 nm) and Q bands were observed by UV-Vis as fast as 10 seconds after mixing (Figure 3.3: top). Similarly fast bathochromic shifts of Soret (from 415 nm to 442 nm) and Q bands were observed by UV-Vis with the use of Co(II) complex of D_2 -symmetric chiral amidoporphyrin [Co(P1)] (Figure 3.3: bottom). This characteristic change in the optical absorption spectra is in agreement with the reported redshifts associated with one-electron oxidation of Co(II) to Co(III) in the metalloporphyrins.^{8b,56}

Figure 3.3| UV-Vis Studies on Activation of NaOCl by [Co(Por)]

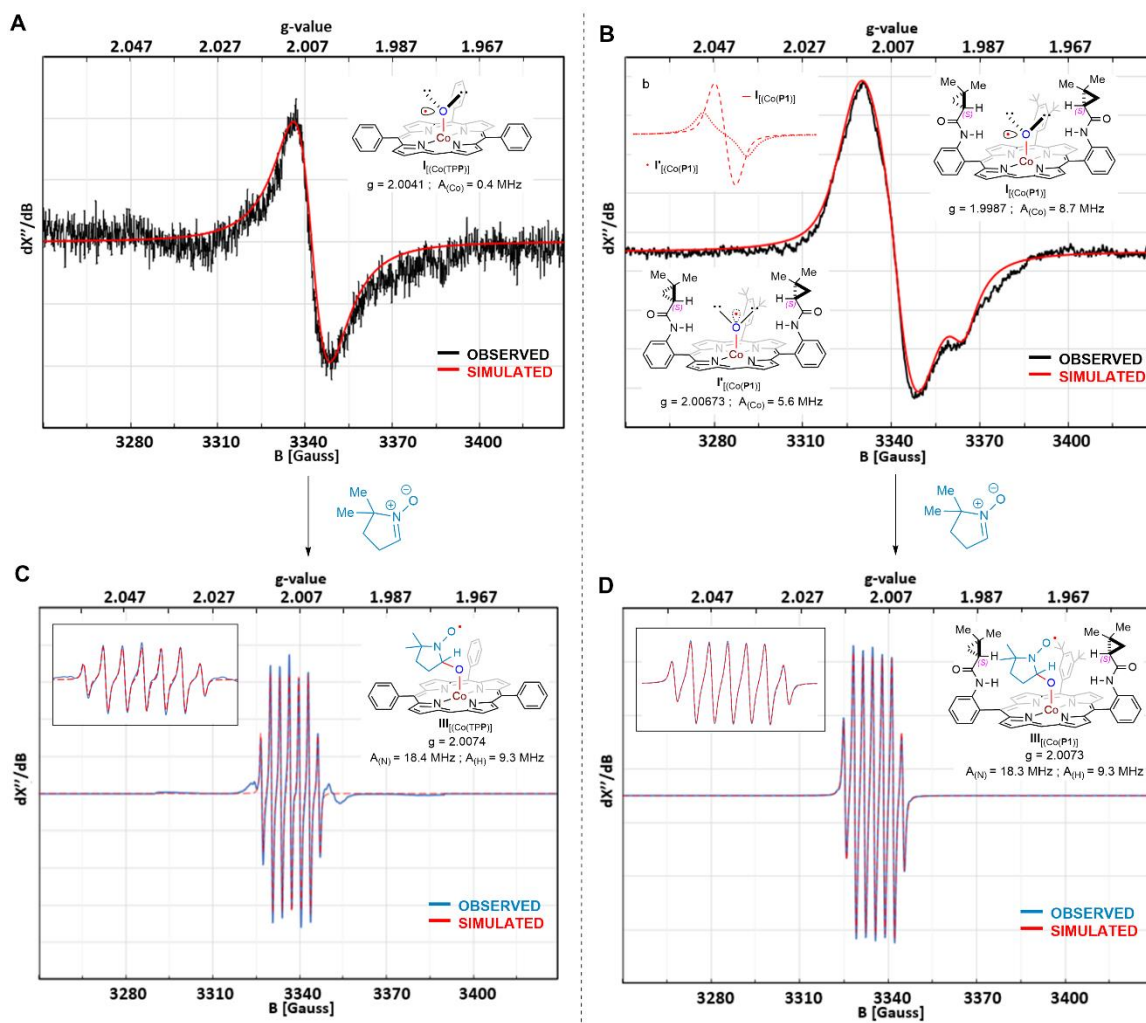


3.2.2.2 Electron Paramagnetic Resonance (EPR)

While [Co(Por)] are EPR silent at room temperature (Figure 3.2(e)),⁷ the EPR spectrum of the reaction mixture between [Co(TPP)] and NaOCl at room temperature showed a diagnostic broad peak, which could be simulated to the corresponding cobalt-supported oxygen-centered radical using SpinFit software on the basis of hyperfine coupling by ⁵⁹Co ($I = 7/2$) (Figure 3.4A; see Experimental Section for details). A similar phenomenon was observed when the experiment was repeated with catalyst [Co(P1)] (Figure 3.4B). The observed diagnostic peak could be simulated using two different radical species, attributed to a different orientation of the radical containing p-orbital. As shown in Figure 3.4b, two different species contribute to the observed signal and simulation of a single species without the other would not afford a fitting simulation. The presence of EPR signal confirms the formation of a new radical species. In both instances (Figure 3.4A and B), the observed isotropic g value of 2.00 is consistent with the formation of organic radical $I_{[Co(Por)]}$ upon spin translocation from the Co(II) to the O-atom during metalloradical activation of NaOCl. It is noteworthy that control experiments in the absence of [Co(Por)] showed no EPR signal, and when [Co(Por)] were exposed to oxygen in the absence of other species under the same reaction conditions, no signal was observed either (Figure 3.2(f)). These data points along with control experiments strongly suggest the formation of a new radical species upon the reaction of [Co(Por)] with NaOCl. To further investigate the nature of the newly-formed radical, we used spin trapping reagent 5,5-dimethyl-1-pyrroline N-oxide (DMPO). As shown in Figure 3.4C and 3.4D, the diagnostic signals associated with α -Co(III)-oxyl radicals (Figure 3.4A and 3.4B), changed drastically upon addition of trapping reagent DMPO. These changes are attributed to the trapping of the metal-

supported oxyl radicals. In both cases (Figure 3.4C and 3.4D), the new signals observed upon addition of DMPO could also be fittingly simulated using SpinFit software as new species **III** based on hyperfine coupling by both ^{14}N ($I = 1$) and ^1H ($I = 1/2$) (See Experimental Section for details).

Figure 3.4| EPR Studies on Activation of NaOCl by Co(II)-Metalloradicals [Co(Por)]

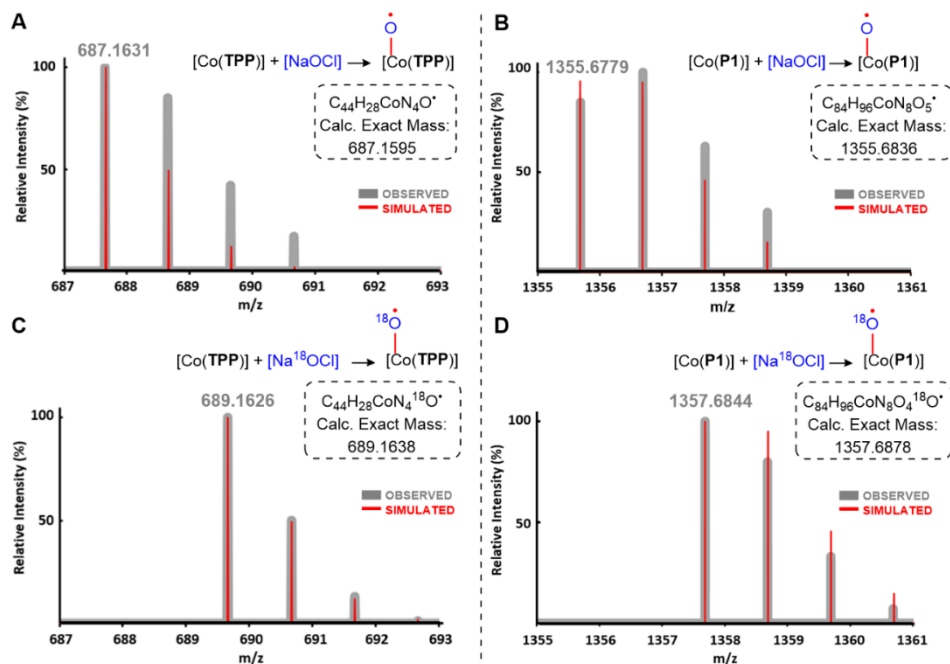


3.2.2.3 High Resolution Mass Spectrometry

Although the UV-vis and EPR spectroscopy results hint a desired interaction between the Co(II) porphyrin and the oxygen radical precursor, they do not provide enough

information about the exact nature of the new radical species. To gain further insight into the nature of the putative reactive intermediates **I** observed by UV-Vis and EPR, we analyzed the interaction of NaOCl and cobalt(II) porphyrins [Co(TPP)] and [Co(**P1**)] by high resolution mass spectrometry (HRMS) (Scheme 3.2; see Experimental Section for details). Notably, the desired α -Co(III)-oxyl radicals were observed as indicated by the characteristic peak in the DART-TOF analysis of the *in situ*-generated mixture of NaOCl with [Co(TPP)] (Scheme 3.2A), and with [Co(**P1**)] (Scheme 3.2B), and its observed isotopic distribution could be fittingly matched with the simulations. To further verify that the new species was generated by the interaction of the [Co(Por)] with NaOCl and rule out other possibilities, the same HRMS experiments were repeated using isotopically labeled Na¹⁸OCl. We were pleased to observe that the desired species containing the incorporated isotope were detected, and the observed isotopic distributions could also be well matched with their simulations (Scheme 3.2C and 3.2D).

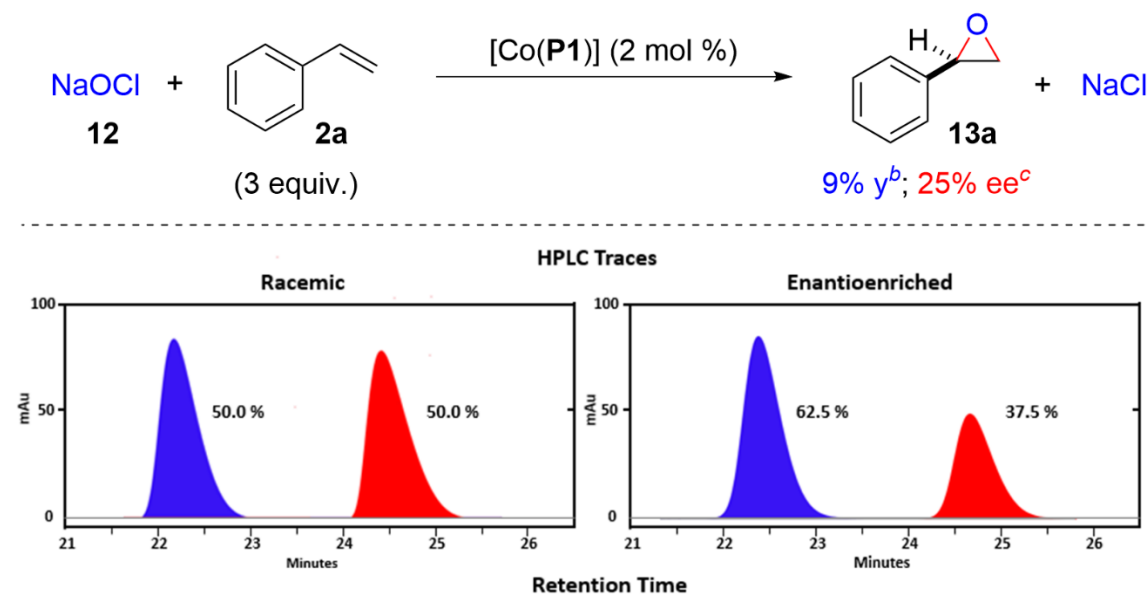
Scheme 3.2| Characterization of α -Co(III)-Oxyl Radicals by Mass Spectrometry



3.2.2.4 Reactivity Towards Epoxidation

Encouraged by the characterization data obtained, we then envisioned that if present in the reaction mixture, the α -Co(III)-oxyl radical could participate in enantioselective radical epoxidation reactions as proposed in the catalytic cycle in Scheme 3.1B. To test the hypothesis, we proceeded with the epoxidation of styrene as a proof-of-concept model reaction (Scheme 3.3). While [Co(TPP)] failed to afford styrene oxide product **13a**, when chiral amidoporphyrin [Co(**P1**)] was exposed to NaOCl in the presence of styrene, the corresponding epoxide **13a** was obtained in low yields but with a noticeable degree of enantioselectivity (Scheme 3.3). It is important to note that only trace amount of product was observed in the absence of any [Co(Por)] under identical reaction conditions. Despite the low yield and enantioselectivity, these results support the involvement of the chiral [Co(**P1**)] in the epoxidation reaction and hence, further bolster the hypothesis instigated by EPR, UV-vis, and HRMS characterization studies of the new radical species. Furthermore, these results show how the new species α -Co(III)-oxyl radicals are relevant to catalytic epoxidation reactions. We envision that the right ligand design and conditions optimization will render this challenging reaction highly efficient and selective.

Scheme 3.3| Relevance of the New α -Co(III)-Oxyl Radicals to Catalytic Radical Epoxidation^a



^aCarried out with NaOCl·5H₂O (**12**; 0.2 mmol) and alkene **2a** (1.0 mmol) in the presence of 4 Å molecular sieves (50 mg) using [Co(**P1**)] (2 mol %) under N₂ atmosphere in acetonitrile (0.5 mL) at -10 °C for 24 h. ^bIsolated yield. ^cEnantiomeric excess (ee) determined by chiral HPLC.

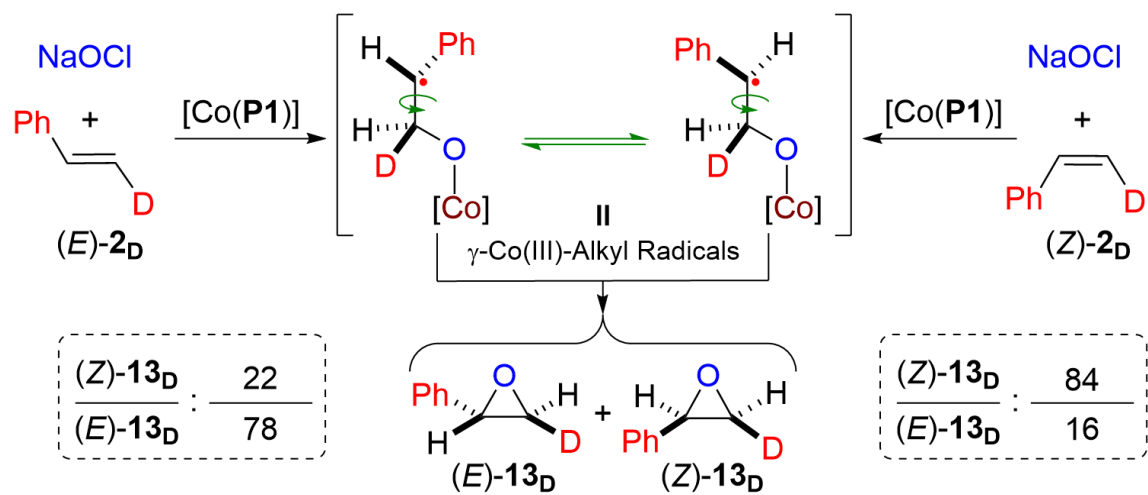
3.2.2.5 Isotope Labeling studies

Deuterostyrenes

To gain more insight on the mechanism of this new radical epoxidation reaction, we explored the epoxidation of both isotopomers of β -deuterostyrenes (*E*)-**2D** and (*Z*)-**2D** (Scheme 3.4). While concerted mechanisms associated with metal-oxo complexes are usually stereospecific, a radical stepwise mechanism as proposed in Scheme 3.1B could result in the formation of different stereoisomers due to the rotation of the β -C-C bond in the γ -Co(III)-alkyl radical (intermediate **II**, Scheme 3.1B, 3.4) before ring closure. When (*E*)-**2D** was used in the presence of catalyst [Co(**P1**)], both (*Z*)-**13D** and (*E*)-**13D** products

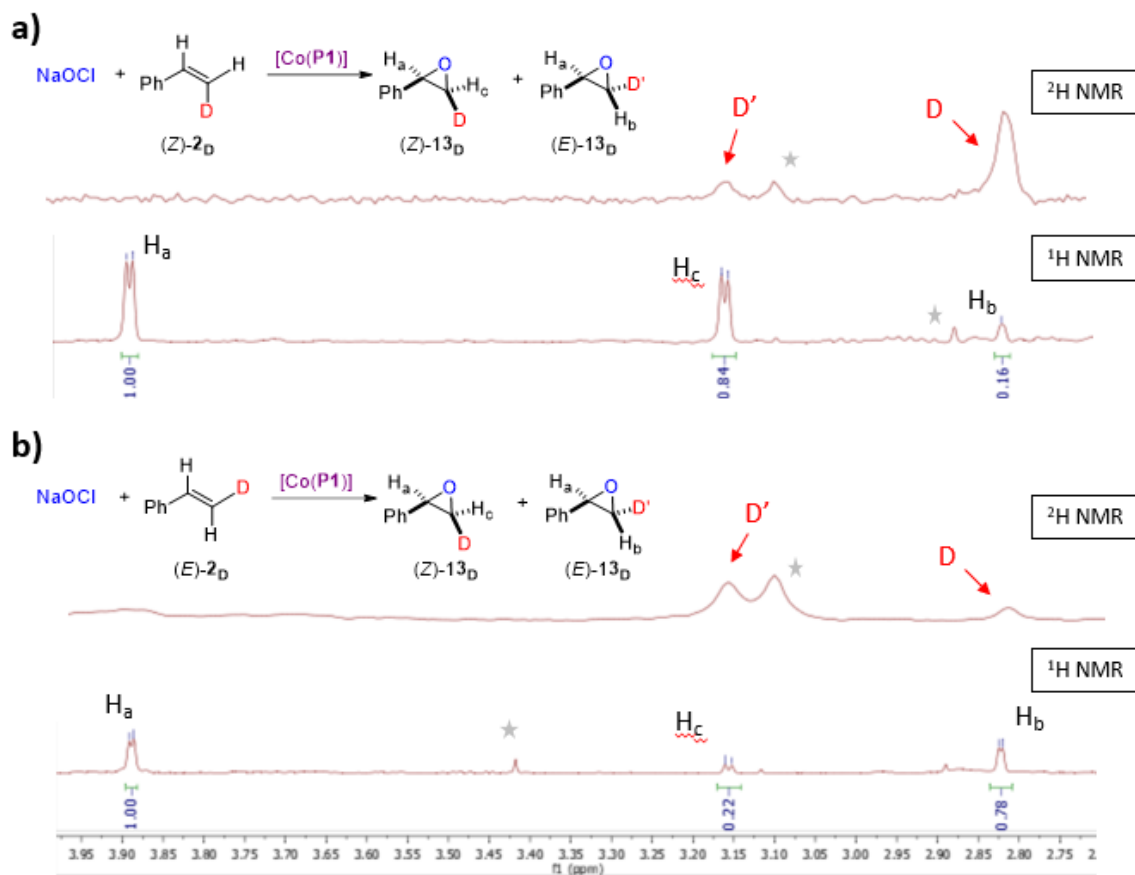
were observed with an isotopomer ratio of 22:78. Under the same conditions, epoxidation of (*Z*)-**2_D** yielded an 84:16 (*Z*)-**13_D** to (*E*)-**13_D** product ratio (Scheme 3.4 and 3.5). It is worth mentioning that no erosion of the original isomeric purity was observed in the recovered starting materials (*E*)-**2_D** and (*Z*)-**2_D** after the reaction. The observation of (*Z*)-**13_D** from isomerically pure (*E*)-**2_D** along with the observation of (*E*)-**13_D** from isomerically pure (*E*)-**2_D** suggests rotation around the β-C–C bond in the γ-Co(III)-alkyl radical intermediate **II** before ring closure. These observations are in sound agreement with the putative stepwise radical mechanism proposed (Scheme 3.1B) and are further consistent with the previous characterization studies supporting the existence of the new α-Co(III)-oxyl radical.

Scheme 3.4| Epoxidation of (*E*)- or (*Z*)-β-Deuterostyrenes to Probe Radical Mechanism^a



^aCarried out with NaOCl·5H₂O (**12**; 0.2 mmol) and **2_D** (1.0 mmol) using [Co(P1)] (2 mol %) in the presence of 4 Å molecular sieves (50 mg) under N₂ atmosphere in acetonitrile (0.5 mL) at room temperature for 16 h. (*Z*)-**13_D**:(*E*)-**13_D** ratio determined by ¹H-NMR and ²H-NMR analysis of crude reaction mixture; see Scheme 3.5.

Scheme 3.5| Upfield ^2H NMR and ^1H NMR for Epoxide Isomers 13_{D} from $[\text{Co}(\text{P1})]$ -Catalyzed Epoxidation between: a) NaOCl (12) and (Z) - β -Deuterostyrene ((Z) - 2_{D}); b) NaOCl (12) and (E) - β -Deuterostyrene ((E) - 2_{D})



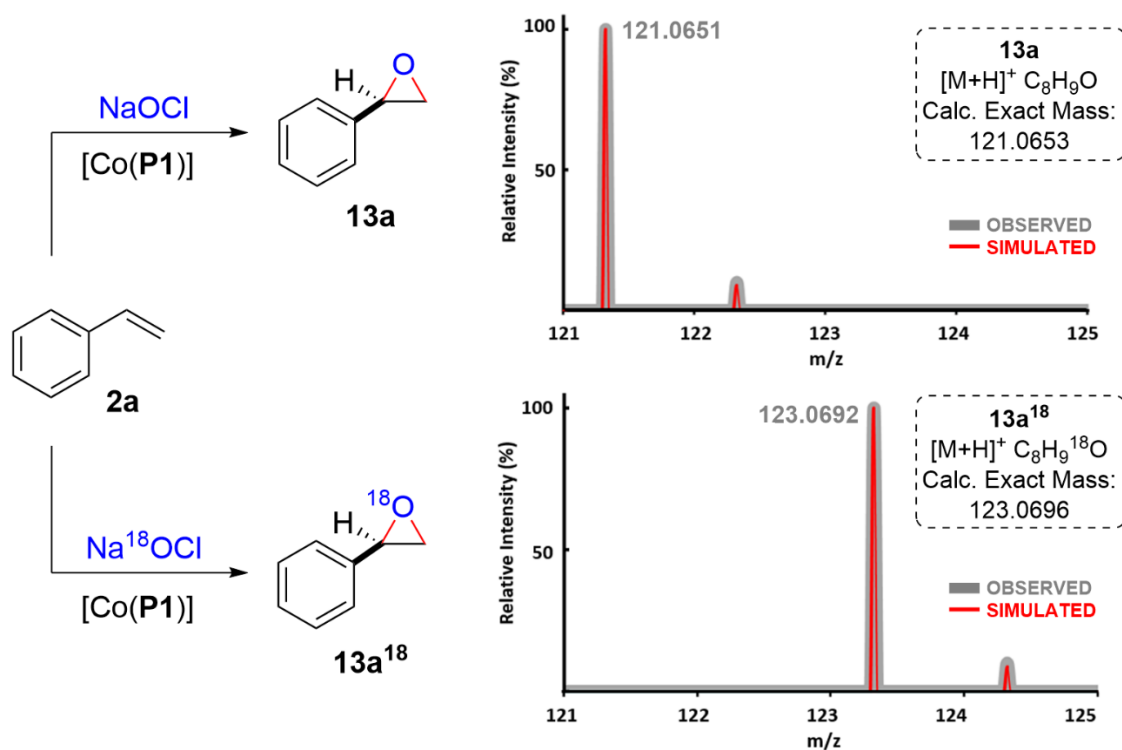
★ Indicates impurity in crude ^1H NMR.

Oxygen 18 Labeled NaOCl

The results obtained by HRMS studies (Scheme 3.2D) of isotopically labeled Na^{18}OCl demonstrated the involvement of the oxidant in the generation of the new radical species. To further test the involvement of the species detected by HRMS in the epoxidation reaction, we used isotopically labeled Na^{18}OCl as oxygen radical precursor for the

epoxidation of styrene. We were pleased to see that isotopically labeled ^{18}O styrene oxide was obtained in 5% yield as confirmed by HRMS (Scheme 3.6).

Scheme 3.6| Oxygen Isotope Labeling Epoxidation: Characterization by HRMS^a



^aSee Experimental Section for experimental procedures details.

3.2.2.6 Computational Studies

Activation Mechanism

In an effort to shine some light into the specific mechanism of the formation of the new α -Co(III)-oxyl radical, with the help of Hao Xu as computational chemist, we carried out DFT calculations on the activation of NaOCl by [Co(Por)] (Por = porphyrin core only, see Experimental Section for details) (Scheme 3.7). Calculations were carried out with the

Gaussian 09⁴⁴ at unrestricted level of B3LYP^{47,57} functional coupled with mixed basis set. The mixed basis set was defined as def2-svp for Co and 6-311G(p) for the rest of the atoms. The calculations indicate the formation of intermediate **B** upon coordination of the oxygen anion to the cobalt center of the catalyst, which is exergonic by -12.8 kcal/mol. Upon further activation, the coordinated NaOCl undergoes NaCl elimination to generate α -Co(III)-oxyl radical **C** in the metalloradical activation step, which is exergonic by -21.0 kcal/mol and has a relative low activation energy (TS1: $\Delta G^\ddagger = 6.8$ kcal/mol). These results suggest an overall thermodynamically and kinetically favorable activation of NaOCl by [Co(Por)], which is consistent with the UV-Vis and EPR data where spectroscopic changes were observed just after seconds of mixing NaOCl and [Co(Por)] (*vide supra*). See Figure 3.5 for optimized geometries of intermediates and transition states.

Scheme 3.7] Calculated Energy Diagram of the [Co(Por)] Activation of NaOCl

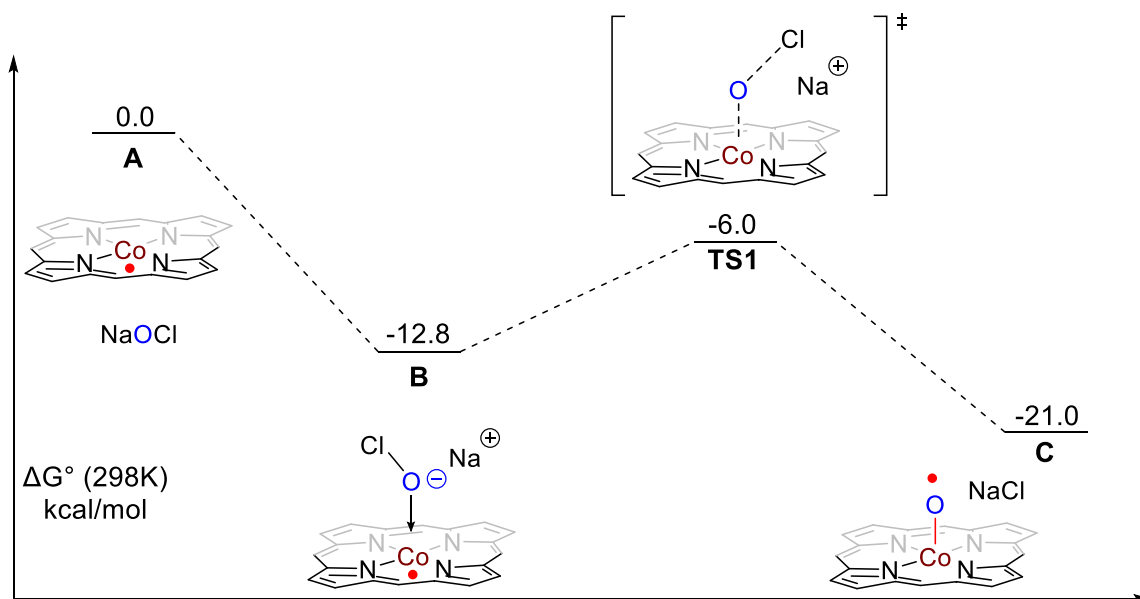
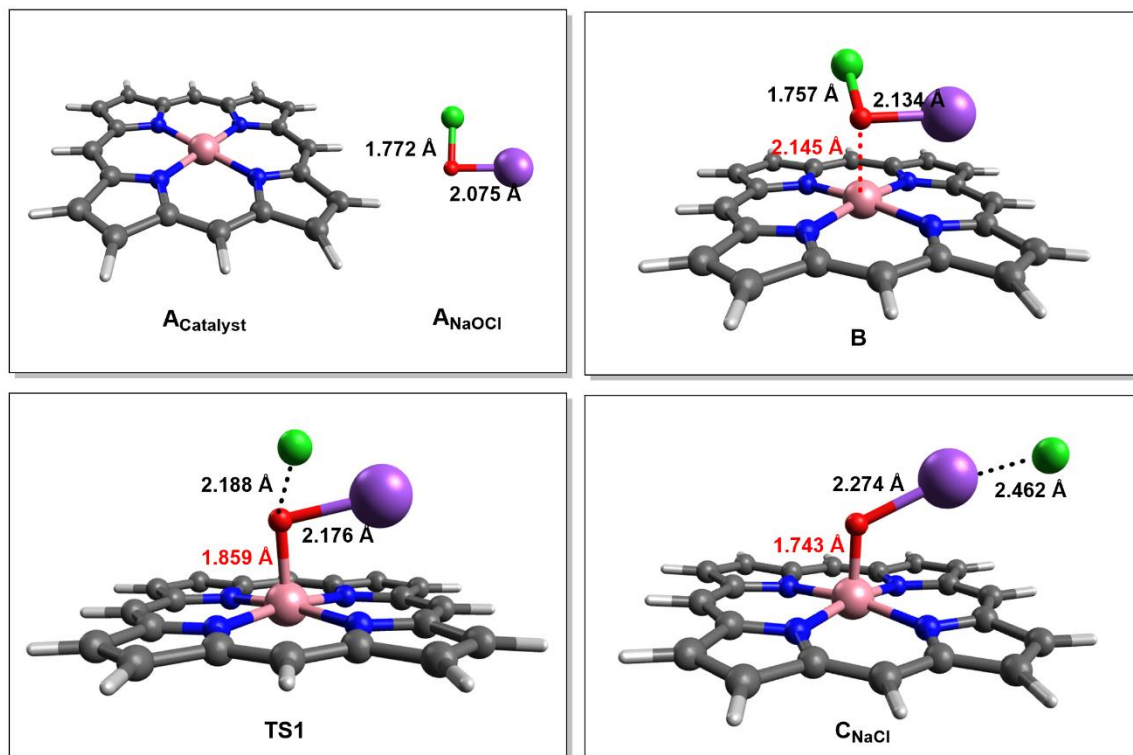


Figure 3.5| Optimized Geometries for Intermediates and Transition States

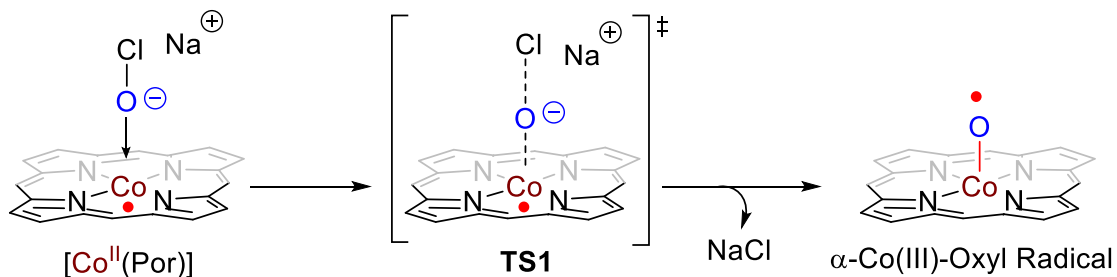


We also performed further DFT calculations to obtain more knowledge about the specific interaction between NaOCl and [Co(Por)] for the generation of the new radical species (see Experimental Section for details). We computationally analyzed the spin density, bond distance, and charge variation of all participant atoms as a function of the calculated reaction coordinate (Scheme 3.8B), with the intent to see whether there could be spin translocation from the [Co(Por)] to the oxygen of NaOCl (Scheme 3.8A). As shown in Scheme 3.8D, the spin density on the Co center goes from its original +1 to zero as the reaction proceeds with the oxygen-chlorine bond length increasing and the cobalt oxygen bond length decreasing. Furthermore, with the same X-axis variation, the spin density on oxygen increases from practically zero to +1 (Scheme 3.8D). These changes are consistent with the postulated spin translocation from the cobalt center to the oxygen anion as the O–

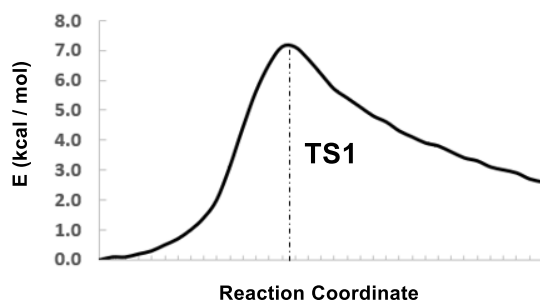
Cl bond is cleaved and the Co–O bond is formed (Scheme 3.8C). This computational study also shows how there is a low but noticeable degree of spin density developing in the chlorine atom during the reaction pathway while there is essentially no spin change in the sodium atom. When the same type of calculation was performed but analyzing the Mulliken charge change (Scheme 3.8E), the results suggest a zero to -1 change for chlorine and from -1 to 0 for oxygen as the reaction proceeds with the O–Cl bond breaking and the Co–O bond forming, while no change in charge occurs for cobalt and sodium. While it is difficult to decipher the exact mechanism of activation, these results are consistent with the idea outlined in Scheme 3.8A, where the spin density in the Co(II) metalloradical is translocated to the oxygen atom with the formation of the NaCl ion pair.

Scheme 3.8| Computational Study on the Generation of α -Co(III)-Oxyl Radicals through [Co(Por)] Activation of NaOCl

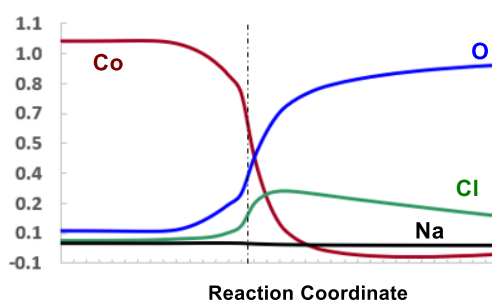
A. Rationale



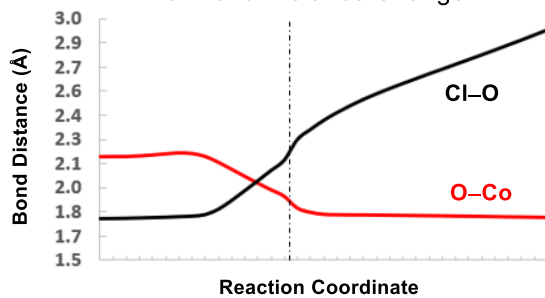
B. Energy Profile



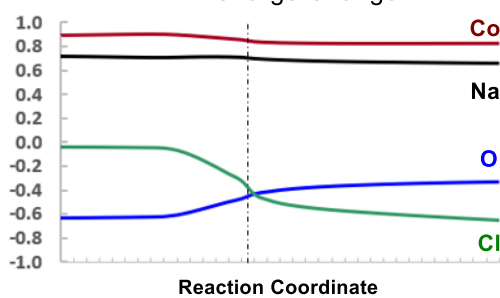
D. Spin Change



C. Bond Distance Change



E. Charge Change



3.3 CONCLUSIONS

In summary, we have demonstrated, for the first time, the generation and characterization of α -Co(III)-oxyl radicals via the reaction of common reagent NaOCl with Co(II) porphyrins. The reactive intermediates have been characterized by UV-vis spectroscopy, EPR, HRMS, and isotope labeling experiments. Computational studies suggest a favorable interaction between NaOCl and Co(II) porphyrins, supporting the feasibility of the generation of α -Co(III)-oxyl radicals as experimentally observed. Furthermore, these unprecedented oxygen-centered radicals have been shown to be competent intermediates for the enantioselective radical epoxidation of styrene. Further mechanistic studies on the epoxidation reaction are in agreement with the proposed stepwise radical mechanism (Scheme 3.1B). We envision that these findings can have potential implications in the design of highly selective oxidation reactions and can open new reactivity modes via Co(II)-Metalloradical epoxidation and C–H hydroxylation.

3.4 EXPERIMENTAL SECTION

3.4.1 General Considerations

Unless otherwise stated, all reactions were carried out under a nitrogen atmosphere in oven-dried glassware following standard Schlenk techniques. Gas tight syringes were used to transfer liquid reagents and solvents in catalytic reactions. 4Å MS were dried in a vacuum oven prior to use. Solvent was freshly distilled/degassed prior to use unless otherwise noted. Thin layer chromatography was performed on Merck TLC plates (silica gel 60 F254), visualizing with UV-light 254 nm. Flash column chromatography was performed with ICN silica gel (60 Å, 230-400 mesh, 32-63 µm). ²H and ¹H NMR, and ¹³C NMR were recorded on a Varian 600 (600 MHz), Varian 500 (500 MHz), Varian Inova 400 (400 MHz) instrument with chemical shifts reported relative to residual solvent. HPLC measurements were carried out on a Shimadzu HPLC system with Chiralcel ID column. The UV-Vis absorption spectra in the range 200-700 nm were measured with an Evolution 300 UV-VIS spectrophotometer using quartz cuvettes with 1.0 cm optical path length. High resolution mass spectra were obtained on an Agilent 6220 using electrospray ionization time-of-flight (ESI-TOF). Co(3,5-Di^tBu-ChenPhyrin) was synthesized following literature reported procedures.^{9b} X-band EPR spectra were recorded on a Bruker EMX-Plus spectrometer (Bruker BioSpin). Simulations of the EPR spectra were performed by iteration of the isotropic g-values and line widths using the EPR simulation program SpinFit in Xenon.

3.4.2 Characterization of α -Co(III)-Oxyl Radicals by UV-Vis Using Different Oxygen Radical Precursors

General Procedure for UV-Vis Experiments

A gas tight sealable quartz cuvette was evacuated and refilled with nitrogen for three times. Under nitrogen, CH₃CN (1 ml) was added via a gas-tight syringe. The background spectrum was collected. During the time, [Co(Por)] (2 mol %) was charged in a Schlenk tube, then evacuated and backfilled with nitrogen for three times (Flask A). In a similar manner, a second Schlenk tube was charged with the solid reagents (0.1 mmol), evacuated, and backfilled with nitrogen for three times (Flask B). Under nitrogen, liquid reagents (0.1 mmol) and CH₃CN (1 ml) were added and stirred at room temperature. Under nitrogen, 10 μ l from flask A were added to the sealed cuvette with a gas-tight syringe. The cuvette was shaken and placed in the instrument for analysis. Once the spectrum for [Co(Por)] only was recorded, 10 μ l from flask B were added to the sealed cuvette with a gas-tight syringe. The cuvette was shaken and placed in the instrument for analysis. The spectra show redshifts after 3 minutes (Figure 3.1).

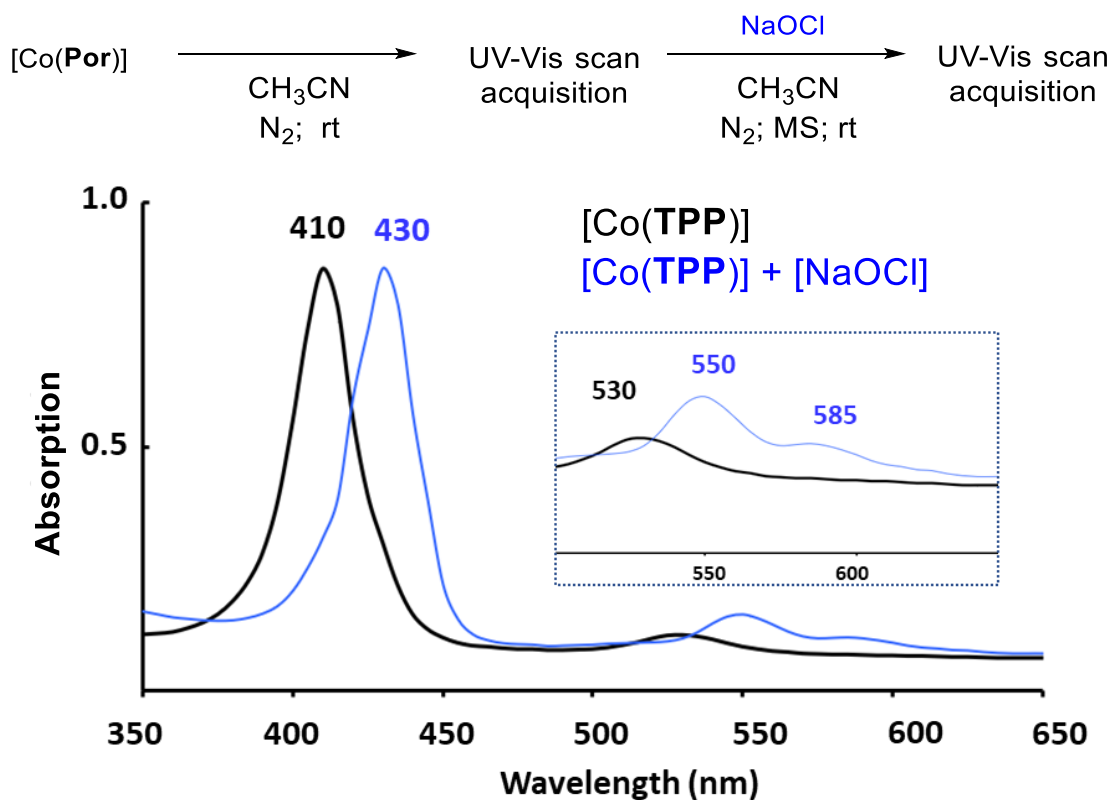
3.4.3 Characterization of α -Co(III)-Oxyl Radicals by UV-Vis Using NaOCl

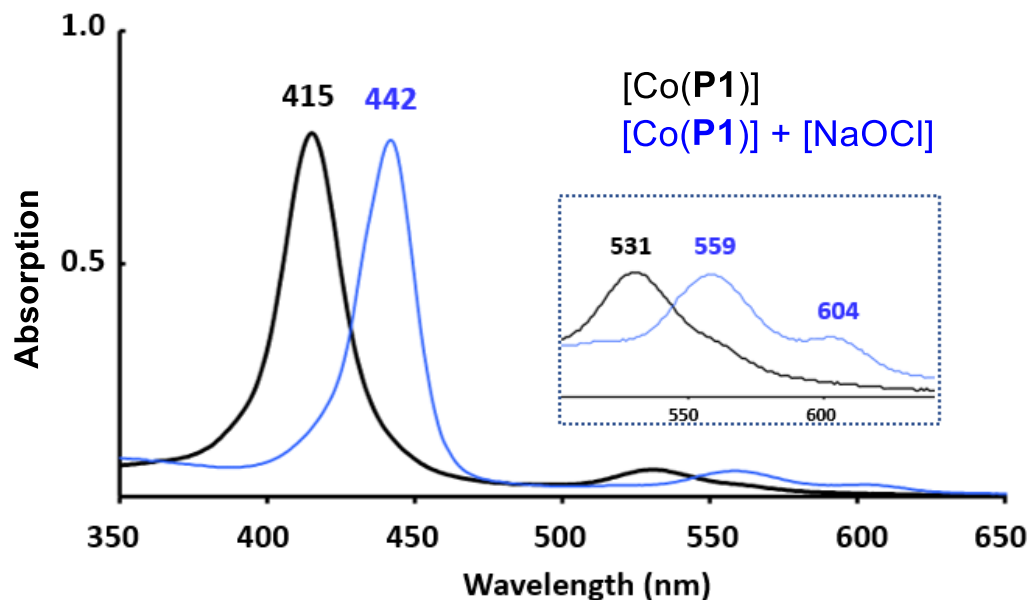
General Procedure for UV-Vis Experiments with NaOCl

A gas tight sealable quartz cuvette was evacuated and refilled with nitrogen for three times. Under nitrogen, CH₃CN (1 ml) was added via a gas-tight syringe. The background spectrum was collected. During the time, [Co(Por)] (2 mol %) was charged in

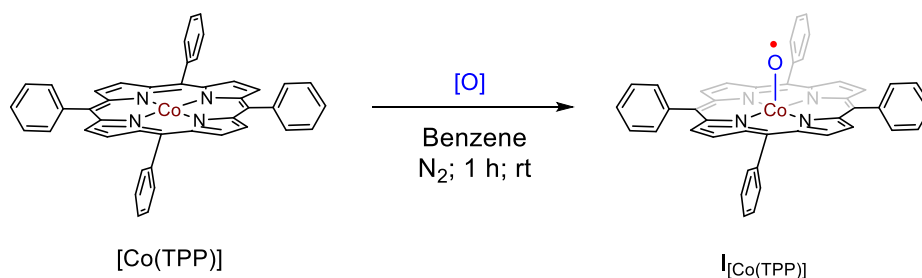
a Schlenk tube, then evacuated and backfilled with nitrogen for three times (Flask A). In a similar manner, a second Schlenk tube was charged with 50mg of 4A MS, evacuated and backfilled with nitrogen for three times (Flask B). Under nitrogen, NaOCl-5H₂O (0.1 mmol) and CH₃CN (1 ml) were added and stirred at room temperature. Under nitrogen, 10 μl from flask A were added to the sealed cuvette with a gas-tight syringe. The cuvette was shaken and placed in the instrument for analysis. Once the spectrum for [Co(Por)] only was recorded, 10 μl from flask B were added to the sealed cuvette with a gas-tight syringe. The cuvette was shaken and placed in the instrument for analysis. The spectrum showed complete redshift after one scan (10 seconds) Figure 3.6.

Figure 3.6| UV-Vis Spectrum for Co(III)-Supported Oxyl Radical Intermediate





3.4.4 Characterization of α -Co(III)-Oxyl Radicals by EPR Using Different Oxygen Radical Precursors



General Procedure for EPR Experiments

To an over-dried Schlenk tube, [Co(TPP)] (2 mol %) was added. The Schlenk tube was then evacuated and backfilled with nitrogen for 3 times. The Teflon screw cap was replaced with a rubber septum, and the oxygen radical precursor (0.1 mmol) [a) mCPBA + K₂CO₃ b) Oxone + K₂CO₃, c) Pyridine N-Oxide, d) NaOCl·5H₂O and Benzene (0.5 mL) were added. The mixture was then stirred at room temperature for 1h and transferred into a

degassed EPR tube (filled with argon) through a gas tight syringe. The sample was then carried out for EPR experiment at room temperature (EPR settings: T = 298 K; microwave frequency: 9.37762 GHz; power: 20 mW; modulation amplitude: 1.0 G).

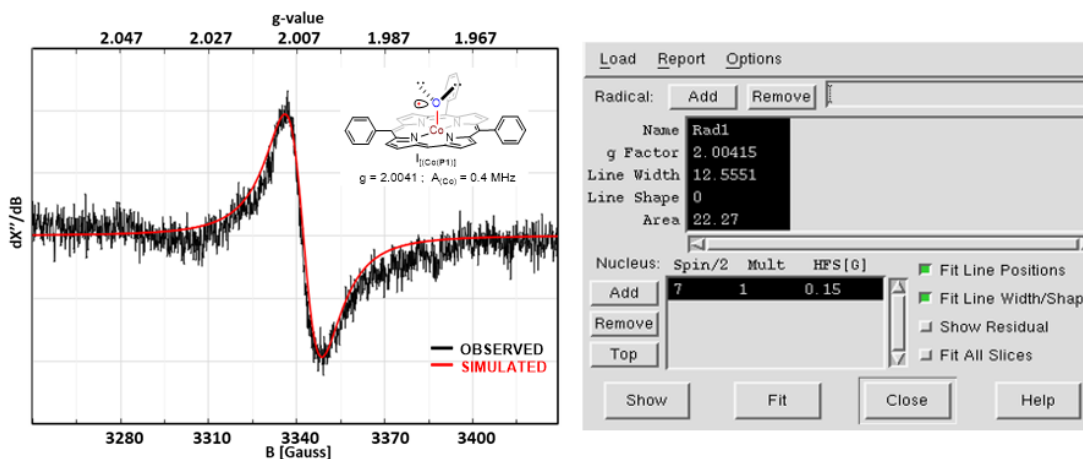
X-band EPR spectra were recorded on a Bruker EMX-Plus spectrometer (Bruker BioSpin). Simulations of the EPR spectra were performed by iteration of the isotropic g-values and line widths using the EPR simulation program SpinFit in Xenon (Figure 3.2).

3.4.5 Characterization of α -Co(III)-Oxyl Radicals by EPR using NaOCl

Procedure for EPR Experiment with NaOCl and [Co(TPP)]

To an over-dried Schlenk tube, [Co(TPP)] (2 mol %) was added. The Schlenk tube was then evacuated and backfilled with nitrogen for 3 times. The Teflon screw cap was replaced with a rubber septum, and NaOCl-5H₂O (0.1 mmol) and Benzene (0.5 mL) were added. The mixture was then stirred at room temperature for 1h and transferred into a degassed EPR tube (filled with argon) through a gas tight syringe. The sample was then carried out for EPR experiment at room temperature (EPR settings: T = 298 K; microwave frequency: 9.37762 GHz; power: 20 mW; modulation amplitude: 1.0 G). X-band EPR spectra were recorded on a Bruker EMX-Plus spectrometer (Bruker BioSpin). Simulations of the EPR spectra were performed by iteration of the isotropic g-values and line widths using the EPR simulation program SpinFit in Xenon.

EPR simulation details:

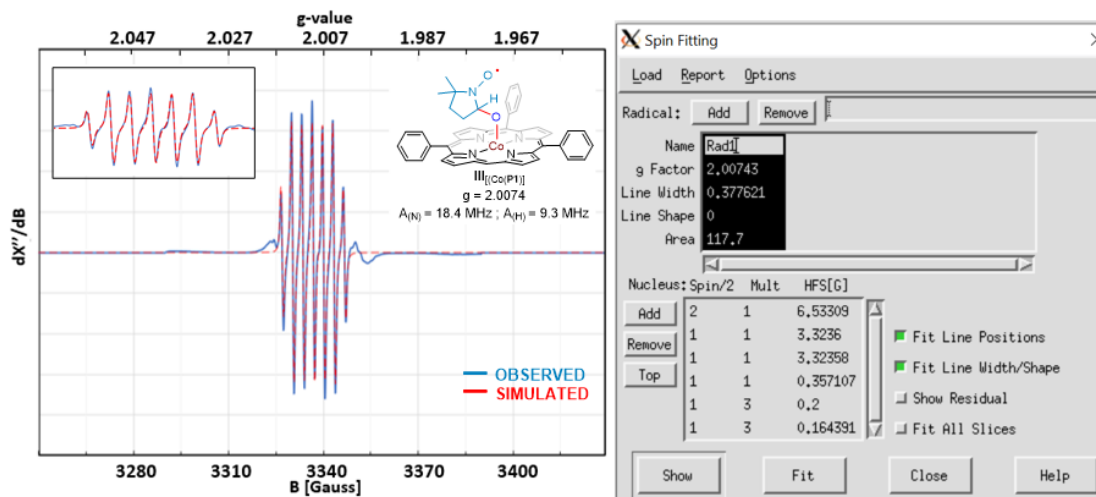


$$g_{\text{iso}} = 2.00415 / A_{\text{iso}}(\text{Co}) = 0.15 \times 2.00415 \times 1.399611451 = 0.4 \text{ MHz}$$

Procedure for EPR Trapping Experiment with DMPO

To an over-dried Schlenk tube, [Co(TPP)] (2 mol %) was added. The Schlenk tube was then evacuated and backfilled with nitrogen for 3 times. The Teflon screw cap was replaced with a rubber septum, and NaOCl-5H₂O (0.1 mmol) and Benzene (0.5 mL) were added. The mixture was then stirred at room temperature for 1h, then DMPO (5,5-Dimethyl-1-Pyrroline-N-Oxide) (0.05mmol) was added to the reaction mixture and stirred at room temperature for 30 min and transferred into a degassed EPR tube (filled with argon) through a gas tight syringe. The sample was then carried out for EPR experiment at room temperature (EPR settings: T = 298 K; microwave frequency: 9.37762 GHz; power: 20 mW; modulation amplitude: 1.0 G). X-band EPR spectra were recorded on a Bruker EMX-Plus spectrometer (Bruker BioSpin). Simulations of the EPR spectra were performed by iteration of the isotropic g-values and line widths using the EPR simulation program SpinFit in Xenon.

EPR simulation details:



$$g_{\text{iso}} = 2.0073$$

$$A_{\text{iso}}(\text{N}) = 6.533090 \times 2.0074 \times 1.399611451 = 18.4 \text{ MHz}$$

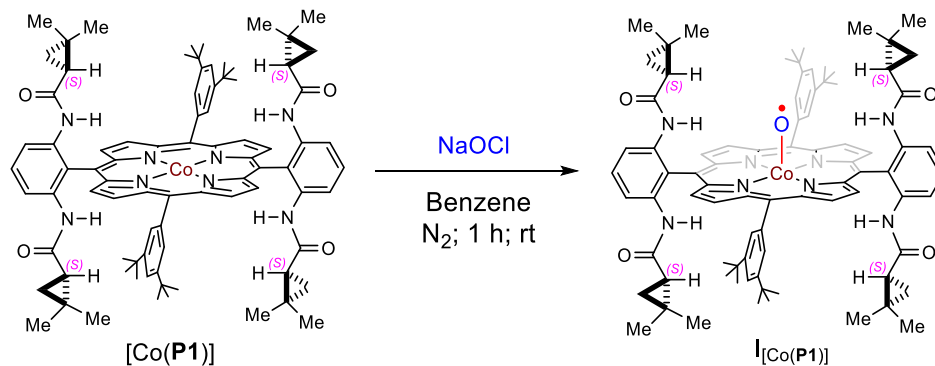
$$A_{\text{iso}}(\text{H}) = 3.323600 \times 2.0074 \times 1.399611451 = 9.3 \text{ MHz}$$

$$A_{\text{iso}}(\text{H}) = 3.323580 \times 2.0074 \times 1.399611451 = 9.3 \text{ MHz}$$

$$A_{\text{iso}}(\text{H}) = 0.357107 \times 2.0074 \times 1.399611451 = 1.0 \text{ MHz}$$

$$A_{\text{iso}}(\text{H}) = 0.200000 \times 2.0074 \times 1.399611451 = 0.6 \text{ MHz}$$

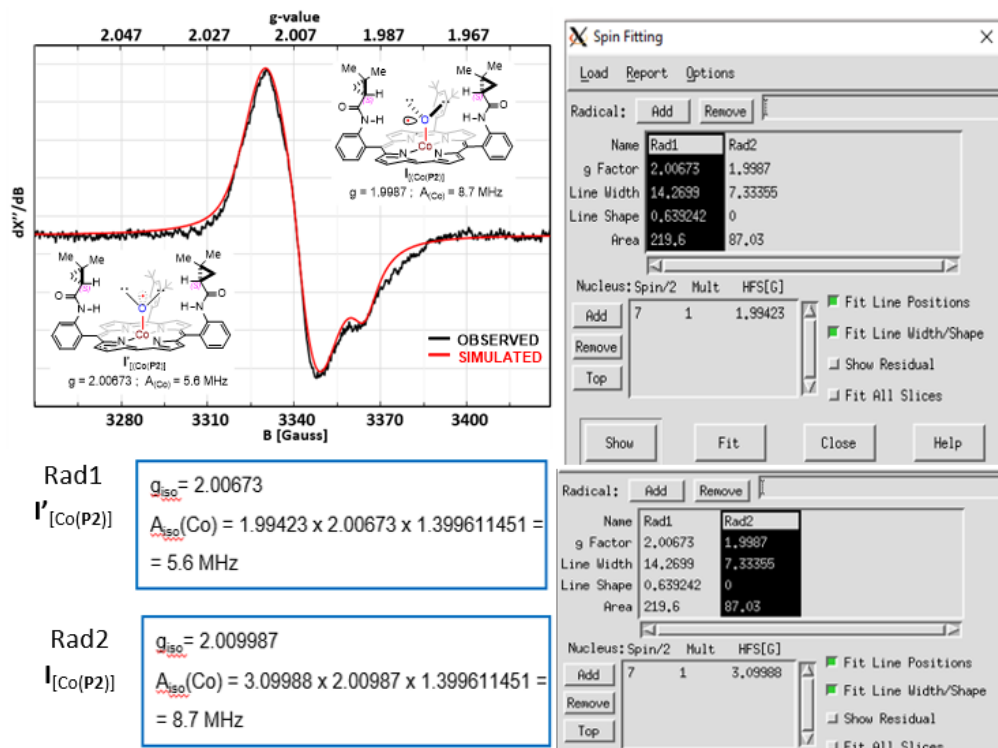
$$A_{\text{iso}}(\text{H}) = 0.164391 \times 2.0074 \times 1.399611451 = 0.5 \text{ MHz}$$



Procedure for EPR Experiment with NaOCl and [Co(P1)]

To an over-dried Schlenk tube, [Co(P1)] (2 mol %) was added. The Schlenk tube was then evacuated and backfilled with nitrogen for 3 times. The Teflon screw cap was replaced with a rubber septum, and NaOCl·5H₂O (0.1 mmol) and Benzene (0.5 mL) were added. The mixture was then stirred at room temperature for 1h and transferred into a degassed EPR tube (filled with argon) through a gas tight syringe. The sample was then carried out for EPR experiment at room temperature (EPR settings: T = 298 K; microwave frequency: 9.37762 GHz; power: 20 mW; modulation amplitude: 1.0 G). X-band EPR spectra were recorded on a Bruker EMX-Plus spectrometer (Bruker BioSpin). Simulations of the EPR spectra were performed by iteration of the isotropic g-values and line widths using the EPR simulation program SpinFit in Xenon.

EPR simulation details:

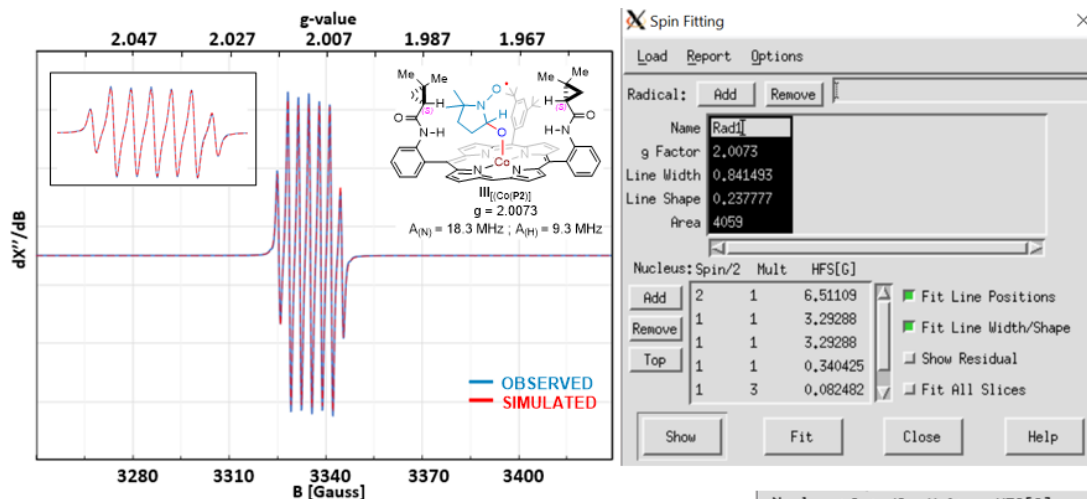


Procedure for EPR Trapping Experiment with DMPO

To an over-dried Schlenk tube, [Co(P1)] (2 mol %) was added. The Schlenk tube was then evacuated and backfilled with nitrogen for 3 times. The Teflon screw cap was replaced with a rubber septum, and NaOCl-5H₂O (0.1 mmol) and Benzene (0.5 mL) were added. The mixture was then stirred at room temperature for 1h, then DMPO (5,5-Dimethyl-1-Pyrroline-N-Oxide) (0.05mmol) was added to the reaction mixture and stirred at room temperature for 30 min and transferred into a degassed EPR tube (filled with argon) through a gas tight syringe. The sample was then carried out for EPR experiment at room temperature (EPR settings: T = 298 K; microwave frequency: 9.37762 GHz; power: 20 mW; modulation amplitude: 1.0 G). X-band EPR spectra were recorded on a Bruker EMX-

Plus spectrometer (Bruker BioSpin). Simulations of the EPR spectra were performed by iteration of the isotropic g-values and line widths using the EPR simulation program SpinFit in Xenon.

EPR simulation details:



$$g_{\text{ISO}} = 2.0073$$

$$A_{\text{ISO}}(\text{N}) = 6.511090 \times 2.0073 \times 1.399611451 = 18.3 \text{ MHz}$$

$$A_{\text{ISO}}(\text{H}) = 3.292880 \times 2.0073 \times 1.399611451 = 9.3 \text{ MHz}$$

$$A_{\text{ISO}}(\text{H}) = 3.292880 \times 2.0073 \times 1.399611451 = 9.3 \text{ MHz}$$

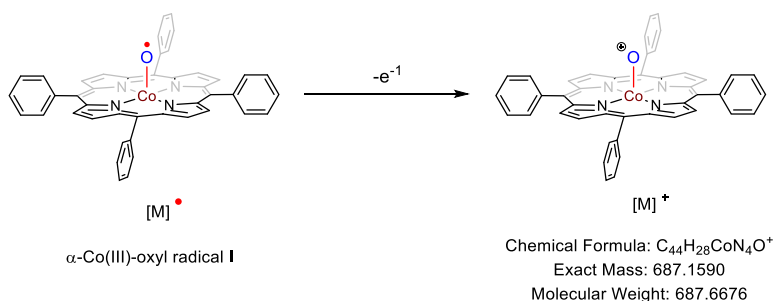
$$A_{\text{ISO}}(\text{H}) = 0.340425 \times 2.0073 \times 1.399611451 = 1.0 \text{ MHz}$$

$$A_{\text{ISO}}(\text{H}) = 0.100000 \times 2.0073 \times 1.399611451 = 0.3 \text{ MHz}$$

$$A_{\text{ISO}}(\text{H}) = 0.082482 \times 2.0073 \times 1.399611451 = 0.2 \text{ MHz}$$

Nucleus: Spin/2 Mult HFS[G]			
Add	1	1	3.29288
Remove	1	1	3.29288
Top	1	3	0.340425
	1	3	0.1

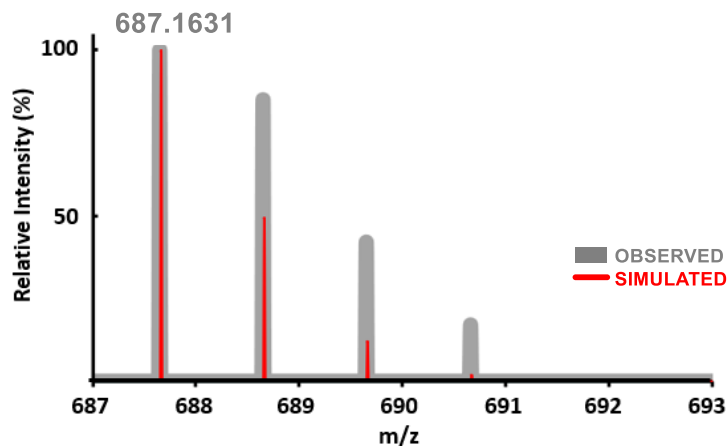
3.4.6 Characterization of α -Co(III)-Oxyl Radicals by HRMS

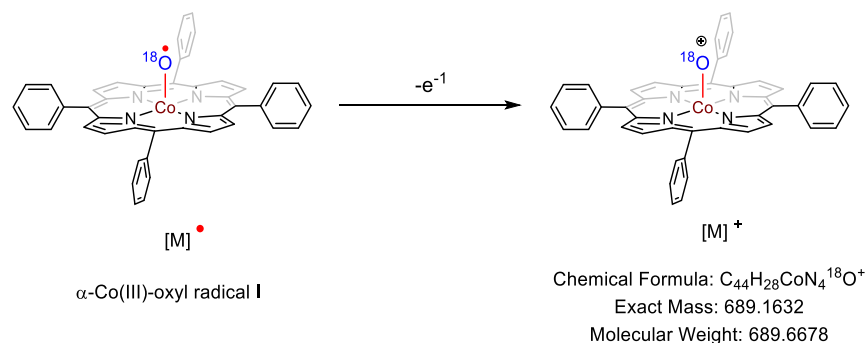


Procedure for HRMS Experiments

Catalyst [Co(TPP)] (2 mol %) was dissolved into 1.0 mL of anhydrous DCM. NaOCl·5H₂O (0.1 mmol) was dissolved into 1.0 mL of acetonitrile. These two solutions were mixed *in situ* on a filter paper for direct detection of molecular ion peak by DART-MS. The high-resolution mass spectra in the absence of any additives such as formic acids that commonly act as electron carriers for ionization allowed for the detection of the molecular ion signals corresponding to the α -Co(III)-oxyl radical I_[Co(TPP)] ([M]⁺ m/z = 687.1631 (observed)), by the loss of one electron, Figure 3.7.

Figure 3.7| High Resolution Mass Spectroscopy (HRMS) Spectrum for α -Co(III)-oxyl radical I_[Co(TPP)]

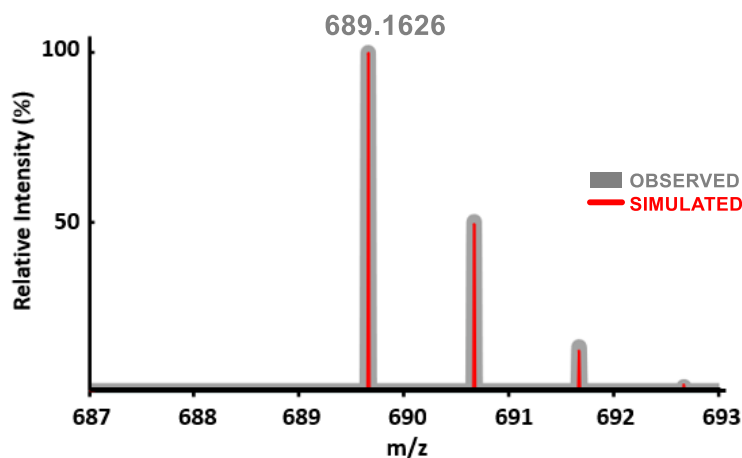


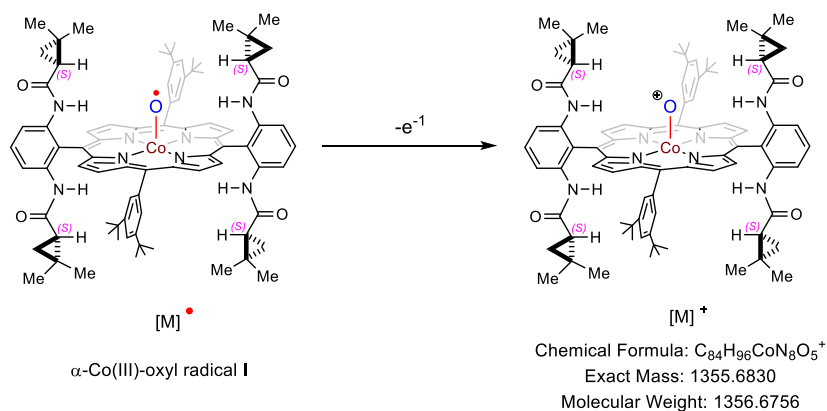


Procedure for HRMS Experiments with Isotopically Labeled Na^{18}OCl

Catalyst $[\text{Co}(\text{TPP})]$ (2 mol %) was dissolved into 1.0 mL of anhydrous DCM. $\text{Na}^{18}\text{OCl}\cdot 5\text{H}_2\text{O}$ was prepared according to the literature.⁵⁸ $\text{Na}^{18}\text{OCl}\cdot 5\text{H}_2\text{O}$ (0.1 mmol) was dissolved into 1.0 mL of acetonitrile. These two solutions were mixed *in situ* on a filter paper for direct detection of molecular ion peak by DART-MS. The high-resolution mass spectra in the absence of any additives such as formic acids that commonly act as electron carriers for ionization allowed for the detection of the molecular ion signals corresponding to the $\alpha\text{-Co(III)-oxyl radical I}_{[\text{Co}(\text{TPP})]}$ ($[\text{M}]^+$ $m/z = 689.1626$ (observed)), by the loss of one electron, Figure 3.8.

Figure 3.8| High Resolution Mass Spectroscopy (HRMS) Spectrum for Isotopically Labeled $\alpha\text{-Co(III)-oxyl radical I}_{[\text{Co}(\text{TPP})]}$

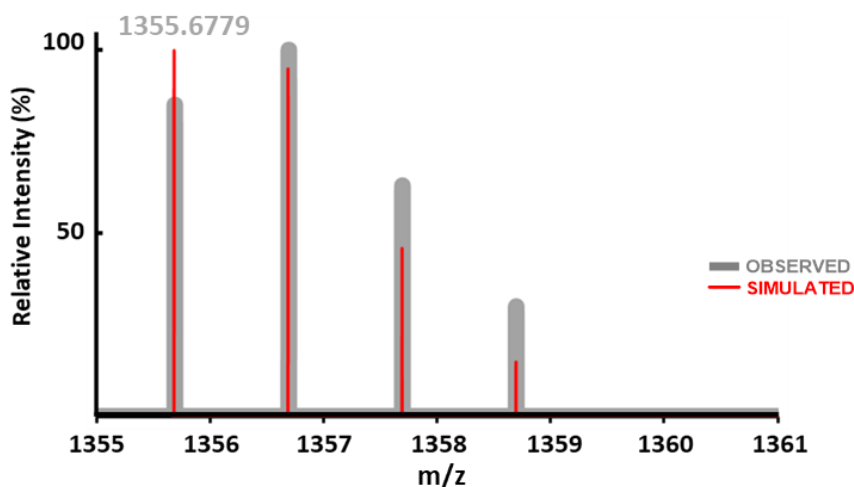


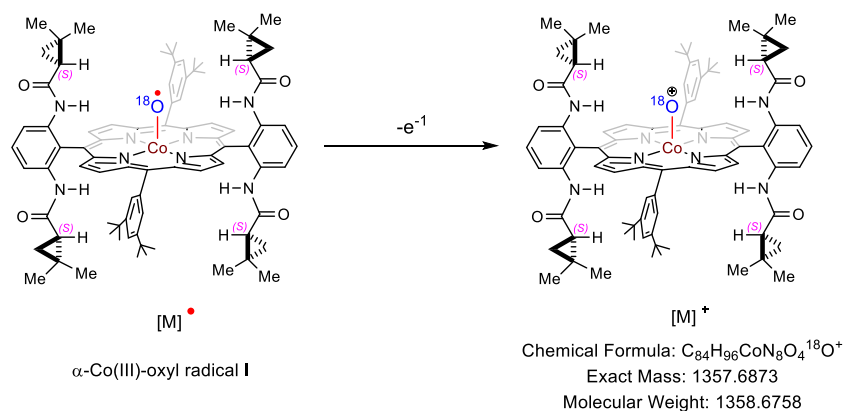


Procedure for HRMS Experiments

Catalyst [Co(P1)] (2 mol %) was dissolved into 1.0 mL of anhydrous DCM. NaOCl-5H₂O (0.1 mmol) was dissolved into 1.0 mL of acetonitrile. These two solutions were mixed *in situ* on a filter paper for direct detection of molecular ion peak by DART-MS. The high-resolution mass spectra in the absence of any additives such as formic acids that commonly act as electron carriers for ionization allowed for the detection of the molecular ion signals corresponding to the α -Co(III)-oxyl radical I_[Co(P1)] ($[M]^+$ $m/z = 1355.6779$ (observed)), by the loss of one electron, Figure 3.9.

Figure 3.9| High Resolution Mass Spectroscopy (HRMS) Spectrum for α -Co(III)-oxyl radical I_[Co(P1)]

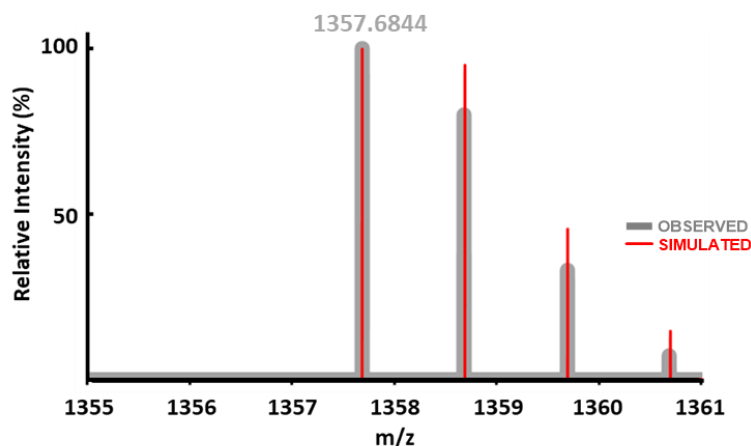




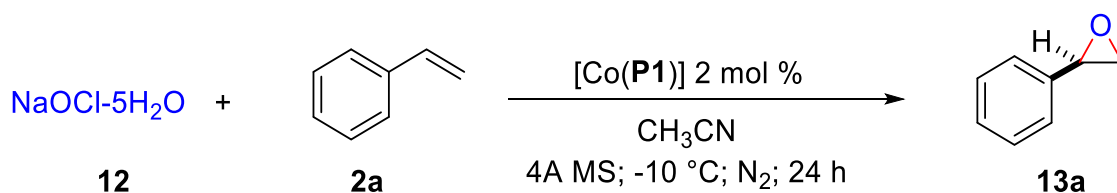
Procedure for HRMS Experiments with Isotopically Labeled $Na^{18}OCl$

Catalyst [Co(P1)] (2 mol %) was dissolved into 1.0 mL of anhydrous DCM. $Na^{18}OCl \cdot 5H_2O$ (0.1 mmol) was dissolved into 1.0 mL of acetonitrile. These two solutions were mixed *in situ* on a filter paper for direct detection of molecular ion peak by DART-MS. The high-resolution mass spectra in the absence of any additives such as formic acids that commonly act as electron carriers for ionization allowed for the detection of the molecular ion signals corresponding to the α -Co(III)-oxyl radical $I_{[Co(P1)]}$ ($[M]^+$ $m/z = 1357.6844$ (observed)), by the loss of one electron, Figure 3.10.

Figure 3.10| High Resolution Mass Spectroscopy (HRMS) Spectrum for Isotopically labeled α -Co(III)-oxyl radical $I_{[Co(P1)]}$



3.4.7 General Procedure for Enantioselective Epoxidation of Styrene



To an over-dried Schlenk tube, [Co(Por)] (2 mol %) and 4A MS (50 mg) were added. The Schlenk tube was then evacuated and backfilled with nitrogen for 3 times. The Teflon screw cap was replaced with a rubber septum and NaOCl-5H₂O (0.2 mmol), styrene (0.6 mmol), and CH₃CN (0.5 mL) were added. The Schlenk tube was then purged with nitrogen for 2 minutes and the rubber septum was replaced with a Teflon screw cap. The mixture was then stirred at -10 °C for 24 h. After the reaction finished, the resulting mixture was passed through a silica gel plug that was pretreated with 1% Et₃N/hexanes. The styrene oxide product was isolated on flash chromatography (9:1 Hexane:Ethyl Acetate) on silica gel that was pretreated with 5% Et₃N/hexanes.

Styrene Oxide (13a), known compound. ¹H NMR (400 MHz, CDCl₃): δ 7.41 – 7.24 (m, 5H), 3.87 (dd, *J* = 3.9, 2.7 Hz, 1H), 3.16 (dd, *J* = 5.5, 4.1 Hz, 1H), 2.81 (dd, *J* = 5.5, 2.6 Hz, 1H). ¹³C NMR (125 MHz, CDCl₃) δ 137.73 (s), 128.63, 128.32, 125.62, 52.50, 51.34. HRMS (DART+) ([M+H]⁺) Calcd. for C₈H₉O: 121.0653, found: 121.0651. HPLC analysis: *ee* = 25%. ID (99% hexanes: 1% isopropanol, 1.0 ml/min) *t*_{major} = 22.41 min, *t*_{minor} = 24.72 min.

3.4.8 DFT Calculations

Calculations were carried out with the Gaussian 09⁴⁴ at unrestricted level of B3LYP^{47,57} functional coupled with mixed basis set. The mixed basis set was defined as def2-svp for Co and 6-311G(p) for the rest of the atoms. The geometry optimizations and energy calculations were performed with simplified catalyst (porphyrin core only, see figure 3.10) in the gas phase at room temperature. Gas-phase Hessian matrix calculations were applied to the characterization of all minima (without imaginary frequency) and transition states (with only one imaginary frequency). Thermochemical parameters such as internal energy, enthalpy, entropy, Gibbs free energy and thermal corrections (entropy and enthalpy, 298.15 K, 1 Atm) were obtained from these calculations.

To investigate the radical activation step (Scheme 3.8), the charge transfer and radical delocalization along with the key bond length were tracked over the reaction path. The atomic charges and spin densities were collected from Mulliken population analysis.⁵⁹

Intermediate A

$A_{[\text{Co(II)}]}$:

Temperature: 298.15 Kelvin

Pressure: 1.0 Atm

G_corr: 0.229531 Hartree

H_corr: 0.29248 Hartree

SCF: -2371.309627 Hartree

S: 132.488 Cal/Mol-Kelvin

H: -2371.017147 Hartree

G: -2371.080096 Hartree

Cartesian Coordinates:

C	2.44162900	1.79515100	0.00056400
N	1.07097800	1.67970800	-0.00003300
H	3.85536500	3.53269100	0.00087200
C	0.59722400	2.97104000	-0.00066200
C	1.68858600	3.91053700	-0.00058100
H	1.57574100	4.98597100	-0.00106000
C	2.83279600	3.18106300	0.00042400
C	-0.73775000	3.33347400	-0.00106300
N	-1.67970800	1.07097800	0.00004500
C	-2.97104000	0.59722400	0.00071700
C	-3.91053700	1.68858600	0.00063400
H	-4.98597100	1.57574100	0.00114300
C	-3.18106300	2.83279600	-0.00041400
H	-3.53269100	3.85536500	-0.00087500
C	-1.79515100	2.44162900	-0.00057900
C	3.33347500	0.73774900	0.00100500
H	3.53269100	-3.85536500	-0.00109800
C	3.18106300	-2.83279600	-0.00059400
C	1.79515100	-2.44162900	-0.00067700

H	4.98597100	-1.57574100	0.00093100
N	1.67970800	-1.07097800	-0.00003500
C	2.97104000	-0.59722400	0.00057800
C	3.91053700	-1.68858600	0.00045400
C	-3.33347400	-0.73774900	0.00116900
H	-1.57574100	-4.98597100	-0.00101400
C	-1.68858600	-3.91053700	-0.00050800
C	-2.83279600	-3.18106300	0.00058400
H	-3.85536500	-3.53269100	0.00110200
C	-2.44162900	-1.79515100	0.00069100
N	-1.07097800	-1.67970800	0.00002200
C	-0.59722400	-2.97104000	-0.00063300
C	0.73774900	-3.33347400	-0.00111000
Co	0.00000000	0.00000000	0.00000000
H	4.39226700	0.97201000	0.00151800
H	0.97201000	-4.39226700	-0.00166300
H	-4.39226700	-0.97201000	0.00173400
H	-0.97201000	4.39226700	-0.00158900

A_{NaOCl} :

Temperature: 298.15 Kelvin

Pressure: 1.0 Atm

G_corr: -0.024264 Hartree

H_corr: 0.007609 Hartree

SCF: -697.730743 Hartree

S: 67.083 Cal/Mol-Kelvin

H: -697.723134 Hartree

G: -697.755007 Hartree

Cartesian Coordinates:

O	0.00000000	1.05721700	0.00000000
Cl	-1.06250200	-0.36025000	0.00000000
Na	1.64204800	-0.21213500	0.00000000

Intermediate B

Temperature: 298.15 Kelvin

Pressure: 1.0 Atm

G_corr: 0.226086 Hartree

H_corr: 0.301583 Hartree

SCF: -3069.081554 Hartree

S: 158.896 Cal/Mol-Kelvin

H: -3068.779971 Hartree

G: -3068.855468 Hartree

Cartesian Coordinates:

C	-2.06513800	2.32793400	-0.25666600
N	-1.78619300	0.98235100	-0.33511400
H	-3.96175200	3.52047600	-0.27002000
C	-3.01056700	0.35826100	-0.45397300
C	-4.07501800	1.32988000	-0.42800300
H	-5.12790600	1.09721500	-0.51265800
C	-3.48686000	2.54960700	-0.30709300
C	-3.19701500	-1.01749100	-0.56275900
N	-0.82854900	-1.67556700	-0.52807100
C	-0.18672500	-2.88756600	-0.64475600
C	-1.14540100	-3.95137000	-0.79311900
H	-0.89420700	-4.99682000	-0.90854800
C	-2.37857100	-3.37976800	-0.77772700
H	-3.34259400	-3.85920700	-0.88116100

C	-2.17493100	-1.96123200	-0.62245500
C	-1.11906800	3.33705200	-0.17969600
H	3.41216700	4.13037700	-0.19779700
C	2.44274600	3.65165600	-0.21598600
C	2.22740900	2.22623800	-0.31464300
H	0.96787900	5.27472600	-0.06947300
N	0.88885700	1.94194700	-0.31970500
C	0.25325600	3.14995800	-0.21194600
C	1.21681500	4.22555000	-0.15084400
C	1.18666900	-3.06646300	-0.66208100
H	5.18485200	-0.79381700	-0.57380500
C	4.13232600	-1.04167200	-0.57174700
C	3.55356900	-2.26493300	-0.64492500
H	4.03084700	-3.23229800	-0.72039600
C	2.12555500	-2.04995500	-0.60223600
N	1.84385000	-0.71275000	-0.50950900
C	3.05792800	-0.08001800	-0.48375000
C	3.24448800	1.28930400	-0.39340900
Co	0.05371700	0.13250200	-0.29939800
H	-1.48253700	4.35654500	-0.10929800
H	4.26525100	1.65553900	-0.38037000
H	1.55530100	-4.08273100	-0.74933000
H	-4.21611900	-1.37812600	-0.65340500
O	0.09060100	0.19454800	1.84442200
Cl	0.78570600	-1.14284500	2.74843500
Na	-1.85071800	-0.69264900	1.83135600

Transition State TS1

Temperature: 298.15 Kelvin

Pressure: 1.0 Atm

Imaginary Frequency: -285.0695 cm^{-1}

G_corr: 0.225095 Hartree

H_corr: 0.300555 Hartree

SCF: -3069.069729 Hartree

S: 158.819 Cal/Mol-Kelvin

H: -3068.769174 Hartree

G: -3068.844634 Hartree

Cartesian Coordinates:

C	-0.04186300	3.10650000	-0.28210000
N	-0.67911200	1.89252500	-0.40495200
H	-0.74625000	5.23162800	-0.26339900
C	-2.01929200	2.19157100	-0.53363600
C	-2.22352200	3.61609100	-0.48081900
H	-3.18317400	4.10665200	-0.57086200
C	-0.99622500	4.18159800	-0.32814000
C	-3.03495900	1.25328300	-0.68061900
N	-1.62526700	-0.75782000	-0.66908300
C	-1.90643300	-2.09831100	-0.77973700
C	-3.32044800	-2.30522700	-0.95432000
H	-3.79189600	-3.27095700	-1.07247100
C	-3.90322800	-1.07918600	-0.94216800
H	-4.94982400	-0.83042600	-1.05255500
C	-2.84269100	-0.11972700	-0.76325500
C	1.32574600	3.28076900	-0.15563500
H	5.30265800	0.98396600	0.03813800
C	4.25445000	1.23763700	-0.03815700
C	3.18587500	0.28069600	-0.18821400

H	4.15490400	3.43042000	0.08686500
N	1.97670800	0.92056100	-0.26827000
C	2.25745300	2.25854000	-0.14758700
C	3.67879900	2.46485100	-0.01355200
C	-0.97124400	-3.11688800	-0.74651100
H	3.53811000	-3.92834200	-0.38278200
C	2.57307400	-3.44521400	-0.44740000
C	1.35138400	-4.01398900	-0.58734300
H	1.10063800	-5.06301200	-0.66094600
C	0.39319000	-2.93484100	-0.61521400
N	1.02827800	-1.72535600	-0.50743000
C	2.36112100	-2.01869500	-0.39017900
C	3.37426300	-1.08878200	-0.24502000
Co	0.18186400	0.06276200	-0.30946100
H	1.69457900	4.29610600	-0.06126900
H	4.38986800	-1.45957300	-0.16378300
H	-1.33570000	-4.13445000	-0.83032700
H	-4.04983400	1.62411800	-0.77601300
O	0.16274700	0.03292200	1.54923000
Cl	-0.80370800	-1.36676800	2.92609600
Na	-1.86820700	0.73432400	1.89028700

Intermedaite C

$C_{[Co(III)]-NaCl}$:

Temperature: 298.15 Kelvin

Pressure: 1.0 Atm

G_{corr} : 0.224172 Hartree

H_{corr} : 0.302612 Hartree

SCF: -3069.092764 Hartree

S: 165.09 Cal/Mol-Kelvin

H: -3068.790152 Hartree

G: -3068.868592 Hartree

Cartesian Coordinates:

C	-0.62005400	2.76614500	-0.75336600
N	-0.80652000	1.40029900	-0.75520800
H	-1.96744600	4.51654000	-1.09610300
C	-2.15292300	1.22024700	-1.00042700
C	-2.80904100	2.48632400	-1.16955500
H	-3.86605400	2.60426100	-1.35839100
C	-1.85650100	3.44318100	-1.03272700
C	-2.79413500	-0.00036800	-1.08818500
N	-0.80618800	-1.40058400	-0.75521700
C	-0.61944300	-2.76639700	-0.75330300
C	-1.85571200	-3.44369900	-1.03273800
H	-1.96642000	-4.51708200	-1.09612800
C	-2.80848200	-2.48705800	-1.16950000
H	-3.86547000	-2.60523400	-1.35833200
C	-2.15264000	-1.22083500	-1.00045900
C	0.57293100	3.40865300	-0.48827200
H	4.90178000	2.61004600	0.82040900
C	3.87271000	2.48776800	0.51289200
C	3.21096700	1.22075100	0.36058000
H	3.09613400	4.51852900	0.17901000
N	1.91345600	1.40187200	-0.06106100
C	1.74625400	2.76605400	-0.14815700
C	2.96743500	3.44529700	0.18939500
C	0.57366500	-3.40864900	-0.48810400
H	4.90233000	-2.60905400	0.82060500
C	3.87323000	-2.48702400	0.51308900

C	2.96813000	-3.44476500	0.18974600
H	3.09704000	-4.51797300	0.17948400
C	1.74682600	-2.76579400	-0.14793800
N	1.91374100	-1.40157700	-0.06090100
C	3.21120000	-1.22015400	0.36073500
C	3.81986300	0.00037100	0.57270200
Co	0.50870000	0.00000700	-0.22072300
H	0.58052600	4.49199500	-0.51984800
H	4.85133200	0.00048600	0.90548200
H	0.58146800	-4.49199100	-0.51962400
H	-3.86726100	-0.00048400	-1.22551200
O	0.07470100	-0.00006500	1.46768200
Cl	-4.59839800	-0.00008200	1.96471100
Na	-2.13680100	0.00012000	1.99592500

4. CHAPTER 4: NEW CATALYTIC SYSTEM FOR ENANTIOSELECTIVE RADICAL EPOXIDATION OF ALKENES: CATALYST DEVELOPMENT, SUBSTRATE SCOPE, AND REACTION MECHANISM

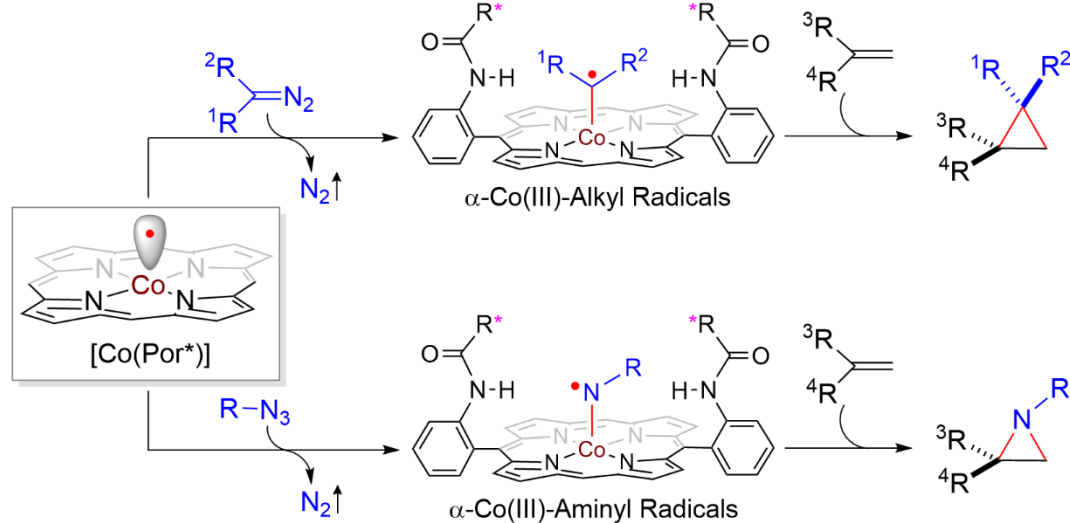
4.1 INTRODUCTION

As mentioned in Chapters 2 and 3, over the years, the well-defined cobalt(porphyrin)-supported carbon- and nitrogen-centered radicals have been demonstrated as key intermediates in several new catalytic asymmetric radical processes. While these distinctive cobalt-supported organic radicals have been successfully utilized for the enantioselective formation of C–C and C–N bonds (Scheme 4.1A), the generation of the analogous α -Co(III)-oxyl radicals **I** and related applications for C–O bond formation, such as olefin epoxidation (Scheme 4.1B), have not been successfully realized. In Chapter 3 (*vide supra*) we reported the generation and characterization of the unprecedented α -Co(III)-oxyl radicals and also demonstrated their competency in participating in asymmetric epoxidation. While the previous chapter focused on the generation and characterization of the new α -Co(III)-oxyl radicals intermediates **I**, it only achieved very minimal reactivity and selectivity towards olefin epoxidation (See Chapter 3). In order to make the previous system relevant for the highly effective and enantioselective epoxidation of alkenes, several questions need to be addressed regarding the catalytic application: i) could the metal-stabilized oxygen-centered radicals **I** act as competent intermediate to undergo effective radical addition with alkenes for the formation of the corresponding α -Co(III)-alkyl radicals **II**? ii) Could the proposed 3-*exo-tet* radical cyclization step of

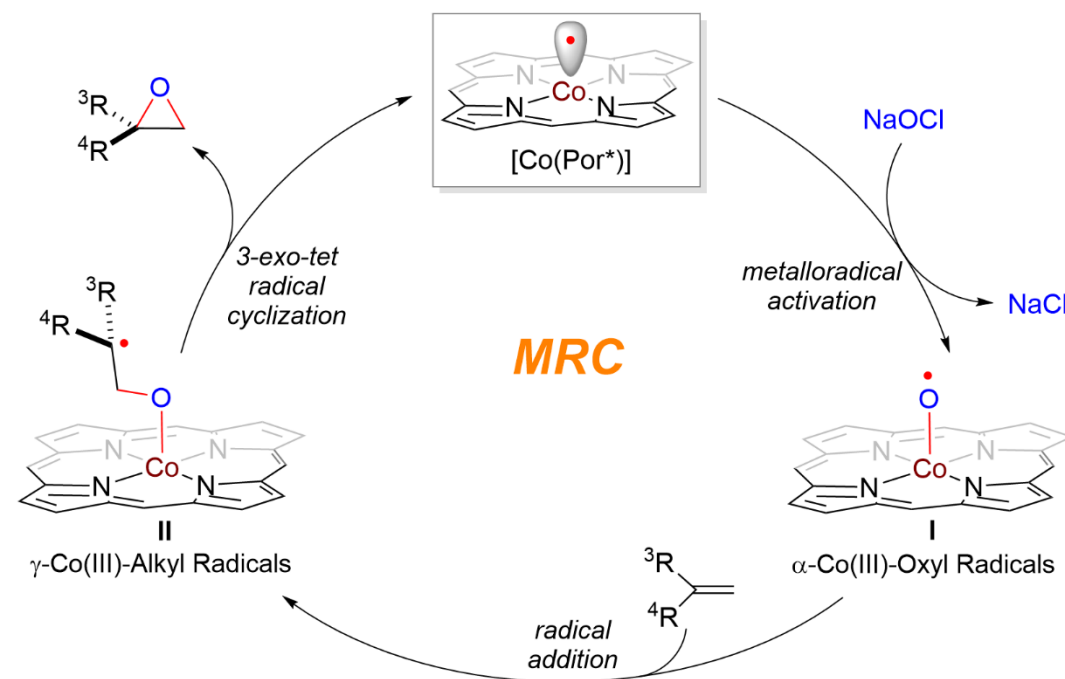
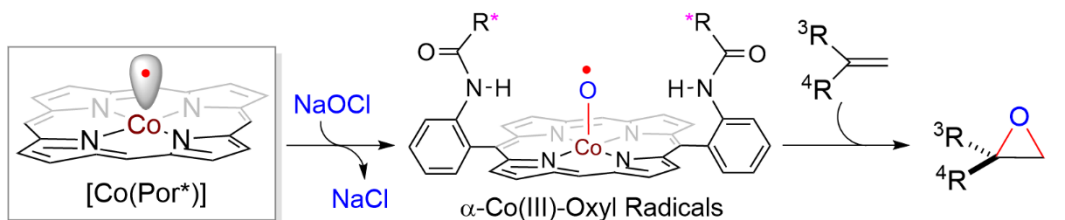
intermediate **II** for C–O bond formation be more efficient and selective? iii) Most importantly, given the absence of substituents in the oxygen-centered radical, which have been effectively utilized for analogous asymmetric radical olefin cyclopropanation^{9b} and aziridination^{11c} (Scheme 4.1A), it is unclear whether the radical epoxidation process could be rendered highly enantioselective. We envisioned the perspective of addressing these and related challenges by catalyst engineering through judicious tuning of the steric, electronic, and chiral environments of the D_2 -symmetric chiral amidoporphyrin ligands. If successful, it would give rise to a fundamentally new radical process for enantioselective olefin epoxidation, one of the most important organic transformations that have several unsolved problems (Scheme 4.1B).

Scheme 4.1 | Working Proposal for Catalytic Radical Epoxidation Involving α -Co(III)-Oxyl Radicals via Co(II)-MRC

A. Co(II)-MRC for Enantioselective Radical Cyclopropanation and Aziridination



B. Co(II)-MRC for Enantioselective Radical Epoxidation (*This Chapter*)



Reactions involving oxygenation of organic molecules play a crucial role in organic synthesis and have been widely employed in the synthesis of natural products.⁵¹ Styrene and its derivatives represent one of the most important prochiral terminal olefins in the chemical industry.⁶⁰ Its derived epoxide, styrene oxide, is furthermore an exceptionally useful building block for the synthesis of organic chiral molecules containing ubiquitous oxygenated motifs.^{13c} Despite significant advances on the asymmetric epoxidation of styrene and derivatives with metal complexes of chiral porphyrins⁶¹ and salen⁶² ligands, as well as with chiral dioxiranes catalyst,⁶³ with isolated examples of highly enantioenriched epoxides, the enantioselective epoxidation of a broad range of styrene derivatives remains a challenge in the field. Herein we wish to report the development of a new enantioselective radical epoxidation process that evolved from the discovery in Chapter 3 and has been realized through the design and development of a novel family of ligands.

4.2 RESULTS AND DISCUSSION

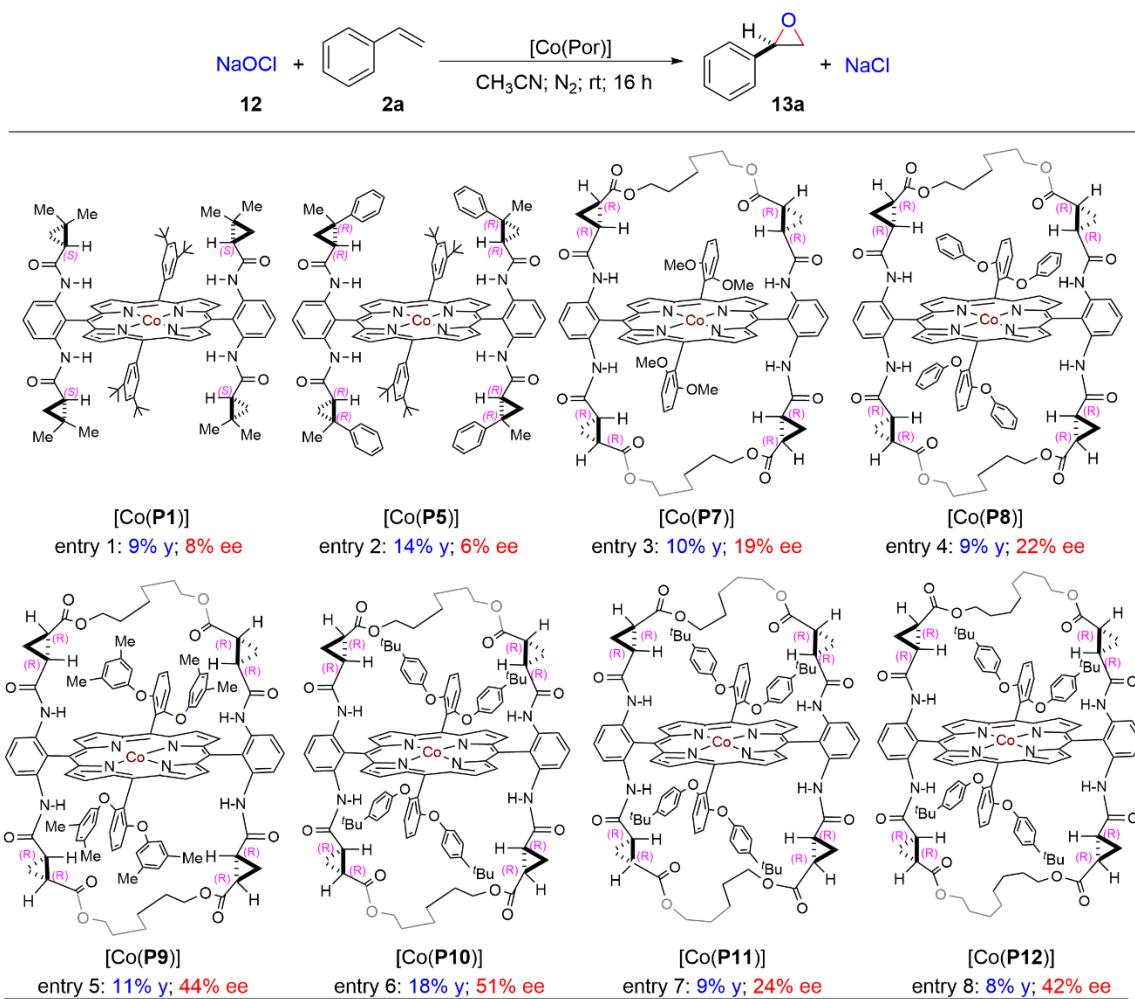
4.2.1 Ligand Screening

Encouraged by the characterization data obtained for the α -Co(III)-oxyl radicals from our previous report (Chapter 3) and the preliminary results obtained with [Co(**P1**)] (Table 4.1, entry 1), we decided to further investigate the ligand effect on the [Co(Por)] catalyzed enantioselective epoxidation of styrene. Compared with the first-generation catalyst [Co(**P1**)], similar results were obtained when the second-generation metalloradical catalyst [Co(**P5**)] (**P5** = 3,5-Di^tBu-QingPhyrin), a [Co(*D*₂-Por*)] complex bearing chiral amides

with two contiguous stereogenic centers (Table 4.1, entry 2), was used. It is important to note that only trace amount of product was observed in the absence of any [Co(Por)] under identical reaction conditions. Despite the modest magnitude of the yields and enantioselectivities (Table 4.1, entries 1–2), these results further support the involvement of the [Co(Por)] in the epoxidation reaction and encouraged us to try different chiral ligand environments to enhance the levels of enantioselectivity. Taking advantage of the tunability of the D_2 -symmetric chiral amidoporphyrins, we explored the recently developed family of ligands that contain an alkyl bridging unit, HuPhyrin,⁶⁴ with the hypothesis that changes in yield and enantioselectivity could further indicate the involvement of the α -Co(III)-oxyl radicals in the radical epoxidation. Indeed, changing the sterics and electronics around the cobalt center had a dramatic effect on the enantioselectivity. When [Co(**P7**)], containing a six-carbon bridging unit and two methoxy groups close to the reaction center was used, the enantioselectivity of the epoxidation reaction increased to 19% ee (Table 4.1, entry 3). At this point, we reasoned that further tuning the steric environment of the non-chiral units in the *meso* position while keeping the same bridge length could influence the yield and enantioselectivity. By changing the two methoxy groups to phenyl groups, [Co(**P8**)], the enantioselectivity increased to 22% ee (Table 4.1, entry 4). Further increasing the steric crowdedness in the phenyl groups resulted in a significant increase in enantioselectivity of up to 51% ee as shown in Table 4.1 by [Co(**P9**)] and [Co(**P10**)]. While keeping the phenoxy groups in the achiral *meso* position, tuning the length of the alkyl bridge to a shorter five-carbon ([Co(**P11**)], Table 4.1 entry 7) or a longer eight-carbon bridge ([Co(**P12**)], Table 4.1 entry 8) enhanced neither the enantioselectivity nor the yield. Although the overall yields of the epoxidation reactions are low, the significant levels of

enantioselectivity observed when using [Co(**P9**)] and [Co(**P10**)] strongly agree with the involvement of the putative α -Co(III)-oxyl radicals **I** as key reactive intermediate in the epoxidation reaction as proposed in Scheme 4.1B, indicating further ligand design as the right approach to achieve high levels of reactivity and enantioselectivity.

Table 4.1| Ligand Effect on the Co(II)-Catalyzed Enantioselective Epoxidation of Styrene with NaOCl^a



^aCarried out with NaOCl·5H₂O (**12**; 0.2 mmol) and styrene (**2a**; 1.0 mmol) in the presence of 4 Å MS (50 mg) using [Co(Por)] (2 mol %) under N₂ atmosphere in acetonitrile (0.5 mL) at room temperature for 16 h. (**P7**) = 2,6-DiMeO-Hu(C₆)Phyrin, (**P8**) = 2,6-DiPhO-Hu(C₆)Phyrin, (**P9**) = 2,6-Di(3',5'-DiMe)PhO-Hu(C₆)Phyrin, (**P10**) = 2,6-Di(4-'Bu)PhO-

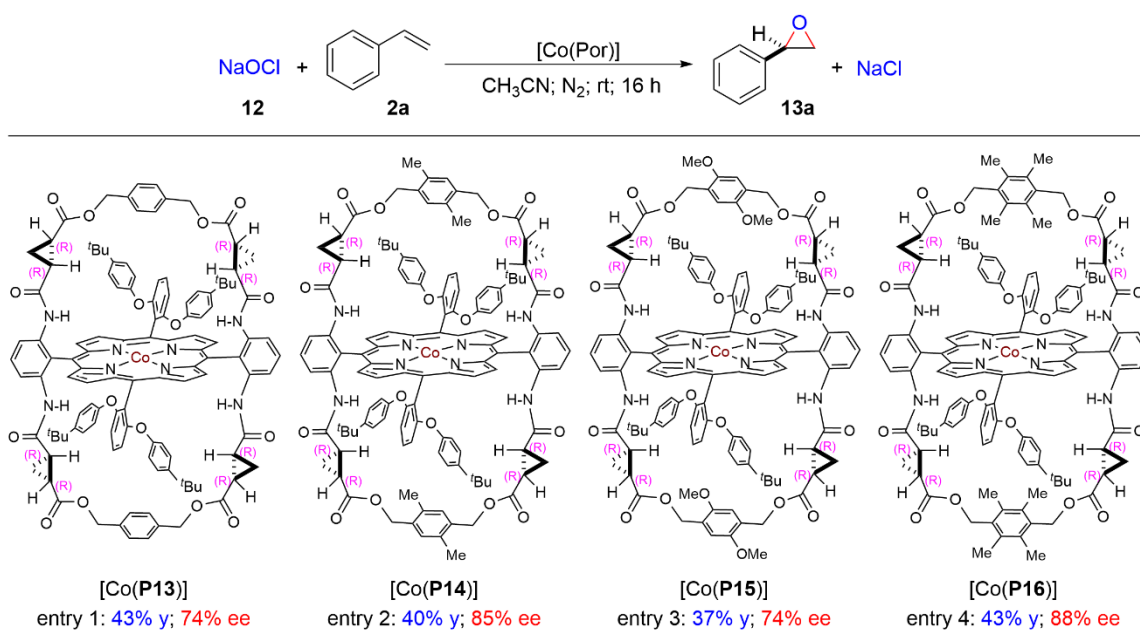
Hu(C₆)Pyrin, (**P11**) = 2,6-Di(4'-*t*Bu)PhO-Hu(C₅)Pyrin, (**P12**) = 2,6-Di(4'-*t*Bu)PhO-Hu(C₈)Pyrin.

4.2.2 Design of New Ligands

Given the dramatic ligand effect observed with the alkyl bridge ligand scaffold HuPyrin, we envisioned that further catalyst engineering could render this process highly asymmetric with synthetically useful yields. To that end, we embarked on developing a new family of porphyrins by further modifying the bridge moiety. Based on the initial screening (Table 4.1), it appeared that the six-carbon alkyl bridge afforded the best results in terms of both yield and enantioselectivity (Table 4.1, entry 6). We reasoned that modifying the alkyl bridge by keeping a pseudo six carbon length while introducing further functionalities could improve the enantioselectivity. Furthermore, it seemed that a more rigid bridge could limit certain conformations compared to the alkyl bridge and have positive effects in the enantioselectivity. With that idea, we decided to introduce a phenyl ring as a bridging unit, further envisioning potential π - π interactions with the aromatic substrates. The new bridge ligand platform, designated “JesuPyrin”, where a phenyl ring is introduced in the bridging unit, resulted in a remarkable increase of the yield to 43% and the enantioselectivity to 74% ee, as exemplified by the use of [Co(**P13**)], (**P13** = 2,6-Di(4'-*t*Bu)PhO-JesuPyrin, Table 4.2, entry 1). Given the divergent synthesis of this new ligand scaffold, (Scheme 4.2), the phenyl bridging unit was easily modified by introducing different groups in the aromatic ring. When [Co(**P14**)] (**P14** = 2,6-Di(4'-*t*Bu)PhO-Jesu(2,5-DiMe)Pyrin), containing two methyl groups in the phenyl ring, was used the

enantioselectivity of the styrene oxide product **13a** increased to 84% ee, maintaining the synthetically useful yield (Table 4.2, entry 2). While changing the methyl groups in the phenyl bridge to methoxy units decreased the enantioselectivity ([Co(**P15**)], **P15** = 2,6-Di(4'-tBu)PhO-Jesu(2,5-DiMeO)Phyrin, Table 4.2, entry 3), the addition of two more methyl units in [Co(**P16**)] (**P16** = 2,6-Di(4'-tBu)PhO-Jesu(2,3,5,6-TetraMe)Phyrin) resulted in the formation of product **13a** in 43% yield and 88% ee (Table 4.2, entry 4).

Table 4.2| Effect of the New Ligands on the Co(II)-Catalyzed Enantioselective Epoxidation of Styrene with NaOCl^a



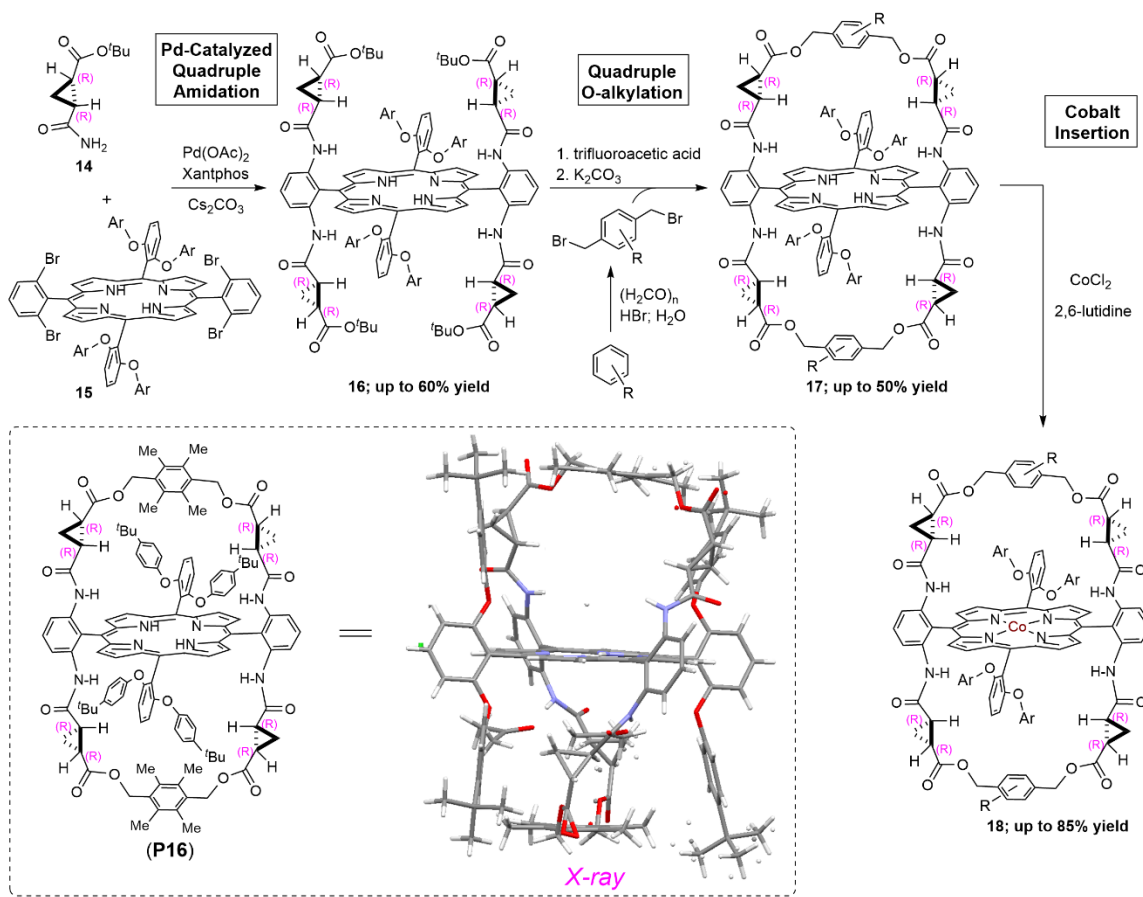
^aCarried out with NaOCl·5H₂O (**12**; 0.2 mmol) and styrene (**2a**; 1.0 mmol) in the presence of 4 Å MS (50 mg) using [Co(Por)] (2 mol %) under N₂ atmosphere in acetonitrile (0.5 mL) at room temperature for 16 h.

4.2.3 New Catalyst Synthesis

For the synthesis of the new family of bridged porphyrins JesuPhyrin, 3,5-Di^tBu-Tao(^tBu)Phyrin (**16**; Scheme 4.2)⁶⁴ was selected as the scaffold structure, considering that the ester functionalities in **16** may serve as convenient handles for building the bridges. Following the previously established procedure,^{9b} **16** was prepared by Pd-catalyzed quadruple amidation reaction of the tetrabromoporphyrin **15** with the optically pure chiral amide **14** (Scheme 4.2). Since the previous established methodology for synthesizing alkyl bridges, which involved a three-step sequence consisting of: i) formal transesterification, ii) olefin metathesis, iii) reduction,⁶⁴ could not be employed for constructing the phenyl bridge, a new pathway was devised. We reasoned that upon hydrolysis, the tert-butyl esters in **16** could undergo subsequent formal transesterification with the corresponding 1,4-dibzenesulfonates in an intramolecular manner, affording the desired phenyl containing bridge. However, the formal transesterification only provided minute yields of desired product. We were please to observed that when 1,4-dibromobenzylys were used as the bridging partners, the quadruple intramolecular O-alkylation proceeded smoothly, affording the new platform of bridge porphyrins **17** (Scheme 4.2). Final metalation afforded the Co(II) complexes of JesuPhyrin **18** (Scheme 4.2)

Scheme 4.2| General Synthesis of the New Family of Bridged Amidoporphyrins

JesuPhyrin^a

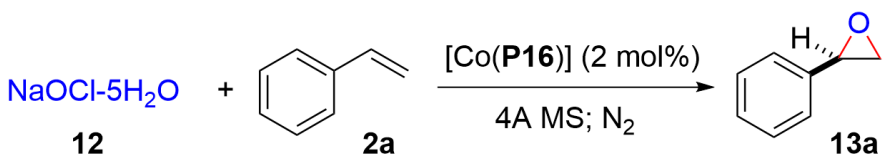


^aCompounds **14** and **15** were synthesized following previously reported methods. See Experimental Section for details and complete X-ray data for **P16**.

4.2.4 Reaction Optimization

Considering the enhancement of reactivity and enantiocontrol achieved with the new ligand scaffold JesuPhyrin (Table 4.2), the original reaction conditions were revisited and further optimized to improve both yield and enantioselectivity. Scrutinous solvent and temperature effects analysis (Table 4.3) revealed the optimal conditions as a solvent mixture of acetonitrile and *n*-Hexane (30:70 ratio) at 4 °C, affording the desired styrene oxide **13a** in 61% yield and 90% ee.

Table 4.3| Optimization of the [Co(P16)] Catalysed Epoxidation of Styrene Reaction^a



entry	12 : 2a ^b	solvent	T (°C)	time (h)	yield (%) ^c	ee (%) ^d
1	3:1	CH ₃ CN	4	24	48	54
2	1:3	CH ₃ CN	4	16	40	88
3	1:3	C ₆ H ₅ F	4	16	2	82
4	1:3	CH ₃ CN/C ₆ H ₆	4	16	56	82
5	1:3	CH ₃ CN/C ₆ F ₆	4	16	42	62
6	1:3	CH ₃ CN/DCM	4	16	38	78
7	1:3	CH ₃ CN/C ₆ H ₅ F	4	16	53	86
8	1:3	CH ₃ CN/pentane	4	16	58	88
9	1:3	CH ₃ CN/Cy-Hex	4	16	37	86
10	1:3	CH ₃ CN/ <i>n</i> -Hex	4	16	61	90
11	1:3	CH ₃ CN/ <i>n</i> -Hex	4	48	63	90

^aReactions were carried out using 2 mol % [Co(P16)] under N₂. Concentration: 0.20 mmol limiting reagent/mL. For solvent mixtures, 1:3 CH₃CN:solvent ratio. ^b Mol ratio of NaOCl to styrene. ^c NMR yields determined by using 0.5 equiv of CH₂Cl₄ as internal standard. ^d Enantiomeric excess determined by chiral HPLC.

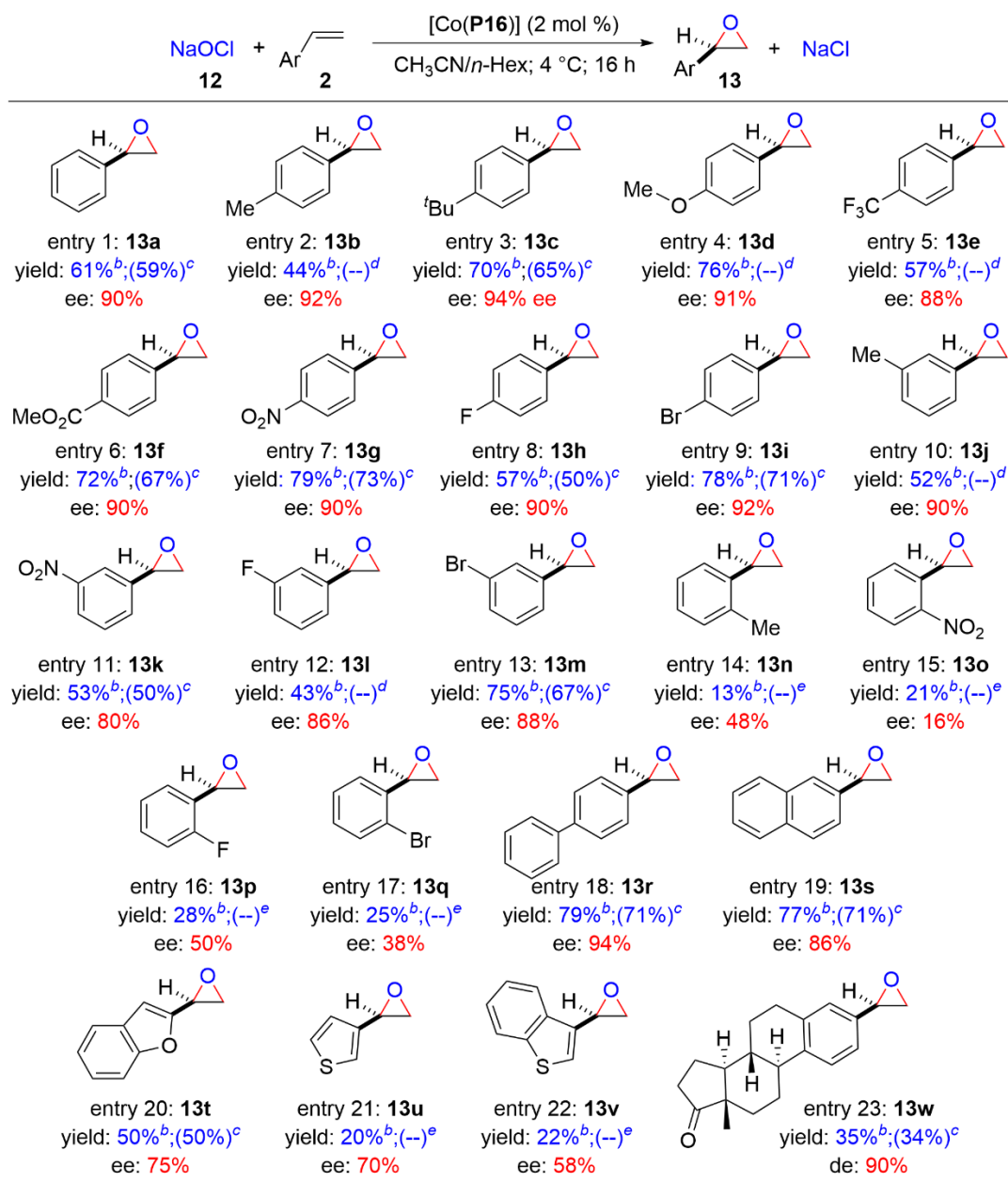
4.2.5 Substrate Scope

Under optimized reaction conditions, the substrate scope of the [Co(**P16**)]-based system for enantioselective radical epoxidation was examined next by employing styrene derivatives with varied steric and electronic properties (Table 4.4). Like styrene, the Co(II)-catalyzed epoxidation was suitable for styrene derivatives bearing alkyl and electron donating substituents at the *para* positions, affording the desired epoxides **13b–13d** in moderate to high yields with excellent enantioselectivities (Table 4.4; entries 2–4). Similarly, styrenes containing electron withdrawing groups (Table 4.4, entries 5–7) and halogens (Table 4.4, entries 8–9) in the *para* position could be employed as effective substrates, providing the corresponding epoxides **13e–13i** in high to moderate yields and excellent enantioselectivities. Of particular interest are the highly enantioenriched halogenated epoxides **13h** and **13i**, which may be potentially transformed to other epoxide derivatives by cross-coupling and related reactions. Furthermore, the Co(II)-based system could tolerate functional groups as exemplified by productive formation of the desired epoxide **13f** and **13g** with high enantioselectivity (Table 4.4; entry 6 and 7, respectively). Interestingly, the position of the substituents in the styrene derivatives seemed to have a significant impact in the levels of reactivity and enantioselectivity. For example, when styrene derivatives containing electron donating substituents (Table 4.4, entry 10), electron withdrawing substituents (Table 4.4, entries 11), or halogens (Table 4.4, entries 12–13) in the *meta* position were employed as substrates, the levels of enantiocontrol dropped slightly while maintaining similar reactivity. However, when the same substituents were moved closer to the reactive double bond at the *ortho* position (Table 4.4, entries 14–17), both the yield and the reactivity decreased significantly, affording epoxides **13n–13q** in low yields

and low levels of enantioselectivity. Given that the same trend is observed for both electron donating and withdrawing substituents, we speculate that the origin of this decrease in reactivity and selectivity is the increase in the steric crowdedness around the active double bond: i) hindering the access of the terminal alkene into the sterically demanding chiral porphyrin pocket containing the oxygen radical, and ii) perturbing potential secondary interactions that increase the enantioselectivity.

The epoxidation system catalyzed by [Co(**P16**)] could be applied to extended aromatic olefins as shown by the effective construction of epoxides **13r–13s** in high yields with excellent enantioselectivities (Table 4.4; entries 18–19). This new Co(II)-catalyzed epoxidation is also suitable for substrates containing heteroatoms, as exemplified by the productive epoxidation of 2-vinylbenzofuran (**13t**, Table 4.4, entry 20) with synthetically useful yields and good levels of enantiocontrol. Interestingly, when substrates containing sulfur atoms were used, the desired product was obtained albeit in reduced yields and enantioselectivities (Table 4.4, entries 21–22). Nitrogen-containing substrates only afforded minimal yields and levels of enantiocontrol as the oxidized byproducts (N-Oxides) were observed as the major product. Finally, this methodology could be successfully applied to more complex molecules as exemplified by the synthesis of estrone derivative **13w** (Table 4.4, entry 23). While this cobalt catalyzed radical epoxidation system failed to yield the desired product when 1,1-disubstituted, 1,2-disubstituted or aliphatic alkenes were employed as substrates, we believe appropriate extensive studies with these types of substrates along with reaction conditions may render this methodology broader in scope.

Table 4.4| [Co(P16)]-Catalyzed Enantioselective Radical Epoxidation of Different Alkenes with NaOCl^a



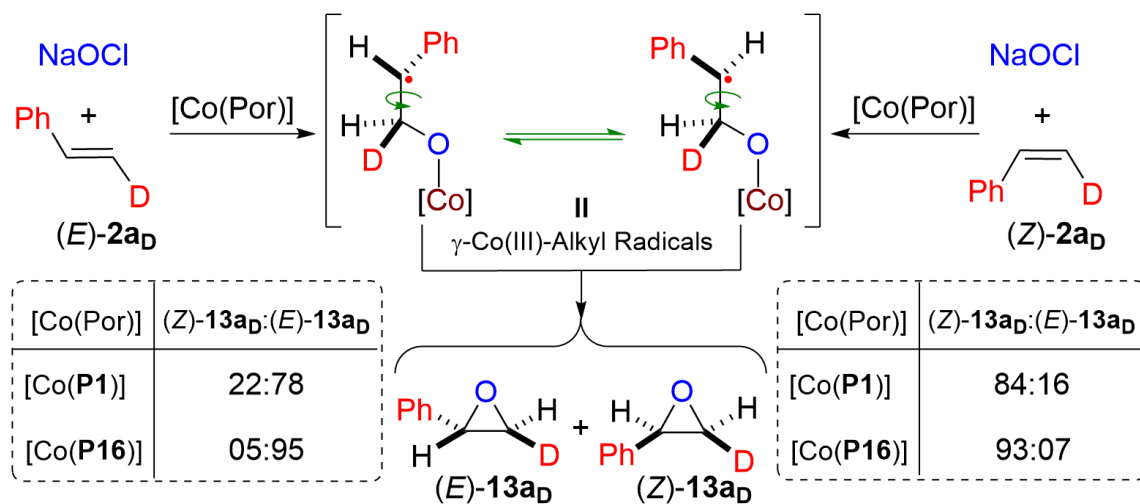
^aCarried out with NaOCl·5H₂O (**12**; 0.1 mmol) and alkene **2** (0.5 mmol) in the presence of 4 Å MS (50 mg) using [Co(P16)] (2 mol %) under N₂ atmosphere in a mixture of acetonitrile (0.15 mL) and n-Hexane (0.35 mL) at 4 °C for 16 h. Enantiomeric excess determined by chiral HPLC analysis. ^bYield based on crude HNMR analysis with internal standard. ^cIsolated yield. ^dIsolation failed due to products low boiling point and decomposition during column chromatography. ^eIsolation not attempted due to low yield.

4.2.6 Mechanistic Studies

To gain further insight on the nature of this new radical reaction with the new ligand scaffold, we explored the epoxidation of both isotopomers of β -deuterostyrenes (*E*)-**2a_D** and (*Z*)-**2a_D** with the same logic explained in section 3.2.2.5. As demonstrated in Chapter 3, when (*E*)-**2a_D** was used in the presence of catalyst [Co(**P1**)], both (*Z*)-**13a_D** and (*E*)-**13a_D** products were observed with an isotopomer ratio of 22:78. Under the same conditions, epoxidation of (*Z*)-**2a_D** yielded an 84:16 (*Z*)-**13a_D** to (*E*)-**13a_D** product ratio (Scheme 4.3). In a similar fashion, when (*E*)-**2a_D** and (*Z*)-**2a_D** were used in the presence of more sterically congested catalyst [Co(**P16**)], both (*Z*)-**13a_D** and (*E*)-**13a_D** products were observed with an isotopomer ratio of 05:95 and 93:07, respectively (Scheme 4.4). While the degree of product distribution decreased when using the optimal and more rigid catalyst compared with [Co(**P1**)], the observation of (*Z*)-**13a_D** from isomerically pure (*E*)-**2a_D** along with the observation of (*E*)-**13a_D** from isomerically pure (*Z*)-**2a_D** still suggest rotation around the β -C–C bond in the γ -Co(III)-alkyl radical intermediate **II** before ring closure, supporting the existence of such intermediate. These observations, along with the characterization data obtained in Chapter 3, are in sound agreement with the putative stepwise radical mechanism proposed (Scheme 4.1B). It is necessary to add that no erosion of the original isomeric purity was observed in the recovered starting materials (*E*)-**2_D** and (*Z*)-**2_D** after the reaction.

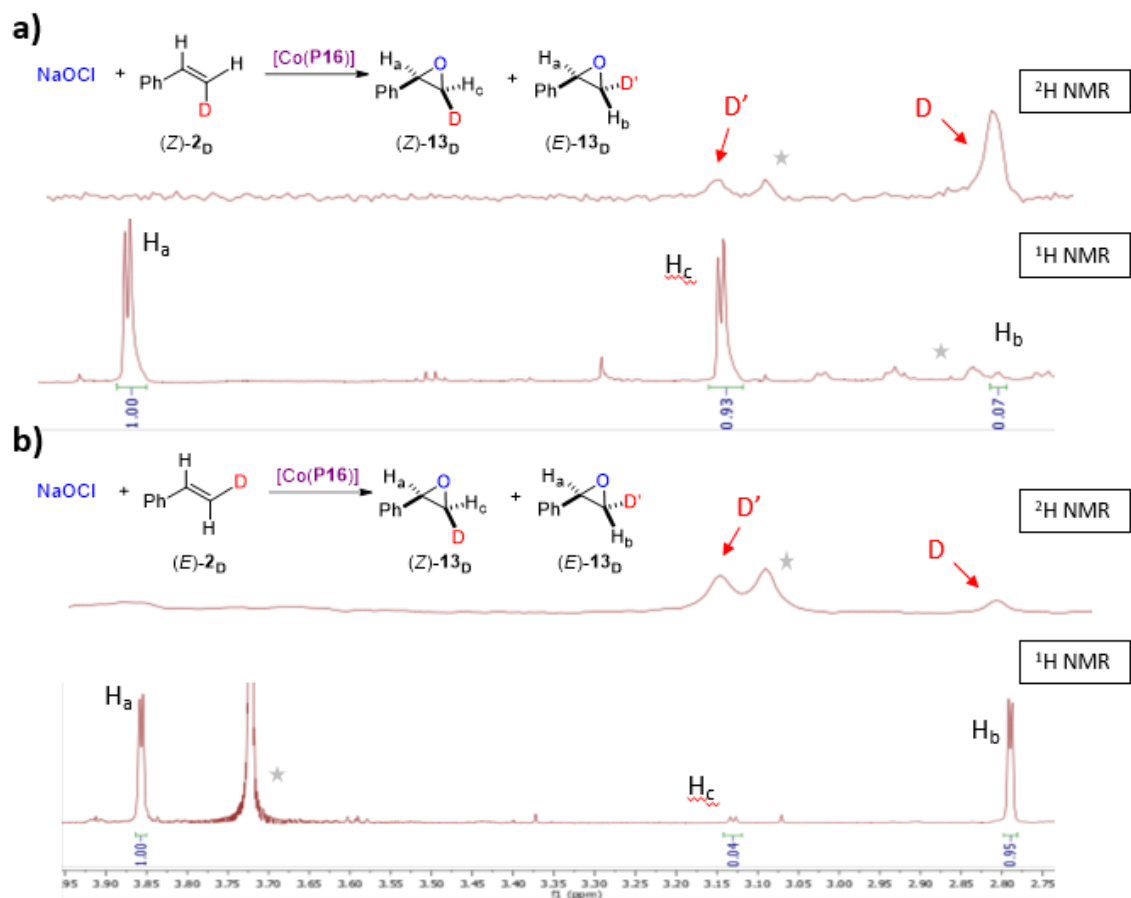
Scheme 4.3| Epoxidation of β -Deuterostyrenes with New Catalyst to Probe Radical

Mechanism^a



^aCarried out with NaOCl-5H₂O (**12**; 0.1 mmol) and **2D** (0.5 mmol) using [Co(Por)] (2 mol %) in the presence of 4 Å molecular sieves (50 mg) under N₂ atmosphere in acetonitrile (0.5 mL) at room temperature for 16 h. (Z)-**13a_D**:(E)-**13a_D** ratio determined by ¹H-NMR and ²H-NMR analysis of crude reaction mixture; see Scheme 4.4.

Scheme 4.4| Upfield ^2H NMR and ^1H NMR for Epoxide Isomers 13_{D} from $[\text{Co}(\text{P16})]$ -Catalyzed Epoxidation between: a) NaOCl (12) and (Z) - β -Deuterostyrene ((Z) - 2_{D}); b) NaOCl (12) and (E) - β -Deuterostyrene ((E) - 2_{D})



★ Indicates impurity in crude ^1H NMR.

4.3 CONCLUSIONS

In summary, we have demonstrated for the first time how the unprecedented oxygen-centered radicals have been used for the highly enantioselective epoxidation of alkenes through the development of a novel scaffold of D_2 -symmetric chiral amidoporphyrins with arene-containing bridges across two chiral amide units on both sides of the porphyrin plane (designated “JesuPhyrin”). The new catalytic system for the enantioselective radical epoxidation affords styrene oxide derivatives with up to 80% yields and 94% ee. Further mechanistic studies with the new ligand scaffold are consistent with the proposed step wise radical mechanism characteristic of MRC. We envision that these findings can have potential implications in the design of highly selective oxidation reactions and can open new reactivity modes via Co(II)-Metalloradical epoxidation and C–H hydroxylation. Furthermore, we hope the new ligand scaffold of bridge porphyrin “JesuPhyrin” will find many applications in the development of new stereoselective radical reactions via Co(II)-MRC.

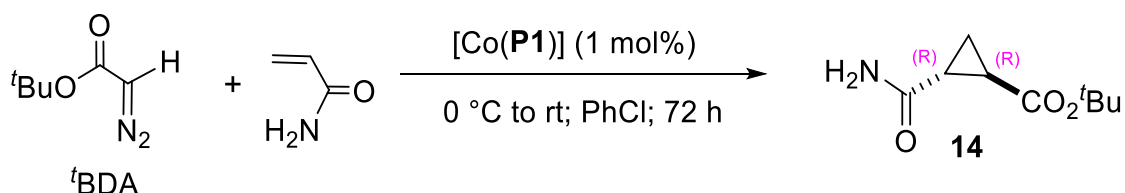
4.4 EXPERIMENTAL SECTION

4.4.1 General Considerations

Unless otherwise stated, all reactions were carried out under a nitrogen atmosphere in oven-dried glassware following standard Schlenk techniques. Gas tight syringes were used to transfer liquid reagents and solvents in catalytic reactions. 4Å MS were dried in a vacuum oven prior to use. Solvent was freshly distilled/degassed prior to use unless otherwise noted. Thin layer chromatography was performed on Merck TLC plates (silica gel 60 F254), visualizing with UV-light 254 nm Flash column chromatography was performed with ICN silica gel (60 Å, 230-400 mesh, 32-63 µm). ²H and ¹H NMR, and ¹³C NMR were recorded on a Varian600 (600 MHz), Varian500 (500 MHz), Varian Inova400 (400 MHz) instrument with chemical shifts reported relative to residual solvent. ¹⁹F spectra were recorded on a Bruker 400 spectrometer (376 MHz), using CFC₃ (δ=0) as internal standard. Infrared spectra were measured with a Nicolet Avatar 320 spectrometer with a Smart Miracle accessory. HPLC measurements were carried out on a Shimadzu HPLC system with Chiralcel OD-H, OJ-H, AD-H, IC, ID and Whelk columns. Optical rotations were measured on a Rudolph Research Analytical AUTOPOL[®] IV digital polarimeter. The UV-Vis absorption spectra in the range 200-700 nm were measured with an Evolution 300 UV-VIS spectrophotometer using quartz cuvettes with 1.0 cm optical path length. High resolution mass spectra were obtained on an Agilent 6220 using electrospray ionization time-of-flight (ESI-TOF). The X-ray diffraction data were collected using Bruker-AXSSMART-APEXII CCD diffractometer (CuKα, λ = 1.54178 Å). Co(3,5-Di^tBu-IbuPyrin), Co(3,5-Di^tBu-ChenPyrin) and Co(3,5-Di^tBu-QingPyrin) were synthesized

following literature reported procedures.^{9b} Co(2,6-DiMeO-Hu(C₆)Phyrin)⁶⁴ [Co(**P7**)], and porphyrin **15a**^{10a} were also synthesized following reported procedures. Mechanistic studies involving deuterated styrenes were carried out using the same procedures and logic as in section 3.4.8 in Chapter 3.

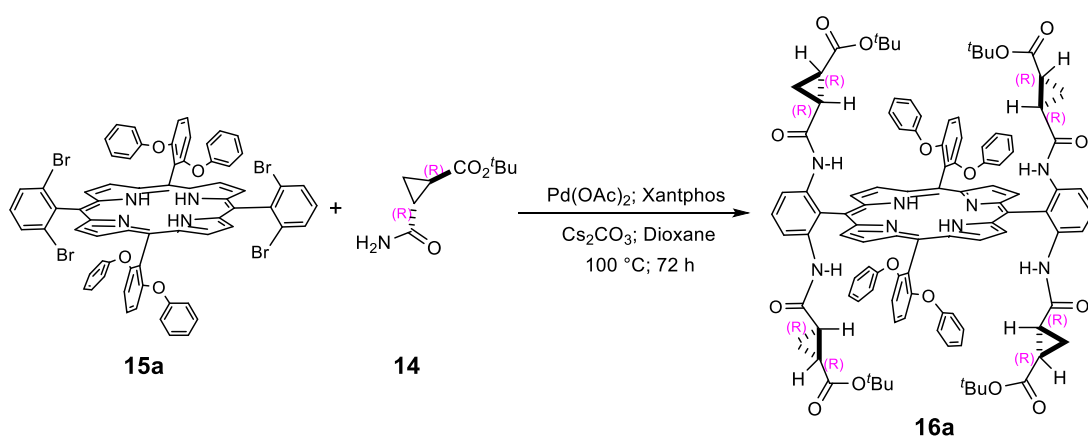
4.4.2 Catalysts Synthesis



(1R,2R)-tert-Butyl 2-carbamoylcyclopropanecarboxylate (14) was synthesized according to our reported procedure.^{9d} (S)-[Co(3,5-ditBu-ChenPhyrin)]([Co(**P1**)]) (200 mg, 0.15 mmol, 0.01 equiv), acryl amide (5.3 g, 75 mmol, 5 equiv) and DMAP (915mg, 7.5 mmol, 0.5 equiv) were placed in an oven dried, resealable Schlenk tube. The tube was capped with a Teflon screw cap, evacuated, and backfilled with nitrogen. The screw cap was replaced with a rubber septum. Chlorobenzene (50 mL) was added via syringe. After the solution was cooled to 0 °C, tBDA (2.2 mL, 15 mmol, 1 equiv) was added dropwise followed by the addition of 10 mL of chlorobenzene. The tube was purged with nitrogen for 1 min and sealed with a Teflon screw cap. The reaction mixture was warmed up to r.t. and stirred for three days. After the reaction finished, the resulting mixture was purified by flash silica gel chromatography (eluent: Hexanes/EtOAc 3:1) to give the title compound (1.80g, 65%) in 98% ee. The following recrystallization gave >99% ee; TLC R_f = 0.25 (Hexanes/EtOAc 3:1). ¹H NMR (400 MHz, CDCl₃) δ 5.84 (s, 1H), 5.76 (s, 1H), 2.07 (ddd,

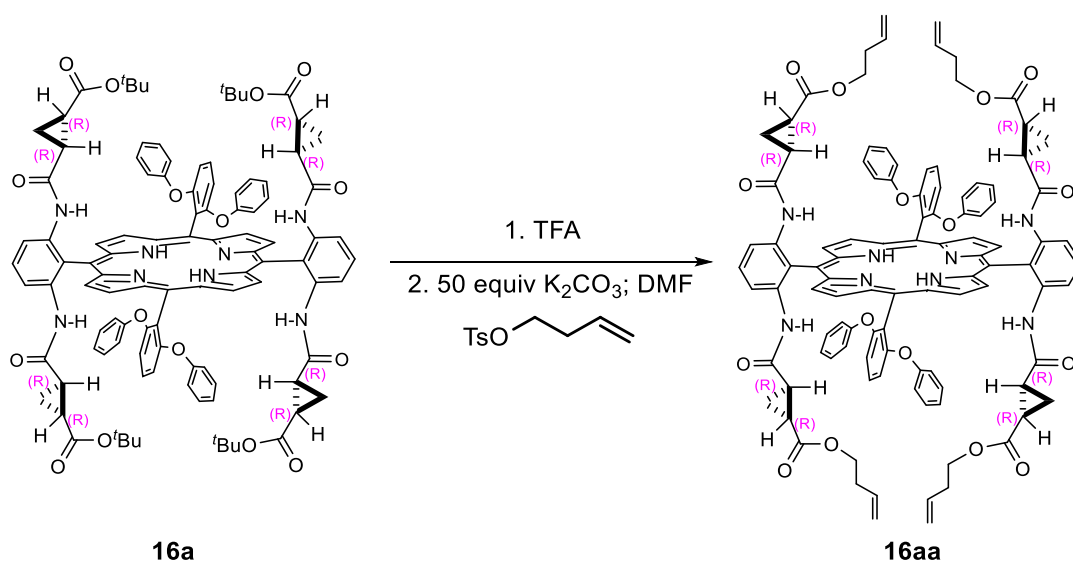
J = 9.5, 5.8, 3.8 Hz, 1H), 1.93 (ddd, J = 9.4, 5.7, 3.8 Hz, 1H), 1.44 (s, 9H), 1.38 (ddd, J = 9.3, 5.7, 3.7 Hz, 1H), 1.28 (ddd, J = 9.4, 5.8, 3.7 Hz, 1H); GC (DCB, 5 °C/min): Major t = 12.95 min., Minor t = 11.77 min. (Note: To build up enough materials, multiple runs were conducted.)

Synthesis of the Catalysts [Co(P8)]



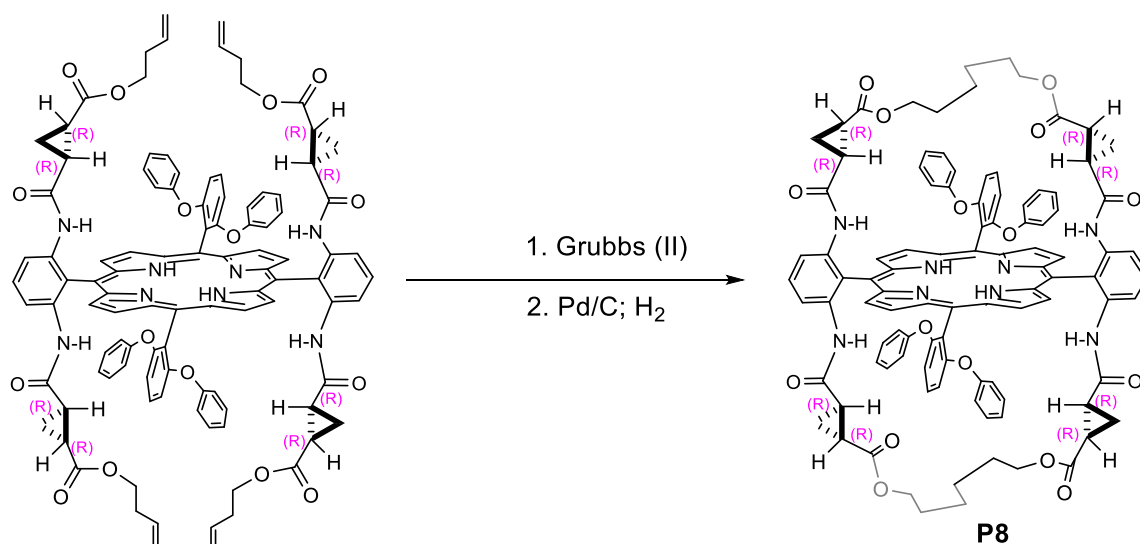
2,6-Bis(phenoxy)-Tao(^tBu)Pyrin, 16a, was synthesized by this procedure with 70% yield. 5,15-bis(2,6-dibromophenyl)-10,20-bis(2,6-diphenoxyphenyl) porphyrin (0.3 mmol), (1R,2R)-*tert*-butyl 2-carbamoylcyclopropanecarboxylate (4.8 mmol), Pd(OAc)₂ (0.08 mmol), Xantphos (0.16 mmol), and Cs₂CO₃ (3.2 mmol) were placed in an oven-dried, resealable Schlenk tube. The tube was capped with a teflon screwcap, evacuated, and backfilled with nitrogen. The screwcap was replaced with a rubber septum, and dioxane (30 mL) was added via a gastight syringe. The tube was purged with nitrogen for 2 minutes, and then the septum was replaced again with the teflon screwcap. The tube was sealed and stirred at 100 °C for 72 h. The resulting mixture was cooled down to room temperature, diluted in EtOAc, filtrated through a silica pad and concentrated under vacuum. The pure

compound was obtained as a purple solid after purification by flash column chromatography (hexanes /ethyl acetate: 3/1 to 2/1). ^1H NMR (500 MHz, CDCl_3) δ 9.11 (d, $J = 4.8$ Hz, 4H), 8.77 (d, $J = 4.7$ Hz, 4H), 8.46 (s, 4H), 7.83 (t, $J = 8.5$ Hz, 2H), 7.62 (t, $J = 8.5$ Hz, 2H), 7.02 (t, $J = 7.6$ Hz, 12H), 6.80 (t, $J = 7.4$ Hz, 4H), 6.77 (d, $J = 8.1$ Hz, 8H), 6.58 (s, 4H), 1.78 – 1.75 (m, 4H), 0.92 (s, 36H), 0.80 (p, $J = 4.7$ Hz, 4H), 0.43 (s, 4H), 0.21 (s, 4H). ^{13}C NMR (125 MHz, CDCl_3): δ 170.34, 169.08, 159.21, 156.32, 139.19, 130.79, 130.39, 129.56, 123.63, 123.46, 119.52, 119.45, 118.01, 112.76, 112.26, 107.13, 80.55, 27.79, 24.00, 22.95, 14.86. UV-vis (CHCl_3), λ_{max} nm (log ϵ): 423(5.51), 515(4.25), 545 (3.33), 589(3.53), 644(3.21). HRMS (ESI): m/z calculated for $[\text{C}_{104}\text{H}_{98}\text{N}_8\text{O}_{16}+\text{H}]^+$, found 1715.7154 $[\text{M}+\text{H}]^+$



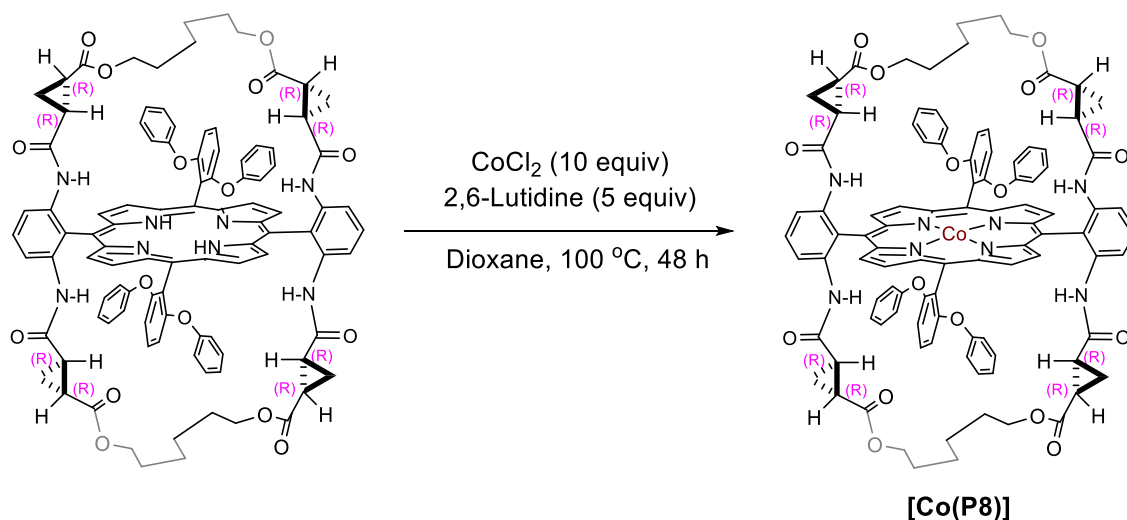
Synthesis of 16aa: TFA (100.0 equiv) was added to a solution of 2,6-bis(phenoxy)-Tao(*t*Bu)Pyrin (1.0 equiv) in DCM (0.5 M) and the reaction mixture was stirred overnight prior to the evaporation of all the volatiles. The residue was dissolved in DMF (0.1 M),

followed by the addition of powdered K_2CO_3 (50.0 equiv) and then followed by the addition of alkylating reagents (20.0 equiv). The reaction mixture was heated at 100 °C for 12 h. After cooling to room temperature, the reaction mixture was diluted with EtOAc and water. The organic layer was separated and washed with brine five times. The organic solvent was removed under vacuum and the resulting oil was then purified by flash column chromatography (eluent: Hexanes/EtOAc 3:1) to afford the pure title compound **16aa** (80% yield). 1H NMR (600 MHz, $CDCl_3$) δ 9.33 (d, $J = 4.5$ Hz, 4H), 8.98 (d, $J = 5.1$ Hz, 4H), 8.68 – 8.59 (m, 4H), 8.00 (t, $J = 8.6$ Hz, 2H), 7.80 (td, $J = 8.5, 2.7$ Hz, 2H), 7.19 (td, $J = 8.2, 2.9$ Hz, 12H), 6.97 (t, $J = 7.4$ Hz, 4H), 6.95 – 6.91 (m, 8H), 6.87 (s, 4H), 5.46 (dq, $J = 17.1, 7.8$ Hz, 4H), 4.81 (t, $J = 15.7$ Hz, 8H), 3.66 (t, $J = 6.5$ Hz, 8H), 2.08 – 1.95 (m, 12H), 1.15 – 1.00 (m, 4H), 0.66 (s, 4H), 0.49 (s, 4H), -2.38 (s, 2H). ^{13}C NMR (150 MHz, $CDCl_3$): δ 171.18, 168.65, 159.18, 156.20, 139.08, 133.64, 130.87, 130.47, 129.59, 123.70, 123.09, 121.89, 119.51, 117.97, 116.99, 112.72, 112.14, 107.16, 63.43, 32.63, 24.33, 21.79, 14.82. UV-vis ($CHCl_3$), λ_{max} nm (log ϵ): 424(5.49), 516(4.21), 546 (3.36), 589(3.57), 644(3.14). HRMS (ESI): m/z calculated for m/z calculated for $[C_{104}H_{91}N_8O_{16}+H]^+$ 1709.6659 found 1709.6531 $[M+H]^+$



Synthesis of P8: Grubbs 2nd generation catalyst (0.1 equiv) was added to a solution of the ester porphyrin (1.0 equiv) in DCM (0.001 M) and the reaction mixture was stirred 12 h at 40 °C. The reaction mixture was directly poured onto a pad of silica gel (Hexanes/EtOAc 1:1) to afford the mixture of trans-cis isomers, which was in turn dissolved in EtOAc-toluene (V/V 2/1, 0.02 M) in the presence of 10% Pd/C (1 mg per mg of porphyrin). Hydrogen gas was bubbled through the reaction mixture for about 10 to 20 min until the reaction is completed based on the crude ¹H NMR. The reaction mixture was filtered, the solvent was removed under vacuum, and the resulting oil was then purified by flash column chromatography (Hexanes/EtOAc/DCM 1:1:1) to afford pure product **P8** (70% yield). ¹H NMR (600 MHz, CDCl₃) δ 9.28 (d, *J* = 4.8 Hz, 4H), 8.96 (d, *J* = 4.8 Hz, 4H), 8.43 (d, *J* = 8.4 Hz, 4H), 7.95 (t, *J* = 8.5 Hz, 2H), 7.72 (t, *J* = 8.6 Hz, 2H), 7.19 – 7.13 (m, 8H), 7.07 (d, *J* = 8.6 Hz, 4H), 6.96 (t, *J* = 7.3 Hz, 4H), 6.92 – 6.84 (m, 8H), 6.70 (s, 4H), 3.59 (dt, *J* = 10.8, 6.9 Hz, 4H), 3.37 (dt, *J* = 10.8, 6.6 Hz, 4H), 1.98 (ddd, *J* = 9.2, 5.9, 3.8 Hz, 4H), 0.99 (dt, *J* = 9.3, 4.5 Hz, 4H), 0.84 (dq, *J* = 25.8, 7.8, 7.2 Hz, 8H), 0.74 – 0.58 (m, 12H), 0.38 – 0.26 (m, 4H), -2.52 (s, 2H). ¹³C NMR (150 MHz, CDCl₃) δ 170.72, 168.57, 159.35, 156.14,

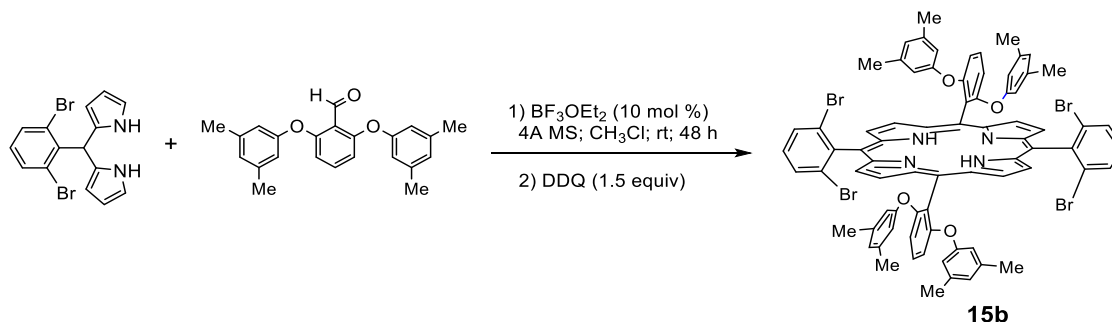
138.79, 132.88, 130.93, 130.46, 129.68, 123.93, 122.96, 122.67, 119.74, 119.55, 112.99, 111.51, 107.67, 77.44, 77.02, 64.19, 27.32, 24.53, 23.77, 22.34, 14.71. UV-vis (CHCl₃), λ_{max} nm (log ϵ): 423(5.40), 515(4.12), 547(3.41), 588(4.62), 642(3.05). HRMS (ESI): m/z calculated for [C₁₀₀H₈₆N₈O₁₆+H]⁺ 1656.6268 found 1656.6264 [M+H]⁺



Synthesis of [Co(P8)]: The desired porphyrin (1.0 equiv) and CoCl₂ (10.0 equiv) were placed in an oven dried, resealable Schlenk tube. The tube was capped with a teflon screw cap, evacuated, and backfilled with nitrogen. The screw cap was replaced with a rubber septum. 2,6-Lutidine (4.0 equiv) and THF (0.05 M) were added and the tube was purged with nitrogen for 1 min and sealed with a teflon screw cap. The reaction mixture was stirred at 100 °C for 48 h prior to being cooled to r.t. The reaction mixture was diluted with DCM and washed with brine. The organic layer was separated, dried, and concentrated. The residue was purified by flash silica gel chromatography (Hexanes:EtOAc: DCM 1:1:1) to give the title compound **[Co(P8)]** (93% yield). UV-vis (CHCl₃), λ_{max} nm (log ϵ): λ_{max}

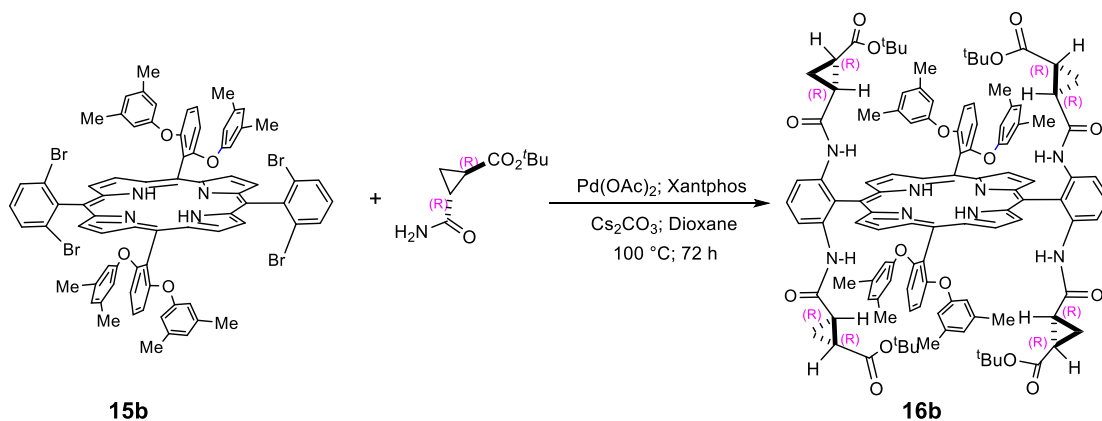
nm (log ϵ): 414(5.30), 530(4.07), 547(3.75). HRMS (ESI): m/z calculated for m/z calculated for $[C_{100}H_{84}CoN_8O_{16}+H]^+$ 1712.5410 found 1712.5341 $[M+H]^+$

Synthesis of the catalysts [Co(P9)]



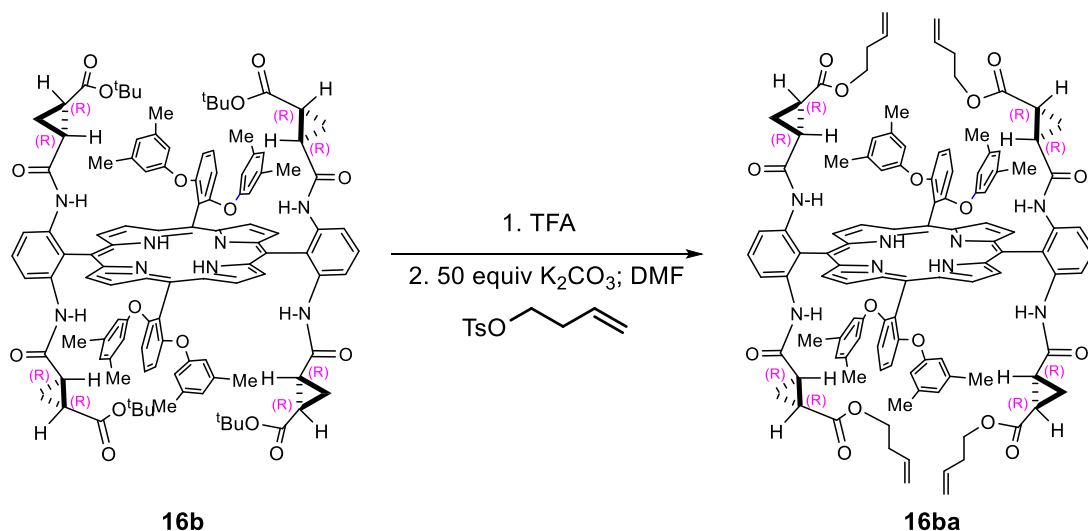
5,15-Bis(2,6-dibromophenyl)-10,20-bis(2,6-di-*m*-xilyloxyphenyl)porphyrin, 15b, was synthesized according to our previous reported procedure^{9b} with 54% yield. A mixture of meso-(2,6-dibromophenyl)dipyrrromethane (5 mmol), 2,6-di-*m*-xilyloxybenzaldehyde (5 mmol) in chloroform (500 mL) was purged with nitrogen for 10 min. The flask was wrapped with aluminum foil to shield it from light. Then boron trifluoride diethyl etherate was added dropwise via a syringe. After the solution was stirred under the nitrogen atmosphere at room temperature for 48 h, 2,3-dichloro-5,6-dicyano-1,4-benzoquinone (DDQ) (7.5 mmol) was added at one time. After 1 h, triethylamine (10 mL) was added. The reaction solution was then directly poured into a silica gel column that was rinsed with dichloromethane. The column was eluted with dichloromethane. The fractions containing the product were collected and concentrated under vacuum. The residue was washed several times with methanol/ dichloromethane mixture to afford the pure compound in 54% yield. 1H NMR (600 MHz, $CDCl_3$): δ 8.95 (d, $J = 4.7$ Hz, 4H), 8.55 (d, $J = 4.7$ Hz,

4H), 8.02 (d, $J = 8.2$ Hz, 5H), 7.61 (t, $J = 8.5$ Hz, 2H), 7.52 (t, $J = 8.2$ Hz, 2H), 7.08 (d, $J = 8.4$ Hz, 4H), 6.22 (s, 8H), 6.15 (s, 4H), 1.79 (s, 24H), -2.67 (s, 2H). ^{13}C NMR (125 MHz, CDCl_3): δ 159.00, 156.44, 143.82, 138.80, 131.59, 131.02, 130.22, 128.88, 124.91, 124.79, 117.69, 116.98, 113.15, 110.77, 21.06. UV-vis (CHCl_3), λ_{max} nm (log ϵ): 425(6.53), 518(5.21), 596(4.77), 606(4.55). HRMS (ESI): m/z calculated for $[\text{C}_{76}\text{H}_{58}\text{Br}_4\text{N}_4\text{O}_4+\text{H}]^+$ 1407.1264, found 1407.1236 $[\text{M}+\text{H}]^+$



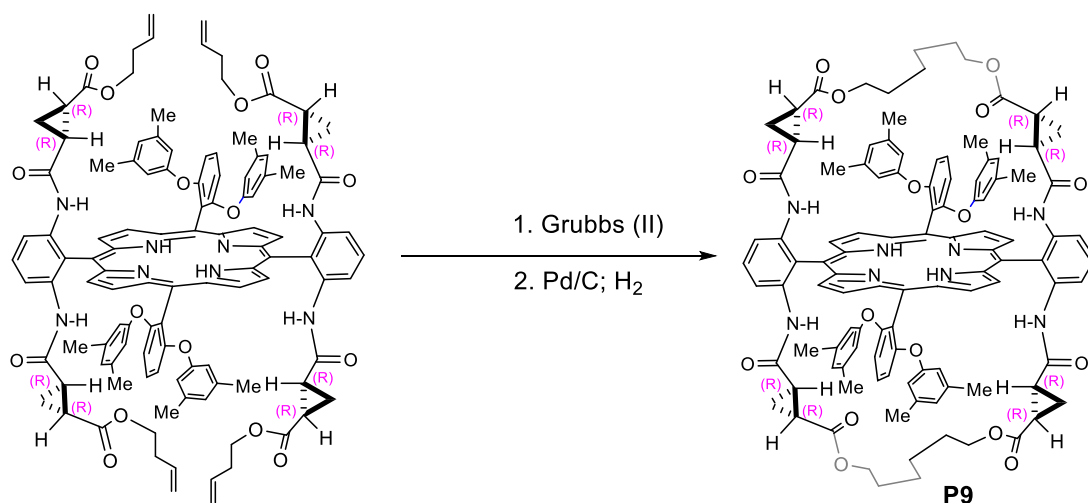
(2,6-Di-*m*-xylyloxy)-Tao(*t*-Bu)Pheyrin, 16b, was synthesized according to our previous reported procedure^{9b} with 58% yield. The 5,15-bis(2,6-dibromophenyl)-10,20-bis(2,6-di-*m*-xylyloxyphenyl)porphyrin (0.3 mmol), (1*R*,2*R*)-*tert*-Butyl 2-carbamoylcyclopropanecarboxylate (4.8 mmol), $\text{Pd}(\text{OAc})_2$ (0.08 mmol), Xantphos (0.16 mmol), and Cs_2CO_3 (3.2 mmol) were placed in an oven-dried, resealable Schlenk tube. The tube was capped with a teflon screwcap, evacuated, and backfilled with nitrogen. The screwcap was replaced with a rubber septum, and dioxane (30 mL) was added via a gastight syringe. The tube was purged with nitrogen for 2 minutes, and then the septum was replaced with the teflon screwcap. The tube was sealed and stirred at 100 °C for 72 h. The

resulting mixture was cooled down to room temperature, diluted in EtOAc, filtrated through a silica pad and concentrated under vacuum. The pure compound was obtained as a purple solid after purification by flash column chromatography (hexanes/ethyl acetate: 3/1 to 2/1). ^1H NMR (500 MHz, CDCl_3): δ 9.14 (d, $J = 3.8$ Hz, 4H), 8.80 (d, $J = 4.9$ Hz, 4H), 8.40 (s, 4H), 7.85 (td, $J = 8.5, 2.4$ Hz, 2H), 7.58 (td, $J = 8.6, 2.7$ Hz, 2H), 6.94 (dd, $J = 8.5, 2.9$ Hz, 4H), 6.65 (s, 4H), 6.48 (s, 4H), 6.43 (s, 8H), 2.05 (s, 24H), 1.79 (q, $J = 5.1$ Hz, 4H), 0.93 (s, 36H), 0.76 (s, 4H), 0.49 (s, 4H), 0.14 (s, 4H), -2.52 (s, 2H). ^{13}C NMR (125 MHz, CDCl_3): δ 170.33, 169.20, 159.48, 156.00, 139.28, 139.11, 132.56, 130.50, 130.25, 130.24, 125.51, 122.86, 122.43, 118.80, 117.42, 113.05, 111.02, 107.18, 80.41, 27.72, 23.88, 22.75, 21.21, 14.64. UV-vis (CHCl_3), λ_{max} nm (log ϵ): 423(5.24), 516(4.03), 546(3.49), 590(3.59), 644(3.22). HRMS (ESI): m/z calculated for $[\text{C}_{112}\text{H}_{114}\text{N}_8\text{O}_{16} + \text{H}]^+$ 1828.8459, found 1828.8458 $[\text{M} + \text{H}]^+$



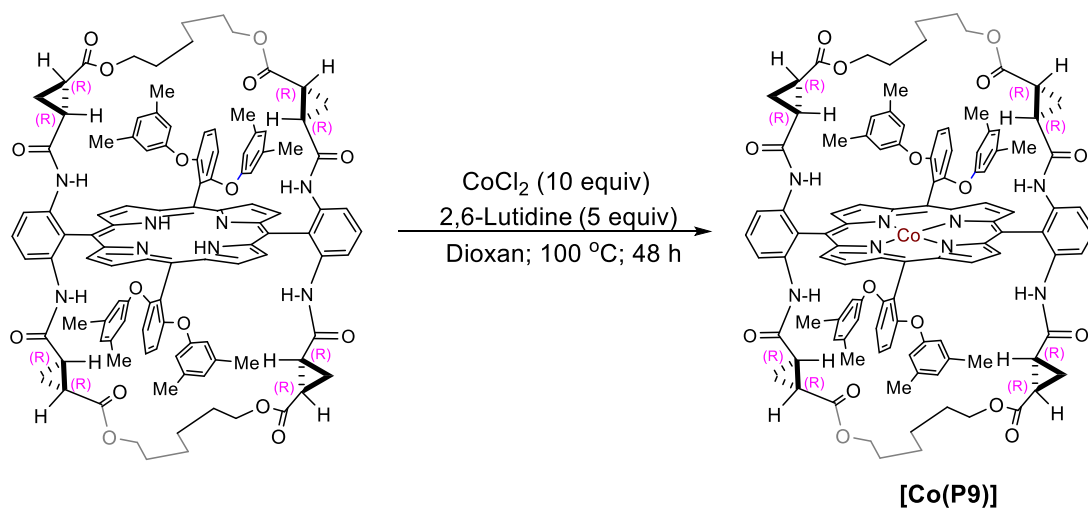
Synthesis of 16ba: TFA (100.0 equiv) was added to a solution of (2,6-di-*m*-xylyloxy)-Tao(*t*Bu)Phyrin (1.0 equiv) in DCM (0.5 M) and the reaction mixture was stirred overnight

prior to the evaporation of all the volatiles. The residue was dissolved in DMF (0.1 M), followed by the addition of powdered K_2CO_3 (50.0 equiv) and then followed by the addition of alkylating reagents (20.0 equiv). The reaction mixture was heated at 100 °C for 12 h. After cooling to rt, the reaction mixture was diluted with EtOAc and water. The organic layer was separated and washed with brine five times. The organic solvent was removed under vacuum and the resulting oil was then purified by flash column chromatography (eluent: Hexanes/EtOAc 3:1) to afford the pure title compound **16ba** (87% yield). 1H NMR (500 MHz, $CDCl_3$): δ 9.15 (d, $J = 4.8$ Hz, 4H), 8.80 (d, $J = 4.8$ Hz, 4H), 8.42 (s, 4H), 7.85 (t, $J = 8.5$ Hz, 2H), 7.56 (t, $J = 8.5$ Hz, 2H), 6.91 (d, $J = 8.5$ Hz, 4H), 6.63 (s, 4H), 6.49 (s, 4H), 6.44 (s, 8H), 5.27 (d, $J = 11.8$ Hz, 4H), 4.60 (t, $J = 16.7$ Hz, 8H), 3.48 (s, 8H), 2.05 (s, 24H), 1.91 – 1.73 (m, 12H), 0.83 (dt, $J = 9.5, 4.8$ Hz, 4H), 0.50 (s, 4H), 0.22 (s, 4H), -2.51 (s, 2H). ^{13}C NMR (125 MHz, $CDCl_3$): δ 171.13, 168.82, 159.65, 155.96, 139.44, 139.09, 133.67, 130.59, 130.46, 125.70, 122.64, 122.02, 118.57, 117.68, 117.00, 113.21, 110.83, 107.04, 63.43, 32.71, 24.33, 21.70, 21.25, 14.72. HRMS (ESI): m/z calculated for $[C_{112}H_{106}N_8O_{16}+H]^+$ 1820.7833, found 1820.7838 $[M+H]^+$ UV-vis ($CHCl_3$), λ_{max} nm (log ϵ): 423(5.73), 515(4.49), 547(3.84), 590(4.0), 644(3.44).



Synthesis of P9: Grubbs 2nd generation catalyst (0.1 equiv) was added to a solution of above ester porphyrin (1.0 equiv) in DCM (0.001 M) and the reaction mixture was stirred 12 h at 40 °C. The reaction mixture was directly poured onto a pad of silica gel (Hexanes/EtOAc 1:1) to afford the mixture of trans-cis isomers, which was in turn dissolved in EtOAc-toluene(V/V 2/1, 0.02 M) in the presence of 10% Pd/C (1 mg per mg of porphyrin). Hydrogen gas was bubbled through the reaction mixture for about 10 to 20 min until the reaction is completed based on the crude ¹H NMR. The reaction mixture was filtered, the solvent was removed under vacuum, and the resulting oil was then purified by flash column chromatography (Hexanes/EtOAc 1:1) to afford pure product **P9** (70% yield). ¹H NMR (500 MHz, CDCl₃): δ 9.18 (d, *J* = 4.8 Hz, 4H), 8.87 (d, *J* = 4.8 Hz, 4H), 8.31 (d, *J* = 8.4 Hz, 4H), 7.87 (t, *J* = 8.4 Hz, 2H), 7.59 (t, *J* = 8.5 Hz, 2H), 6.92 (d, *J* = 8.5 Hz, 4H), 6.60 (s, 4H), 6.53 (dt, *J* = 1.6, 0.7 Hz, 4H), 6.44 (dt, *J* = 1.5, 0.7 Hz, 8H), 3.46 (dt, *J* = 10.8, 6.9 Hz, 4H), 3.29 (dt, *J* = 10.8, 6.7 Hz, 4H), 2.07 (s, 24H), 1.92 (ddd, *J* = 8.9, 5.9, 3.8 Hz, 4H), 0.86 (ddd, *J* = 9.2, 5.5, 4.0 Hz, 4H), 0.72 (m, 8H), 0.60 (ddd, *J* = 9.1, 5.5, 3.8 Hz, 4H), 0.57 – 0.40 (m, 8H), 0.17 (ddd, *J* = 8.7, 5.9, 4.0 Hz, 4H), -2.61 (s, 2H). ¹³C NMR (125 MHz, CDCl₃): δ 170.66, 168.61, 159.56, 155.90, 139.42, 138.76, 130.67, 130.38, 125.68,

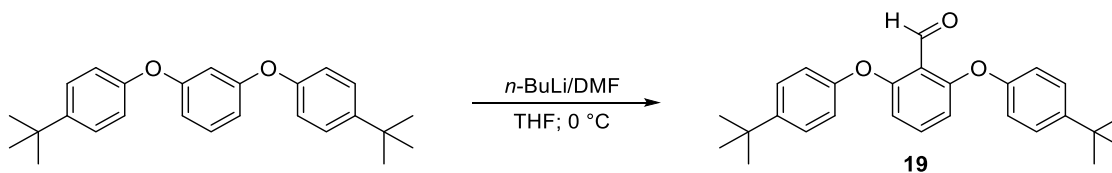
123.45, 121.88, 119.87, 117.57, 113.33, 110.66, 107.57, 64.21, 27.34, 24.63, 23.72, 22.22, 21.25, 14.55. UV-vis (CHCl_3), λ_{max} nm (log ϵ): 424(5.75), 516(4.49), 550(3.87), 590(4.0), 643(3.50). HRMS (ESI): m/z calculated for $[\text{C}_{108}\text{H}_{102}\text{N}_8\text{O}_{16}+\text{H}]^+$ 1768.7520, found 1768.7516 $[\text{M}+\text{H}]^+$



Synthesis of [Co(P9)]: The desired porphyrin (1.0 equiv) and CoCl_2 (10.0 equiv) were placed in an oven dried, resealable Schlenk tube. The tube was capped with a teflon screw cap, evacuated, and backfilled with nitrogen. The screw cap was replaced with a rubber septum. 2,6-Lutidine (4.0 equiv) and THF (0.05 M) were added and the tube was purged with nitrogen for 1 min and sealed with a teflon screw cap. The reaction mixture was stirred at 100 °C for 48 h prior to being cooled to r.t. The reaction mixture was diluted with DCM and washed with brine. The organic layer was separated, dried, and concentrated. The residue was purified by flash silica gel chromatography (Hexanes:EtOAc:DCM 1:1:1) to give the title compound **[Co(P9)]** (90% yield). UV-vis (CHCl_3), λ_{max} nm (log ϵ): 415

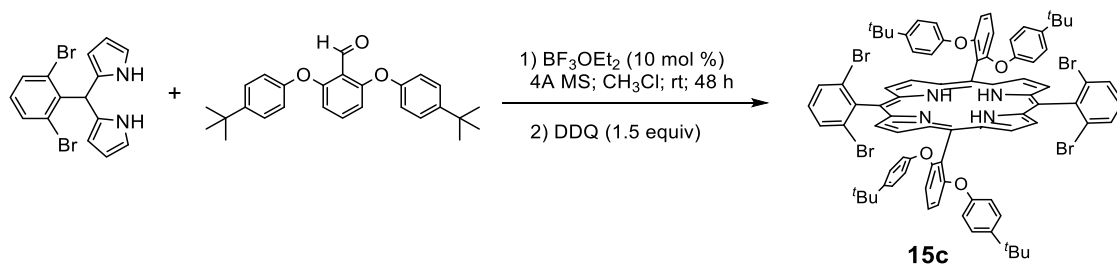
(4.38), 529 (4.11), 544 (3.44). HRMS (ESI): m/z calculated for $[C_{108}H_{100}CoN_8O_{16}+H]^+$ 1824.6662, found 1824.6606 $[M+H]^+$

Synthesis of the catalysts [Co(P10)]



2,6-bis(4-(*tert*-butyl)phenoxy)benzaldehyde (19). To a stirred solution of 1,3-bis(4-(*tert*-butyl)phenoxy)benzene (10 mmol) in dry THF (60 mL) at $0\text{ }^\circ\text{C}$, $n\text{-BuLi}$ (8 mL, 1.5 M in hexanes) was added dropwise for 1 h. Then the mixture was stirred at room temperature for 2 h and followed by the slow addition of DMF (1.83 g, 25 mmol). After 2 h, the mixture was poured into ice water. The organic phase was separated and the aqueous phase was extracted with ether ($3\times 30\text{ mL}$). The combined organic layer was dried over anhydrous Na_2SO_4 . After the removal of solvent under vacuum, the product was purified by column chromatography with hexanes/ethyl acetate (9:1 to 6:1) as eluent to afford the aldehyde as a white solid in 70% yield.

^1H NMR (600 MHz, CDCl_3) δ 10.63 (s, 1H), 7.43 – 7.38 (m, 4H), 7.29 (dd, $J = 18.0, 9.6$ Hz, 1H), 7.05 – 7.00 (m, 4H), 6.57 (d, $J = 8.4$ Hz, 2H), 1.35 (s, 18H). ^{13}C NMR (150 MHz, CDCl_3) δ 188.47, 160.35, 153.79, 147.38, 135.10, 126.89, 119.32, 118.30, 112.30, 34.53, 31.60. IR (neat, cm^{-1}): 2964.39, 1692.72, 1598.69, 1507.03, 1458.88, 1214.59, 1026.95, 846.57. HRMS (DART) ($[M+H]^+$) Calcd. for $\text{C}_{27}\text{H}_{31}\text{O}_3^+$: 403.2268, found 403.2278.

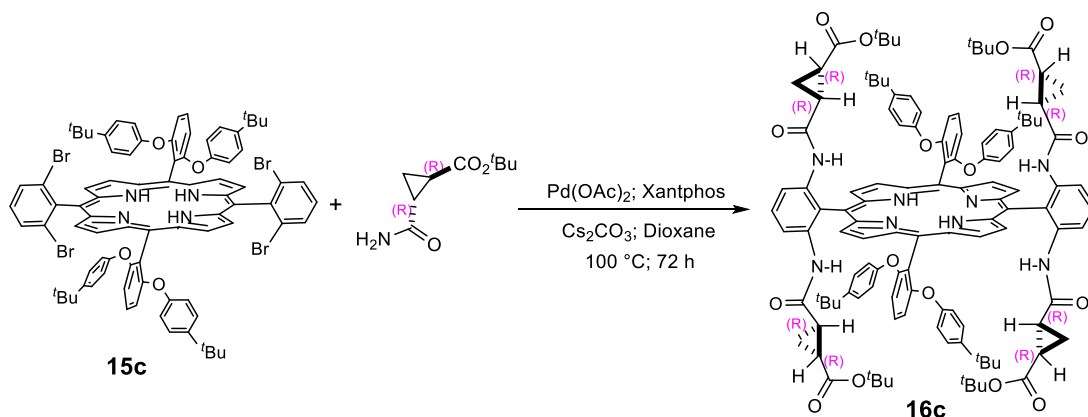


5,15-bis(2,6-bis(4-(*tert*-butyl)phenoxy)phenyl)-10,20-bis(2,6-

dibromophenyl)porphyrin, **15c**, was synthesized according to our previous reported

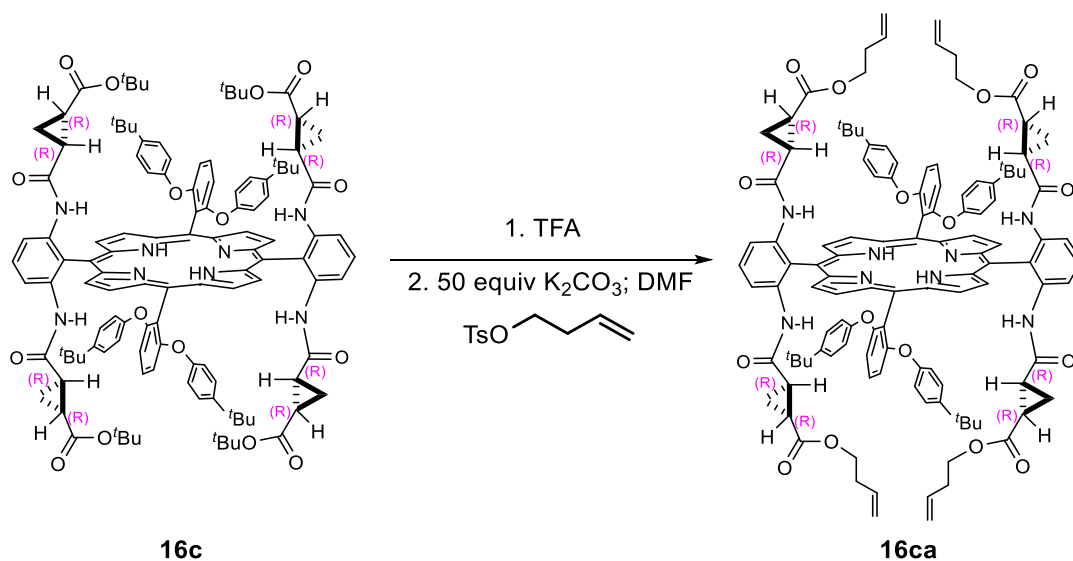
procedure^{9b} with 58% yield. A mixture of meso-(2,6-dibromophenyl)dipyrrromethane (5 mmol), 2,6-bis(4-(*tert*-butyl)phenoxy)benzaldehyde (5 mmol) in chloroform (500 mL) was purged with nitrogen for 10 min. The flask was wrapped with aluminum foil to shield it from light. Then boron trifluoride diethyl etherate was added dropwise via a syringe. After the solution was stirred under the nitrogen atmosphere at room temperature for 48 h, 2,3-dichloro5,6-dicyano-1,4-benzoquinone (DDQ) (7.5 mmol) was added at one time. After 1 h, triethylamine (10 mL) was added. The reaction solution was then directly poured into a silica gel column that was rinsed with dichloromethane. The column was eluted with dichloromethane. The fractions containing the product were collected and concentrated under vacuum. The residue was washed several times with methanol/ dichloromethane mixture to afford the pure porphyrin compound in 58% yield. ¹H NMR (600 MHz, CDCl_3) δ 8.97 (d, $J = 4.7$ Hz, 4H), 8.57 (d, $J = 4.7$ Hz, 4H), 8.01 (d, $J = 8.2$ Hz, 4H), 7.58 (t, $J = 8.5$ Hz, 2H), 7.51 (t, $J = 8.2$ Hz, 2H), 7.03 (d, $J = 8.4$ Hz, 4H), 6.95 – 6.86 (m, 8H), 6.68 – 6.60 (m, 8H), 0.98 (s, 36H), -2.61 (s, 2H). ¹³C NMR (150 MHz, CDCl_3): δ 159.30, 154.22, 145.97, 143.77, 131.58, 131.02, 130.11, 128.91, 126.06, 124.47, 118.89, 117.76, 112.44, 111.06, 34.16, 31.42. UV-vis (CHCl_3), λ_{max} nm (log ϵ): 424 (5.54), 518 (4.21), 593 (3.54),

649 (3.12). HRMS (ESI): m/z calculated for $[C_{84}H_{74}Br_4N_4O_4 + H]^+$ 1519.2475, found 1519.2486 $[M+H]^+$



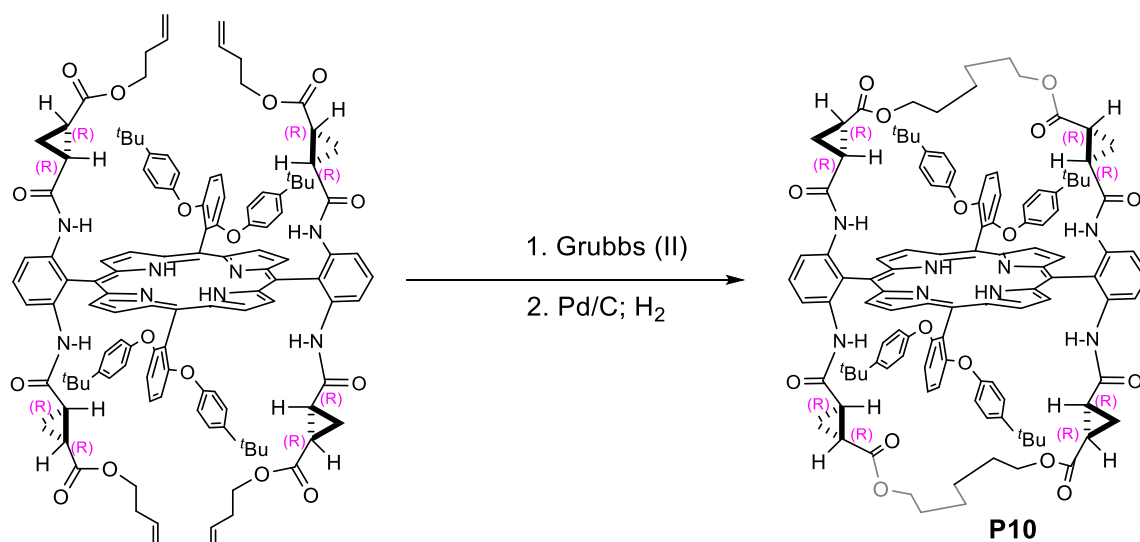
2,6-Bis(4-(*tert*-butyl)phenoxy)-Tao(*tert*-Bu)Pheyrin, 16c, was synthesized according to our previous reported procedure with 61% yield. The 5,15-bis(2,6-dibromophenyl)-10,20-bis(2,6-di-*m*-xylyloxyphenyl)porphyrin (0.3 mmol), (1*R*,2*R*)-*tert*-butyl 2-carbamoylcyclopropanecarboxylate (4.8 mmol), Pd(OAc)₂ (0.08 mmol), Xantphos (0.16 mmol), and Cs₂CO₃ (3.2 mmol) were placed in an oven-dried, resealable Schlenk tube. The tube was capped with a teflon screwcap, evacuated, and backfilled with nitrogen. The screwcap was replaced with a rubber septum, and dioxane (30 mL) was added via a gastight syringe. The tube was purged with nitrogen for 2 minutes, and then the septum was replaced with the teflon screwcap. The tube was sealed and stirred at 100 °C for 72 h. The resulting mixture was cooled down to room temperature, diluted in EtOAc, filtered through a silica pad and concentrated under vacuum. The pure compound was obtained as a purple solid after purification by flash column chromatography (hexanes/dichloromethane/ethyl acetate: 3/3/1 to 2/2/1). ¹H NMR (500 MHz, CDCl₃) δ

9.14 (t, $J = 4.1$ Hz, 4H), 8.80 (d, $J = 5.1$ Hz, 4H), 8.39 (s, 4H), 7.84 (t, $J = 8.4$ Hz, 2H), 7.55 (t, $J = 8.5$ Hz, 2H), 7.09 (dtd, $J = 9.6, 4.6, 2.3$ Hz, 8H), 6.92 (d, $J = 8.5$ Hz, 4H), 6.81 – 6.71 (m, 8H), 6.63 (s, 4H), 1.77 (p, $J = 5.0, 4.6$ Hz, 4H), 1.13 (s, 36H), 0.93 (s, 36H), 0.68 (s, 4H), 0.46 (s, 4H), 0.10 – 0.03 (m, 4H), -2.47 (s, 2H). ^{13}C NMR (125 MHz, CDCl_3) δ 170.36, 169.20, 159.90, 153.73, 146.78, 139.07, 130.43, 130.26, 126.49, 122.86, 121.99, 119.60, 118.78, 113.21, 110.48, 107.14, 80.46, 34.34, 31.51, 27.80, 23.89, 22.77, 14.84. UV-vis (CHCl_3), λ_{max} nm (log ϵ): 424 (5.53), 515 (4.32), 548 (3.71), 589 (3.86), 644 (3.37). HRMS (ESI): m/z calculated for $[\text{C}_{120}\text{H}_{130}\text{N}_8\text{O}_{16}+\text{H}]^+$ 1939.9678 found 1939.9676 $[\text{M}+\text{H}]^+$



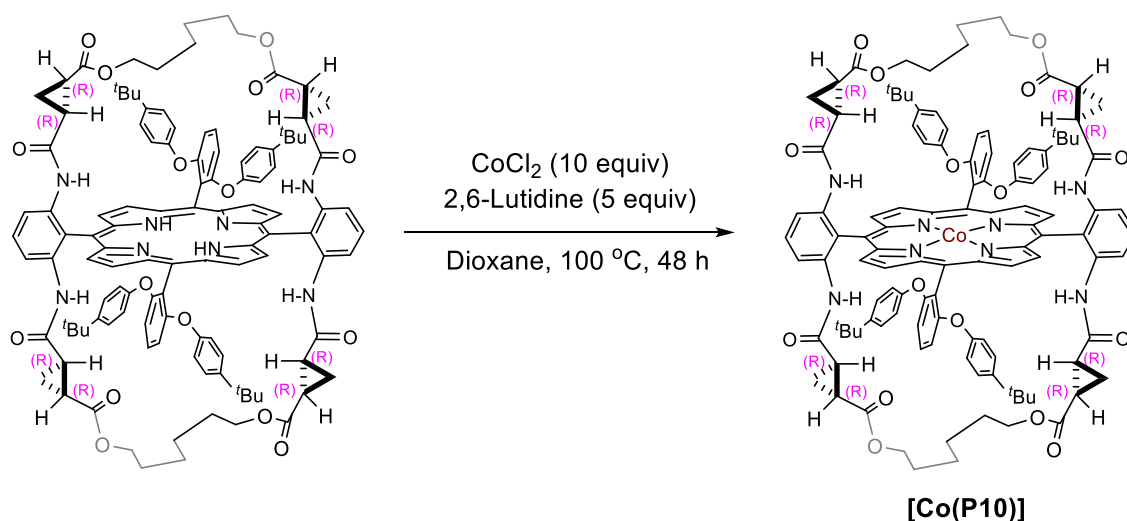
Synthesis of 16ca: TFA (100.0 equiv) was added to a solution of 2,6-bis(4-(*tert*-butyl)phenoxy)-Tao(*t*Bu)Phyrin (1.0 equiv) in DCM (0.5 M) and the reaction mixture was stirred overnight prior to the evaporation of all the volatiles. The residue was dissolved in DMF (0.1 M), followed by the addition of powdered K_2CO_3 (50.0 equiv) and then followed

by the addition of alkylating reagents (20.0 equiv). The reaction mixture was heated at 100 °C for 12 h. After cooling to rt, the reaction mixture was diluted with EtOAc and water. The organic layer was separated and washed with brine five times. The organic solvent was removed under vacuum and the resulting oil was then purified by flash column chromatography (eluent: Hexanes/EtOAc/DCM 3:3:1) to afford the pure title compound **16ca** (78% yield). ¹H NMR (500 MHz, CDCl₃) δ 9.16 (d, *J* = 4.8 Hz, 4H), 8.80 (d, *J* = 4.6 Hz, 4H), 8.41 (s, 4H), 7.85 (t, *J* = 8.4 Hz, 2H), 7.55 (t, *J* = 8.5 Hz, 2H), 7.14 – 7.06 (m, 8H), 6.90 (d, *J* = 8.5 Hz, 4H), 6.81 – 6.73 (m, 8H), 6.63 (s, 4H), 5.33 – 5.20 (m, 4H), 4.60 (dd, *J* = 23.8, 13.7 Hz, 8H), 3.49 (s, 8H), 1.98 – 1.68 (m, 12H), 1.13 (s, 36H), 0.81 – 0.67 (m, 4H), 0.47 (s, 4H), 0.07 (s, 4H), -2.47 (s, 2H). ¹³C NMR (125 MHz, CDCl₃) δ 171.14, 168.76, 159.95, 153.67, 146.95, 139.02, 133.66, 130.53, 130.41, 126.57, 122.52, 121.68, 119.70, 118.44, 117.02, 113.26, 110.44, 107.00, 63.43, 34.37, 32.70, 31.50, 24.30, 21.66, 14.80. UV-vis (CHCl₃), λ_{max} nm (log ε): 423 (5.55), 514 (4.33), 549 (3.70), 590 (3.86), 644 (3.50). HRMS (ESI): *m/z* calculated for [C₁₂₀H₁₂₂N₈O₁₆+H]⁺ 1932.9085 found 1932.9081 [M+H]⁺



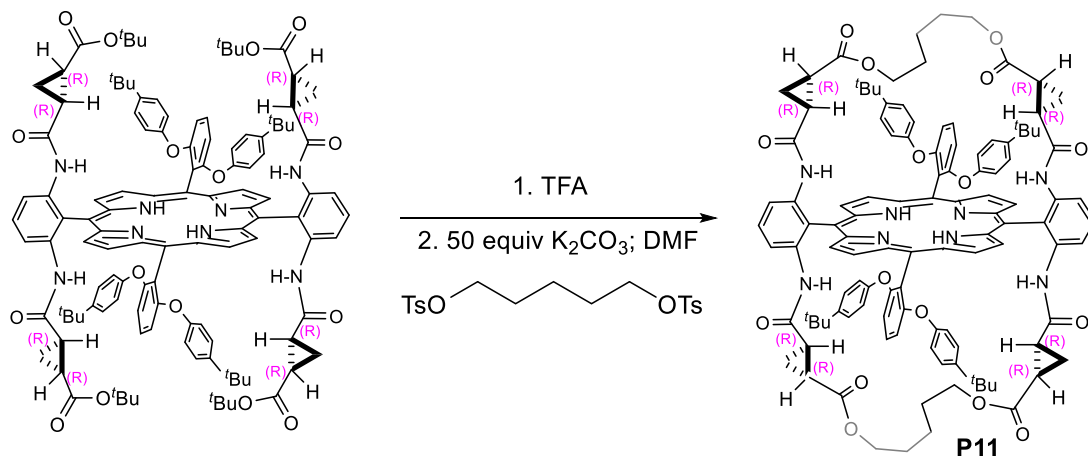
Synthesis of P10: Grubbs 2nd generation catalyst (0.1 equiv) was added to a solution of above ester porphyrin (1.0 equiv) in DCM (0.001 M) and the reaction mixture was stirred 12 h at 40 °C. The reaction mixture was directly poured onto a pad of silica gel (Hexanes/EtOAc 1:1) to afford the mixture of trans-cis isomers, which was in turn dissolved in EtOAc-toluene (V/V 2/1, 0.02 M) in the presence of 10% Pd/C (1 mg per mg of porphyrin). Hydrogen gas was bubbled through the reaction mixture for about 10 to 20 min until the reaction is completed based on the crude ¹H NMR. The reaction mixture was filtered, the solvent was removed under vacuum, and the resulting oil was then purified by flash column chromatography (Hexanes/EtOAc/DCM 1:1:1) to afford pure product **P10** (75% yield). ¹H NMR (500 MHz, CDCl₃) δ 9.19 (d, *J* = 4.8 Hz, 4H), 8.87 (d, *J* = 4.8 Hz, 4H), 8.32 (d, *J* = 8.4 Hz, 4H), 7.87 (t, *J* = 8.4 Hz, 2H), 7.58 (t, *J* = 8.5 Hz, 2H), 7.14 – 7.06 (m, 8H), 6.93 (d, *J* = 8.5 Hz, 4H), 6.80 – 6.70 (m, 8H), 3.47 (dt, *J* = 10.7, 6.9 Hz, 4H), 3.29 (dt, *J* = 10.8, 6.7 Hz, 4H), 1.92 – 1.84 (m, 4H), 1.12 (s, 36H), 0.81 (ddd, *J* = 9.2, 5.6, 4.2 Hz, 4H), 0.74 (dt, *J* = 13.5, 6.7 Hz, 8H), 0.60 – 0.50 (m, 12H), 0.07 (ddd, *J* = 9.1, 5.7, 4.1 Hz, 4H), -2.57 (s, 2H). ¹³C NMR (125 MHz, CDCl₃) δ 170.66, 168.57, 159.79, 153.65, 146.94, 138.76, 130.69, 130.40, 126.51, 123.12, 121.78, 119.60, 119.49, 113.33, 110.56,

107.48, 64.17, 34.34, 31.47, 27.29, 24.58, 23.77, 22.22, 14.64. UV-vis (CHCl₃), λ_{max} nm (log ε): 424 (5.63), 517 (4.37), 549 (3.77), 590 (3.89), 640 (3.21). HRMS (ESI): m/z calculated for [C₁₁₆H₁₁₈N₈O₁₆+H]⁺ 1880.8772 found 1880.8762 [M+H]⁺



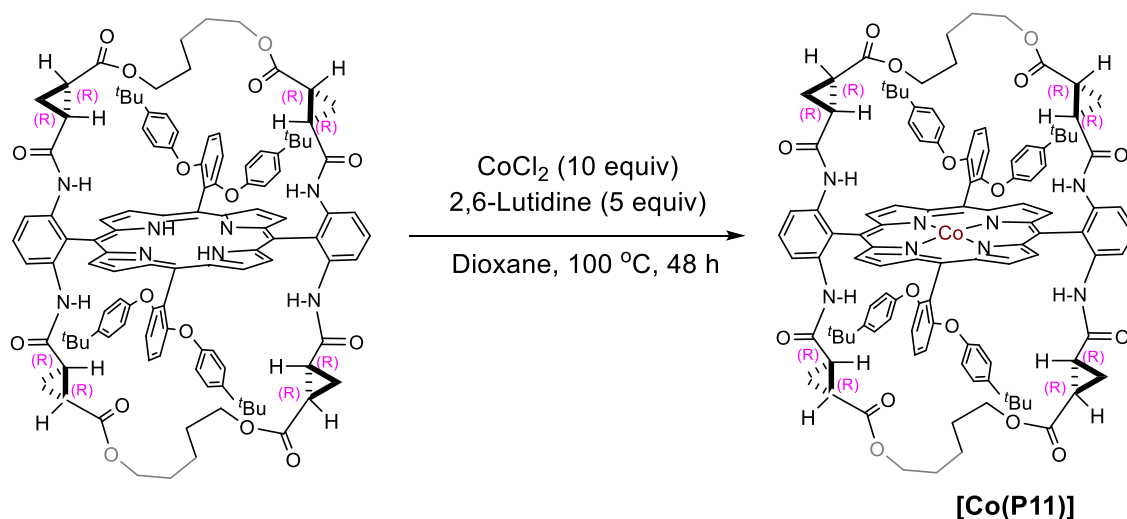
Synthesis of [Co(P10)]: The desired porphyrin (1.0 equiv) and CoCl₂ (10.0 equiv) were placed in an oven dried, resealable Schlenk tube. The tube was capped with a teflon screw cap, evacuated, and backfilled with nitrogen. The screw cap was replaced with a rubber septum. 2,6-Lutidine (5.0 equiv) and THF (0.05 M) were added and the tube was purged with nitrogen for 1 min and sealed with a teflon screw cap. The reaction mixture was stirred at 100 °C for 48 h prior to being cooled to r.t. The reaction mixture was diluted with EtOAc and washed with brine. The organic layer was separated, dried, and concentrated. The residue was purified by flash silica gel chromatography (Hexanes:EtOAc: DCM 1:1:1) to give the title compound **[Co(P10)]** (92% yield). UV-vis (CHCl₃), λ_{max} nm (log ε): 417 (5.05), 529 (4.53), 557 (4.18). HRMS (ESI): m/z calculated for [C₁₁₆H₁₁₆CoN₈O₁₆+H]⁺ 1936.7914 found 1936.7849 [M+H]⁺

Synthesis of the catalysts [Co(P11)]



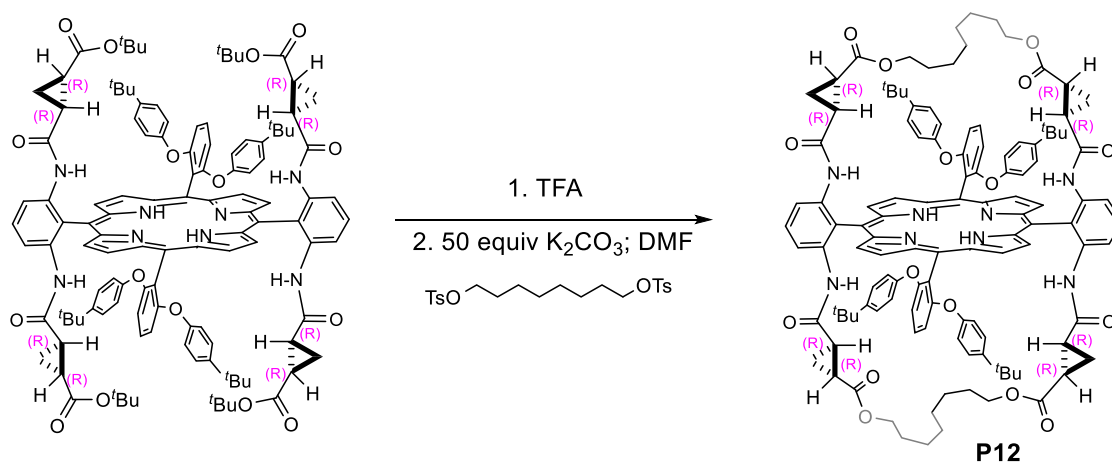
Synthesis of (P11): TFA (100.0 equiv) was added to a solution of **2,6-Di(4'-^tBu)-(^tBu)TaoPyrin (16c)** (1.0 equiv) in DCM (0.5 M) and the reaction mixture was stirred overnight prior to the evaporation of all the volatiles. The residue was dissolved in DMF (0.1 M), followed by the addition of powdered K₂CO₃ (50 equiv) and then followed by the addition of alkylating reagents (20.0 equiv). The reaction mixture was heated at 100 °C for 24 h. After cooling to rt, the reaction mixture was diluted with EtOAc and water. The organic layer was separated and washed with brine ten times. The organic solvent was removed under vacuum and the resulting mixture was then purified by flash column chromatography (eluent: Hexanes/DCM/EtOAc 5:5:1) to afford the pure title compound **P11** (45% yield). ¹H NMR (500 MHz, CDCl₃) δ 9.22 (d, J = 4.7 Hz, 4H), 8.88 (d, J = 4.7 Hz, 4H), 8.51 (d, J = 8.5 Hz, 4H), 7.86 (s, 2H), 7.56 (d, J = 8.5 Hz, 2H), 7.11 (d, J = 8.9 Hz, 8H), 6.91 (d, J = 8.5 Hz, 4H), 6.75 (d, J = 8.8 Hz, 8H), 6.65 (s, 4H), 3.40 (dt, J = 10.7, 7.1 Hz, 4H), 3.02 (dt, J = 10.6, 7.1 Hz, 4H), 1.82 – 1.77 (m, 4H), 1.13 (s, 36H), 0.92 (dt, J = 9.2, 4.6 Hz, 4H), 0.76 – 0.63 (m, 8H), 0.46 (ddd, J = 17.5, 11.4, 6.6 Hz, 8H), 0.26 – 0.20 (m, 4H), -2.59 (s, 2H). ¹³C NMR (100 MHz, CDCl₃) δ δ 170.38, 168.42, 159.79, 153.55,

147.00, 139.03, 130.74, 130.70, 126.50, 121.49, 120.98, 119.58, 117.77, 113.63, 110.43, 107.09, 63.32, 34.35, 31.46, 29.86, 26.81, 24.14, 22.41, 20.73, 14.60. HRMS (ESI) ($[M+H]^+$) Calcd. for $C_{114}H_{115}N_8O_{16}^+$: 1850.8353, found 1851.8436. UV-vis (CH_3Cl), λ_{max} nm (log ϵ): 423(4.78), 515(3.56), 547(2.94), 587(3.10), 642(2.65).



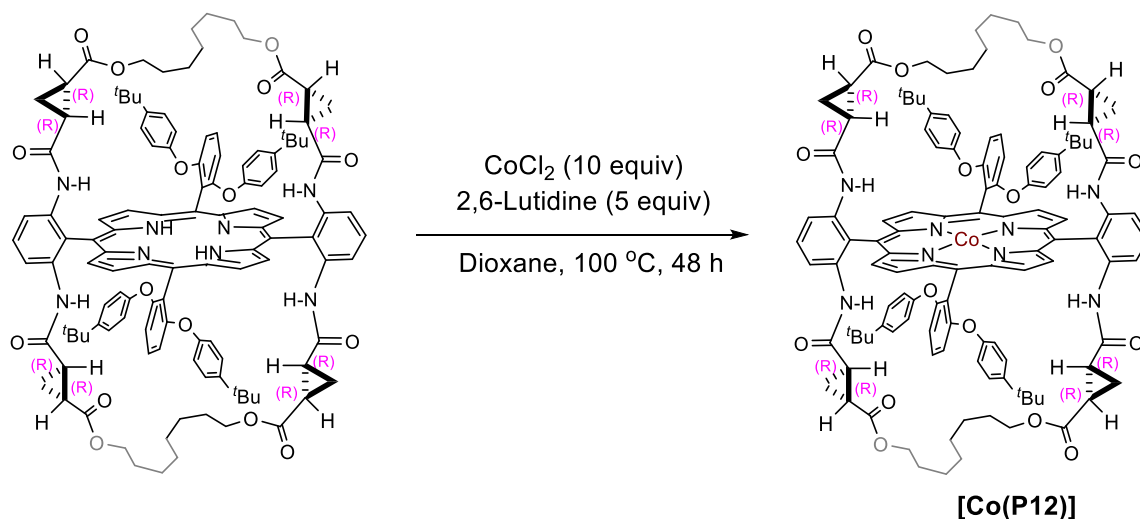
Synthesis of [Co(P11)]: The desired porphyrin (1.0 equiv) and $CoCl_2$ (10.0 equiv) were placed in an oven dried, resealable Schlenk tube. The tube was capped with a teflon screw cap, evacuated, and backfilled with nitrogen. The screw cap was replaced with a rubber septum. 2,6-Lutidine (5.0 equiv) and dioxane (0.05 M) were added and the tube was purged with nitrogen for 1 min and sealed with a teflon screw cap. The reaction mixture was stirred at 100 °C for 48 h prior to being cooled to r.t. The reaction mixture was diluted with EtOAc and washed with brine. The organic layer was separated, dried, and concentrated. The residue was purified by flash silica gel chromatography (Hexanes:EtOAc: DCM 1:1:1) to give the title compound **[Co(P11)]** (90% yield). UV-vis ($CHCl_3$), λ_{max} nm (log ϵ): 434 (4.00), 545 (3.04). HRMS (ESI) $[M]^+$: m/z calculated for $[C_{114}H_{112}CoN_8O_{16}]^+$ 1907.7528, found 1907.7664.

Synthesis of the catalysts [Co(P12)]



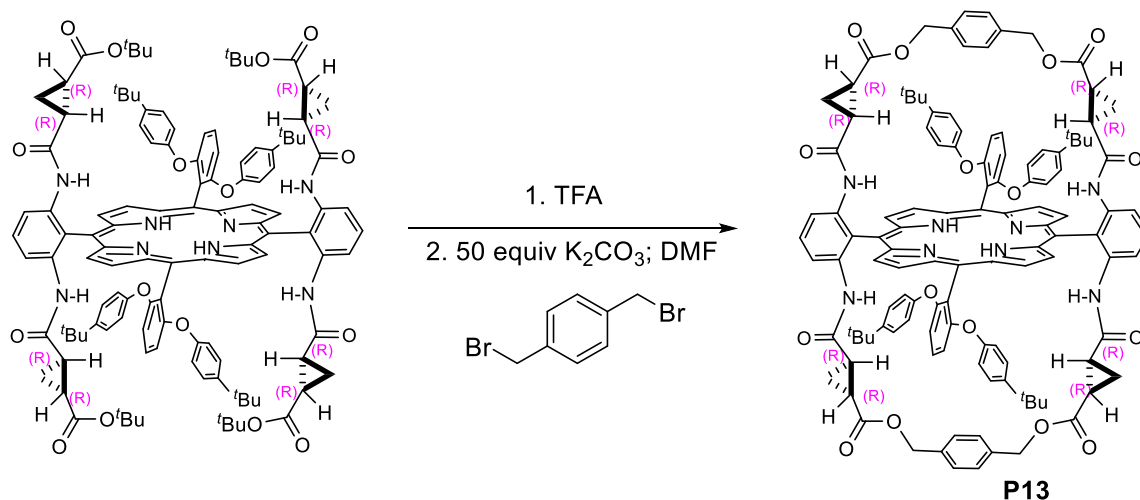
Synthesis of (P12). TFA (100.0 equiv) was added to a solution of **2,6-Di(4'-^tBu)-(^tBu)TaoPyrin (16c)** (1.0 equiv) in DCM (0.5 M) and the reaction mixture was stirred overnight prior to the evaporation of all the volatiles. The residue was dissolved in DMF (0.1 M), followed by the addition of powdered K₂CO₃ (50 equiv) and then followed by the addition of alkylating reagents (20.0 equiv). The reaction mixture was heated at 100 °C for 24 h. After cooling to rt, the reaction mixture was diluted with EtOAc and water. The organic layer was separated and washed with brine ten times. The organic solvent was removed under vacuum and the resulting mixture was then purified by flash column chromatography (eluent: Hexanes/DCM/EtOAc 5:5:1) to afford the pure title compound **P12** (44% yield). ¹H NMR (500 MHz, CDCl₃) δ 9.16 (d, J = 4.7 Hz, 4H), 8.83 (d, J = 4.6 Hz, 4H), 8.30 (d, J = 8.4 Hz, 4H), 7.86 (t, J = 8.4 Hz, 2H), 7.56 (t, J = 8.5 Hz, 2H), 7.10 (d, J = 8.8 Hz, 8H), 6.91 (d, J = 8.5 Hz, 4H), 6.76 (d, J = 8.8 Hz, 8H), 6.63 (s, 4H), 3.55 (dt, J = 10.8, 7.2 Hz, 4H), 3.39 (dt, J = 10.8, 7.0 Hz, 4H), 1.93 – 1.86 (m, 4H), 1.12 (s, 36H), 0.95 (dd, J = 12.1, 6.3 Hz, 8H), 0.81 (dt, J = 9.1, 4.6 Hz, 4H), 0.70 (m, 16H), 0.61 – 0.55 (m, 4H), 0.14 – 0.08 (m, 4H), -2.51 (s, 2H). ¹³C NMR (100 MHz, CDCl₃) δ 170.95, 168.74,

159.90, 153.67, 146.90, 138.71, 130.51, 130.28, 126.50, 123.47, 121.74, 119.78, 119.61, 113.11, 110.48, 107.21, 63.90, 34.32, 31.44, 27.21, 26.98, 24.35, 23.88, 21.93, 14.76. HRMS (ESI) ($[M+H]^+$) Calcd. for $C_{120}H_{127}N_8O_{16}^+$: 1935.9292, found 1935.9350. UV-vis (CH_3Cl), λ_{max} nm (log ϵ): 424(4.72), 517(3.45), 549(2.86), 589(2.95), 644(2.49).



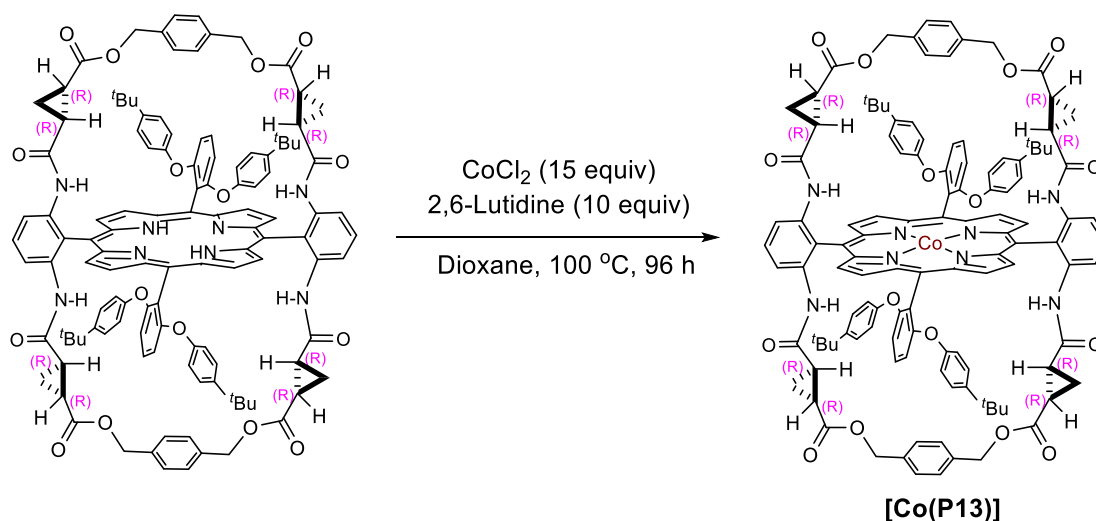
Synthesis of [Co(P12)]: The desired porphyrin (1.0 equiv) and $CoCl_2$ (10.0 equiv) were placed in an oven dried, resealable Schlenk tube. The tube was capped with a teflon screw cap, evacuated, and backfilled with nitrogen. The screw cap was replaced with a rubber septum. 2,6-Lutidine (5.0 equiv) and dioxane (0.05 M) were added and the tube was purged with nitrogen for 1 min and sealed with a teflon screw cap. The reaction mixture was stirred at 100 °C for 48 h prior to being cooled to r.t. The reaction mixture was diluted with EtOAc and washed with brine. The organic layer was separated, dried, and concentrated. The residue was purified by flash silica gel chromatography (Hexanes:EtOAc: DCM 1:1:1) to give the title compound **[Co(P12)]** (93% yield). UV-vis ($CHCl_3$), λ_{max} nm (log ϵ): 436 (4.25), 547 (3.27). HRMS (ESI) $[M]^+$: m/z calculated for $[C_{120}H_{124}CoN_8O_{16}]^+$ 1991.8467, found 1991.8431

Synthesis of the catalysts [Co(P13)]



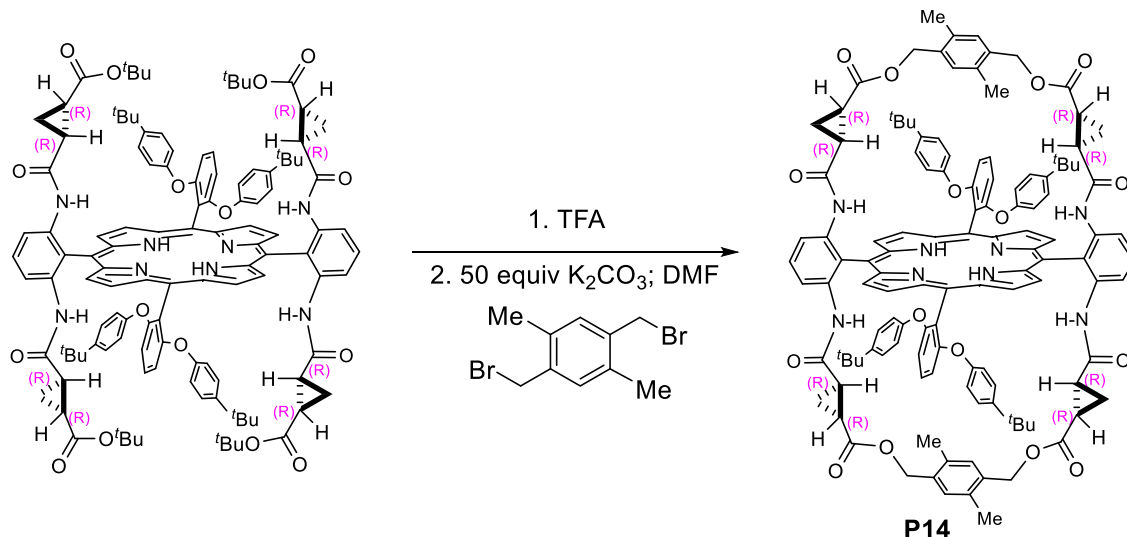
Synthesis of P13: TFA (100.0 equiv) was added to a solution of **2,6-Di(4'-*t*Bu)-(*t*Bu)TaoPhyrin (16c)** (1.0 equiv) in DCM (0.5 M) and the reaction mixture was stirred overnight prior to the evaporation of all the volatiles. The residue was dissolved in DMF (0.1 M), followed by the addition of powdered K₂CO₃ (50 equiv) and then followed by the addition of alkylating reagents (20.0 equiv). The reaction mixture was heated at 100 °C for 24 h. After cooling to rt, the reaction mixture was diluted with EtOAc and water. The organic layer was separated and washed with brine ten times. The organic solvent was removed under vacuum and the resulting oil was then purified by flash column chromatography (eluent: Hexanes/DCM/EtOAc 5:5:1) to afford the pure title compound **2,6-Di(4'-*t*Bu)PhO-JesuPhyrin (P13)** (38% yield.) TLC R_f = 0.3 (Hexanes/DCM/EtOAc 4:4:1). ¹H NMR (500 MHz, CDCl₃) δ 9.12 (d, J = 4.7 Hz, 4H), 8.80 (d, J = 4.7 Hz, 4H), 8.23 (d, J = 8.4 Hz, 4H), 7.87 (t, J = 8.4 Hz, 2H), 7.56 (t, J = 8.5 Hz, 2H), 7.15 – 7.07 (m, 8H), 6.92 (d, J = 8.5 Hz, 4H), 6.78 – 6.71 (m, 8H), 6.58 (s, 4H), 6.33 (s, 8H), 4.40 (ABq, J = 12.7 Hz, 8H), 2.07 – 2.02 (m, 4H), 1.12 (s, 36H), 0.81 (m, 4H), 0.68 (m, 4H), 0.10 – 0.02 (m, 4H), -2.61 (s, 2H). ¹³C NMR (150 MHz, CDCl₃) δ ppm: 170.55, 168.38, 159.78,

153.58, 147.01, 138.57, 134.50, 130.53, 130.23, 127.33, 126.48, 124.05, 121.68, 120.28, 119.60, 113.14, 110.28, 107.38, 65.93, 34.35, 31.46, 23.75, 22.00, 14.92. HRMS (ESI) ($[M+H]^+$) Calcd. for $C_{120}H_{111}N_8O_{16}^+$: 1919.8040, found: 1919.8144.; UV-vis ($CHCl_3$), λ_{max} nm (log ϵ): 424(4.87), 516(3.62), 548(3.00), 589(3.12), 643(2.53).



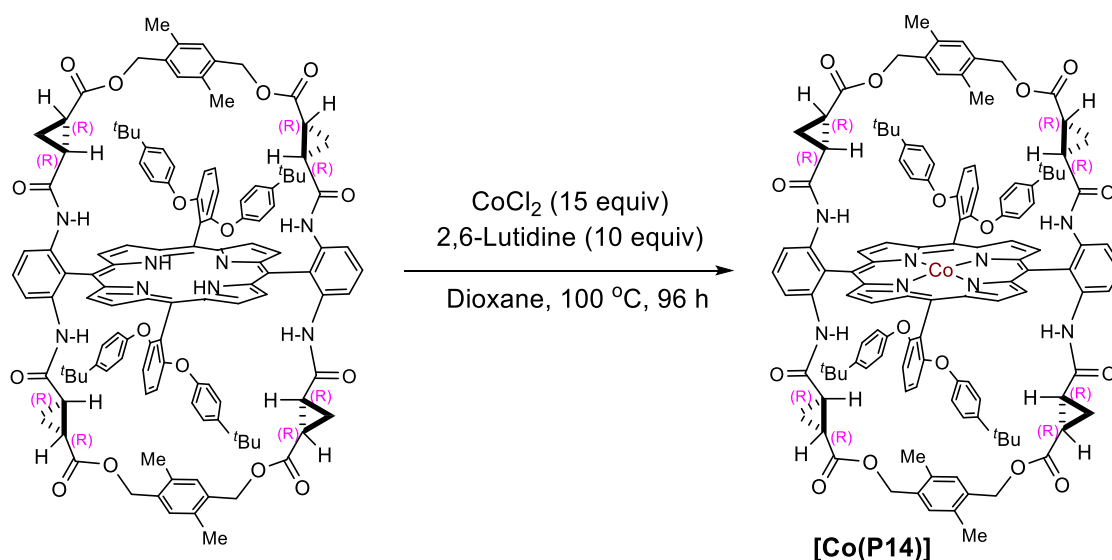
Synthesis of [Co(P13)]: The desired porphyrin (1.0 equiv) and $CoCl_2$ (15.0 equiv) were placed in an oven dried, resealable Schlenk tube. The tube was capped with a teflon screw cap, evacuated, and backfilled with nitrogen. The screw cap was replaced with a rubber septum. 2,6-Lutidine (10.0 equiv) and dioxane (0.05 M) were added and the tube was purged with nitrogen for 1 min and sealed with a teflon screw cap. The reaction mixture was stirred at 100 °C for 96 h prior to being cooled to r.t. The reaction mixture was diluted with EtOAc and washed with brine. The organic layer was separated, dried, and concentrated. The residue was purified by flash silica gel chromatography (Hexanes:EtOAc: DCM 4:4:1) to give **[Co(2,6-Di(4'-tBu)PhO-JesuPhyrin)]**, **[Co(P13)]** (80% yield). HRMS (ESI) ($[M]^+$) Calcd. for $C_{120}H_{108}N_8O_{16}Co^+$: 1975.7215, found: 1975.7157.; UV-vis ($CHCl_3$), λ_{max} nm (log ϵ): 435(4.82), 545(3.77).

Synthesis of the catalysts [Co(P14)]



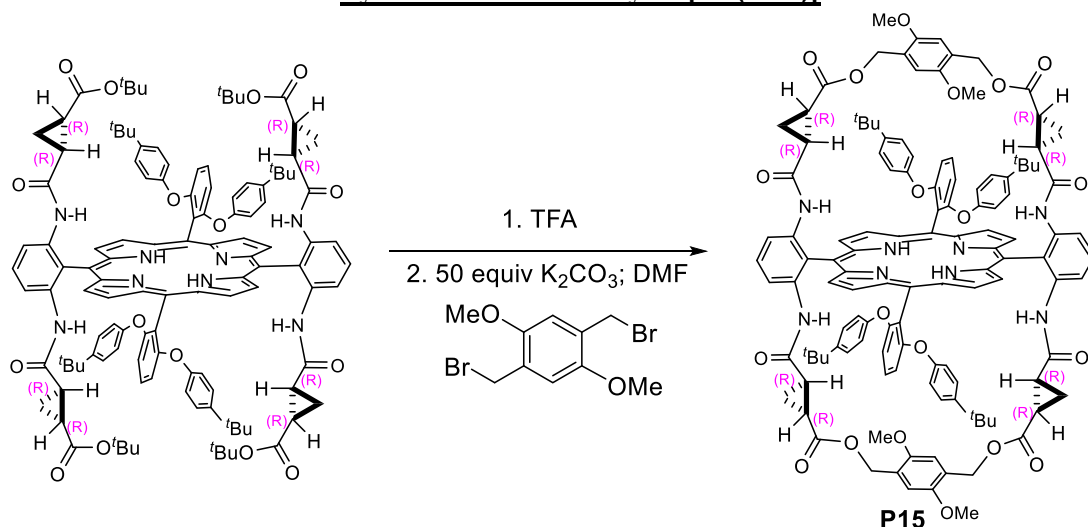
Synthesis of P14: TFA (100.0 equiv) was added to a solution of **2,6-Di(4'-*t*Bu)-(*t*Bu)TaoPhyrin (16c)** (1.0 equiv) in DCM (0.5 M) and the reaction mixture was stirred overnight prior to the evaporation of all the volatiles. The residue was dissolved in DMF (0.1 M), followed by the addition of powdered K₂CO₃ (50 equiv) and then followed by the addition of alkylating reagents (20.0 equiv). The reaction mixture was heated at 100 °C for 24 h. After cooling to rt, the reaction mixture was diluted with EtOAc and water. The organic layer was separated and washed with brine ten times. The organic solvent was removed under vacuum and the resulting oil was then purified by flash column chromatography (eluent: Hexanes/DCM/EtOAc 5:5:1) to afford the pure title compound **2,6-Di(4'-*t*Bu)PhO-Jesu(2,5-DiMe)Phyrin (P14)** (44% yield.) TLC R_f = 0.3 (Hexanes/DCM/EtOAc 4:4:1). ¹H NMR (500 MHz, CDCl₃) δ 9.09 (d, J = 4.7 Hz, 4H), 8.77 (d, J = 4.6 Hz, 4H), 8.17 (d, J = 8.4 Hz, 4H), 7.87 (s, 2H), 7.53 (s, 2H), 7.20 – 7.14 (m, 8H), 6.83 (d, J = 8.6 Hz, 4H), 6.79 – 6.74 (m, 8H), 6.51 (s, 4H), 6.13 (s, 4H), 4.38 – 4.31 (m, 8H), 2.06 – 2.01 (m, 4H), 1.40 (s, 12H), 1.19 (s, 36H), 0.73 (dt, J = 9.2, 4.8 Hz, 5H), 0.65 (ddd, J = 9.3, 5.6, 4.0 Hz, 4H), -0.04 – -0.13 (m, 4H), -2.61 (s, 2H). ¹³C NMR (150

MHz, CDCl₃) δ ppm δ 170.63, 168.38, 160.16, 153.59, 147.21, 138.42, 134.16, 132.71, 131.17, 130.40, 130.08, 126.61, 124.80, 121.19, 120.86, 119.95, 112.98, 109.84, 107.43, 64.86, 34.42, 31.53, 23.59, 21.93, 17.85, 14.85. HRMS (ESI) ($[M+H]^+$) Calcd. for C₁₂₄H₁₁₉N₈O₁₆⁺: 1975.8739, found: 1975.8661.; UV-vis (CHCl₃), λ_{\max} nm (log ϵ): 423(4.98), 516(4.01), 549(3.47), 590(3.55), 644(3.14).



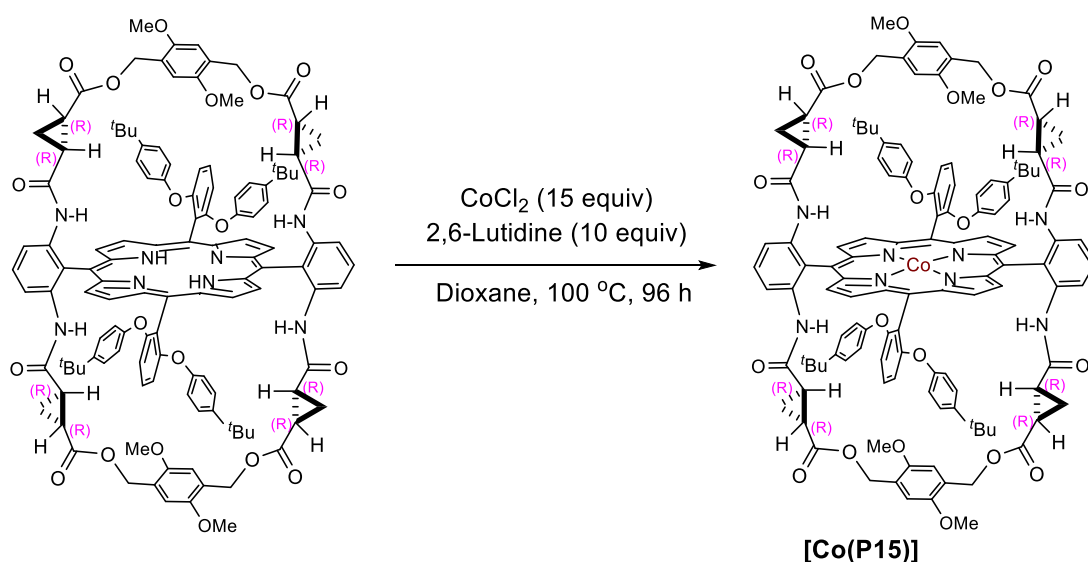
Synthesis of [Co(P14)]: The desired porphyrin (1.0 equiv) and CoCl₂ (15.0 equiv) were placed in an oven dried, resealable Schlenk tube. The tube was capped with a teflon screw cap, evacuated, and backfilled with nitrogen. The screw cap was replaced with a rubber septum. 2,6-Lutidine (10.0 equiv) and dioxane (0.05 M) were added and the tube was purged with nitrogen for 1 min and sealed with a teflon screw cap. The reaction mixture was stirred at 100 °C for 96 h prior to being cooled to r.t. The reaction mixture was diluted with EtOAc and washed with brine. The organic layer was separated, dried, and concentrated. The residue was purified by flash silica gel chromatography (Hexanes:EtOAc: DCM 4:4:1) to give **[Co(2,6-Di(4'-tBu)PhO-Jesu(2,5-DiMe)Phyrin)]**, **[Co(P14)]** (85% yield). HRMS (ESI) ($[M]^+$) Calcd. for C₁₂₄H₁₁₆N₈O₁₆Co⁺: 2031.7841, found: 2031.7790.; UV-vis (CHCl₃), λ_{\max} nm (log ϵ): 434(4.82), 542(3.85).

Synthesis of the catalysts [Co(P15)]



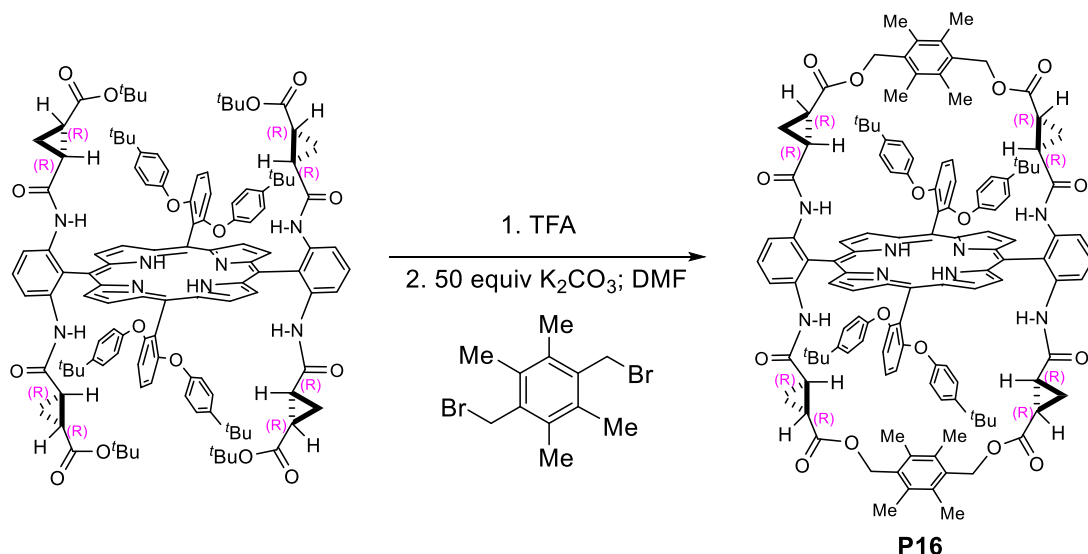
Synthesis of P15: TFA (100.0 equiv) was added to a solution of **2,6-Di(4'-*t*Bu)-(*t*Bu)TaoPhyrin (16c)** (1.0 equiv) in DCM (0.5 M) and the reaction mixture was stirred overnight prior to the evaporation of all the volatiles. The residue was dissolved in DMF (0.1 M), followed by the addition of powdered K_2CO_3 (50 equiv) and then followed by the addition of alkylating reagents (20.0 equiv). The reaction mixture was heated at 100 °C for 24 h. After cooling to rt, the reaction mixture was diluted with EtOAc and water. The organic layer was separated and washed with brine ten times. The organic solvent was removed under vacuum and the resulting oil was then purified by flash column chromatography (eluent: Hexanes/DCM/EtOAc 4:4:1) to afford the pure title compound **2,6-Di(4'-*t*Bu)PhO-Jesu(2,5-DiMeO)Phyrin (P15)** (38% yield.) TLC $R_f = 0.3$ (Hexanes/DCM/EtOAc 4:4:2). 1H NMR (600 MHz, $CDCl_3$) δ ppm δ 9.12 (d, $J = 4.5$ Hz, 4H), 8.80 (d, $J = 4.3$ Hz, 4H), 8.19 (d, $J = 8.4$ Hz, 4H), 7.87 (t, $J = 8.4$ Hz, 2H), 7.52 (t, $J = 8.6$ Hz, 2H), 7.15 (d, $J = 8.9$ Hz, 8H), 6.81 (d, $J = 8.6$ Hz, 4H), 6.76 (d, $J = 8.9$ Hz, 8H), 6.51 (s, 4H), 5.83 (s, 4H), 4.38 (dd, $J = 117.2, 12.3$ Hz, 8H), 2.85 (s, 12H), 2.04 – 1.99 (m, 4H), 1.18 (s, 36H), 0.73 (dt, $J = 9.0, 4.4$ Hz, 4H), 0.68 – 0.60 (m, 4H), 0.01 – -0.08 (m, 4H), -2.62 (s, 2H).; ^{13}C NMR (150 MHz, $CDCl_3$) δ 170.59, 168.49, 160.23, 153.53, 150.84,

147.33, 138.54, 130.43, 130.15, 126.59, 124.43, 123.65, 120.93, 120.55, 120.05, 113.02, 112.30, 109.78, 107.55, 61.91, 55.38, 34.41, 31.50, 23.60, 22.81, 22.10. HRMS (ESI) ($[M+H]^+$) Calcd. for $C_{124}H_{119}N_8O_{20}^+$: 2039.8481, found: 2039.8482.; UV-vis ($CHCl_3$), λ_{max} nm (log ϵ): 423(4.92), 516(3.86), 548(3.32), 588(3.42), 645(2.99).



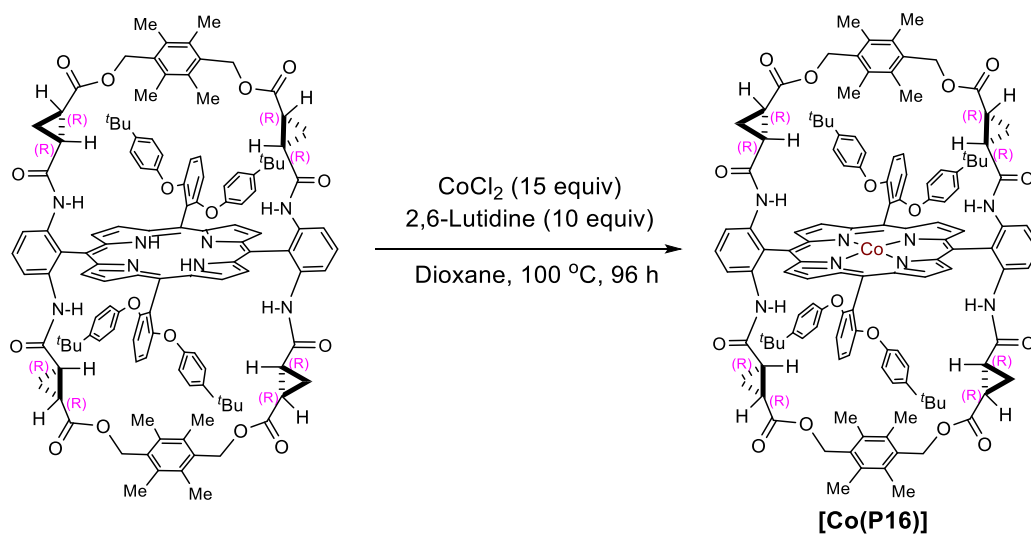
Synthesis of [Co(P15)]: The desired porphyrin (1.0 equiv) and $CoCl_2$ (15.0 equiv) were placed in an oven dried, resealable Schlenk tube. The tube was capped with a teflon screw cap, evacuated, and backfilled with nitrogen. The screw cap was replaced with a rubber septum. 2,6-Lutidine (10.0 equiv) and dioxane (0.05 M) were added and the tube was purged with nitrogen for 1 min and sealed with a teflon screw cap. The reaction mixture was stirred at 100 °C for 96 h prior to being cooled to r.t. The reaction mixture was diluted with EtOAc and washed with brine. The organic layer was separated, dried, and concentrated. The residue was purified by flash silica gel chromatography (Hexanes:EtOAc: DCM 4:4:2) to give **[Co(2,6-Di(4'-tBu)PhO-Jesu(2,5-DiMeO)Phyrin)]**, **[Co(P15)]** (84% yield). HRMS (ESI) ($[M]^+$) Calcd. for $C_{124}H_{116}N_8O_{20}Co^+$: 2095.7638, found: 2095.7583.; UV-vis ($CHCl_3$), λ_{max} nm (log ϵ): 434(4.86), 544(3.87).

Synthesis of the catalysts [Co(P16)]



Synthesis of P16: TFA (100.0 equiv) was added to a solution of **2,6-Di(4'-*t*Bu)-(*t*Bu)TaoPhyrin (16c)** (1.0 equiv) in DCM (0.5 M) and the reaction mixture was stirred overnight prior to the evaporation of all the volatiles. The residue was dissolved in DMF (0.1 M), followed by the addition of powdered K₂CO₃ (50 equiv) and then followed by the addition of alkylating reagents (20.0 equiv). The reaction mixture was heated at 100 °C for 24 h. After cooling to rt, the reaction mixture was diluted with EtOAc and water. The organic layer was separated and washed with brine ten times. The organic solvent was removed under vacuum and the resulting oil was then purified by flash column chromatography (eluent: Hexanes/DCM/EtOAc 4:4:1.5) to afford the pure title compound **2,6-Di(4'-*t*Bu)PhO-Jesu(2,3,5,6-TetraMe)Phyrin (P16)** (52% yield.) TLC R_f = 0.3 (Hexanes/DCM/EtOAc 4:4:1.5). ¹H NMR (500 MHz, CDCl₃) δ 9.09 (d, J = 4.4 Hz, 4H), 8.78 (d, J = 4.2 Hz, 4H), 8.09 (d, J = 8.3 Hz, 4H), 7.89 (d, J = 8.3 Hz, 2H), 7.50 (t, J = 8.6 Hz, 2H), 7.21 (d, J = 8.7 Hz, 8H), 6.79 (d, J = 8.7 Hz, 8H), 6.75 (d, J = 8.6 Hz, 4H), 6.46 (s, 4H), 4.63 (d, J = 12.5 Hz, 4H), 4.29 (d, J = 12.5 Hz, 4H), 2.10 – 2.05 (m, 4H), 1.35 (s,

24H), 1.23 (s, 36H), 0.68 (m, 8H), -0.23 (m, 4H), -2.59 (s, 2H). ^{13}C NMR (100 MHz, CDCl_3) δ 170.82, 168.42, 160.54, 153.63, 147.43, 138.18, 133.87, 131.03, 130.26, 129.94, 126.73, 125.54, 121.65, 120.82, 120.24, 112.91, 109.46, 107.41, 61.74, 34.46, 31.56, 23.40, 21.87, 15.61, 15.04. HRMS (ESI) ($[\text{M}+\text{H}]^+$) Calcd. for $\text{C}_{128}\text{H}_{127}\text{N}_8\text{O}_{16}^+$: 2031.9325, found: 2031.9251.; UV-vis (CHCl_3), λ_{max} nm (log ϵ): 420(5.29), 516(4.35), 550(3.83), 590(3.89), 644(3.46).



Synthesis of [Co(P16)]: The desired porphyrin (1.0 equiv) and CoCl_2 (15.0 equiv) were placed in an oven dried, resealable Schlenk tube. The tube was capped with a teflon screw cap, evacuated, and backfilled with nitrogen. The screw cap was replaced with a rubber septum. 2,6-Lutidine (10.0 equiv) and dioxane (0.05 M) were added and the tube was purged with nitrogen for 1 min and sealed with a teflon screw cap. The reaction mixture was stirred at 100 °C for 96 h prior to being cooled to r.t. The reaction mixture was diluted with EtOAc and washed with brine. The organic layer was separated, dried, and concentrated. The residue was purified by flash silica gel chromatography (Hexanes:EtOAc: DCM 4:4:2) to give **[Co(2,6-Di(4'-tBu)PhO)-Jesu(2,3,5,6-**

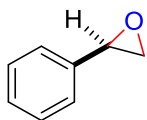
TetraMe)Phyrin)], [Co(P16)] (88% yield). HRMS (ESI) ($[M]^+$) Calcd. for $C_{128}H_{124}CoN_8O_{16}^+$: 2087.8467, found: 2087.8501.; UV-vis ($CHCl_3$), λ_{max} nm (log ϵ): 434(4.19), 543(3.18).

4.4.3 General Procedure for Enantioselective Epoxidation of Styrenes

To an over-dried Schlenk tube, [Co(Por)] (2 mol %) and 4A MS (50 mg) were added. The Schlenk tube was then evacuated and backfilled with nitrogen for 3 times. The Teflon screw cap was replaced with a rubber septum and NaOCl-5H₂O (0.1 mmol), styrene (0.3 mmol), *n*-Hexane (0.35 mL) and CH₃CN (0.15 mL) were added. The Schlenk tube was then purged with nitrogen for 2 minutes and the rubber septum was replaced with a Teflon screw cap. The mixture was then stirred at 4 °C for 16 h. After the reaction finished, the resulting mixture was passed through a silica gel plug that was pretreated with 5% Et₃N/hexanes. The collected mixture was reduced in vacuo to afford the crude product, which was analyzed by HNMR. NMR yields were calculated using 0.5 equiv of internal standard CH₂Cl₄. Isolation of the resulting products was afforded by flash chromatography on silica gel pretreated with 5% Et₃N, using hexanes and ethyl acetate as eluents.

4.4.4 Characterization of Styrene Oxide Products

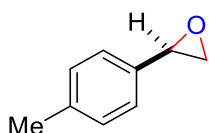
2-Phenylloxirane (13a), $R_f = 0.5$ (Eluent: hexanes/ethyl acetate 9:1) $[\alpha]_D^{20} = -10.325$ ($c =$



1.0, CHCl_3). $^1\text{H NMR}$ (500 MHz, CDCl_3): δ 7.25 – 7.38 (m, 5H), δ 3.89 (dd, $J = 3.9, 2.7$ Hz, 1H), 3.17 (dd, $J = 5.5, 4.1$ Hz, 1H), 2.83 (dd, $J = 5.5, 2.6$ Hz,

1H). HRMS (DART) ($[\text{M}+\text{H}]^+$) Calcd. for $\text{C}_8\text{H}_9\text{O}^+$: 121.0653, found: 121.0651. HPLC analysis: $ee = 90\%$. ID (99% hexanes: 1% isopropanol, 1.0 ml/min) $t_{\text{major}} = 19.50$ min, $t_{\text{minor}} = 22.65$ min.

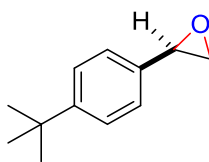
2-(p-tolyl)oxirane (13b), known compound.⁶⁵ Yield based on crude $^1\text{H NMR}$ by



integration of oxirane peaks with internal standard. $R_f = 0.4$ (Eluent: hexanes/ethyl acetate 10:1). HRMS (DART) ($[\text{M}+\text{H}]^+$) Calcd. for

$\text{C}_9\text{H}_{11}\text{O}^+$: 153.0804, found: 153.0803. HPLC analysis: $ee = 92\%$. ID (99% hexanes: 1% isopropanol, 1.0 ml/min) $t_{\text{major}} = 18.67$ min, $t_{\text{minor}} = 21.67$ min.

2-(4-(tert-butyl)phenyl)oxirane (13c), $R_f = 0.4$ (Eluent: hexanes/ethyl acetate 10:1) $[\alpha]_D^{20}$



$= -3.599$ ($c = 0.5$, CHCl_3). $^1\text{H NMR}$ (600 MHz, CDCl_3): δ 7.38 (d, $J = 8.3$ Hz, 2H), 7.22 (d, $J = 8.3$ Hz, 2H), 3.87 – 3.82 (m, 1H), 3.13 (dd, $J =$

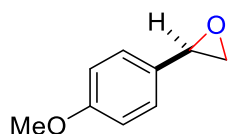
5.4, 4.1 Hz, 1H), 2.82 (dd, $J = 5.4, 2.6$ Hz, 1H), 1.32 (s, 9H). $^{13}\text{C NMR}$ (150 MHz, CDCl_3)

δ 151.47, 134.67, 125.60, 125.44, 52.42, 51.20, 34.75, 31.46. HRMS (DART) ($[\text{M}+\text{H}]^+$)

Calcd. for $\text{C}_{12}\text{H}_{17}\text{O}^+$: 177.1274, found: 177.1269 HPLC analysis: $ee = 94\%$. IF (99%

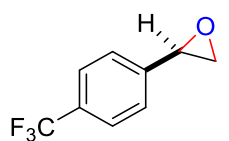
hexanes: 1% isopropanol, 1.0 ml/min) $t_{\text{major}} = 17.23$ min, $t_{\text{minor}} = 16.15$ min.

2-(4-methoxyphenyl)oxirane (13d), known compound.⁶⁶ Yield based on crude ¹H NMR



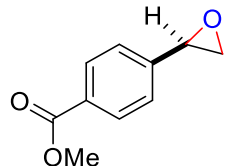
by integration of oxirane peaks with internal standard. $R_f = 0.5$ (Eluent: hexanes/ethyl acetate 5:1). HRMS (DART) ($[M+H]^+$) Calcd. for $C_9H_{11}O_2^+$: 151.0754, found: 151.0755. HPLC analysis: $ee = 92\%$. ADH (98% hexanes: 2% isopropanol, 1.0 ml/min) $t_{major} = 14.02$ min, $t_{minor} = 15.30$ min.

2-(4-(trifluoromethyl)phenyl)oxirane (13e), known compound.⁶⁷ Yield based on crude



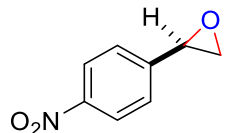
¹H NMR by integration of oxirane peaks with internal standard. $R_f = 0.4$ (Eluent: hexanes/ethyl acetate 15:1). HRMS (DART) ($[M+H]^+$) Calcd. for $C_9H_8F_3O^+$: 189.0522, found: 189.0518. HPLC analysis: $ee = 88\%$. IC (99% hexanes: 1% isopropanol, 1.0 ml/min) $t_{major} = 11.10$ min, $t_{minor} = 12.17$ min.

methyl 4-(oxiran-2-yl)benzoate (13f), $R_f = 0.5$ (Eluent: hexanes/ethyl acetate 10:1). $[\alpha]_D^{20}$



$= -5.718$ ($c = 0.5$, $CHCl_3$). ¹H NMR (500 MHz, $CDCl_3$): δ 8.04 – 7.99 (m, 2H), 7.37 – 7.33 (m, 2H), 3.94 – 3.88 (m, 4H), 3.19 (dd, $J = 5.6$, 4.1 Hz, 1H), 2.79 (dd, $J = 5.6$, 2.5 Hz, 1H). ¹³C NMR (125 MHz, $CDCl_3$) δ 166.89, 143.03, 130.15, 129.96, 125.54, 52.28, 52.08, 51.58. HRMS (DART) ($[M+H]^+$) Calcd. for $C_{10}H_{11}O^+$: 179.0702, found: 179.0703. HPLC analysis: $ee = 90\%$. IF (98% hexanes: 2% isopropanol, 1.0 ml/min) $t_{major} = 31.13$ min, $t_{minor} = 29.63$ min.

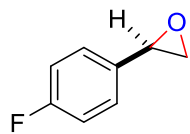
2-(4-nitrophenyl)oxirane (13g), $R_f = 0.3$ (Eluent: hexanes/ethyl acetate 10:1). $[\alpha]_D^{20} = -$



11.198 ($c = 0.5$, $CHCl_3$). ¹H NMR (600 MHz, $CDCl_3$): δ 8.24 – 8.19 (m, 2H), 7.48 – 7.42 (m, 2H), 3.96 (dd, $J = 4.0$, 2.5 Hz, 1H), 3.23 (dd, $J = 5.5$, 4.1 Hz, 1H), 2.78 (dd, $J = 5.5$, 2.5 Hz, 1H). ¹³C NMR (150 MHz, $CDCl_3$) δ 148.00, 145.37, 126.36, 123.98, 51.82, 51.60. HRMS (DART) ($[M+H]^+$) Calcd. for $C_8H_8NO_3^+$:

166.0498, found: 166.0499 HPLC analysis: *ee* = 90%. IF (97% hexanes: 3% isopropanol, 1.0 ml/min) t_{major} = 23.42 min, t_{minor} = 24.95 min.

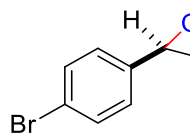
2-(4-fluorophenyl)oxirane (13h), R_f = 0.4 (Eluent: hexanes/ethyl acetate 10:1). $[\alpha]_D^{20}$ = -



9.998 (c = 0.5, CHCl_3). $^1\text{H NMR}$ (600 MHz, CDCl_3): δ 7.26 – 7.22 (m, 2H), 7.06 – 7.02 (m, 2H), 3.87 – 3.81 (m, 1H), 3.14 (dd, J = 5.1, 4.4 Hz,

1H), 2.77 (dd, J = 5.4, 2.5 Hz, 1H). $^{19}\text{F NMR}$ (470 MHz, CFCl_3 , CDCl_3): -113.9 (m). HRMS (DART) ($[\text{M}+\text{H}]^+$) Calcd. for $\text{C}_8\text{H}_8\text{OF}^+$: 139.05537, found: 139.0557. HPLC analysis: *ee* = 90%. ID (99% hexanes: 1% isopropanol, 1.0 ml/min) t_{major} = 13.73 min, t_{minor} = 16.04 min.

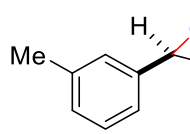
2-(4-bromophenyl)oxirane (13i), R_f = 0.4 (Eluent: hexanes/ethyl acetate 10:1). $[\alpha]_D^{20}$ = -



8.399 (c = 0.5, CHCl_3). $^1\text{H NMR}$ (600 MHz, CDCl_3): δ 7.47 (d, J = 8.5 Hz, 2H), 7.15 (d, J = 8.4 Hz, 2H), 3.83 (dd, J = 4.0, 2.6 Hz, 1H), 3.15

(dd, J = 5.4, 4.1 Hz, 1H), 2.75 (dd, J = 5.4, 2.5 Hz, 1H). $^{13}\text{C NMR}$ (150 MHz, CDCl_3) δ 136.88, 131.81, 127.30, 122.18, 51.99, 51.38. HRMS (DART) ($[\text{M}+\text{H}]^+$) Calcd. for $\text{C}_8\text{H}_8\text{BrO}^+$: 198.9753, found: 198.9754. HPLC analysis: *ee* = 92%. IF (99% hexanes: 1% isopropanol, 1.0 ml/min) t_{major} = 25.39 min, t_{minor} = 29.48 min.

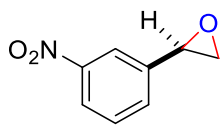
2-(*m*-tolyl)oxirane (13j), known compound.⁶⁸ Yield based on crude $^1\text{H NMR}$ by



integration of oxirane peaks with internal standard. R_f = 0.5 (Eluent: hexanes/ethyl acetate 15:1). HRMS (DART) ($[\text{M}+\text{H}]^+$) Calcd. for

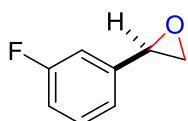
$\text{C}_9\text{H}_{11}\text{O}^+$: 153.0804, found: 153.0806. HPLC analysis: *ee* = 90%. ASH (99% hexanes: 1% isopropanol, 1.0 ml/min) t_{major} = 13.83 min, t_{minor} = 17.06 min.

2-(3-nitrophenyl)oxirane (13k), $R_f = 0.3$ (Eluent: hexanes/ethyl acetate 10:1). $[\alpha]_D^{20} = -$



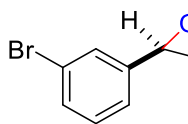
3.991 ($c = 0.5$, CHCl_3). $^1\text{H NMR}$ (500 MHz, CDCl_3): δ 8.20 – 8.12 (m, 2H), 7.62 (dt, $J = 7.8, 1.2$ Hz, 1H), 7.53 (td, $J = 7.6, 0.9$ Hz, 1H), 3.97 (dd, $J = 4.0, 2.5$ Hz, 1H), 3.22 (dd, $J = 5.4, 4.0$ Hz, 1H), 2.81 (dd, $J = 5.4, 2.5$ Hz, 1H). $^{13}\text{C NMR}$ (150 MHz, CDCl_3) δ 148.70, 140.25, 131.58, 129.72, 123.28, 120.76, 51.58, 51.57. HRMS (DART) ($[\text{M}+\text{H}]^+$) Calcd. for $\text{C}_8\text{H}_8\text{NO}_3^+$: 166.0498, found: 166.0496. HPLC analysis: $ee = 80\%$. IF (97% hexanes: 3% isopropanol, 1.0 ml/min) $t_{\text{major}} = 27.26$ min, $t_{\text{minor}} = 21.25$ min.

2-(3-fluorophenyl)oxirane (13l), known compound.⁶⁹ Yield based on crude $^1\text{H NMR}$ by



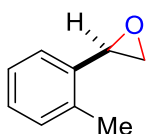
integration of oxirane peaks with internal standard. $R_f = 0.4$ (Eluent: hexanes/ethyl acetate 10:1). HRMS (DART) ($[\text{M}+\text{H}]^+$) Calcd. for $\text{C}_8\text{H}_8\text{FO}^+$: 139.0554, found: 139.0559. HPLC analysis: $ee = 86\%$. ID (99% hexanes: 1% isopropanol, 1.0 ml/min) $t_{\text{major}} = 18.69$ min, $t_{\text{minor}} = 17.74$ min.

2-(3-bromophenyl)oxirane (13m), $R_f = 0.4$ (Eluent: hexanes/ethyl acetate 10:1). $[\alpha]_D^{20} =$



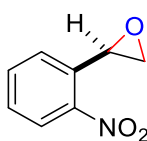
-6.665 ($c = 0.5$, CHCl_3). $^1\text{H NMR}$ (600 MHz, CDCl_3): δ 7.45 – 7.41 (m, 2H), 7.24 – 7.19 (m, 2H), 3.83 (dd, $J = 4.0, 2.6$ Hz, 1H), 3.15 (dd, $J = 5.4, 4.1$ Hz, 1H), 2.76 (dd, $J = 5.5, 2.5$ Hz, 1H). $^{13}\text{C NMR}$ (150 MHz, CDCl_3) δ 140.24, 131.41, 130.21, 128.60, 124.35, 122.87, 51.78, 51.41. HRMS (DART) ($[\text{M}+\text{H}]^+$) Calcd. for $\text{C}_8\text{H}_8\text{BrO}^+$: 198.9753, found: 198.9754. HPLC analysis: $ee = 80\%$. IF (99% hexanes: 1% isopropanol, 1.0 ml/min) $t_{\text{major}} = 22.02$ min, $t_{\text{minor}} = 19.40$ min.

2-(o-tolyl)oxirane (13n), known compound.⁶⁵ Yield based on crude ¹H NMR by



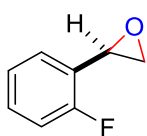
integration of oxirane peaks with internal standard. $R_f = 0.5$ (Eluent: hexanes/ethyl acetate 15:1). HRMS (DART) ($[M+H]^+$) Calcd. for $C_9H_{11}O^+$: 153.0804, found: 153.080. HPLC analysis: $ee = 48\%$. ID (100% hexanes, 1.0 ml/min) $t_{major} = 24.20$ min, $t_{minor} = 26.02$ min.

2-(2-nitrophenyl)oxirane (13o), known compound.⁷⁰ Yield based on crude ¹H NMR by



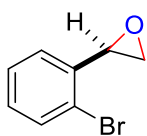
integration of oxirane peaks with internal standard. $R_f = 0.3$ (Eluent: hexanes/ethyl acetate 10:1). HRMS (DART) ($[M+H]^+$) Calcd. for $C_8H_8NO_3^+$: 166.0499, found: 166.0501. HPLC analysis: $ee = 16\%$. IF (97% hexanes: 3% isopropanol, 1.0 ml/min) $t_{major} = 28.05$ min, $t_{minor} = 20.34$ min.

2-(2-fluorophenyl)oxirane (13p), known compound.⁷¹ Yield based on crude ¹H NMR by



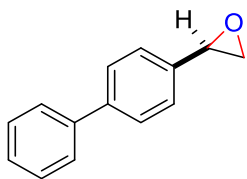
integration of oxirane peaks with internal standard. $R_f = 0.4$ (Eluent: hexanes/ethyl acetate 10:1). HRMS (DART) ($[M+H]^+$) Calcd. for $C_8H_8FO^+$: 139.0554, found: 139.0558. HPLC analysis: $ee = 52\%$. ID (99% hexanes: 1% isopropanol, 1.0 ml/min) $t_{major} = 16.19$ min, $t_{minor} = 18.23$ min.

2-(2-bromophenyl)oxirane (13q), known compound.⁷² Yield based on crude ¹H NMR by



integration of oxirane peaks with internal standard. $R_f = 0.4$ (Eluent: hexanes/ethyl acetate 10:1). HRMS (DART) ($[M+H]^+$) Calcd. for $C_8H_8BrO^+$: 198.9753, found: 198.9751. HPLC analysis: $ee = 38\%$. ADH (100% hexanes, 1.0 ml/min) $t_{major} = 12.51$ min, $t_{minor} = 14.08$ min.

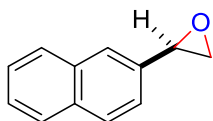
2-([1,1'-biphenyl]-4-yl)oxirane (13r), $R_f = 0.4$ (Eluent: hexanes/ethyl acetate 15:1). $[\alpha]_D^{20} =$



$[\alpha]_D^{20} = -4.799$ ($c = 0.5$, CHCl_3). $^1\text{H NMR}$ (600 MHz, CDCl_3): δ 7.61 – 7.57 (m, 4H), 7.44 (t, $J = 7.7$ Hz, 2H), 7.36 (d, $J = 8.0$ Hz, 3H), 3.91 (dd, $J = 3.8, 2.8$ Hz, 1H), 3.19 (dd, $J = 5.4, 4.1$ Hz, 1H), 2.85 (dd, $J = 5.4,$

2.6 Hz, 1H). $^{13}\text{CNMR}$ (150 MHz, CDCl_3) δ 141.35, 140.83, 136.78, 128.94, 127.55, 127.42, 127.22, 126.11, 52.37, 51.39. HRMS (DART) ($[\text{M}+\text{H}]^+$) Calcd. for $\text{C}_{14}\text{H}_{13}\text{O}^+$: 197.0961, found: 197.0956. HPLC analysis: $ee = 94\%$. ODH (98.5% hexanes: 1.5% isopropanol, 1.0 ml/min) $t_{\text{major}} = 26.86$ min, $t_{\text{minor}} = 18.92$ min.

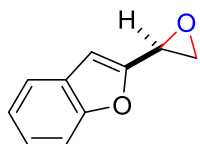
2-(naphthalen-2-yl)oxirane (13s), $R_f = 0.4$ (Eluent: hexanes/ethyl acetate 15:1). $[\alpha]_D^{20} =$



$[\alpha]_D^{20} = -6.255$ ($c = 0.5$, CHCl_3). $^1\text{H NMR}$ (600 MHz, CDCl_3): δ 7.86 – 7.80 (m, 4H), 7.52 – 7.46 (m, 2H), 7.34 (dd, $J = 8.5, 1.6$ Hz, 1H), 4.04 (dd, $J =$

3.9, 2.7 Hz, 1H), 3.23 (dd, $J = 5.3, 4.2$ Hz, 1H), 2.92 (dd, $J = 5.4, 2.6$ Hz, 1H). $^{13}\text{C NMR}$ (150 MHz, CDCl_3) δ 135.18, 133.44, 133.30, 128.52, 127.88, 127.88, 126.47, 126.19, 125.29, 122.77, 52.73, 51.39. HRMS (DART) ($[\text{M}+\text{H}]^+$) Calcd. for $\text{C}_{12}\text{H}_{11}\text{O}^+$: 171.0804, found: 171.0813. HPLC analysis: $ee = 86\%$. IF (98% hexanes: 2% isopropanol, 1.0 ml/min) $t_{\text{major}} = 12.22$ min, $t_{\text{minor}} = 11.59$ min.

2-(oxiran-2-yl)benzofuran (13t), $R_f = 0.5$ (Eluent: hexanes/ethyl acetate 5:1). $[\alpha]_D^{20} = -$

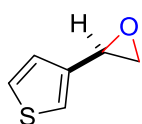


$[\alpha]_D^{20} = -7.599$ ($c = 0.5$, CHCl_3). $^1\text{H NMR}$ (600 MHz, CDCl_3): δ 7.54 (d, $J = 7.8$ Hz, 1H), 7.45 (d, $J = 8.2$ Hz, 1H), 7.30 – 7.27 (m, 1H), 7.22 (t, $J = 7.5$

Hz, 1H), 6.83 (s, 1H), 4.01 (dd, $J = 4.0, 2.7$ Hz, 1H), 3.37 (dd, $J = 5.5, 2.6$ Hz, 1H), 3.23 (dd, $J = 5.4, 4.2$ Hz, 1H). $^{13}\text{C NMR}$ (150 MHz, CDCl_3) δ 155.06, 153.02, 128.13, 124.88, 123.12, 121.14, 111.50, 106.63, 48.50, 46.80. HRMS (DART) ($[\text{M}+\text{H}]^+$) Calcd. for

$C_{10}H_9O_2^+$: 161.0597, found: 161.0594. HPLC analysis: $ee = 75\%$. ID (99% hexanes: 1% isopropanol, 1.0 ml/min) $t_{major} = 10.65$ min, $t_{minor} = 11.63$ min.

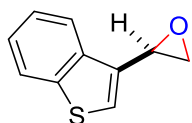
2-(thiophen-3-yl)oxirane (13u), Yield based on crude 1H NMR by integration of oxirane



peaks with internal standard. HRMS (DART) ($[M+H]^+$) Calcd. for $C_6H_7SO^+$: 127.0212, found: 127.0221. HPLC analysis: $ee = 70\%$. ADH (99% hexanes:

1% isopropanol, 1.0 ml/min) $t_{major} = 8.85$ min, $t_{minor} = 10.62$ min.

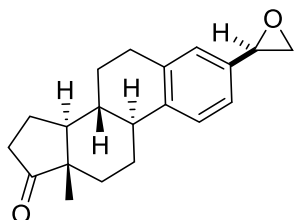
2-(benzo[b]thiophen-3-yl)oxirane (13v), Yield based on crude 1H NMR by integration of



oxirane peaks with internal standard. HRMS (DART) ($[M+H]^+$) Calcd. for $C_{10}H_9SO^+$: 177.0369, found: 177.0368. HPLC analysis: $ee = 58\%$.

ODH (99.5% hexanes: 0.5% isopropanol, 1.0 ml/min) $t_{major} = 22.16$ min, $t_{minor} = 31.28$ min.

(8R,9S,13S,14S)-13-methyl-3-((R)-oxiran-2-yl)-6,7,8,9,11,12,13,14,15,16-decahydro-



17H-cyclopenta[a]phenanthren-17-one (13w), $R_f = 0.4$

(Eluent: hexanes/ethyl acetate 5:1). $[\alpha]_D^{20} = 13.598$ ($c = 0.5$,

$CHCl_3$). 1H NMR (600 MHz, $CDCl_3$): δ 7.27 (d, $J = 8.1$ Hz, 1H),

7.07 (d, $J = 7.8$ Hz, 1H), 7.00 (s, 1H), 3.84 – 3.76 (m, 1H), 3.11 (dd, $J = 5.2, 4.3$ Hz, 1H),

2.90 (dd, $J = 8.7, 3.9$ Hz, 2H), 2.79 (dd, $J = 5.4, 2.5$ Hz, 1H), 2.50 (dd, $J = 19.0, 8.7$ Hz,

1H), 2.41 (dd, $J = 12.0, 4.7$ Hz, 1H), 2.30 (s, 1H), 2.18 – 2.09 (m, 1H), 2.09 – 1.99 (m, 2H),

1.98 – 1.93 (m, 1H), 1.66 – 1.40 (m, 7H), 0.90 (s, 3H). ^{13}C NMR (150 MHz, $CDCl_3$): δ

220.90, 140.03, 136.96, 135.15, 126.08, 125.72, 123.27, 52.31, 51.16, 50.65, 48.11, 44.54,

38.25, 35.99, 31.73, 29.47, 26.57, 25.90, 21.74, 13.98. HRMS (DART) ($[M+H]^+$) Calcd.

for $C_{20}H_{25}O_2^+$: 297.1849, found: 297.1855. HPLC analysis: $de = 90\%$. OJH (96% hexanes:

4% isopropanol, 1.0 ml/min) $t_{major} = 73.06$ min, $t_{minor} = 61.75$ min.

4.4.5 X-ray Crystallographic Information

The X-ray diffraction data for **P16** was measured on a Bruker D8 Venture PHOTON 100 CMOS system equipped with a Cu K α INCOATEC Imus micro-focus source ($\lambda = 1.54178 \text{ \AA}$). Indexing was performed using *APEX2*³⁸ (Difference Vectors method). Data integration and reduction were performed using SaintPlus 6.01³⁹. Absorption correction was performed by multi-scan method implemented in SADABS⁴⁰. Space groups were determined using XPREP implemented in *APEX2*³⁸. The structure was solved using SHELXS-97 (direct methods) and refined using SHELXL-2013³⁸ (full-matrix least-squares on F^2) contained in *APEX2*^{38,41} WinGX v1.70.01⁴¹⁻⁴² and OLEX2.⁴³

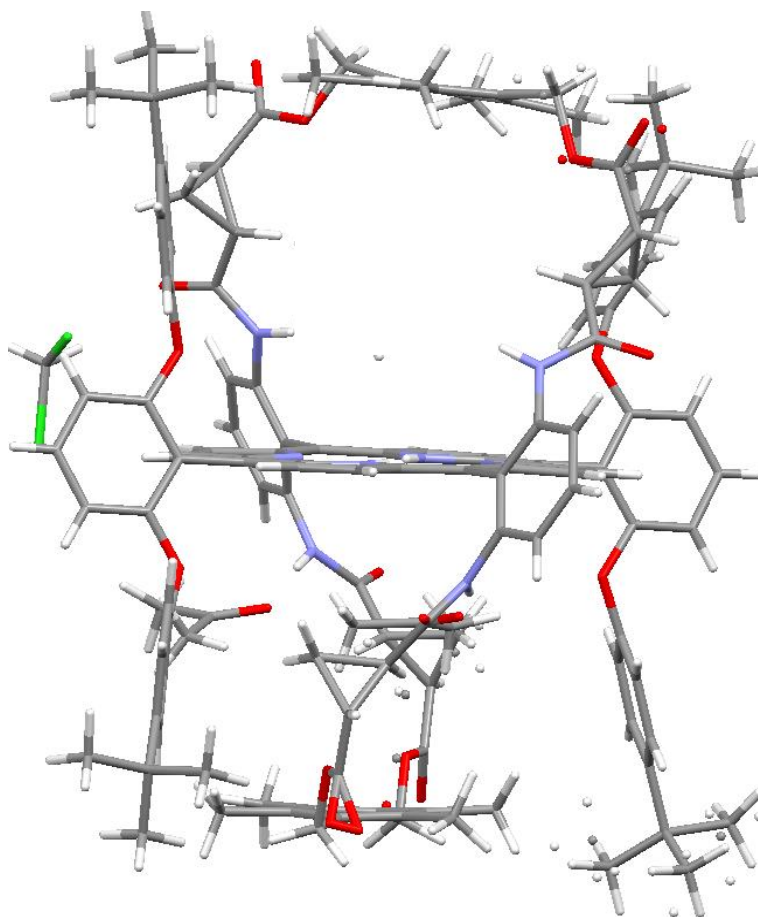


Table 4.5| Crystal Data and Structure Refinement for P16

Identification code	C128H126N8O16	
Empirical formula	C141 H152 Cl2 N8 O20	
Formula weight	2349.60	
Temperature	173(2) K	
Wavelength	1.54178 Å	
Crystal system	Monoclinic	
Space group	P2 ₁	
Unit cell dimensions	a = 14.1153(9) Å	$\alpha = 90^\circ$.
	b = 27.4900(15) Å	$\beta = 109.337(4)^\circ$.
	c = 18.5337(12) Å	$\gamma = 90^\circ$.
Volume	6785.9(7) Å ³	
Z	2	
Density (calculated)	1.150 Mg/m ³	
Absorption coefficient	0.964 mm ⁻¹	
F(000)	2496	
Crystal size	0.320 x 0.180 x 0.120 mm ³	
Theta range for data collection	2.526 to 66.666°.	
Index ranges	-16 ≤ h ≤ 16, -31 ≤ k ≤ 32, -21 ≤ l ≤ 21	
Reflections collected	190103	
Independent reflections	23702 [R(int) = 0.0691]	
Completeness to theta = 66.666°	99.5 %	
Absorption correction	Semi-empirical from equivalents	
Max. and min. transmission	0.7528 and 0.6396	
Refinement method	Full-matrix least-squares on F ²	
Data / restraints / parameters	23702 / 2888 / 1671	
Goodness-of-fit on F ²	1.048	
Final R indices [I > 2σ(I)]	R1 = 0.0688, wR2 = 0.1852	
R indices (all data)	R1 = 0.0882, wR2 = 0.2088	
Absolute structure parameter	0.048(12)	
Extinction coefficient	n/a	
Largest diff. peak and hole	0.604 and -0.605 e.Å ⁻³	

5. REFERENCES

1. Chatgililoglu, C.; Studer, A. *Encyclopedia of Radicals in Chemistry, Biology and Materials*; John Wiley & Sons, 2012.
2. (a) Zard, S. Z. Radical Alliances: Solutions and Opportunities for Organic Synthesis. *Helv. Chim. Acta* **2019**, *102*, e1900134. (b) Huang, H.-M.; Garduño-Castro, M. H.; Morrill, C.; Procter, D. J. Catalytic Cascade Reactions by Radical Relay. *Chem. Soc. Rev.* **2019**, *48*, 4626–4638. (c) Studer, A.; Curran, D. P. Catalysis of Radical Reactions: A Radical Chemistry Perspective. *Angew. Chem. Int. Ed.* **2016**, *55*, 58–102. (d) Brimiouille, R.; Lenhart, D.; Maturi, M. M.; Bach, T. Enantioselective Catalysis of Photochemical Reactions. *Angew. Chem. Int. Ed.* **2015**, *54*, 3872–3890. (e) Prier, C. K.; Rankic, D. A.; MacMillan, D. W. C. Visible Light Photoredox Catalysis with Transition Metal Complexes: Applications in Organic Synthesis. *Chem. Rev.* **2013**, *113*, 5322–5363. (f) Quiclet-Sire, B. Z., S. Z Fun with Radicals: Some New Perspectives for Organic Synthesis. *Pure Appl. Chem.* **2011**, *83*, 519–551. (g) Narayanam, J. M. R.; Stephenson, C. R. J. Visible Light Photoredox Catalysis: Applications in Organic Synthesis. *Chem. Soc. Rev.* **2011**, *40*, 102–113. (h) Zard, S. Z. Recent Progress in the Generation and Use of Nitrogen-Centred Radicals. *Chem. Soc. Rev.* **2008**, *37*, 1603–1618. (i) Curran, D. P.; Porter, N. A.; Giese, B. *Stereochemistry of Radical Reactions: Concepts, Guidelines, and Synthetic Applications*; John Wiley & Sons, 2008. . (j) Zard, S. Z. *Radical Reactions in Organic Synthesis*; Oxford University Press, 2003.
3. (a) Du, J.; Skubi, K. L.; Schultz, D. M.; Yoon, T. P. A Dual-Catalysis Approach to Enantioselective [2 + 2] Photocycloadditions Using Visible Light. *Science* **2014**, *344*, 392–

396. (b) Huo, H.; Shen, X.; Wang, C.; Zhang, L.; Röse, P.; Chen, L.-A.; Harms, K.; Marsch, M.; Hilt, G.; Meggers, E. Asymmetric Photoredox Transition-Metal Catalysis Activated by Visible Light. *Nature* **2014**, *515*, 100–103. (c) Hoyt, J. M.; Schmidt, V. A.; Tondreau, A. M.; Chirik, P. J. Iron-Catalyzed Intermolecular [2+2] Cycloadditions of Unactivated Alkenes. *Science* **2015**, *349*, 960–963. (d) Brill, Z. G.; Grover, H. K.; Maimone, T. J. Enantioselective Synthesis of an Ophiobolin Sesterterpene Via a Programmed Radical Cascade. *Science* **2016**, *352*, 1078–1082. (e) Funken, N.; Mühlhaus, F.; Gansäuer, A. General, Highly Selective Synthesis of 1,3- and 1,4-Difunctionalized Building Blocks by Regiodivergent Epoxide Opening. *Angew. Chem. Int. Ed.* **2016**, *55*, 12030–12034. (f) Kainz, Q. M.; Matier, C. D.; Bartoszewicz, A.; Zultanski, S. L.; Peters, J. C.; Fu, G. C. Asymmetric Copper-Catalyzed C–N Cross-Couplings Induced by Visible Light. *Science* **2016**, *351*, 681–684. (g) Zhang, W.; Wang, F.; McCann, S. D.; Wang, D.; Chen, P.; Stahl, S. S.; Liu, G. Enantioselective Cyanation of Benzylic C–H Bonds Via Copper-Catalyzed Radical Relay. *Science* **2016**, *353*, 1014–1018. (h) Kern, N.; Plesniak, M. P.; McDouall, J. J. W.; Procter, D. J. Enantioselective Cyclizations and Cyclization Cascades of Samarium Ketyl Radicals. *Nat. Chem.* **2017**, *9*, 1198–1204. (i) Morrill, C.; Jensen, C.; Just-Baringo, X.; Grogan, G.; Turner, N. J.; Procter, D. J. Biocatalytic Conversion of Cyclic Ketones Bearing A-Quaternary Stereocenters into Lactones in an Enantioselective Radical Approach to Medium-Sized Carbocycles. *Angew. Chem. Int. Ed.* **2018**, *57*, 3692–3696. (j) Huang, H.-M.; McDouall, J. J. W.; Procter, D. J. Sm₂-Catalysed Cyclization Cascades by Radical Relay. *Nat. Catal.* **2019**, *2*, 211–218. (k) Cheng, Y.-F.; Liu, J.-R.; Gu, Q.-S.; Yu, Z.-L.; Wang, J.; Li, Z.-L.; Bian, J.-Q.; Wen, H.-T.; Wang, X.-J.; Hong, X.; Liu, X.-Y. Catalytic Enantioselective Desymmetrizing Functionalization of Alkyl Radicals Via

Cu(I)/Cpa Cooperative Catalysis. *Nat. Catal.* **2020**. (l) Perego, L. A.; Bonilla, P.; Melchiorre, P. Photo-Organocatalytic Enantioselective Radical Cascade Enabled by Single-Electron Transfer Activation of Allenes. *Adv. Synth. Catal.* **2020**, *362*, 302–307.

(m) Roos, C. B.; Demaerel, J.; Graff, D. E.; Knowles, R. R. Enantioselective Hydroamination of Alkenes with Sulfonamides Enabled by Proton-Coupled Electron Transfer. *J. Am. Chem. Soc.* **2020**, *142*, 5974–5979. (n) Ye, L.; Tian, Y.; Meng, X.; Gu, Q.-S.; Liu, X.-Y. Enantioselective Copper(I)/Chiral Phosphoric Acid Catalyzed Intramolecular Amination of Allylic and Benzylic C–H Bonds. *Angew. Chem., Int. Ed.* **2020**, *59*, 1129–1133. (o) Zhang, X.; Wu, W.; Cao, W.; Yu, H.; Xu, X.; Liu, X.; Feng, X. Enantioselective Radical-Polar Crossover Reactions of Indanonecarboxamides with Alkenes. *Angew. Chem., Int. Ed.* **2020**, *59*, 4846–4850.

4. (a) Singh, R.; Mukherjee, A. Metalloporphyrin Catalyzed C–H Amination. *ACS Catal.* **2019**, *9*, 3604–3617. (b) Demarteau, J.; Debuigne, A.; Detrembleur, C. Organocobalt Complexes as Sources of Carbon-Centered Radicals for Organic and Polymer Chemistries. *Chem. Rev.* **2019**, *119*, 6906–6955. (c) Roy, S.; Das, S. K.; Chattopadhyay, B. Cobalt(II)-Based Metalloradical Activation of 2-(Diazomethyl)Pyridines for Radical Transannulation and Cyclopropanation. *Angew. Chem., Int. Ed.* **2018**, *57*, 2238–2243. (d) Kuijpers, P. F.; Tiekink, M. J.; Breukelaar, W. B.; Broere, D. L. J.; van Leest, N. P.; van der Vlugt, J. I.; Reek, J. N. H.; de Bruin, B. Cobalt-Porphyrin-Catalysed Intramolecular Ring-Closing C–H Amination of Aliphatic Azides: A Nitrene-Radical Approach to Saturated Heterocycles. *Chem. Eur. J.* **2017**, *23*, 7945–7952. (e) Gu, Z.-Y.; Liu, Y.; Wang, F.; Bao, X.; Wang, S.-Y.; Ji, S.-J. Cobalt(II)-Catalyzed Synthesis of Sulfonyl Guanidines Via Nitrene Radical Coupling with Isonitriles:

A Combined Experimental and Computational Study. *ACS Catal.* **2017**, *7*, 3893-3899. (f) Chirila, A.; Gopal Das, B.; Paul, N. D.; de Bruin, B. Diastereoselective Radical-Type Cyclopropanation of Electron-Deficient Alkenes Mediated by the Highly Active Cobalt(Ii) Tetramethyltetraaza[14]Annulene Catalyst. *ChemCatChem* **2017**, *9*, 1413-1421. (g) Reddy, A. R.; Hao, F.; Wu, K.; Zhou, C.-Y.; Che, C.-M. Cobalt(Ii) Porphyrin-Catalyzed Intramolecular Cyclopropanation of N-Alkyl Indoles/Pyrroles with Alkylcarbene: Efficient Synthesis of Polycyclic N-Heterocycles. *Angew. Chem., Int. Ed.* **2016**, *55*, 1810-1815. (h) Pellissier, H.; Clavier, H. Enantioselective Cobalt-Catalyzed Transformations. *Chem. Rev.* **2014**, *114*, 2775–2823. (i) Lu, H.; Zhang, X. P. Catalytic C–H Functionalization by Metalloporphyrins: Recent Developments and Future Directions. *Chem. Soc. Rev.* **2011**, *40*, 1899–1909. (j) Che, C.-M.; Lo, V. K.-Y.; Zhou, C.-Y.; Huang, J.-S. Selective Functionalisation of Saturated C–H Bonds with Metalloporphyrin Catalysts. *Chem. Soc. Rev.* **2011**, *40*, 1950-1975. (k) Driver, T. G. Recent Advances in Transition Metal-Catalyzed N-Atom Transfer Reactions of Azides. *Org. Biomol. Chem.* **2010**, *8*, 3831-3846. (l) Fantauzzi, S.; Caselli, A.; Gallo, E. Nitrene Transfer Reactions Mediated by Metallo-Porphyrin Complexes. *Dalton Trans.* **2009**, *28*, 5434-5443. (m) Doyle, M. P. Exceptional Selectivity in Cyclopropanation Reactions Catalyzed by Chiral Cobalt(Ii)–Porphyrin Catalysts. *Angew. Chem. Int. Ed.* **2009**, *48*, 850-852.

5. (a) Ye, K.-Y.; McCallum, T.; Lin, S. Bimetallic Radical Redox-Relay Catalysis for the Isomerization of Epoxides to Allylic Alcohols. *J. Am. Chem. Soc.* **2019**, *141*, 9548-9554. (b) Yao, C.; Dahmen, T.; Gansäuer, A.; Norton, J. Anti-Markovnikov Alcohols Via Epoxide Hydrogenation through Cooperative Catalysis. *Science* **2019**, *364*, 764–767. (c) McCallum, T.; Wu, X.; Lin, S. Recent Advances in Titanium Radical Redox Catalysis. *J.*

Org. Chem. **2019**, *84*, 14369-14380. (d) Klare, S.; Gordon, J. P.; Gansäuer, A.; RajanBabu, T. V.; Nugent, W. A. The Reaction of β,γ -Epoxy Alcohols with Titanium(III) Reagents. A Proposed Role for Intramolecular Hydrogen Bonding. *Tetrahedron* **2019**, *75*, 130662. (e) Hao, W.; Wu, X.; Sun, J. Z.; Siu, J. C.; MacMillan, S. N.; Lin, S. Radical Redox-Relay Catalysis: Formal [3+2] Cycloaddition of N-Acylaziridines and Alkenes. *J. Am. Chem. Soc.* **2017**, *139*, 12141-12144. (f) Gansäuer, A.; Hildebrandt, S.; Vogelsang, E.; Flowers II, R. A. Tuning the Redox Properties of the Titanocene(III)/(IV)-Couple for Atom-Economical Catalysis in Single Electron Steps. *Dalton Trans.* **2016**, *45*, 448–452. (g) Gansäuer, A.; Hildebrandt, S.; Michelmann, A.; Dahmen, T.; von Laufenberg, D.; Kube, C.; Fianu, G. D.; Flowers II, R. A. Cationic Titanocene(III) Complexes for Catalysis in Single-Electron Steps. *Angew. Chem., Int. Ed.* **2015**, *54*, 7003-7006. (h) Gansäuer, A.; Fleckhaus, A.; Lafont, M. A.; Okkel, A.; Kotsis, K.; Anoop, A.; Neese, F. Catalysis Via Homolytic Substitutions with C–O and Ti–O Bonds: Oxidative Additions and Reductive Eliminations in Single Electron Steps. *J. Am. Chem. Soc.* **2009**, *131*, 16989-16999. (i) Gansäuer, A.; Fan, C.-A.; Keller, F.; Keil, J. Titanocene-Catalyzed Regiodivergent Epoxide Openings. *J. Am. Chem. Soc.* **2007**, *129*, 3484-3485. (j) Gansäuer, A.; Rinker, B.; Pierobon, M.; Grimme, S.; Gerenkamp, M.; Mück-Lichtenfeld, C. A Radical Tandem Reaction with Homolytic Cleavage of a Ti–O Bond. *Angew. Chem., Int. Ed.* **2003**, *42*, 3687-3690. (k) RajanBabu, T. V.; Nugent, W. A. Selective Generation of Free Radicals from Epoxides Using a Transition-Metal Radical. A Powerful New Tool for Organic Synthesis. *J. Am. Chem. Soc.* **1994**, *116*, 986-997. (l) Nugent, W. A.; RajanBabu, T. V. Transition-Metal-Centered Radicals in Organic Synthesis. Titanium(III)-Induced Cyclization of Epoxy Olefins. *J. Am. Chem. Soc.* **1988**, *110*, 8561–8562.

6. (a) Smith, D. M.; Pulling, M. E.; Norton, J. R. Tin-Free and Catalytic Radical Cyclizations. *J. Am. Chem. Soc.* **2007**, *129*, 770-771. (b) Estes, D. P.; Norton, J. R.; Jockusch, S.; Sattler, W. Mechanisms by Which Alkynes React with $\text{Cp}^*(\text{Co})_3\text{H}$. Application to Radical Cyclization. *J. Am. Chem. Soc.* **2012**, *134*, 15512–15518. (c) Li, G.; Han, A.; Pulling, M. E.; Estes, D. P.; Norton, J. R. Evidence for Formation of a Co–H Bond from $(\text{H}_2\text{O})_2\text{Co}(\text{Dmgbf}_2)_2$ under H_2 : Application to Radical Cyclizations. *J. Am. Chem. Soc.* **2012**, *134*, 14662–14665. (d) Kuo, J. L.; Hartung, J.; Han, A.; Norton, J. R. Direct Generation of Oxygen-Stabilized Radicals by $\text{H}\cdot$ Transfer from Transition Metal Hydrides. *J. Am. Chem. Soc.* **2015**, *137*, 1036-1039.
7. Dzik, W. I.; Xu, X.; Zhang, X. P.; Reek, J. N. H.; de Bruin, B. ‘Carbene Radicals’ in $\text{Co}^{\text{II}}(\text{Por})$ -Catalyzed Olefin Cyclopropanation. *J. Am. Chem. Soc.* **2010**, *132*, 10891-10902.
8. (a) Lyaskovskyy, V.; Suarez, A. I. O.; Lu, H.; Jiang, H.; Zhang, X. P.; de Bruin, B. Mechanism of Cobalt(II) Porphyrin-Catalyzed C–H Amination with Organic Azides: Radical Nature and H-Atom Abstraction Ability of the Key Cobalt(III)–Nitrene Intermediates. *J. Am. Chem. Soc.* **2011**, *133*, 12264-12273. (b) Goswami, M.; Lyaskovskyy, V.; Domingos, S. R.; Buma, W. J.; Woutersen, S.; Troeppner, O.; Ivanović-Burmazović, I.; Lu, H.; Cui, X.; Zhang, X. P.; Reijerse, E. J.; DeBeer, S.; van Schooneveld, M. M.; Pfaff, F. F.; Ray, K.; de Bruin, B. Characterization of Porphyrin-Co(III)-‘Nitrene Radical’ Species Relevant in Catalytic Nitrene Transfer Reactions. *J. Am. Chem. Soc.* **2015**, *137*, 5468-5479. (c) Hu, Y.; Lang, K.; Li, C.; Gill, J. B.; Kim, I.; Lu, H.; Fields, K. B.; Marshall, M.; Cheng, Q.; Cui, X.; Wojtas, L.; Zhang, X. P. Enantioselective Radical

Construction of 5-Membered Cyclic Sulfonamides by Metalloradical C–H Amination. *J. Am. Chem. Soc.* **2019**, *141*, 18160-18169.

9. (a) Huang, L.; Chen, Y.; Gao, G.-Y.; Zhang, X. P. Diastereoselective and Enantioselective Cyclopropanation of Alkenes Catalyzed by Cobalt Porphyrins. *J. Org. Chem.* **2003**, *68*, 8179-8184. (b) Chen, Y.; Fields, K. B.; Zhang, X. P. Bromoporphyrins as Versatile Synthons for Modular Construction of Chiral Porphyrins: Cobalt-Catalyzed Highly Enantioselective and Diastereoselective Cyclopropanation. *J. Am. Chem. Soc.* **2004**, *126*, 14718-14719. (c) Chen, Y.; Zhang, X. P. Vitamin B12 Derivatives as Natural Asymmetric Catalysts: Enantioselective Cyclopropanation of Alkenes. *J. Org. Chem.* **2004**, *69*, 2431-2435. (d) Chen, Y.; Ruppel, J. V.; Zhang, X. P. Cobalt-Catalyzed Asymmetric Cyclopropanation of Electron-Deficient Olefins. *J. Am. Chem. Soc.* **2007**, *129*, 12074-12075. (e) Zhu, S.; Perman, J. A.; Zhang, X. P. Acceptor/Acceptor-Substituted Diazo Reagents for Carbene Transfers: Cobalt-Catalyzed Asymmetric Z-Cyclopropanation of Alkenes with A-Nitrodiazoacetates. *Angew. Chem. Int. Ed.* **2008**, *47*, 8460-8463. (f) Zhu, S.; Ruppel, J. V.; Lu, H.; Wojtas, L.; Zhang, X. P. Cobalt-Catalyzed Asymmetric Cyclopropanation with Diazosulfones: Rigidification and Polarization of Ligand Chiral Environment Via Hydrogen Bonding and Cyclization. *J. Am. Chem. Soc.* **2008**, *130*, 5042-5043. (g) Ruppel, J. V.; Gauthier, T. J.; Snyder, N. L.; Perman, J. A.; Zhang, X. P. Asymmetric Co(II)-Catalyzed Cyclopropanation with Succinimidyl Diazoacetate: General Synthesis of Chiral Cyclopropyl Carboxamides. *Org. Lett.* **2009**, *11*, 2273-2276. (h) Zhu, S.; Xu, X.; Perman, J. A.; Zhang, X. P. A General and Efficient Cobalt(II)-Based Catalytic System for Highly Stereoselective Cyclopropanation of Alkenes with A-Cyanodiazoacetates. *J. Am. Chem. Soc.* **2010**, *132*, 12796-12799. (i) Xu, X.; Lu, H.;

Ruppel, J. V.; Cui, X.; Lopez de Mesa, S.; Wojtas, L.; Zhang, X. P. Highly Asymmetric Intramolecular Cyclopropanation of Acceptor-Substituted Diazoacetates by Co(Ii)-Based Metalloradical Catalysis: Iterative Approach for Development of New-Generation Catalysts. *J. Am. Chem. Soc.* **2011**, *133*, 15292-15295. (j) Xu, X.; Zhu, S.; Cui, X.; Wojtas, L.; Zhang, X. P. Cobalt(Ii)-Catalyzed Asymmetric Olefin Cyclopropanation with α -Ketodiazoacetates. *Angew. Chem. Int. Ed.* **2013**, *52*, 11857-11861. (k) Wang, Y.; Wen, X.; Cui, X.; Wojtas, L.; Zhang, X. P. Asymmetric Radical Cyclopropanation of Alkenes with in Situ-Generated Donor-Substituted Diazo Reagents Via Co(Ii)-Based Metalloradical Catalysis. *J. Am. Chem. Soc.* **2017**, *139*, 1049-1052. (l) Xu, X.; Wang, Y.; Cui, X.; Wojtas, L.; Zhang, X. P. Metalloradical Activation of α -Formyldiazoacetates for the Catalytic Asymmetric Radical Cyclopropanation of Alkenes. *Chem. Sci.* **2017**, *8*, 4347-4351.

10. (a) Cui, X.; Xu, X.; Jin, L.-M.; Wojtas, L.; Zhang, X. P. Stereoselective Radical C–H Alkylation with Acceptor/Acceptor-Substituted Diazo Reagents Via Co(Ii)-Based Metalloradical Catalysis. *Chem. Sci.* **2015**, *6*, 1219–1224. (b) Wang, Y.; Wen, X.; Cui, X.; Zhang, X. P. Enantioselective Radical Cyclization for Construction of 5-Membered Ring Structures by Metalloradical C–H Alkylation. *J. Am. Chem. Soc.* **2018**, *140*, 4792-4796. (c) Wen, X.; Wang, Y.; Zhang, X. P. Enantioselective Radical Process for Synthesis of Chiral Indolines by Metalloradical Alkylation of Diverse C(Sp³)–H Bonds. *Chem. Sci.* **2018**, *9*, 5082–5086.

11. (a) Gao, G.-Y.; Jones, J. E.; Vyas, R.; Harden, J. D.; Zhang, X. P. Cobalt-Catalyzed Aziridination with Diphenylphosphoryl Azide (Dppa): Direct Synthesis of N-Phosphorus-Substituted Aziridines from Alkenes. *J. Org. Chem.* **2006**, *71*, 6655-6658. (b) Jones, J. E.; Ruppel, J. V.; Gao, G.-Y.; Moore, T. M.; Zhang, X. P. Cobalt-Catalyzed Asymmetric

Olefin Aziridination with Diphenylphosphoryl Azide. *J. Org. Chem.* **2008**, *73*, 7260-7265.

(c) Ruppel, J. V.; Jones, J. E.; Huff, C. A.; Kamble, R. M.; Chen, Y.; Zhang, X. P. A Highly Effective Cobalt Catalyst for Olefin Aziridination with Azides: Hydrogen Bonding Guided Catalyst Design. *Org. Lett.* **2008**, *10*, 1995-1998. (d) Subbarayan, V.; Ruppel, J. V.; Zhu, S.; Perman, J. A.; Zhang, X. P. Highly Asymmetric Cobalt-Catalyzed Aziridination of Alkenes with Trichloroethoxysulfonyl Azide (Tcesn₃). *Chem. Commun.* **2009**, 4266-4268.

(e) Jin, L.-M.; Xu, X.; Lu, H.; Cui, X.; Wojtas, L.; Zhang, X. P. Effective Synthesis of Chiral N-Fluoroaryl Aziridines through Enantioselective Aziridination of Alkenes with Fluoroaryl Azides. *Angew. Chem. Int. Ed.* **2013**, *52*, 5309-5313. (f) Subbarayan, V.; Jin, L.-M.; Cui, X.; Zhang, X. P. Room Temperature Activation of Aryloxysulfonyl Azides by [Co(Ii)(Tpp)] for Selective Radical Aziridination of Alkenes Via Metalloradical Catalysis. *Tetrahedron Lett.* **2015**, *56*, 3431-3434. (g) Jiang, H.; Lang, K.; Lu, H.; Wojtas, L.; Zhang, X. P. Intramolecular Radical Aziridination of Allylic Sulfamoyl Azides by Cobalt(Ii)-Based Metalloradical Catalysis: Effective Construction of Strained Heterobicyclic Structures. *Angew. Chem. Int. Ed.* **2016**, *55*, 11604-11608. (h) Jiang, H.; Lang, K.; Lu, H.; Wojtas, L.; Zhang, X. P. Asymmetric Radical Bicyclization of Allyl Azidoformates Via Cobalt(Ii)-Based Metalloradical Catalysis. *J. Am. Chem. Soc.* **2017**, *139*, 9164-9167.

12. (a) Harden, J. D.; Ruppel, J. V.; Gao, G.-Y.; Zhang, X. P. Cobalt-Catalyzed Intermolecular C–H Amination with Bromamine-T as Nitrene Source. *Chem. Commun.* **2007**, 4644-4646. (b) Ruppel, J. V.; Kamble, R. M.; Zhang, X. P. Cobalt-Catalyzed Intramolecular C–H Amination with Arylsulfonyl Azides. *Org. Lett.* **2007**, *9*, 4889-4892. (c) Lu, H.; Jiang, H.; Wojtas, L.; Zhang, X. P. Selective Intramolecular C–H Amination through the Metalloradical Activation of Azides: Synthesis of 1,3-Diamines under Neutral

and Nonoxidative Conditions. *Angew. Chem. Int. Ed.* **2010**, *49*, 10192-10196. (d) Lu, H.; Subbarayan, V.; Tao, J.; Zhang, X. P. Cobalt(Ii)-Catalyzed Intermolecular Benzylic C–H Amination with 2,2,2-Trichloroethoxycarbonyl Azide (Trocn₃). *Organometallics* **2010**, *29*, 389-393. (e) Lu, H.; Tao, J.; Jones, J. E.; Wojtas, L.; Zhang, X. P. Cobalt(Ii)-Catalyzed Intramolecular C–H Amination with Phosphoryl Azides: Formation of 6- and 7-Membered Cyclophosphoramidates. *Org. Lett.* **2010**, *12*, 1248-1251. (f) Lu, H.; Jiang, H.; Hu, Y.; Wojtas, L.; Zhang, X. P. Chemoselective Intramolecular Allylic C–H Amination Versus C=C Aziridination through Co(Ii)-Based Metalloradical Catalysis. *Chem. Sci.* **2011**, *2*, 2361-2366. (g) Lu, H.; Hu, Y.; Jiang, H.; Wojtas, L.; Zhang, X. P. Stereoselective Radical Amination of Electron-Deficient C(Sp³)–H Bonds by Co(Ii)-Based Metalloradical Catalysis: Direct Synthesis of α -Amino Acid Derivatives Via α -C–H Amination. *Org. Lett.* **2012**, *14*, 5158-5161. (h) Jin, L.-M.; Lu, H.; Cui, Y.; Lizardi, C. L.; Arzua, T. N.; Wojtas, L.; Cui, X.; Zhang, X. P. Selective Radical Amination of Aldehydic C(Sp²)–H Bonds with Fluoroaryl Azides Via Co(Ii)-Based Metalloradical Catalysis: Synthesis of N-Fluoroaryl Amides from Aldehydes under Neutral and Nonoxidative Conditions. *Chem. Sci.* **2014**, *5*, 2422-2427. (i) Lu, H.; Li, C.; Jiang, H.; Lizardi, C. L.; Zhang, X. P. Chemoselective Amination of Propargylic C(Sp³)–H Bonds by Cobalt(Ii)-Based Metalloradical Catalysis. *Angew. Chem. Int. Ed.* **2014**, *53*, 7028-7032. (j) Lu, H.; Lang, K.; Jiang, H.; Wojtas, L.; Zhang, X. P. Intramolecular 1,5-C(Sp³)–H Radical Amination Via Co(Ii)-Based Metalloradical Catalysis for Five-Membered Cyclic Sulfamides. *Chem. Sci.* **2016**, *7*, 6934-6939. (k) Li, C.; Lang, K.; Lu, H.; Hu, Y.; Cui, X.; Wojtas, L.; Zhang, X. P. Catalytic Radical Process for Enantioselective Amination of C(Sp³)–H Bonds. *Angew. Chem. Int. Ed.* **2018**, *57*, 16837-16841. (l) Lang, K.; Torker, S.; Wojtas, L.; Zhang, X. P.

Asymmetric Induction and Enantiodivergence in Catalytic Radical C–H Amination Via Enantiodifferentiative H-Atom Abstraction and Stereoretentive Radical Substitution. *J. Am. Chem. Soc.* **2019**, *141*, 12388-12396. (m) Jin, L.-M.; Xu, P.; Xie, J.; Zhang, X. P. Enantioselective Intermolecular Radical C–H Amination. *J. Am. Chem. Soc.* **2020**, *142*, 20828-20836. (n) Lang, K.; Li, C.; Kim, I.; Zhang, X. P. Enantioconvergent Amination of Racemic Tertiary C–H Bonds. *J. Am. Chem. Soc.* **2020**, *142*, 20902-20911.

13. (a) Zwanenburg, B.; ten Holte, P., The Synthetic Potential of Three-Membered Ring Aza-Heterocycles. In *Stereoselective Heterocyclic Synthesis Iii*; Metz, P., Ed. Springer Berlin Heidelberg: Berlin, Heidelberg, 2001; pp 93-124. (b) Sweeney, J. B. Aziridines: Epoxides' Ugly Cousins? *Chem. Soc. Rev.* **2002**, *31*, 247-258. (c) Lowden, P. A. S., Aziridine Natural Products – Discovery, Biological Activity and Biosynthesis. In *Aziridines and Epoxides in Organic Synthesis*; Yudin, A. K., Ed. Wiley-VCH: Germany, 2006; pp 399-442. (d) Jiang, H.; Zhang, X. P., Oxidation: C–N Bond Formation by Oxidation (Aziridines). In *Comprehensive Chirality*; Carreira, E. M.; Yamamoto, H., Eds. Elsevier: Amsterdam, 2012; Vol. 5, pp 168-182.

14. (a) Tanner, D. Chiral Aziridines—Their Synthesis and Use in Stereoselective Transformations. *Angew. Chem. Int. Ed. Engl.* **1994**, *33*, 599-619. (b) Osborn, H. M. I.; Sweeney, J. The Asymmetric Synthesis of Aziridines. *Tetrahedron: Asymmetry* **1997**, *8*, 1693-1715. (c) Müller, P.; Fruit, C. Enantioselective Catalytic Aziridinations and Asymmetric Nitrene Insertions into C–H Bonds. *Chem. Rev.* **2003**, *103*, 2905-2920. (d) Pellissier, H. Recent Developments in Asymmetric Aziridination. *Tetrahedron* **2010**, *66*, 1509-1555. (e) Degennaro, L.; Trinchera, P.; Luisi, R. Recent Advances in the Stereoselective Synthesis of Aziridines. *Chem. Rev.* **2014**, *114*, 7881-7929.

15. Sweeney, J. B., Synthesis of Aziridines. In *Aziridines and Epoxides in Organic Synthesis*; 2006; pp 117-144.
16. (a) Richardson, R. D.; Desai, M.; Wirth, T. Hypervalent Iodine-Mediated Aziridination of Alkenes: Mechanistic Insights and Requirements for Catalysis. *Chem. Eur. J.* **2007**, *13*, 6745-6754. (b) Brown, M.; Farid, U.; Wirth, T. Hypervalent Iodine Reagents as Powerful Electrophiles. *Synlett* **2013**, *24*, 424-431. (c) Muñiz, K., Aminations with Hypervalent Iodine. In *Hypervalent Iodine Chemistry*; Wirth, T., Ed. Springer International Publishing: Cham, 2016; pp 105-133.
17. (a) Gao, G.-Y.; Harden, J. D.; Zhang, X. P. Cobalt-Catalyzed Efficient Aziridination of Alkenes. *Org. Lett.* **2005**, *7*, 3191-3193. (b) Fructos, M. R.; Trofimenko, S.; Díaz-Requejo, M. M.; Pérez, P. J. Facile Amine Formation by Intermolecular Catalytic Amidation of Carbon-Hydrogen Bonds. *J. Am. Chem. Soc.* **2006**, *128*, 11784-11791. (c) Fantauzzi, S.; Caselli, A.; Gallo, E. Nitrene Transfer Reactions Mediated by Metalloporphyrin Complexes. *Dalton Trans.* **2009**, 5434-5443.
18. (a) Lebel, H.; Huard, K.; Lectard, S. N-Tosylloxycarbamates as a Source of Metal Nitrenes: Rhodium-Catalyzed C-H Insertion and Aziridination Reactions. *J. Am. Chem. Soc.* **2005**, *127*, 14198-14199. (b) Lebel, H.; Spitz, C.; Leogane, O.; Trudel, C.; Parmentier, M. Stereoselective Rhodium-Catalyzed Amination of Alkenes. *Org. Lett.* **2011**, *13*, 5460-5463. (c) Lebel, H.; Parmentier, M.; Leogane, O.; Ross, K.; Spitz, C. Copper Bis(Oxazolines) as Catalysts for Stereoselective Aziridination of Styrenes with N-Tosylloxycarbamates. *Tetrahedron* **2012**, *68*, 3396-3409.
19. (a) Bräse, S.; Gil, C.; Knepper, K.; Zimmermann, V. Organic Azides: An Exploding Diversity of a Unique Class of Compounds. *Angew. Chem. Int. Ed.* **2005**, *44*, 5188-5240.

- (b) Katsuki, T. Azide Compounds: Nitrogen Sources for Atom-Efficient and Ecologically Benign Nitrogen-Atom-Transfer Reactions. *Chem. Lett.* **2005**, *34*, 1304-1309.
20. (a) Caselli, A.; Gallo, E.; Ragaini, F.; Ricatto, F.; Abbiati, G.; Cenini, S. Chiral Porphyrin Complexes of Cobalt(II) and Ruthenium(II) in Catalytic Cyclopropanation and Amination Reactions. *Inorg. Chim. Acta* **2006**, *359*, 2924-2932. (b) Tao, J.; Jin, L.-M.; Zhang, X. P. Synthesis of Chiral N-Phosphoryl Aziridines through Enantioselective Aziridination of Alkenes with Phosphoryl Azide Via Co(II)-Based Metalloradical Catalysis. *Beilstein Journal of Organic Chemistry* **2014**, *10*, 1282-1289.
21. Greene, T. W.; Wutts, P. G., Protection for the Amino Group. In *Greene's Protective Groups in Organic Synthesis*; 4th ed.; John Wiley & Sons: New York, 2006; pp 696-926.
22. Yamamoto, Y. From Σ - to Π -Electrophilic Lewis Acids. Application to Selective Organic Transformations. *J. Org. Chem.* **2007**, *72*, 7817-7831.
23. (a) Ametamey, S. M.; Honer, M.; Schubiger, P. A. Molecular Imaging with Pet. *Chem. Rev.* **2008**, *108*, 1501-1516. (b) Purser, S.; Moore, P. R.; Swallow, S.; Gouverneur, V. Fluorine in Medicinal Chemistry. *Chem. Soc. Rev.* **2008**, *37*, 320-330. (c) Amii, H.; Uneyama, K. C-F Bond Activation in Organic Synthesis. *Chem. Rev.* **2009**, *109*, 2119-2183.
24. Lu, H.; Subbarayan, V.; Tao, J.; Zhang, X. P. Cobalt(II)-Catalyzed Intermolecular Benzylic C-H Amination with 2,2,2-Trichloroethoxycarbonyl Azide (Trocn₃). *Organometallics* **2010**, *29*, 389-393.
25. Cui, X.; Xu, X.; Wojtas, L.; Kim, M. M.; Zhang, X. P. Regioselective Synthesis of Multisubstituted Furans Via Metalloradical Cyclization of Alkynes with A-

Diazocarbonyls: Construction of Functionalized A-Oligofurans. *J. Am. Chem. Soc.* **2012**, *134*, 19981-19984.

26. (a) Jat, J. L.; Paudyal, M. P.; Gao, H.; Xu, Q.-L.; Yousufuddin, M.; Devarajan, D.; Ess, D. H.; Kürti, L.; Falck, J. R. Direct Stereospecific Synthesis of Unprotected N-H and N-Me Aziridines from Olefins. *Science* **2014**, *343*, 61–65. (b) Watson, I. D. G.; Yu, L.; Yudin, A. K. Advances in Nitrogen Transfer Reactions Involving Aziridines. *Acc. Chem. Res.* **2006**, *39*, 194-206.

27. (a) Rhouati, S.; Bernou, A. Cyclisation of Azidoformates, Formation of Aziridines. *J. Chem. Soc., Chem. Commun.* **1989**, 730–732. (b) Bergmeier, S. C.; Stanchina, D. M. Synthesis of Vicinal Amino Alcohols Via a Tandem Acylnitrene Aziridination–Aziridine Ring Opening. *J. Org. Chem.* **1997**, *62*, 4449-4456. (c) Bergmeier, S. C.; Stanchina, D. M. Acylnitrene Route to Vicinal Amino Alcohols. Application to the Synthesis of (–)-Bestatin and Analogues. *J. Org. Chem.* **1999**, *64*, 2852-2859. (d) Kan, C.; Long, C. M.; Paul, M.; Ring, C. M.; Tully, S. E.; Rojas, C. M. Photo Amidoglycosylation of an Allal Azidoformate. Synthesis of B-2-Amido Allopyranosides. *Org. Lett.* **2001**, *3*, 381-384. (e) Yoshimitsu, T.; Ino, T.; Tanaka, T. Total Synthesis of (–)-Agelastatin A. *Org. Lett.* **2008**, *10*, 5457-5460. (f) Chang, Y.-J.; Hsuan, Y.-C.; Lai, A. C.-Y.; Han, Y.-C.; Hou, D.-R. Synthesis of A-C-Galactosylceramide Via Diastereoselective Aziridination: The New Immunostimulant 4'-Epi-C-Glycoside of Krm7000. *Org. Lett.* **2016**, *18*, 808-811. (g) Zhang, Y.; Dong, X.; Wu, Y.; Li, G.; Lu, H. Visible-Light-Induced Intramolecular C(Sp²)–H Amination and Aziridination of Azidoformates Via a Triplet Nitrene Pathway. *Org. Lett.* **2018**, *20*, 4838–4842.

28. (a) Curtius, T. Hydrazoic Acid. *Ber.* **1890**, *23*, 3023-3033. (b) Smith, P. A. The Curtius Reaction. *Org. React.* **1946**, 337-449.
29. Scholz, S. O.; Farney, E. P.; Kim, S.; Bates, D. M.; Yoon, T. P. Spin-Selective Generation of Triplet Nitrenes: Olefin Aziridination through Visible-Light Photosensitization of Azidoformates. *Angew. Chem. Int. Ed.* **2016**, *55*, 2239-2242.
30. (a) Heine, H.; Proctor, Z. Notes - Isomerization of N-P-Ethoxybenzolethylenimine. *J. Org. Chem.* **1958**, *23*, 1554-1556. (b) Nishimura, M.; Minakata, S.; Takahashi, T.; Oderaotoshi, Y.; Komatsu, M. Asymmetric N1 Unit Transfer to Olefins with a Chiral Nitridomanganese Complex: Novel Stereoselective Pathways to Aziridines or Oxazolines. *J. Org. Chem.* **2002**, *67*, 2101-2110. (c) Luppi, G.; Tomasini, C. A New Entry to Polyfunctionalized 4,5-Trans Disubstituted Oxazolidin-2-Ones from L-Aspartic Acid. *Synlett* **2003**, 0797-0800.
31. (a) Olivos Suarez, A. I.; Jiang, H.; Zhang, X. P.; de Bruin, B. The Radical Mechanism of Cobalt(Ii) Porphyrin-Catalyzed Olefin Aziridination and the Importance of Cooperative H-Bonding. *Dalton Trans.* **2011**, *40*, 5697-5705. (b) Hopmann, K. H.; Ghosh, A. Mechanism of Cobalt-Porphyrin-Catalyzed Aziridination. *ACS. Catal.* **2011**, *1*, 597-600.
32. (a) Lu, Z.; Zhang, Y.; Wulff, W. D. Direct Access to N-H-Aziridines from Asymmetric Catalytic Aziridination with Borate Catalysts Derived from Vaulted Binaphthol and Vaulted Biphenanthrol Ligands. *J. Am. Chem. Soc.* **2007**, *129*, 7185-7194. (b) Ismail, F. M. D.; Levitsky, D. O.; Dembitsky, V. M. Aziridine Alkaloids as Potential Therapeutic Agents. *Eur. J. Med. Chem.* **2009**, *44*, 3373-3387. (c) Thibodeaux, C. J.;

Chang, W.-c.; Liu, H.-w. Enzymatic Chemistry of Cyclopropane, Epoxide, and Aziridine Biosynthesis. *Chem. Rev.* **2012**, *112*, 1681-1709.

33. (a) Alonso, D. A.; Andersson, P. G. Deprotection of Sulfonyl Aziridines. *J. Org. Chem.* **1998**, *63*, 9455-9461. (b) Ankner, T.; Hilmersson, G. Instantaneous Deprotection of Tosylamides and Esters with $\text{SmI}_2/\text{Amine}/\text{Water}$. *Org. Lett.* **2009**, *11*, 1865-1865.

34. Lebel, H.; Lectard, S.; Parmentier, M. Copper-Catalyzed Alkene Aziridination with N-Tosylloxycarbamates. *Org. Lett.* **2007**, *9*, 4797-4800.

35. (a) Lucet, D.; Le Gall, T.; Mioskowski, C. The Chemistry of Vicinal Diamines. *Angew. Chem. Int. Ed.* **1998**, *37*, 2580-2627. (b) Saibabu Kotti, S. R. S.; Timmons, C.; Li, G. Vicinal Diamino Functionalities as Privileged Structural Elements in Biologically Active Compounds and Exploitation of Their Synthetic Chemistry. *Chemical Biology & Drug Design* **2006**, *67*, 101-114.

36. (a) Breuzard, J. A. J.; Christ-Tommasino, M. L.; Lemaire, M., Chiral Ureas and Thioureas in Asymmetric Catalysis. In *Chiral Diazaligands for Asymmetric Synthesis*; Lemaire, M.; Mangeney, P., Eds. Springer Berlin Heidelberg: Berlin, Heidelberg, 2005; pp 231-270. (b) Doyle, A. G.; Jacobsen, E. N. Small-Molecule H-Bond Donors in Asymmetric Catalysis. *Chem. Rev.* **2007**, *107*, 5713-5743. (c) Xu, H.; Zuend, S. J.; Woll, M. G.; Tao, Y.; Jacobsen, E. N. Asymmetric Cooperative Catalysis of Strong Brønsted Acid-Promoted Reactions Using Chiral Ureas. *Science* **2010**, *327*, 986-990.

37. Hill, J. E.; Matlock, J. V.; Lefebvre, Q.; Cooper, K. G.; Clayden, J. Consecutive Ring Expansion and Contraction for the Synthesis of 1-Aryl Tetrahydroisoquinolines and Tetrahydrobenzazepines from Readily Available Heterocyclic Precursors. *Angew. Chem. Int. Ed.* **2018**, *57*, 5788-5791.

38. Bruker (2013). Apex2 (Version 2013.6-2). Bruker Axs Inc., Madison, Wisconsin, USA.
39. Bruker (2013). Saint-V8.32a. Data Reduction Software.
40. Sheldrick, G. M. (1996). Sadabs. Program for Empirical Absorption Correction. University of Gottingen, Germany.
41. Hubschle, C. B.; Sheldrick, G. M.; Dittrich, B. Shelxle: A Qt Graphical User Interface for Shelxl. *J. Appl. Crystallogr.* **2011**, *44*, 1281-1284.
42. (a) Farrugia, L. Wingx Suite for Small-Molecule Single-Crystal Crystallography. *J. Appl. Crystallogr.* **1999**, *32*, 837-838. (b) Sheldrick, G. Phase Annealing in Shelx-90: Direct Methods for Larger Structures. *Acta Crystallographica Section A* **1990**, *46*, 467-473. (c) Sheldrick, G.M. (1997) Shelxl-97. Program for the Refinement of Crystal.
43. Dolomanov, O. V.; Bourhis, L. J.; Gildea, R. J.; Howard, J. A. K.; Puschmann, H. Olex2: A Complete Structure Solution, Refinement and Analysis Program. *J. Appl. Crystallogr.* **2009**, *42*, 339-341.
44. Frisch. M. J., (2009). Gaussian 09, Revision D.01, Gaussian, Inc., Wallingford Ct.
45. Schultz, N. E.; Zhao, Y.; Truhlar, D. G. Density Functionals for Inorganometallic and Organometallic Chemistry. *J. Phys. Chem. A* **2005**, *109*, 11127-11143.
46. Eichkorn, K.; Weigend, F.; Treutler, O.; Ahlrichs, R. Auxiliary Basis Sets for Main Row Atoms and Transition Metals and Their Use to Approximate Coulomb Potentials. *Theor. Chem. Acc.* **1997**, *97*, 119-124.
47. Furche, F.; Perdew, J. P. The Performance of Semilocal and Hybrid Density Functionals in 3d Transition-Metal Chemistry. *J. Chem. Phys.* **2006**, *124*, 044103.

48. Grimme, S.; Antony, J.; Ehrlich, S.; Krieg, H. A Consistent and Accurate Ab Initio Parametrization of Density Functional Dispersion Correction (Dft-D) for the 94 Elements H-Pu. *J. Chem. Phys.* **2010**, *132*, 154104.
49. Marenich, A. V.; Cramer, C. J.; Truhlar, D. G. Universal Solvation Model Based on Solute Electron Density and on a Continuum Model of the Solvent Defined by the Bulk Dielectric Constant and Atomic Surface Tensions. *J. Phys. Chem. B* **2009**, *113*, 6378-6396.
50. (a) Denisov, I. G.; Makris, T. M.; Sligar, S. G.; Schlichting, I. Structure and Chemistry of Cytochrome P450. *Chem. Rev.* **2005**, *105*, 2253-2278. (b) Ortiz de Montellano, P. R. Hydrocarbon Hydroxylation by Cytochrome P450 Enzymes. *Chem. Rev.* **2010**, *110*, 932-948. (c) Monti, D.; Ottolina, G.; Carrea, G.; Riva, S. Redox Reactions Catalyzed by Isolated Enzymes. *Chem. Rev.* **2011**, *111*, 4111-4140. (d) Oloo, W. N.; Que, L. Bioinspired Nonheme Iron Catalysts for C–H and C=C Bond Oxidation: Insights into the Nature of the Metal-Based Oxidants. *Acc. Chem. Res.* **2015**, *48*, 2612-2621. (e) Rudolf, J. D.; Chang, C.-Y.; Ma, M.; Shen, B. Cytochromes P450 for Natural Product Biosynthesis in Streptomyces: Sequence, Structure, and Function. *Nat. Prod. Rep.* **2017**, *34*, 1141-1172.
51. (a) Epoxides and Aziridines in Click Chemistry. In *Aziridines and Epoxides in Organic Synthesis*; pp 443-477. (b) Que Jr, L.; Tolman, W. B. Biologically Inspired Oxidation Catalysis. *Nature* **2008**, *455*, 333. (c) Newhouse, T.; Baran, P. S. If C–H Bonds Could Talk: Selective C–H Bond Oxidation. *Angew. Chem. Int. Ed.* **2011**, *50*, 3362-3374. (d) Qiu, Y.; Gao, S. Trends in Applying C–H Oxidation to the Total Synthesis of Natural Products. *Nat. Prod. Rep.* **2016**, *33*, 562-581.
52. (a) Chan, S. L.-F.; Kan, Y.-H.; Yip, K.-L.; Huang, J.-S.; Che, C.-M. Ruthenium Complexes of 1,4,7-Trimethyl-1,4,7-Triazacyclononane for Atom and Group Transfer

Reactions. *Coord. Chem. Rev.* **2011**, *255*, 899-919. (b) Nam, W. High-Valent Iron(IV)-Oxo Complexes of Heme and Non-Heme Ligands in Oxygenation Reactions. *Acc. Chem. Res.* **2007**, *40*, 522-531. (c) Punniyamurthy, T.; Velusamy, S.; Iqbal, J. Recent Advances in Transition Metal Catalyzed Oxidation of Organic Substrates with Molecular Oxygen. *Chem. Rev.* **2005**, *105*, 2329-2364.

53. Shimoyama, Y.; Kojima, T. Metal-Oxyl Species and Their Possible Roles in Chemical Oxidations. *Inorg. Chem.* **2019**, *58*, 9517-9542.

54. (a) Wang, C.-C.; Chang, H.-C.; Lai, Y.-C.; Fang, H.; Li, C.-C.; Hsu, H.-K.; Li, Z.-Y.; Lin, T.-S.; Kuo, T.-S.; Neese, F.; Ye, S.; Chiang, Y.-W.; Tsai, M.-L.; Liaw, W.-F.; Lee, W.-Z. A Structurally Characterized Nonheme Cobalt-Hydroperoxo Complex Derived from Its Superoxo Intermediate Via Hydrogen Atom Abstraction. *J. Am. Chem. Soc.* **2016**, *138*, 14186-14189. (b) Jones, R. D.; Summerville, D. A.; Basolo, F. Synthetic Oxygen Carriers Related to Biological Systems. *Chem. Rev.* **1979**, *79*, 139-179.

55. (a) Teruaki, M.; Shigeru, I.; Satoshi, I.; Koji, K.; Tohru, Y.; Toshihiro, T. Oxidation-Reduction Hydration of Olefins with Molecular Oxygen and 2-Propanol Catalyzed by Bis(Acetylacetonato)Cobalt(II). *Chem. Lett.* **1989**, *18*, 449-452. (b) Tung, H. C.; Sawyer, D. T. Cobalt-Induced Activation of Hydrogen Peroxide for the Direct Ketonization of Methylenic Carbons [C-C₆H₁₂ → C-C₆H₁₀(O)], the Oxidation of Alcohols and Aldehydes, and the Dioxygenation of Aryl Olefins and Acetylenes. *J. Am. Chem. Soc.* **1990**, *112*, 8214-8215. (c) Jeet Singh Kalra, S.; Punniyamurthy, T.; Iqbal, J. Cobalt Catalyzed Oxidation of Secondary Alcohols with Dioxygen in the Presence of 2-Methylpropanal. *Tetrahedron Lett.* **1994**, *35*, 4847-4850. (d) Crandell, D. W.; Ghosh, S.; Berlinguette, C. P.; Baik, M. H. How a [Co(IV) a Bond and a Half O](2+) Fragment

Oxidizes Water: Involvement of a Biradicaloid [Co(Ii)-(O)](2+) Species in Forming the O–O Bond. *ChemSusChem* **2015**, *8*, 844-852. (e) Andris, E.; Navrátil, R.; Jašík, J.; Srnec, M.; Rodríguez, M.; Costas, M.; Roithová, J. M–O Bonding Beyond the Oxo Wall: Spectroscopy and Reactivity of Cobalt(Iii)-Oxyl and Cobalt(Iii)-Oxo Complexes. *Angew. Chem. Int. Ed.* **2019**, *58*, 9619-9624.

56. (a) Campo Dall'Orto, V.; Carballo, R.; Hurst, J. A.; Rezzano, I. Uv–Vis Spectroscopic Study of Co(Ii)/Co(Iii) Oxidation in Poly[M-Protoporphyrins] Films and Their Interaction with Axial Ligands. *Spectrochim. Acta A* **2005**, *61*, 2089-2093. (b) Mu, X. H.; Kadish, K. M. Oxidative Electrochemistry of Cobalt Tetraphenylporphyrin under a Co Atmosphere. Interaction between Carbon Monoxide and Electrogenenerated [(Tpp)Co]⁺ in Nonbonding Media. *Inorg. Chem.* **1989**, *28*, 3743-3747.

57. Lee, C.; Yang, W.; Parr, R. G. Development of the Colle-Salvetti Correlation-Energy Formula into a Functional of the Electron Density. *Phys. Rev. B* **1988**, *37*, 785-789.

58. Padamati, S. K.; Angelone, D.; Draksharapu, A.; Primi, G.; Martin, D. J.; Tromp, M.; Swart, M.; Browne, W. R. Transient Formation and Reactivity of a High-Valent Nickel(Iv) Oxido Complex. *J. Am. Chem. Soc.* **2017**, *139*, 8718-8724.

59. (a) Savarese, M.; Brémond, É.; Ciofini, I.; Adamo, C. Electron Spin Densities and Density Functional Approximations: Open-Shell Polycyclic Aromatic Hydrocarbons as Case Study. *J. Chem. Theory Comput.* **2020**, *16*, 3567-3577. (b) Giner, E.; Angeli, C. Spin Density and Orbital Optimization in Open Shell Systems: A Rational and Computationally Efficient Proposal. *J. Chem. Phys.* **2016**, *144*, 104104.

60. Szmant, H. H. *Organic Building Blocks of the Chemical Industry*; John Wiley & Sons, New York, 1989.

61. (a) Collman, J. P.; Lee, V. J.; Zhang, X.; Ibers, J. A.; Brauman, J. I. Enantioselective Epoxidation of Unfunctionalized Olefins Catalyzed by Threitol-Strapped Manganese Porphyrins. *J. Am. Chem. Soc.* **1993**, *115*, 3834–3835. (b) Yoshinori, N.; Nobuo, I.; Fumito, T.; Kazuhiro, M. Asymmetric Epoxidation of Simple Olefins by Chiral Bitetralin-Linked “Twin-Coronet” Porphyrin Catalysts. *Bull. Chem. Soc. Jpn.* **1993**, *66*, 158-166. (c) Rose, E.; Ren, Q.-Z.; Andrioletti, B. A Unique Binaphthyl Strapped Iron–Porphyrin Catalyst for the Enantioselective Epoxidation of Terminal Olefins. *Chem. Eur. J.* **2004**, *10*, 224-230.
62. (a) Palucki, M.; Pospisil, P. J.; Zhang, W.; Jacobsen, E. N. Highly Enantioselective, Low-Temperature Epoxidation of Styrene. *J. Am. Chem. Soc.* **1994**, *116*, 9333-9334. (b) Matsumoto, K.; Sawada, Y.; Saito, B.; Sakai, K.; Katsuki, T. Construction of Pseudo-Heterochiral and Homochiral Di-M-Oxotitanium(Schiff Base) Dimers and Enantioselective Epoxidation Using Aqueous Hydrogen Peroxide. *Angew. Chem. Int. Ed.* **2005**, *44*, 4935-4939.
63. Goedel, D.; Shu, L.; Yuan, Y.; Wong, O. A.; Wang, B.; Shi, Y. Effective Asymmetric Epoxidation of Styrenes by Chiral Dioxirane. *J. Org. Chem.* **2006**, *71*, 1715-1717.
64. Hu, Y.; Lang, K.; Tao, J.; Marshall, M. K.; Cheng, Q.; Cui, X.; Wojtas, L.; Zhang, X. P. Next-Generation D2-Symmetric Chiral Porphyrins for Cobalt(Ii)-Based Metalloradical Catalysis: Catalyst Engineering by Distal Bridging. *Angew. Chem. Int. Ed.* **2019**, *58*, 2670-2674.

65. von Keutz, T.; Cantillo, D.; Kappe, C. O. Organomagnesium Based Flash Chemistry: Continuous Flow Generation and Utilization of Halomethylmagnesium Intermediates. *Org. Lett.* **2020**, *22*, 7537-7541.
66. Chandra, B.; K. M, H.; Pattanayak, S.; Gupta, S. S. Oxoiron(V) Mediated Selective Electrochemical Oxygenation of Unactivated C–H and C=C Bonds Using Water as the Oxygen Source. *Chem. Sci.* **2020**, *11*, 11877-11885.
67. Liu, W.; Li, W.; Spannenberg, A.; Junge, K.; Beller, M. Iron-Catalysed Regioselective Hydrogenation of Terminal Epoxides to Alcohols under Mild Conditions. *Nat. Catal.* **2019**, *2*, 523-528.
68. van Schie, M. M. C. H.; Paul, C. E.; Arends, I. W. C. E.; Hollmann, F. Photoenzymatic Epoxidation of Styrenes. *Chem. Commun.* **2019**, *55*, 1790-1792.
69. Tian, Y.; Jürgens, E.; Kunz, D. Regio- and Chemoselective Rearrangement of Terminal Epoxides into Methyl Alkyl and Aryl Ketones. *Chem. Commun.* **2018**, *54*, 11340-11343.
70. Ji, Y.; Yang, J.; Wu, L.; Yu, L.; Tang, X. Photochemical Regulation of Gene Expression Using Caged Sirnas with Single Terminal Vitamin E Modification. *Angew. Chem. Int. Ed.* **2016**, *55*, 2152-2156.
71. Ma, X.; Pan, S.; Wang, H.; Chen, W. Rhodium-Catalyzed Transannulation of N-Sulfonyl-1,2,3-Triazoles and Epoxides: Regioselective Synthesis of Substituted 3,4-Dihydro-2h-1,4-Oxazines. *Org. Lett.* **2014**, *16*, 4554-4557.
72. Shing, K.-P.; Cao, B.; Liu, Y.; Lee, H. K.; Li, M.-D.; Phillips, D. L.; Chang, X.-Y.; Che, C.-M. Arylruthenium(III) Porphyrin-Catalyzed C–H Oxidation and Epoxidation at

Room Temperature and [Ru^v(Por)(O)(Ph)] Intermediate by Spectroscopic Analysis and Density Functional Theory Calculations. *J. Am. Chem. Soc.* **2018**, *140*, 7032-7042.

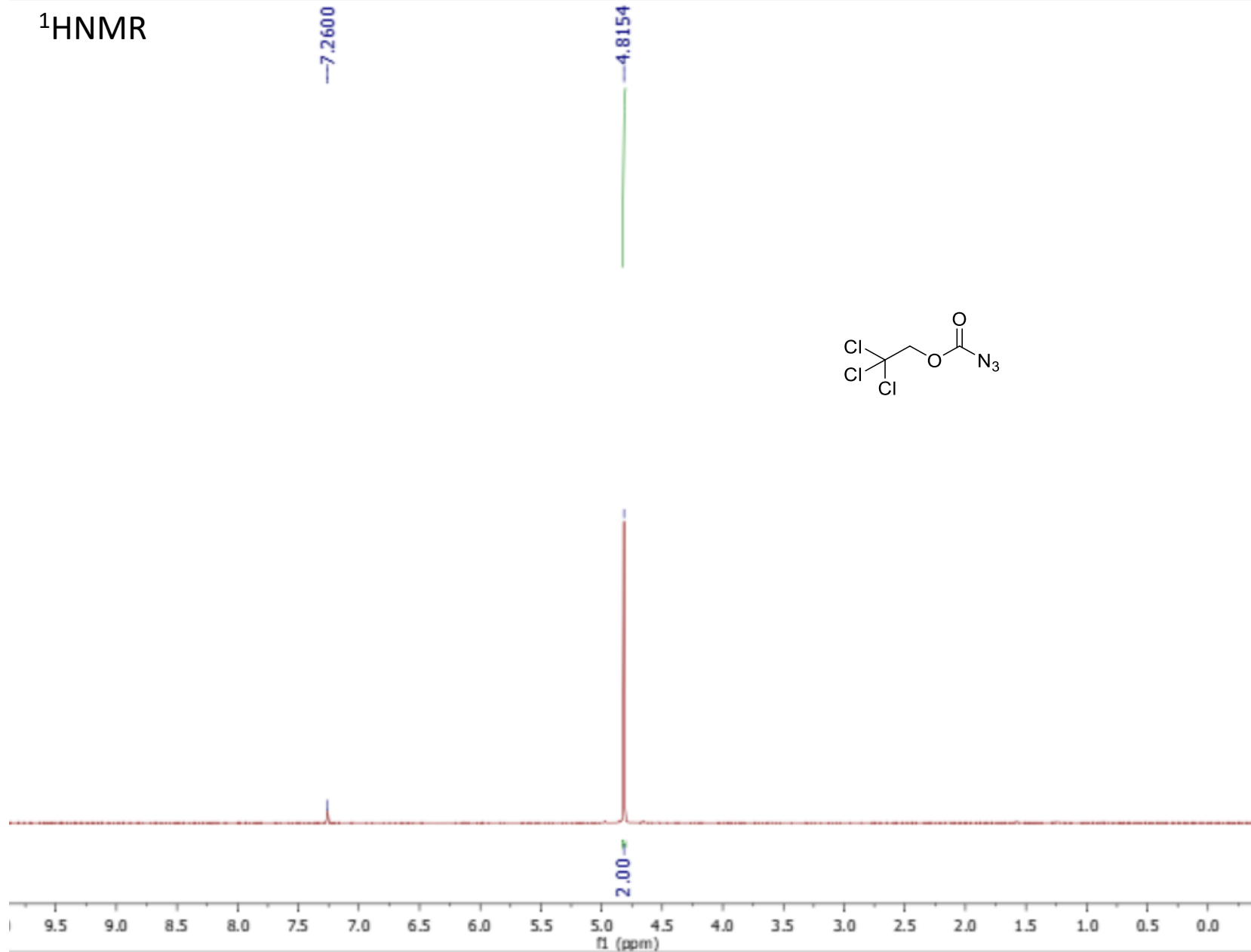
6. SPECTRAL DATA

6.1 Spectral Data for Chapter 2

Enantioselective Radical Aziridination of Alkenes with Carbonyl Azides

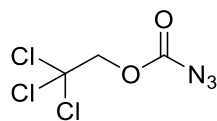
2,2,2-Trichloroethyl carbonazidate (Trocn₃)

¹HNMR



2,2,2-Trichloroethyl carbonazidate (TrocN₃)

¹³CNMR



—156.6921

—93.9469

77.4148

77.1604

76.9061

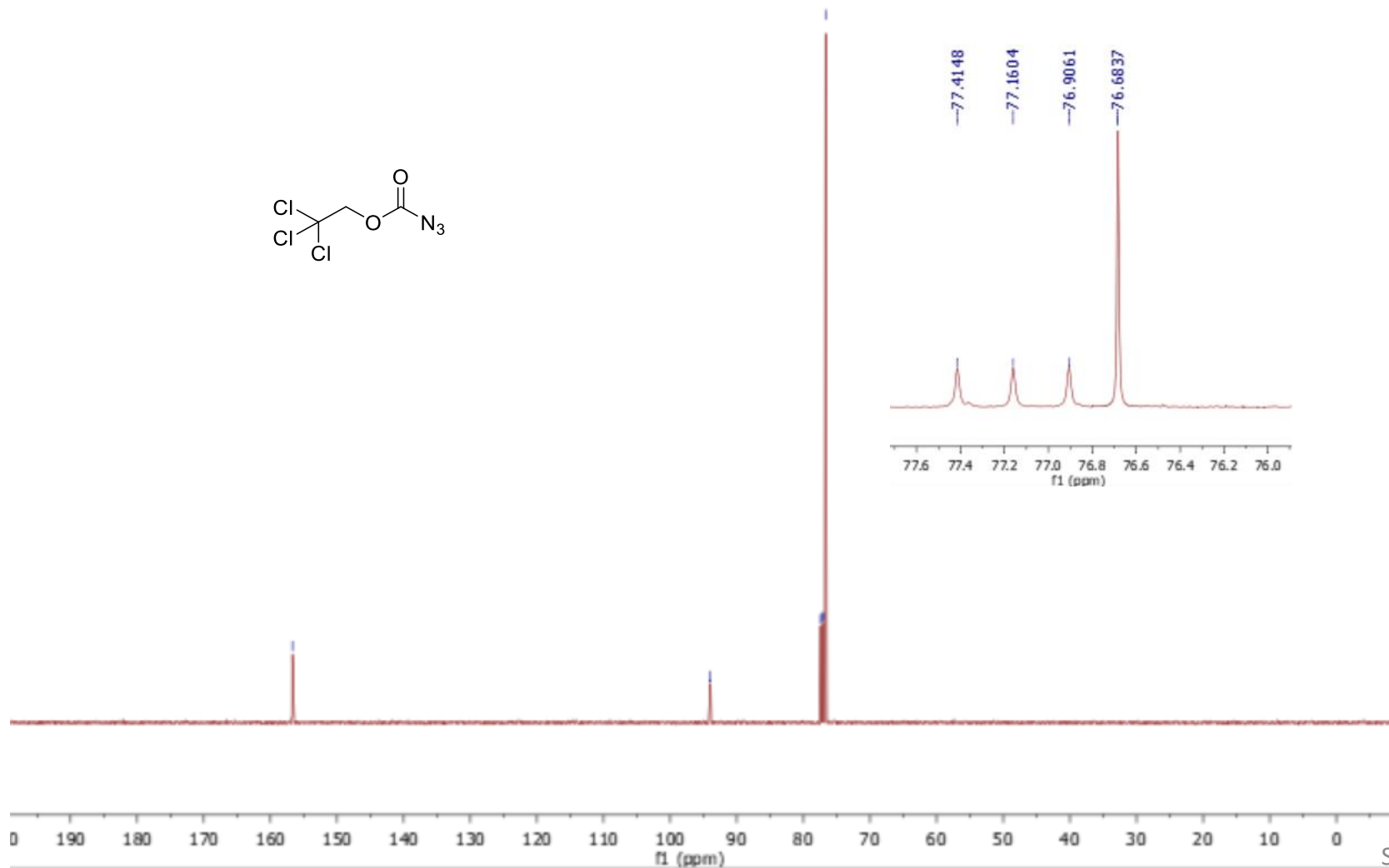
76.6837

—77.4148

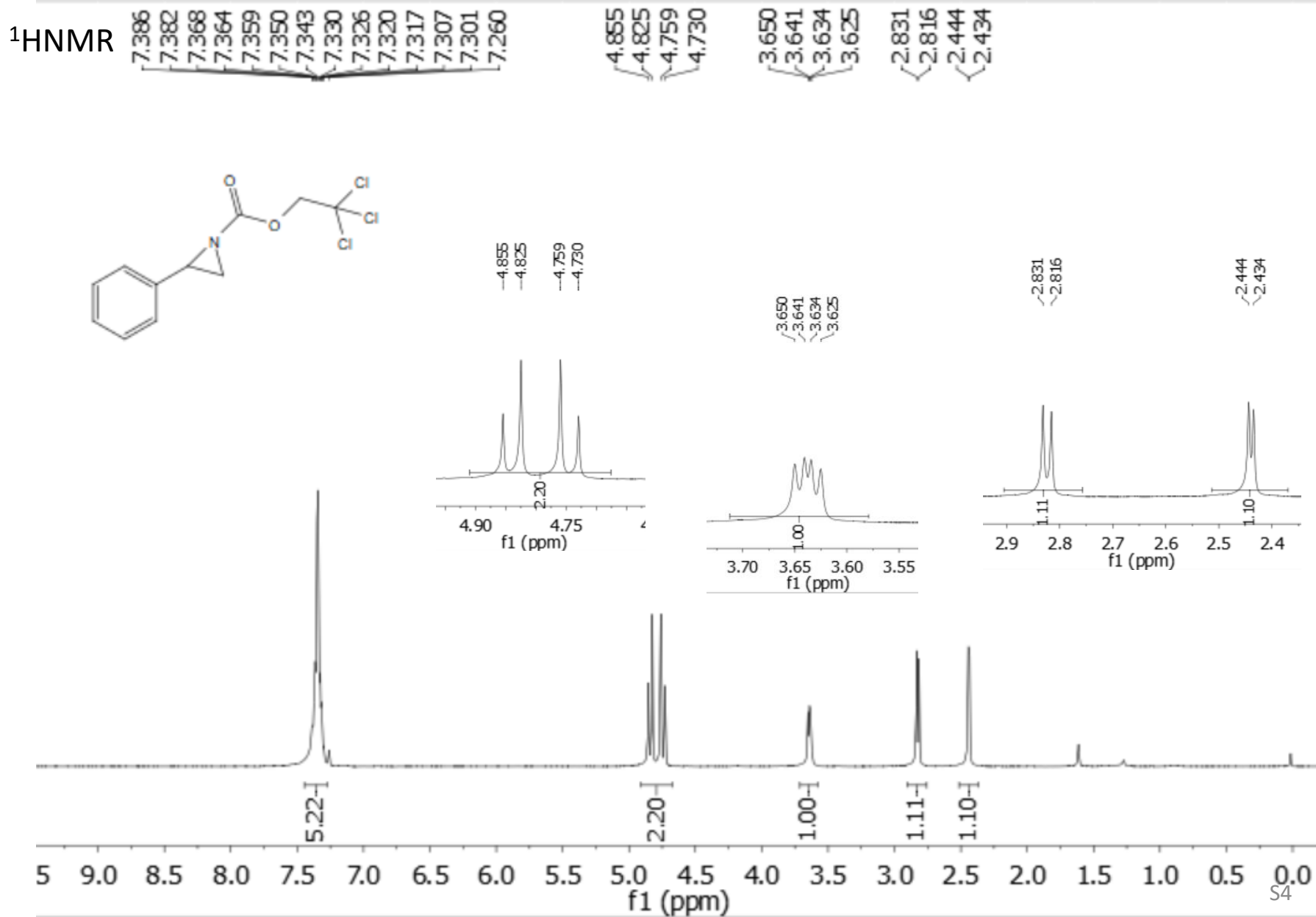
—77.1604

—76.9061

—76.6837



2,2,2-Trichloroethyl 2-phenylaziridine-1-carboxylate (3a)



2,2,2-Trichloroethyl 2-phenylaziridine-1-carboxylate (3a)

^{13}C NMR

-161.414

136.240

128.583

128.118

126.271

-94.905

77.339

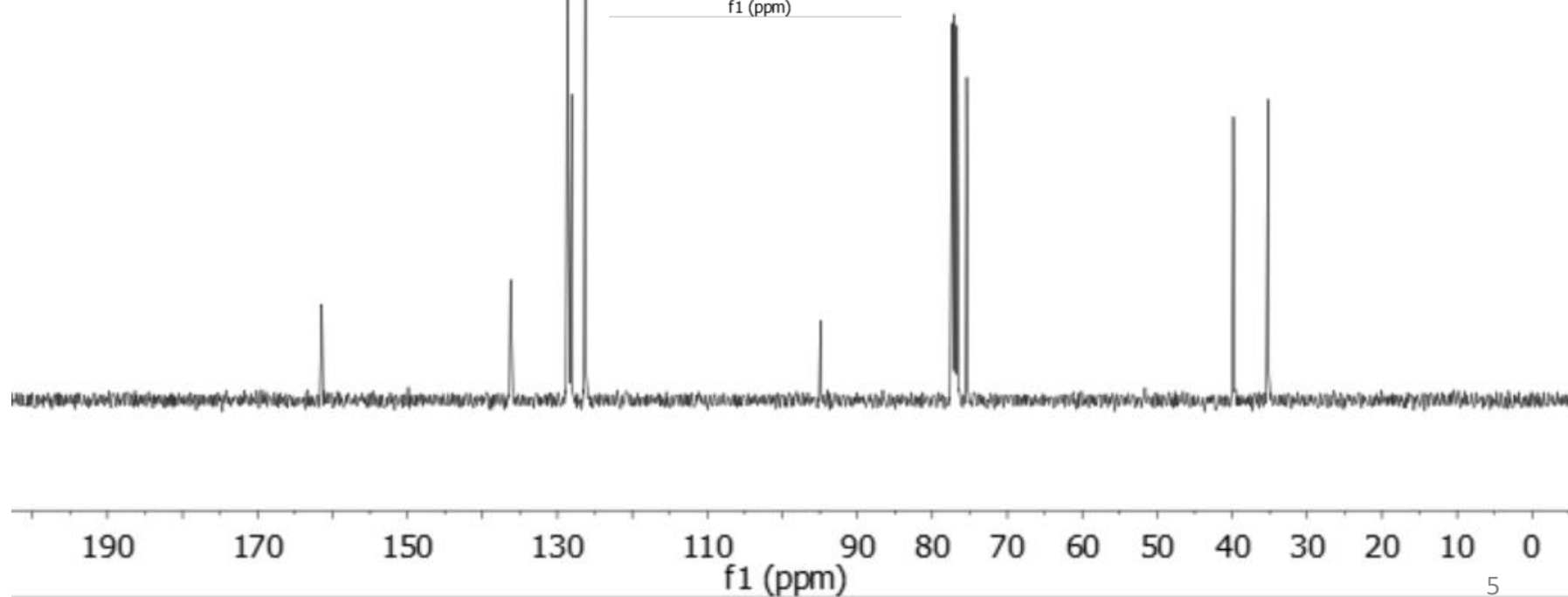
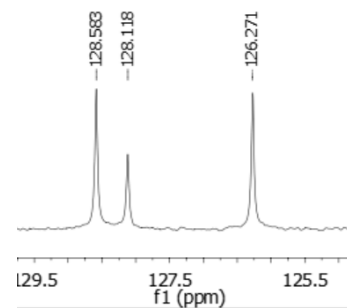
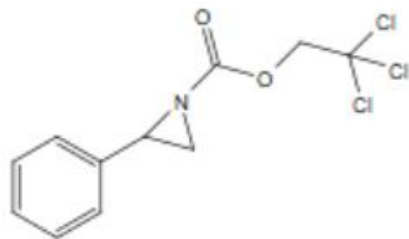
77.021

76.703

75.409

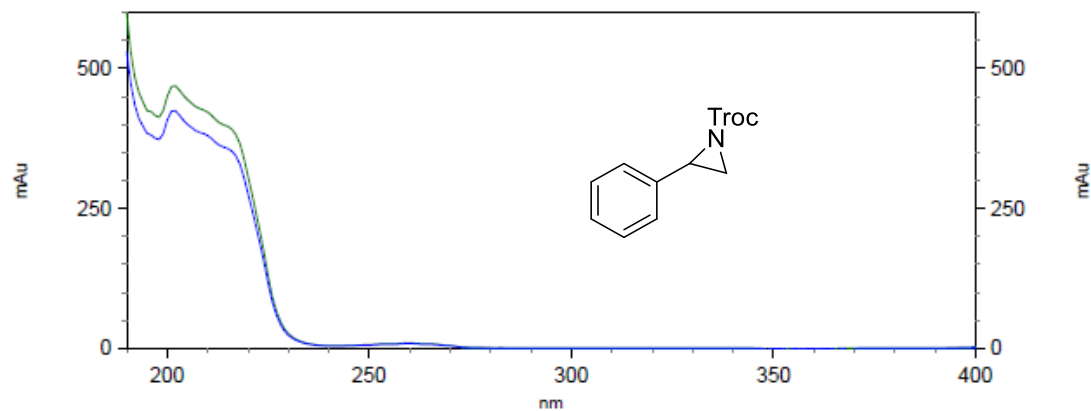
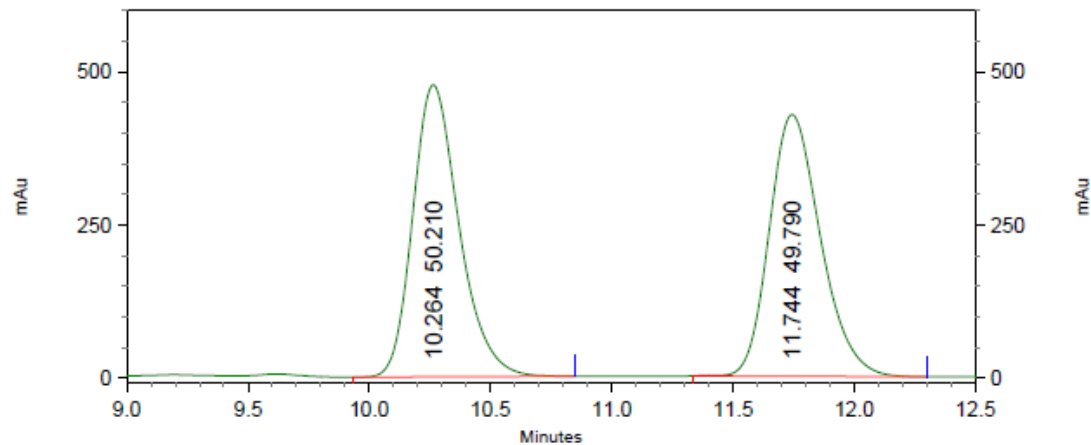
-39.849

-35.204



2,2,2-Trichloroethyl 2-phenylaziridine-1-carboxylate (3a)

HPLC trace
racemic



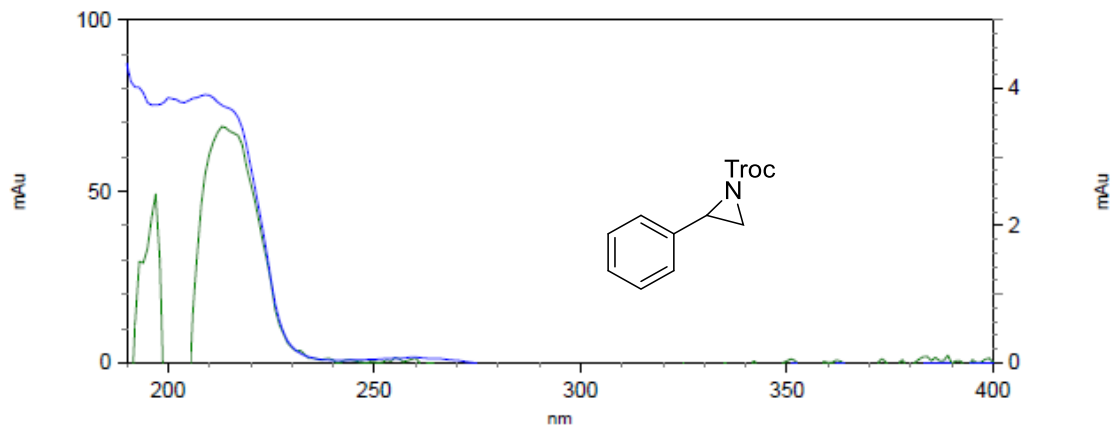
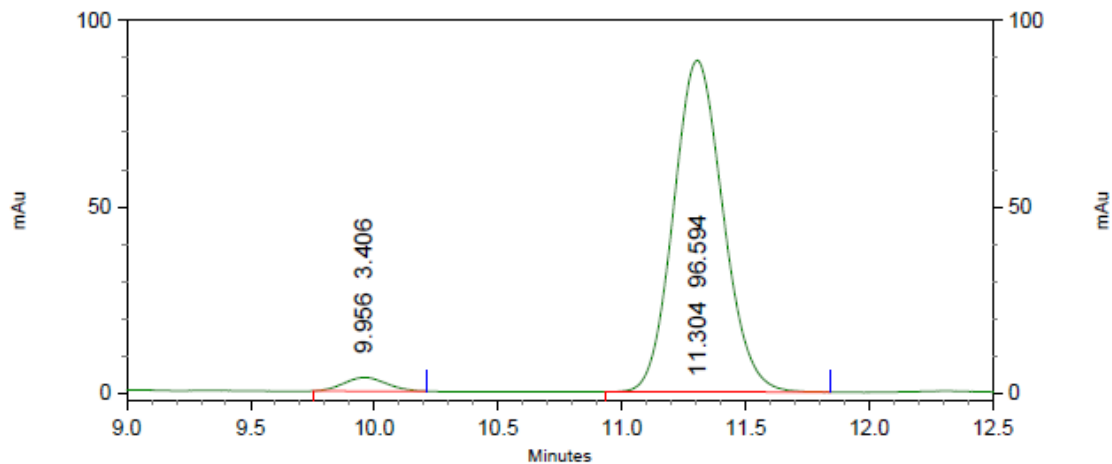
4: 222 nm, 4
nm Results

Pk #	Retention Time	Area Percent
1	10.264	50.210
2	11.744	49.790

Totals		100.000
--------	--	---------

2,2,2-Trichloroethyl 2-phenylaziridine-1-carboxylate (3a)

HPLC trace



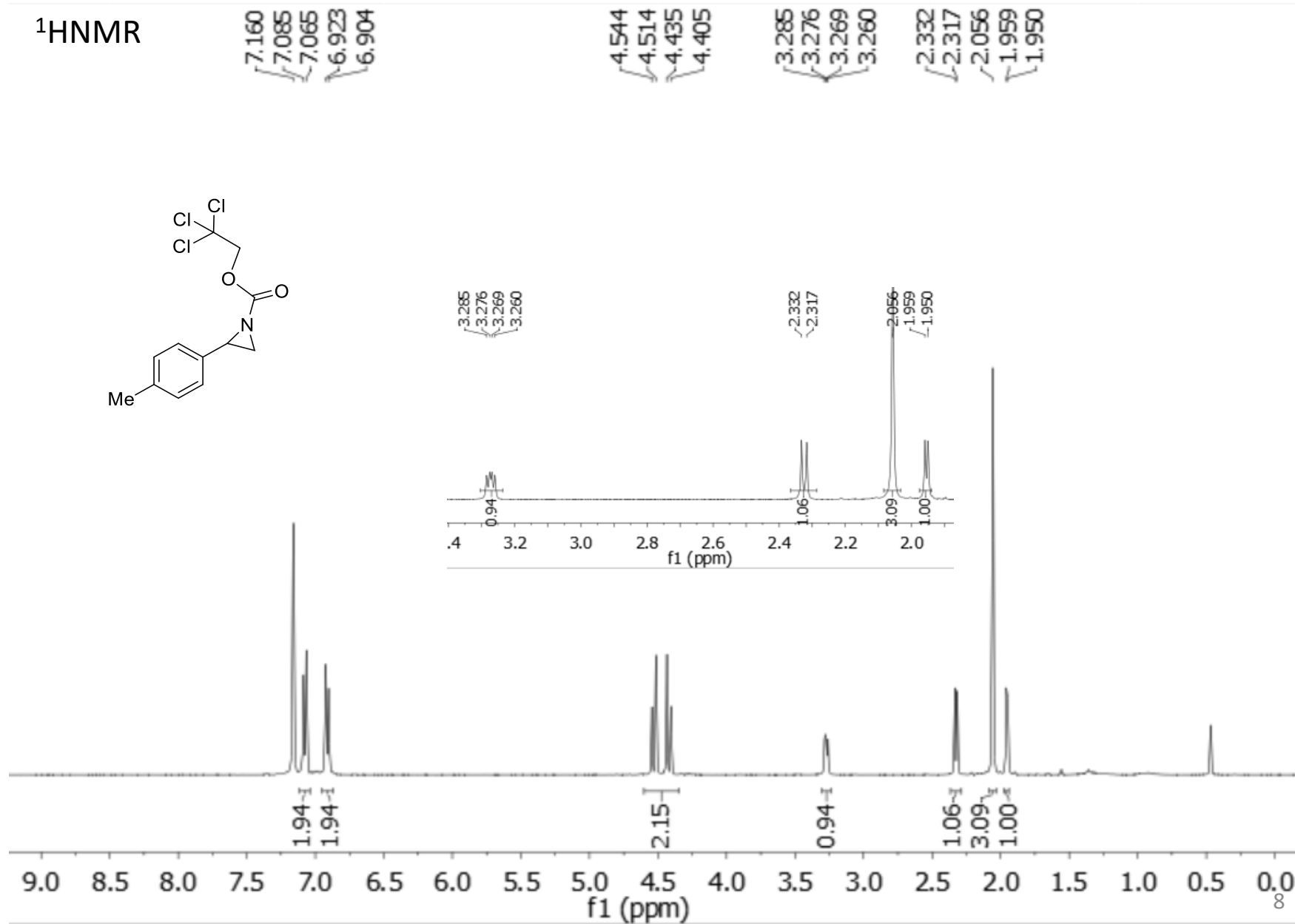
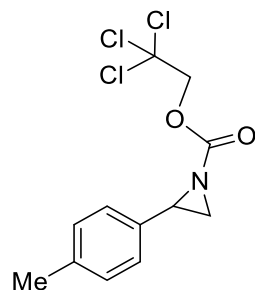
4: 222 nm, 4
nm Results

Pk #	Retention Time	Area Percent
1	9.956	3.406
2	11.304	96.594

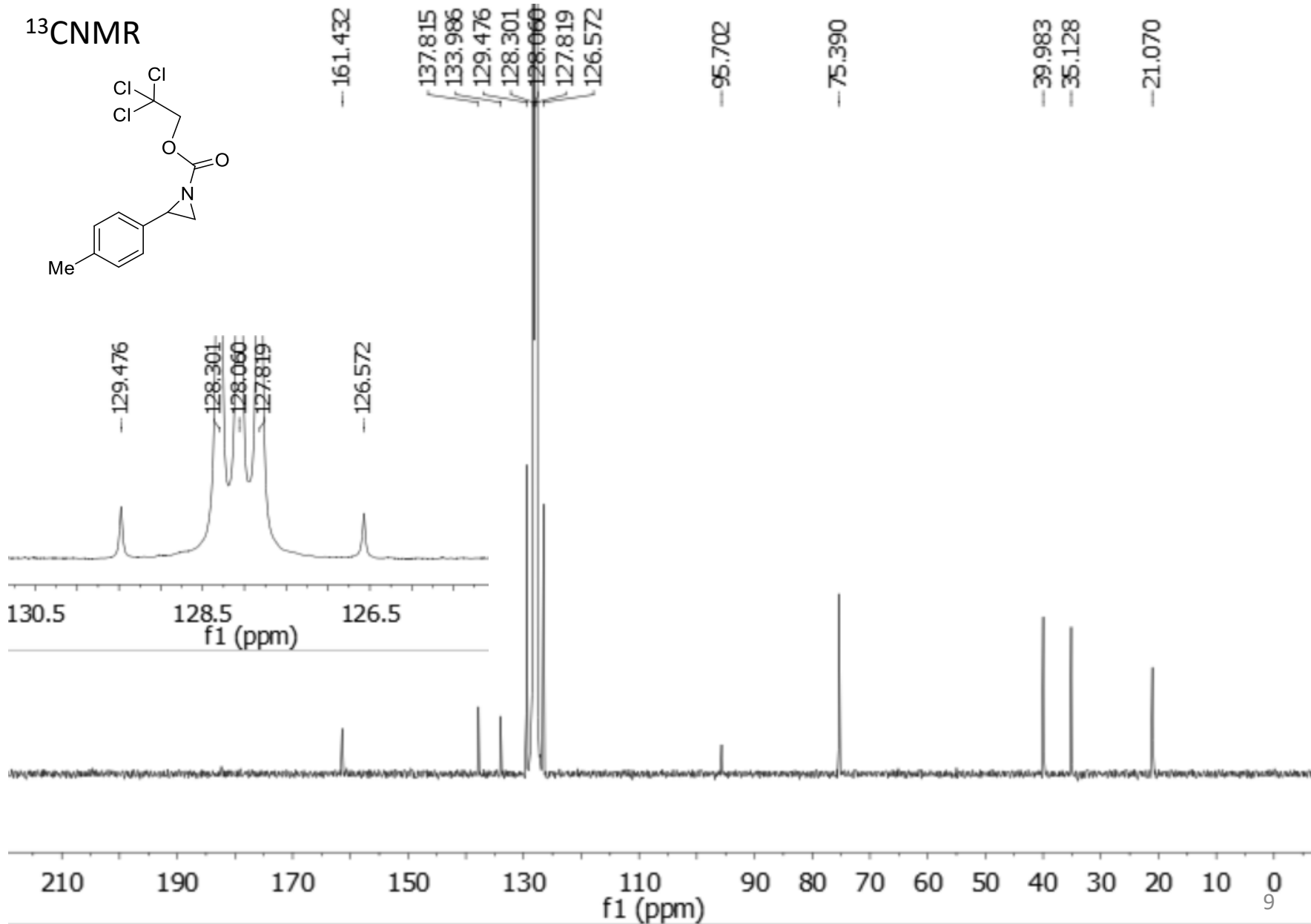
Totals		100.000
--------	--	---------

2,2,2-Trichloroethyl 2-*p*-tolylaziridine-1-carboxylate (3b)

¹H NMR

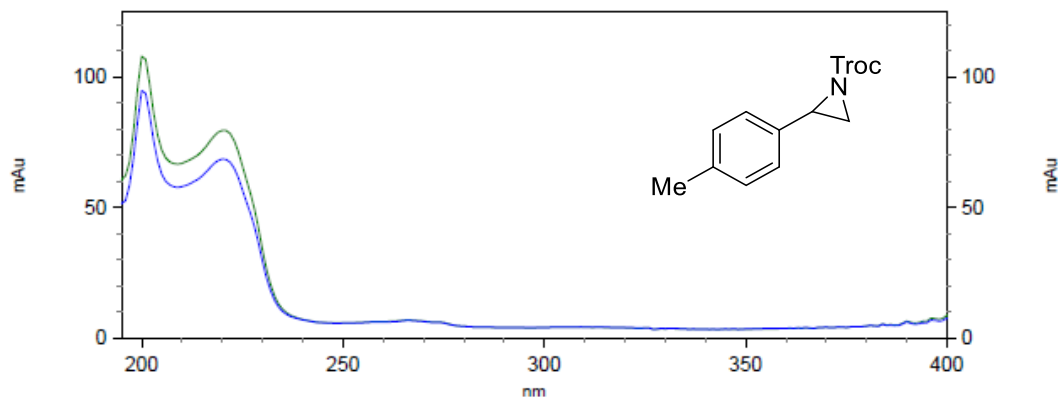
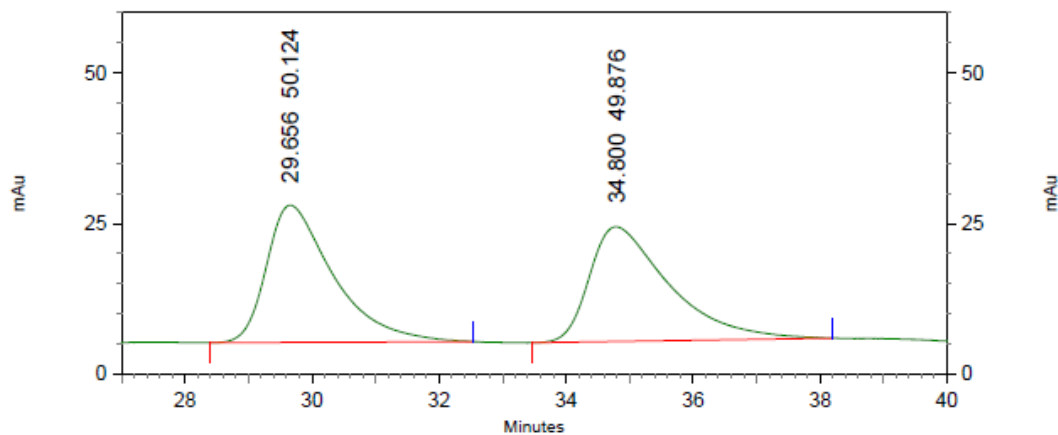


2,2,2-Trichloroethyl 2-*p*-tolylaziridine-1-carboxylate (3b)



2,2,2-Trichloroethyl 2-*p*-tolylaziridine-1-carboxylate (3b)

HPLC trace
racemic



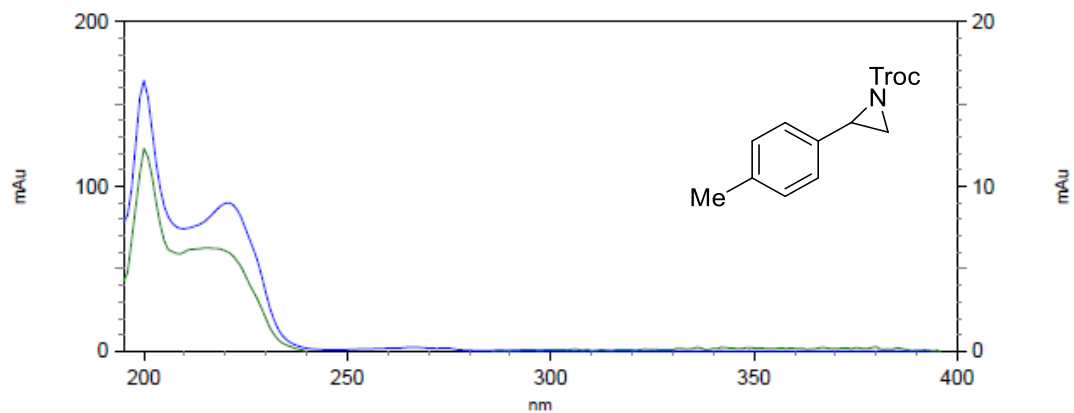
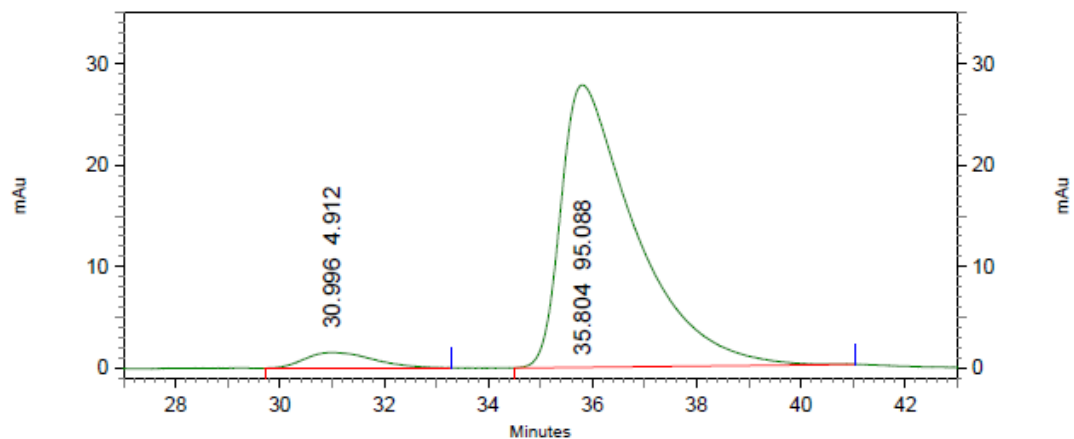
2: 231 nm, 4
nm Results

Pk #	Retention Time	Area Percent
1	29.656	50.124
2	34.800	49.876

Totals		100.000
--------	--	---------

2,2,2-Trichloroethyl 2-*p*-tolylaziridine-1-carboxylate (3b)

HPLC trace

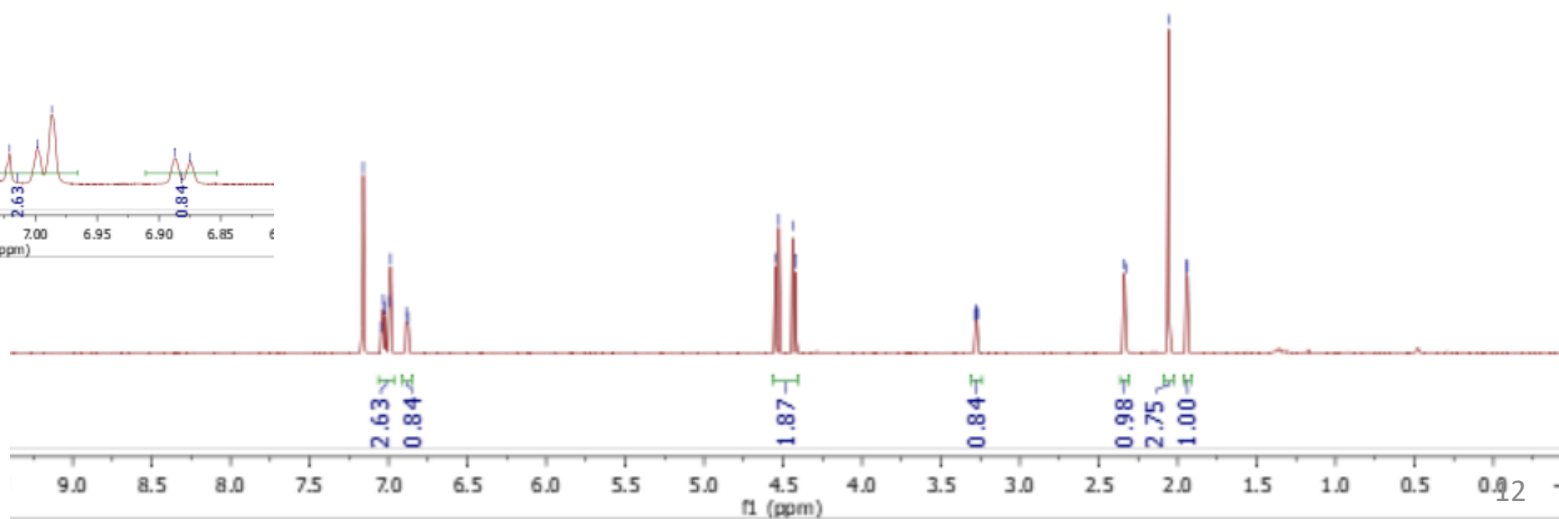
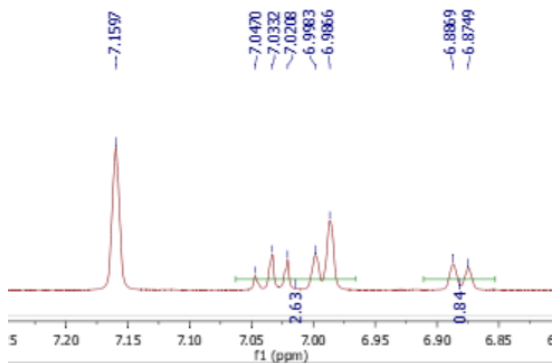
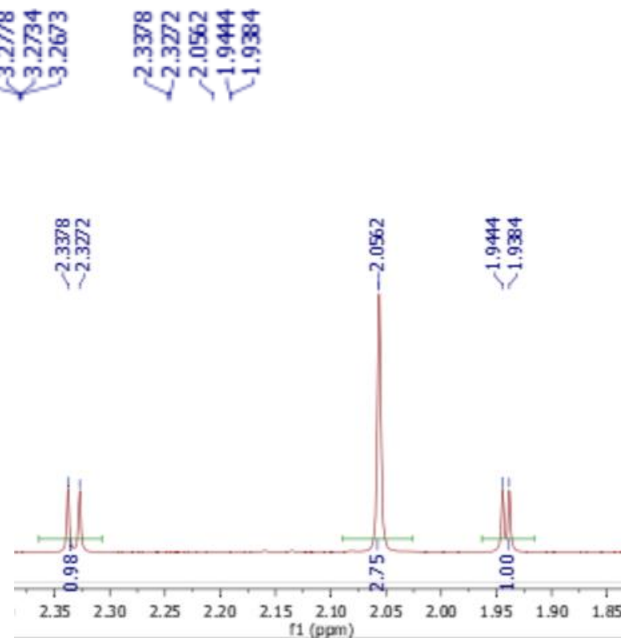
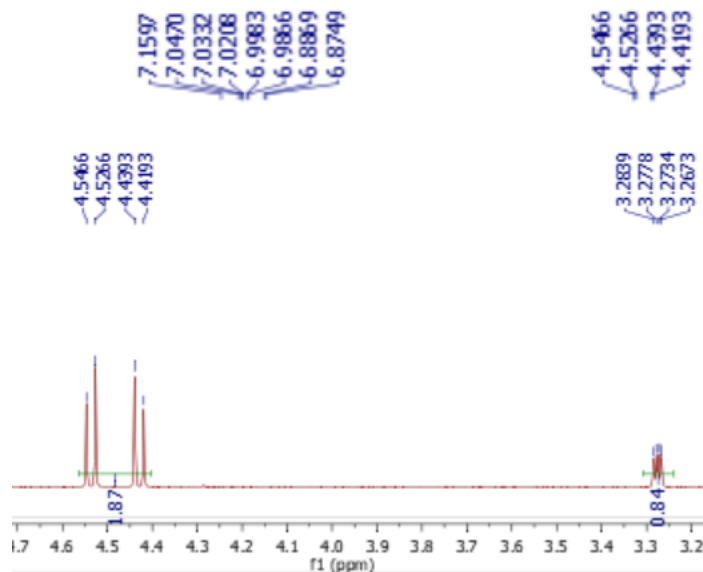
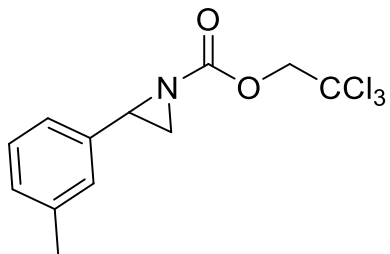


2: 231 nm, 4
nm Results

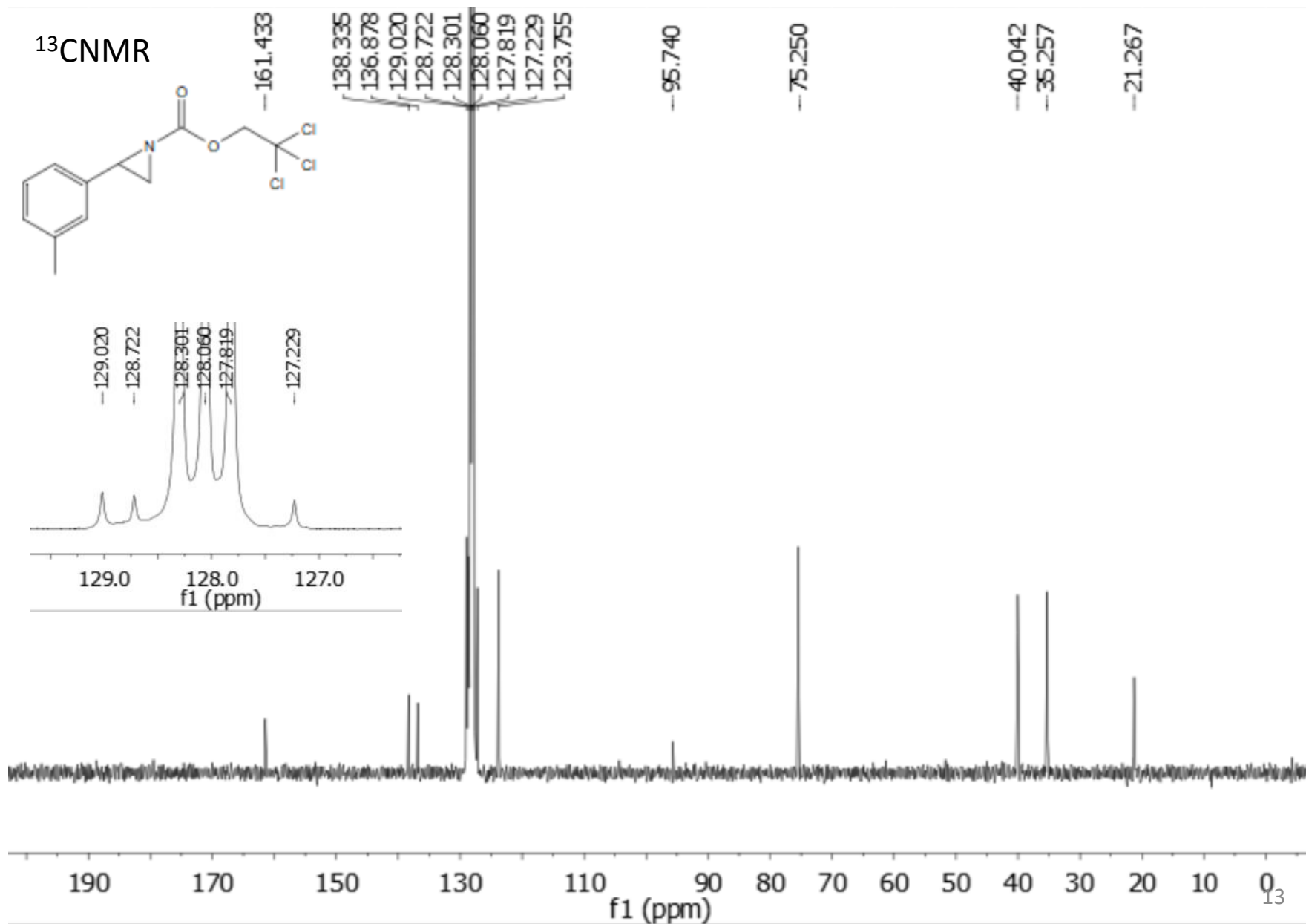
Pk #	Retention Time	Area Percent
1	30.996	4.912
2	35.804	95.088
Totals		100.000

2,2,2-Trichloroethyl 2-*m*-tolylaziridine-1-carboxylate (3c)

$^1\text{H NMR}$

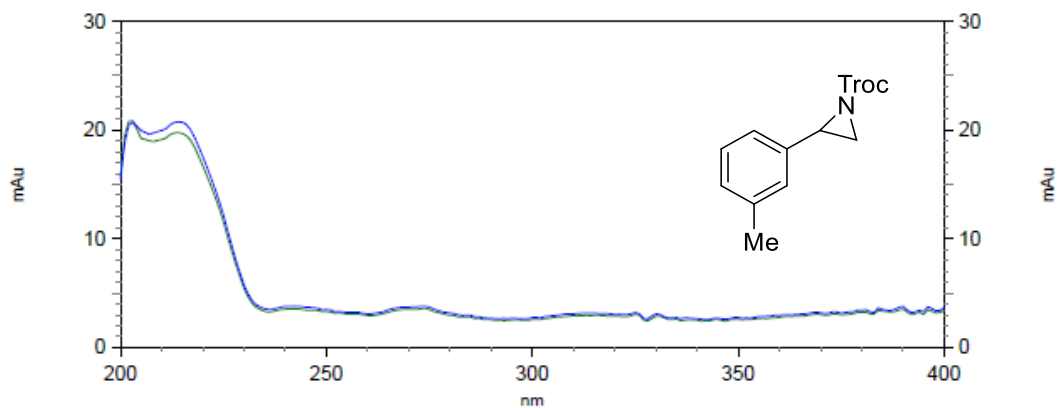
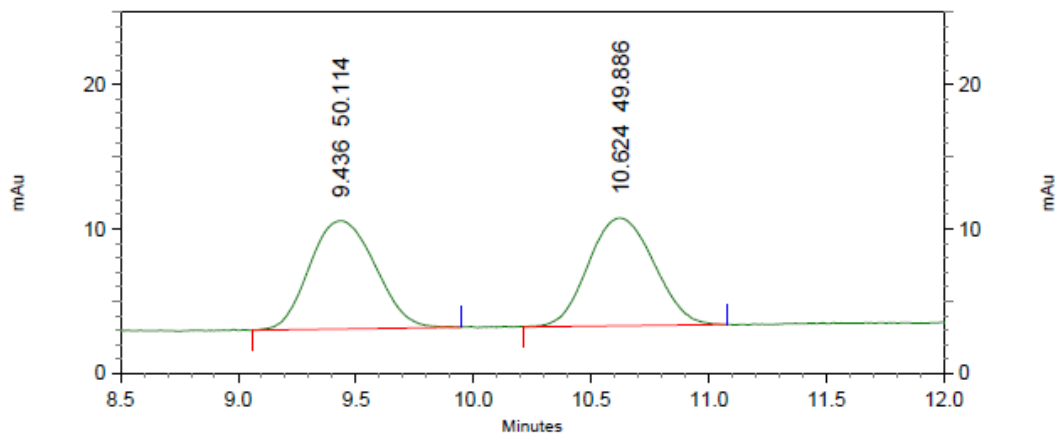


2,2,2-Trichloroethyl 2-*m*-tolylaziridine-1-carboxylate (3c)



2,2,2-Trichloroethyl 2-*m*-tolylaziridine-1-carboxylate (3c)

HPLC trace
racemic



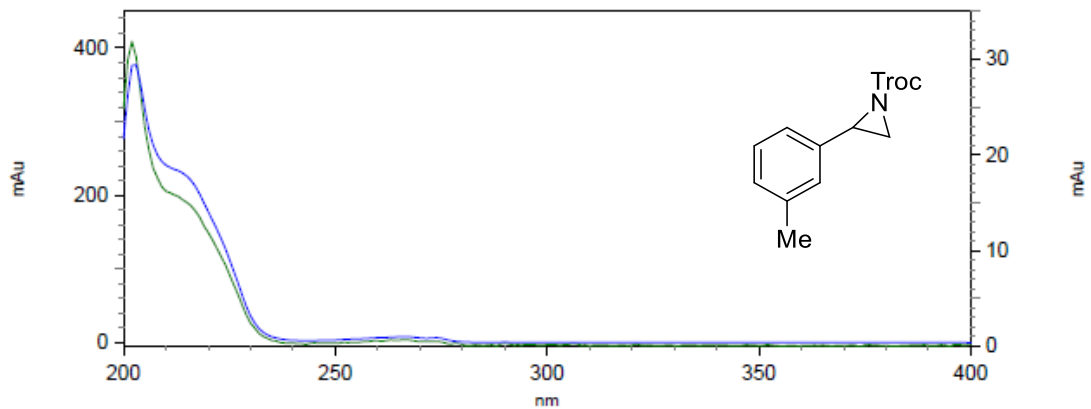
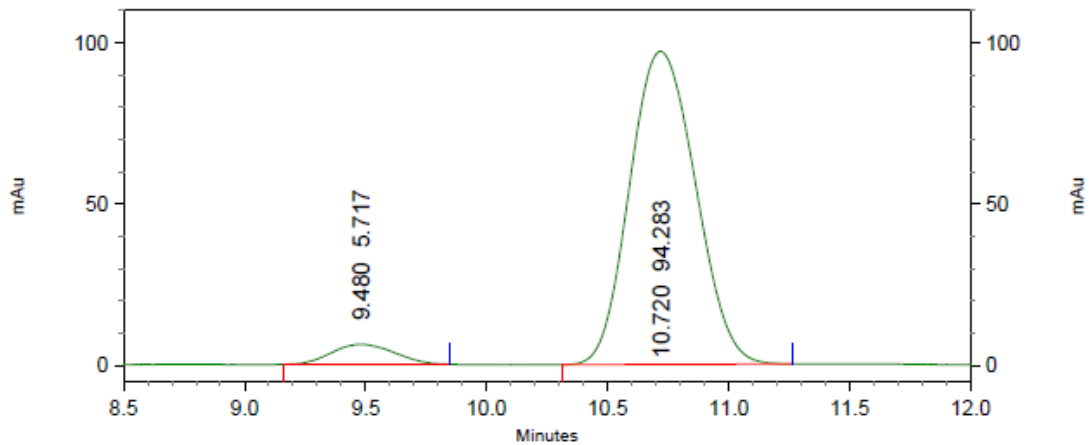
4: 226 nm, 4
nm Results

Pk #	Retention Time	Area Percent
1	9.436	50.114
2	10.624	49.886

Totals	100.000
--------	---------

2,2,2-Trichloroethyl 2-*m*-tolylaziridine-1-carboxylate (3c)

HPLC trace

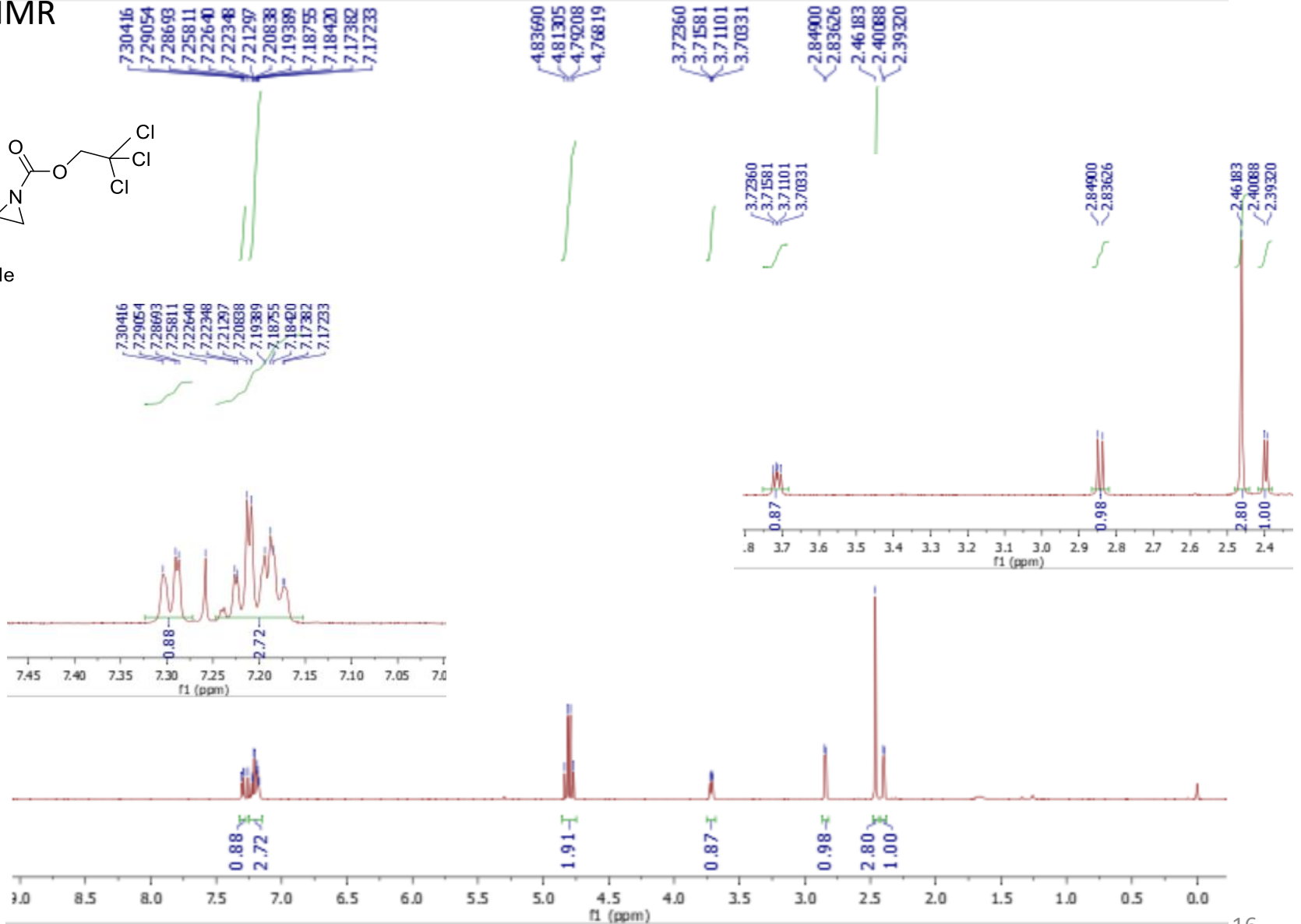
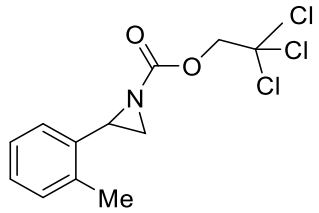


4: 226 nm, 4
nm Results

Pk #	Retention Time	Area Percent
1	9.480	5.717
2	10.720	94.283
Totals		100.000

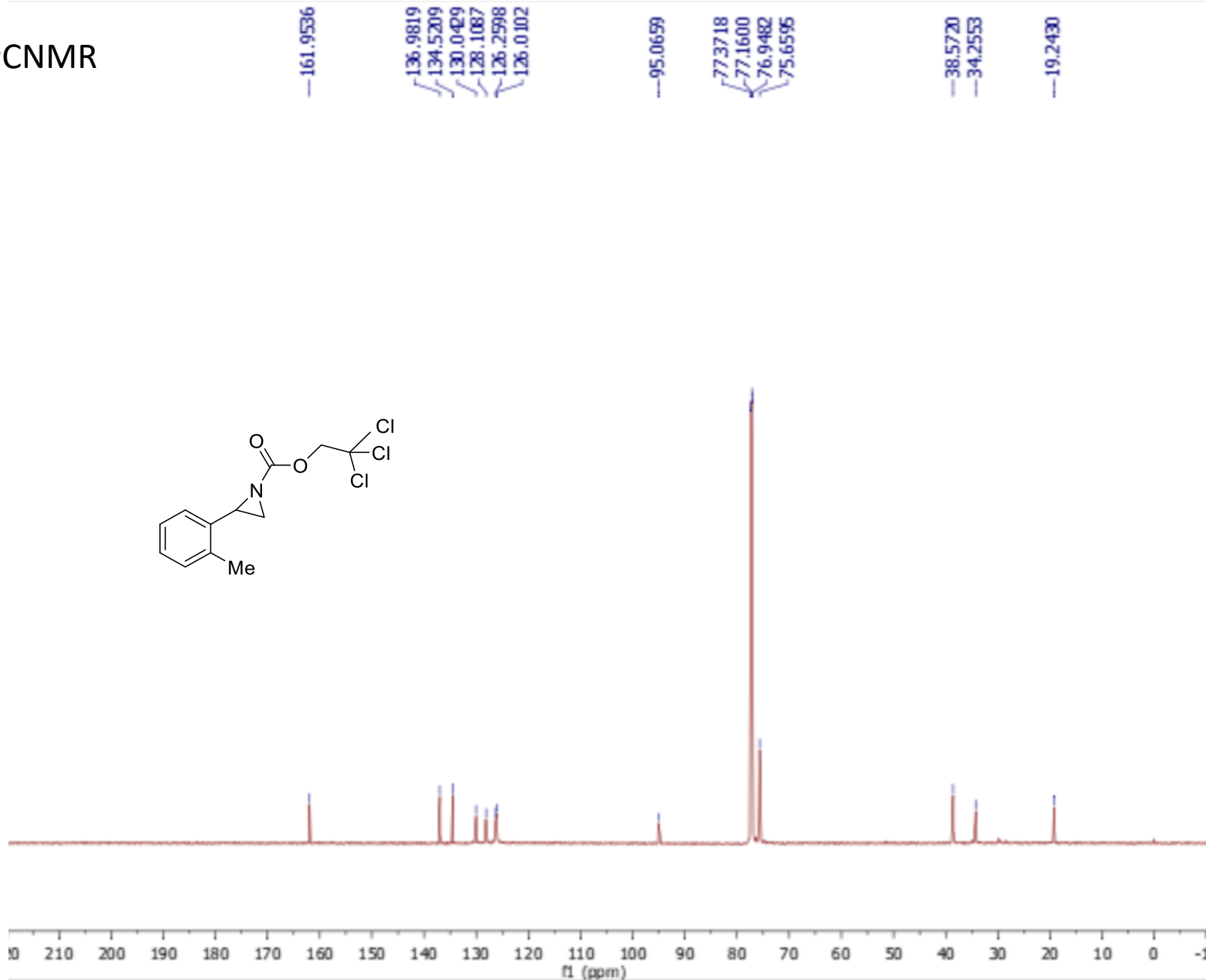
2,2,2-Trichloroethyl 2-*o*-tolylaziridine-1-carboxylate (3d)

¹H NMR



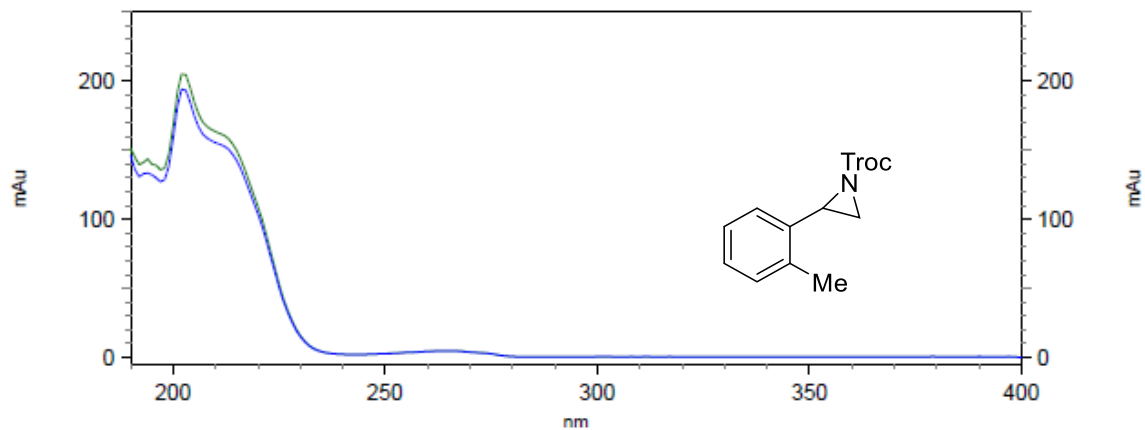
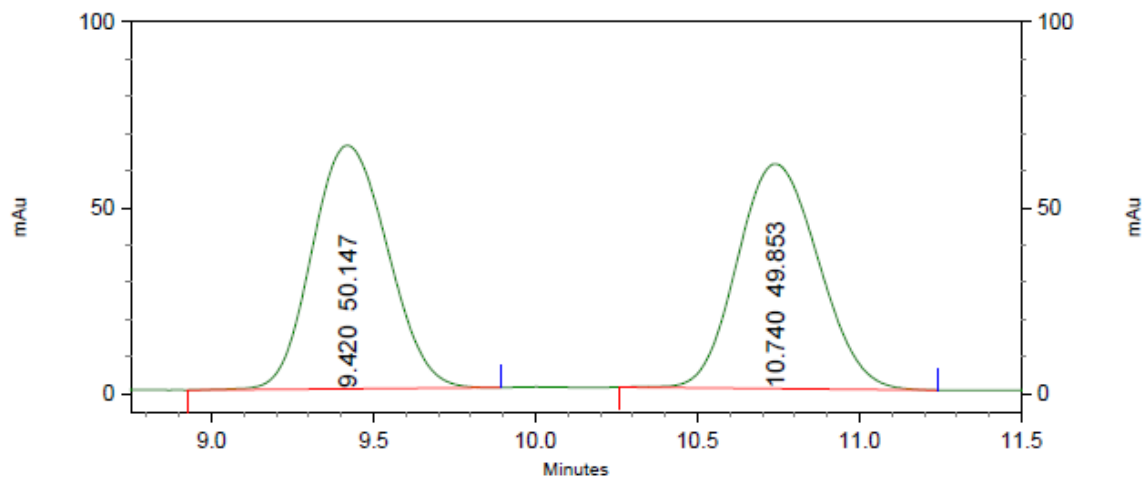
2,2,2-Trichloroethyl 2-*o*-tolylaziridine-1-carboxylate (3d)

^{13}C NMR



2,2,2-Trichloroethyl 2-*o*-tolylaziridine-1-carboxylate (3d)

HPLC trace
racemic



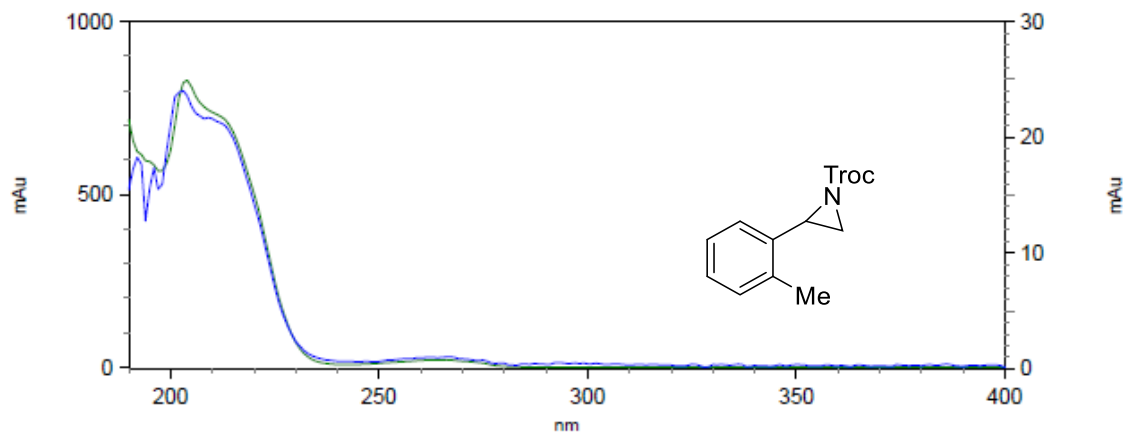
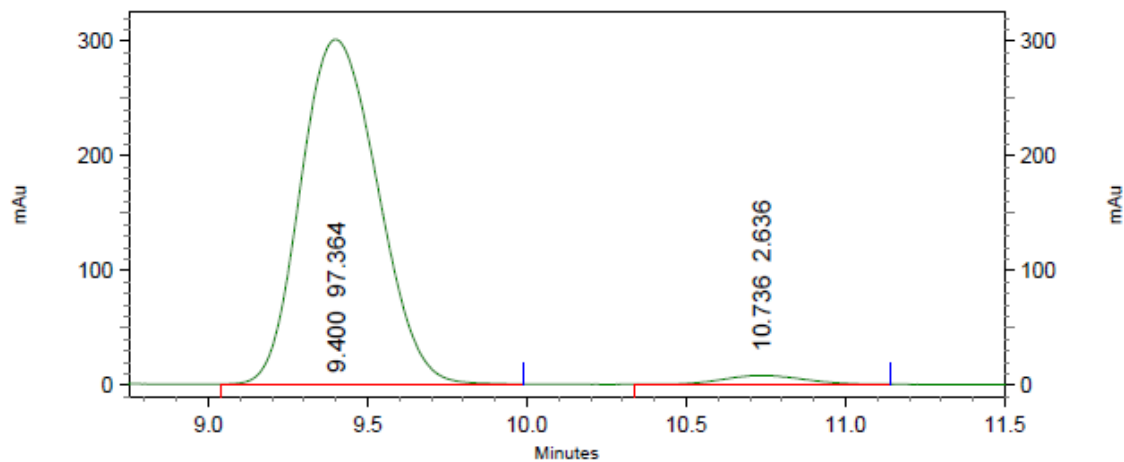
4: 224 nm, 4
nm Results

Pk #	Retention Time	Area Percent
1	9.420	50.147
2	10.740	49.853

Totals	100.000
--------	---------

2,2,2-Trichloroethyl 2-*o*-tolylaziridine-1-carboxylate (3d)

HPLC trace



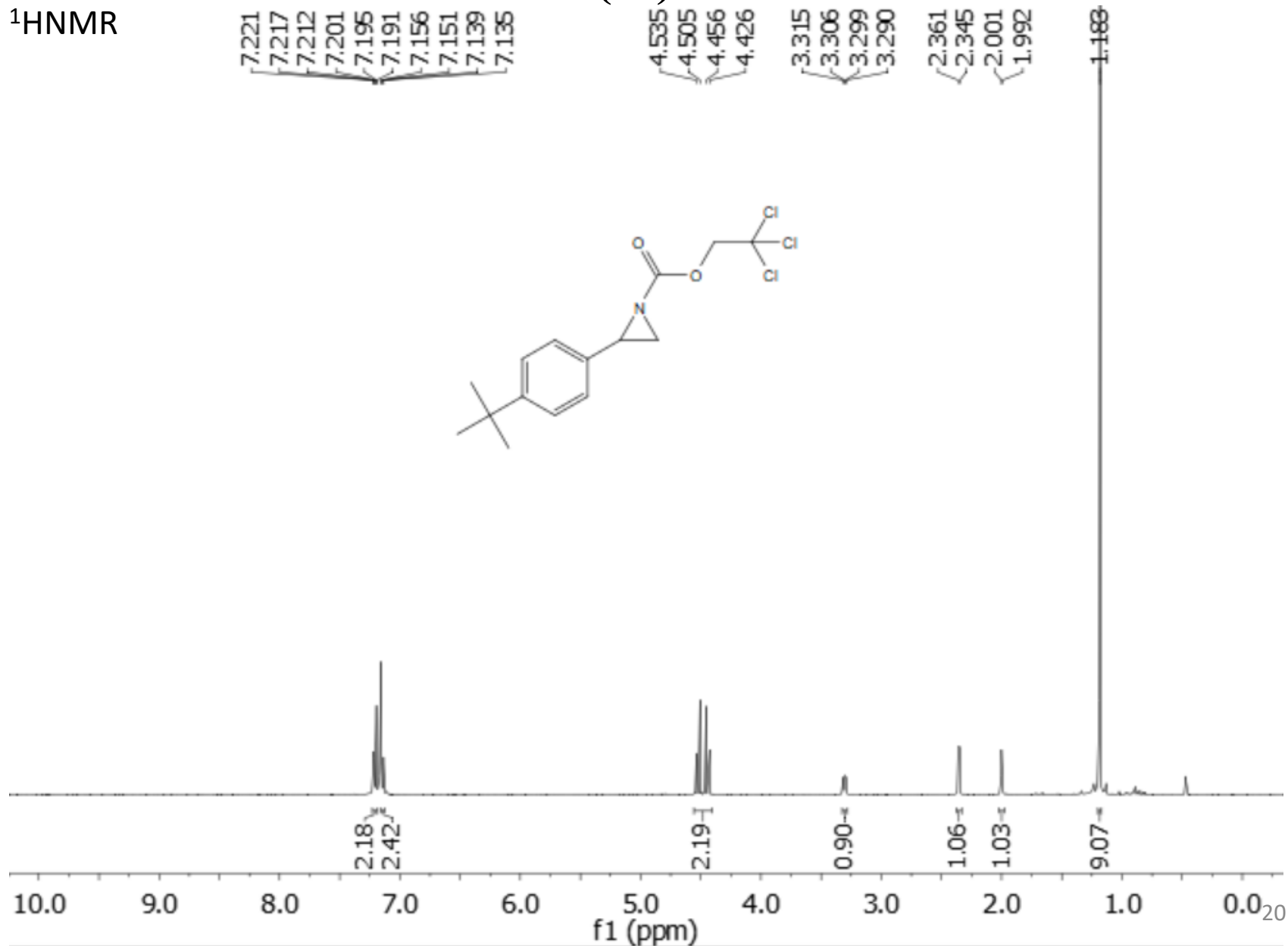
4: 224 nm, 4
nm Results

Pk #	Retention Time	Area Percent
1	9.400	97.364
2	10.736	2.636

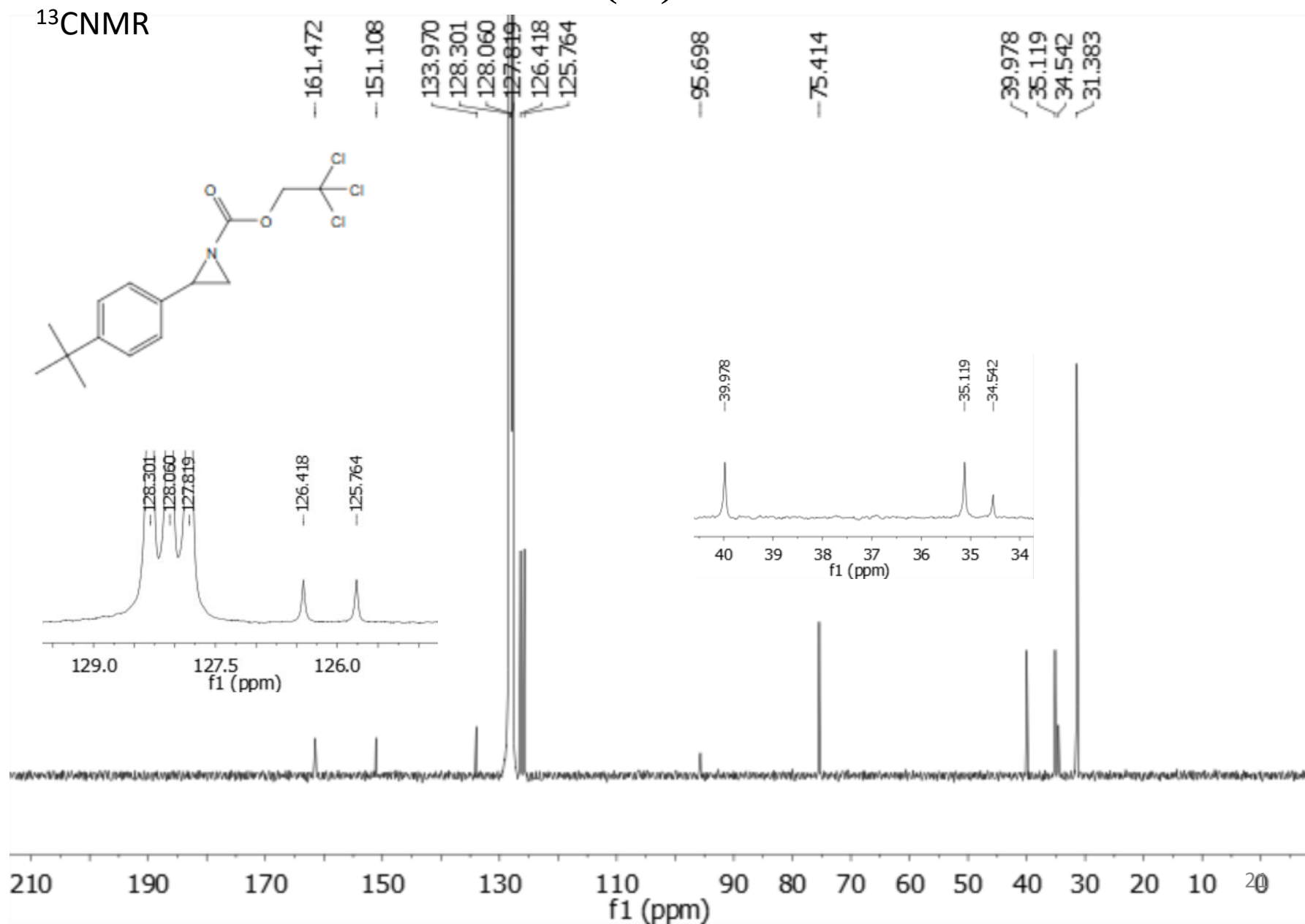
Totals		100.000
--------	--	---------

2,2,2-Trichloroethyl 2-(4-*tert*-butylphenyl)aziridine-1-carboxylate (3e)

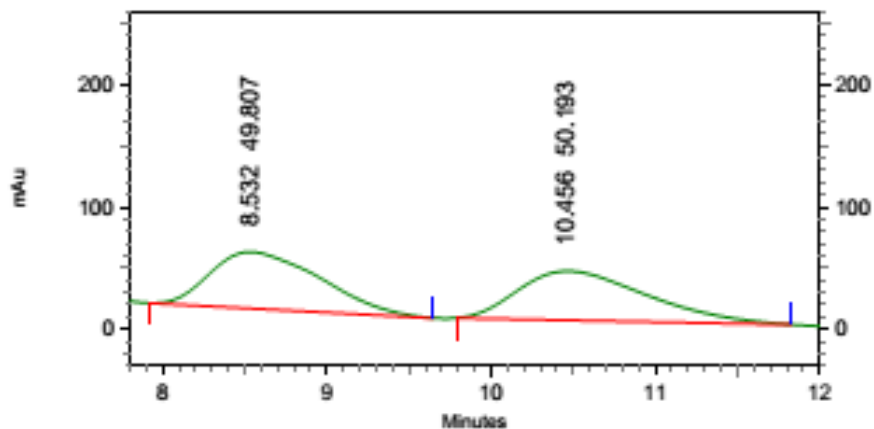
$^1\text{H NMR}$



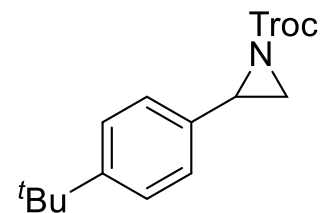
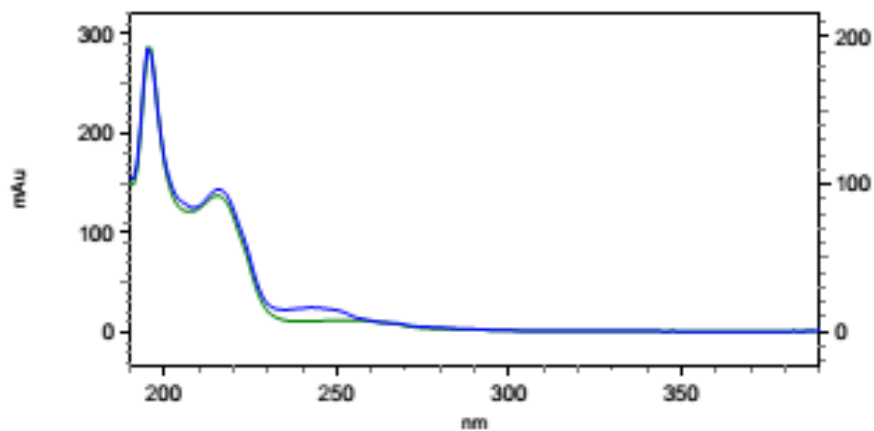
2,2,2-Trichloroethyl 2-(4-*tert*-butylphenyl)aziridine-1-carboxylate (3e)



2,2,2-Trichloroethyl 2-(4-*tert*-butylphenyl)aziridine-1-carboxylate (3e)



HPLC trace
racemic



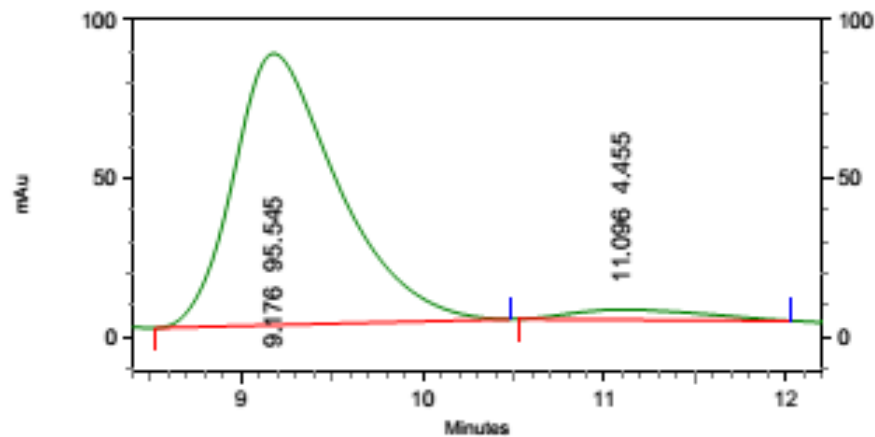
3: 230 nm, 4 nm

Results

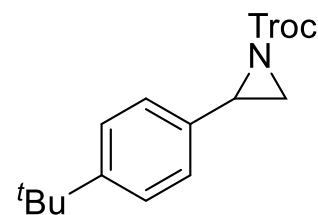
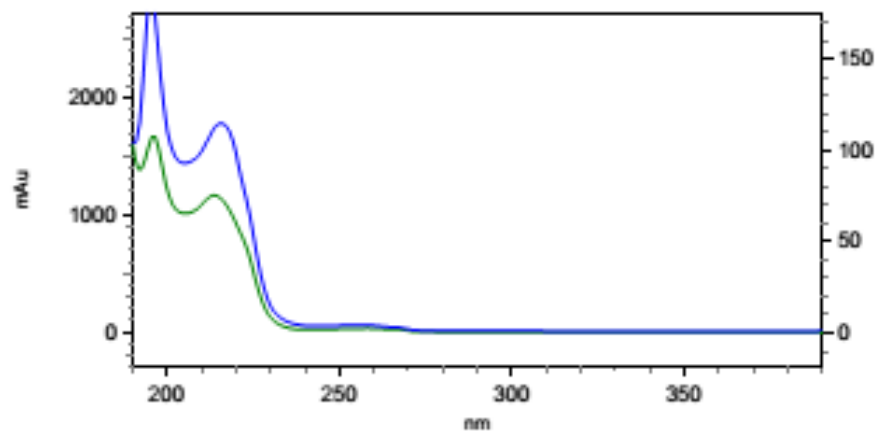
Name	Retention Time	Area Percent	Pk #
	8.532	49.807	1
	10.456	50.193	2

Totals		100.000	
--------	--	---------	--

2,2,2-Trichloroethyl 2-(4-*tert*-butylphenyl)aziridine-1-carboxylate (3e)



HPLC trace



3: 237 nm, 4 nm

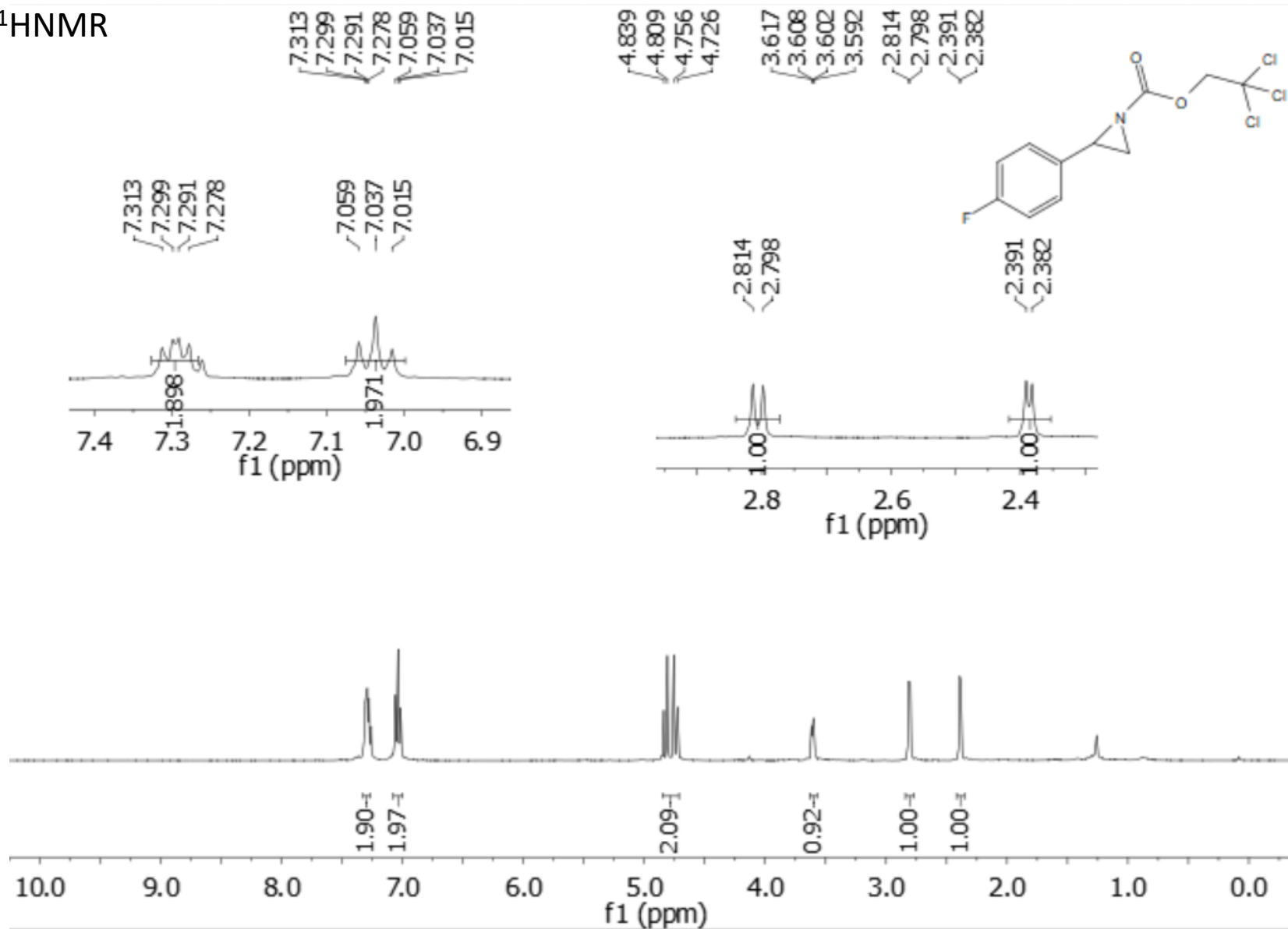
Results

Name	Retention Time	Area Percent	Pk #
	9.176	95.545	1
	11.096	4.455	2

Totals		100.000	
--------	--	---------	--

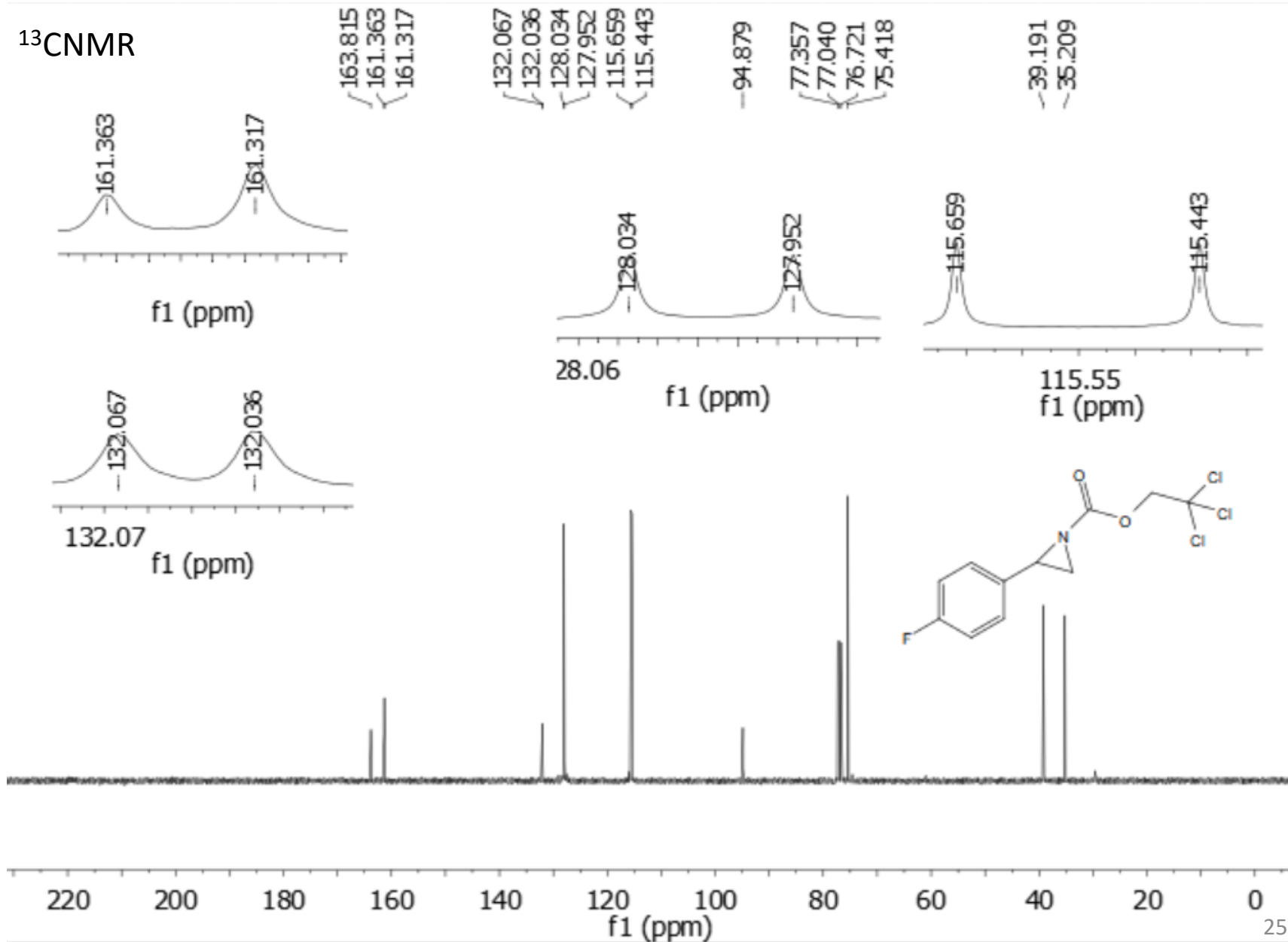
2,2,2-Trichloroethyl 2-(4-fluorophenyl)aziridine-1-carboxylate (3f)

$^1\text{H NMR}$



2,2,2-Trichloroethyl 2-(4-fluorophenyl)aziridine-1-carboxylate (3f)

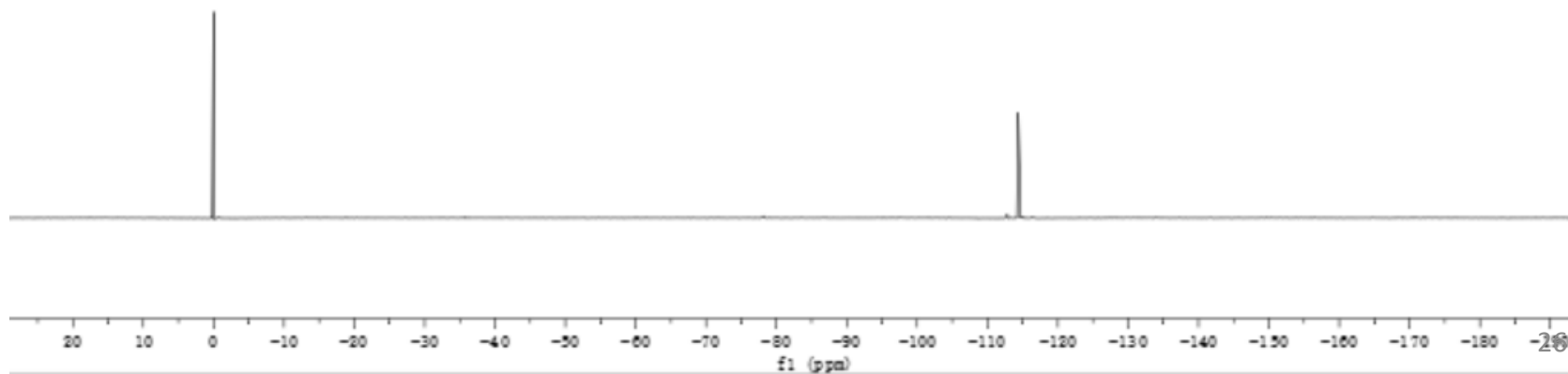
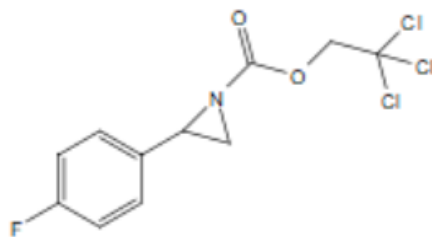
^{13}C NMR



2,2,2-Trichloroethyl 2-(4-fluorophenyl)aziridine-1-carboxylate (3f)

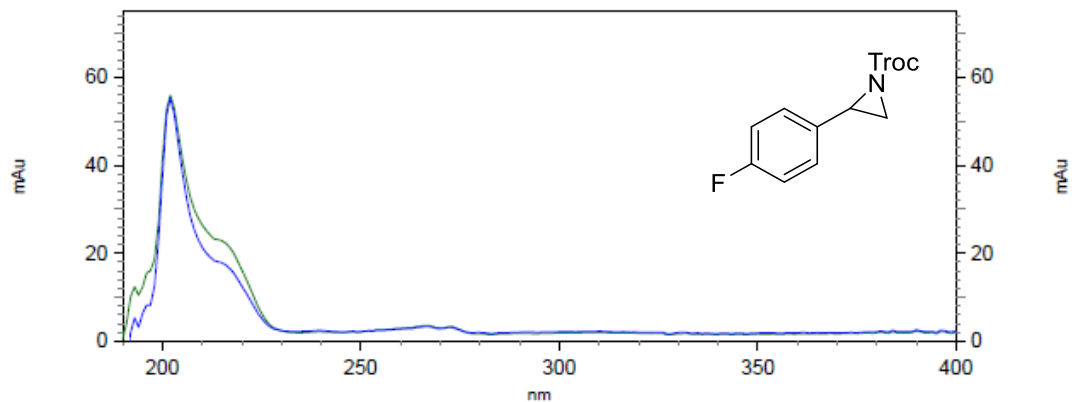
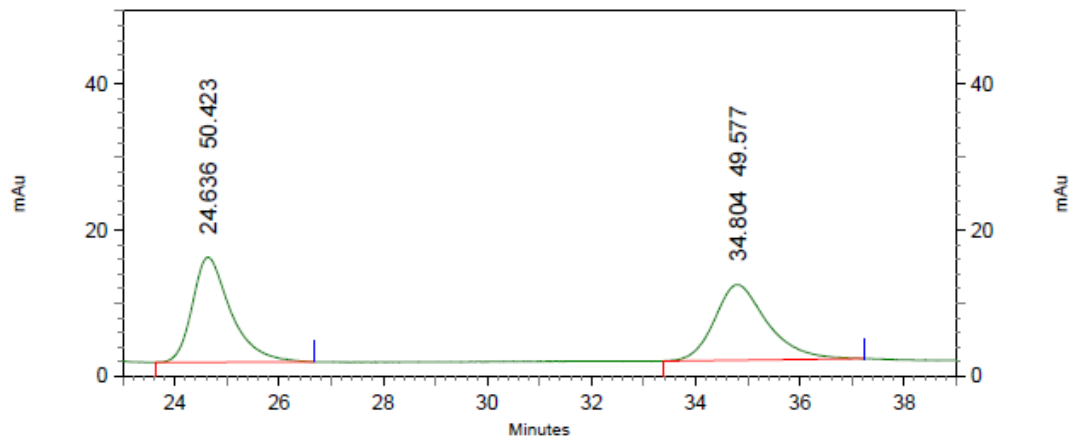
^{19}F NMR

-- 114.373



2,2,2-Trichloroethyl 2-(4-fluorophenyl)aziridine-1-carboxylate (3f)

HPLC trace
racemic

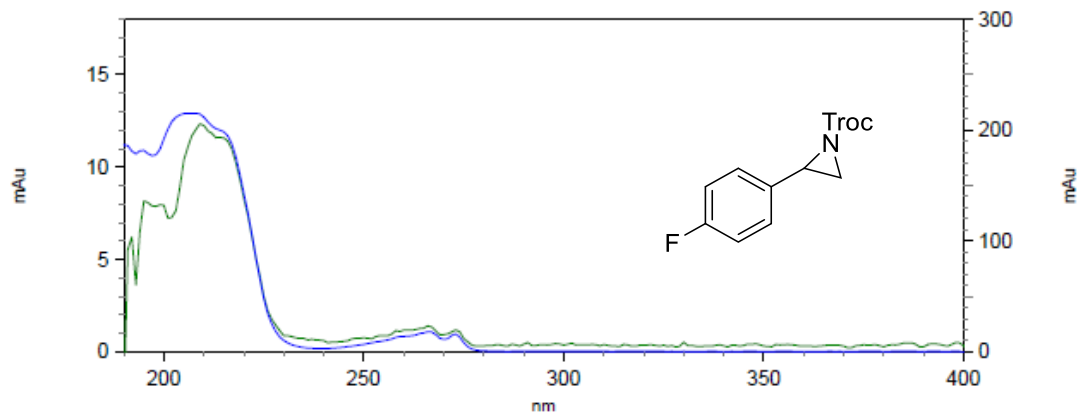
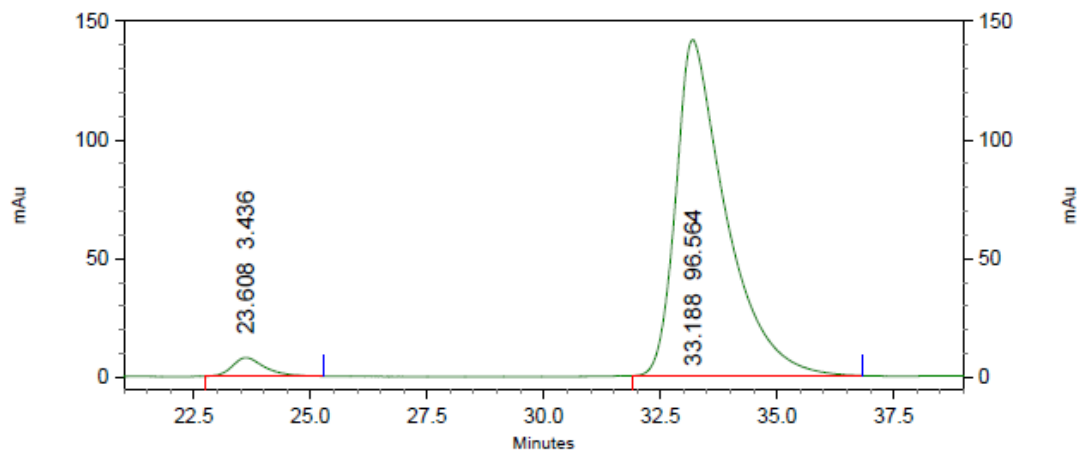


2: 220 nm, 4
nm Results

Pk #	Retention Time	Area Percent
1	24.636	50.423
2	34.804	49.577
Totals		100.000

2,2,2-Trichloroethyl 2-(4-fluorophenyl)aziridine-1-carboxylate (3f)

HPLC trace



2: 220 nm, 4
nm Results

Pk #	Retention Time	Area Percent
1	23.608	3.436
2	33.188	96.564

Totals	100.000
--------	---------

2,2,2-Trichloroethyl 2-(3-fluorophenyl)aziridine-1-carboxylate (3g)

$^1\text{H NMR}$

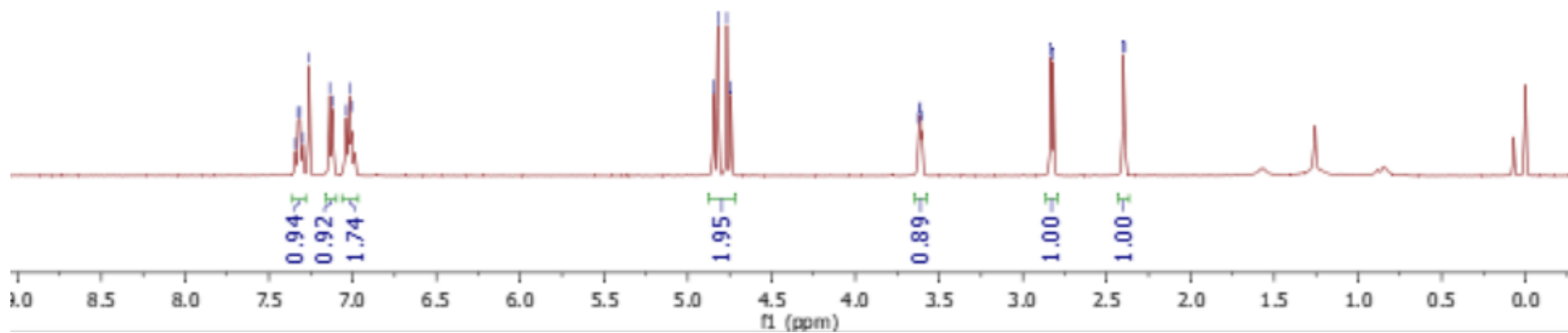
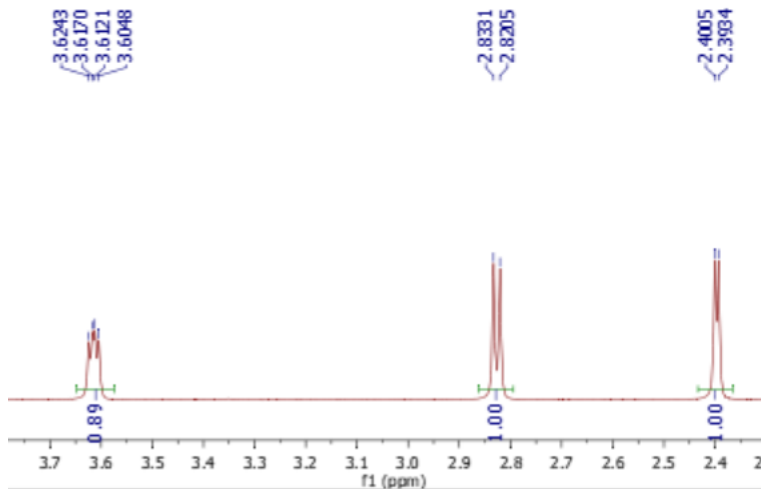
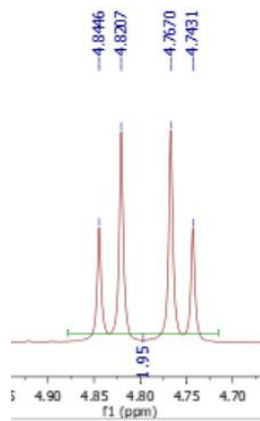
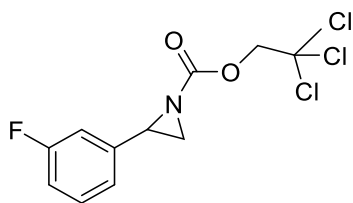
7.3415
7.3259
7.3139
7.2983
7.2605
7.1366
7.1213
7.0384
7.0195
7.0072

4.8446
4.8207
4.7670
4.7431

3.6243
3.6170
3.6121
3.6048

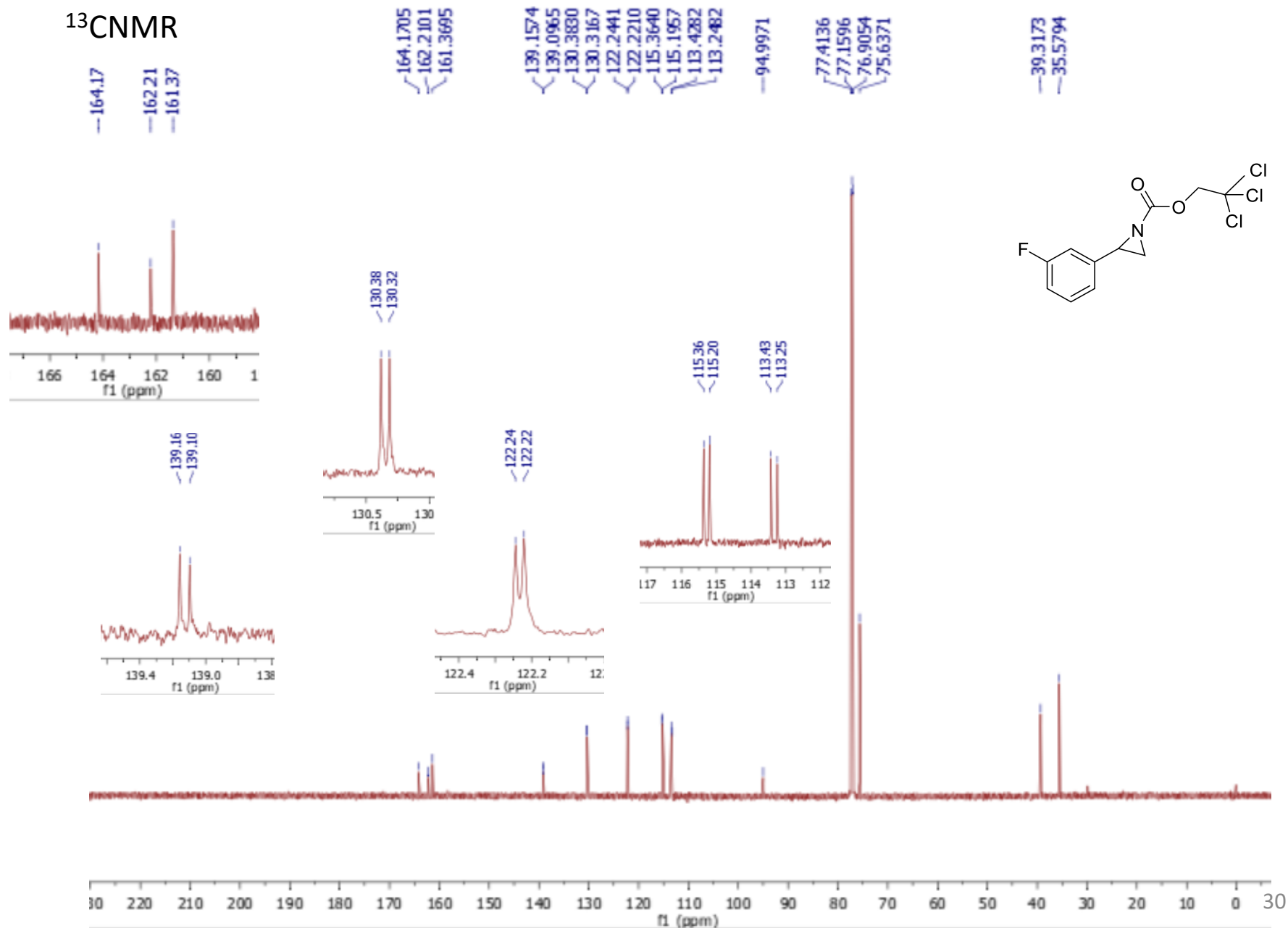
2.8331
2.8205

2.4005
2.3934



2,2,2-Trichloroethyl 2-(3-fluorophenyl)aziridine-1-carboxylate (3g)

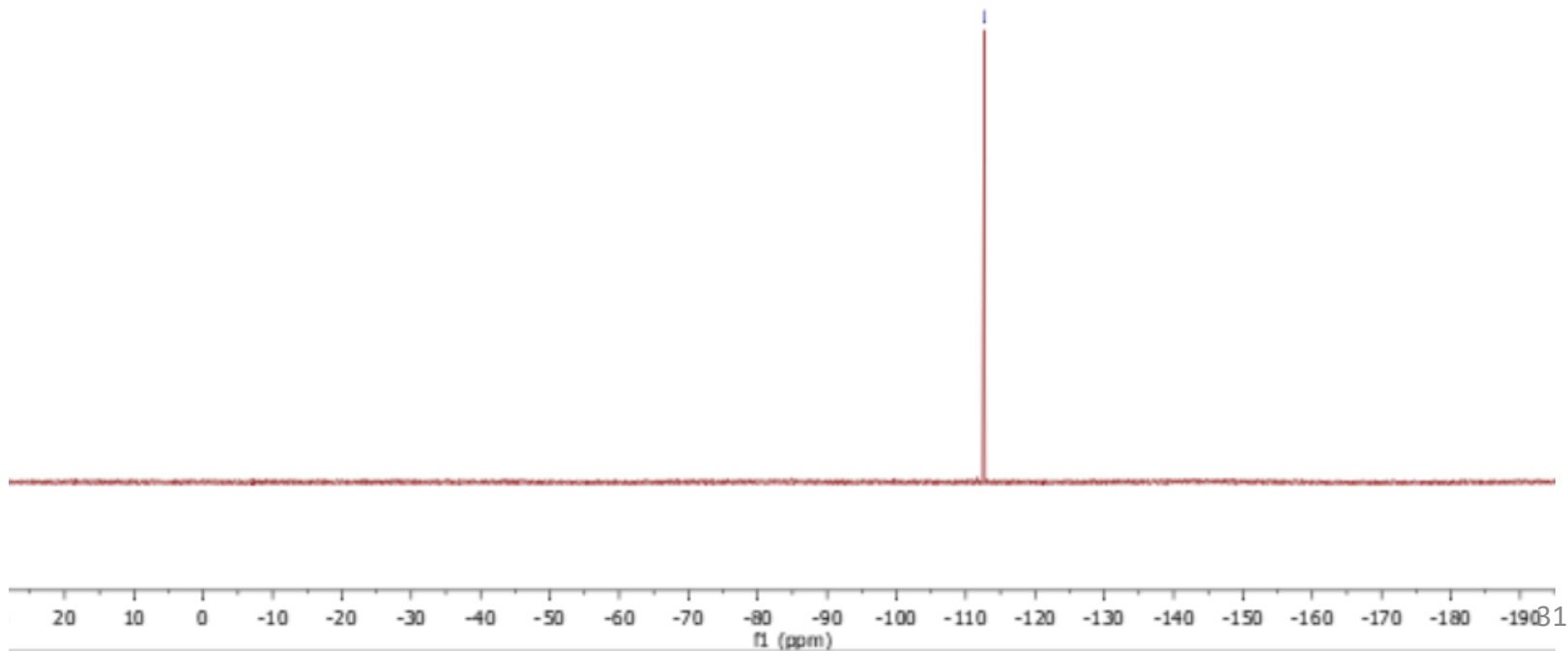
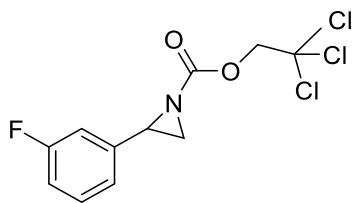
¹³CNMR



2,2,2-Trichloroethyl 2-(3-fluorophenyl)aziridine-1-carboxylate (3g)

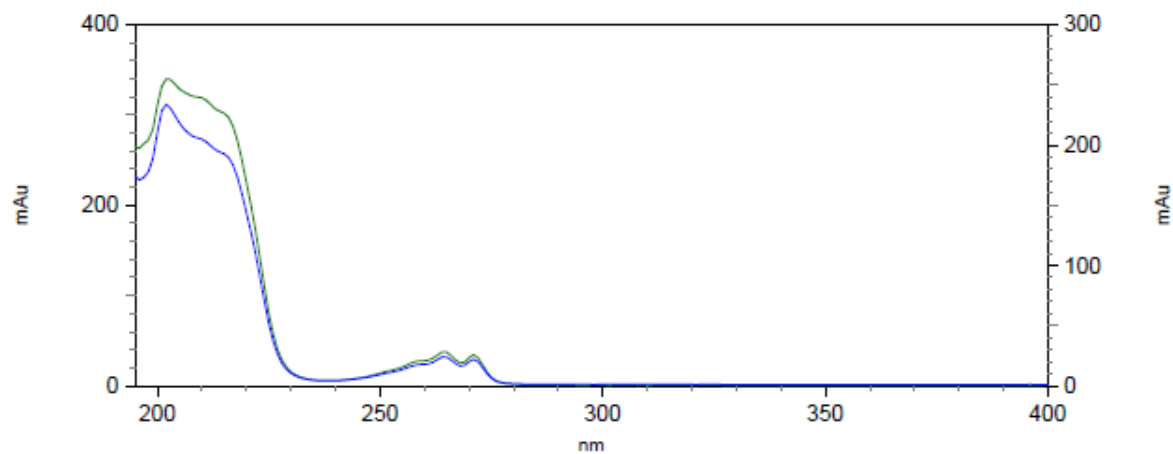
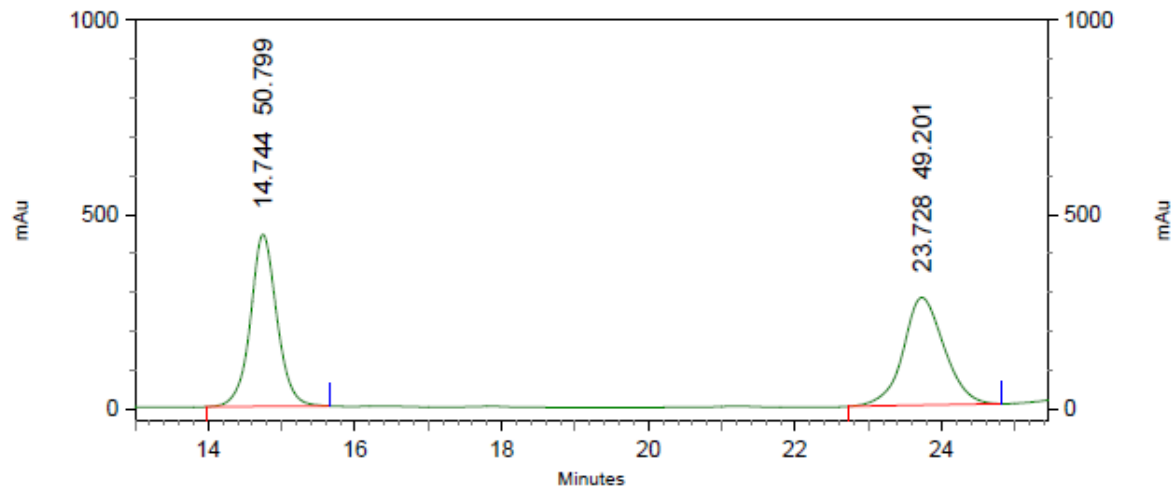
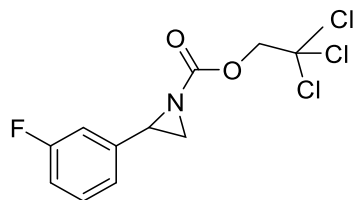
^{19}F NMR

---112.65



2,2,2-Trichloroethyl 2-(3-fluorophenyl)aziridine-1-carboxylate (3g)

HPLC trace
racemic

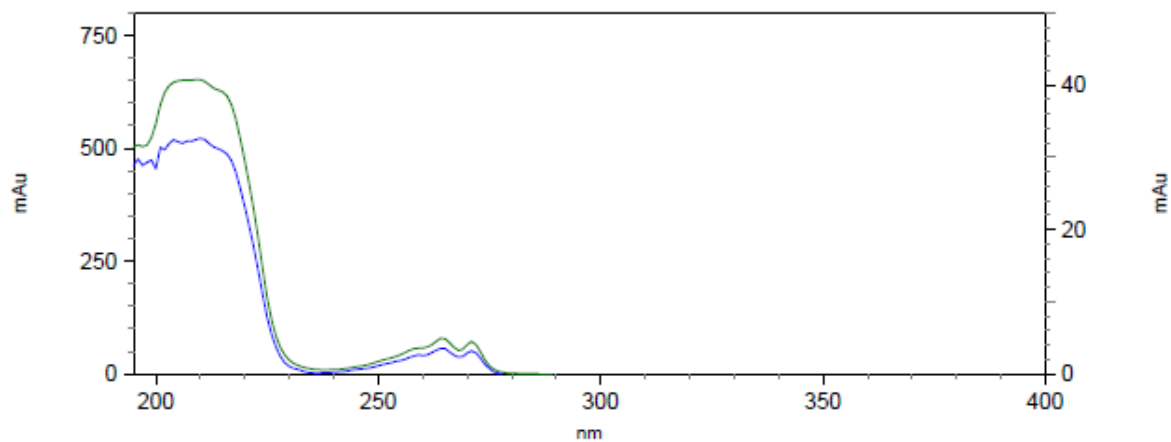
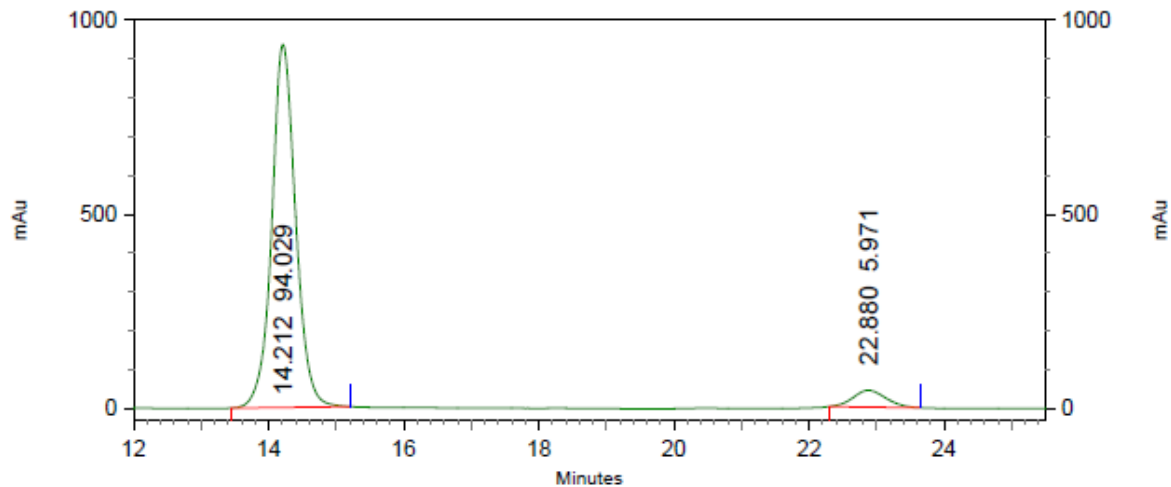
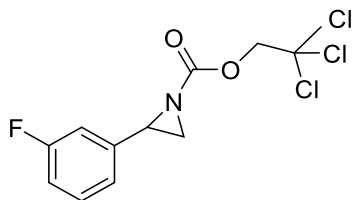


3: 220 nm, 4
nm Results

Pk #	Retention Time	Area Percent
1	14.744	50.799
2	23.728	49.201
Totals		100.000

2,2,2-Trichloroethyl 2-(3-fluorophenyl)aziridine-1-carboxylate (3g)

HPLC trace

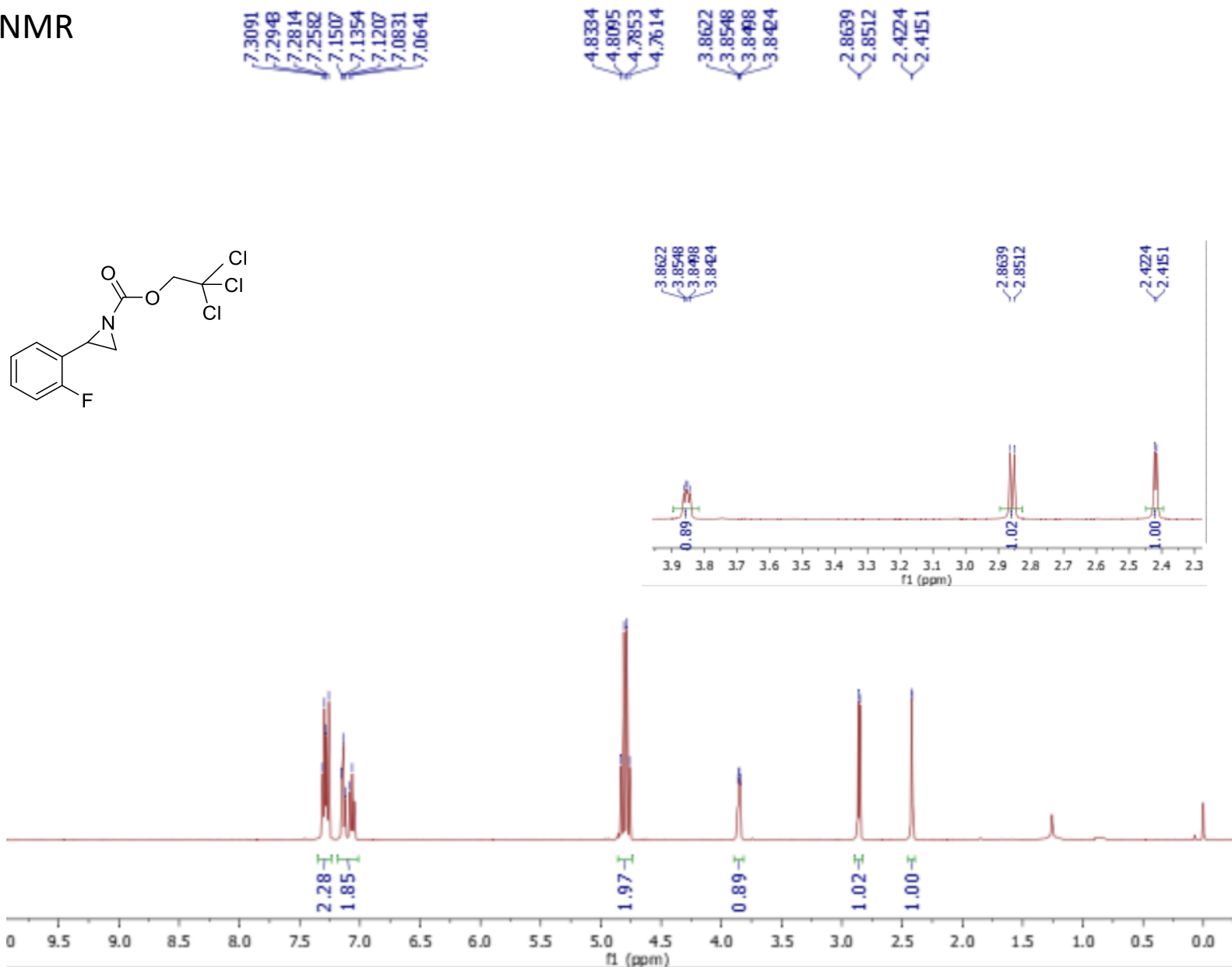


3: 220 nm, 4
nm Results

Pk #	Retention Time	Area Percent
1	14.212	94.029
2	22.880	5.971
Totals		100.000

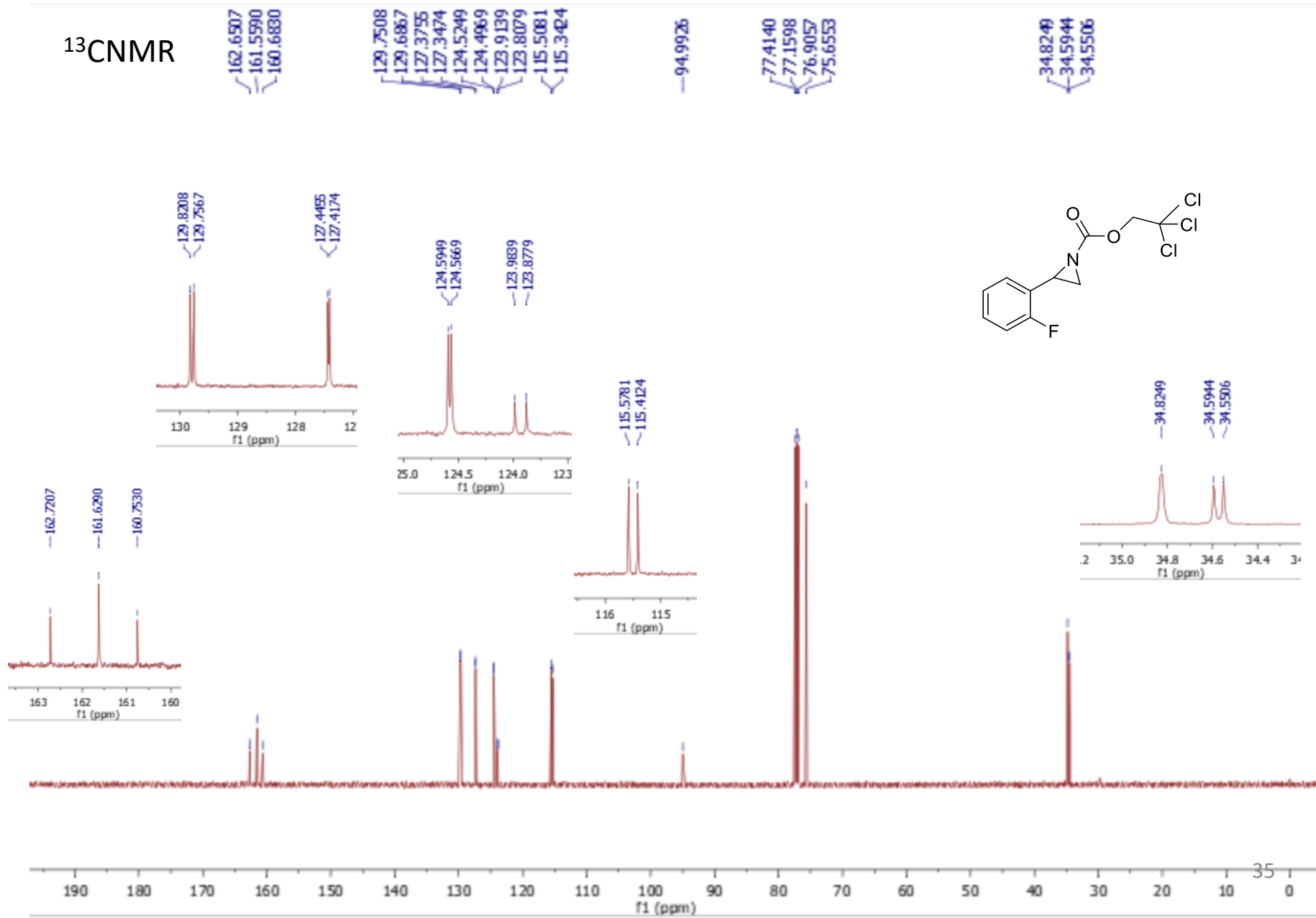
2,2,2-Trichloroethyl 2-(2-fluorophenyl)aziridine-1-carboxylate (3h)

$^1\text{H NMR}$



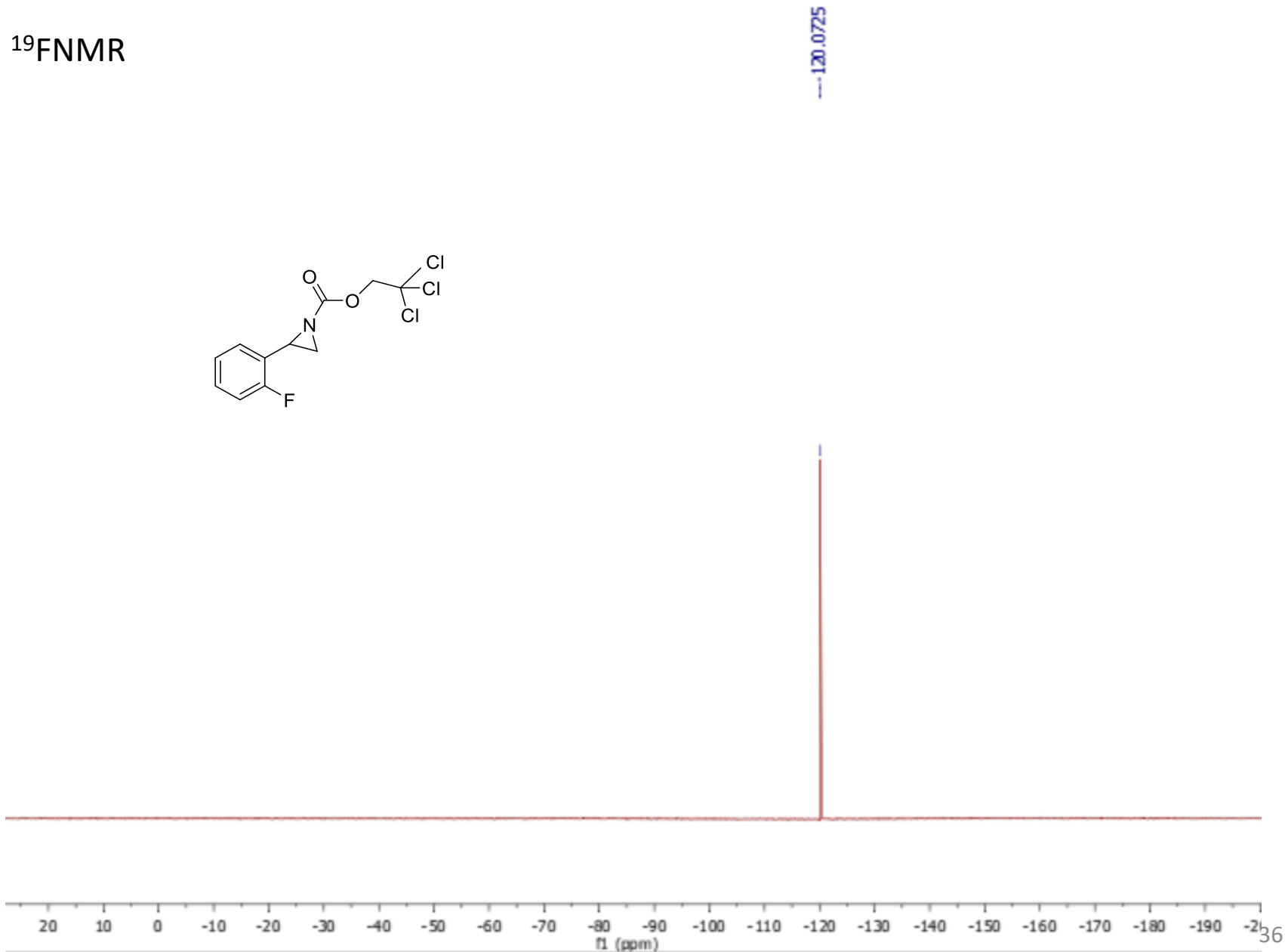
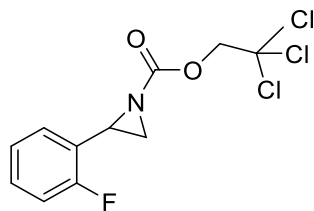
2,2,2-Trichloroethyl 2-(2-fluorophenyl)aziridine-1-carboxylate (3h)

^{13}C NMR



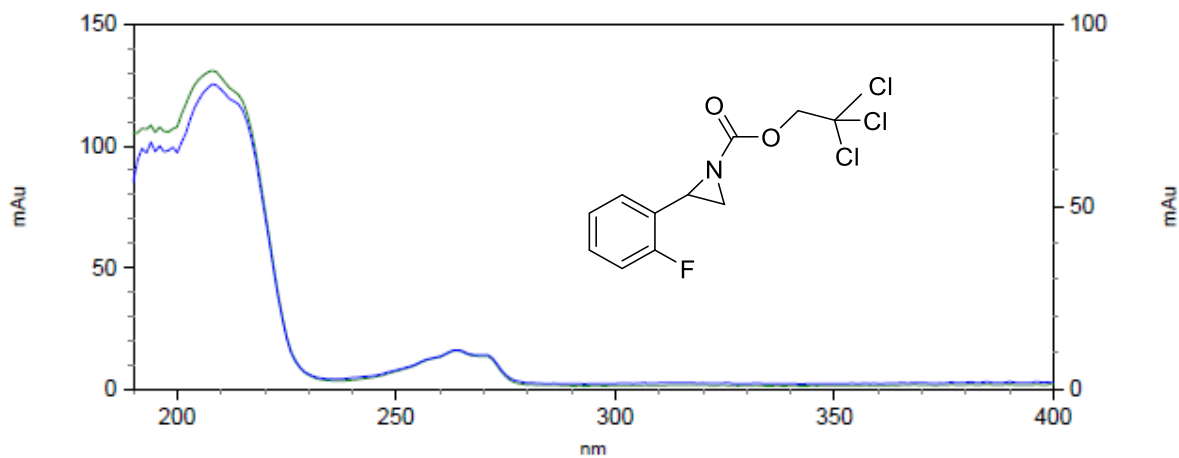
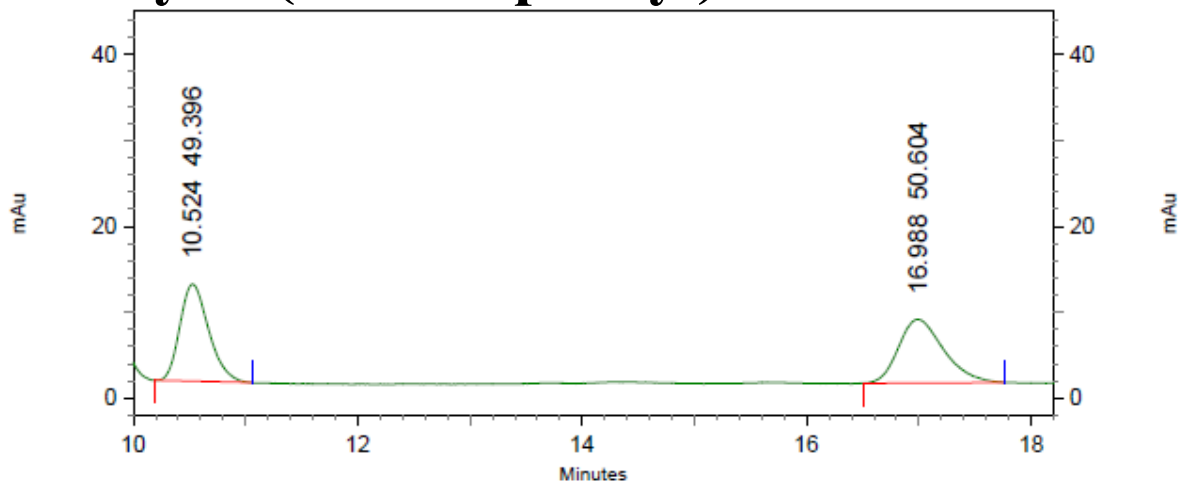
2,2,2-Trichloroethyl 2-(2-fluorophenyl)aziridine-1-carboxylate (3h)

^{19}F NMR



2,2,2-Trichloroethyl 2-(2-fluorophenyl)aziridine-1-carboxylate (3h)

HPLC trace
racemic

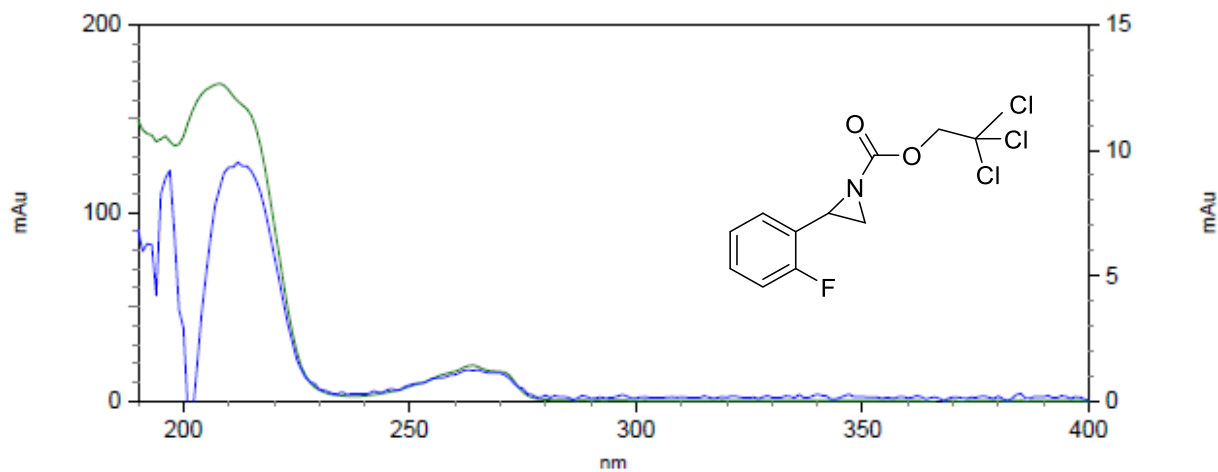
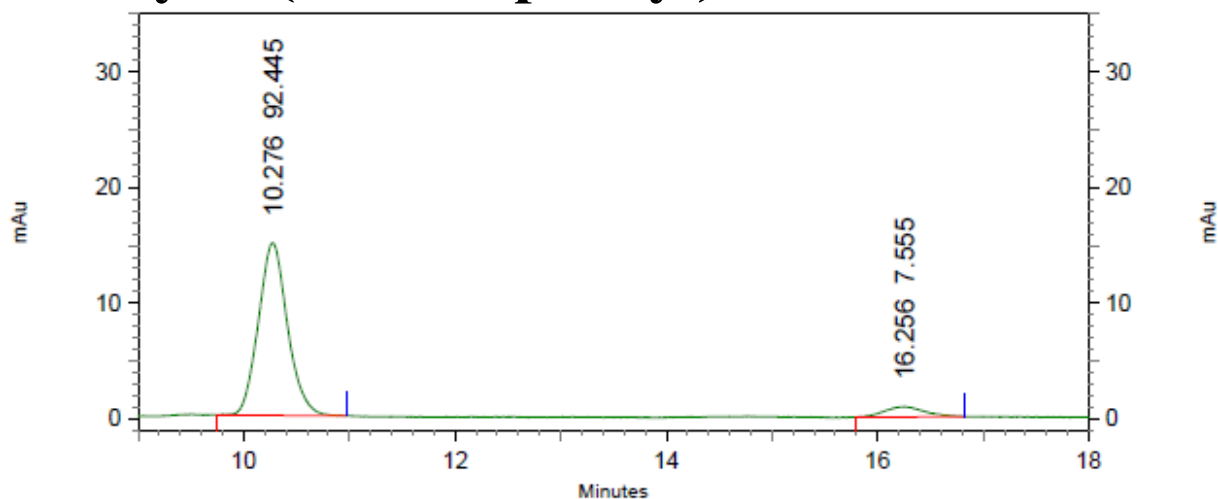


4: 270 nm, 4
nm Results

Pk #	Retention Time	Area Percent
1	10.524	49.396
2	16.988	50.604
Totals		100.000

2,2,2-Trichloroethyl 2-(2-fluorophenyl)aziridine-1-carboxylate (3h)

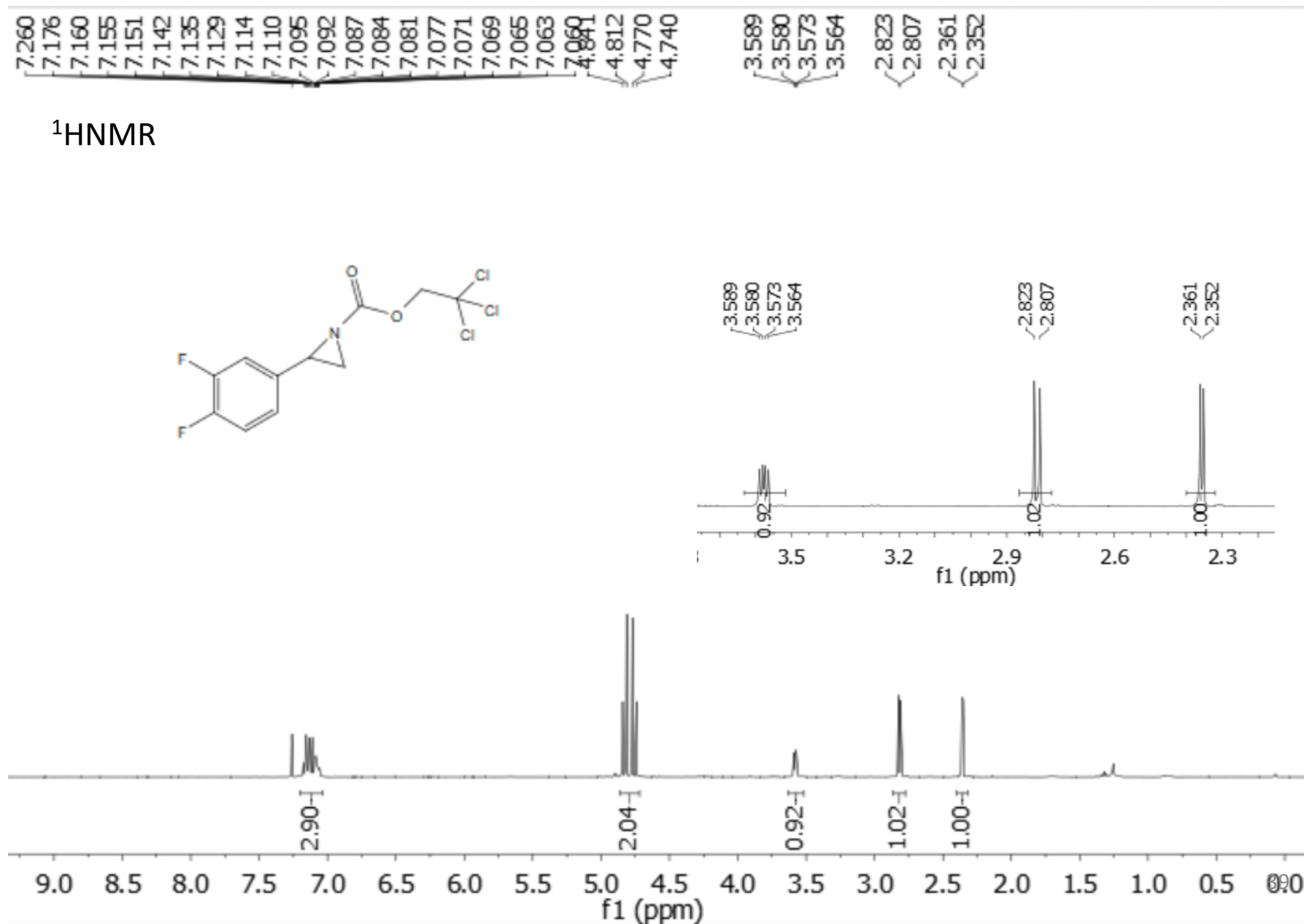
HPLC trace



4: 270 nm, 4
nm Results

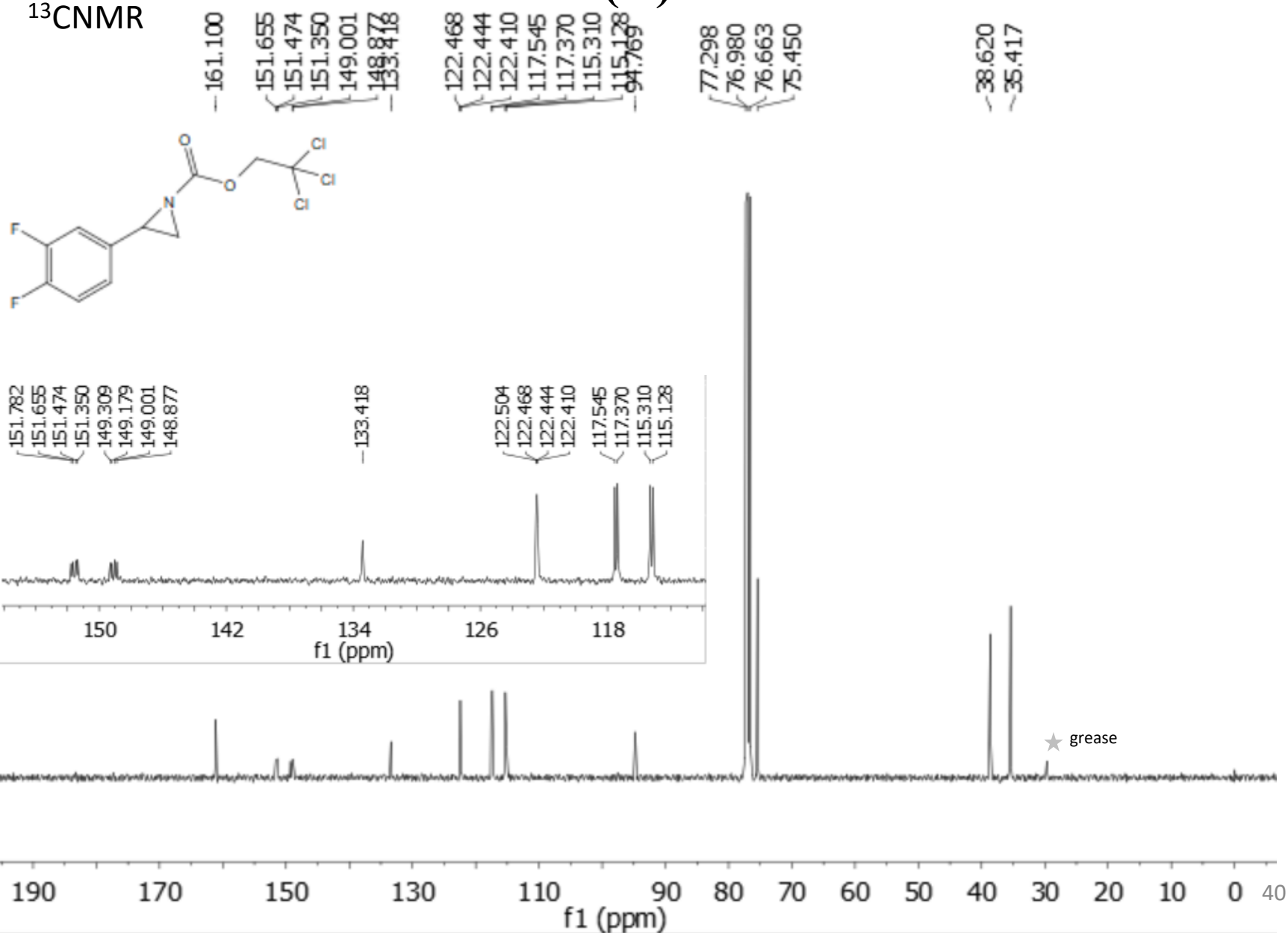
Pk #	Retention Time	Area Percent
1	10.276	92.445
2	16.256	7.555
Totals		100.000

2,2,2-Trichloroethyl 2-(3,4-difluorophenyl)aziridine-1-carboxylate (3i)



2,2,2-Trichloroethyl 2-(3,4-difluorophenyl)aziridine-1-carboxylate (3i)

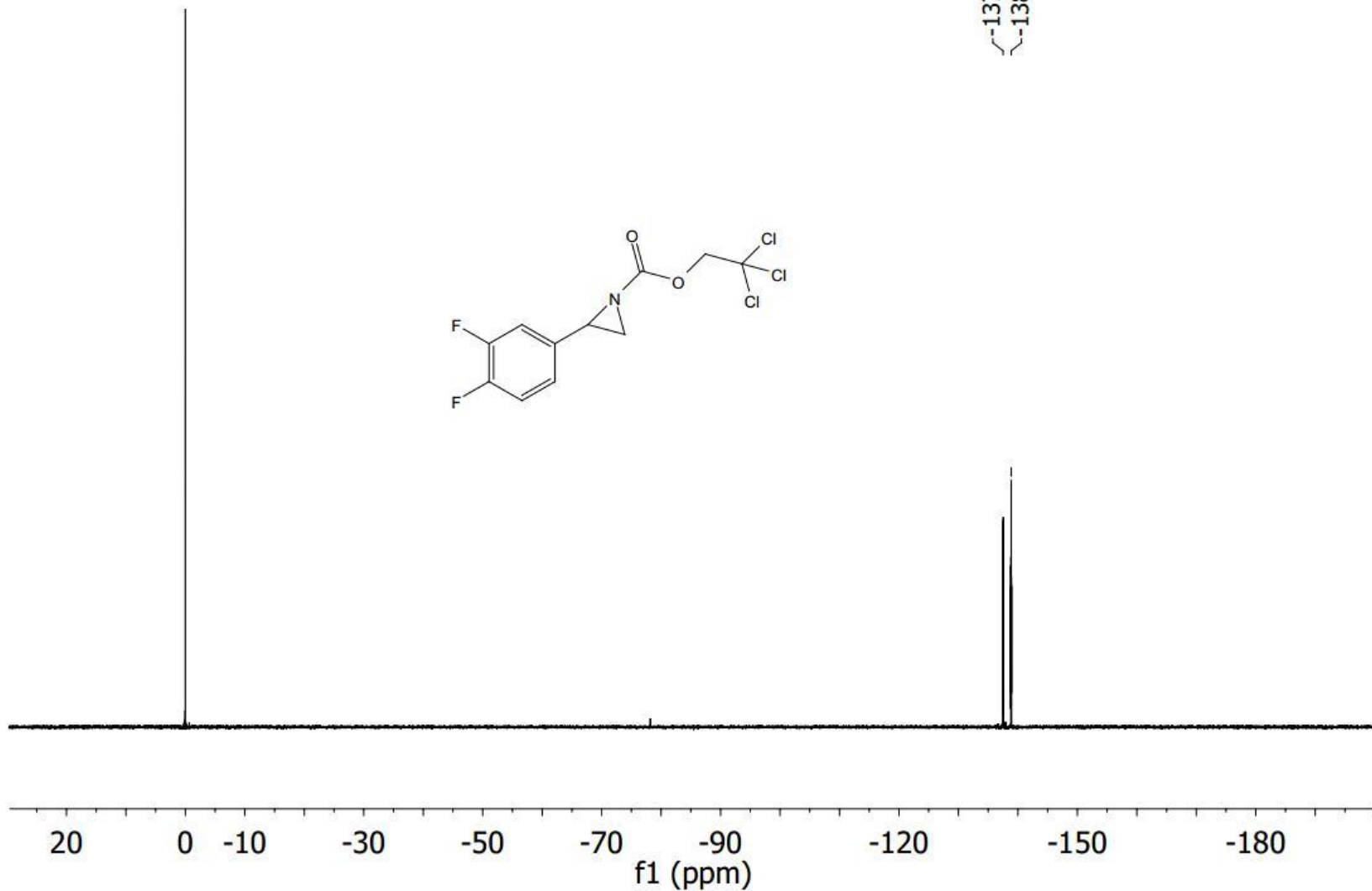
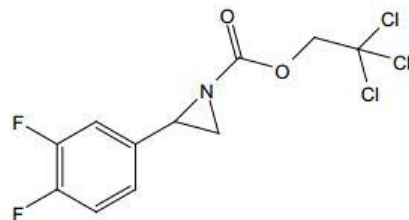
¹³CNMR



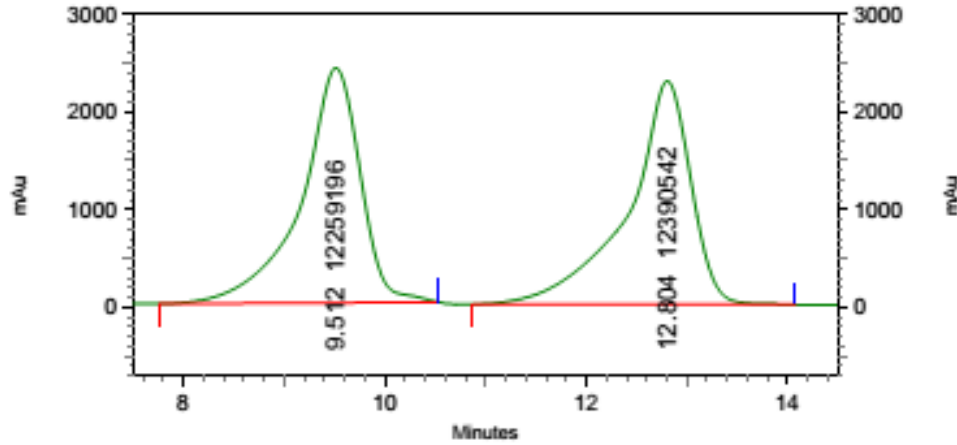
2,2,2-Trichloroethyl 2-(3,4-difluorophenyl)aziridine-1-carboxylate (3i)

^{19}F NMR

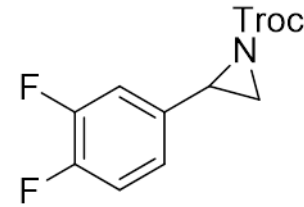
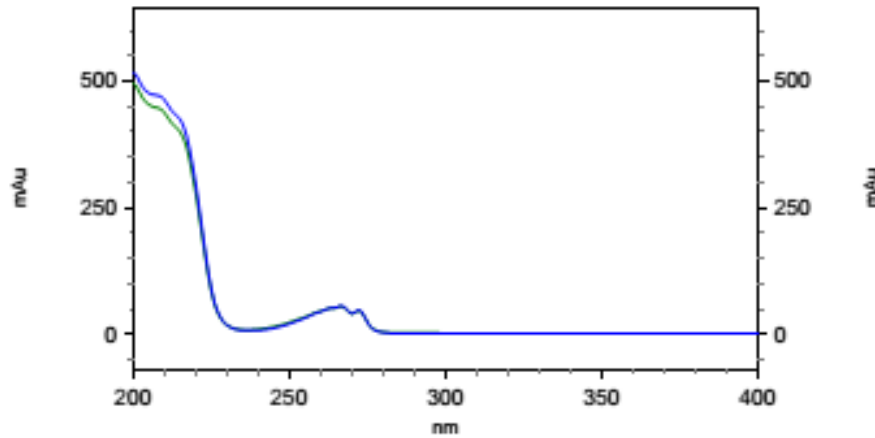
137.509
138.872



2,2,2-Trichloroethyl 2-(3,4-difluorophenyl)aziridine-1-carboxylate (3i)



HPLC trace
racemic

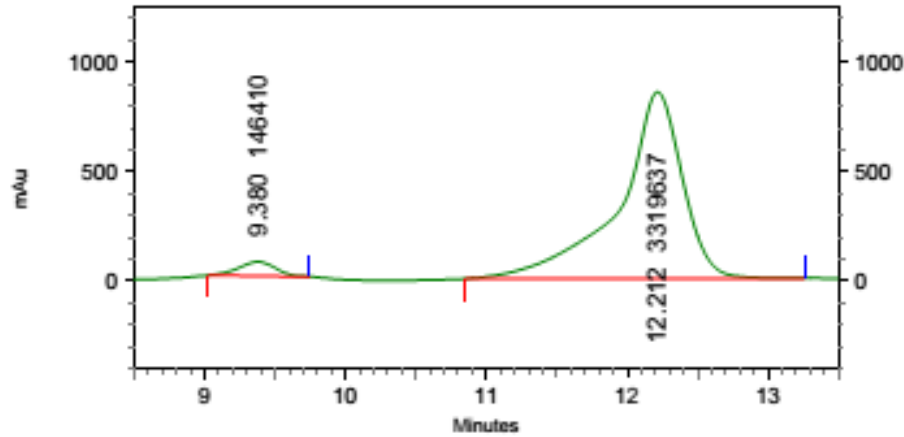


4: 220 nm, 4 nm

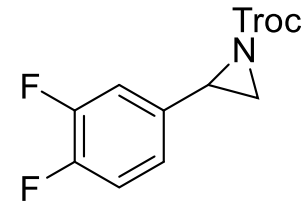
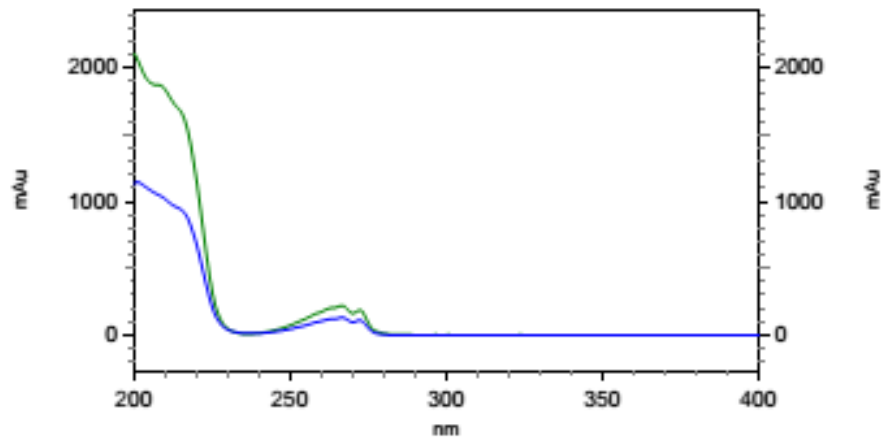
Results

Pk #	Name	Retention Time	Area Percent
1		9.512	49.734
2		12.804	50.266
Totals			100.000

2,2,2-Trichloroethyl 2-(3,4-difluorophenyl)aziridine-1-carboxylate (3i)



HPLC trace



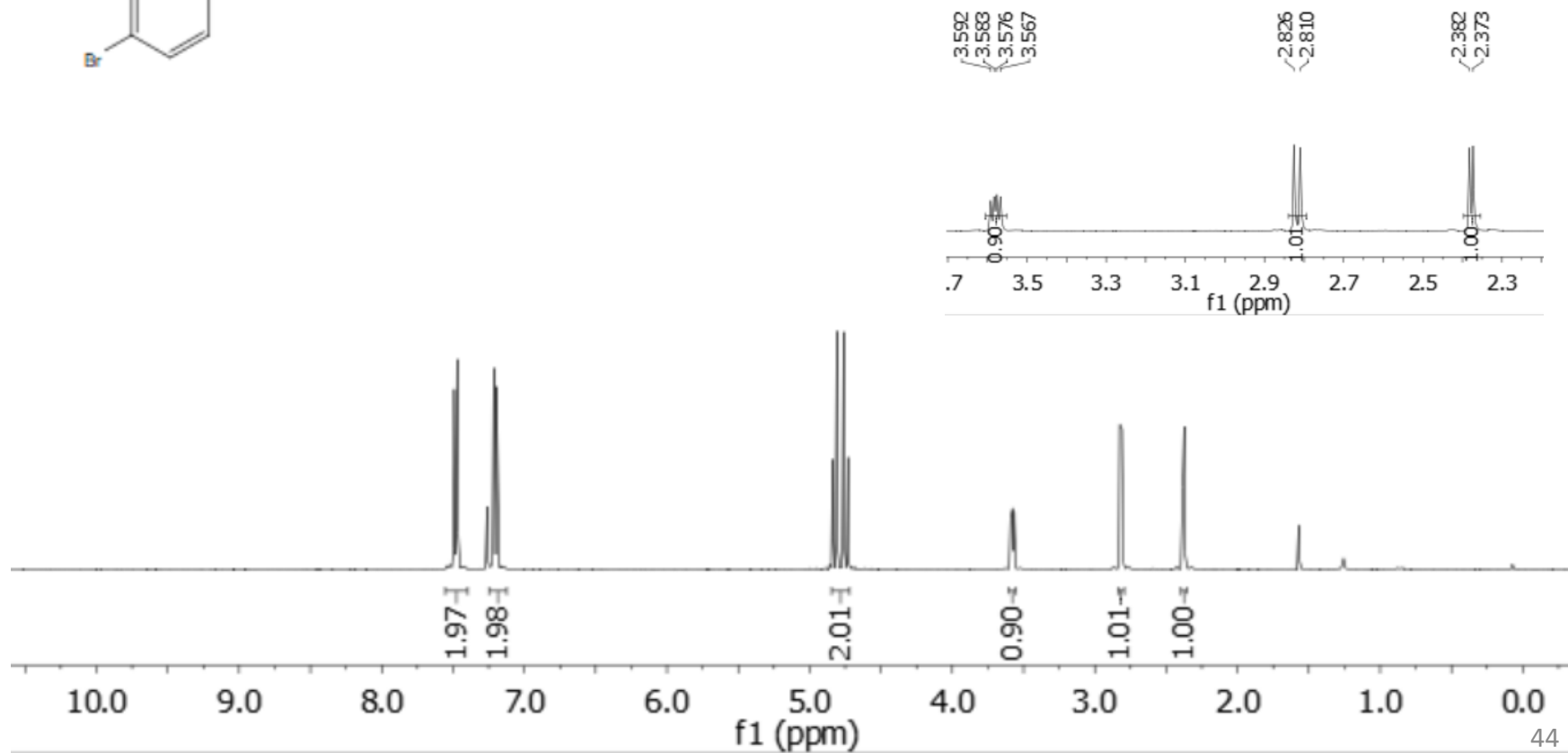
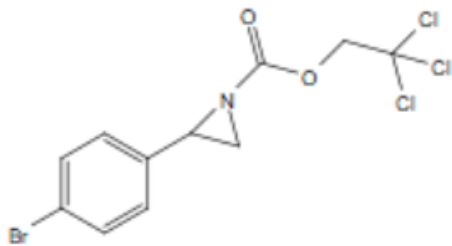
4: 260 nm, 4 nm
Results

Pk #	Name	Retention Time	Area Percent
1		9.380	4.224
2		12.212	95.776
Totals			100.000

2,2,2-Trichloroethyl 2-(4-bromophenyl)aziridine-1-carboxylate (3j)

$^1\text{H NMR}$

7.498
7.492
7.475
7.471
7.260
7.219
7.213
7.192
4.838
4.809
4.761
4.731
3.592
3.583
3.576
3.567
2.826
2.810
2.382
2.373



2,2,2-Trichloroethyl 2-(4-bromophenyl)aziridine-1-carboxylate (3j)

^{13}C NMR

-161.207

-135.360

-131.713

-127.941

-122.064

-94.711

77.307

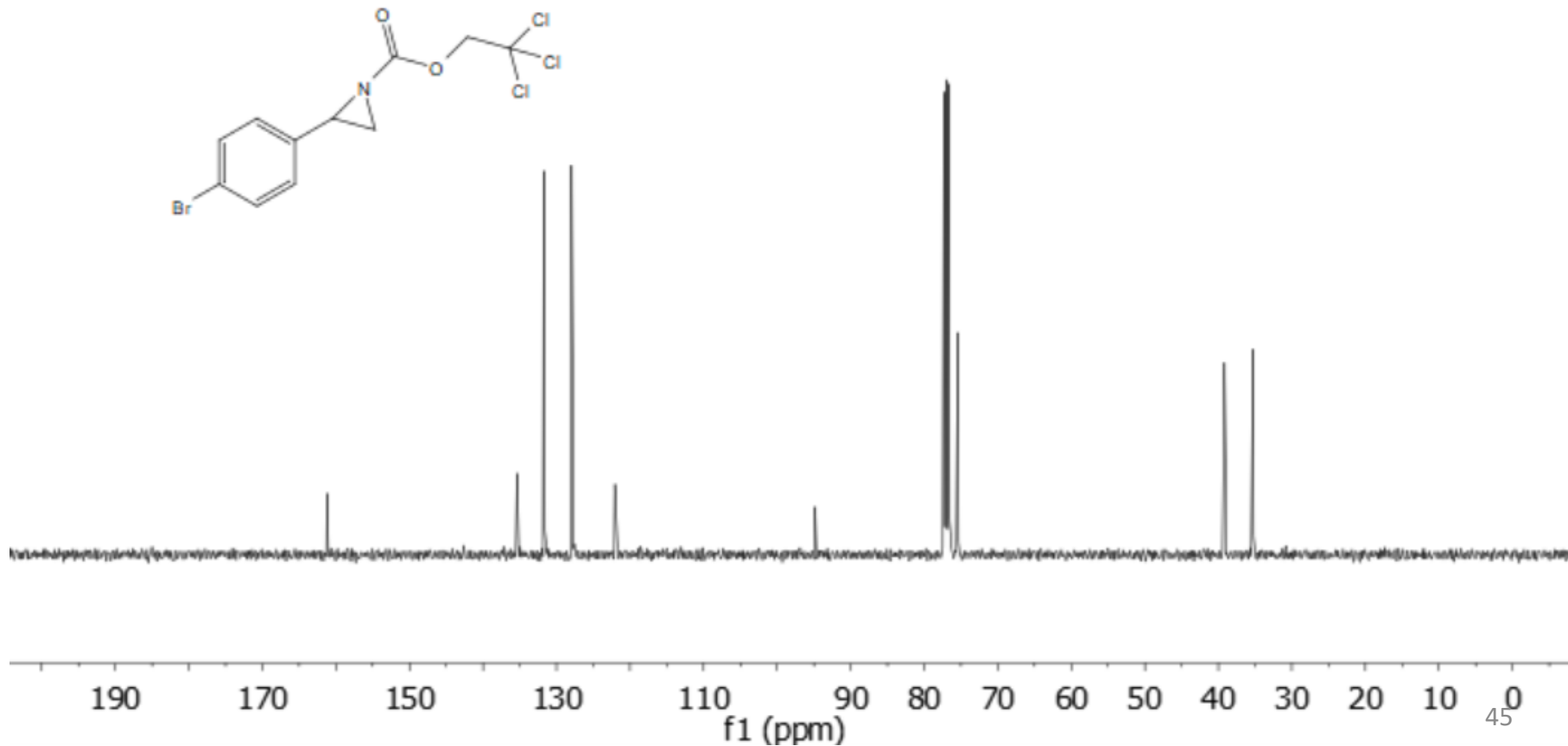
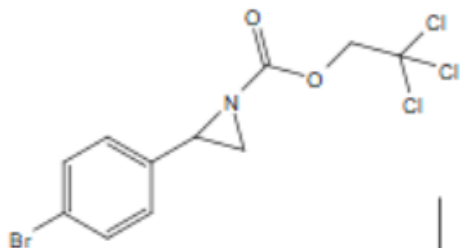
76.989

76.672

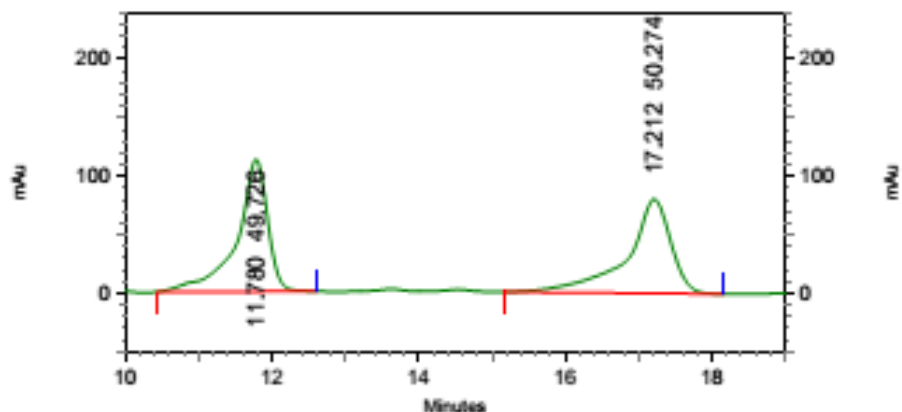
75.430

-39.166

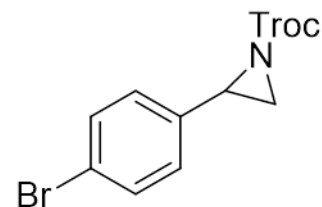
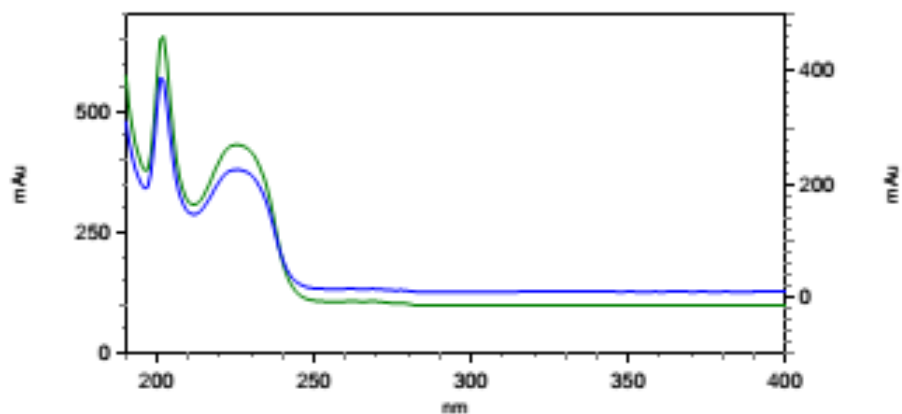
-35.290



2,2,2-Trichloroethyl 2-(4-bromophenyl)aziridine-1-carboxylate (3j)



HPLC trace
racemic

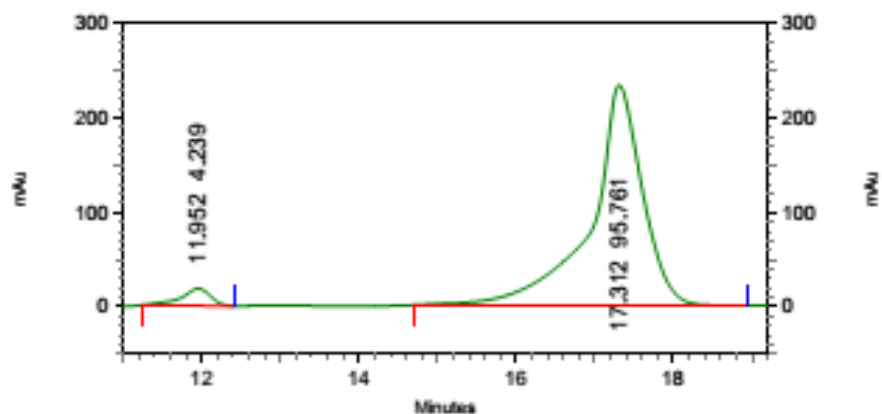


6: 236 nm, 4 nm

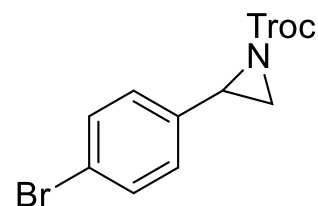
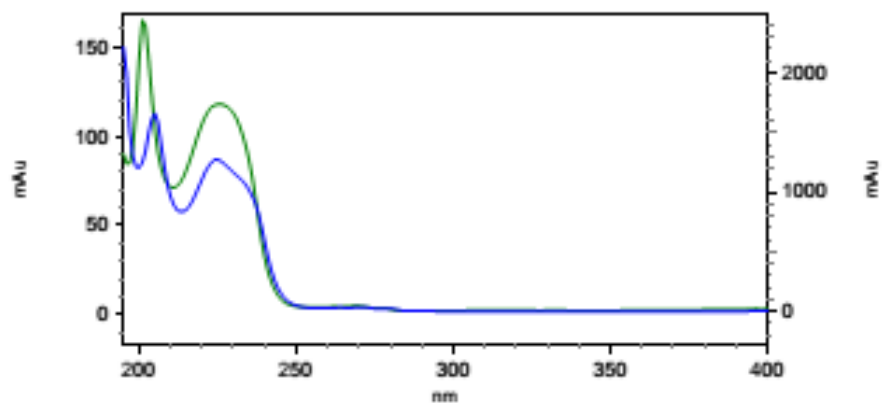
Results

Pk #	Name	Retention Time	Area Percent
1		11.780	49.726
2		17.212	50.274
Totals			100.000

2,2,2-Trichloroethyl 2-(4-bromophenyl)aziridine-1-carboxylate (3j)



HPLC trace



3: 239 nm, 4 nm

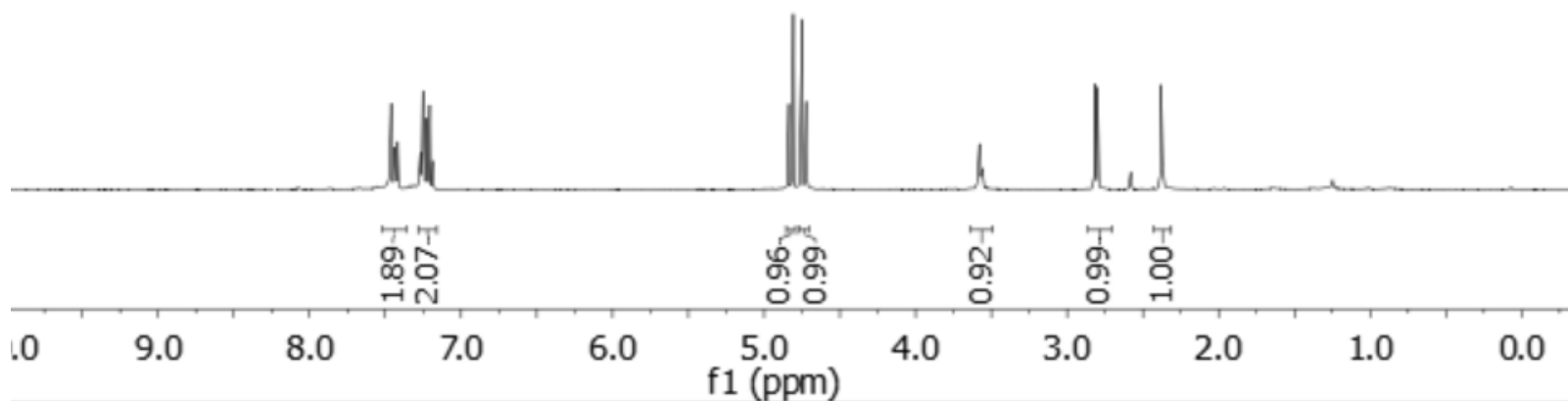
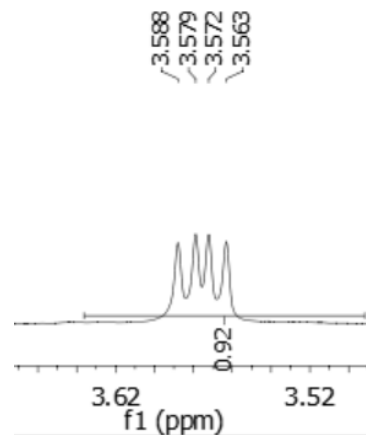
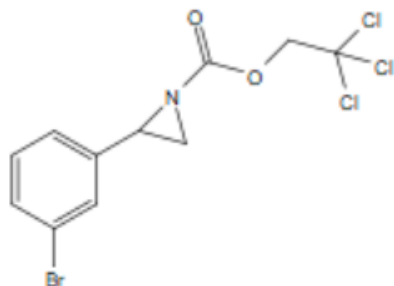
Results

Pk #	Name	Retention Time	Area Percent
1		11.952	4.239
2		17.312	95.761
Totals			100.000

2,2,2-Trichloroethyl 2-(3-bromophenyl)aziridine-1-carboxylate (3k)

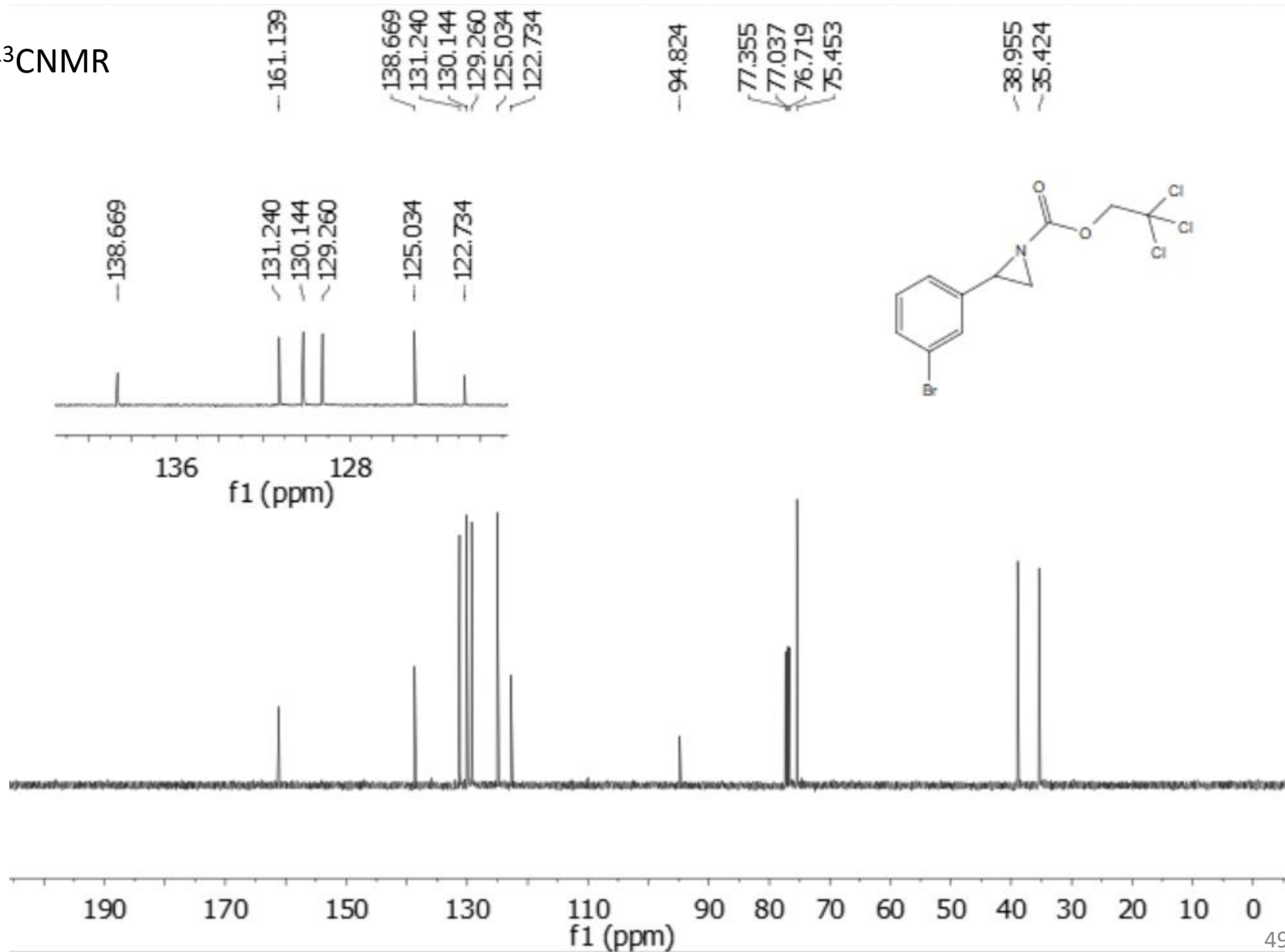
7.466
7.461
7.457
7.441
7.438
7.433
7.422
7.418
7.414
7.270
7.267
7.263
7.251
7.247
7.244
7.226
7.207
7.188
4.837
4.807
4.753
4.723
3.588
3.579
3.572
3.563
2.816
2.800
2.381
2.372

¹H NMR



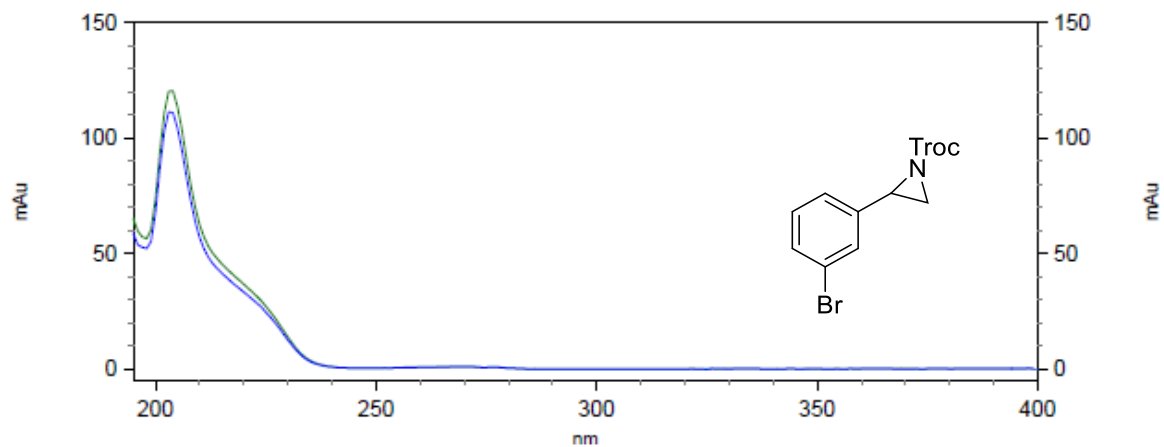
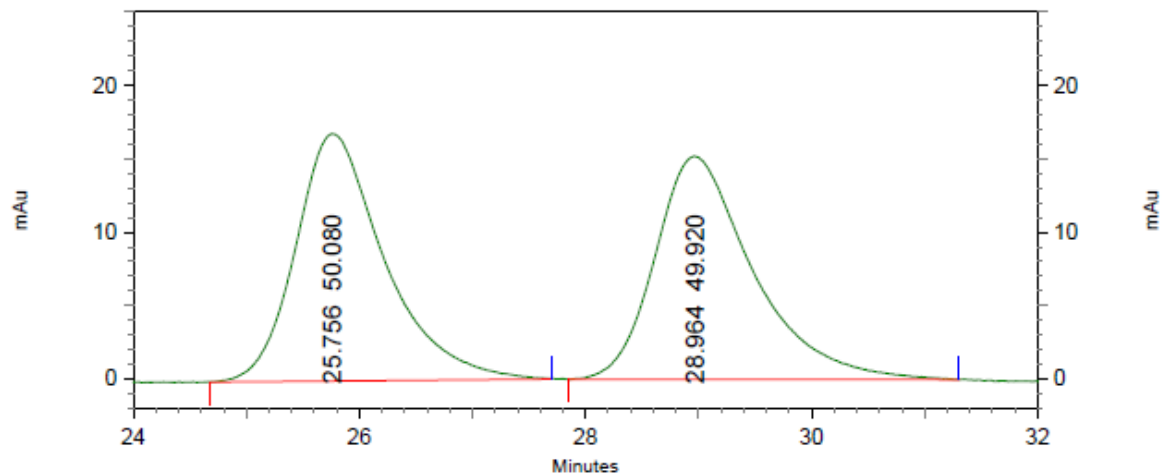
2,2,2-Trichloroethyl 2-(3-bromophenyl)aziridine-1-carboxylate (3k)

^{13}C NMR



2,2,2-Trichloroethyl 2-(3-bromophenyl)aziridine-1-carboxylate (3k)

HPLC trace
racemic



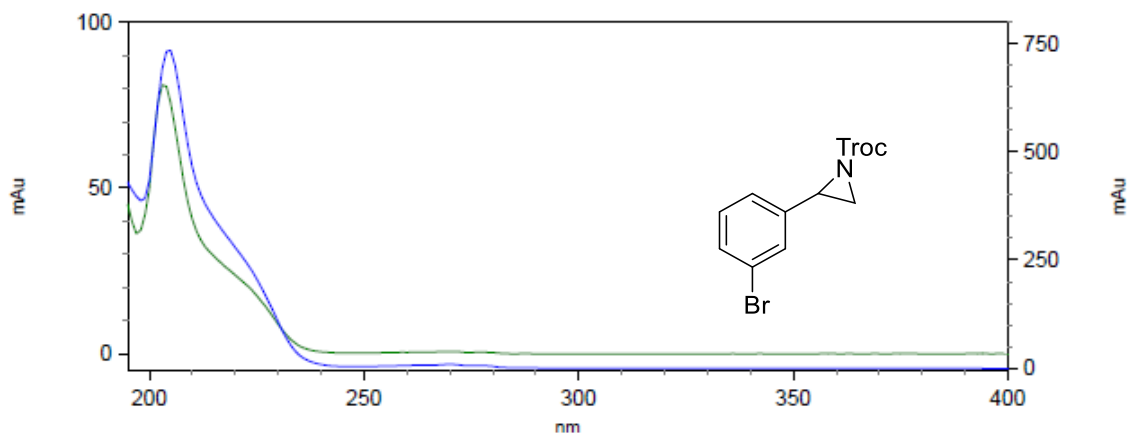
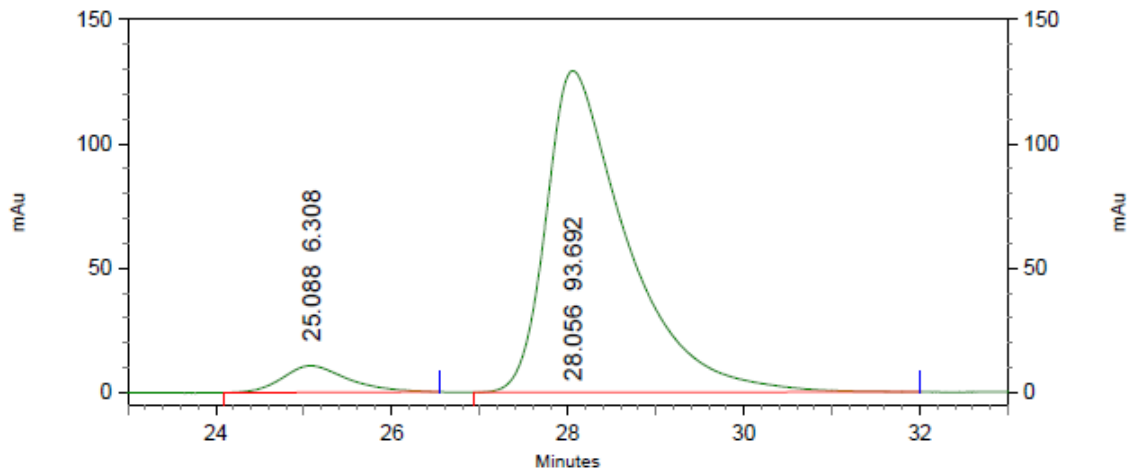
2: 229 nm, 4
nm Results

Pk #	Retention Time	Area Percent
1	25.756	50.080
2	28.964	49.920

Totals	100.000
--------	---------

2,2,2-Trichloroethyl 2-(3-bromophenyl)aziridine-1-carboxylate (3k)

HPLC trace

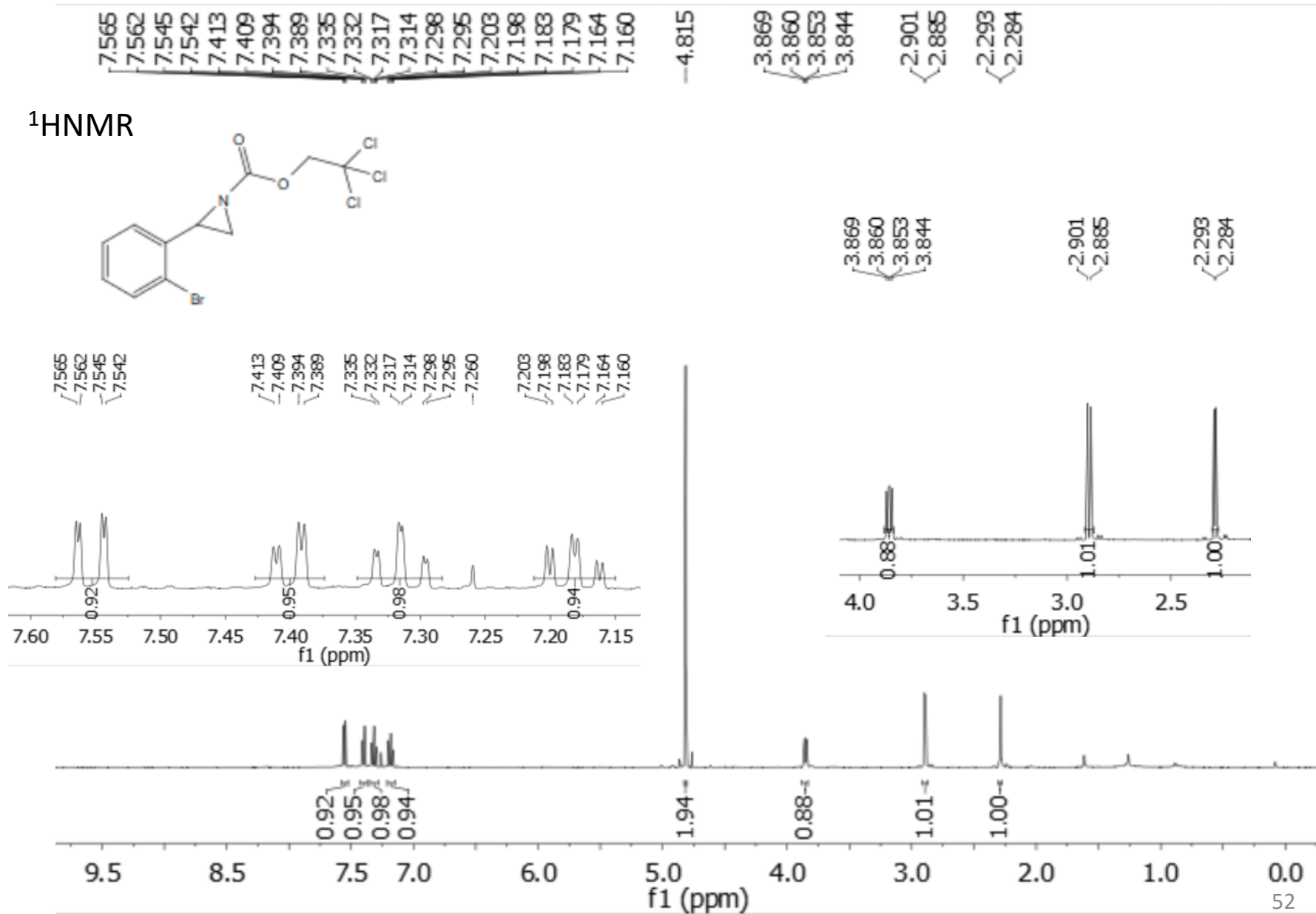


2: 229 nm, 4
nm Results

Pk #	Retention Time	Area Percent
1	25.088	6.308
2	28.056	93.692

Totals	100.000
--------	---------

2,2,2-Trichloroethyl 2-(2-bromophenyl)aziridine-1-carboxylate (3l)



2,2,2-Trichloroethyl 2-(2-bromophenyl)aziridine-1-carboxylate (3l)

^{13}C NMR

-161.423

135.919

132.333

129.415

127.721

127.665

122.721

-94.827

77.332

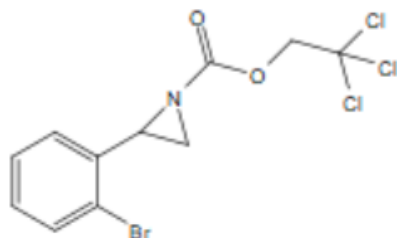
77.014

76.696

75.493

-39.787

-34.899



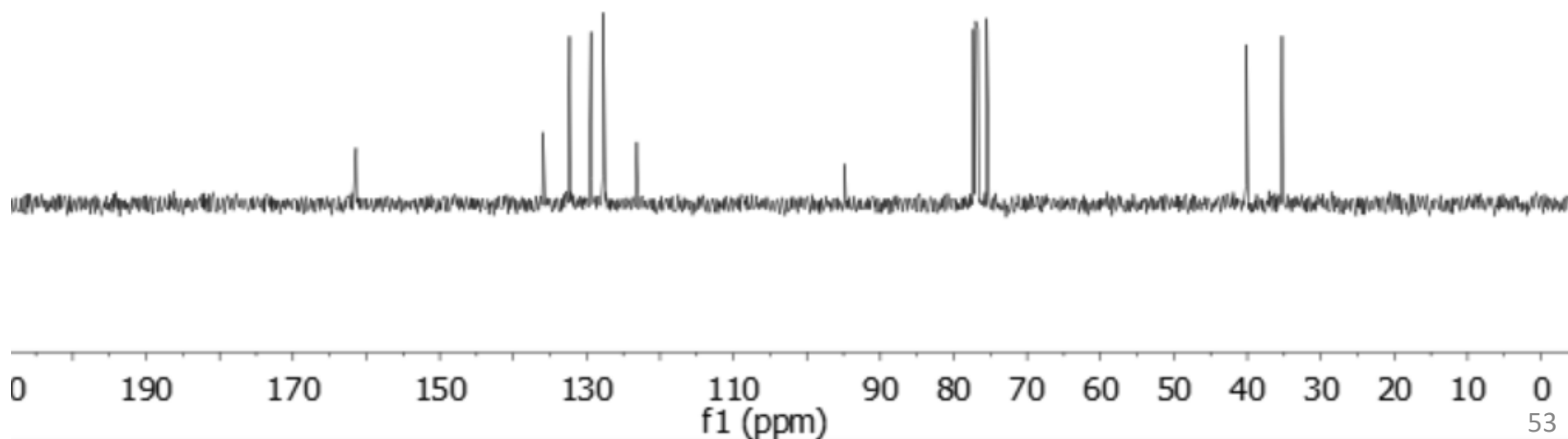
-129.415

127.721

127.665

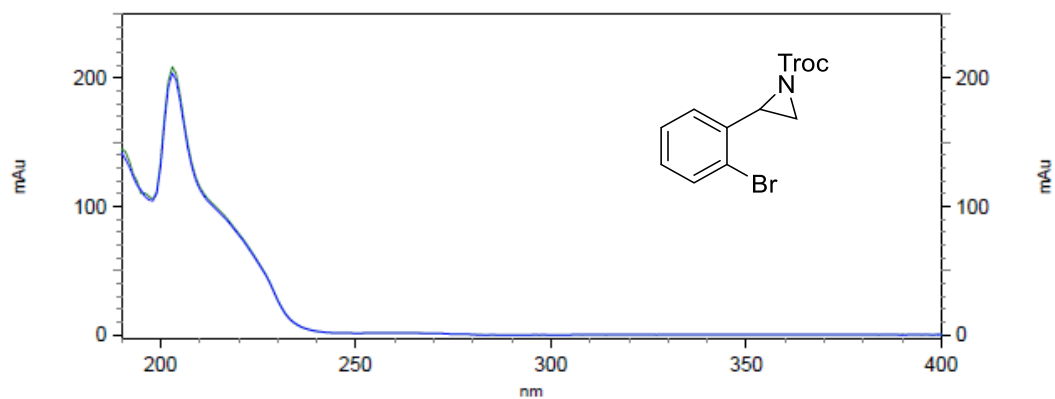
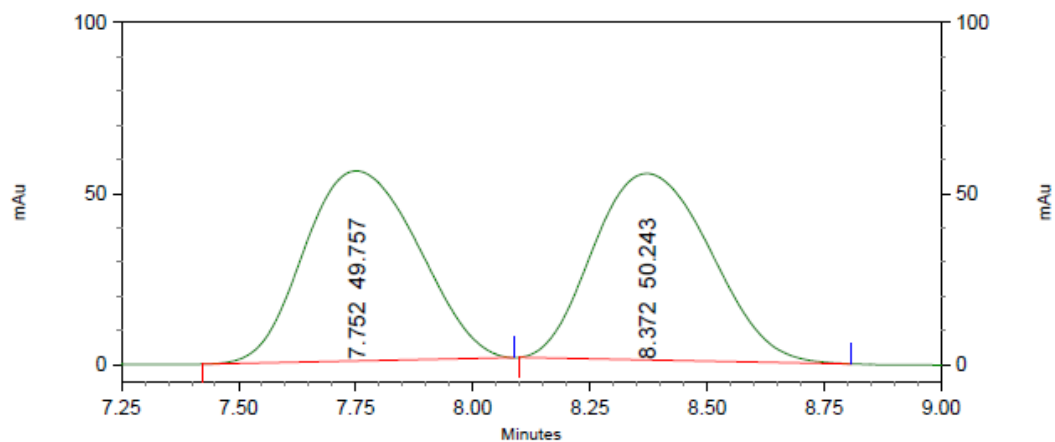


129.5
f1 (ppm)
127.5



2,2,2-Trichloroethyl 2-(2-bromophenyl)aziridine-1-carboxylate (31)

HPLC trace
racemic



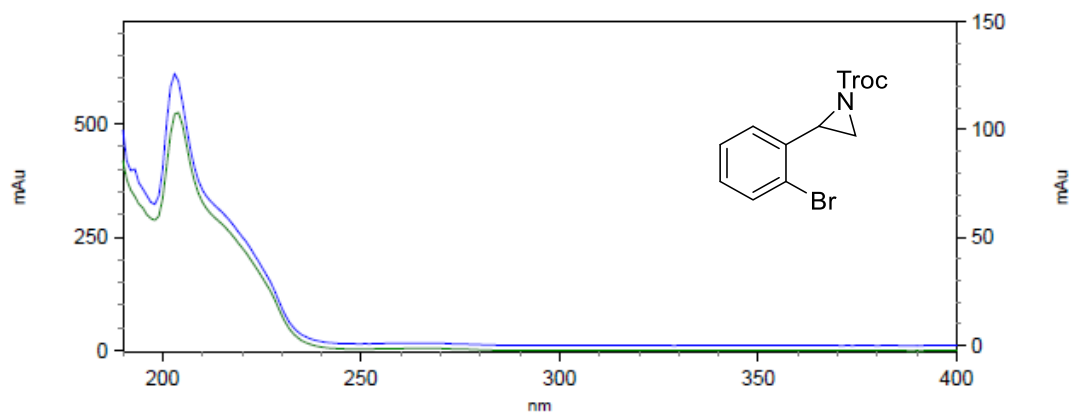
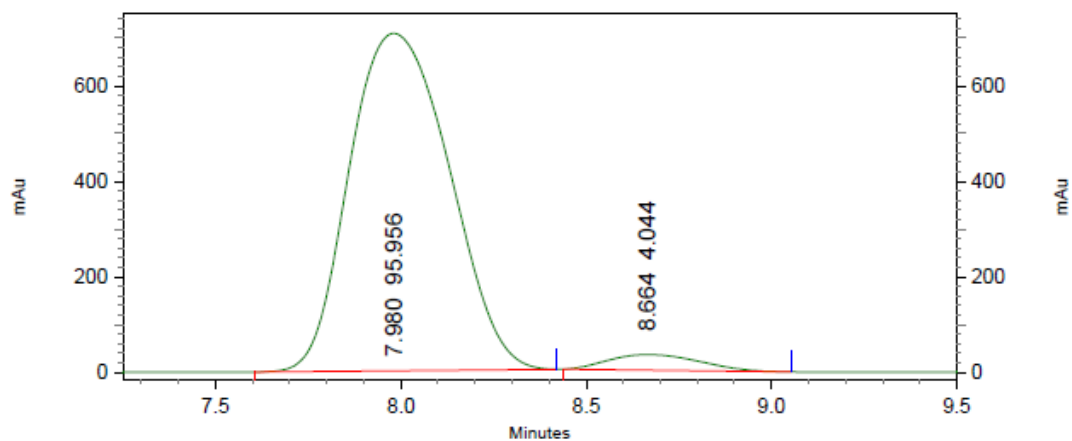
4: 225 nm, 4
nm Results

Pk #	Retention Time	Area Percent
1	7.752	49.757
2	8.372	50.243

Totals	100.000
--------	---------

2,2,2-Trichloroethyl 2-(2-bromophenyl)aziridine-1-carboxylate (3I)

HPLC trace



4: 225 nm, 4
nm Results

Pk #	Retention Time	Area Percent
1	7.980	95.956
2	8.664	4.044
Totals		100.000

2,2,2-Trichloroethyl 2-(3,5-dibromophenyl)aziridine-1-carboxylate (3m)

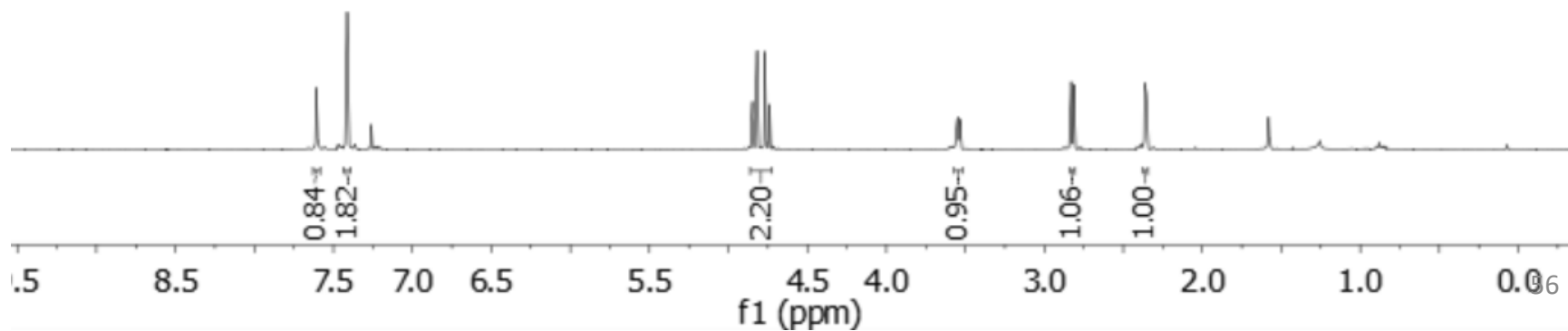
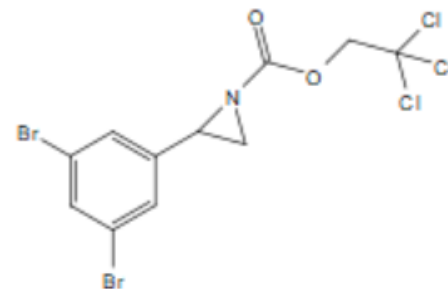
7.612
7.607
7.605
7.603
7.601
7.416
7.415
7.413
7.412
7.260

4.848
4.818
4.766
4.737

3.559
3.550
3.543
3.536

2.829
2.814
2.365
2.357

¹HNMR



2,2,2-Trichloroethyl 2-(3,5-dibromophenyl)aziridine-1-carboxylate (3m)

^{13}C NMR

-161.055

-140.530

-133.945

-128.333

-123.341

-94.873

77.478

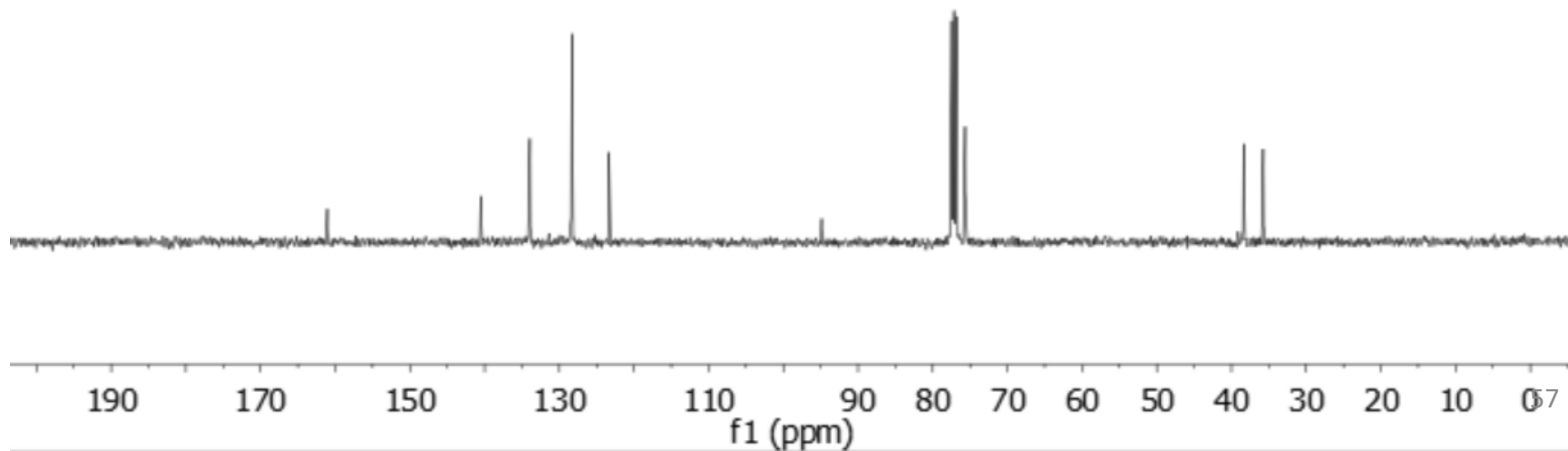
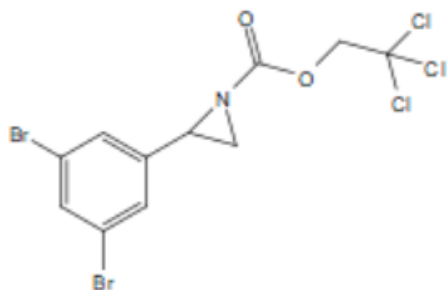
77.160

76.842

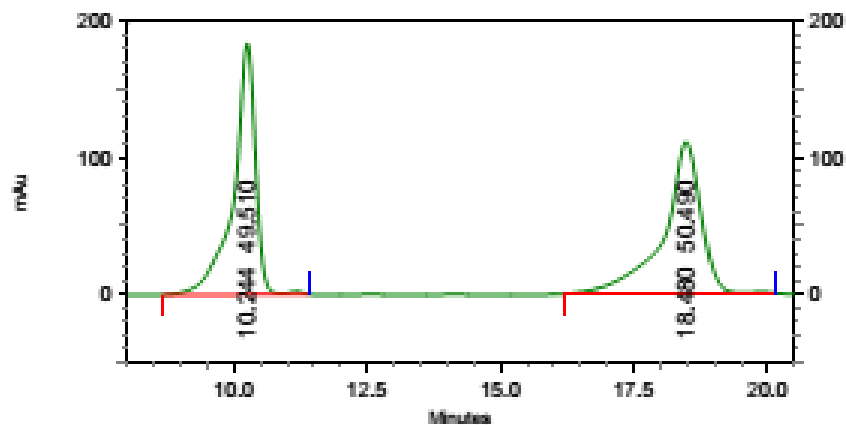
75.667

38.373

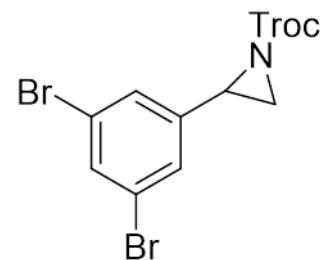
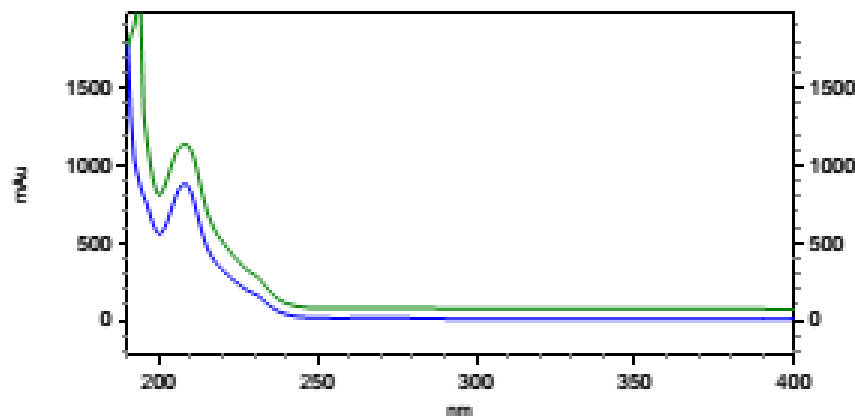
35.748



2,2,2-Trichloroethyl 2-(3,5-dibromophenyl)aziridine-1-carboxylate (3m)



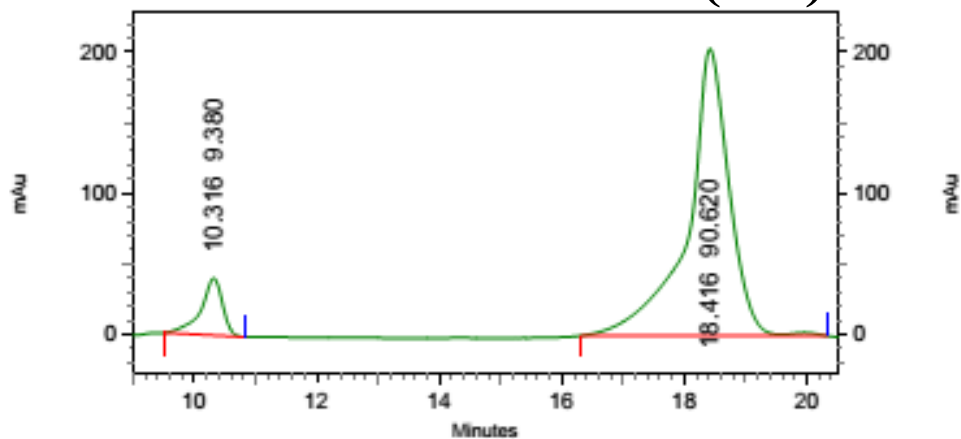
HPLC trace
racemic



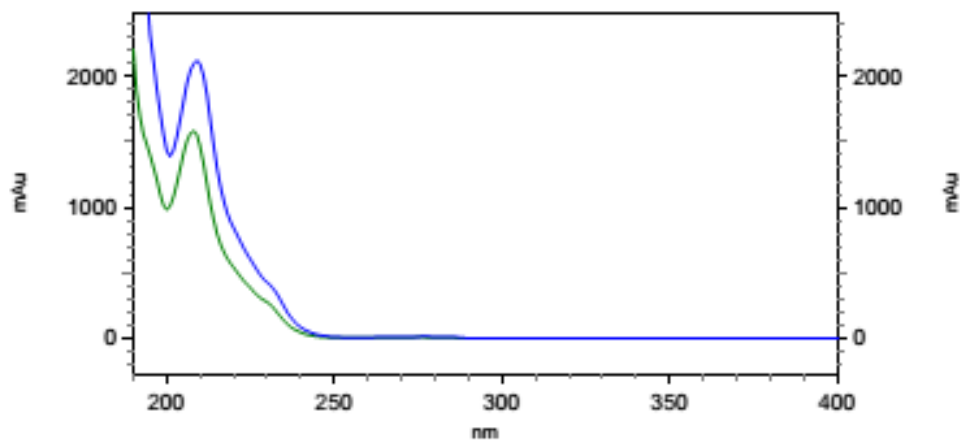
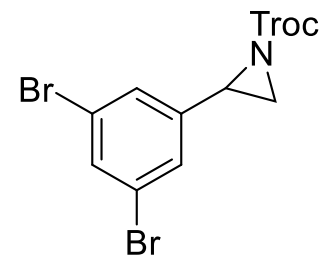
6: 228 nm, 4 nm
Results

Pk #	Name	Retention Time	Area Percent
1		10.244	49.510
2		18.480	50.490
Totals			100.000

2,2,2-Trichloroethyl 2-(3,5-dibromophenyl)aziridine-1-carboxylate (3m)



HPLC trace



3: 237 nm, 4 nm

Results

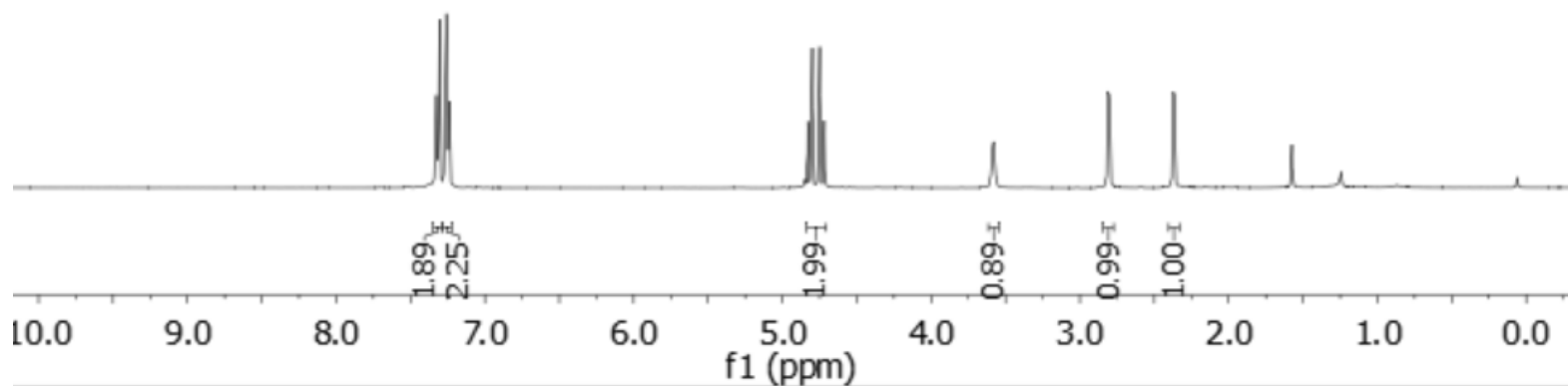
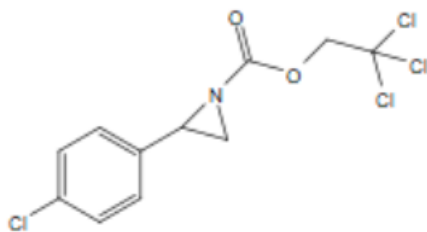
Name	Retention Time	Area Percent	Pk #
	10.316	9.380	1
	18.416	90.620	2

Totals		100.000	
--------	--	---------	--

2,2,2-Trichloroethyl 2-(4-chlorophenyl)aziridine-1-carboxylate (3n)

$^1\text{H NMR}$

7.326
7.321
7.310
7.305
7.300
7.259
7.254
7.249
7.243
7.238
4.828
4.798
4.749
4.719
3.595
3.586
3.579
3.570
2.814
2.798
2.374
2.365



2,2,2-Trichloroethyl 2-(4-chlorophenyl)aziridine-1-carboxylate (3n)

^{13}C NMR

-161.238

134.882

133.978

128.778

127.630

-94.828

77.318

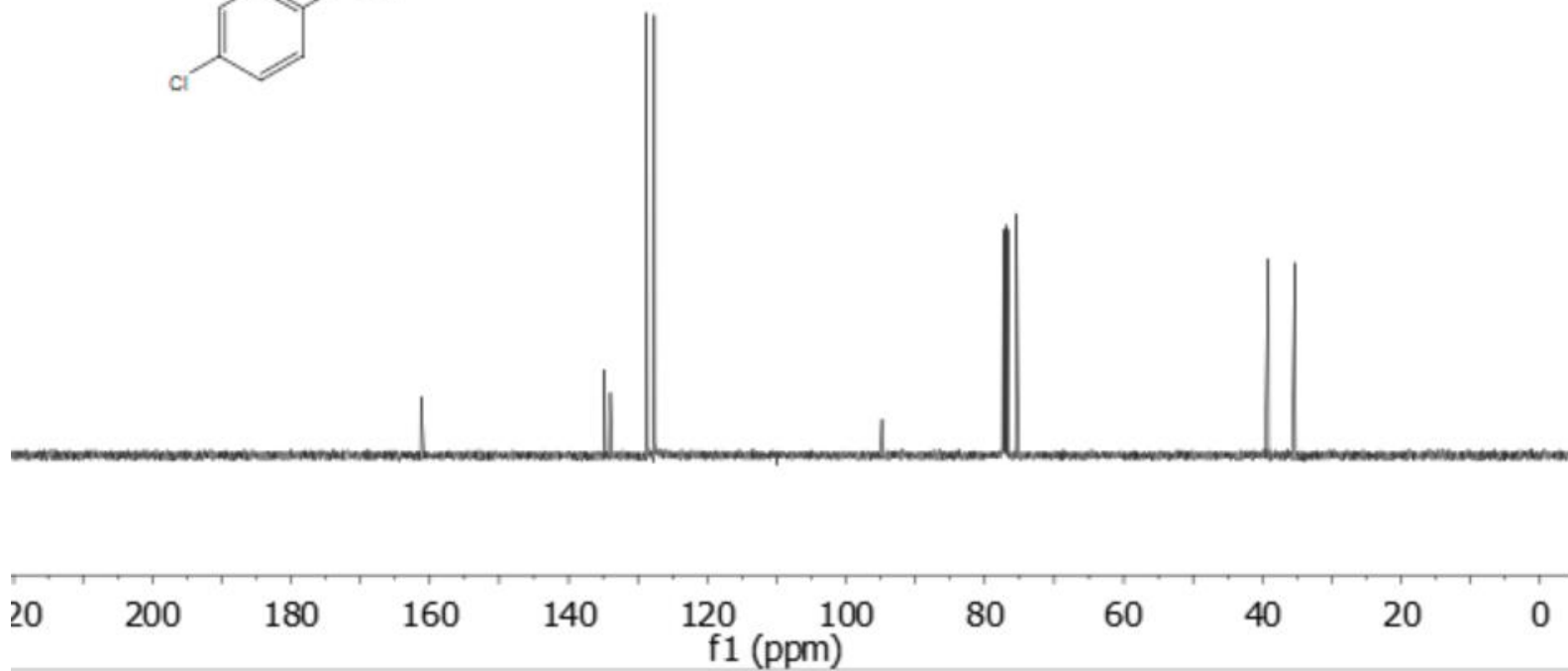
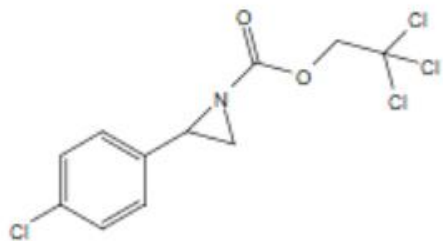
77.001

76.682

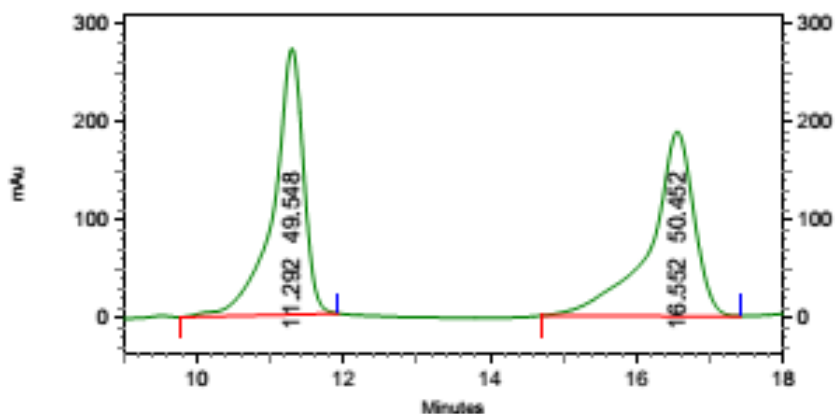
75.435

-39.128

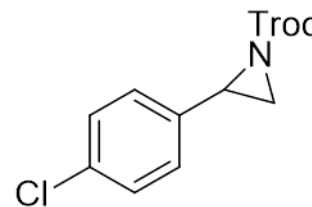
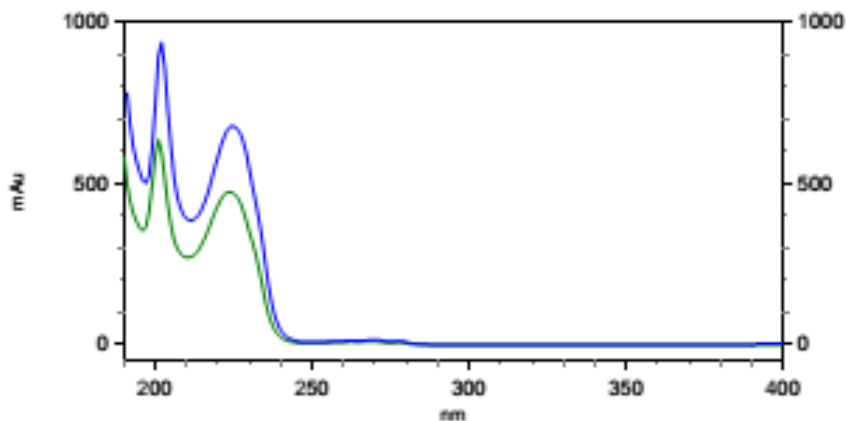
-35.318



2,2,2-Trichloroethyl 2-(4-chlorophenyl)aziridine-1-carboxylate (3n)



HPLC trace
racemic



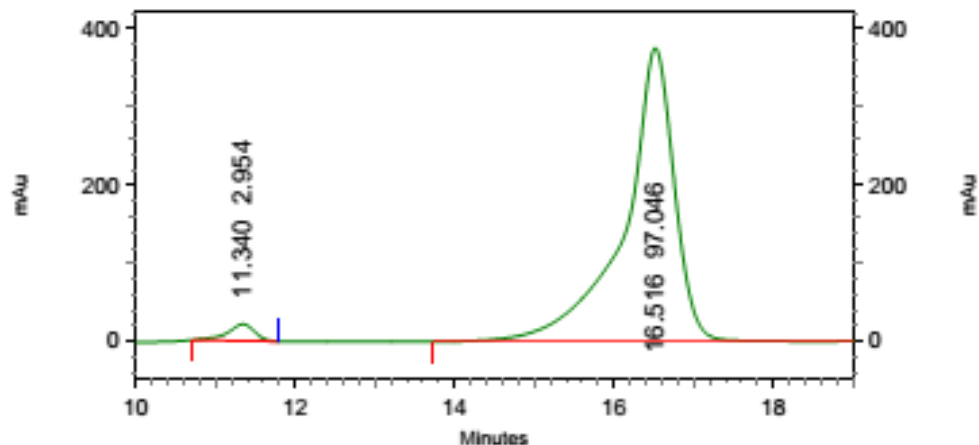
3: 232 nm, 4 nm

Results

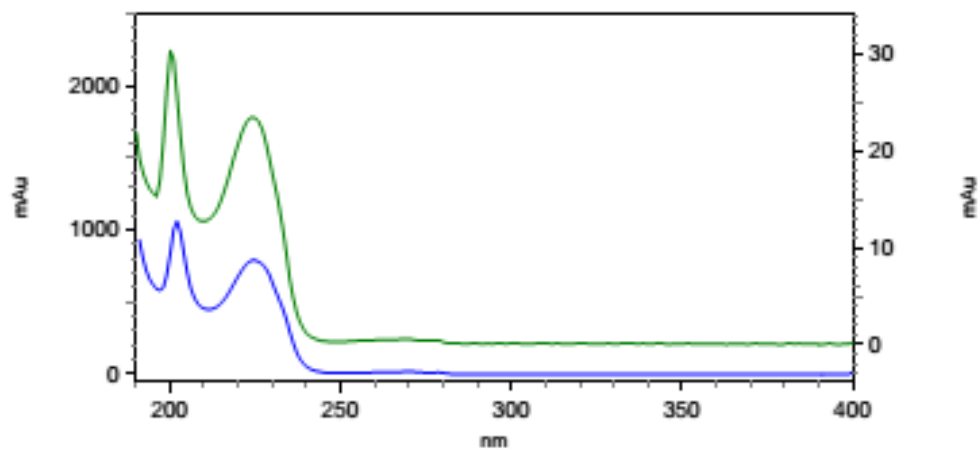
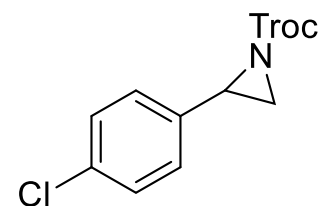
Name	Retention Time	Area Percent	Pk #
	11.292	49.548	1
	16.552	50.452	2

Totals	100.000
--------	---------

2,2,2-Trichloroethyl 2-(4-chlorophenyl)aziridine-1-carboxylate (3n)



HPLC trace



3: 226 nm, 4 nm

Results

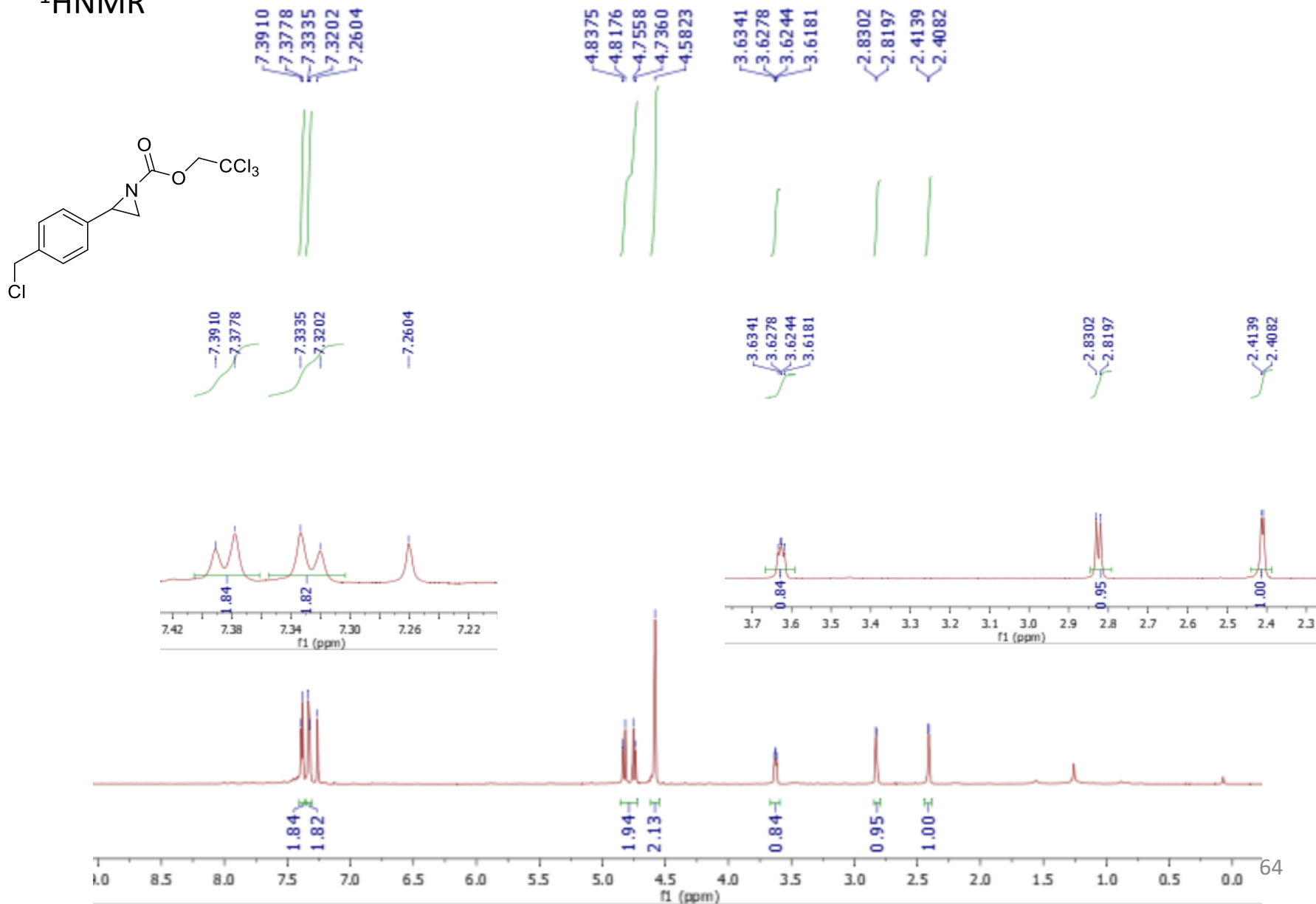
Name	Retention Time	Area Percent	Pk #
	11.340	2.954	1
	16.516	97.046	2

Totals

100.000

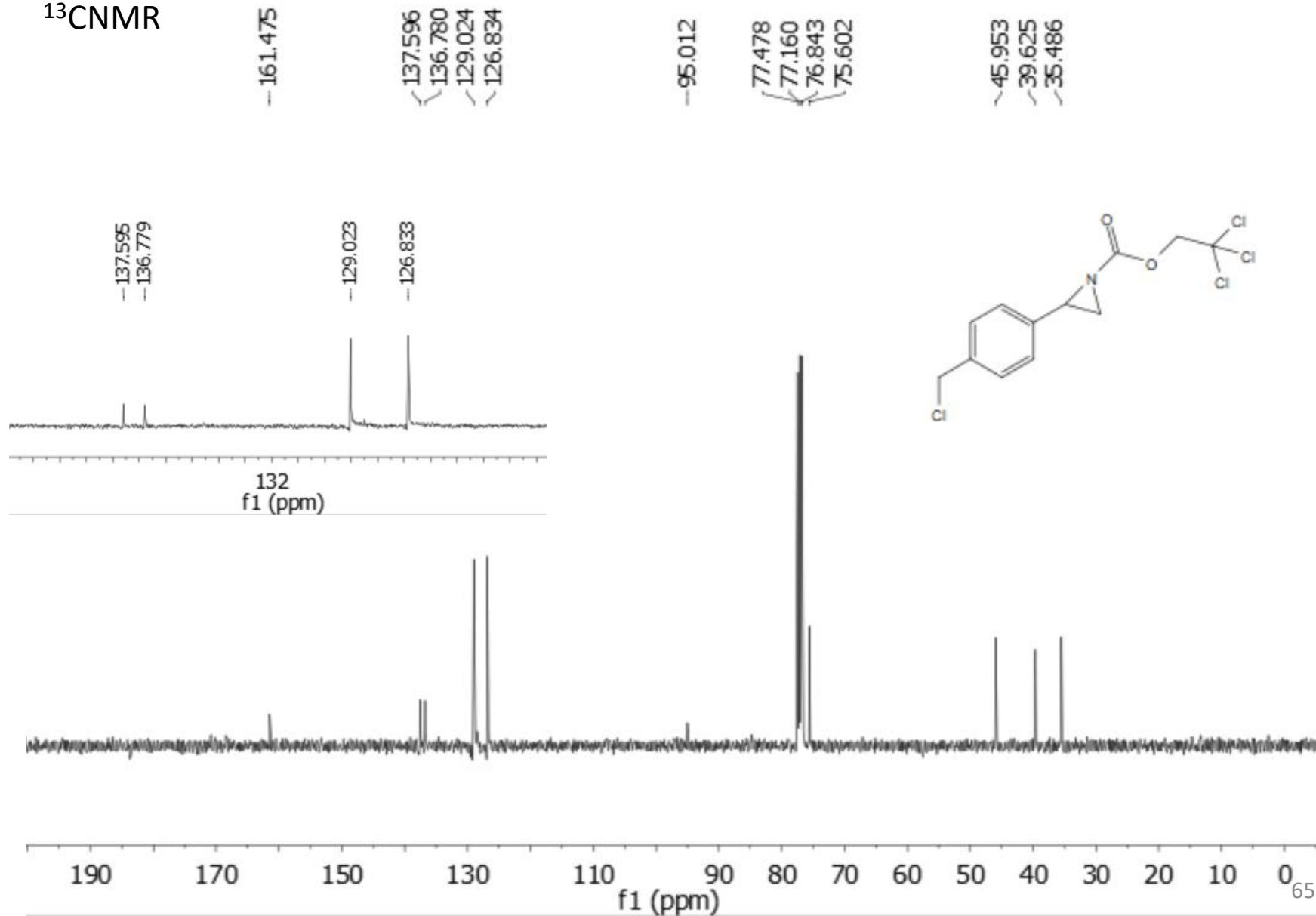
2,2,2-Trichloroethyl 2-(4-(chloromethyl)phenyl)aziridine-1-carboxylate (30)

^1H NMR



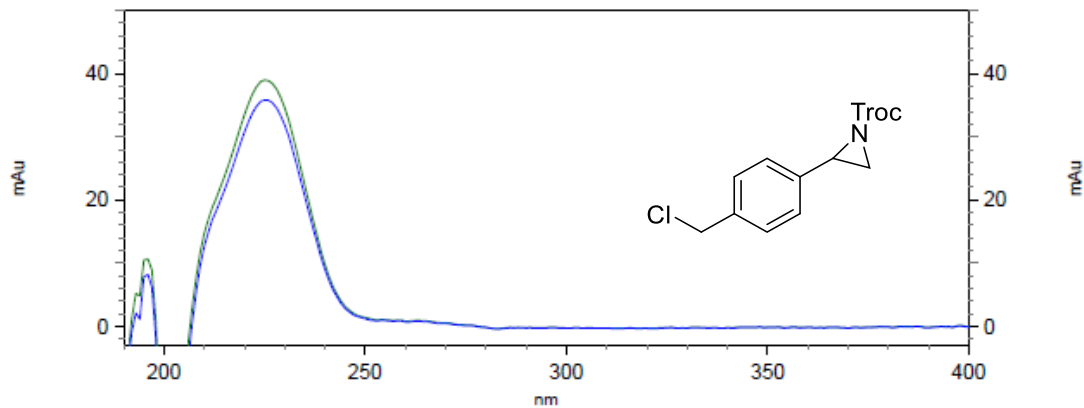
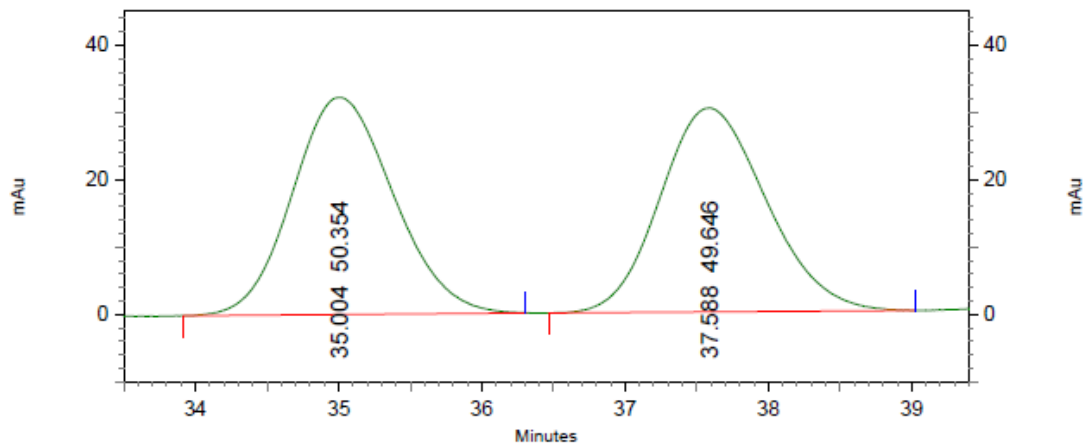
2,2,2-Trichloroethyl 2-(4-(chloromethyl)phenyl)aziridine-1-carboxylate (30)

^{13}C NMR



2,2,2-Trichloroethyl 2-(4-(chloromethyl)phenyl)aziridine-1-carboxylate (30)

HPLC trace
racemic

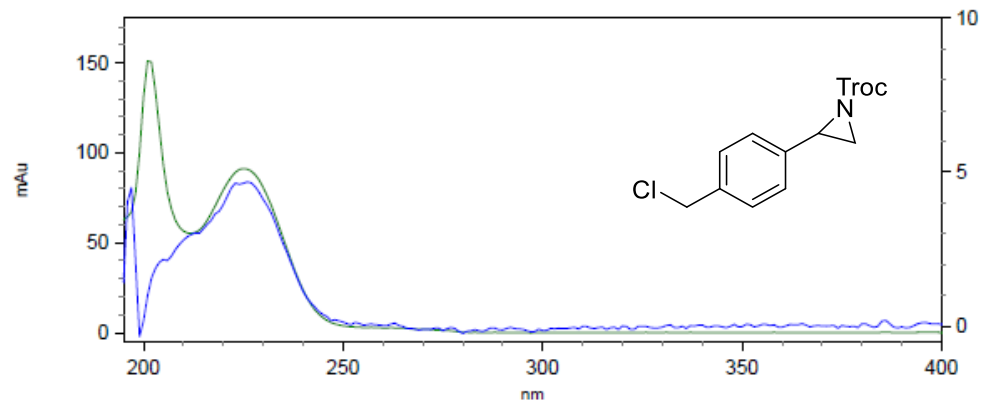
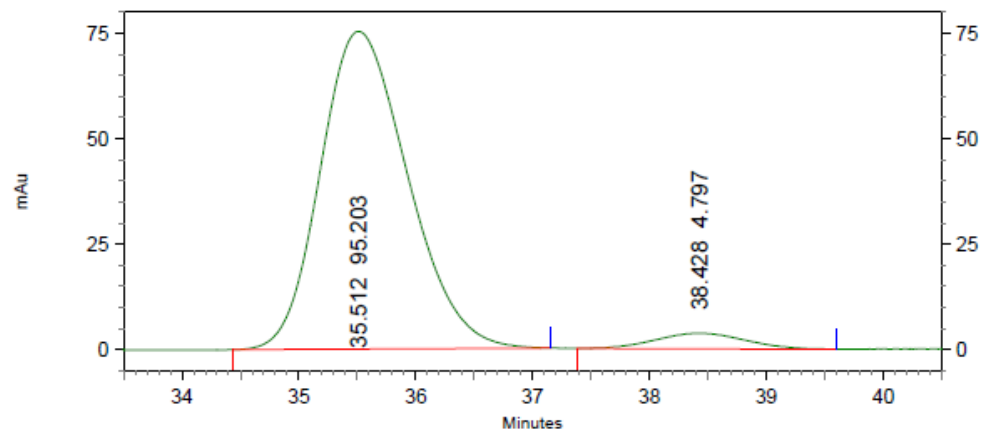


4: 231 nm, 4
nm Results

Pk #	Retention Time	Area Percent
1	35.004	50.354
2	37.588	49.646
Totals		100.000

2,2,2-Trichloroethyl 2-(4-(chloromethyl)phenyl)aziridine-1-carboxylate (30)

HPLC trace

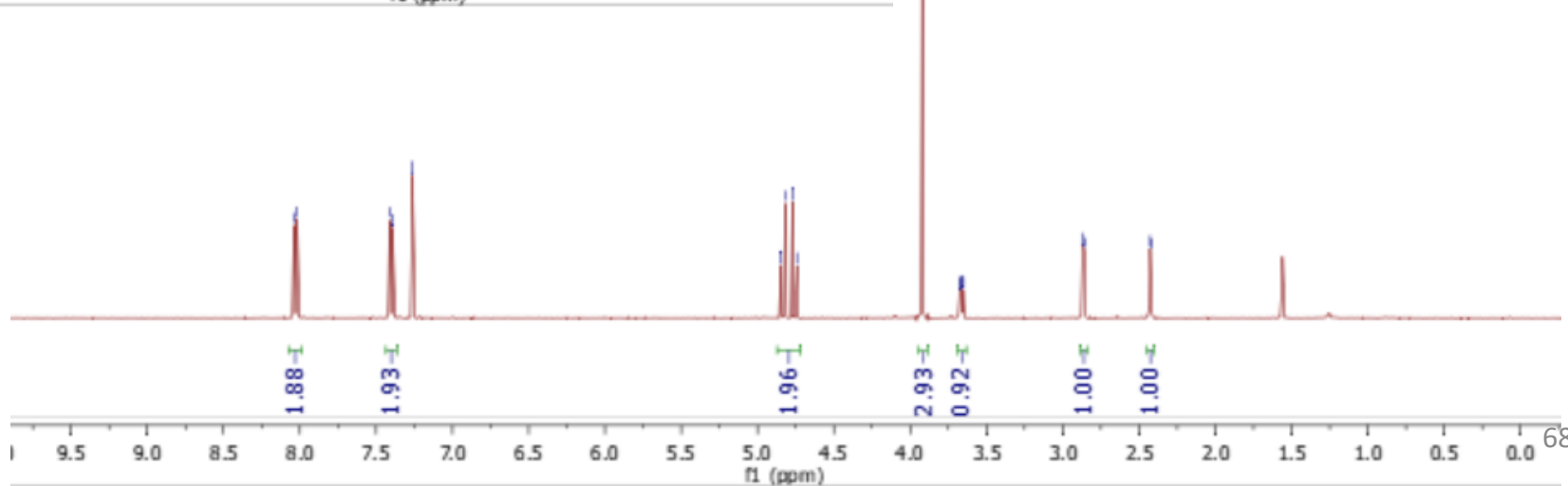
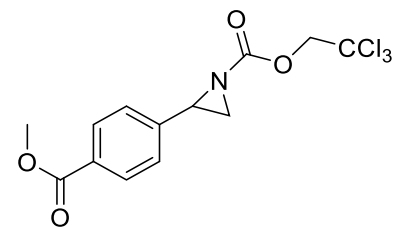
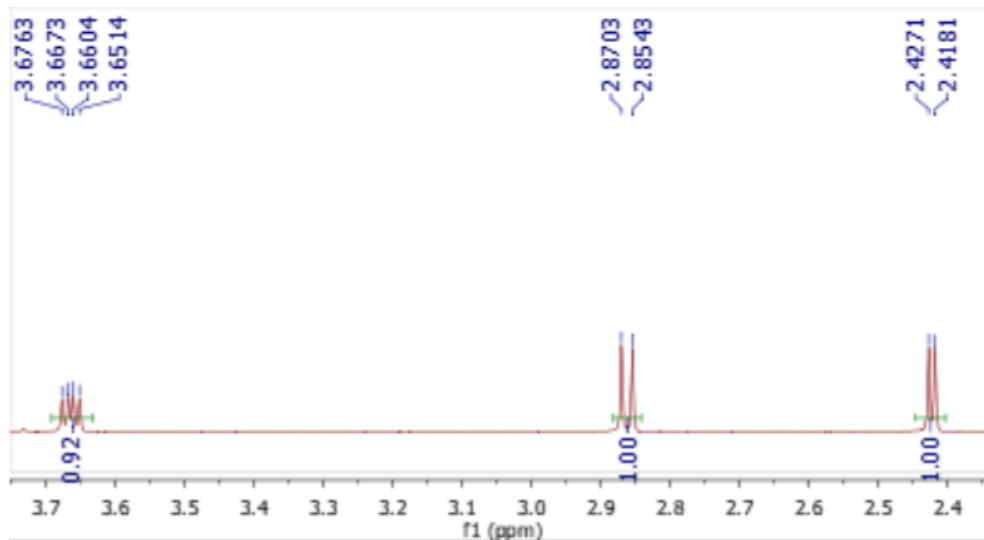


4: 231 nm, 4
nm Results

Pk #	Retention Time	Area Percent
1	35.512	95.203
2	38.428	4.797
Totals		100.000

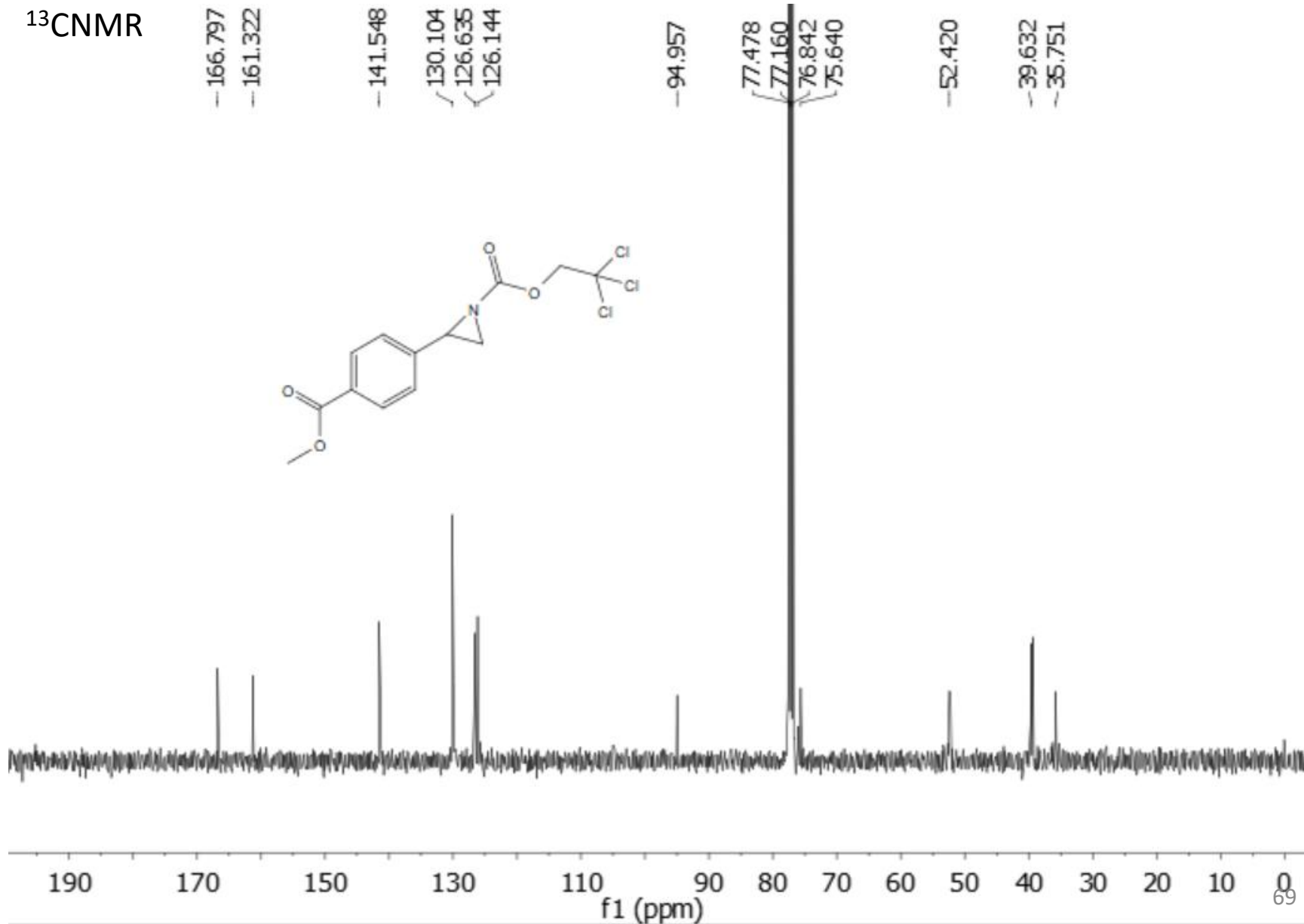
2,2,2-Trichloroethyl 2-(4-(methoxycarbonyl)phenyl)aziridine-1-carboxylate (3p)

$^1\text{H NMR}$



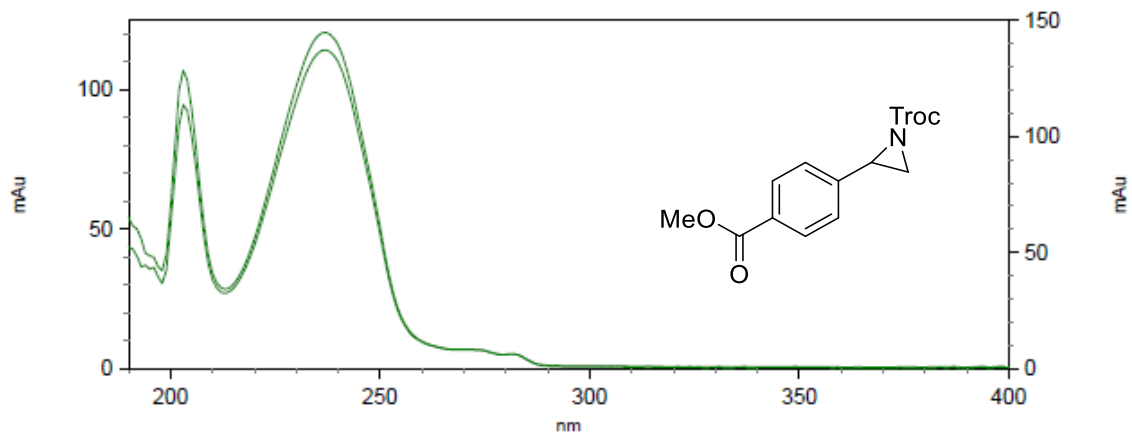
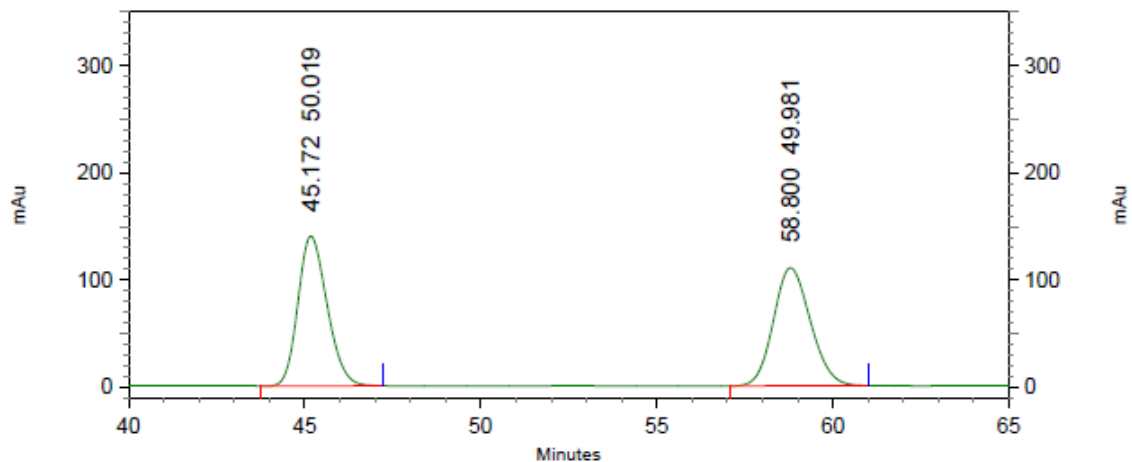
2,2,2-Trichloroethyl 2-(4-(methoxycarbonyl)phenyl)aziridine-1-carboxylate (3p)

¹³CNMR



2,2,2-Trichloroethyl 2-(4-(methoxycarbonyl)phenyl)aziridine-1-carboxylate (3p)

HPLC trace
racemic

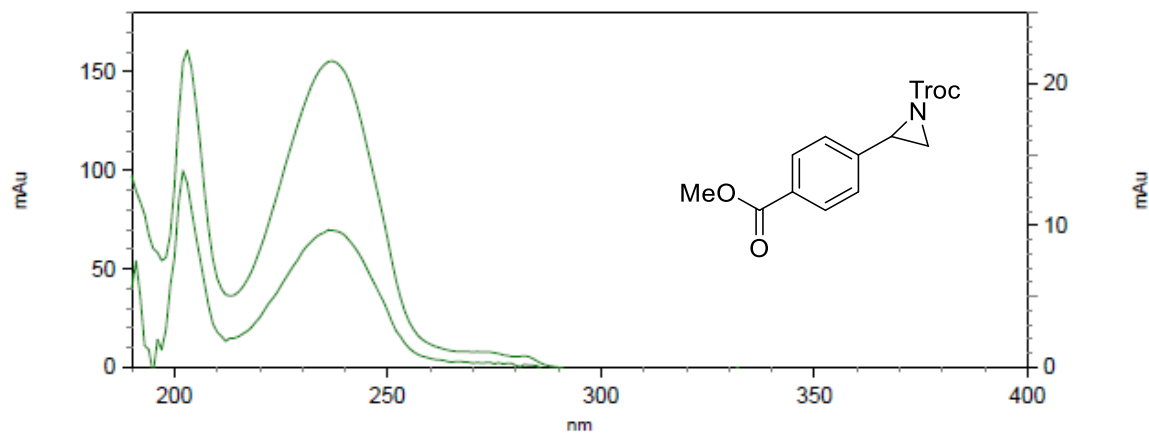
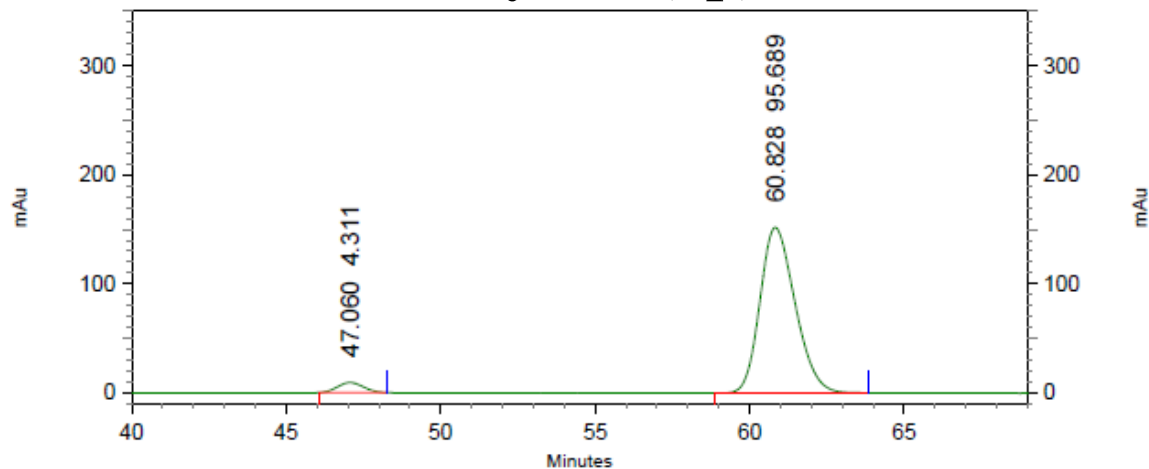


4: 239 nm, 4
nm Results

Pk #	Retention Time	Area Percent
1	45.172	50.019
2	58.800	49.981
Totals		100.000

2,2,2-Trichloroethyl 2-(4-(methoxycarbonyl)phenyl)aziridine-1-carboxylate (3p)

HPLC trace



4: 239 nm, 4
nm Results

Pk #	Retention Time	Area Percent
1	47.060	4.311
2	60.828	95.689
Totals		100.000

2,2,2-Trichloroethyl 2-(4-(trifluoromethyl)phenyl)aziridine-1-carboxylate (3q)

¹HNMR

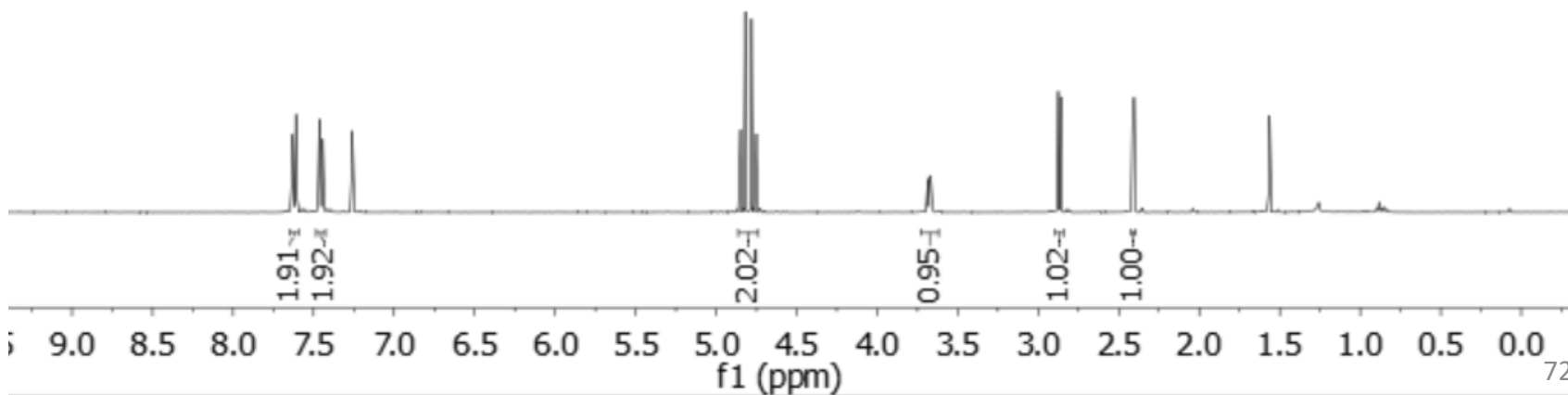
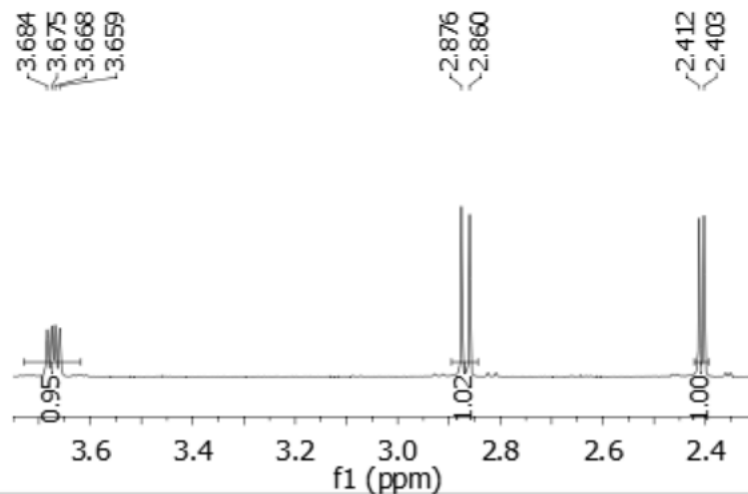
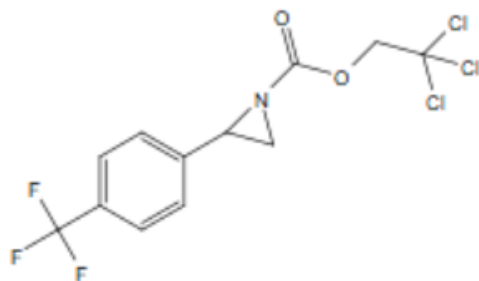
7.629
7.609
7.463
7.443
7.260

4.849
4.819
4.780
4.750

3.684
3.675
3.668
3.659

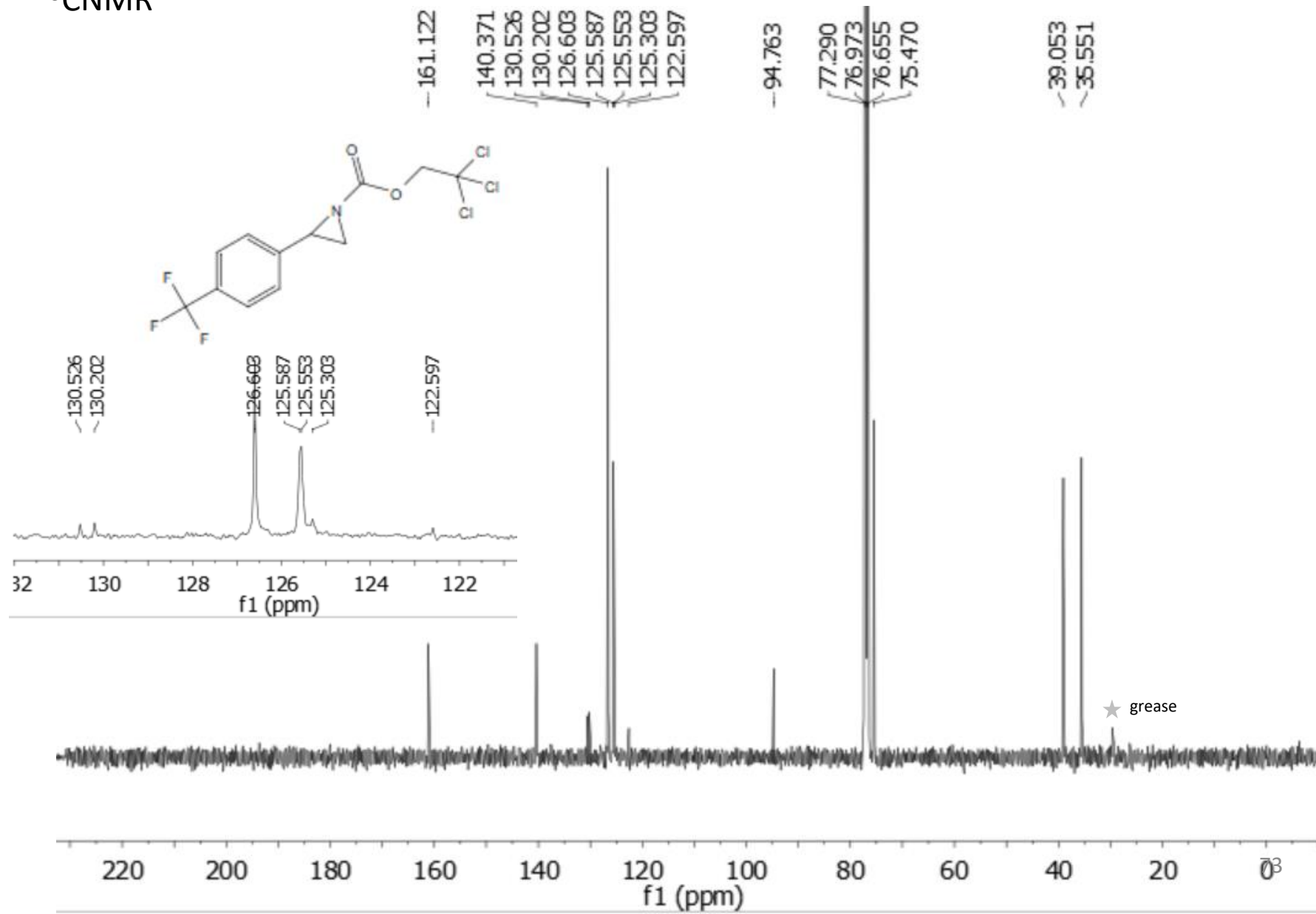
2.876
2.860

2.412
2.403



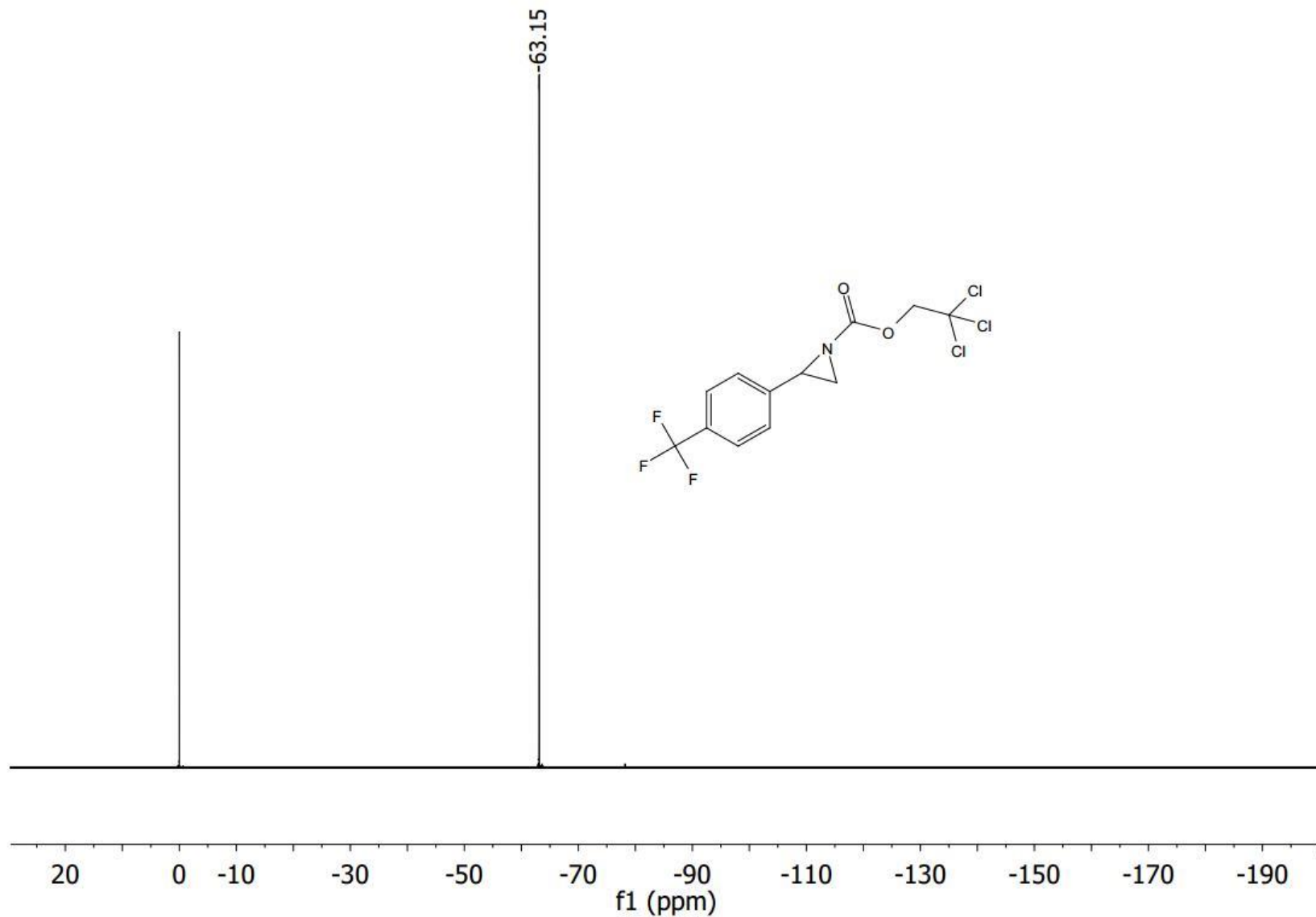
2,2,2-Trichloroethyl 2-(4-(trifluoromethyl)phenyl)aziridine-1-carboxylate (3q)

¹³CNMR



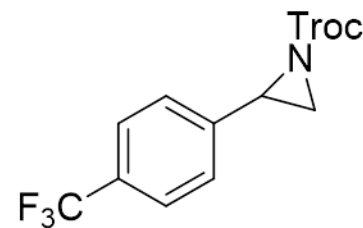
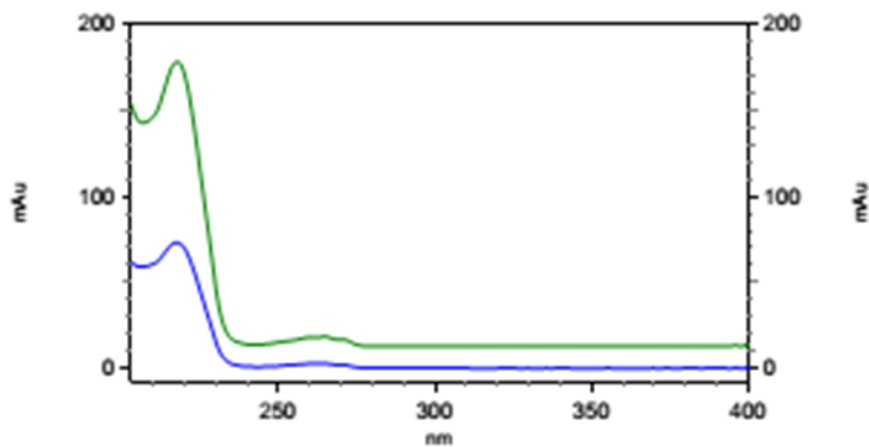
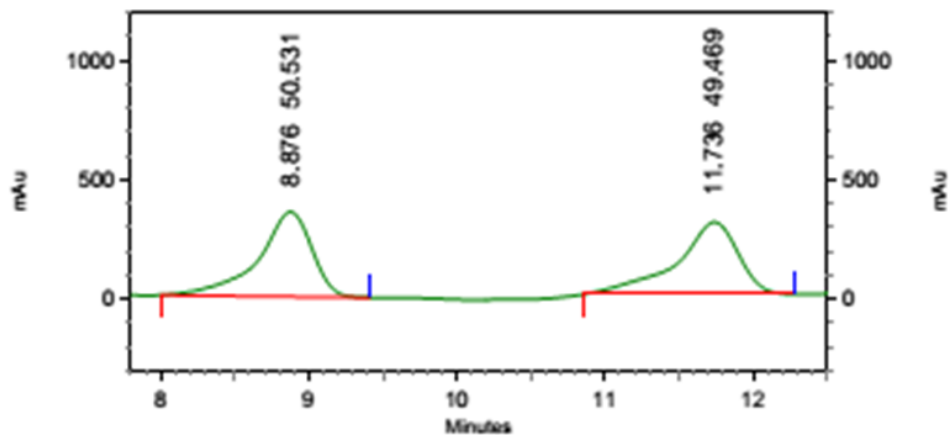
2,2,2-Trichloroethyl 2-(4-(trifluoromethyl)phenyl)aziridine-1-carboxylate (3q)

^{19}F NMR



2,2,2-Trichloroethyl 2-(4-(trifluoromethyl)phenyl)aziridine-1-carboxylate (3q)

HPLC trace
racemic



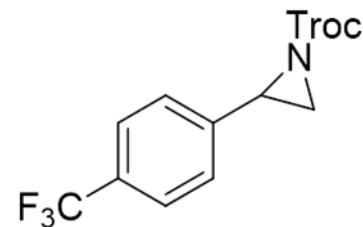
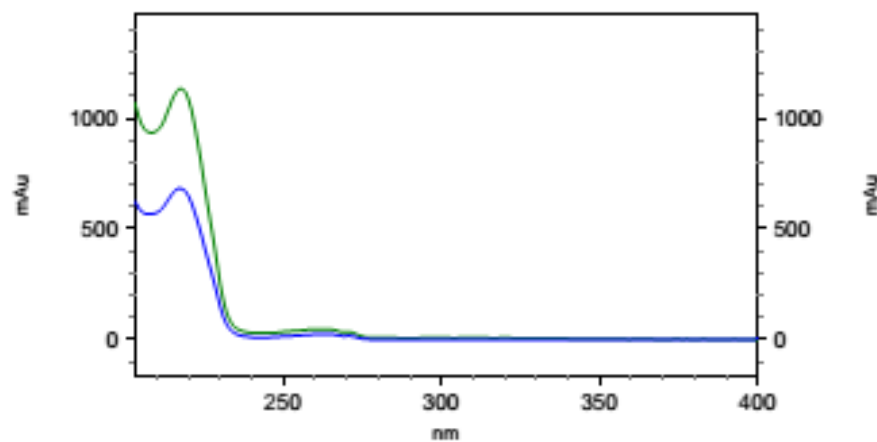
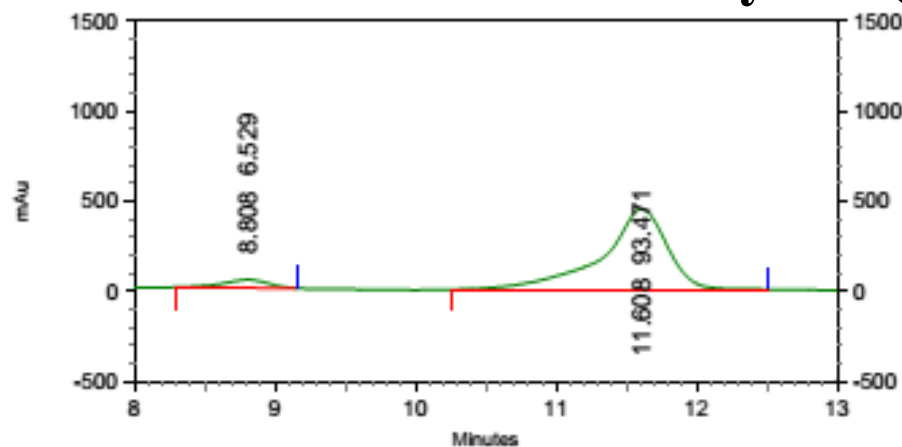
4: 226 nm, 4 nm

Results

Pk #	Name	Retention Time	Area Percent
1		8.876	50.531
2		11.736	49.469
Totals			100.000

2,2,2-Trichloroethyl 2-(4-(trifluoromethyl)phenyl)aziridine-1-carboxylate (3q)

HPLC trace



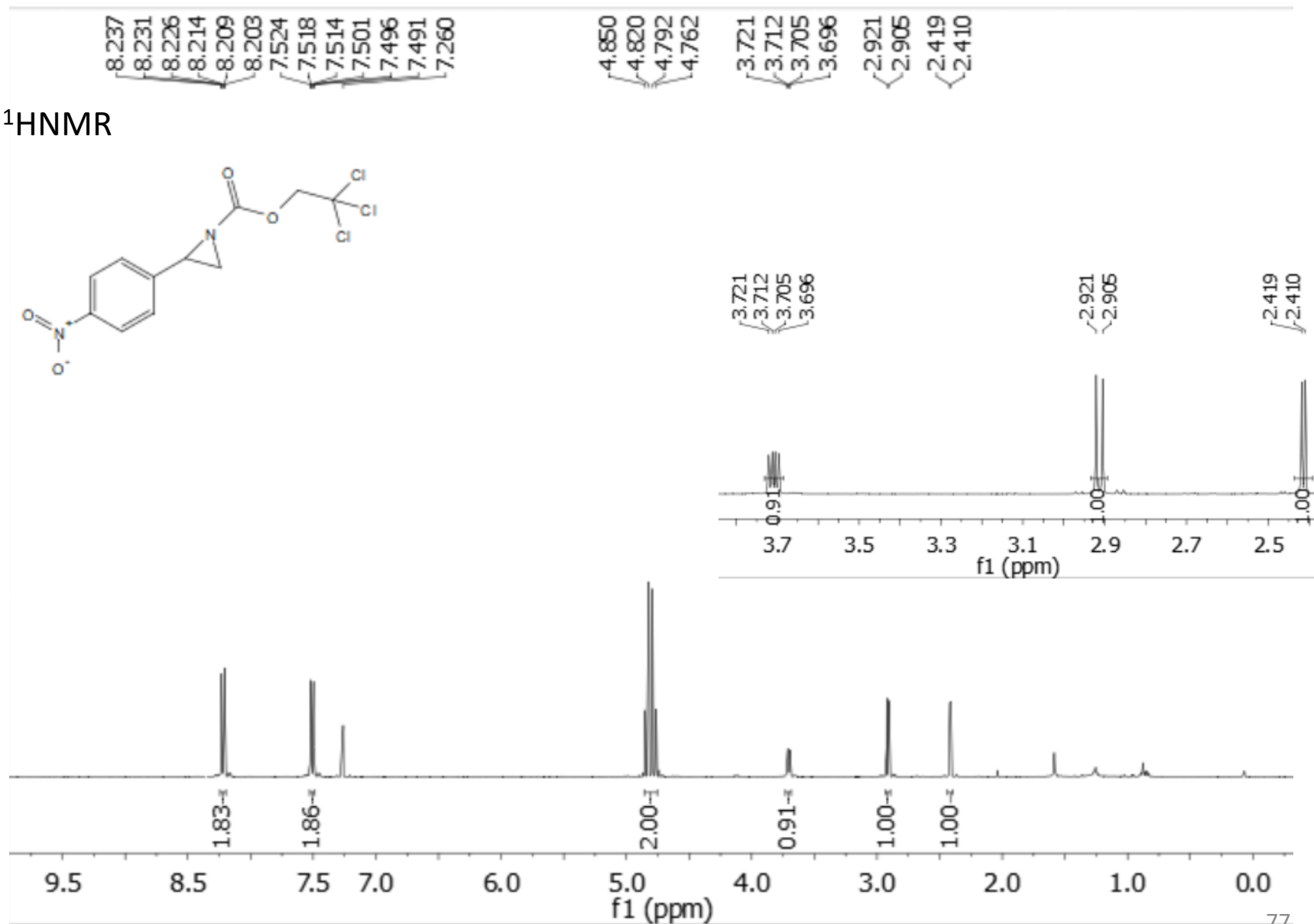
4: 233 nm, 4 nm

Results

Pk #	Name	Retention Time	Area Percent
1		8.808	6.529
2		11.608	93.471
Totals			100.000

2,2,2-Trichloroethyl 2-(4-nitrophenyl)aziridine-1-carboxylate (3r)

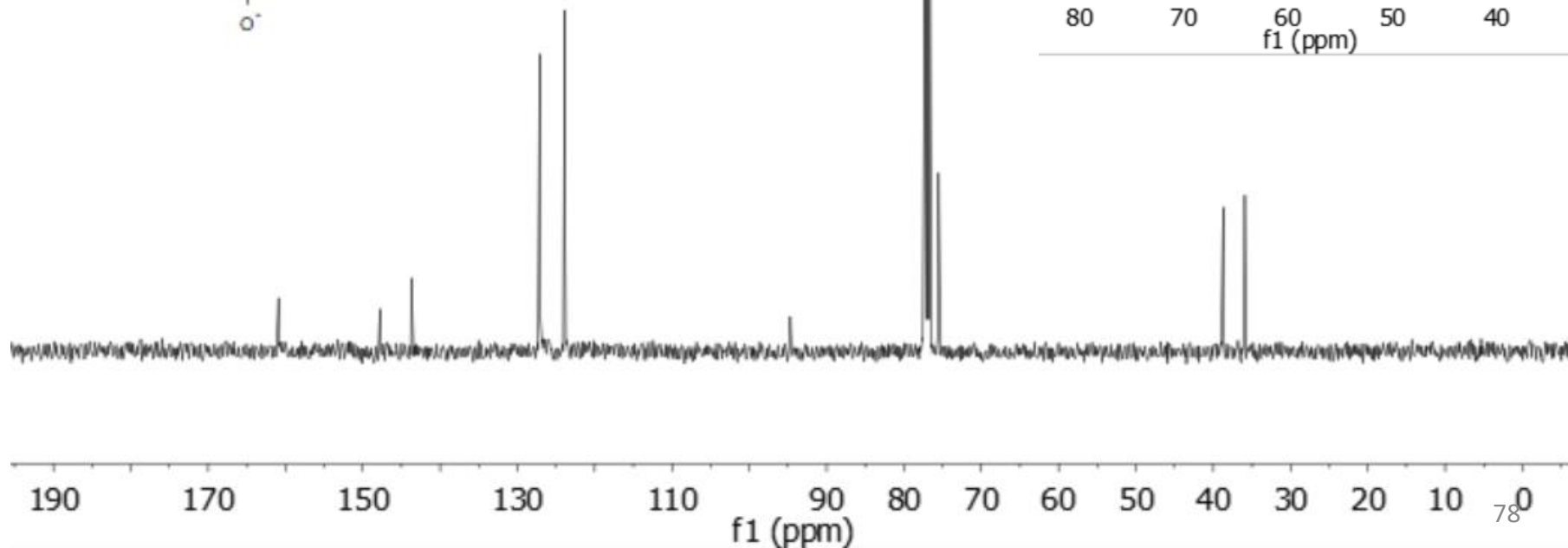
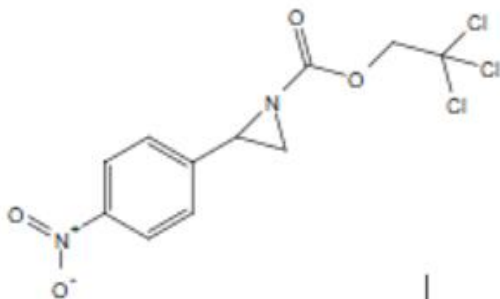
$^1\text{H NMR}$



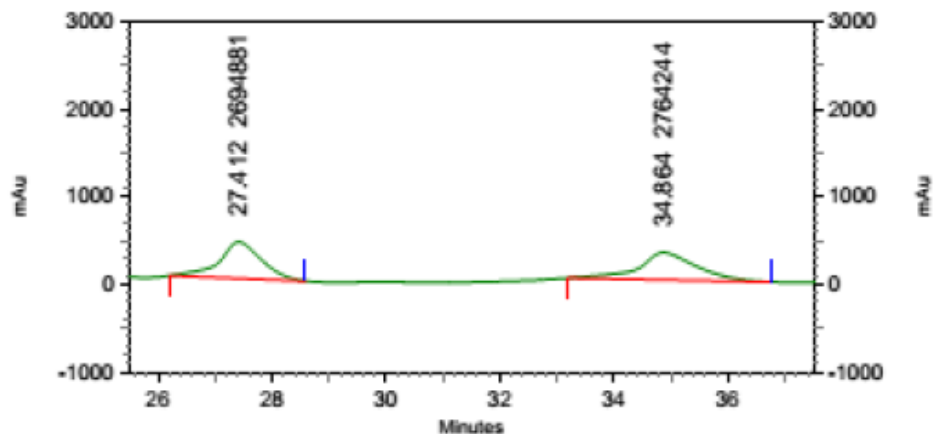
2,2,2-Trichloroethyl 2-(4-nitrophenyl)aziridine-1-carboxylate (3r)

^{13}C NMR

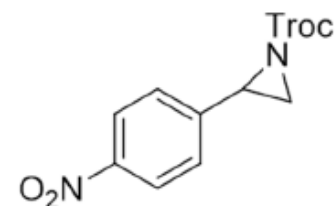
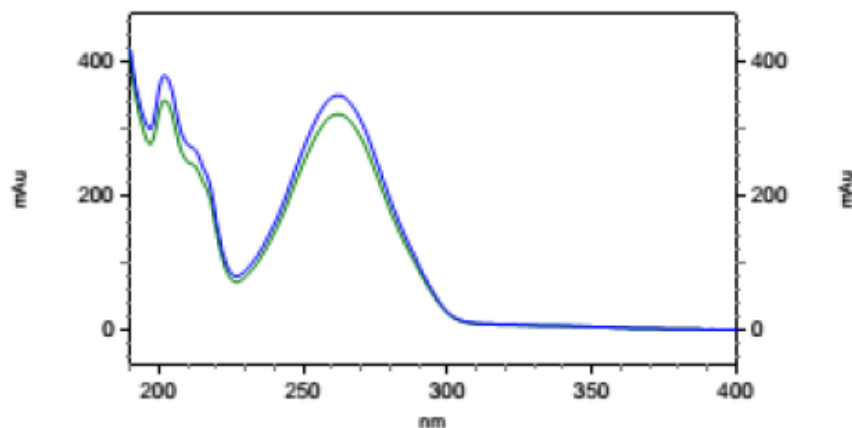
-160.903
-147.760
-143.693
-127.116
-123.873
-94.695
77.304
76.986
76.669
75.513
-38.713
-35.915



2,2,2-Trichloroethyl 2-(4-nitrophenyl)aziridine-1-carboxylate (3r)



HPLC trace
racemic

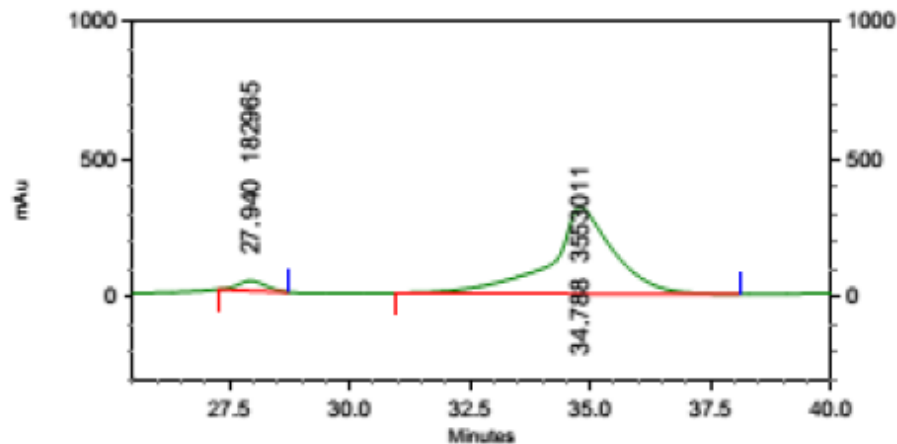


4: 297 nm, 4 nm

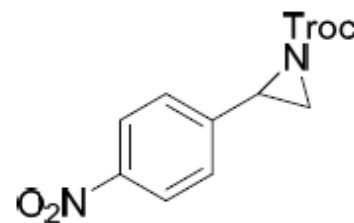
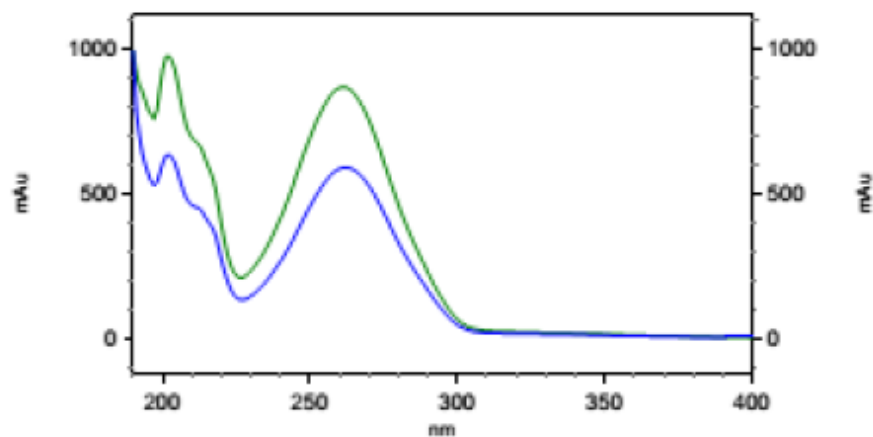
Results

Pk #	Name	Retention Time	Area Percent
1		27.412	49.365
2		34.864	50.635
Totals			100.000

2,2,2-Trichloroethyl 2-(4-nitrophenyl)aziridine-1-carboxylate (3r)



HPLC trace



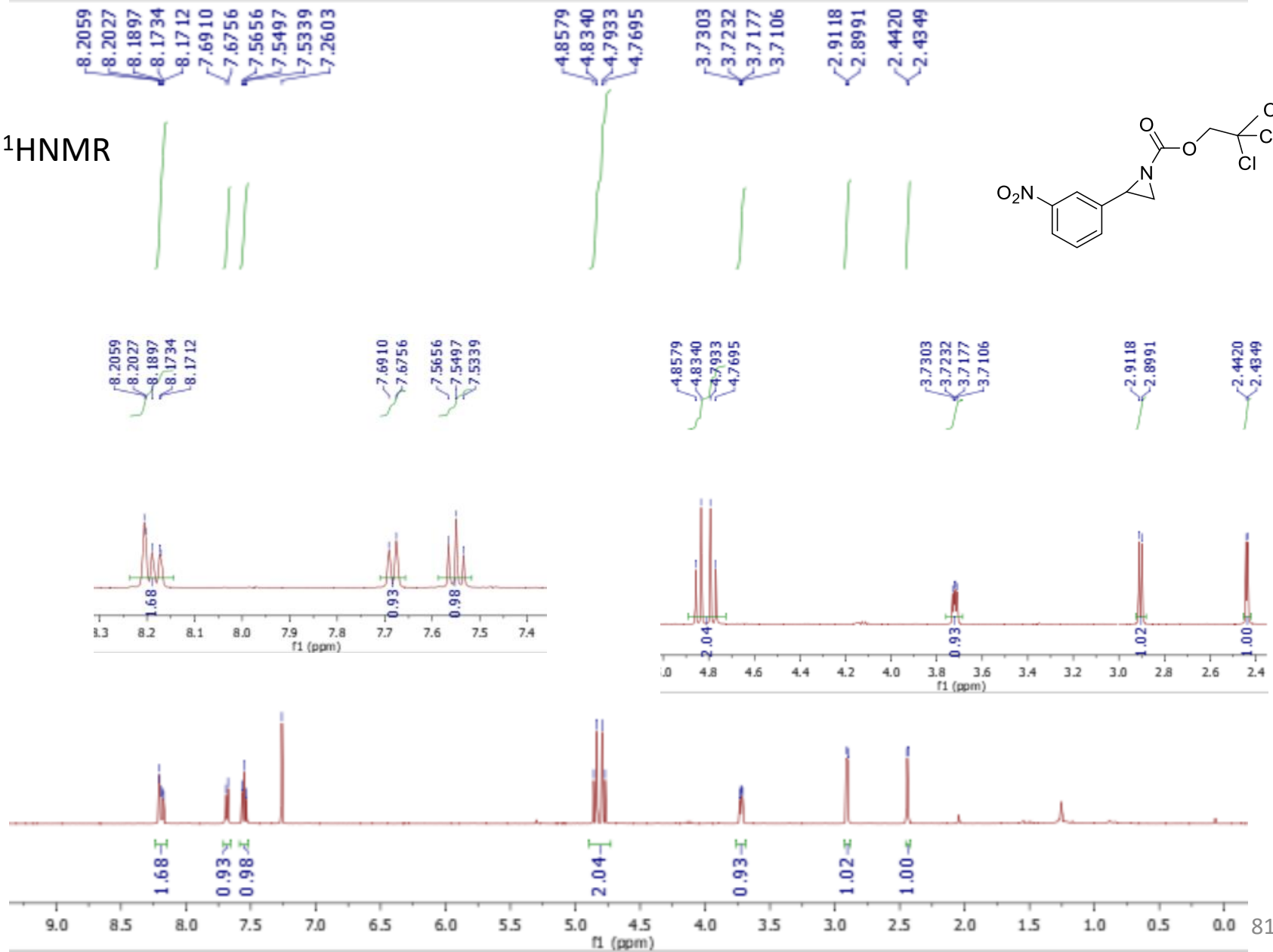
4: 301 nm, 4 nm

Results

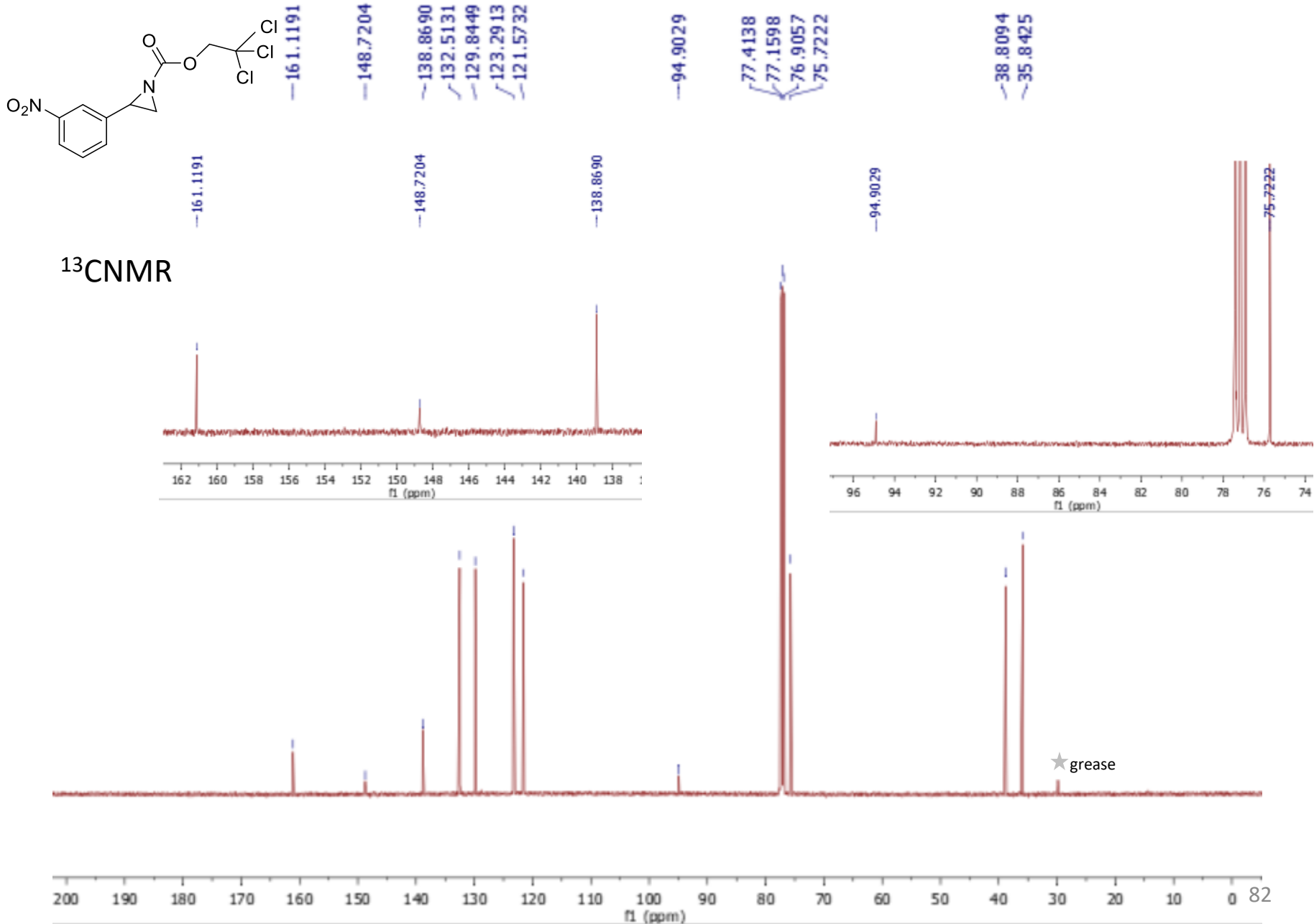
Pk #	Name	Retention Time	Area Percent
1		27.940	4.897
2		34.788	95.103
Totals			100.000

2,2,2-Trichloroethyl 2-(3-nitro)aziridine-1-carboxylate (3s)

¹HNMR

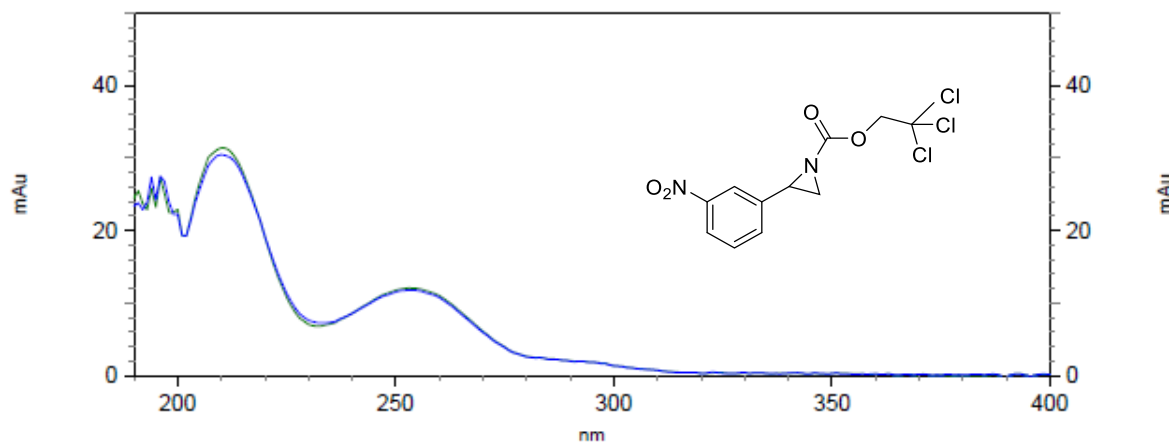
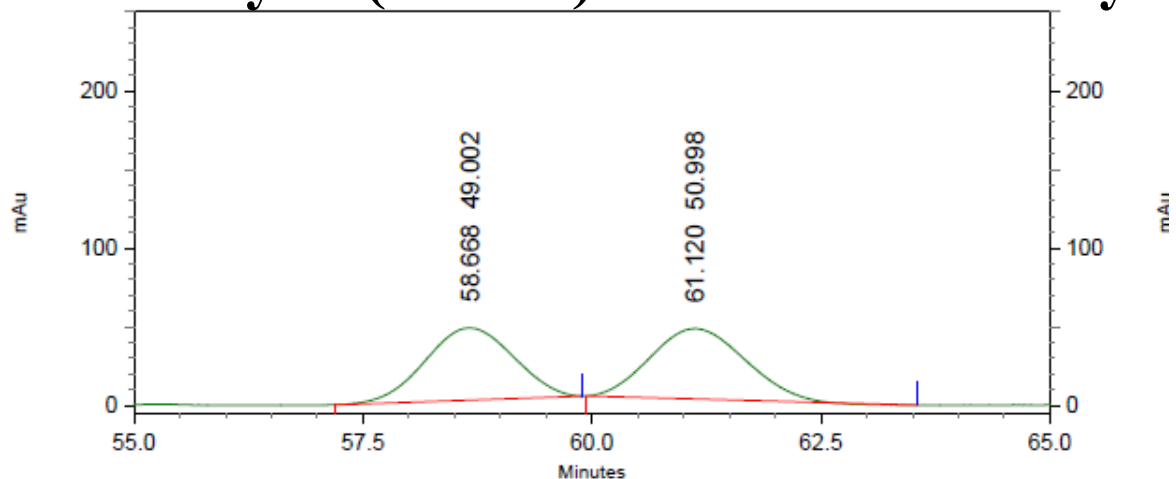


2,2,2-Trichloroethyl 2-(3-nitro)aziridine-1-carboxylate (3s)



2,2,2-Trichloroethyl 2-(3-nitro)aziridine-1-carboxylate (3s)

HPLC trace
racemic



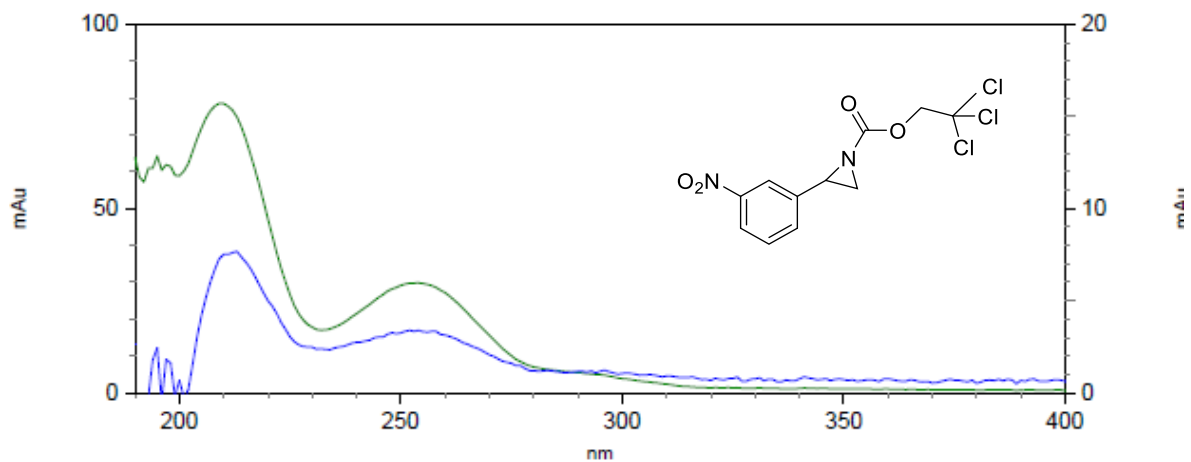
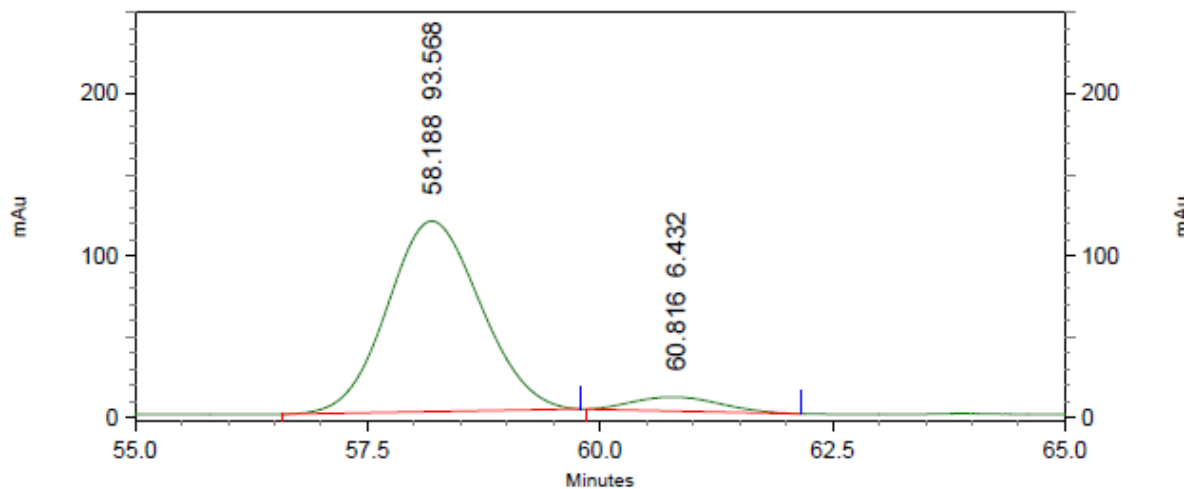
2: 217 nm, 4
nm Results

Pk #	Retention Time	Area Percent
1	58.668	49.002
2	61.120	50.998

Totals		100.000
--------	--	---------

2,2,2-Trichloroethyl 2-(3-nitro)aziridine-1-carboxylate (3s)

HPLC trace

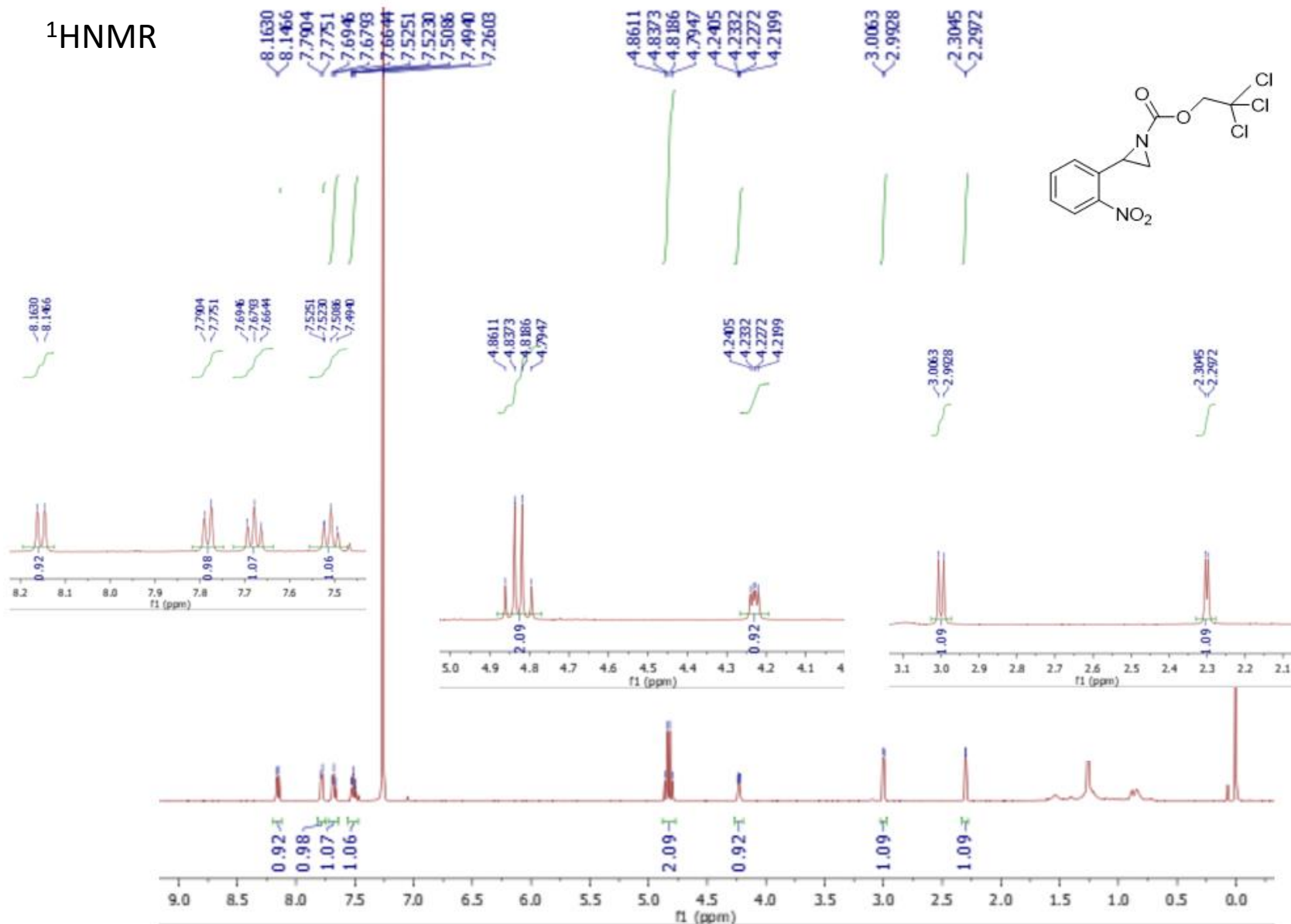


2: 217 nm, 4
nm Results

Pk #	Retention Time	Area Percent
1	58.188	93.568
2	60.816	6.432
Totals		100.000

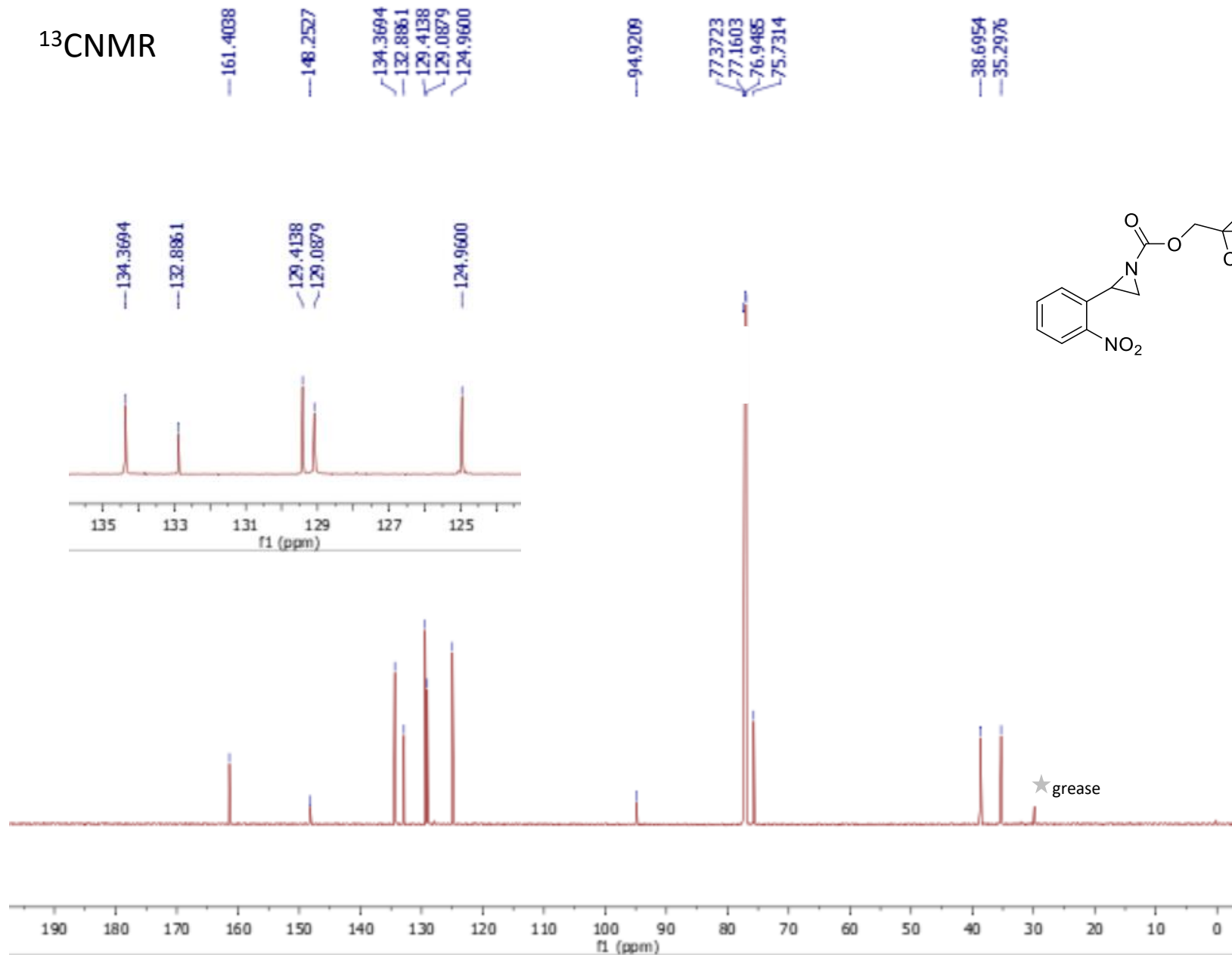
2,2,2-Trichloroethyl 2-(2-nitro)aziridine-1-carboxylate (3t)

¹H NMR



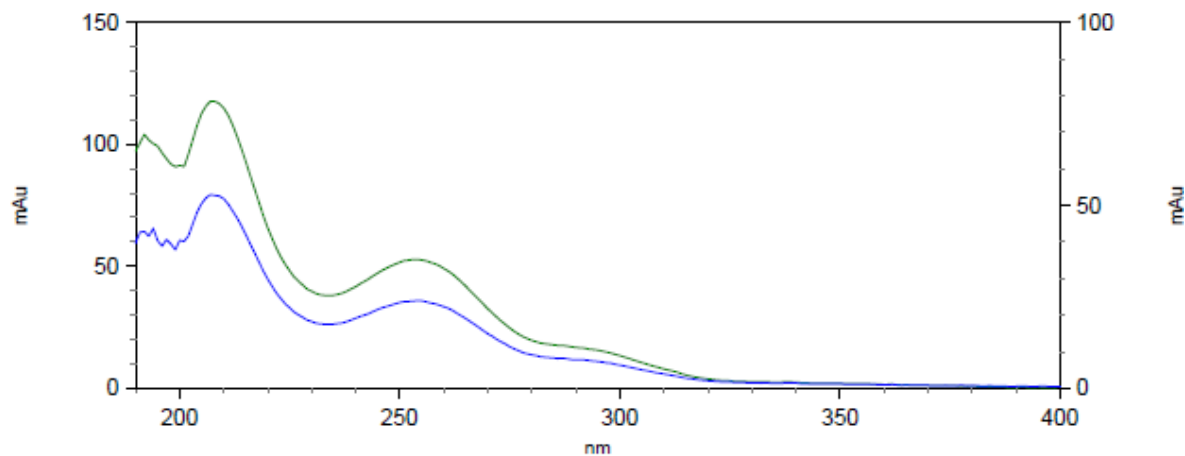
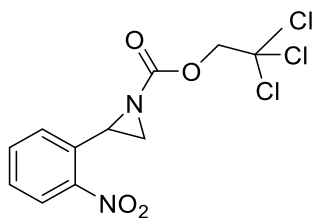
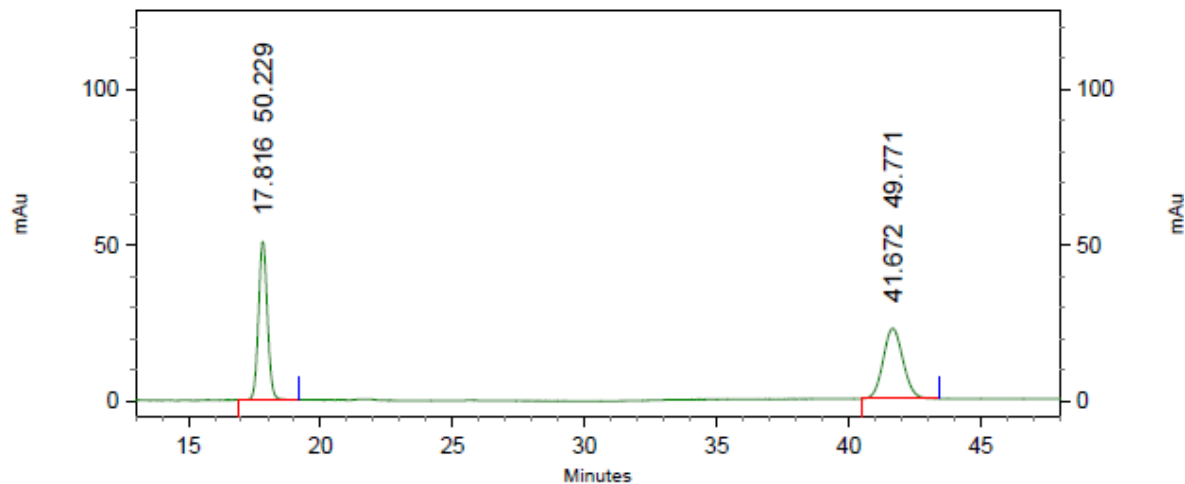
2,2,2-Trichloroethyl 2-(2-nitro)aziridine-1-carboxylate (3t)

¹³CNMR



2,2,2-Trichloroethyl 2-(2-nitro)aziridine-1-carboxylate (3t)

HPLC trace
racemic



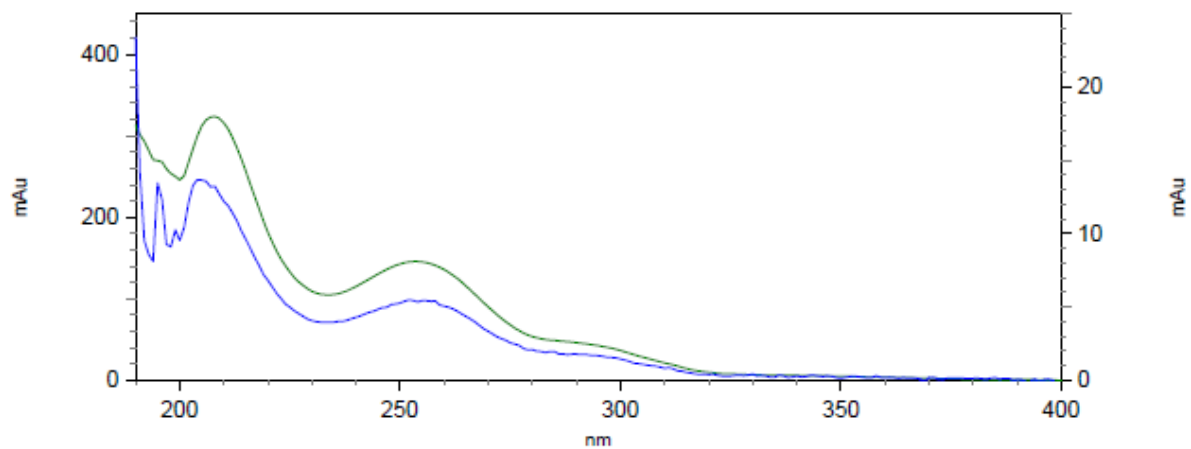
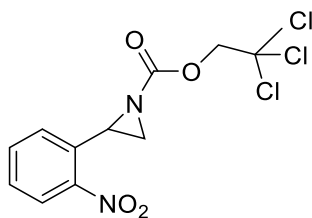
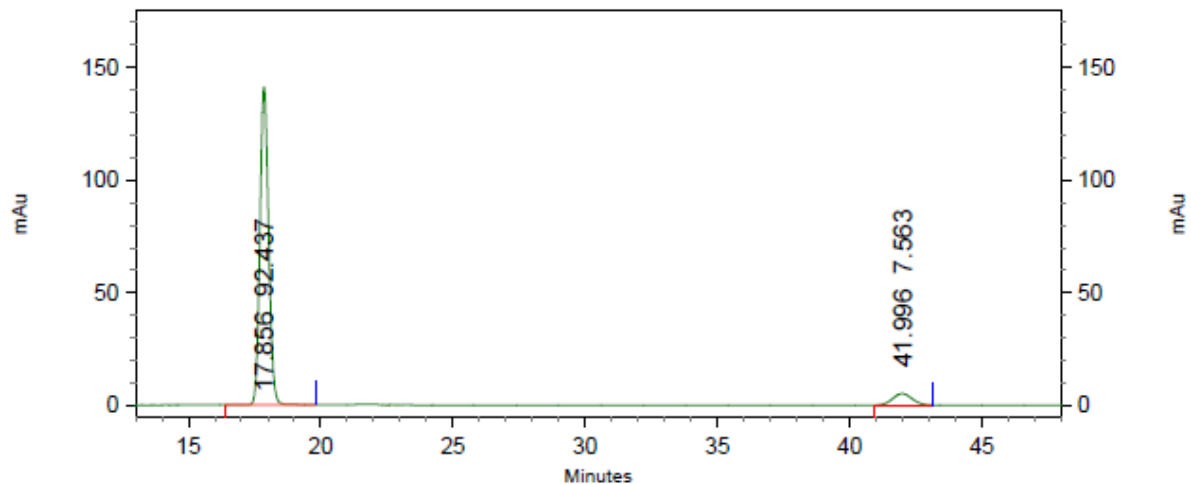
4: 224 nm, 4
nm Results

Pk #	Retention Time	Area Percent
1	17.816	50.229
2	41.672	49.771

Totals		100.000
--------	--	---------

2,2,2-Trichloroethyl 2-(2-nitro)aziridine-1-carboxylate (3t)

HPLC trace

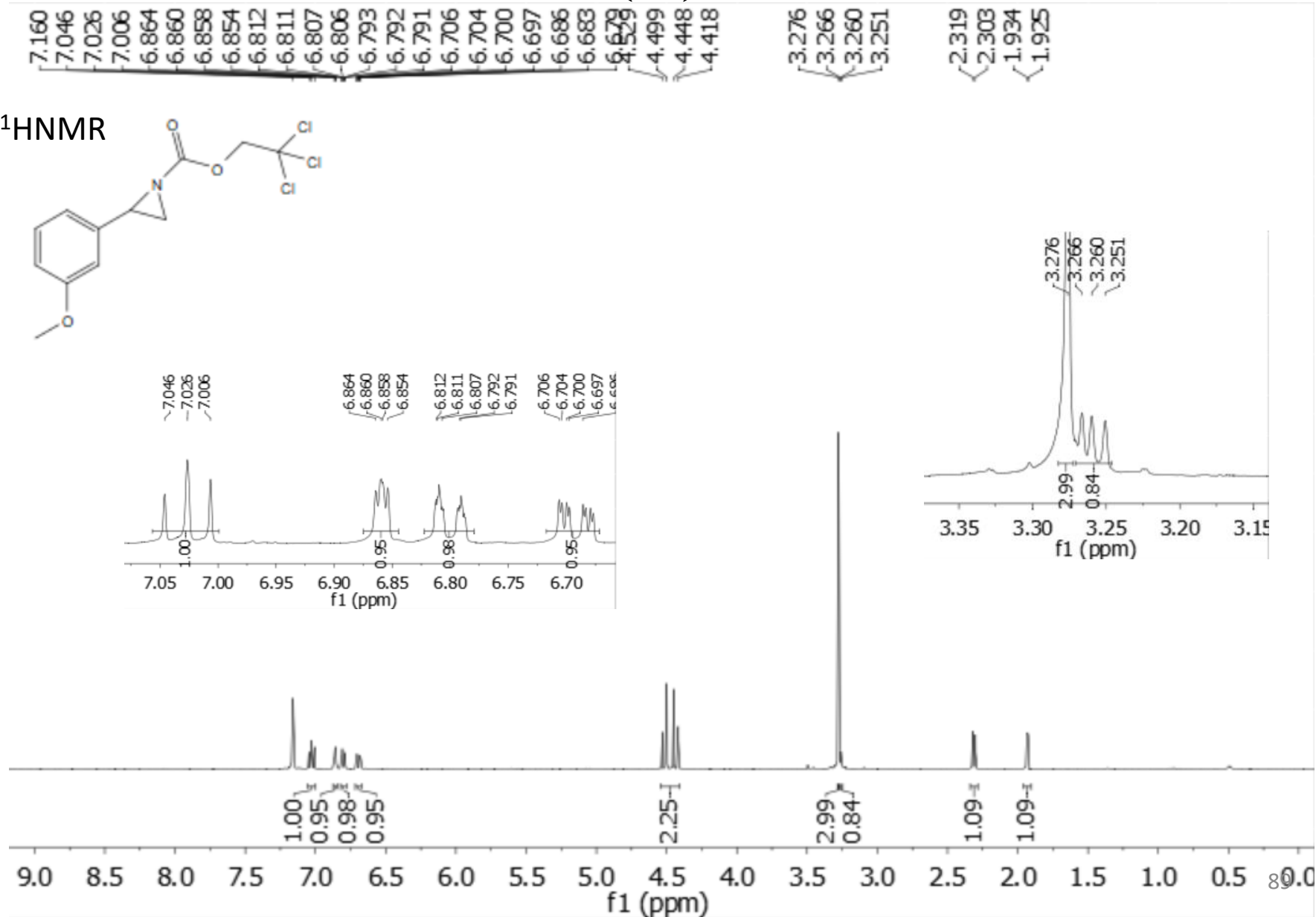
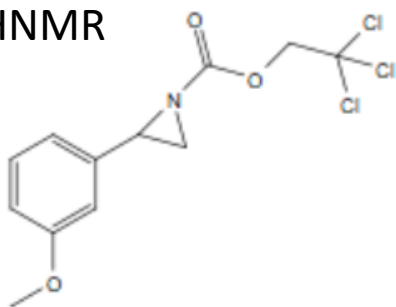


4: 224 nm, 4
nm Results

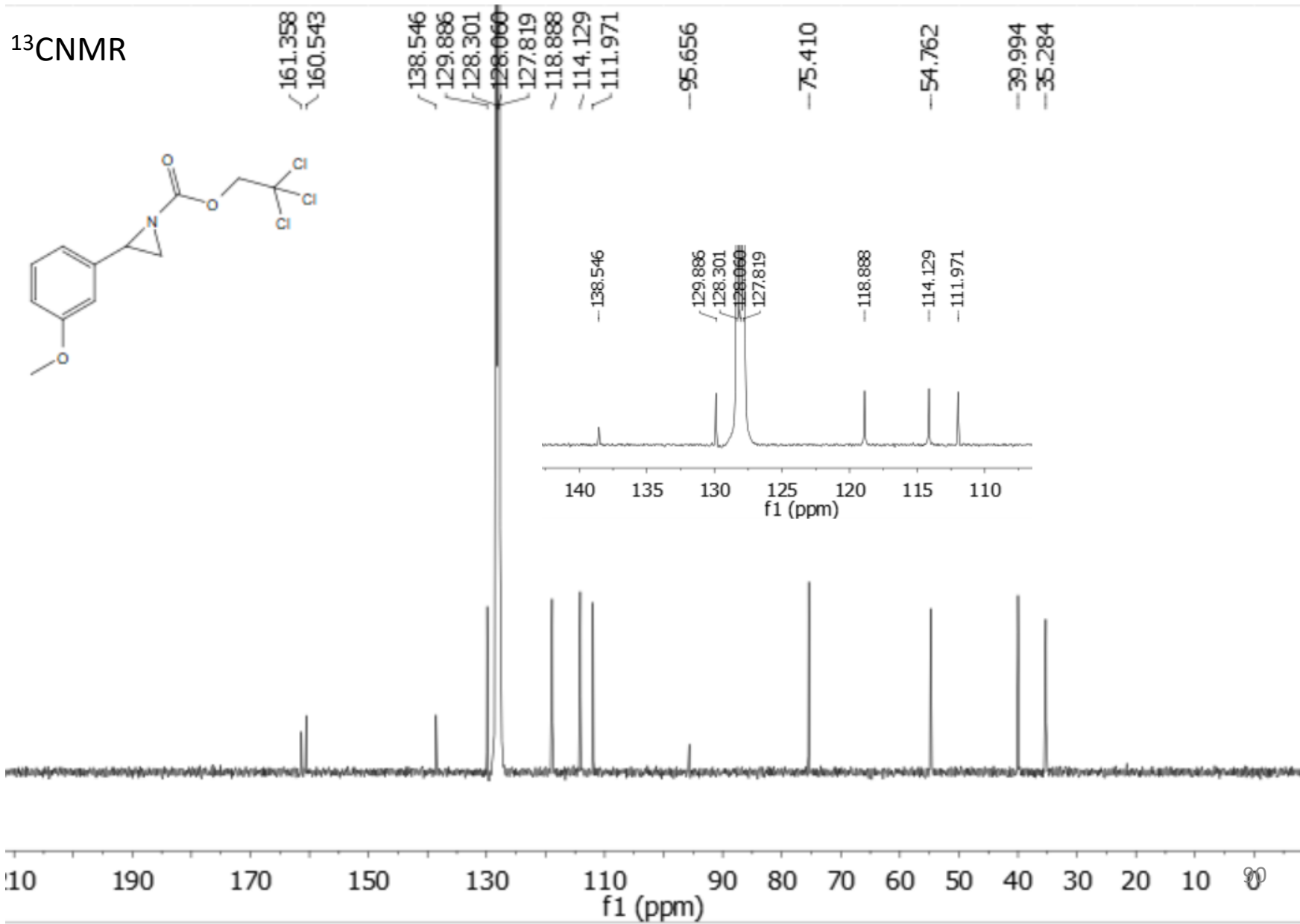
Pk #	Retention Time	Area Percent
1	17.856	92.437
2	41.996	7.563
Totals		100.000

2,2,2-Trichloroethyl 2-(3-methoxyphenyl)aziridine-1-carboxylate (3u)

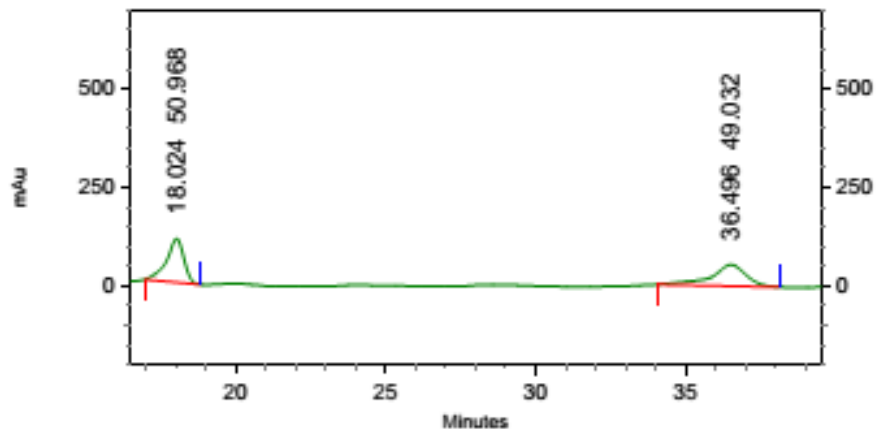
¹H NMR



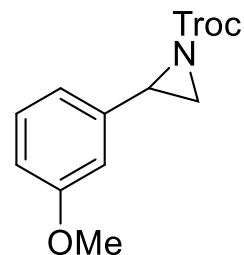
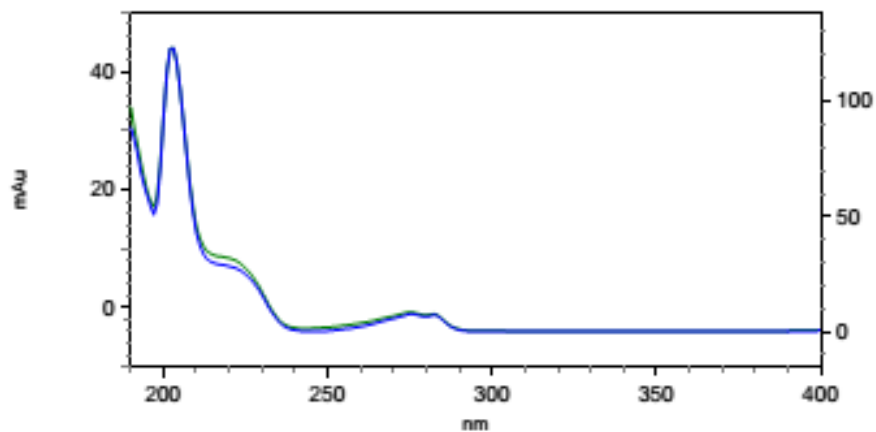
2,2,2-Trichloroethyl 2-(3-methoxyphenyl)aziridine-1-carboxylate (3u)



2,2,2-Trichloroethyl 2-(3-methoxyphenyl)aziridine-1-carboxylate (3u)



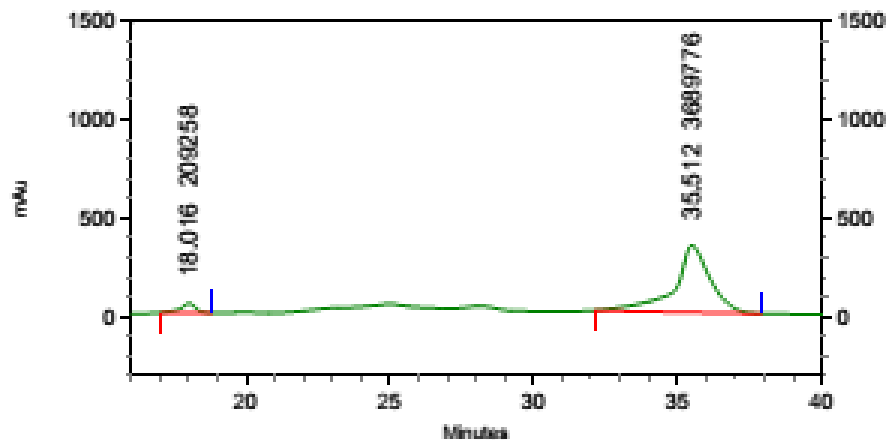
HPLC trace
racemic



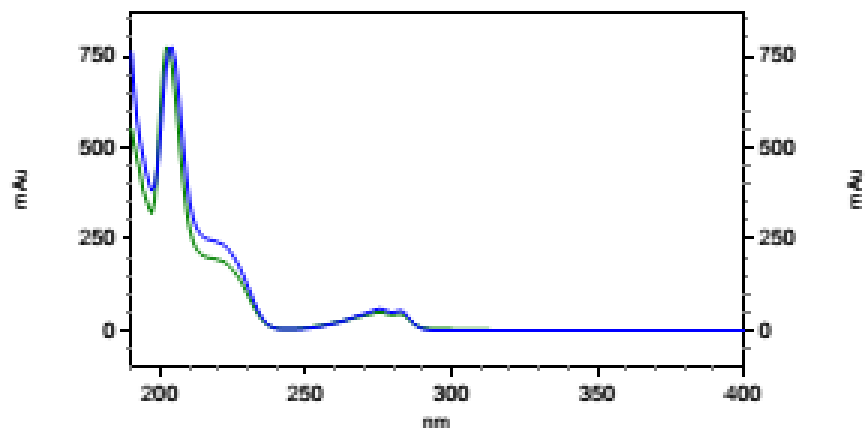
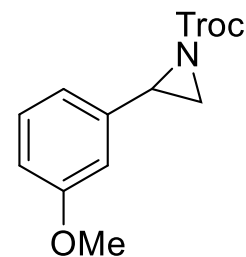
3: 206 nm, 4 nm
Results

Pk #	Name	Retention Time	Area Percent
1		18.024	50.968
2		36.496	49.032
Totals			100.000

2,2,2-Trichloroethyl 2-(3-methoxyphenyl)aziridine-1-carboxylate (3u)



HPLC trace



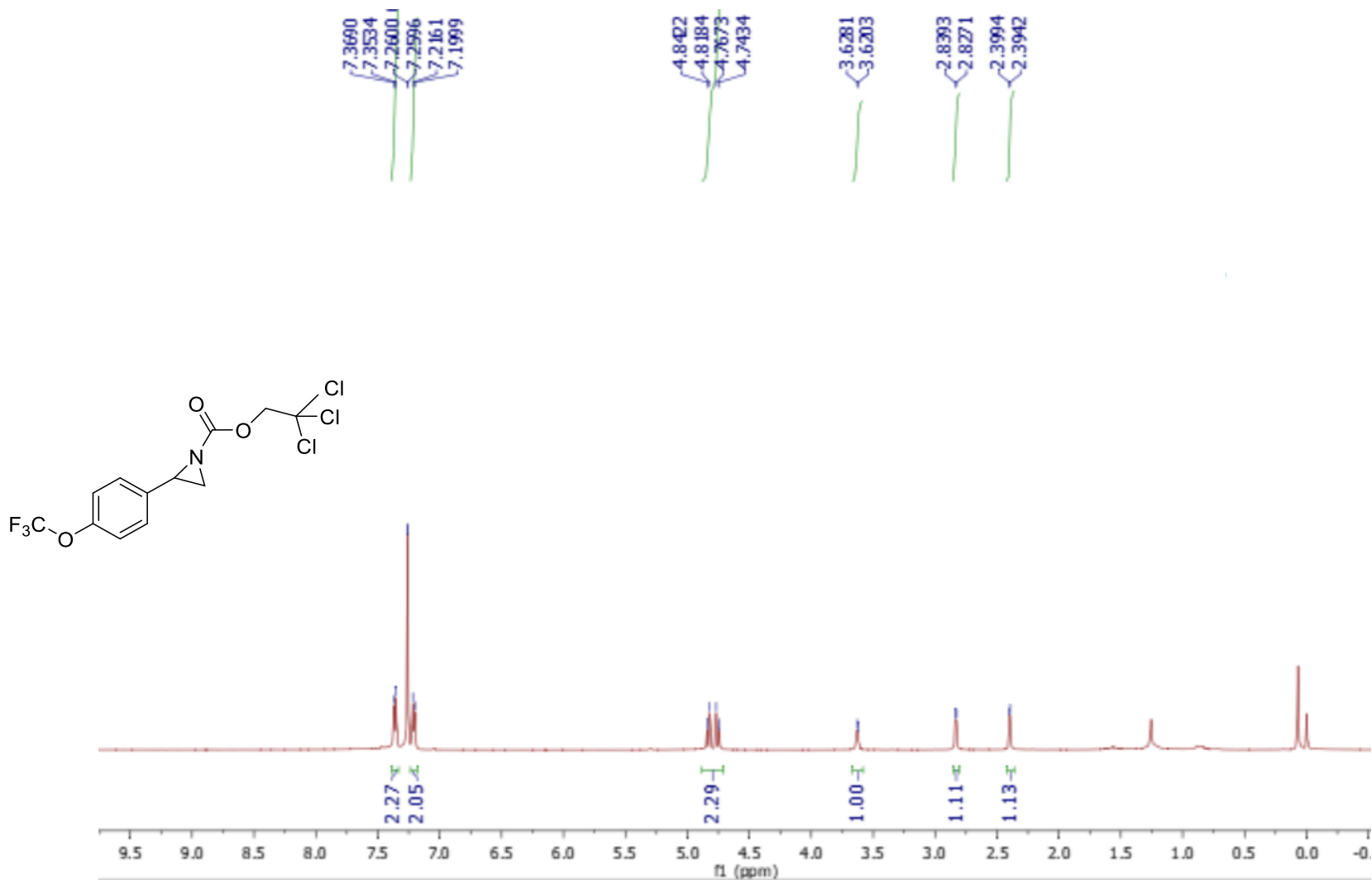
4: 269 nm, 4 nm

Results

Pk #	Name	Retention Time	Area Percent
1		18.016	5.367
2		35.512	94.633
Totals			100.000

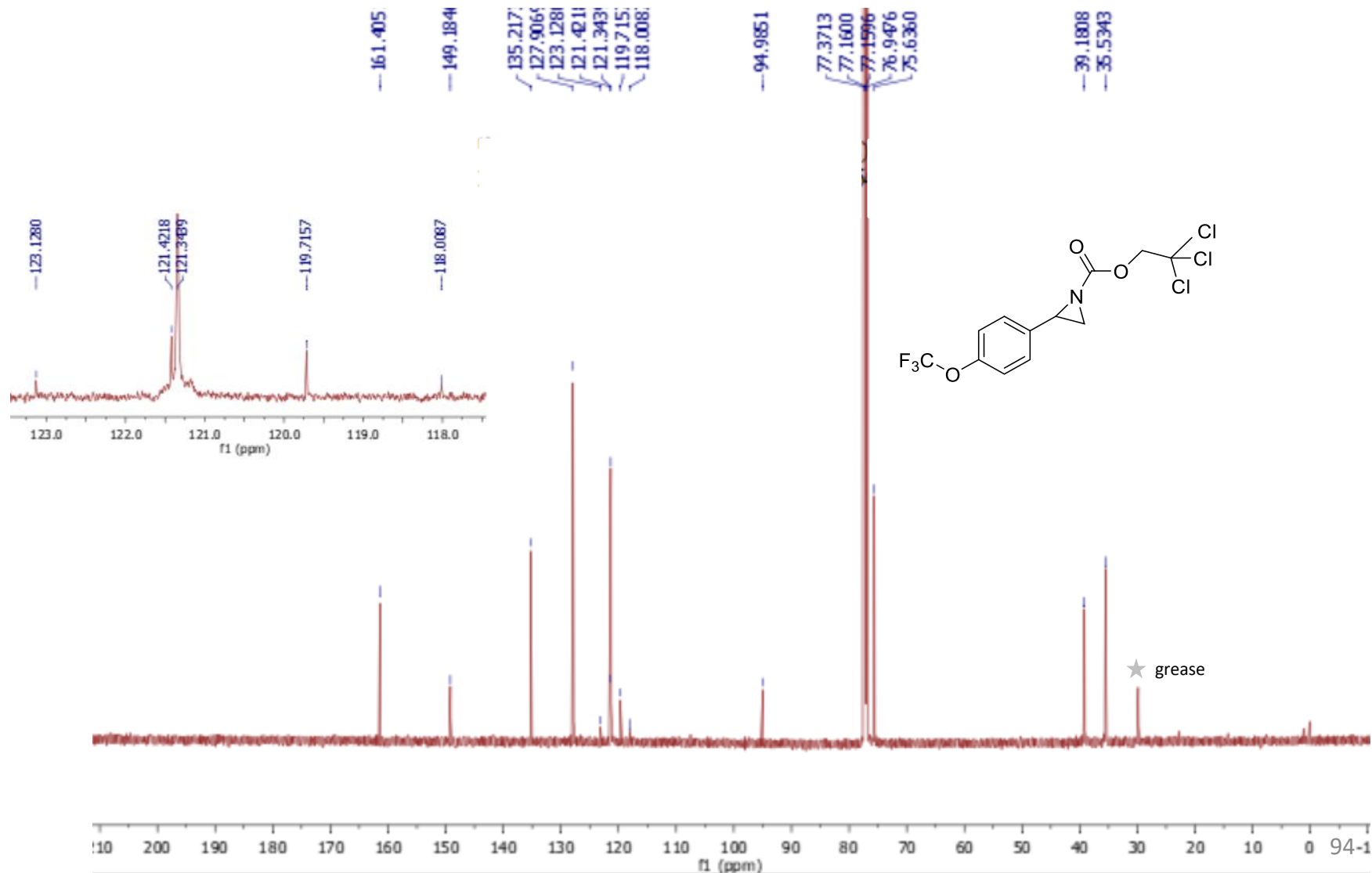
2,2,2-Trichloroethyl 2-(4-trifluoromethoxyphenyl)aziridine-1-carboxylate (3v)

$^1\text{H NMR}$



2,2,2-Trichloroethyl 2-(4-trifluoromethoxyphenyl)aziridine-1-carboxylate (3v)

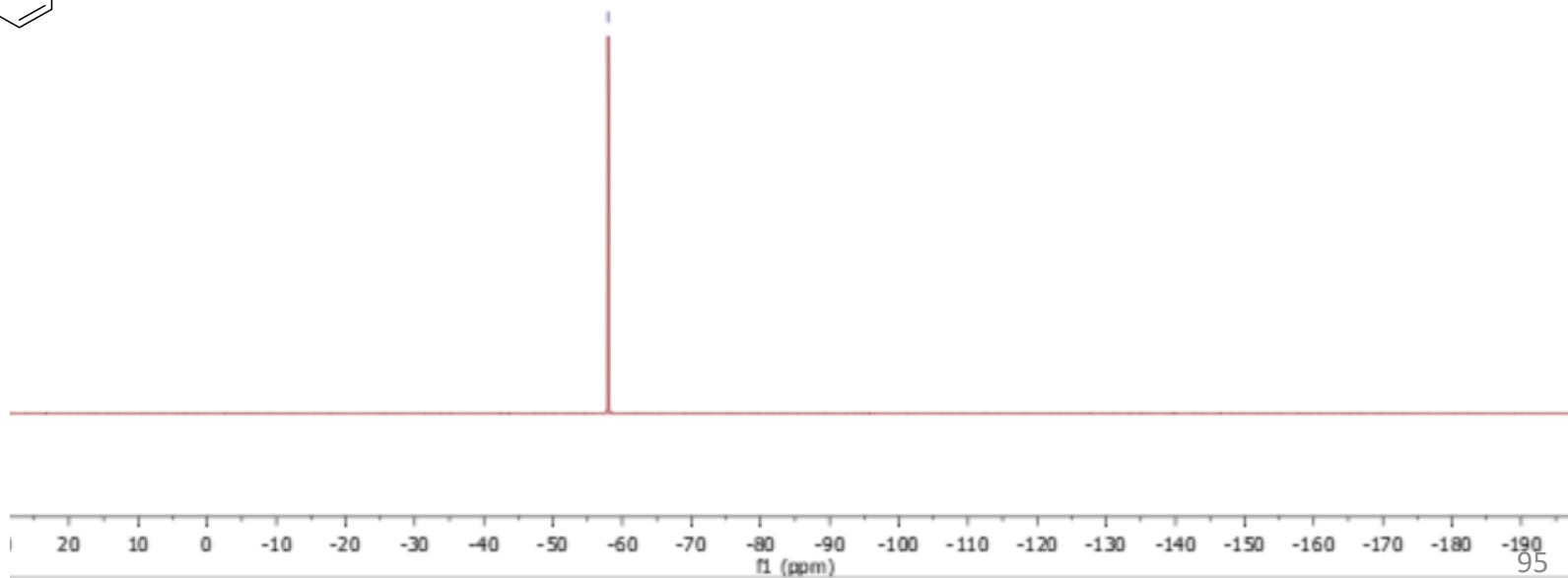
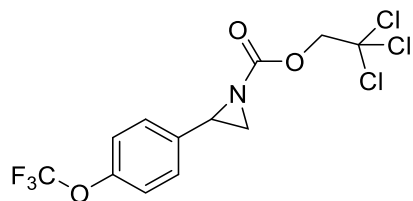
^{13}C NMR



2,2,2-Trichloroethyl 2-(4-trifluoromethoxyphenyl)aziridine-1-carboxylate (3v)

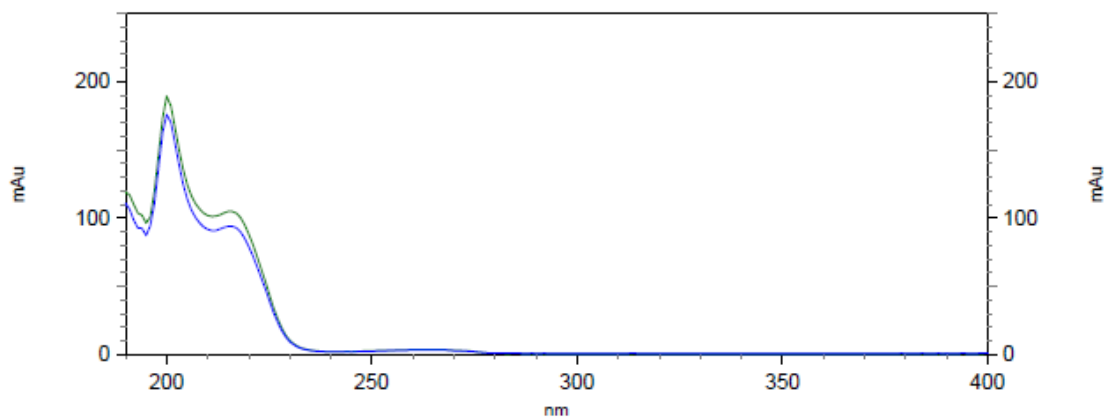
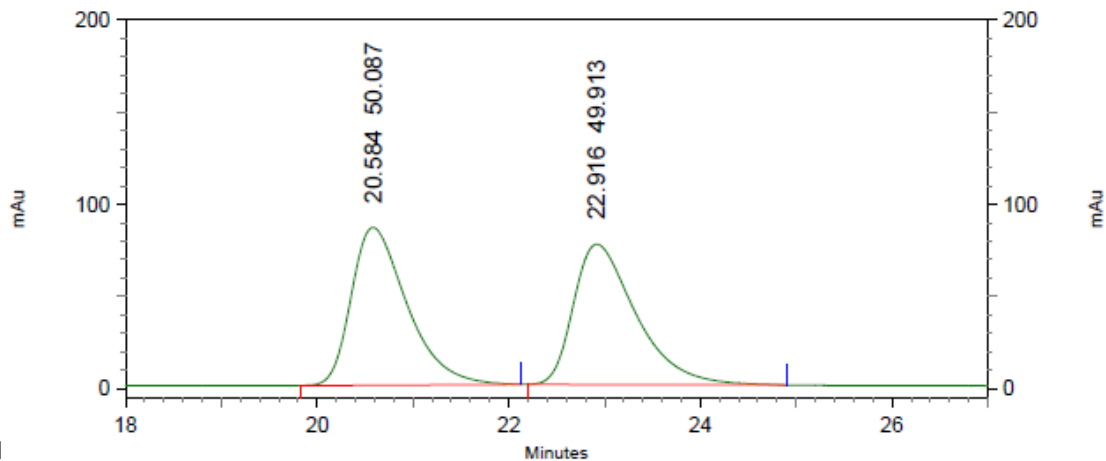
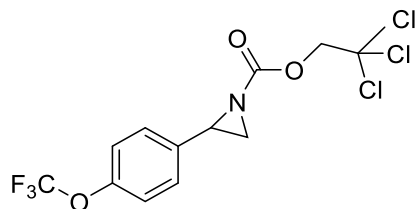
^{19}F NMR

57.933



2,2,2-Trichloroethyl 2-(4-trifluoromethoxyphenyl)aziridine-1-carboxylate (3v)

HPLC trace
racemic

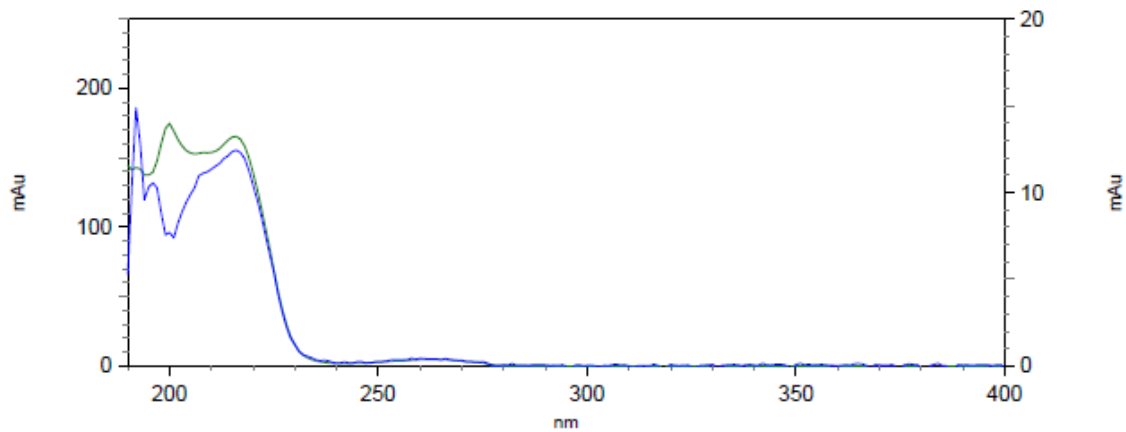
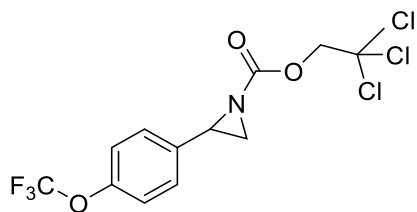
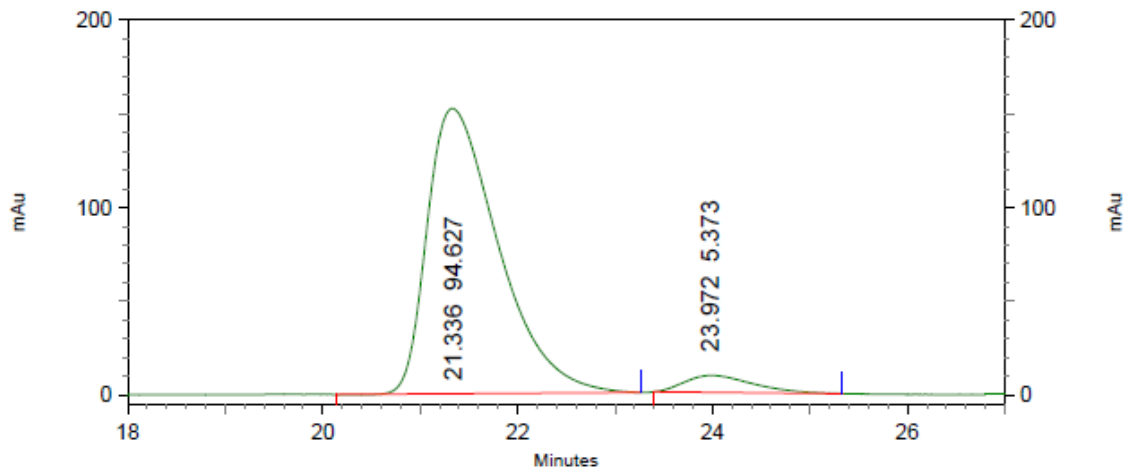


4: 220 nm, 4
nm Results

Pk #	Retention Time	Area Percent
1	20.584	50.087
2	22.916	49.913
Totals		100.000

2,2,2-Trichloroethyl 2-(4-trifluoromethoxyphenyl)aziridine-1-carboxylate (3v)

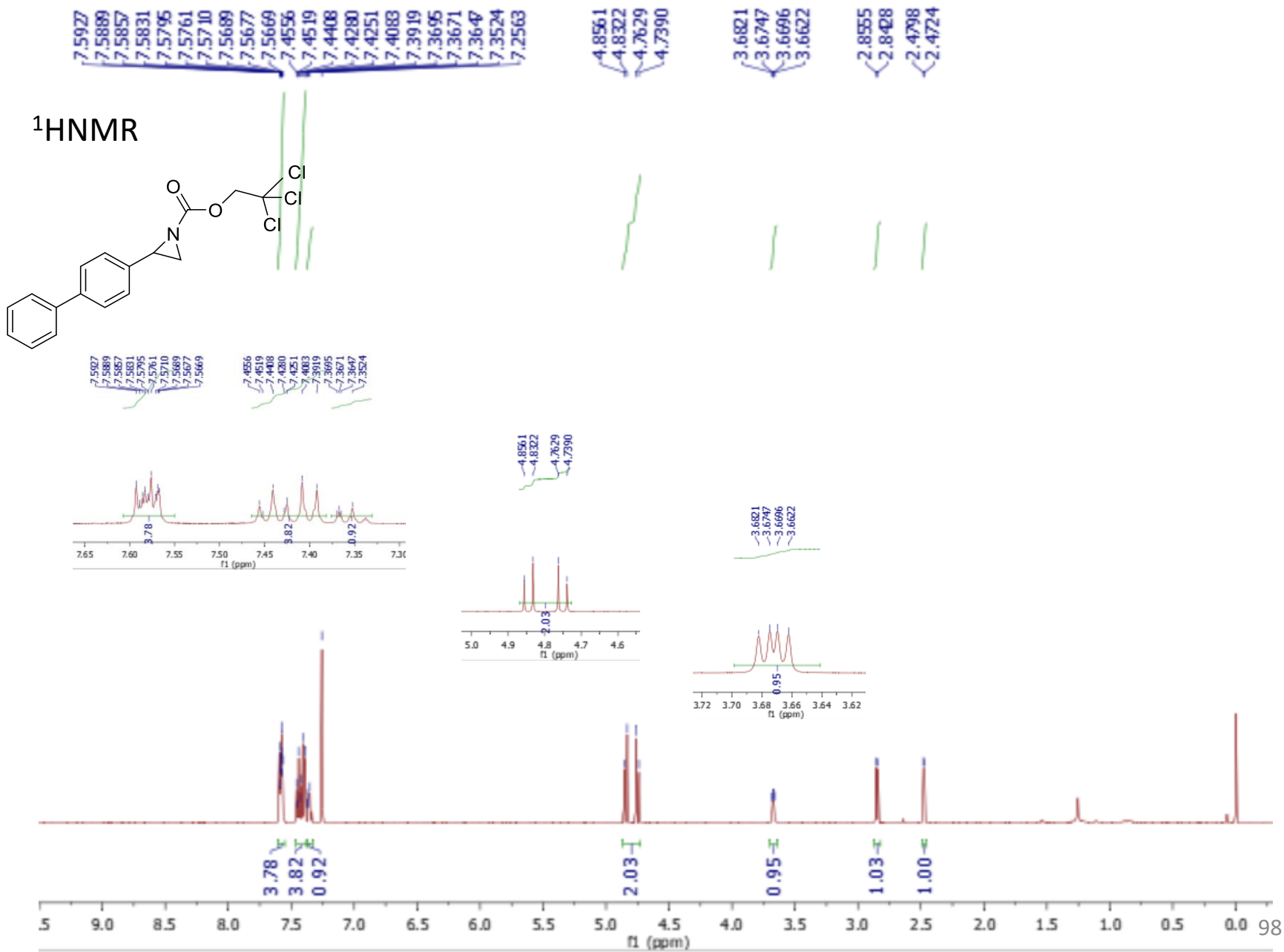
HPLC trace



4: 220 nm, 4
nm Results

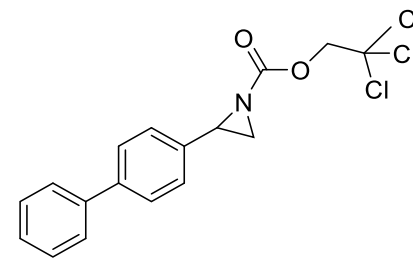
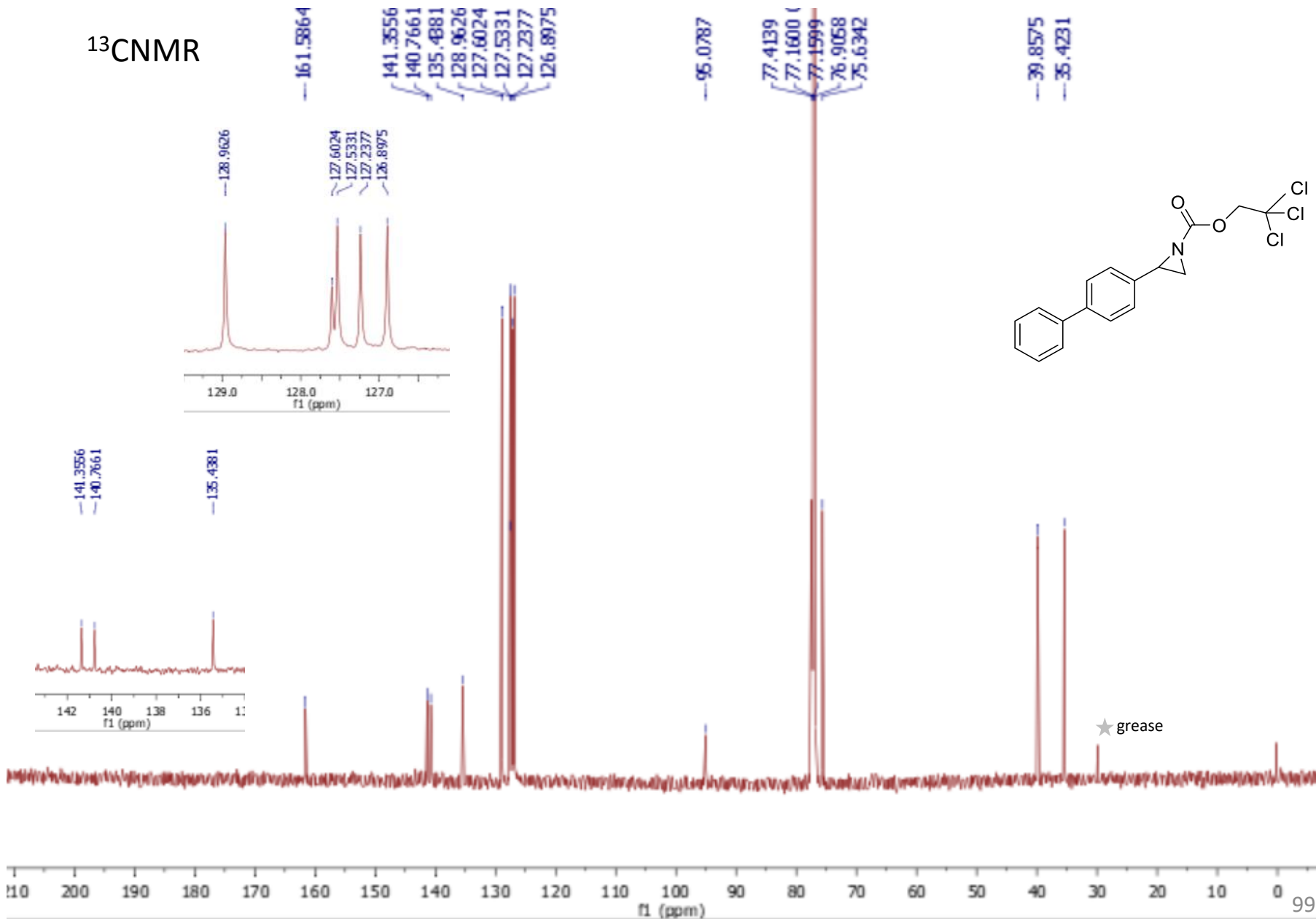
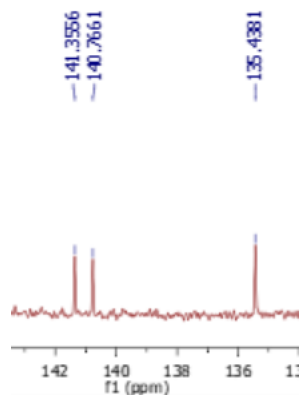
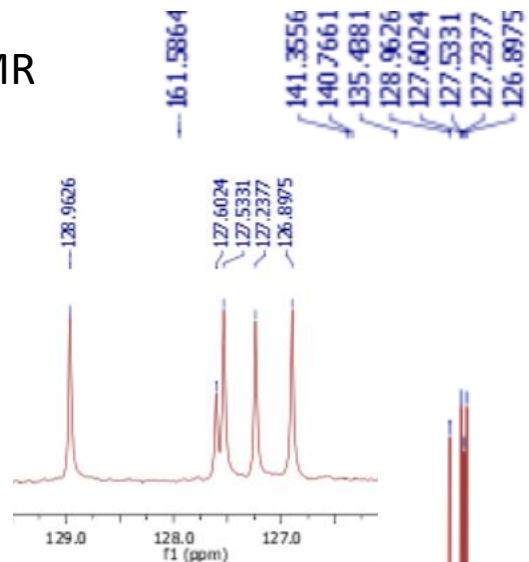
Pk #	Retention Time	Area Percent
1	21.336	94.627
2	23.972	5.373
Totals		100.000

2,2,2-Trichloroethyl 2-(4-phenyl)aziridine-1-carboxylate (3w)



2,2,2-Trichloroethyl 2-(4-phenyl)aziridine-1-carboxylate (3w)

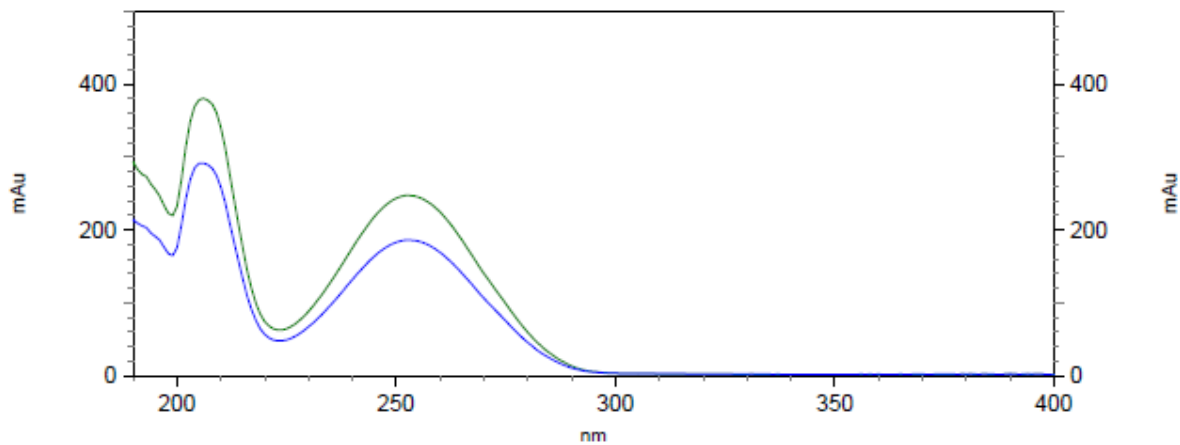
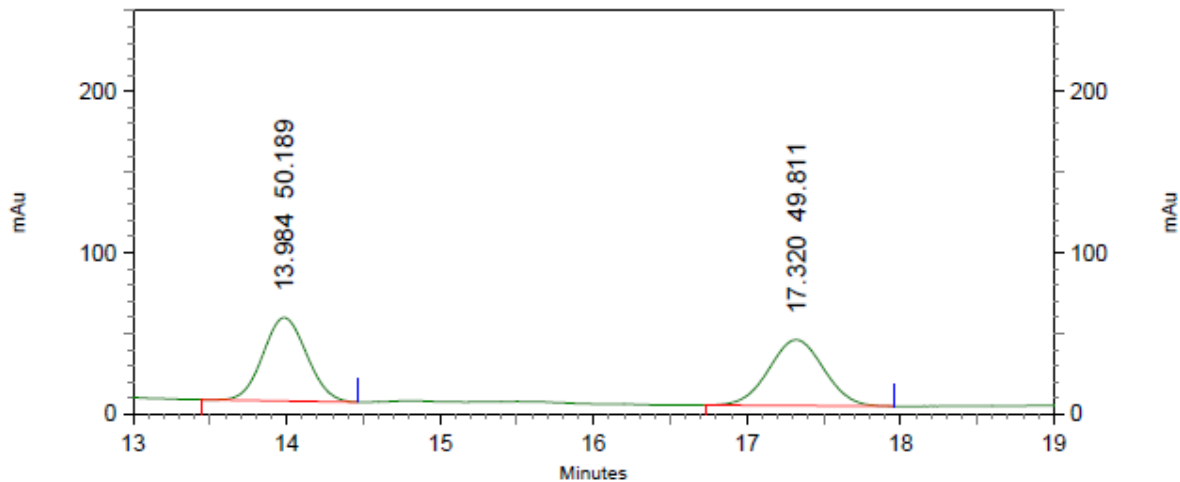
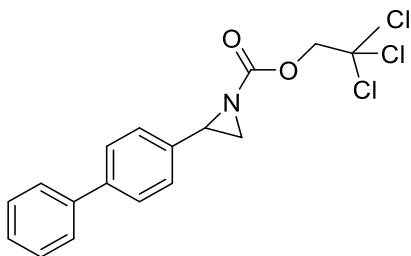
^{13}C NMR



★ grease

2,2,2-Trichloroethyl 2-(4-phenyl)aziridine-1-carboxylate (3w)

HPLC trace
racemic

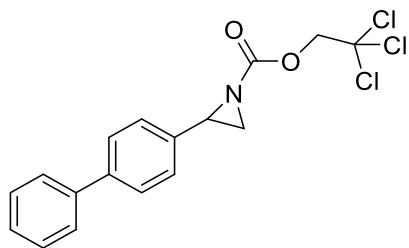


4: 280 nm, 4

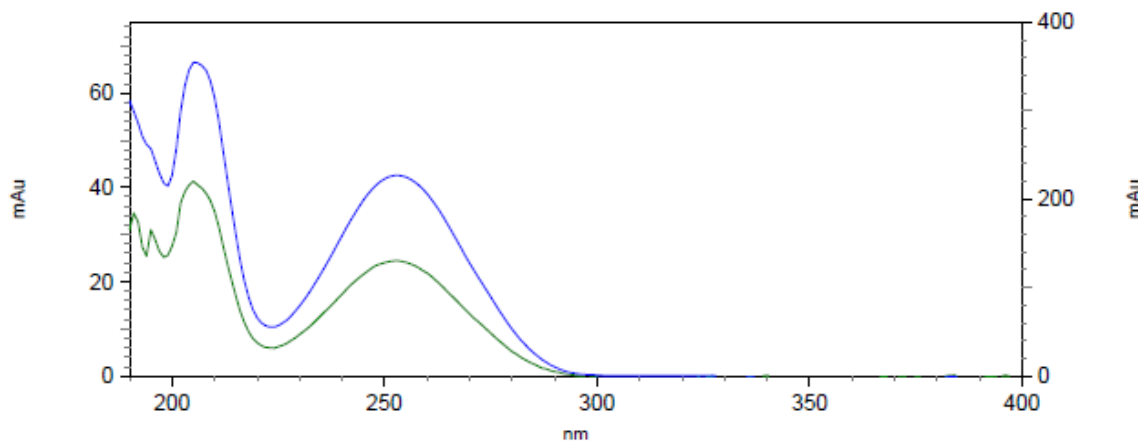
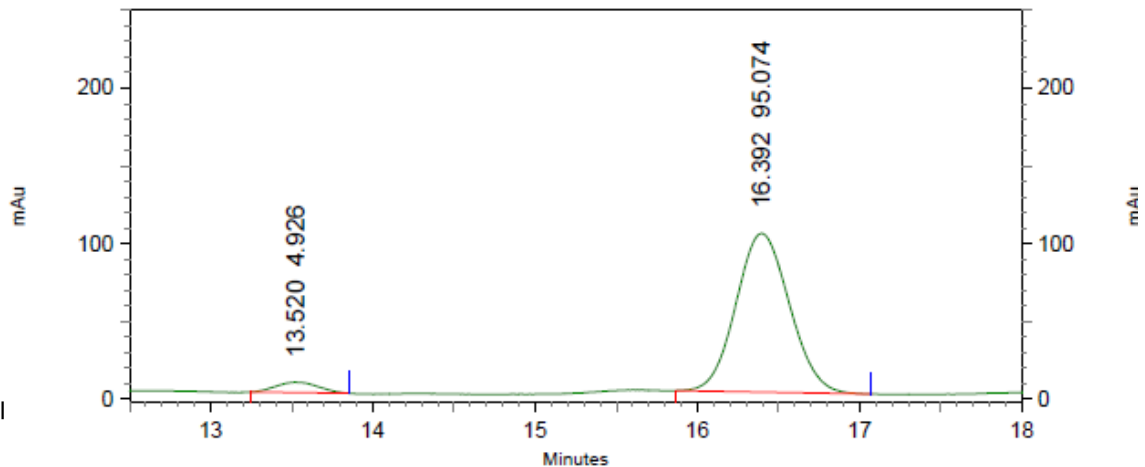
nm Results

Pk #	Retention Time	Area Percent
1	13.984	50.189
2	17.320	49.811
Totals		100.000

2,2,2-Trichloroethyl 2-(4-phenyl)aziridine-1-carboxylate (3w)



HPLC trace



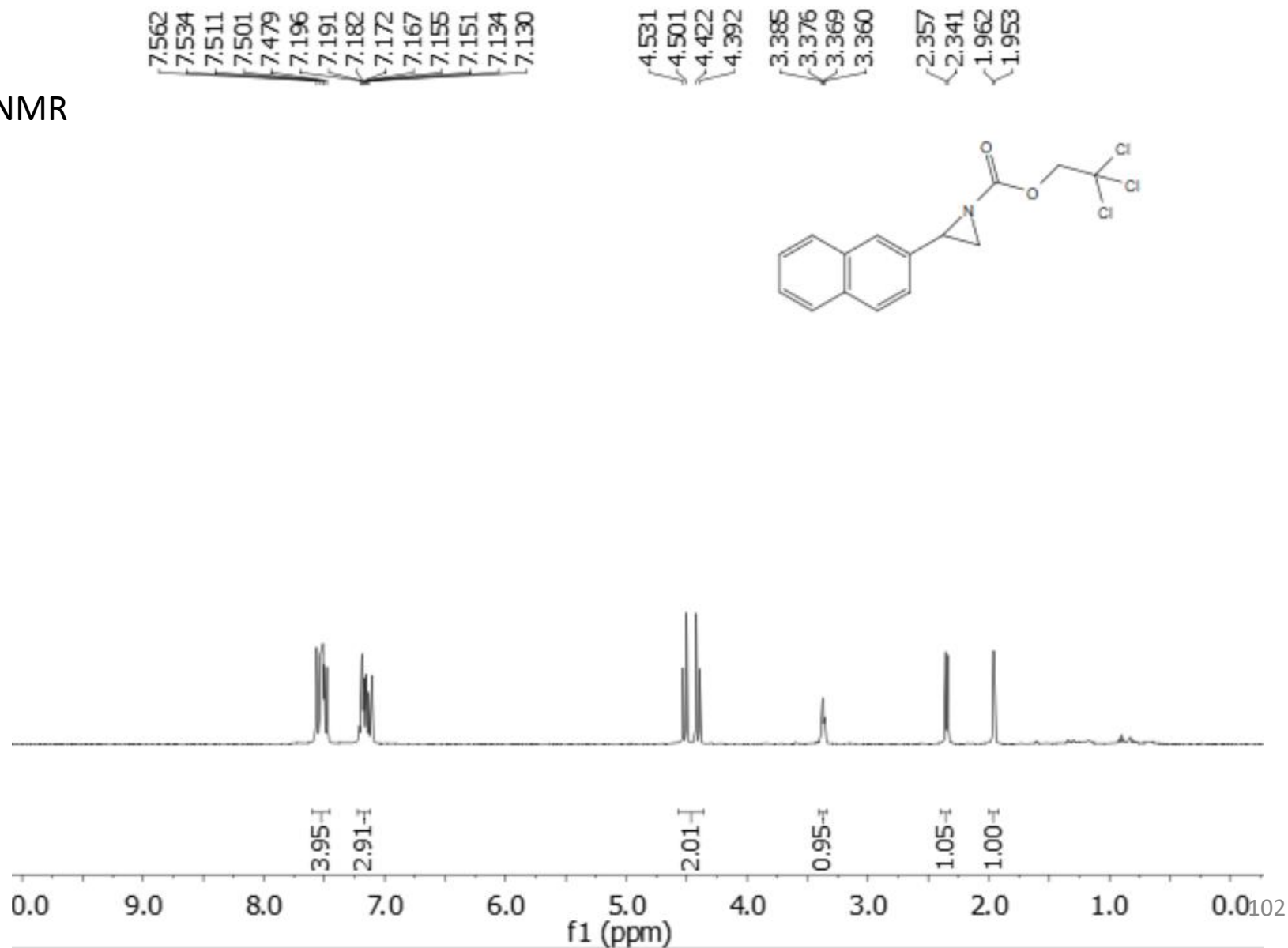
3: 280 nm, 4
nm Results

Pk #	Retention Time	Area Percent
1	13.520	4.926
2	16.392	95.074

Totals		100.000
--------	--	---------

2,2,2-Trichloroethyl 2-(naphthalen-2-yl)aziridine-1-carboxylate (3x)

¹HNMR



7.562
7.534
7.511
7.501
7.479
7.196
7.191
7.182
7.172
7.167
7.155
7.151
7.134
7.130

4.531
4.501
4.422
4.392

3.385
3.376
3.369
3.360

2.357
2.341
1.962
1.953

3.95H

2.91H

2.01H

0.95H

1.05H

1.00H

0.0 9.0 8.0 7.0 6.0 5.0 4.0 3.0 2.0 1.0 0.0

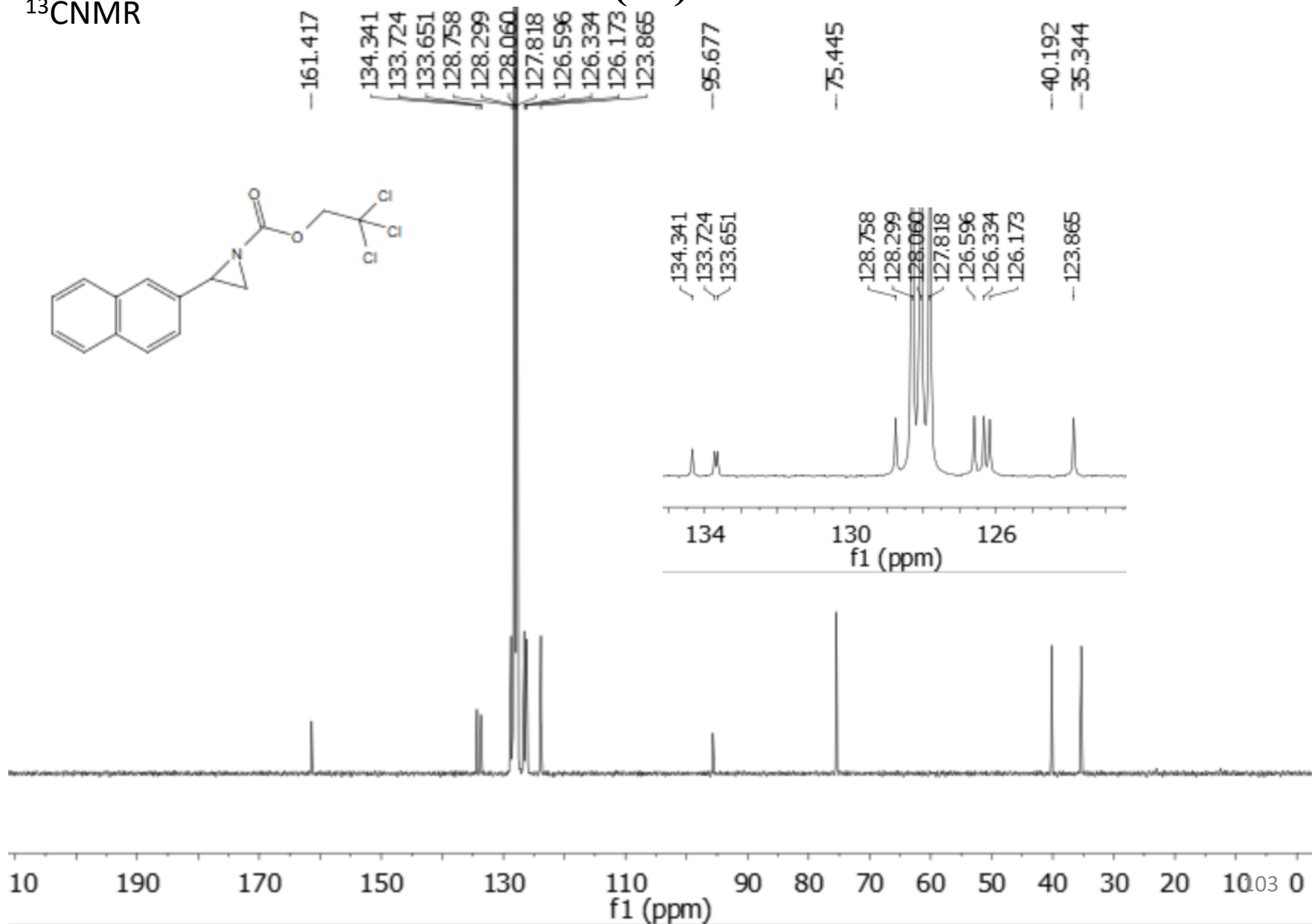
f1 (ppm)

102

2,2,2-Trichloroethyl 2-(naphthalen-2-yl)aziridine-1-carboxylate

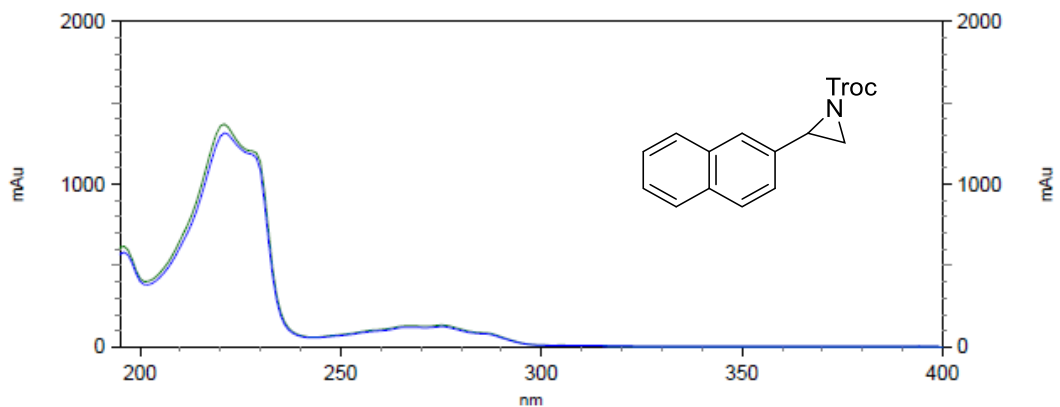
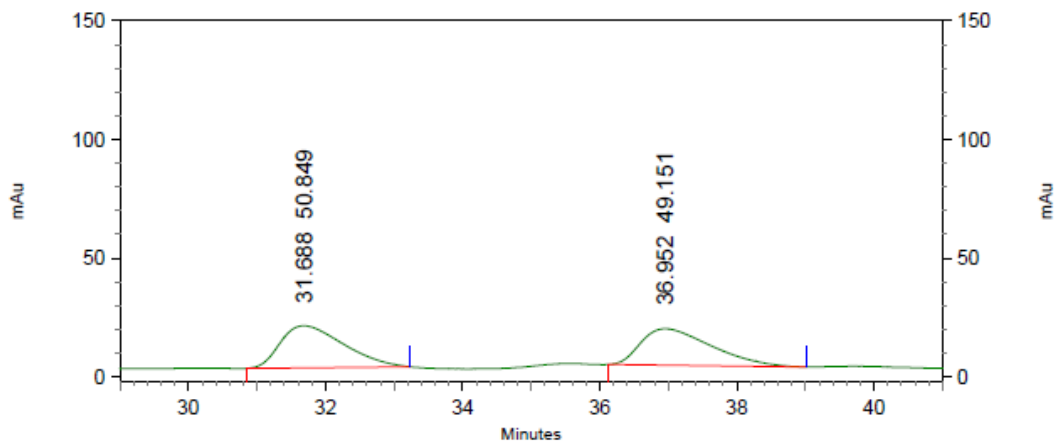
(3x)

¹³CNMR



2,2,2-Trichloroethyl 2-(naphthalen-2-yl)aziridine-1-carboxylate (3x)

HPLC trace
racemic



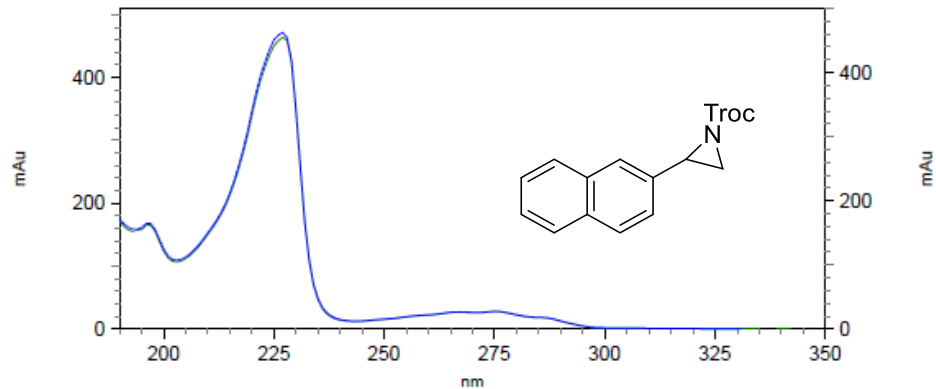
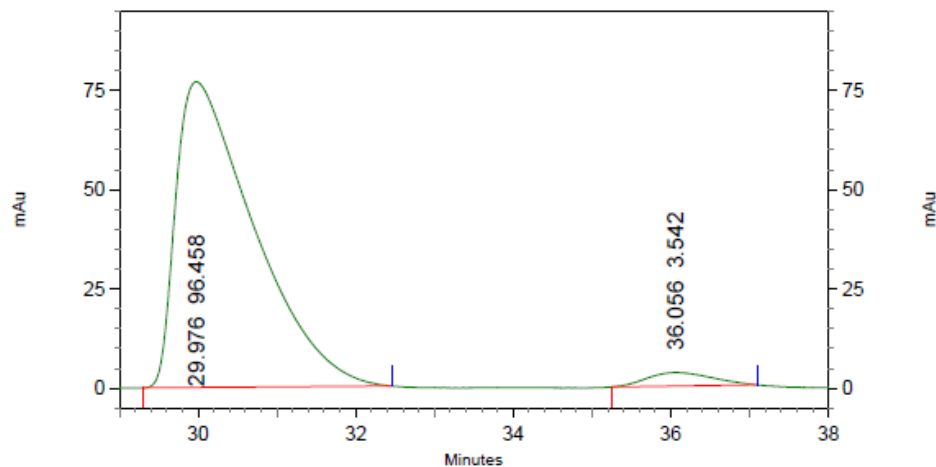
2: 296 nm, 4
nm Results

Pk #	Retention Time	Area Percent
1	31.688	50.849
2	36.952	49.151

Totals	100.000
--------	---------

2,2,2-Trichloroethyl 2-(naphthalen-2-yl)aziridine-1-carboxylate (3x)

HPLC trace

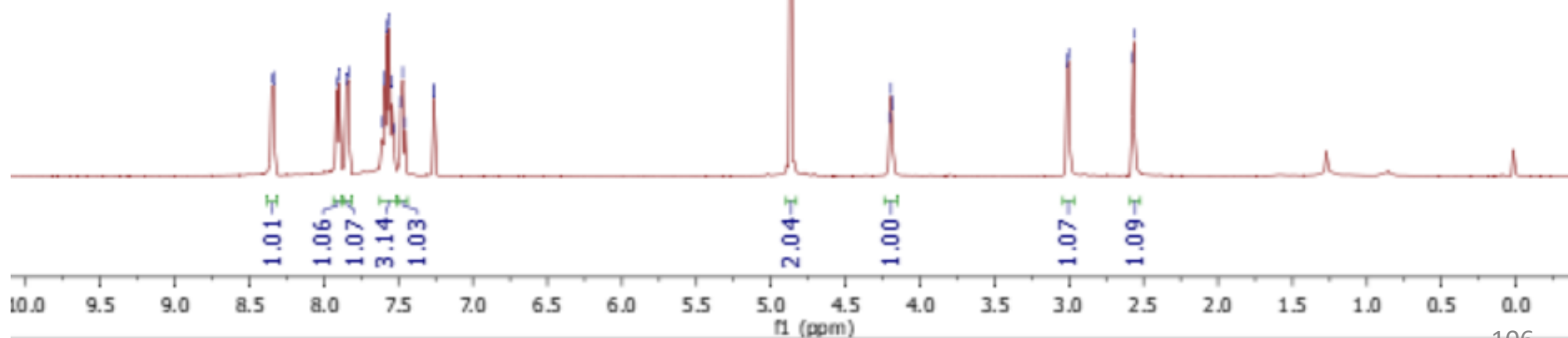
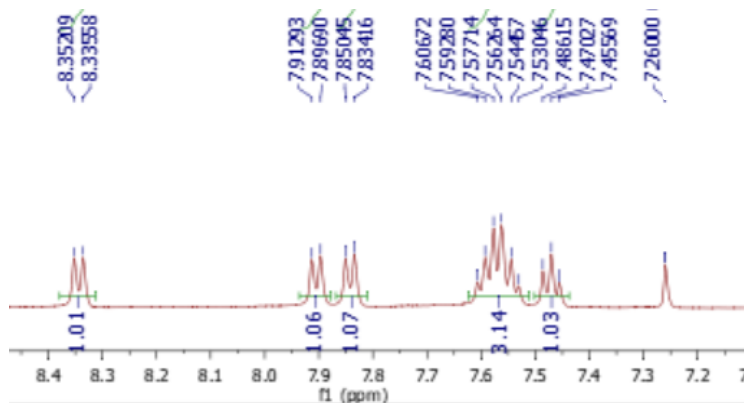
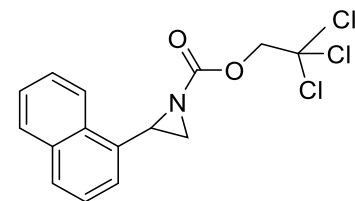


1: 296 nm, 4
nm Results

Pk #	Retention Time	Area Percent
1	29.976	96.458
2	36.056	3.542
Totals		100.000

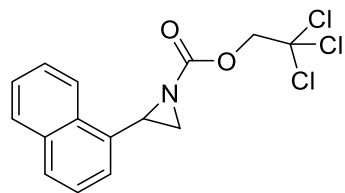
2,2,2-Trichloroethyl 2-(naphthalen-1-yl)aziridine-1-carboxylate (3y)

$^1\text{H NMR}$

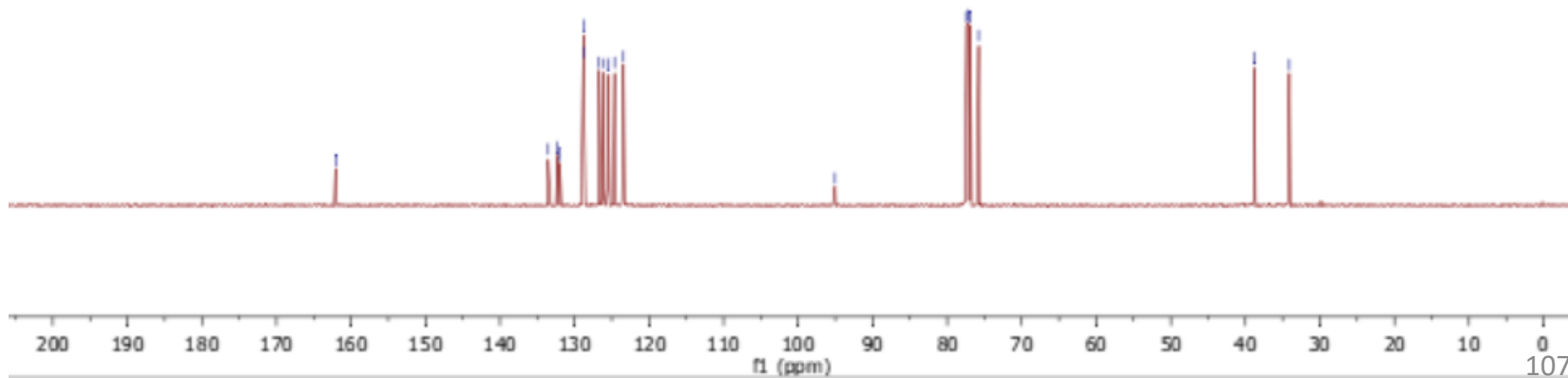
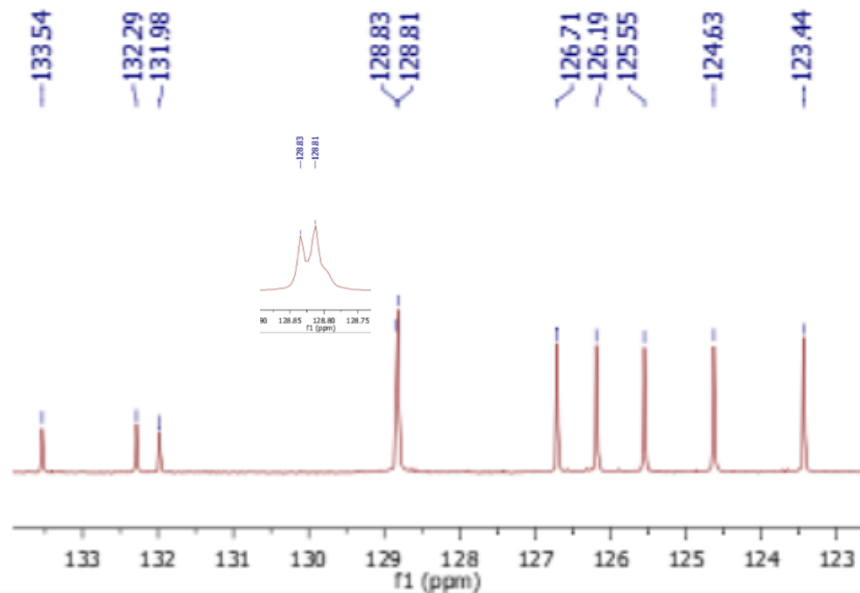


2,2,2-Trichloroethyl 2-(naphthalen-1-yl)aziridine-1-carboxylate (3y)

^{13}C NMR

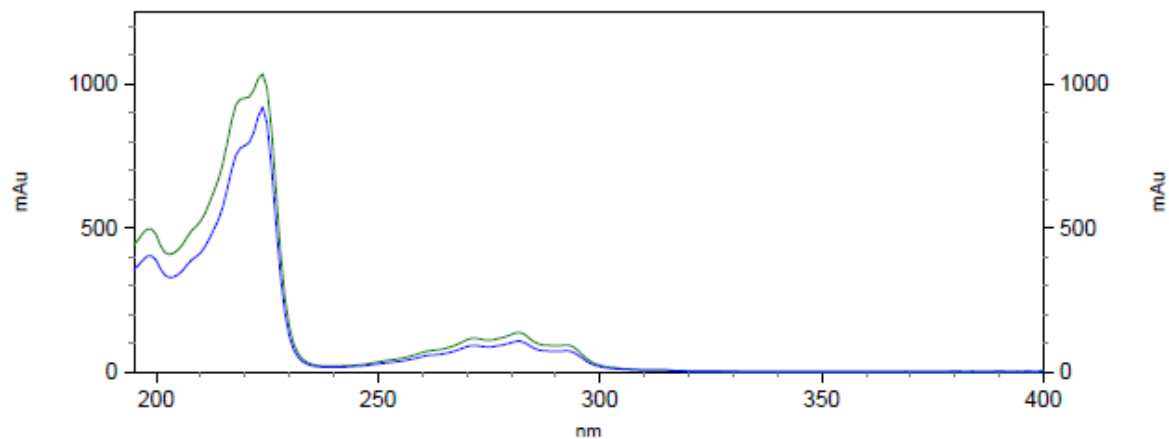
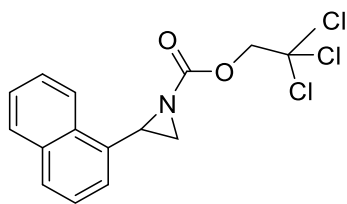
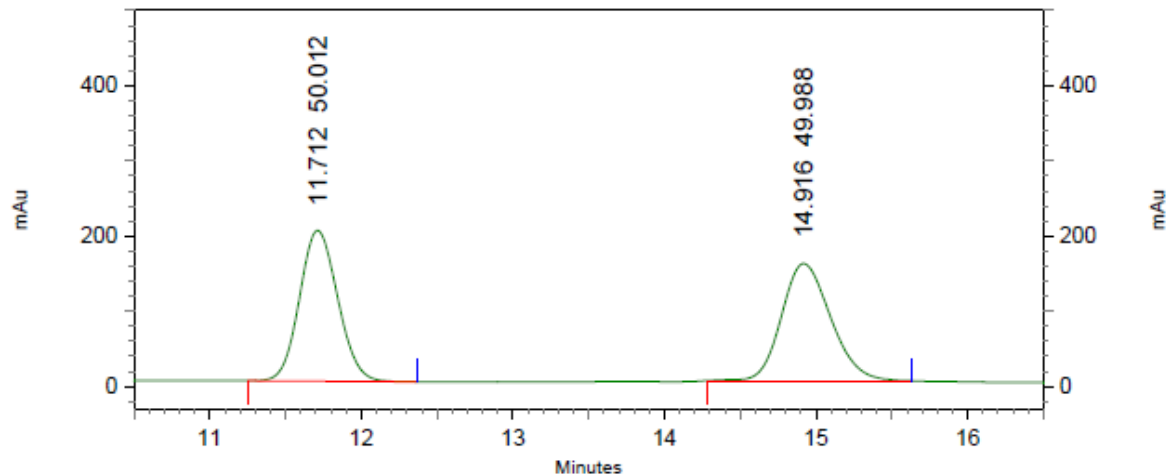


162.07
133.54
132.29
131.98
128.83
128.81
126.71
126.19
125.55
124.63
123.44
95.05
77.41
77.16
76.91
75.78
38.77
34.10



2,2,2-Trichloroethyl 2-(naphthalen-1-yl)aziridine-1-carboxylate (3y)

HPLC trace
racemic

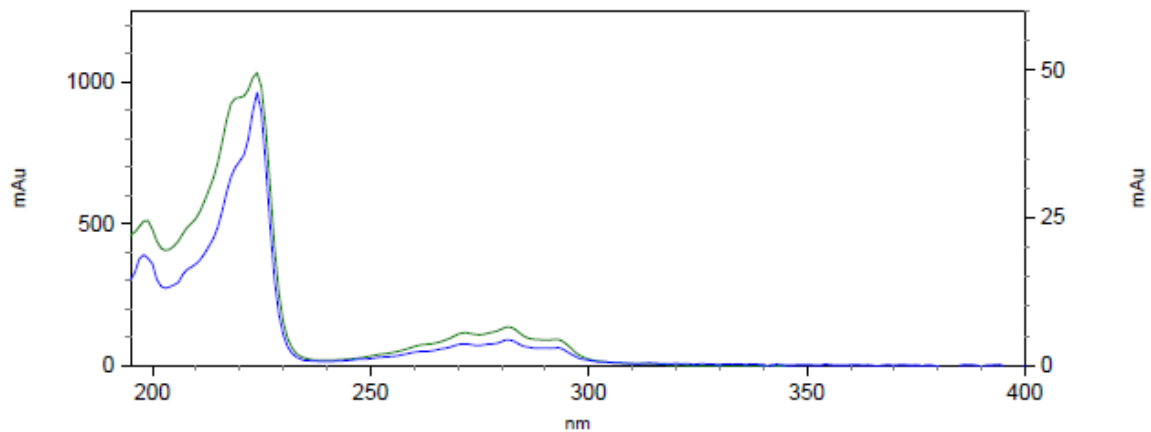
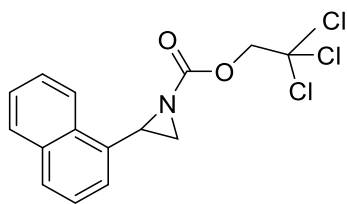
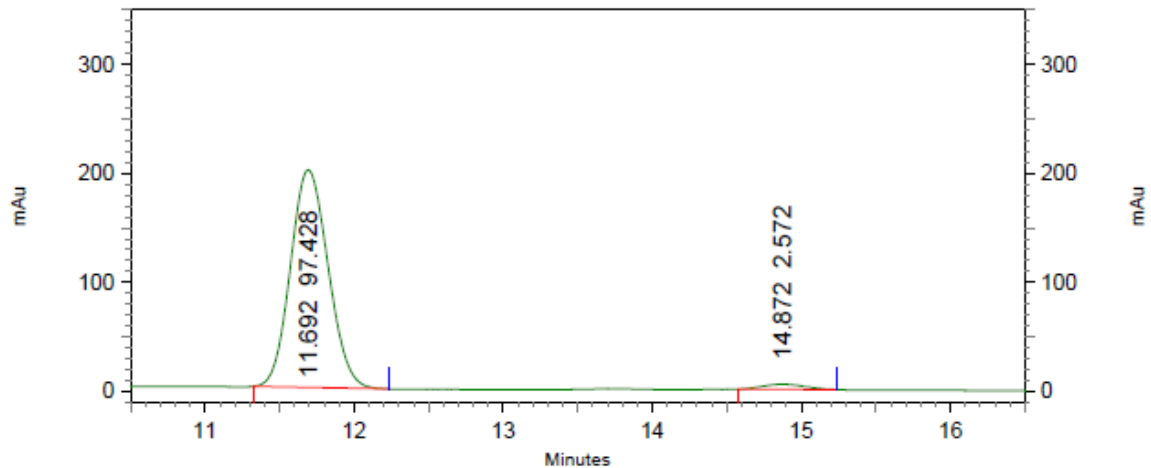


3: 269 nm, 4
nm Results

Pk #	Retention Time	Area Percent
1	11.712	50.012
2	14.916	49.988
Totals		100.000

2,2,2-Trichloroethyl 2-(naphthalen-1-yl)aziridine-1-carboxylate (3y)

HPLC trace



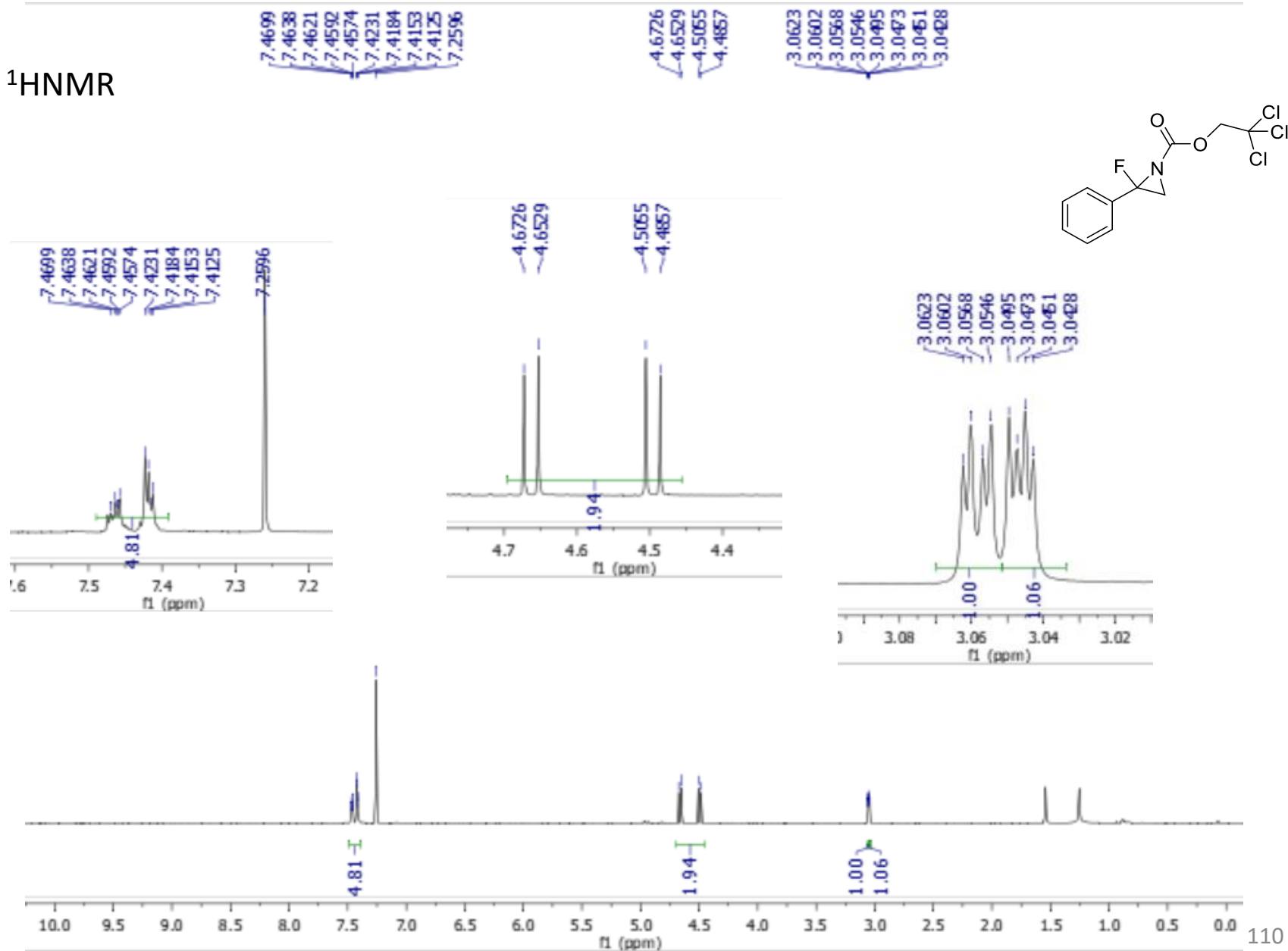
3: 269 nm, 4
nm Results

Pk #	Retention Time	Area Percent
1	11.692	97.428
2	14.872	2.572

Totals	100.000
--------	---------

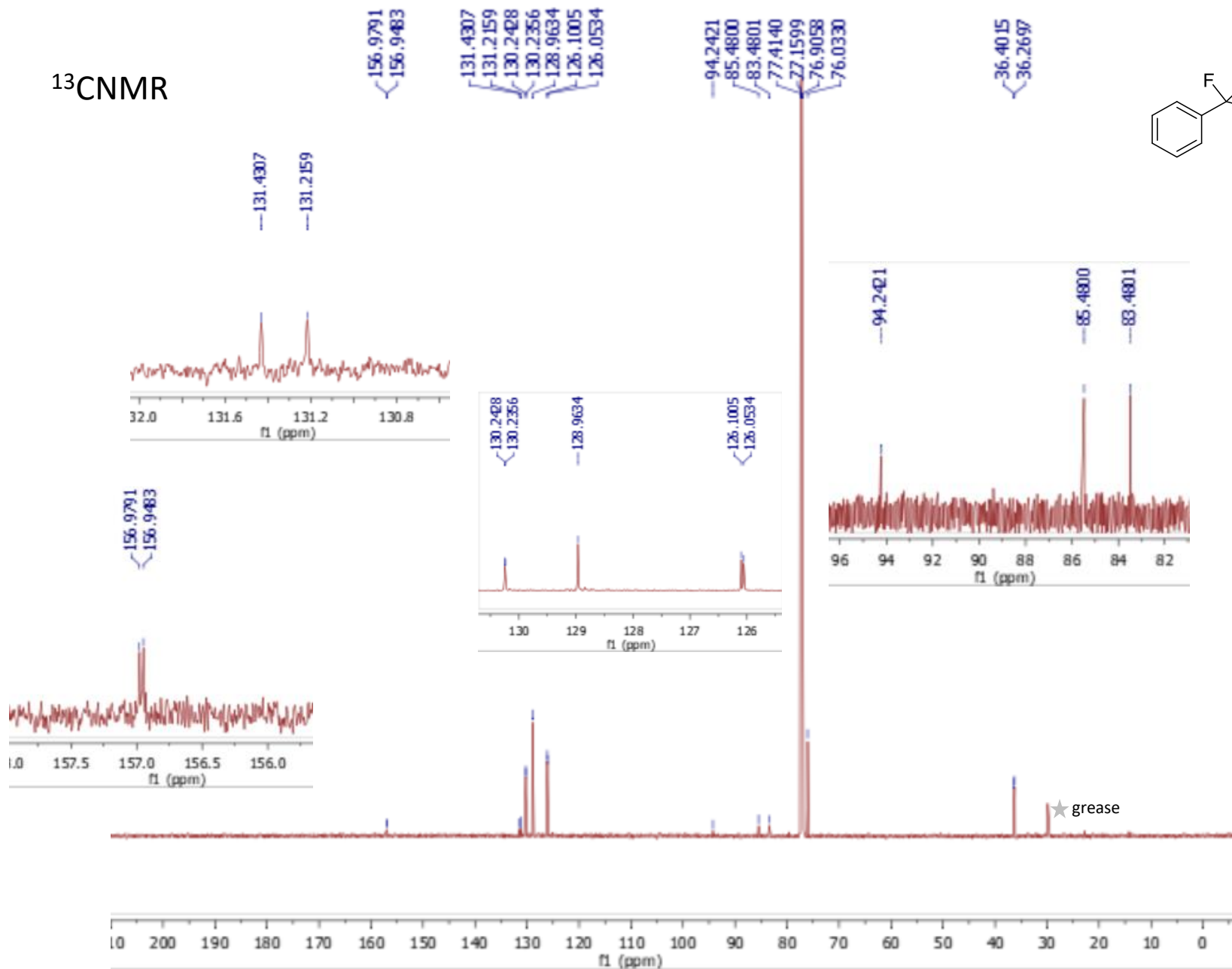
2,2,2-trichloroethyl 2-fluoro-2-phenylaziridine-1-carboxylate (3z)

¹HNMR



2,2,2-trichloroethyl 2-fluoro-2-phenylaziridine-1-carboxylate (3z)

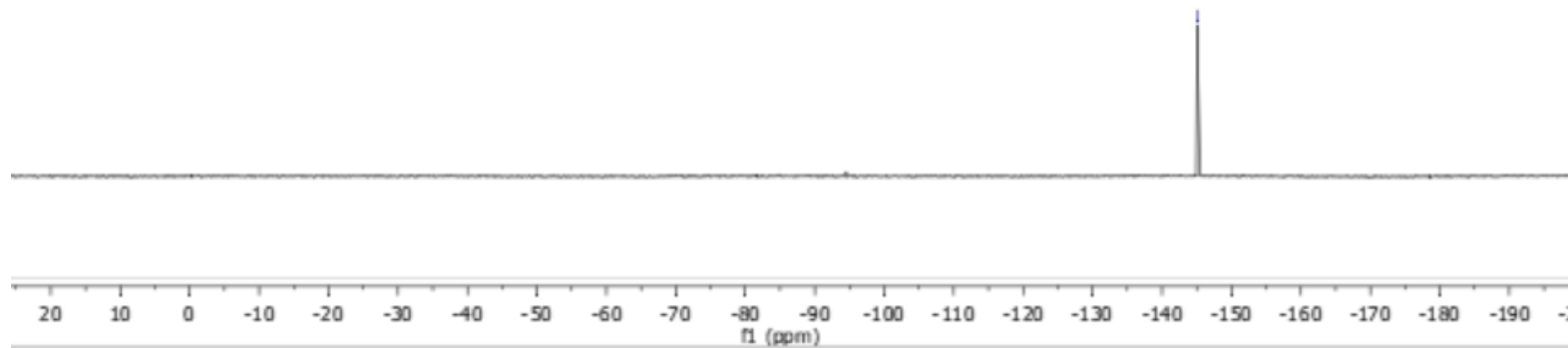
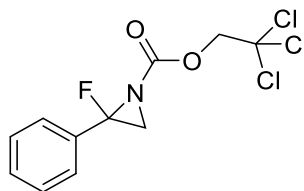
^{13}C NMR



2,2,2-trichloroethyl 2-fluoro-2-phenylaziridine-1-carboxylate (3z)

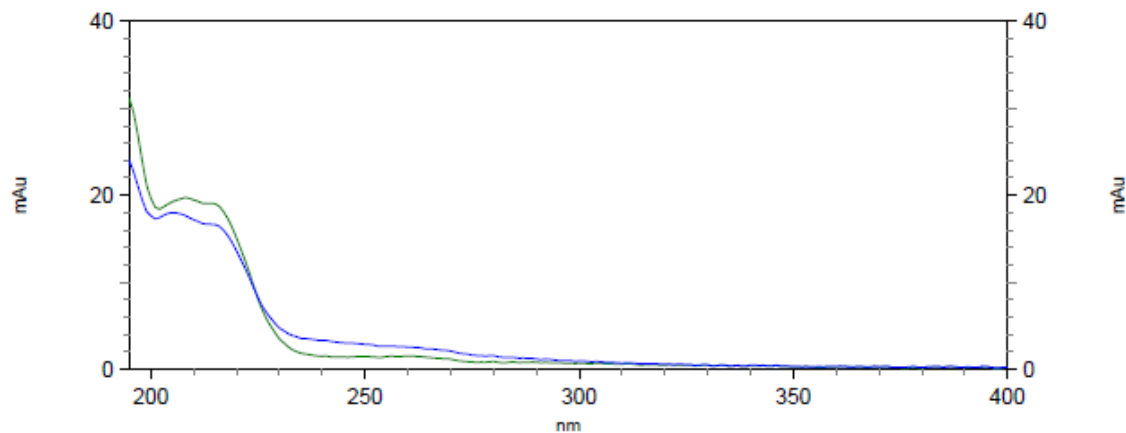
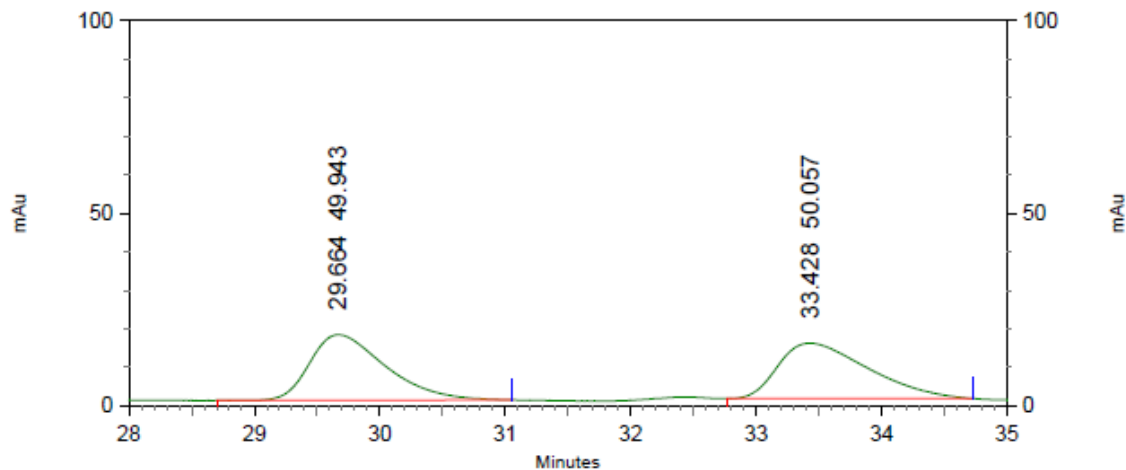
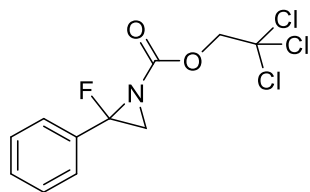
^{19}F NMR

---145.0632



2,2,2-trichloroethyl 2-fluoro-2-phenylaziridine-1-carboxylate (3z)

HPLC trace
racemic

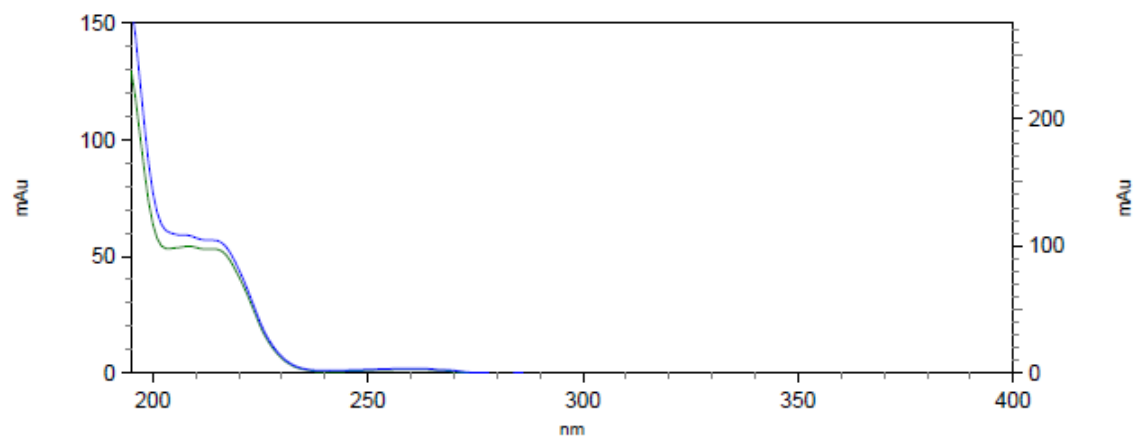
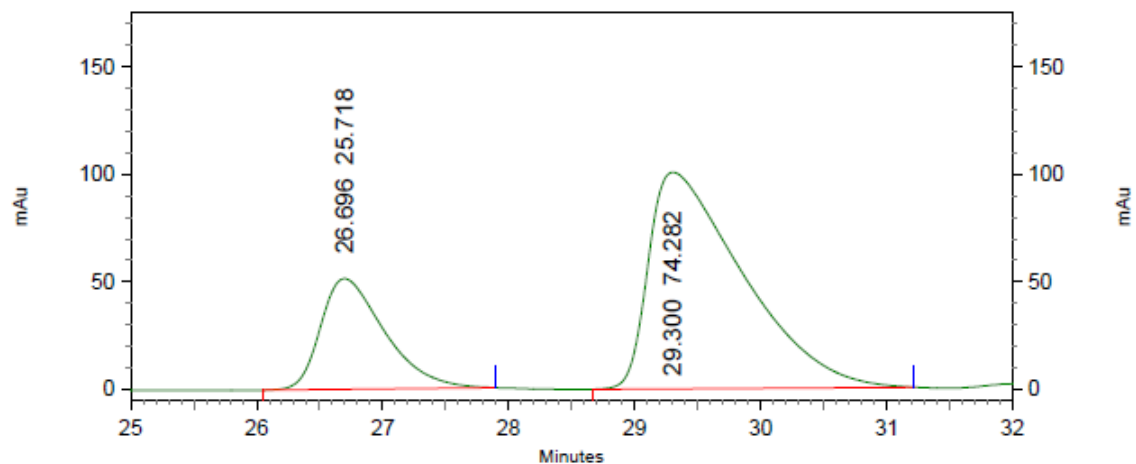
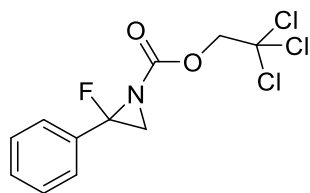


6: 216 nm, 4
nm Results

Pk #	Retention Time	Area Percent
1	29.664	49.943
2	33.428	50.057
Totals		100.000

2,2,2-trichloroethyl 2-fluoro-2-phenylaziridine-1-carboxylate (3z)

HPLC trace



6: 216 nm, 4
nm Results

Pk #	Retention Time	Area Percent
1	26.696	25.718
2	29.300	74.282

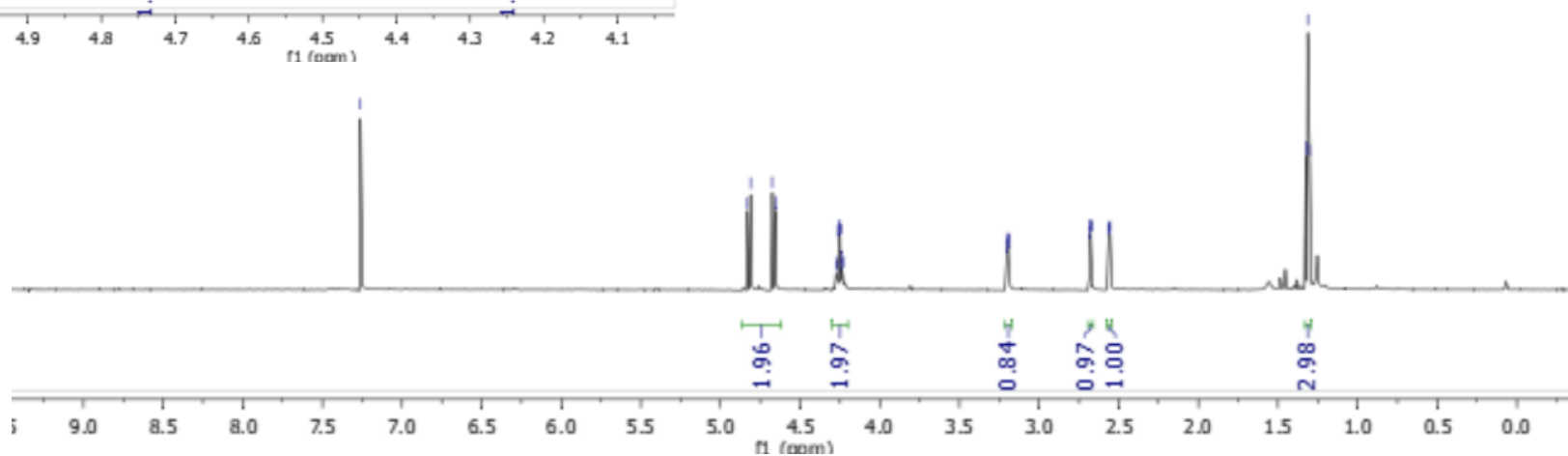
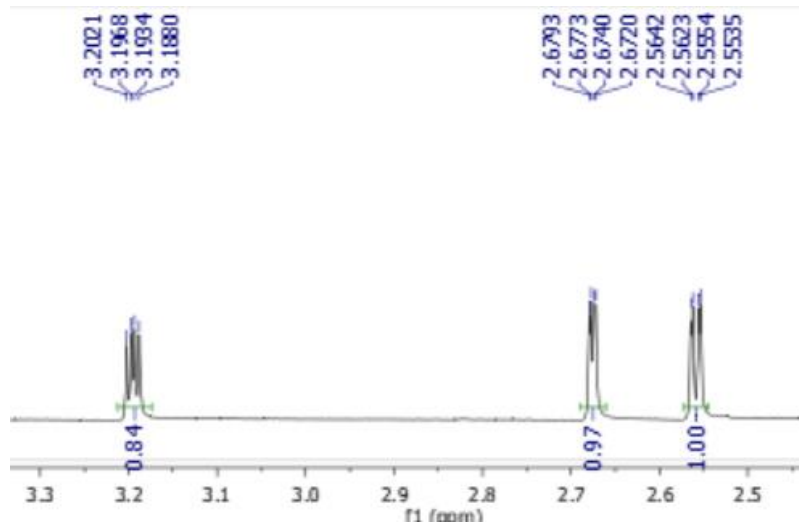
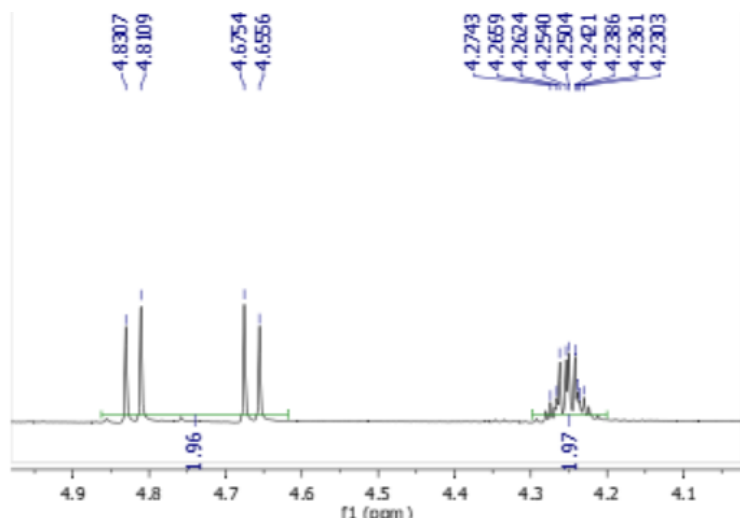
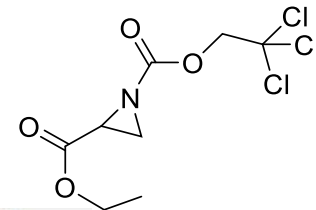
Totals		100.000
--------	--	---------

2-ethyl 1-(2,2,2-trichloroethyl) aziridine-1,2-dicarboxylate (3aa)

$^1\text{H NMR}$

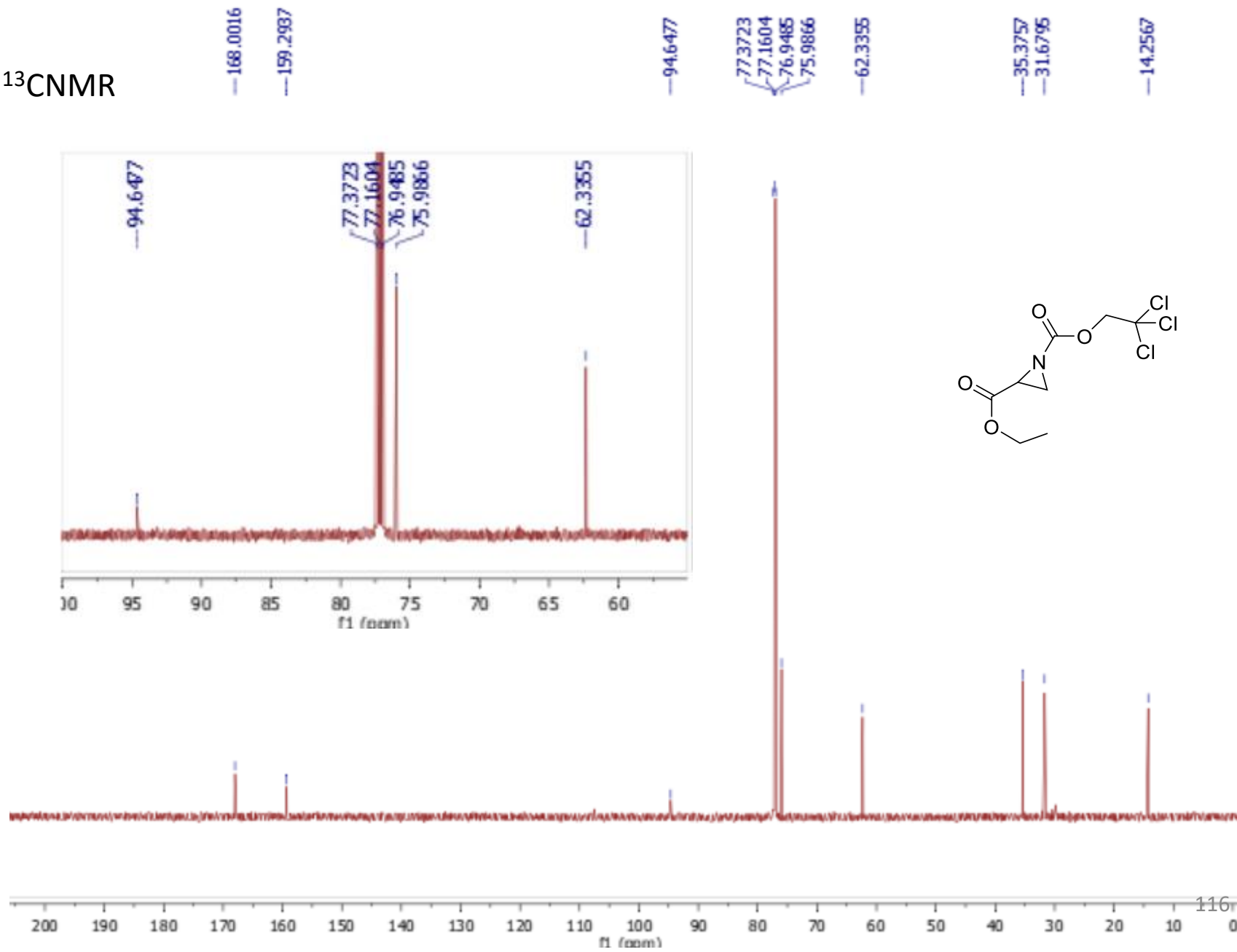
7.2605

4.8307
4.8109
4.6754
4.6556
4.2624
4.2540
4.2504
4.2421
3.2021
3.1968
3.1934
3.1880
2.6793
2.6773
2.6740
2.6720
2.5642
2.5623
2.5554
2.5535
1.3242
1.3123
1.3004



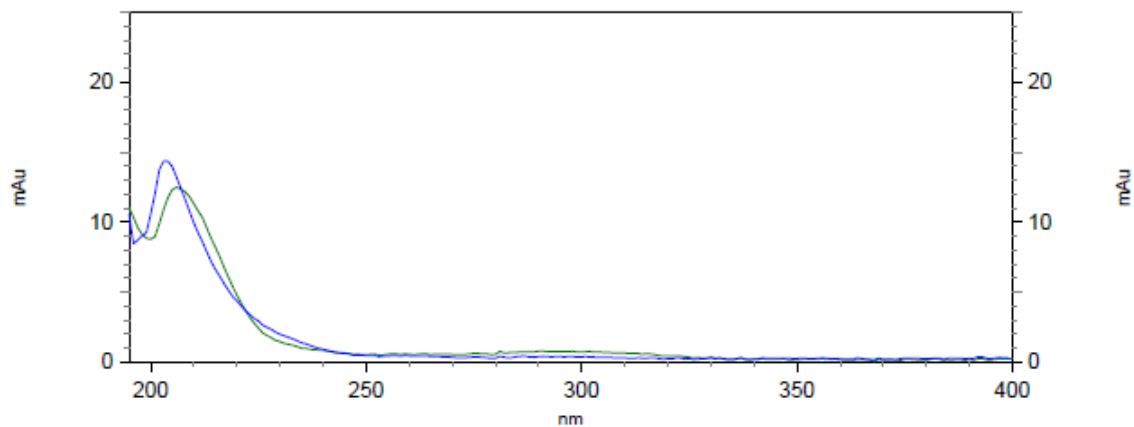
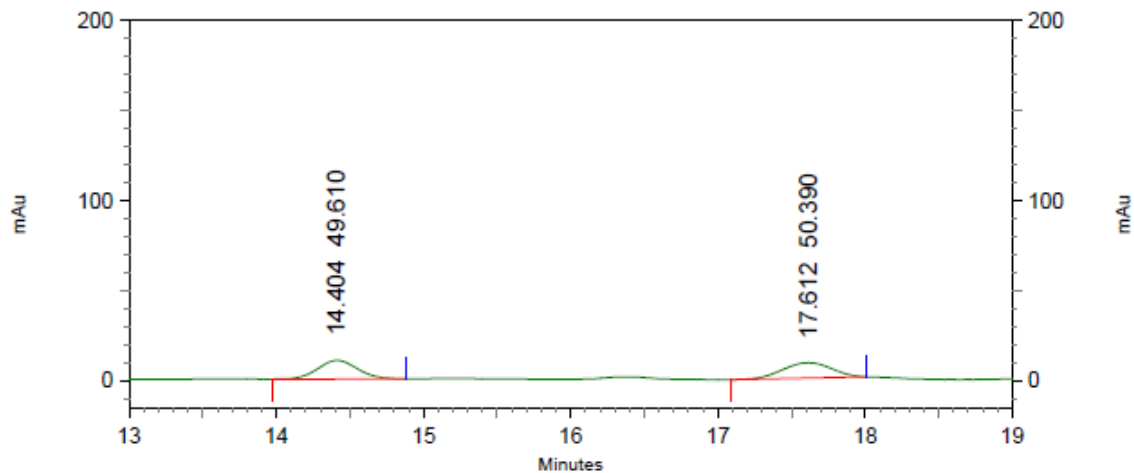
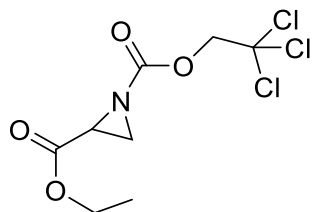
2-ethyl 1-(2,2,2-trichloroethyl) aziridine-1,2-dicarboxylate (3aa)

^{13}C NMR



2-ethyl 1-(2,2,2-trichloroethyl) aziridine-1,2-dicarboxylate (3aa)

HPLC trace
racemic

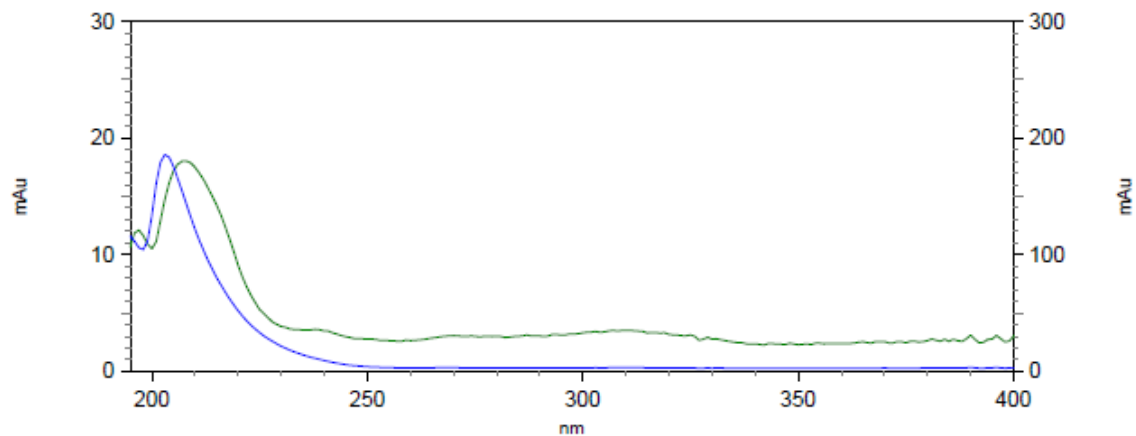
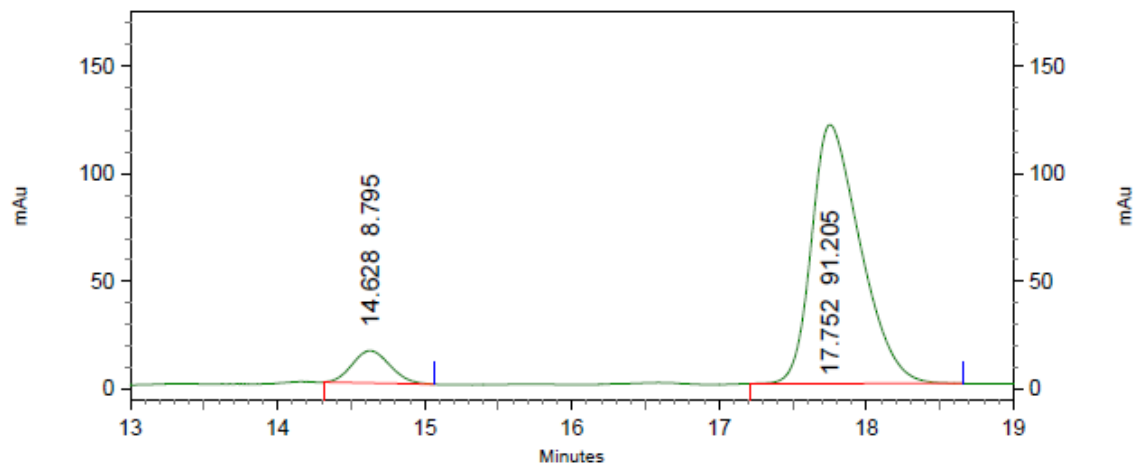
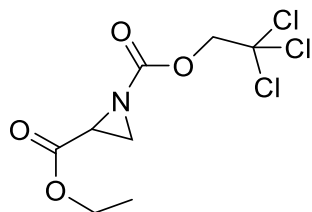


4: 210 nm, 4
nm Results

Pk #	Retention Time	Area Percent
1	14.404	49.610
2	17.612	50.390
Totals		100.000

2-ethyl 1-(2,2,2-trichloroethyl) aziridine-1,2-dicarboxylate (3aa)

HPLC trace



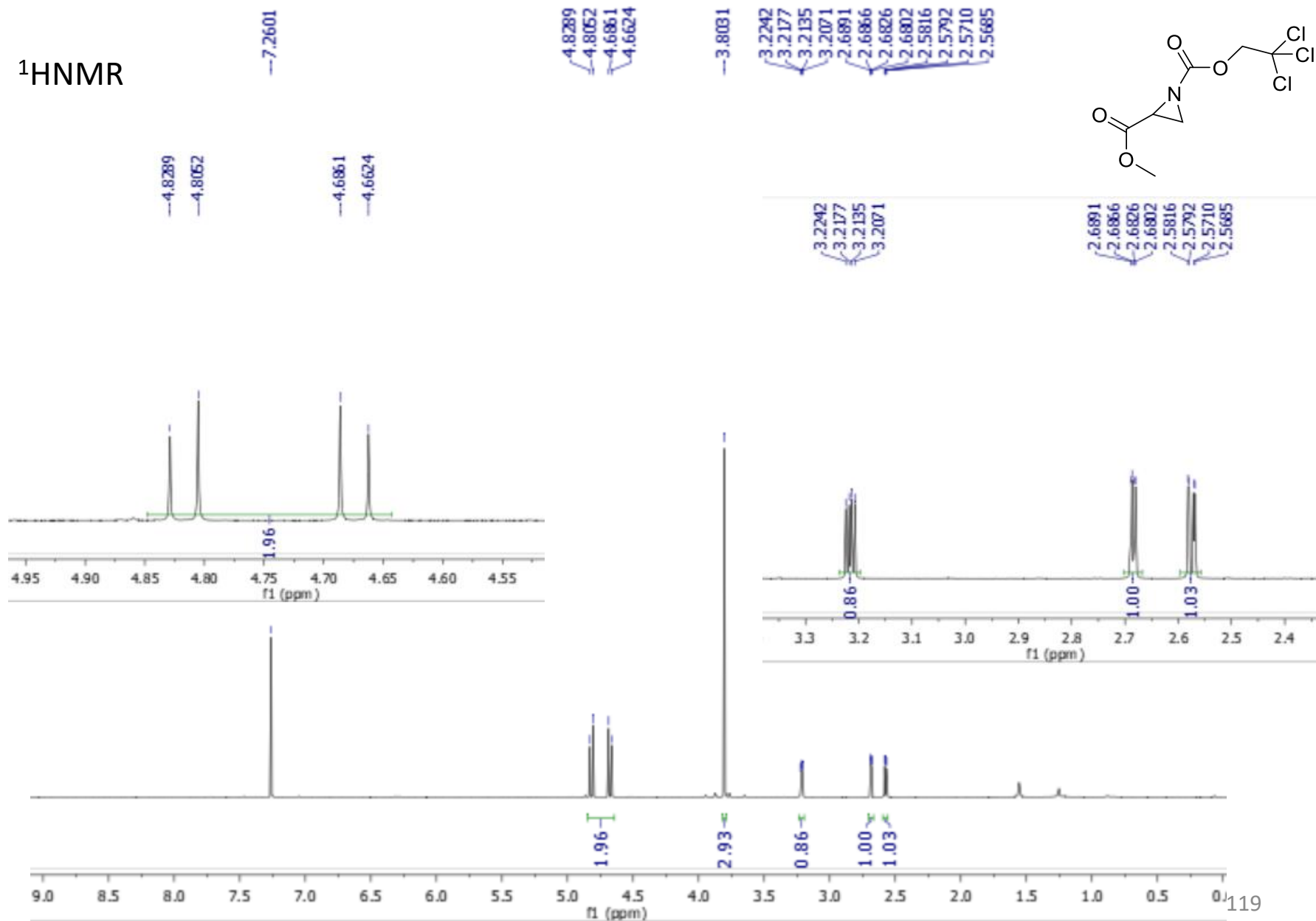
4: 210 nm, 4
nm Results

Pk #	Retention Time	Area Percent
1	14.628	8.795
2	17.752	91.205

Totals		100.000
--------	--	---------

2-methyl 1-(2,2,2-trichloroethyl) aziridine-1,2-dicarboxylate (3ab)

$^1\text{H NMR}$



2-methyl 1-(2,2,2-trichloroethyl) aziridine-1,2-dicarboxylate (3ab)

^{13}C NMR

168.4489

159.2563

94.6393

77.4146

77.1604

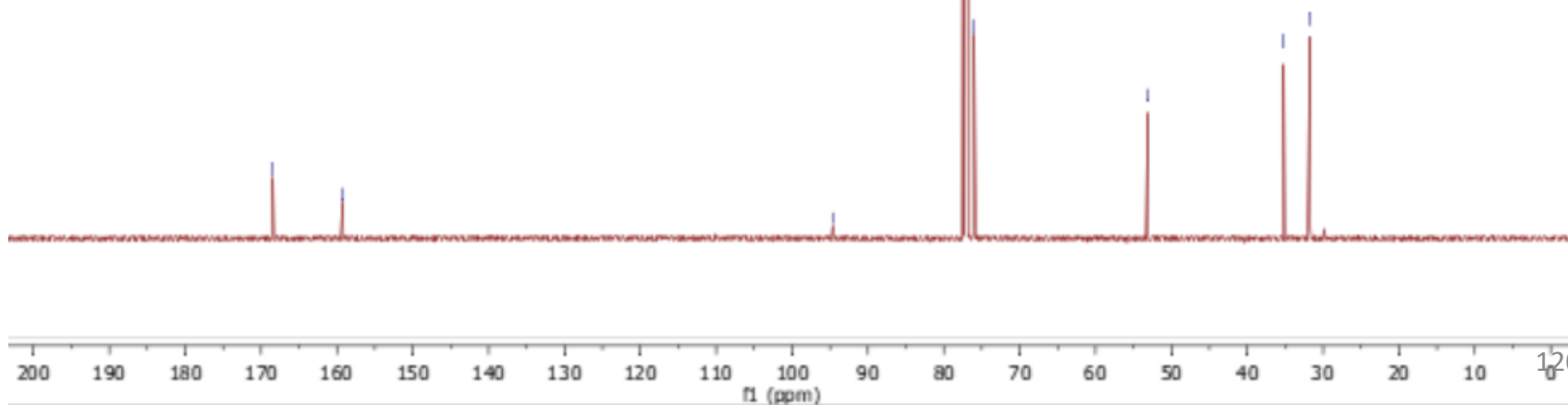
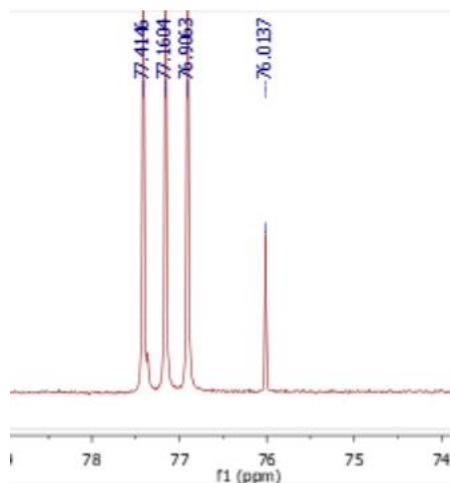
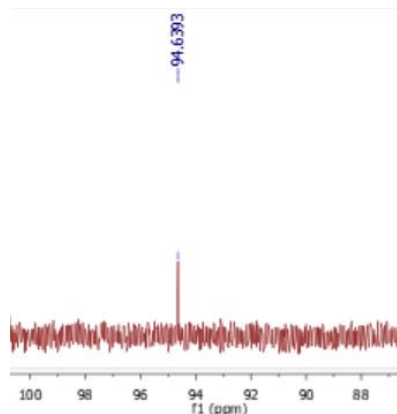
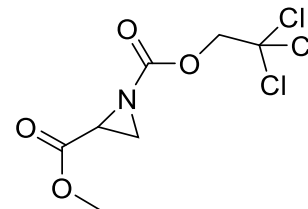
76.9063

76.0137

53.0935

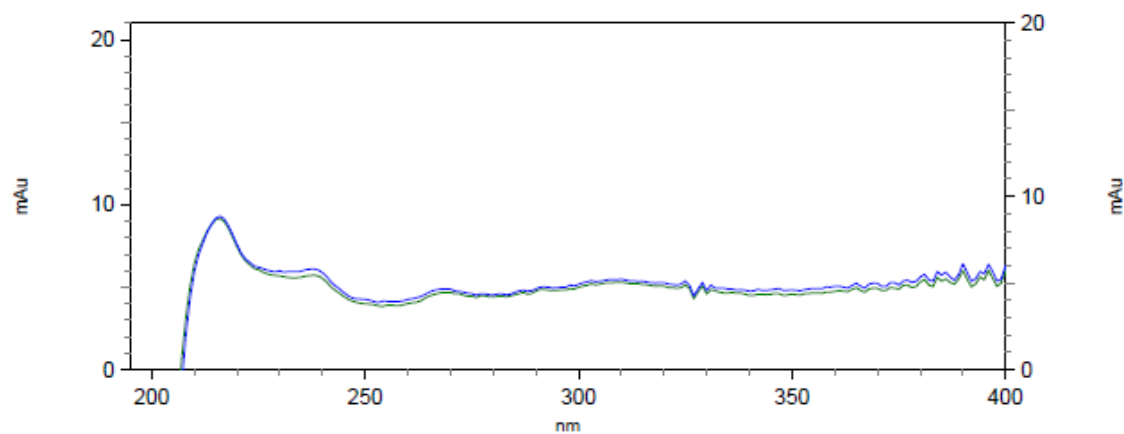
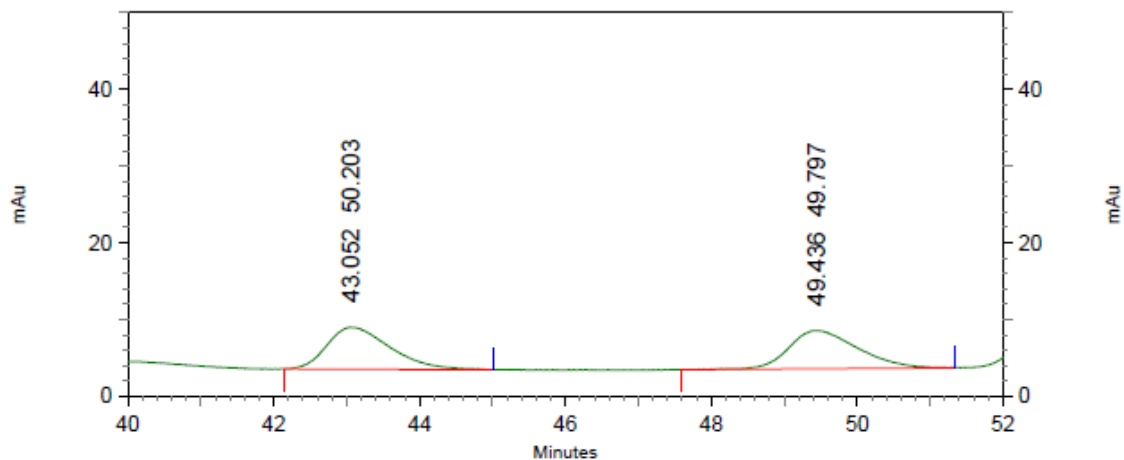
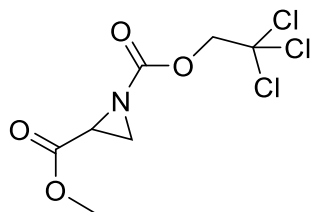
35.1970

31.7343



2-methyl 1-(2,2,2-trichloroethyl) aziridine-1,2-dicarboxylate (3ab)

HPLC trace
racemic



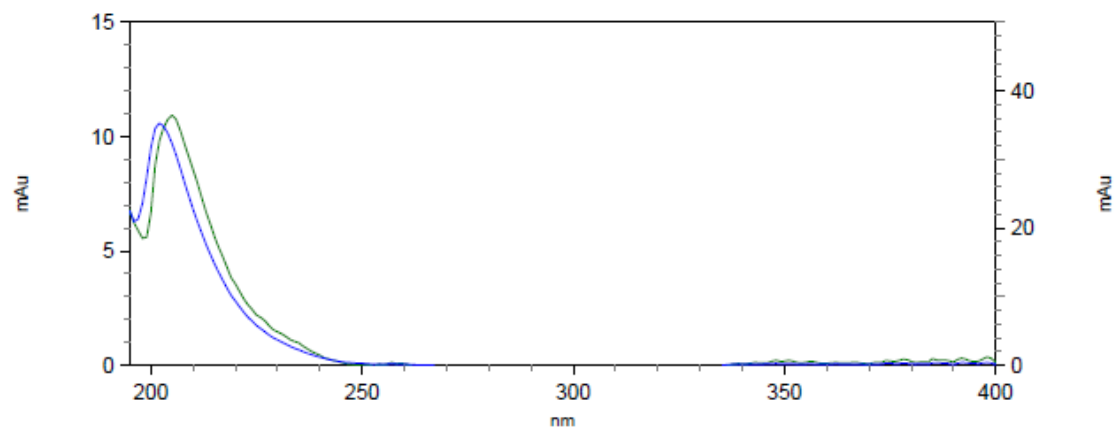
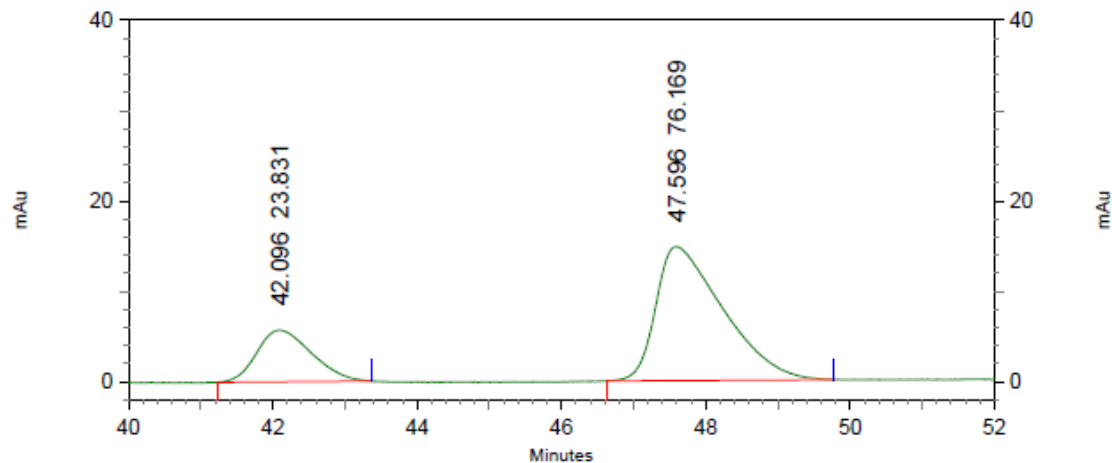
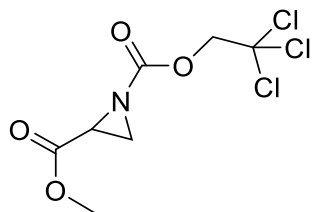
6: 215 nm, 4
nm Results

Pk #	Retention Time	Area Percent
1	43.052	50.203
2	49.436	49.797

Totals	100.000
--------	---------

2-methyl 1-(2,2,2-trichloroethyl) aziridine-1,2-dicarboxylate (3ab)

HPLC trace
racemic



6: 215 nm, 4
nm Results

Pk #	Retention Time	Area Percent
1	42.096	23.831
2	47.596	76.169
Totals		100.000

2-(4-Nitrophenyl)aziridine (4r)

$^1\text{H NMR}$

8.1547
8.1329

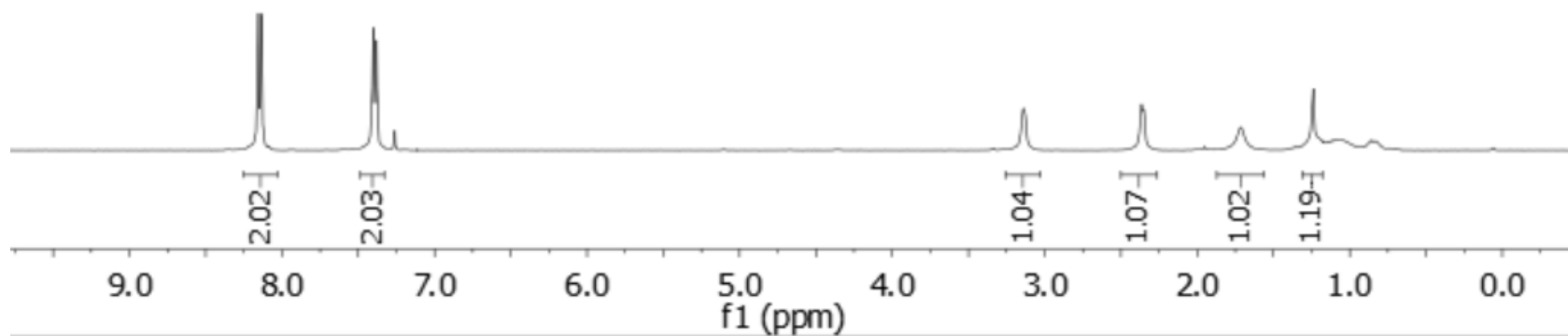
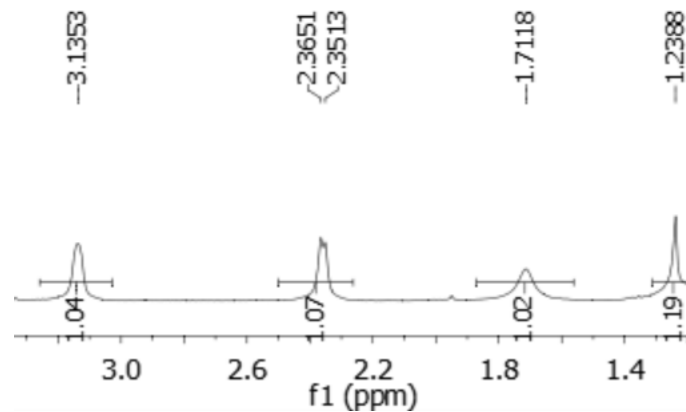
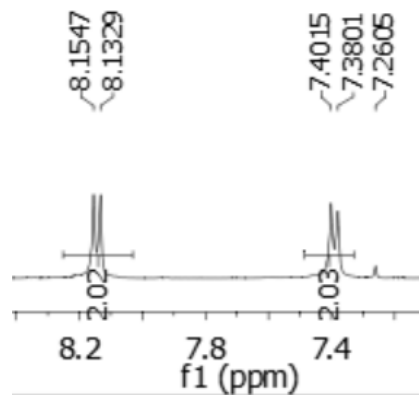
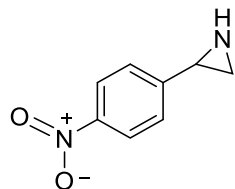
7.4015
7.3801
7.2605

-3.1353

2.3651
2.3513

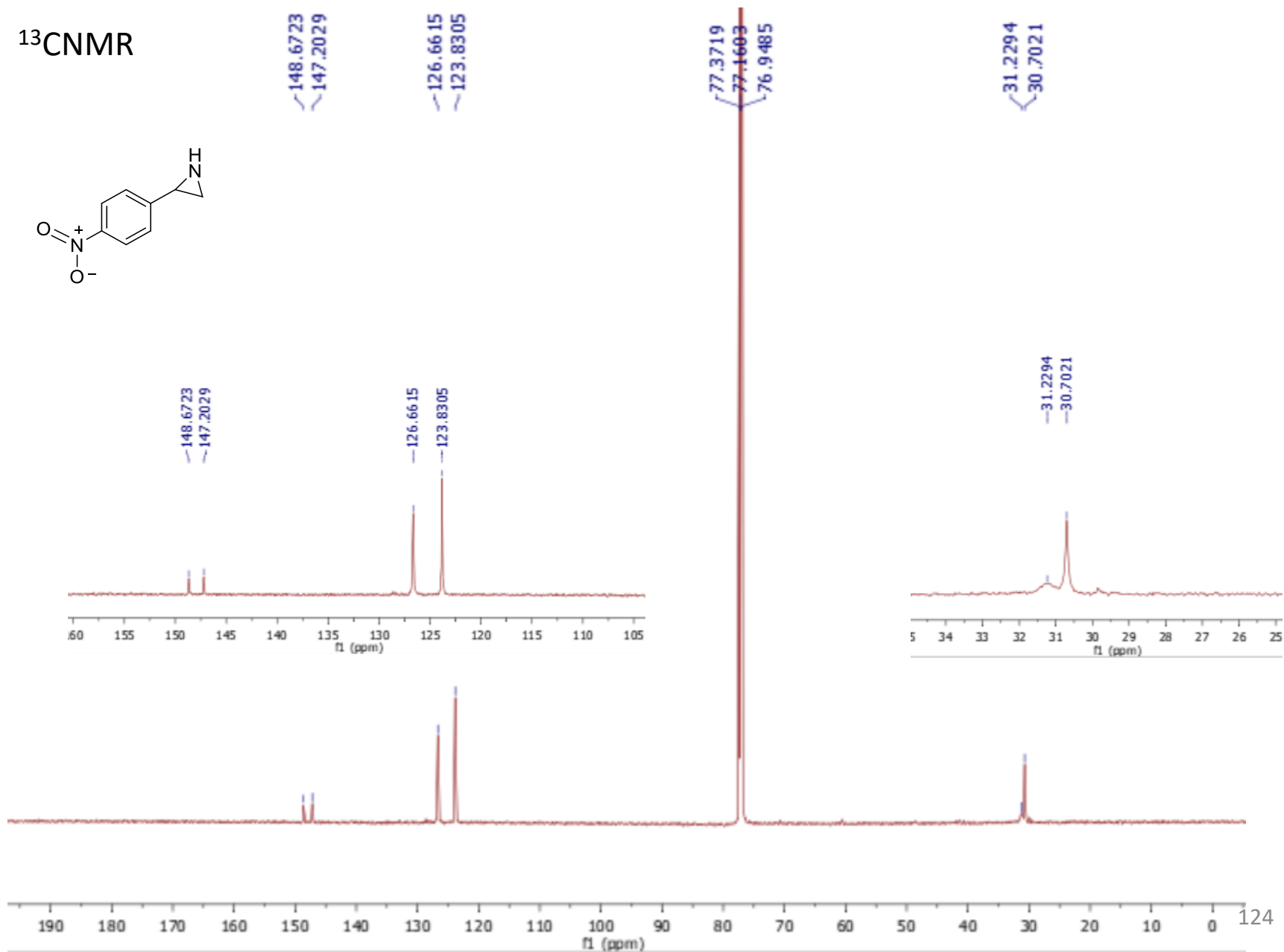
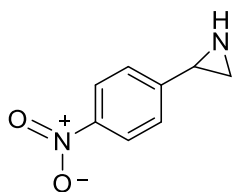
-1.7118

-1.2388

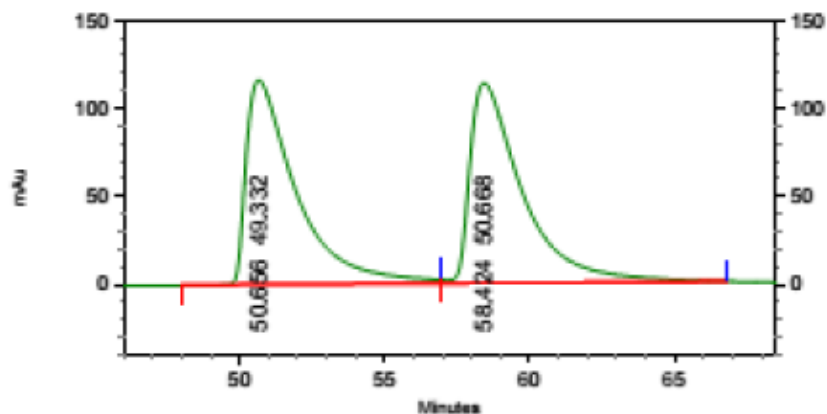


2-(4-Nitrophenyl)aziridine (4r)

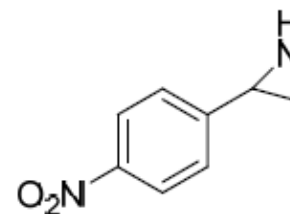
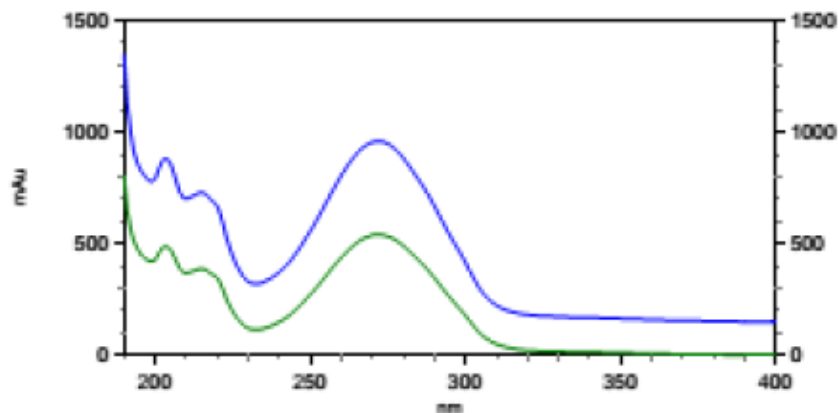
^{13}C NMR



2-(4-Nitrophenyl)aziridine (4r)



HPLC trace
racemic



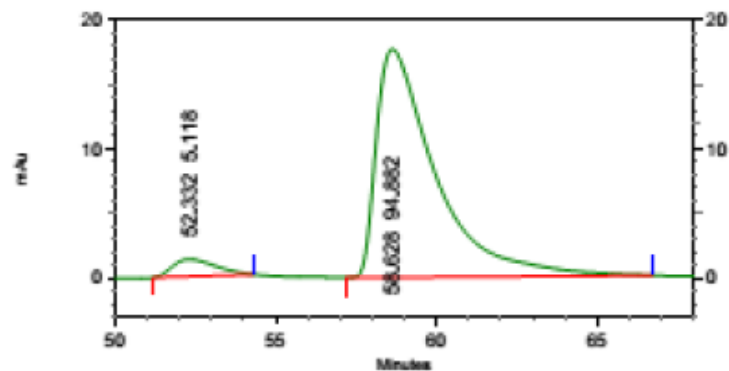
6: 282 nm, 4 nm

Results

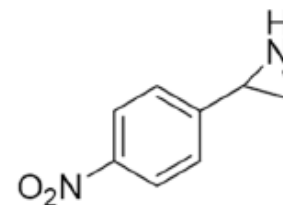
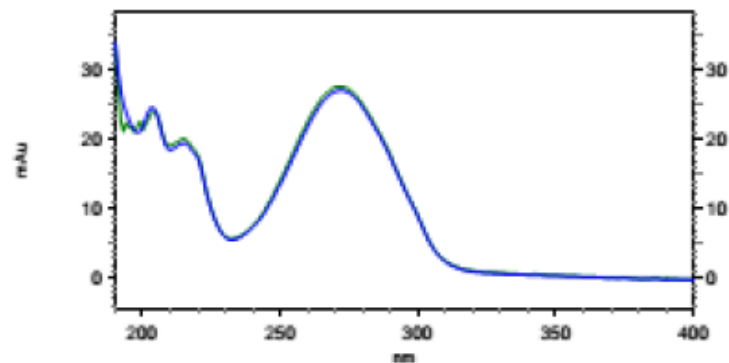
Name	Retention Time	Area Percent	Pk #
	50.656	49.332	1
	58.424	50.668	2

Totals	100.000
--------	---------

2-(4-Nitrophenyl)aziridine (4r)



HPLC trace



6: 233 nm, 4 nm

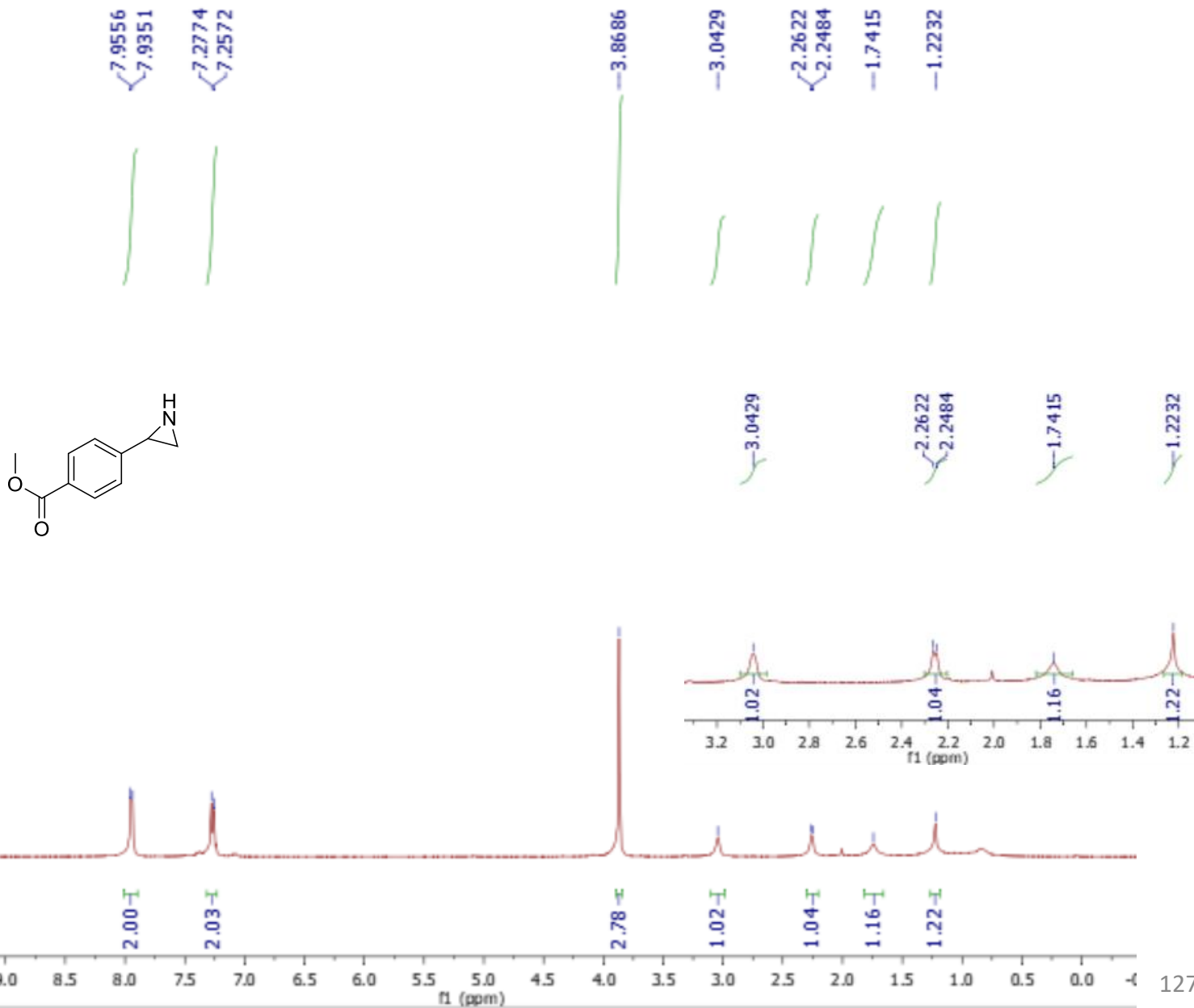
Results

Name	Retention Time	Area Percent	Pk #
	52.332	5.118	1
	58.628	94.882	2

Totals		100.000	
--------	--	---------	--

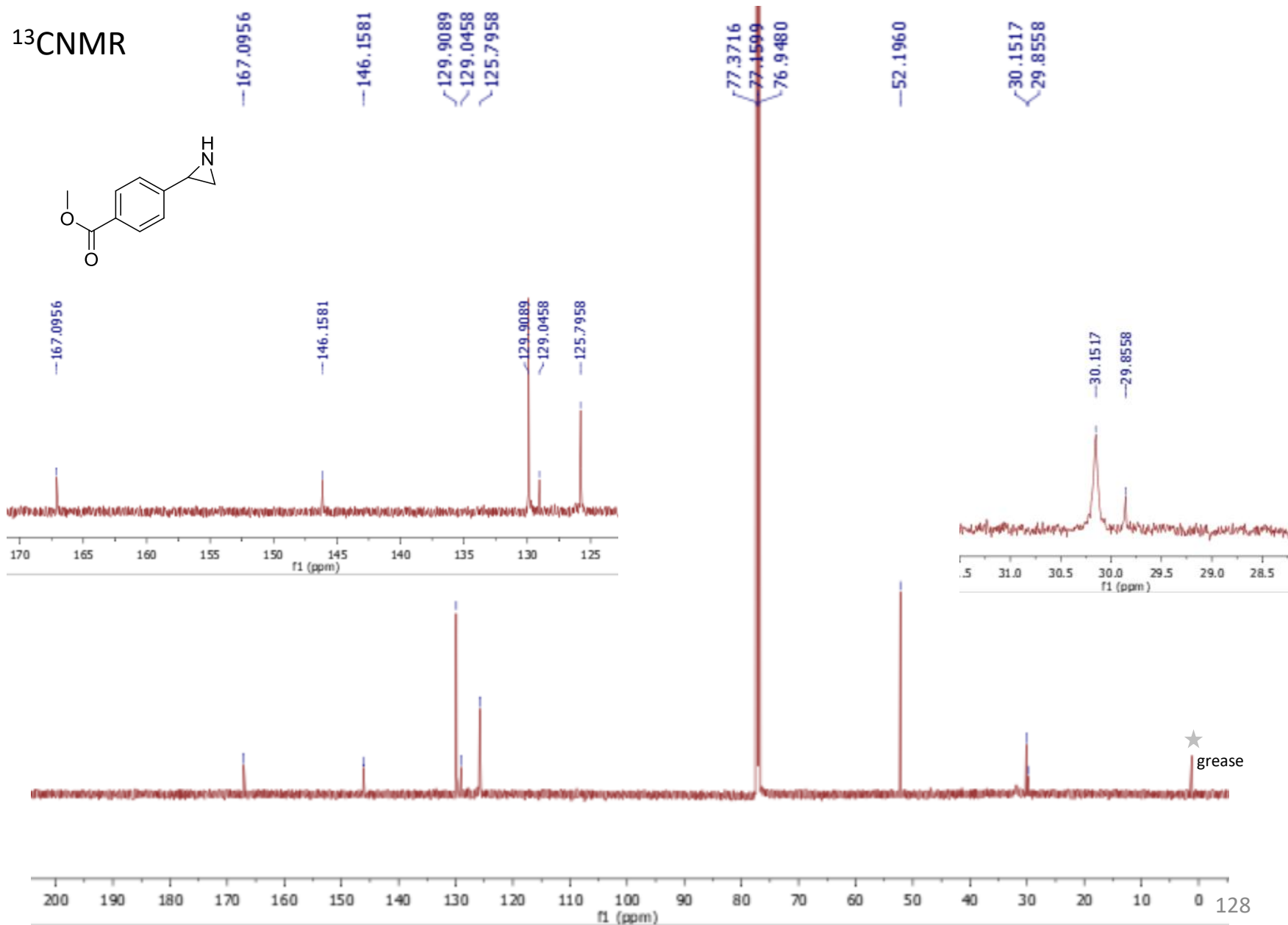
Methyl 4-(aziridin-2-yl)benzoate (4p)

¹HNMR

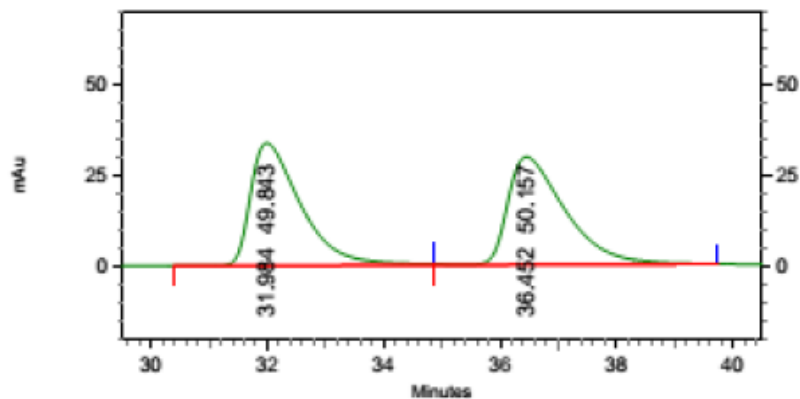


Methyl 4-(aziridin-2-yl)benzoate (4p)

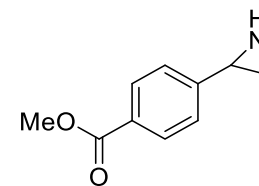
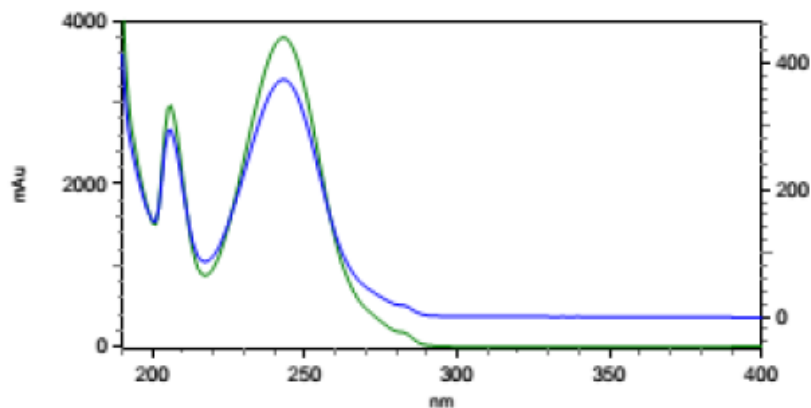
^{13}C NMR



Methyl 4-(aziridin-2-yl)benzoate (4p)



HPLC trace
racemic

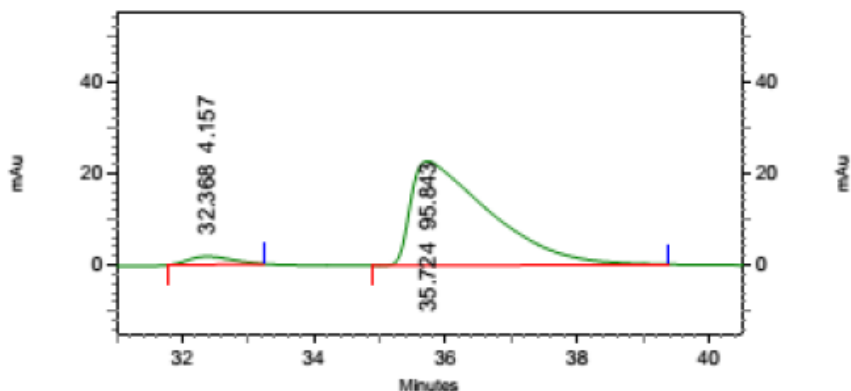


2: 265 nm, 4 nm

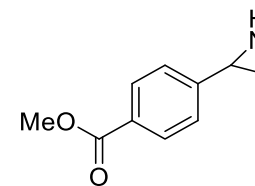
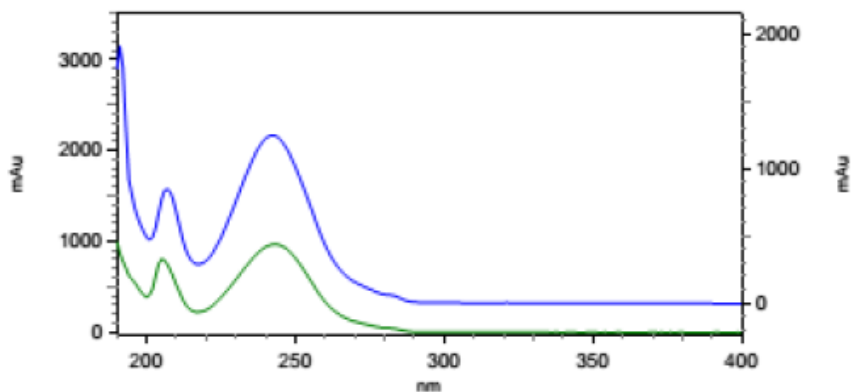
Results

Name	Retention Time	Area Percent	Pk #
	31.984	49.843	1
	36.452	50.157	2
Totals		100.000	

Methyl 4-(aziridin-2-yl)benzoate (4p)



HPLC trace



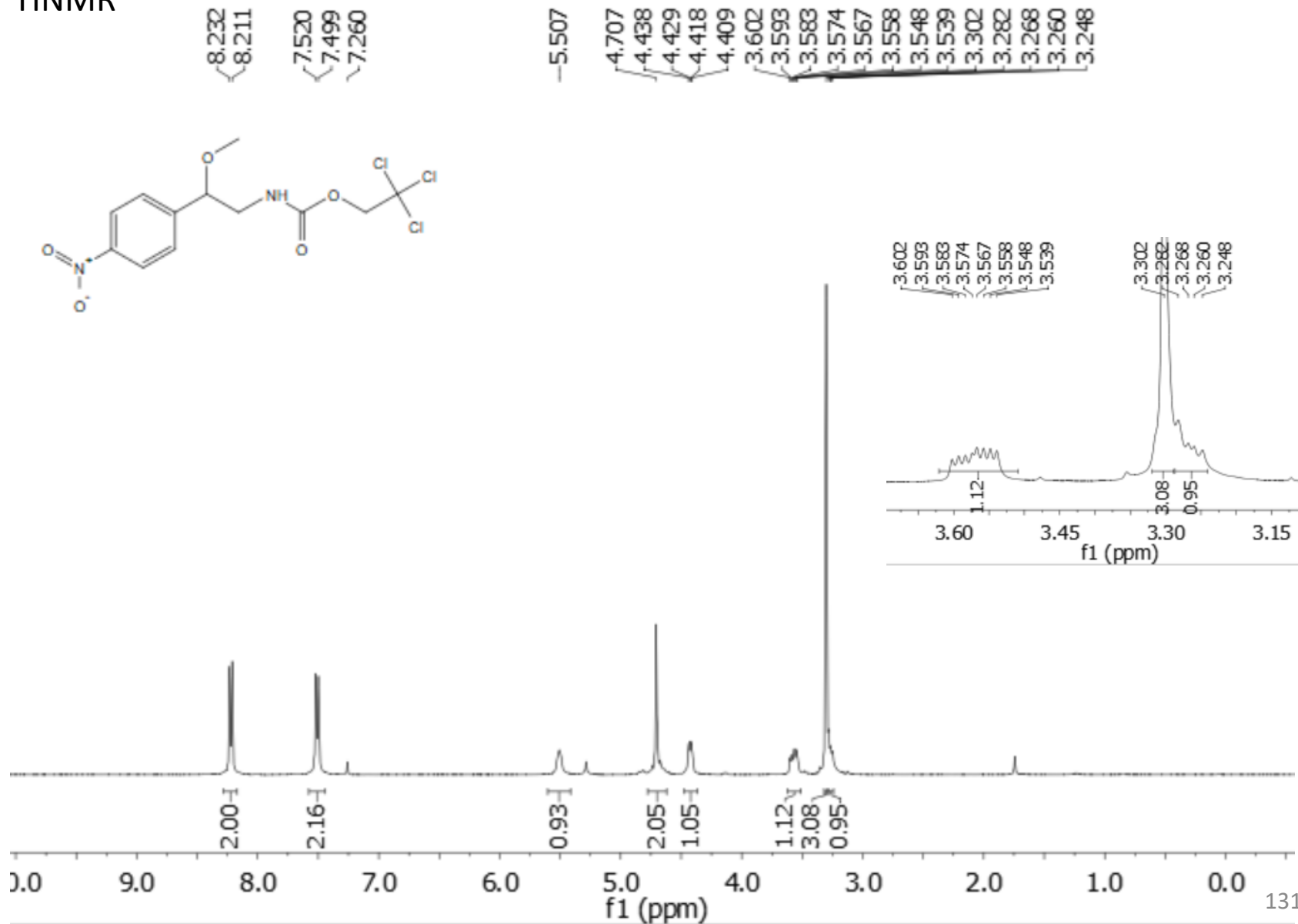
2: 282 nm, 4 nm

Results

Name	Retention Time	Area Percent	Pk #
	32.368	4.157	1
	35.724	95.843	2
Totals		100.000	

2,2,2-Trichloroethyl 2-methoxy-2-(4-nitrophenyl)ethylcarbamate (5r)

¹HNMR



2,2,2-Trichloroethyl 2-methoxy-2-(4-nitrophenyl)ethylcarbamate (5r)

^{13}C NMR

154.550
147.875
146.266

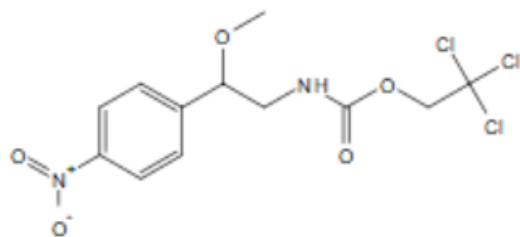
127.488
123.887

95.454

81.597
77.345
77.027
76.709
74.532

57.429

47.083

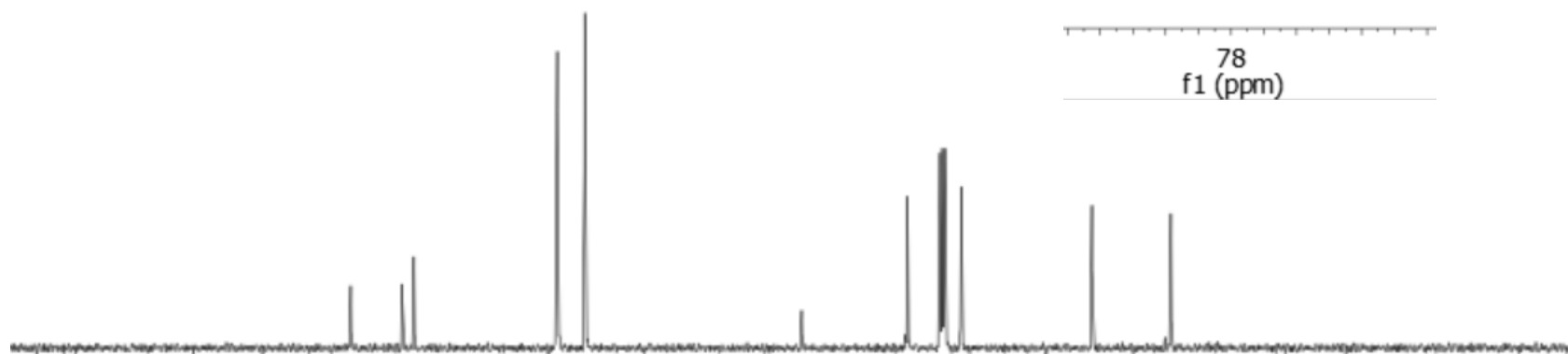
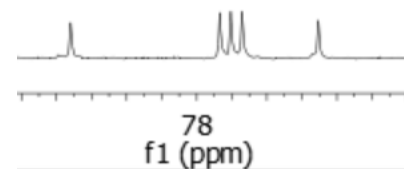


81.597

77.345
77.027

76.709

74.532



190

170

150

130

110

90

80

70

60

50

40

30

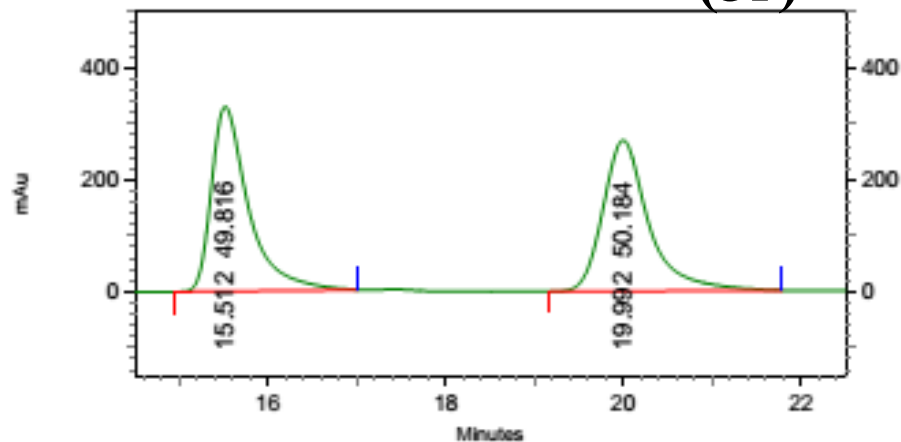
20

10

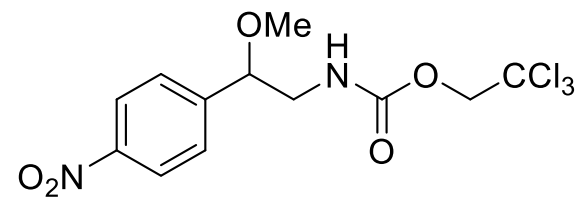
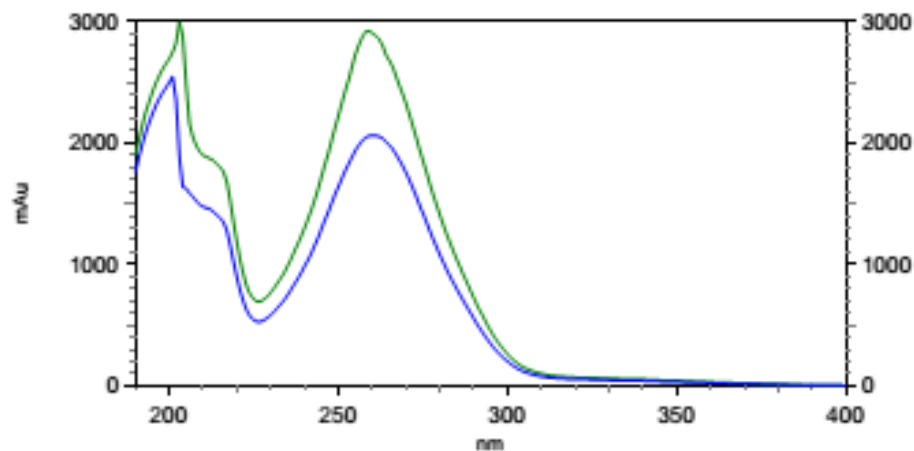
0

f1 (ppm)

2,2,2-Trichloroethyl 2-methoxy-2-(4-nitrophenyl)ethylcarbamate (5r)



HPLC trace
racemic



2: 233 nm, 4 nm

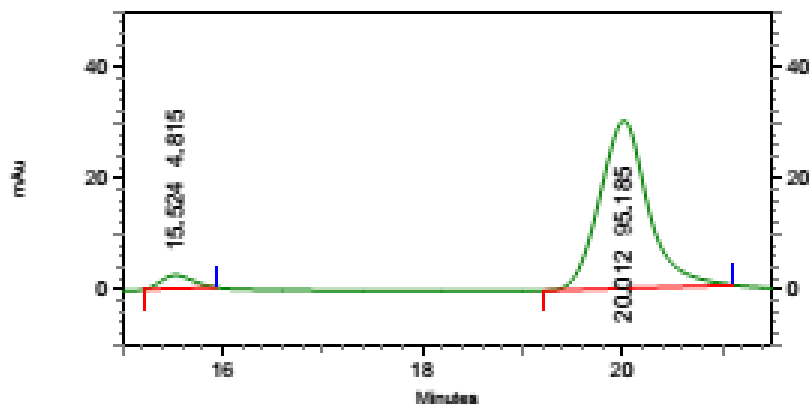
Results

Name	Retention Time	Area Percent	Pk #
	15.512	49.816	1
	19.992	50.184	2

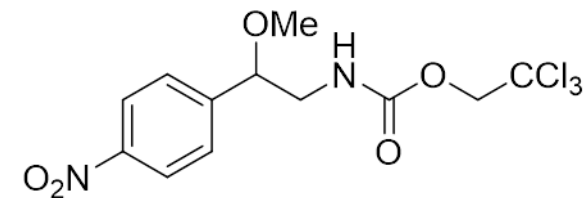
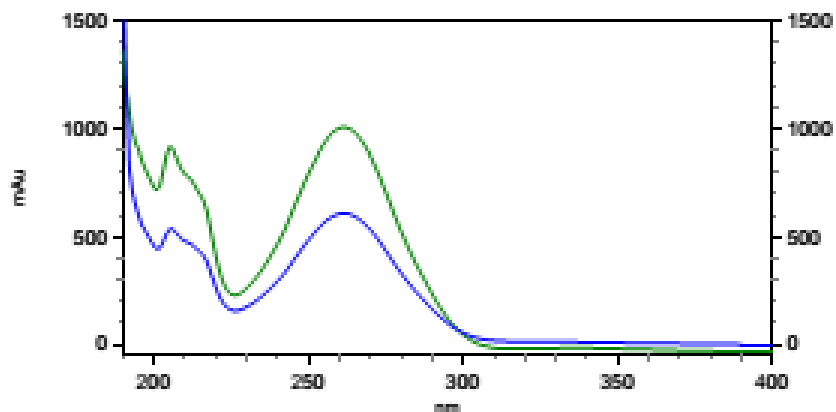
Totals

100.000

2,2,2-Trichloroethyl 2-methoxy-2-(4-nitrophenyl)ethylcarbamate (5r)



HPLC trace



2: 343 nm, 4 nm

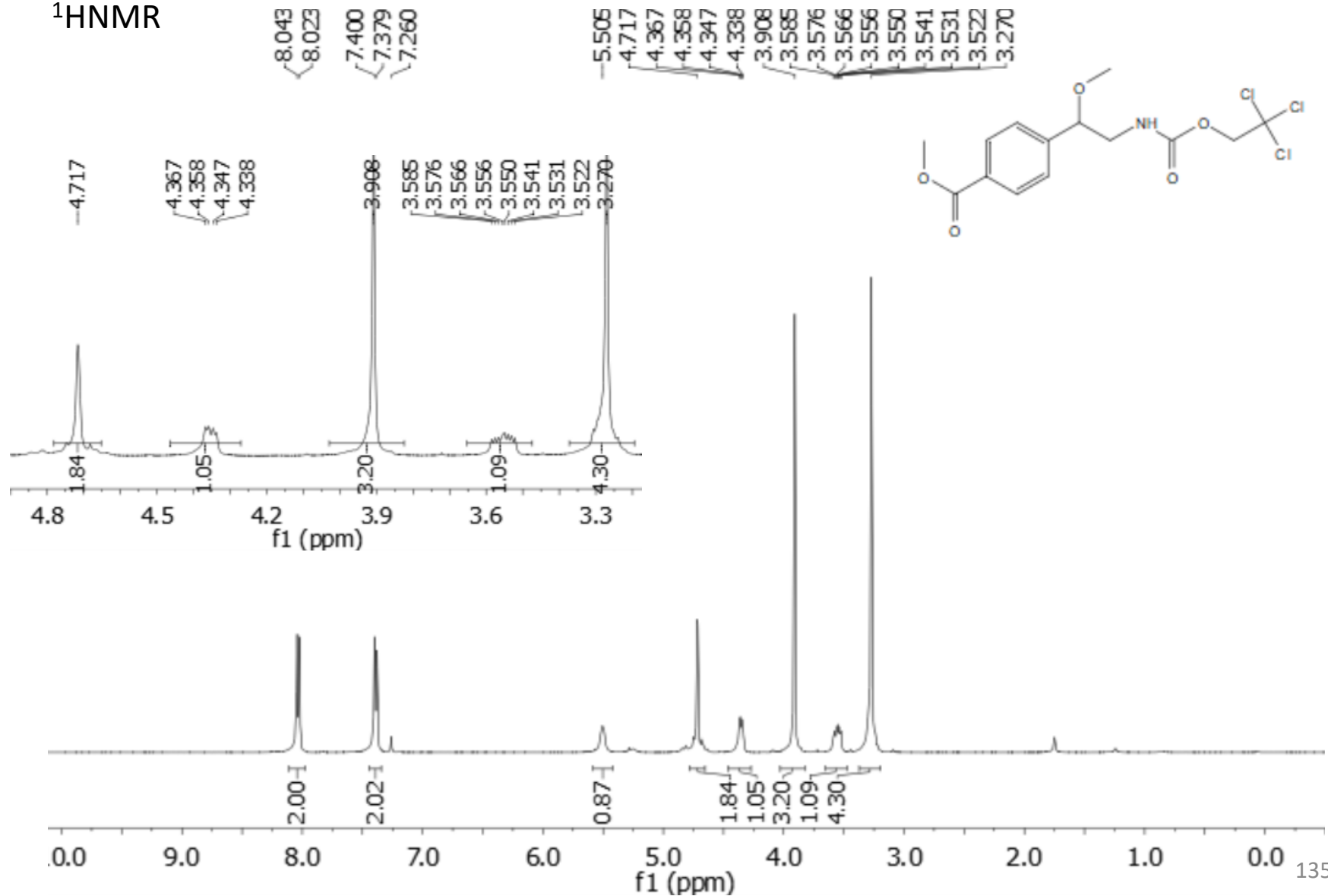
Results

Name	Retention Time	Area Percent	Pk #
	15.524	4.815	1
	20.012	95.185	2

Totals	100.000
--------	---------

Methyl 4-(1-methoxy-2-((2,2,2-trichloroethoxy)carbonylamino)ethyl)benzoate (5p)

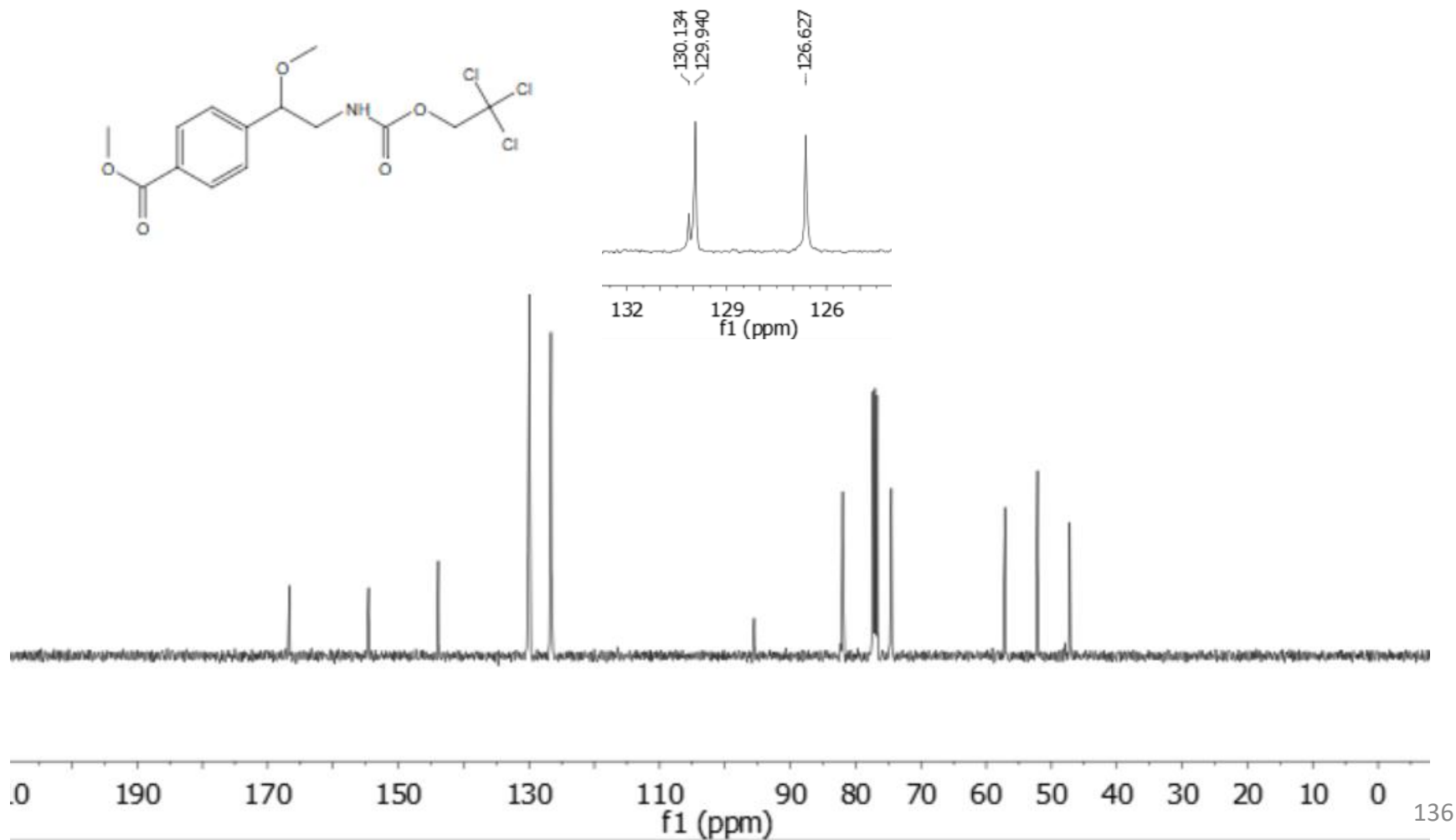
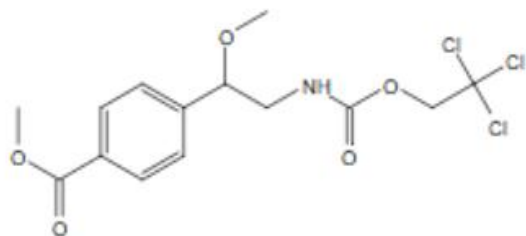
¹H NMR



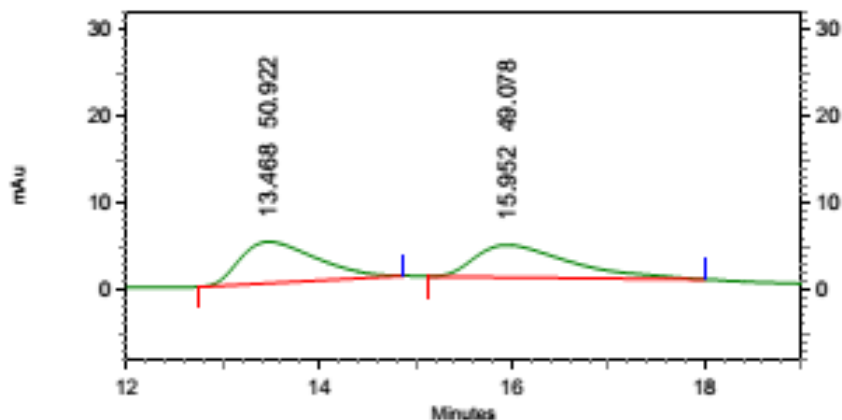
Methyl 4-(1-methoxy-2-((2,2,2-trichloroethoxy)carbonylamino)ethyl)benzoate (5p)

^{13}C NMR

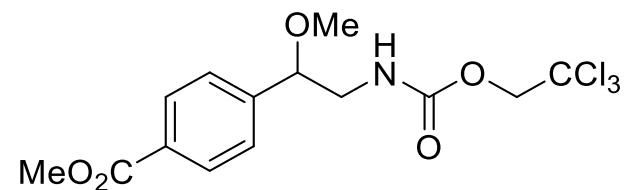
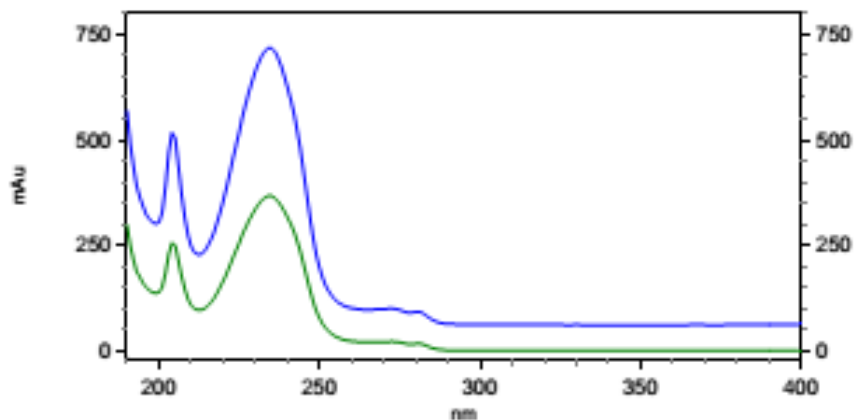
-166.680	-154.549	-143.894	130.134	129.940	126.627	-95.520	81.974	77.332	77.013	76.696	74.515	-57.130	-52.138	-47.206
----------	----------	----------	---------	---------	---------	---------	--------	--------	--------	--------	--------	---------	---------	---------



Methyl 4-(1-methoxy-2-((2,2,2-trichloroethoxy)carbonylamino)ethyl)benzoate (5p)



HPLC trace
racemic



6: 272 nm, 4 nm

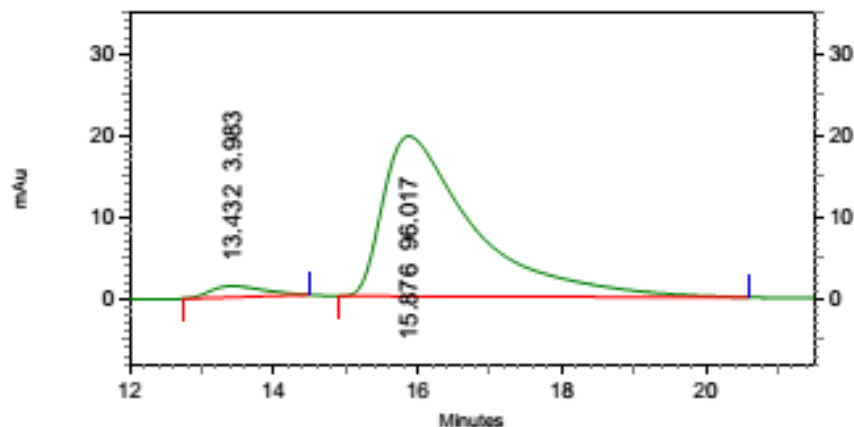
Results

Name	Retention Time	Area Percent	Pk #
	13.468	50.922	1
	15.952	49.078	2

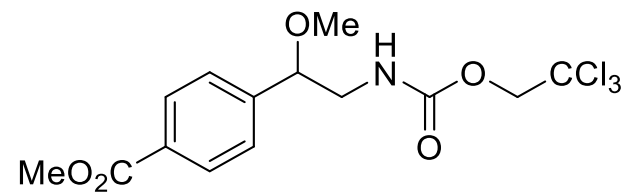
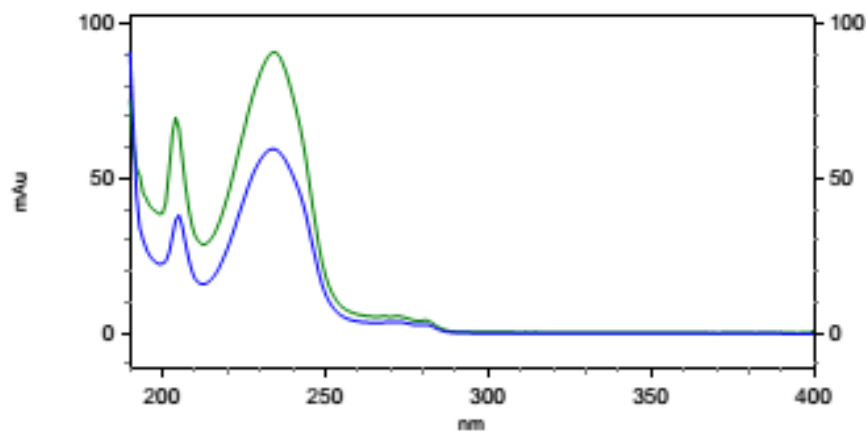
Totals

100.000

Methyl 4-(1-methoxy-2-((2,2,2-trichloroethoxy)carbonylamino)ethyl)benzoate (5p)



HPLC trace



6: 259 nm, 4 nm

Results

Name	Retention Time	Area Percent	Pk #
	13.432	3.983	1
	15.876	96.017	2

Totals	100.000
--------	---------

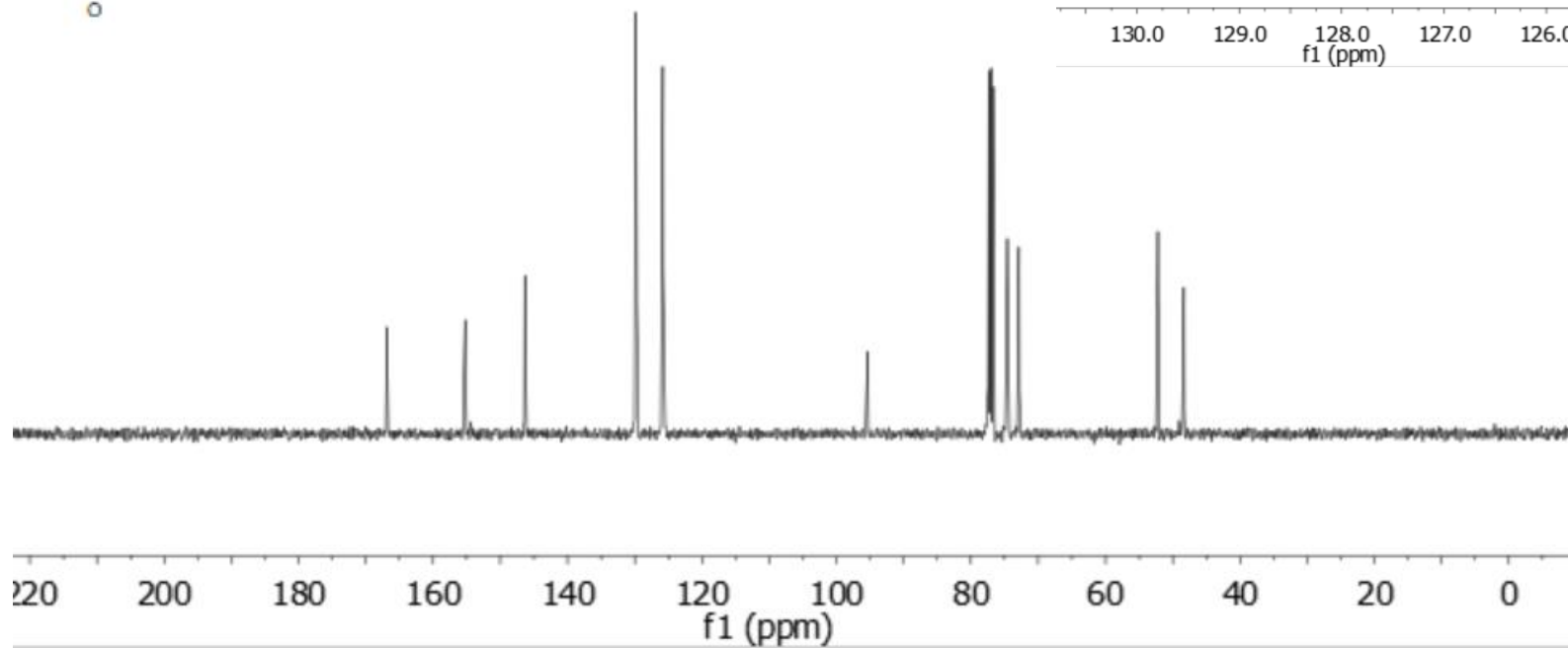
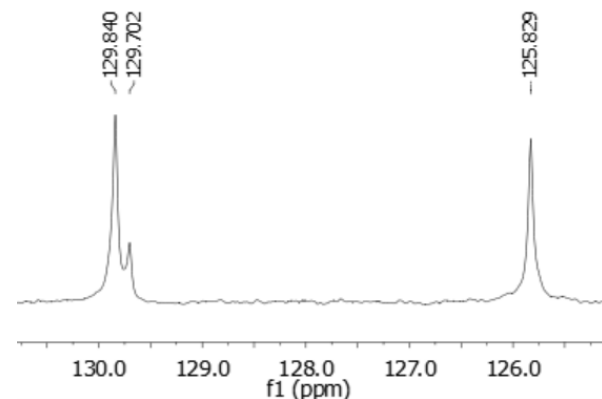
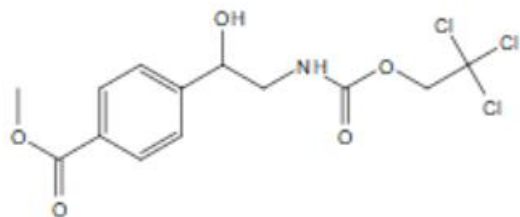
Methyl 4-(1-hydroxy-2-((2,2,2-trichloroethoxy)carbonylamino)ethyl)benzoate (6p)



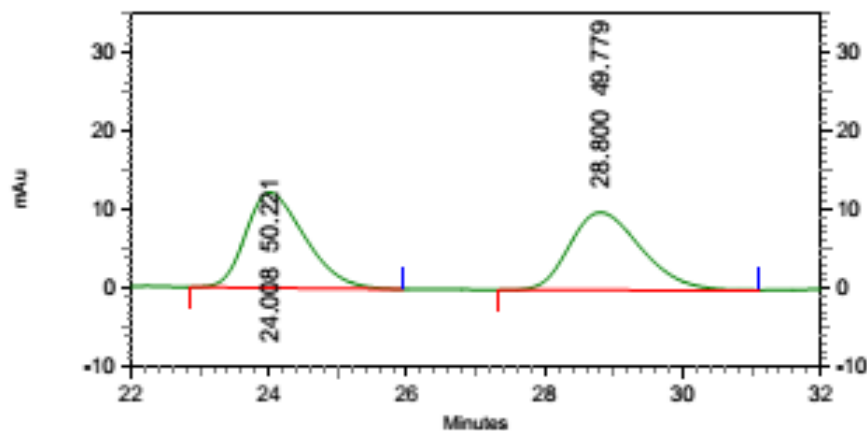
Methyl 4-(1-hydroxy-2-((2,2,2-trichloroethoxy)carbonylamino)ethyl)benzoate (6p)

¹³CNMR

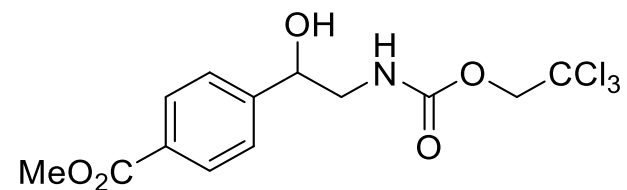
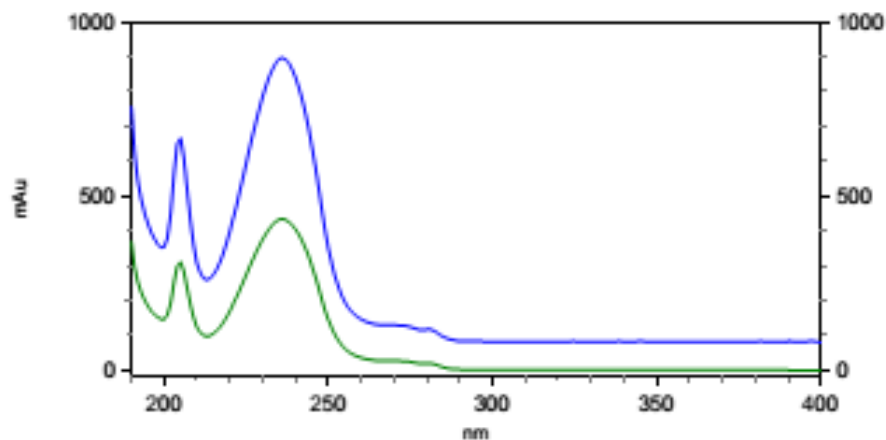
Chemical shift values (ppm):
-166.861, -155.235, -146.344, -129.840, -129.702, -125.829, -95.376, 77.347, 77.029, 76.711, 74.595, 72.874, 52.195, 48.335



Methyl 4-(1-hydroxy-2-((2,2,2-trichloroethoxy)carbonylamino)ethyl)benzoate (6p)



HPLC trace
racemic



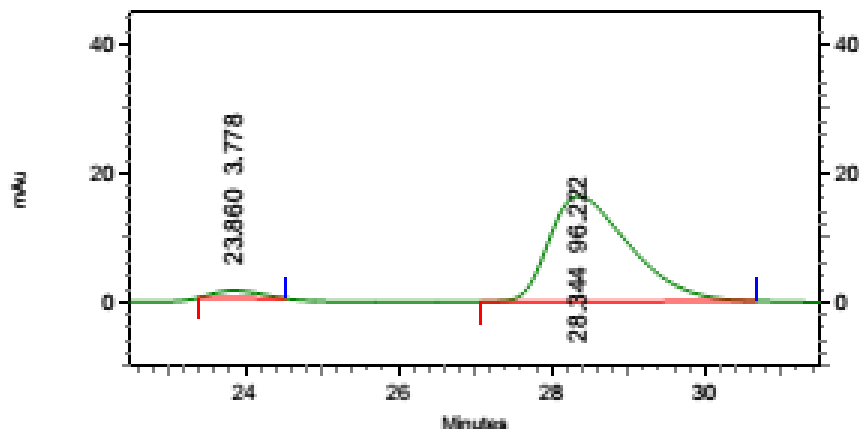
3: 257 nm, 4 nm

Results

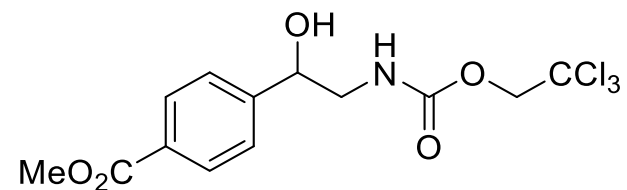
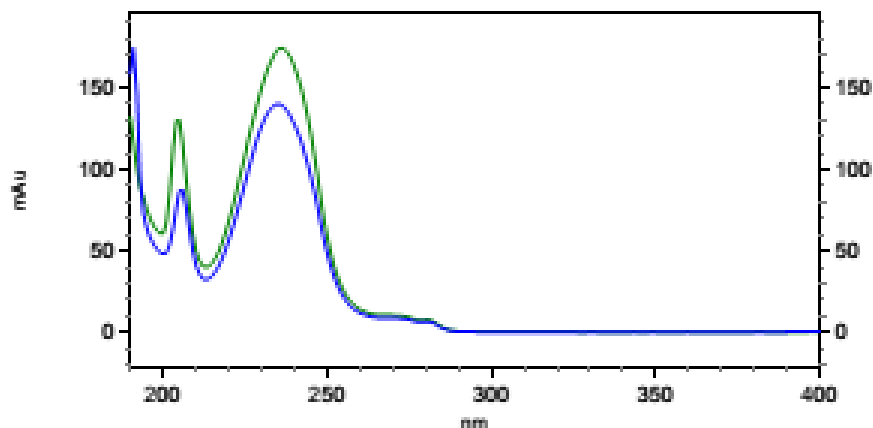
Name	Retention Time	Area Percent	Pk #
	24.008	50.221	1
	28.800	49.779	2

Totals		100.000	
--------	--	---------	--

Methyl 4-(1-hydroxy-2-((2,2,2-trichloroethoxy)carbonylamino)ethyl)benzoate (6p)



HPLC trace



3: 281 nm, 4 nm

Results

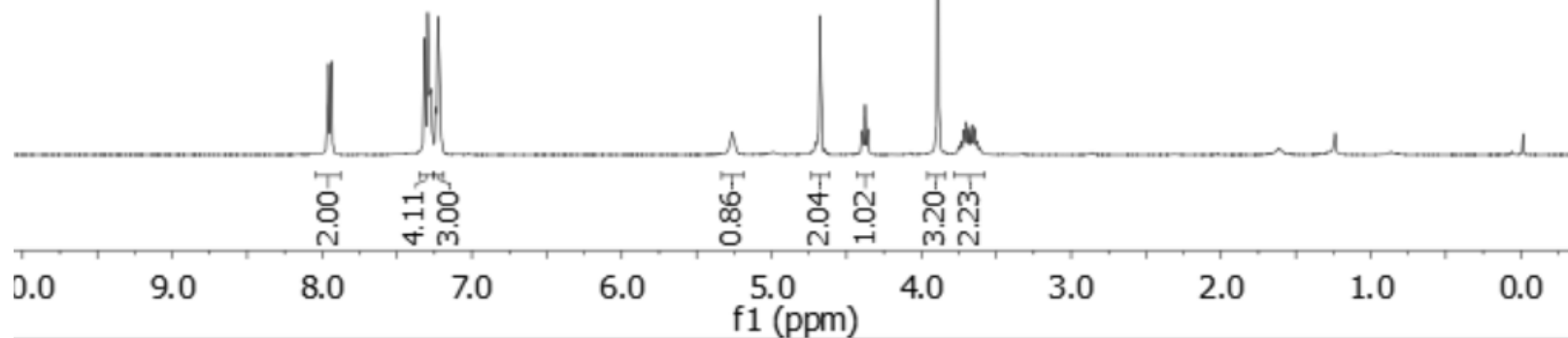
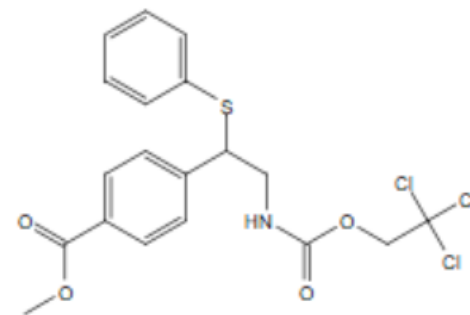
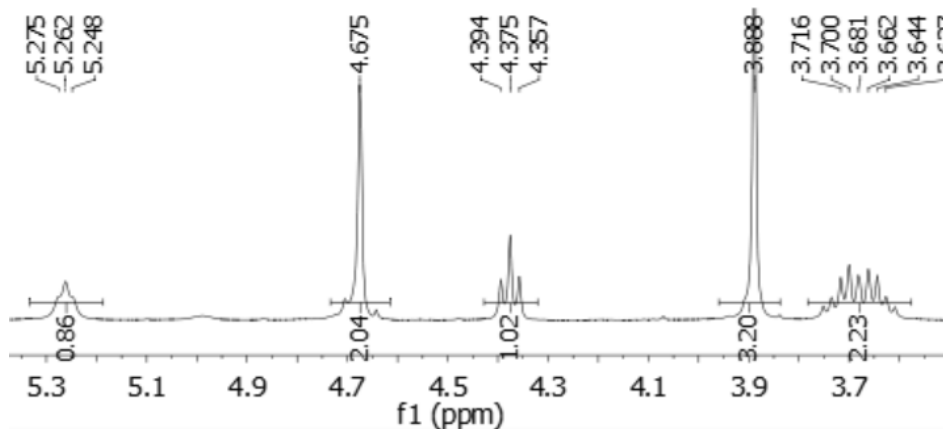
Name	Retention Time	Area Percent	Pk #
	23.860	3.778	1
	28.344	96.222	2

Totals		100.000	
--------	--	---------	--

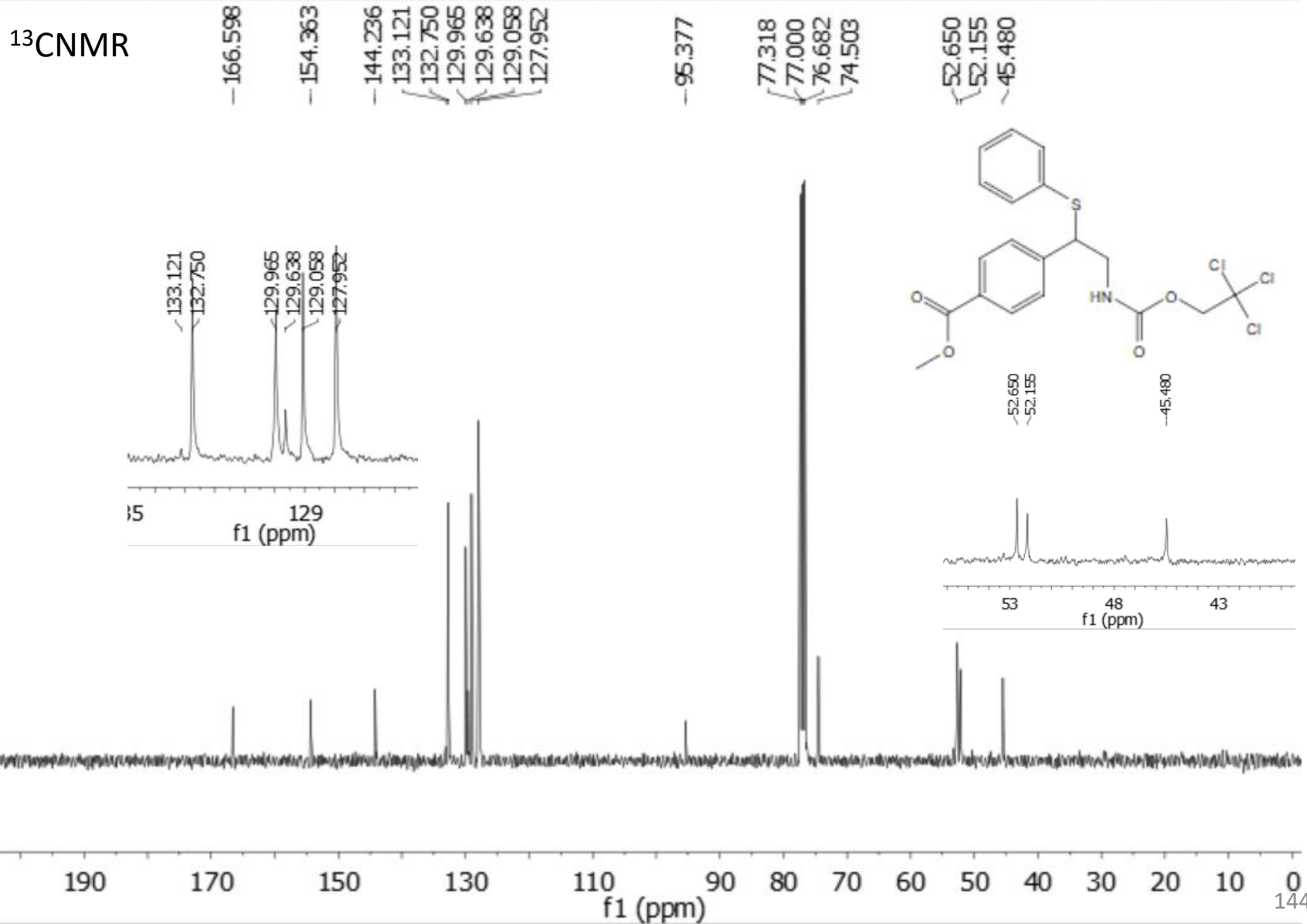
Methyl 4-(1-(phenylthio)-2-((2,2,2-trichloroethoxy)carbonylamino)ethyl)benzoate (7p)

¹HNMR

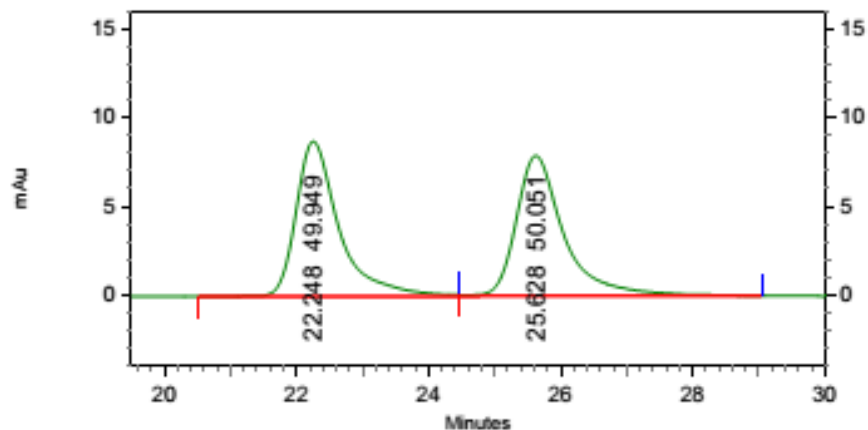
7.958, 7.937, 7.316, 7.295, 7.278, 7.271, 7.244, 7.228, 7.220, 7.212, 5.275, 5.262, 5.248, 4.675, 4.375, 4.357, 3.888, 3.751, 3.735, 3.716, 3.700, 3.681, 3.662, 3.644, 3.627, 3.609



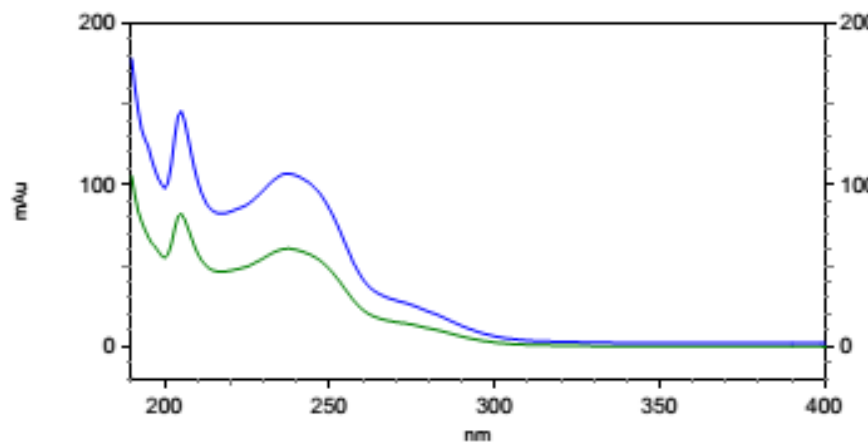
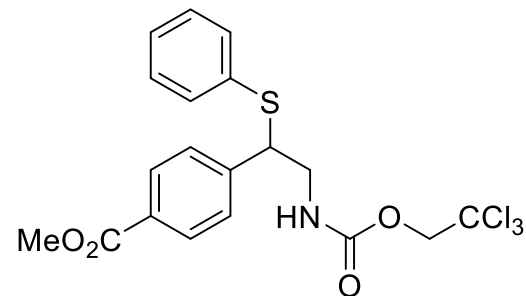
Methyl 4-(1-(phenylthio)-2-((2,2,2-trichloroethoxy)carbonylamino)ethyl)benzoate (7p)



Methyl 4-(1-(phenylthio)-2-((2,2,2-trichloroethoxy)carbonylamino)ethyl)benzoate (7p)



HPLC trace
racemic



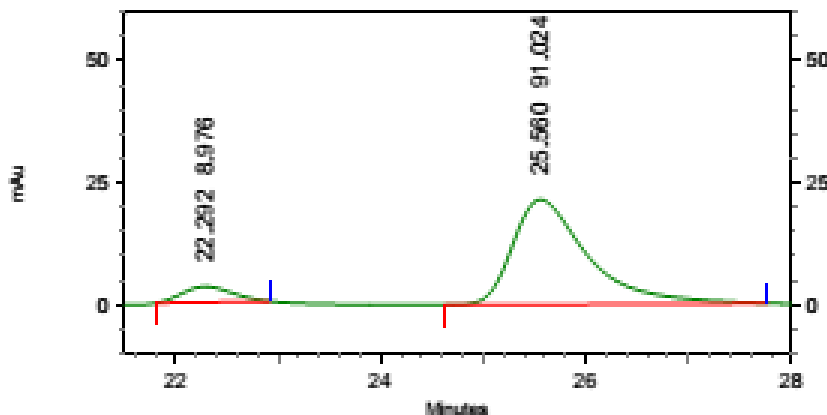
3: 255 nm, 4 nm

Results

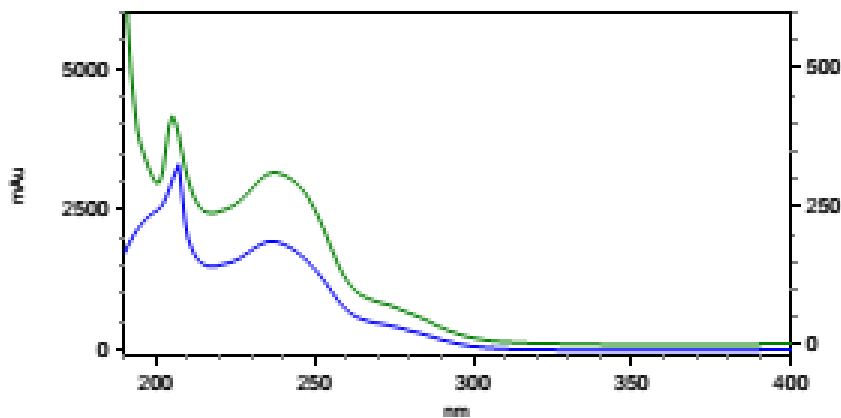
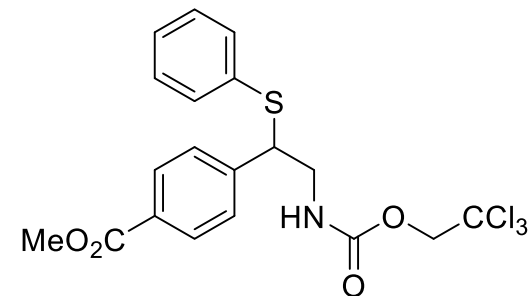
Name	Retention Time	Area Percent	Pk #
	22.248	49.949	1
	25.628	50.051	2

Totals		100.000	
--------	--	---------	--

Methyl 4-(1-(phenylthio)-2-((2,2,2-trichloroethoxy)carbonylamino)ethyl)benzoate (7p)



HPLC trace



3: 298 nm, 4 nm

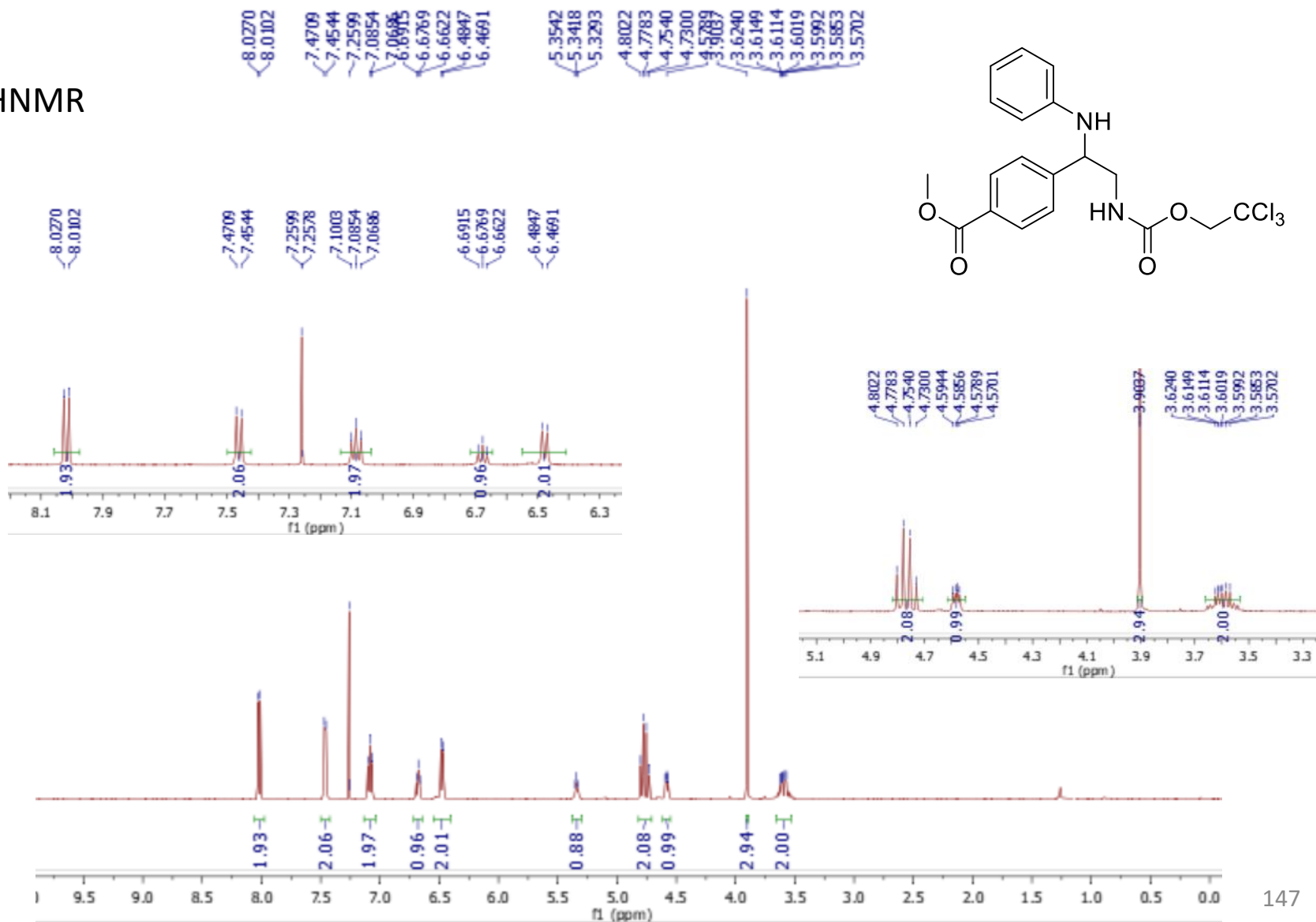
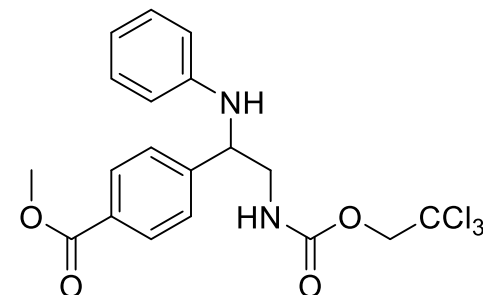
Results

Name	Retention Time	Area Percent	Pk #
	22.292	8.976	1
	25.560	91.024	2

Totals	Area Percent
	100.000

Methyl 4-(1-(phenylamino)-2-((2,2,2-trichloroethoxy)carbonylamino)ethyl)benzoate (8p)

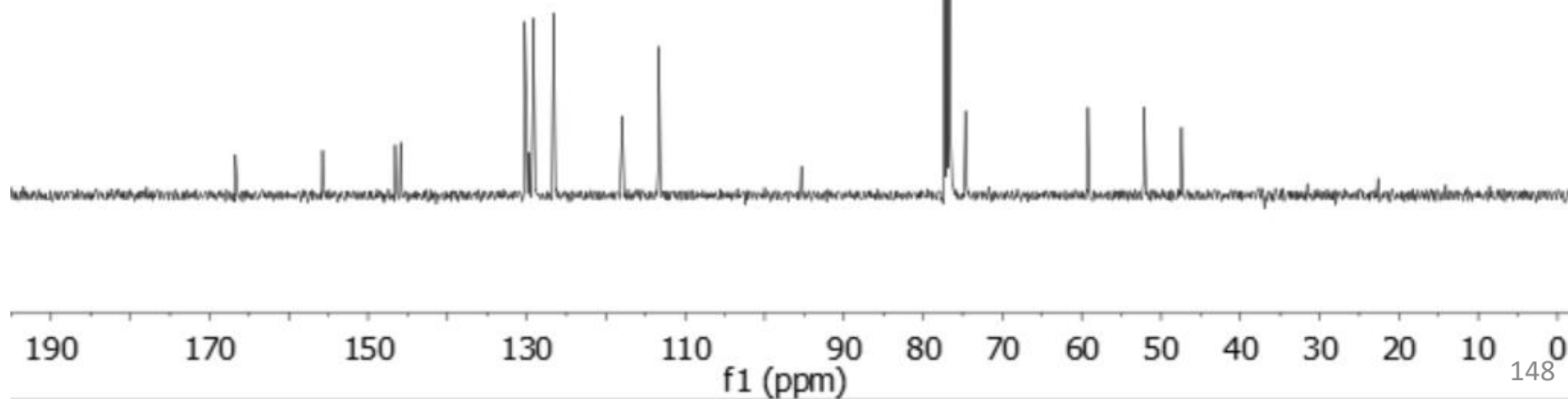
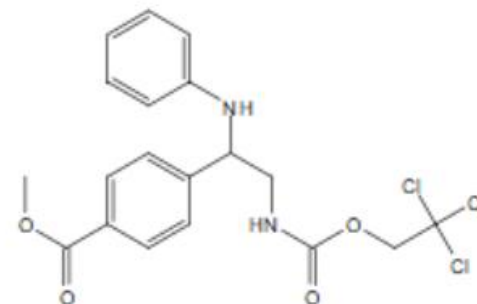
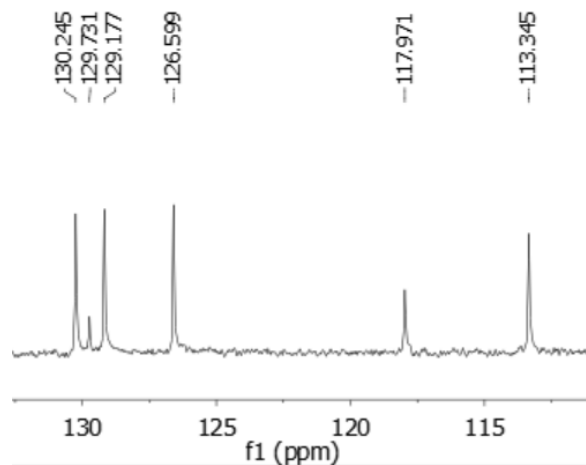
¹HNMR



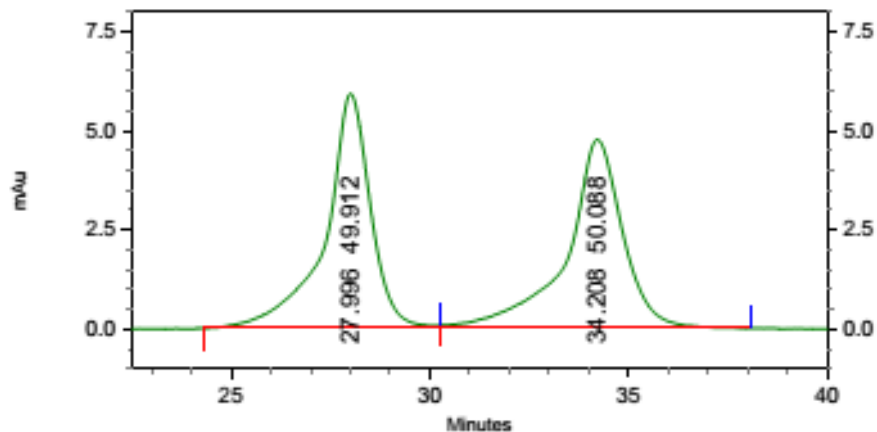
Methyl 4-(1-(phenylamino)-2-((2,2,2-trichloroethoxy)carbonylamino)ethyl)benzoate (8p)

¹³CNMR

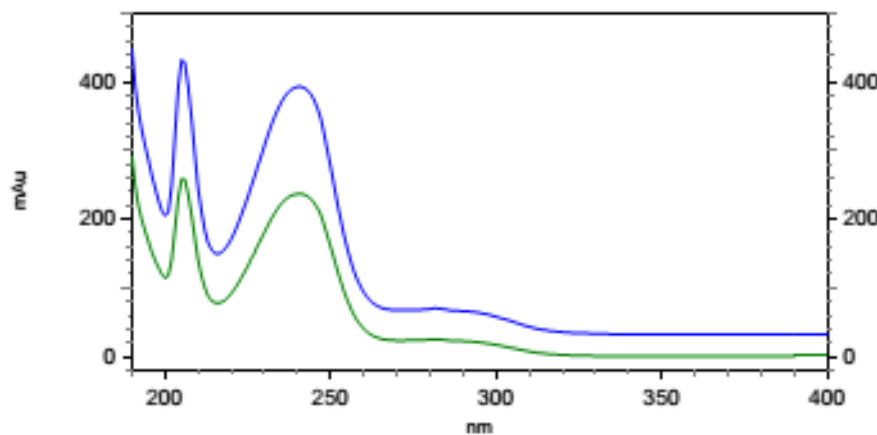
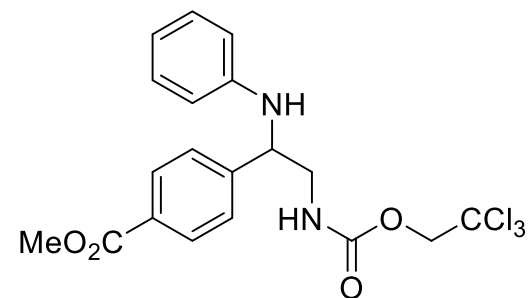
-166.730
-155.736
146.567
145.885
130.245
129.731
129.177
126.599
-117.971
-113.345
-95.342
77.311
76.994
76.676
74.652
59.215
52.131
47.427



Methyl 4-(1-(phenylamino)-2-((2,2,2-trichloroethoxy)carbonylamino)ethyl)benzoate (8p)



HPLC trace
racemic



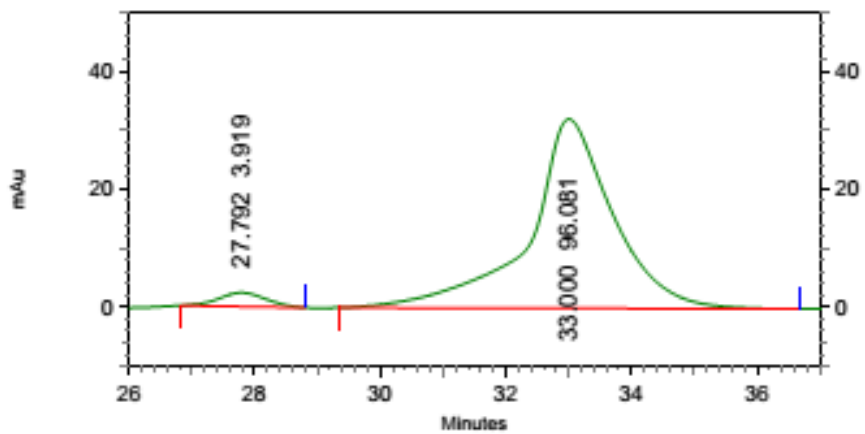
3: 273 nm, 4 nm

Results

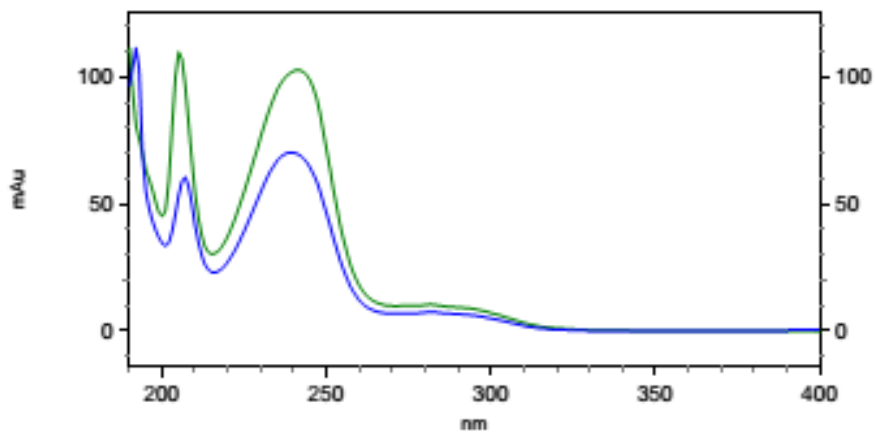
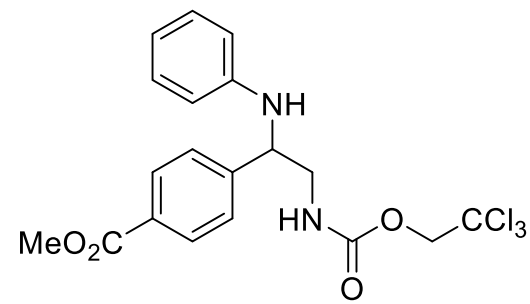
Name	Retention Time	Area Percent	Pk #
	27.996	49.912	1
	34.208	50.088	2

Totals		100.000	
--------	--	---------	--

Methyl 4-(1-(phenylamino)-2-((2,2,2-trichloroethoxy)carbonylamino)ethyl)benzoate (8p)



HPLC trace



3: 275 nm, 4 nm

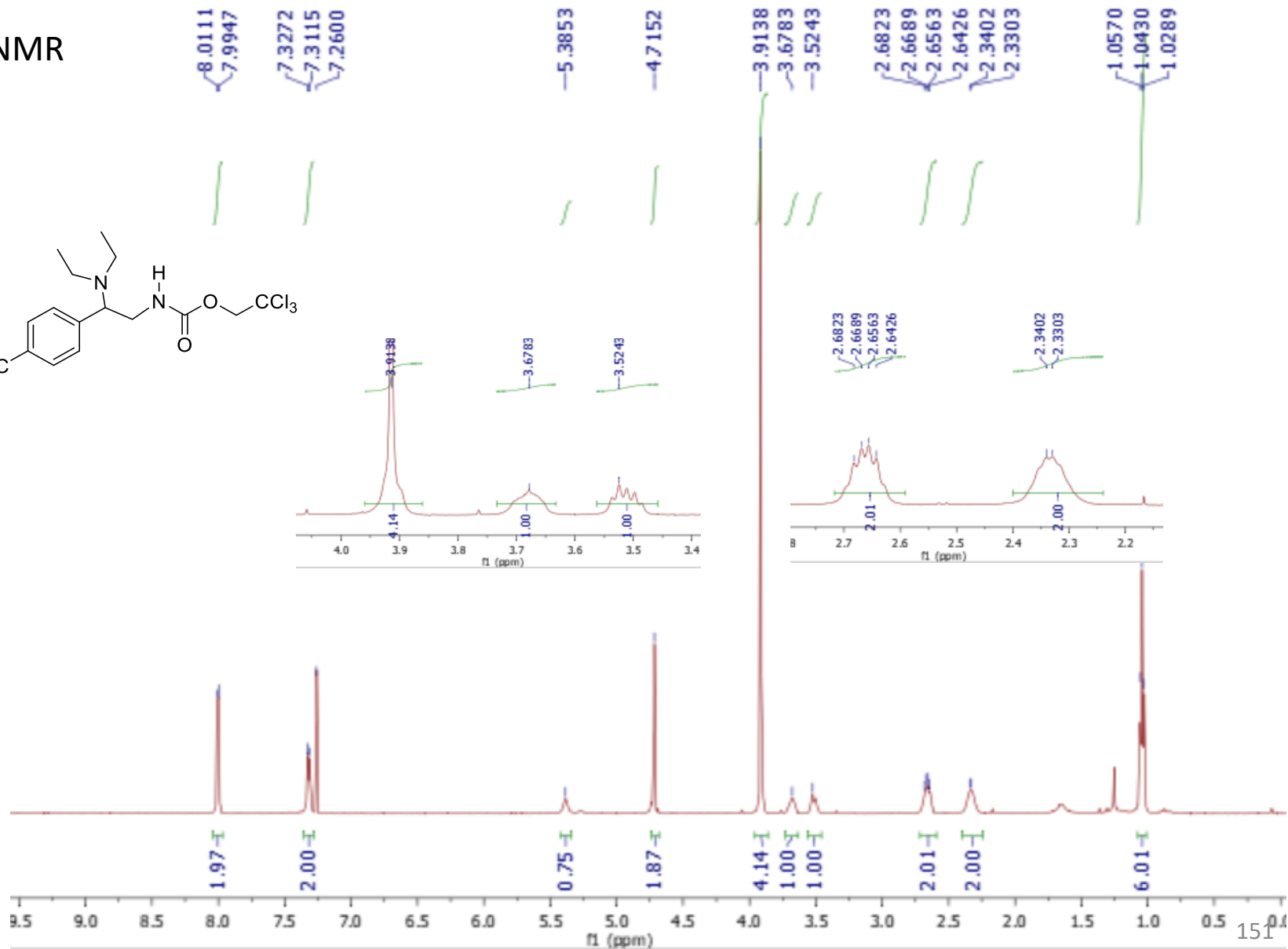
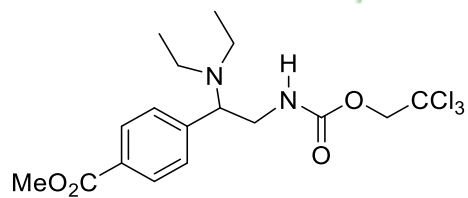
Results

Name	Retention Time	Area Percent	Pk #
	27.792	3.919	1
	33.000	96.081	2

Totals		100.000	
--------	--	---------	--

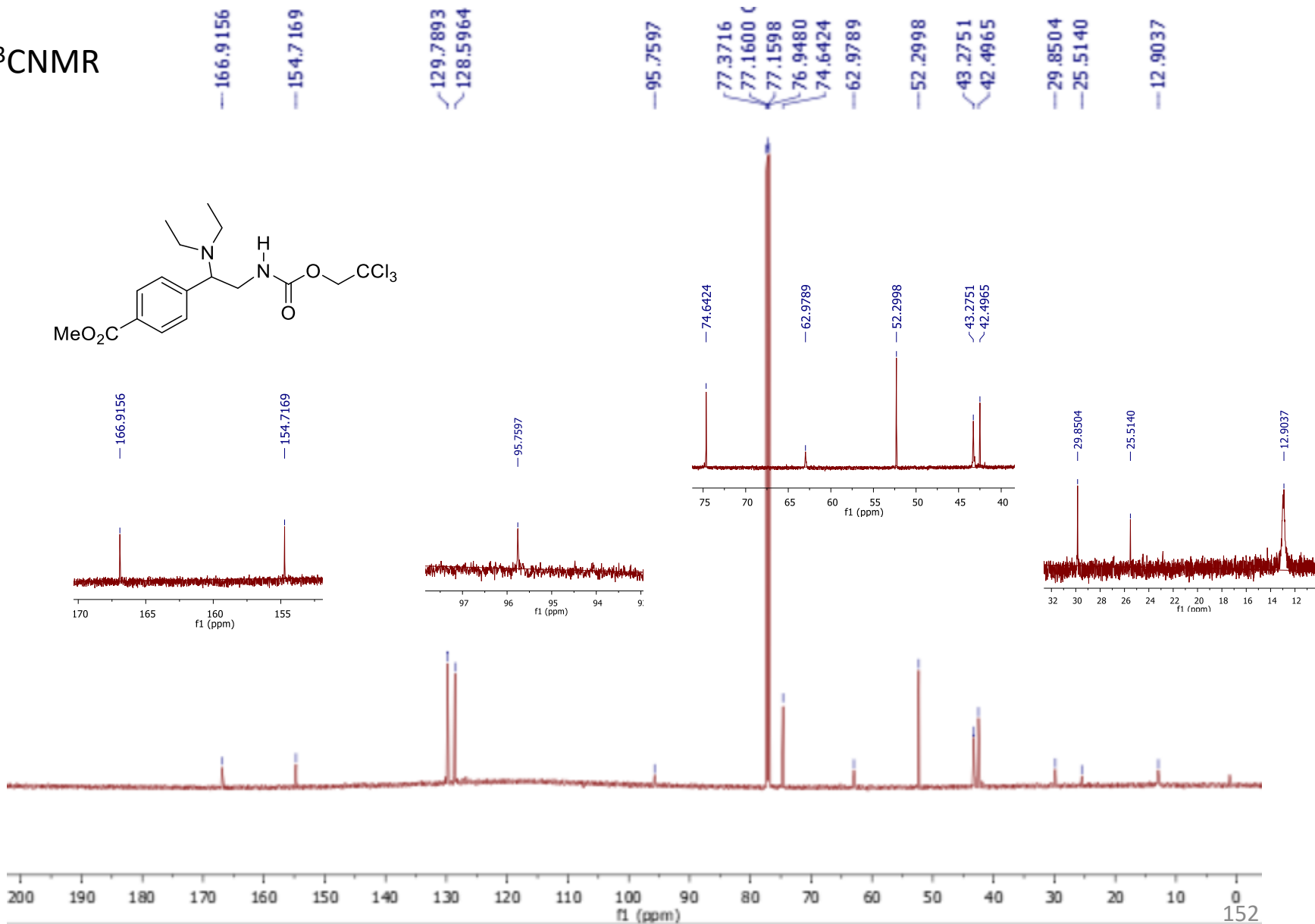
Methyl 4-(1-(N,N-diethyl)-2-((2,2,2-trichloroethoxy)carbonylamino)ethyl)benzoate(9p)

¹HNMR



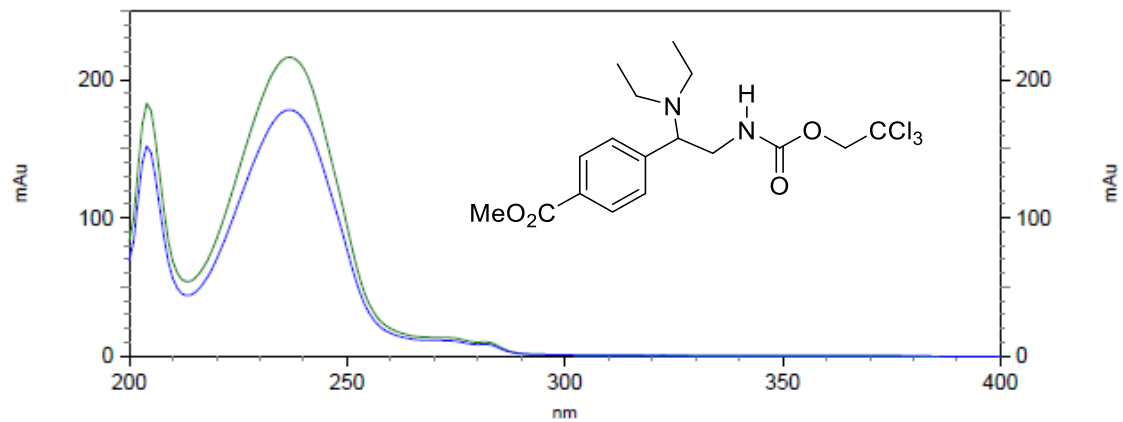
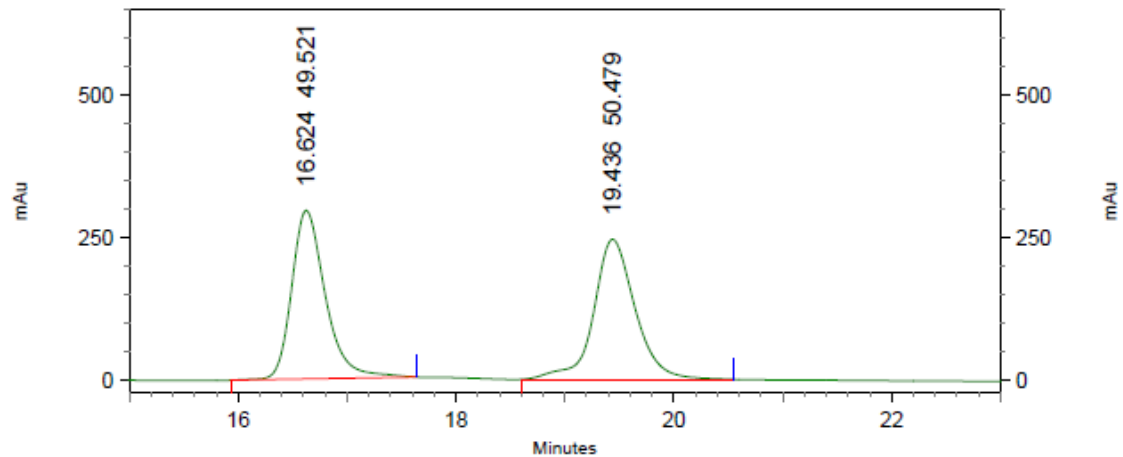
Methyl 4-(1-(N,N-diethyl)-2-((2,2,2-trichloroethoxy)carbonylamino)ethyl)benzoate (9p)

^{13}C NMR



Methyl 4-(1-(N,N-diethyl)-2-((2,2,2-trichloroethoxy)carbonylamino)ethyl)benzoate(9p)

HPLC trace
racemic

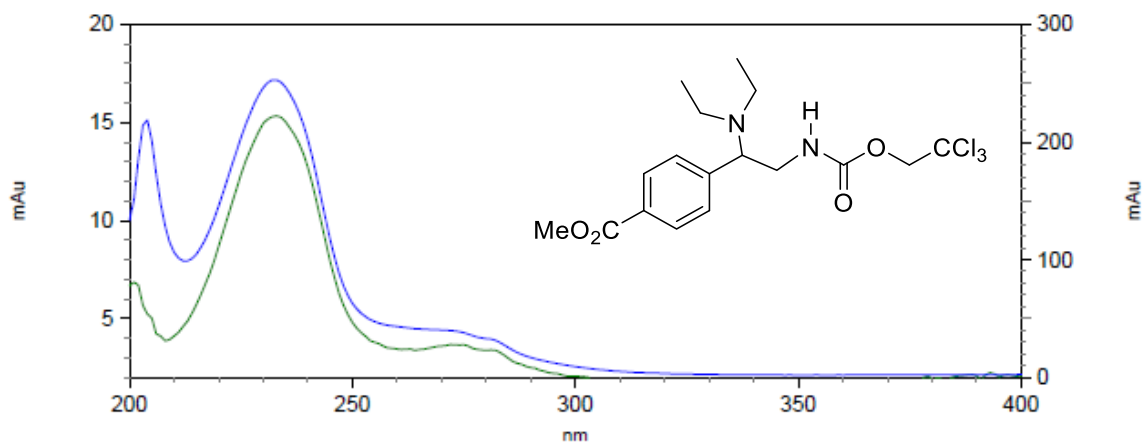
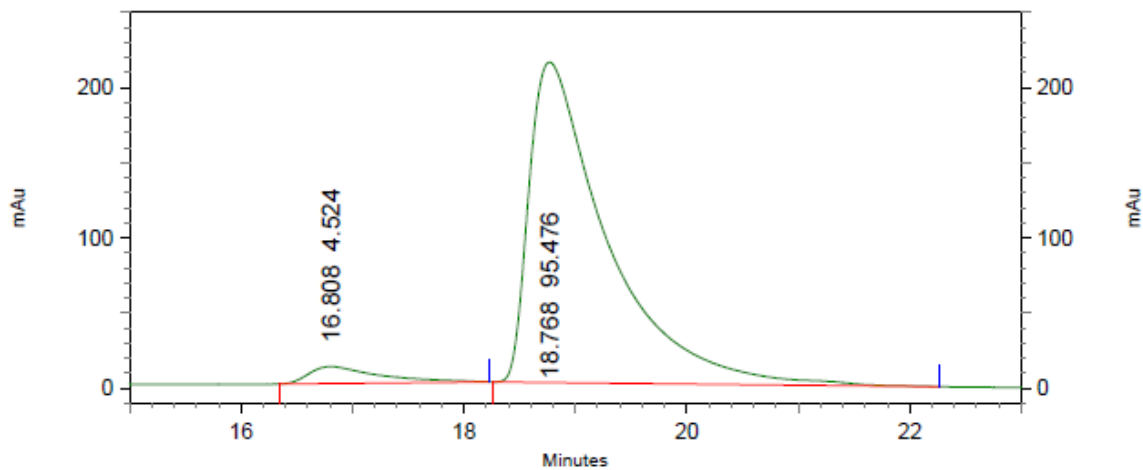


3: 246 nm, 4
nm Results

Pk #	Retention Time	Area Percent
1	16.624	49.521
2	19.436	50.479
Totals		100.000

Methyl 4-(1-(N,N-diethyl)-2-((2,2,2-trichloroethoxy)carbonylamino)ethyl)benzoate(9p)

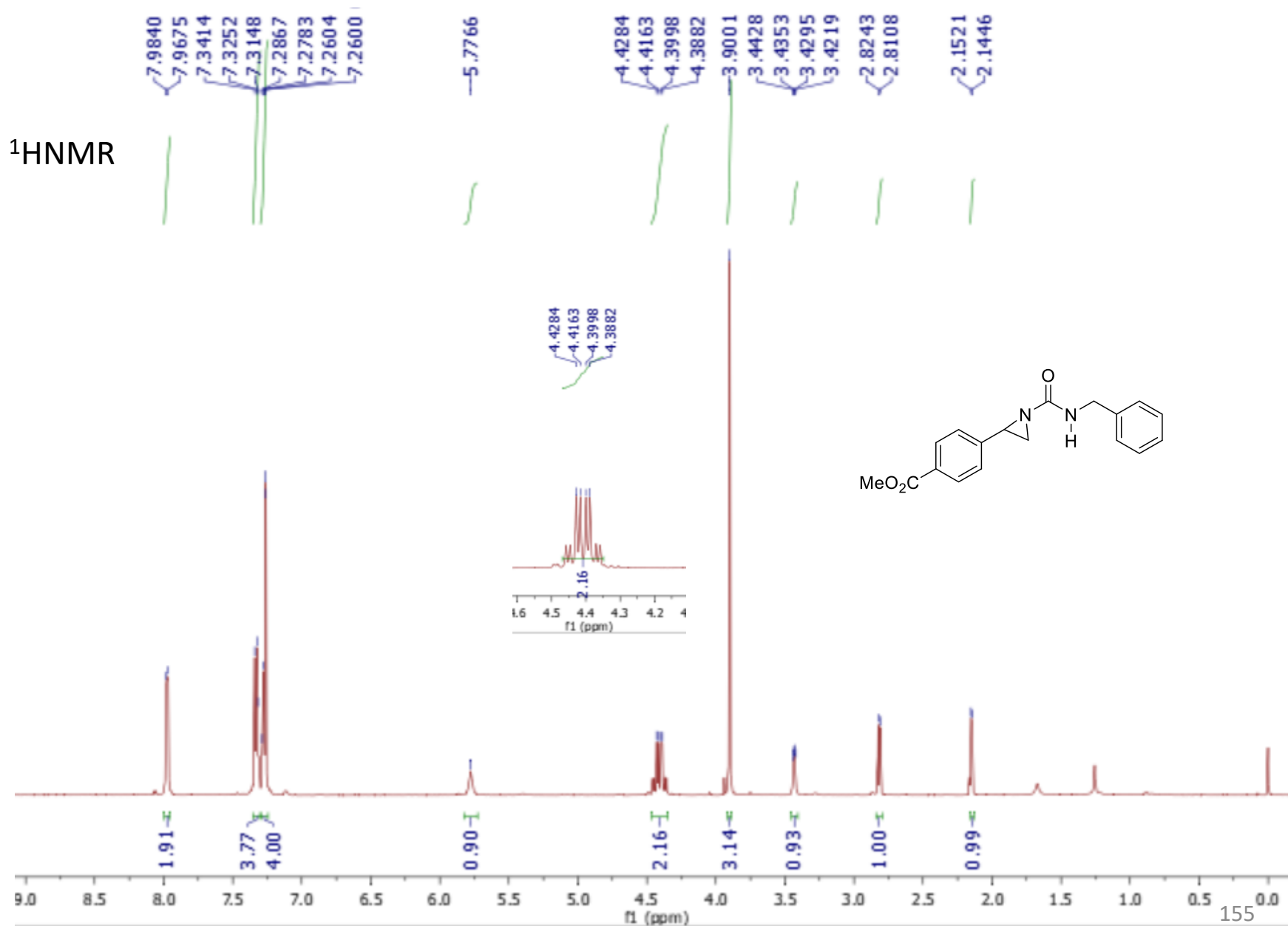
HPLC trace



3: 246 nm, 4
nm Results

Pk #	Retention Time	Area Percent
1	16.808	4.524
2	18.768	95.476
Totals		100.000

Methyl 4-(3-benzyl-2-oxoimidazolidin-4-yl)benzoate (10p)



Methyl 4-(3-benzyl-2-oxoimidazolidin-4-yl)benzoate (10p)

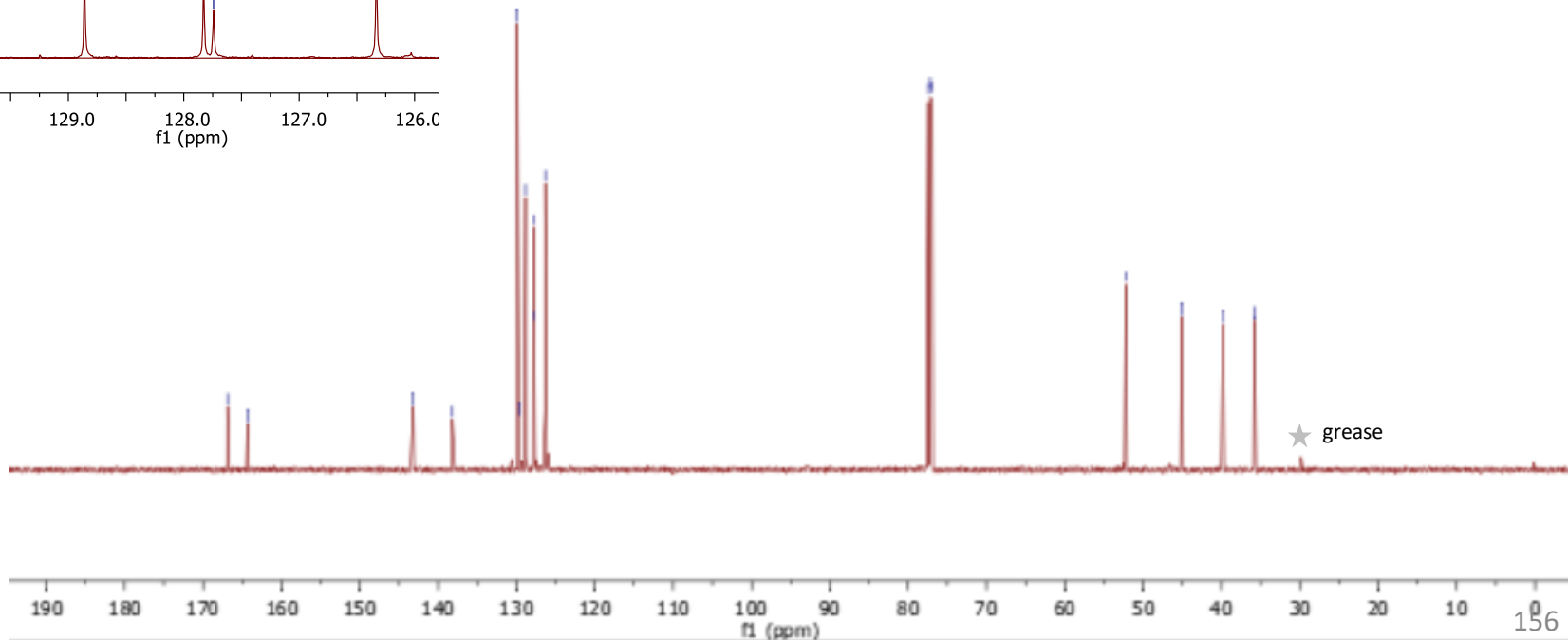
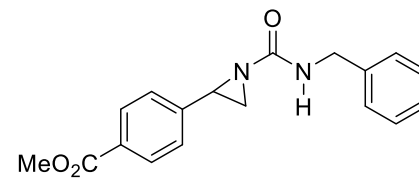
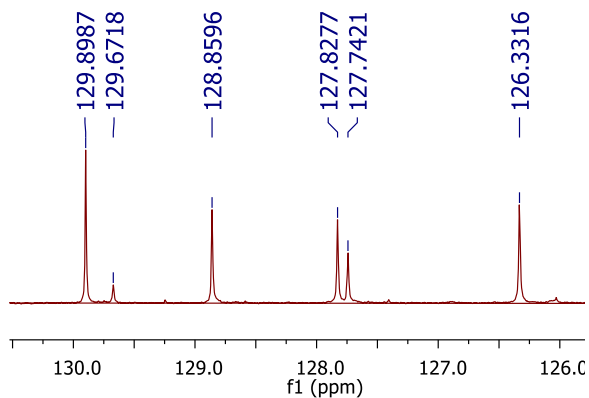
¹³CNMR

166.8982
164.3645

143.1906
138.2133
129.8987
129.6718
128.8596
127.8277
127.7421
126.3316

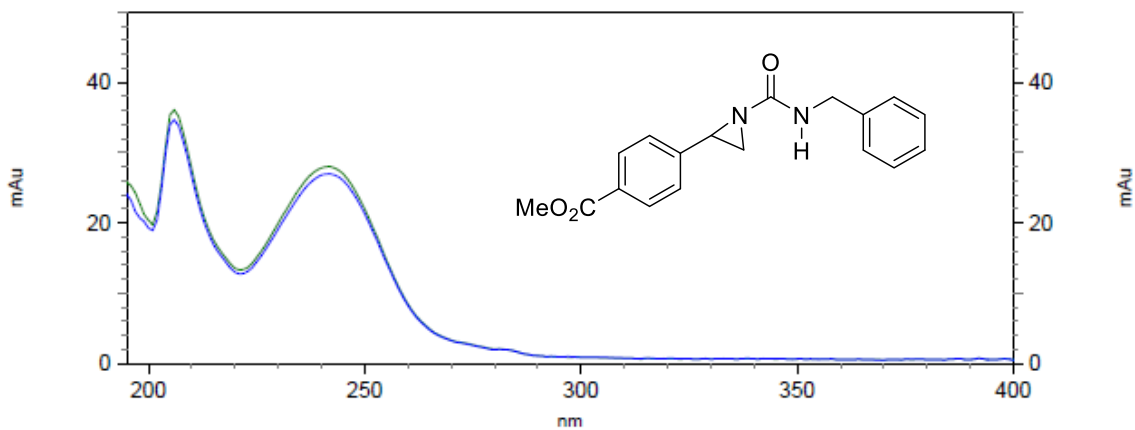
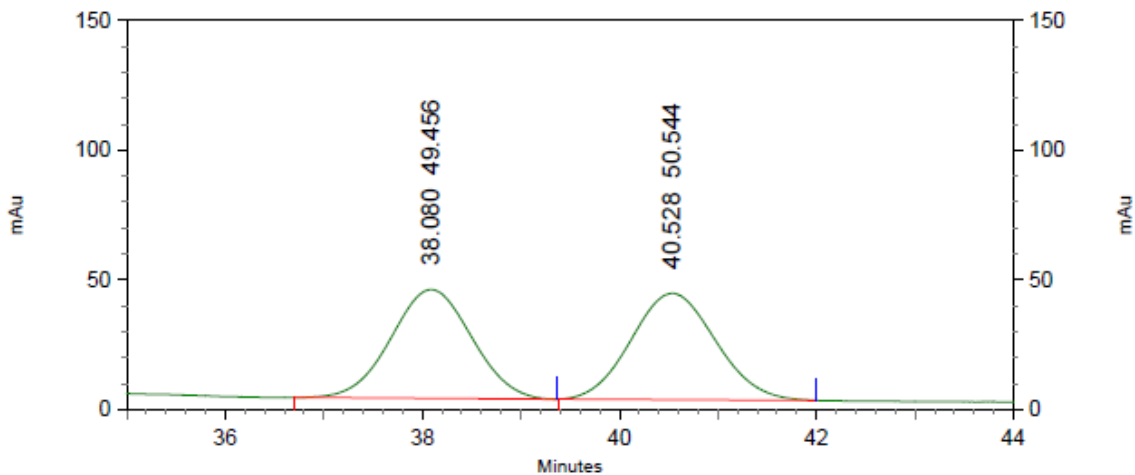
77.4144
77.1602
76.9061

52.2403
45.1023
39.8229
35.8151



Methyl 4-(3-benzyl-2-oxoimidazolidin-4-yl)benzoate (10p)

HPLC trace
racemic



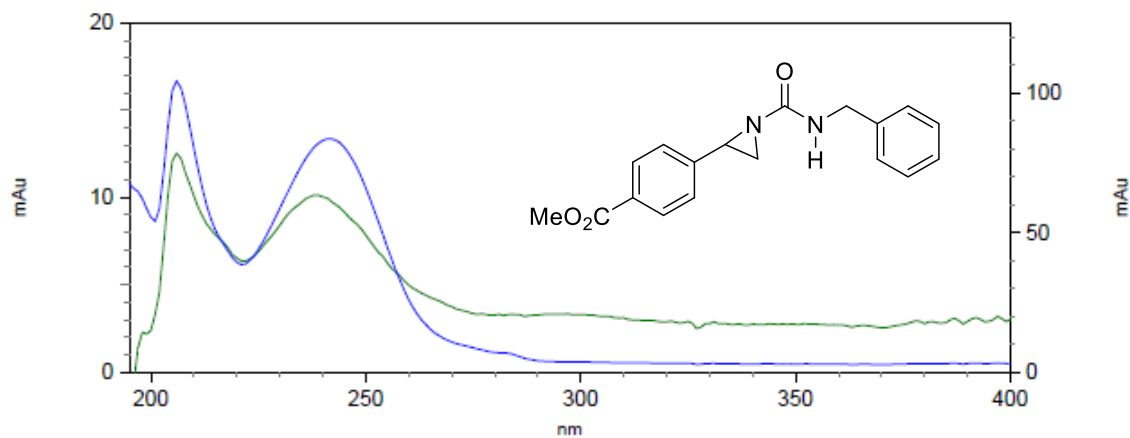
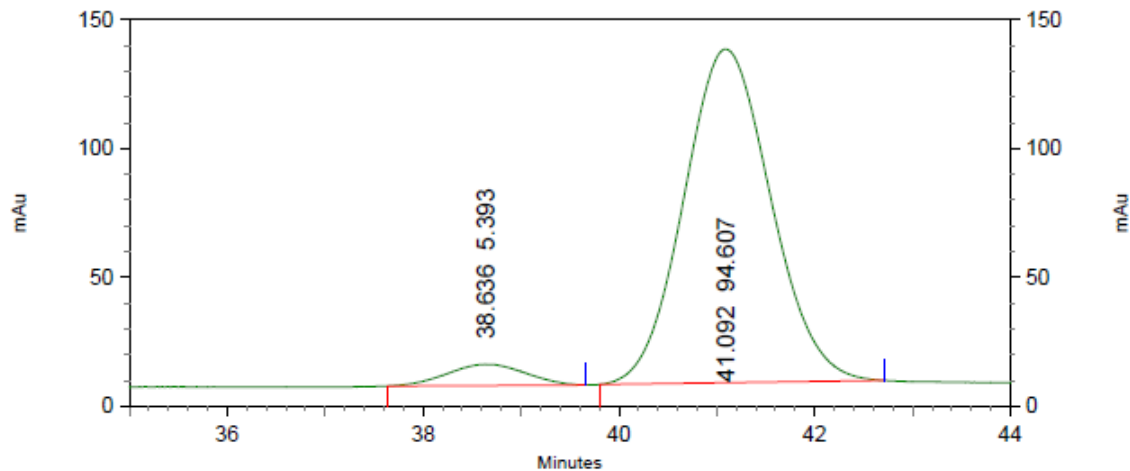
3: 249 nm, 4
nm Results

Pk #	Retention Time	Area Percent
1	38.080	49.456
2	40.528	50.544

Totals	100.000
--------	---------

Methyl 4-(3-benzyl-2-oxoimidazolidin-4-yl)benzoate (10p)

HPLC trace

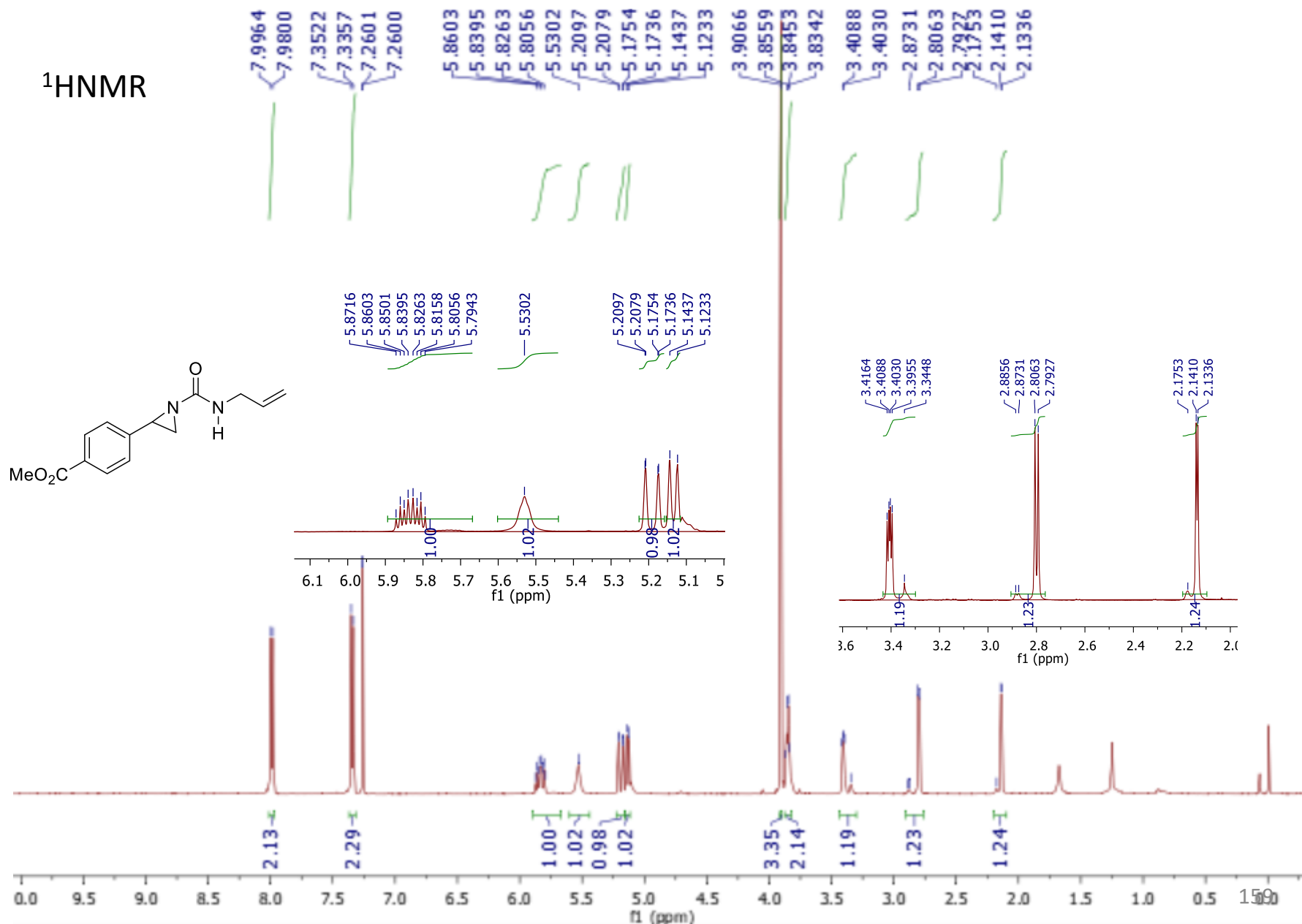


3: 249 nm, 4
nm Results

Pk #	Retention Time	Area Percent
1	38.636	5.393
2	41.092	94.607

Totals	100.000
--------	---------

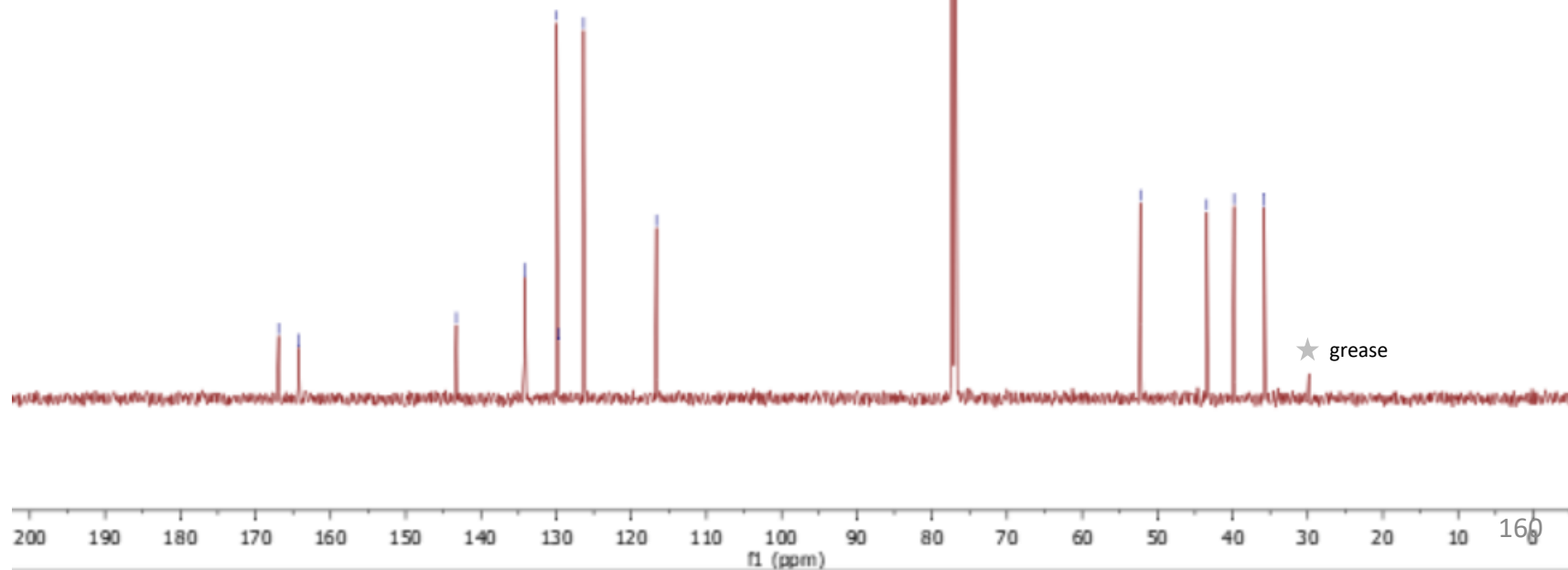
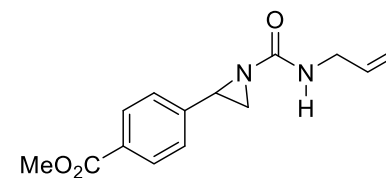
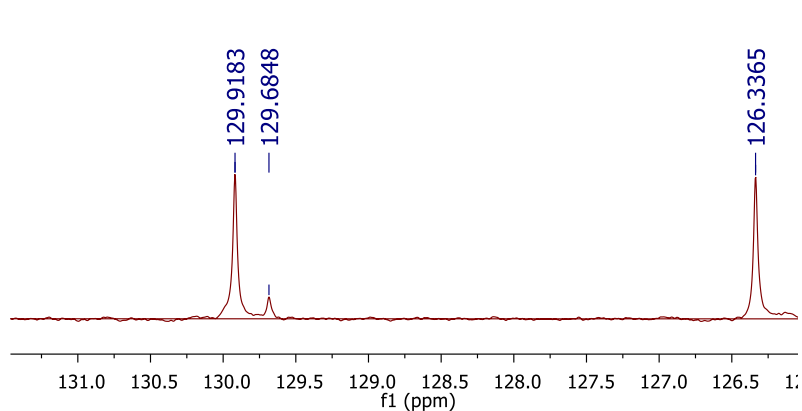
Methyl 4-(3-allyl-2-oxoimidazolidin-4-yl)benzoate (11p)



Methyl 4-(3-allyl-2-oxoimidazolidin-4-yl)benzoate (11p)

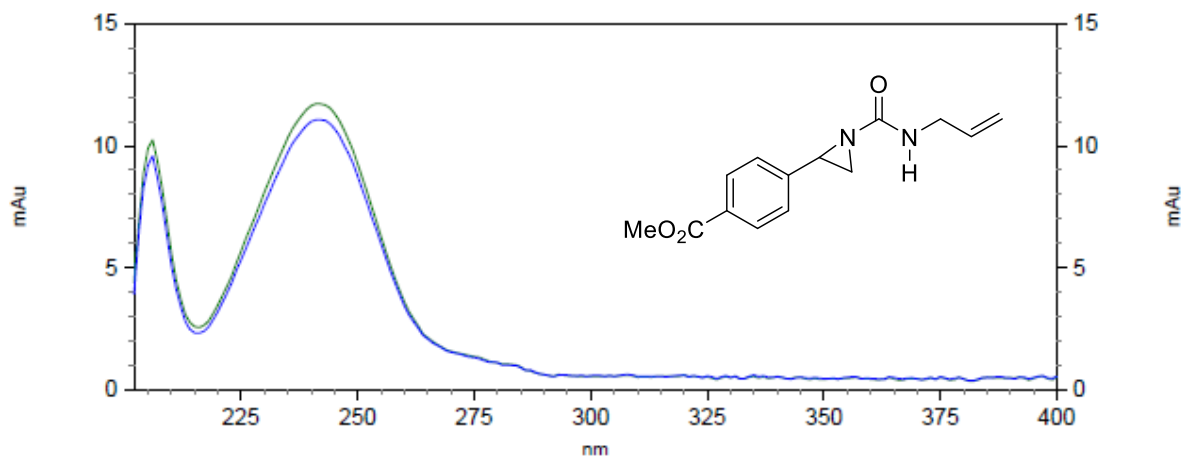
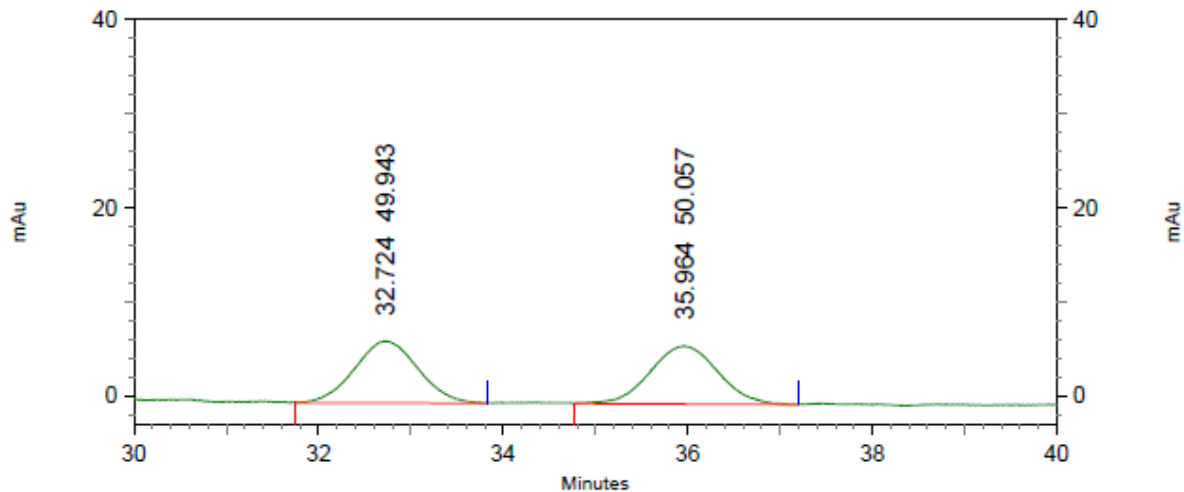
¹³CNMR

~166.9187
~164.2920
-143.2747
~134.1932
~129.9183
~129.6848
~126.3365
-116.6520
77.4145
77.1605
76.9062
-52.2607
-43.4305
-39.8110
-35.7964



Methyl 4-(3-allyl-2-oxoimidazolidin-4-yl)benzoate (11p)

HPLC trace
racemic

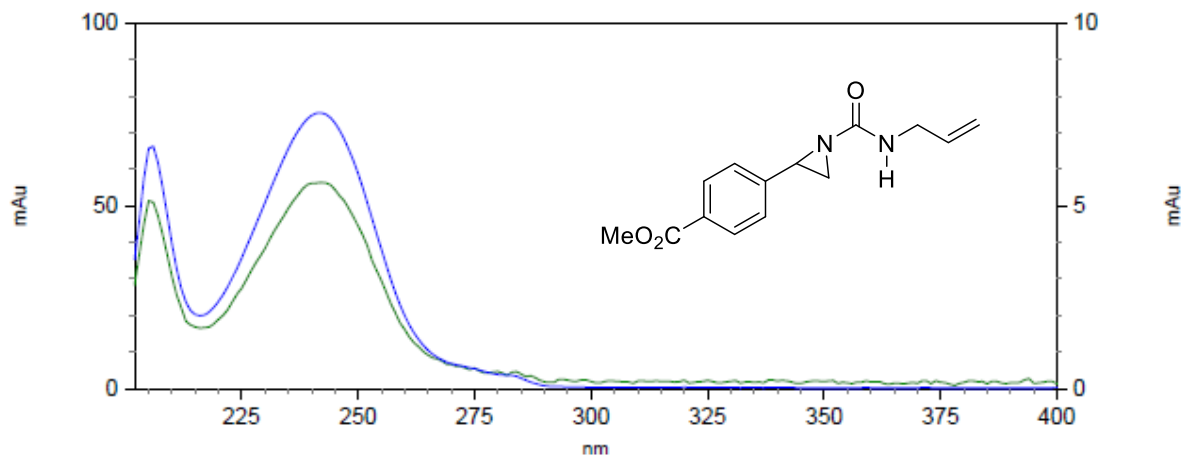
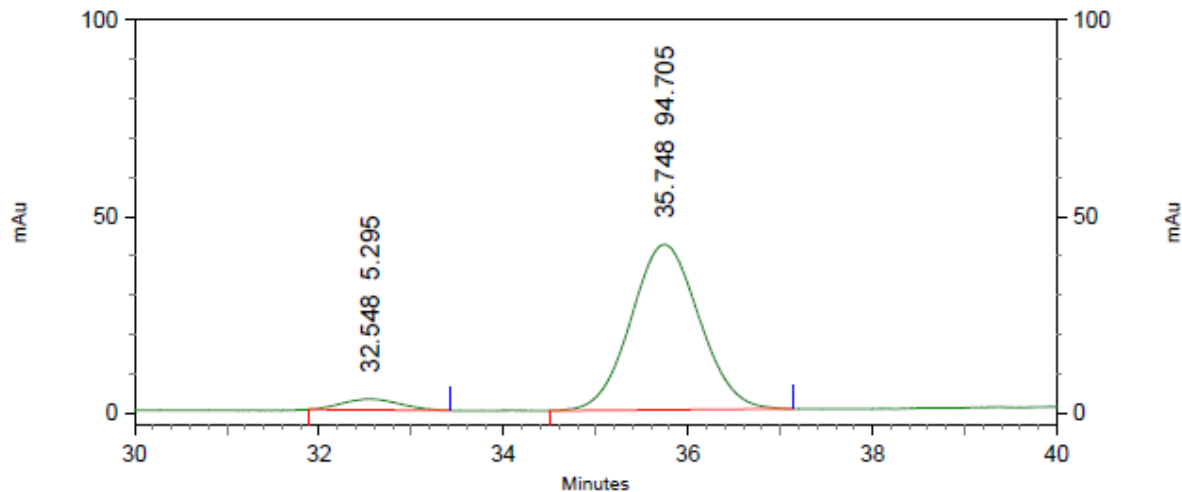


4: 218 nm, 4
nm Results

Pk #	Retention Time	Area Percent
1	32.724	49.943
2	35.964	50.057
Totals		100.000

Methyl 4-(3-allyl-2-oxoimidazolidin-4-yl)benzoate (11p)

HPLC trace

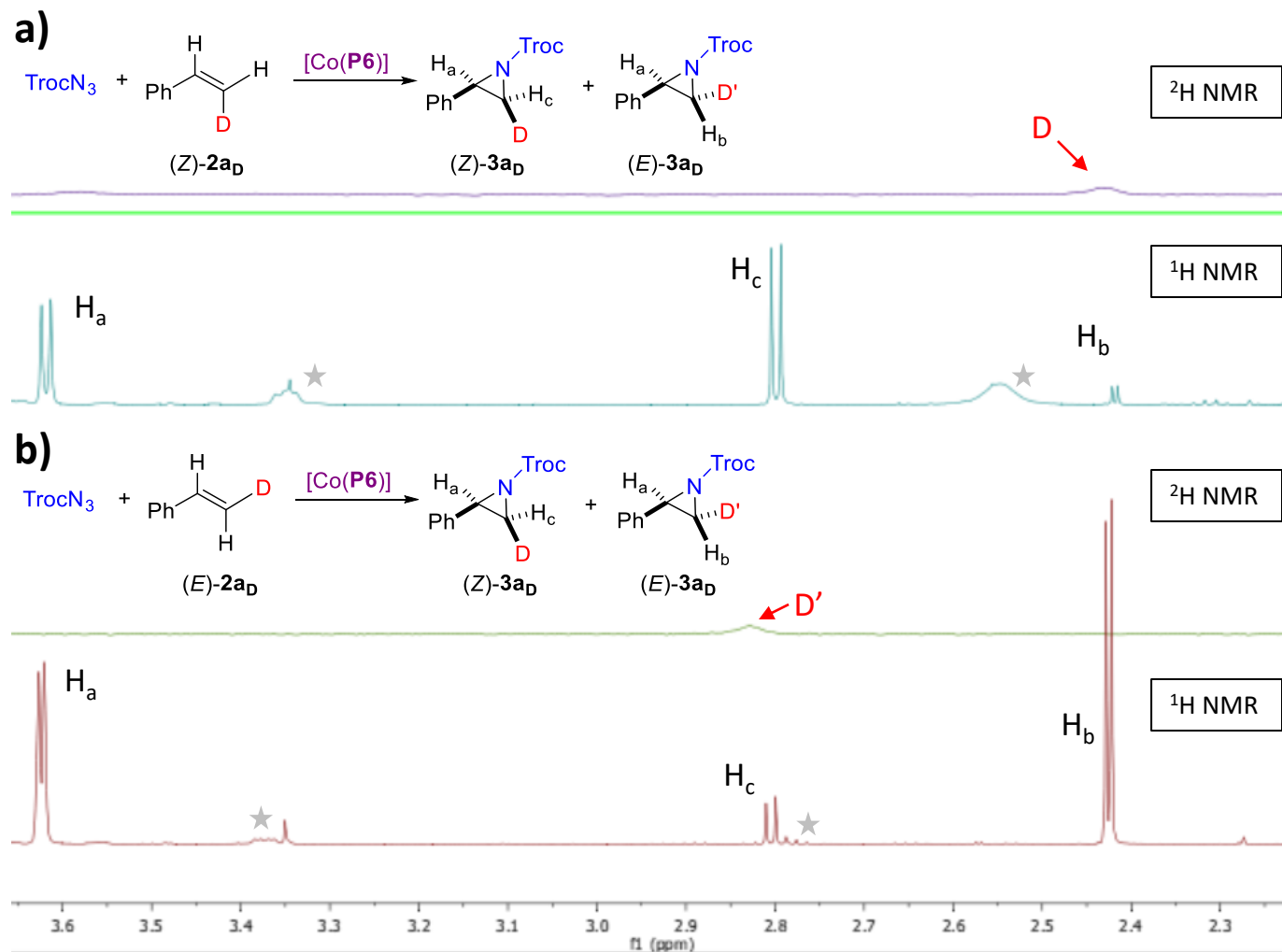


4: 218 nm, 4
nm Results

Pk #	Retention Time	Area Percent
1	32.548	5.295
2	35.748	94.705

Totals	100.000
--------	---------

Scheme 2.10

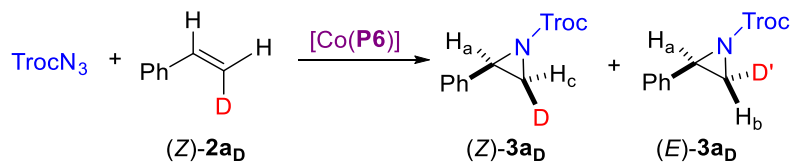


★ Indicates impurity in crude $^1\text{H NMR}$

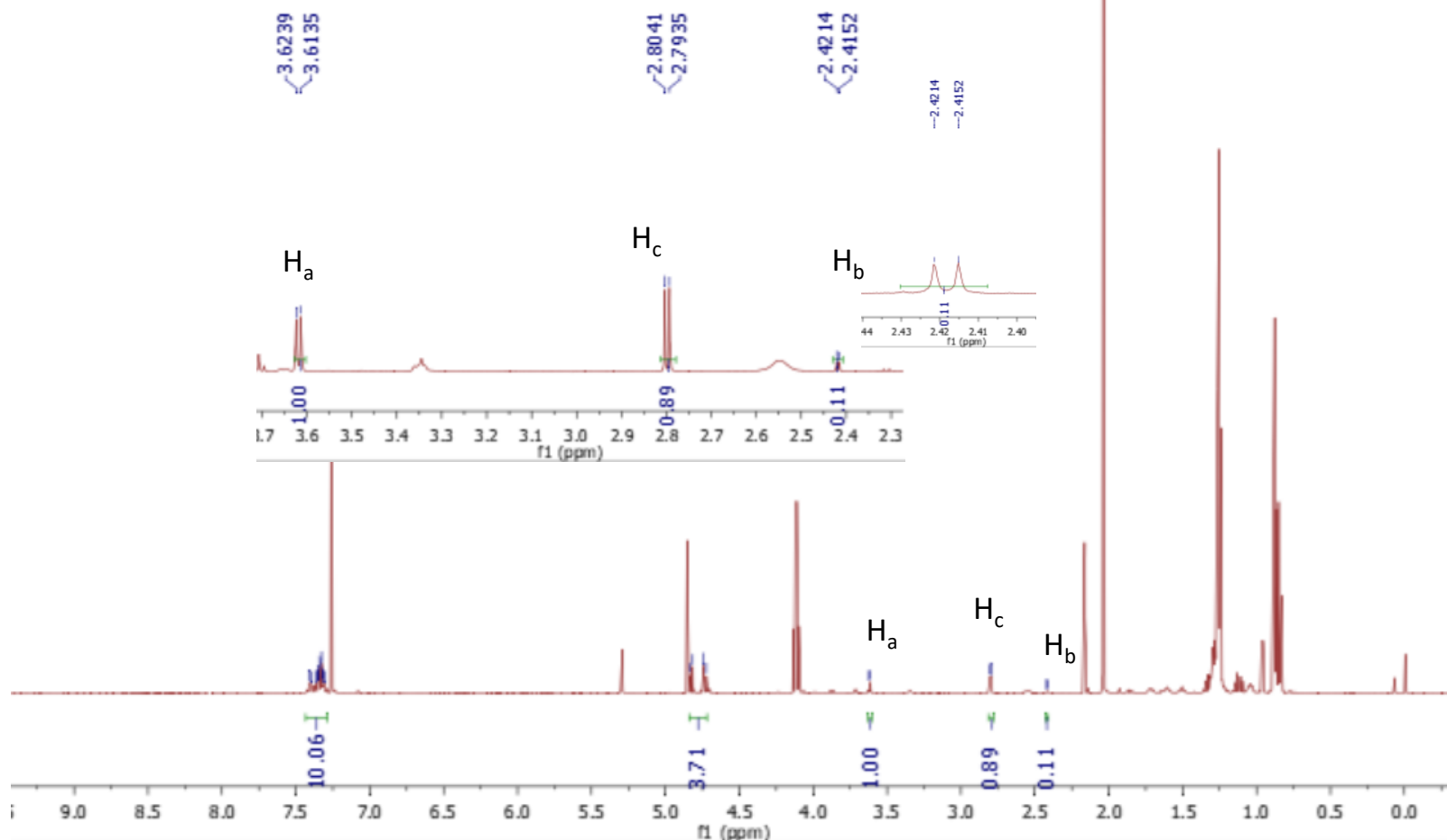
Scheme 2.10-Full spectrum

a)

¹H NMR

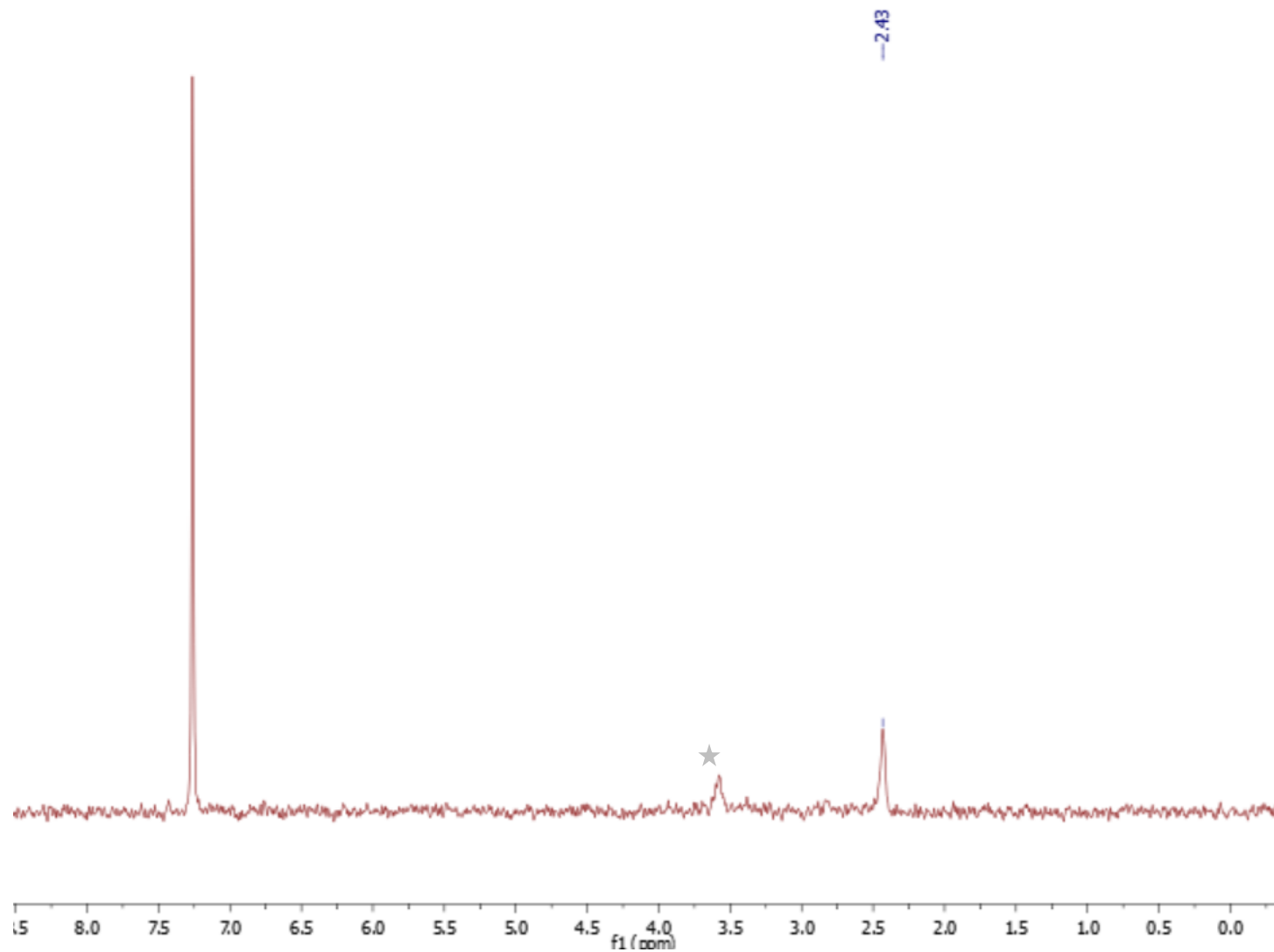
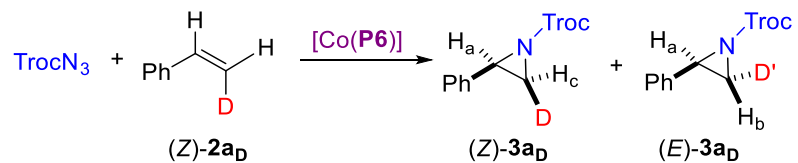


¹H NMR (600 MHz, CDCl₃) δ 7.37 – 7.29 (m, 7H), 4.78 (AB q, *J* = 11.9 Hz, 2H), 3.62 (d, *J* = 6.3 Hz, 1H), 2.80 (d, *J* = 6.4 Hz, 1H), 2.42 (d, *J* = 3.7 Hz, 1H).

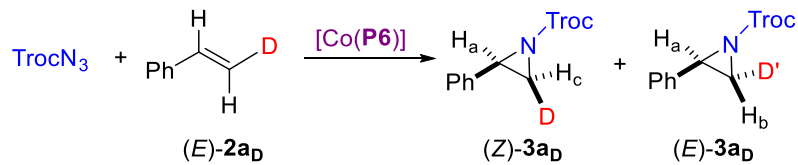


Scheme 2.10-Full spectrum

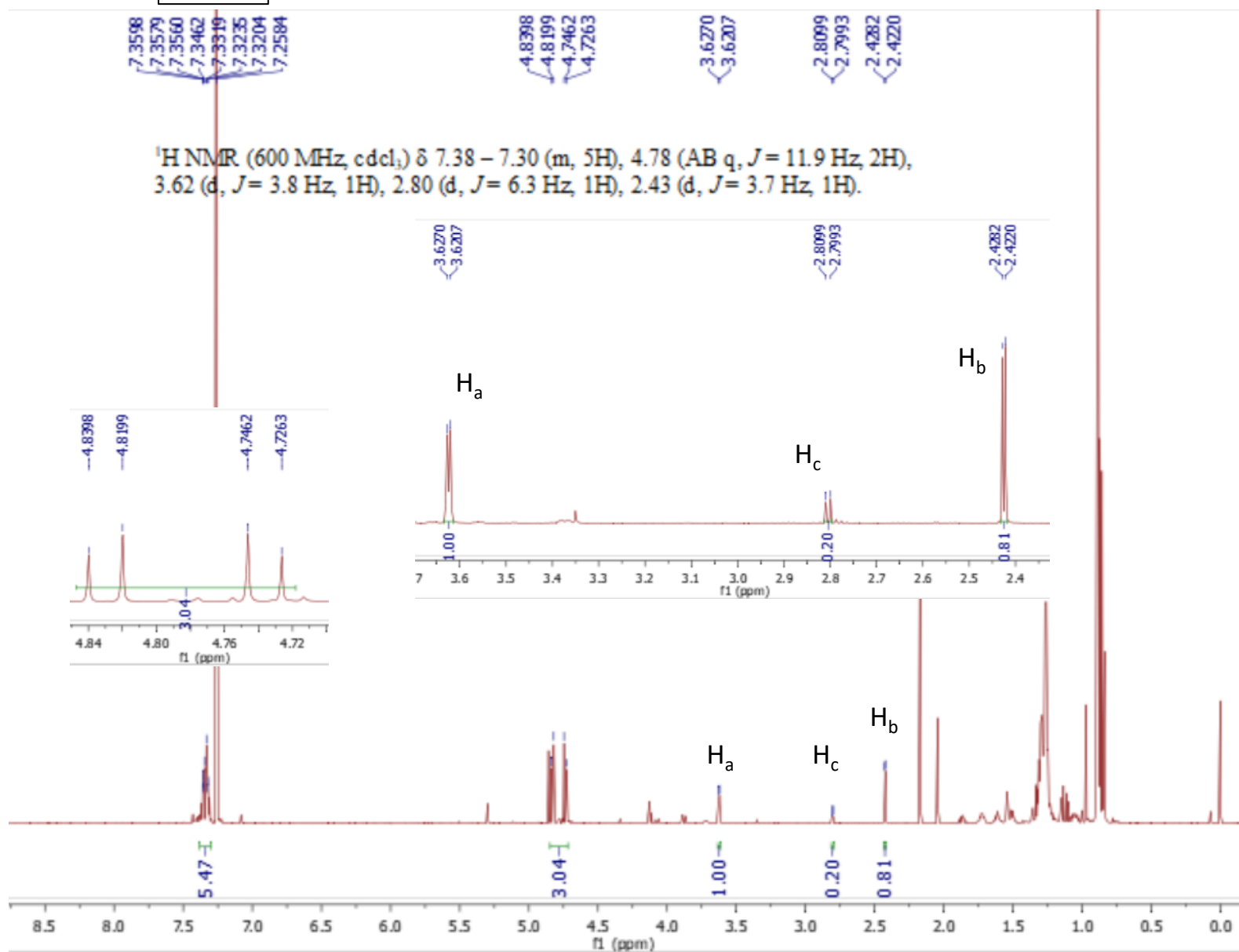
a) ^2H NMR



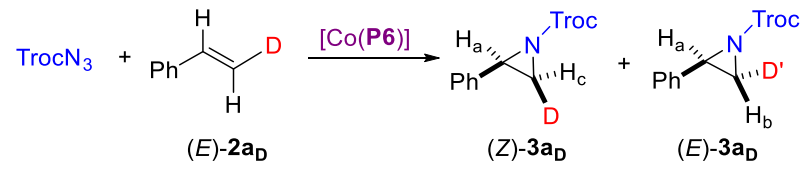
Scheme 2.10-Full spectrum



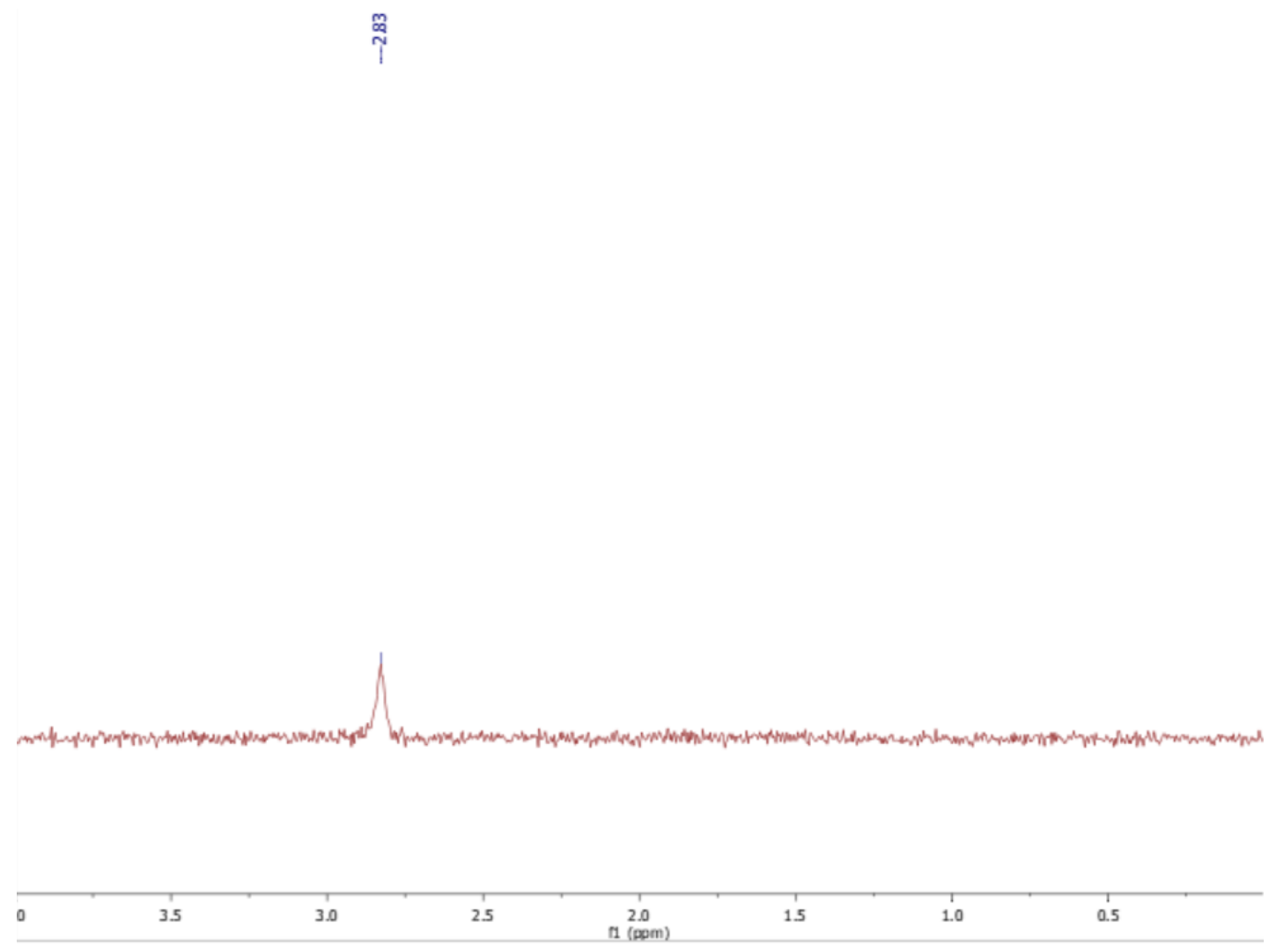
b) $^1\text{H NMR}$



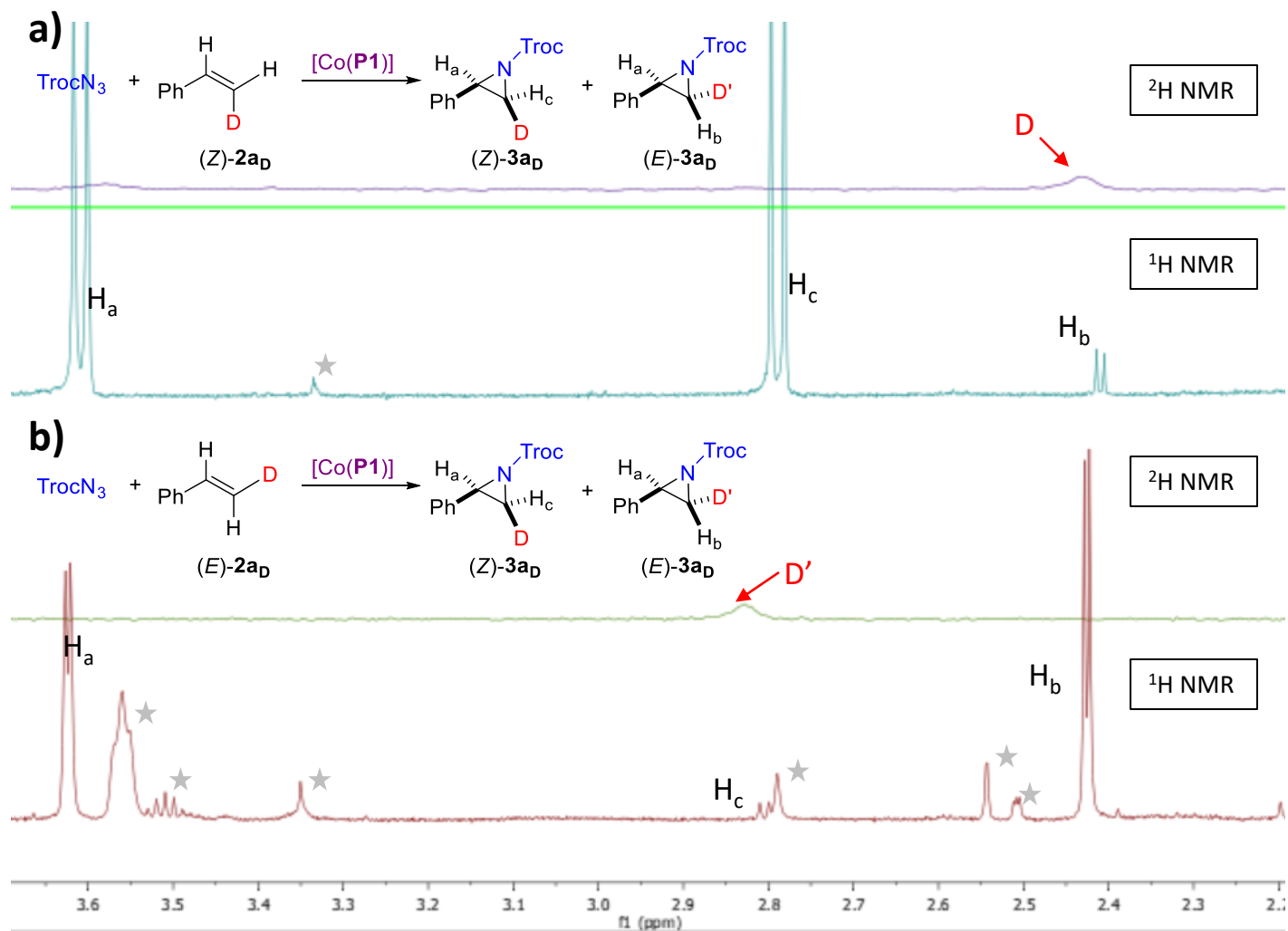
Scheme 2.10-Full spectrum



b) ^2H NMR



Scheme 2.11

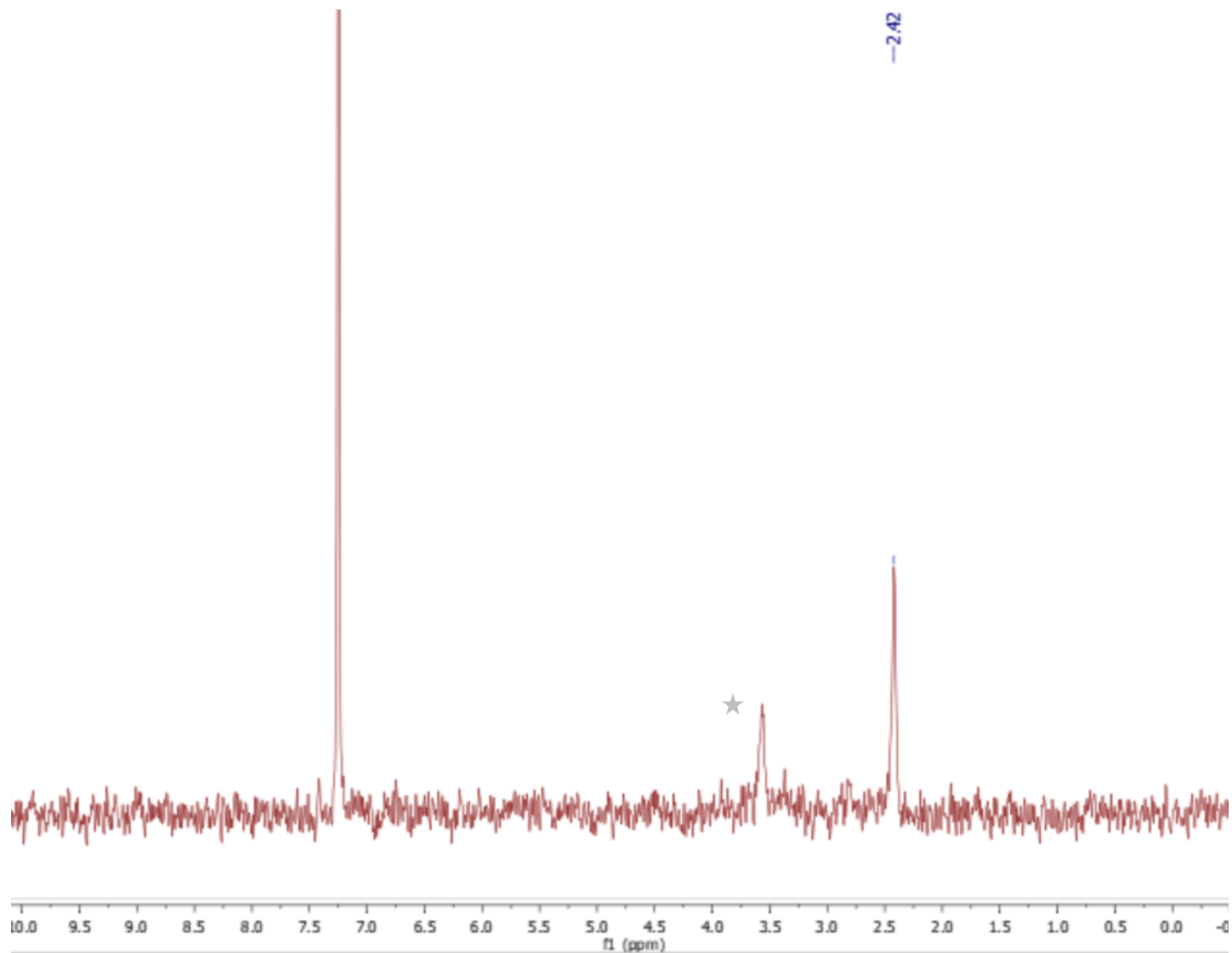
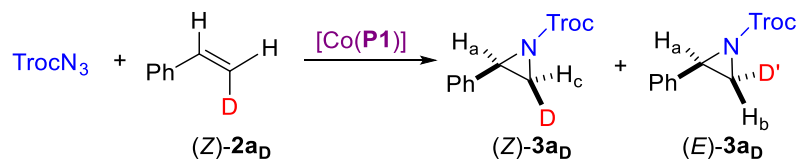


★ Indicates impurity in crude $^1\text{H NMR}$

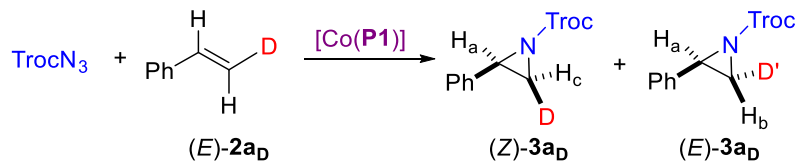
Scheme 2.11-Full spectrum

a)

^2H NMR

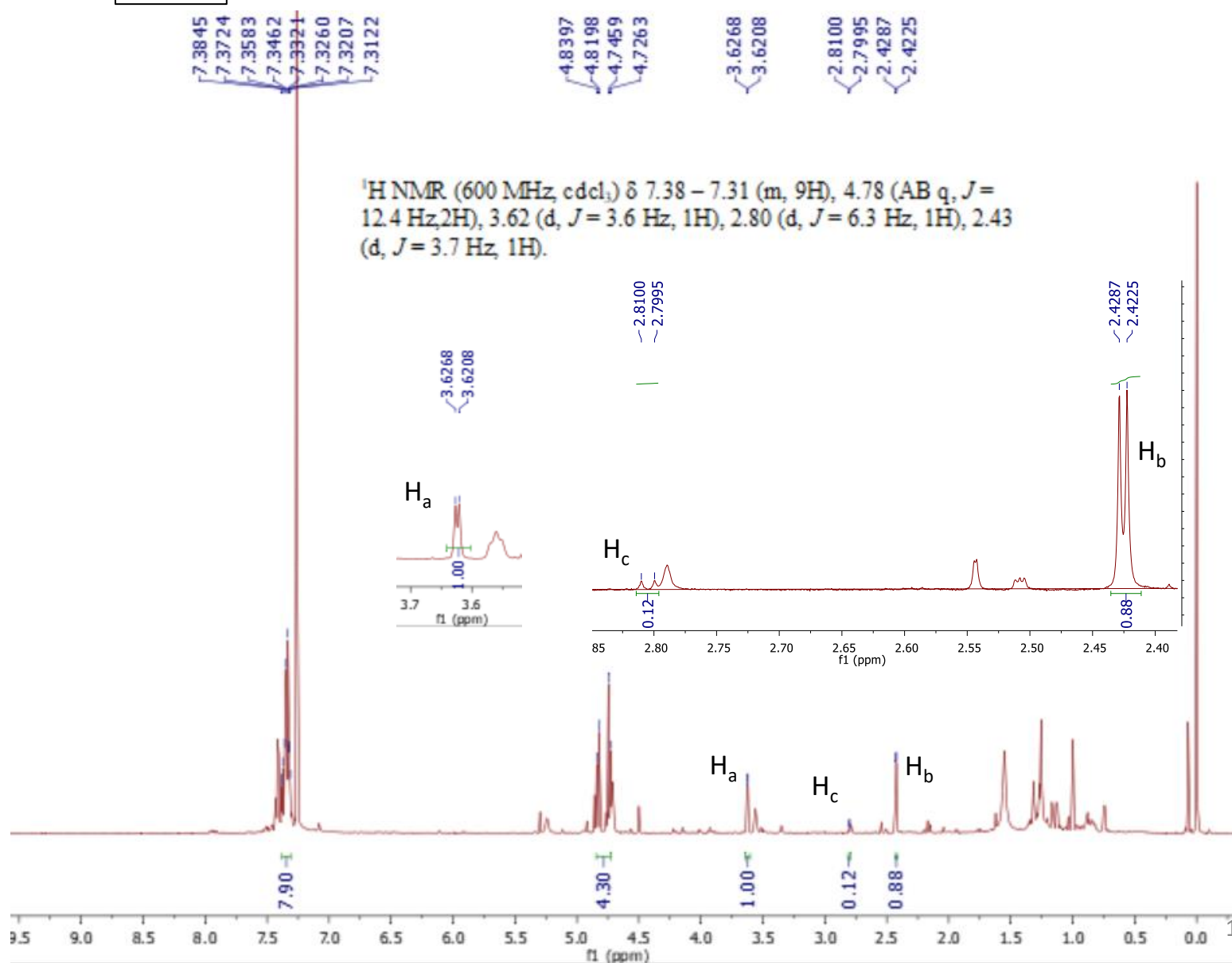


Scheme 2.11-Full spectrum

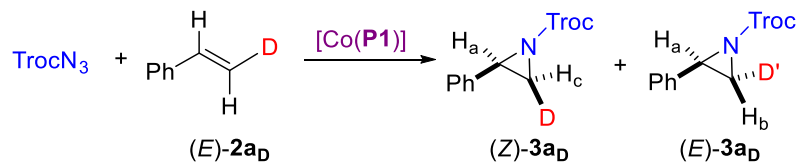


b)

$^1\text{H NMR}$

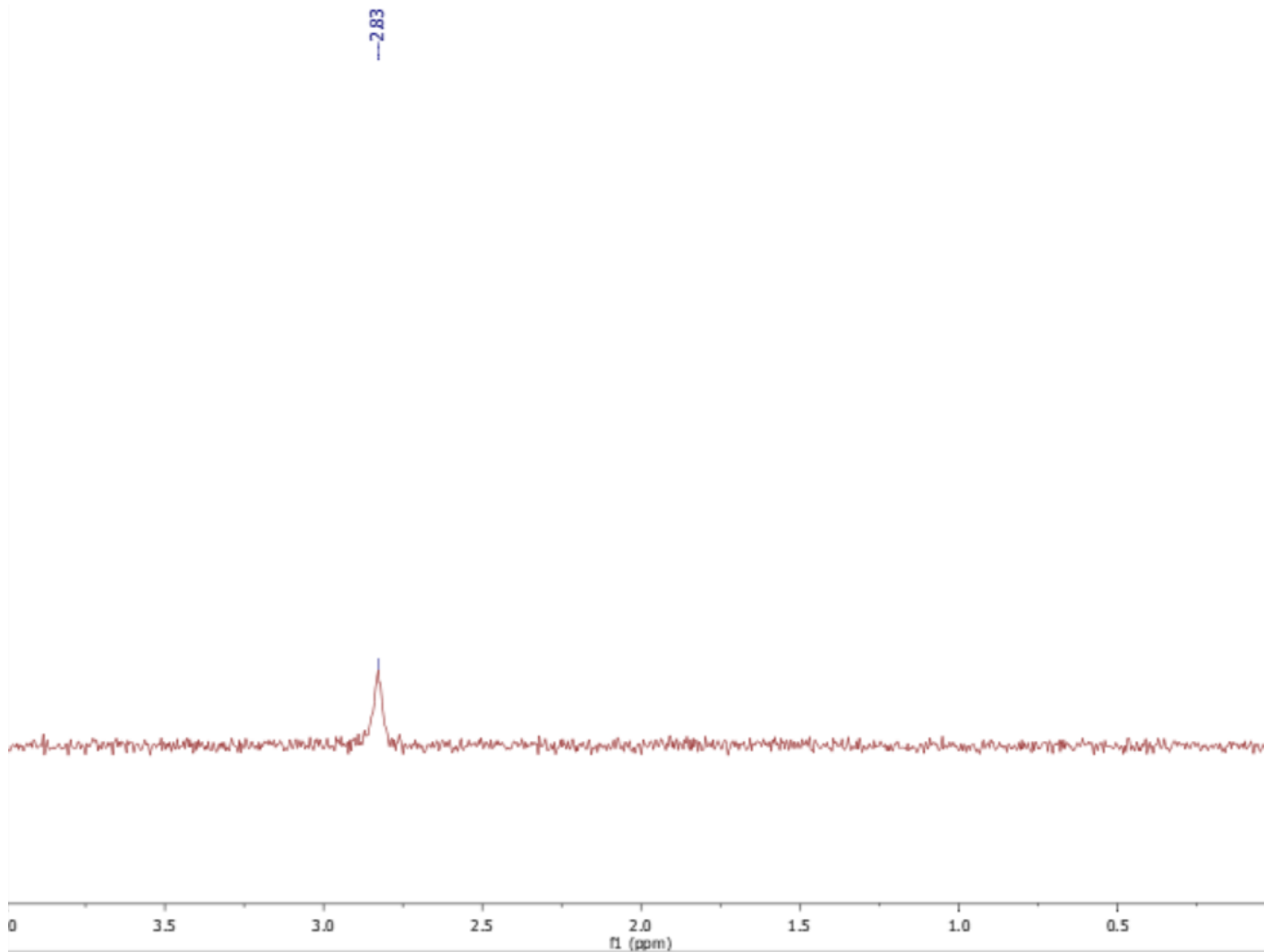


Scheme 2.11-Full spectrum

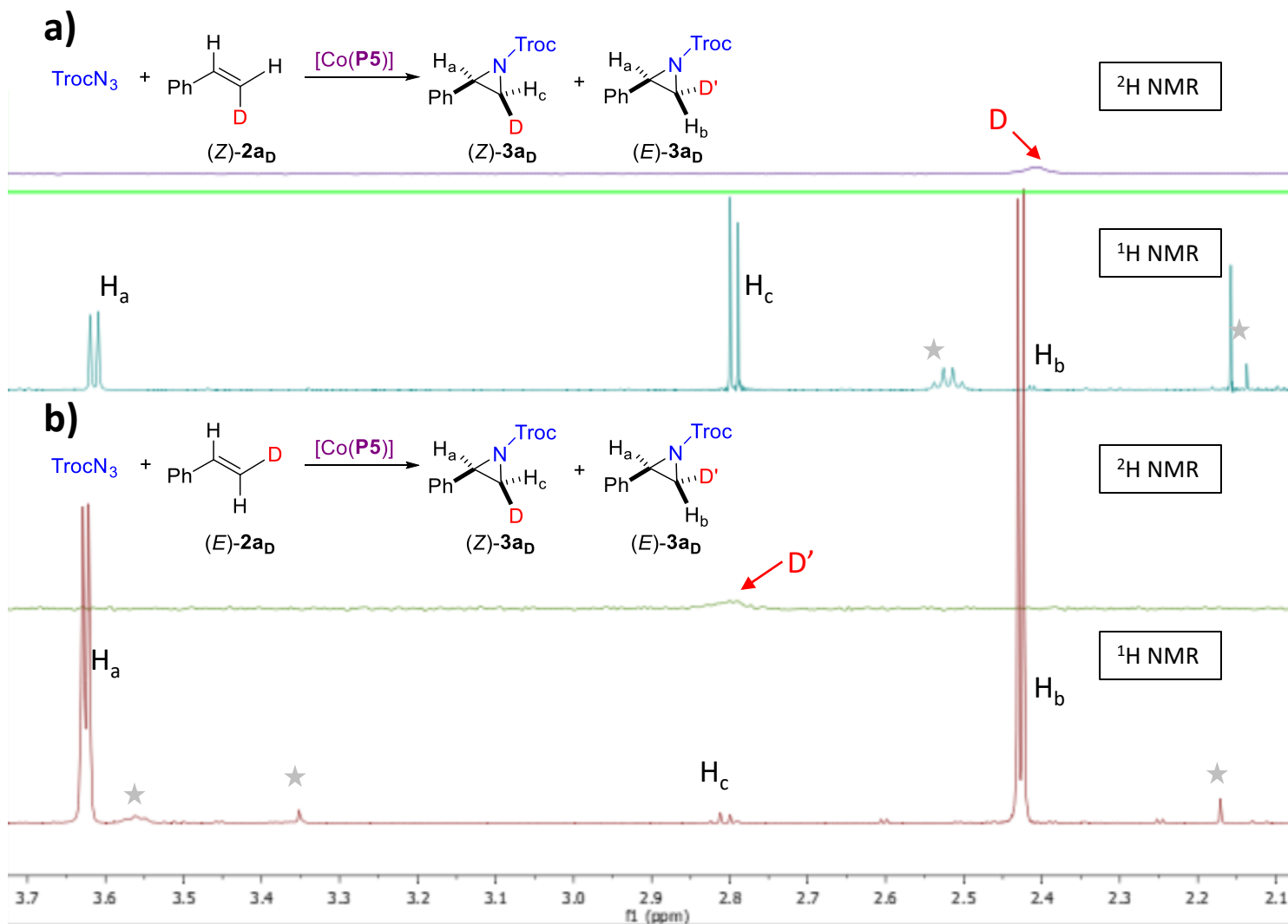


b)

²H NMR

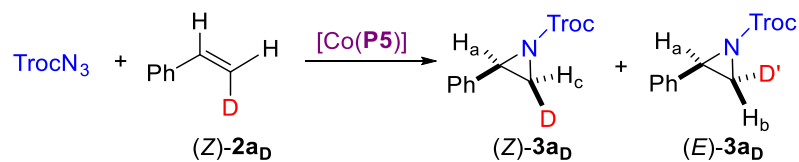


Scheme 2.12

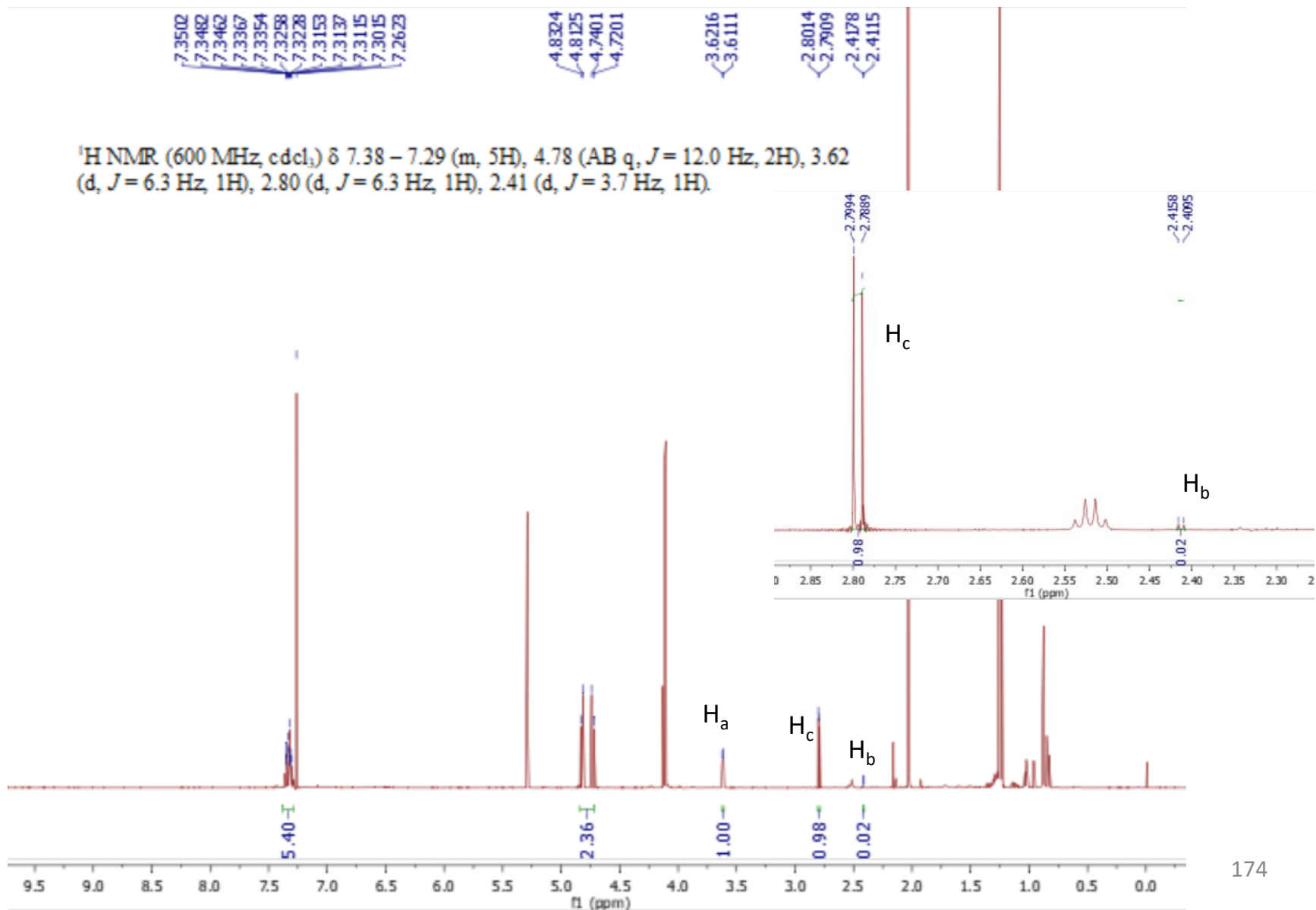


★ Indicates impurity in crude ¹H NMR

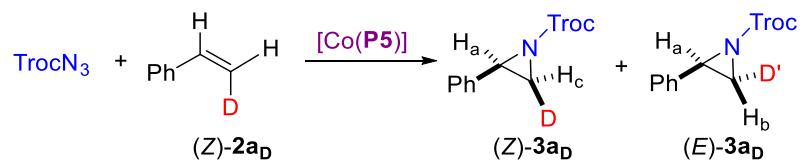
Scheme 2.12-Full spectrum



a) $^1\text{H NMR}$

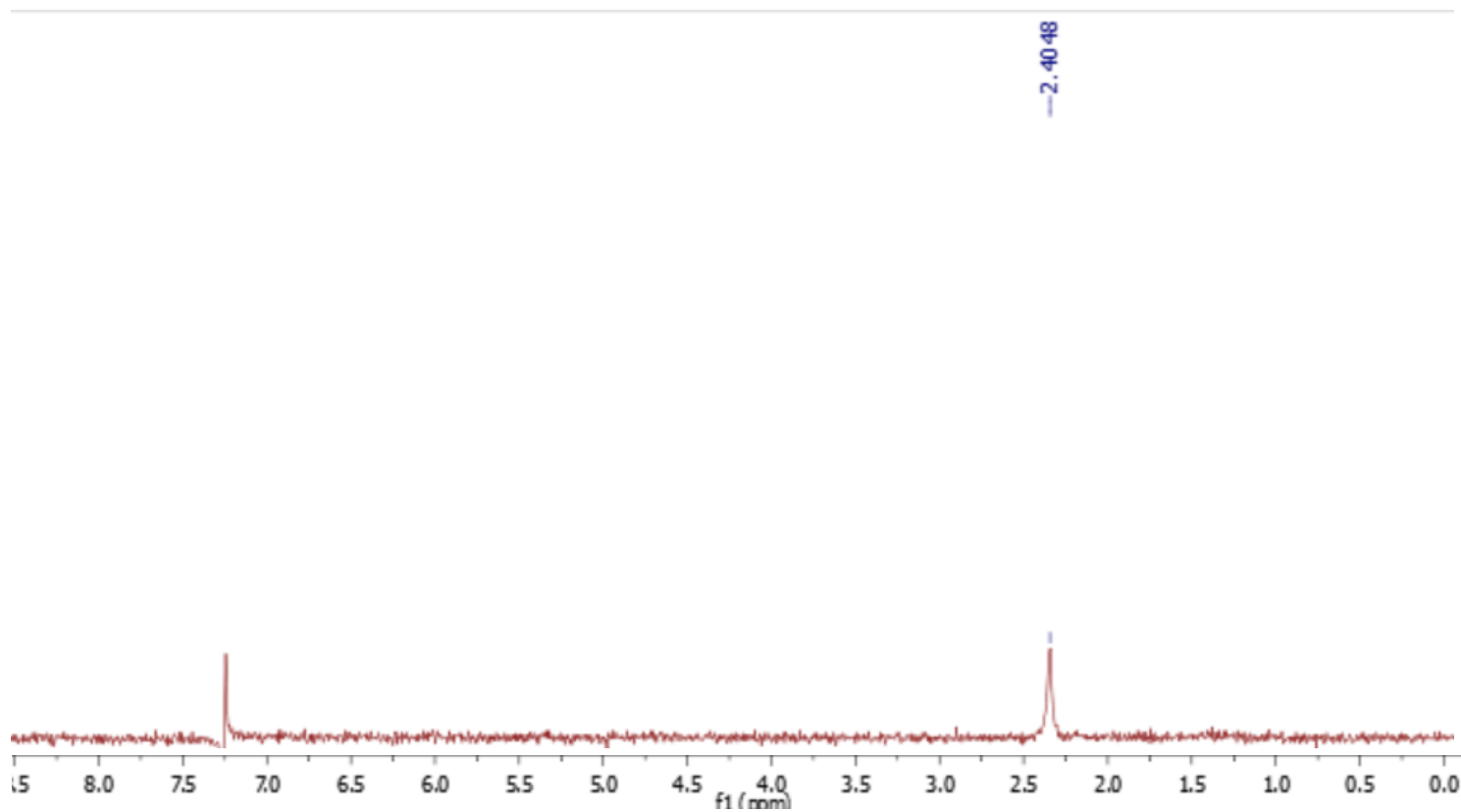


Scheme 2.12-Full spectrum

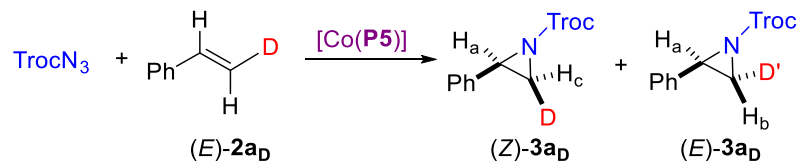


a)

$^2\text{H NMR}$

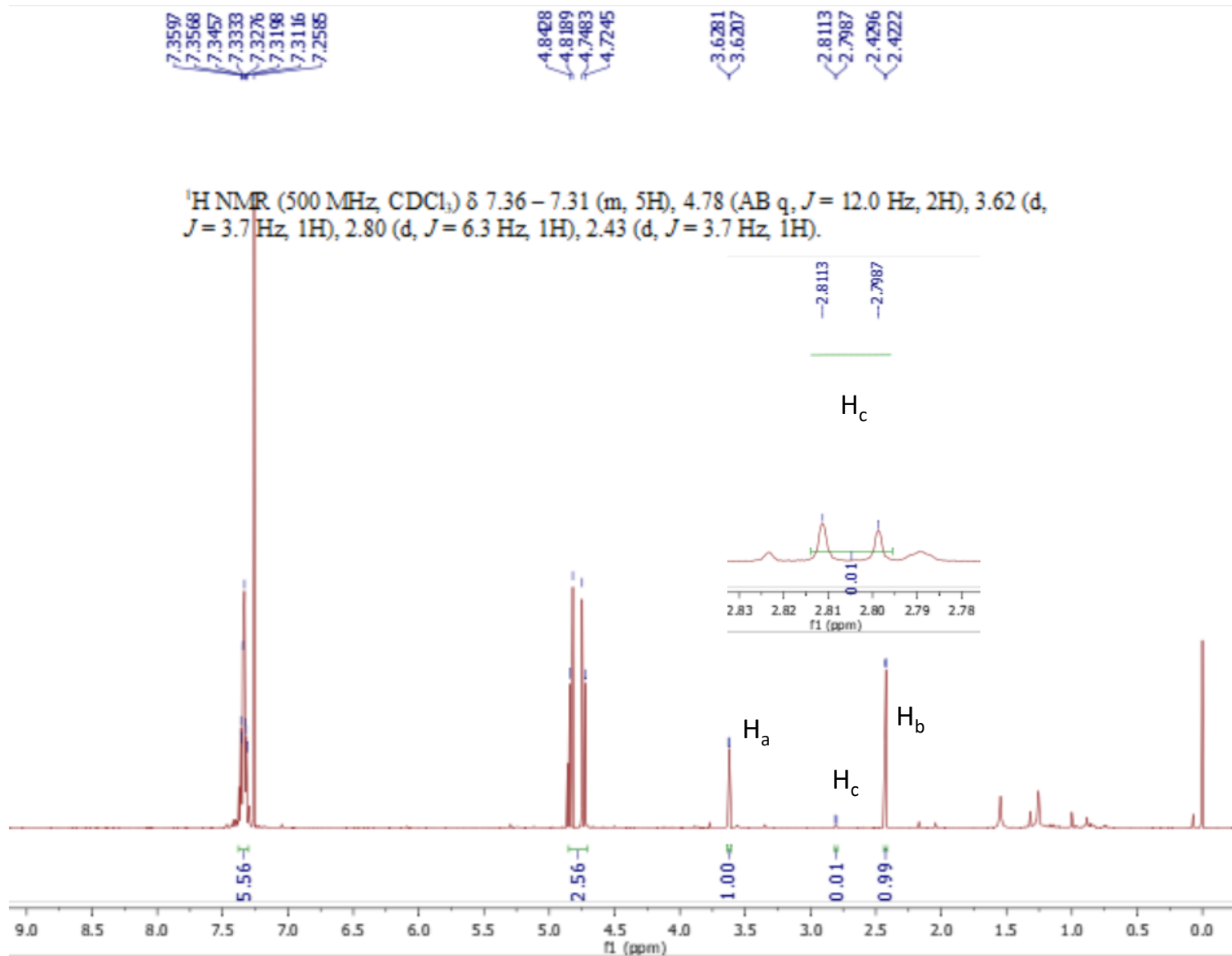


Scheme 2.12-Full spectrum

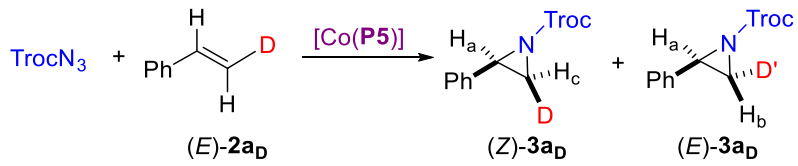


b)

$^1\text{H NMR}$

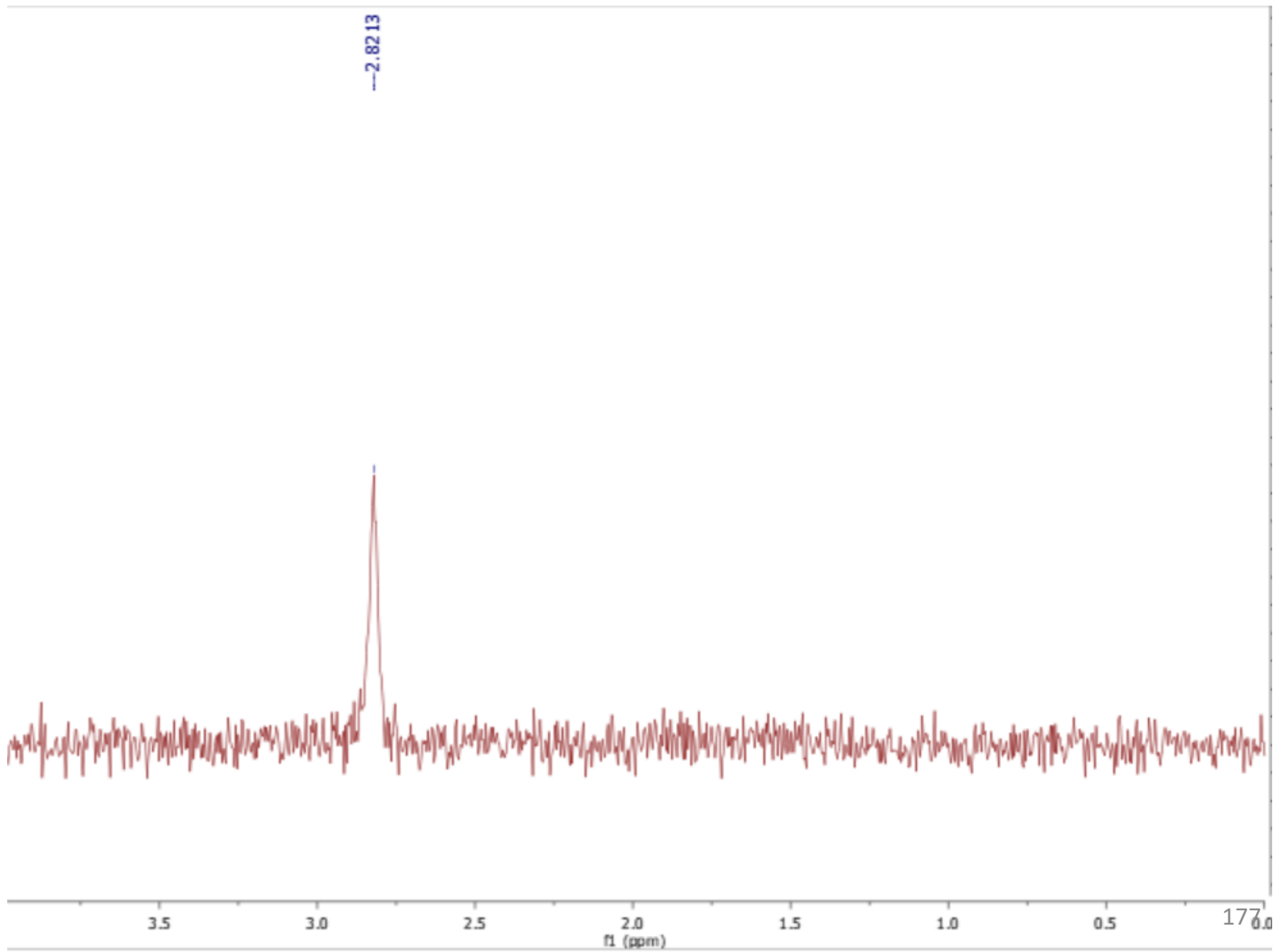


Scheme 2.12-Full spectrum



b)

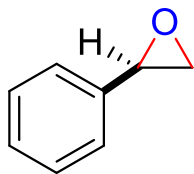
$^2\text{H NMR}$



6.2 Spectral Data for Chapter 3

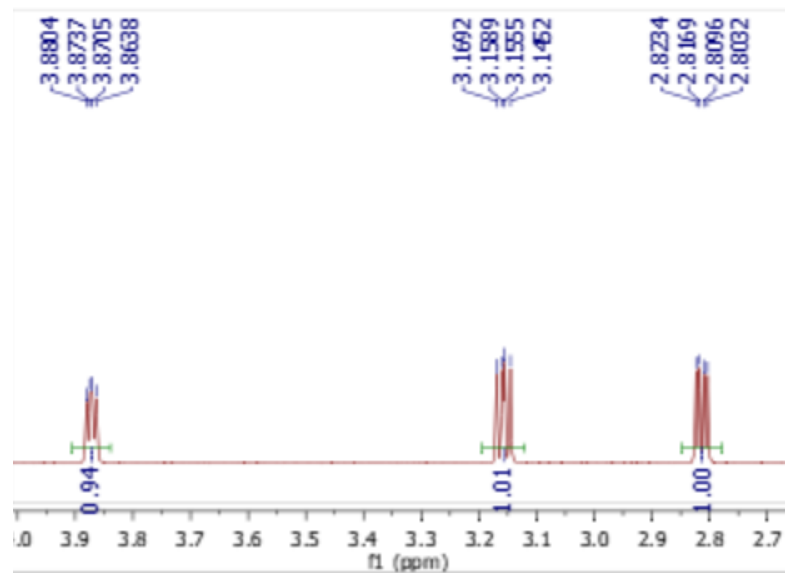
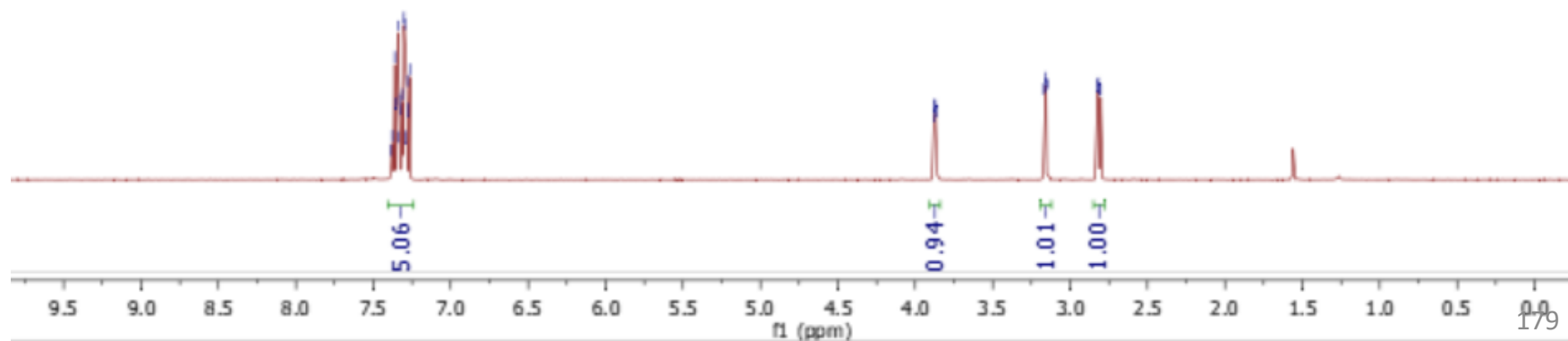
**Generation and Characterization of Unprecedented α -Co(III)-
Oxyl Radicals by Metalloradical Activation of Oxygen Radical
Precursors**

^1H NMR

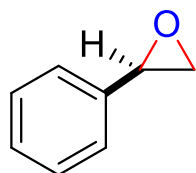


7.3826
7.3777
7.3615
7.3570
7.3432
7.3350
7.3303
7.3262
7.3136
7.3018
7.2974
7.2915
7.2815
7.2780
7.2644

3.8804
3.8737
3.8705
3.8638
3.1692
3.1589
3.1555
3.1452
2.8234
2.8169
2.8096
2.8032



^{13}C NMR



137.7311

128.6341

128.3151

125.6235

77.4143

77.1601

76.9059

52.5001

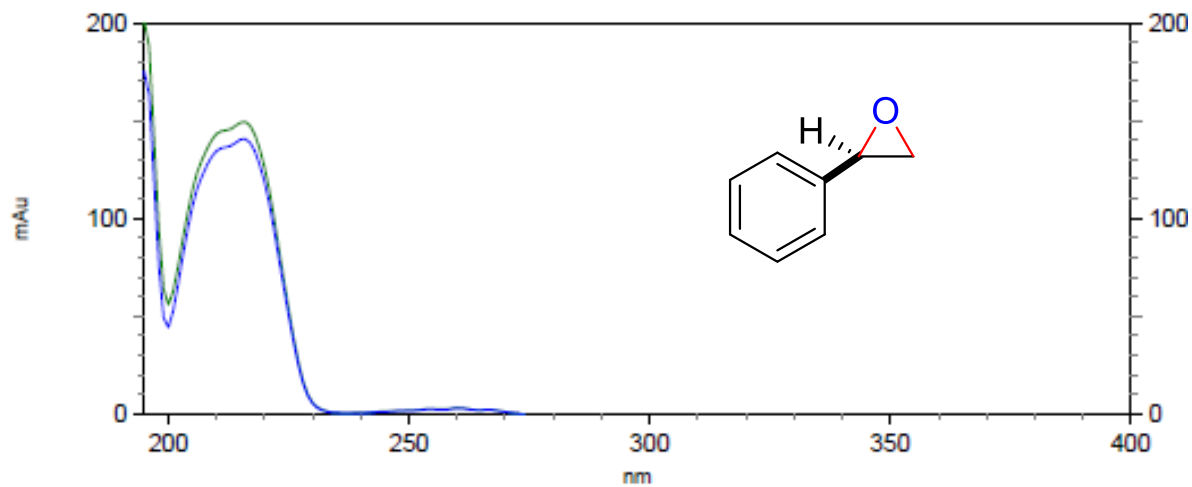
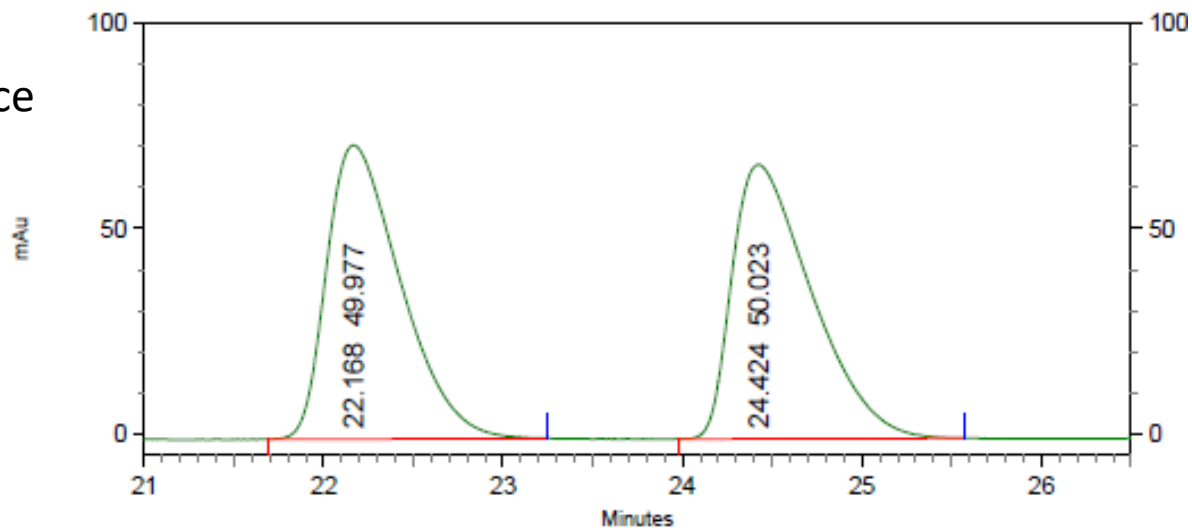
51.3359

180 170 160 150 140 130 120 110 100 90 80 70 60 50 40 30 20 10 0

f1 (ppm)

180

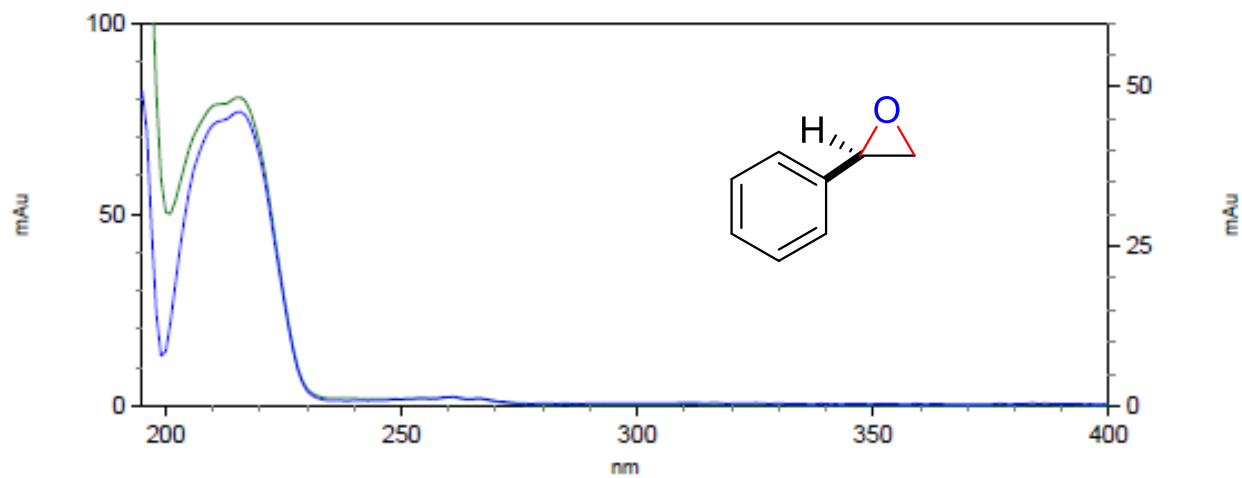
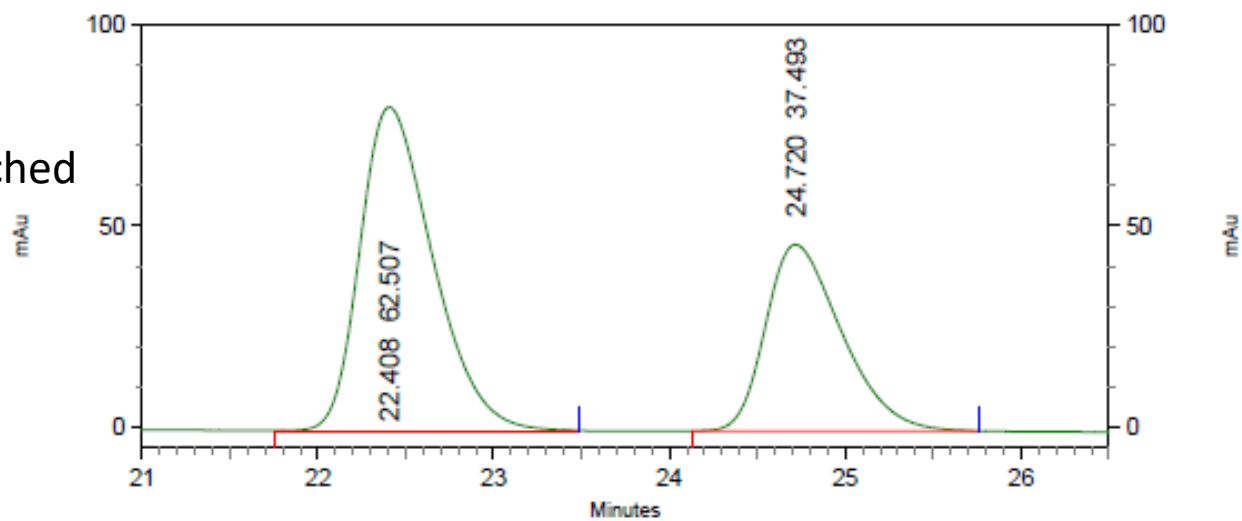
HPLC Trace Racemic



4: 224 nm, 4
nm Results

Pk #	Retention Time	Area Percent
1	22.168	49.977
2	24.424	50.023
Totals		100.000

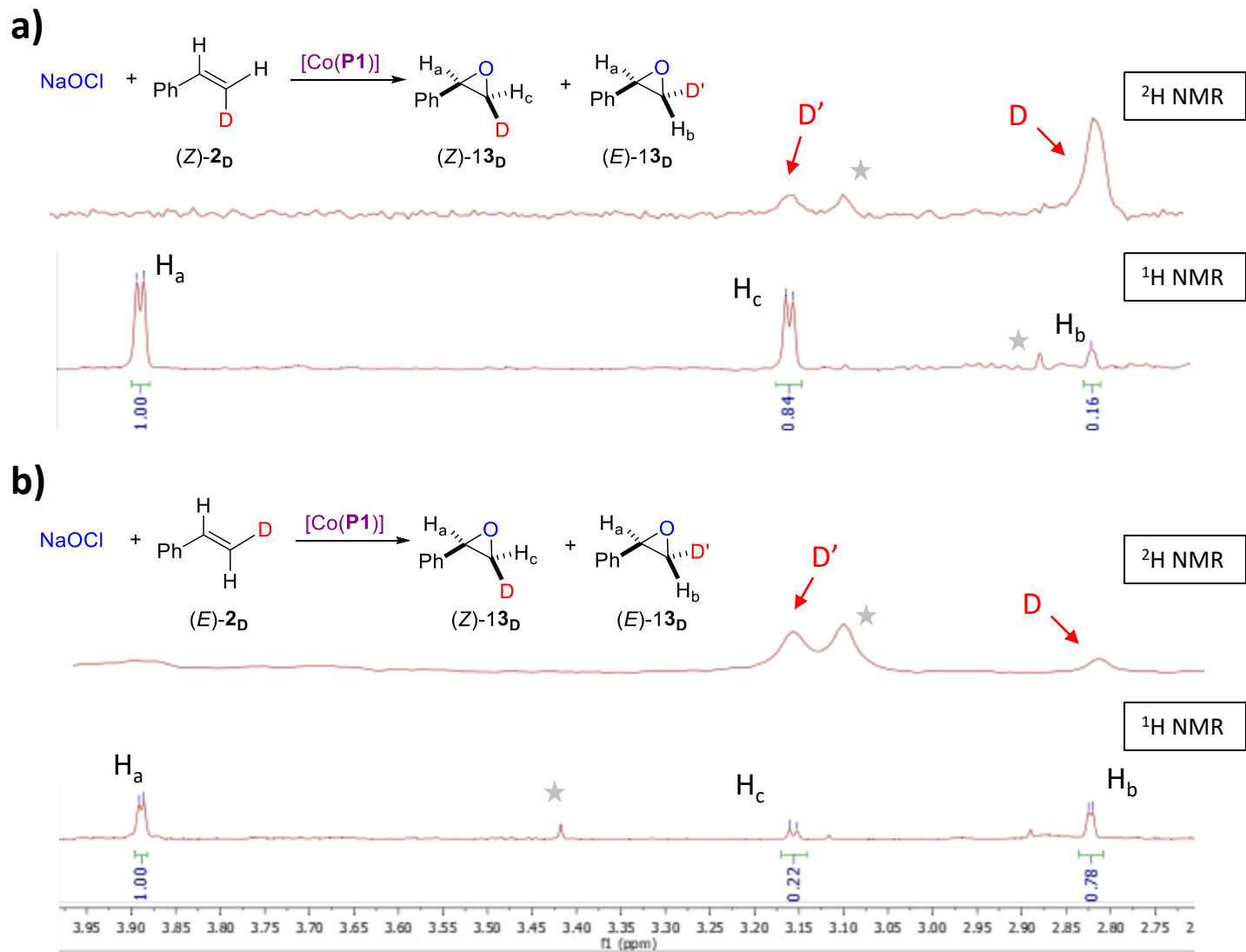
HPLC Trace Enantioenriched



4: 213 nm, 4
nm Results

Pk #	Retention Time	Area Percent
1	22.408	62.507
2	24.720	37.493
Totals		100.000

Scheme 3.10

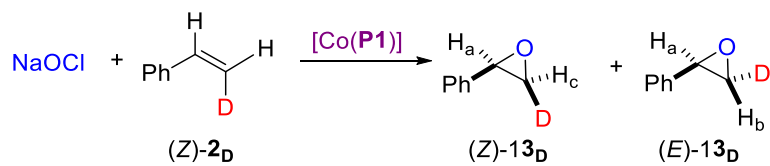


★ Indicates impurity in crude ^1H NMR

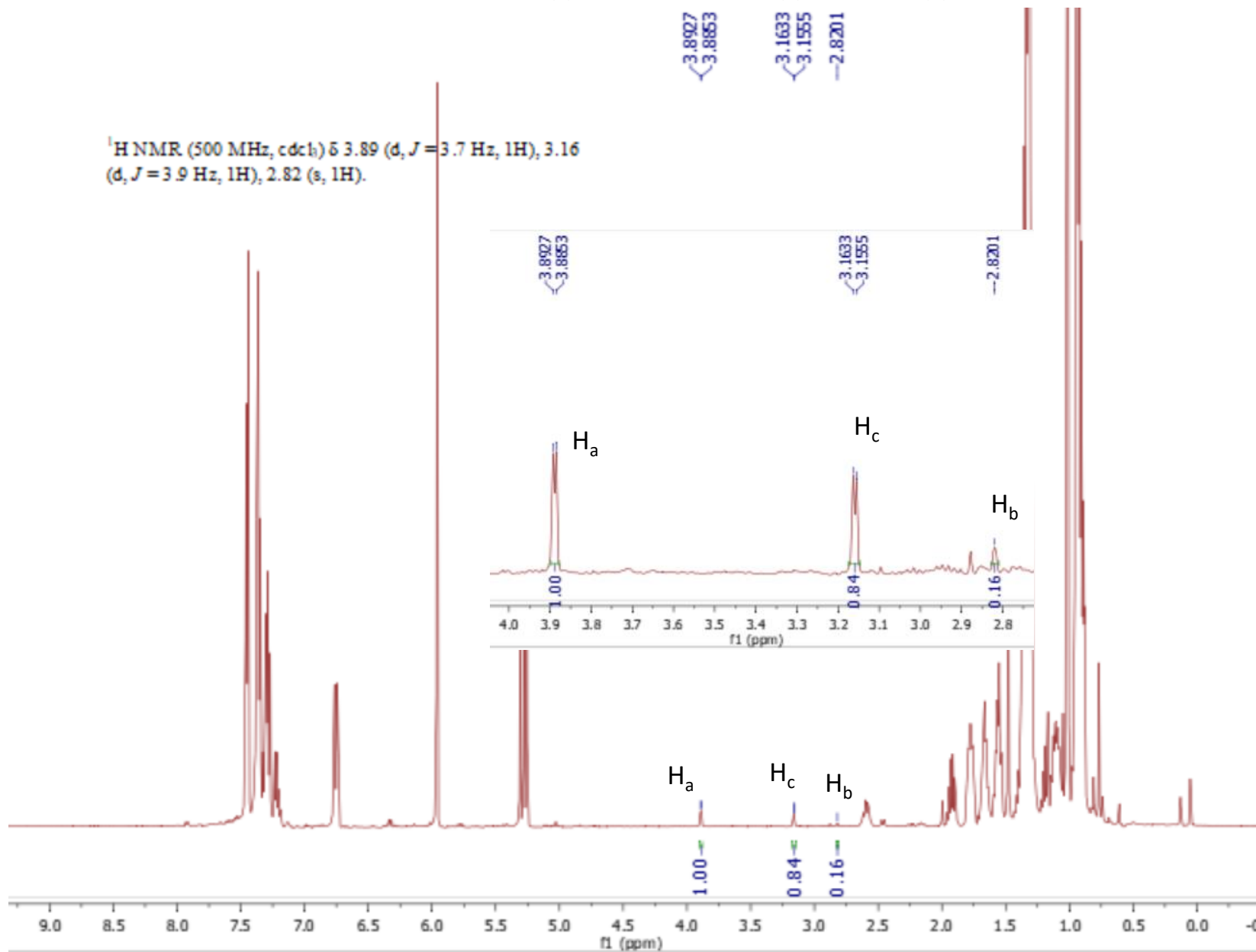
Scheme 3.10-Full spectrum

a)

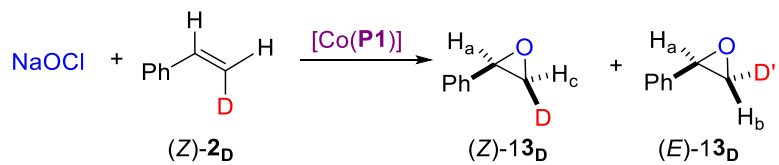
$^1\text{H NMR}$



$^1\text{H NMR}$ (500 MHz, cdcl_3) δ 3.89 (d, $J=3.7$ Hz, 1H), 3.16 (d, $J=3.9$ Hz, 1H), 2.82 (s, 1H).

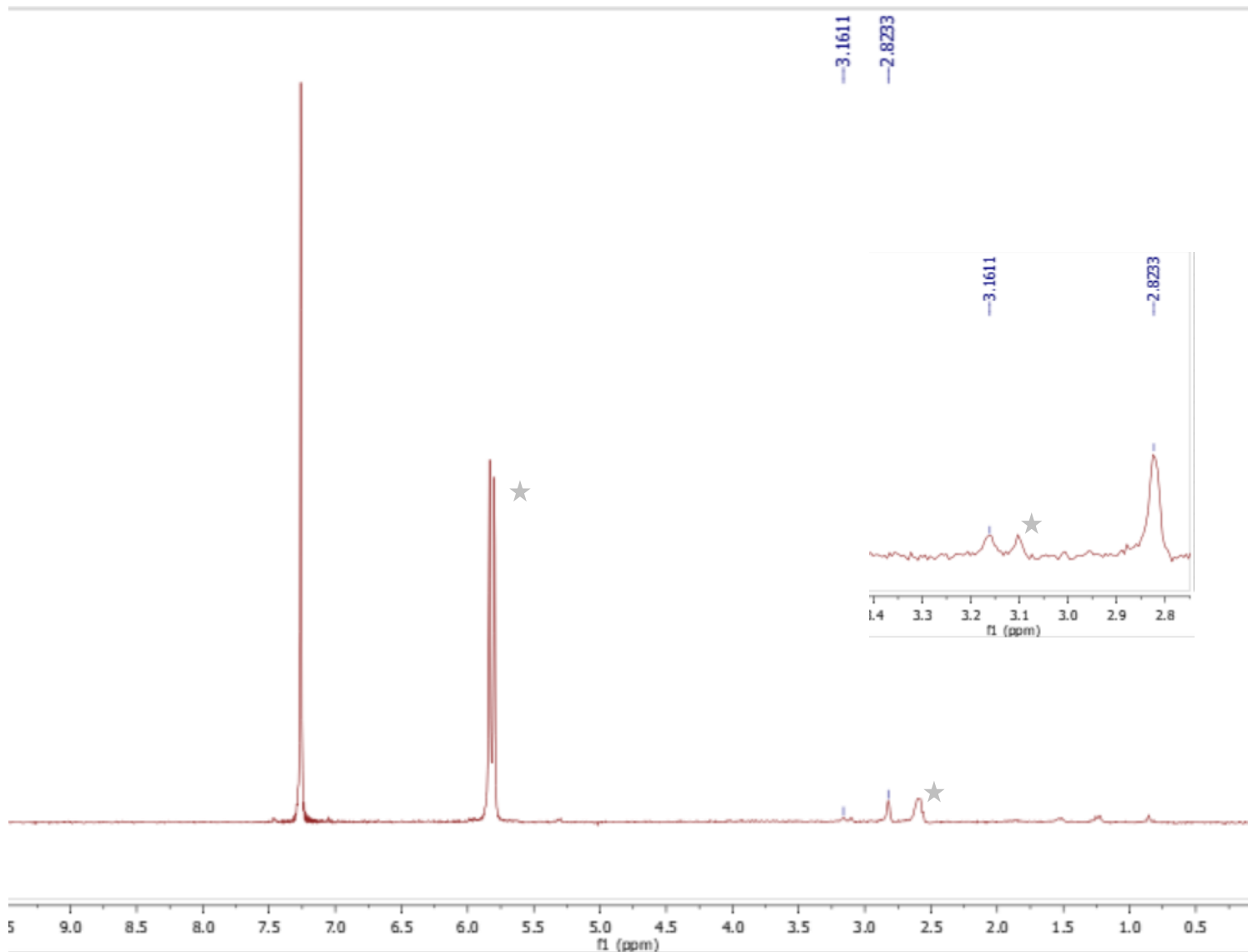


Scheme 3.10-Full spectrum

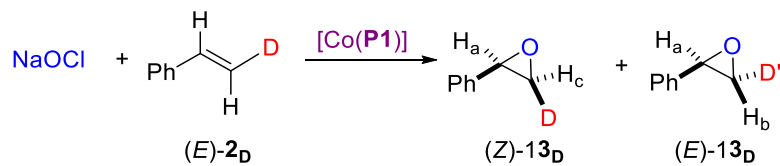


a)

²H NMR

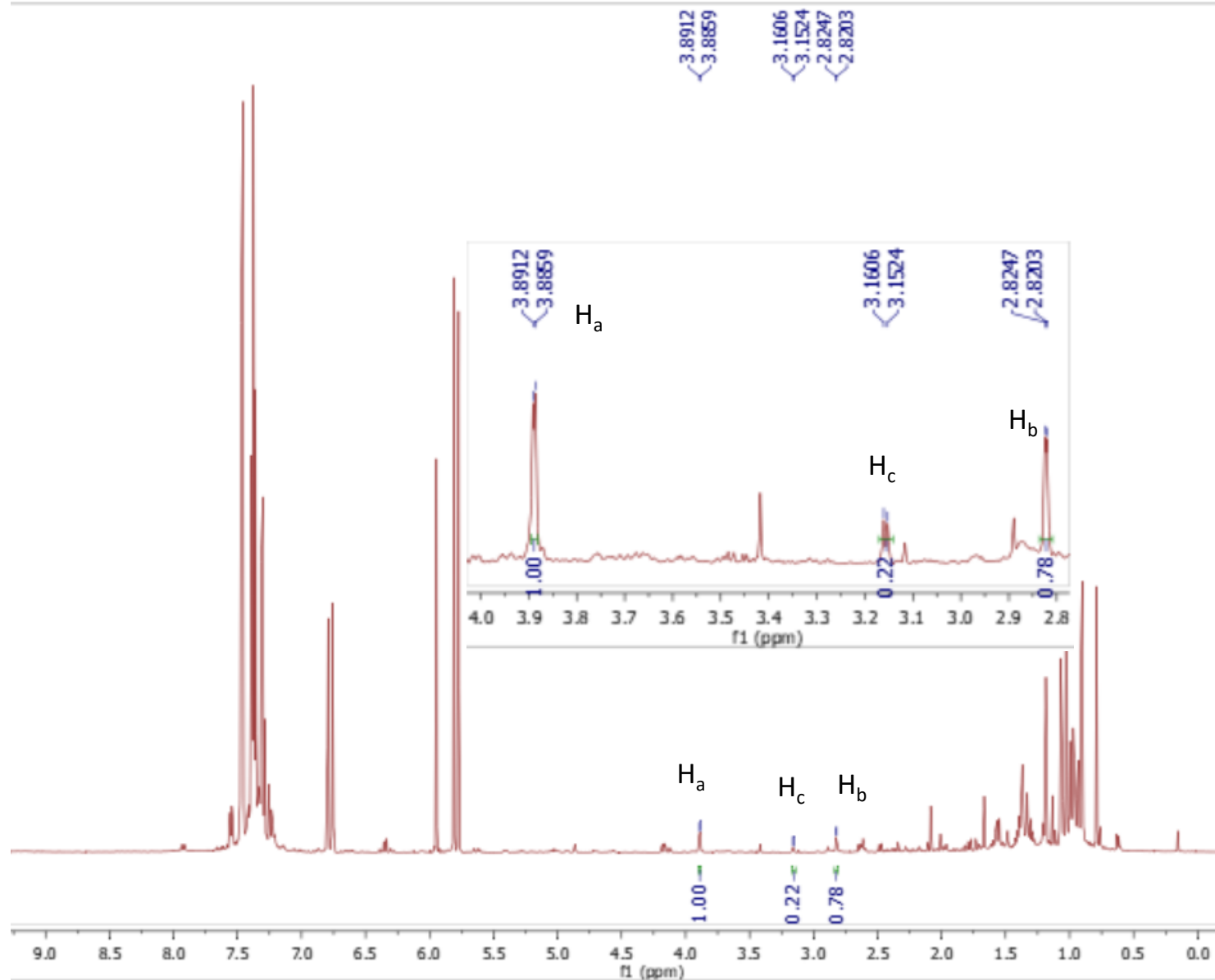


Scheme 3.10-Full spectrum

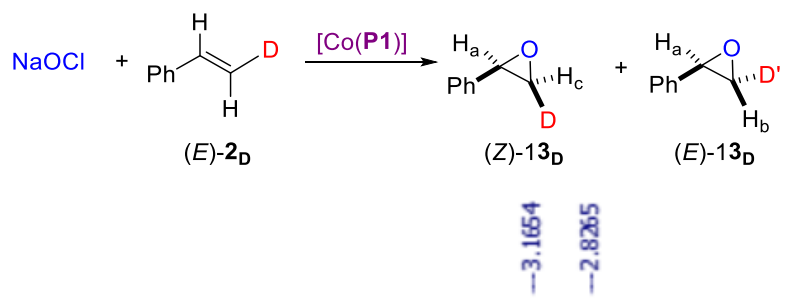


b)

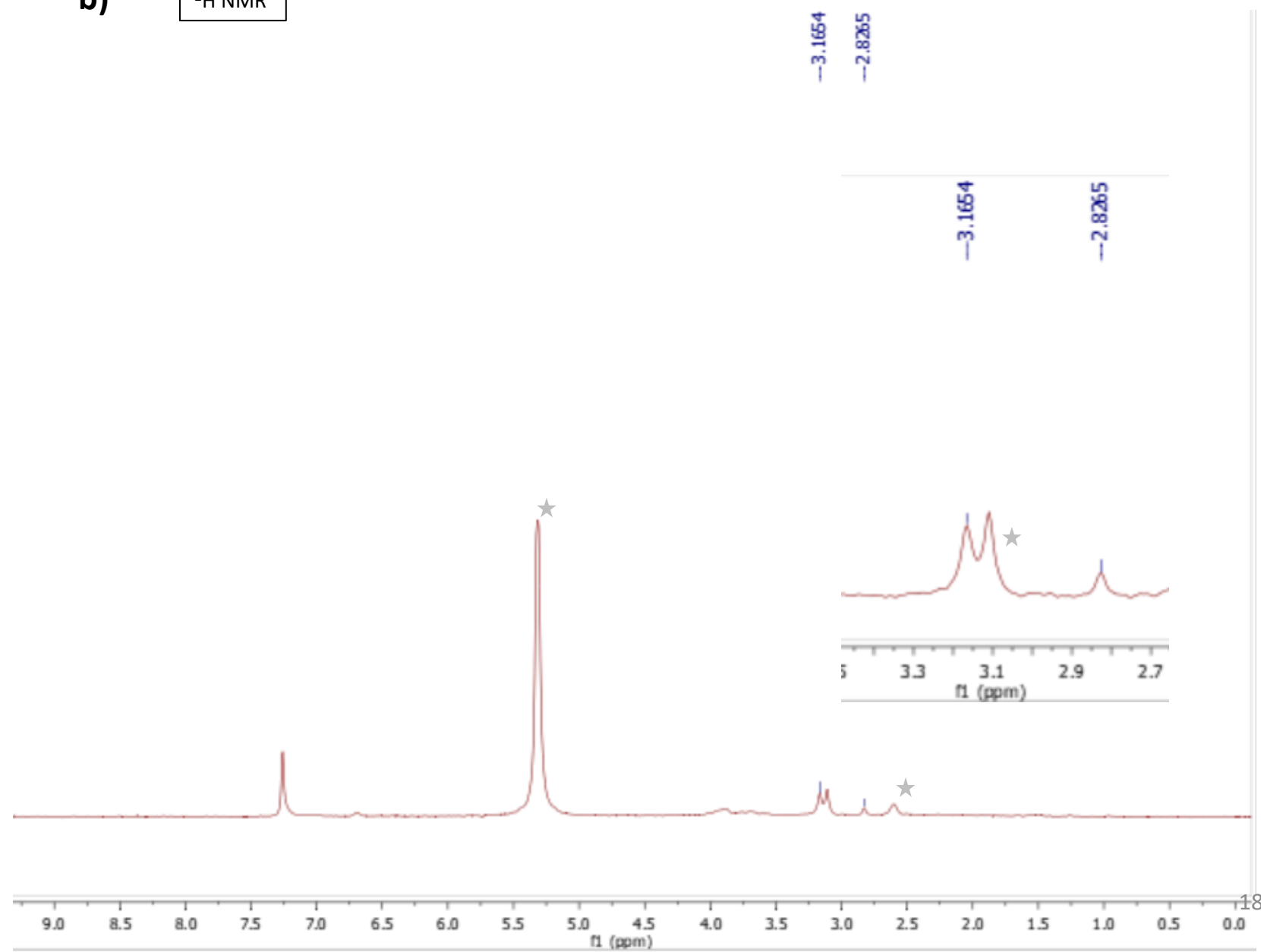
¹H NMR



Scheme 3.10-Full spectrum



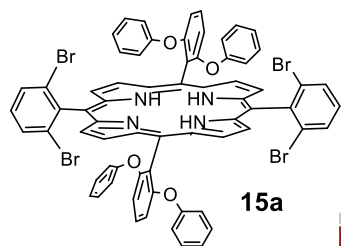
b) $^2\text{H NMR}$



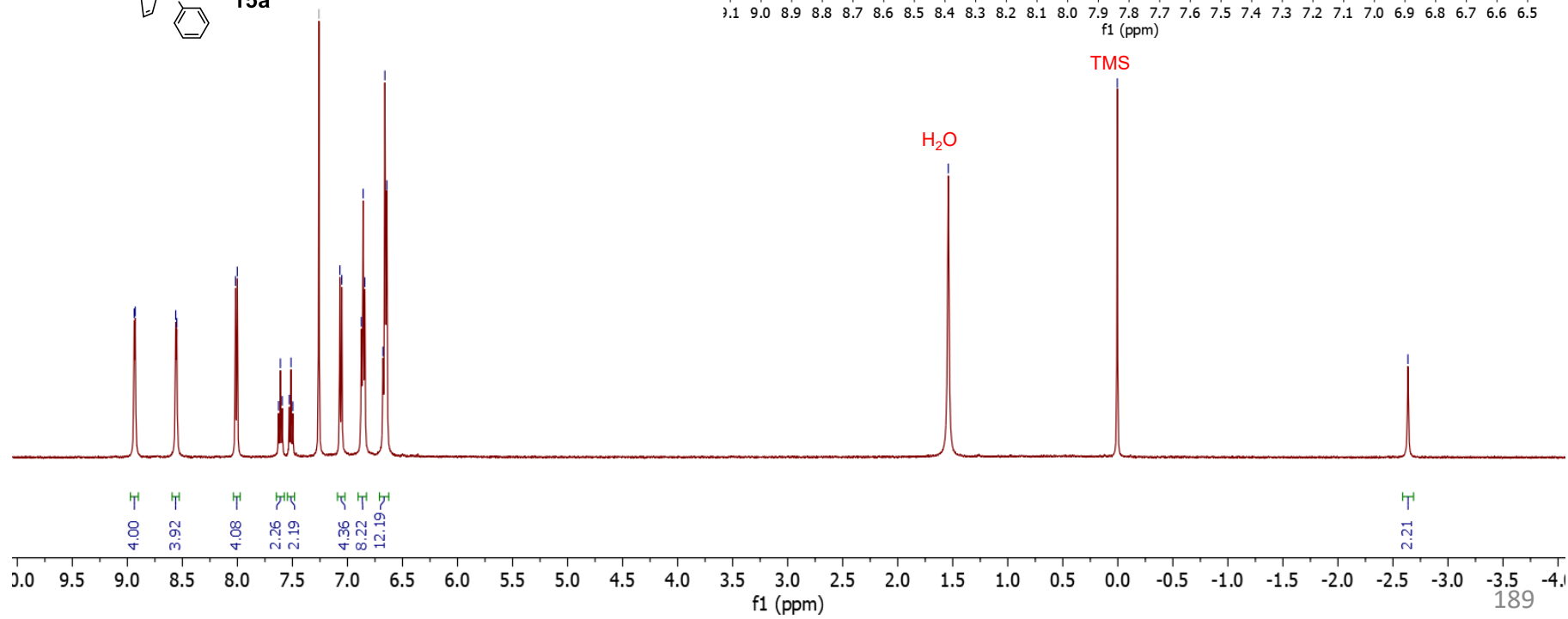
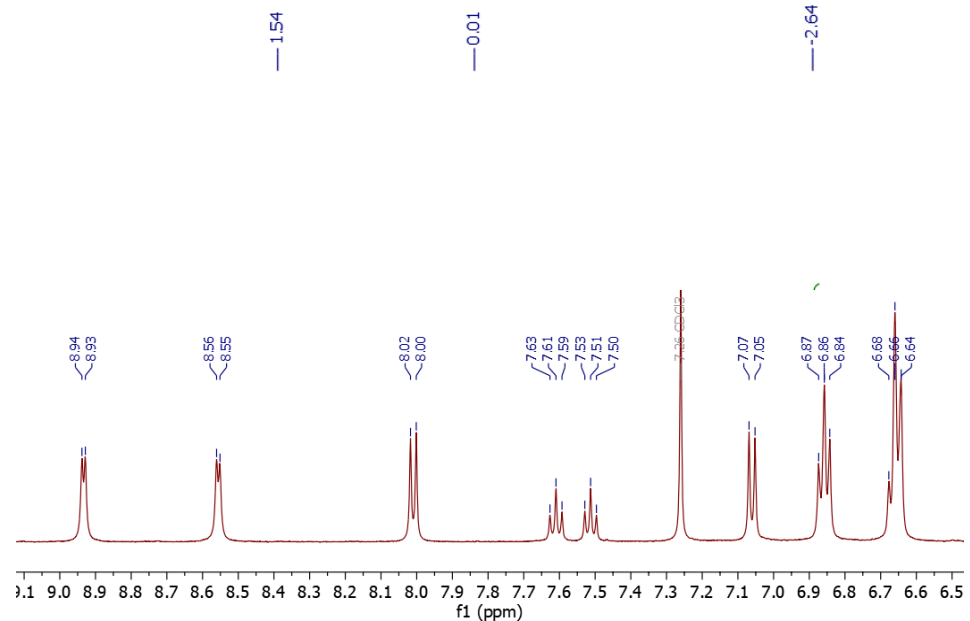
6.3 Spectral Data for Chapter 4

**New Catalytic System for Enantioselective Radical
Epoxidation of Alkenes: Catalyst Development, Substrate
Scope, and Reaction Mechanism**

¹H NMR



8.94
8.93
8.56
8.55
8.02
8.00
7.63
7.61
7.59
7.53
7.51
7.50
7.26 CDCl₃
7.07
7.05
6.87
6.86
6.84
6.68
6.66
6.64



¹³C NMR

— 159.19
— 156.61

— 131.60
— 131.06
— 130.23
— 129.30
— 128.86
— 123.31
— 119.49
— 117.87
— 112.97

— 77.48
— 77.23 CDCl₃
— 76.98

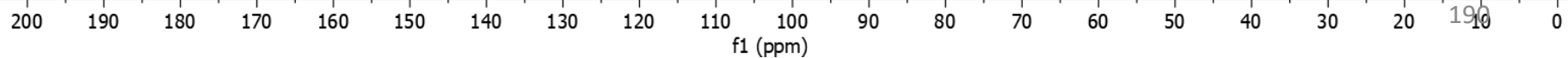
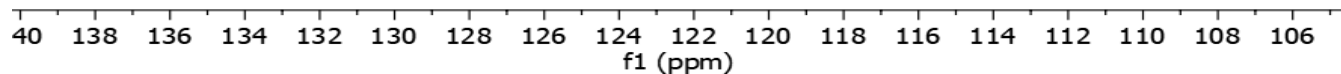
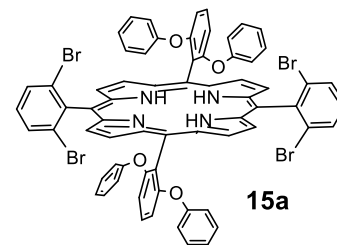
— 131.60
— 131.06
— 130.23
— 129.30
— 128.86

— 123.31

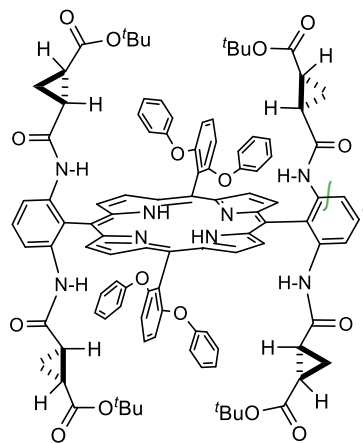
— 119.49

— 117.87

— 112.97



¹H NMR



9.14
9.11
9.10
9.07
8.78
8.77
8.46
7.85
7.83
7.82
7.64
7.62
7.61
7.26 CDCl₃
7.02
7.01
7.00
6.99
6.99
6.98
6.97
6.81
6.80
6.79
6.78
6.74
6.74
6.72
6.58

1.78
1.78
1.77
1.77
1.76
1.75
1.75
1.52
1.51
0.92
0.80
0.43
0.21

-2.55

TMS

H₂O

4.00
4.09
4.04

2.15
2.04

11.72
3.98
8.12
4.03

4.01

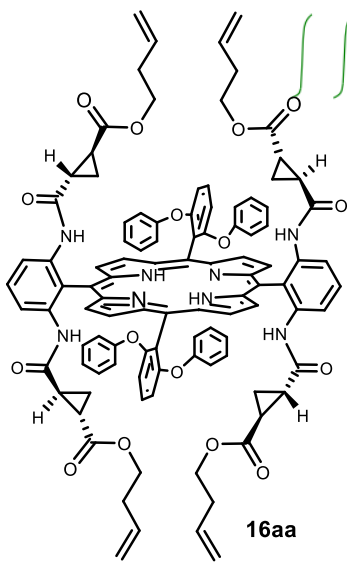
36.14
4.10
4.13
3.91

2.16

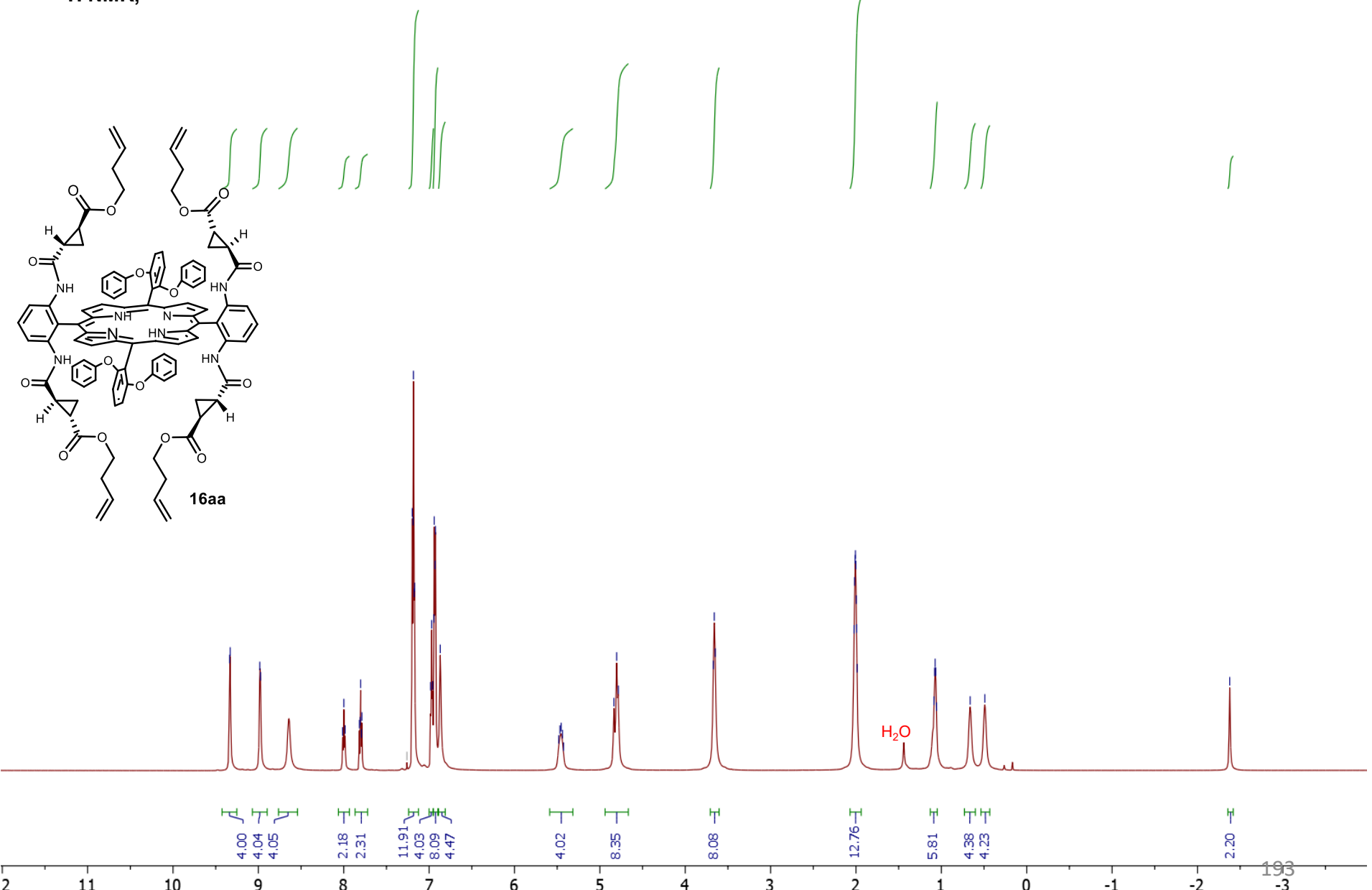
11 10 9 8 7 6 5 4 3 2 1 0 -1 -2 -3 -4

f1 (ppm)

¹H NMR,



9.34
9.33
8.98
8.01
8.00
7.98
7.82
7.81
7.80
7.79
7.79
7.26 CDCl₃
7.20
7.19
7.18
7.18
7.17
6.98
6.97
6.96
6.94
6.94
6.93
6.87
5.48
5.47
5.45
5.44
5.43
4.84
4.80
4.78
3.67
3.66
3.65
2.02
2.02
2.01
2.01
2.00
2.00
1.99
1.99
1.09
1.08
1.07
1.06
1.06
0.66
0.49



-2.38

¹³C NMR

— 171.18
— 168.65

— 159.18
— 156.20

— 139.08
— 133.64
— 130.87
— 130.47
— 129.59
— 123.70
— 123.09
— 121.89
— 119.51
— 117.97
— 116.99
— 112.72
— 112.14
— 107.16

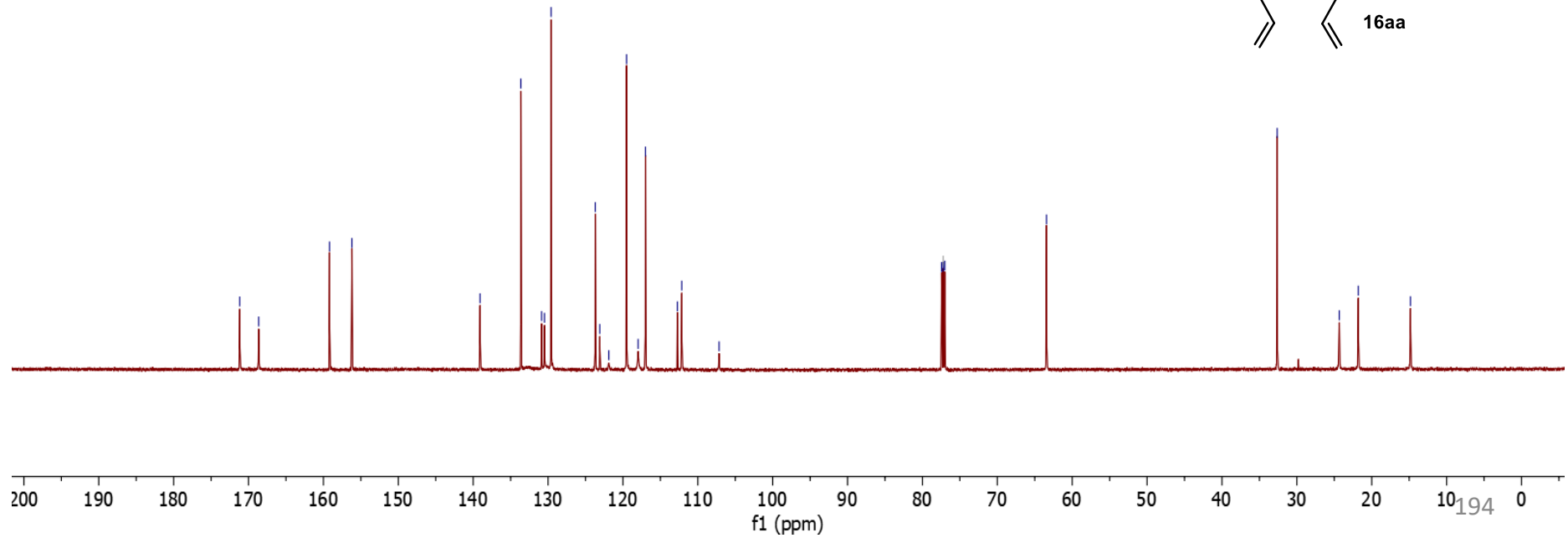
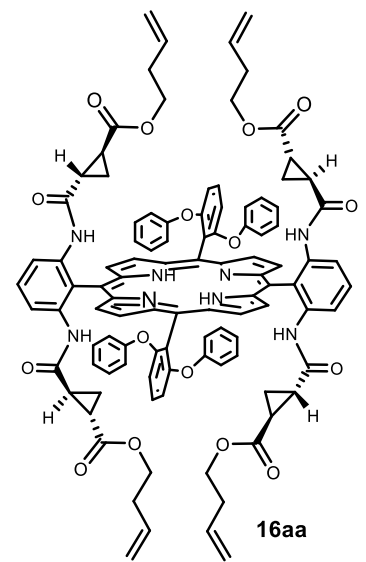
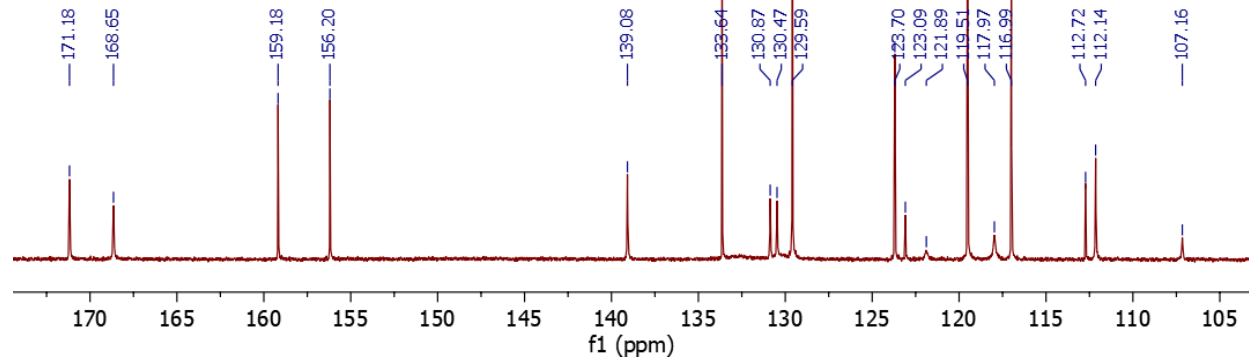
77.44
77.23 CDCl₃
77.23
77.02

— 63.43

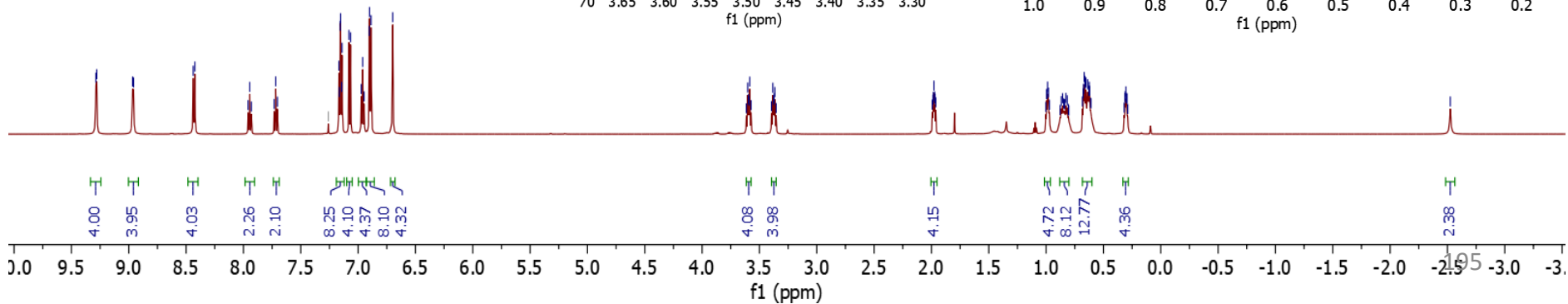
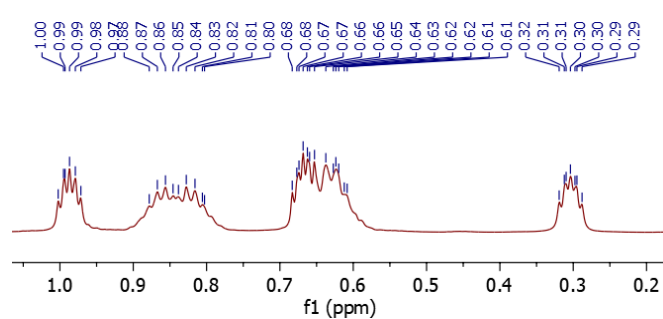
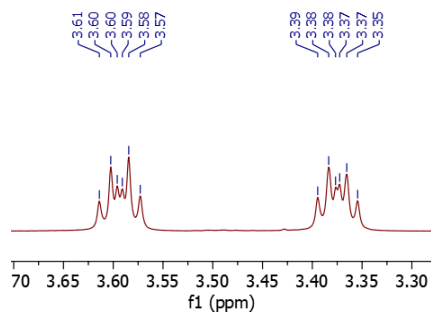
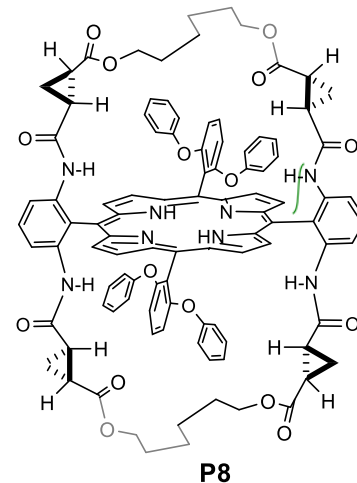
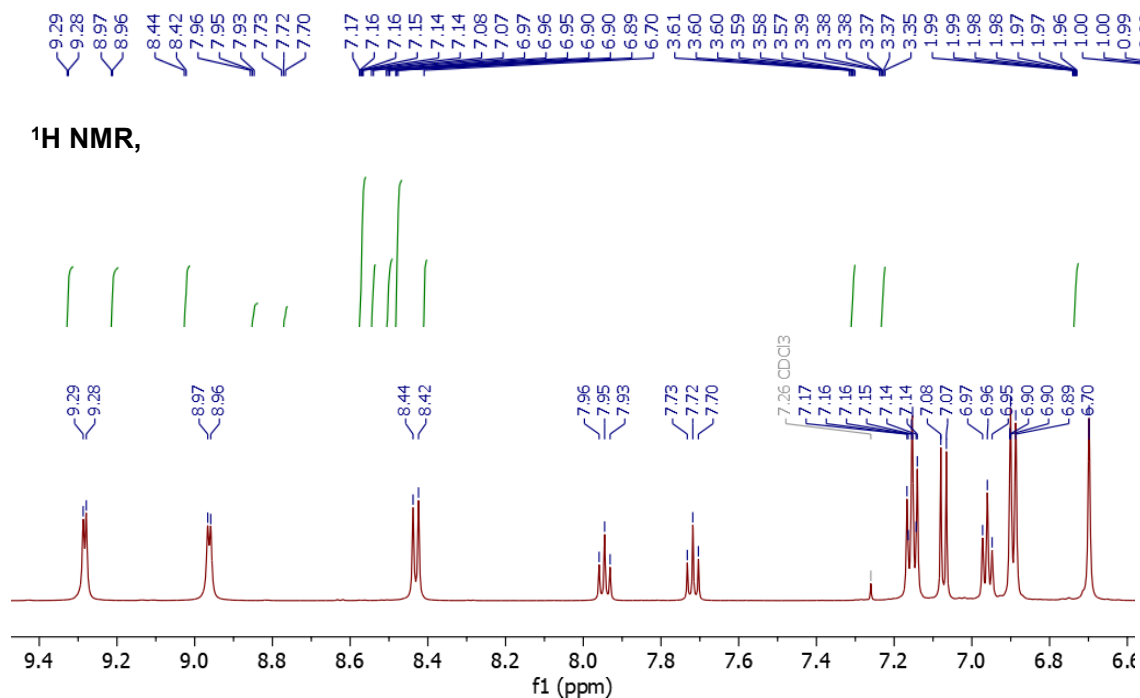
— 32.63

— 24.33
— 21.79

— 14.82



¹H NMR,



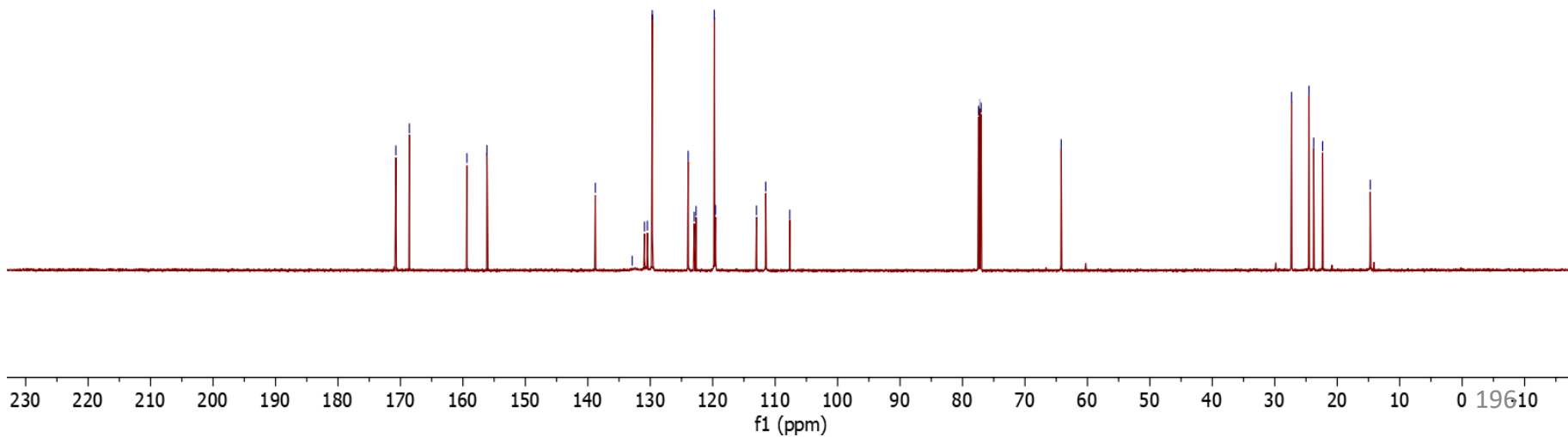
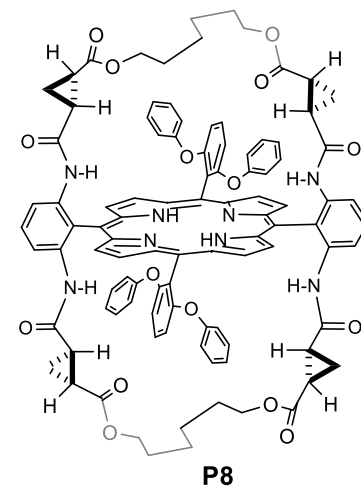
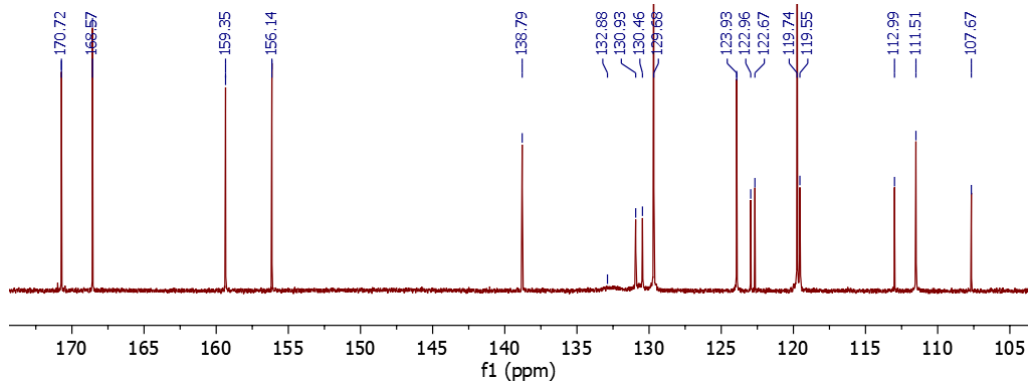
¹³C NMR

170.72
168.57
159.35
156.14
138.79
132.88
130.93
130.46
129.68
123.93
122.96
122.67
119.74
119.55
112.99
111.51
107.67

77.44
77.23 CDCl₃
77.02

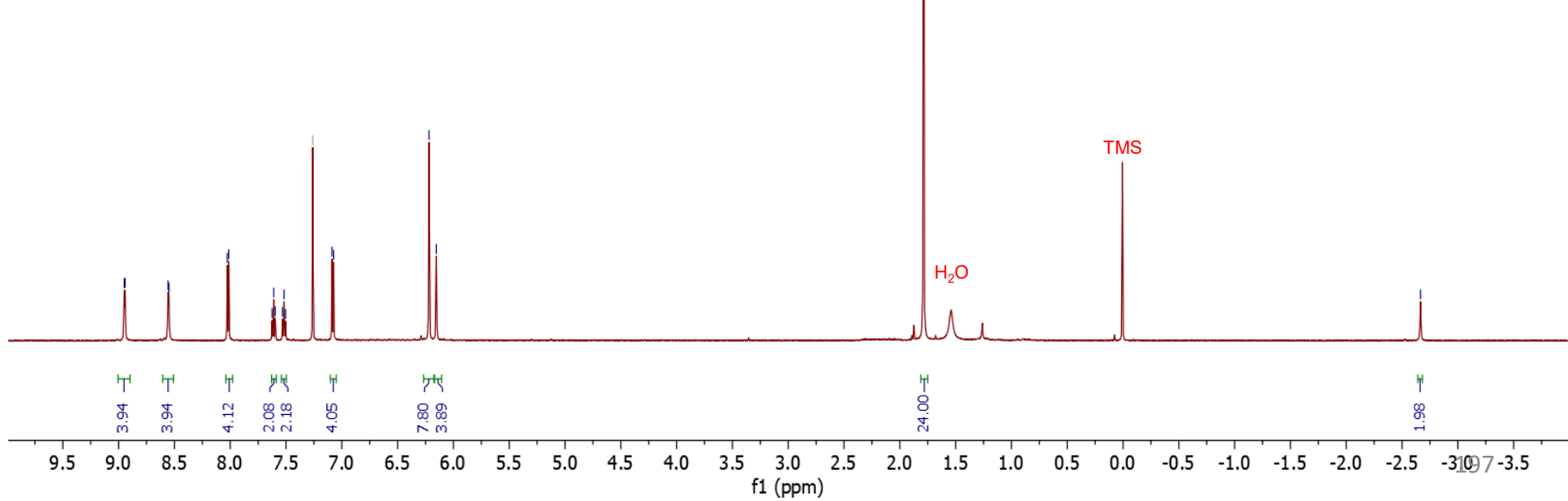
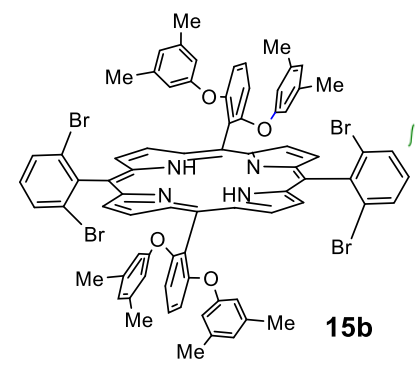
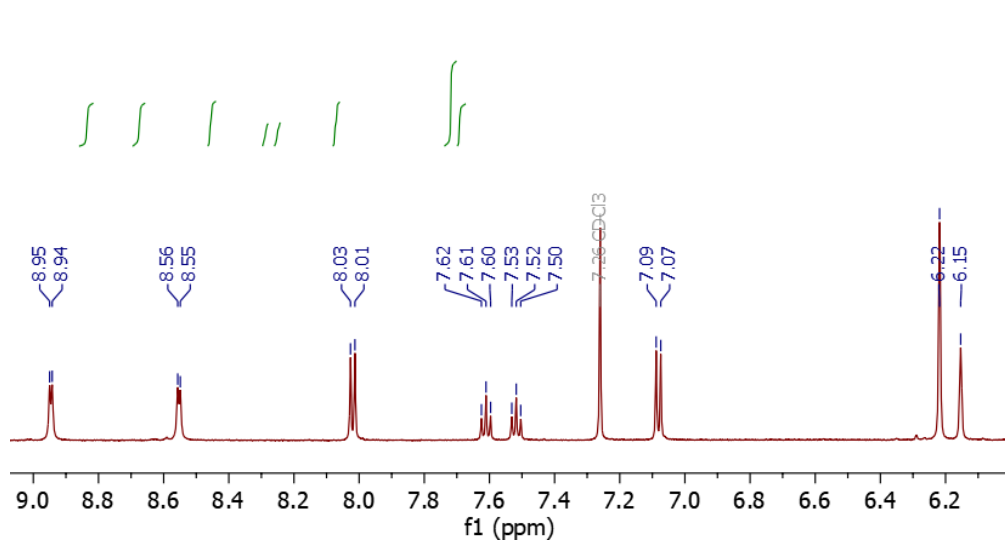
64.19

27.32
24.53
23.77
22.34
14.71

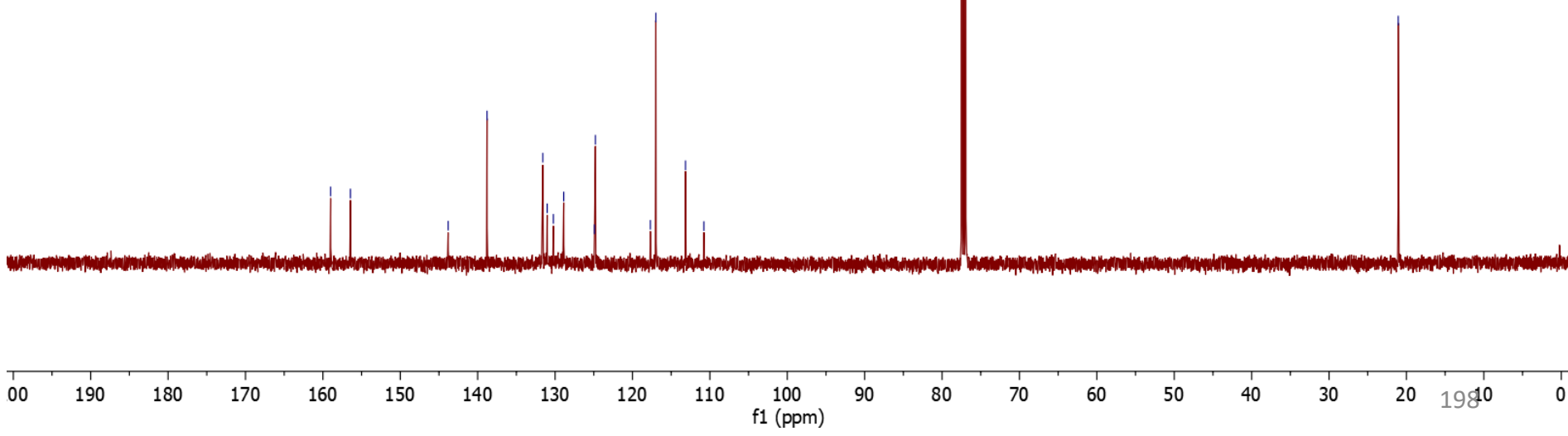
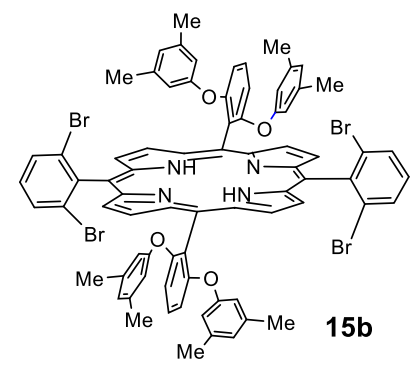
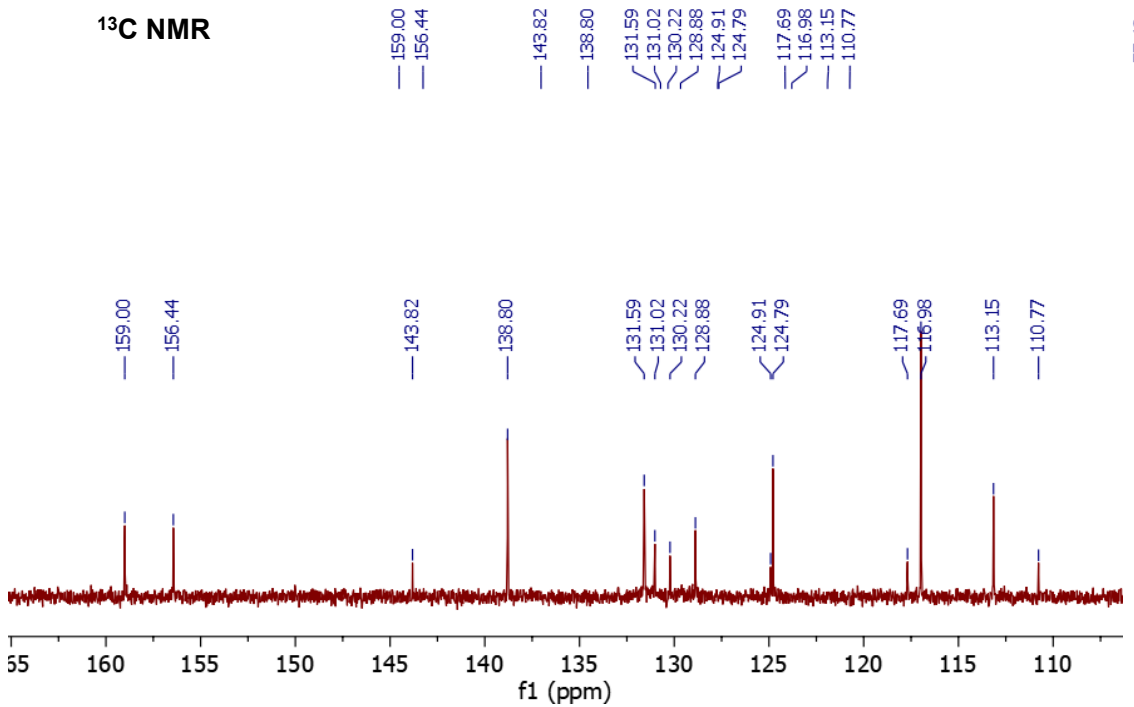


¹H NMR,

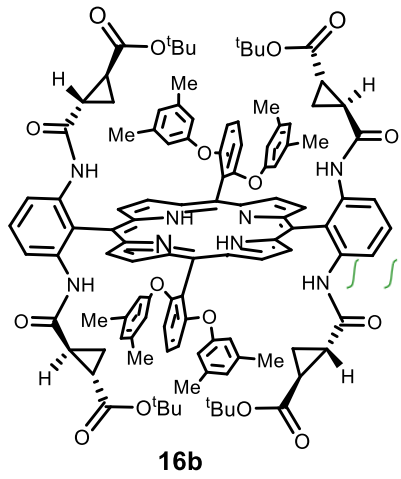
8.95
8.94
8.56
8.55
8.03
8.01
7.62
7.61
7.60
7.53
7.52
7.50
7.26 CDCl₃
7.09
7.07
6.22
6.15



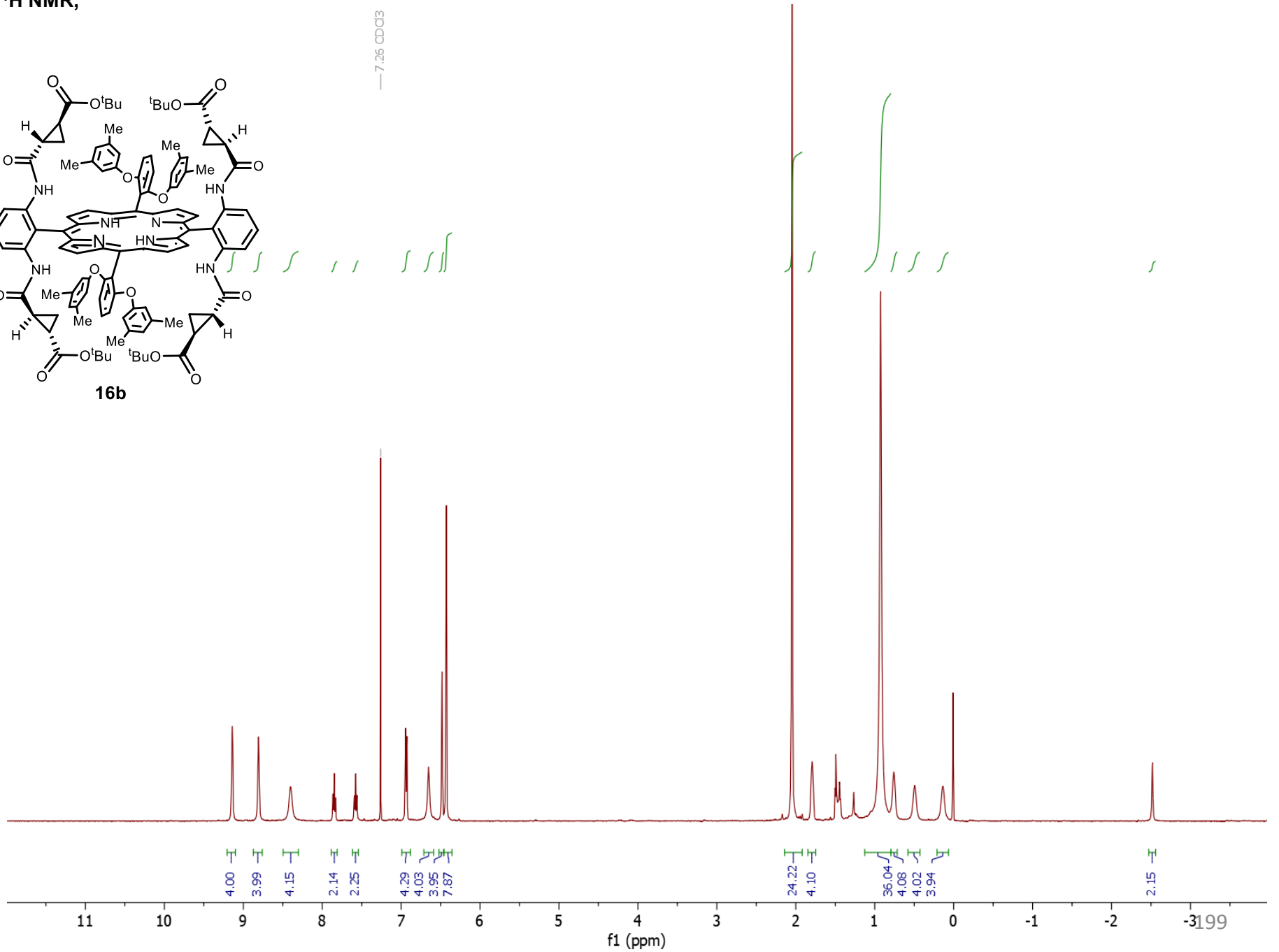
¹³C NMR



¹H NMR,



—7.26 CDCl₃



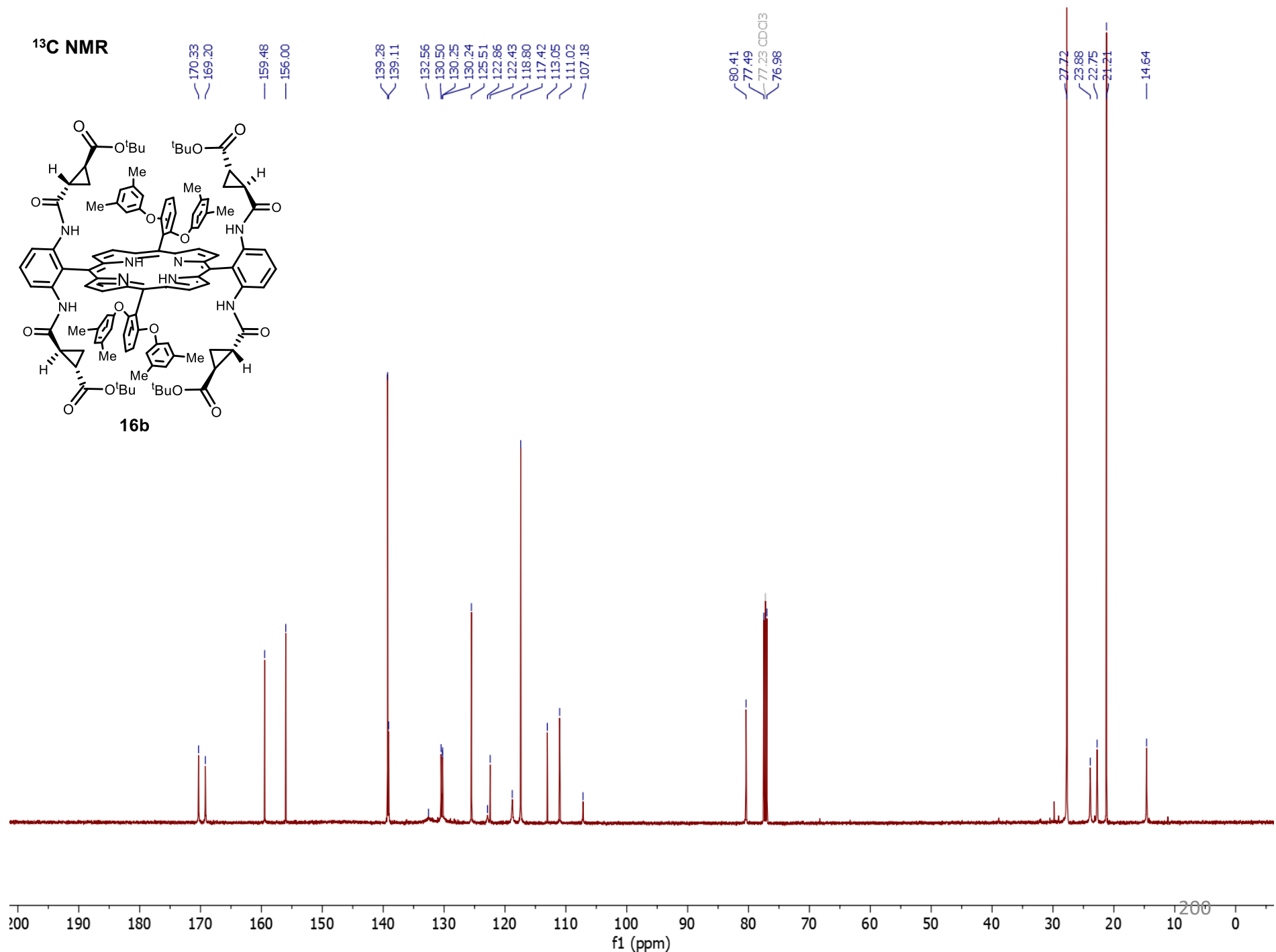
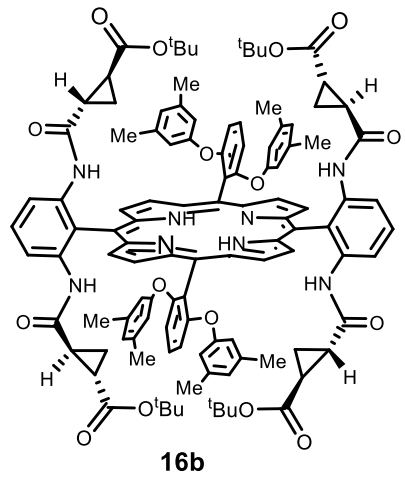
¹³C NMR

170.33
169.20
159.48
156.00

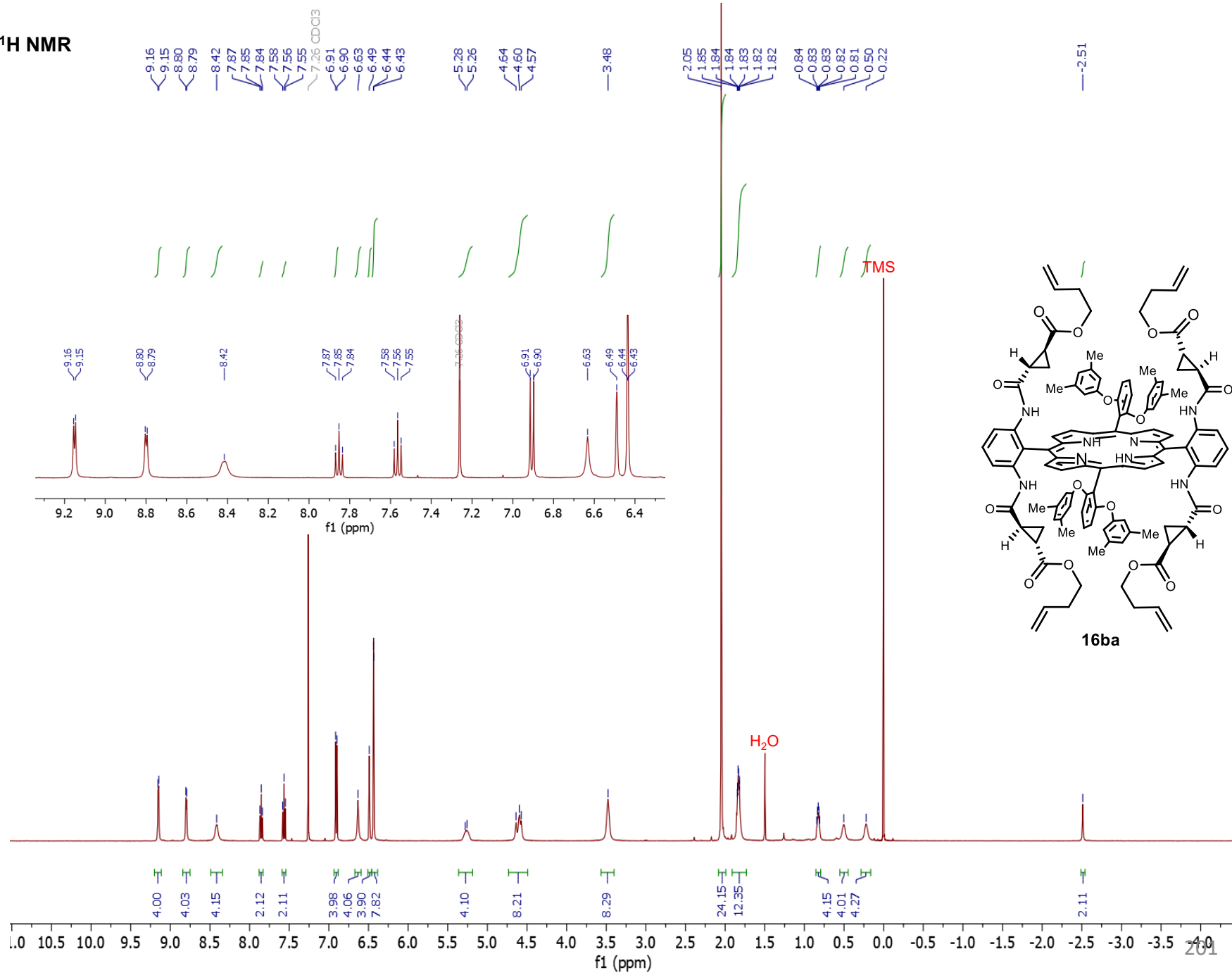
139.28
139.11
132.56
130.50
130.25
130.24
125.51
122.86
122.43
118.80
117.42
113.05
111.02
107.18

80.41
77.49
77.23 CDCl₃
76.98

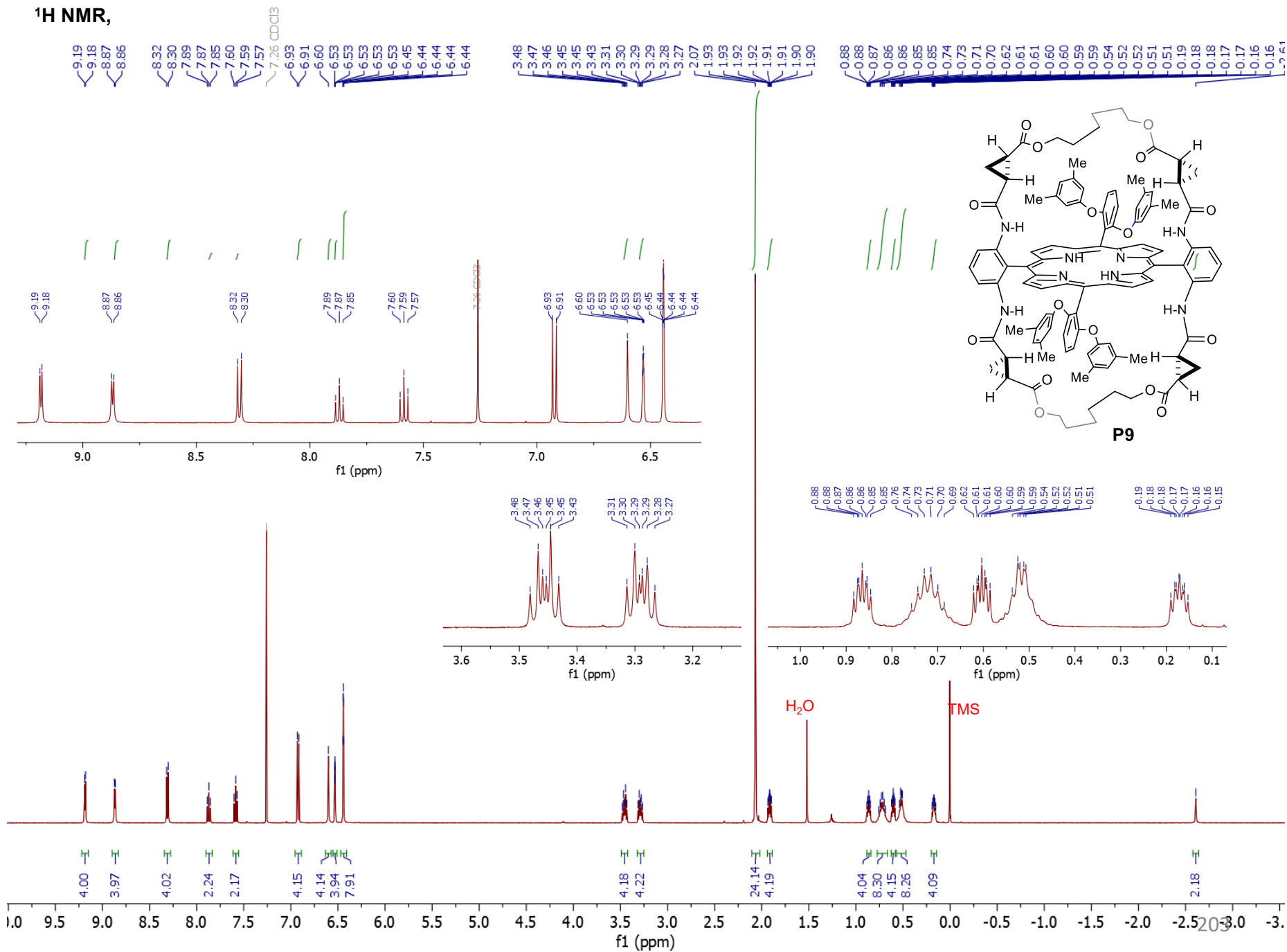
27.72
23.88
22.75
21.51
14.64



¹H NMR



¹H NMR,



¹³C NMR

— 170.66
— 168.61

— 159.56
— 155.90

— 139.42
— 138.76

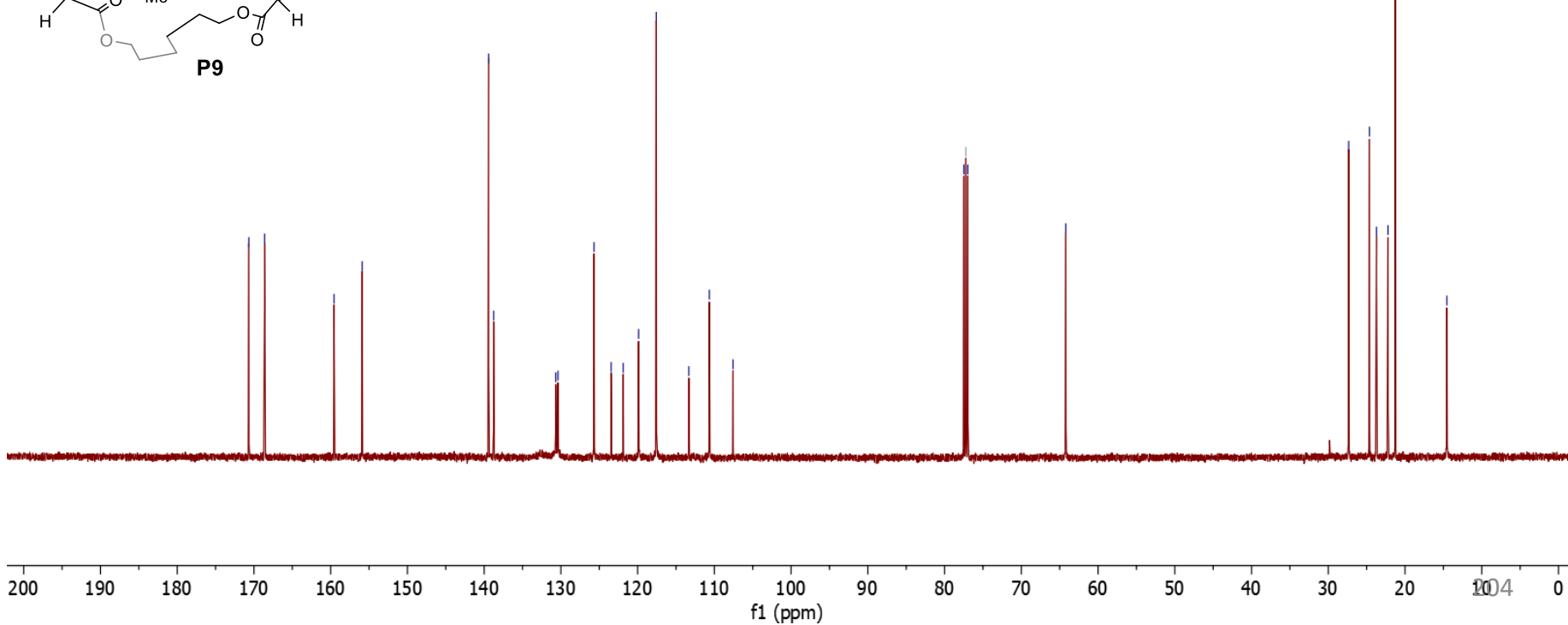
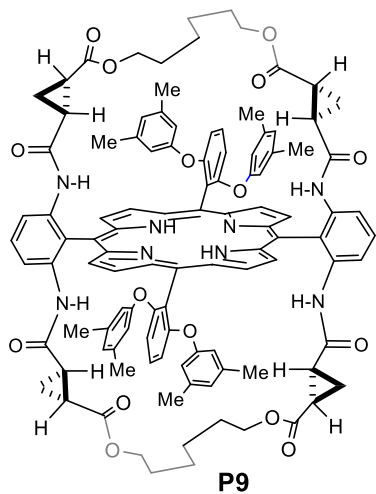
— 130.67
— 130.38

— 125.68
— 123.45
— 121.88
— 119.87
— 117.57
— 113.33
— 110.66
— 107.57

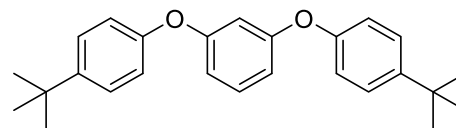
77.48
77.23 CDCl₃
76.98

— 64.21

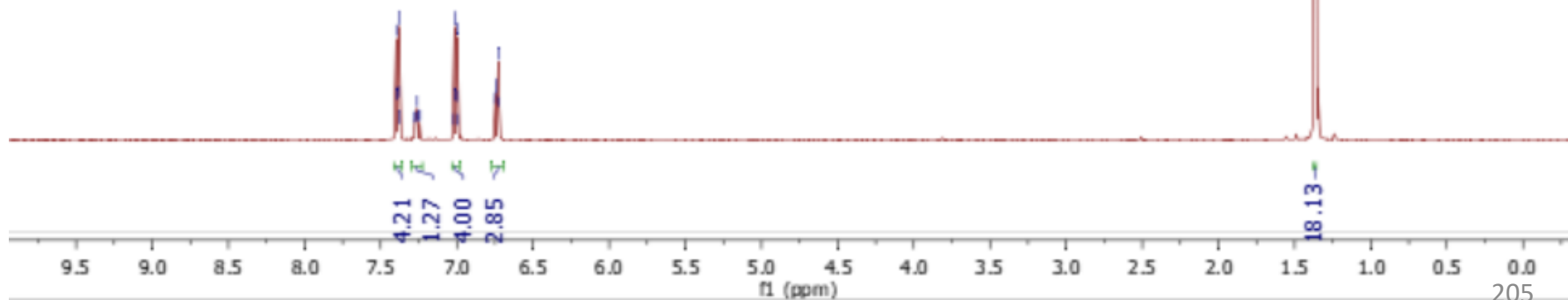
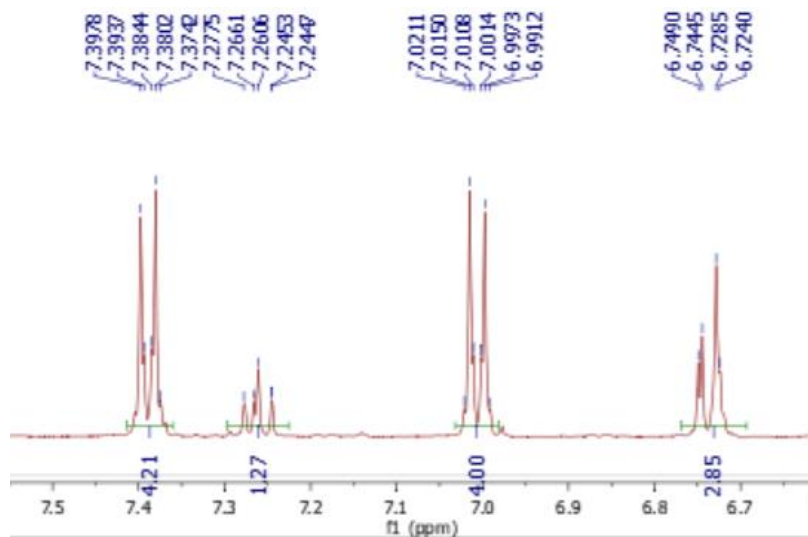
— 27.34
— 24.63
— 23.72
— 22.22
— 21.25
— 14.55



¹H NMR

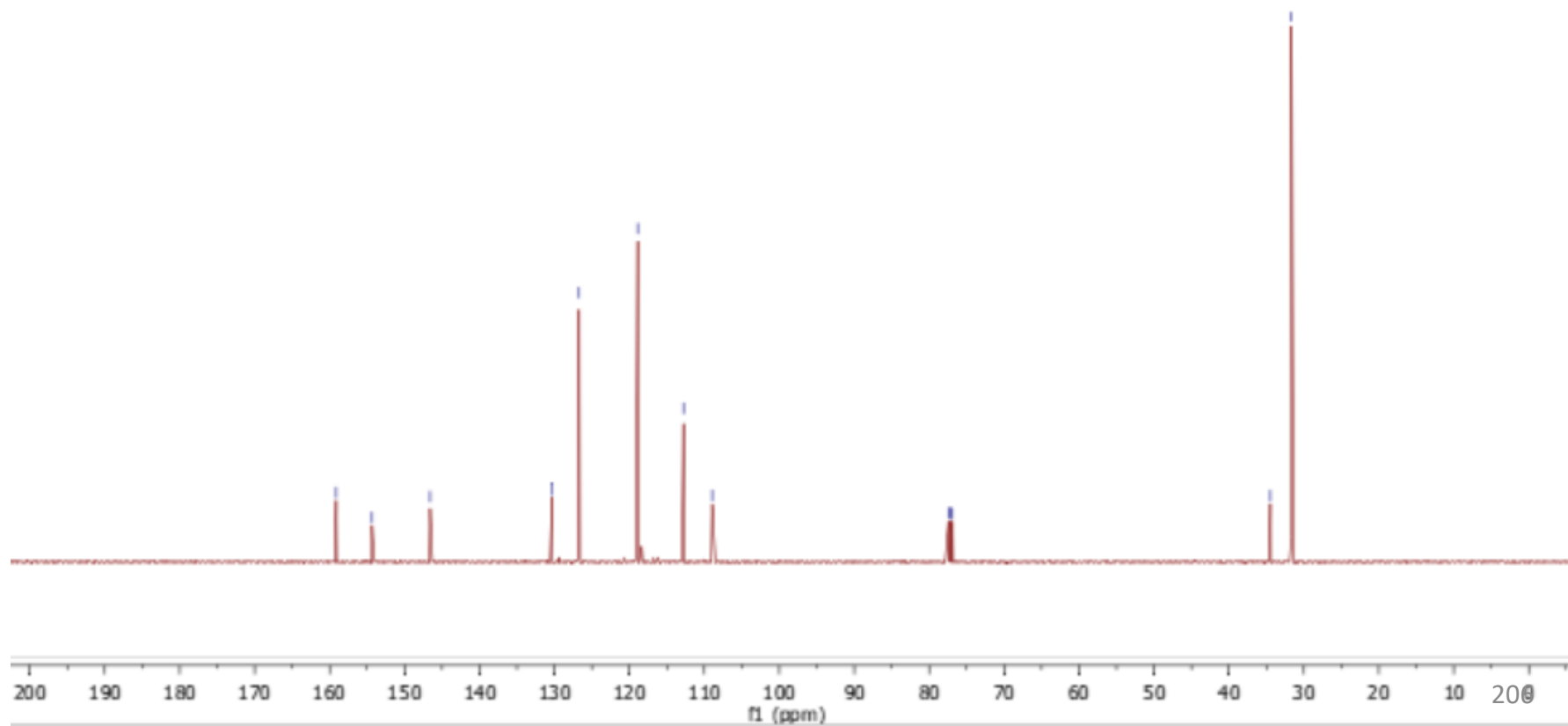
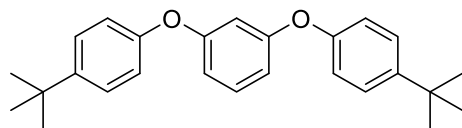


—1.3654

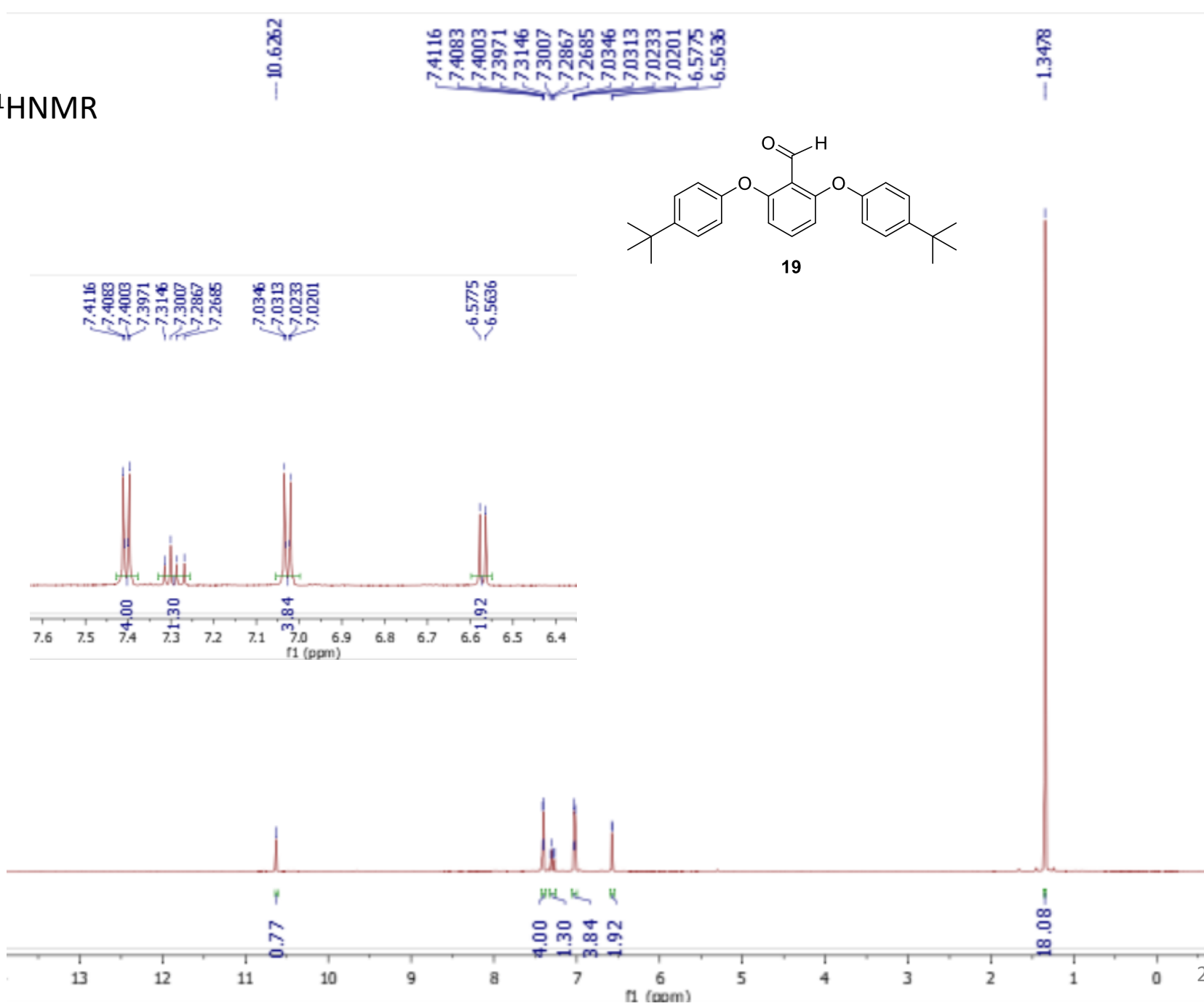
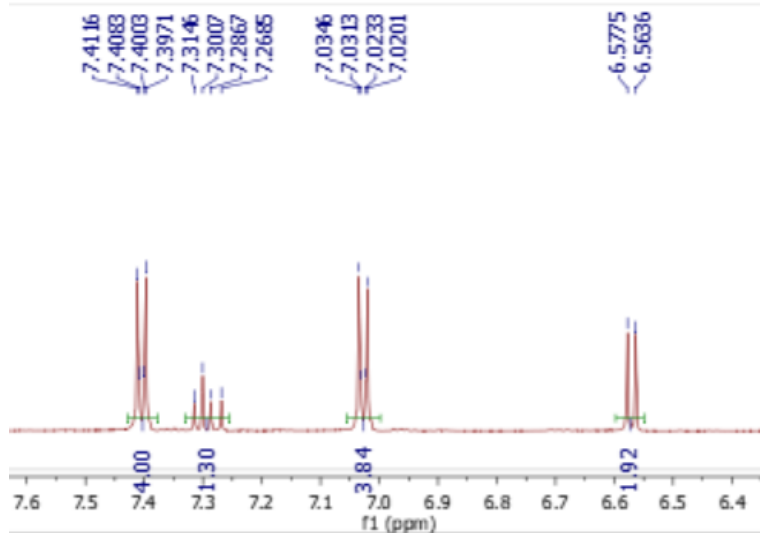
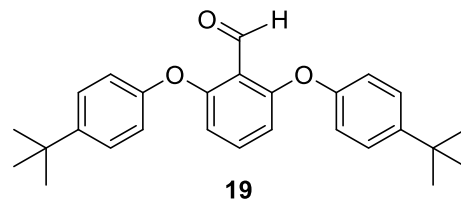


^{13}C NMR

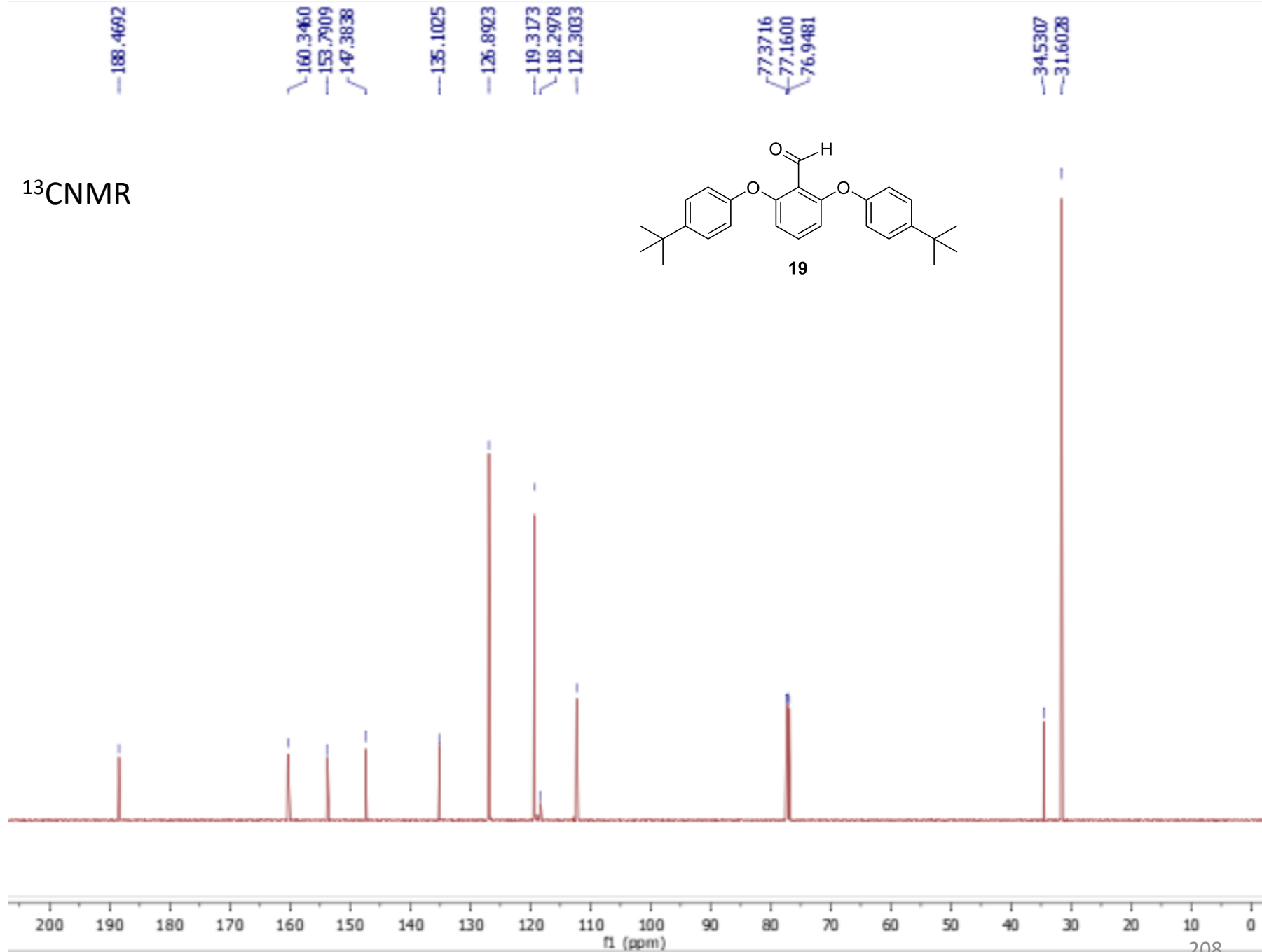
- 159.1261
- 154.3331
- 146.5842
- 130.3128
- 126.7111
- 118.8888
- 112.7751
- 108.9449
- 77.4142
- 77.1600
- 76.9058
- 34.4693
- 31.6448



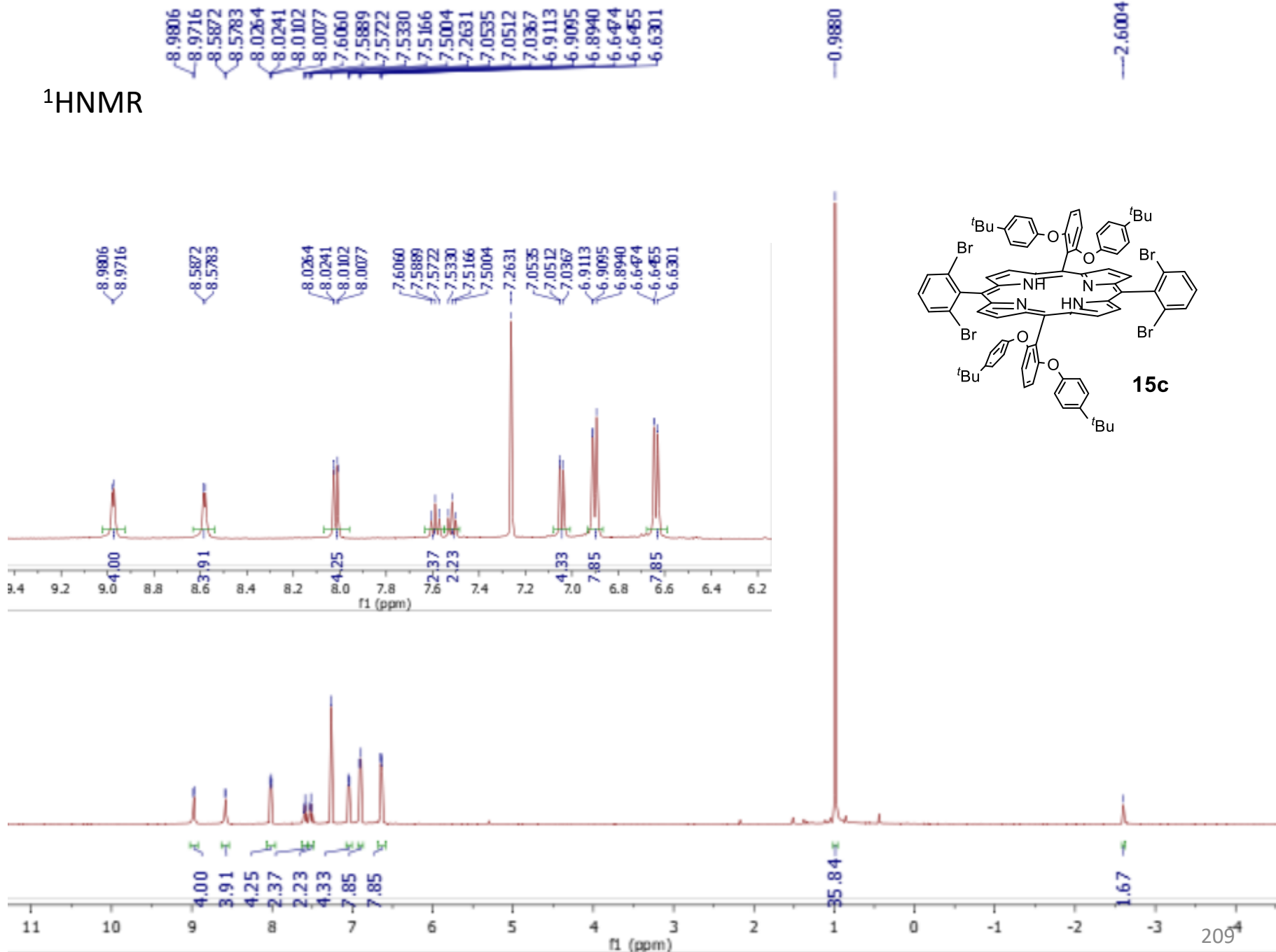
¹H NMR



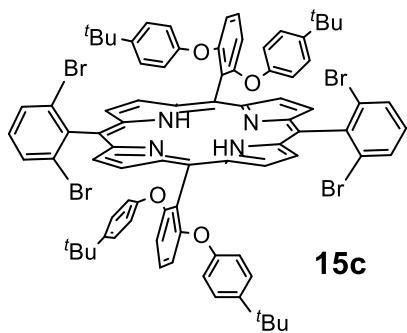
^{13}C NMR



^1H NMR



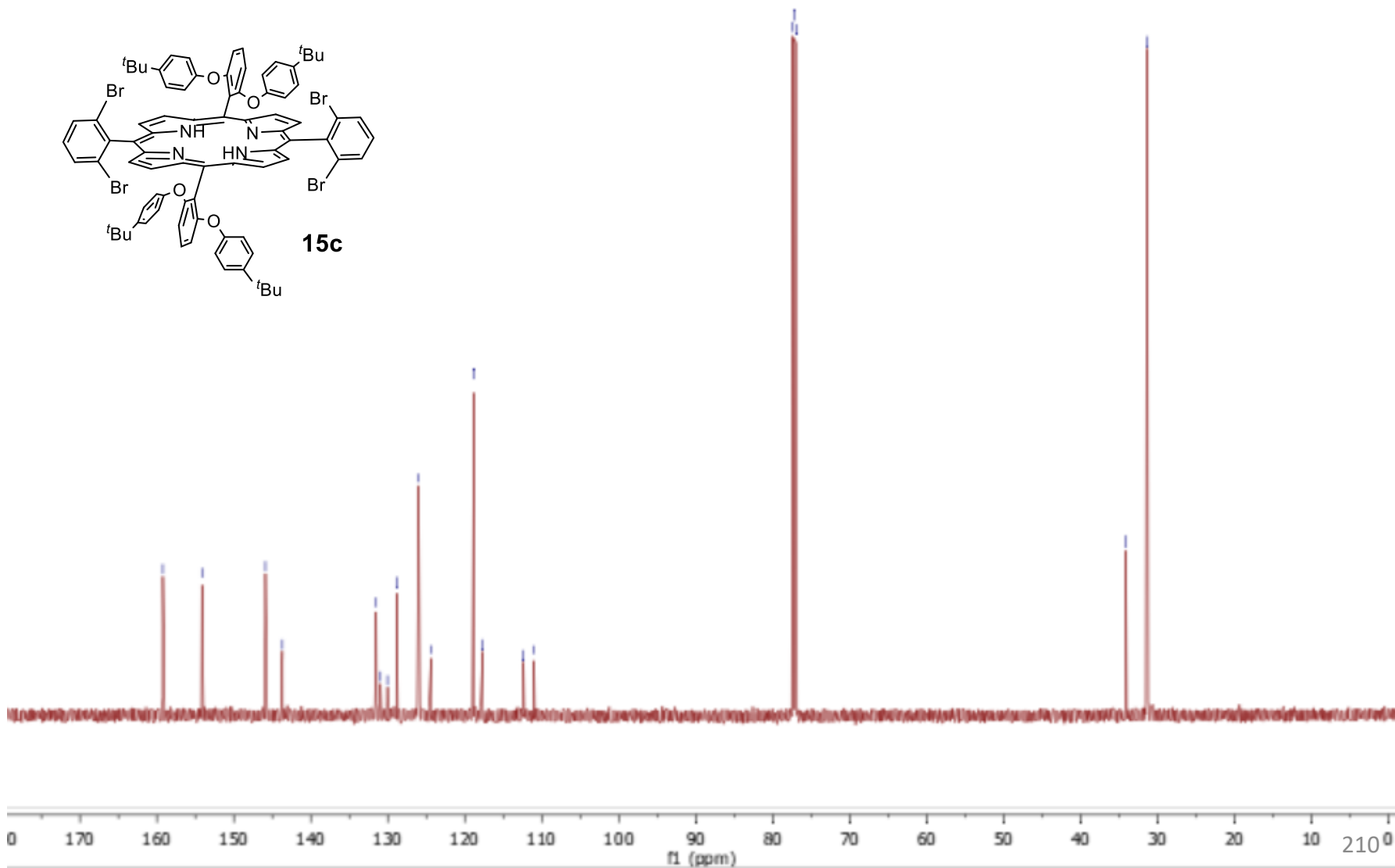
¹³CNMR



- 159.2226
- 154.1427
- 146.8889
- 148.6964
- 131.5062
- 130.9428
- 130.0336
- 128.8320
- 125.9813
- 124.3900
- 118.8162
- 117.6844
- 112.3643
- 110.9904

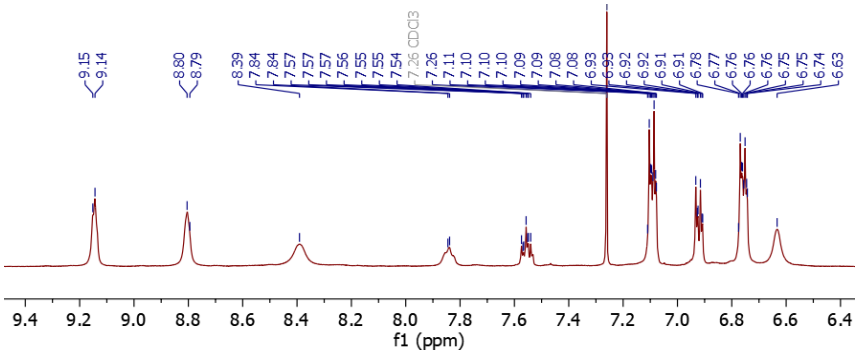
- 77.3718
- 77.1601
- 76.9482

- 34.0899
- 31.3503

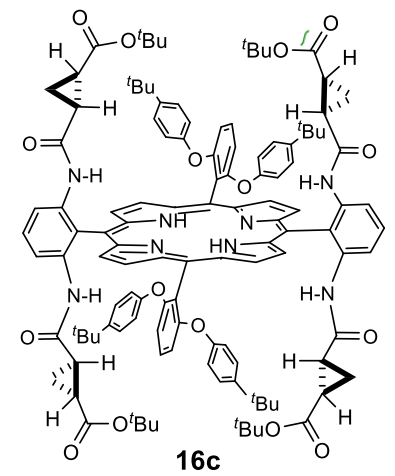
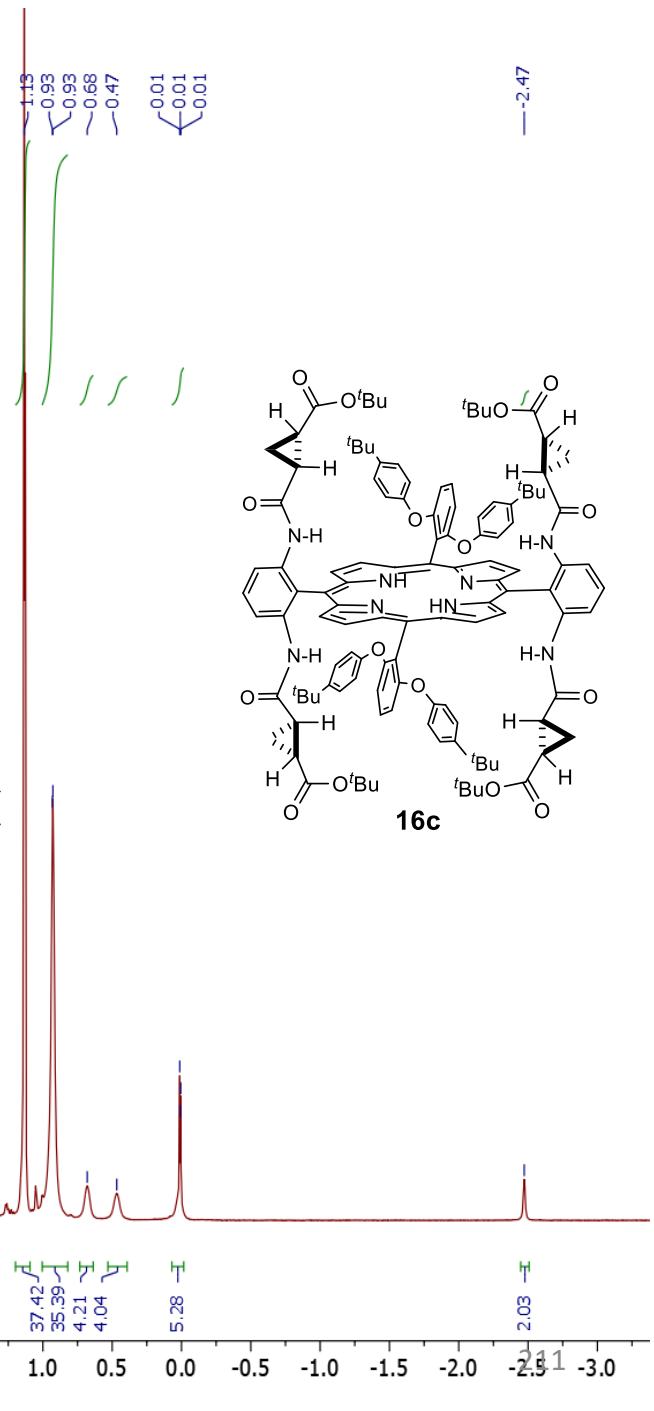
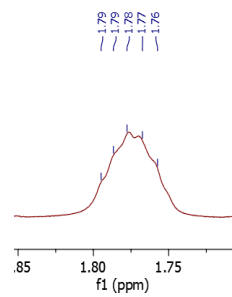


¹H NMR,

9.15
9.14
9.14
8.80
8.79
8.39
7.84
7.84
7.57
7.57
7.56
7.55
7.54
7.26 CDCl3
7.11
7.10
7.10
7.09
7.09
7.08
7.08
6.93
6.92
6.92
6.91
6.91
6.78
6.77
6.76
6.76
6.75
6.75
6.74
6.63



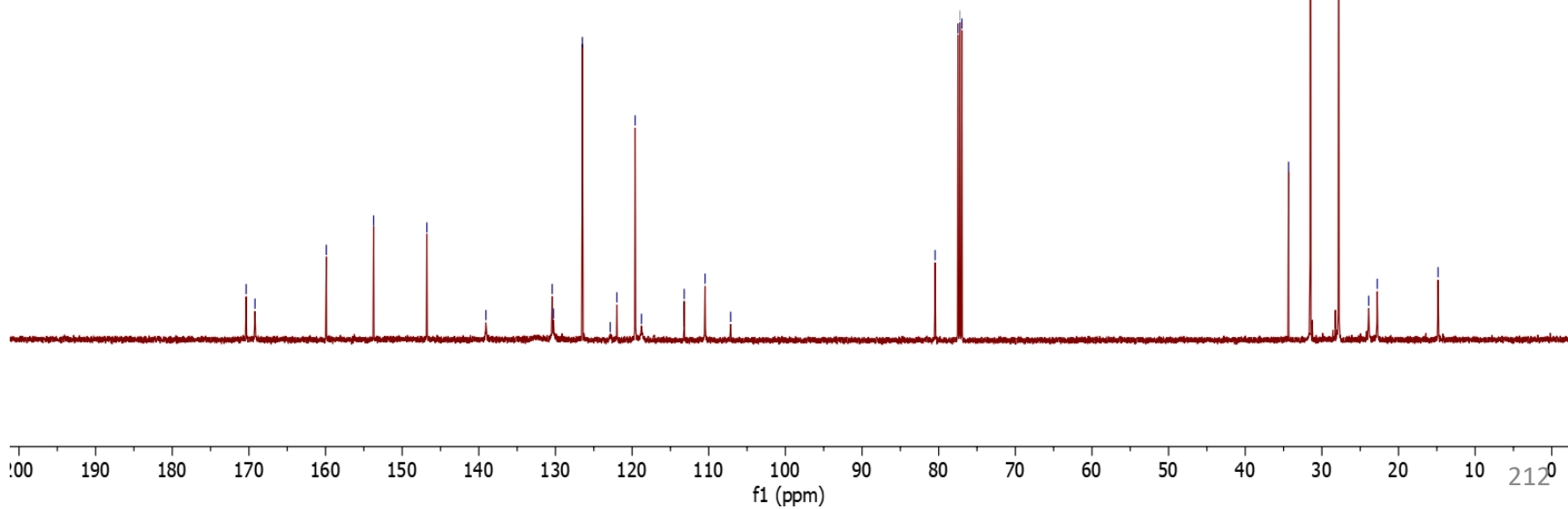
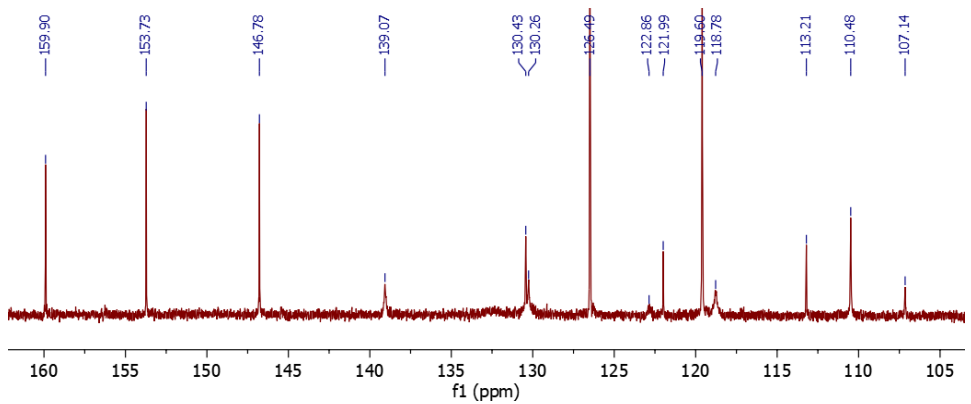
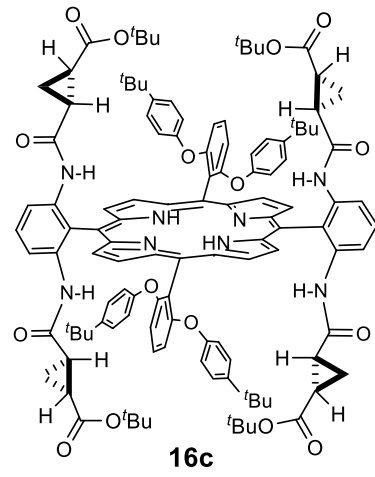
1.79
1.78
1.77
1.76



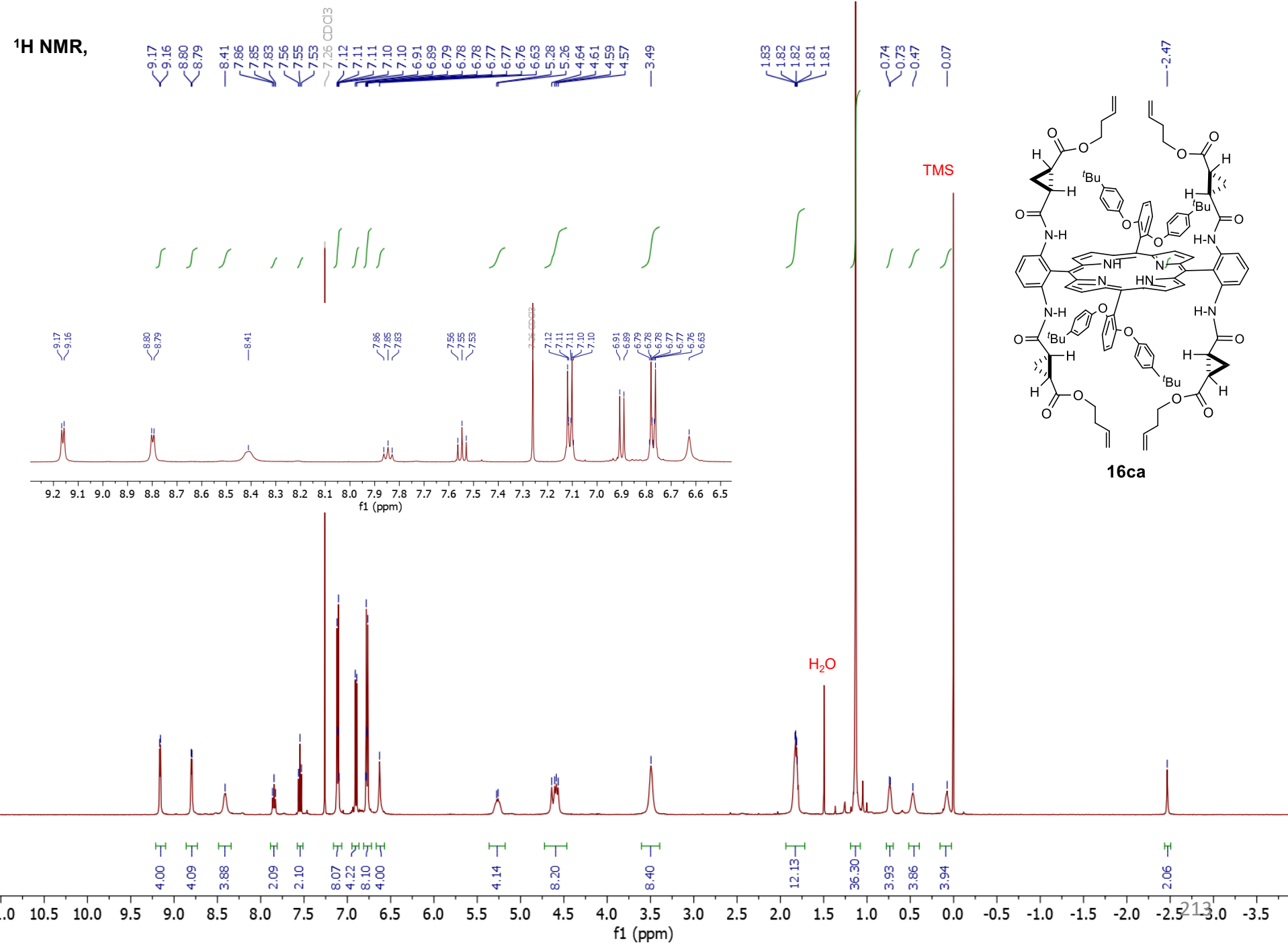
¹³C NMR

- 170.36
- 169.20
- 159.90
- 153.73
- 146.78
- 139.07
- 130.43
- 130.26
- 126.49
- 122.86
- 121.99
- 119.60
- 118.78
- 113.21
- 110.48
- 107.14

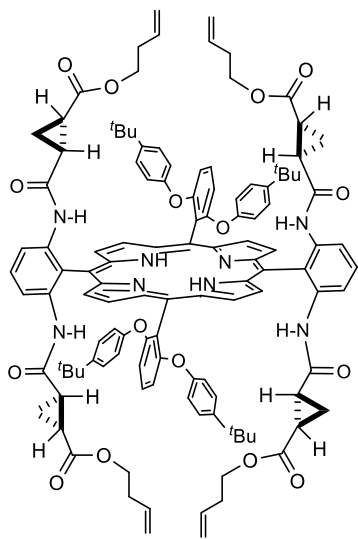
- 80.46
- 77.48
- 77.23
- 76.98
- 34.34
- 31.51
- 27.80
- 23.89
- 22.77
- 14.84



¹H NMR,



¹³C NMR

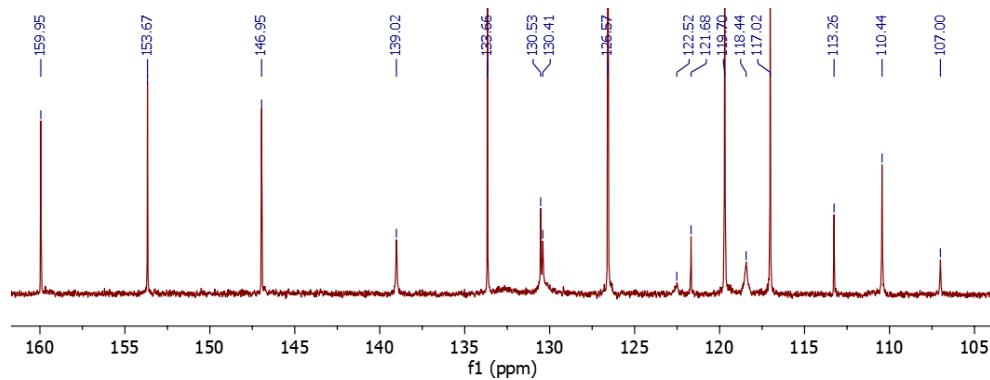


16ca

— 171.14
— 166.76

— 159.95
— 153.67
— 146.95

— 139.02
— 133.66
— 130.53
— 130.41
— 126.57
— 122.52
— 121.68
— 119.70
— 118.44
— 117.02
— 113.26
— 110.44
— 107.00



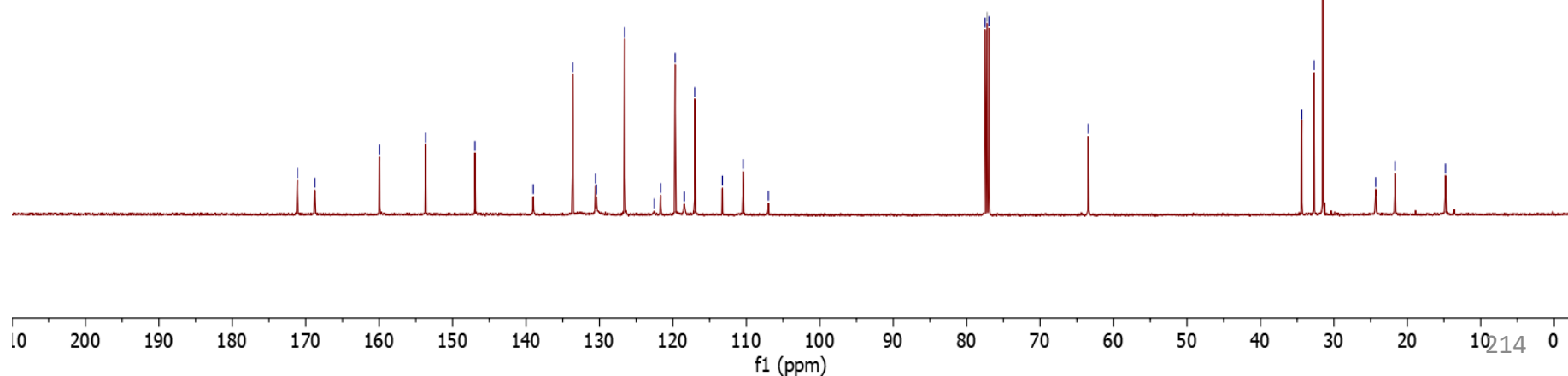
77.48
77.23 CDCl₃
76.98

63.43

34.37
32.70
31.50

24.30
21.66

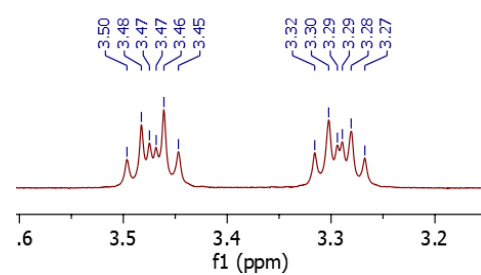
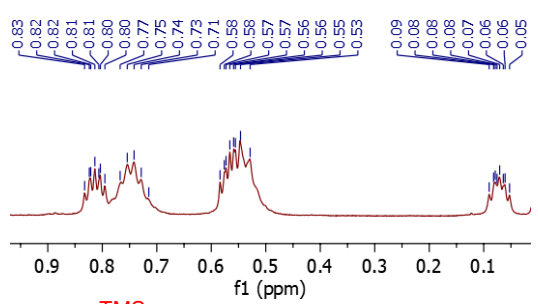
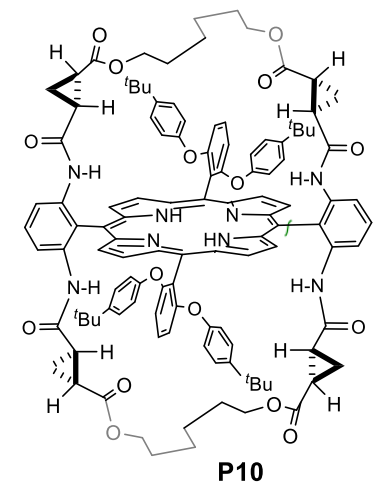
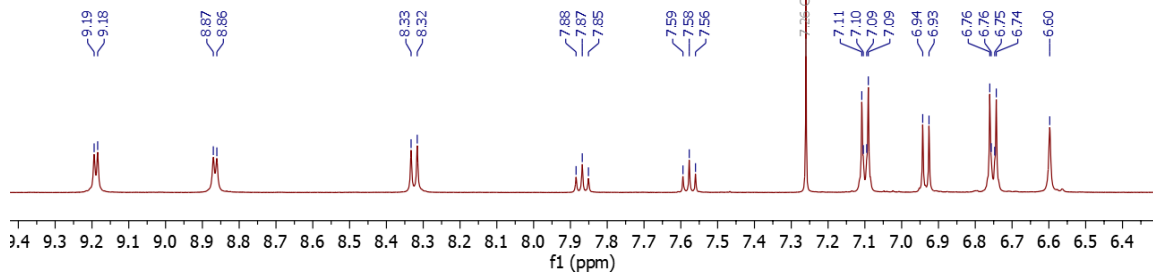
14.80



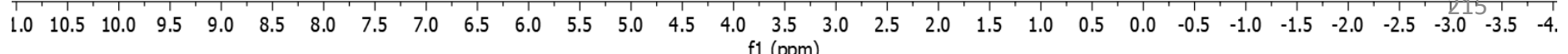
¹H NMR,

9.19, 9.18, 8.87, 8.86, 8.33, 8.32, 7.88, 7.87, 7.85, 7.59, 7.58, 7.56, 7.26 CDCl₃, 7.11, 7.10, 7.09, 7.09, 6.94, 6.93, 6.76, 6.75, 6.74, 6.60, 3.50, 3.48, 3.47, 3.47, 3.46, 3.45, 3.32, 3.30, 3.29, 3.28, 3.27, 1.90, 1.89, 1.89, 1.89, 1.88, 1.88, 1.87, 1.87, 1.12, 0.83, 0.82, 0.82, 0.81, 0.81, 0.80, 0.80, 0.77, 0.75, 0.74, 0.74, 0.73, 0.71, 0.58, 0.58, 0.57, 0.57, 0.56, 0.56, 0.55, 0.53, 0.09, 0.08, 0.08, 0.08, 0.07, 0.06, 0.06, 0.05, -2.57

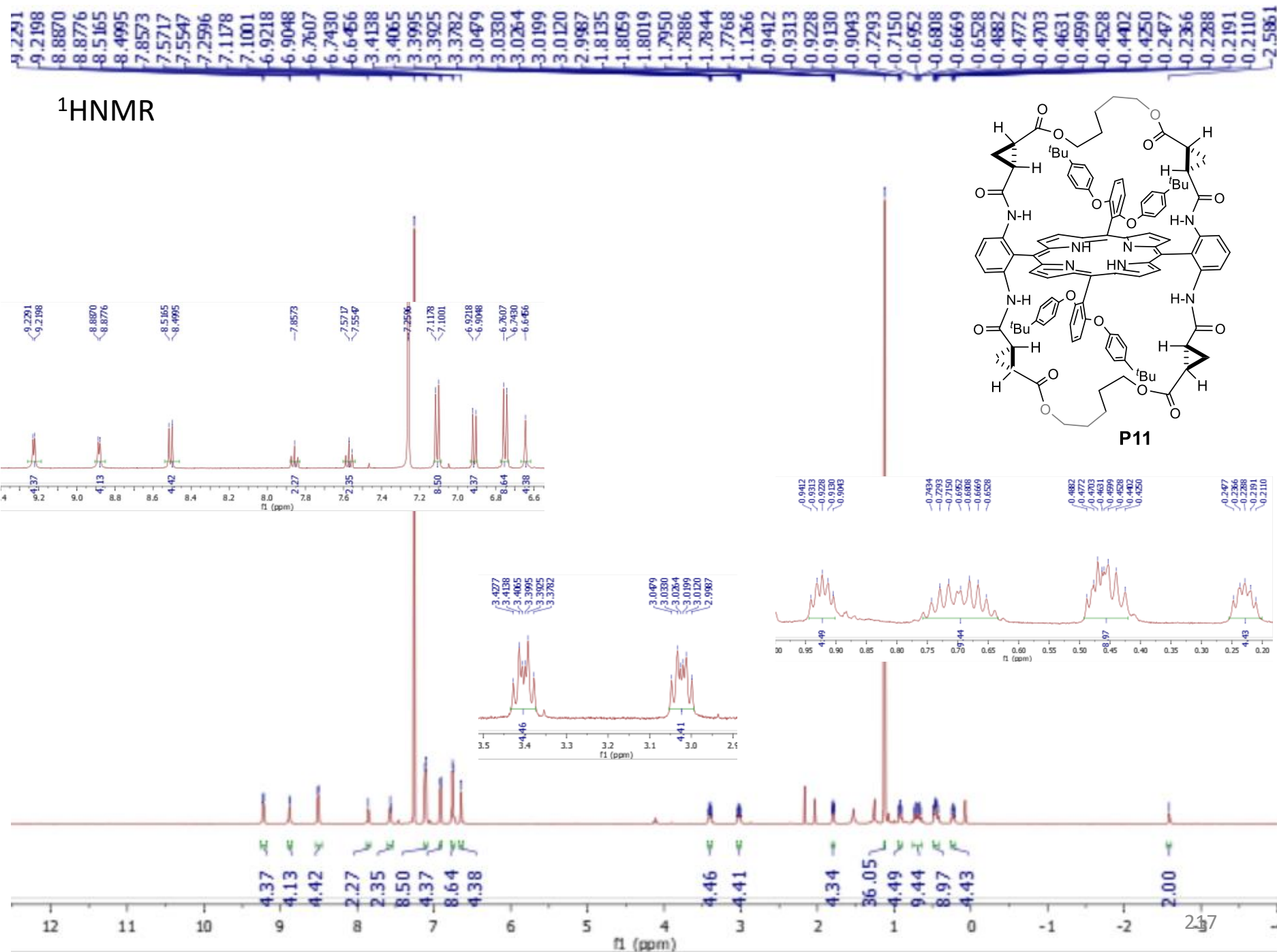
9.19, 9.18, 8.87, 8.86, 8.33, 8.32, 7.88, 7.87, 7.85, 7.59, 7.58, 7.56, 7.11, 7.10, 7.09, 7.09, 6.94, 6.93, 6.76, 6.75, 6.74, 6.60, 3.50, 3.48, 3.47, 3.47, 3.46, 3.45, 3.32, 3.30, 3.29, 3.28, 3.27, 1.90, 1.89, 1.89, 1.89, 1.88, 1.88, 1.87, 1.87, 1.12, 0.83, 0.82, 0.82, 0.81, 0.81, 0.80, 0.80, 0.77, 0.75, 0.74, 0.74, 0.73, 0.71, 0.58, 0.58, 0.57, 0.57, 0.56, 0.56, 0.55, 0.53, 0.09, 0.08, 0.08, 0.08, 0.07, 0.06, 0.06, 0.05, -2.57



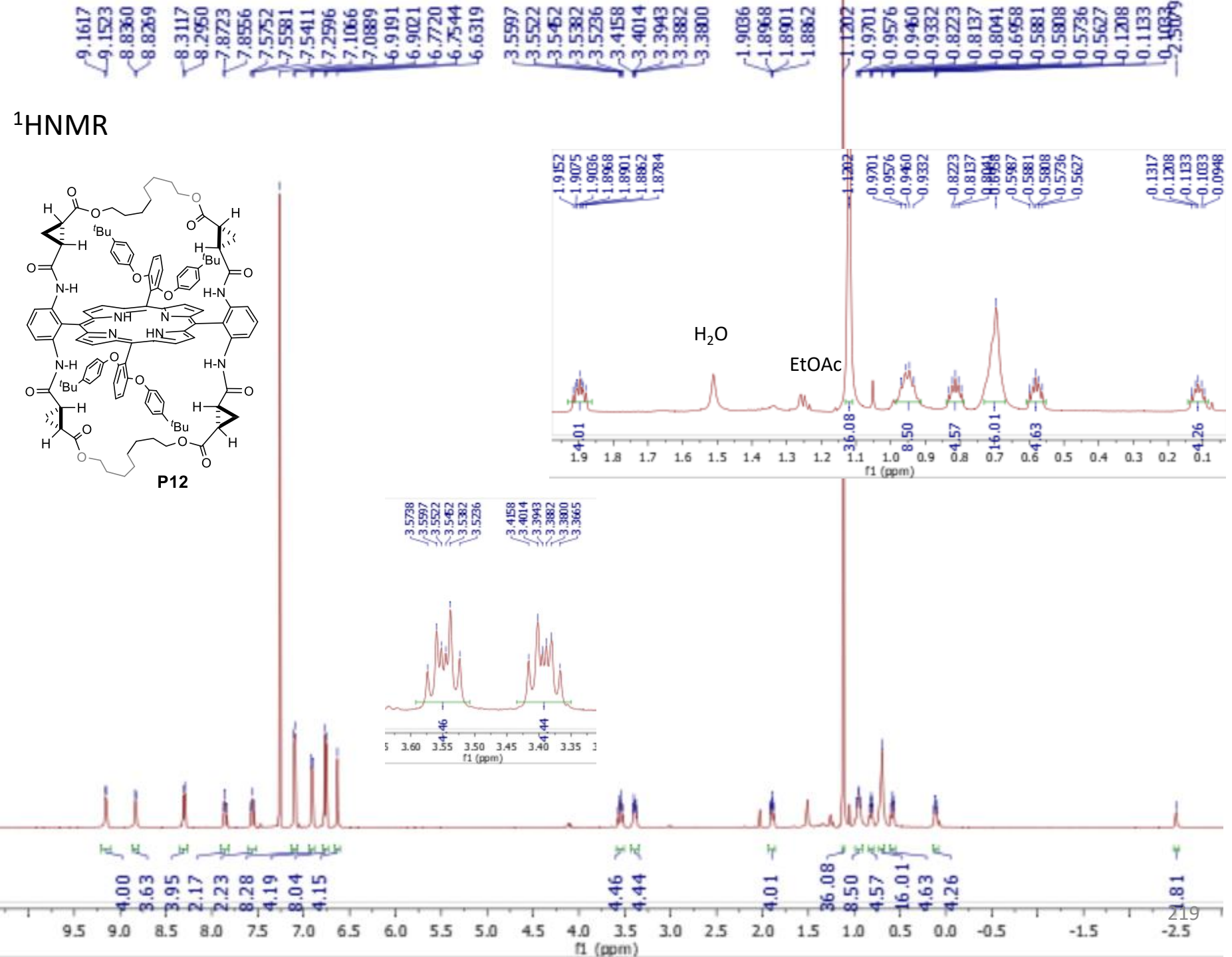
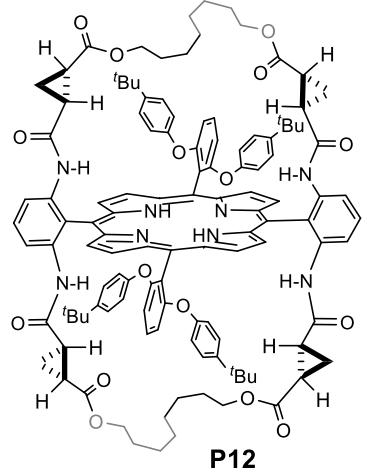
4.08, 4.11, 4.00, 2.19, 2.10, 8.03, 4.21, 7.92, 3.97, 4.20, 4.19, 4.09, 36.11, 4.10, 8.20, 12.25, 4.11, 2.07



¹H NMR

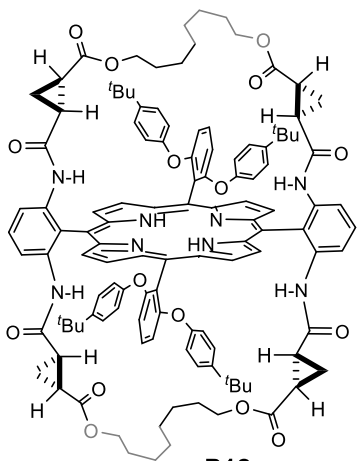


¹H NMR

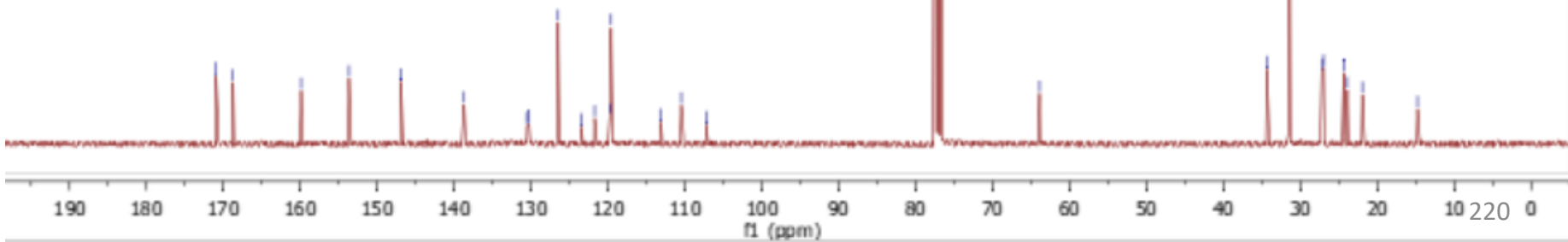
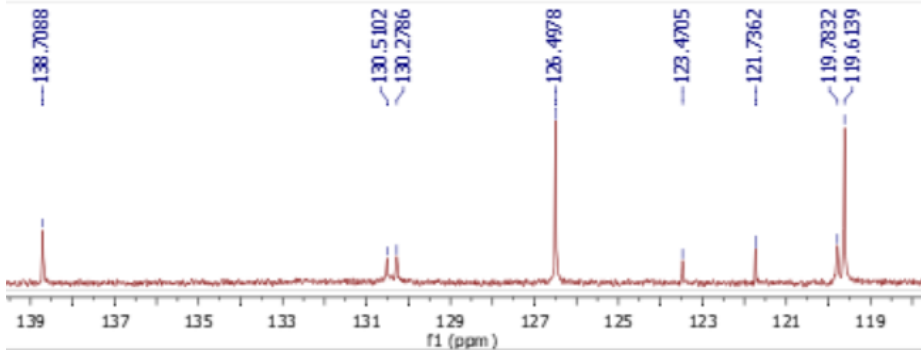
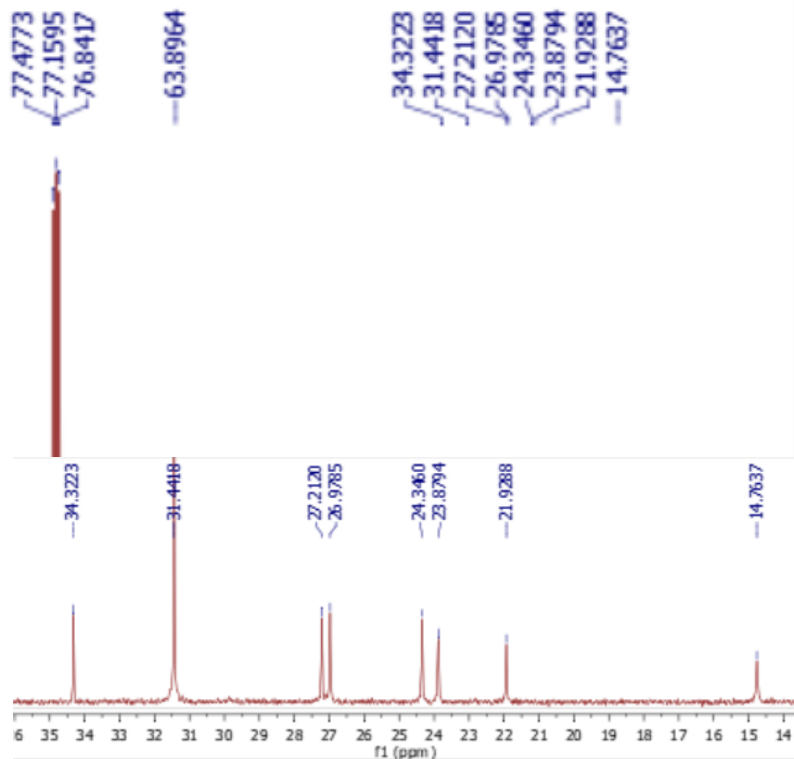


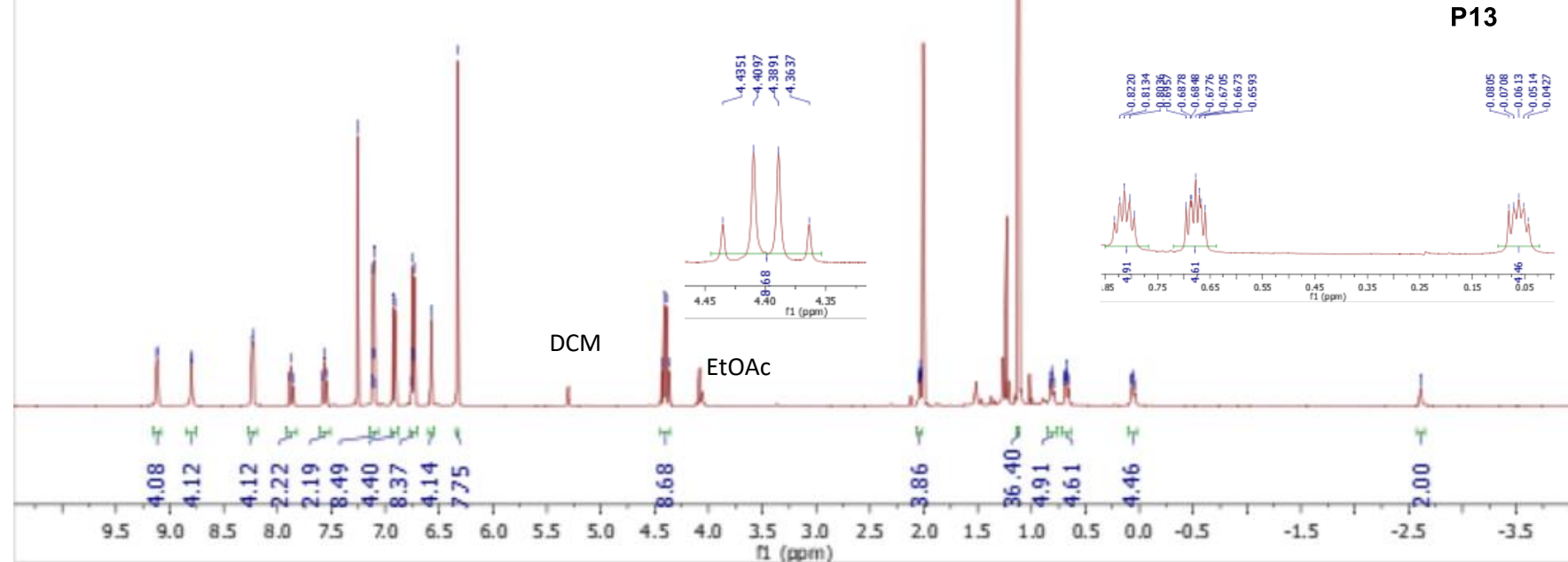
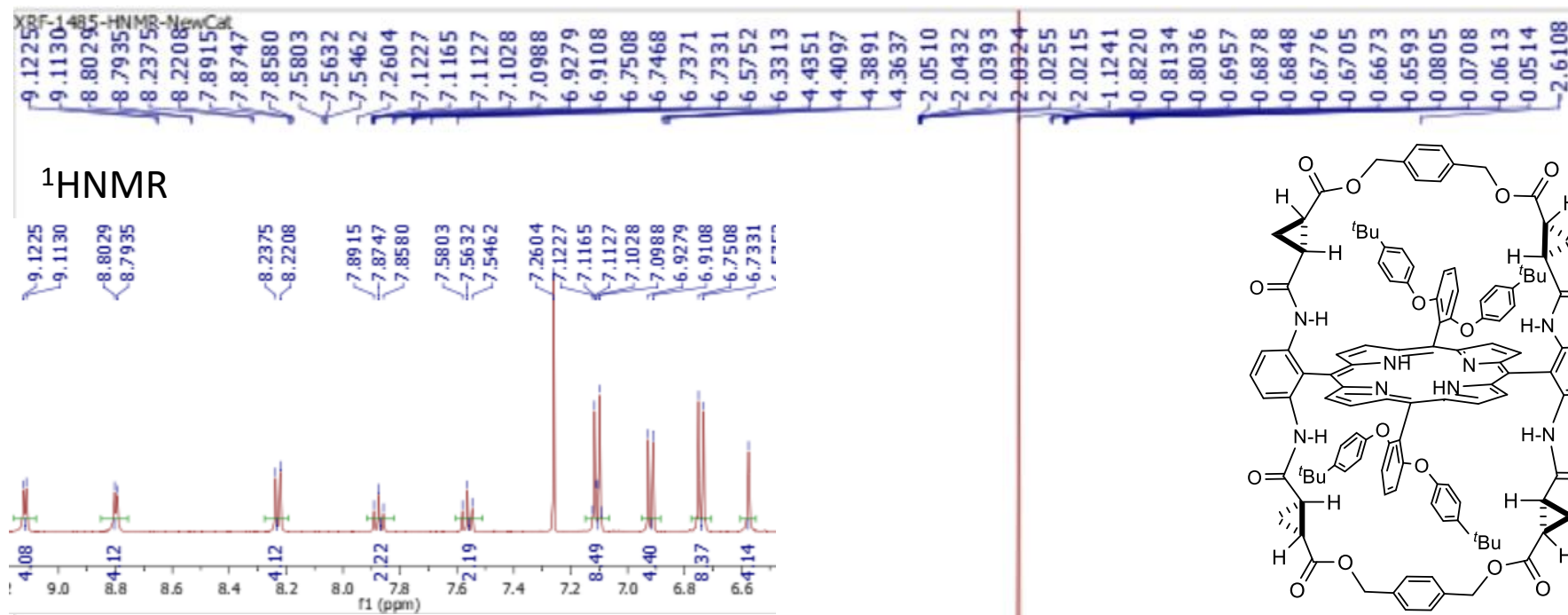
¹³CNMR

- 170.9476
- 168.7420
- 159.8982
- 153.6690
- 146.9020
- 138.7088
- 130.5102
- 130.2786
- 126.4978
- 123.4705
- 121.7362
- 119.7832
- 119.6139
- 113.1139
- 110.4752
- 107.2052

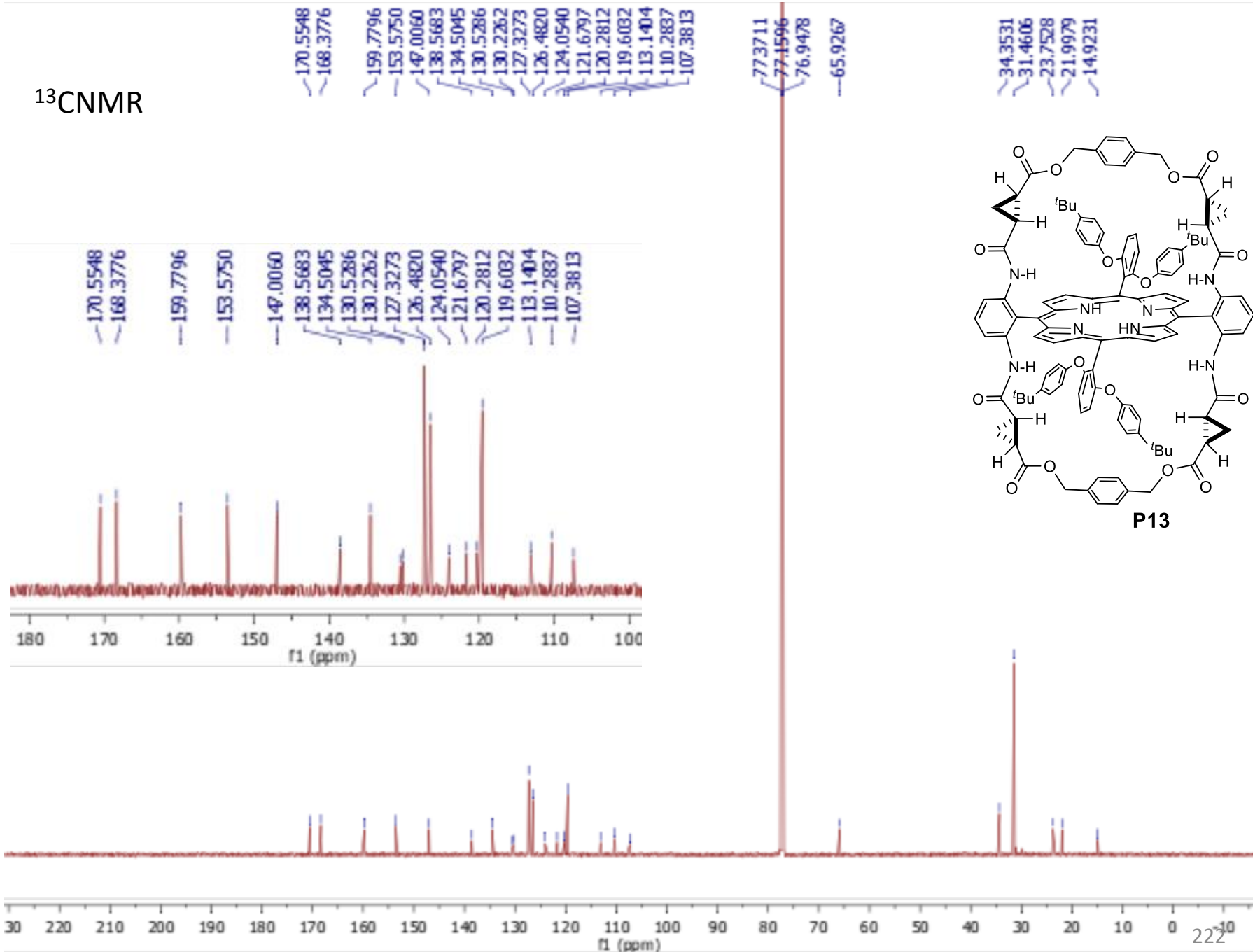


P12

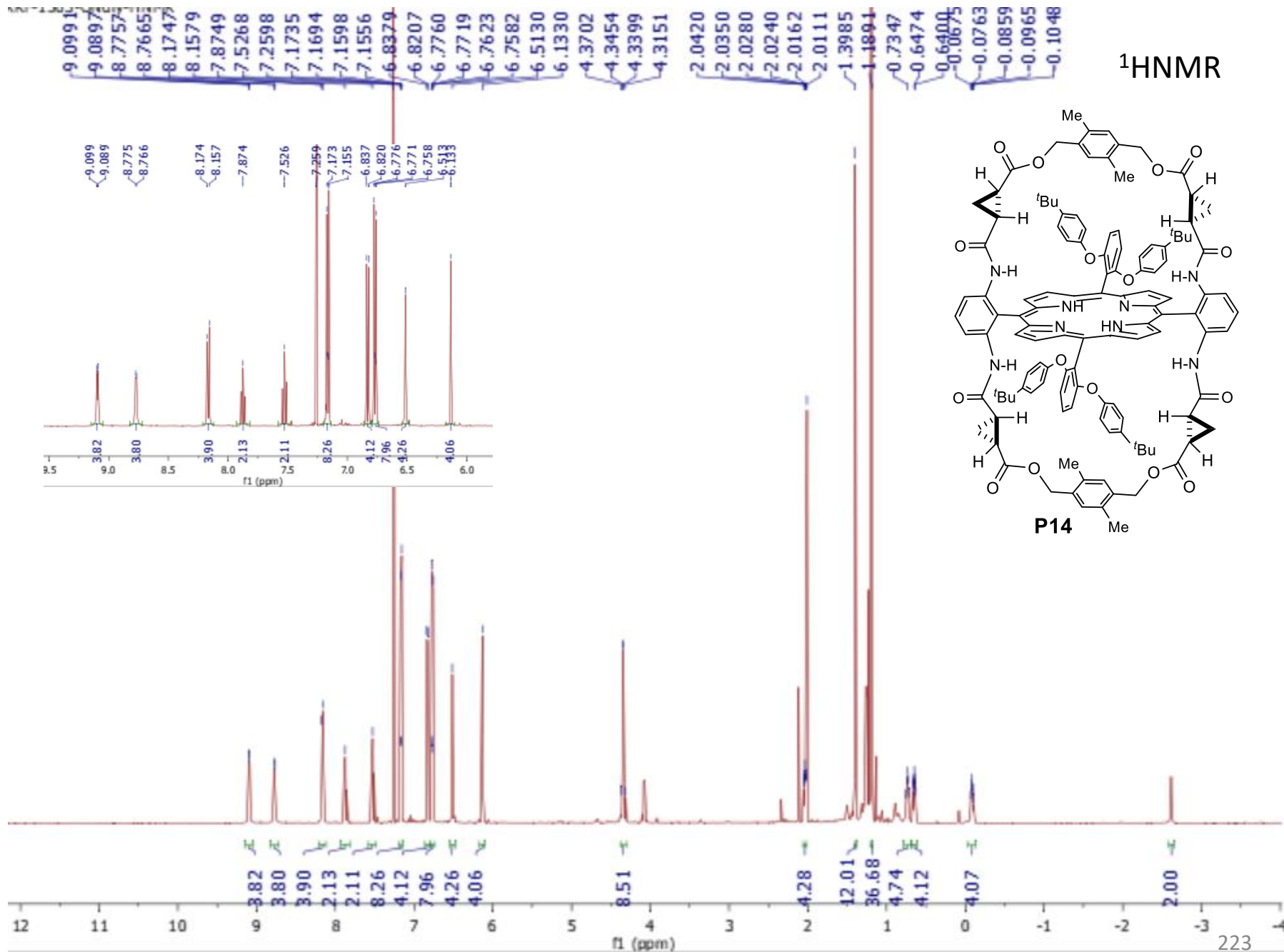




¹³CNMR



¹H NMR



¹³CNMR

170.6282
168.3778

160.1639
153.5854
149.2071

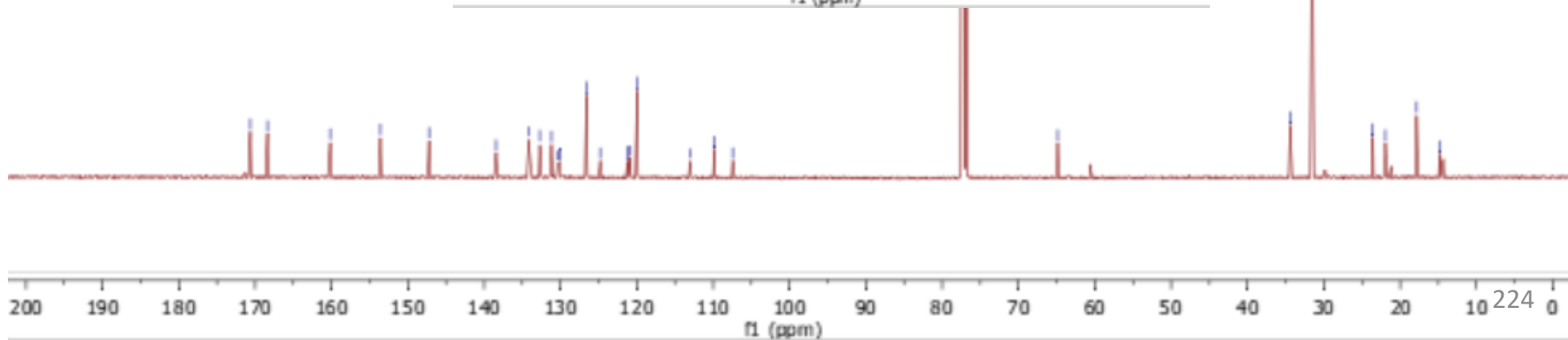
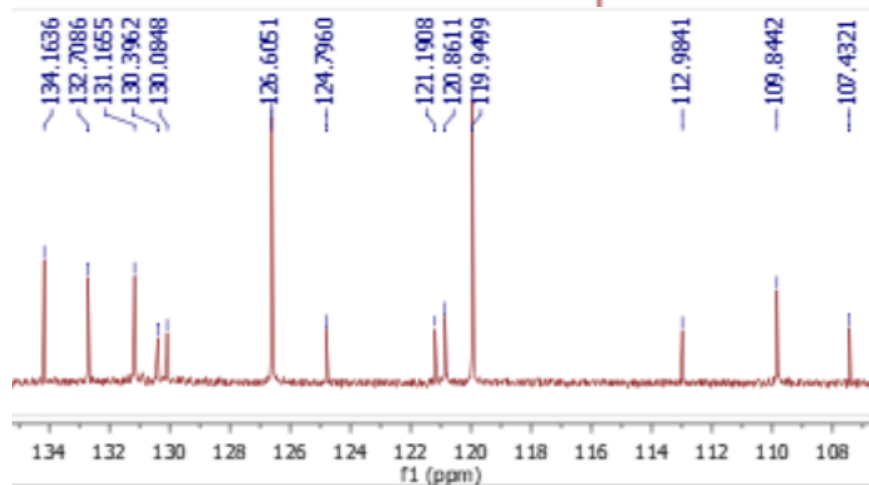
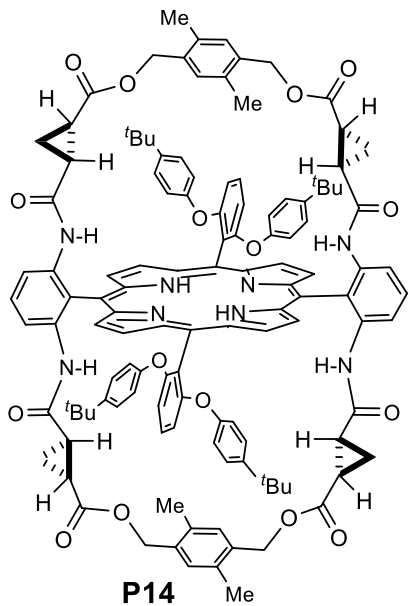
138.4245
134.1636
132.7086
131.1655
126.6051
124.7960
121.1908
120.8611
119.9499
109.8442
107.4321

77.3717
77.1601
76.9482

64.8574

34.4194
31.5332

23.5859
21.9320
17.8536
14.8455



9.1200
9.1129
8.7987
8.7915
8.2014
8.1874
7.8853
7.8712
7.8572
7.5343
7.5199
7.5055
7.2588
7.1558
7.1409
6.8179
6.8036
6.7700
6.7551
6.5125
-5.8298

4.4904
4.4699
4.2950
4.2744

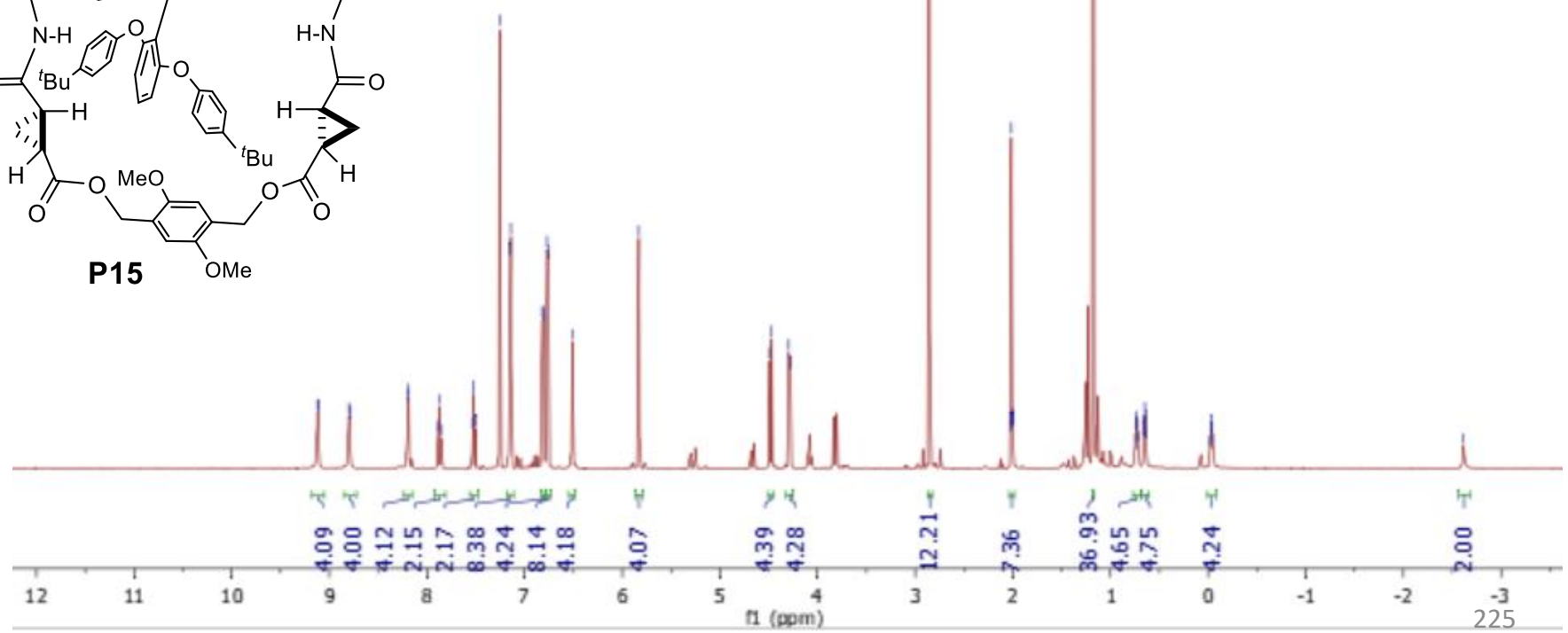
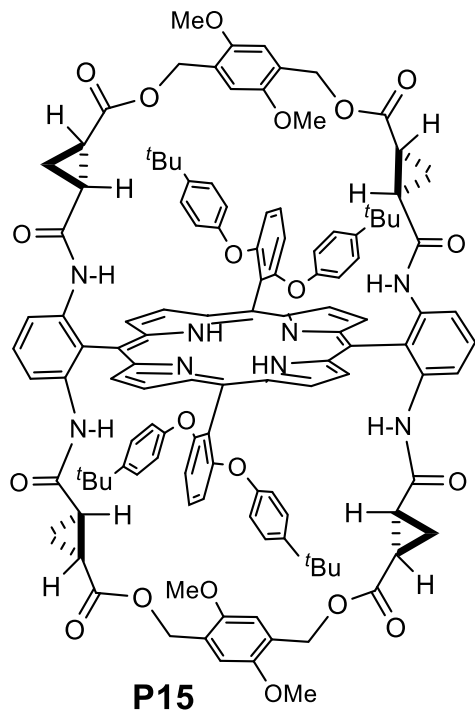
-2.8548

2.0148
2.0063
2.0031

1.1778
-0.7314
-0.6473
-0.6417
-0.0177
-0.0265
-0.0331
-0.0406
-0.0482

-2.6151

¹H NMR



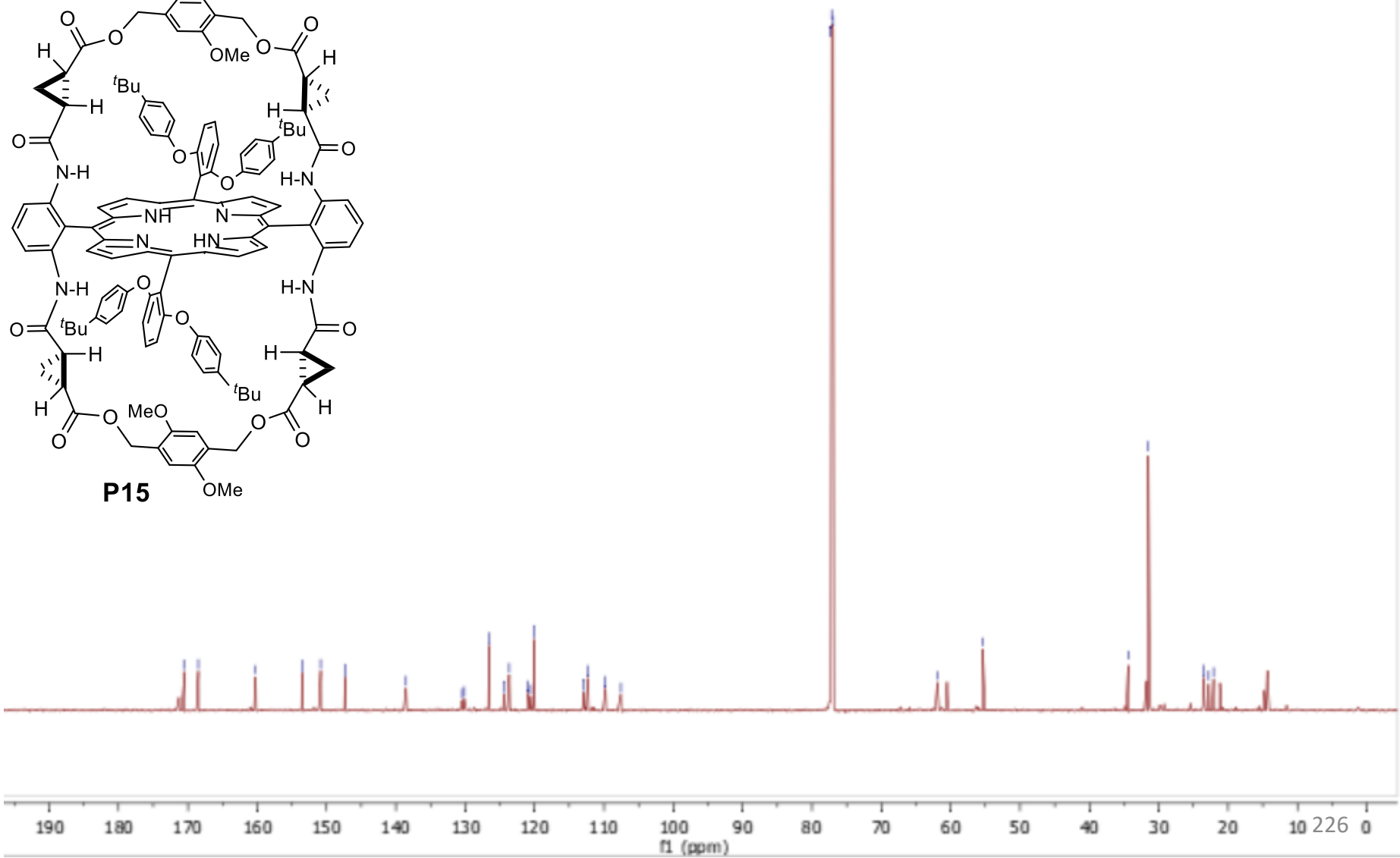
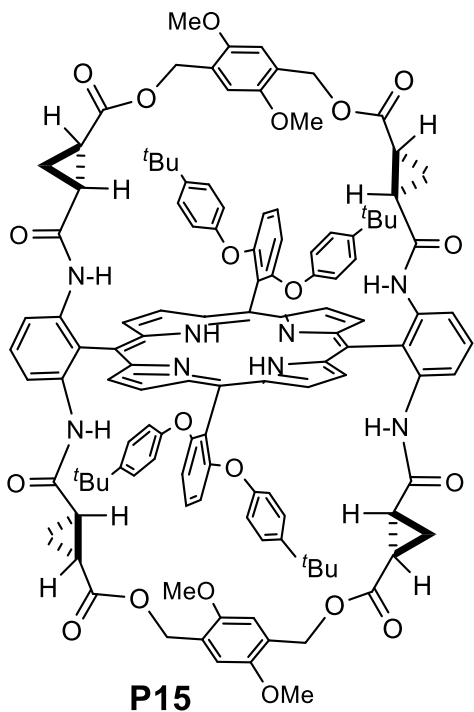
¹³CNMR

- 170.5877
- 168.4865
- 160.2324
- 153.5283
- 150.8416
- 147.3274
- 138.5363
- 126.5854
- 124.4349
- 123.6492
- 120.9272
- 120.5526
- 118.8217
- 112.3015
- 109.7814
- 107.5474

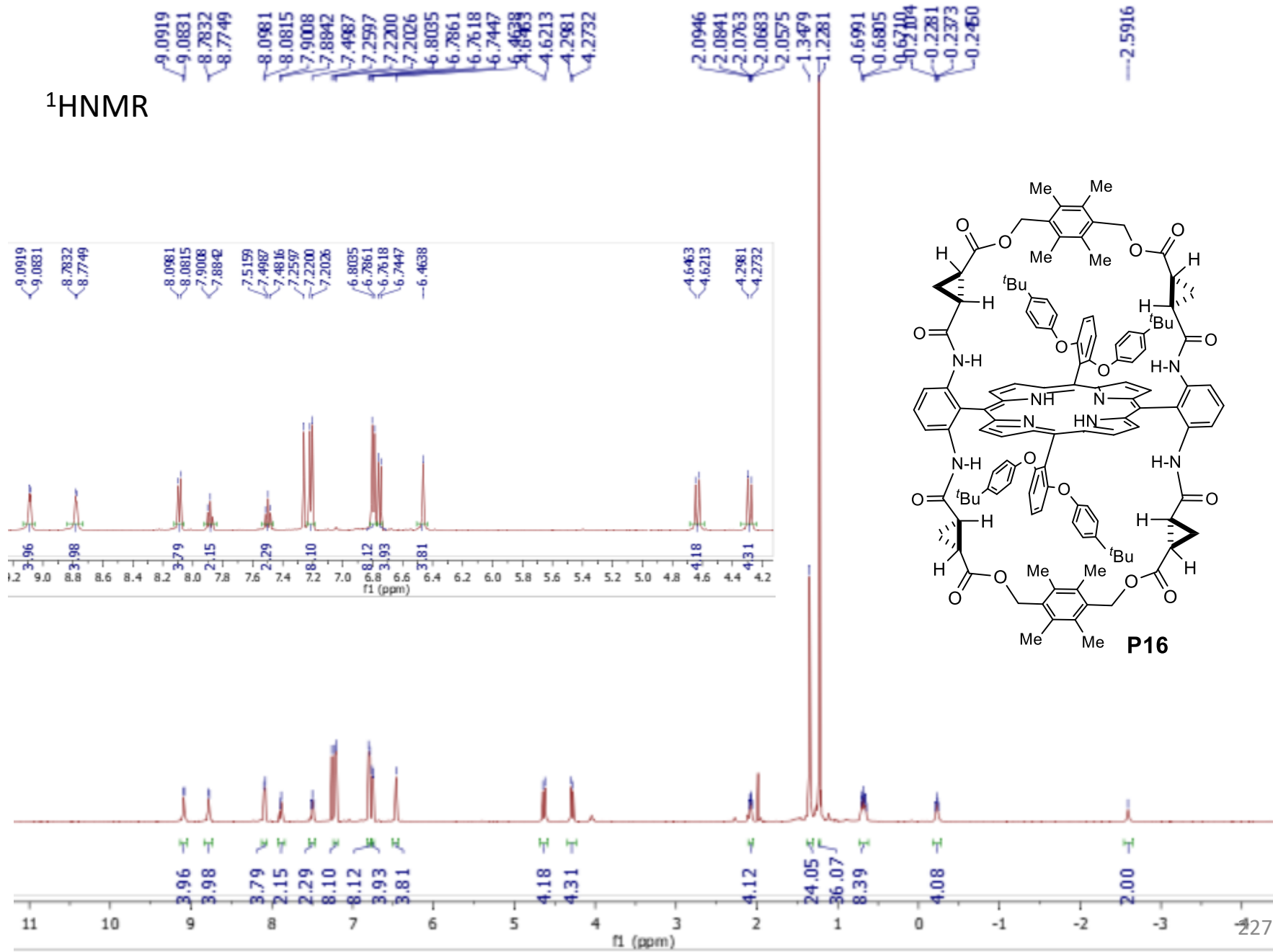
- 77.3715
- 77.1597
- 76.9479

- 61.9128
- 55.3813

- 34.4076
- 31.4963
- 23.6007
- 22.8069
- 22.1023

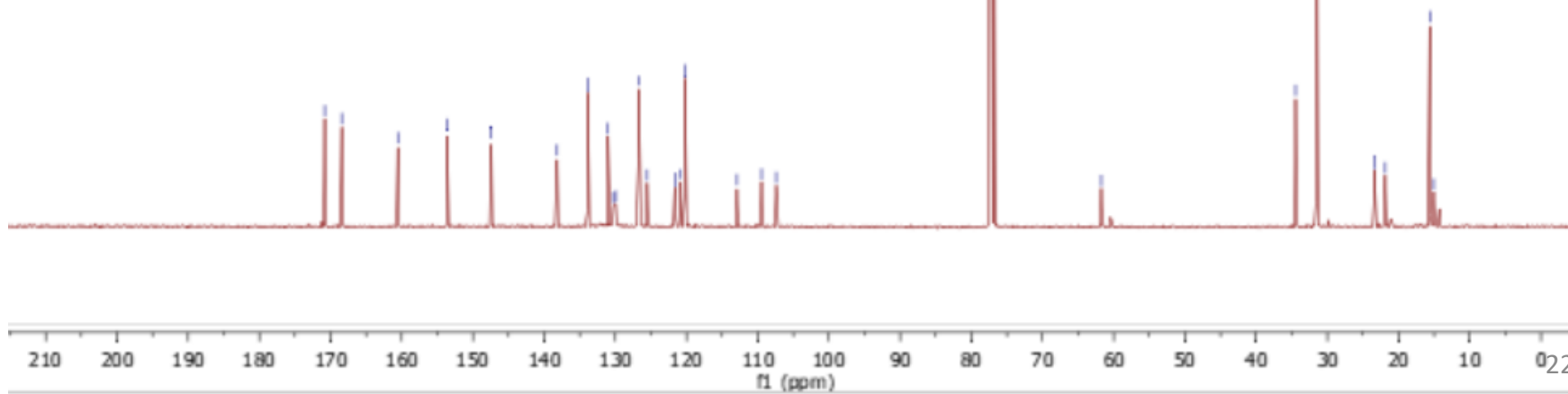
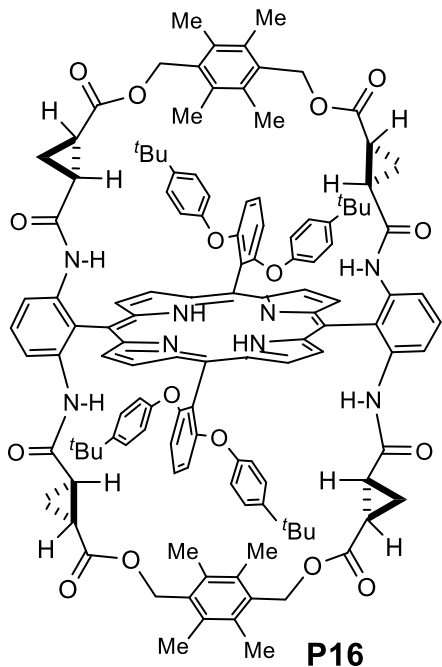


¹H NMR

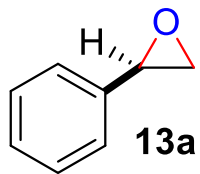


¹³CNMR

- 170.8209
- 168.4155
- 160.5398
- 153.6336
- 147.4255
- 138.1780
- 133.8736
- 131.0315
- 130.2613
- 129.9423
- 126.7251
- 125.5398
- 121.6464
- 120.8156
- 120.2353
- 112.9142
- 109.4624
- 107.4057
- 77.4780
- 77.1600
- 76.8421
- 61.7416
- 34.4563
- 31.5587
- 23.4039
- 21.8748
- 15.6141
- 15.0403

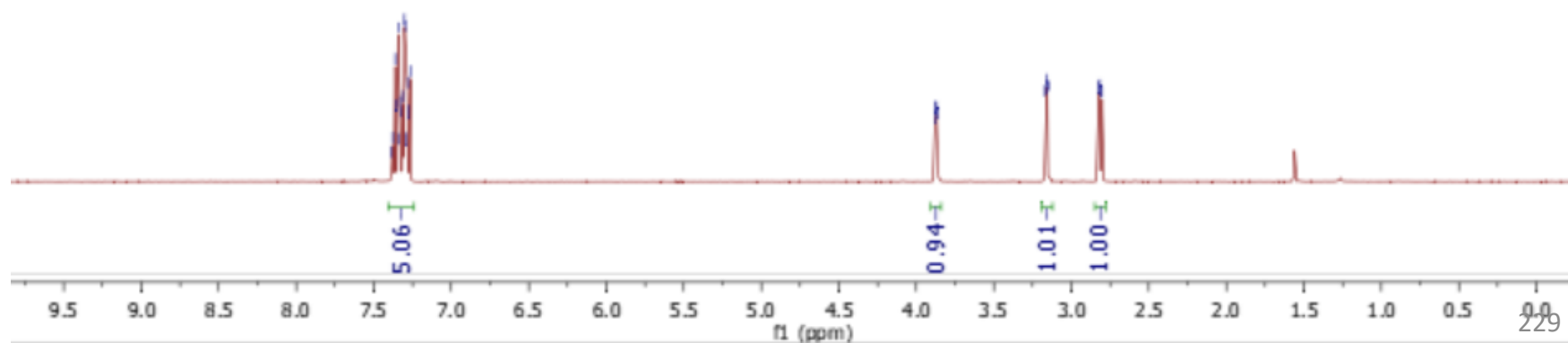
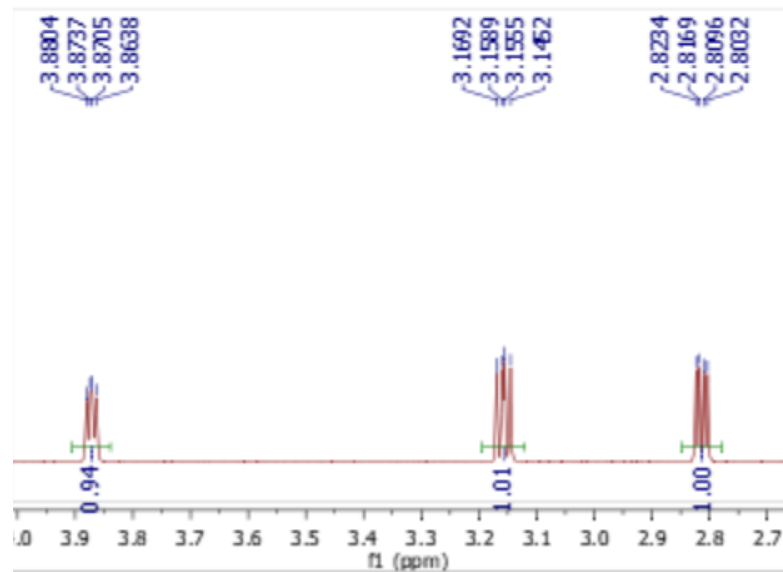


^1H NMR

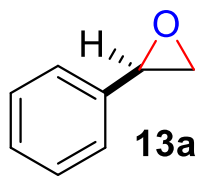


7.3826
7.3777
7.3615
7.3570
7.3432
7.3350
7.3303
7.3262
7.3136
7.3018
7.2974
7.2915
7.2815
7.2780
7.2644

3.8804
3.8737
3.8705
3.8638
3.1692
3.1589
3.1555
3.1452
2.8234
2.8169
2.8096
2.8032



^{13}C NMR



137.7311

128.6341

128.3151

125.6235

77.4143

77.1601

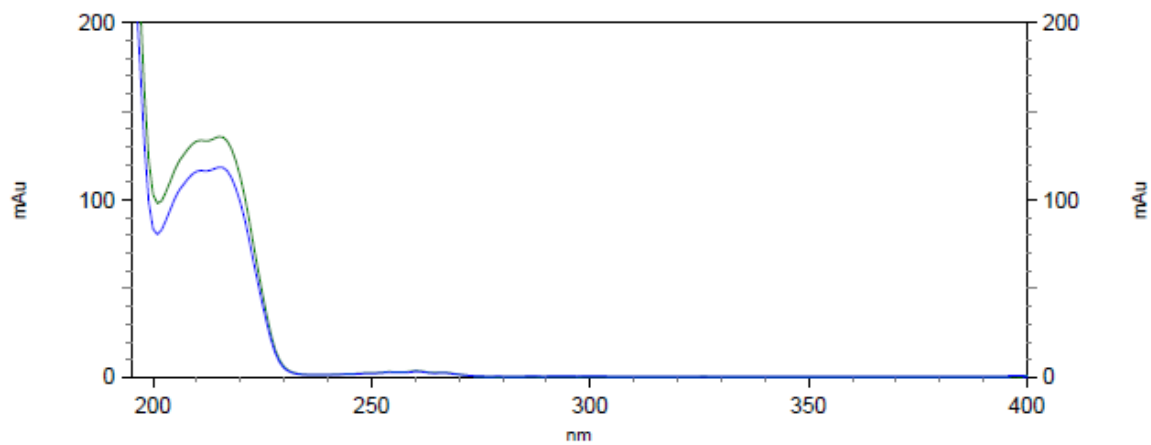
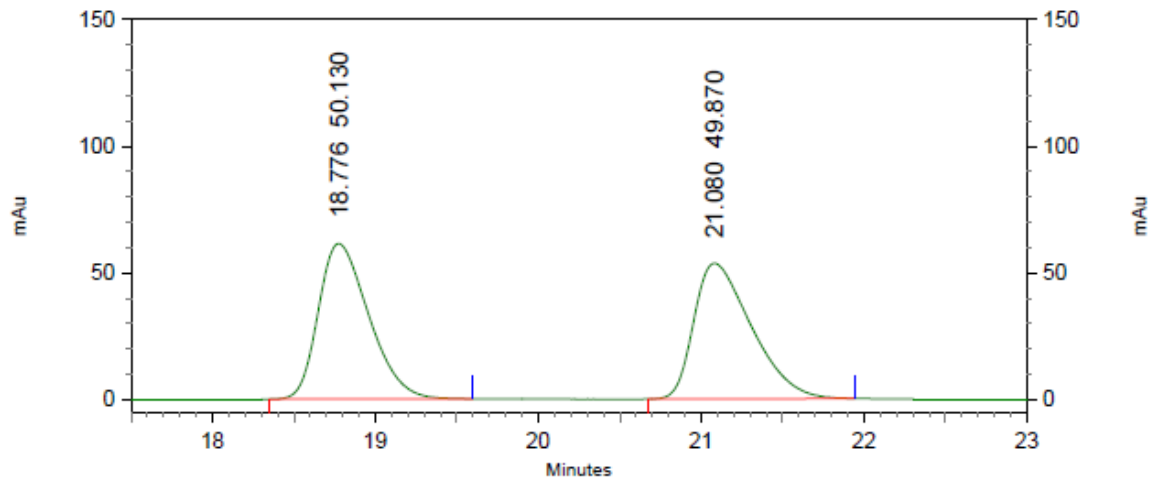
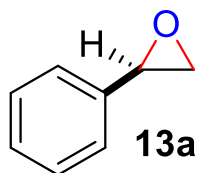
76.9059

52.5001

51.3359



Racemic 13a

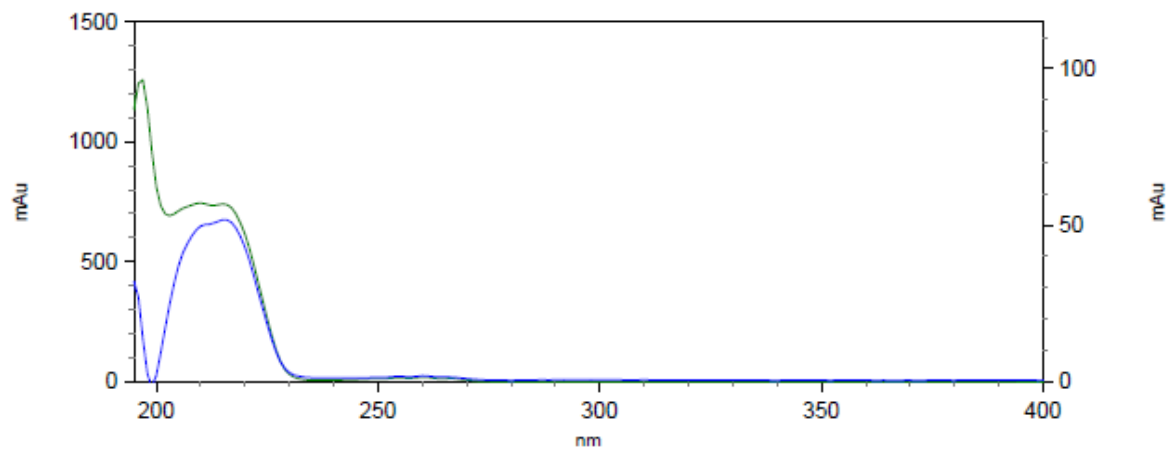
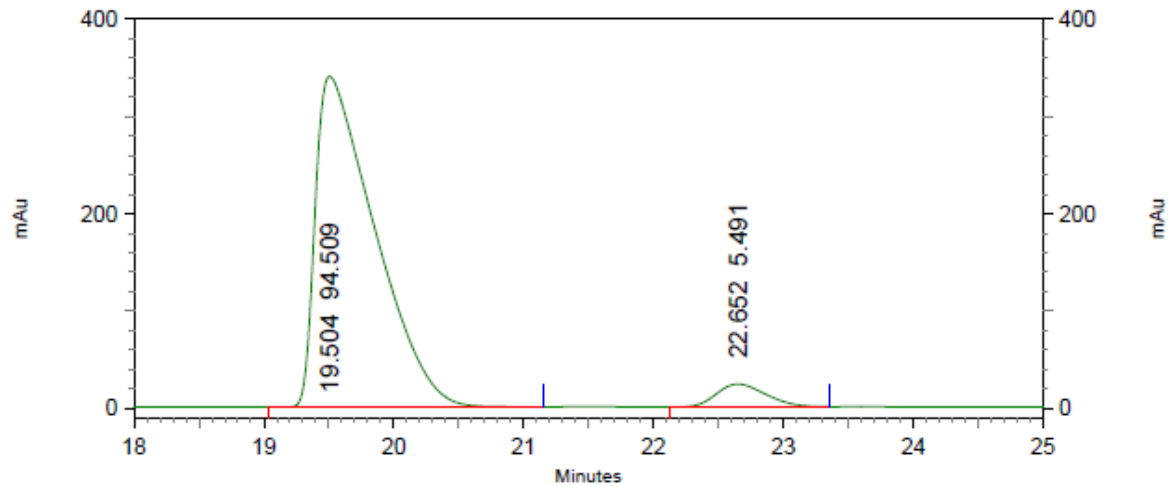
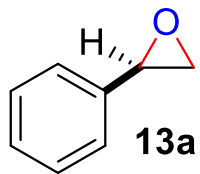


2: 224 nm, 4
nm Results

Pk #	Retention Time	Area Percent
1	18.776	50.130
2	21.080	49.870

Totals		100.000
--------	--	---------

Enantioenriched 13a

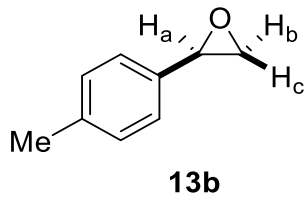


2: 224 nm, 4
nm Results

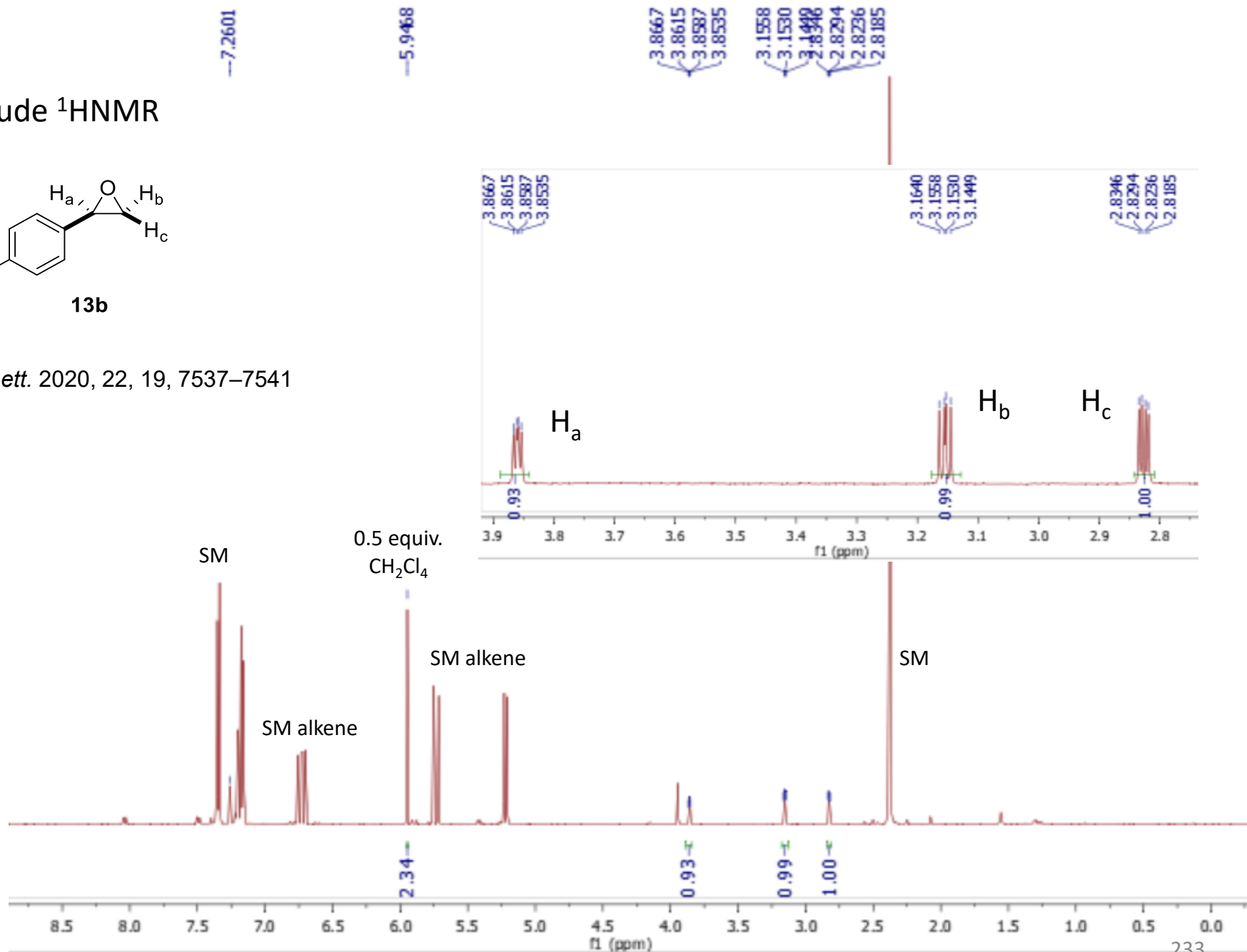
Pk #	Retention Time	Area Percent
1	19.504	94.509
2	22.652	5.491

Totals	100.000
--------	---------

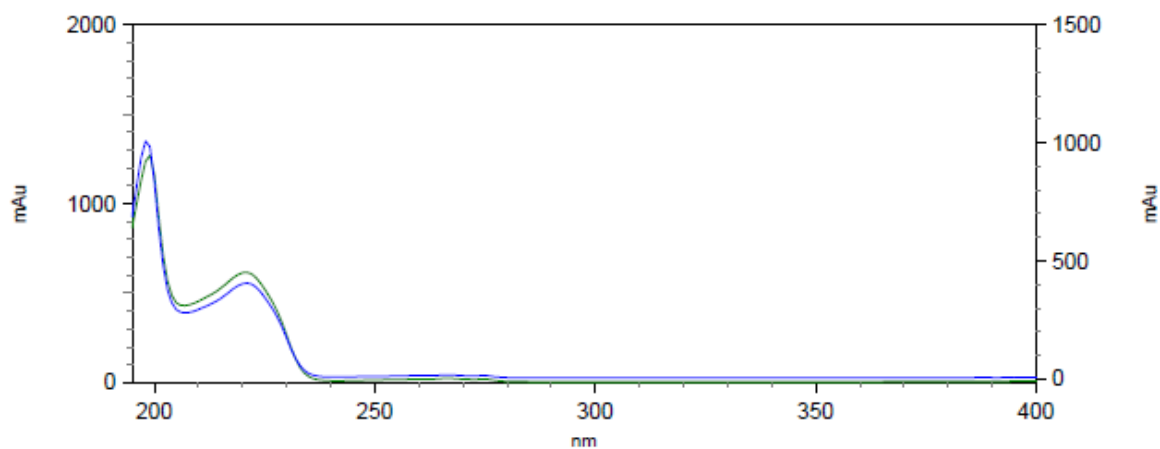
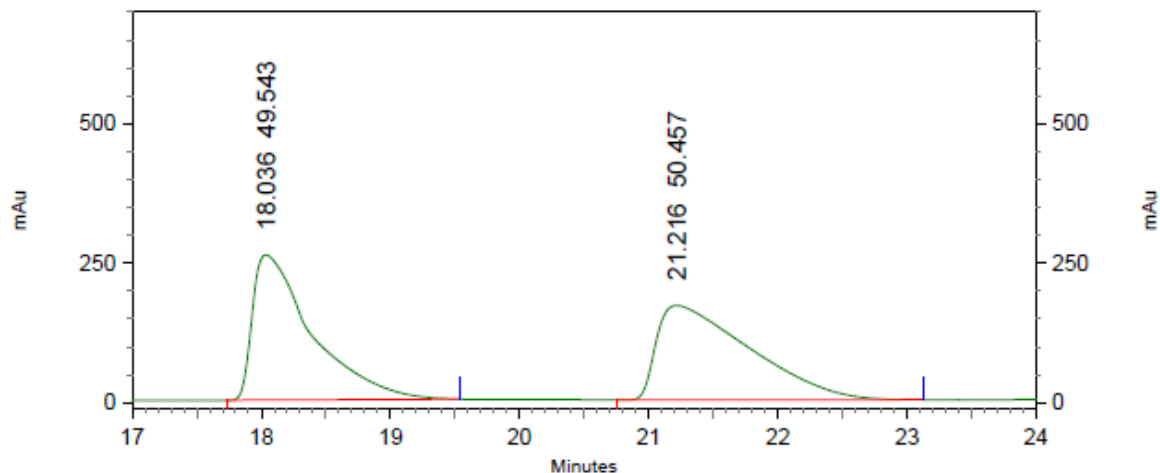
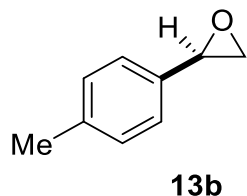
Crude ¹H NMR



Org. Lett. 2020, 22, 19, 7537–7541



Racemic
HPLC trace

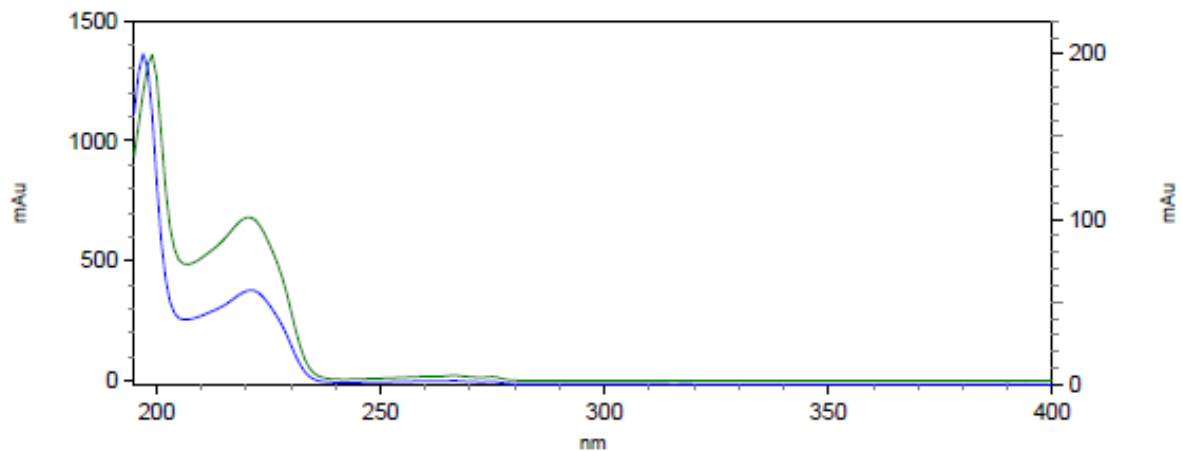
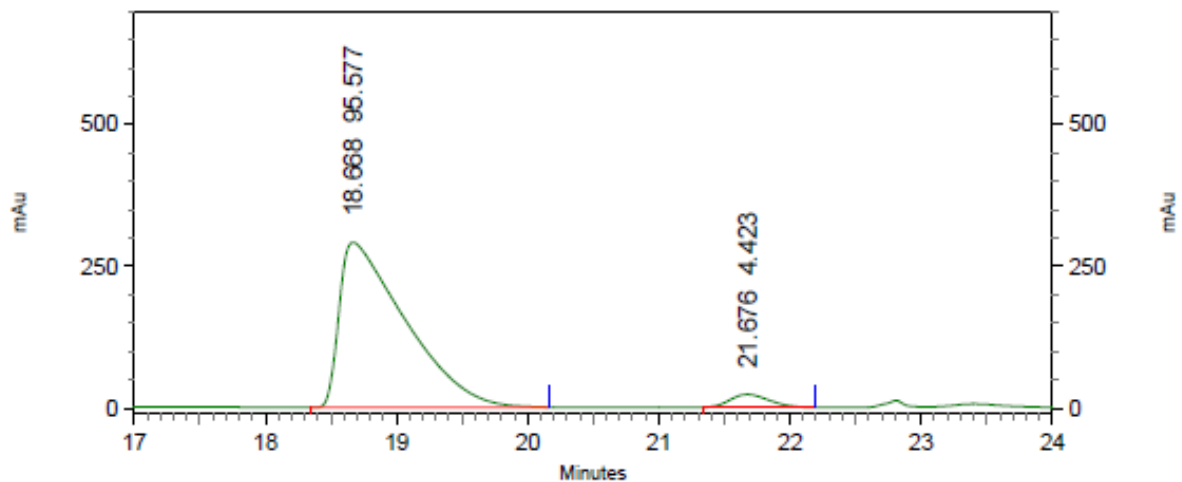
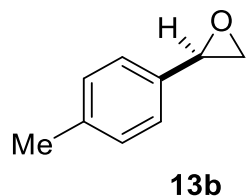


4: 230 nm, 4
nm Results

Pk #	Retention Time	Area Percent
1	18.036	49.543
2	21.216	50.457

Totals	100.000
--------	---------

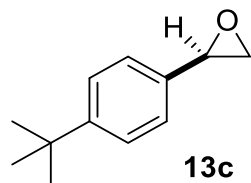
HPLC trace



4: 230 nm, 4
nm Results

Pk #	Retention Time	Area Percent
1	18.668	95.577
2	21.676	4.423
Totals		100.000

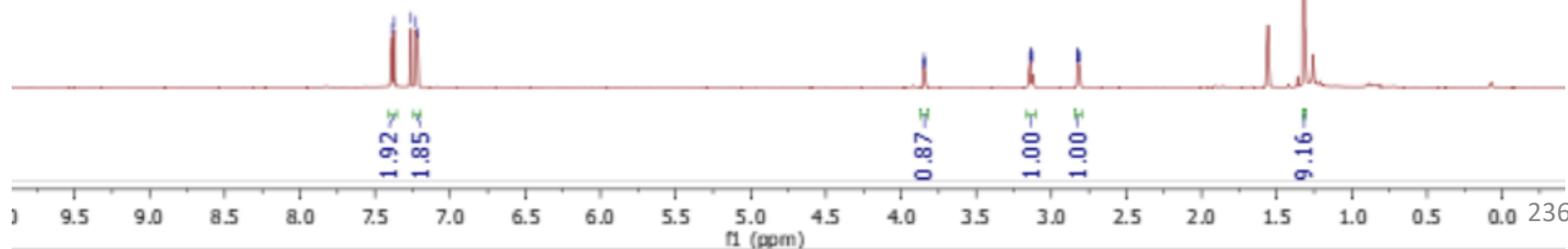
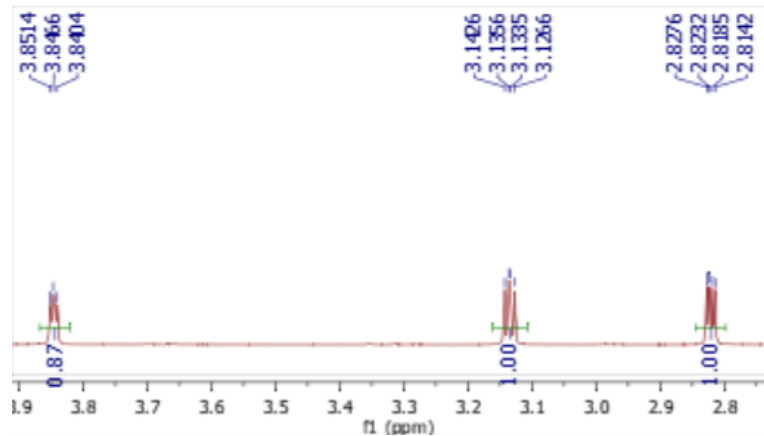
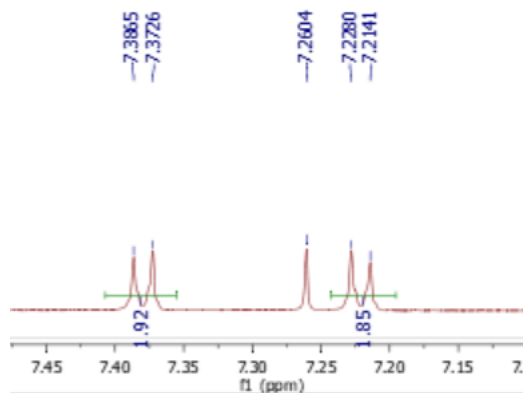
¹H NMR



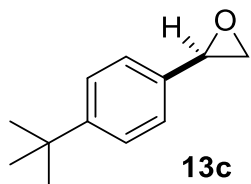
7.3865
7.3726
7.2604
7.2280
7.2141

3.8514
3.8466
3.8404
3.1426
3.1356
3.1335
3.1266
2.8276
2.8232
2.8185
2.8142

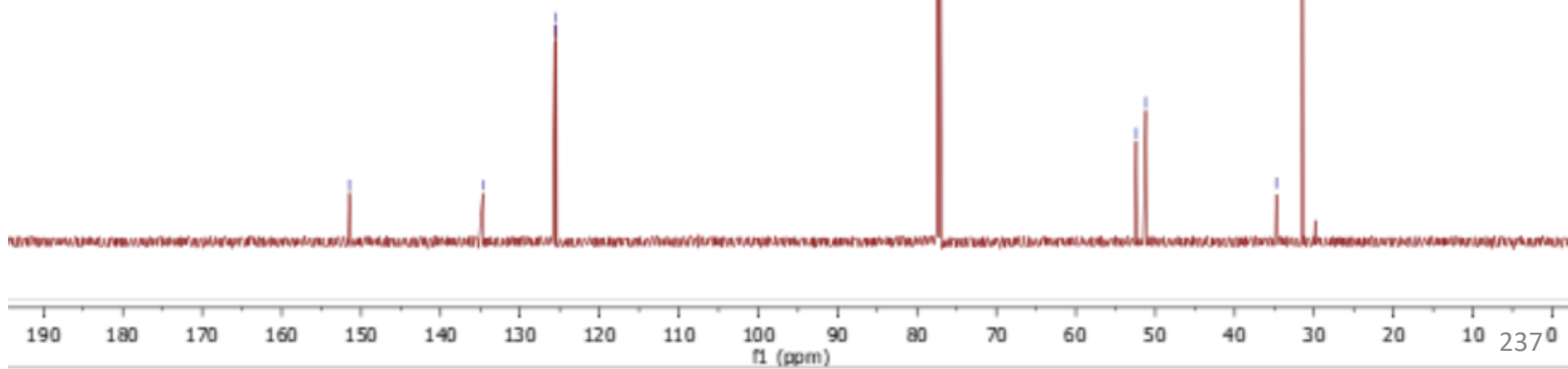
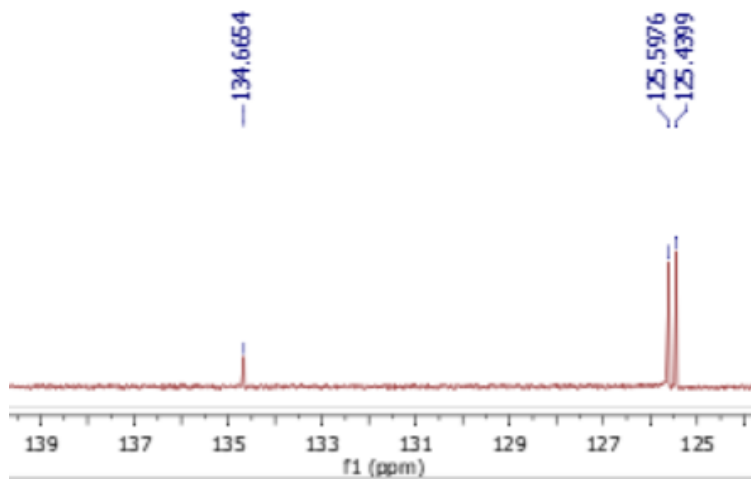
1.3175



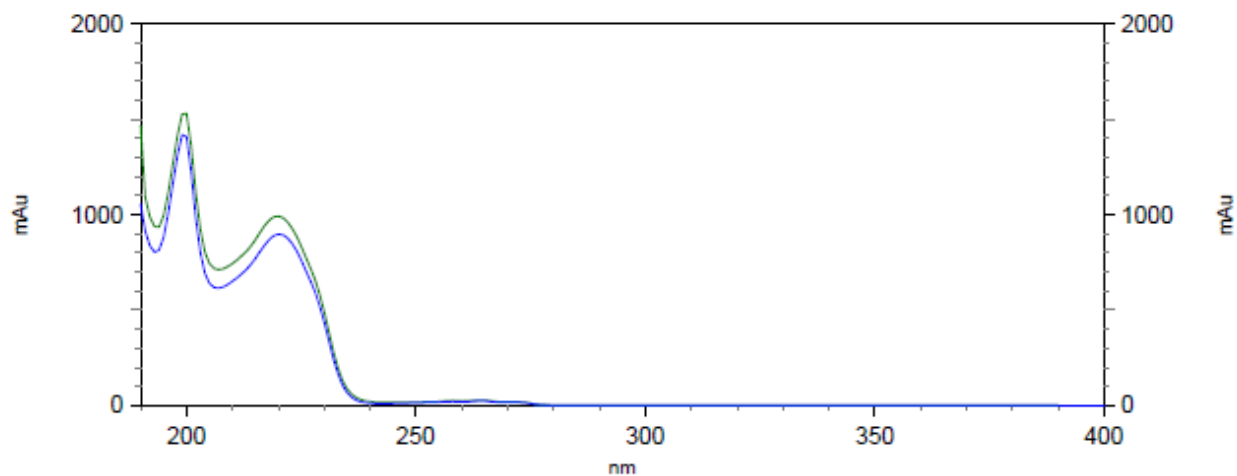
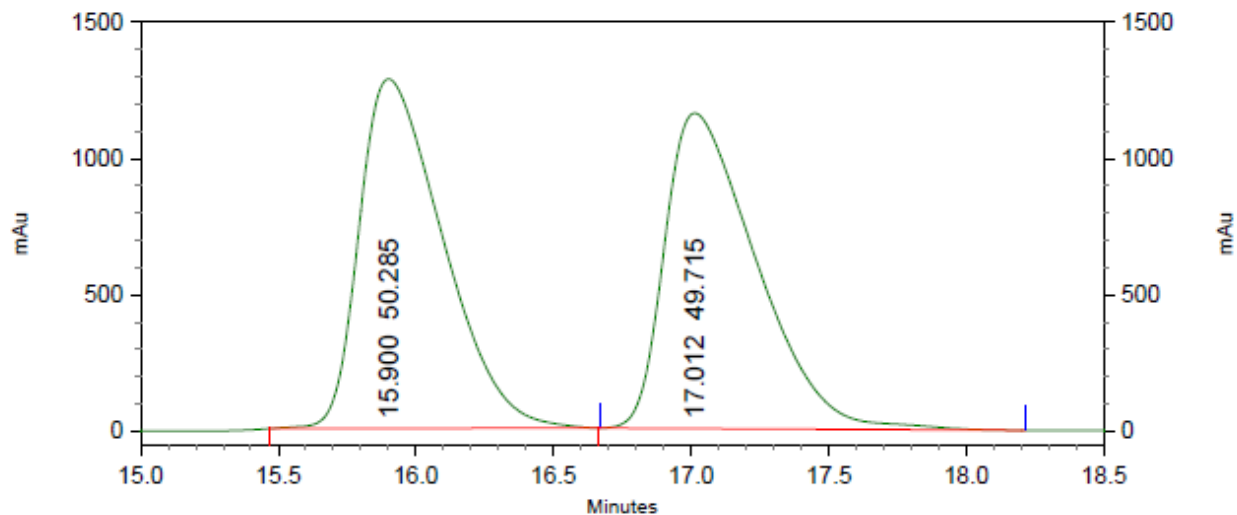
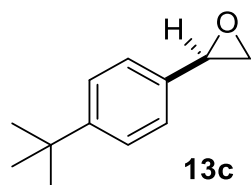
^{13}C NMR



- 151.4714
- 134.6654
- 125.5976
- 125.4399
- 77.3720
- 77.1603
- 76.9485
- 52.4238
- 51.1981
- 34.7465
- 31.4607



Racemic
HPLC trace

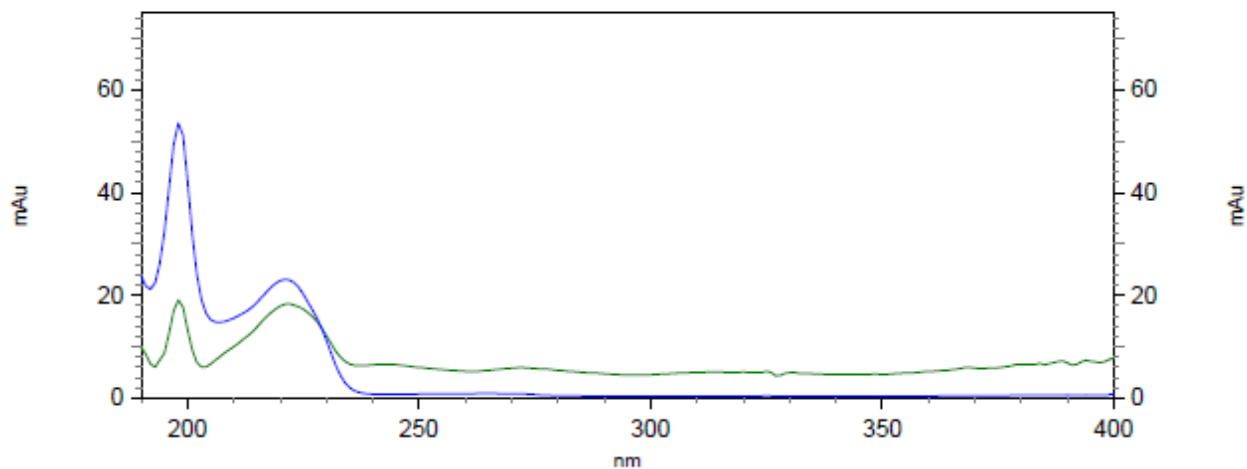
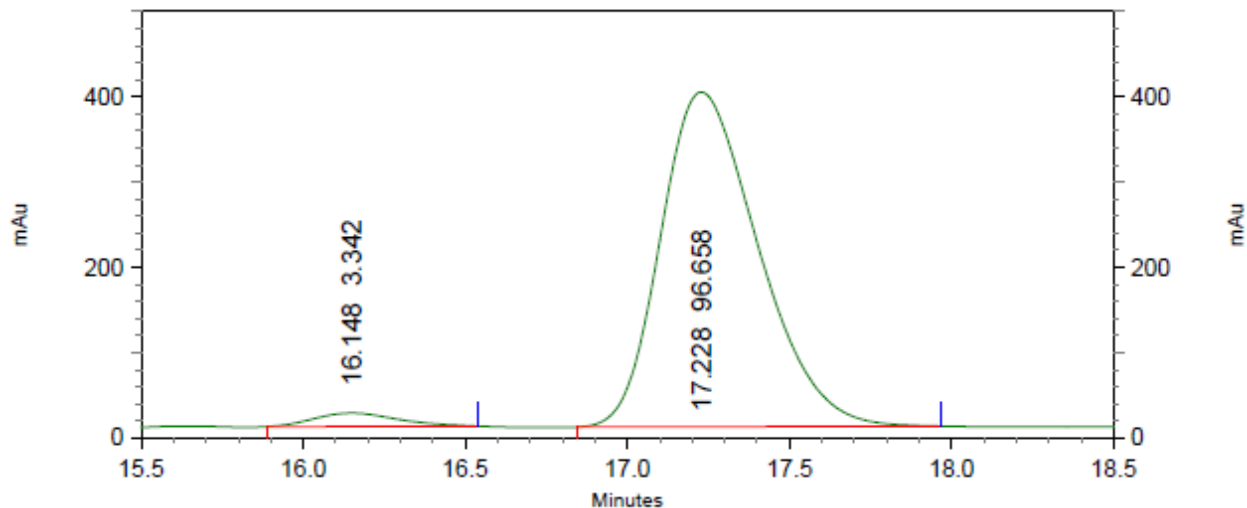
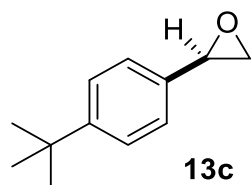


4: 228 nm, 4
nm Results

Pk #	Retention Time	Area Percent
1	15.900	50.285
2	17.012	49.715

Totals	100.000
--------	---------

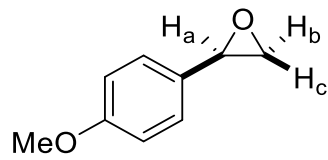
HPLC trace



4: 228 nm, 4
nm Results

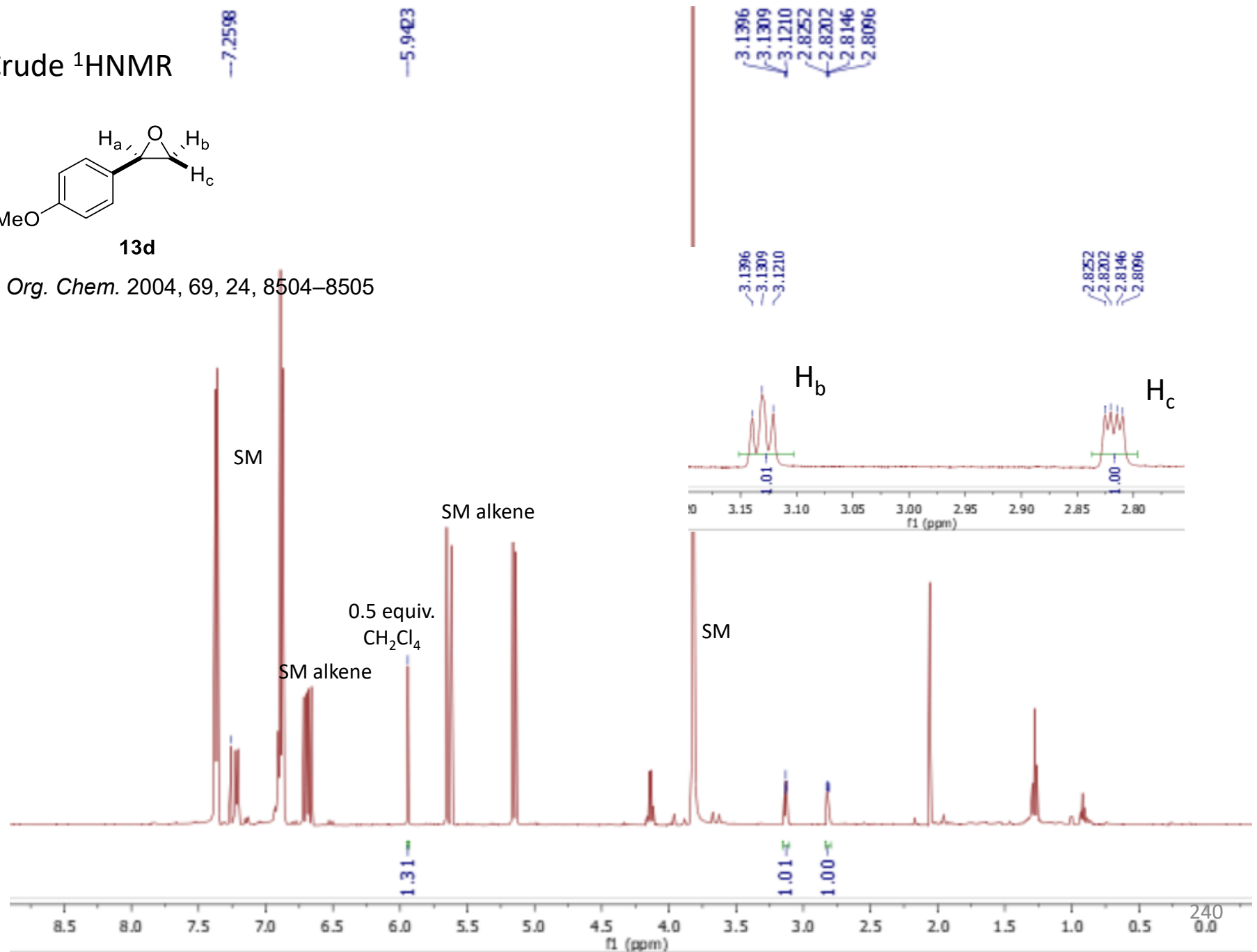
Pk #	Retention Time	Area Percent
1	16.148	3.342
2	17.228	96.658
Totals		100.000

Crude ¹H NMR



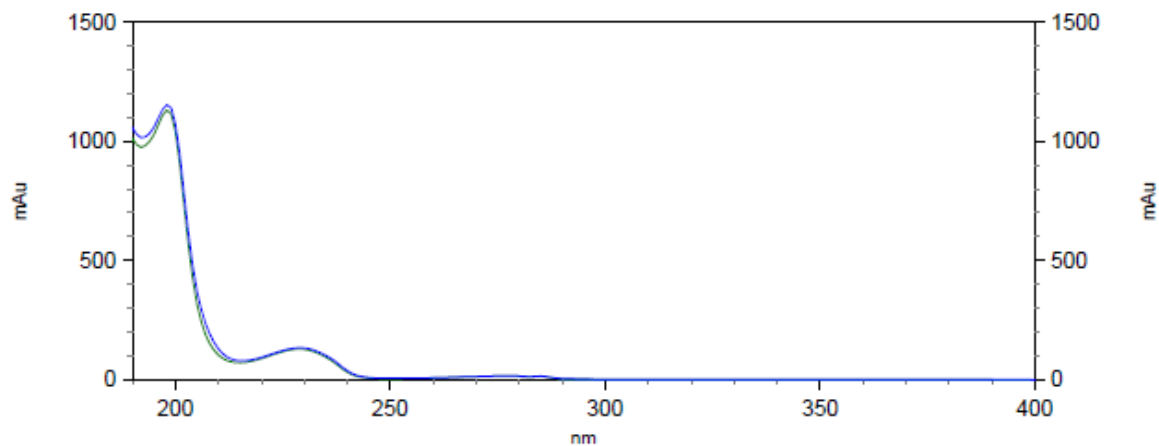
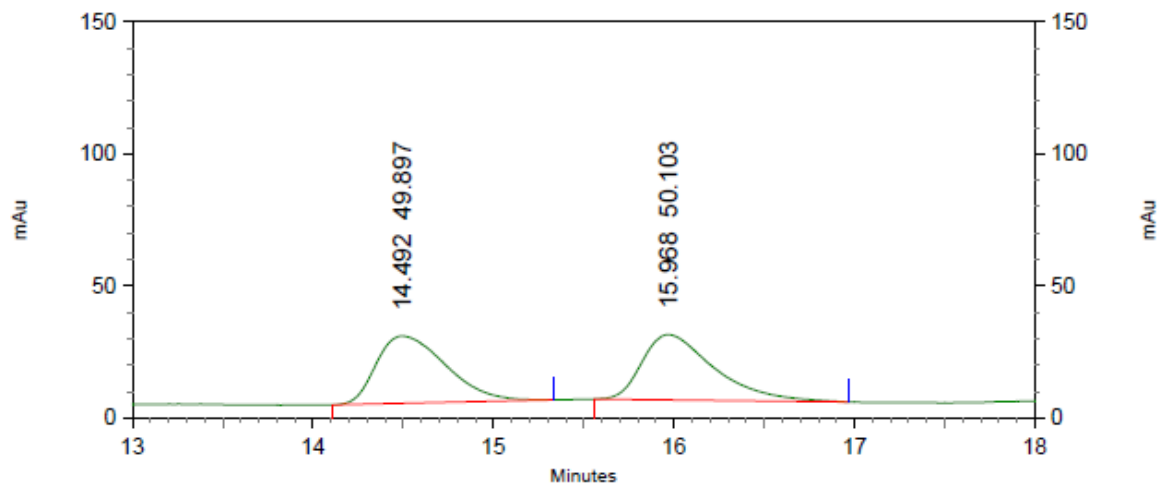
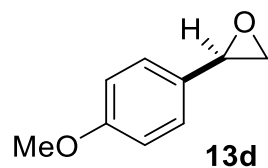
13d

J. Org. Chem. 2004, 69, 24, 8504–8505



C:\EZStart\Projects\Default\Data\XRF-1698-RAC-ADH-2%
C:\Documents and Settings\zhang\Desktop\WCL\Method.met

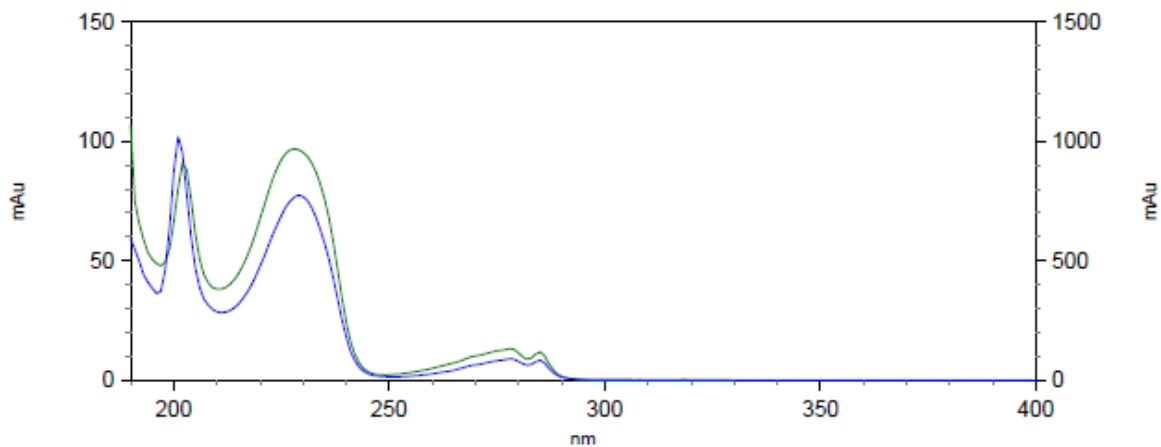
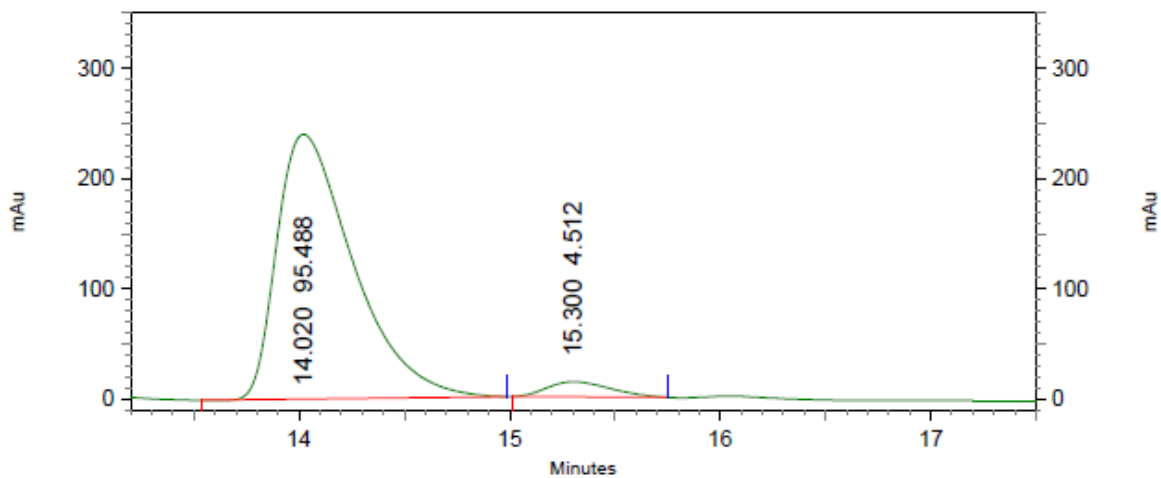
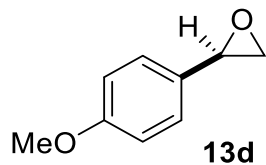
Racemic HPLC trace



4: 274 nm, 4
nm Results

Pk #	Retention Time	Area Percent
1	14.492	49.897
2	15.968	50.103
Totals		100.000

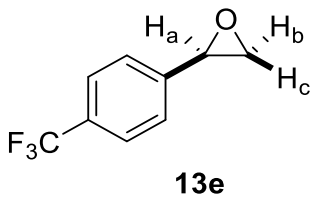
HPLC trace



4: 274 nm, 4
nm Results

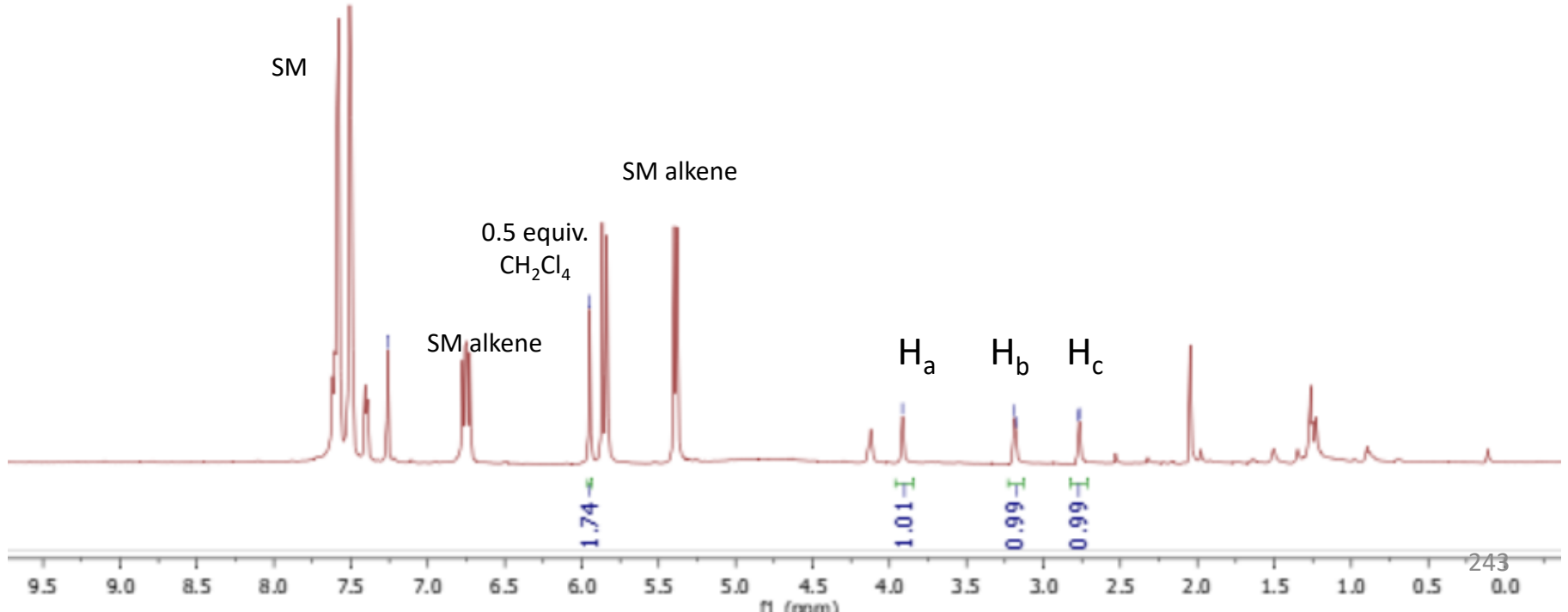
Pk #	Retention Time	Area Percent
1	14.020	95.488
2	15.300	4.512
Totals		100.000

Crude ¹H NMR

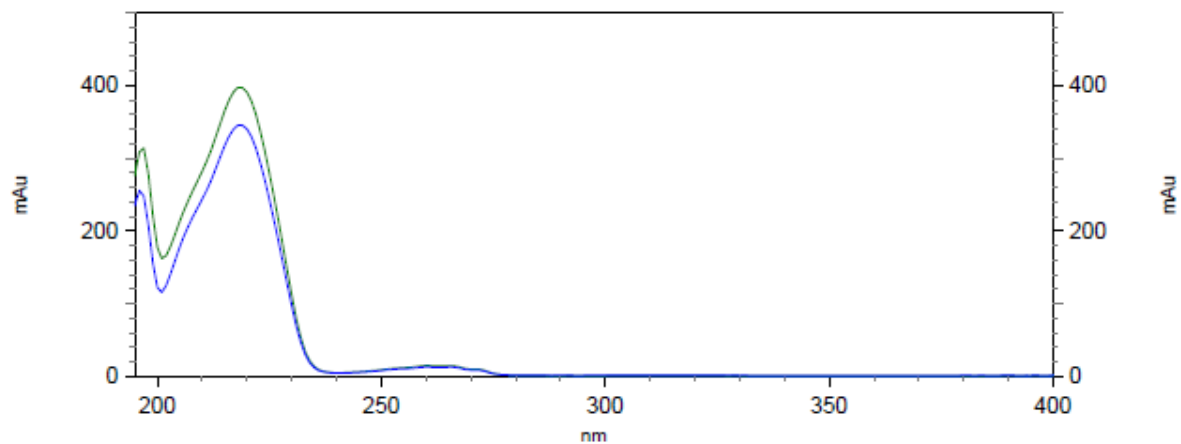
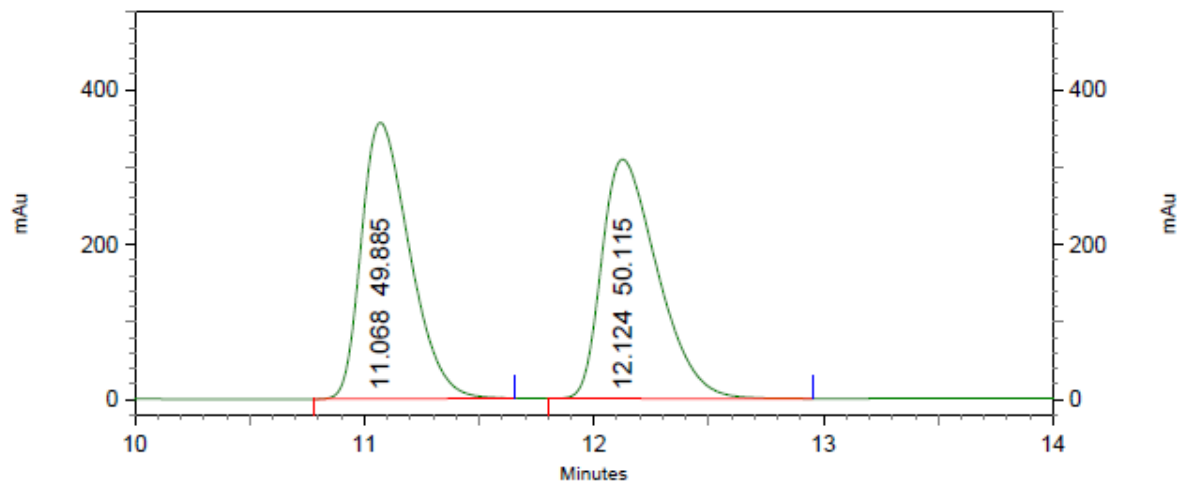
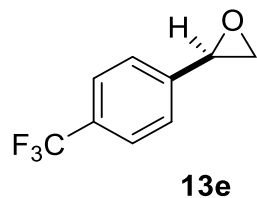


Org. Lett. 2005, 7, 6, 987-990

7.2602
5.9489
3.9160
3.1872
3.1805
2.7716
2.7667



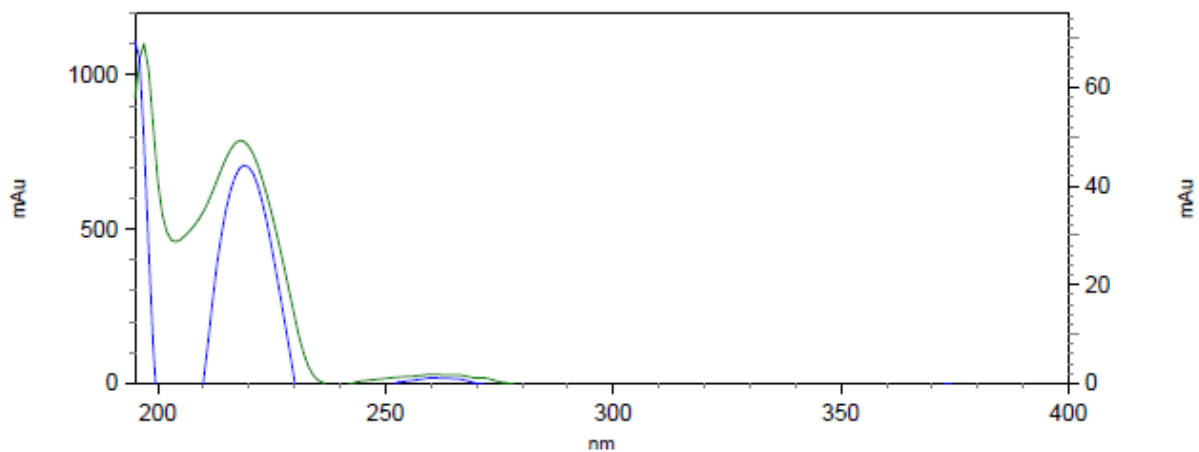
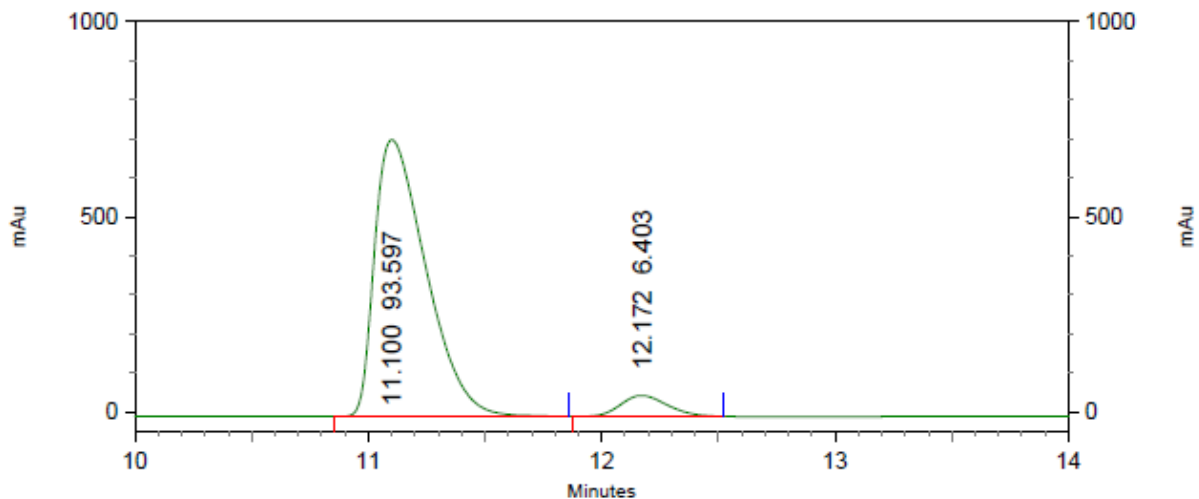
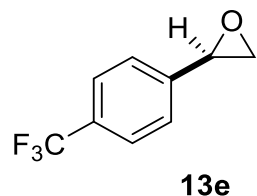
Racemic HPLC trace



2: 222 nm, 4
nm Results

Pk #	Retention Time	Area Percent
1	11.068	49.885
2	12.124	50.115
Totals		100.000

HPLC trace

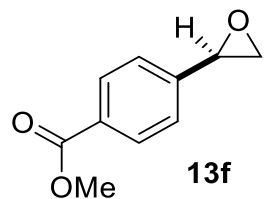


2: 222 nm, 4
nm Results

Pk #	Retention Time	Area Percent
1	11.100	93.597
2	12.172	6.403

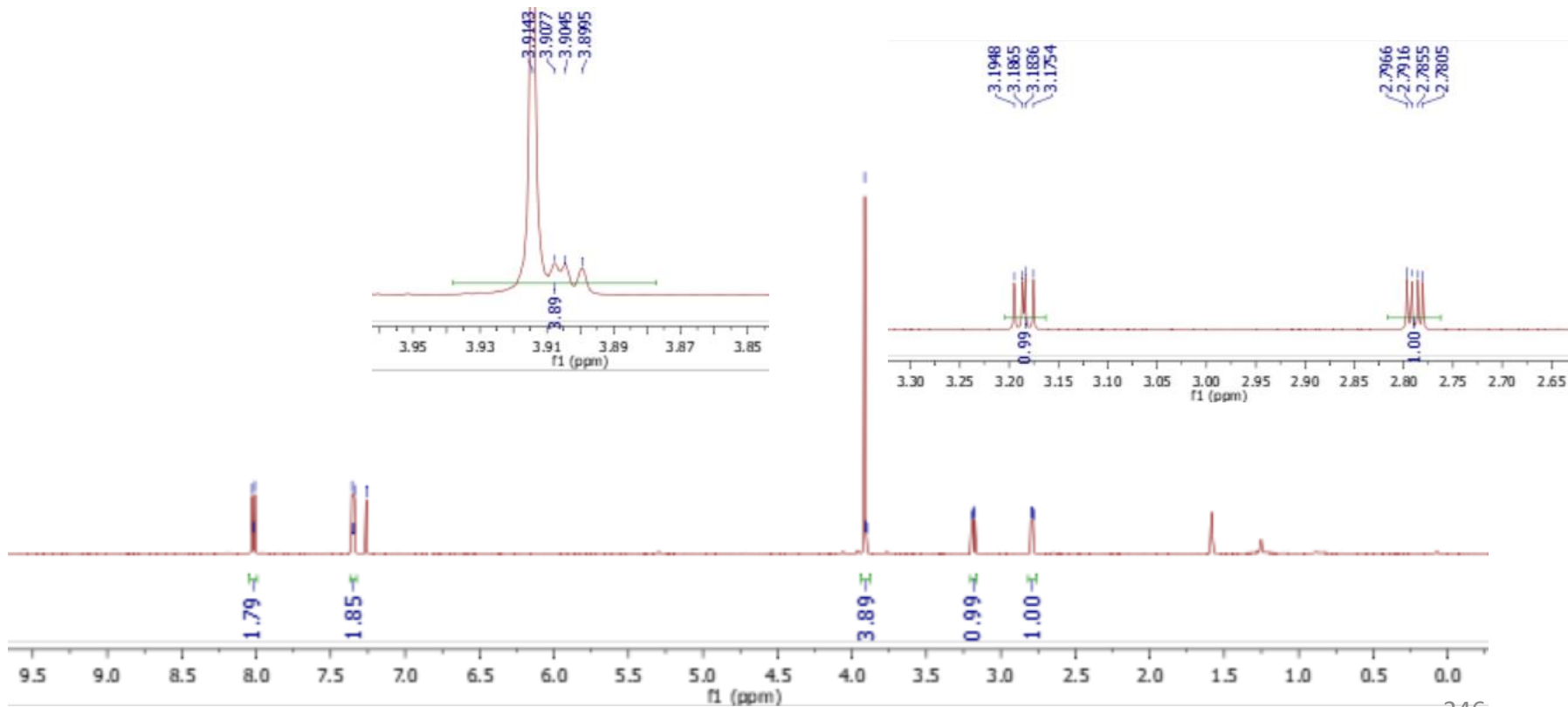
Totals	100.000
--------	---------

¹H NMR

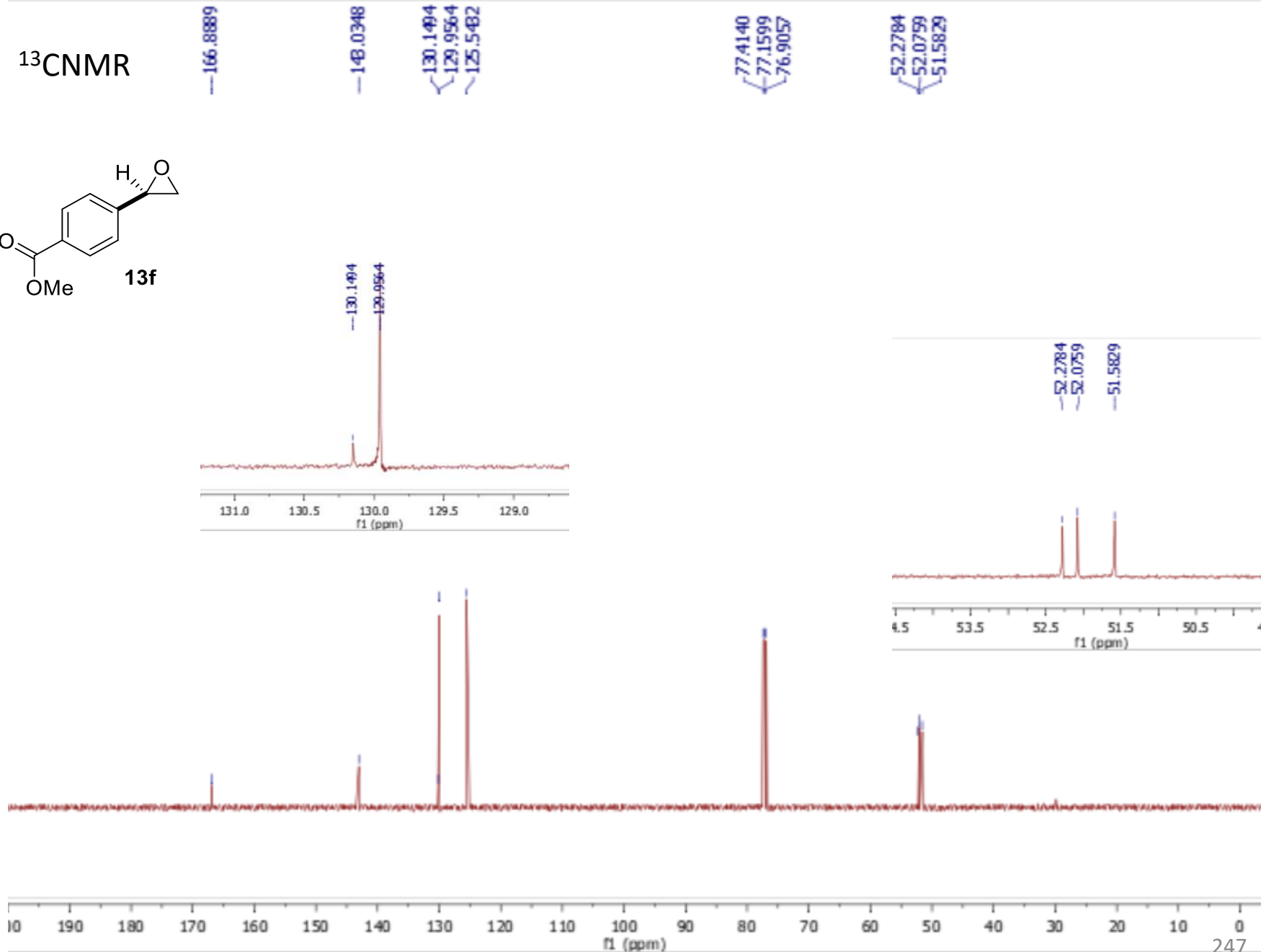
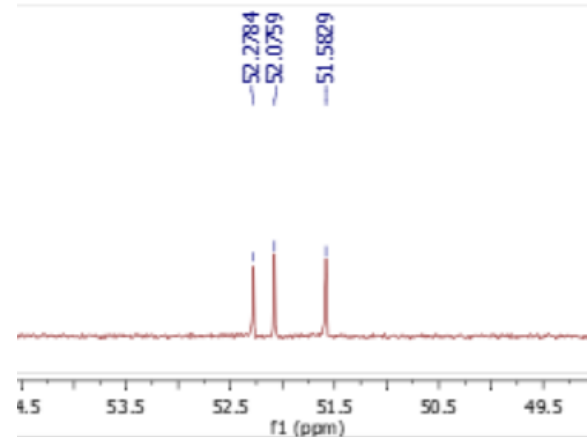
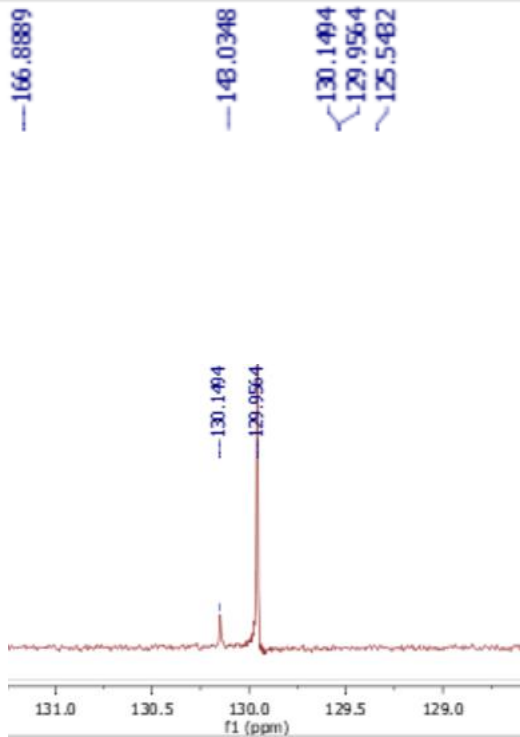
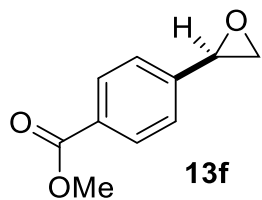


8.0255
8.0219
8.0123
8.0087
7.3560
7.3525
7.3428
7.3394
7.2601

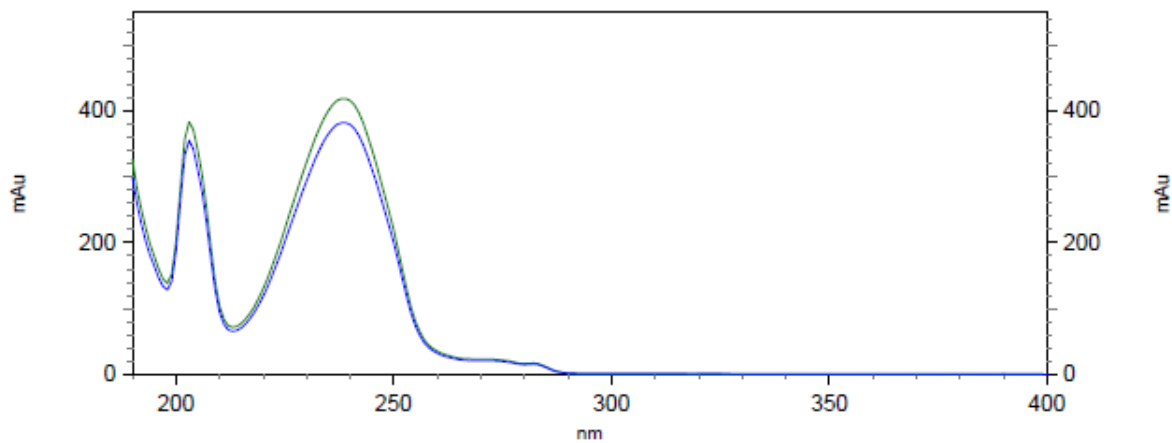
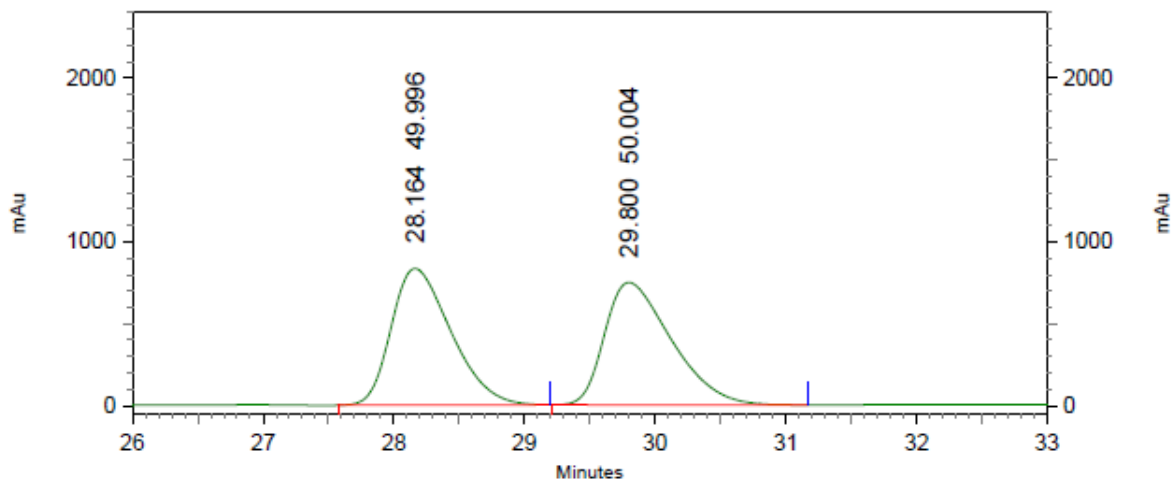
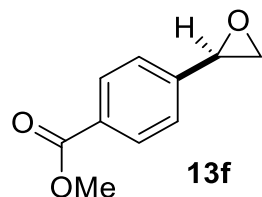
3.9143
3.9077
3.9045
3.8995
3.1865
3.1836
3.1768
2.7916
2.7855
2.7805



¹³CNMR



Racemic HPLC trace

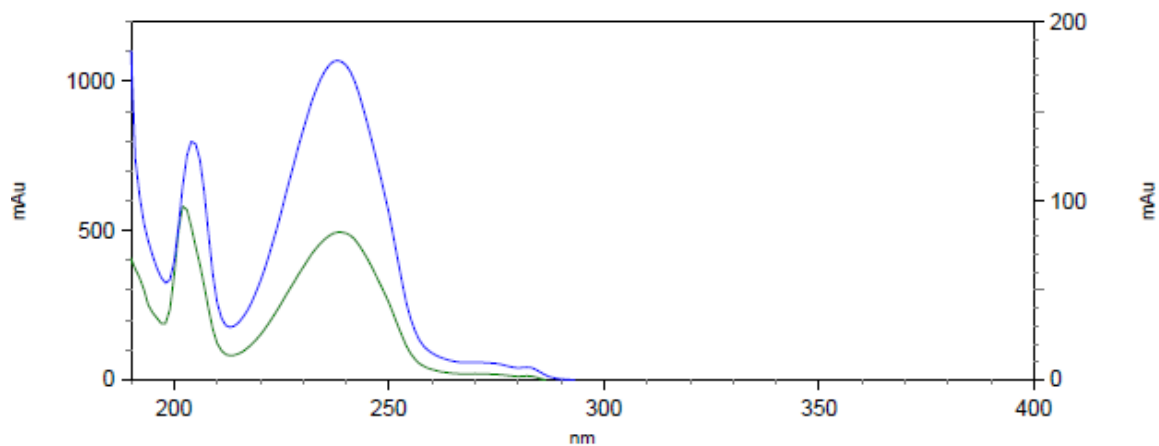
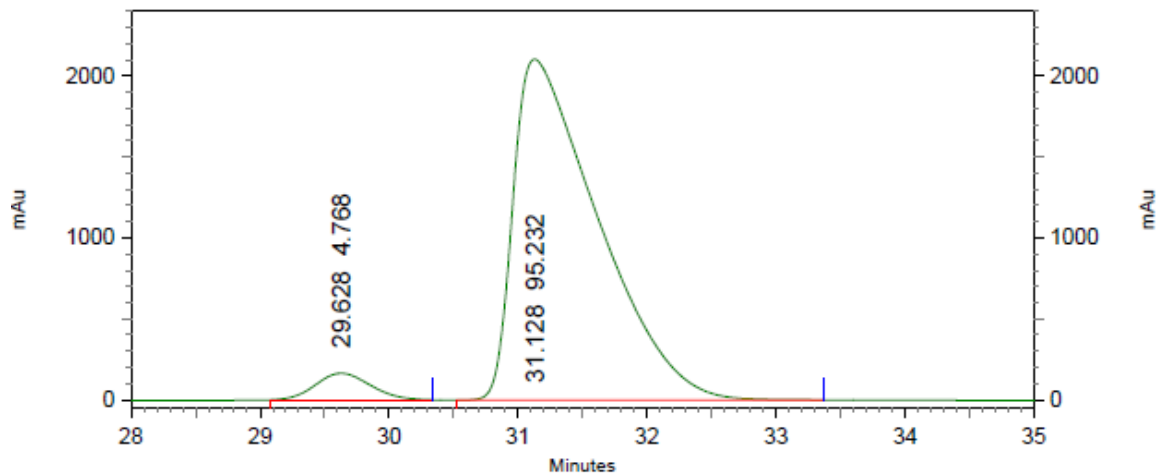
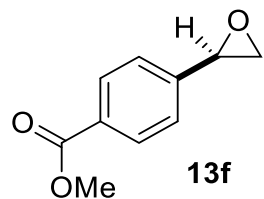


4: 240 nm, 4
nm Results

Pk #	Retention Time	Area Percent
1	28.164	49.996
2	29.800	50.004
Totals		100.000

C:\EZStart\Projects\Default\Data\XRF-1704--IF-2%-1
C:\Documents and Settings\zhang\Desktop\WCL\Method.met

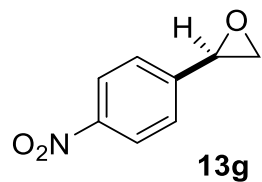
HPLC trace



4: 240 nm, 4
nm Results

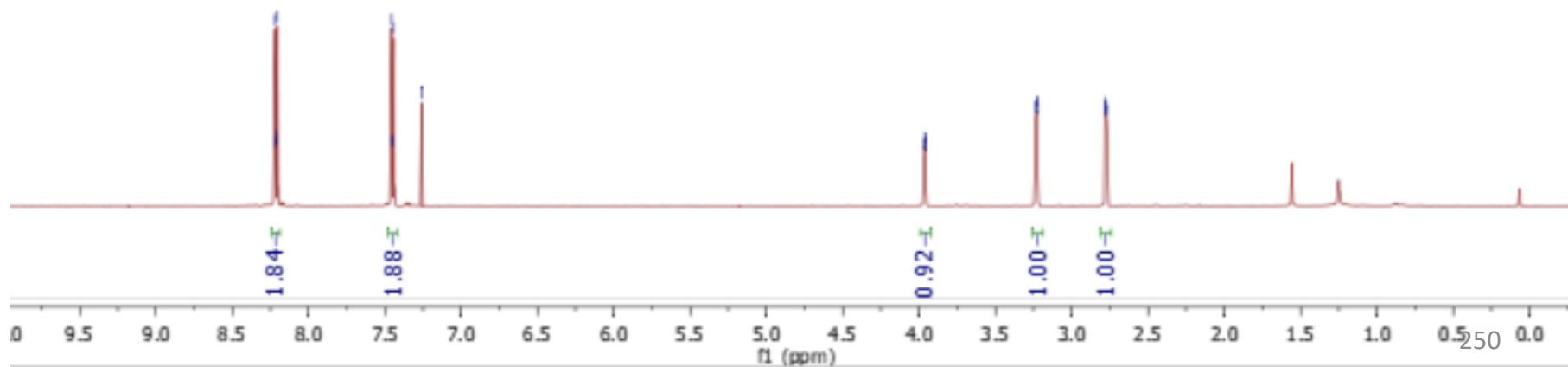
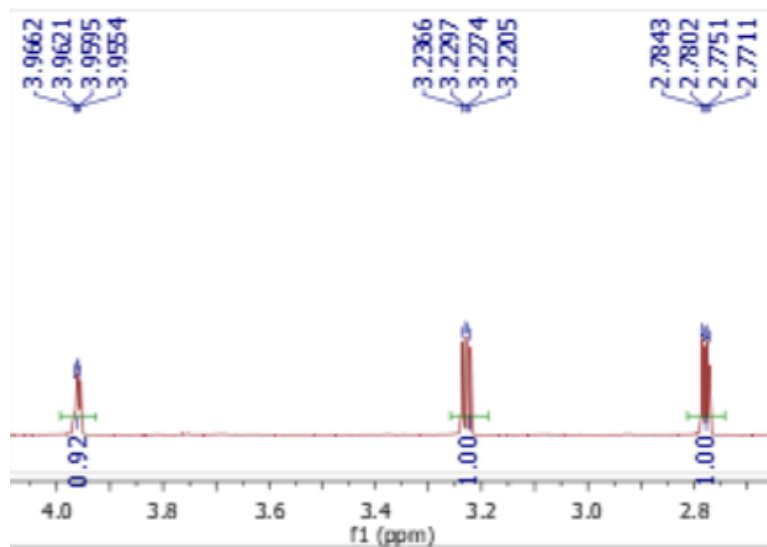
Pk #	Retention Time	Area Percent
1	29.628	4.768
2	31.128	95.232
Totals		100.000

¹H NMR

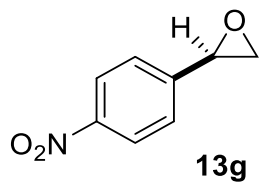


8.2194
8.2162
8.2079
8.2047
7.4570
7.4538
7.4455
7.4424
7.2596

3.9662
3.9621
3.9595
3.9554
3.2366
3.2297
3.2274
2.7843
2.7802
2.7751
2.7711



¹H NMR

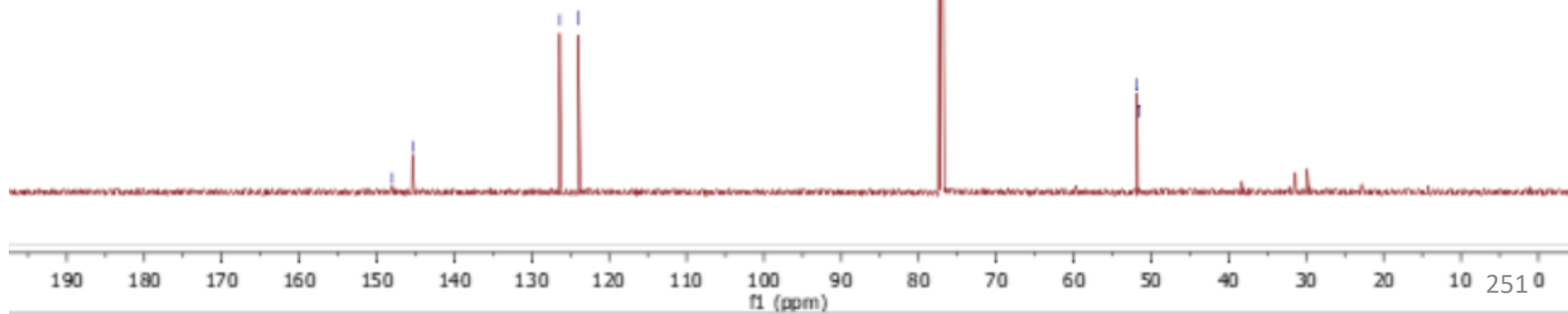
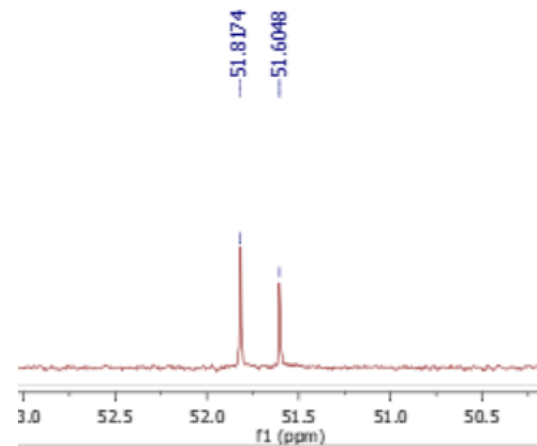
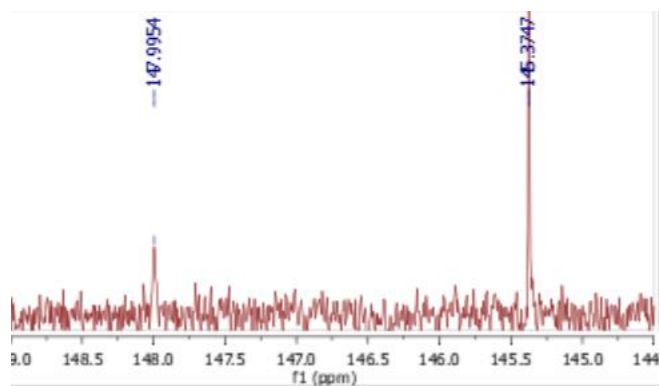


147.9954
145.3747

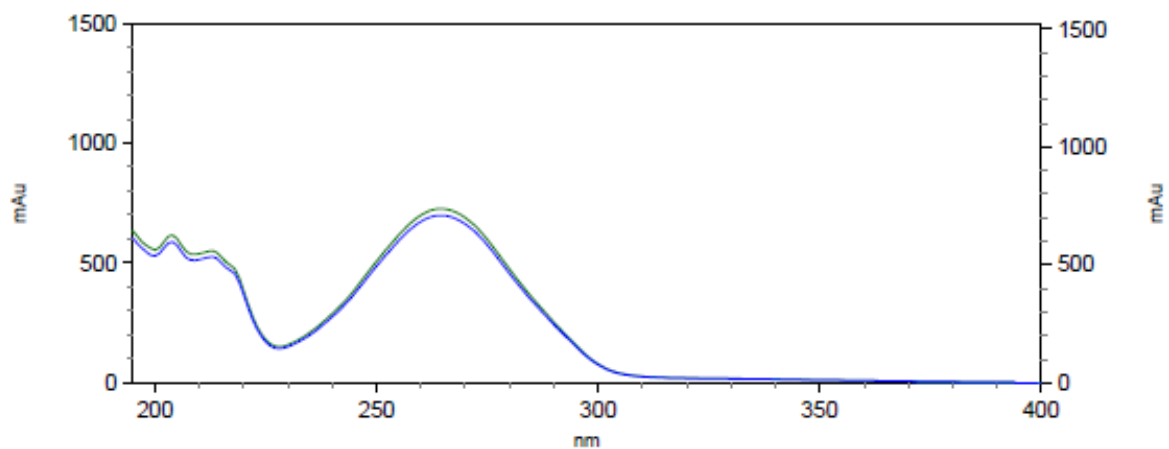
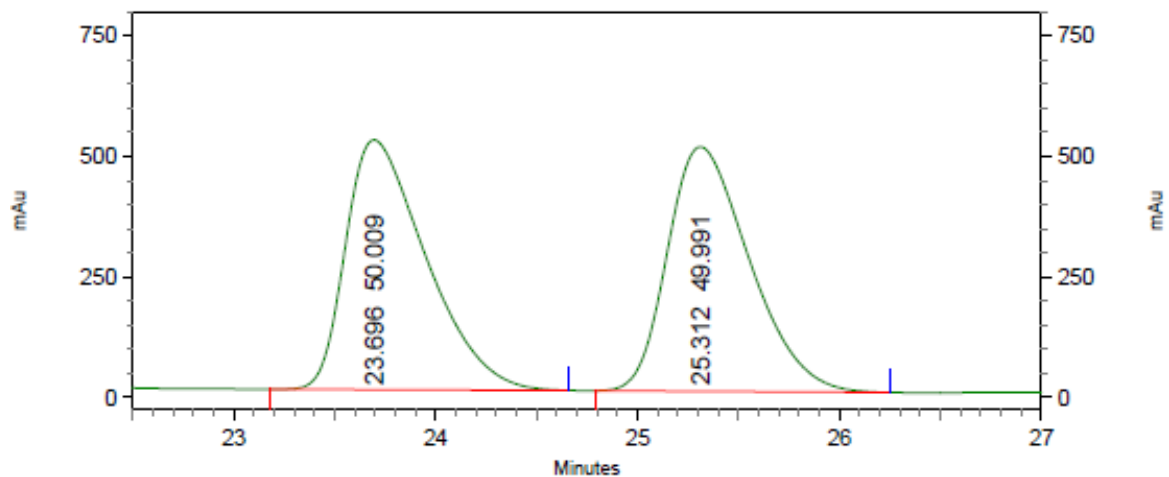
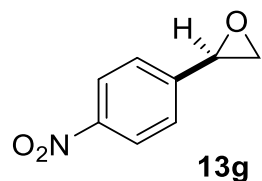
126.3644
123.9754

77.3717
77.1600
76.9481

51.8174
51.6048



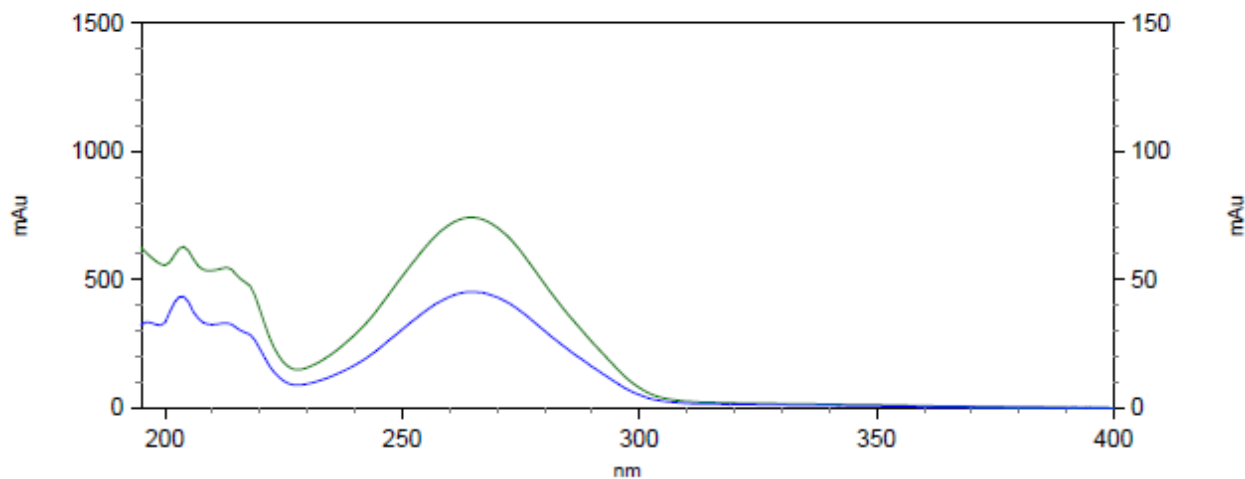
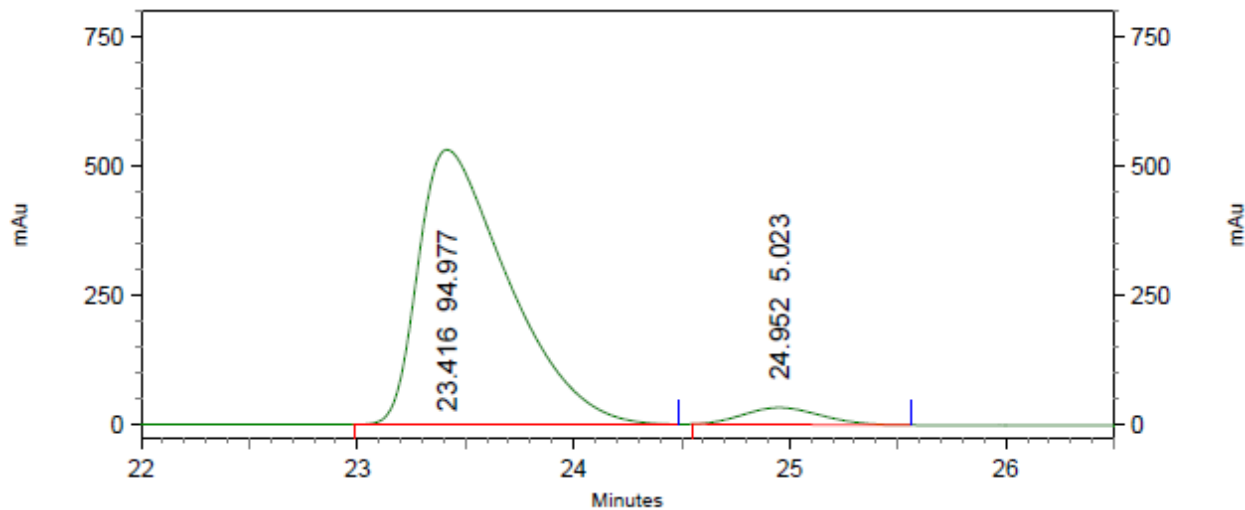
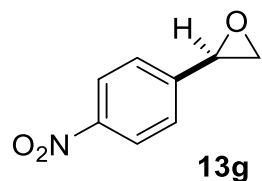
Racemic HPLC trace



2: 214 nm, 4
nm Results

Pk #	Retention Time	Area Percent
1	23.696	50.009
2	25.312	49.991
Totals		100.000

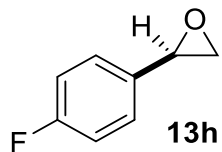
HPLC trace



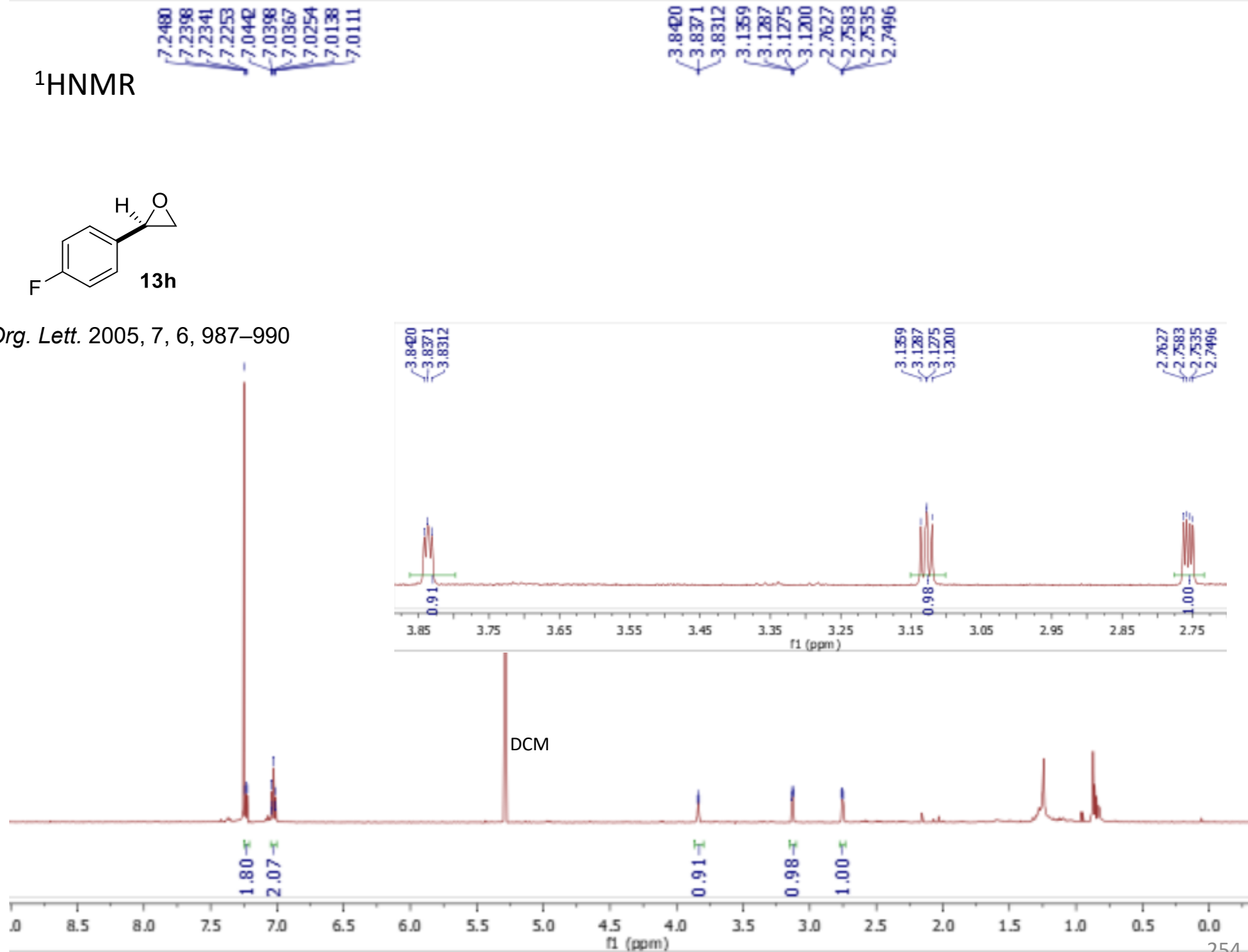
2: 214 nm, 4 nm Results

Pk #	Retention Time	Area Percent
1	23.416	94.977
2	24.952	5.023
Totals		100.000

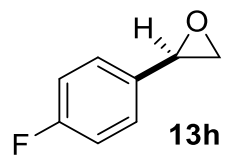
¹H NMR



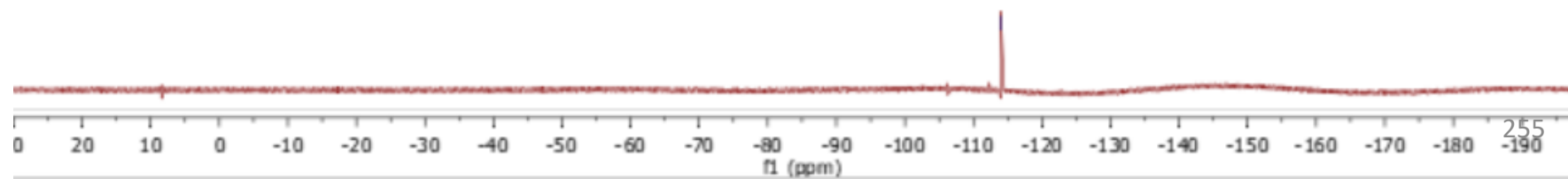
Org. Lett. 2005, 7, 6, 987–990



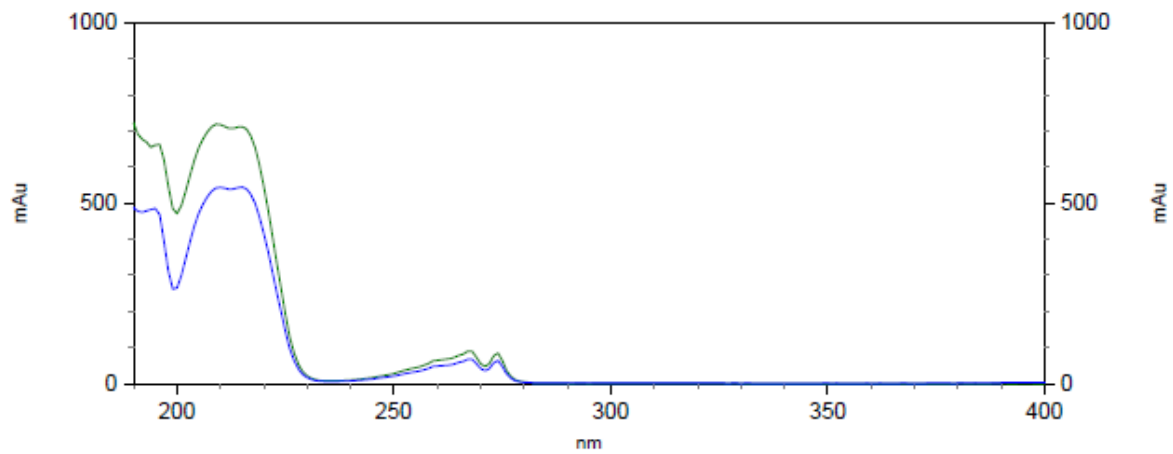
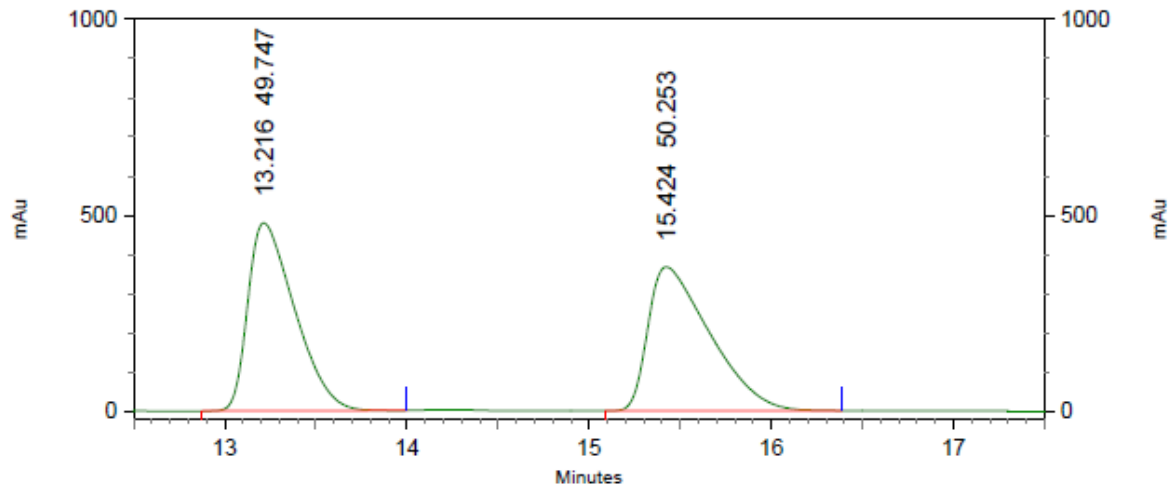
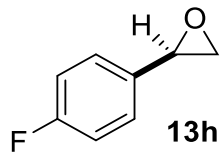
^{19}F NMR



-113.9785



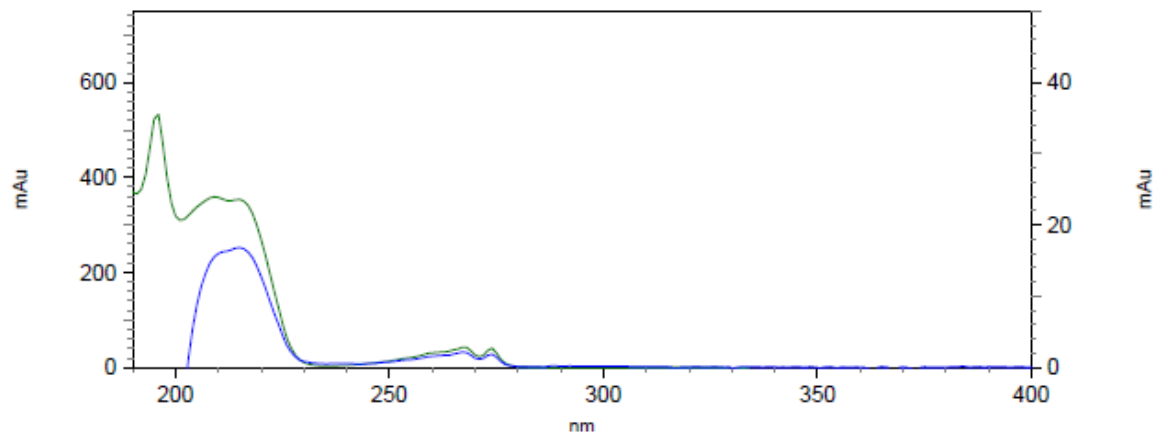
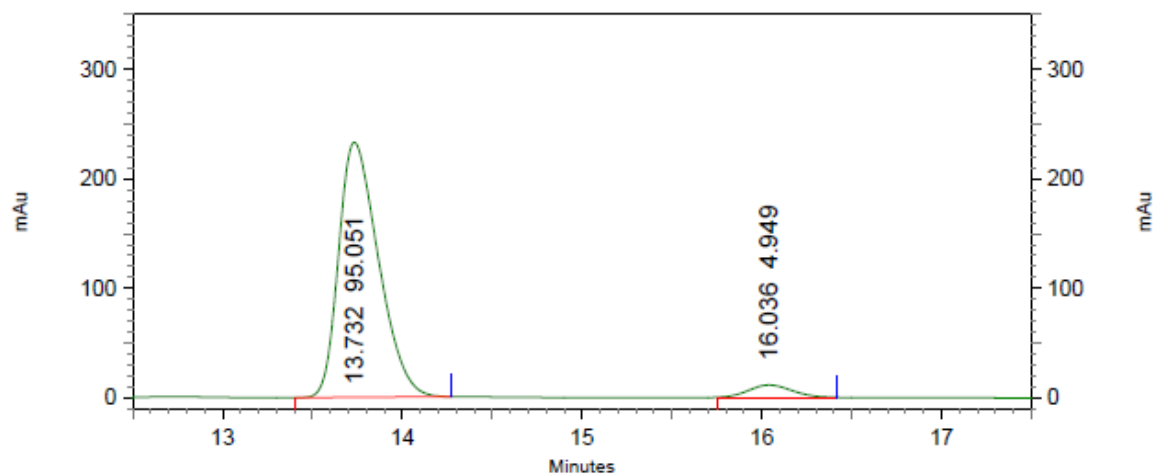
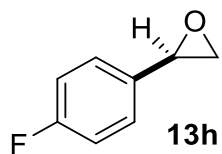
Racemic
HPLC trace



4: 221 nm, 4
nm Results

	Pk #	Retention Time	Area Percent
	1	13.216	49.747
	2	15.424	50.253
Totals			100.000

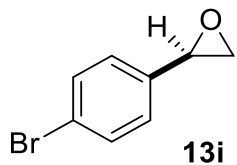
HPLC trace



4: 221 nm, 4
nm Results

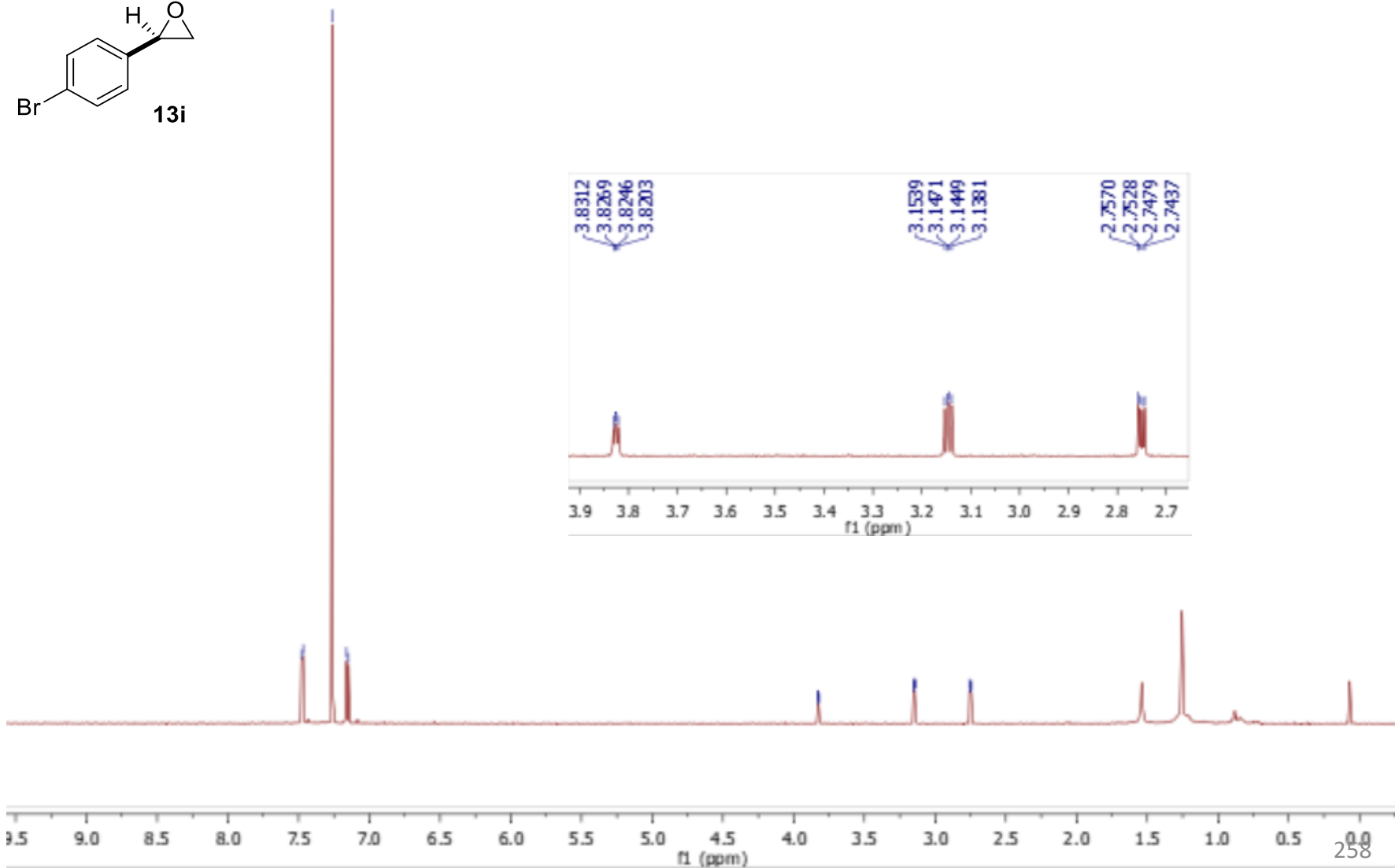
Pk #	Retention Time	Area Percent
1	13.732	95.051
2	16.036	4.949
Totals		100.000

¹H NMR

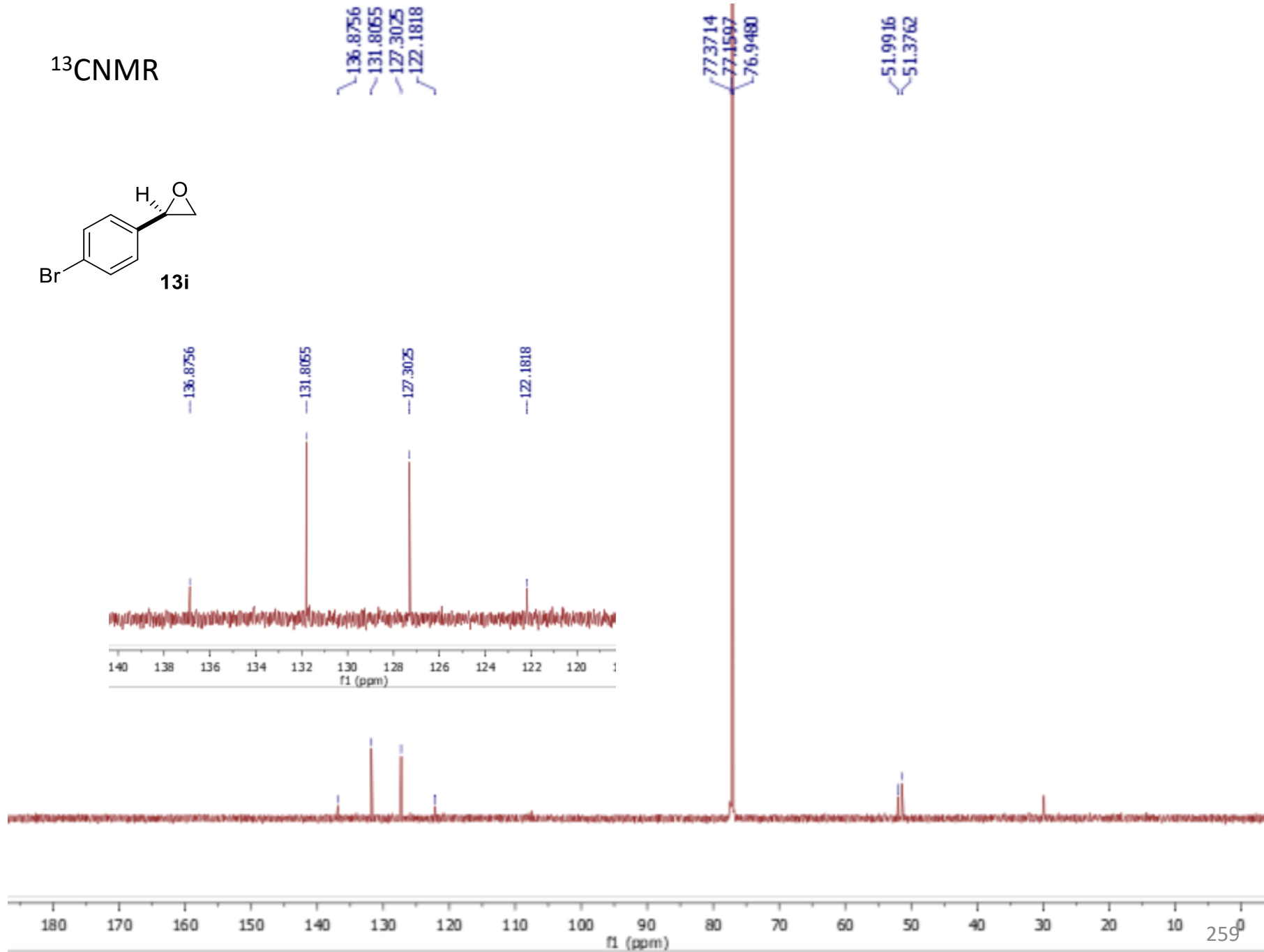
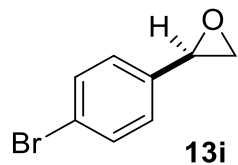


7.4809
7.4667
7.2597
7.1616
7.1475

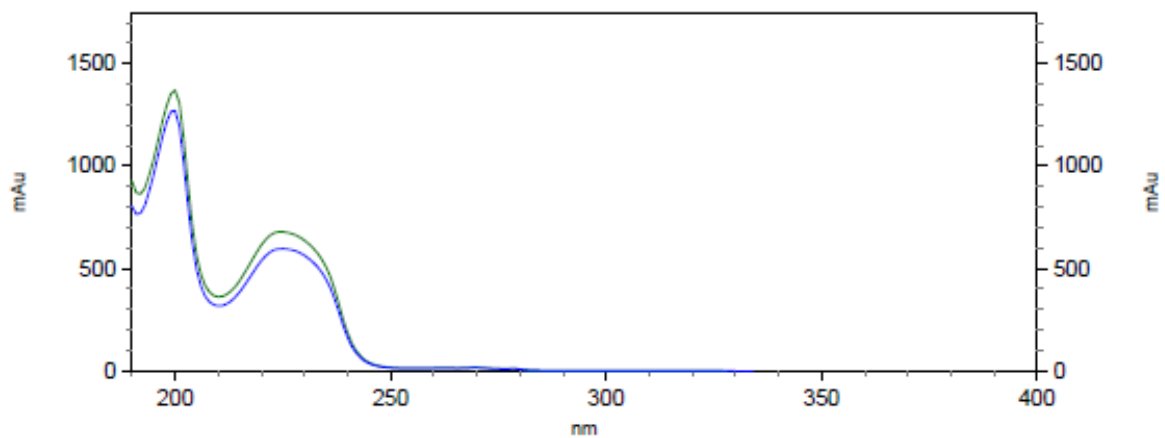
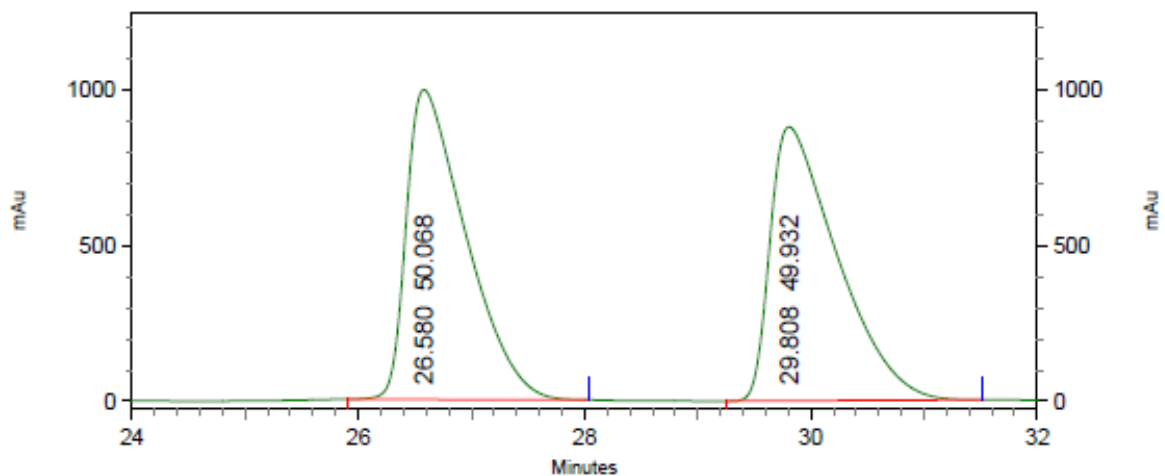
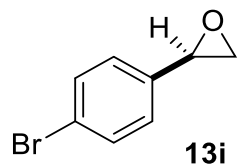
3.8312
3.8269
3.8246
3.8203
3.1471
3.1449
3.1381
2.7570
2.7528
2.7479
2.7437



^{13}C NMR



Racemic HPLC trace



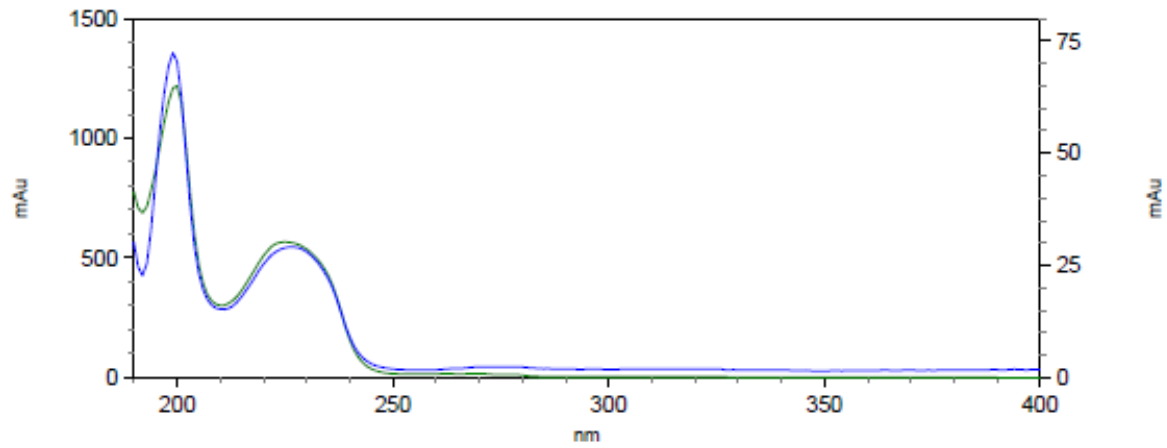
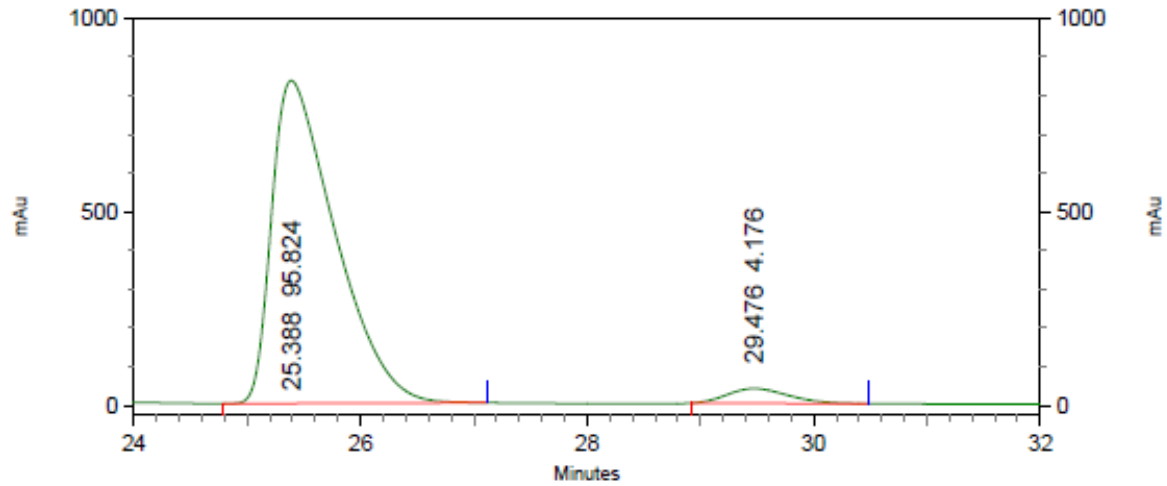
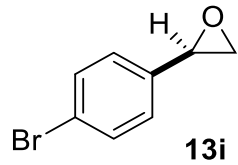
4: 235 nm, 4
nm Results

Pk #	Retention Time	Area Percent
1	26.580	50.068
2	29.808	49.932

Totals	
	100.000

C:\EZStart\Projects\Default\Data\XRF-1689-IF-1%-1
C:\Documents and Settings\zhang\Desktop\WCL\Method.met

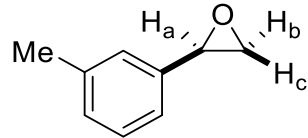
HPLC trace



4: 235 nm, 4
nm Results

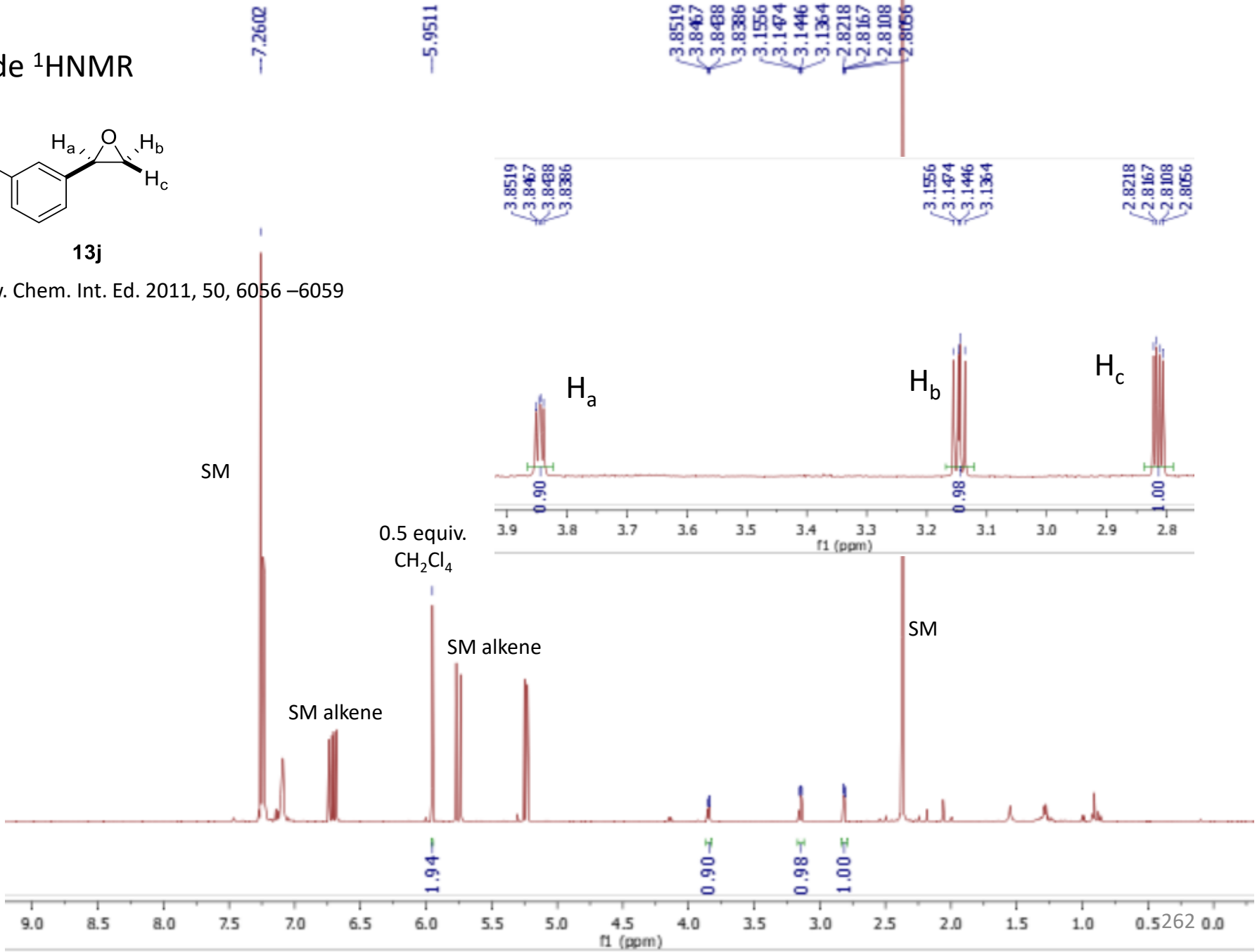
Pk #	Retention Time	Area Percent
1	25.388	95.824
2	29.476	4.176
Totals		100.000

Crude ¹H NMR

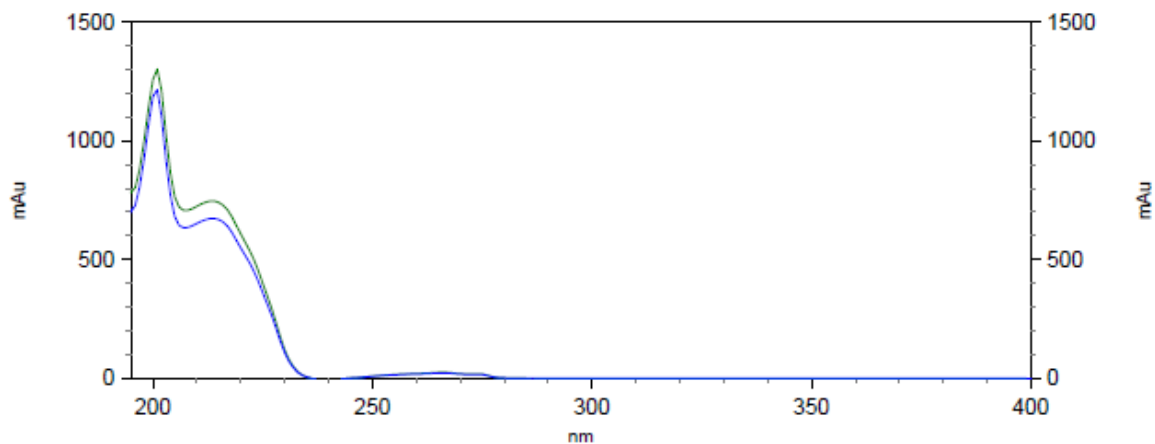
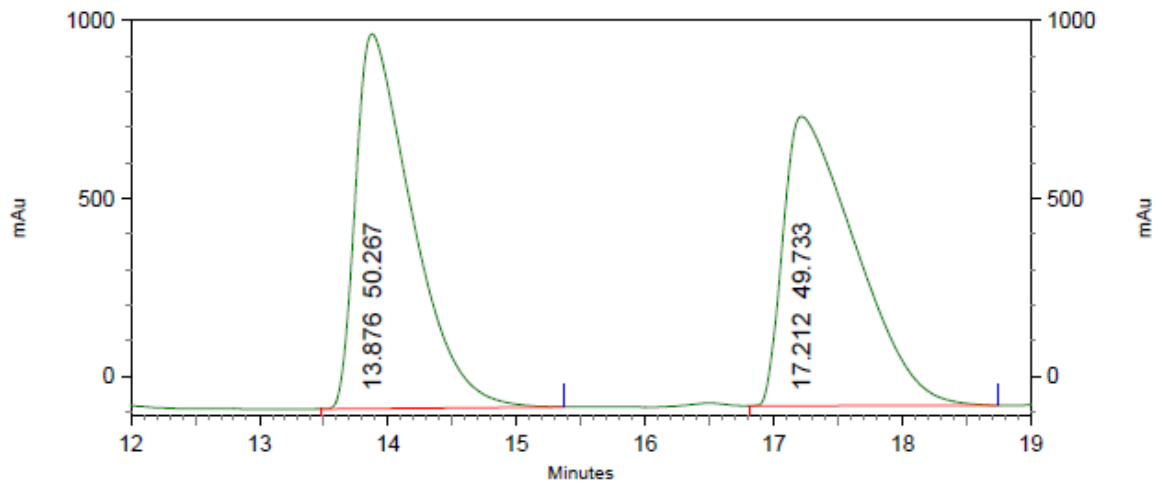
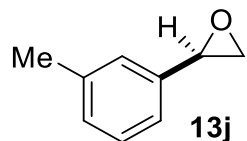


13j

Angew. Chem. Int. Ed. 2011, 50, 6056 –6059



Racemic
HPLC trace

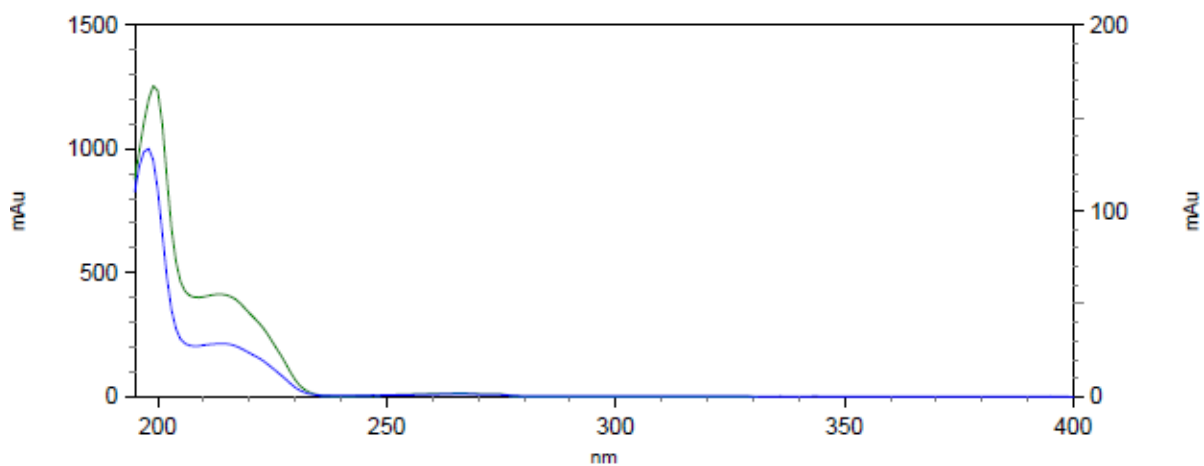
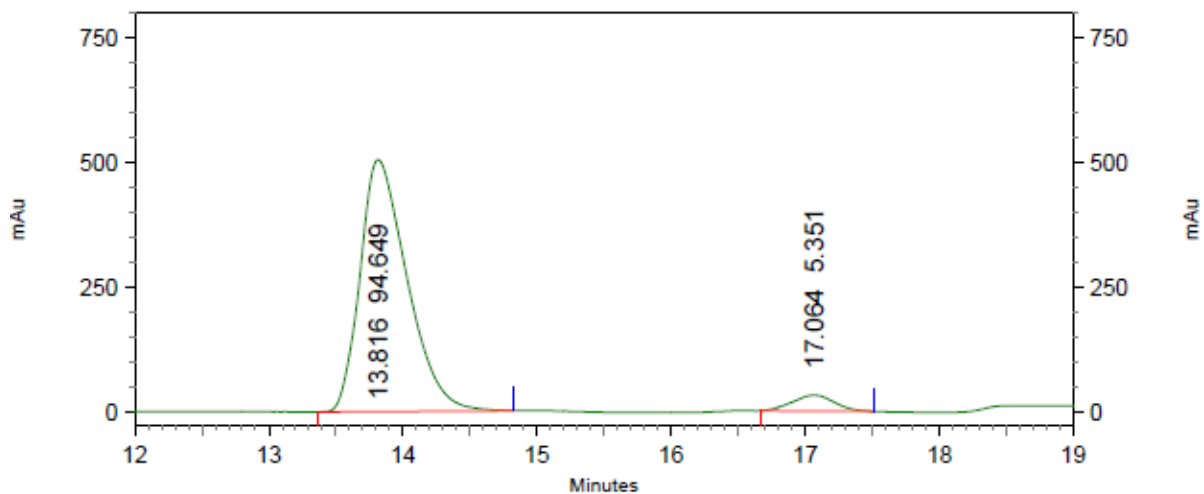
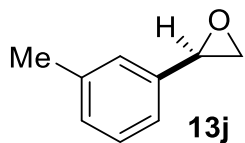


2: 205 nm, 4
nm Results

Pk #	Retention Time	Area Percent
1	13.876	50.267
2	17.212	49.733

Totals		100.000
--------	--	---------

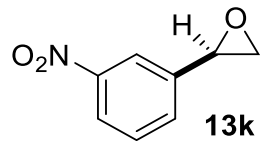
HPLC trace



2: 205 nm, 4
nm Results

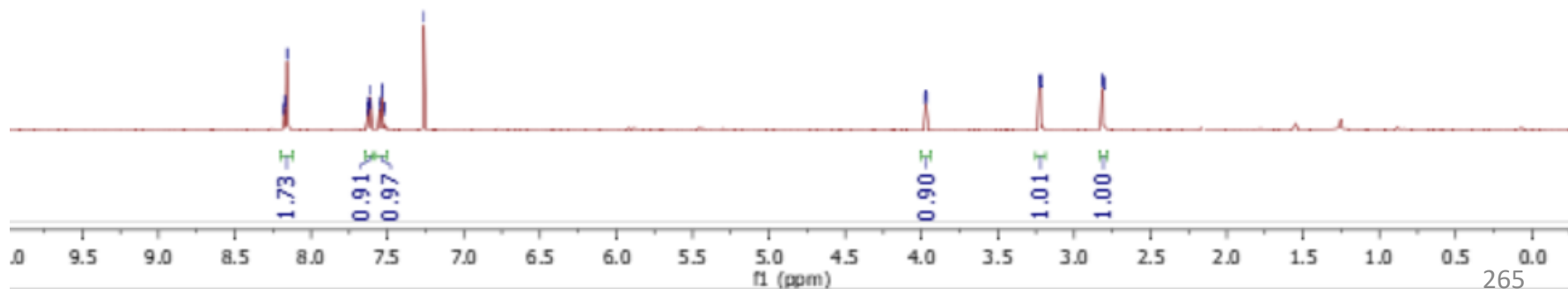
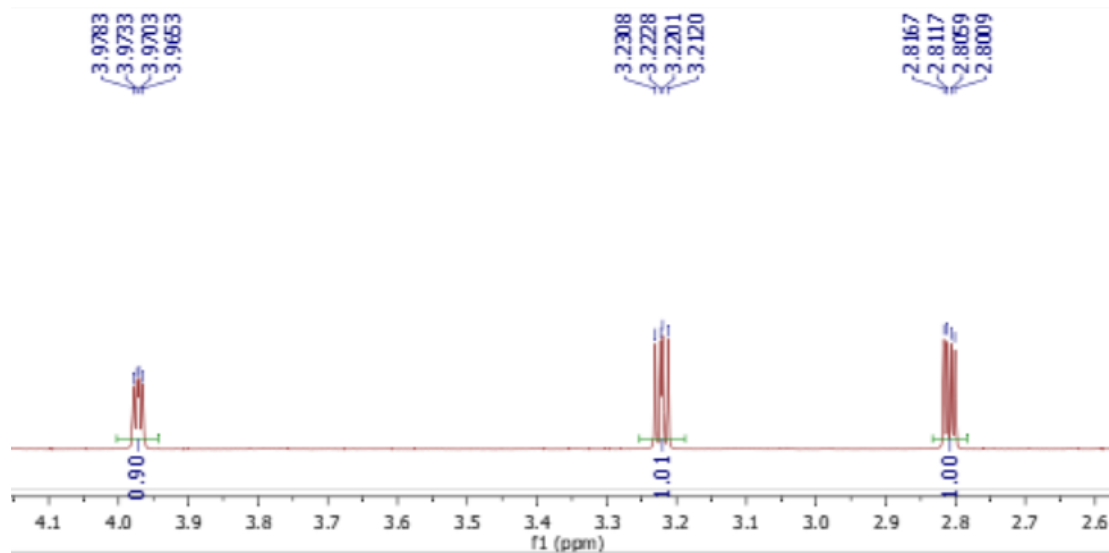
Pk #	Retention Time	Area Percent
1	13.816	94.649
2	17.064	5.351
Totals		100.000

¹HNMR

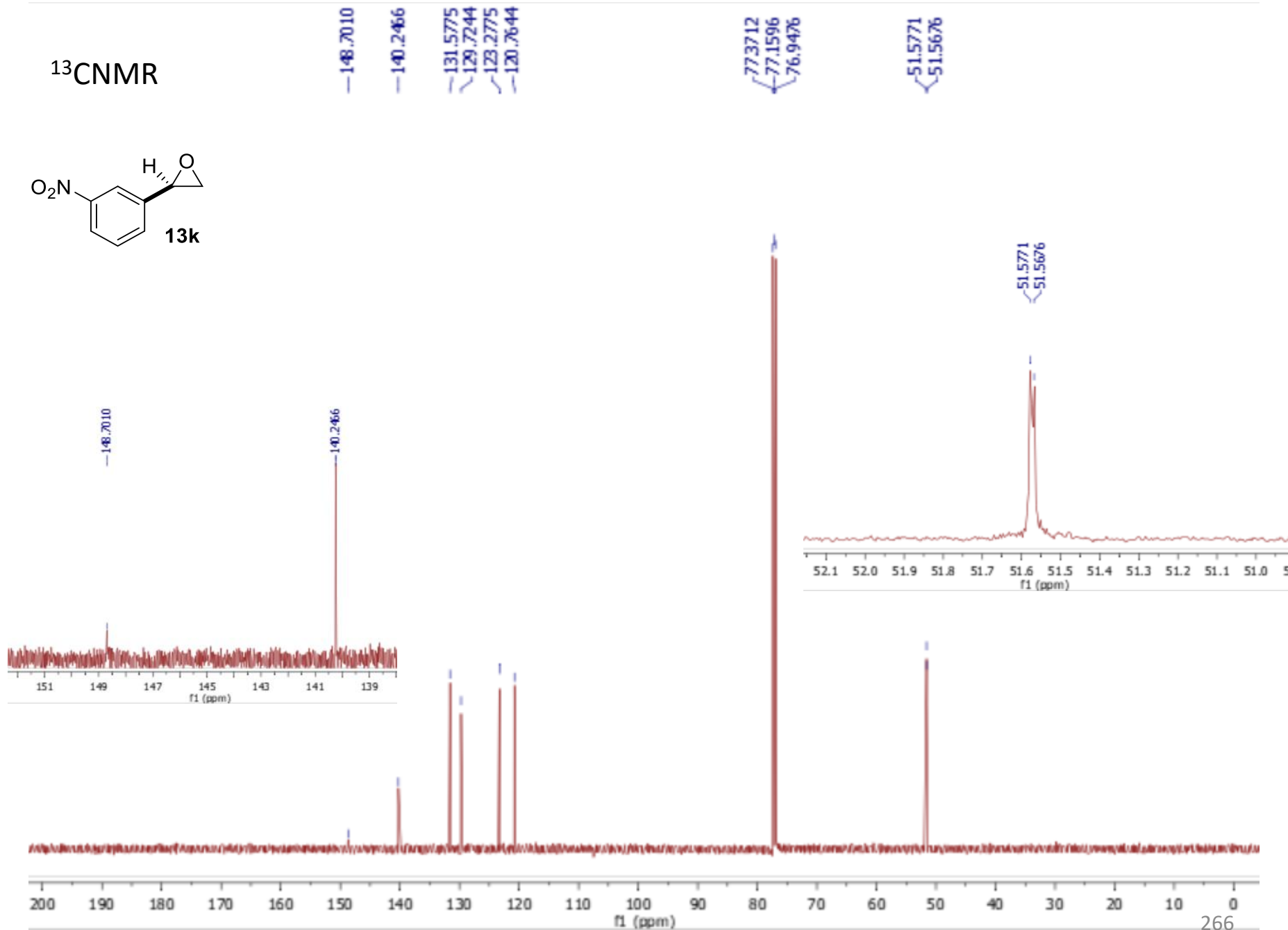
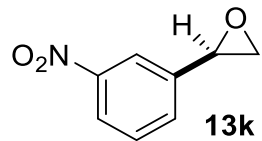


8.1780
8.1757
8.1734
8.1712
8.1581
8.1558
7.6286
7.6263
7.6239
7.6135
7.6109
7.6084
7.5507
7.5488
7.5355
7.5336
7.5200
7.5183
7.2605

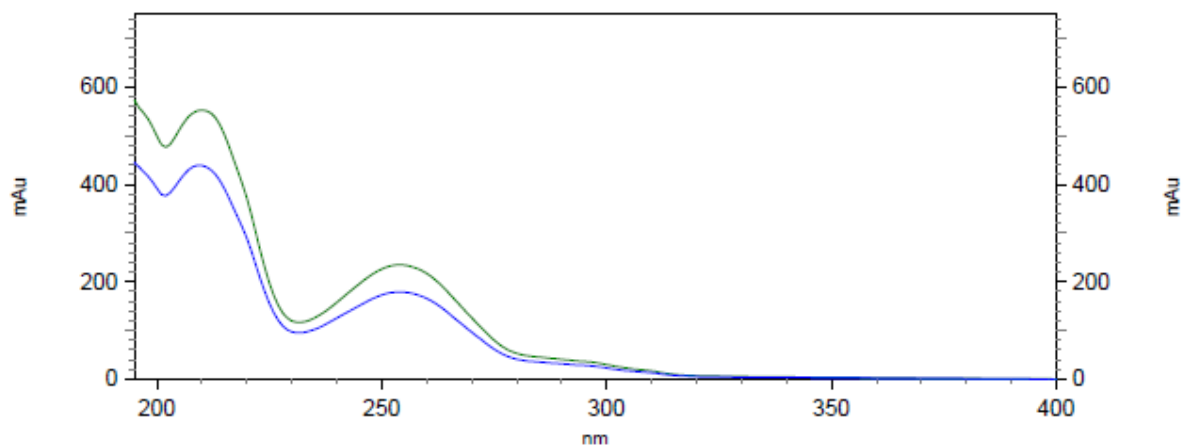
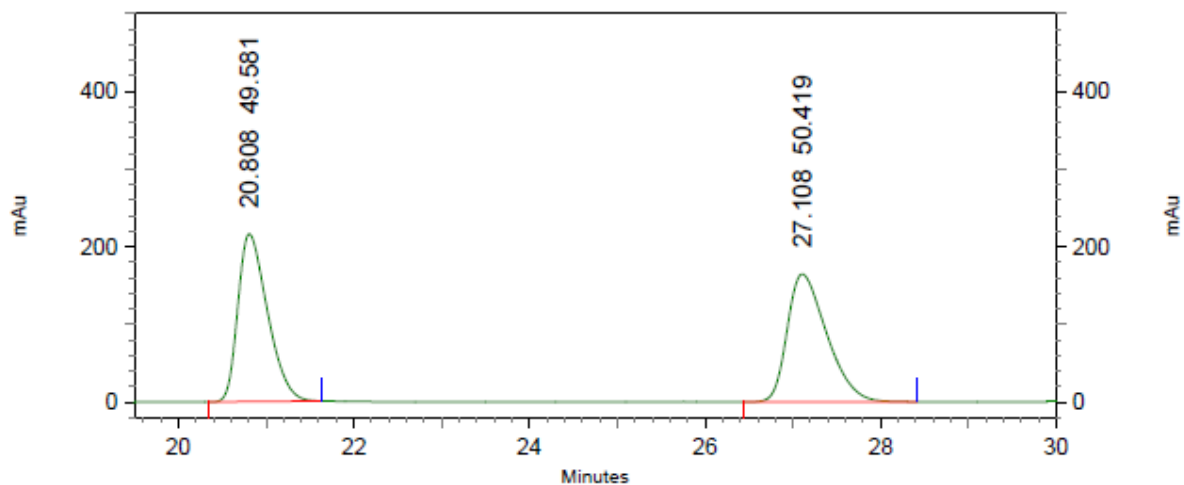
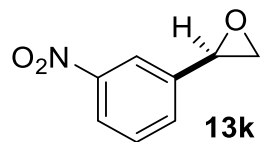
3.9783
3.9733
3.9703
3.9653
3.2228
3.2201
3.2129
2.8117
2.8059
2.8009



^{13}C NMR



Racemic
HPLC trace

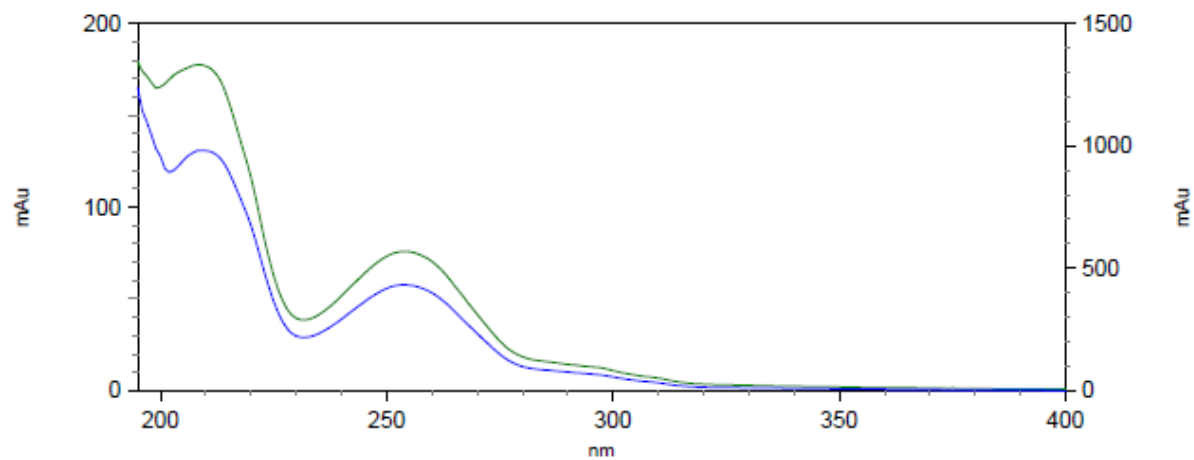
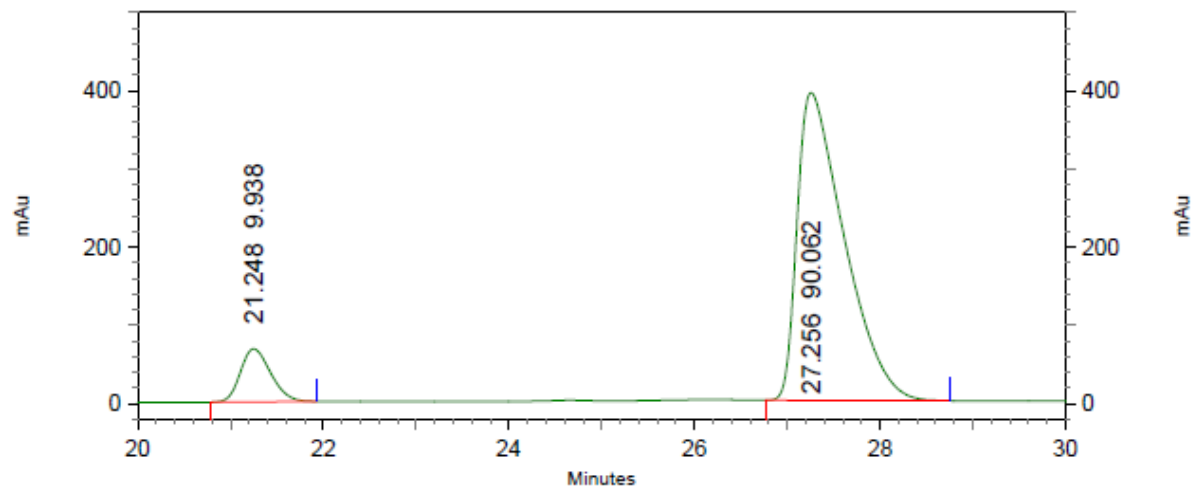
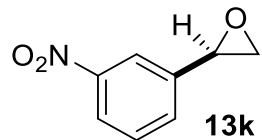


2: 260 nm, 4
nm Results

Pk #	Retention Time	Area Percent
1	20.808	49.581
2	27.108	50.419

Totals	100.000
--------	---------

HPLC trace

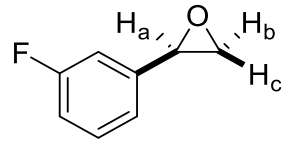


2: 260 nm, 4
nm Results

Pk #	Retention Time	Area Percent
1	21.248	9.938
2	27.256	90.062

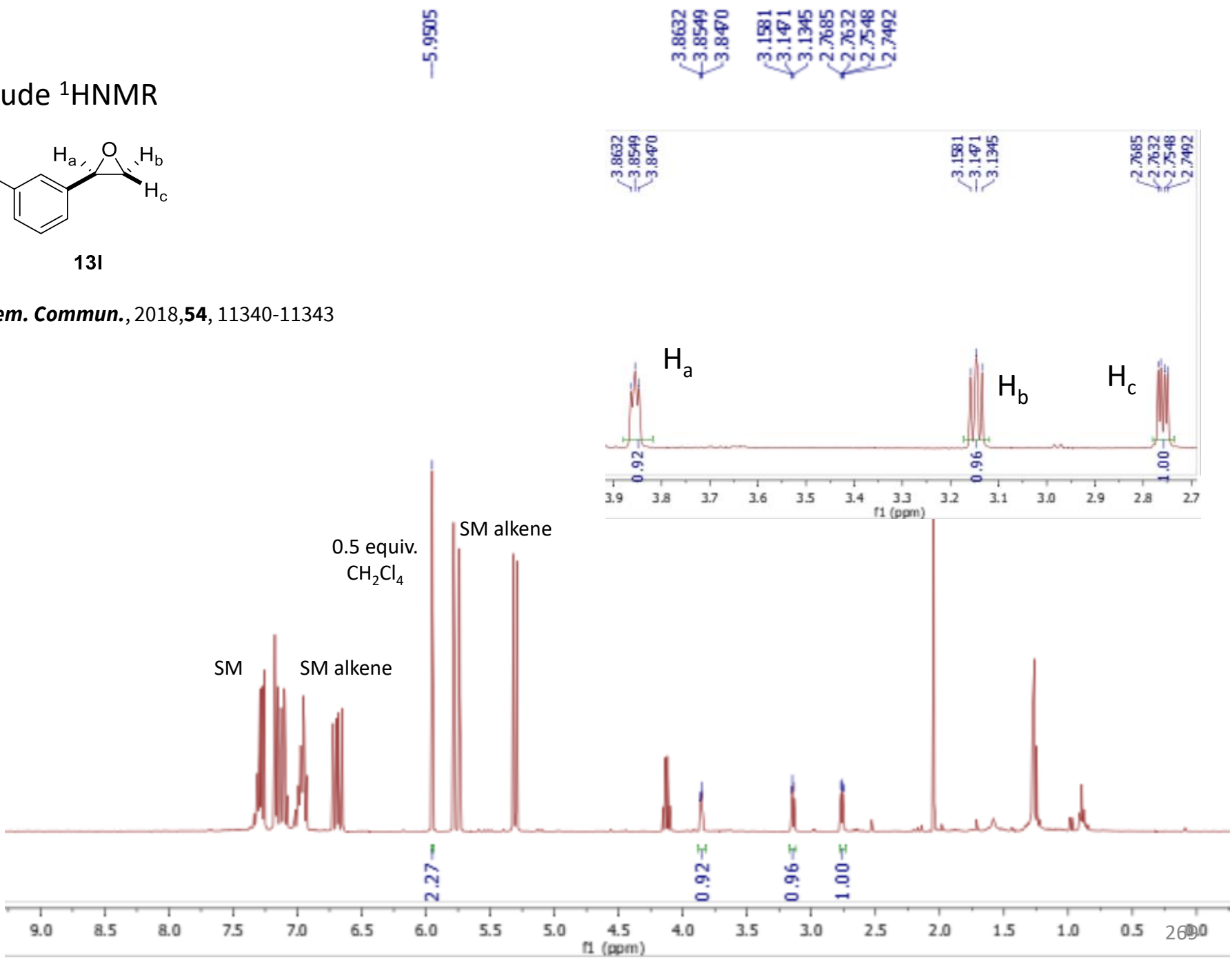
Totals		100.000
--------	--	---------

Crude ¹HNMR

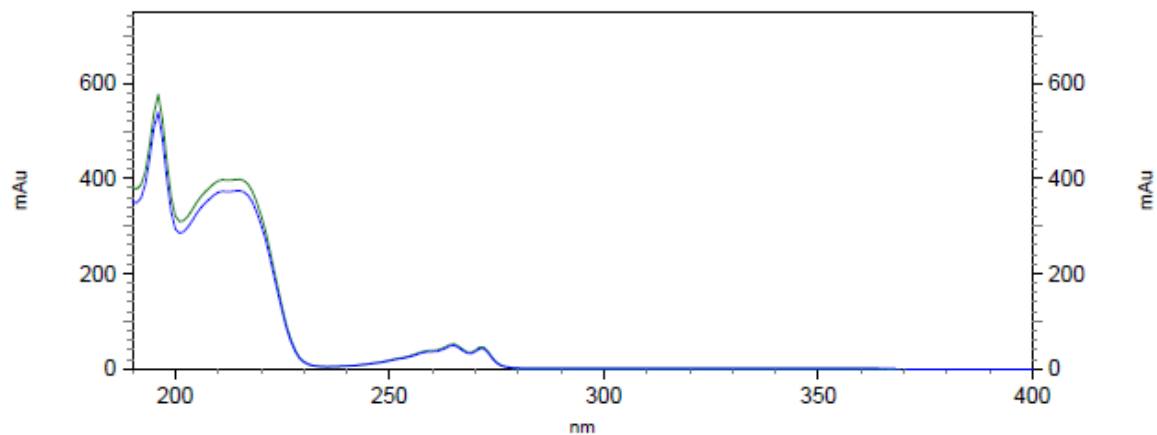
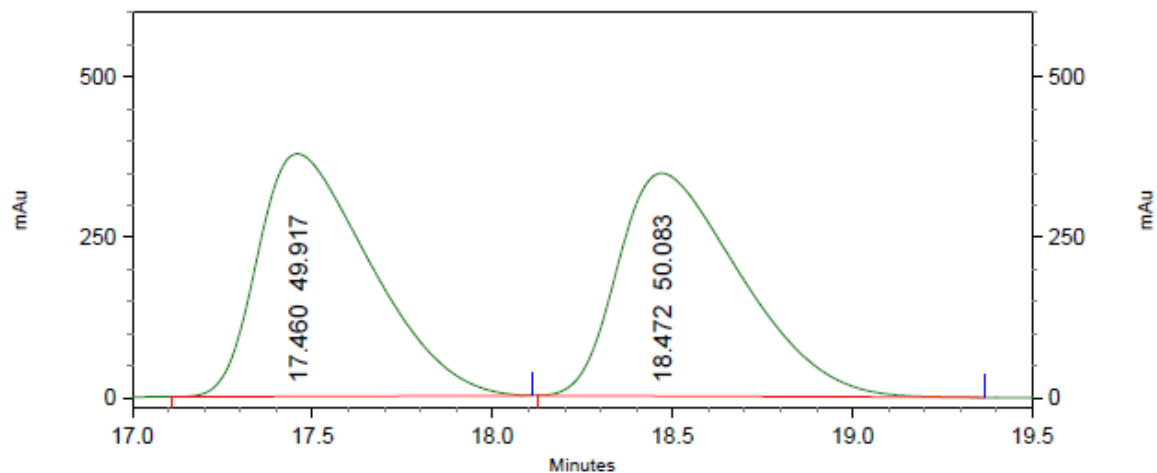
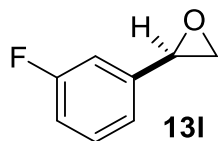


13I

Chem. Commun., 2018, 54, 11340-11343



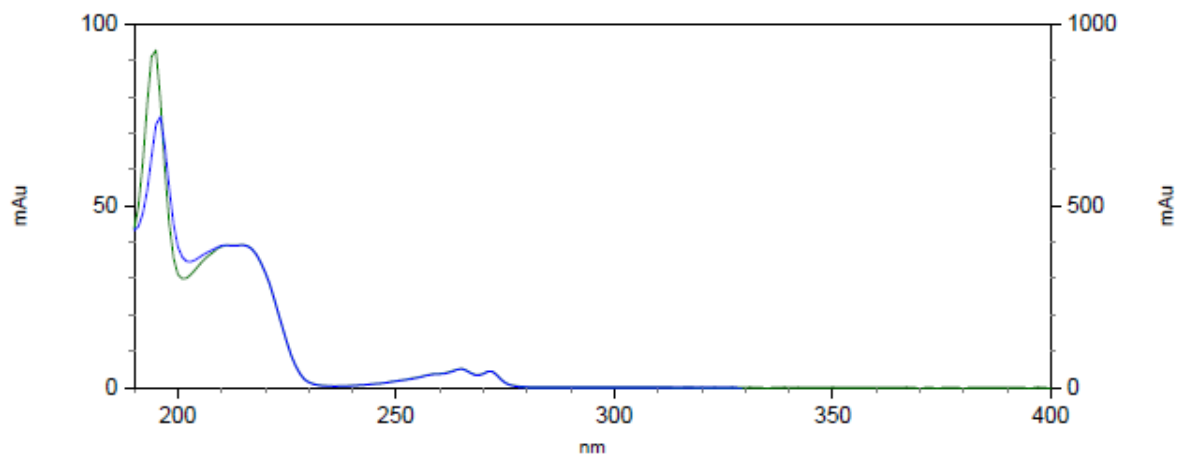
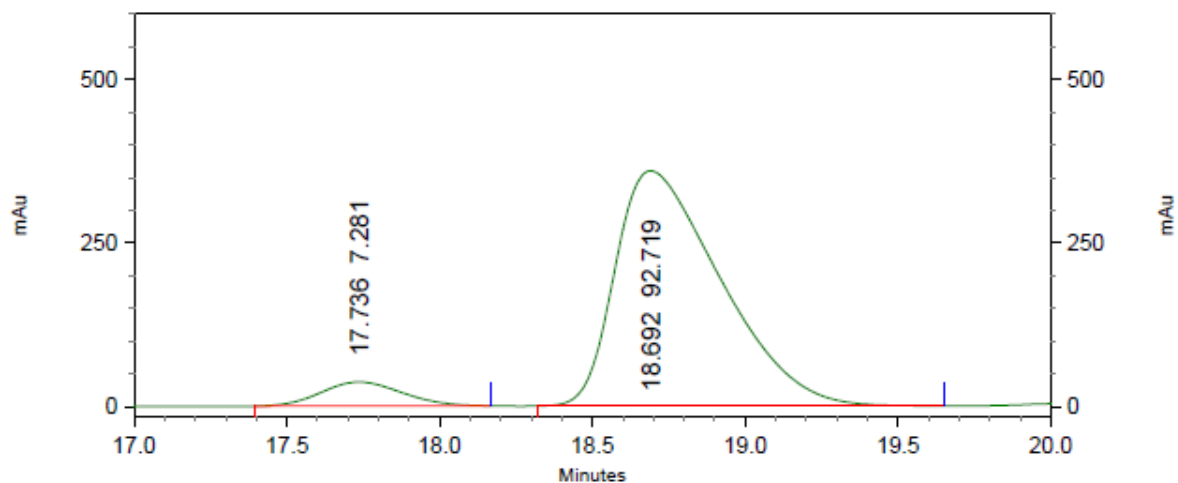
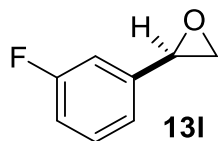
Racemic HPLC trace



4: 218 nm, 4
nm Results

Pk #	Retention Time	Area Percent
1	17.460	49.917
2	18.472	50.083
Totals		100.000

HPLC trace

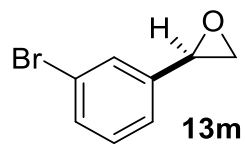


4: 218 nm, 4
nm Results

Pk #	Retention Time	Area Percent
1	17.736	7.281
2	18.692	92.719

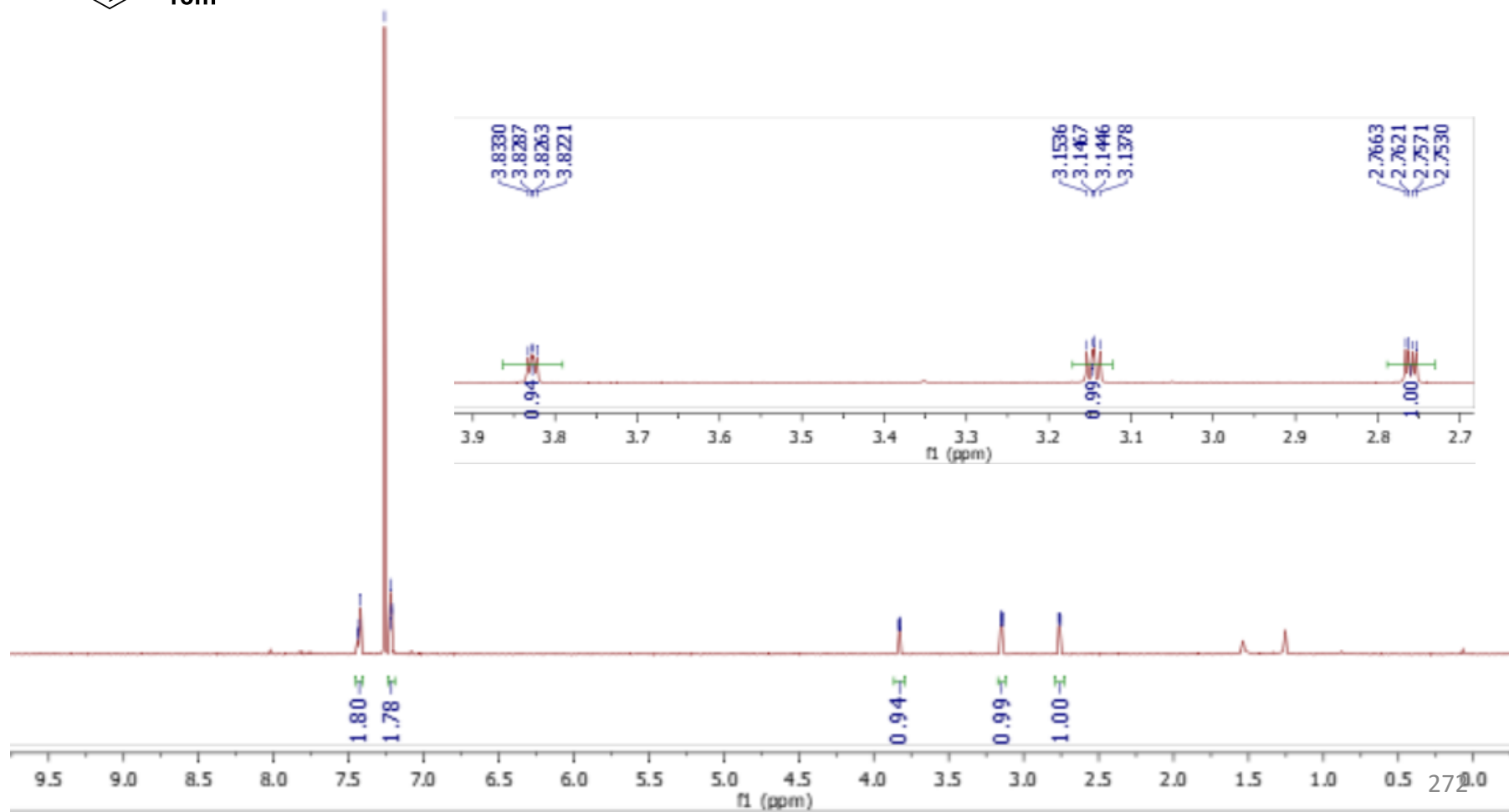
Totals	100.000
--------	---------

¹H NMR

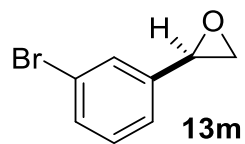


7.4429
7.4395
7.4316
7.4202
7.2601
7.2219
7.2170
7.2142
7.2123

3.8330
3.8287
3.8263
3.8221
3.1467
3.1446
3.1378
2.7621
2.7571
2.7530



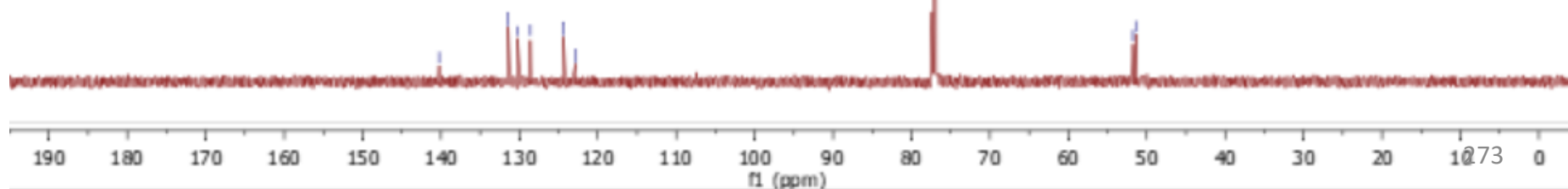
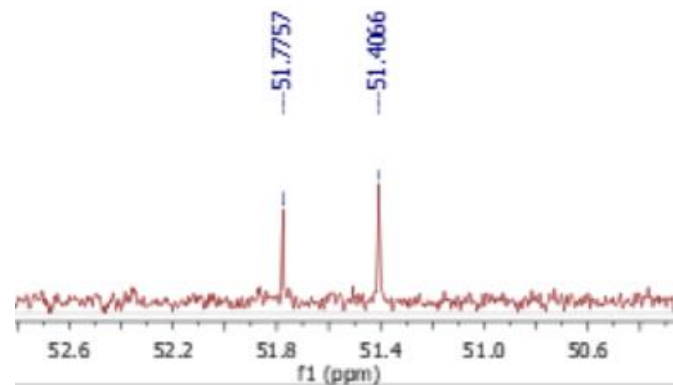
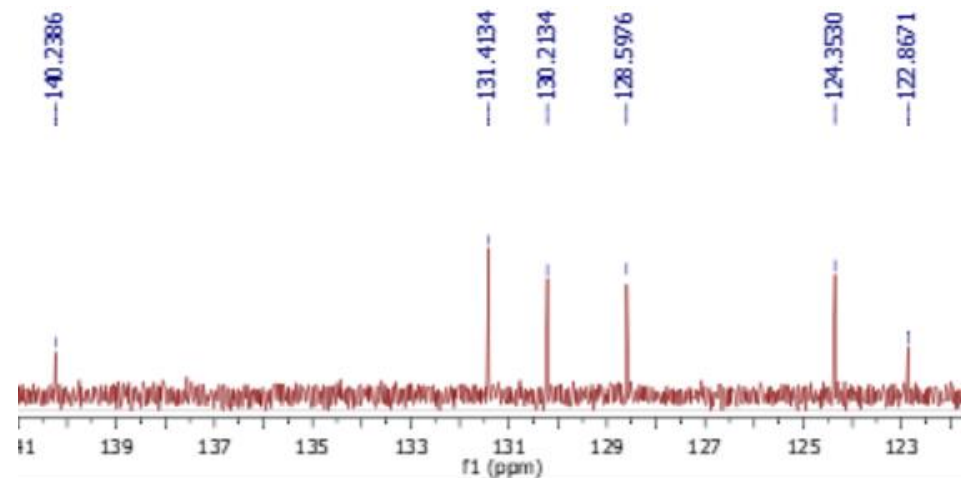
¹³CNMR



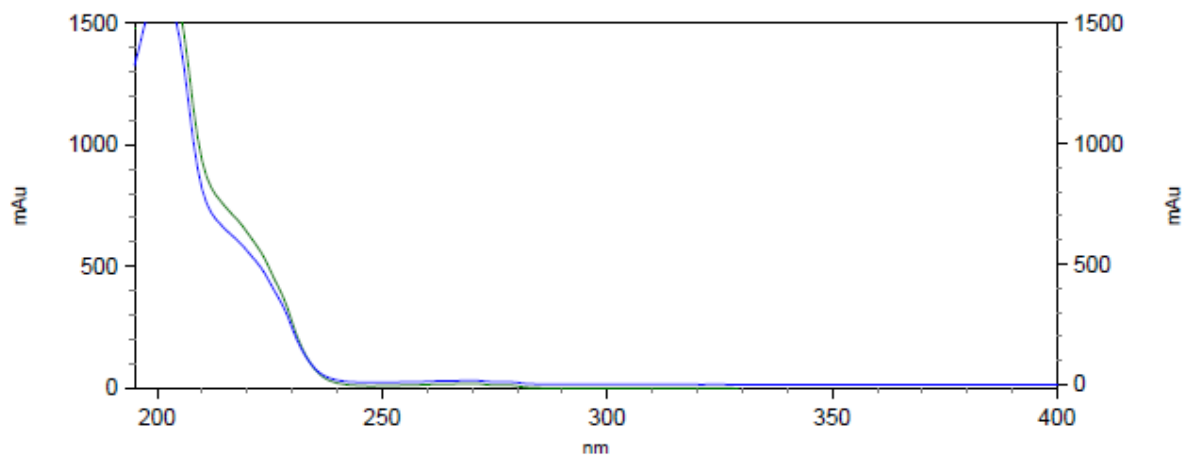
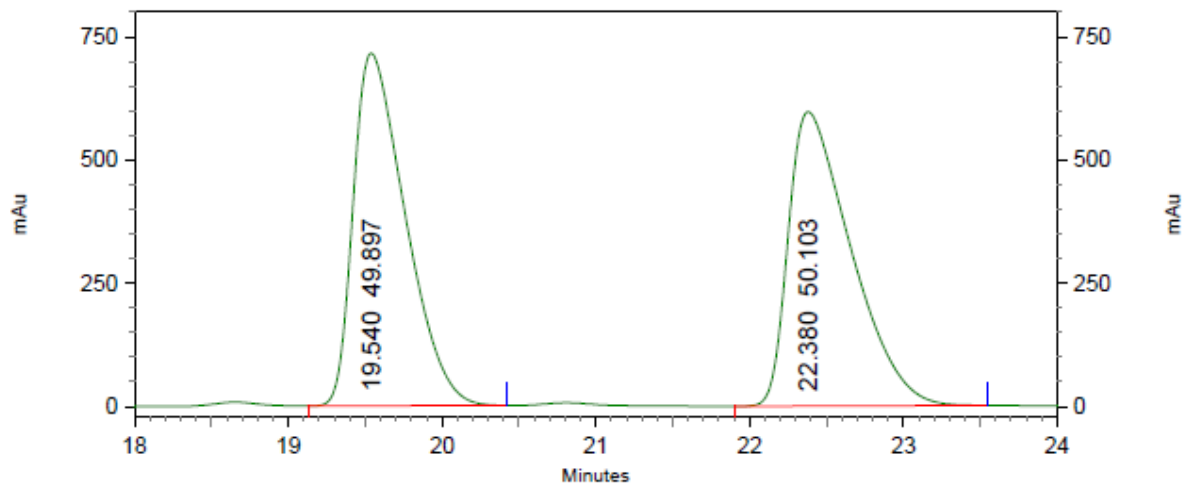
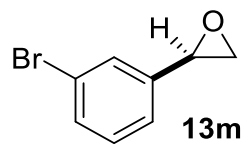
140.2386
131.4134
130.2134
128.5976
124.3530
122.8671

77.3712
77.1595
76.9477

51.7757
51.4066



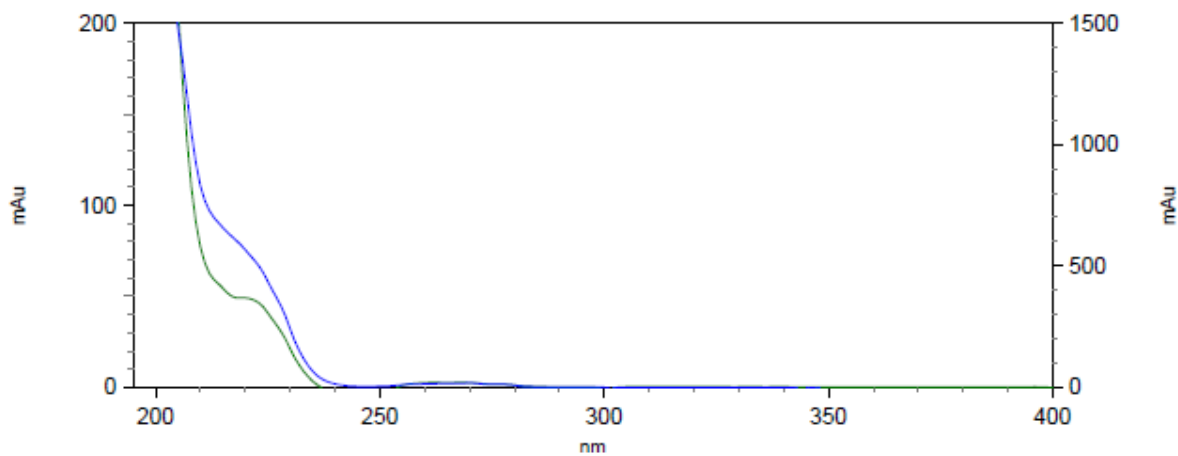
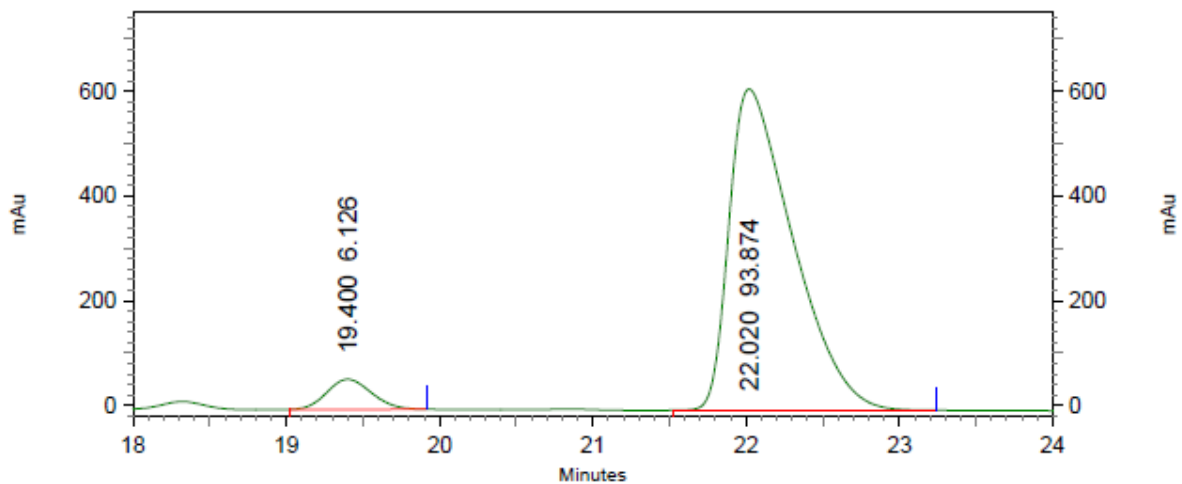
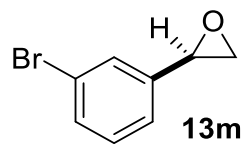
Racemic
HPLC trace



2: 218 nm, 4
nm Results

Pk #	Retention Time	Area Percent
1	19.540	49.897
2	22.380	50.103
Totals		100.000

HPLC trace

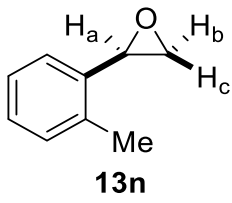


2: 218 nm, 4
nm Results

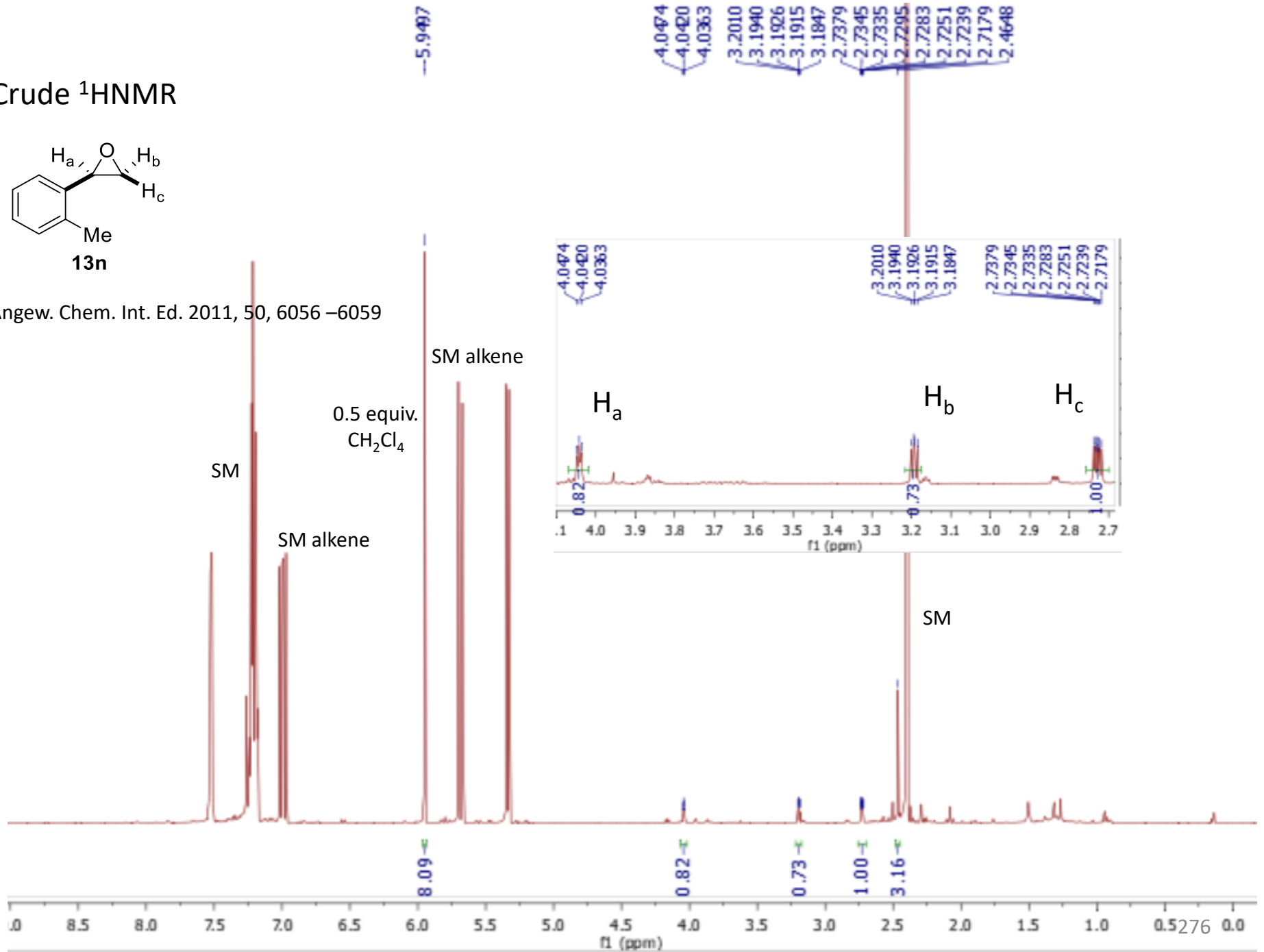
Pk #	Retention Time	Area Percent
1	19.400	6.126
2	22.020	93.874

Totals		100.000
--------	--	---------

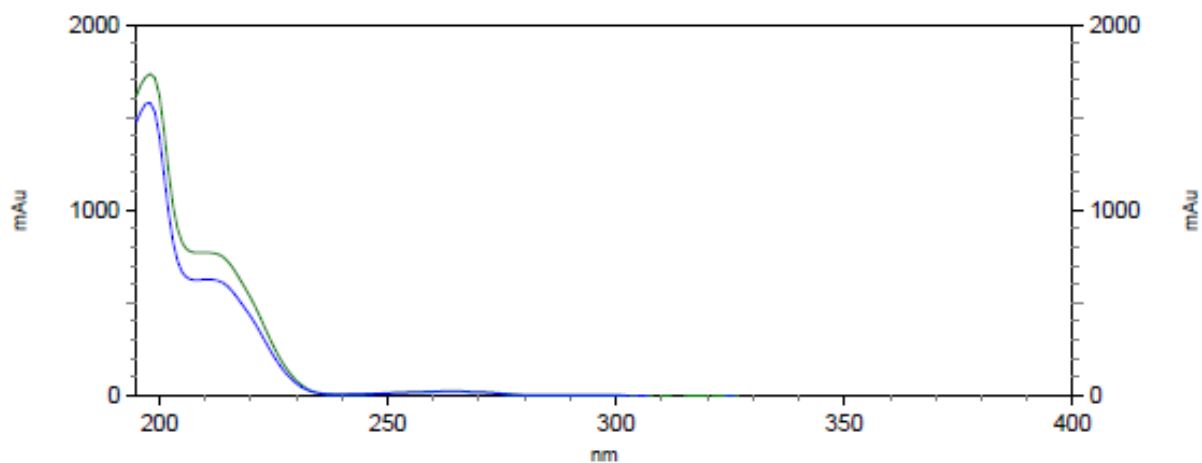
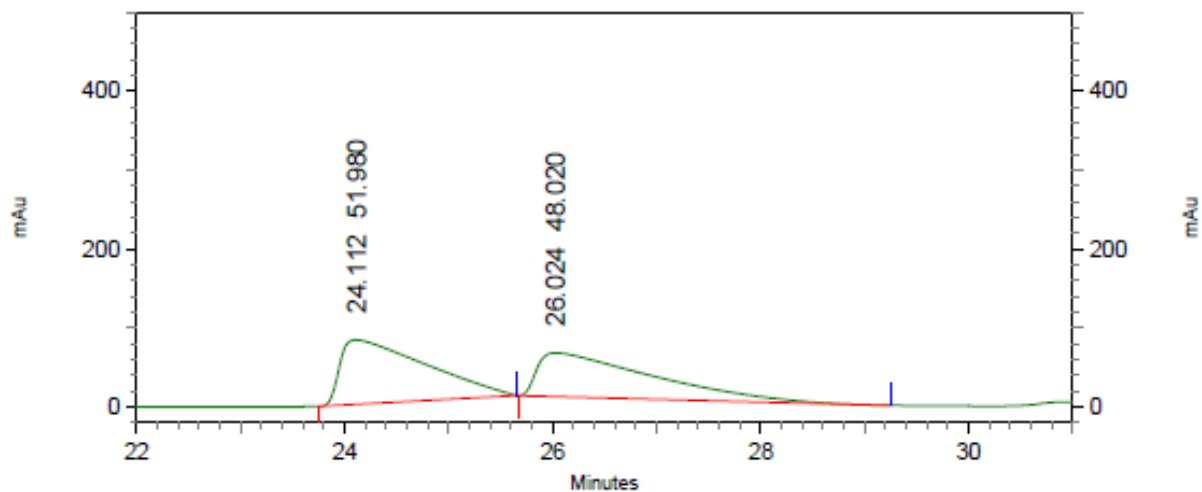
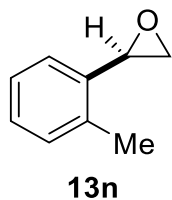
Crude ¹HNMR



Angew. Chem. Int. Ed. 2011, 50, 6056 –6059



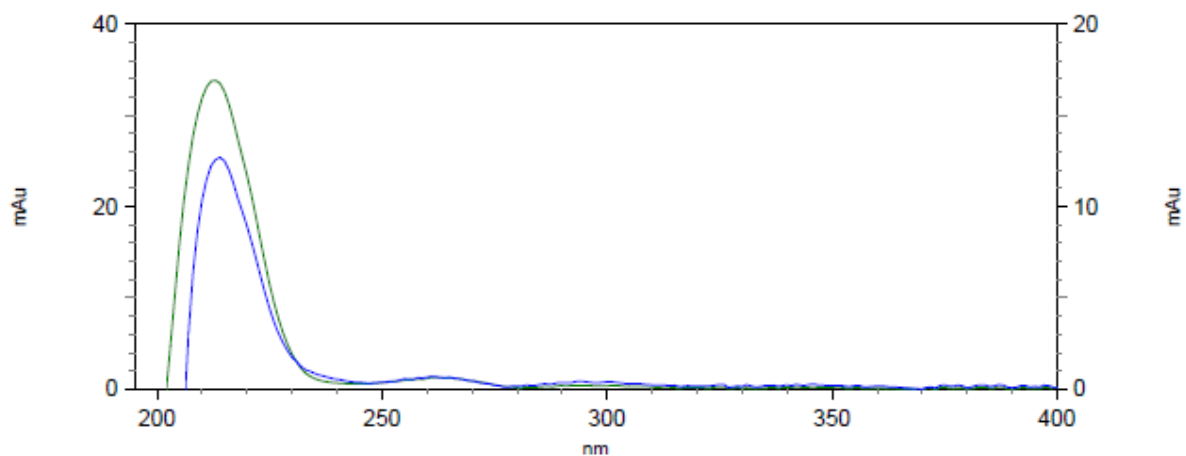
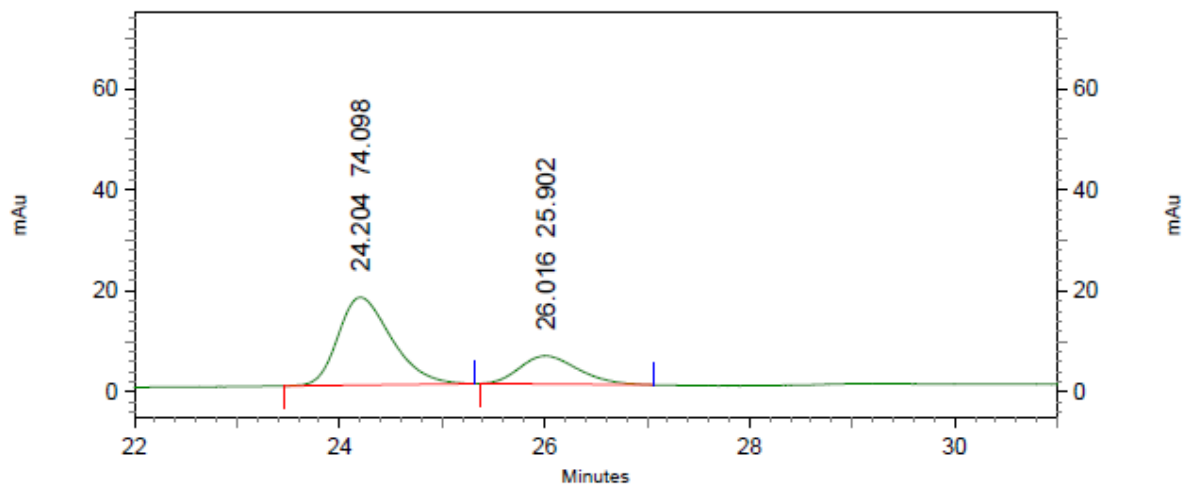
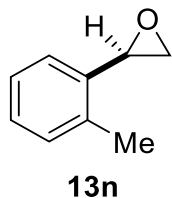
Racemic HPLC trace



4: 230 nm, 4
nm Results

Pk #	Retention Time	Area Percent
1	24.112	51.980
2	26.024	48.020
Totals		100.000

HPLC trace

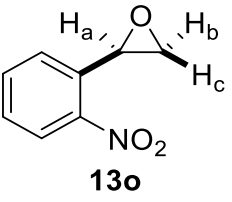


4: 222 nm, 4
nm Results

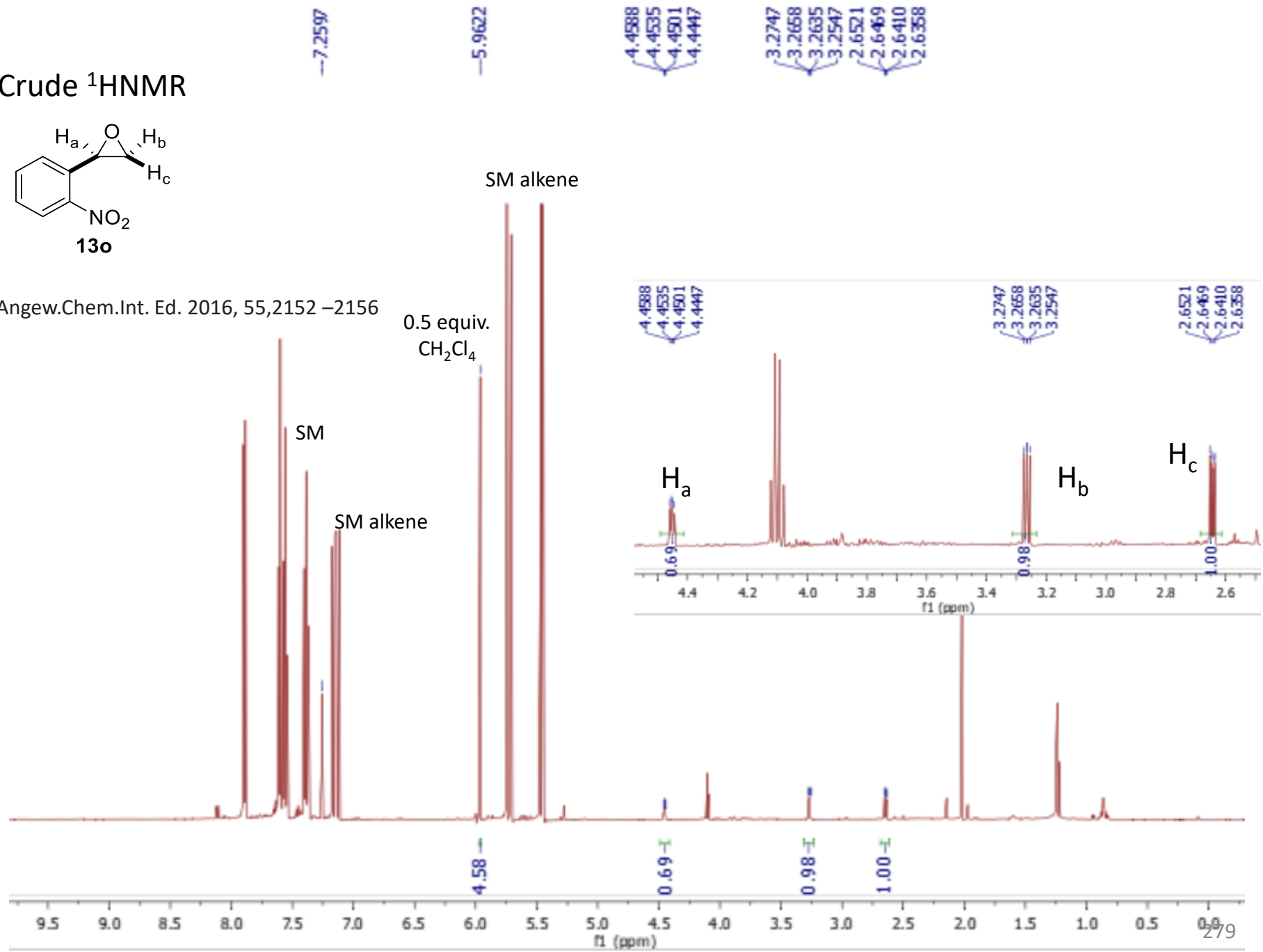
Pk #	Retention Time	Area Percent
1	24.204	74.098
2	26.016	25.902

Totals	100.000
--------	---------

Crude ¹H NMR

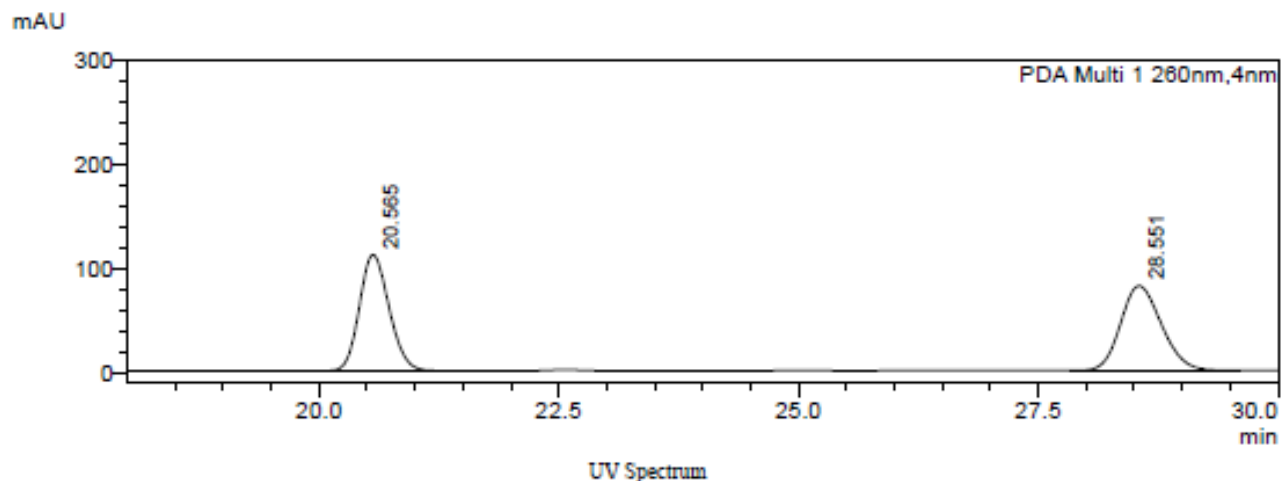
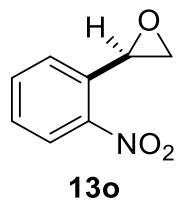


Angew.Chem.Int. Ed. 2016, 55,2152 –2156

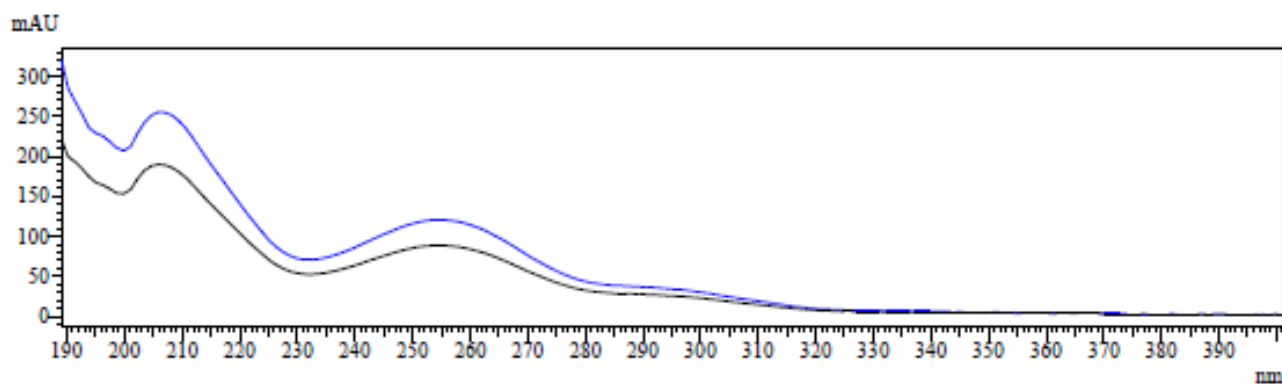


Sample Name : XRF-1852-RAC-IF-3%

Racemic
HPLC trace



XRF-1852-RAC-IF-3%_001.lcd



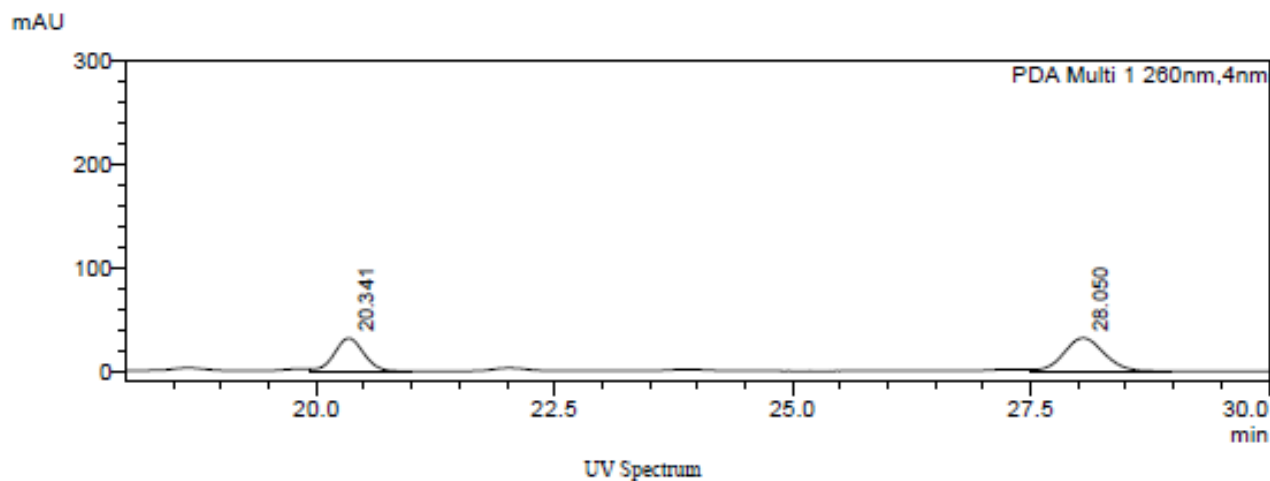
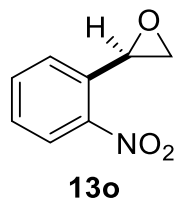
Peak Table

PDA Ch1 260nm

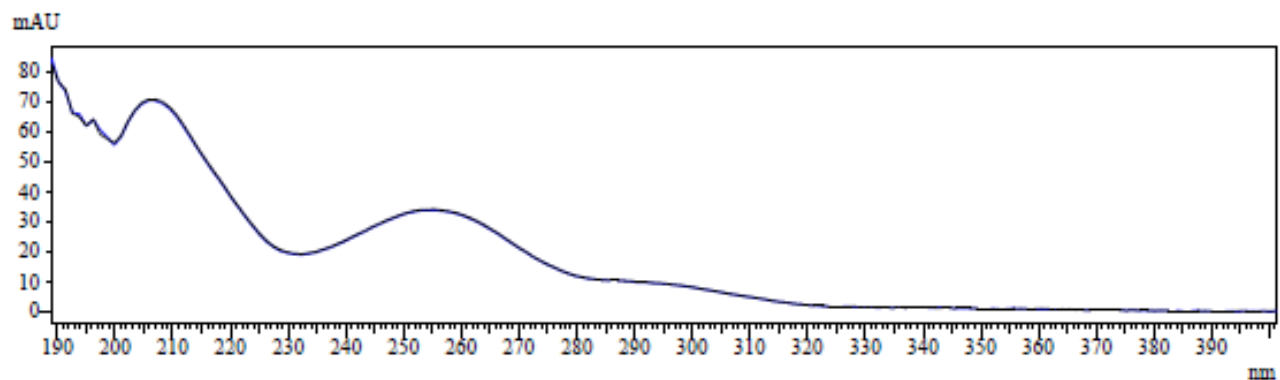
Peak#	Ret. Time	Area%
1	20.565	49.961
2	28.551	50.039
Total		100.000

Sample Name : XRF-1852-IF-3%

HPLC trace



XRF-1852-IF-3%_002.lcd

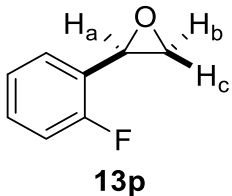


Peak Table

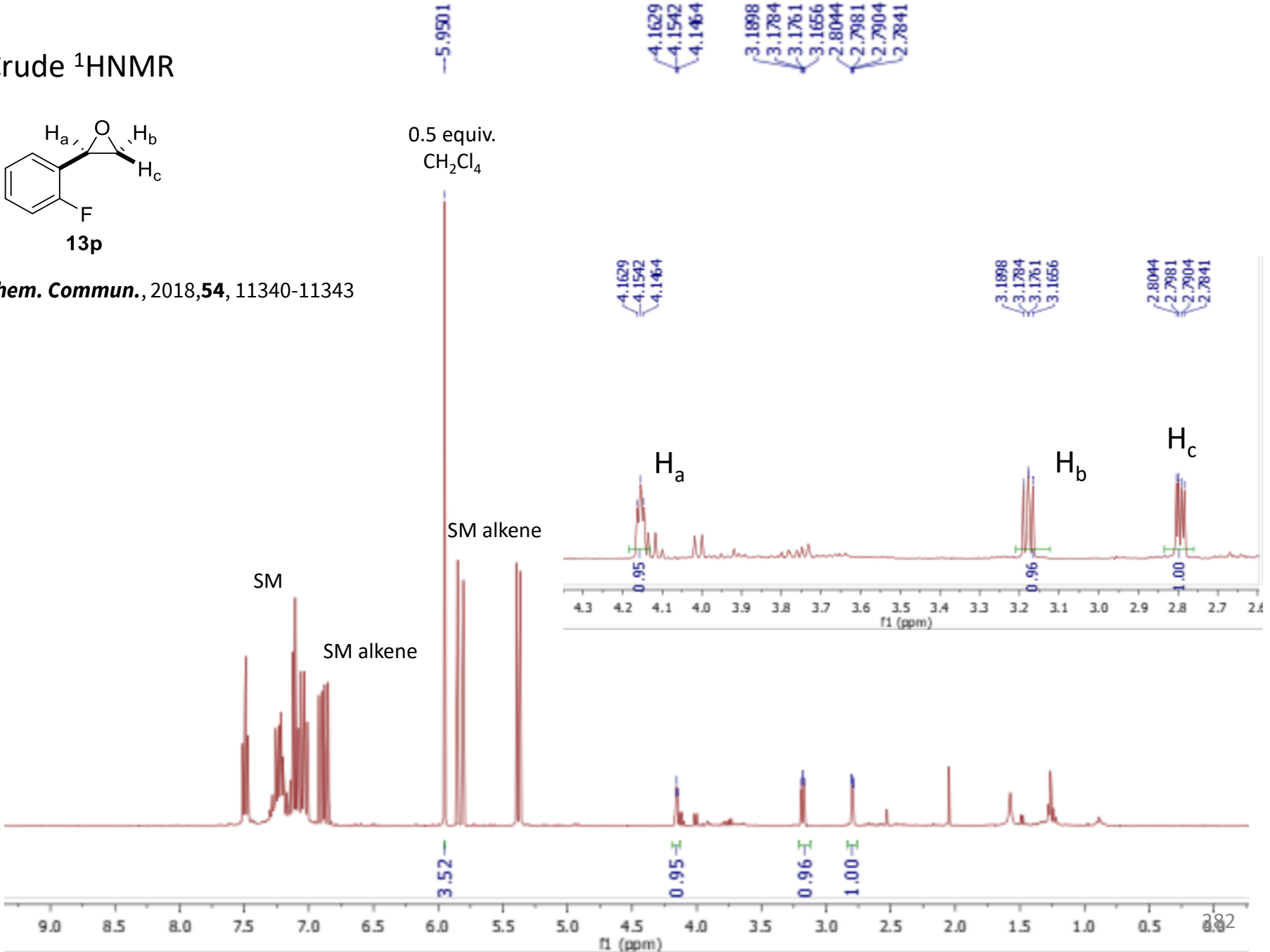
PDA Ch1 260nm

Peak#	Ret. Time	Area%
1	20.341	42.344
2	28.050	57.656
Total		100.000

Crude ¹HNMR

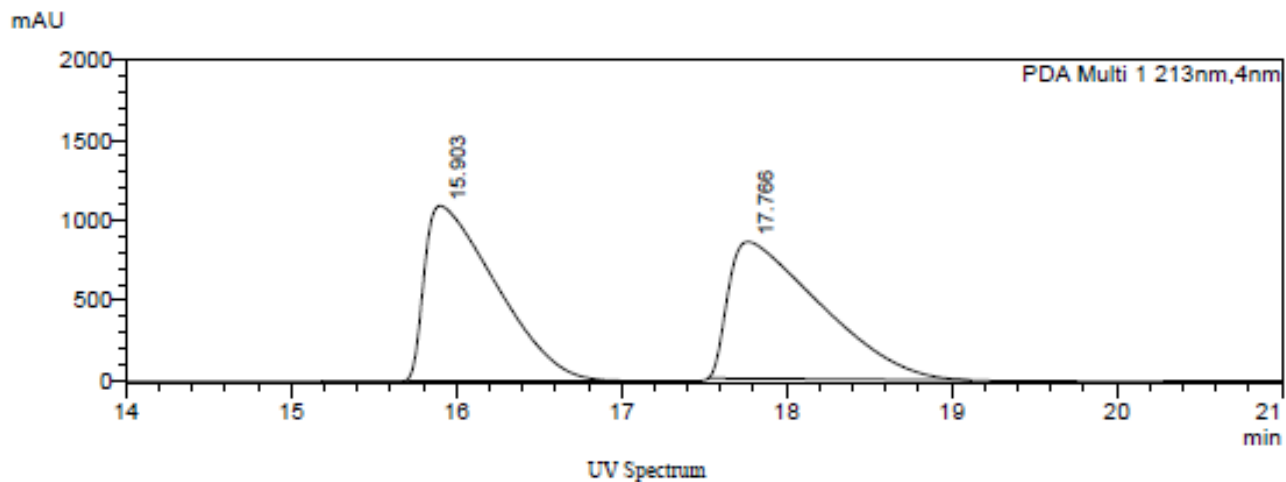
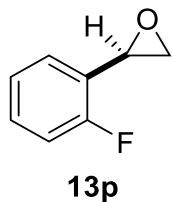


Chem. Commun., 2018, **54**, 11340-11343

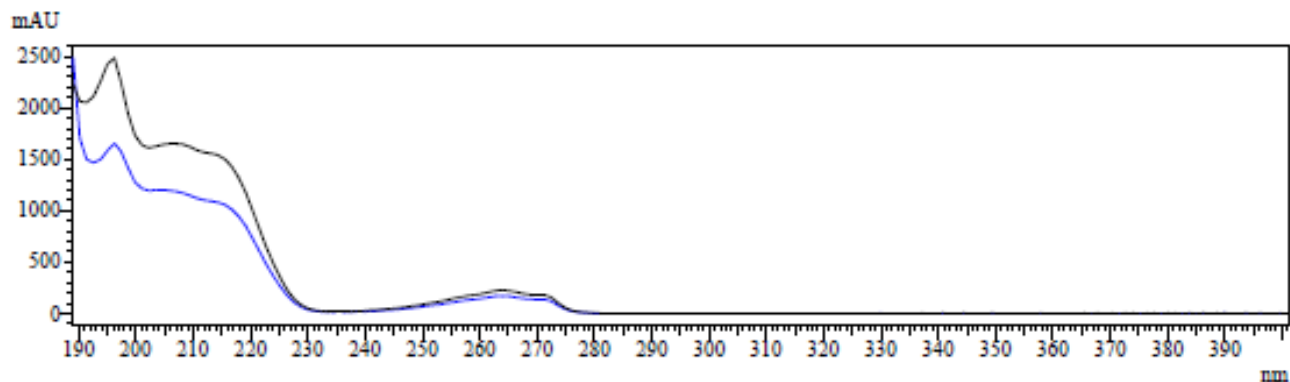


Sample Name : XRF-1709-RAC-ID-1%-2

Racemic
HPLC trace



XRF-1709-RAC-ID-1%-2_002.lcd



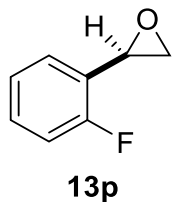
Peak Table

PDA Ch1 213nm

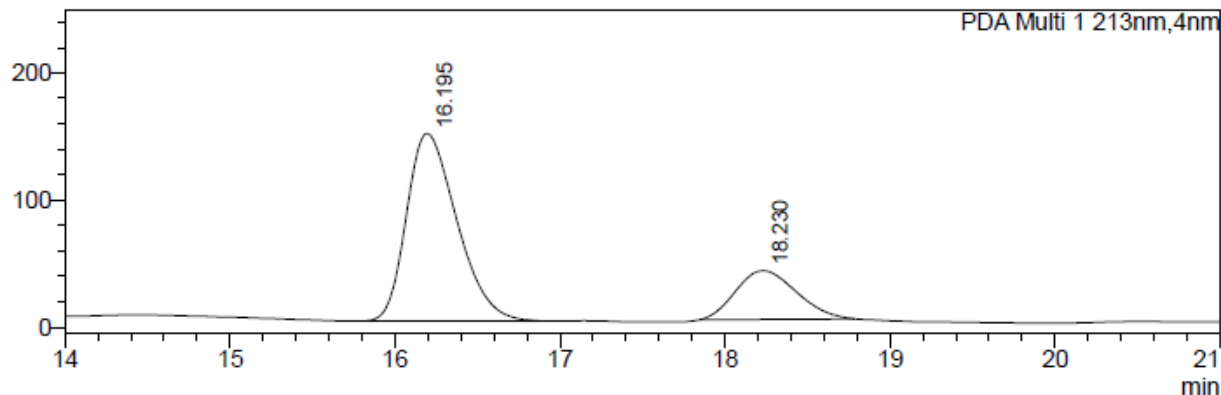
Peak#	Ret. Time	Area%
1	15.903	49.857
2	17.766	50.143
Total		100.000

Sample Name : XRF-1709-ID-1%-2

HPLC trace

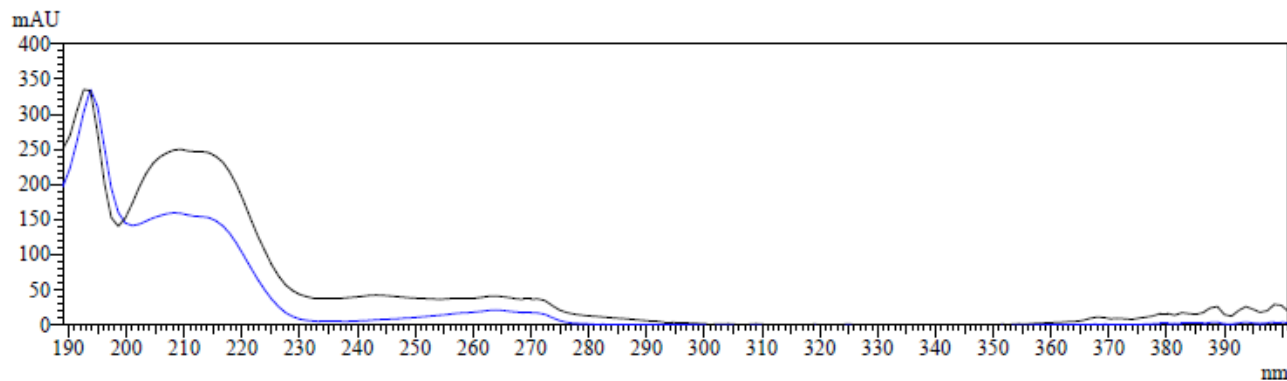


mAU



UV Spectrum

XRF-1709-ID-1%-2_001.lcd

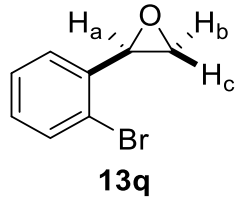


Peak Table

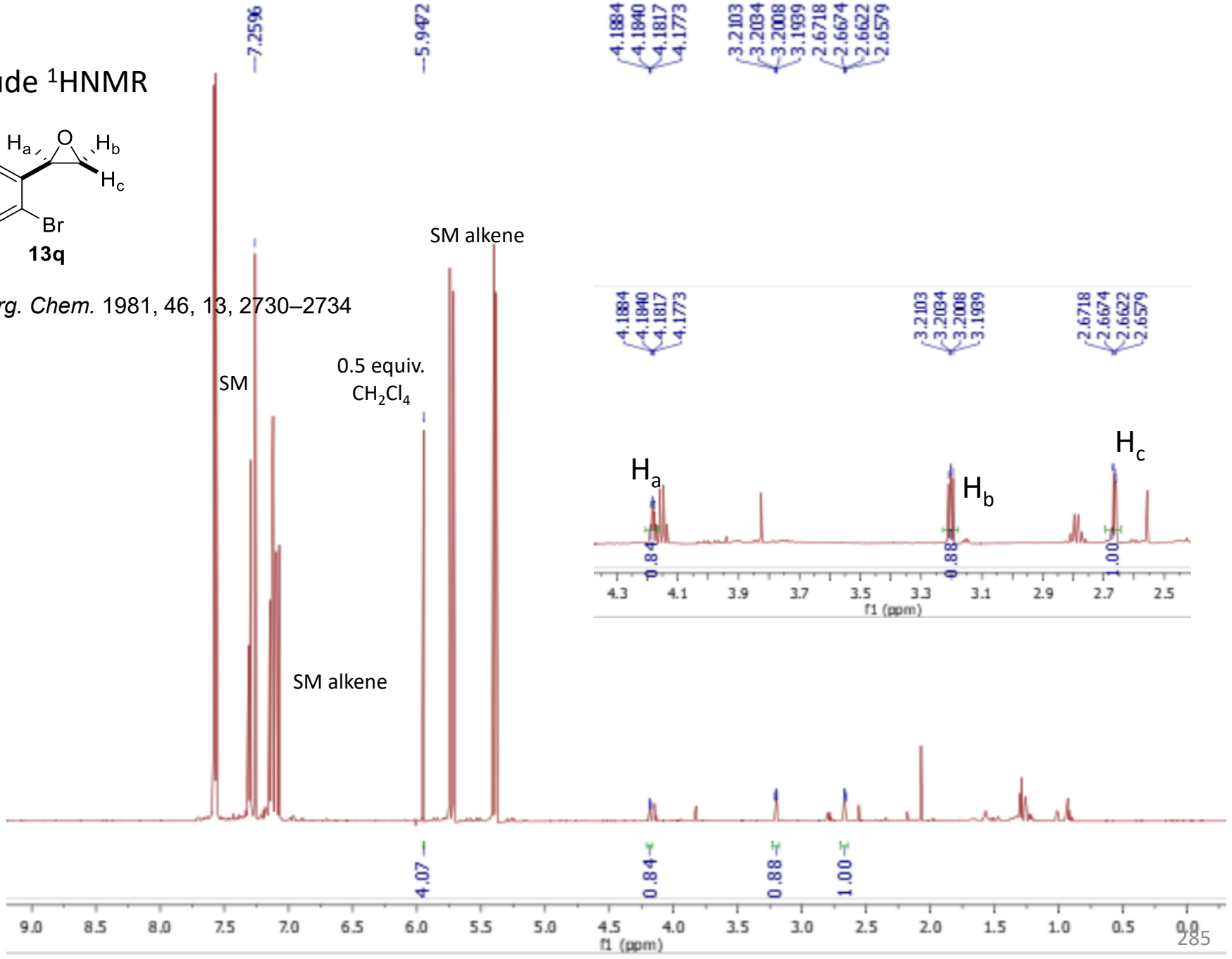
PDA Ch1 213nm

Peak#	Ret. Time	Area%
1	16.195	76.143
2	18.230	23.857
Total		100.000

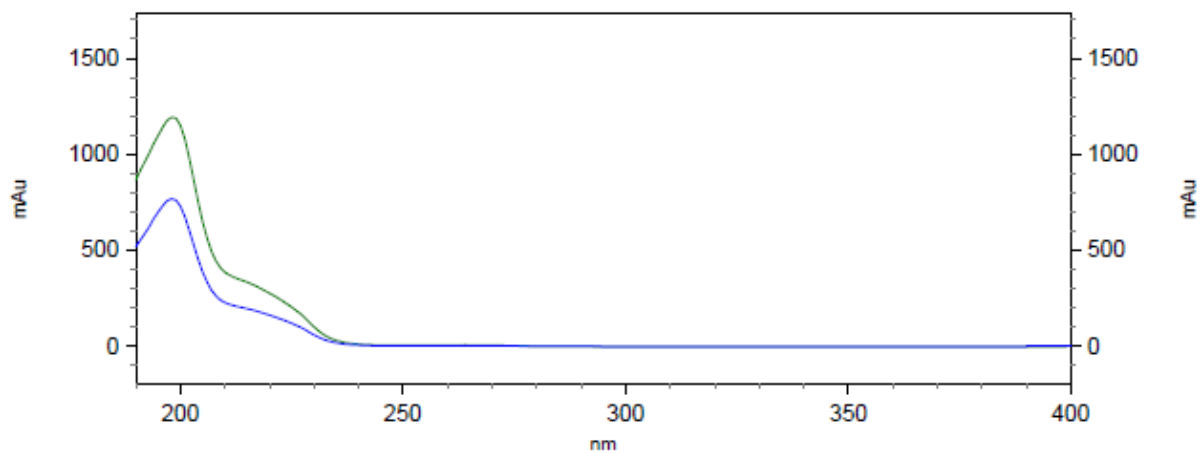
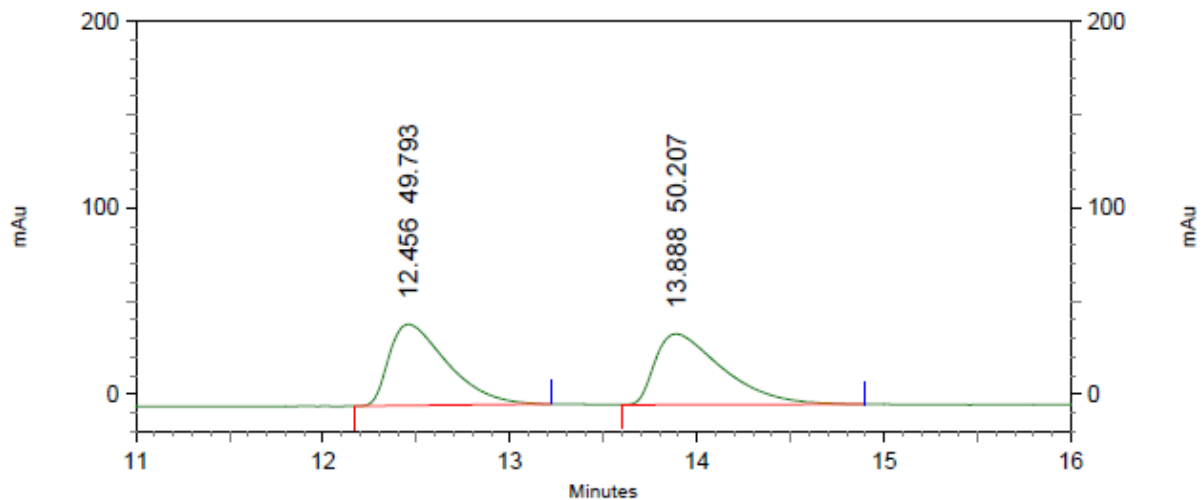
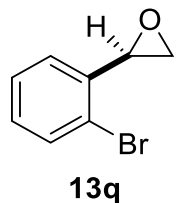
Crude ¹H NMR



J. Org. Chem. 1981, 46, 13, 2730–2734



Racemic HPLC trace

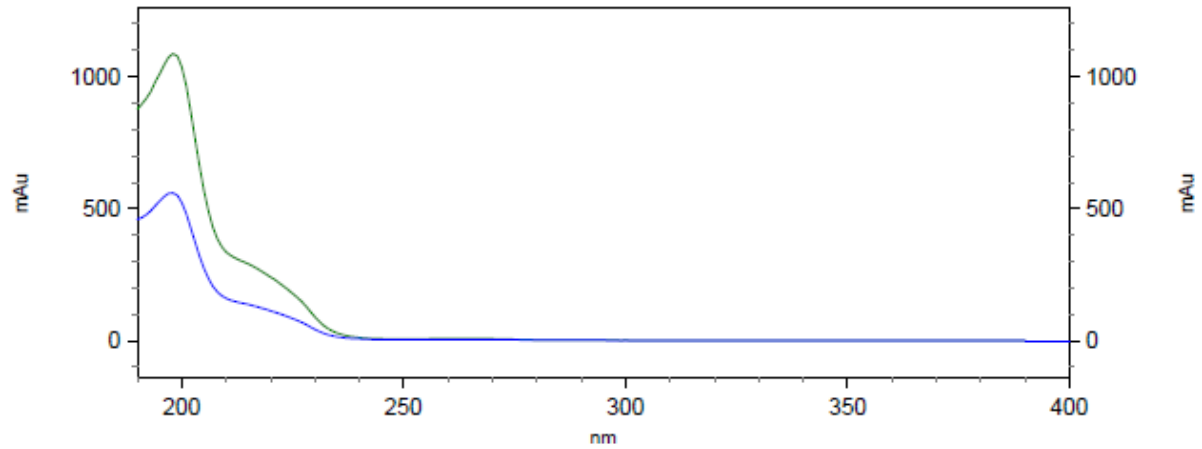
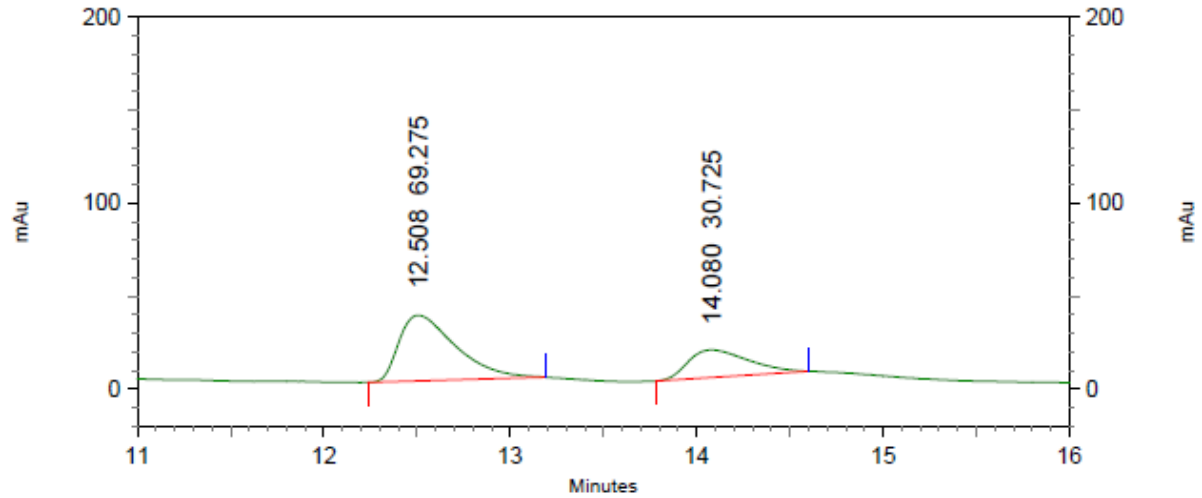
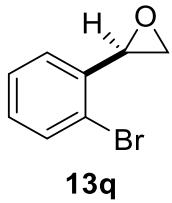


4: 237 nm, 4
nm Results

Pk #	Retention Time	Area Percent
1	12.456	49.793
2	13.888	50.207

Totals		100.000
--------	--	---------

HPLC trace

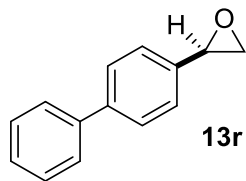


4: 237 nm, 4
nm Results

Pk #	Retention Time	Area Percent
1	12.508	69.275
2	14.080	30.725

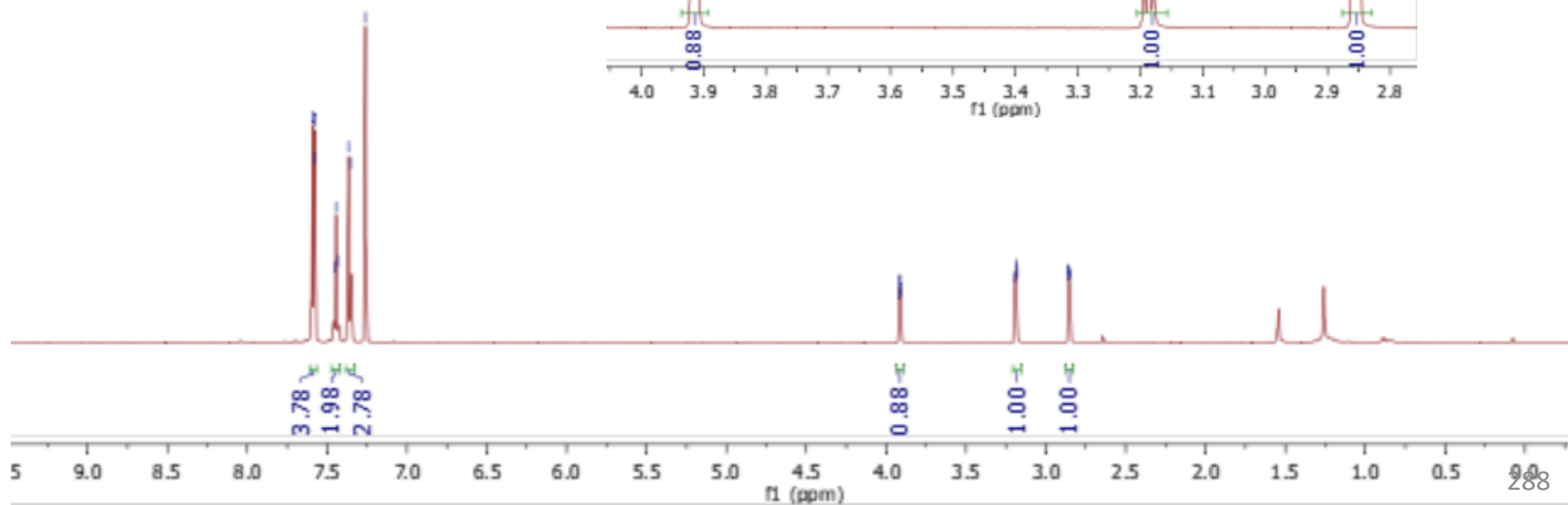
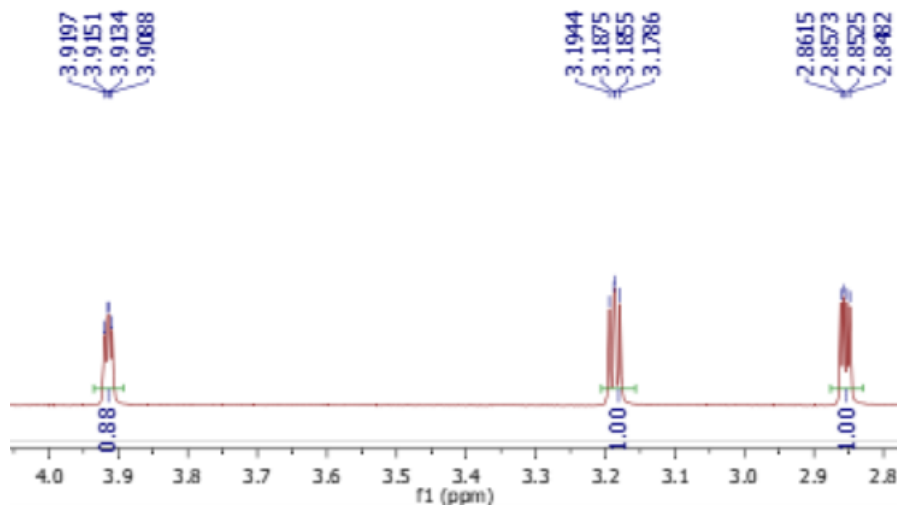
Totals		100.000
--------	--	---------

^1H NMR



7.5915
7.5801
7.5780
7.4556
7.4431
7.4300
7.3657
7.3523
7.2596

3.9197
3.9151
3.9134
3.9088
3.1944
3.1875
3.1855
3.1786
2.8615
2.8573
2.8525
2.8482

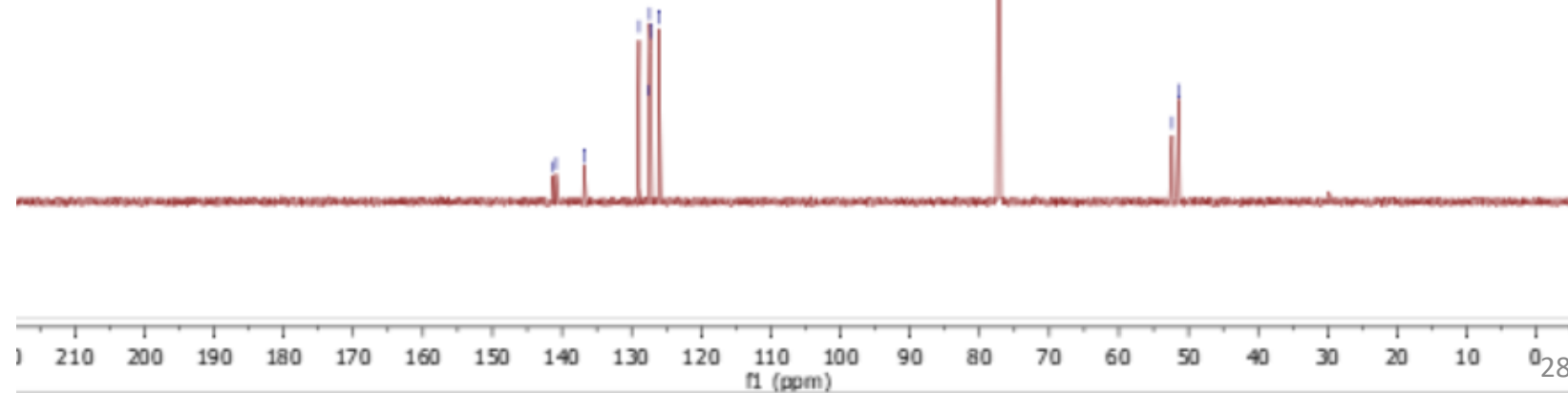
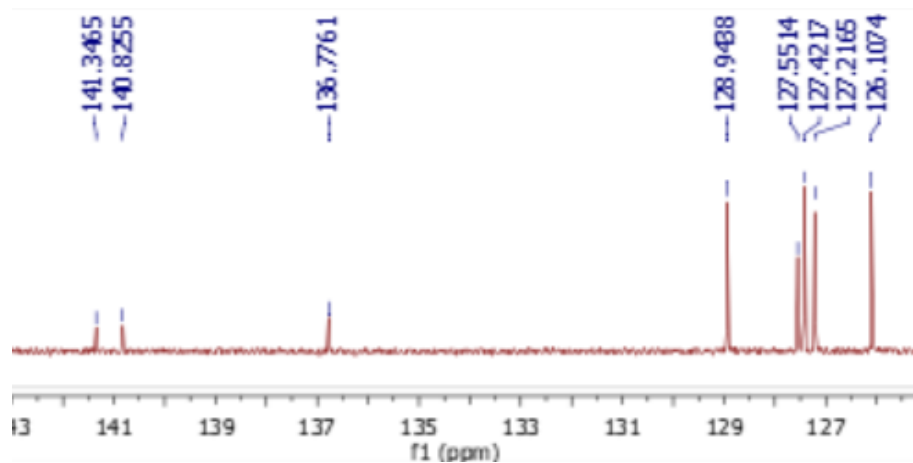
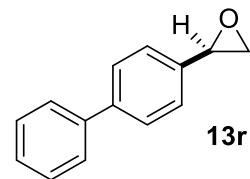


¹³CNMR

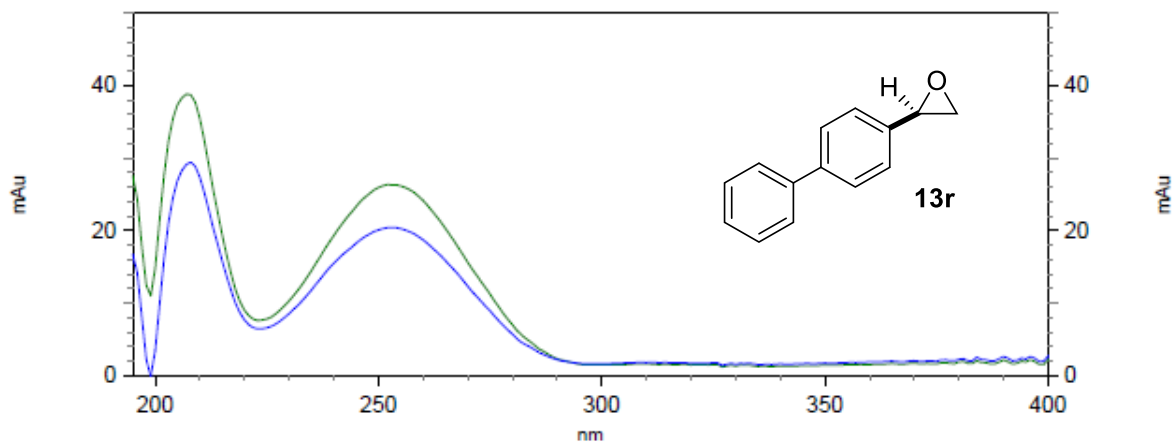
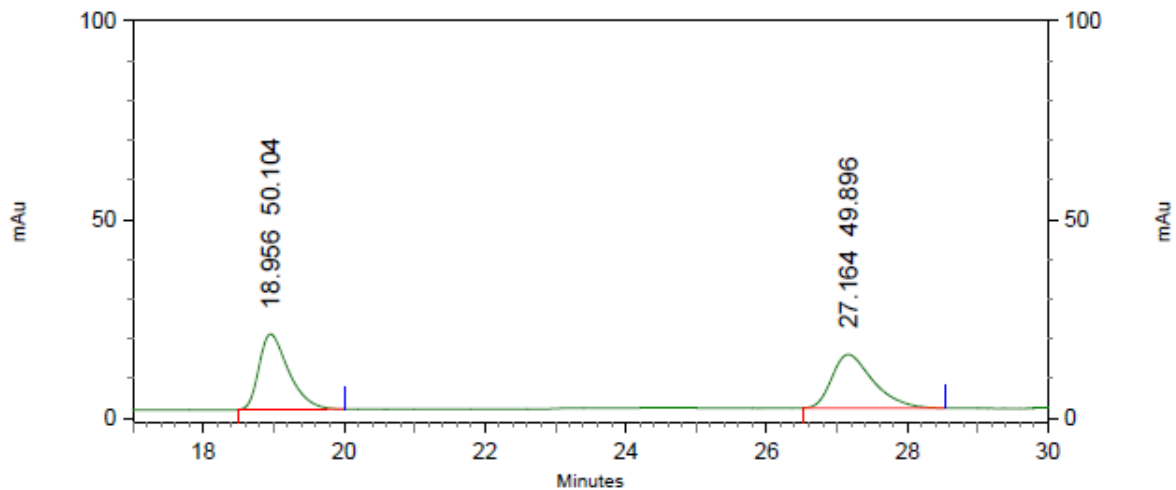
141.3465
140.8255
136.7761
128.9488
127.5514
127.4217
127.2165
126.1074

77.3714
77.1598
76.9481

52.3682
51.3932



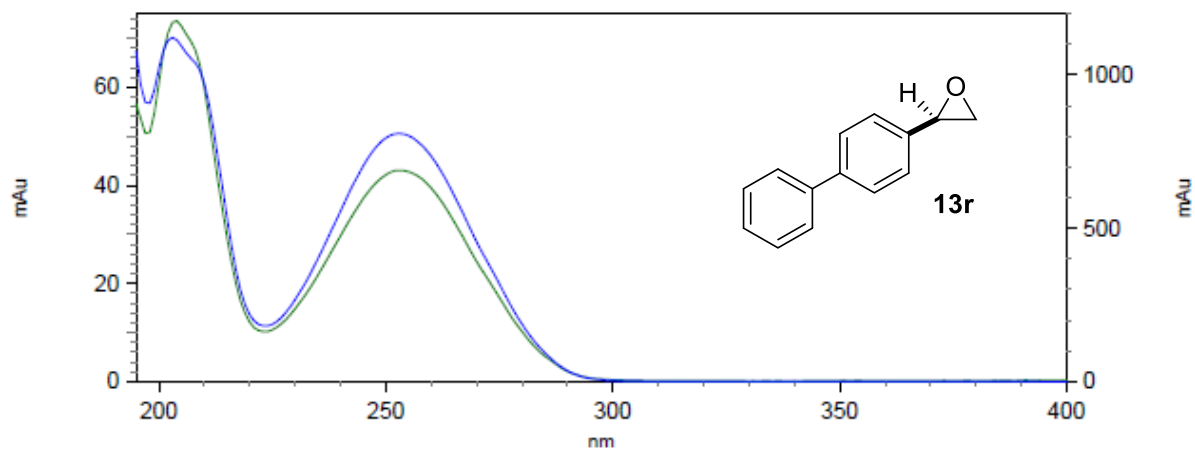
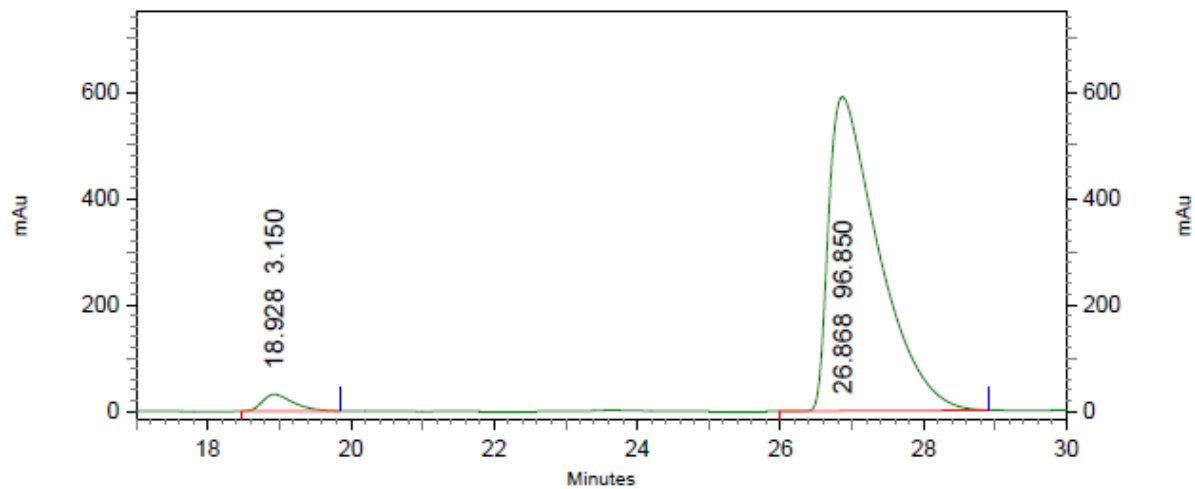
Racemic



6: 241 nm, 4
nm Results

Pk #	Retention Time	Area Percent
1	18.956	50.104
2	27.164	49.896
Totals		100.000

Enantioenriched

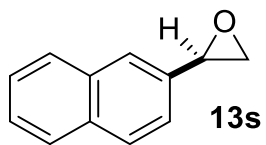


6: 241 nm, 4
nm Results

Pk #	Retention Time	Area Percent
1	18.928	3.150
2	26.868	96.850

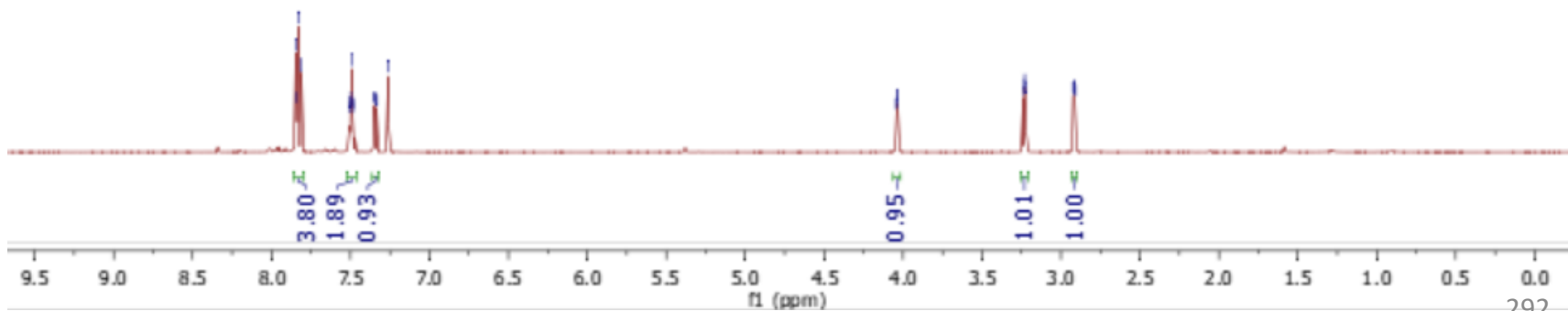
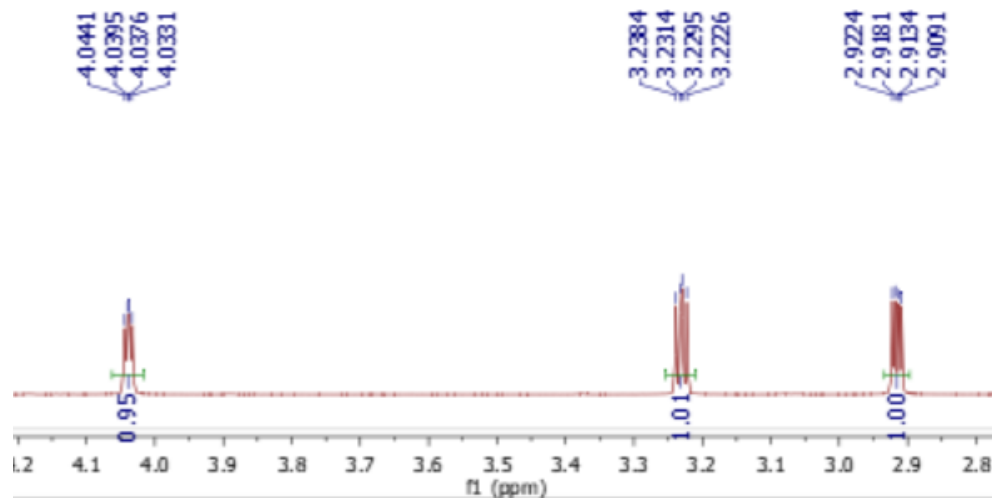
Totals		100.000
--------	--	---------

¹H NMR

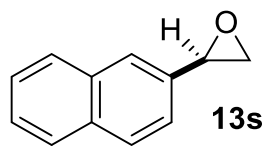


7.8456
7.8393
7.8315
7.8111
7.5048
7.5018
7.4970
7.4928
7.4886
7.4839
7.4814
7.3490
7.3463
7.3349
7.3321
7.2605

4.0441
4.0395
4.0376
4.0331
3.2384
3.2314
3.2295
3.2226
2.9224
2.9181
2.9134
2.9091



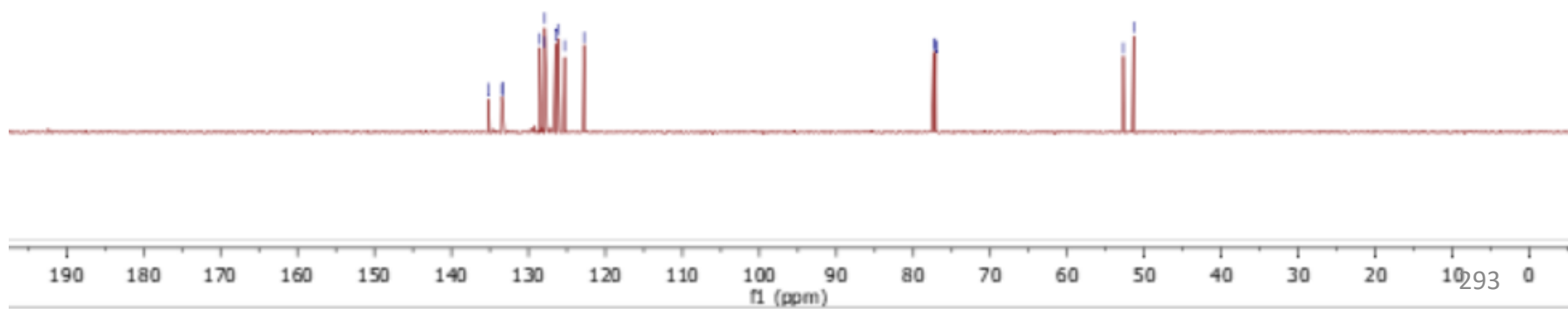
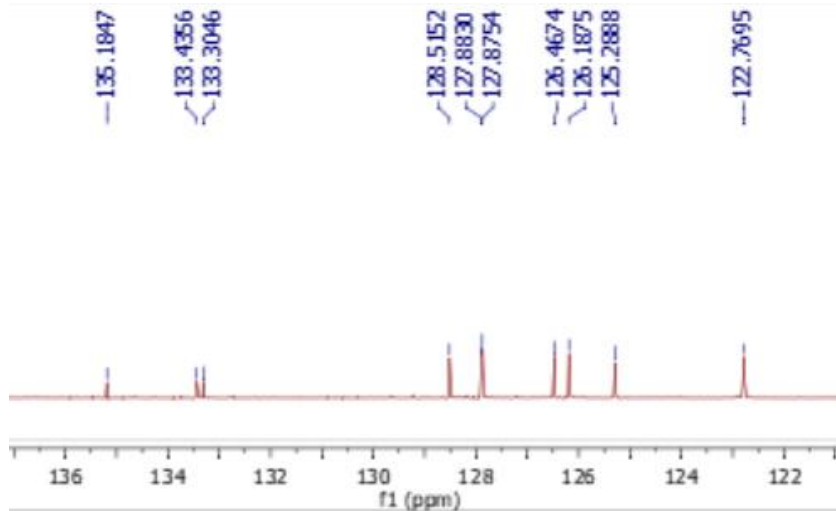
¹³CNMR



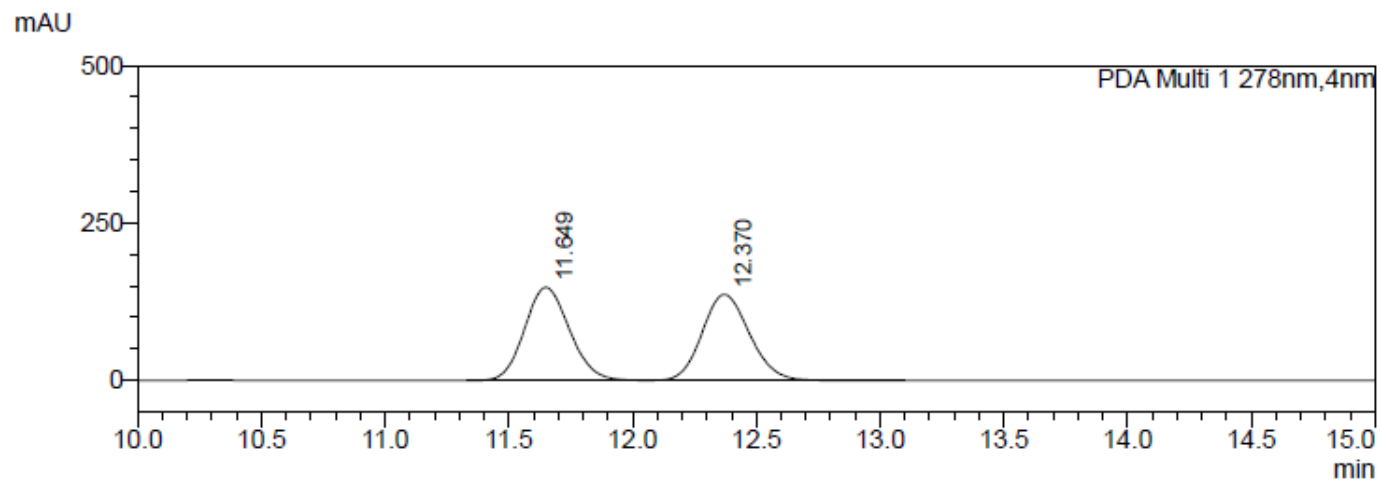
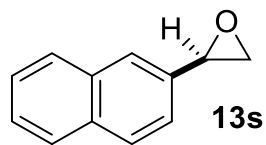
135.1847
133.4356
133.3046
128.5152
127.8830
127.8754
126.4674
126.1875
125.2888
122.7695

77.3713
77.1598
76.9477

52.7313
51.3910

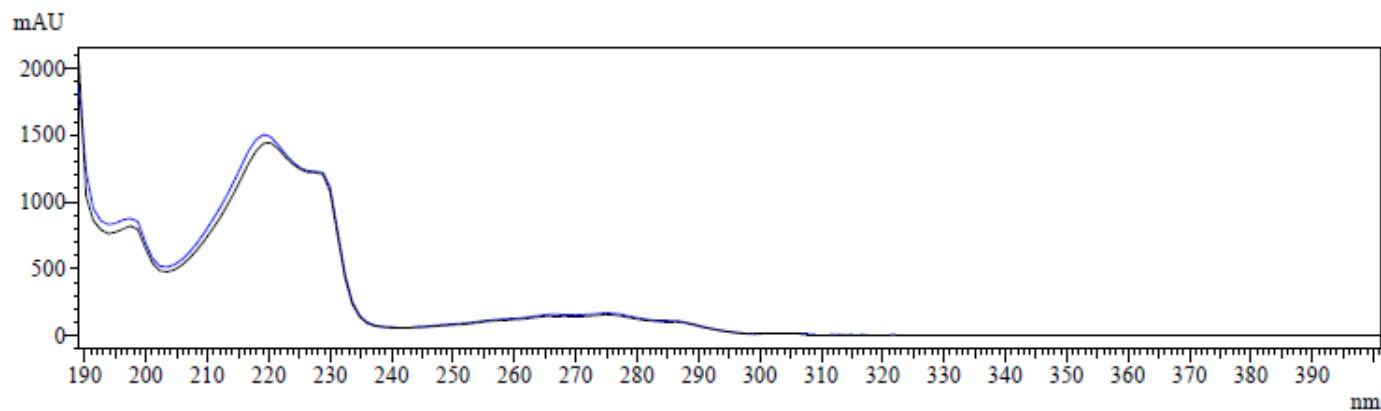


Racemic
HPLC trace



UV Spectrum

XRF-RAC-Naph-IF-2%-1_004.lcd

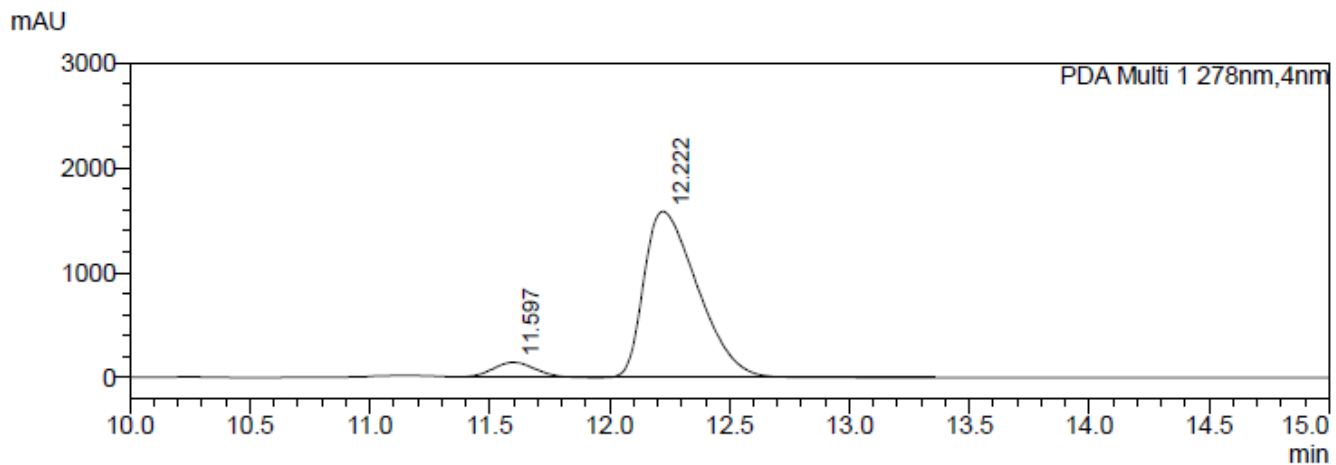
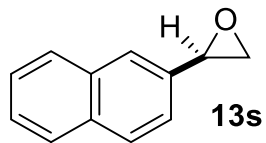


Peak Table

PDA Ch1 278nm

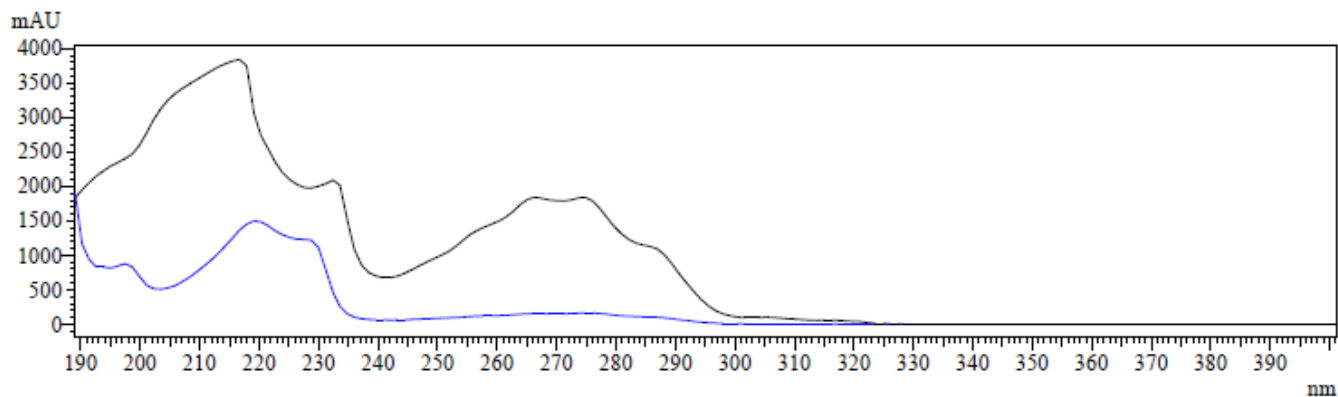
Peak#	Ret. Time	Area%
1	11.649	50.655
2	12.370	49.345
Total		100.000

HPLC trace



UV Spectrum

XRF-Naph-IF-2%_005.lcd

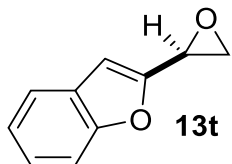


Peak Table

PDA Ch1 278nm

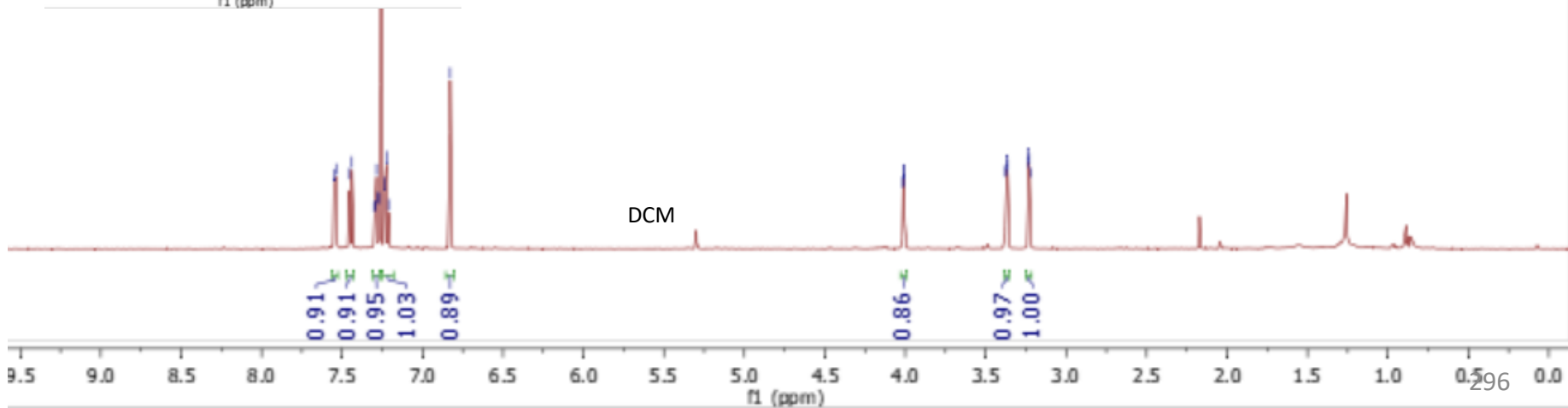
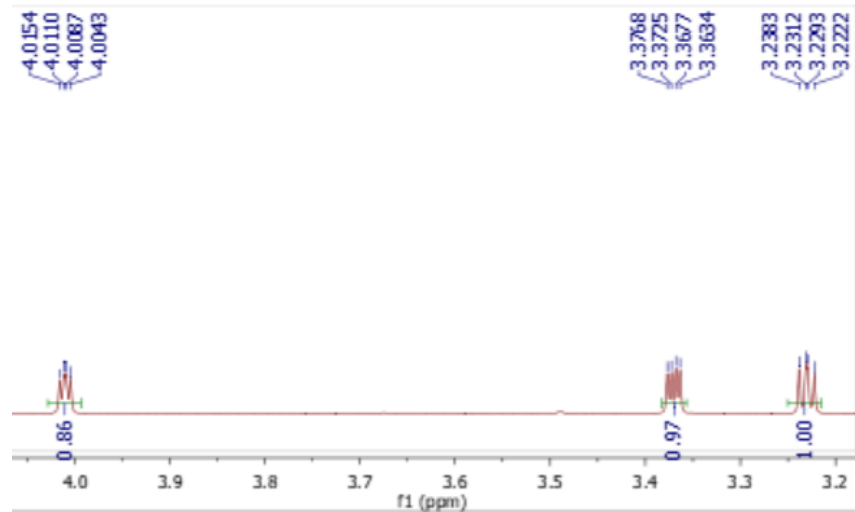
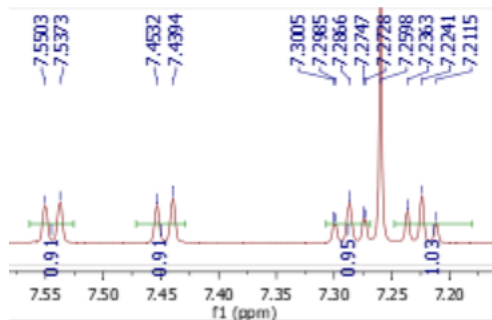
Peak#	Ret. Time	Area%
1	11.597	7.021
2	12.222	92.979
Total		100.000

¹H NMR

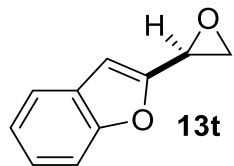


7.5503
7.5373
7.4532
7.4394
7.3005
7.2985
7.2866
7.2747
7.2728
7.2598
7.2363
7.2241
7.2115
6.8281

4.0154
4.0110
4.0087
4.0043
3.3768
3.3725
3.3677
3.3634
3.2383
3.2312
3.2293
3.2222



¹³CNMR



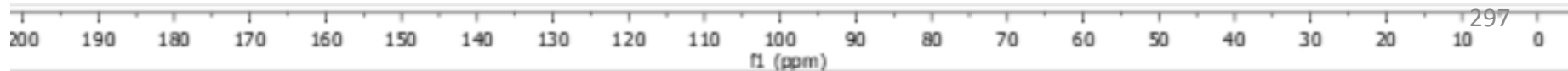
155.0561
153.0239

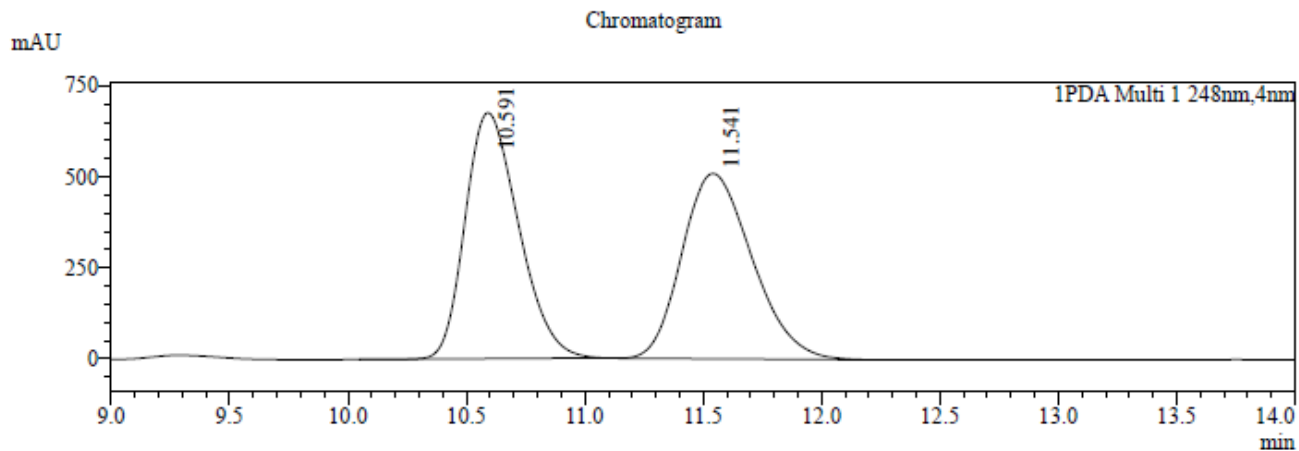
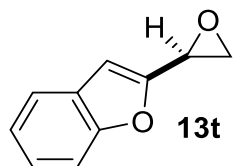
128.1345
124.8848
123.1188
121.1350

111.4959
106.6264

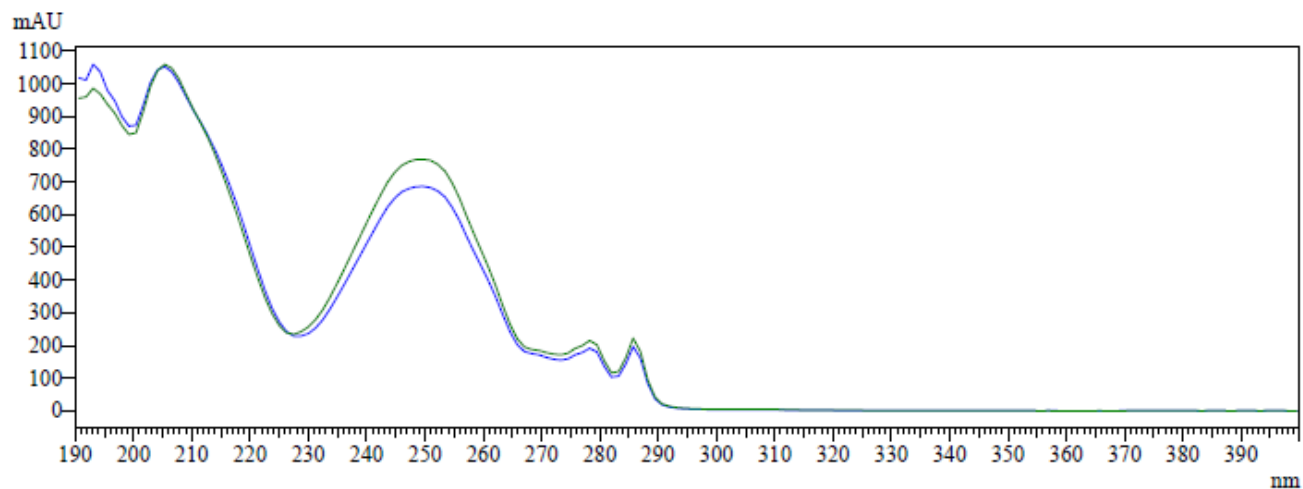
77.3712
77.1597
76.9477

48.4999
46.8013



Racemic
HPLC trace

XRF-1855-RAC-ID-1%.lcd

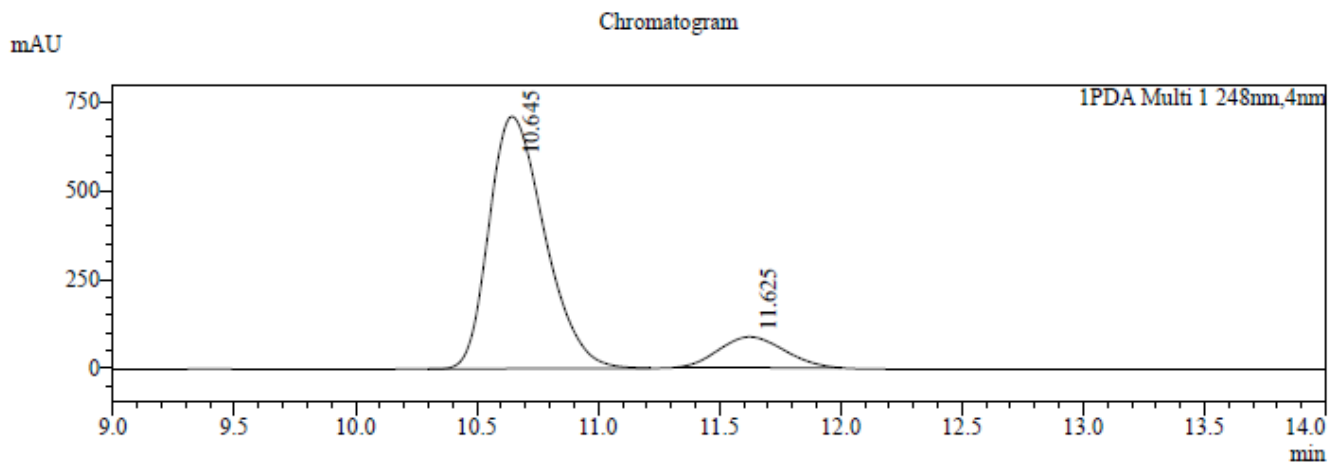
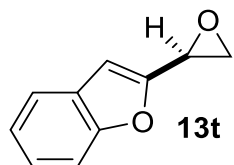


Peak Table

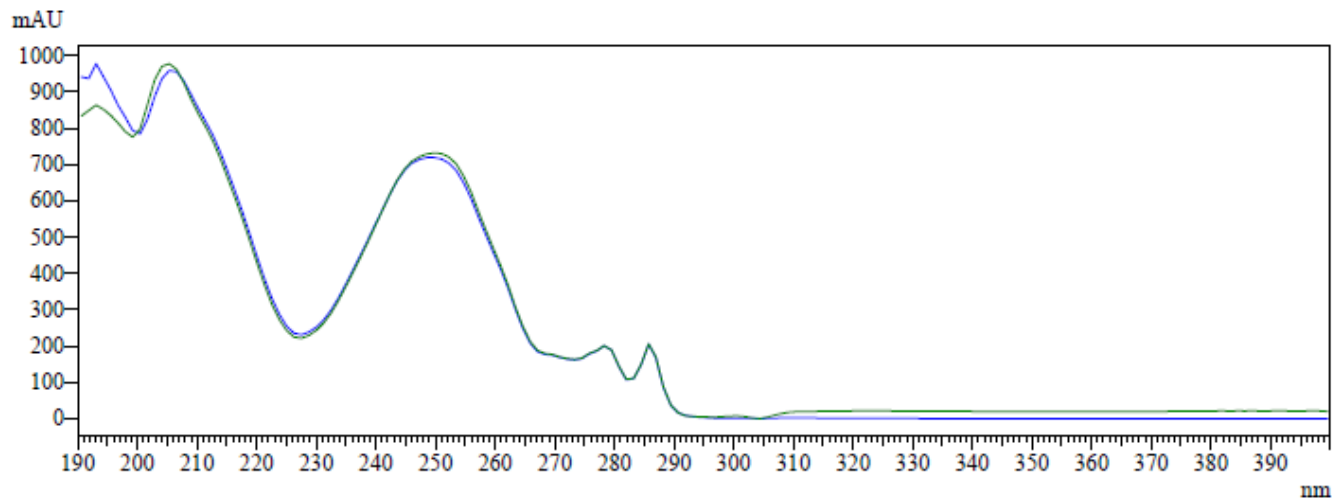
PDA Ch1 248nm

Peak#	Ret. Time	Area	Area%
1	10.591	10593076	50.170
2	11.541	10521167	49.830
Total		21114243	100.000

HPLC trace



XRF-1855-ID-1%.lcd

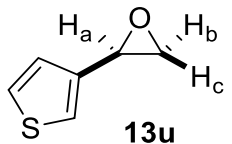


Peak Table

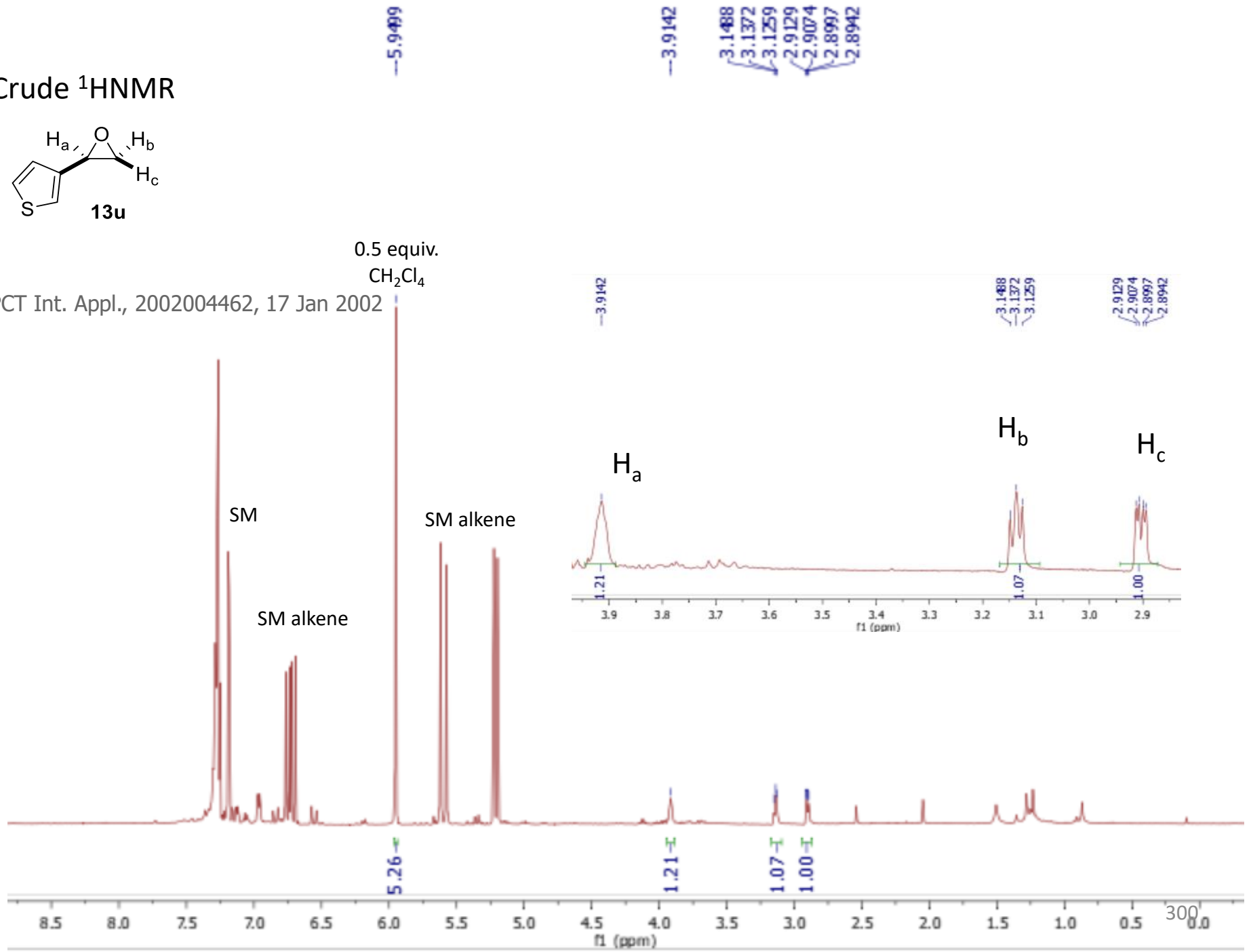
PDA Ch1 248nm

Peak#	Ret. Time	Area	Area%
1	10.645	11309609	87.500
2	11.625	1615667	12.500
Total		12925276	100.000

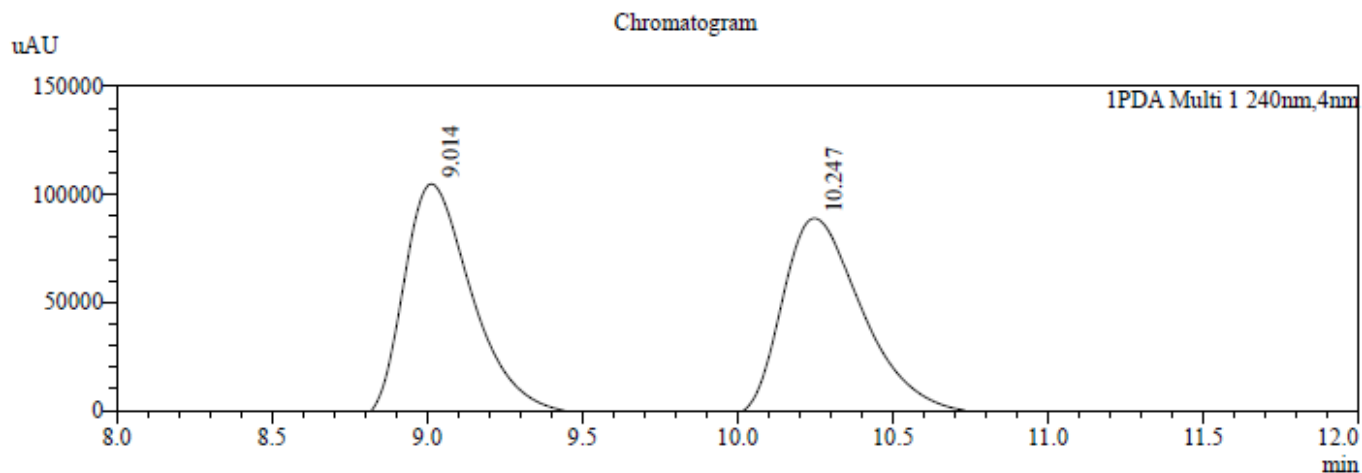
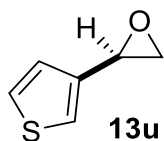
Crude ¹HNMR



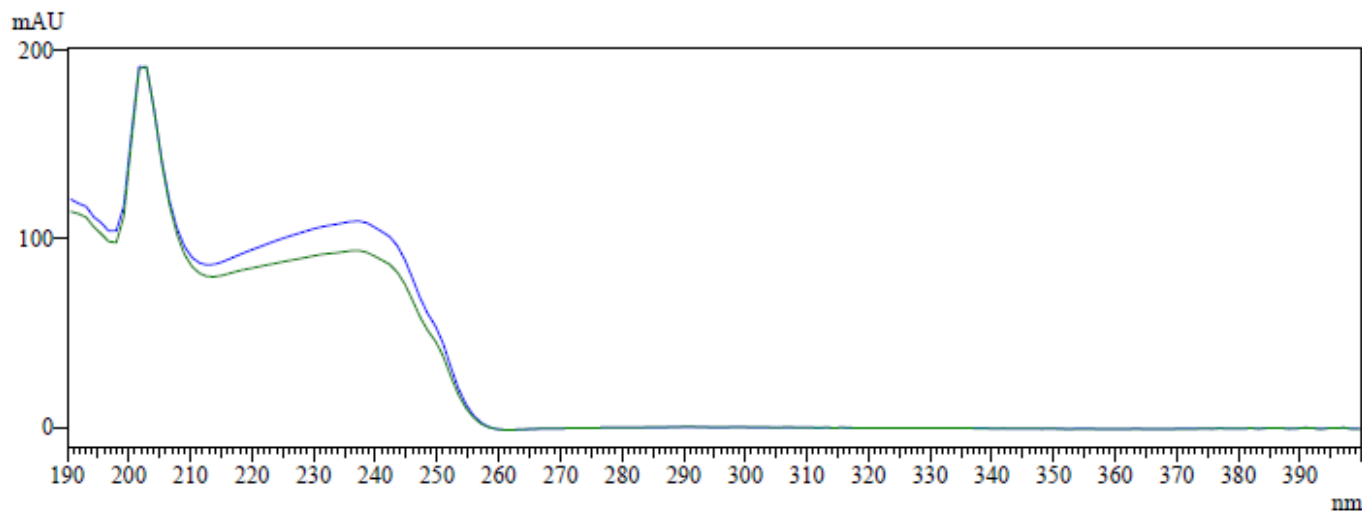
0.5 equiv.
CH₂Cl₄
PCT Int. Appl., 2002004462, 17 Jan 2002



Racemic
HPLC trace



XRF-1726-RAC-ADH-1%.lcd

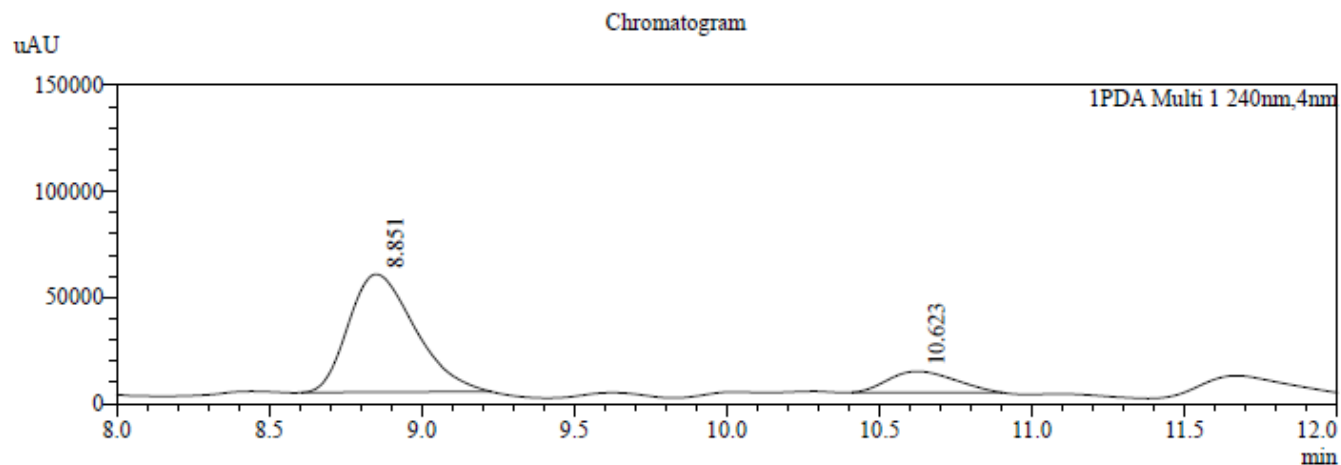
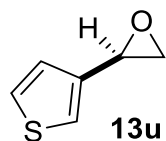


Peak Table

PDA Ch1 240nm

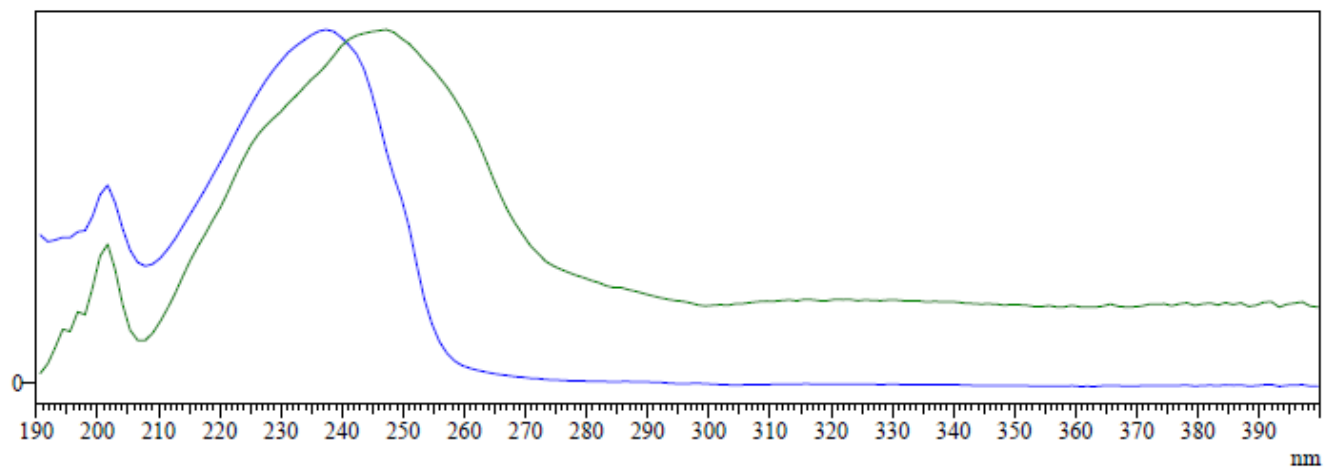
Peak#	Ret. Time	Area	Area%
1	9.014	1684024	50.081
2	10.247	1678558	49.919
Total		3362583	100.000

HPLC trace



XRF-1726-ADH-1%.lcd

mAU

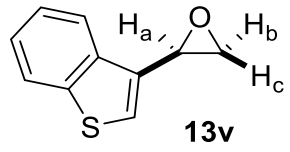


Peak Table

PDA Ch1 240nm

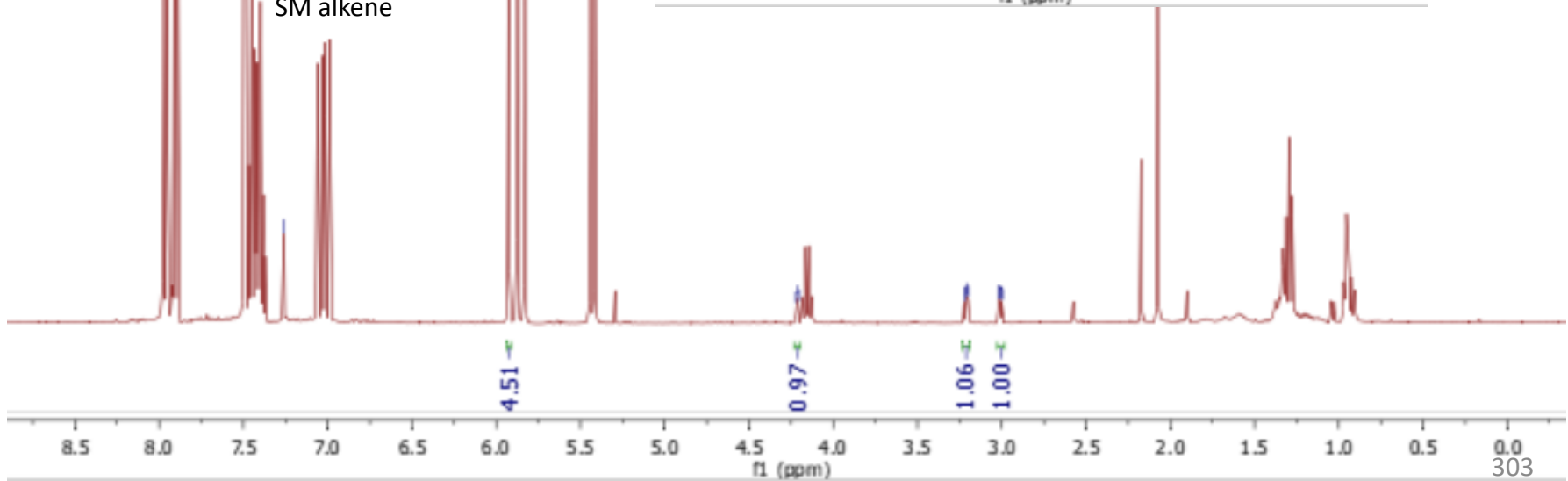
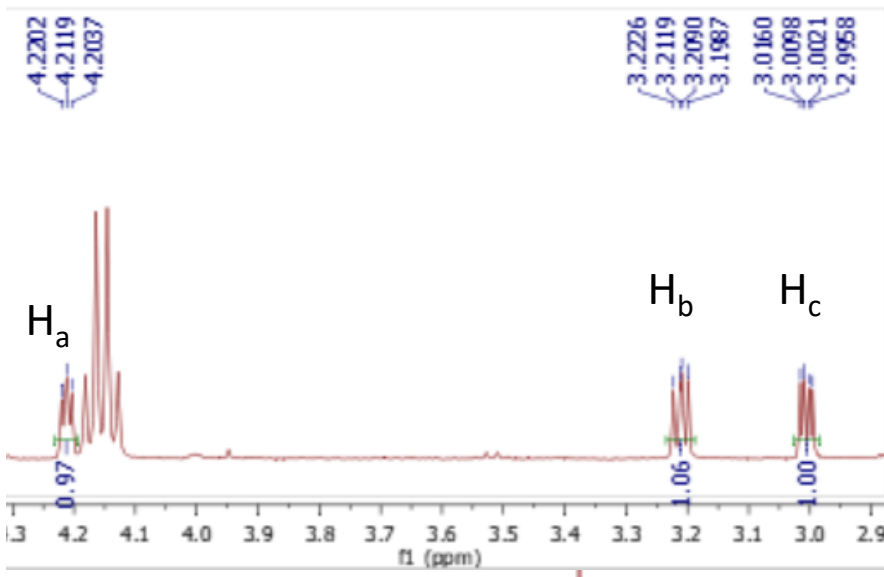
Peak#	Ret. Time	Area	Area%
1	8.851	843271	84.721
2	10.623	152082	15.279
Total		995353	100.000

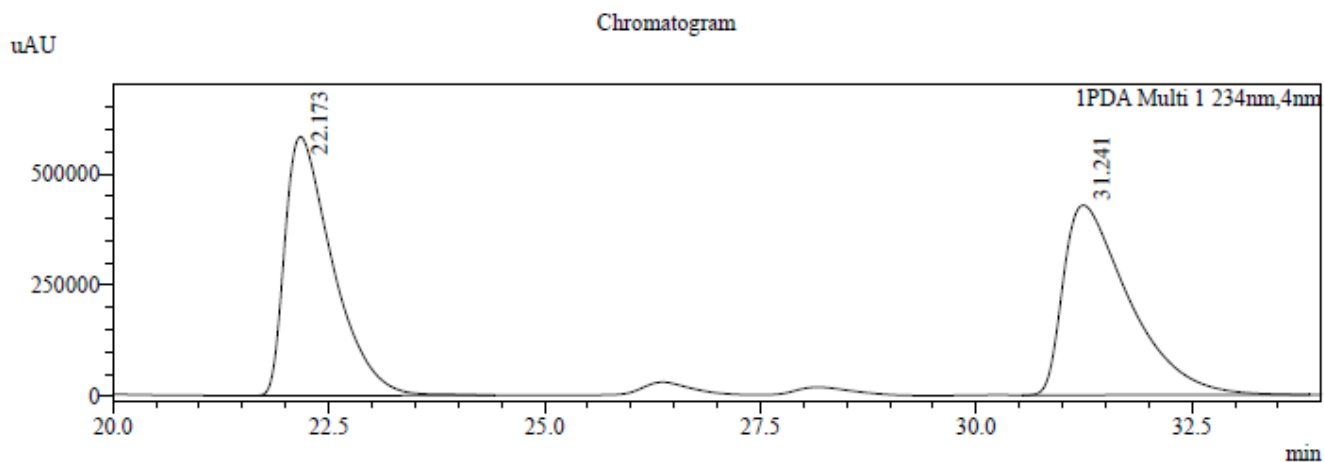
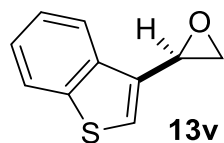
Crude ¹HNMR



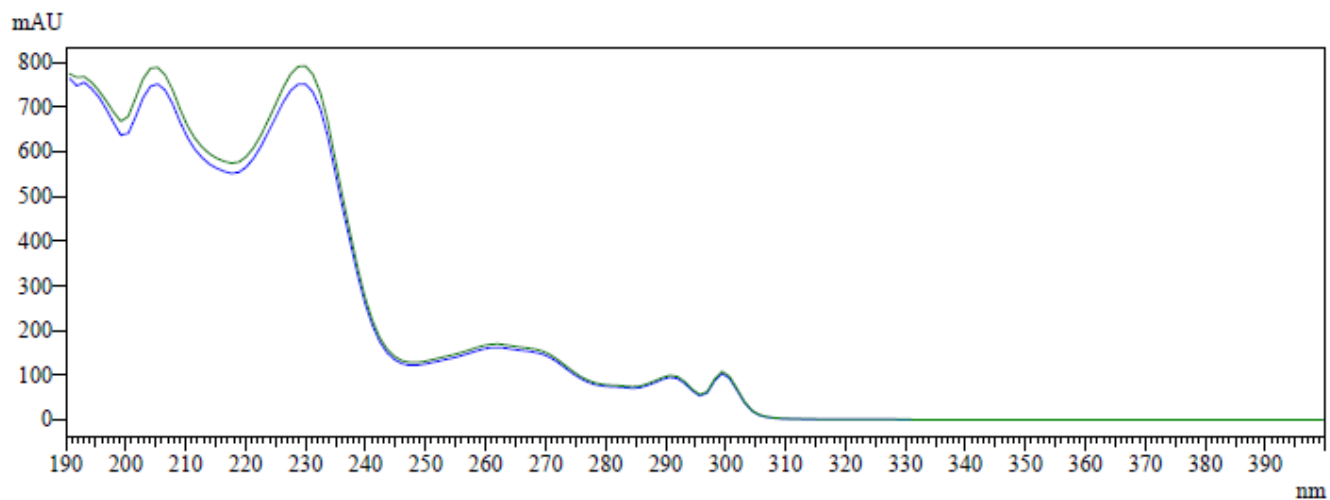
-7.2595
-5.9253
4.2202
4.2119
4.2037
3.2226
3.2119
3.2090
3.1987
3.0160
3.0098
3.0021
2.9958

SM
SM alkene
0.5 equiv.
CH₂Cl₄
SM alkene



Racemic
HPLC trace

XRF-1856-RAC-ODH-0.5%.lcd

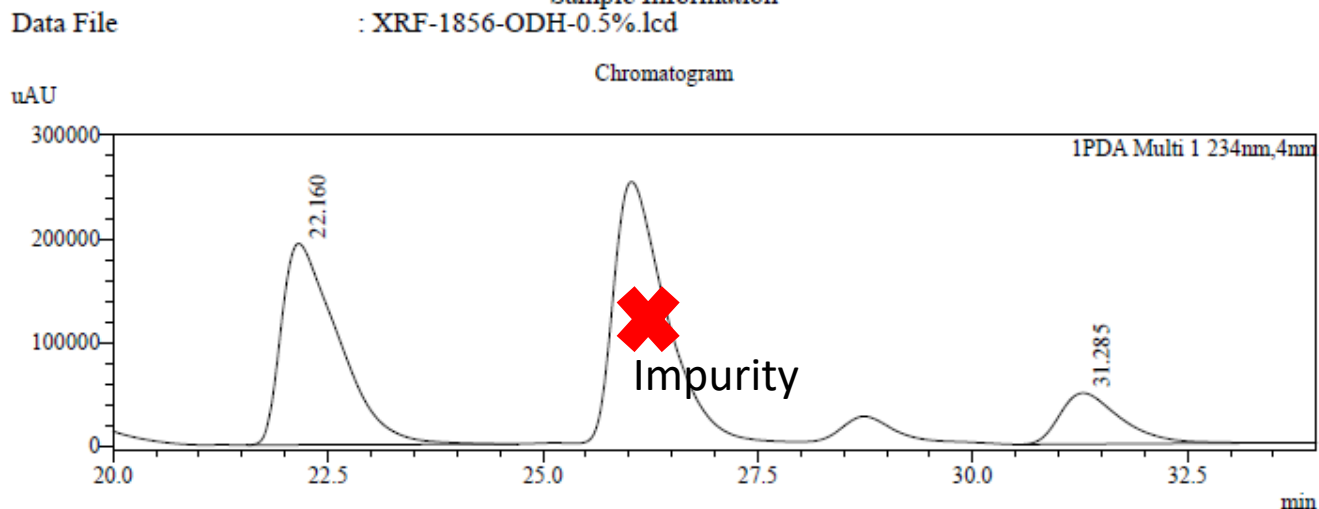
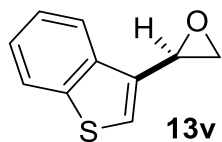


Peak Table

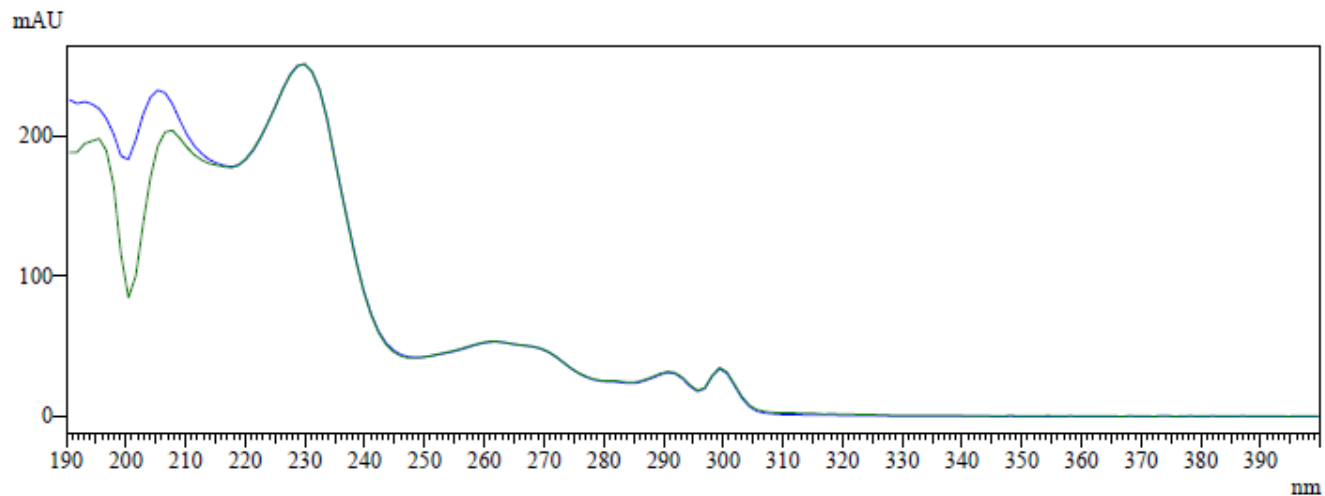
PDA Ch1 234nm

Peak#	Ret. Time	Area	Area%
1	22.173	22401093	49.693
2	31.241	22677688	50.307
Total		45078782	100.000

HPLC trace



XRF-1856-ODH-0.5%.lcd



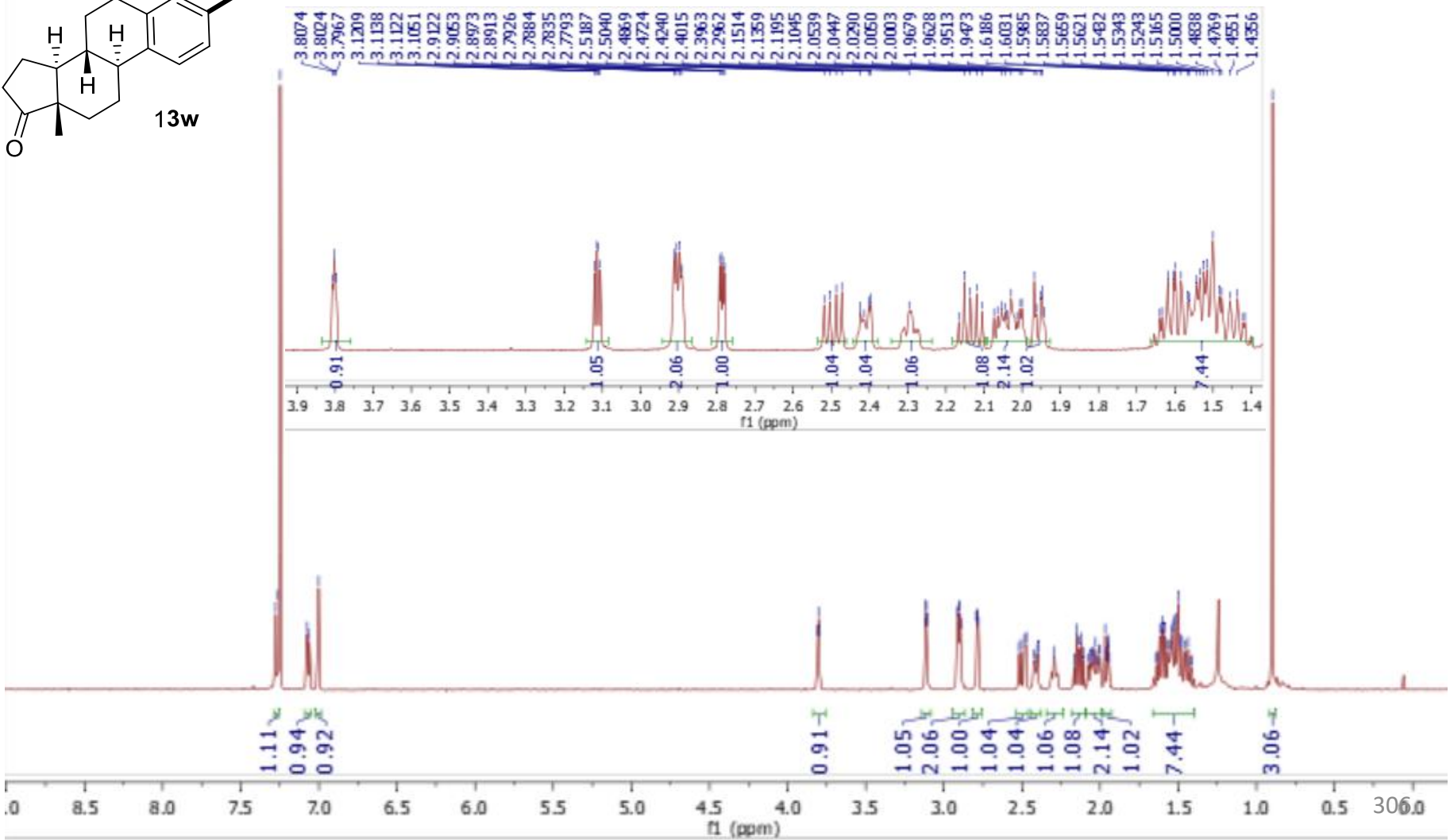
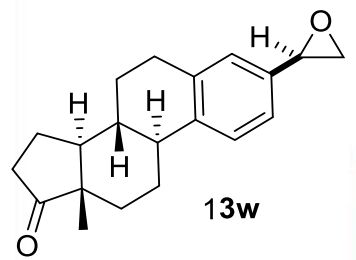
Peak Table

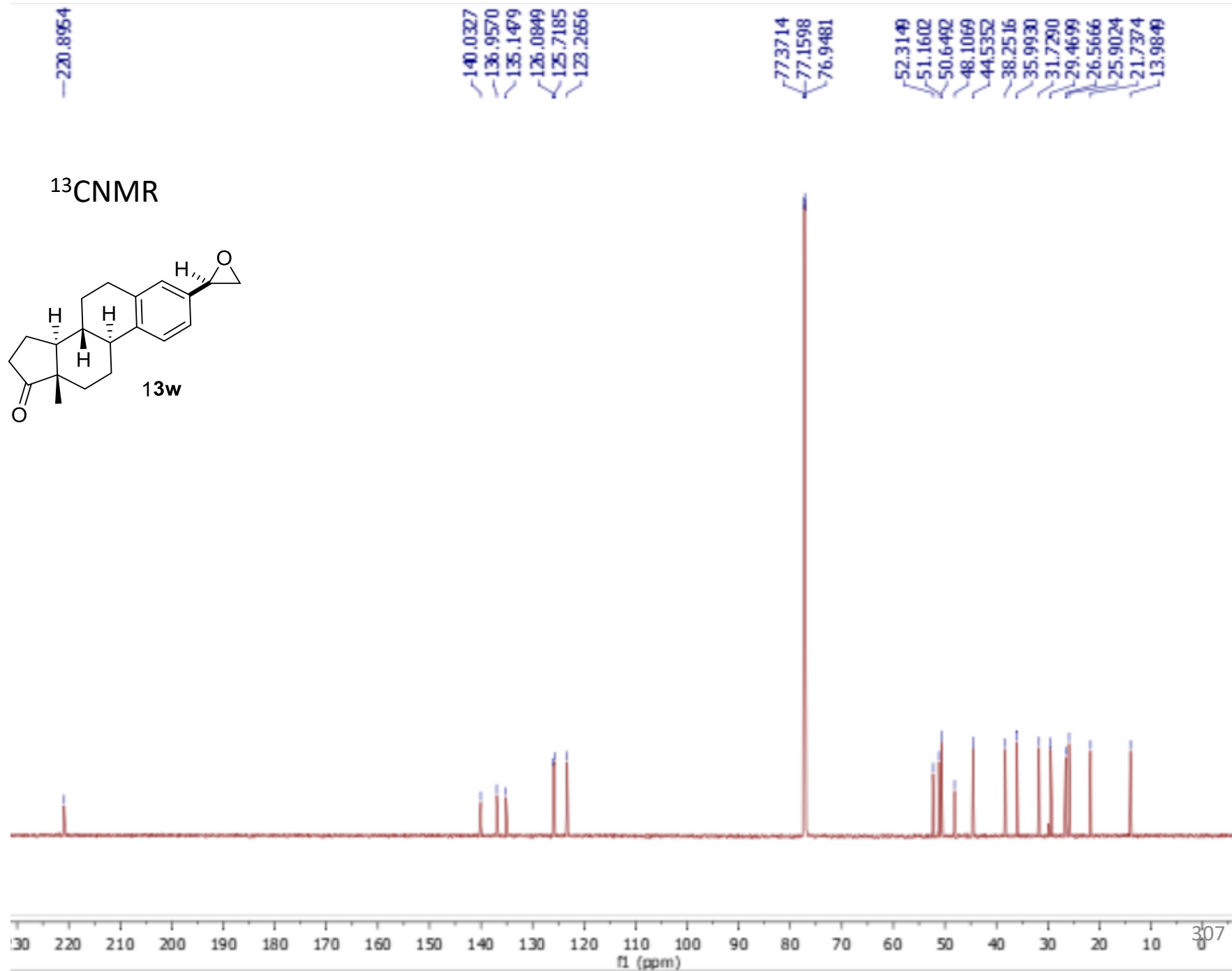
PDA Ch1 234nm

Peak#	Ret. Time	Area	Area%
1	22.160	8977139	78.680
2	31.285	2432601	21.320
Total		11409740	100.000

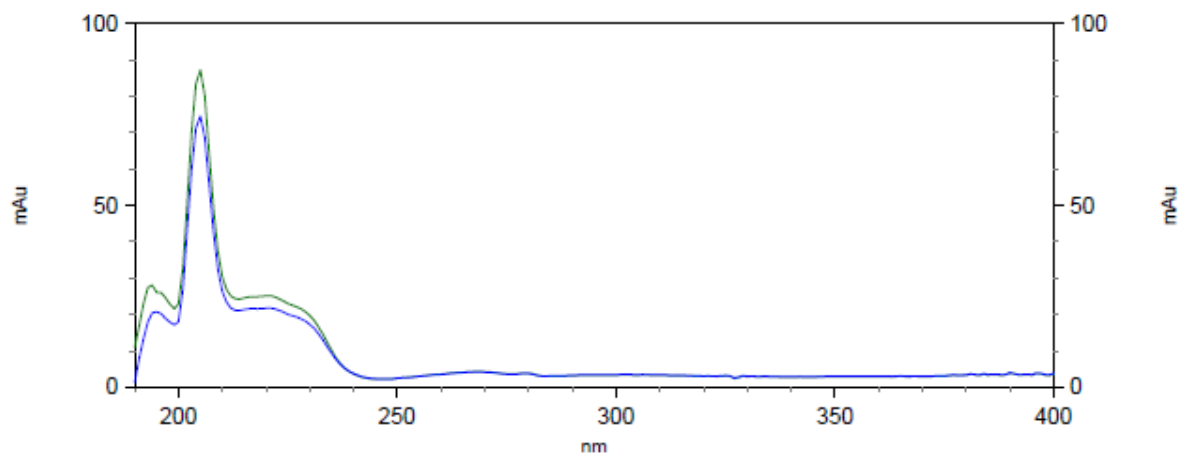
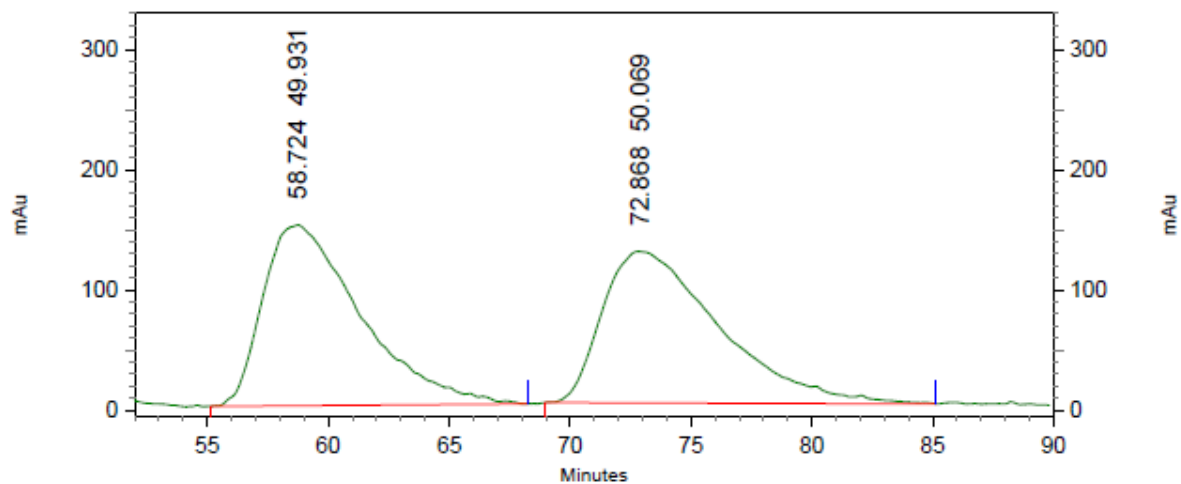
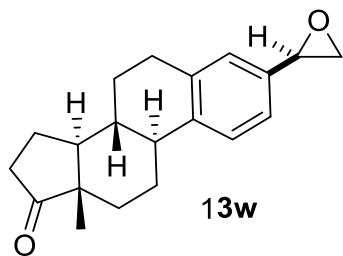
7.2762
7.2627
7.2475
7.0749
7.0617
7.0016
3.8074
3.8024
3.7967
3.1209
3.1138
3.1122
3.1051
2.9122
2.9122
2.9053
2.8973
2.8913
2.7926
2.7884
2.7835
2.7793
2.5187
2.5040
2.4859
2.4724
2.4240
2.4015
2.3963
2.2962
2.1514
2.1359
2.1195
2.1045
2.0644
2.0539
2.0447
2.0290
2.0050
2.0003
2.0003
1.9679
1.9628
1.9513
1.9473
1.9419
1.6336
1.6186
1.6031
1.5985
1.5837
1.5659
1.5621
1.5482
1.5243
1.5165
1.5000
1.4838
1.4769
1.4551
1.4356

¹H NMR





Racemic
HPLC trace

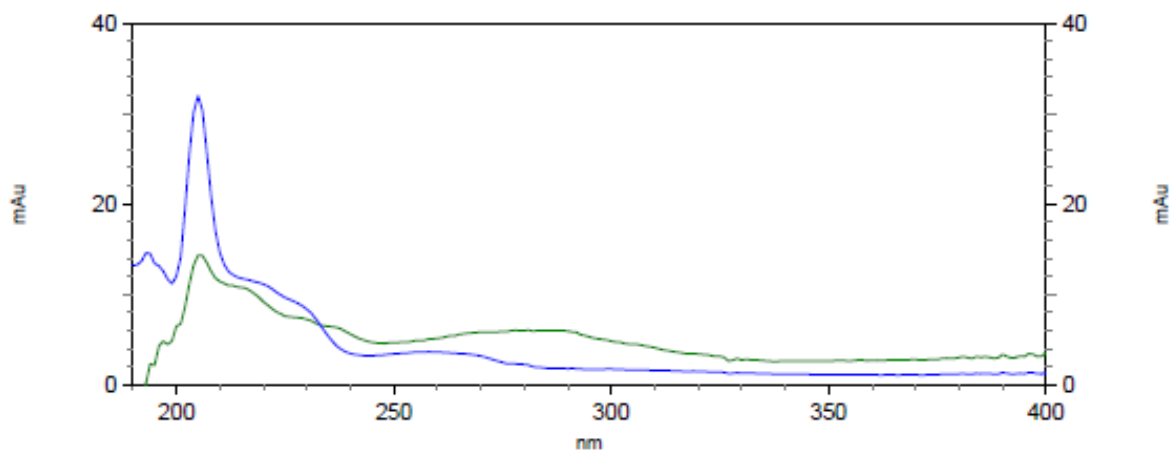
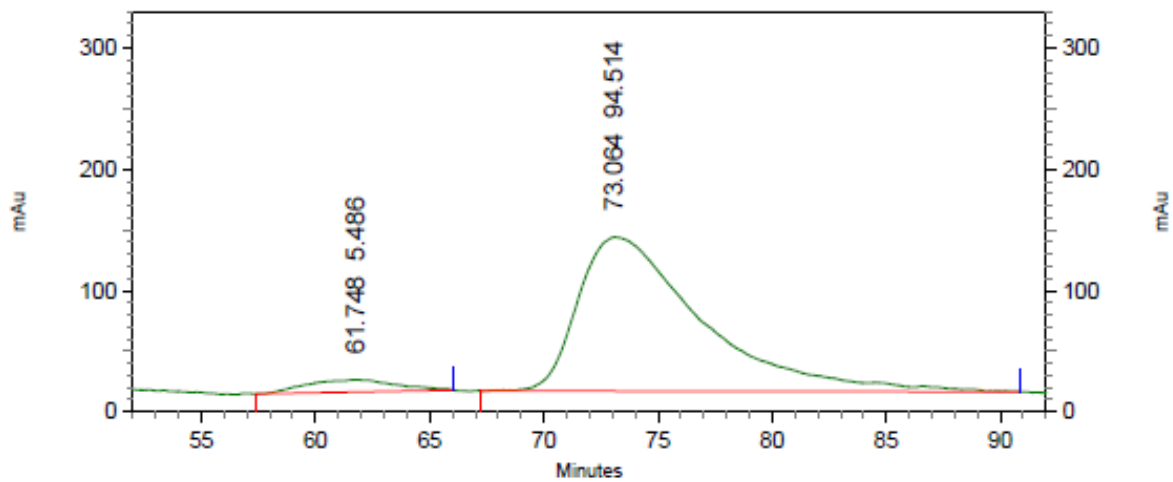
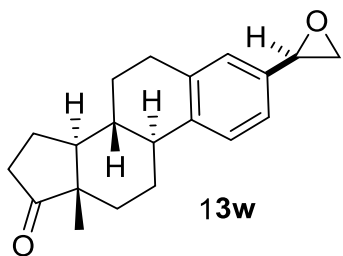


4: 205 nm, 4
nm Results

Pk #	Retention Time	Area Percent
1	58.724	49.931
2	72.868	50.069
Totals		100.000

C:\EZStart\Projects\Default\Data\XRF-1703-OJH-4%
 C:\Documents and Settings\zhang\Desktop\WCL\Method.met

HPLC trace



4: 205 nm, 4
 nm Results

Pk #	Retention Time	Area Percent
1	61.748	5.486
2	73.064	94.514
Totals		100.000

